ADVANCES IN BEHAVIORAL BIOLOGY • VOLUME 56

THE BASAL GANGLIA VIII

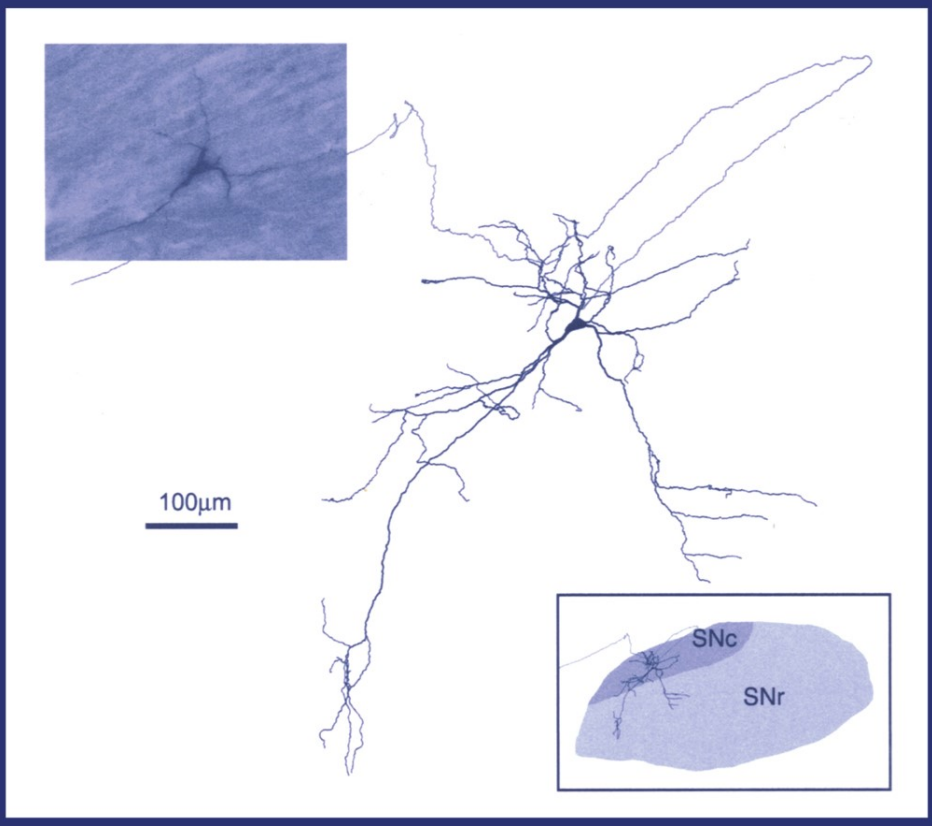

Edited by
J. Paul Bolam, Cali A. Ingham,
and Peter J. Magill

THE BASAL GANGLIA VIII

ADVANCES IN BEHAVIORAL BIOLOGY

Recent Volumes in This Series

Volume 39	THE BASAL GANGLIA III Edited by Giorgio Bernardi, Malcolm B. Carpenter, Gaetano Di Chiara, Micaela Morelli, and Paolo Stanzione
Volume 40	TREATMENT OF DEMENTIAS: A New Generation of Progress Edited by Edwin M. Meyer, James W. Simpkins, Jyunji Yamamoto, and Fulton T. Crews
Volume 41	THE BASAL GANGLIA IV: New Ideas and Data on Structure and Function Edited by Gérard Percheron, John S. McKenzie, and Jean Féger
Volume 42	CALLOSAL AGENESIS: A Natural Split Brain? Edited by Maryse Lassonde and Malcolm A. Jeeves
Volume 43	NEUROTRANSMITTERS IN THE HUMAN BRAIN Edited by David J. Tracey, George Paxinos, and Jonathan Stone
Volume 44	ALZHEIMER'S AND PARKINSON'S DISEASES: Recent Developments Edited by Israel Hanin, Mitsuo Yoshia, and Abraham Fisher
Volume 45	EPILEPSY AND THE CORPUS CALLOSUM 2 Edited by Alexander G. Reeves and David W. Roberts
Volume 46	BIOLOGY AND PHYSIOLOGY OF THE BLOOD-BRAIN BARRIER: Transport, Cellular Interactions, and Brain Pathologies Edited by Pierre-Olivier Couraud and Daniel Scherman
Volume 47	THE BASAL GANGLIA V Edited by Chihoto Ohye, Minoru Kimura, and John S. McKenzie
Volume 48	KINDLING 5 Edited by Michael E. Corcoran and Solomon Moshé
Volume 49	PROGRESS IN ALZHEIMER'S AND PARKINSON'S DISEASES Edited by Abraham Fisher, Israel Hanin, and Mitsuo Yoshida
Volume 50	NEUROPSYCHOLOGY OF CHILDHOOD EPILEPSY Edited by Isabelle Jambaqué, Maryse Lassonde, and Olivier Dulac
Volume 51	MAPPING THE PROGRESS OF ALZHEIMER'S AND PARKINSON'S DISEASE Edited by Yoshikuni Mizuno, Abraham Fisher, and Israel Hanin
Volume 52	THE BASAL GANGLIA VII Edited by Louise F.B. Nicholson and Richard L.M. Faull
Volume 53	CATECHOLAMINE RESEARCH: From Molecular Insights to Clinical Medicine Edited by Toshiharu Nagatsu, Toshitaka Nabeshima, Richard McCarty, and David S. Goldstein
Volume 54	THE BASAL GANGLIA VI Edited by Ann M. Graybiel, Mahlon R. Delong, and Stephen T. Kitai
Volume 55	KINDLING 6 Edited by Michael E. Corcoran and Solomon L. Moshé

THE BASAL GANGLIA VIII

Edited by

J. Paul Bolam
MRC Anatomical Neuropharmacology Unit
University of Oxford
UK

Cali A. Ingham
Division of Veterinary Biomedical Science
University of Edinburgh
UK

and

Peter J. Magill
MRC Anatomical Neuropharmacology Unit
University of Oxford
UK

Springer

J.P. Bolam
MRC Anatomical Neuropharmacology Unit
Oxford
United Kingdom

C.A. Ingham
University of Edinburgh
Edinburgh
United Kingdom

P.J. Magill
MRC Anatomical Neuropharmacology Unit
Oxford
United Kingdom

Library of Congress Control Number: 2005931829

ISBN-10: 0-387-28065-0 e-ISBN 0-387-28066-9
ISBN-13: 978-0387-28065-3

Printed on acid-free paper.

Printed in Singapore. (BS/KYO)

9 8 7 6 5 4 3 2 1

springeronline.com

INTERNATIONAL BASAL GANGLIA SOCIETY OFFICERS (2001–2004)

President
J. Paul Bolam (England)

Past President
Richard L.M. Faull (New Zealand)

President Elect
Henk J. Groenewegen (The Netherlands)

Secretary
Cali A. Ingham (Scotland)

Secretary Elect
Henk Berendse (The Netherlands)

Treasurer
Yoland Smith (USA)

Council
Marianne Amalric (France)
Gordon Arbuthnott (Scotland)
Alan Crossman (England)
Gaetano Di Chiara (Italy)
Glenda Halliday (Australia)
Katsuma Nakano (Japan)
Louise F.B. Nicholson (New Zealand)
Charles J Wilson (USA)

IBAGS VIII

The 8th Triennial Meeting of the International Basal Ganglia Society was held at the Crieff Hydro Hotel, Crieff, Scotland
5th–9th September 2004

President	J. Paul Bolam
Secretary	Cali A. Ingham

Local Committee

J. Paul Bolam
Cali A. Ingham
Peter J. Magill
Gordon Arbuthnott

Scientific organising committee

J.P. Bolam
G. Arbuthnott
P.J. Magill
A. Crossman
E. Abercrombie
D. Brooks
T. Aziz
C.A. Ingham
P. Emson
W. Schultz
J. Tepper
Y. Smith
P. Redgrave

The following organisations are gratefully acknowledged for their financial assistance

AFFINITI Research Products, Kenneth and Ellen Aidekman, Alpha Omega Egineering, British Neuroscience Association, Cambridge Electronic Design Ltd, Crieff Hydro Hotel, Dalwhinnie Distillery, Eli Lilly & Co, Elsevier Ireland, Elsevier Life Science Marketing, GlaxoSmithKline, International Brain Research Organization, Medtronic Ltd, Novartis Institute for Biomedical Research Inc, Parkinson's Disease Society (UK), PGRD Groton Laboratories, The Wellcome Trust.

PREFACE

This volume, The Basal Ganglia VIII, is derived from the proceedings of the Eighth Triennial Meeting of the International Basal Ganglia Society (IBAGS). The meeting was held from 5th–9th September 2004 at the Crieff Hydro Hotel, Crieff, Scotland. Over 270 delegates from 16 countries (Argentina, Australia, Austria, Canada, Hong Kong, France, Germany, Israel, Italy, Japan, The Netherlands, New Zealand, Spain, Sweden, United Kingdom and USA) attended the meeting, and there were over 54 oral presentations and 186 poster presentations. In keeping with the traditions of IBAGS meetings inclusion of chapters in this book was open to all presenters. In the event, we have 59 contributions. The Scientific Organising Committee of the meeting had identified several themes of outstanding interest to the basal ganglia researcher and we are pleased to say that three of them, 'Oscillations in the basal ganglia: The good, the bad and the unexpected', 'The ventral/dorsal divide: To integrate or separate' and 'Cholinergic mechanisms in the striatum', are featured here. The remaining sections of the book do not necessarily reflect the sessions organised for the meeting, but rather, the chapters have been grouped according to more general research topics. Timed to coincide with the meeting were two special issues of *Trends in Neurosciences*, 'Current Thinking in Basal Ganglia Research', designed to highlight key issues in contemporary basal ganglia research.

The triennial meetings of IBAGS are traditionally organised to enable young and (more) senior scientists to interact at both scientific and social levels, and we hope that the eighth meeting fulfilled this role. The beautiful Scottish setting of the meeting presented the ideal opportunity for delegates to exchange ideas on an informal basis, which variously included bracing countryside walks, ferocious *ceilidh* dancing, and plenty of whisky! A particularly pleasing event was the 'opening lecture' given by Oleh Hornykiewicz, who took us through forty years of dopamine research, thus enabling the younger scientists to put their work in an historical perspective. For his contributions to neuroscience, and in particular to dopamine research, he was elected as an Honorary Member of the society, as were Ann Graybiel and Anne Young for their long and continuing contributions to basal ganglia research. They join John McKenzie and Gerard Percheron, both long-standing honorary members.

The next meeting will take place in The Netherlands in 2007 under the watchful eyes of 'The Henks', Henk Groenewegen and Henk Berendse. We all look forward to the ninth meeting with eager anticipation.

Paul Bolam, Cali Ingham and Pete Magill

Photos from the 8th Triennial Meeting of IBAGS (5th–9th September 2004, Crieff, Scotland). *Upper left*, one of the poster sessions. *Top middle*, lunch-time discussions. *Top right*, Oleh Hornykiewicz gives the "Opening Lecture". *Bottom left*, Anne Young introduces Oleh Hornykiewicz. *Bottom middle*, the conference dinner. *Bottom right*, piping in the haggis.

CONTENTS

SECTION I
Oscillations in the Basal Ganglia

SECTION II
Cholinergic Mechanisms in the Striatum

SECTION III
Pharmacological and Receptor Studies of the Basal Ganglia

SECTION V
Disorders of Basal Ganglia Function II: Clinical Studies

SECTION VI
Physiological and Anatomical Studies of the Functional Organisation of the Basal Ganglia

Section I

OSCILLATIONS IN THE BASAL GANGLIA

OSCILLATIONS IN THE BASAL GANGLIA:
The good, the bad, and the unexpected

Thomas Boraud, Peter Brown, Joshua A. Goldberg, Ann M. Graybiel, and Peter J. Magill*

1. INTRODUCTION

Oscillations are present at many levels in the basal ganglia (BG), and can describe regular fluctuations in, for example, gene expression, current flow across the plasma membrane, the firing rate of a single neuron, the activity within and between small networks of neurons, and activity at the level of whole nuclei. Many BG neurons, including those of the subthalamic nucleus, globus pallidus (both segments), substantia nigra (both divisions), and some striatal interneurons, are endowed with a battery of intrinsic membrane properties that promote the expression of oscillatory discharge at both 'rest' (or in functional isolation) and in response to organized synaptic input (Richards et al., 1997; Bennett and Wilson, 1999; Bevan et al., 2002). The oscillatory activity of a single cell may or may not be synchronized with the oscillatory activity of another cell or network of cells. Indeed, oscillation and synchronization are distinct properties of neuronal networks. This is well illustrated in the BG; while the firing patterns of pallidal neurons are strongly periodic, the discharges of pairs of these neurons are typically uncorrelated (Bergman et al., 1998; Boraud et al., 2002). Conversely, the activity of BG neurons may be synchronized to within milliseconds but without being strongly periodic. These facts aside, it may be that *synchronized oscillations* offer the BG, and indeed the whole brain, something more than the simple sum of the parts (Steriade, 2000; Engel et al., 2001; Buzsáki and Draguhn, 2004). For example, they may provide the brain with a mechanism to execute tasks that require the combined

* Thomas Boraud, Basal Gang., Laboratoire de Neurophysiologie, CNRS UMR 5543, Université Victor Segalen Bordeaux, 33076 Bordeaux, France. Peter Brown, Sobell Dept. of Motor Neuroscience and Movement Disorders, Institute of Neurology, London, WC1N 3BG, UK. Joshua A. Goldberg, Dept. of Biology, University of Texas at San Antonio, San Antonio, TX 78249, USA. Ann M. Graybiel, Dept. of Brain & Cognitive Sciences, Massachusetts Institute of Technology, Cambridge, MA 02139, USA. Peter J. Magill, MRC Anatomical Neuropharmacology Unit, University of Oxford, Oxford, OX1 3TH, UK.

function of distant and disparate neural networks (Engel et al., 2001). This premise is of great importance in terms of cultivating research on the candidate mechanisms that underlie the elusive 'neural code'.

In this chapter, we will explore the evidence for synchronized network oscillations in the BG. We will focus on those oscillations that are generated by the coordinated and correlated activity of populations of neurons in the BG and their afferent partners *in vivo*. Research on synchronized network oscillations in the BG is still at an early stage. Perhaps as a consequence of this, the intrinsic cellular and circuit mechanisms that must underlie such oscillations remain obscure. Whilst it is conceivable that the intrinsic oscillations of single BG neurons can serve as the basis for collective synchrony and thus, the expression of such network oscillations, we will not venture further than to highlight this interesting possibility. We discuss the hypothetical roles played by synchronized network oscillations that permeate cortico-basal ganglia circuits during motor and cognitive behaviours, and we will re-examine the common view that synchronized network oscillations are primarily a feature of the diseased BG. New data suggest that oscillatory activity within the BG, and particularly the striatum and subthalamic nucleus, is prevalent during, and thus, may be important for, normal behaviour (the "Good"). We also take into account recent studies in humans, specifically patients with Parkinson's disease, that have reinforced the idea that BG population activity synchronized in certain frequency bands may be counter-productive or pathological in the truest sense (the "Bad"). Finally, we synthesise these discussion points in the context of fresh insight into the co-evolution of parkinsonian motor symptoms and BG oscillations (the "Unexpected").

2. PREVALENCE OF SYNCHRONIZED OSCILLATIONS IN CORTICO-BASAL GANGLIA CIRCUITS

All oscillations have a frequency associated with them. Oscillatory activities with a wide ranged of frequencies have been reported to occur in the healthy and diseased BG, with examples reported for each constituent nucleus. Thus, oscillations in the subthreshold and suprathreshold activities of single neurons or networks of neurons have been reported to occur at 'ultra-slow' frequencies (0.05–0.5 Hz; Allers et al., 2002; Ruskin et al., 2003) and at frequencies commonly associated with sleep rhythms, such as 'slow-wave activity' (~1 Hz: Stern et al., 1998; Magill et al., 2000, 2001, 2004b; Goto and O'Donnell, 2001a) and 'spindles' (5–12 Hz: Magill et al., 2000, 2004b, 2005; Berke et al., 2004). Some BG oscillations are synchronized within other frequency bands, such as the 'theta' band (4–10 Hz: Brown et al., 2002; Berke et al., 2004; DeCoteau et al., 2004, 2005), the 'alpha' or 'mu' band (8–15 Hz: Raz et al., 2000; Goldberg et al., 2002, 2004), the 'beta' band (15–30 Hz: Levy et al., 2000, 2002b; Brown et al., 2001; Williams et al., 2002; Courtemanche et al., 2003; Magill et al., 2004b; Sharott et al., 2005a), and the 'gamma' band (30–90 Hz: Brown, 2003; Brown et al., 2002; Berke et al., 2004; Masimore et al., 2004). The gamut of synchronized oscillations that occur in the BG extends to 'ultra-fast' frequencies at around 300 Hz (Foffani et al., 2003).

Oscillations in the BG are often defined according to frequency bands that were established decades ago to distinguish between the oscillatory phenomena that are widespread in the neocortex, thalamus and hippocampus (Steriade, 2000; Buzsáki, 2002, Buzsáki and Draguhn, 2004). The functions that may be subserved by synchronized oscillatory activity

within and between ensembles of cortical and thalamic neurons have received much attention over the last twenty years (for reviews, see MacKay, 1997; DeCharms and Zador, 2000; Steriade, 2000; Engel and Singer, 2001; Engel et al., 2001; Buzsáki, 2002; Buzsáki and Draguhn, 2004). It is now well established that neurons in both cortical and subcortical structures can synchronize their discharges to within a few milliseconds, and that such synchrony is often subject to oscillatory modulation. Importantly, synchronized network oscillations are present across systems and species, and the degree and/or frequency of synchronization is often task-dependent or at least dependent on behaviour (see Steriade, 2000; Engel and Singer, 2001). The existence of complex, brain state-dependent synchronizations of neuronal activity in different frequency bands raises the possibility that synchronization itself may be mechanistically important in the functional organization of these circuits. In particular, oscillatory synchronization of activity at frequencies of >20 Hz has been suggested to offer one solution to the so-called 'binding problem' (Engel and Singer, 2001; Engel et al., 2001). That is to say the problem of how to define dynamic functional relations between anatomically-distributed neuronal networks. The functional coupling of circuits through coherent oscillations may facilitate the binding together of distributed neural assemblies during, for example, sensory-motor integration (MacKay, 1997; Roelfsema et al., 1997; Engel and Singer, 2001; Engel et al., 2001). Entrainment of afferents and their targets during synchronous network oscillations could also underlie the cooperativity that is thought to be essential for the long-term modification of synaptic weights (Buzsáki, 2002).

One fundamental issue is whether the BG employ the same strategy for information processing that has been hypothesized to be favoured in the cortex and thalamus, the two structures that together provide the bulk of the extrinsic input to the BG. There is some evidence to suggest that the BG do not encode information in the same way as the cortex, and that the BG might instead perform some sort of active desynchronizing process, as a function of a 'dimensional reduction' of their cortical input (Bar-Gad et al., 2003). The idea that the BG and cortex use distinct mechanisms for information processing seems logical enough in the face of such striking differences in their physiological and anatomical properties. Yet, it would be somewhat surprising if BG networks could not at least distinguish between synchronous oscillatory inputs and a bombardment of uncorrelated and/or arrhythmic inputs. The mechanisms that may underlie the (presumably) meaningful dialogue between the oscillating circuits of the thalamus/cortex and the neuronal networks of the BG are unknown, although the finding of coherent network oscillations in cortico-basal ganglia circuits supports the idea that a dialogue founded on oscillatory activity could take place (Marsden et al., 2001; Williams et al., 2002; Magill et al., 2004b, Sharott et al., 2005b). To determine whether synchronized network oscillations carry information or serve some other computational role, the description of a feasible 'readout' mechanism for the information is required. One hypothetical readout mechanism, as proposed for the hippocampus, is founded on differences in frequency and phase between the subthreshold membrane oscillations of a select few neurons and the synchronized oscillations of the network in which they are embedded (Buzsáki, 2002; Buzsáki and Draguhn, 2004). It is not known whether a readout mechanism exists in the BG or, if it does exist, how it operates. However, with a viable readout mechanism, it is possible that synchronized oscillations in cortico-basal ganglia networks could solve the binding problem by creating a common temporal reference or 'master clock' for the computations carried out in distant regions. The idea that the BG could encode or transfer information in synchronized oscillations (for better or worse) will be discussed below in more detail.

3. RECORDING AND ANALYZING SYNCHRONOUS OSCILLATIONS

Before exploring synchronized oscillations in the BG in more detail, it is important to consider the methods that may be employed to record and analyze oscillatory and synchronized activity. Two distinct, but largely complementary measures, single-/multi-unit activity and local field potentials (LFPs), are most commonly used to determine the prevalence of synchronized and/or oscillatory activity in networks of neurons. The former represents the suprathreshold activity *i.e.*, action potential discharges, of one cell or a small group of neurons. In contrast, LFPs are dominated by synchronized, subthreshold and, to a lesser extent, suprathreshold events in much larger populations of neurons (see section 3.1). In practical terms, single-/multi-unit activity and LFPs may be recorded simultaneously or independently. Single-/multi-unit activity is typically recorded with electrodes of relatively high impedance (*e.g.* 0.5–20 MΩ), whereas LFPs can also be recorded with electrodes of much lower impedance (*e.g.* >0.05 MΩ). The major frequency components of single-/multi-unit activity are at least an order of magnitude faster than those of LFPs and, as such, these signals can be isolated from each other with appropriate high-pass and low-pass filtering.

We must defer to statistics to determine whether a given stationary stochastic process, which might be a *point process* (*e.g.* a 'spike train' derived from unit activity) or a *time series* (*e.g.* LFP), is oscillatory. Analyses can be based in either the time domain or frequency domain. In the time domain, *auto-correlograms* can be constructed to test for oscillations in the spike train of a single neuron (Fig. 1A; Perkel et al., 1967a; Abeles, 1982; but see Bar-Gad et al., 2001). Similarly, *autocovariance sequences* can be computed in search of periodicities in time series, such as LFPs or the electroencephalogram (EEG). However, spectral analysis in the frequency domain is preferable over time-domain analyses because the estimation of oscillatory activity at each frequency is, in principle, independent of any other. The statistical significance and frequency of rhythmic activity can be assessed in the frequency domain using spectral analysis methods, most commonly based on the discrete or finite Fourier transform (FFT: Brillinger, 1975; Halliday et al., 1995). The *power spectrum* displays the frequency decomposition of the stationary process.

The occurrence of significant peaks in the power spectrum of the LFP is indicative of synchronized network oscillations, because LFPs likely reflect the synchronous activity of many neurons. The principal statistical tool used for determining the relationship between pairs of spike trains in the time domain is the cross-correlation histogram or *cross-correlogram* (Perkel et al., 1967b). The presence of a significant peak and/or trough in these histograms can indicate a firing rate co-variation, or even spike-to-spike synchronization, between the pair of neurons (Fig. 1B). The deviation of the centre peak from zero time shows the latency of interaction between the pair. Importantly, cross-correlograms can be used to discriminate between non-oscillatory and oscillatory firing relationships. Indeed, synchronous oscillations are reflected as side peaks or lobes in the histogram (Fig. 1C).

Analyses of mixed point process/time series data describing two stochastic processes can also be performed in either the time or frequency domains (Halliday et al., 1995; also see the chapter by Goldberg and Bergman in this volume for a formalism for such mixed processes). Thus, in the time domain, *spike-triggered averages* or *cumulant density estimates* may be calculated to characterise the relationship between the activity of a single neuron and that of the greater neuronal population, as reflected in the LFP. These measures are particularly useful because they provide information on the relative timing of synchronized oscillatory activity. A useful frequency-domain measure of synchronized oscillations is *coherence* (Halliday et al., 1995). Coherence is a measure of the linear association

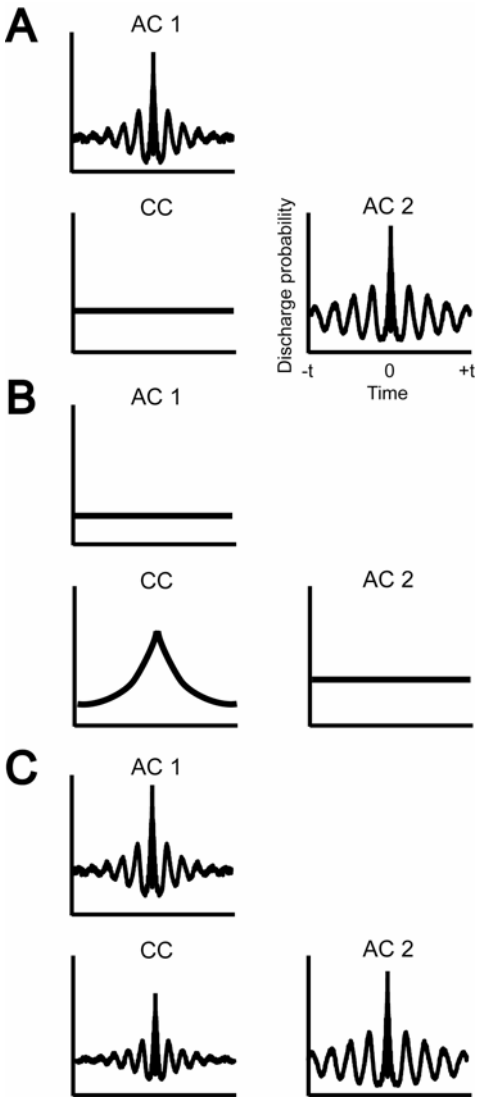

Figure 1. Permutations of auto-correlograms and cross-correlograms. *A:* Multiple peaks/troughs in the auto-correlograms of neurons 1 and 2 (AC1 and AC2, respectively) indicate that the firing of each neuron is oscillatory. However, the flat cross-correlogram (CC) suggests that the firing of the pair is not related. *B:* The flat auto-correlograms in this example imply that neither cell is engaged in oscillatory activity. However, the single peak in the CC indicates that there is a non-oscillatory co-variation in the firing of the pair. *C:* In this case, both neurons discharge in an oscillatory manner. The multiple side peaks/troughs in the corresponding CC suggest that there is also an oscillatory firing relationship between this pair of neurons.

between two stochastic processes and thus, oscillations must be temporally coupled (phase locked) and their amplitudes must have a constant ratio to be coherent at any given frequency. The relative timing of synchronized (coherent) oscillations can be extrapolated from the related *phase* estimates (Halliday et al., 1995). Unfortunately, paradoxical phase

estimates can arise when different coherent activities have overlapping frequency components, which is particularly likely in highly interconnected circuits, such as the cortico-basal ganglia loops. In some cases, difficulties in assessing the effective timing or direction of coherent activity may be overcome with other statistical methods, such as the Directed Transfer Function (Sharott et al., 2005b).

It should be noted that local stationarity of data is a prerequisite for these statistical analyses. Because most contemporary methods require the averaging of data gathered over relatively long periods of time, measures of apparent synchrony, coherence and oscillatory power are often challenged by oscillations that are fleeting, weak or highly dynamic (*e.g.* phase-variable). The successful detection and analysis of synchronized oscillations will be a direct function of the networks examined. Studies in awake and anesthetized animals have shown that high-frequency oscillations can be effete and focal in nature, especially in sensorimotor systems (Murthy and Fetz, 1992, 1996a; Sanes and Donoghue, 1993; MacKay, 1997; Donoghue et al., 1998; Destexhe et al., 1999). Indeed, correlations between single unit and population activities are sometimes elusive, perhaps as a consequence of the rapid recruitment of neurons to, and release from, the population oscillation (Murthy and Fetz, 1992, 1996b; Donoghue et al., 1998).

3.1. The Nature of Local Field Potentials Recorded in the Basal Ganglia

The last five years has seen renewed interest in the recording of LFPs in the BG (Brown, 2003). Recordings of single-/multi-unit activity and LFPs are complementary, both in terms of the different scales of synchronized activity that are reflected by these measures and the distinct mechanistic insights that are offered. There is much evidence from studies of laminated structures, such as the neocortex, hippocampus, olfactory bulb, and cerebellum, that LFPs are representative of the aggregate activity of local neuronal populations (Creutzfeldt et al., 1966a,b; Frost, 1968; Hubbard et al., 1969; Mitzdorf, 1985). Currents must be synchronized in time and space in order to significantly influence the field potential. The spatiotemporal summation of currents in a neuronal network is promoted by a regular arrangement of the constituent elements *e.g.* the regimented apical dendrites of principal neurons of the cerebral cortex. Although synchronized action currents or presynaptic currents can be observed in the LFP, as a 'population spike' or a 'fiber volley', respectively, it is almost certainly the case that LFPs better reflect synchronized, subthreshold currents generated in the somata and dendrites of local neuronal elements (Hubbard et al., 1969; Mitzdorf, 1985).

Although the neural basis of LFPs recorded in layered structures is reasonably well characterized, we currently lack a clear mechanistic understanding of how LFPs are generated in non-layered structures, such as the BG. In fact, it is somewhat surprising that such potentials exist in regions like the BG because their anatomy would be predicted to oppose the generation of strong fields. This of course raises the possibility that LFPs recorded in the BG are the result of the passive spread of currents generated in other brain areas (so-called 'volume conduction'), rather than the subthreshold and suprathreshold activities of local networks of BG neurons. Nevertheless, there is evidence to support the notion that LFPs recorded in the BG also reflect synchronized aggregate activity. Local field potentials can be registered in the BG using a differential recording configuration, with a near-field reference, which would be predicted to minimize contamination by volume conduction (Brown et al., 2001, 2002; Courtemanche et al., 2003; DeCoteau et al., 2005; Sharott et al., 2005a). Moreover, LFPs recorded across BG nuclei can show a phase shift or polarity

reversal, which would not be expected for volume-conducted potentials (Brown et al., 2001). In defining a population oscillation, it is important to demonstrate a relationship between synaptic activity (presumed to be reflected globally in the LFP) and the output of active cells (as reflected in spike trains). Temporal coupling of single-/multi-unit activity to the LFP has been reported for several different oscillations in the BG, thereby substantiating the idea that LFPs can be generated locally by BG neurons (Goto and O'Donnell, 2001a; Levy et al., 2002a; Courtemanche et al., 2003; Berke et al., 2004; Goldberg et al., 2004; Magill et al., 2004a,b; DeCoteau et al., 2005; Kühn et al., 2005). These issues are discussed in more detail by Walters et al. and Berke elsewhere in this volume. This temporal coupling of input and output activities in the BG further suggests that their targets could receive synchronized oscillatory inputs.

Despite, or perhaps because of, the limitations and uncertainties that are commonly assigned to recordings of LFPs in the BG, it is important to ascertain what LFPs can tell us about the dynamics of neuronal activity in these structures. To refine our understanding of the LFPs, we can study their relationship to another widely-used measure of collective synchrony, the pair-wise cross-correlogram. Elsewhere in this volume, Goldberg and Bergman describe a partial-spectra based method for using the LFP to predict the pairwise cross-correlograms between pairs of neurons. They have recently applied this method to predict cross-correlograms of neurons recorded in the cortex and BG of 1-methyl-4-phenyl-1,2,3,6-tetrahydropyridine (MPTP)-treated parkinsonian primates (Goldberg et al., 2004). They found that the LFP was a better predictor of the cross-correlograms in the MPTP-treated monkeys than the cross-correlograms in the healthy control animals. This was true regarding neuronal correlations in cortex, among the tonically active neurons (TANs) of the striatum, among pallidal neurons, and between TANs and pallidal neurons. Thus, LFPs may be a useful indicator of the synchronized activity of BG neurons. These findings further suggest that brain dynamics become more 'globalized' in the MPTP-treated parkinsonian condition. In addition, several of the cross-correlograms and spike-triggered averages of the LFPs that were generated following the MPTP treatment showed the presence of oscillatory activity at 10 Hz, indicating a propensity for global, albeit intermittent, oscillations in the diseased condition (see section 5 below).

4. THE GOOD: SYNCHRONIZED OSCILLATIONS IN THE HEALTHY BASAL GANGLIA

In contrast to the extensive experimental evidence that oscillatory activity is a prominent feature of the thalamus, neocortex and hippocampus in the normal state, most studies, until very recently, suggested only low levels of oscillatory activity in the BG under normal conditions. This situation has changed, and this change has brought the challenge of trying to determine the functional significance of such oscillatory activity. The paucity of evidence for oscillatory activity in the BG of behaving animals stands in contrast to growing evidence that oscillatory activity is a property of subthalamo-pallidal circuit neurons, key modulators not only of the output of the BG to the thalamus, but also of other parts of the BG circuitry, including the striatum (Bevan et al., 2002). Yet all studies agree that only small numbers of striatal neurons have oscillatory spike activity in the normal state. As LFP recordings have been re-introduced into the study of BG circuitry, however, it has become evident that there is indeed robust oscillatory activity in the striatum (and subthalamic nucleus) when animals are alert and behaving, and that this activity is modulated as the animals perform

behavioral tasks (Brown et al., 2002; Courtemanche et al., 2003; Berke et al., 2004; DeCoteau et al., 2004, 2005; Gervasoni et al., 2004; Masimore et al., 2004; Sharott et al., 2005a). The evidence for striatal network oscillations comes from experiments both in primates and in rodents.

In macaque monkeys, LFP recordings have been made in the caudate nucleus and putamen with chronically-implanted multiple electrodes while monkeys, seated in primate chairs with their heads fixed, are observed under a variety of behavioral conditions (Courtemanche et al., 2003). Low-frequency large-amplitude activity dominates during resting and dozing states. But when the monkeys become alert, and as they perform visuomotor tasks, prominent beta-band activity (ca. 10–25 Hz, average near 15 Hz) appears, along with lower levels of oscillatory activity in other frequency bands (Fig. 2A). This oscillatory activity is present with local (near-field) referencing, as well as with distant referencing, indicating that it is not the result of volume conduction (see section 3.1 above).

This 10–25 Hz LFP oscillatory activity in the striatum has several striking features. First, the oscillations are episodic, not continuous. The episodes last for less than a second (average of ~600 msec) and they occur about 20 times a minute, but irregularly, with inter-episode intervals ranging from less than 1 second to about 3 seconds. This suggests that they are related to shifting activity states in the system. The origin of these activity shifts is not known, but it was found that some striatal neurons (classified as either projection neurons, or as TANs) have spiking activity that is in-phase or in anti-phase with the LFP oscillations. In the total population of neurons, there is a discernable tendency for spiking to be related to the LFP oscillations. These findings suggest that the oscillations, in part at least, reflect local neuronal activity in the striatum.

Second, the striatal LFP oscillations are highly synchronous across the caudate nucleus and putamen, with near sites more highly coherent than far sites. For example, in paired two-site recordings, cross-covariance values at zero lag ranged from 0.93 for sites 2 mm apart to 0.63 for sites 10 mm apart, and across all recorded sites in the caudate nucleus and putamen, values ranged with distance from almost 1.0 (sites were relatively near) to ~0.2 (relatively far). This finding suggests that large parts of the striatum can come into synchronous states of beta-band activity episodically, and repeatedly, at irregular intervals averaging half a second or so (Courtemanche et al., 2003).

Third, and perhaps most interestingly, the level of synchrony, as well as the content of these striatal beta-band oscillations, can vary depending on the behavior of the monkey (Fig. 2B). In the experiments reported by Courtemanche et al. (2003), macaques were trained to fixate a target light on a screen in front of them and then to perform single saccades in response to visual targets briefly presented at varying locations. Local field potentials were recorded simultaneously from up to five microelectrodes implanted in and near the oculomotor zone of the striatum. Single-unit and multi-unit activity was recorded from the same electrodes, and LFPs that were recorded at sites with saccade-related unit activity were compared with those simultaneously recorded at sites lacking such saccade-related unit activity (Fig. 2B). When the monkeys fixated the fixation point, the level of cross-covariance between pairs of recording sites was consistently high (0.8–0.9). This level remained high for sites at which saccade-related activity was not recorded. But the oscillatory activity at some sites with saccade-related unit activity fell out of such strict synchrony during the peri- and post-saccadic period, only to return afterwards. This finding suggests that the high levels of synchrony in striatal oscillatory LFP activity in the normal monkey can be modulated locally according to the particular activity of units at the sites of recorded LFPs.

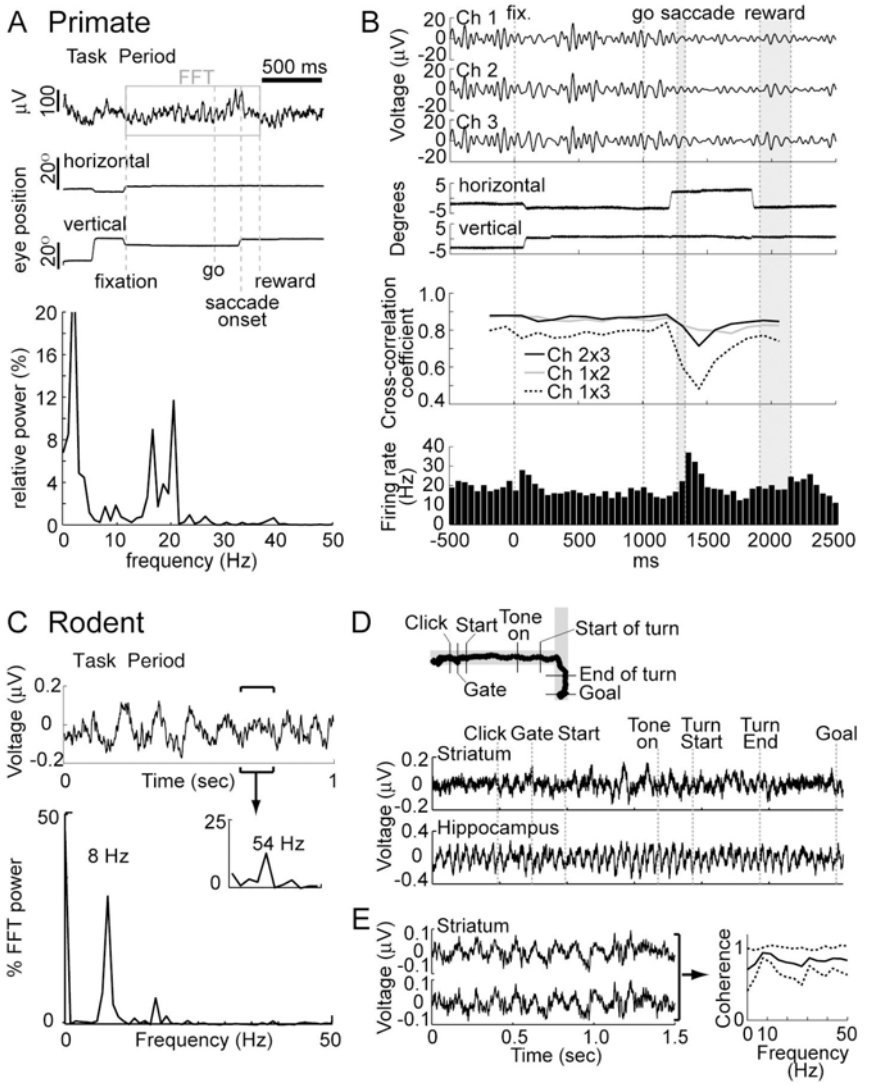

Figure 2. Oscillatory activity in the striatum of macaque monkey (A–B) and rat (C–E). *A:* Example of beta-band LFP oscillation in the oculomotor striatum of a macaque monkey performing a single saccade task. Horizontal and vertical eye position is shown below the trace of a raw LFP (*top*). Spectral plot (*bottom*) shows the relative power of oscillatory activity in the 0–50 Hz range. *B:* Raw LFP traces recorded on three electrodes (Ch1, Ch2, Ch3) in the oculomotor striatum during a single saccade task (eye positions shown in degrees under the LFP traces). *Middle* plot shows cross-correlation coefficients calculated for different pairings of the three electrodes. One pair (1 × 3) falls out of the otherwise tight synchrony. There was saccade-related unit activity on electrode 3 (*bottom* plot), in contrast to electrodes 1 and 2. Modified from Courtemanche et al. (2003). *C–E:* LFPs recorded in rats running in a simple T-maze. *C:* illustrates a raw LFP trace recorded as a rat ran down the maze illustrated in D. Power spectra are shown below. *D:* An example of a run trajectory in the T-maze task and, below, the raw LFP traces simultaneously recorded in the striatum and hippocampus during this maze run. Note that striatal and hippocampal theta are not identical. *E:* LFPs recorded from two sites in the lateral striatum as a rat spontaneously moved along the maze (*left*) and the coherogram calculated for these traces, illustrating the high level of cohernce of oscillatory activity in the rat striatum (*right*). Modified from DeCoteau et al. (2005).

The working model prompted by these experiments is that LFP activity in the normal primate striatum is characterized by widespread, coordinated, episodic oscillatory activity, and that local sites in the striatum can 'pop out' of this synchrony when task demands engage the striatal neurons at the pop-out sites. These local sites were estimated to be on the order of a millimeter in diameter, suggesting that they could be related to the compartmental architecture of the striatum. In the oculomotor zone, as elsewhere in the striatum, functionally-related sets of input fibers converge on zones roughly 0.5–1 millimeter wide ("matrisomes") and output neurons in these small regions can in turn project to similar small sites in the pallidum. This model suggests that one function of the oscillatory activity in the primate striatum may be to serve as a thresholding device. If, and only if, activity in a local region exceeds the level of synchronous oscillatory activity would the threshold for exciting spike activity in striatal projection neurons be crossed. These are the neurons responsible for sending outputs to the pallidum and substantia nigra. Thus, the modulatory control over oscillatory activity in the striatum could be part of a dynamic and state-dependent filter mechanism in the striatum, biasing attention and action. If such a filter were set at too high a threshold (as in the exaggerated oscillatory states characteristic of Parkinson's disease), activation of striato-pallidal and striato-nigral outputs could be impaired, contributing to the parkinsonian syndrome.

Oscillatory LFP activity has also been observed in the normal state as rats behave in task paradigms (Berke et al., 2004; DeCoteau et al., 2004; Masimore et al., 2004). Recordings in the striatum (Fig. 2C–E) show that the dominant frequency band for these oscillations is in the theta range (4–10 Hz), but activity at lower (<4 Hz; 'delta') and higher (30–50 Hz; 'gamma') ranges is also observed. In the rat, some of this activity has been associated with the activity of (presumed) fast-spiking striatal interneurons, thought to correspond to the parvalbumen-containing GABAergic interneurons of the striatum (Berke et al., 2004). When rats were trained to run mazes, such as simple T-mazes (Fig. 2D), robust theta-band oscillatory activity is apparent in striatal recordings made with multiple chronically-implanted tetrodes (DeCoteau et al., 2004, 2005). By contrast, when the rats are grooming or resting, this activity is relatively weak.

Like the beta-band oscillations in the macaque striatum, these theta oscillations in the rodent are highly synchronous across the striatum. In the ventral striatum, theta oscillations are synchronous with those in the hippocampus (Goto and O'Donnell, 2001b; Berke et al., 2004), but the theta oscillations in the dorsal striatum can be uncoupled from those in the hippocampus (Fig. 2D), and they occur robustly with local referencing, suggesting their independence from oscillations generated in the hippocampus or other sources (DeCoteau et al., 2004, 2005). As for the beta-band LFP activity in the macaque striatum, local inhomogeneities are found in the theta oscillations in the rat striatum. Furthermore, theta-band activity is modulated during task performance in trained animals. For example, when rats are trained to run a T-maze in order to receive a reward, theta-band oscillations are highest during the outbound (straight) part of the runs, but they decline before reaching the goal, at which point gamma-band oscillatory activity sharply increases. Interestingly, although the spectral peak of the striatal theta oscillation is near 8 Hz, the highest coherence of unit activity with the LFP oscillations is approximately 4 Hz (DeCoteau et al., 2005).

These and other recent studies raise a number of important questions. If such oscillatory activity is important for normal striatal function, why are the dominant frequencies in rats and monkeys different? What could set up such synchronous network activity? Are these activities actually devices for facilitating network communication with other brain regions? Are they internally generated or predominantly dictated by afferents? Ample

evidence suggests that both afferents and local interneuronal networks might be responsible for the activities recorded. What functions do these oscillations serve? As stated at the outset of this chapter, this is a question relevant to all brain regions in which oscillatory activity has been recorded. The perturbations of these oscillations in dopamine-depleted parkinsonian states, however, may offer a special clue to their function in the BG and, at the least, provide a clear indication that when oscillatory activity in the BG is aberrant, then abnormal behavioural states are likely to occur.

5. THE BAD: SYNCHRONIZED OSCILLATIONS IN THE PARKINSONIAN BASAL GANGLIA

The chronic loss of dopamine from the forebrain, as occurs in idiopathic Parkinson's disease (PD) and its animal models, is associated with profound changes in the patterning of activity in the BG and their afferent/efferent networks. Much of the early evidence for this was derived from studies of animal models of PD, most often MPTP-lesioned primates and the 6-hydroxydopamine-lesioned rat (Bergman et al., 1998; Bevan et al., 2002; Boraud et al., 2002). Thus, along with the changes in the firing rates of BG neurons that were posited by the now-classic model of BG dysfunction (DeLong, 1990), increases in oscillatory activity and synchronized firing (rate co-variations) have been frequently reported to occur in the BG, most notably in the subthalamic nucleus-pallidum network, and the cortex of parkinsonian animals (Bergman et al., 1994; Nini et al., 1995; Raz et al. 2000, 2001, Magill et al., 2001; Goldberg et al., 2002, 2004; Heimer et al., 2002). In terms of increases in the power and prevalence of oscillations, these studies have emphasized the role of (pathological) activity that is synchronized at frequencies below 15 Hz, including those frequencies associated with parkinsonian tremor, although exaggerated oscillations at higher frequencies have also been reported (Vorobyov et al., 2003; Sharott et al., 2005a). Taken together, data from animal models of PD serve to further highlight the potentially critical roles played by synchronized oscillatory activity in the function and dysfunction of cortico-basal ganglia-thalamocortical circuits.

The recent renaissance in functional neurosurgery has provided an opportunity to record neuronal activity directly from the subthalamic nucleus (STN) and internal pallidum (GPi) in patients with PD. Unit activity, with or without LFPs, can be recorded intra-operatively through microelectrodes, or LFPs (only) may be recorded directly from the deep brain stimulation electrode (DBS-electrode). In the latter case, LFPs may be recorded intra-operatively, or after implantation surgery while the electrode leads are externalized and prior to connection to the subcutaneous stimulator. Such recordings have demonstrated that oscillatory activity is synchronized in two major frequency bands in PD patients withdrawn from dopaminergic therapy (as is the case intra-operatively). The first band contains activity in the frequency range of parkinsonian rest and action tremor (3–12 Hz). This is seen in microelectrode recordings of pairs of units drawn from the same electrode or electrodes in close proximity to each other (Hurtado et al., 1999; Levy et al., 2000). Paradoxically, however, this form of synchronization is neither a consistent nor strong feature of LFPs recorded in the basal ganglia (but see Liu et al., 2002), perhaps because synchronization between neurons occurs within small local ensembles, thereby mirroring the multiple peripheral oscillators manifest in parkinsonian rest tremor (Hurtado et al., 2000). Moreover, neurons oscillating at tremor frequency tend to vary their phase relationships with one another over time, so that spectral analysis methods that average LFPs over time would

tend to underestimate the strength of such synchronized activity when it occurs (Hurtado et al., 1999, 2004; Levy et al., 2000).

The second major band of synchronized oscillatory activity evident in recordings from the STN or GPi of patients with PD is 13–32 Hz, often termed the 'beta' band (Fig. 3). It is manifest in single-unit activity and in the cross-correlograms of pairs of neurons (Levy et al., 2002a,b; Amirnovin et al., 2004; Kühn et al., 2005), but is particularly prominent in the LFPs recorded from subthalamic (Brown et al., 2001; Priori et al., 2002; Williams et al., 2002, 2003, 2005; Kühn et al., 2004; Priori et al., 2004) and pallidal (Brown et al., 2001; Priori et al., 2002; Silberstein et al., 2003) DBS-electrodes. Indeed, subthalamic and pallidal LFPs are coherent (*i.e.*, show linear amplitude and phase co-variation) in the beta band (Brown et al., 2001), and, in turn, are coherent with EEG activity recorded over cortical motor areas at the same frequencies (Marsden et al., 2001; Williams et al., 2002). Thus, synchronized beta-band activity, as indexed by the LFP, is a physiological hallmark of cortico-basal ganglia-thalamocortical circuits in PD.

Synchronized oscillatory activity in the STN and GPi of patients with PD may also occur at frequencies in excess of 65 Hz, which, for convenience, we will term the 'gamma' band (Fig. 3). In particular, after treatment with dopamine agonists or the dopamine precursor, levodopa, some PD patients develop a new pattern of LFP oscillation at 65–85 Hz (Brown et al., 2001; Cassidy et al., 2002; Williams et al., 2002; Brown, 2003). This high-frequency activity is observed at rest and is increased with movement (Cassidy et al., 2002; Brown et al., 2002) and may therefore have some similarities to the cortical activity of similar frequency that has been implicated in the planning of movement (Crone et al., 1998). There is a single report of a further band of activity at 200 to 350 Hz in the LFP recorded from the STN region that behaves in a similar manner (Foffani et al., 2003).

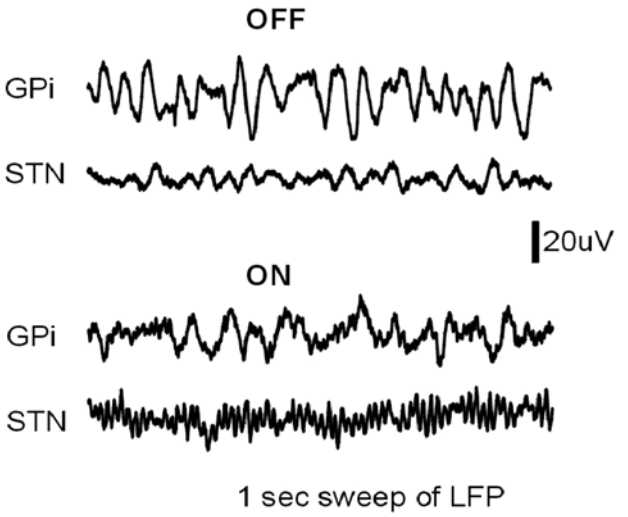

Figure 3. Example of LFP activities recorded by DBS-electrodes in the subthalamic nucleus (STN) and globus pallidus interna (GPi) of a patient with PD when withdrawn from antiparkinsonian treatment (OFF levodopa) and following restitution of treatment (ON levodopa). Off medication, there are prominent oscillations at around 20 Hz. These beta-band oscillations are suppressed by treatment with levodopa, which also promotes the expression of higher frequency oscillations at around 70 Hz.

However, activities above 65 Hz are an inconsistent feature of BG LFP recordings in patients with PD, and have not been detected in the cross-correlation of pairs of neurons, or in correlations between unit activity and the LFP. In the absence of direct evidence that such oscillations are coupled to neuronal activity in the BG, we will not consider these activities in any further detail, other than to highlight their potential interest in the future.

5.1. Do Synchronized Oscillations in the Parkinsonian Basal Ganglia Contribute to Motor Abnormalities?

Oscillatory synchronization at tremor frequencies might be related to the genesis of tremor, but the same neurons that synchronize at these frequencies also tend to be activated by passive movements, raising the possibility that some of this activity may be afferent rather than efferent in nature. Both oscillations at tremor-related frequencies (Volkmann et al., 1996) and those in the beta band (Brown, 2003) have been implicated in the sparsity and slowness of movements in PD. The evidence is strongest in the case of activity in the beta band, which generally exhibits an inverse relationship with motor function. Thus, a reduction in the power of beta oscillations is often coincident with the improvement of motor symptoms that is seen after levodopa administration (Fig. 3) or high-frequency (>70 Hz) stimulation of the STN region (Brown et al., 2004). Furthermore, beta oscillations in the STN are suppressed prior to, and during, self- and externally-paced voluntary movements, and following environmental cues informative of subsequent movement demands (Cassidy et al., 2002; Levy et al., 2002a; Priori et al., 2002; Williams et al., 2003, 2005; Kühn et al., 2004; Doyle et al., 2005). In reaction-time tasks, the timing of the reduction in power of beta activity positively correlates with both the mean reaction time across patients (Kühn et al., 2004; see also Fig. 4) and the reaction time across single trials within a single patient (Williams et al., 2005). Similarly, in self-paced movements, the onset of suppression of beta oscillations in STN can be used to predict the timing of voluntary movements on-line (Loukas and Brown, 2004). The critical feature in these paradigms is that oscillatory activity fluctuates with motor-related information processing, rather than any non-specific changes in attention. Thus, in reaction-time tasks, warning cues that allow premovement motor selection are associated with more frequent and prominent suppression of beta-band LFP activity in STN than those warning cues that are uninformative and do not allow premovement motor selection (Williams et al., 2003). Such warning cues do not vary in their attentional demands.

The above indicates a strong relationship between the onset of suppression of beta-band activity in STN and the timing of subsequent voluntary movements. If such a reduction in the power of beta oscillations is linked specifically to the facilitation of subsequent movement, an augmentation of power might also be predicted when a pre-prepared movement requires cancellation and, indeed, this also seems to be the case (Kühn et al., 2004).

The inverse relationship between beta-band activity and motor function suggests that the information processing necessary for renewed movement may be actively antagonized by the synchronization of activity in this band. Recent recordings in primates confirm an inverse relationship between oscillatory LFP activity in the beta band and task-related coding of movement by neurons, so that oscillations are preferentially suppressed in the local area of the striatum that contains neurons exhibiting task-related increases in discharge rate (Courtemanche et al., 2003; see section 4 above). Parallel observations have been made in the primate motor cortex, as exemplified by the ‘clamping’ of single-unit firing rates during periods of 20–40 Hz oscillatory synchrony (Murthy and Fetz, 1996b)

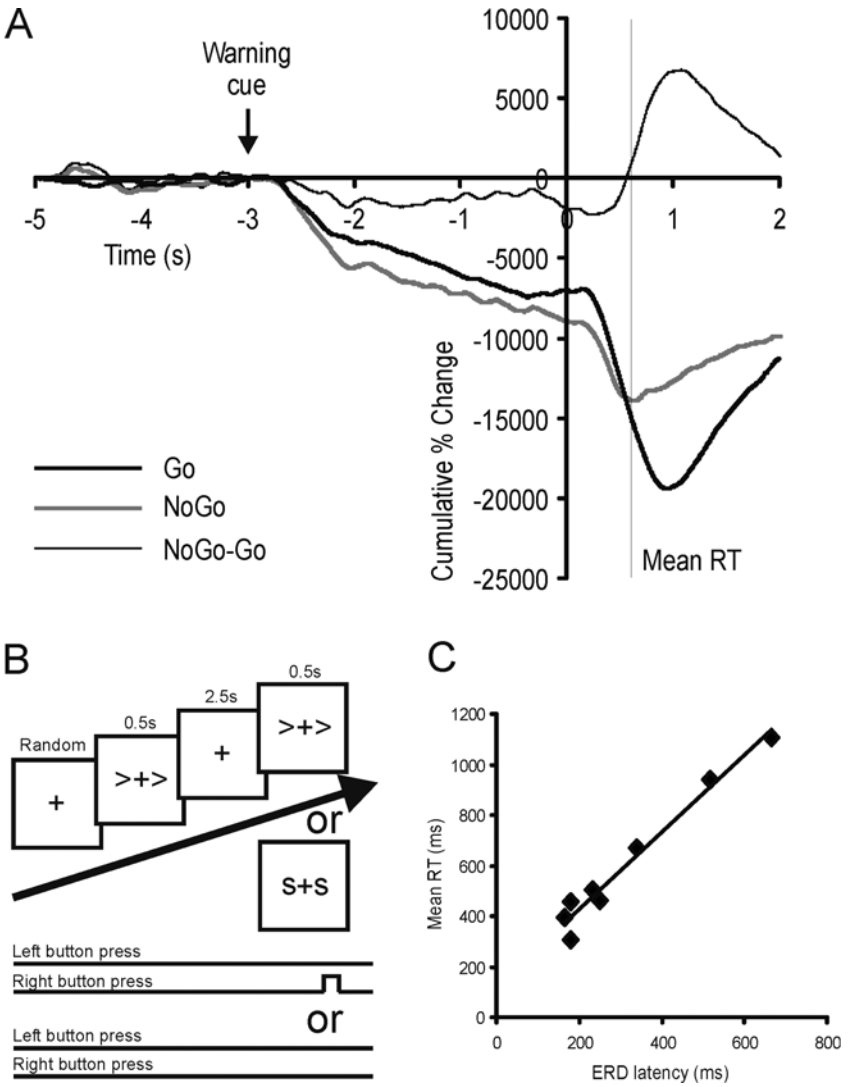

Figure 4. Change in the power of beta activity (13–30 Hz) in the STN LFP while PD patients are engaged in a Go No-Go task. *A*: Averaged power changes represented in the form of a cumulative sum (8 patients, 16 STN). In such cumulative sums, periods of zero, negative and positive gradients demonstrate no change, power decreases and power increases, with respect to baseline, respectively. *B*: Paradigm. Patients sat with a button device held in each hand and an imperative 'go' signal on a computer screen instructed patients to press the button with either their left or right hand as fast as possible. Under these circumstances (*thick black* trace in *A*), there is a drop in beta power after the warning signal, and an even more marked drop following the go signal, but preceding the mean reaction time (RT), as indicated by the thin vertical line in *A*. The 'go' cue was preceded by a warning cue that correctly anticipated the form of the 'go' signal. In 20% of trials, however, the 'go' signal was substituted by a stop signal (S), instructing the subject not to make a movement. In these circumstances, the drop in power after the imperative cue was abbreviated, and followed by an early increase in beta power (*grey trace* in *A*). This is best seen in the trace illustrating the difference between the average 'go' and 'no-go' cusums (*thin black trace* in *A*). *C*: Correlation between latency of onset of 'go' cue (event)-related desynchronization (ERD) of beta activity and mean reaction time (RT) across eight patients. Note the highly significant correlation ($r = 0.986$, $p < 0.001$). Adapted with permission from Kühn et al. (2004).

and the tendency of firing rate modulation to occur as oscillations decrease in motor cortical LFP (Donoghue et al., 1998).

In summary, activity synchronized in the beta band is prominent in the STN and GPi of parkinsonian patients and inversely correlates with motor-related information processing, or at least motor function. Studies in the striatum of healthy rats (Vorobyov et al., 2003; Berke et al., 2004) and monkeys (Courtemanche et al., 2003), and recordings in the putamen of a patient without PD (Sochurkova & Rektor, 2003), suggest that synchronized beta oscillations, and their task-related suppression, are not a *de novo* feature of parkinsonism. However, the parkinsonian state certainly seems to be associated with an exaggeration of this form of synchronized activity, as demonstrated by comparisons of activity in the cortex and STN of healthy and 6-hydroxydopamine-lesioned rats (Sharott et al., 2005a), and PD patients before and after treatment with levodopa (Brown et al., 2001; Silberstein et al., 2003; Priori et al., 2004). This exaggeration of an activity that is inversely related to motor information processing might contribute to a lack of movement (akinesia) in untreated PD. In addition, the elevated beta-band activity in PD seems less easily suppressed when movements are made after withdrawal of levodopa (Doyle et al., 2005). Restoration of levodopa treatment improves movement-related suppression of beta LFP activity in the STN. Thus, an impaired ability to suppress the synchronization of activity in the beta band might also contribute to the slowness of movement (bradykinesia) in untreated PD.

6. THE UNEXPECTED: WHICH DATA CHALLENGE OUR VIEWS ON THE ROLES SUBSERVED BY OSCILLATIONS IN THE BASAL GANGLIA?

A key question remains as to the functional significance of synchronized oscillations in the human BG. One possibility is that they are a passive characteristic of BG and cortical neuronal networks when they are not engaged in active information processing. In this formulation, the oscillatory activity is viewed as a characteristic of the resting or idling state, as proposed for cortical alpha-band activity (Pfurtscheller et al., 1996), rather than a phenomenon that may actively impede novel processing. Although this possibility has not been completely refuted, several observations would argue against it. First, there is the rebound synchronization of beta activity above resting levels following movement, and there is a premature synchronization of this activity when movement is to be voluntarily suppressed (Cassidy et al., 2002; Kühn et al., 2004). Although there may be degrees of active suppression of dynamic movement-related processing, it seems unlikely that the BG and cortex would enter into a deeper idling state than that present at rest when movement has to be actively inhibited or terminated (Fig. 4). Second, direct stimulation of the BG at tremor and beta frequencies may exacerbate parkinsonism. The worsening of bradykinesia in PD patients has been reported following 5 Hz (Moro et al., 2002), 10 Hz (Timmermann et al., 2004) and 20 Hz (Fogelson et al., 2005) stimulation in the region of the STN. Similarly, stimulation of the putamen in healthy cats at 30 Hz leads to akinesia (Hassler and Dieckmann, 1967). It is important to note, however, that these stimulation experiments were conducted with square-wave current pulses of short duration (<100 μs). Such artificial trains of oscillatory stimuli can differ dramatically from the oscillations in unit activity and LFPs that can be recorded in the parkinsonian BG and thus, the two may engage different mechanisms in producing their effects.

If pathological synchronized oscillations do indeed underlie motor abnormalities in PD, then we can expect that the two will co-evolve during disease progression. In a recent

study (Leblois et al., submitted) designed to characterize the evolution of spontaneous and movement-related neuronal activity in the GPi of rhesus monkeys during a slow dopamine depletion induced by daily injections of small doses of MPTP, abnormal synchronized oscillatory activity (10–20 Hz) at rest appeared significantly later in the depletion process than did the first parkinsonian symptoms (Fig. 5). Moreover, the appearance of these

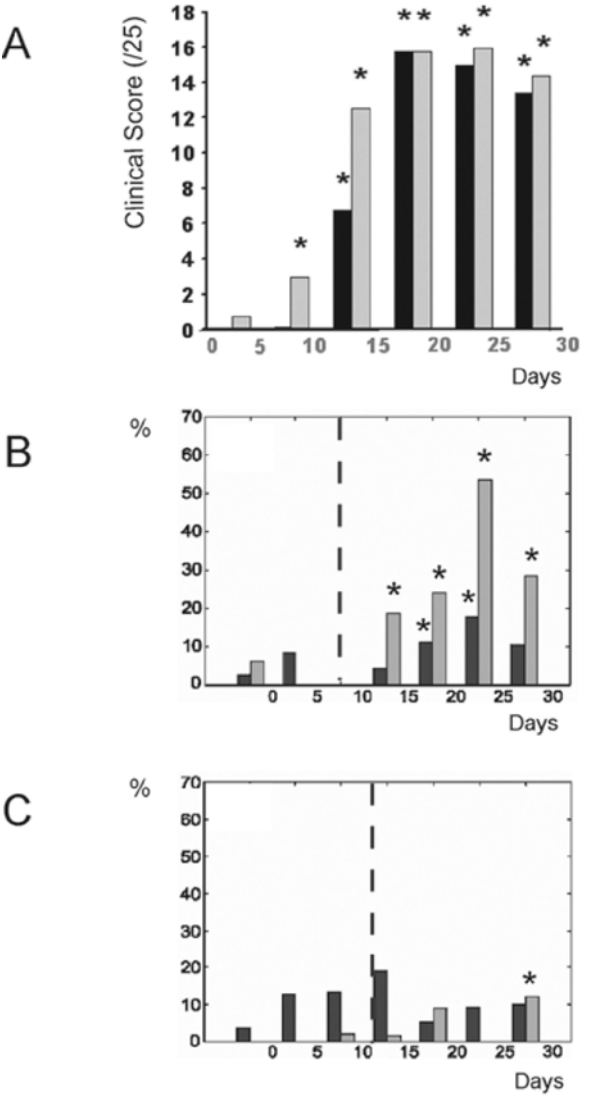

Figure 5. Comparison of the evolution of the clinical scores (*A*) and synchronized oscillations in the pallidum (*B* and *C*) during the slow development of a parkinsonian syndrome in 2 monkeys. *A:* Clinical scores of monkey J (*grey*) and M (*black*). *B:* Evolution of the percentage of auto-correlograms (*black*) and cross-correlograms (*grey*) containing significant oscillations with a frequency of between 10 and 20 Hz for monkey J. The dashed line indicates the appearance of significant parkinsonian feature in the animal. *C:* The same for monkey M. *, $p < 0.05$, as compared to control situation before MPTP treatment.

oscillations was preceded by a drastic change in the movement-related neuronal activity; pallidal neurons responded less specifically to active movement during a motor task, while reaction and movement times increased significantly. In these experiments, the monkeys displayed a pure akinetic-rigid form of the parkinsonian syndrome, without tremor, which is the rule for this species.

The above study determined the level of synchronization through cross-correlation analysis of the discharges of pairs of pallidal neurons. It may be that LFPs provide a more sensitive measure of synchronized activity at the network level. Nevertheless, the data as they stand argue against a strong causative influence of synchronized oscillations upon the bradykinetic symptoms of PD. Instead, the primate data suggest a more complex model in which dopamine depletion leads to the loss of some specific function of the BG yet to be determined, whether related to pure motor control (Mink, 1996) or information processing (Bar-Gad et al., 2003). Moreover, the appearance of oscillations synchronized at mu/beta frequencies in the BG may be related to the progression (worsening), rather than establishment, of the parkinsonian syndrome.

7. FUTURE DIRECTIONS

A number of fundamental issues concerning synchronized network oscillations in the BG remain unresolved. Perhaps most importantly, the complex cellular and network mechanisms underlying these oscillations must be further elucidated. With the proven utility of LFP recordings in the BG coming to the fore, there also remains a pressing need for further studies of their neural basis.

Many of the synchronized network oscillations described here are not found (or at least have not been reported to occur) *in vitro*. One possible explanation for this is that the necessary levels of connectivity between the BG and their afferent/efferent partners are not maintained *ex vivo*. This would in turn suggest that some or all of the circuit elements of the intact cortico-basal ganglia-thalamocortical loops are required for the generation and/or maintenance of these synchronized oscillations in the BG. A critical question arises as to which circuit element(s) lie at the heart of the oscillations. The network formed by the reciprocally-connected neurons of the STN and external pallidum is one candidate pacemaker, although a mechanism that might generate oscillations at >5 Hz is currently lacking (Bevan et al., 2002; also see Stanford et al. elsewhere in this volume). It has also been proposed that oscillations arise from competition between two feedback loops, namely the cortex-STN-GPi-thalamocortical loop and the cortex-striatal-GPi-thalamocortical loop (Leblois et al., 2005). The cerebral cortex itself may drive much of the synchronous oscillatory activity in the BG (Magill et al., 2000, 2001; Brown, 2003), yet there are clear contradictions (Courtemanche et al., 2003; Goldberg et al., 2004). The thalamus is implicated in several brain rhythms, and most prominently those related to states of vigilance (Steriade, 2000). The ventral nuclei of the dorsal thalamus provide the final connection in the loop circuit, whereas the intralaminar thalamic nuclei provide direct inputs to the BG, notably the striatum (Smith et al., 1998). The physiological and anatomical properties of the thalamic neuronal networks place them in an ideal position to play a lead role in modulating synchronized oscillatory activity in the BG, yet little is known about how and when they might do this. One possibility is that oscillatory activity in the striatum is strongly influenced by the conjoint effects of thalamic and cortical inputs to striatal interneurons; thalamic input to the (cholinergic) TANs and cortical input to the (GABAergic) fast-spiking

interneurons (Courtemanche et al., 2003). The contribution of such thalamic and cortical inputs to the physiological and pathophysiological rhythms in the BG is arguably one of the most important scientific issues that face us. The roles played by other structures that are interconnected with the BG, such as the pedunculopontine tegmental nucleus (Mena-Segovia et al., 2004), should also be considered.

Electrophysiological investigations in PD patients have focused on the synchronization of oscillatory activity in the beta band, and the frequencies associated with resting tremor. Synchronized oscillations at >60 Hz have received far less attention. These fast oscillations are an inconsistent finding in recordings of LFPs from the STN of patients with PD (Brown, 2003; Foffani et al., 2003) and thus, their nature remains obscure. Further investigation is warranted as to how they may relate to specific coding of movement-related parameters and how they might contribute to dyskinesias. Beta-band oscillations at 20–30 Hz are a predominant activity pattern in patients with idiopathic PD and thus, it is perhaps surprising that, with only one published exception (Sharott et al., 2005a), similar activity patterns are not widespread in experimental PD. The reasons for this inconsistency are unknown but it calls for a careful re-examination of the pathophysiology of animal models of PD.

Finally, it must not be forgotten that much of the evidence linking synchronized network oscillations and function in the BG is correlative in nature and there remains the need for a direct demonstration of a causal relationship. One experimental approach (yet to be attempted) would be to induce, in a physiologically relevant manner, oscillations in the networks of BG and subsequently correlate neuronal activity patterns with behavioral performance.

8. ACKNOWLEDGEMENTS

This work was supported by CNRS CTI01_01, CTI02_14 and ACI-NIC0013 (T.B.), Medical Research Council UK (P.B. and P.J.M.), and NIH EY12848, NIH NS25529 and NIH MH60379 (A.M.G.).

9. REFERENCES

Abeles, M., 1982, Quantification, smoothing and confidence limits for single-units' histograms. *J. Neurosci. Methods* **5**:317.

Allers, K.A., Ruskin, D.N., Bergstrom, D.A., Freeman, L.E., Ghazi, L.J., Tierney, P.L., and Walters, J.R., 2002, Multisecond periodicities in basal ganglia firing rates correlate with theta bursts in transcortical and hippocampal EEG. *J. Neurophysiol.* **87**:1118.

Amirnovin, R., Williams, Z.M., Cosgrove, G.R., and Eskandar, E.N., 2004, Visually guided movements suppress subthalamic oscillations in Parkinson's disease patients. *J. Neurosci.* **24**:11302.

Bar-Gad, I., Ritov, Y., and Bergman, H., 2001, The neuronal refractory period causes a short-term peak in the autocorrelation function. *J. Neurosci. Methods* **104**:155.

Bar-Gad, I., Morris, G., and Bergman, H., 2003, Information processing, dimensionality reduction and reinforcement learning in the basal ganglia. *Prog. Neurobiol.* **71**:439.

Bennett, B.D., and Wilson, C.J., 1999, Spontaneous activity of neostriatal cholinergic interneurons *in vitro*. *J. Neurosci.* **19**:5586.

Bergman, H., Wichmann, T., Karmon, B., and DeLong, M.R., 1994, The primate subthalamic nucleus. II. Neuronal activity in the MPTP model of parkinsonism. *J. Neurophysiol.* **72**:507.

Bergman, H., Feingold, A., Nini, A., Raz, A., Slovin, H., Abeles, M., and Vaadia, E., 1998, Physiological aspects of information processing in the basal ganglia of normal and parkinsonian primates. *Trends Neurosci.* **21**:32.

Berke, J.D., Okatan, M., Skurski, J., and Eichenbaum, H.B., 2004, Oscillatory entrainment of striatal neurons in freely moving rats. *Neuron* **43**:883.

Bevan, M.D., Magill, P.J., Terman, D., Bolam, J.P., and Wilson, C.J., 2002, Move to the rhythm: oscillations in the subthalamic nucleus-external globus pallidus network. *Trends Neurosci.* **25**:525.

Boraud, T., Bezard, E., Bioulac, B., and Gross, C.E., 2002, From single extracellular unit recording in experimental and human Parkinsonism to the development of a functional concept of the role played by the basal ganglia in motor control. *Prog. Neurobiol.* **66**:265.

Brillinger, D.R., 1975, Statistical inference for stationary point processes, in: *Stochastic Processes and Related Topics*, *Vol.1*, M.I. Puri, ed., Academic Press, New York, pp. 55–79.

Brown, P., 2003, The oscillatory nature of human basal ganglia activity: relationship to the pathophysiology of Parkinson's disease. *Mov. Disord.* **18**:357.

Brown, P., Oliviero, A., Mazzone, P., Insola, A., Tonali, P., and Di Lazzaro, V., 2001, Dopamine dependency of oscillations between subthalamic nucleus and pallidum in Parkinson's disease. *J. Neurosci.* **21**:1033.

Brown, P., Mazzone, P., Oliviero, A., Altibrandi, M.G., Pilato, F., Tonali, P.A., and Di Lazzaro, V., 2004, Effects of stimulation of the subthalamic area on oscillatory pallidal activity in Parkinson's disease. *Exp. Neurol.* **188**:480.

Buzsáki, G., 2002, Theta oscillations in the hippocampus. *Neuron* **33**:325.

Buzsáki, G., and Draguhn, A., 2004, Neuronal oscillations in cortical networks. *Science* **304**:1926.

Cassidy, M., Mazzone, P., Oliviero, A., Insola, A., Tonali, P., Di Lazzaro, V., and Brown, P., 2002, Movement-related changes in synchronization in the human basal ganglia. *Brain* **125**:1235.

Courtemanche, R., Fujii, N., and Graybiel, A.M., 2003, Synchronous, focally modulatedβ-band oscillations characterize local field potential activity in the striatum of awake behaving monkeys. *J. Neurosci.* **23**:11741.

Creutzfeld, O.D., Watanabe, S., and Lux, H.D., 1966a, Relations between EEG phenomena and potentials of single cortical cells. I. Evoked responses after thalamic and epicortical stimulation. *Electroencephalogr. Clin. Neurophysiol.* **20**:1.

Creutzfeld, O.D., Watanabe, S., and Lux, H.D., 1966b, Relations between EEG phenomena and potentials of single cortical cells. II. Spontaneous and convulsoid activity. *Electroencephalogr. Clin. Neurophysiol.* **20**:19.

Crone, N.E., Migloiretti, D.L., Gordon, B., and Lesser, R.P., 1998, Functional mapping of human sensorimotor cortex with electroencephalographic analysis. 2. Event related synchronisation in the gamma band. *Brain* **121**:2301.

DeCharms, R.C., and Zador, A., 2000, Neural representation and the cortical code. *Annu. Rev. Neurosci.* **23**:613.

DeCoteau, W.E., Mao, J., Gibson, D.J., Courtemanche, R., Kubota, Y., and Graybiel, A.M., 2004, Striatal theta-gamma local field potential oscillations coordinate with hippocampus rhythms in behaviorally selective patterns. *Soc. Neurosci. Abstr.* Program No. 70.4.

DeCoteau, W.E., Mao, J., Gibson, D.J., Courtemanche, R., Kubota, Y., and Graybiel, A.M, 2005, Theta-gamma oscillations in local field potentials are prominent in the rat striatum and are coordinated with hippocampal rhythms in behaviorally selective patterns. Submitted.

DeLong, M.R., 1990, Primate models of movement disorders of basal ganglia origin. *Trends Neurosci.* **13**:281.

Destexhe, A., Contreras, D., and Steriade, M., 1999, Spatiotemporal analysis of local field potentials and unit discharges in cat cerebral cortex during natural wake and sleep states. *J. Neurosci.* **19**:4595.

Donoghue, J.P., Sanes, J.N., Hastopoulos, N.G., and Gaál, G., 1998, Neural discharge and local field potential oscillations in primate motor cortex during voluntary movements. *J. Neurophysiol.* **79**:159.

Doyle, L.M.F., Kühn A.A., Hariz, M., Kupsch, A., Schneider, G-H., and Brown, P., 2005, Levodopa-induced modulation of subthalamic beta oscillations during self-paced movements in patients with Parkinson's disease. *Eur. J. Neurosci.* **21**:1403.

Engel, A.K., Fries, P., and Singer, W., 2001, Dynamic predictions: oscillations and synchrony in top-down processing. *Nat. Rev. Neurosci.* **10**:704.

Engel, A.K., and Singer, W., 2001, Temporal binding and the neural correlates of sensory awareness. *Trends Cog. Sci.* **5**:16–25.

Foffani, G., Priori, A., Egidi, M., Rampini, P., Tamma, F., Caputo, E., Moxon, K.A., Cerutti, S., and Barbieri, S., 2003, 300-Hz subthalamic oscillations in Parkinson's disease. *Brain* **126**:2153.

Fogelson, N., Kühn, A.A., Silberstein, P., Dowsey Limousin, P., Hariz, M., Trottenberg, T., Kupsch, A., and Brown, P., 2005, Frequency dependent effects of subthalamic nucleus stimulation in Parkinson's disease. *Neurosci. Lett*., in press.

Frost, J.D., 1968, EEG-intracellular potential relationships in isolated cerebral cortex. *Electroencephalogr. Clin. Neurophysiol.* **24**:434.

Gervasoni, D., Lin, S.C., Ribeiro, S., Soares, E.S., Pantoja, J., and Nicolelis, M.A., 2004, Global forebrain dynamics predict rat behavioral states and their transitions. *J. Neurosci.* **24**:11137.

Goldberg, J.A., Boraud, T., Maraton, S., Haber, S.N., Vaadia, E., and Bergman, H., 2002, Enhanced synchrony among primary motor cortex neurons in the 1-methyl-4-phenyl-1,2,3,6-tetrahydropyridine primate model of Parkinson's disease. *J. Neurosci.* **22**:4639.

Goldberg, J.A., Rokni, U., Boraud, T., Vaadia, E., and Bergman, H., 2004, Spike synchronization in the cortex-basal ganglia networks of parkinsonian primates reflects global dynamics of the local field potentials. *J. Neurosci.* **24**:6003.

Goto, Y., and O'Donnell, P., 2001a, Network synchrony in the nucleus accumbens *in vivo*. *J. Neurosci.* **21**:4498.

Goto, Y., and O'Donnell, P., 2001b, Synchronous activity in the hippocampus and nucleus accumbens *in vivo*. *J. Neurosci.* **21**:RC131.

Halliday, D.M., Rosenberg, J.R., Amjad, A.M., Breeze, P., Conway, B.A., and Farmer, S.F., 1995, A framework for the analysis of mixed time series/point process data – theory and application to the study of physiological tremor, single motor unit discharges and electromyograms. *Prog. Biophys. Mol. Biol.* **64**:237.

Hassler, R., and Dieckmann, G., 1967, Arrest reaction, delayed inhibition and unusual gaze behaviour resulting from stimulation of the putamen in awake unrestrained cats. *Brain Res.* **5**:504.

Heimer, G., Bar-Gad, I., Goldberg, J.A., and Bergman, H., 2002, Dopamine replacement therapy reverses abnormal synchronization of pallidal neurons in the 1-methyl-4-phenyl-1,2,3,6-tetrahydropyridine primate model of parkinsonism. *J. Neurosci.* **22**:7850.

Hubbard, J.I., Llinás, R., and Quastel, D.M.J., 1969, Extracellular field potentials in the central nervous system, in: *Electrophysiological Analysis of Synaptic Transmission*, Edward Arnold (Publishers) Ltd., London, pp. 265–293.

Hurtado, J.M., Gray, C.M., Tamas, L.B., and Sigvardt, K.A., 1999, Dynamics of tremor-related oscillations in the human globus pallidus: a single study. *Proc. Natl. Acad. Sci. USA.* **96**:1674.

Hurtado, J.M., Lachaux, J.P., Beckley, D.J., Gray, C.M., and Sigvardt, K.A., 2000, Inter- and intralimb oscillator coupling in Parkinsonian tremor. *Mov. Disord.* **15**:683.

Hurtado, J.M., Rubchinsky, L.L., and Sigvardt, K.A., 2004, Statistical method for detection of phase-locking episodes in neural oscillations. *J. Neurophysiol.* **91**:1883.

Kühn, A.A., Williams, D., Kupsch, A., Limousin, P., Hariz, M., Schneider, G-H., Yarrow, K., and Brown, P., 2004, Event-related beta synchronization in human subthalamic nucleus correlates with motor performance. *Brain* **127**:735.

Kühn, A.A., Trottenberg, T., Kivi, A., Kupsch, A., Schneider, G-H., and Brown, P., 2005, The relationship between local field potential and neuronal discharge in the subthalamic nucleus of patients with Parkinson's disease. *Exp. Neurol.*, in press.

Leblois, A., Meissner, W., Bezard, E., Bioulac, B., Gross, C., and Boraud, T., Evolution of the activity of GPi neurons during a slow dopamine depletion process. Submitted.

Leblois, A., Boraud, T., Bergman, H., and Hansel, D., 2005, Basal ganglia physiology is built on competition between feedback loops, in: *Recent Breakthroughs in Basal Ganglia Research*, E. Bezard, ed., Nova Science Publishers, New York, in press.

Levy, R., Hutchison, W.D., Lozano, A.M., and Dostrovsky, J.O., 2000, High-frequency synchronisation of neuronal activity in the subthalamic nucleus of parkinsonian patients with limb tremor. *J. Neurosci.* **20**:7766.

Levy, R., Ashby, P., Hutchinson, W.D., Lang, A.E., Lozano, A.M., and Dostrovsky, J.O., 2002a, Dependence of subthalamic nucleus oscillations on movement and dopamine in Parkinson's disease. *Brain* **125**:1196.

Levy, R., Hutchison, W.D., Lozano, A.M., and Dostrovsky, J.O., 2002b, Synchronized neuronal discharge in the basal ganglia of parkinsonian patients is limited to oscillatory activity. *J. Neurosci.* **22**:2855.

Liu, X., Ford-Dunn, H.L., Hayward, G.N., Nandi, D., Miall, R.C., Aziz, T.Z., and Stein, J.F., 2002, The oscillatory activity in the parkinsonian subthalamic nucleus investigated using the macro-electrodes for deep brain stimulation. *Clin. Neurophysiol.* **113**:1667.

Loukas, C., and Brown, P., 2004, Online prediction of self-paced hand movements from subthalamic activity using neural networks in Parkinson's disease. *J. Neurosci. Methods.* **137**:193.

MacKay, W.A., 1997, Synchronised neuronal oscillations and their role in motor processes. *Trends Cog. Sci.* **1**:176.

Magill, P.J., Bolam, J.P., and Bevan, M.D., 2000, Relationship of activity in the subthalamic nucleus-globus pallidus network to cortical electroencephalogram. *J. Neurosci.* **20**:820.

Magill, P.J., Bolam, J.P., and Bevan, M.D., 2001, Dopamine regulates the impact of the cerebral cortex on the subthalamic nucleus-globus pallidus network. *Neuroscience* **106**:313.

Magill, P.J., Sharott, A., Bevan, M.D., Brown, P., and Bolam, J.P., 2004a, Synchronous unit activity and local field potentials evoked in the subthalamic nucleus by cortical stimulation. *J. Neurophysiol.* **92**:700.

Magill, P.J., Sharott, A., Bolam, J.P., and Brown, P., 2004b, Brain state-dependency of coherent oscillatory activity in the cerebral cortex and basal ganglia of the rat. *J. Neurophysiol.* **92**:2122.

Magill, P.J., Sharott, A., Harnack, D., Kupsch, A., Meissner, W., and Brown, P., 2005, Coherent spike-wave oscillations in the cortex and subthalamic nucleus of the freely moving rat. *Neuroscience* **132**:659.

Masimore, B., Kakalios, J., and Redish, A.D., 2004, Measuring fundamental frequencies in local field potentials. *J. Neurosci. Methods* **138**:97.

Marsden, J.F., Limousin-Dowsey, P., Ashby, P., Pollak, P., and Brown, P., 2001, Subthalamic nucleus, sensorimotor cortex and muscle interrelationships in Parkinson's disease. *Brain* **124**:378.

Mena-Segovia, J., Bolam, J.P., and Magill, P.J., 2004, Pedunculopontine nucleus and basal ganglia: distant relatives or part of the same family? *Trends Neurosci.* **27**:585.

Mink, J.W., 1996, The basal ganglia: focused selection and inhibition of competing motor programs. *Prog. Neurobiol.* **50**:381.

Mitzdorf, U., 1985, Current-source density method and application in cat cerebral cortex: investigation of evoked potentials and EEG phenomena. *Physiol. Rev.* **65**:37.

Moro, E., Esselink, R.J.A., Xie, J., Hommel, M., Benabid, A.L., and Pollak, P., 2002, The impact on Parkinson's disease of electrical parameter settings in STN stimulation. *Neurology* **59**:706.

Murthy, V.N., and Fetz, E.E., 1992, Coherent 25- and 35-Hz oscillations in the sensorimotor cortex of awake behaving monkeys. *Proc. Natl. Acad. Sci. USA.* **89**:5670.

Murthy, V.N., and Fetz, E.E, 1996a, Oscillatory activity in sensorimotor cortex of awake monkeys: synchronization of local field potentials and relation to behavior. *J. Neurophysiol.* **76**:3949.

Murthy, V.N., and Fetz, E.E., 1996b, Synchronization of neurons during local field potential oscillations in sensorimotor cortex of awake monkeys. *J. Neurophysiol.* **76**: 3968.

Nini, A., Feingold, A., Slovin, H., and Bergman, H., 1995, Neurons in the globus pallidus do not show correlated activity in the normal monkey, but phase-locked oscillations appear in the MPTP model of parkinsonism. *J. Neurophysiol.* **74**:1800.

Perkel, D.H., Gerstein, G.L., and Moore, G.P., 1967a, Neuronal spike trains and stochastic point processes. I. The single spike train. *Biophys. J.* **7**:391.

Perkel, D.H., Gerstein, G.L., and Moore, G.P., 1967b, Neuronal spike trains and stochastic point processes. II. Simultaneous spike trains. *Biophys. J.* **7**:419.

Pfurtscheller, G., Stancak, A., and Neuper, C., 1996, Post-movement beta synchronization. A correlate of an idling motor area? *Electroencephalogr. Clin. Neurophysiol.* **98**:281.

Priori, A., Foffani, G., Pesenti, A., Bianchi, A., Chiesa, V., Baselli, G., Caputo, E., Tamma, F., Rampini, P., Egidi, M., Locatelli, M., Barbieri, S., and Scarlato, G., 2002, Movement-related modulation of neural activity in human basal ganglia and its L-DOPA dependency: recordings from deep brain stimulation electrodes in patients with Parkinson's disease. *Neurol. Sci.* **23**:S101.

Priori, A., Foffani, G., Pesenti, A., Tamma, F., Bianchi, A.M., Pellegrini, M., Locatelli, M., Moxon, K.A., and Villani, R.M., 2004, Rhythm-specific pharmacological modulation of subthalamic activity in Parkinson's disease. *Exp. Neurol.* **189**:369.

Raz, A., Vaadia, E., and Bergman, H., 2000, Firing patterns and correlations of spontaneous discharge of pallidal neurons in the normal and the tremulous 1-methyl-4-phenyl-1,2,3,6-tetrahydropyridine vervet model of parkinsonism. *J. Neurosci.* **20**:8559.

Raz, A., Frechter-Mazar, V., Feingold, A., Abeles, M., Vaadia, E., and Bergman, H., 2001, Activity of pallidal and striatal tonically active neurons is correlated in MPTP-treated monkeys but not in normal monkeys. *J. Neurosci.* **21**:RC128.

Richards, C.D., Shiroyama, T., and Kitai, S.T., 1997, Electrophysiological and immunocytochemical characterization of GABA and dopamine neurons in the substantia nigra of the rat. *Neuroscience* **80**:557.

Roelfsema, P.R., Engel, A.K., König, P., and Singer, W., 1997, Visuomotor integration is associated with zero time-lag synchronization among cortical areas. *Nature* **385**:157.

Ruskin, D.N., Bergstrom, D.A., Tierney, P.L., and Walters, J.R., 2003, Correlated multisecond oscillations in firing rate in the basal ganglia: modulation by dopamine and the subthalamic nucleus. *Neuroscience* **117**:427.

Sanes, J.N., and Donoghue, J.P., 1993, Oscillations in local field potentials of the primate motor cortex during voluntary movement. *Proc. Natl. Acad. Sci. USA.* **90**:4470.

Sharott, A., Magill, P.J., Harnack, D., Kupsch, A., Meissner, W., and Brown, P., 2005a, Dopamine depletion increases the power and coherence of β-oscillations in the cerebral cortex and subthalamic nucleus of the awake rat. *Eur. J. Neurosci.* **21**:1413.

Sharott, A., Magill, P.J., Bolam, J.P., and Brown, P., 2005b, Directional analysis of coherent oscillatory field potentials in the cerebral cortex and basal ganglia of the rat. *J. Physiol.* **562**:951.

Silberstein, P., Kühn, A.A., Kupsch, A., Trottenberg, T., Krauss, J., Wöhrle, J.C., Mazzone, P., Insola, A., Di Lazzaro, V., Oliviero, A., Aziz, T., and Brown, P., 2003, Patterning of globus pallidus local field potentials differs between Parkinson's disease and dystonia. *Brain* **126**:2597.

Sochurkova, D., and Rektor, I., 2003, Event-related desynchronization/synchronization in the putamen. An SEEG case study. *Exp. Brain. Res.* **149**:401.

Smith, Y., Bevan, M.D., Shink, E., and Bolam, J.P., 1998, Microcircuitry of the direct and indirect pathways of the basal ganglia. *Neuroscience* **86**:353.

Steriade, M., 2000, Corticothalamic resonance, states of vigilance and mentation. *Neuroscience* **101**:243.

Stern, E.A., Jaeger, D., and Wilson, C.J., 1998, Membrane potential synchrony of simultaneously recorded striatal spiny neurons *in vivo*. *Nature* **394**:475.

Timmermann, L., Wojtecki, L., Gross, J., Lehrke, R., Voges, J., Maarouf, M., Treuer, H., Sturm, V., and Schnitzler, A., 2004, Ten-Hertz stimulation of subthalamic nucleus deteriorates motor symptoms in Parkinson's disease. *Mov. Disord.* **19**:1328.

Volkmann, J., Joliot, M., Mogilner, A., Ioannides, A.A., Lado, F., Fazzini, E., Ribary, U., and Llinás, R., 1996, Central motor loop oscillations in parkinsonian resting tremor revealed by magnetoencephalography. *Neurology* **46**:1359.

Vorobyov, V.V., Schibaev, N.V., Morelli, M., and Carta, A.R., 2003, EEG modifications in the cortex and striatum after dopaminergic priming in the 6-hydroxydopamine rat model of Parkinson's disease. *Brain Res.* **972**:177.

Williams, D., Tijssen, M., van Bruggen, G., Bosch, A., Insola, A., Di Lazzaro, V., Mazzone, P., Oliviero, A., Quartarone, A., Speelman, H., and Brown, P., 2002, Dopamine dependent changes in the functional connectivity between basal ganglia and cerebral cortex in the human. *Brain* **125**:1558.

Williams, D., Kühn, A., Kupsch, A., Tijssen, M., van Bruggen, G., Speelman, H., Hotton, G., Yarrow, K., and Brown, P., 2003, Behavioural cues are associated with modulations of synchronous oscillations in the human subthalamic nucleus. *Brain* **126**:1975.

Williams, D., Kühn, A., Kupsch, A., Tijssen, M., van Bruggen, G., Speelman, H., Hotton, G., Loukas, C., Brown, P., 2005, The relationship between oscillatory activity and motor reaction time in the parkinsonian subthalamic nucleus. *Eur. J. Neurosci.* **21**:249.

PARTICIPATION OF STRIATAL NEURONS IN LARGE-SCALE OSCILLATORY NETWORKS

Joshua D. Berke

1. INTRODUCTION

In recent years basal ganglia physiologists have become increasingly interested in oscillations and synchrony (Bevan et al., 2002; see also chapters by Boraud et al., and Walters et al., this volume). This reflects a now broad recognition that "box-and-arrow" models of the basal ganglia based upon simple inhibition and excitation are inadequate to explain current data, and too conceptually limited to serve as a basis for further experimentation. In this brief chapter I shall address some recent observations while recording local field potentials (LFPs) and single-units in the striatum of awake, unrestrained rats (Berke et al., 2004). Rather than reiterating previously published points, I shall focus on some *difficulties* encountered in interpretation of field potential recordings, and some (incomplete) solutions to these problems.

The striatum is just one component of the cortex – basal ganglia – thalamus – cortex loops, and may or may not reflect all the dynamic activity seen in subsequent nuclei such as the globus pallidus. However, it will be difficult to understand oscillations in such other structures without considering oscillations in their inputs – so the striatum, together with its relationships to cortex, is a reasonable place to begin.

2. WHAT IS A LOCAL FIELD POTENTIAL, AND WHAT IS IT GOOD FOR?

Extracellular recordings are made by measuring the potential difference between the tip of an electrode in the brain, and some reference location. Fluctuations in this potential difference can be filtered into either higher-frequency (e.g. 300–6000 Hz) or lower-frequency (e.g. 0.1–300 Hz) components. The higher frequency parts of the signal can include brief action potentials (spikes) from individual neurons ("single-units") or groups of cells ("multi-unit activity"). The lower frequencies are called the local field potential

* Joshua D. Berke, Department of Psychology, University of Michigan, Ann Arbor, Michigan 48109, USA.

(for some examples, see Figs. 1,3), and can be an indication of the collective activity of large populations of neurons and/or synapses. Such population activity may be of interest in itself, especially in a structure such as striatum where individual neurons tend to have highly diverse behavioral correlates (Schultz, 1995). Even more importantly, the relationships between single-units and LFPs may give us useful clues to the phenotypes, connectivity, and temporal coding properties of individual neurons, as discussed below.

3. STRIATAL LFPs ARE TOPOGRAPHICALLY ORGANIZED AND BEHAVIORALLY CONTINGENT

Oscillatory activity is readily apparent in LFPs recorded from rat striatum. The types of oscillation observed reflect both the behavioral state of the animal, and the location within the striatum (Fig. 1). High-voltage spindles (HVSs, ~8 Hz), which engage broad regions of neocortex, are also strongly present in the dorsal/lateral striatum. These oscillations occur in awake but immobile animals, and have increased incidence following striatal dopamine depletion or blockade (Buonamici et al., 1986; Buzsáki et al., 1990). In ventral striatum strong ~50 Hz gamma oscillations are frequently observed in alert rats (whether moving or not), and these are sometimes accompanied by beta oscillations (~20 Hz; Berke and Kunec, 2004). During maze running ventral striatum also shows the ~8 Hz theta rhythm that is widespread in limbic brain regions (Buzsáki, 2002).

4. HOW LOCAL IS THE STRIATAL LOCAL FIELD POTENTIAL?

To understand the significance of such striatal LFP oscillations, we need to know how they arise. Firstly we should establish which components of the striatal LFP signal are actually being generated in striatum, rather than some other structure. While all LFPs rely on conduction through the extracellular medium to some extent, under some conditions electrical field changes generated in one brain area can be detected in another, quite distant, location. This volume conduction is a serious concern when interpreting LFP signals. Secondly, if the LFP is indeed locally generated, we would like to know which neural elements are responsible, and over what spatial scale they contribute to the LFP. Unfortunately, despite a number of useful clues, neither question can currently be answered to our full satisfaction in any brain nuclei, including the basal ganglia.

To address the first question we must rely heavily on mapping out the amplitude and phase of oscillations, within and around the structure of interest. Recording from multiple brain regions and subregions simultaneously can be helpful in establishing the spatial extent of oscillatory activity, and in adding or excluding candidate structures that may be generating rhythmic activity. For example, ~50 Hz gamma oscillations appear very similar in ventral striatum and in nearby piriform cortex, but not in medial prefrontal cortex or hippocampal CA1 (Fig. 3A). Recording different signals from many distinct sites, all using the same (distant) reference location, also adds confidence that the signals observed are not actually being detected at the reference site. Similarly, moving an electrode progressively through a structure and observing that a signal disappears at the structure's boundaries can increase confidence that a signal is local. On the other hand, even in large-scale electrophysiological recording one is limited in the number of recording sites, so often it remains possible to argue that another, non-sampled location is actually generating the observed signal.

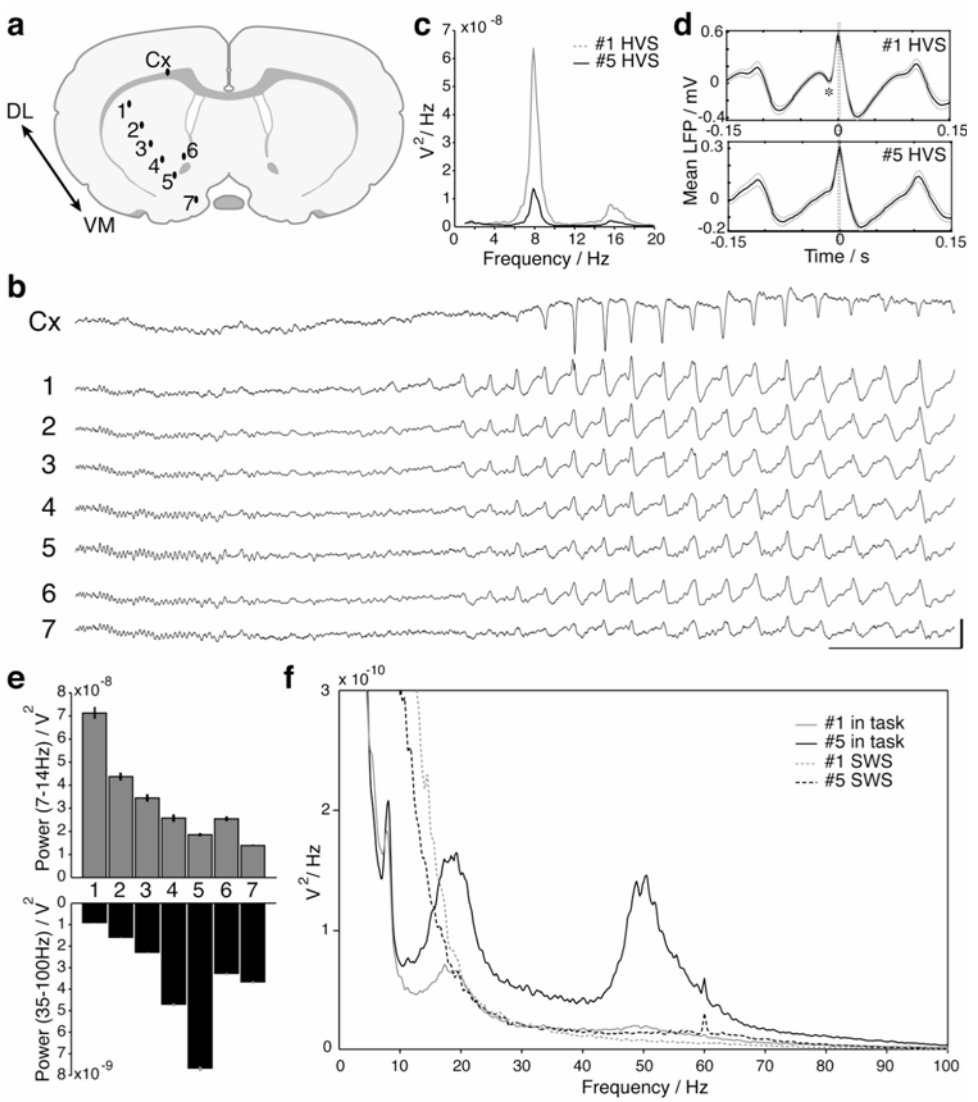

Figure 1. Graded distributions of striatal oscillations. **a)** Example of tetrode recording positions. "1"–"5" were positioned along the dorsal/lateral to ventral/medial axis, "Cx" was on the boundary between deep cortical layers and the white matter of the corpus callosum. **b)** Example of LFPs recorded from the sites shown in a, in an awake but immobile rat. Gamma oscillations (~50 Hz) are visible early in some traces, a high-voltage spindle (~8 Hz) is present on the right hand side. Scale bars: 0.5 s, 1 mV. **c)** Power spectral density for LFPs from tetrodes 1,5 during HVSs. **d)** Averaged shape of HVS cycles from tetrodes 1,5. HVS peaks in ventral-medial striatum lag slightly behind those in dorsal-lateral striatum. In addition to smaller amplitude, they also lack the clear negative deflection (marked by asterisk) slightly before the peak. **e)** HVS (top), and gamma (bottom) power for each striatal location, during detected HVS and gamma epochs respectively. There are opposite gradients of HVS and gamma power between dorsal/lateral and ventral/medial striatum. **f)** Power spectral densities for electrodes 1,5 during well-practiced performance of a radial maze task (solid lines) or slow-wave sleep (dashed lines). Ventral/medial striatum shows pronounced theta (~8 Hz), beta (~20 Hz) and gamma oscillations (~50 Hz). For more details and methods see Berke et al., 2004. Parts of this figure and the next were modified from that work, with permission from Elsevier.

Signals that are the result of volume conduction should propagate at the speed of light (in brain), and hence have no detected phase lag. This is not the case for striatal high-voltage spindles (Fig. 1d), which show a small but measurable phase-lag between dorsal-lateral and ventral-medial sites, as well as a pronounced change in shape (more on this below). This is fairly good evidence that the high-voltage spindles in striatum actually do reflect local processes.

Usually, some of the strongest evidence for local generation of LFPs is the observation of complete phase reversals within the structure. Note that there are two quite distinct meanings of phase reversal (Duffy et al., 1989). "Instrumental" phase reversal can be observed when a series of electrode contacts are placed in a line, with each contact serving as the reference point for the next. A single focus of current can produce voltage deflections in opposite directions for two adjacent channels in this chain of bipolar recordings, simply as a result of the referencing arrangement. Such useful evidence for focal oscillatory activity located between two contacts has been obtained in macroelectrode investigations of the human subthalamic nucleus (e.g. Brown et al., 2001). However, such electrode and recording configurations are not well suited for mapping out oscillations. For example if two adjacent contacts are both located within similar parts of the same structure, or in two structures oscillating in phase, the bipolar arrangement can make it appear as if there is no oscillation present at all. In addition these human recordings have so far suffered from the limitations of low spatial resolution and imprecise electrode localization without post-mortem data.

"True" phase reversal occurs between recording sites whose local potential changes are truly out of phase – because of opposite directions of current flow at the two locations. One of the best-studied examples is the hippocampal CA1 region (see Fig. 3A). Here the phase of theta oscillations changes systematically with depth (Brankack et al., 1993; Buzsáki, 2002), as electrodes pass through successive layers of synapses from distinct afferents, and cell bodies. The organized separation of these current "sources" and "sinks" in coherently aligned neurons allows large electrical fields to be generated. High-density recording methods, together with current-source-density analysis, have now allowed systematic investigation of current sources and sinks within such laminar structures (e.g. Kandel and Buzsáki, 1997; Csicsvari et al., 2003).

Our understanding of LFPs in structures such as striatum, in which cells have radial morphology and lack organized orientation, is far more limited. Current theories that treat neurons as electric dipoles (balanced sources and sinks) would predict that the electric fields generated by a set of randomly arranged dipoles should cancel one another out, unless the LFP signal reflected activity from just one or a small number of cells (this would be a "very local" field potential). This is not the case, since striatum LFPs can remain nearly unchanged during electrode movements of a millimeter or more, while extracellular spikes from individual units typically disappear with electrode movements of 100 μm or less. Thus, in so far as the LFPs within striatum are indeed being striatally-generated, they are reflecting synchronized population activity of many neural elements. In cortex it has long been believed that the longer duration of synaptic currents (especially EPSCs) compared to spikes results in synaptic activity dominating the LFP (Mitzdorf, 1985). More recent work suggests that other cellular processes that affect membrane potentials may also make a substantial contribution (Nadasdy et al., 1998; Logothetis, 2003). It would be useful to have more theoretical analyses to tell us what processes may contribute to the striatal LFP, and over what spatial scales.

If striatal LFPs are generated largely by EPSCs, one could conceivably observe substantial LFP phase changes in striatum if there were sharp boundaries between the terminal

fields of distinct afferents, and these afferents oscillated with different phases. For the most part, the divergent nature of corticostriatal innervation would seem to discourage this – corticostriatal axons tend to innervate rather wide areas within striatum, and make only a small number of synapses on each striatal neuron they pass (e.g. Cowan and Wilson, 1994; Zheng and Wilson, 2002). Although focal zones within striatum can receive rather different innervation (e.g. Gerfen, 1989; Ragsdale and Graybiel, 1990), we have not yet observed any sharp transitions in the striatal LFP during electrode movements that might correspond to distinct LFPs in these zones.

To summarize so far, while we have observed phase changes within striatum that are suggestive of a local origin, we have not observed the sort of LFP phase reversals that are used to make inferences about LFP generators in laminar structures. Nor, given the microanatomical organization of the striatum, would one necessarily expect to. On the other hand, one at least has the consolation of never being in the "wrong" layer within striatum – allowing useful analyses of LFP–single unit phase relationships with only moderately precise anatomical reconstruction.

5. RELATIONSHIP BETWEEN INDIVIDUAL STRIATAL NEURONS AND LFPs

In the absence of extracellular phase reversals, some of the best evidence for local generation of striatal LFPs comes from examination of the timing relationships between LFPs and the activity of individual cells. Some useful demonstrations that the local field potential in the striatum can closely mirror local individual neuronal potentials have come from combined intracellular and extracellular recordings in ventral striatum (Leung and Yim, 1993; Goto and O'Donnell, 2001). In these anesthetized rats, prominent slow-wave/delta (~1 Hz) oscillations were seen in both types of recording, but inverted with respect to each other. This may reflect current flow between the intracellular and extracellular compartments. Such slow membrane changes occur simultaneously across populations of medium-spiny striatal neurons, showing a greater degree of synchrony than individual action potentials (Stern et al., 1998). Hence the striatal LFP may be a good indicator of striatal population changes in intracellular membrane potential.

However, as such slow-wave oscillations are synchronously present across wide regions of the brain during sleep and anesthesia, the causal relationship between intracellular and extracellular potentials could in principle be indirect (Tseng et al., 2001). Further, intracellular recording is currently limited to anesthetized and/or head-restrained preparations. As the rhythms observed in the basal ganglia are highly dependent on behavioral state, it is hard to gain intracellular data on the faster rhythms associated with active behaviors – a particular problem when investigating the functional roles of the basal ganglia in action selection and learning.

We have therefore focused on the relationship between extracellularly-recorded single-units and LFPs (Fig. 2) To briefly address one methodological point first: Magill and colleagues have argued that ". . . the utility of analyses of the correlation or coherence between units and LFPs recorded through the same electrode is limited by overlaps in the frequency content of the two signals, which may lead to the spurious detection of temporal coupling" (Magill et al., 2004). There is indeed a potential pitfall, but this can be readily avoided. One common method of relating spikes to LFP oscillations is to find the peaks (or troughs) of the rhythm, and for each single-unit spike that falls between two peaks calculate the corresponding phase. This produces a phase histogram (e.g. Fig. 2e) and one can use standard circular statistics to calculate the significance of any entrainment. A problem can

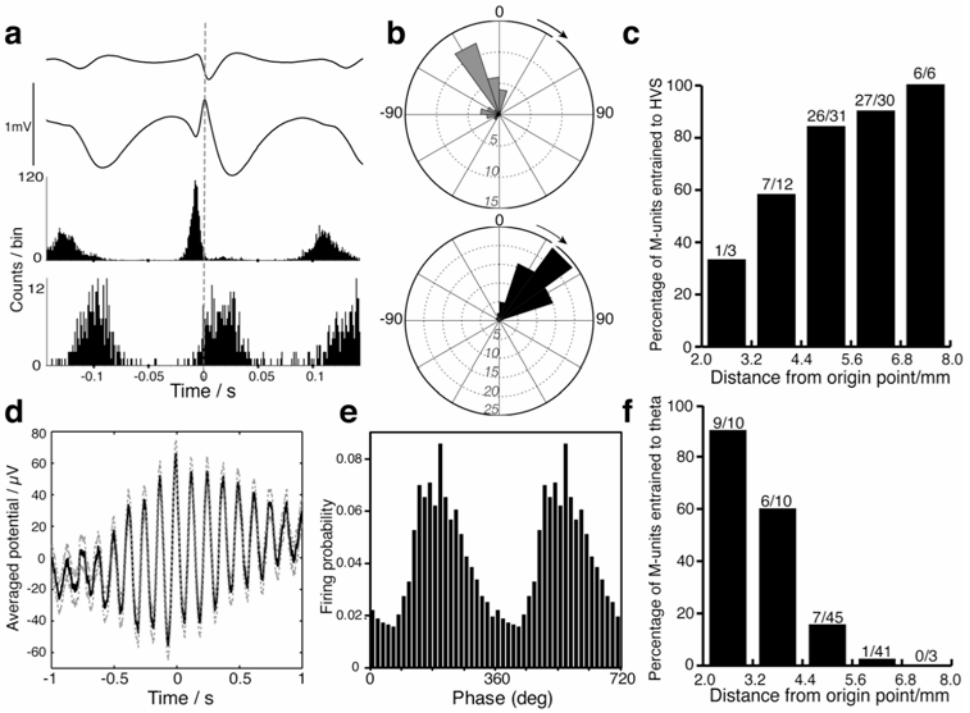

Figure 2. Single-unit entrainment to HVS and theta oscillations. **a)** Upper traces: EEG from frontal cortex (top) and dorsal/lateral striatal LFP (bottom), averaged around the peak of the striatal HVS cycles. Bottom: Perievent spike histograms for two single-units, triggered by the same HVS peaks. Top unit is a presumed fast-spiking interneuron ("F-unit"), bottom is a presumed medium-spiny cell ("M-unit"). **b)** Firing phase for all entrained F-units (top) and M-units (bottom). F-units as a population fire with distinct phase to the M-unit population. **c)** Distribution of HVS-entrained M-units, relative to an arbitrary origin point on the ventral midline. Increasing distance from this point indicates more dorsal, lateral, and/or posterior locations. **d)** Spike-triggered average between a medial striatal M-unit and LFP recorded in dorsal hippocampus. Dashed lines indicate ±2 × S.E.M. The strong oscillation centered around zero indicates that this unit tends to fire at a specific phase of the hippocampal theta rhythm. **e)** Phase histogram for the same unit and hippocampal LFP (theta troughs are at 0°/360°/720°). This cell tends to fire at or shortly after hippocampal theta peaks. Entrainment was significant at $p < 10^{-57}$. **f)** Distribution of theta-entrained M-units, relative to same origin as in c. Note opposite gradients of entrainment to HVS and hippocampal theta.

arise when, depending on the signal filtering and the peak detection algorithm, the action-potentials of a single-unit contribute transients to the LFP that are falsely detected as peaks of the LFP oscillation under investigation. The result can be the incorrect assignment of these spikes as having a zero-phase relationship to the LFP oscillation. Therefore any phase histogram showing just a narrow peak of high entrainment precisely at zero phase should be viewed with considerable scepticism. In a similar way, spike-triggered averages of LFPs can show the averaged action potential contribution to the LFP – though only at time zero, so oscillations on either side of this are not affected. One can, of course, escape any such problems altogether by correlating units recorded on one electrode to the LFP recorded on another. As field potentials change only slowly with distance in the striatum (as discussed above), clear oscillatory entrainment of single-units is easily detected even when using LFPs from a considerable distance away (e.g. Figs. 3c,d).

We observed that at least some properties of the striatal local field potential do closely reflect striatal spike activity (Fig. 2). High-voltage spindles (HVS) are strong in dorsal-lateral striatum, and almost all single-units recorded there are strongly entrained to this rhythm. The proportion of entrained units drops off medially and ventrally, along with the HVS power in the LFP. By contrast, ventral-medial striatum contains a high proportion of units that are entrained to hippocampal theta rhythm, and the LFP there shows a theta peak with clear coherence to hippocampus. Thus there are opposite gradients of single-unit entrainment between sensorimotor and cognitive/limbic striatum, which match the properties of the LFP.

Further, the shape, as well as power, of striatal HVS oscillations reflects local unit properties. The striatum shows a graded distribution of tonically-active, brief-waveform cells that are probably parvalbumin-staining, fast-spiking GABAergic interneurons (see Fig. 1 of Berke et al., 2004). Given that fast-spiking interneurons have been shown to strongly influence the spike timing of wide populations of spiny neurons *in vitro* (Koos and Tepper, 1999), it is quite likely that they play an important role in entraining the wider population of spiny neurons into the HVS oscillation *in vivo* – though this remains to be directly demonstrated. These cells fire just before the peak of the HVS oscillation, while the main population of single-units (almost certainly medium-spiny cells) fire after the peak. The activity of the two populations corresponds to two negative deflections in the LFP; in ventral-medial striatum, where there are relatively few fast-spiking units, there is a corresponding relative loss of power of the first deflection (Fig. 1d). As this dip has a similar width to the HVS peak itself, and thus contributes similar frequency components to the LFP, this waveform change is unlikely to be the result of some passive filtering property of the striatal neuropil.

Such close correlations between such HVS variations in the striatal LFP and the variation in the single-unit properties strongly support the view that at least this oscillation is locally generated in striatum. It may be possible to gain further confirmatory evidence by, for example, a selective lesion of striatal fast-spiking interneurons – though there is always the possibility that this would alter the incidence or nature of the oscillation too much to be useful. The very high proportion of theta-entrained units in ventral striatum, the fact that these cells as a population fire with coherent phase (Berke et al., 2004), and the spatially graded decrease of unit entrainment, LFP theta power, and LFP theta coherence with hippocampus argues for local generation of striatal LFP theta as well.

However, there are also some dissociations between spike activity and LFP, both in the striatum and in other structures (Logothetis, 2003). Consider the rather complex case of striatal beta and gamma oscillations (Fig. 3). These rhythms show interesting power changes over the course of habit learning, as well as frequency modulations in response to both dopaminergic drug manipulations and behavioral task features such as reward receipt (Berke et al., 2003; Berke and Kunec, 2004). However, the evidence for these LFP oscillations reflecting local striatal activity is decidedly mixed. It is possible to findsingle-units in striatum that are strongly entrained to gamma and beta oscillations (e.g. Figs. 3c, d), so these rhythms undoubtedly have some impact on striatal activity. On the other hand, the proportion of clearly entrained units is very small compared to (for example) theta-entrained units, even though ~50 Hz gamma oscillations in particular are very prominent in the LFP. In addition, extremely similar beta and gamma oscillations are observed in the adjacent piriform cortex (e.g. Fig. 3a), as well as related structures such as endopiriform cortex (unpublished observations). Given the potential for large electric field generation by the laminar piriform cortex, it seems quite likely that a large component of the LFP gamma

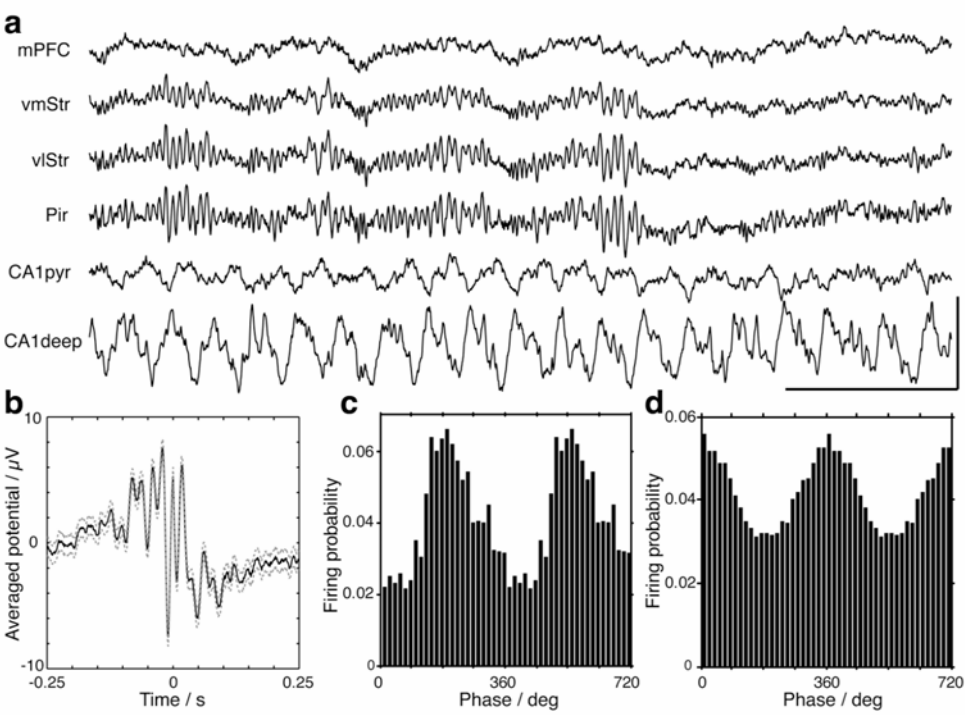

Figure 3. Gamma oscillations in striatum and piriform cortex. **a)** Simultaneously recorded LFPs from medial prefrontal cortex ("mPFC"), ventral-medial striatum ("vmStr"), ventral-lateral striatum ("vlStr"), piriform cortex ("Pir"), cell body layer of dorsal hippocampal CA1 ("CA1pyr"), and deep dorsal hippocampal CA1 ("CA1deep"). All signals were referenced to the same skull screw at a distant, posterior midline location. Scale bars, 0.5 s, 1 mV. Note phase reversal of hippocampal theta between the two hippocampal recording sites, and that the large gamma oscillations are very similar in both ventral striatum and piriform cortex. **b)** Spike-triggered average between spikes from an F-unit recorded at one location in ventral striatum and the LFP recorded at another ventral striatal site. Dashed lines indicate ±2 × S.E.M. The complex-appearing averaged signal reflects entrainment to multiple oscillations. **c)** Phase histogram showing entrainment of the same F-unit to beta oscillations (LFP filtered at 12–25 Hz before peak detection). Entrainment is significant at $p < 10^{-62}$. **d)** Phase histogram showing entrainment of the same F-unit to ~50 Hz gamma oscillations (LFP filtered at 42–58 Hz before peak detection). Entrainment is significant at $p < 10^{-147}$.

oscillations recorded in striatum is not produced there. We will need to complete phase mapping and possibly lesion studies before drawing any firm conclusions; initial analyses suggest that piriform cortex and striatum may have zero phase difference most of the time, but not under all behavioral conditions. In any case, it appears that at least a large part of rat striatal beta and gamma oscillations are a manifestation of olfactory information processing (e.g. Kay and Freeman, 1998) (Vanderwolf, 2000; Neville and Haberly, 2003; Ravel et al., 2003) rather than some particular striatal mechanism.

Another unresolved observation is that the few gamma-entrained striatal units recorded so far have all been presumed fast-spiking interneurons (Berke and Kunec, 2004). These cells may receive a more convergent pattern of afferents from cortical structures (Ramanathan et al., 2002) that contributes to higher sensitivity (Parthasarathy and Graybiel, 1997). It is also easier to detect oscillatory entrainment in tonically active units simply due to a larger number of spikes available for analysis. Nonetheless, given the tight control

these interneurons can exert over the spike timing of nearby medium spiny cells, it would be interesting to know what membrane properties or other factors prevent the clear entrainment of projection neuron spikes. Reduced synaptic efficacy at gamma frequencies might also contribute (Thomson and West 2003).

6. CONCLUSIONS

Given our limited understanding of LFP generation (and not just in the striatum), one might ask why it is worth recording the LFP at all, rather than just oscillations in spike trains. One major reason is that the LFP serves as a form of temporal reference. By comparing spike times to the LFP, one can indirectly compare the timing properties of individual neurons recorded from different sessions or even different rats. This has allowed us to confirm that groups of units with different waveforms and firing patterns actually do represent functionally distinct neuronal subpopulations. The relationship between individual neurons and particular rhythms may also give clues as to the sorts of information they are receiving. For example, both theta-entrained and -unentrained neurons can be recorded simultaneously from the same electrode. It would be interesting to know whether neurons that are more entrained to hippocampal theta have behavioral correlates that are more closely related to hippocampal representations than those that are not.

Recording of striatal LFPs may also be useful when attempting to make connections to the human neuroimaging literature. Recent studies have found that (at least in cortex) the fMRI BOLD signal is much more closely related to the LFP than to neuronal spiking (Logothetis, 2003). Both signals appear to more closely reflect synaptic input and local processing than the output of a brain structure, which is encoded in the activity of projection neurons. Because of this, the LFP may contribute useful information about population-wide subthreshold changes in membrane potential – if we can learn more about how it is generated.

The oscillatory entrainment of striatal units shows that oscillations are indeed a feature of rat striatal activity. Do such oscillations play an important role in the functional properties of the basal ganglia? The significance of neural oscillations has been the subject of much debate, and the possible advantages of organizing neural information processing using oscillations have been recently reviewed (Engel et al., 2001; Buzsaki and Draguhn, 2004). While mechanisms for oscillatory pacemaking may exist within striatum (Wilson, 2005), our current evidence suggests that most oscillatory activity found within the normal rat striatum is instead the result of oscillations in striatal afferents. Hence, theta oscillations in striatum are found in striatal areas that receive afferents from theta-entrained brain regions, including hippocampus and medial prefrontal cortex. While there have been few studies of olfactory innervation of striatal regions (e.g. Haberly and Price, 1978; Luskin and Price, 1983), it appears that striatal ~50 Hz gamma oscillations are another manifestation of the widespread olfaction-related gamma. And sensorimotor striatum shows the high-voltage spindles that are most reliably initiated in sensorimotor cortex (Meeren et al., 2002). Intrastriatal circuit properties may, however, influence the spread, extent, and occurrence of oscillations both locally and in other brain structures. For example, high-voltage spindles are far more synchronized in striatum than between cortical EEGs, which likely reflects both divergence of corticostriatal pathways and the coupled activity of striatal fast-spiking interneurons (Berke et al., 2004). The fact that loss of striatal dopamine alters the nature and incidence of oscillations in the basal ganglia and cortex (e.g. Buonamici et al.,

1986; Magill et al., 2001; Goldberg et al., 2002; Belluscio et al., 2003) demonstrates the influence of basal ganglia mechanisms over the dynamic activity of cortex – basal ganglia – thalamus – cortex loops. We have a long way to go, however, before we are able to prove or disprove the intriguing hypothesis of Brown and Marsden (1998) that basal ganglia control of oscillatory activity is central to their functional role in action selection and initiation.

7. ACKNOWLEDGEMENTS

I thank György Buzsáki for insightful comments at conference presentations.

8. REFERENCES

Belluscio, M.A., Kasanetz, F., Riquelme, L.A., and Murer, M.G., 2003, Spreading of slow cortical rhythms to the basal ganglia output nuclei in rats with nigrostriatal lesions, *Eur. J. Neurosci.* **17**:1046–1052.

Berke, J.D., and Kunec, S., 2004, Behavioral correlates of beta and gamma oscillations in the rat striatum. *Soc. Neurosci. Abstr.* 70.21.

Berke, J.D., Okatan, M., Skurski, J., and Eichenbaum, H.B., 2003, Synchronous striatal spindles and gamma-oscillations in freely-moving rats. *Soc. Neurosci. Abstr.* 390.16.

Berke, J.D., Okatan, M., Skurski, J., and Eichenbaum, H.B., 2004, Oscillatory entrainment of striatal neurons in freely moving rats, *Neuron* **43**:883–896.

Bevan, M.D., Magill, P.J., Terman, D., Bolam, J.P., and Wilson, C.J., 2002, Move to the rhythm: oscillations in the subthalamic nucleus-external globus pallidus network, *Trends Neurosci.* **25**:525–531.

Brankack, J., Stewart, M., and Fox, S.E., 1993, Current source density analysis of the hippocampal theta rhythm: associated sustained potentials and candidate synaptic generators, *Brain Res.* **615**:310–327.

Brown, P., Oliviero, A., Mazzone, P., Insola, A., Tonali, P., and Di Lazzaro, V., 2001, Dopamine dependency of oscillations between subthalamic nucleus and pallidum in Parkinson's disease, *J. Neurosci.* **21**:1033–1038.

Buonamici, M., Maj, R., Pagani, F., Rossi, A.C., and Khazan, N., 1986, Tremor at rest episodes in unilaterally 6-OHDA-induced substantia nigra lesioned rats: EEG-EMG and behavior, *Neuropharmacology* **25**:323–325.

Buzsaki, G., and Draguhn, A., 2004, Neuronal oscillations in cortical networks, *Science* **304**:1926–1929.

Buzsáki, G., 2002, Theta oscillations in the hippocampus, *Neuron* **33**:325–340.

Buzsáki, G., Smith, A., Berger, S., Fisher, L.J., and Gage, F.H., 1990, Petit mal epilepsy and parkinsonian tremor: hypothesis of a common pacemaker, *Neuroscience* **36**:1–14.

Cowan, R.L., and Wilson, C.J., 1994, Spontaneous firing patterns and axonal projections of single corticostriatal neurons in the rat medial agranular cortex, *J. Neurophysiol.* **71**:17–32.

Csicsvari, J., Jamieson, B., Wise, K.D., and Buzsaki, G., 2003, Mechanisms of gamma oscillations in the hippocampus of the behaving rat, *Neuron* **37**:311–322.

Duffy, F.H., Iyer, V.G., and Surwillo, W.W., 1989, Clinical Electroencephalography and Topographic Brain Mapping. New York: Springer-Verlag.

Engel, A.K., Fries, P., and Singer, W., 2001, Dynamic predictions: oscillations and synchrony in top-down processing, *Nat. Rev. Neurosci.* **2**:704–716.

Gerfen, C.R., 1989, The neostriatal mosaic: striatal patch-matrix organization is related to cortical lamination, *Science* **246**:385–388.

Goldberg, J.A., Boraud, T., Maraton, S., Haber, S.N., Vaadia, E., and Bergman, H., 2002, Enhanced synchrony among primary motor cortex neurons in the 1-methyl-4-phenyl-1,2,3,6-tetrahydropyridine primate model of Parkinson's disease, *J. Neurosci.* **22**:4639–4653.

Goto, Y., and O'Donnell, P., 2001, Network synchrony in the nucleus accumbens in vivo, *J. Neurosci.* **21**:4498–4504.

Haberly, L.B., and Price, J.L., 1978, Association and commissural fiber systems of the olfactory cortex of the rat, *J. Comp. Neurol.* **178**:711–740.

Kandel, A., and Buzsáki, G., 1997, Cellular-synaptic generation of sleep spindles, spike-and-wave discharges, and evoked thalamocortical responses in the neocortex of the rat, *J. Neurosci.* **17**:6783–6797.

Kay, L.M., and Freeman, W.J., 1998, Bidirectional processing in the olfactory-limbic axis during olfactory behavior, *Behav. Neurosci.* **112**:541–553.

Koos, T., and Tepper, J.M., 1999, Inhibitory control of neostriatal projection neurons by GABAergic interneurons, *Nat. Neurosci.* **2**:467–472.

Leung, L.S., and Yim, C.Y., 1993, Rhythmic delta-frequency activities in the nucleus accumbens of anesthetized and freely moving rats, *Can J. Physiol. Pharmacol.* **71**:311–320.

Logothetis, N.K., 2003, MR imaging in the non-human primate: studies of function and of dynamic connectivity, *Curr. Opin. Neurobiol.* **13**:630–642.

Luskin, M.B., and Price, J.L., 1983, The topographic organization of associational fibers of the olfactory system in the rat, including centrifugal fibers to the olfactory bulb, *J. Comp. Neurol.* **216**:264–291.

Magill, P.J., Bolam, J.P., and Bevan, M.D., 2001, Dopamine regulates the impact of the cerebral cortex on the subthalamic nucleus-globus pallidus network, *Neuroscience* **106**:313–330.

Magill, P.J., Sharott, A., Bolam, J.P., and Brown, P., 2004, Brain state-dependency of coherent oscillatory activity in the cerebral cortex and basal ganglia of the rat, *J. Neurophysiol.* **92**:2122–2136.

Meeren, H.K., Pijn, J.P., Van Luijtelaar, E.L., Coenen, A.M., and Lopes da Silva, F.H., 2002, Cortical focus drives widespread corticothalamic networks during spontaneous absence seizures in rats, *J. Neurosci.* **22**:1480–1495.

Mitzdorf, U., 1985, Current source-density method and application in cat cerebral cortex: investigation of evoked potentials and EEG phenomena, *Physiol. Rev.* **65**:37–100.

Nadasdy, Z., Csicsvari, J., Penttonen, M., Hetke, J., Wise, K., and Buzsaki, G., 1998, Extracellular Recording and Analysis of Neuronal Activity: From Single Cells to Ensembles, In: *Neuronal Ensembles: Strategies for Recording and Decoding* (Eichenbaum HB, Davis JL, eds), pp 17–55. New York: Wiley-Liss.

Neville, K.R., and Haberly, L.B., 2003, Beta and gamma oscillations in the olfactory system of the urethaneanesthetized rat, *J. Neurophysiol.* **90**:3921–3930.

Parthasarathy, H.B., and Graybiel, A.M., 1997, Cortically driven immediate-early gene expression reflects modular influence of sensorimotor cortex on identified striatal neurons in the squirrel monkey, *J. Neurosci.* **17**:2477–2491.

Ragsdale, C.W., Jr., and Graybiel, A.M., 1990, A simple ordering of neocortical areas established by the compartmental organization of their striatal projections, *Proc. Natl. Acad. Sci. U. S. A.* **87**:6196–6199.

Ramanathan, S., Hanley, J.J., Deniau, J.M., and Bolam, J.P., 2002, Synaptic convergence of motor and somatosensory cortical afferents onto GABAergic interneurons in the rat striatum, *J. Neurosci.* **22**:8158–8169.

Ravel, N., Chabaud, P., Martin, C., Gaveau, V., Hugues, E., Tallon-Baudry, C., Bertrand, O., and Gervais, R., 2003, Olfactory learning modifies the expression of odour-induced oscillatory responses in the gamma (60–90 Hz) and beta (15–40 Hz) bands in the rat olfactory bulb, *Eur. J. Neurosci.* **17**:350–358.

Schultz, W., Apicella, P., Romo, R., and Scarnati, E., 1995, Context-dependent activity in primate striatum reflecting past and future behavioral events, In: *Models of Information Processing in the Basal Ganglia* (Houk JC, Davis, J.L., Beiser, D.G., ed). Cambridge, MA: MIT Press.

Stern, E.A., Jaeger, D., and Wilson, C.J., 1998, Membrane potential synchrony of simultaneously recorded striatal spiny neurons in vivo, *Nature* **394**:475–478.

Thomson, A.M., and West, D.C., 2003, Presynaptic frequency filtering in the gamma frequency band; dual intracellular recordings in slices of adult rat and cat neocortex, *Cereb Cortex* **13**:136–143.

Tseng, K.Y., Kasanetz, F., Kargieman, L., Riquelme, L.A., and Murer, M.G., 2001, Cortical slow oscillatory activity is reflected in the membrane potential and spike trains of striatal neurons in rats with chronic nigrostriatal lesions, *J. Neurosci.* **21**:6430–6439.

Vanderwolf, C.H., 2000, What is the significance of gamma wave activity in the pyriform cortex?, *Brain Res.* **877**:125–133.

Wilson, C.J., 2005, The mechanism of intrinsic amplification of hyperpolarizations and spontaneous bursting in striatal cholinergic interneurons, *Neuron* **45**:575–585.

Zheng, T., Wilson, C.J., 2002, Corticostriatal combinatorics: the implications of corticostriatal axonal arborizations, *J. Neurophysiol.* **87**:1007–1017.

DO LOCAL FIELD POTENTIALS REFLECT SYNCHRONIZED SPIKING ACTIVITY OF NEURONAL POPULATIONS IN THE BASAL GANGLIA?

Studies in a rodent model of Parkinson's disease

Judith R. Walters, Dan Hu, Christy A. Itoga, Louise C. Parr-Brownlie, and Debra A. Bergstrom*

1. INTRODUCTION

The ability to record neuronal activity during placement of deep brain stimulation electrodes in the basal ganglia of parkinsonian patients has provided unique opportunities for exploring relationships between brain activity and movement-related dysfunction. One issue relevant to the interpretation of the data made available by these procedures is the extent to which local field potential (LFP) recordings can compliment and extend perspectives obtained from single unit recordings. As LFPs reflect net changes in pre- and post-synaptic currents in tissue surrounding the recording electrode (for recent discussion of relevant literature, see Goldberg et al., 2004; Logothetis and Pfeuffer, 2004), it has been proposed that they may provide insight into wide-spread changes in firing pattern and synchronization of activity in the basal ganglia after loss of dopamine (Brown et al., 2001; Levy et al., 2002; Goldberg et al., 2004). The present chapter discusses an approach to exploring the usefulness of LFP as a predictor of change in neuronal population activity through investigation of relationships between LFP and spiking activity in the subthalamic nucleus (STN) in a rodent model of Parkinson's disease.

A number of investigators have reported that, in anesthetized rats, neurons in several basal ganglia nuclei exhibit altered firing patterns after unilateral 6-hydroxydopamine (6-OHDA)-mediated dopamine cell lesion. One site where firing pattern changes have frequently been noted in anesthetized 6-OHDA-treated rats is the STN, where an increase in

* Neurophysiological Pharmacology Section, National Institute of Neurological Disorders and Stroke, National Institutes of Health, Porter Neuroscience Center, Bethesda, MD 20892-3702, USA. Dan Hu, Current address: McGovern Institute for Brain Research, MIT, Cambridge, MA 02139, USA

bursting activity has been described (Hollerman and Grace, 1992; Hassani et al., 1996; Perier et al., 2000; Vila et al., 2000; Magill et al., 2001; Ni et al., 2001; Tai et al., 2003; Hu et al., 2004). This phenomenon provides an opportunity to examine the extent to which changes in LFP correlate with changes in neuronal firing pattern under conditions where LFP, firing pattern, and behavior are all relatively stable. To take advantage of this, simultaneous recordings of LFP and spike activity were obtained from STN in intact rats and in rats with unilateral 6-OHDA-mediated lesions of the medial forebrain bundle under urethane anesthesia. Effort was made to sample LFP and spiking activity at multiple sites in each STN studied. Spectral analysis techniques were used to permit quantitative comparisons of LFP and spike train patterns to examine the extent to which LFP recordings were predictive of changes in firing patterns in STN neurons induced by dopamine cell lesion. Fast Fournier transform and Lomb periodogram based techniques were applied to the frequency range with the most prominent oscillations in LFPs and spike trains in urethane anesthetized rats. Results show that relatively dramatic changes in STN firing pattern are associated with modest but significant changes in STN LFP power. In addition, a significant increase in coherence between LFPs and spike train waveforms was noted after dopamine cell lesion. These observations suggest that LFP-spike train relationships in the STN are affected by loss of dopaminergic basal ganglia innervation.

2. METHODS

2.1. Nigrostriatal Lesions

Male Sprague-Dawley rats (275–325 g at time of surgery) were anesthetized with ketamine (100 mg/kg, i.p.) and xylazine (10 mg/kg, i.p.) and placed in a stereotaxic apparatus. Six μg of 6-OHDA HBr in 3 μl of 0.9% saline containing 0.1% ascorbic acid were infused via a cannula into the left medial forebrain bundle. Rats were injected with desmethylimipramine (15 mg/kg, i.p.) 30 min prior to the intracerebral infusion to protect noradrenergic neurons. Five to 10 days after surgery, rats were screened for lesion efficacy by step testing (Olsson et al., 1995). Only rats that demonstrated a strong lesion effect in behavior (number of steps by contralateral limb/number of steps by ipsilateral limb < 15%) were used for electrophysiology.

2.2. Single Unit and LFP Recordings

Seven to 13 days after lesion, extracellular single unit activity and LFPs of STN neurons ipsilateral to 6-OHDA-induced dopamine cell lesion were recorded through the same electrode. STN recordings were also performed in intact rats. Recordings were conducted under urethane anesthesia (1.25 g/kg, i.p., with additional supplement as needed). LFPs were filtered with a 0.1–100 Hz band pass filter and spike trains with a 250–5000 Hz band pass filter. Signals were sampled at 1 KHz (LFP) or 24 KHz (single unit). Glass microelectrodes had resistances of ~4 MΩ (measured at 135 Hz) with tip diameter 1–2 μm. Discriminated signals were stored and analyzed using Spike2 data acquisition and analysis software (Cambridge Electronic Design, Cambridge, UK). Recording sites and extent of neuronal loss in substantia nigra pars compacta were histologically verified.

Respiration was monitored via a force sensing resistor (406, Interlink Electronics) placed under the animals, which registered contact-force variations due to breathing.

Cardiac activity was monitored with surface EKG electrodes, lead II (Grass, West Warwick, RI, USA). All experiments were conducted in accordance with the NIH Guide for Care and Use of Laboratory Animals and approved by the NINDS Animal Care and Use Committee.

2.3. Data Analysis

STN spike train burstiness was assessed by the density discharge histogram method of Kaneoke and Vitek (1996) as described previously (Kreiss et al., 1997; Allers et al., 2000, 2005). A discharge density histogram with a bin width equal to twice the mean ISI was used, providing a 'burstiness index' = 0.5 (see Magill et al., 2000; Wilson et al., 2004). A spike train was identified as bursty if its discharge density histogram distribution was significantly different from a Poisson distribution of the discharge density histogram ($\chi 2$ test set at a significance level of 0.05) and positively skewed, and the number of bursts/1000 spikes was >5. Analyses were conducted on 300 sec epochs.

Oscillatory characteristics of spiking activity and LFPs were analyzed over 300 sec epochs for the frequency range of 0.3–2.5 Hz using either Lomb periodogram analysis of autocorrelograms or fast Fourier transforms (FFT) with a resolution of 0.08 Hz. Lomb periodogram based analysis of interspike interval (ISI) autocorrelograms (50 msec bins, 10 sec lag) were performed according to the method of Kaneoke and Vitek (1996). For FFT based analyses, spike trains were transformed from events to a series of Gaussian curves (50 msec duration) and summed to provide a continuous waveform smoothed to 20 Hz. LFPs were smoothed to 20 Hz and high pass filtered at 0.2 Hz. Total power of LFPs and spike waveforms in the 0.3–2.5 Hz range were calculated from FFT based power spectra, generated using Spike2 software scripts.

Coherence between LFPs and spike train waveforms was calculated using 23 non-overlapping windows with a 12.8 sec bin. A coherence confidence level for these parameters was 0.13, as determined by the equation: $1-(1-\forall)^{1/(L-1)}$ where $\forall$ is 0.95 and L is the number of windows used (Rosenberg et al., 1989). Coherences were averaged over the 0.3–2.5 Hz range.

Data were collected from 5 intact and 7 lesioned rats with ~4 cells/LFPs recorded on average per rat. To assess total power, each spike train was analyzed individually while LFPs were assessed per track. Lesion effects on incidence of spike train oscillations and burstiness were analyzed with $\chi 2$ test. Lesion effects on mean coherence between spike train waveforms and LFPs, and total power of LFPs and spike train waveforms were analyzed using Student's t test or ANOVA with Student-Newman-Keuls post-hoc comparisons. The criterion for significance was $p < 0.05$.

3. RESULTS

3.1. STN Spike Trains: Changes in Firing Pattern after Dopamine Cell Lesion

Seven to 13 days after unilateral dopamine cell lesion, most (94%) STN spike trains recorded ipsilateral to the lesion showed a bursty firing pattern (Figure 1A), as previously reported in studies in anesthetized rats (Hollerman and Grace, 1992; Hassani et al., 1996; Perier et al., 2000; Vila et al., 2000; Magill et al., 2001; Ni et al., 2001; Tai et al., 2003; Hu et al., 2004). Bursts occurred at an average rate of ~50 bursts/1000 spikes when assessed

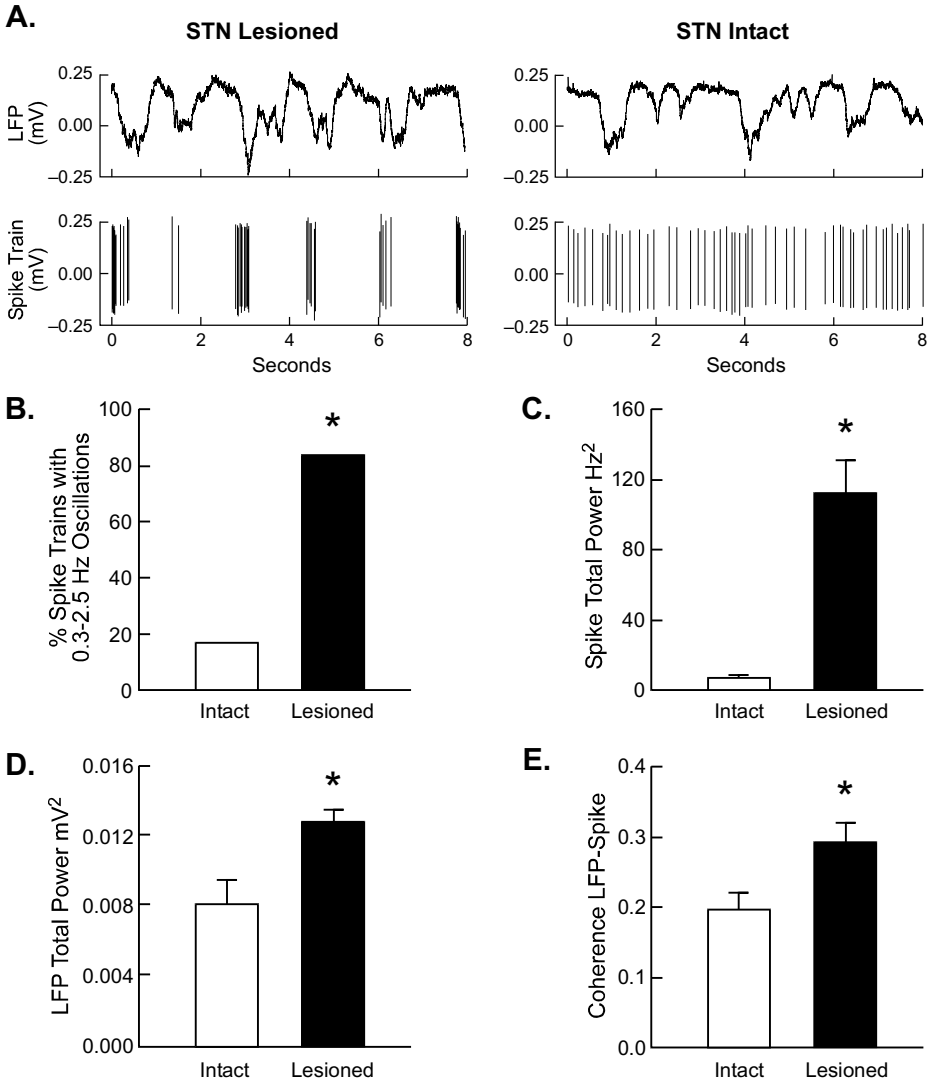

Figure 1. A. STN LFP and spike train recordings. Traces are typical of simultaneously recorded LFP and spike train data from STNs ipsilateral to a unilateral dopamine cell lesion (left) and in a neurologically intact rat (right) under urethane anesthesia. Most STN spike trains recorded ipsilateral to lesion showed a bursty firing pattern that was rarely seen in the intact rodent STN. LFPs showed slow oscillations in both intact and lesioned preparations. B. Incidence of slow periodic oscillations in STN spike trains as determined by Lomb periodogram based analyses. STN spike trains from lesioned rats had significantly more periodic oscillations in the 0.3–2.5 Hz range than STN spike trains from intact rats. C. Total power in the frequency range of 0.3–2.5 Hz of STN spike train waveforms as determined by FFT analyses. STN spike train power was 13-fold greater in the lesioned animal. D. Total power of STN LFPs as determined by FFT analyses for the 0.3–2.5 Hz range. STN LFP power in the lesioned animal was significantly greater than in controls. E. Mean coherence for the 0.3–2.5 Hz frequency range between STN LFPs and STN spike trains. Coherences were significant in both preparations and were significantly greater in lesioned animals compared to intact animals. * $p < 0.05$ compared with intact.

with a burstiness index of 0.5, as described in methods. In contrast, no STN spike trains recorded in the intact rats were bursty; none showed more than 5 bursts/1000 spikes. The more regular firing pattern observed in the intact rat was reflected in the comparison of the coefficient of variation (CV) of the ISI from the two groups; ISI CV of the intact STN spike trains was 43% that of the lesioned STN spike trains.

The temporal dynamics and rhythmicity of the bursty pattern observed in the STN spike trains were assessed using a) Lomb periodogram based spectral analysis of spike train ISI autocorrelograms and b) FFT based analysis of spike trains converted to waveforms. Incidence of significant oscillations, peak oscillatory frequencies, and total power over the 0.3–2.5 Hz range were compared for recordings in intact and lesioned animals. While it is certainly possible for neurons to have a firing pattern that is bursty but not significantly periodic or oscillatory, or vice versa, the bursts observed in the STN spike trains in 6-OHDA lesioned, anesthetized rats tended to occur in a significantly periodic manner. Significant oscillations were observed in the 0.3–2.5 Hz range in 84% of spike train autocorrelograms (n = 32) from STN neurons recorded ipsilateral to the dopamine cell lesion (Figure 1B). Peak frequencies of firing rate oscillations were most commonly in the range of 0.6–1.0 Hz, although a few spike train oscillations had main peak frequencies ranging up to 2.5 Hz. In intact animals, notably fewer spike trains, only 17%, yielded autocorrelograms that were significantly periodic in the 0.3–2.5 Hz range (n = 23). FFT analyses of spike trains converted to waveforms gave results concordant with the Lomb based analyses. Total power in the 0.3–2.5 Hz range in spike train waveforms FFTs was 13-fold greater in lesioned animals than in intact animals (Figure 1C). Firing rates of STN neurons ipsilateral to dopamine cell lesions were significantly greater (67%) than those in intact animals.

3.2. STN LFP: Power of Slow Oscillations after Dopamine Cell Lesion

In contrast to the marked differences in firing patterns in STN spike trains recorded in the intact and lesioned hemispheres, STN LFPs recorded in intact hemispheres appeared relatively similar to those recorded in lesioned hemispheres. LFPs recorded in both lesioned and intact STN in urethane anesthetized rats showed prominent slow oscillations. Peak frequencies of STN LFP oscillations from both intact and lesioned rats were in the same range as the firing rate oscillations observed in the lesioned rats as described above: 0.6–1.0 Hz. Notable in the lesioned rats, moreover, was the correlation between the oscillations in LFPs and the periodic burstiness evident in most STN spike trains. Bursts typically occurred during the troughs of the LFP oscillations, corresponding to periods of net increased depolarization in the surrounding neuronal tissue (Figure 1A). This phase relationship between bursting activity and LFP oscillations in the dopamine lesioned rats was confirmed using spike-triggered waveform analysis (data not shown).

The contrast between the apparent similarity between STN LFPs in intact and lesioned brains and the marked differences in spike firing patterns in the two preparations prompted a further investigation into whether quantitative measures of LFP pattern could, in the rodent STN, provide an indication of the dramatic alterations in firing pattern in the population of recorded STN neurons. To address this question, total power in the 0.3–2.5 Hz range was assessed in LFP recordings. LFP total power was significantly greater in the lesioned hemisphere, consistent with the prominent differences in oscillatory spiking activity in STN neurons in the lesioned hemisphere (Figure 1D). However, the increase in LFP power of 57% in the lesioned hemisphere relative to the intact was notably less than the ~1300% increase in spike power.

3.3. STN LFP – Spike Train Relationships: Effects of Dopamine Cell Lesion

The results described above indicated that the striking changes in firing pattern in STN spike trains were associated with relatively modest changes in simultaneously recorded LFP. To further explore this apparent nonlinear relationship between LFP and spike pattern, coherence between LFP and spike waveforms was assessed in recordings from intact and lesioned animals. Peak coherence was in the 0.7–1.0 Hz range and mean coherence was significant in the 0.3–2.5 Hz range in both preparations. Moreover, loss of dopamine was associated with a significant increase of 50% in mean coherence between LFPs and spike train waveforms from the lesioned hemispheres (Figure 1E).

4. DISCUSSION

This study explores the effect of dopamine cell lesion on LFP – single unit activity relationships in the rodent STN. As a number of investigators have reported and results discussed in this chapter further highlight, single unit activity is notably more bursty in the STN of anesthetized rats after dopamine depletion (Hollerman and Grace, 1992; Hassani et al., 1996; Perier et al., 2000; Vila et al., 2000; Magill et al., 2001; Ni et al., 2001; Tai et al., 2003; Hu et al., 2004). Spectral analysis of STN spike trains recorded in the present study has shown (Hu et al., 2004), moreover, that this bursty activity is strongly periodic: STN spike train ISI autocorrelograms were significantly more oscillatory, and total power in spike train waveforms in the 0.3–2.5 Hz range was increased 13-fold in recordings from lesioned rats, relative to controls. The bursts also appear to occur in a relatively synchronized manner, as they show a consistent phase relationship with the LFP over a range of recordings sites within the STN.

This effect of dopamine cell lesion on STN neuronal firing pattern provides an opportunity to compare properties of LFPs from nuclei in the basal ganglia with comparable anatomy but different neuronal activity. While it remains to be determined whether conclusions drawn from a study of slow oscillations in LFPs in anesthetized preparations are relevant to the awake state where faster frequencies are more dominant, the observations discussed in this chapter are both encouraging and cautionary with respect to the question of whether changes in LFP oscillations can provide insight into dopamine lesioned induced changes in firing patterns and synchronization of spike trains in the basal ganglia. The recordings described here do show that peak frequencies in spike train oscillations recorded in rats with dopamine cell lesions correspond with peak frequencies in LFP oscillations. In addition, changes in power in LFP oscillations in lesioned animals are consistent with the direction of change in power of spike train oscillations in the lesioned animals with respect to slow oscillatory activity. Total power in the 0.3–2.5 Hz range from LFPs recorded in lesioned animals with oscillatory STN spike trains was significantly greater than in intact animals where STN bursting and oscillatory firing patterns were infrequent or absent. However, the differences in LFP properties in the intact and lesioned animals were quite modest, relative to the very substantial differences in firing pattern in the two populations.

These results can be viewed from two perspectives. On the one hand, the relatively small change in LFP power in conjunction with a robust change in spike train oscillations could be taken as support for the view that LFP, recorded under conditions discussed here, is not a sensitive tool for probing population activity in a small structure like the STN of

the rat. Historically, researchers have focused on LFPs in structures such as the cortex and hippocampus, where the more organized topography contributes to a relatively more amplified and interpretable LFP signal. The significance of LFP signals recorded in areas where neurons are positioned in a less ordered manner is more controversial, leaving room for concern that LFPs recorded in structures like the rodent STN may reflect or be diluted by volume-conducted higher amplitude signals from structures outside the area of the nucleus. Estimates of the radius of tissue contributing to these signals in the cortex are in the range of 0.5–3 mm (Mitzdorf, 1987) – an area clearly exceeding that of the rat STN. Thus, it is certainly a concern that LFPs recorded in the STN region may be contaminated by volume-conducted signals and inaccurately reflect local changes in synaptic input and postsynaptic neuronal potential.

On the other hand, recent studies have provided support for the view that a substantial component of the LFP recorded in the STN reflects local changes in STN neuronal transmembrane potential triggered by synaptic input (Magill et al., 2004a,b). Viewed from this perspective, the data have interesting implications with respect to the consequences of dopamine cell lesion. The results suggest that loss of dopamine has a modulatory effect on the tendency of STN neurons to generate spikes in response to a given net change in transmembrane potential. This perspective is supported by the robust increase in bursts in the STN spike train in conjunction with the LFP oscillations, as well as the increase in coherence between LFPs and spike train waveforms observed after dopamine cell lesion in the present study. A variety of direct or indirect effects could alter net input-output relationships in the STN after loss of dopaminergic innervation in the basal ganglia. A different mix of excitatory and inhibitory synaptic inputs could produce different intracellular consequences with respect to spiking activity, but similar fluctuations in net LFP. In addition, loss of dopamine might directly or indirectly affect expression of ion channels or other processes regulating spiking activity in STN neurons in the frequency range examined.

Thus, to the extent that LFPs do reflect local changes in the basal ganglia neuronal populations, the present results suggest that, when considered in the context of parallel recordings of spiking activity, LFPs can provide insight into the modulatory effects of a manipulation such as dopamine cell lesion. Similarly, the data predict that LFPs should reflect population-based firing patterns in the basal ganglia in dopamine lesioned preparations, as demonstrated by Goldberg and colleagues (2004), more effectively than in intact preparations. It is interesting to note, in this regard, the literature reflects an extensive range of studies regarding relationships between single- and multi-unit spike patterns and LFP (for examples, see Fromm and Bond, 1964, 1967; Marsan, 1965; Weber and Buchwald, 1965; Buchwald et al., 1966; Legatt et al., 1980; Kamondi et al., 1998; Engel and Singer, 2001; Engel et al., 2001; Fries et al., 2001; Buzsaki, 2002; Magill et al., 2004b). Of special interest is a recent study comparing stimulus-induced changes in LFP oscillations, multi-unit spiking patterns and BOLD signal from the visual cortex (Logothetis et al., 2001). Discrepancies were noted between the time courses of LFP change and firing pattern change, with the BOLD signal being more correlated with changes in LFP than spike pattern.

Finally, the present results also shed some light on an inconsistency in the literature regarding the extent to which bursting activity occurs in the STN after dopamine cell lesion. As referenced above, the observation that STN spike trains exhibit altered firing patterns after unilateral dopamine cell lesion in anesthetized rats is consistent with a series of previous observations. However, these observations are strikingly at odds with other observations from our own laboratory obtained from awake locally anesthetized rats (Kreiss et al., 1997;

Allers et al., 2005). In these two separate studies in the awake, immobilized, locally anesthetized preparation, STN neurons were found to be relatively bursty in both intact and dopamine lesioned rats 6 or more weeks post lesion. Moreover, burstiness was actually decreased after dopamine lesion in the awake preparation, in marked contrast to results observed in anesthetized rats. While the interval between lesion and recording in the study with awake immobilized rats was longer than the 1–2 week period used in the anesthetized study discussed here, increases in STN burstiness after dopamine cell lesion have also been reported in the 4–6 week time period in recordings from anesthetized rats (Hollerman and Grace, 1996; Magill et al., 2001; Ni et al., 2001; Tai et al., 2003). This argues against time-dependent compensatory mechanisms accounting for the inconsistent observations in the different preparations. The present results suggest this discrepancy in effects of dopamine cell lesion on STN burstiness in the two preparations is related to the fact that in the anesthetized rat, slow oscillations are the dominant feature of cortical activity. The coherence between the oscillatory burstiness of the STN neurons in the anesthetized preparation and the slow oscillations in the LFP argues strongly that the temporal dynamics of the bursty pattern is determined by the slow oscillations in synaptic input to these neurons associated with the global effects of the anesthetic. In the awake, locally anesthetized preparation, synaptic input to the STN would be dominated by higher frequency activity. While STN firing patterns might well be altered by loss of dopamine in the awake preparation, effects of higher frequency oscillations in synaptic input would likely be less notable than the effects of the relatively stable 1 Hz oscillation dominant in the anesthetized state.

5. SUMMARY

Simultaneous recordings of STN LFPs and single unit activity were obtained from urethane anesthetized rats in order to explore the effects of dopamine cell loss on relationships between these two indices of neuronal activity, and on the usefulness of LFPs as a means of estimating changes in temporal dynamics of firing patterns in STN neuronal populations. In both preparations, STN LFPs were characterized by slow oscillations in the 0.3–2.5 Hz frequency range, with peak frequencies typically between 0.6–1.0 Hz. Spectral analysis showed that the power of LFP oscillations in the 0.3–2.5 Hz range was approximately 57% greater in recordings obtained 1–2 weeks after dopamine cell lesion than in controls. Power in the corresponding frequency range in simultaneously recorded STN spike trains was more dramatically increased, by approximately 1300%, and incidence of bursty activity in spike trains was increased by 94% by dopamine cell lesion.

These observations argue that LFPs are substantially more predictive of STN spike train firing patterns in 6-OHDA lesioned rats than in intact rats, and they raise a note of caution with respect to the general usefulness of LFPs as a quantitative measure of population-based changes in STN firing patterns across a range of manipulations. On the other hand, the results support the view that LFPs can be predictive of population based firing patterns in the STN of dopamine lesioned preparations. A similar conclusion was drawn in a recent study in the globus pallidus of parkinsonian monkeys (Goldberg et al., 2004), indicating that these observations are relevant across a range of frequencies and preparations, and at least two basal ganglia nuclei. Finally, the results focus attention on the interesting question of the mechanism(s) underlying this effect of dopamine loss on input/output relationships in the STN, and the extent to which it involves an alteration in the composition of synaptic input or more local changes in the processing of the input.

6. REFERENCES

Allers, K.A., Kreiss, D.S., and Walters, J.R., 2000, Multisecond oscillations in the subthalamic nucleus: effects of apomorphine and dopamine cell lesion, *Synapse* **38**:38–50.

Allers, K.A., Bergstrom, D.A., Ghazi, L.J., Kreiss, D.S., and Walters, J.R., 2005, MK801 and amantadine exert different effects on subthalamic neuronal activity in a rodent model of Parkinson's disease, *Exp. Neurol.* **191**:104–118.

Brown, P., Oliviero, A., Mazzone, P., Insola, A., Tonali, P., and Di Lazzaro, V., 2001, Dopamine dependency of oscillations between subthalamic nucleus and pallidum in Parkinson's disease, *J. Neurosci.* **21**:1033–1038.

Buchwald, J.S., Halas, E.S., and Schramm, S., 1966, Relationships of neuronal spike populations and EEG activity in chronic cats, *Electroencephalogr. Clin. Neurophysiol.* **21**:227–238.

Buzsaki, G., 2002, Theta oscillations in the hippocampus, *Neuron* **33**:325–340.

Engel, A.K., Fries, P., and Singer, W., 2001, Dynamic predictions: oscillations and synchrony in top-down processing, *Nat. Rev. Neurosci.* **2**:704–716.

Engel, A.K., and Singer, W., 2001, Temporal binding and the neural correlates of sensory awareness, *Trends Cogn. Sci.* **5**:16–25.

Fries, P., Reynolds, J.H., Rorie, A.E., and Desimone, R., 2001, Modulation of oscillatory neuronal synchronization by selective visual attention, *Science* **291**:1560–1563.

Fromm, G.H., and Bond, H.W., 1964, Slow changes in the electrocorticogram and the activity of cortical neurons, *Electroencephalogr. Clin. Neurophysiol.* **17**:520–523.

Fromm, G.H., and Bond, H.W., 1967, The relationship between neuron activity and cortical steady potentials, *Electroencephalogr. Clin. Neurophysiol.* **22**:159–166.

Goldberg, J.A., Rokni, U., Boraud, T., Vaadia, E., and Bergman, H., 2004, Spike synchronization in the cortex-basal ganglia networks of parkinsonian primates reflects global dynamics of the local field potentials, *J. Neurosci.* **24**:6003–6010.

Hassani, O.K., Mouroux, M., and Féger, J., 1996, Increased subthalamic neuronal activity after nigral dopaminergic lesion independent of disinhibition via the globus pallidus, *Neuroscience* **72**:105–115.

Hollerman, J.R., and Grace, A.A., 1992, Subthalamic nucleus cell firing in the 6-OHDA-treated rat: basal activity and response to haloperidol, *Brain Res.* **590**:291–299.

Hu, D., Itoga, C.A., Bergstrom, D.A., Parr-Brownlie, L.C., Ghiglieri, V., and Walters, J.R., 2004, Increased patterned activity in basal ganglia output in anesthetized rats after dopamine loss is organized by coordinated oscillations in the indirect pathway nuclei, *Soc. Neurosci. Abstr.* 309.8.

Kamondi, A., Acsady, L., and Buzsaki, G., 1998, Dendritic spikes are enhanced by cooperative network activity in the intact hippocampus, *J. Neurosci.* **18**:3919–3928.

Kaneoke, Y., and Vitek, J.L., 1996, Burst and oscillation as disparate neuronal properties, *J. Neurosci. Meth.* **68**:211–223.

Kreiss, D.S., Mastropietro, C.W., Rawji, S.S., and Walters, J.R., 1997, The response of subthalamic nucleus neurons to dopamine receptor stimulation in a rodent model of Parkinson's disease, *J. Neurosci.* **17**:6807–6819.

Legatt, A.D., Arezzo, J., and Vaughan, H.G., Jr., 1980, Averaged multiple unit activity as an estimate of phasic changes in local neuronal activity: effects of volume-conducted potentials, *J. Neurosci. Methods* **2**:203.

Levy, R., Ashby, P., Hutchison, W.D., Lang, A.E., Lozano, A.M., and Dostrovsky, J.O., 2002, Dependence of subthalamic nucleus oscillations on movement and dopamine in Parkinson's disease, *Brain* **125**:1196–1209.

Logothetis, N.K., Pauls, J., Augath, M., Trinath, T., and Oeltermann, A., 2001, Neurophysiological investigation of the basis of the fMRI signal, *Nature* **412**:150–157.

Logothetis, N.K., and Pfeuffer, J., 2004, On the nature of the BOLD fMRI contrast mechanism, *Magn. Reson. Imaging* **22**:1517–1531.

Magill, P.J., Bolam, J.P., and Bevan, M.D., 2000, Relationship of activity in the subthalamic nucleus-globus pallidus network to cortical electroencephalogram, *J. Neurosci.* **20**:820–833.

Magill, P.J., Bolam, J.P., and Bevan, M.D., 2001, Dopamine regulates the impact of the cerebral cortex on the subthalamic nucleus-globus pallidus network, *Neuroscience* **106**:313–330.

Magill, P.J., Sharott, A., Bolam, J.P., and Brown, P., 2004a, Brain state-dependency of coherent oscillatory activity in the cerebral cortex and basal ganglia of the rat, *J. Neurophysiol.* **92**:2122–2136.

Magill, P.J., Sharott, A., Bevan, M.D., Brown, P., and Bolam, J.P., 2004b, Synchronous unit activity and local field potentials evoked in the subthalamic nucleus by cortical stimulation, *J. Neurophysiol.* **92**:700–714.

Marsan, C.A., 1965, Electrical activity of the brain: slow waves and neuronal activity, *Isr. Med. J.* **20**:104–117.

Mitzdorf, U., 1987, Properties of the evoked-potential generators – current source-density analysis of visually evoked-potentials in the cat cortex, *Intern. J. Neurosci.* **33**:33–59.

Ni, Z.G., Bouali-Benazzouz, R., Gao, D.M., Benabid, A.L., and Benazzouz, A., 2001, Time-course of changes in firing rates and firing patterns of subthalamic nucleus neuronal activity after 6-OHDA-induced dopamine depletion in rats, *Brain Res.* **899**:142–147.

Olsson, M., Nikkhah, G., Bentlage, C., and Bjorklund, A., 1995, Forelimb akinesia in the rat Parkinson model – differential-effects of dopamine agonists and nigral transplants as assessed by a new stepping test, *J. Neurosci.* **15**:3863–3875.

Perier, C., Agid, Y., Hirsch, E.C., and Feger, J., 2000, Ipsilateral and contralateral subthalamic activity after unilateral dopaminergic lesion, *Neuroreport* **11**:3275–3278.

Rosenberg, J.R., Amjad, A.M., Breeze, P., Brillinger, D.R., and Halliday, D.M., 1989, The Fourier approach to the identification of functional coupling between neuronal spike trains, *Prog. Biophys. Mol. Biol.* **53**:1–31.

Tai, C.H., Boraud, T., Bezard, E., Bioulac, B., Gross, C., and Benazzouz, A., 2003, Electrophysiological and metabolic evidence that high-frequency stimulation of the subthalamic nucleus bridles neuronal activity in the subthalamic nucleus and the substantia nigra reticulata, *FASEB, J.* **17**:1820–1830.

Vila, M., Perier, C., Feger, J., Yelnik, J., Faucheux, B., Ruberg, M., Raisman-Vozari, R., Agid, Y., and Hirsch, E. C., 2000, Evolution of changes in neuronal activity in the subthalamic nucleus of rats with unilateral lesion of the substantia nigra assessed by metabolic and electrophysiological measurements, *Eur. J. Neurosci.* **12**:337–344.

Weber, D.S., and Buchwald, J.S., 1965, A technique for recording and integrating multiple unit activity simultaneously with the EEG in chronic animals, *Electroencephalogr. Clin. Neurophysiol.* **19**:190–192.

Wilson, C.L., Puntis, M., and Lacey, M.G., 2004, Overwhelmingly asynchronous firing of rat subthalamic nucleus neurones in brain slices provides little evidence for intrinsic interconnectivity, *Neuroscience* **123**:187–200.

A PARTIAL SPECTRA METHOD FOR PREDICTING SPIKE CORRELATIONS FROM LOCAL FIELD POTENTIALS

Application to MPTP induced synchronization

Joshua A. Goldberg and Hagai Bergman*

1. INTRODUCTION

The basic tool for measuring collective synchrony in a network of neurons is the pair-wise cross-correlation histogram (CCH) (Perkel et al., 1967; Eggermont, 1990). Using this technique we have demonstrated dramatic changes in the patterns of synchronization among neurons in the basal ganglia and cortex of 1-methyl-4-phenyl-1,2,3,6-tetrahydropyridine (MPTP)-treated parkinsonian primates (Nini et al., 1995; Raz et al., 2000; Raz et al., 2001; Goldberg et al., 2002). Another signal that is related to collective network dynamics is the local field potential (LFP). Models that explain the source and structure of hippocampal and cortical LFPs rely on the regular layout of pyramidal neurons (Klee and Rall, 1977; Mitzdorf, 1985), which is essential to the emergence of a summated macropotential. Thus, in these structures the LFP results from collective neuronal activity of many neurons. The microanatomy of the basal ganglia does not fit these models, but nevertheless LFPs are readily recorded from these structures (Brown et al., 2001; Marsden et al., 2001; Cassidy et al., 2002; Magill et al., 2004; Sharott et al., 2005). Two properties of the LFP recorded in the basal ganglia suggest that it reflects some global mode of network activity: a) it is correlated with the discharge of nearby neurons (Levy et al., 2002; Goldberg et al., 2004); and b) it is coherent across distances of several millimeters in the brain (Courtemanche et al., 2003; Goldberg et al., 2004).

Armed with these two measures of collective network dynamics – the pair-wise CCH and the LFP – we need to address the question of the relationship between them. Specifically, because the LFP is spatially coherent we may be faced with the situation wherein the discharge of two neurons (that may be several millimeters apart) is correlated

* Joshua A. Goldberg, University of Texas at San Antonio, San Antonio, Texas, 78249. Hagai Bergman, The Hebrew University of Jerusalem, Jerusalem, Israel, 91120.

with the LFP that is common to both. This implies that the discharge of these neurons will be correlated with each other by virtue of the coupling of each one to the LFP. We therefore seek a method to quantify what part of the association observed between the two neurons (measured using the CCH) can be attributed to the coupling between each neuron and the LFP. In a recent paper (Goldberg et al., 2004), we constructed an LFP-predicted CCH using the method of partial spectral analysis (Halliday et al., 1995) to address this question.

The main purpose of this chapter is to present the mathematical derivation of the LFP-predicted CCH. We will then apply this analysis to a trivariate data set composed of simultaneous recordings from three separate electrodes – distanced 1–2 millimeters from each other – of a) a striatal tonically active neuron (TAN); b) a pallidal border cell; and C) the LFP from an MPTP-treated monkey. Additionally, we hope in this chapter to outline how to conduct spectral analysis of mixed data sets of analog signals (e.g., the LFP) and point-processes (e.g., spike trains). A comprehensive treatment of this subject appears in Halliday et al. (1995). We have structured our presentation around the very lucid formalism of Percival and Walden (Percival and Walden, 1993) which deals with univariate time series. This formalism is also easily implemented in Matlab (The Mathworks, Natick, MA) as is outlined in the Appendix to this chapter.

2. STATISTICAL MODEL OF LFP AND SPIKE TRAINS

We begin with a description of our statistical model. We assume that the band-pass filtered LFP is a real-valued zero-mean second-order stationary process, denoted $X(t)$. According to the spectral representation theorem (Percival and Walden, 1993) (under some mild assumptions) X(t) can be expressed using a stochastic form of the Riemann-Stieltjes integral as

$$X(t) = \int_{-\infty}^{\infty} e^{i2\pi ft} d\tilde{X}(f) \tag{1}$$

where the increments of the orthogonal process $\tilde{X}(f)$ have the following properties:

a) $E[d\tilde{X}(f)] = 0$ for all f ($E[\cdot]$ denotes the expectation operator); and

b) $E[d\tilde{X}^*(f)d\tilde{X}(f')] = \delta_{f,f'}\sigma^2(f)df$ where $\delta_{f,f'}$ is the Kronecker delta function; i.e., it equals 1 if $f = f'$ and 0 otherwise. The asterisk denotes complex conjugation.

We further assume that the instantaneous firing rate (or intensity) of the j^{th} neuron, denoted $r_j(t)$, has a time-invariant linear relationship to the LFP of the form

$$r_j(t) = r_j^0 + \int_{-\infty}^{\infty} a_j(u) X(t-u)\, du \tag{2}$$

In the frequency domain this relationship becomes

$$d\tilde{r}_j(f) = r_j^0 \delta(f) df + \tilde{a}_j(f) d\tilde{X}(f) \tag{3}$$

where $\delta(f)$ is the Dirac delta function. From Eq. (3) we can derive an expression for $\tilde{a}_j(f)$ by multiplying both sides by $d\tilde{X}^*(f)$ and evaluating the expectation

$$\tilde{a}_j(f) df = \frac{E\left[d\tilde{r}_j(f) d\tilde{X}^*(f)\right]}{\sigma^2(f)} \tag{4}$$

The cross-correlation function of the rates of the j^{th} and k^{th} neuron is defined as

$$C_{jk}(\tau) = E[r_j(t) r_k(t+\tau)] \tag{5}$$

which is independent of t due to the stationarity of the firing rates. Substituting Eq. (2) into Eq. (5) and using the spectral representation of the rates (Eq. (3)) yields

$$\begin{aligned} C_{jk}(\tau) - r_j^0 r_k^0 &= \int_{-\infty}^{\infty}\int_{-\infty}^{\infty} e^{i2\pi[ft+f'(t+\tau)]}\tilde{a}_j(f) E\left[d\tilde{X}(f) d\tilde{X}(f')\right]\tilde{a}_k(f') \\ &= \int_{-\infty}^{\infty} \tilde{a}_j^*(f)\sigma^2(f)\tilde{a}_k(f) e^{i2\pi f\tau} df = \int_{-\infty}^{\infty} \frac{\chi_j(f)\chi_k^*(f)}{\sigma^2(f)} e^{i2\pi f\tau} df \end{aligned} \tag{6}$$

where

$$\chi_j(f) df \equiv E\left[d\tilde{r}_j^*(f) d\tilde{X}(f)\right] \tag{7}$$

3. ESTIMATION OF THE LFP-PREDICTED CCH

The estimates of these quantities are constructed as follows. We assume that the spike trains and the LFP are sampled at a intervals of Δt. They are denoted by r_t and X_t, respectively, where t is an integer and we have suppressed the index of the neuron. Care must be taken that no more than one spike falls into each Δt interval. The data are then divided into L segments of T samples (using zero padding if necessary). We define the following quantity for the LFP

$$d_X^T(f,l) \equiv \sum_{t=(l-1)T}^{lT-1} e^{-i2\pi ft\Delta t} X_t h_t \tag{8}$$

where X_t has had its empirical mean over the l^{th} segment removed and h_t is a data taper normalized such that $\sum_{t=1}^{T} h_t^2 = 1$ (Percival and Walden, 1993). We would like to define the analogous quantity for the spike trains. The estimate for the instantaneous firing rate is given by the spike train itself. We represented this as a sum of impulses (formally, Dirac delta functions) occurring at the times t_s of the spikes

$$\hat{r}(t) = \sum_{t_s} \delta(t - t_s) \tag{9}$$

The proper way to discretize this sum of Dirac delta functions is by using the Kronecker delta function and normalizing by Δt, as follows

$$r_t = \sum_{t_s} \frac{\delta_{t,t_s}}{\Delta t} \tag{10}$$

Now, analogously to Eq. (8), we define for the spike trains

$$d_r^T(f,l) = \sum_{t=(l-1)T}^{lT-1} e^{-i2\pi ft\Delta t} r_t h_t \tag{11}$$

To calculate the LFP-predicted CCH (Eq. (6)), we estimate $\chi(f)$, which is the cross spectral density (csd) of the spike train and the LFP, by

$$\hat{\chi}(f) = \frac{\Delta t}{L} \sum_{l=1}^{L} (d_r^T(f,l))^* \, d_X^T(f,l) \tag{12}$$

The power spectrum density (psd) of the LFP can be estimated by

$$\hat{\sigma}^2(f) = \frac{\Delta t}{L} \sum_{l=1}^{L} |d_X^T(f,l)|^2 \tag{13}$$

The psd of the spike train can be calculated analogously using Eq. (11). However, the resulting psd will not include the required *line spectrum* (or Dirac delta function) at zero frequency, $(r^0)^2 \delta(f)$, which must be added by hand. Unlike the psd of a time series that tends to zero at high frequencies (Fig. 1a) the psd of a point process tends to its mean intensity (Fig. 1e,f). Equations (12) and (13) (without the Δt pre-factor) are computed in Matlab with the CSD and PSD functions, respectively (see Appendix). These functions return only the estimate for the frequencies up to the Nyquist frequency. The estimates for the other frequencies (sometimes considered negative frequencies) are the complex conjugates of these ones, and must be added by hand, in order to complete the next step. The rightmost hand side of Eq. (6) can then be estimated as follows

$$\frac{1}{T\Delta t} \sum_{n=0}^{T-1} \frac{\hat{\chi}_j(f_n) \hat{\chi}_k^*(f_n)}{\hat{\sigma}^2(f_n)} e^{i2\pi f_n \tau \Delta t} \tag{14}$$

where $f_n = n/T\Delta t$, and τ is some integer time lag. Eq. (14), save the $1/\Delta t$ pre-factor, is computed in Matlab using the IFFT function.

4. EXAMPLE: LFP MEDIATED COUPLING BETWEEN A STRIATAL TAN AND A PALLIDAL BORDER CELL

Figure 1 depicts the result of this analysis performed on a 13.5 minute long trivariate data set composed of spikes trains of a TAN, a border cell, and the LFP (1–150 Hz) recorded from three neighboring electrodes. Panel (a) shows the psd of the LFP. The low-frequency peak results from the high-pass cuttoff at 1 Hz. There is substantial power at ~10 Hz although there is no distinct peak there. Panels (b),(c) depict the absolute values of the csds of the TAN and the border (bor.) cell with the LFP, respectively. Both csds display a marked peak at 10 Hz indicating that both neurons are correlated with the LFP. From these three spectral densities we construct, using Eq. (14), the LFP-predicted CCH, depicted by a thick gray line in panel (d). The small amplitude of modulation relative to baseline indicates that the linearity assumption of Eq. (2) is acceptable. A smoothed estimate of the observed CCH is depicted by the thin black line. It is clear that while the predicted CCH underestimates the central peak of the observed one, it nevertheless captures the oscillatory nature of the correlation. Panels (e) and (f) display the psds (without the DC line spectrum) of the two neurons. Indeed, the psd of the TAN is itself periodic at 10 Hz. However, the border cell does not exhibit any peak in the 10 Hz range. This result is interesting as it demonstrates that the synchronization of a neuron's discharge to the LFP can be a more robust measure

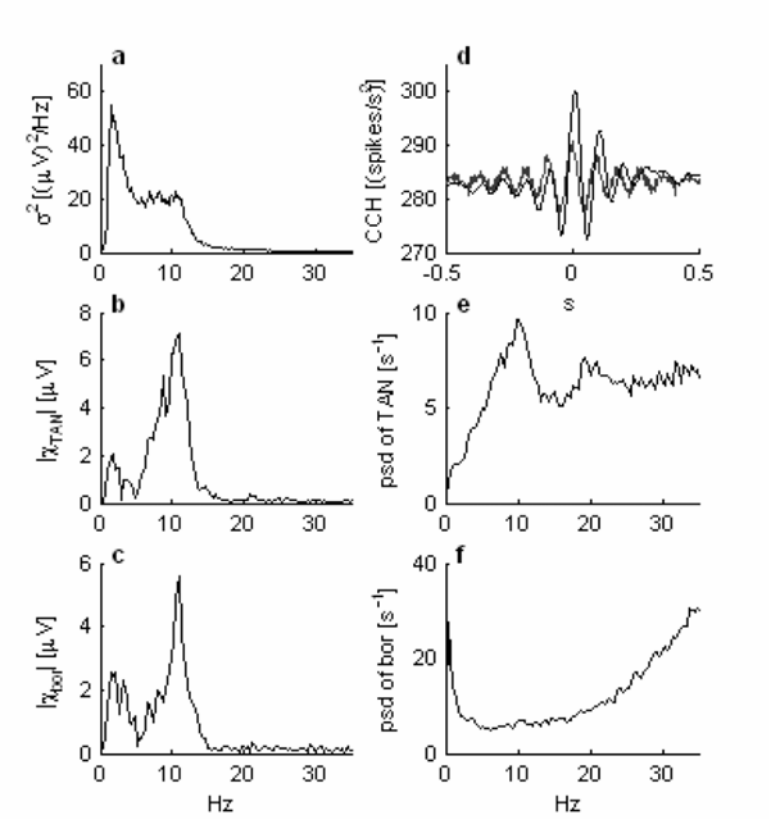

Figure 1. Construction of the LFP-predicted CCH. a. Power spectral density (psd) of the LFP. b. Absolute value of the cross spectral density (csd) of the striatal TAN and the LFP. c. Absolute value of the csd of the pallidal border (bor.) cell and the LFP. d. The LFP-predicted CCH of the TAN and the border cell (thick gray line) is constructed from the spectral densities of panels (a)–(c) as described in the text. The observed CCH is depicted by the thin black line. e. psd of the TAN. f. psd of the border cell. Line spectra at zero frequency are not shown in panels (e) and (f). Note that while the psd of the LFP (panel a) decays to zero for large frequencies, as expected for time-series, the psds of the spike trains [panels (e) and (f)] tend to their mean firing rates, as expected for point processes.

of oscillatory neuronal activity, than a measure that depends solely on the neuron's discharge, or solely on the LFP (panel (a)).

How are we to interpret these results? Strictly speaking, as a correlation-based analysis we cannot conclude anything about causality among these three signals. We cannot argue that this analysis proves that the LFP represents some common drive to both neurons. Nevertheless, this interpretation is the most straightforward one, because the LFP presumably represents some global mode that results from the collective activity of many neurons, in contrast to the spike trains of single neurons. The fact that the overall discharge of the border cell is not oscillatory, whereas its coupling to the LFP oscillations is, further strengthens this interpretation.

In a recent study we applied this methodology to LFPs and multiple single unit recordings from two MPTP-treated primates. We found that several CCHs and spike triggered averages (which are related to the csds) of the LFP recorded in these structures became oscillatory at 10 Hz following the MPTP treatment, indicating a propensity for global albeit intermittent oscillations in the diseased condition. Moreover, we found that the LFP-predicted CCHs in the MPTP-treated condition better matched the observed CCH than in the pre-MPTP condition. This was true for neuronal correlations in cortex, among the tonically active neurons (TANs) of the striatum, in the GP and between TANs and GP units. We interpret these results as indicating that brain dynamics become more globalized in the MPTP-treated condition (Goldberg et al., 2004).

5. APPENDIX: MATLAB CODE

```
function [pCCH,lags]=predcch(lfp,st1,st2,dt);
% [pCCH,lags]=predcch(lfp,st1,st2,dt)returns the LFP-predicted CCH of two spike trains
%ST1 and ST2 given the LFP. DT is the sampling interval of the data. ST1, ST2 and LFP
%must be vectors of equal length. ST1 and ST2 must be vectors whose components are
%zeros except where a spike occurs in which case the component equals 1/DT. LAGS is
%a vector of time lags.

lfp=lfp(:);
st1=st1(:);
st2=st2(:);
nfft=1024;
r1=length(find(st1))/length(st1)/dt;
r2=length(find(st2))/length(st2)/dt;
chi1=csd(lfp,st1,nfft,1/dt,'mean')*dt;
chi=csd(st2,lfp,nfft,1/dt,'mean')*dt;
lspec=psd(lfp,nfft,1/dt,'mean')*dt;
arg=chi1.*chi2./lspec;
linCC=real(ifft([arg;flipud(arg(2:end))]))/dt;
linCC=[linCC(nfft/2+2:end);linCC(1:nfft/2+1)];
pCCH=r1*r2+linCC;
lags=(-nfft/2:nfft/2)*dt;
```

6. REFERENCES

Brown, P., Oliviero, A., Mazzone, P., Insola, A., Tonali, P., and Di Lazzaro, V., 2001, Dopamine dependency of oscillations between subthalamic nucleus and pallidum in Parkinson's disease, *J. Neurosci*. **21**:1033.

Cassidy, M., Mazzone, P., Oliviero, A., Insola, A., Tonali, P., Lazzaro, V.D., and Brown, P., 2002, Movementrelated changes in synchronization in the human basal ganglia, *Brain* **125**:1235.

Courtemanche, R., Fujii, N., and Graybiel, A.M., 2003, Synchronous, focally modulated beta-band oscillations characterize local field potential activity in the striatum of awake behaving monkeys, *J. Neurosci*. **23**:11741.

Eggermont, J.J., 1990, *The Correlative Brain*. *Theory and Experiment in Neuronal Interaction*, Springer-Verlag, Berlin.

Goldberg, J.A., Boraud, T., Maraton, S., Haber, S.N., Vaadia, E., and Bergman, H., 2002, Enhanced synchrony among primary motor cortex neurons in the 1-methyl-4-phenyl-1,2,3,6-tetrahydropyridine primate model of Parkinson's disease, *J. Neurosci*. **22**:4639.

Goldberg, J.A., Rokni, U., Boraud, T., Vaadia, E., and Bergman, H., 2004, Spike synchronization in the cortexbasal ganglia networks of parkinsonian primates reflects global dynamics of the local field potentials, *J. Neurosci*. **24**:6003.

Halliday, D.M., Rosenberg, J.R., Amjad, A.M., Breeze, P., Conway, B.A., and Farmer, S.F., 1995, A framework for the analysis of mixed time series/point process data – theory and application to the study of physiological tremor, single motor unit discharges and electromyograms, *Prog Biophys Mol. Biol*. **64**:237.

Klee, M., and Rall, W., 1977, Computed potentials of cortically arranged populations of neurons. *J. Neurophysiol*. **40**:647.

Levy, R., Ashby, P., Hutchison, W.D., Lang, A.E., Lozano, A.M., and Dostrovsky, J.O., 2002, Dependence of subthalamic nucleus oscillations on movement and dopamine in Parkinson's disease, *Brain* **125**:1196.

Magill, P.J., Sharott, A., Bolam, J.P., and Brown, P., 2004, Brain state-dependency of coherent oscillatory activity in the cerebral cortex and basal ganglia of the rat, *J. Neurophysiol*. **92**:2122.

Marsden, J.F., Limousin-Dowsey, P., Ashby, P., Pollak, P., and Brown, P., 2001, Subthalamic nucleus, sensorimotor cortex and muscle interrelationship in Parkinson's disease, Brain **124**:378–388.

Mitzdorf, U., 1985, Current source-density method and application in cat cerebral cortex: investigation of evoked potentials and EEG phenomena, *Physiol Rev*. **65**:37.

Nini, A., Feingold, A., Slovin, H., and Bergman, H., 1995, Neurons in the globus pallidus do not show correlated activity in the normal monkey, but phase-locked oscillations appear in the MPTP model of parkinsonism, *J. Neurophysiol*. **74**:1800.

Percival, D.B., and Walden, A.T., 1993, *Spectral Analysis for Physical Applications: Multitaper and Conventional Univariate Techniques*, Cambridge University Press, Cambridge.

Perkel, D.H., Gerstein, G.L., and Moore, G.P., 1967, Neuronal spike trains and stochastic point processes. II. Simultaneous spike trains, *Biophys J*. **7**:419.

Raz, A., Frechter-Mazar, V., Feingold, A., Abeles, M., Vaadia, E., and Bergman, H., 2001, Activity of pallidal and striatal tonically active neurons is correlated in MPTP-treated monkeys but not in normal monkeys, *J. Neurosci*. **21**:RC128.

Raz, A., Vaadia, E., and Bergman, H., 2000, Firing patterns and correlations of spontaneous discharge of pallidal neurons in the normal and the tremulous 1-methyl-4-phenyl-1,2,3,6-tetrahydropyridine vervet model of parkinsonism, *J. Neurosci*. **20**:8559.

Sharott, A., Magill, P.J., Bolam, J.P., and Brown, P., 2005, Directional analysis of coherent oscillatory field potentials in the cerebral cortex and basal ganglia of the rat, *J. Physiol*. **562**:951.

PROPAGATION OF CORTICAL PAROXYSMS IN BASAL GANGLIA CIRCUITS DURING ABSENCE SEIZURES

Jeanne T. Paz, Pierre-Olivier Polack, Seán J. Slaght, Jean-Michel Deniau, and Stéphane Charpier*

1. INTRODUCTION

Typical absence, which is a nonconvulsive generalized epileptic seizure, provides the common symptom of genetic epileptic syndromes such as childhood absence epilepsy and juvenile absence epilepsy (Panayiotopoulos, 1997). An absence seizure is characterized by a sudden impairment of consciousness, evident by a brief unresponsiveness to environmental stimuli and cessation of activity, concomitant with bilateral synchronized spike-and-wave discharges (SWDs) in the electroencephalogram (EEG) (Panayiotopoulos, 1997). Electrophysiological recordings in patients (Williams, 1953) and in various animal models (for review, see Danober et al., 1998; Crunelli and Leresche, 2002) revealed that SWDs result from abnormal oscillations in the thalamocortical networks.

In the WAG/Rij rat, a genetic model of absence epilepsy (Coenen et al., 1992), nonlinear association analysis of EEG signals from both thalamic and cortical structures during spontaneous SWDs demonstrated an initial burst of activity in the peri-oral region of the primary somatosensory cortex (S1po), which promote paroxysms in other cortical and thalamic areas (Meeren et al., 2002). Consistent with this finding, local injection of ethosuximide into S1po, a first choice anti-absence drug, specifically suppresses SWDs (Manning et al., 2004) in genetic absence epilepsy rats from Strasbourg (GAERS), another validated genetic model of absence epilepsy (Marescaux et al., 1992; Danober et al., 1998). Recent intracellular investigations performed in our laboratory strongly support the hypothesis that a cortical focus is a dominant factor in initiating the paroxysmal oscillation within the corticothalamic loop. Indeed, we found that S1po neurons in GAERS exhibit a sustained repetitive firing at the onset of the SWD (Fig. 1A), which starts shortly before the surface paroxysms recorded from a distant cortical region (Fig. 1B, unpublished data).

* J. T. Paz, PO Polack, JM Deniau and S Charpier, Institut National de la Santé et de la Recherche Médicale, U 667, Dynamique et Physiopathologie des Réseaux Neuronaux, Collège de France, 11, place Marcelin Berthelot 75231 Paris Cedex 05, France. S.J. Slaght, School of Biosciences, Cardiff University, Cardiff CF10 3US, Wales, United Kingdom.

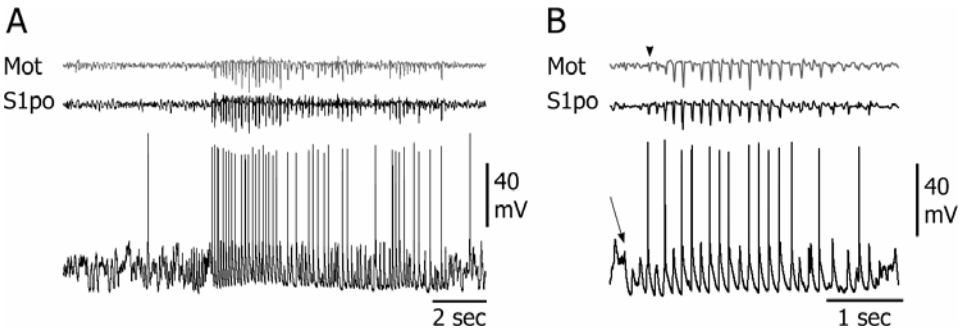

Figure 1. Intracellular recording from the presumed cortical focus during SWDs in GAERS. (A) Intracellular activity of a GAERS pyramidal neuron located in the peri-oral region of the primary somatosensory cortex (S1po) (bottom trace) simultaneously recorded with the corresponding surface EEG (middle trace, S1po) and the ipsilateral motor cortex EEG (top trace, Mot). (B) Multiple recording during another seizure (same representation as in A). The rhythmic cellular oscillations in the S1po neuron (oblique arrow) starts clearly before the first EEG spike occurring in the motor cortex (arrowhead).

Besides the central role of the corticothalamic networks in the generation and the expression of SWDs, recent pharmacological studies in GAERS suggest that the basal ganglia circuits could act as a remote control system for absence seizures via a modulation of activity in the striatonigral and subthalamonigral pathways (Depaulis et al., 1988; Depaulis et al., 1989; Danober et al., 1998; Deransart et al., 1998, 2000, 2001; Deransart and Depaulis, 2002). Specifically, the occurrence of absence seizures is significantly decreased by the activation of GABAergic striatonigral neurons (Depaulis et al., 1988; Deransart et al., 1998) or following an inhibition of the glutamatergic subthalamonigral pathway (Deransart et al., 1996; Vercueil et al., 1998). Consistent with the anti-epileptic effect induced by a reinforced inhibition of the SNr, intranigral injection of $GABA_A$ receptor antagonists increases the occurrence of SWDs (Danober et al., 1998; Deransart et al., 1998).

Taken together, these findings suggest that an alteration in the balance between synaptic excitation and inhibition in the SNr provides an endogenous control process for SWDs, a relative increase in inhibition or excitation having anti- or pro-epileptic effects, respectively. Such a differential control of SWDs, which could prolong or interrupt the seizure, could originate from distinct patterns of activity in the cortico-striato-nigral and cortico-subthalamo-nigral pathways. Because the mechanisms of propagation of cortical epileptic discharges in these subcortical nuclei remained unknown, we have recently undertaken a systematic study of the electrical events occurring in the basal ganglia circuits during spontaneous SWDs in the GAERS. In this chapter, we summarize the work from our laboratory on this important issue relative to the role of the basal ganglia in the control of epileptic seizures.

2. ACTIVITY IN THE CORTICOSTRIATAL NETWORK DURING SPIKE-AND-WAVE DISCHARGES

Given the functional impact of the corticostriatal projections on the excitability of striatal output neurons (SONs) (Wilson, 1995; Mahon et al., 2001, 2004), the cortical

paroxysms associated with absence seizures might produce significant changes in the firing pattern of SONs which could, in turn, modulate SWDs. The initial step of our work devoted to the elucidation of the role of basal ganglia in the control of absence seizures was to determine how these epileptic activities propagate from the cortex to the striatum.

2.1. Corticostriatal Neurons

In corticostriatal (CS) neurons from the GAERS motor cortex (Fig. 2A1), the firing pattern evoked by intracellular injection of positive current pulses (Fig. 2A1, *inset*) is

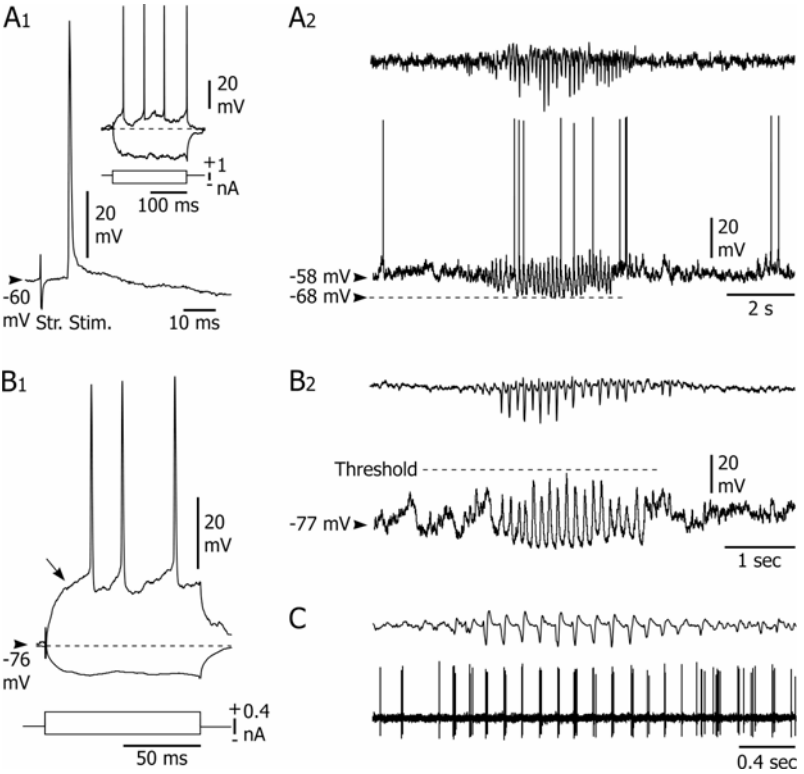

Figure 2. Striatal output neurons are silenced during absence seizures in GAERS. (A1) CS neurons are identified by their antidromic activation after electrical stimulation of the contralateral striatum (Str. Stim.). Inset, voltage responses of the CS cell (top traces) to intracellular injections of square current pulses (bottom traces). (A2) Spontaneous intracellular activity of a CS neuron (bottom trace) simultaneously recorded with the corresponding surface EEG (top trace). The occurrence of the SWD is accompanied in the CS cell by rhythmic suprathreshold depolarizations, which are superimposed on a tonic membrane hyperpolarization (dashed line). (B1) Voltage responses of a SON (top traces) to intracellular injections of square current pulses (bottom traces). Note the ramp-like depolarization (arrow) that precedes the action potential discharge. (B2) The occurrence of a SWD in the EEG (top trace) is accompanied in the recorded SON (bottom trace) with rhythmic depolarizations that remain subthreshold for action potential firing (dashed line). (C) The EEG paroxysms (top trace) are associated with bursting activity in extracellularly recorded GABAergic striatal interneurons (bottom trace). In A and B, the values of the membrane potential are indicated on the left. Results presented in A1 and A2 are from the same CS cell.

characteristic of "regular-spiking" neocortical neurons (Connor and Gutnick, 1990; Slaght et al., 2004). The basic electrophysiological properties of these cells (Slaght et al., 2002, 2004), including resting membrane potential, apparent input resistance and firing threshold, are similar to those described in CS neurons from non-epileptic rats (Cowan and Wilson, 1994; Mahon et al., 2001). This important observation indicates that the intrinsic excitability of CS neurons is not altered in our genetic model of absence epilepsy.

The occurrence of SWDs in the EEG is concomitant in CS neurons with rhythmic depolarizing synaptic potentials superimposed on a tonic membrane hyperpolarization (Slaght et al., 2004) (Fig. 2A2), which probably results from a synaptic disfacilitation (Charpier et al., 1999; Slaght et al., 2002), i.e. a reduction of the tonic excitatory synaptic drive. Because the large-amplitude EEG waves reflect a synchronization of synaptic potentials in many cortical neurons, and given the relatively homogeneous behaviour of CS neurons during SWDs, it is presumable that CS neurons are engaged, during seizures, in a tightly synchronized rhythmic excitation leading to coherent firing.

2.2. Striatal Output Neurons

The membrane properties of SONs recorded in GAERS (Slaght et al. 2004) are similar to those previously described from non-epileptic rats (Wilson 1995; Mahon et al., 2001, 2003, 2004). In particular, these neurons exhibit a highly polarized resting membrane potential (~−80 mV), a relatively low apparent input resistance and the "classical" slow ramp-like membrane depolarization in response to a suprathreshold current pulse (Fig. 2B1, arrow).

Consistent with the synchronized firing in their excitatory cortical afferents, SONs exhibit, during SWDs, large-amplitude rhythmic synaptic depolarizations (Slaght et al., 2004) (Fig. 2B2). However, their spontaneous firing rate is dramatically decreased by the SWD, the majority of cells being silenced during the cortical paroxysms (Fig. 2B2). This finding was unexpected and surprising. Indeed, it is well established that action potential firing in SONs is naturally and consistently initiated by synchronized corticostriatal excitatory synaptic inputs (Wilson, 1995; Wilson and Kawaguchi, 1996; Stern et al., 1997; Mahon et al., 2001, 2004). What is the origin of the collapse in SON firing during SWDs? Because the electrical membrane properties of SONs are not altered in GAERS, their inability to generate action potential during SWDs is not due to a reduced intrinsic excitability. Therefore, we searched for a possible implication of the intrastriatal inhibitory synaptic networks, which could be activated by the cortical inputs during the seizure (Kita, 1993). First, we found that the membrane oscillations in SONs during SWDs are associated with a powerful chloride-dependent increase in membrane conductance able to preclude the generation of action potentials during direct stimulation (Slaght et al., 2004). Second, extracellular striatal recordings revealed a close temporal overlap, during SWDs, between burst firing in GABAergic interneurons (Fig. 2C) and the rising phase of the rhythmic depolarizations in SONs. According to these findings, we propose the following scenario explaining the occurrence of subthreshold synaptic depolarizations in SONs during cortical seizures: [1] the cortical synchronization during SWDs induces, almost simultaneously, bursts of action potentials in striatal GABAergic interneurons and glutamatergic synaptic depolarizations in SONs, [2] because the membrane potential reached in SONs during SWDs is markedly more negative than the equilibrium potential of chloride, GABA-mediated currents induced by the activation of inhibitory interneurons are likely to have

depolarizing action and, [3] the associated increase in membrane conductance, coincident with the cortical inputs, produces a robust shunting inhibition that limits membrane depolarization positive to the equilibrium potential of chloride and, consequently, prevents SON firing.

3. ACTIVITY IN THE CORTICOSUBTHALAMIC NETWORK DURING SPIKE-AND-WAVE DISCHARGES

Since the GABAergic striatonigral pathway is transiently silenced during SWDs, it was essential to determine the corresponding activity in the subthalamic nucleus (STN), which integrates monosynaptic glutamatergic cortical inputs and relays these excitatory signals to the SNr and the globus pallidus (GP) (Deniau et al., 1978; Van der Kooy and Hattori, 1980; Kitai and Deniau, 1981; Magill et al., 2000). Our experimental strategy was similar to that used for the study of the corticostriatal pathway. First, we examined the cellular events occurring in the corticosubthalamic (CSth) neurons during cortical seizures in GAERS. Then, we determined the corresponding activity in the subthalamopallidal network by means of extracellular and intracellular recordings (Paz et al., 2005).

3.1. Corticosubthalamic Neurons

As observed in CS neurons (Fig. 2A1), the firing pattern evoked in motor cortex CSth neurons (Fig. 3A1) by intracellular injection of positive current pulses (Fig. 3A1, *inset*) is characteristic of "regular-spiking" neocortical neurons (Paz et al., 2005). However, these neurons exhibit additional active membrane properties responsible for an elevated intrinsic excitability. In particular, CSth neurons display, in response to hyperpolarizing current injection, a depolarizing "sag" of membrane potential followed by a post-anodal rebound of excitation. These observations indicate that CSth neurons express a hyperpolarization-activated inward cationic current and a low-voltage activated calcium current (Fig. 3A1, *inset*).

The occurrence of SWDs in the EEG is concomitant with a sudden and pronounced modification in the activity of CSth neurons (Paz et al., 2005). The interictal, small-amplitude, irregular synaptic activity in CSth neurons, generating an erratic firing pattern, is converted by the SWD into a step-like behaviour with suprathreshold depolarizations eliciting bursts of action potentials (Fig. 3A2). This synaptic activity, and its associated firing profile, remarkably differ from those of CS neurons, which exhibit oscillatory membrane depolarizations that remain subthreshold, or elicit single action potential during seizures (Slaght et al., 2002, 2004) (see Fig. 2A2). The relatively high firing rate in CSth neurons during SWDs could result from dynamic interactions between synaptic inputs and the specific set of voltage-gated currents present in these neurons.

3.2. Subthalamic Neurons

The intracellularly recorded GAERS STN neurons display passive and active membrane properties consistent with those described *in vitro* from normal rats (Beurrier et al., 1999; Bevan and Wilson, 1999; Bevan et al., 2002). In particular, the current-driven discharge of STN neurons was characterized by peak firing rates as high as 500 Hz with a slight spike frequency adaptation (Fig. 3B1).

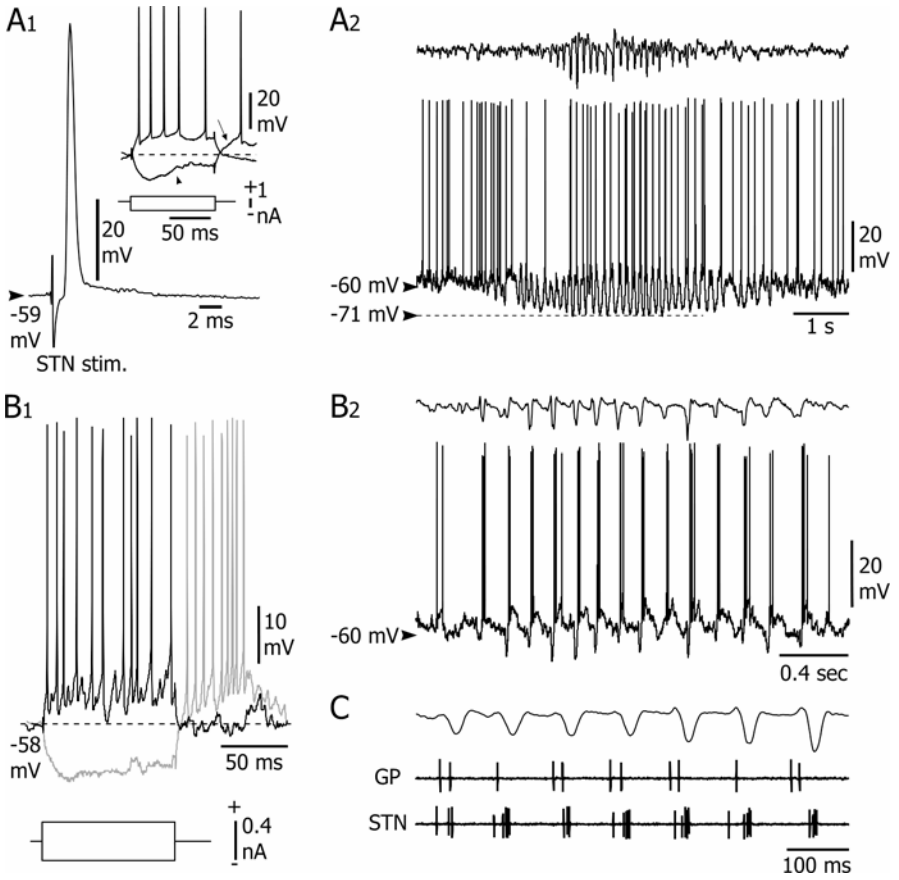

Figure 3. Rhythmic bursting in the corticosubthalamic pathway during SWDs in GAERS. (A) CSth neurons are identified by their antidromic activation after electrical stimulation of the ipsilateral STN (STN stim.). Inset, voltage responses of the CSth cell (top traces) to intracellular injections of square current pulses (bottom traces) from rest (−60 mV, dashed line). Note the "sag" in membrane voltage (arrowhead) during the −1.0 nA-induced hyperpolarization. (A2) Spontaneous intracellular activity of a CSth neuron (bottom trace) simultaneously recorded with the EEG (top trace). The occurrence of a SWD in the EEG was accompanied in the CSth cell by rhythmic suprathreshold depolarizations, which were superimposed on a tonic membrane hyperpolarization (dashed line). (B1) Voltage responses (top traces) of a STN neuron to intracellular injections of square current pulses (bottom traces) from rest (−58 mV, dashed line). After the termination of the hyperpolarizing current step, an excitatory rebound initiated a burst of action potentials (grey trace). (B2) Spontaneous intracellular activity of a STN neuron (bottom trace) during a SWD showing rhythmic burst firing concomitant with the EEG spike (top trace). (C) Simultaneous extracellular recordings of GP and STN neurons during EEG paroxysm. Results depicted in B1 and B2 are from the same STN neuron.

Contrasting with what we observed in SONs, the spontaneous firing rate of STN neurons doubles during SWDs (Paz et al., 2005). The corresponding firing profile is also dramatically modified, switching from an irregular interictal pattern to high-frequency bursts of action potentials during the cortical paroxysms (Figs. 3B2, C). Intracellular recordings from STN neurons reveal that the intra-burst pattern in STN neurons is sculpted

by a complex sequence of synaptic and intrinsic events: an early depolarizing synaptic potential, followed by a short hyperpolarization and a rebound of excitation, which is mainly due to the activation of a low-voltage activated calcium current (Fig. 3B2). Simultaneous extracellular recordings from GP and STN neurons indicate that the rhythmic hyperpolarizations in STN neurons during SWDs are likely to originate from a subpopulation of pallidal neurons exhibiting rhythmic bursting temporally correlated with the EEG spikes (Fig. 3C). Taken together, these findings suggest that cortical seizures promote rhythmic activity in STN neurons via a complex interplay between active membrane properties, corticosubthalamic inputs and reciprocal synaptic connections with GP cells.

4. PROPAGATION OF CORTICAL SEIZURES IN THE BASAL GANGLIA CIRCUITS AND POSSIBLE FEED-BACK CONTROL ON CORTICAL PAROXYSMS

The novel results described above provide the first description of the electrical events occurring in the basal ganglia circuits during absence seizures. The most important finding is that spontaneous, genetically determined, SWDs are associated with a transient interruption of SONs firing and a synchronized rhythmic bursting in STN neurons. These distinct modifications of activity in the striatonigral and subthalamonigral pathways during absence seizures might produce a dramatic change in the balance between excitation and inhibition in the SNr, which should lead to a powerful reinforcement of the synaptic excitation originating from the STN. This hypothesis is supported by a recent study in freely moving GAERS showing a synchronized bursting firing of SNr neurons in phase with the spike-wave complexes in the EEG (Deransart et al., 2003).

Since a relative increase in SNr excitation (as well as a relative decrease in inhibition) induces pro-epileptic effects (see Introduction), the synchronized bursting of glutamatertic subthalamonigral neurons during SWDs, associated with the electrical silence of GABAergic striatonigral cells, could provide a endogenous mechanism controlling positively the maintenance and the duration of the seizure.

Interestingly, we observed in most SONs a rebound of excitation at the end of SWDs (Slaght et al., 2004). As a consequence, the transient increase in the activity of striatonigral pathway, which is consistent with the decrease of SNr activity at the end of cortical paroxysms (Deransart et al., 2003), might have a negative modulatory effect on SWDs and thus, could contribute to the resolution of the absence seizure.

5. SPECULATIONS AND PERSPECTIVES

The cellular and network mechanisms by which the SNr can amplify or attenuate absence seizures remain unknown. However, it is plausible that the bidirectional modulation of SWDs by the basal ganglia is governed, at least in part, by distinct changes in the synaptic inhibition of thalamocortical neurons by SNr. For instance, if the nigral-induced thalamic inhibition promotes a thalamocortical rhythmicity in-phase with SWDs, the cortical paroxysms could be amplified via a resonance mechanism. In contrast, a phase-lag activity in the thalamocortical loop due to a temporal shift in the nigrothalamic activity might suppress the seizure at the cortical level. This positive or negative control of cortical SWDs by the basal ganglia output nuclei could result in an alteration of the epileptogenic processes at

the cortical focus and/or in a perturbation in the propagation mechanisms of paroxysms in widespread cortical areas. Experiments specifically designed to resolve this fascinating issue are currently underway in our laboratory.

6. ACKNOWLEDGEMENTS

We thank Dr S. Mahon for encouragements and thoughtful comments. This work was supported by the Ministère Français de la Recherche and the Institut National de la Santé et de la Recherche Médicale.

7. REFERENCES

Beurrier, C., Congar, P., Bioulac, B., and Hammond, C., 1999, Subthalamic nucleus neurons switch from single-spike activity to burst-firing mode. *J. Neurosci* **19**:599–609.

Bevan, M.D., and Wilson, C.J., 1999, Mechanisms underlying spontaneous oscillation and rhythmic firing in rat subthalamic neurons. *J. Neurosci.* **19**:7617–7628.

Bevan, M.D., Magill, P.J., Terman, D., Bolam, J.P., and Wilson, C.J., 2002, Move to the rhythm: oscillations in the subthalamic nucleus-external globus pallidus network. *Trends Neurosci.* **25**:525–531.

Charpier, S., Lereshe, N., Deniau, J.M., Mahon, S., Hughes, S.W., and Crunelli, V., 1999, On the putative contribution of GABAB receptors to the electrical events occurring during spontaneous spike and waves discharges. *Neuropharmacology*. **38**:1699–1706.

Coenen, A.M., Drinkenburg, W.H., Inoue, M., and van Luijtelaar, E.L., 1992, Genetic models of absence epilepsy, with emphasis on the WAG/Rij strain of rats. *Epilepsy Res.* **12**(2):75–86.

Connors, B.W., and Gutnick, M.J., 1990, Intrinsic firing patterns of diverse neocortical neurons. *Trends Neurosci.* **13**:99–104.

Cowan, R.L., and Wilson, C.J., 1994, Spontaneous firing patterns and axonal projections of single corticostriatal neurons in the rat medial agranular cortex. *J. Neurophysiol* **71**:17–32.

Crunelli, V., and Leresche, N., 2002, Childhood absence epilepsy: genes, channels, neurons and networks. *Nat Rev Neurosci*. **3**:371–382.

Danober, L., Deransart, C., Depaulis, A., Vergnes, M., and Marescaux, C., 1998, Pathophysiological mechanisms of genetic absence epilepsy in the rat. *Prog Neurobiol.* **55**:27–57.

Deniau, J.M., Hammond, C., Chevalier, G., and Feger, J., 1978, Evidence for branched subthalamic nucleus projections to substantia nigra, entopeduncular nucleus and globus pallidus. *Neuroscience Letters.* **9**:117–121.

Depaulis, A., Vergnes, M., Marescaux, C., Lannes, B., and Warter, J., 1988, Evidence that activation of GABA receptors in the substantia nigra suppresses spontaneous spike-and-wave discharges in the rat. *Brain Res.* **448**:20–29.

Depaulis, A., Snead, O.I., Marescaux, C., and Vergnes, M., 1989, Suppressive effects of intranigral injection of muscimol in three models of generalized non-convulsive epilepsy induced by chemical agents. *Brain Res.* **498**:64–72.

Deransart, C., Marescaux, C., and Depaulis, A., 1996, Involvement of nigral glutamatergic inputs in the control of seizures in a genetic model of absence epilepsy in the rat. *Neuroscience.* **71**:721–728.

Deransart, C., Vercueil, L., Marescaux, C., and Depaulis, A., 1998, The role of basal ganglia in the control of generalized absence seizures. *Epilepsy Res.* **32**:213–223.

Deransart, C., Riban, V., Le, B., Marescaux, C., and Depaulis, A., 2000, Dopamine in the striatum modulates seizures in a genetic model of absence epilepsy in the rat. *Neuroscience.* **100**:335–344.

Deransart, C., Le-Pham, B.T., Hirsch, E., Marescaux, C., and Depaulis, A., 2001, Inhibition of the substantia nigra suppresses absences and clonic seizures in audiogenic rats, but not tonic seizures: evidence for seizure specificity of the nigral control. *Neuroscience*. **105**:203–211.

Deransart, C., and Depaulis, A., 2002, The control of seizures by the basal ganglia? A review of experimental data. *Epileptic Disord.* **4** Suppl **3**:S61–72.

Deransart, C., Hellwig, B., Heupel-Reuter, M., Leger, J.F., Heck, D., and Lucking, C.H., 2003, Single-unit analysis of substantia nigra pars reticulata neurons in freely behaving rats with genetic absence epilepsy. *Epilepsia*. **44**(12):1513–1520.

Kita, H., 1993, GABAergic circuits of the striatum., *Prog Brain Res.* **99**:51–72.

Kitai, S.T., and Deniau, J.M., 1981, Cortical inputs to the subthalamus: intracellular analysis. *Brain Res*. **214**:411–415.

Magill, P.J., Bolam, J.P., and Bevan, M.D., 2000, Relationship of activity in the subthalamic nucleus-globus pallidus network to cortical electroencephalogram. *J. Neurosci*. **20**:820–833.

Mahon, S., Deniau, J.M., and Charpier, S., 2001, Relationship between EEG potentials and intracellular activity of striatal and cortico-striatal neurons: an in vivo study under different anesthetics. *Cereb Cortex*. **11**:360–373.

Mahon, S., Casassus, G., Mulle, C., and Charpier, S., 2003, Spike-dependent intrinsic plasticity increases firing probability in rat striatal neurons in vivo. *J. Physiol* (*London*) **550**:947–959.

Mahon, S., Deniau, J.M., and Charpier, S., 2004, Corticostriatal plasticity: life after the depression. *Trends Neurosci.* **27**(8):460–467.

Manning, J.P., Richards, D.A., Leresche, N., Crunelli, V., and Bowery, N.G., 2004, Cortical-area specific block of genetically determined absence seizures by ethosuximide. *Neuroscience.* **123**:5–9.

Marescaux, C., Vergnes, M., and Depaulis, A.,1992, Genetic absence epilepsy in rats from Strasbourg-a review. *J. Neural Transm Suppl.* **35**:37–69.

Meeren, H.K., Pijn, J.P., van Luijtelaar, E.L., Coenen, A.M., and Lopes da Silva, F.H., 2002, Cortical focus drives widespread corticothalamic networks during spontaneous absence seizures in rats. *J. Neurosci.* **22**(4): 1480–1495.

Panayiotopoulos, C.P., 1997, Absences epilepsies, in: *Epilepsy: A Comprehensive Textbook*. J. Jr. Engel, and T.A. Pedley, eds, Lippincott-Raven, Philadelphia, pp 2327–2346.

Paz, J.T., Deniau, J.M., and Charpier, S., 2005, Rhythmic bursting in the cortico-subthalamo-pallidal network during spontaneous genetically determined spike and wave discharges. *J. Neurosci.* **25**:2092–2101.

Slaght, S.J., Paz, T., Mahon, S., Maurice, N., Charpier, S., and Deniau, J.M., 2002, Functional organization of the circuits connecting the cerebral cortex and the basal ganglia: implications for the role of the basal ganglia in epilepsy. *Epileptic Disord*. **4** Suppl 3:S9–22.

Slaght, S.J., Paz, T., Chavez, M., Deniau, J.M., Mahon, S., and Charpier, S., 2004, On the activity of the cortico-striatal networks during spike-and-wave discharges in a genetic model of absence epilepsy. *J. Neurosci*. **24**:6816–6825.

Stern, E.A., Kincaid, A.E., and Wilson, C.J., 1997, Spontaneous subthreshold membrane potential fluctuations and action potential variability of rat corticostriatal and striatal neurons in vivo. *J. Neurophysiol.* **77**: 1697–1715.

Van Der Kooy, D., and Hattori, T., 1980, Single subthalamic nucleus neurons project to both the globus pallidus and substantia nigra in rat. *J. Comp Neurol.* **192**:751–768.

Vercueil, L., Benazzouz, A., Deransart, C., Bressand, K., Marescaux, C., Depaulis, A., and Benabid, A.L., 1998, High-frequency stimulation of the subthalamic nucleus suppresses absence seizures in the rat: comparison with neurotoxic lesions. *Epilepsy Res*. **31**(1):39–46.

Williams, D., 1953, A study of thalamic and cortical rhythms in petit mal. *Brain* **76**:56–69.

Wilson, C.J., 1995, The contribution of cortical neurons to the firing pattern of striatal spiny neurons. In: *Models of Information Processing in the Basal Ganglia.* J.C. Houk, J.L. Davies, and D.G. Beiser, eds., MIT Press, Cambridge, pp 29–50.

Wilson, C.J., and Kawaguchi, Y., 1996, The origins of two-state spontaneous membrane potential fluctuations of neostriatal spiny neurons. *J. Neurosci*. **16**:2397–2410.

LIMITATIONS OF THE ISOLATED GP-STN NETWORK

Ian M. Stanford, Krim C. Loucif, Claire L. Wilson, Diana Cash, and Michael G. Lacey*

1. INTRODUCTION

Activity of the globus pallidus (GP) – subthalamic nucleus (STN) network plays a pivotal role in movement disorders of the basal ganglia. Thus, during dopamine depletion, in idiopathic and animal models of Parkinson's disease, there is an increase in oscillatory burst firing and synchronisation of GP and STN neurons (Bergman et al., 1994, Nini et al., 1995 Raz et al., 2000, 2001). This activity is transmitted to basal ganglia output stations contributing to the excessive inhibition of the thalamocortical motor loop and thus, the symptoms of akinesia and rigidity (Albin et al., 1989, DeLong 1990) and muscle tremor (Filion and Tremblay 1991, Bergman et al., 1994, Magnin et al., 2002). But how does this activity arise and can it be sustained in the isolated GP-STN network?

Using a culture preparation, Plenz and Kitai (1999) proposed that the GP and STN form a central pacemaker responsible for oscillatory activity in the basal ganglia. Brief applications of GABA (to mimic pallidal synaptic input) were able to promote burst firing in the STN, through the de-inactivation of a low-threshold calcium conductance, while STN activity reverted to tonic firing once the pallidal input was disconnected. Therefore, it appeared that viable reciprocal connectivity between the GABAergic GP and glutamatergic STN may be sufficient for the generation and recruitment of the STN rebound burst activity and thus support regenerative oscillatory activity (Plenz and Kitai, 1999; Bevan et al., 2000).

However, *in vivo* experiments have indicated that rhythmic activity in GP and STN neurons is driven by the cortex (Magill et al., 2000), with dopamine depletion sensitizing the system further (Magill et al., 2001). Therefore, aside from in the culture preparation, is there evidence that the GP and STN in isolation can maintain such activity? Indeed, such

* Ian M. Stanford, Krim C. Loucif, Claire L. Wilson. School of Life and Health Sciences, Aston University, Birmingham B4 7ET. U.K. Diana Cash, Neuroimaging Research Group, Institute of Psychiatry, London SE5 8AF, U.K. Michael G. Lacey, The Division of Neuroscience, The Medical School, The University of Birmingham, Edgbaston, Birmingham. B15 2TT. U.K.

a hypothesis would gain credibility if reproduced *in situ*. This chapter details the search for such evidence in a mouse brain slice preparation in which reciprocal connectivity between the GP and the STN is maintained.

2. THE PREPARATION

In order to optimize the extent of the interconnectivity between the GP and the STN we developed a parasagittal mouse slice preparation cut at 20° to the midline, in which the distance between the two brain nuclei is about 1 mm. Connectivity was then demonstrated morphologically, using biocytin-tracing techniques, and by electrical stimulation in either nucleus to evoke inhibitory GABA or excitatory glutamate mediated post-synaptic currents (I/EPSCs) respectively. In addition, spontaneous IPSCs (which can only emanate from the GP) and EPSCs (from the cortex, pedunculopontine nucleus or thalamus) were also observed in the STN. This preparation was then used to directly investigate the role of GABA and glutamate release in shaping and modulating neuronal activity in slices taken from control and MPTP-treated mice.

2.1. Biocytin Tracer Studies

Slices (300 µm thick) were obtained from CB57BL/6JGL male mice at 21–40 days of age. In order to assess the anatomical connectivity between the GP and STN we exploited the retrograde and anterograde transport of the neuroanatomical tracer biocytin. Biocytin (Sigma Chemicals, Poole, UK) was mixed with 20% gelatin (Fisher Scientific, Loughborough, UK) in Tris-buffered saline to a final concentration of 50%. Pellets were injected into GP and STN in horizontal (cut at 10° to true) or parasagittal (cut at 20° to the midline) sections using either a 1µl Hamilton syringe or glass pipette attached to a Picospritzer II (General Valve Corporation, NJ, USA) pressure ejection system. Following 8–10 hours of continuous perfusion with aCSF, slices were fixed in 4% paraformaldehyde in 0.1 M phosphate buffered saline (PBS) at 4°C for several days. Biocytin was revealed with avidin biotin complex (Elite ABC kit, Vector Laboratories). Although axonal labelling between the GP and STN was observed in both planes of section, the most robust connectivity, including labelling of axonal tracts and cell bodies, was observed in 20° parasagittal sections (Figure 1A). This plane of section was used for all subsequent electrophysiological recordings.

2.2. Evoked Synaptic Currents

Whole-cell recordings coupled with electrical stimulation were used to show connectivity between the GP and the STN. Whole-cell recordings were made using borosilicate glass pipettes of 3–6 MΩ resistance containing (in mM) K-gluconate 125, NaCl 10, $CaCl_2$ 1, $MgCl_2$ 2, EGTA 0.5, HEPES 10, GTP 0.3, Mg-ATP 2, biocytin 5, adjusted to pH 7.25 with KOH. Individual neurons were visualized (×40 water immersion objective) using differential interference contrast infa-red microscopy (Olympus BX 501, Japan) with CCD camera (Hitachi KP-M1, Japan) and contrast enhancement system (ADV-2, Brian Reece Scientific Ltd, Newbury, UK). Membrane currents and potentials were monitored using an Axopatch 200B patch-clamp amplifier (Axon Instruments, Foster City, CA, USA). Synaptic

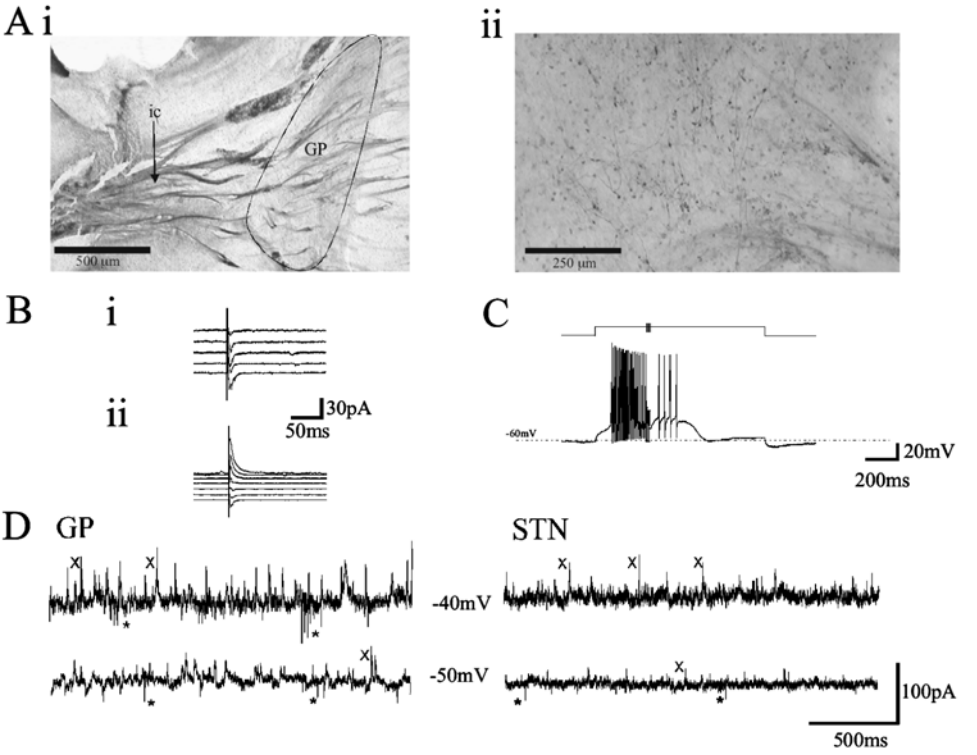

Figure 1. Ai. A parasagittal slice in which the STN was injected with biocytin showing labelled fibre tracts heading towards the GP and striatum. **Aii** Biocytin labelled cell bodies of the GP from the slice shown in Ai **Bi.** EPSCs, recorded in the GP in response to single shock electrical stimulation in the STN and **Bii** IPSCs, recorded in the STN in response to single shock electrical stimulation in the GP. Holding potentials ranged from −90 to −30 mV **C.** Voltage records from a STN cell held at −60 mV. A 300 ms step depolarisation promoted fast action potential firing. 5 shocks at 200 Hz in the GP evoked IPSPs, which summated and blocked action potential firing. Following this inhibition there was a rebound depolarisation, which promoted further action potential firing. **D.** Spontaneous inward (*) and outward (^{X}) currents recorded from a GP cell and a STN cell at holding potentials −40 and −50 mV.

events were evoked by bipolar single-shock stimulation (0.2 ms, 1–3 mA) using a constant current stimulation unit (Digitimer, DS2A).

Most GP cells recorded (>90% of the population) corresponded to Type A neurons of the rat (Cooper and Stanford, 2000), the type II cells of guinea pig (Nambu & Llinás, 1994) and bursting cells of Nakanishi et al., (1987). They were easily identified by the presence of a time- and voltage-dependent 'sag' of membrane potential evoked by hyperpolarising current steps, indicative of I_h, and anodal break rebound depolarisations, often accompanied by action potential firing (Cooper and Stanford, 2000). All STN cells displayed both I_h and rebound depolarisations, typical characteristics of STN neurons (Beurrier et al., 1999, Bevan and Wilson, 1999, Bevan et al., 2000).

As there is no anatomical evidence for a GABA projection to the STN, other than from the GP, or a glutamate projection to the GP, other than the STN, which courses through the STN, we used single shock electrical stimulation (0.2 ms, 1–3 mA) within the STN or within the GP to evoke excitatory and inhibitory postsynaptic potentials respectively.

Stimulation of the STN evoked bicuculline-resistant EPSCs in the GP in 22/33 cells (66%) (Figure 1Bi), which were blocked by co-application of the glutamate antagonists CNQX (10 μM) and AP5 (100 μM) (n = 5). Often responses with double peaks could be observed which could be due to the activation of polysynaptic circuitry, asynchronous release following single stimuli or the promotion of a somatic spike that may evoke further release.

Stimulation of the GP in the presence of CNQX (10 μM) and AP5 (100 μM) evoked $GABA_A$ receptor mediated IPSCs in the STN in 44/59 slices (75%) which reversed close to theoretical equilibrium potential for chloride (Figure 1Bii). These postsynaptic currents were blocked by the $GABA_A$ antagonist bicuculline (10 μM, n = 7). In 2 of 2 slices evoked IPSCs, and evoked EPSCs were recorded, indicative of reciprocal connectivity.

2.3. Functional Connectivity

STN-evoked EPSPs were able to trigger action potentials in GP neurons while single-shock simulation in the GP evoked a single IPSP in STN neurons. Increasing the number of shocks induced IPSP summation and inhibition of STN action potential firing. The following rebound depolarisations were then able to elicit further action potential firing (n = 4, Figure 1C). These rebound depolarisations were not found to produce action potentials at any consistent frequency but may provide recurrent excitation of the GP in a reciprocally connected network required for reverberating oscillatory activity, as previously proposed (Plenz and Kitai, 1999, Bevan et al., 2000). However, *regenerative* rebound depolarisations were never observed, even when using stimulus trains.

2.4. Spontaneous Synaptic Currents

Evidence for spontaneous release of GABA and glutamate on both GP and STN cells was also observed. At a holding potential of −50 mV, spontaneous outward currents indicative of sIPSCs (from the GP) were observed in 85/150 (57%) STN cells. Inward currents indicative of sEPSCs (from the cortex, thalamus, pedunculopontine nucleus) were observed in 106/150 (71%) cells. Inward and outward currents were often observed in the same recording (Figure 1D). In GP cells, sEPSCs (presumably from the STN) were observed in 26/43 cells (60%) while sIPSCs (likely from GP axon collaterals) were observed in all 43 cells recorded (Figure 1D).

3. SPIKE FIRING PATTERNS IN THE STN ARE INDEPENDENT OF GABA OR GLUTAMATE RELEASE IN CONTROL CONDITIONS

Does the connectivity and GABA release from the GP play a role in the rate and pattern of spontaneous STN activity in the mouse brain slice preparation? To address this question, we used extracellular single-unit recordings of STN activity using borosilicate glass pipettes of resistance 6–10 MΩ filled with 2 M NaCl and bath application of the $GABA_A$ antagonist picrotoxin (50 μM) in order to eliminate any effects of synaptically released GABA. Single units were detected and amplified ×10,000 with Axon Cyberamp 380 and AL402 differential amplifiers. Data acquisition and analysis was performed with a Micro-1401 *mkII* and Spike2 software (Cambridge Electronic Design). Single unit waveforms were discriminated from noise and sorted off-line.

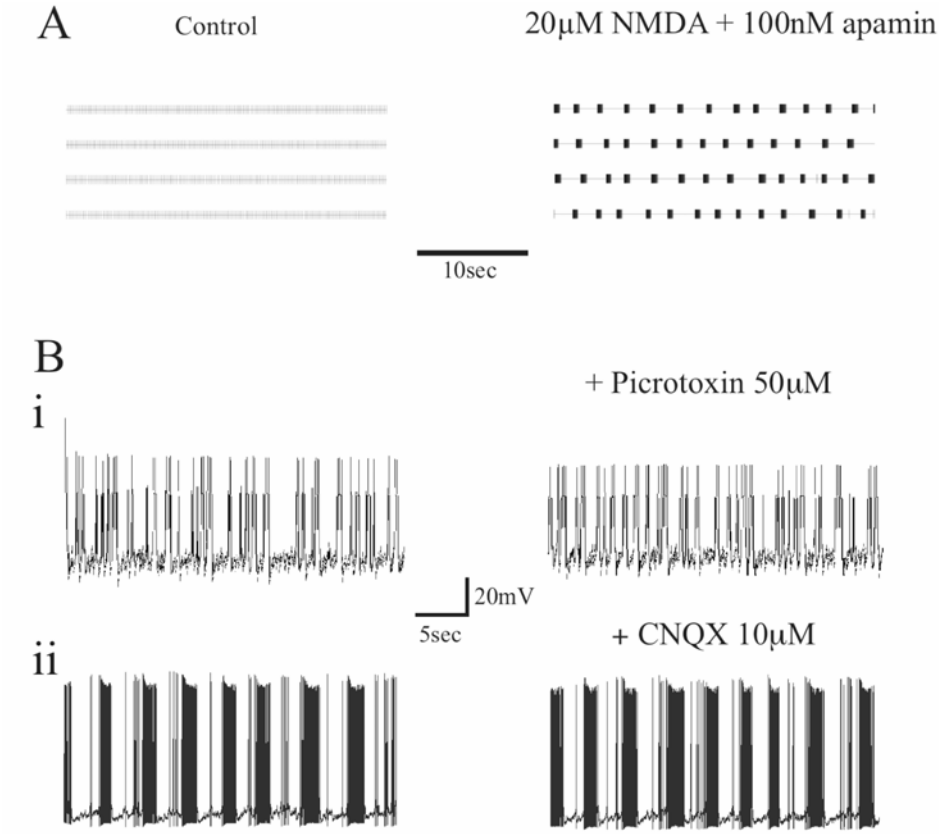

Figure 2. A. Extracellular single-unit recording from a spontaneously firing STN neuron in control and following perfusion with NMDA (20 μM) and apamin (100 nM). **B.** Whole cell recording from two STN cells bursting in the presence of NMDA and apamin. Bath application of **Bi** picrotoxin (50 μM) or **Bii** CNQX (10 μM) had no effect on the oscillation frequency, number of spikes per burst or the interspike interval (ISI) within bursts.

In control slices, STN cells fire action potentials at a tonic rate of 9.24 ± 0.92 Hz. (n = 82) (Figure 2A). Application of picrotoxin resulted in no effect on the frequency of all 9 STN cells tested indicating that at least under control conditions the tonic release of GABA has no effect on firing rate. To block any glutamatergic tone the glutamate antagonist CNQX (10μM) was applied. No change of firing rate was observed in all 8 STN cells indicating that at least under control conditions the tonic release of glutamate has no effect on firing rate. These data also suggest that the GP-STN network is not engaged in oscillatory bursting in the connected slice preparation under control conditions.

4. NMDA- AND APAMIN-INDUCED BURST FIRING IN THE STN IS ALSO INDEPENDENT OF GLUTAMATE AND GABA RELEASE

In an attempt to replicate the bursting activity observed in STN neurons during dopamine depletion *in vivo*, and also to increase the release of GABA from the GP, we bath

applied the ionotropic glutamate receptor agonist NMDA (Zhu et al., 2004). NMDA (20 μM) induced an increase in firing rate of 415 ± 103% (n = 15). However, only 3/18 cells (17%) changed the firing pattern from regular to a burst-firing. Bursting activity was much more reproducible if NMDA (20 μM) was applied in conjunction with the calcium-activated potassium channel blocker, apamin (20–100 nM). Apamin has previously been shown to enhance NMDA-mediated burst firing, both in dopaminergic neurons et al., 1993) and in the rat STN (Wilson et al., 2004b). Addition of 20 nM apamin to NMDA (20 μM) induced bursting in 5/19 STN cells (26%), while 50 nM apamin induced bursting in 12/25 cells (48%), and 100 nM apamin in 24/44 cells (55%).

The burst parameters of 25 STN cells were analysed using the program of Kaneoke and Vitek (1996). This burst detection algorithm identifies cells which fire in patterns which differed significantly from the Poisson distribution with a mean of 2, thus giving a burst index >0.5. No differences in the burst firing induced by different concentrations of apamin were observed. Thus, analysis of pooled data revealed slow oscillatory bursting at a frequency of 0.46 ± 0.06 Hz, each burst containing 31.7 ± 5.35 spikes, the interspike interval within bursts being 24.2 ± 3.73 ms (n = 25). Such bursting activity would be expected to promote increased GABA or glutamate release in the STN and GP respectively. Indeed, 6/12 single unit recordings from GP cells show NMDA/apamin induced burst firing.

As burst firing induces the release of more transmitter than single spiking (Lisman, 1997) and because STN cells display a reverse spike-frequency adaptation and a steep secondary range in their frequency-intensity curves (Wilson et al., 2004a) and are therefore more sensitive to synaptic input when excited in the burst range, we expected to observe more pronounced effects of applied picrotoxin and CNQX. However, this was not the case. Using the whole cell technique, picrotoxin (50 μM) was applied to 5 NMDA/apamin induced bursting cells, which all continued to burst fire with no significant change in oscillation frequency ($P = 0.86$), spikes per burst ($P = 0.86$), or ISI within bursts ($P = 0.5$). CNQX (100 μM) was added to 6 bursting cells. All cells continued to burst fire with no significant change in oscillation frequency ($P = 0.32$), spikes per burst ($P = 0.44$), or ISI within bursts ($P = 0.22$). Thus, despite 75% of our GP cells being connected to the STN and 66% of STN cells being connected to the GP and extensive evidence for sIPSCs and sEPSCs in our mouse slice preparation, we have no evidence that GABA or glutamate has any role in promoting, shaping or modulating the NMDA/apamin induced burst-firing patterns in STN neurons**.** Rather, the bursting observed is likely to be purely intrinsically driven from within the somatodendritic segments of the individual cells studied.

4.1. Paired Recordings

Simultaneous single unit recordings of neuronal activity were made from a number of cells in the STN and the GP. Seven pairs of regularly firing STN/GP neurons were recorded. In the presence of NMDA (20 μM) and apamin (100 nM), bursting of both cells was observed in 3 of the 7 pairs (Figure 3A). In 3 pairs, only the STN exhibited bursting activity and in one pair bursting was promoted only in the GP unit. In all cases the activity observed remained uncorrelated. Seven pairs of bursting STN neurons were also recorded. In each pair, the regular/tonic activity in control conditions was uncorrelated as was the bursting activity induced by NMDA (20 μM) and apamin (100 nM) application (Figure 3B).

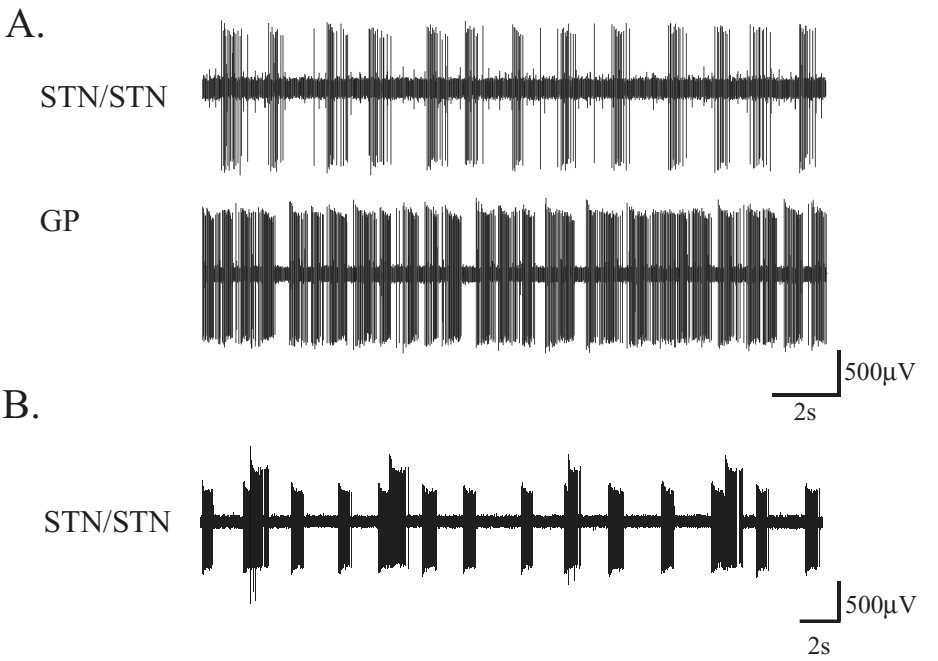

Figure 3. Simultaneous single-unit recordings from STN and GP neurons in the presence of NMDA (20 μM) and apamin (100 nM) showing uncorrelated bursting activity. **A.** A bursting STN cell and a bursting GP cell. Note the presence of a second non-bursting unit within the STN recording. **B.** Two bursting STN units recorded on a single electrode.

5. STUDIES IN DOPAMINE DELETED ANIMALS

As adaptive changes caused by chronic dopamine depletion may be a fundamental requirement for the manifestation of synchronous oscillatory activity we repeated the extracellular studies in slices obtained from mice treated with the dopamine neurotoxin 1-methyl-4-phenyl-1,2,3,6-tetrahydropyridine (MPTP), using the regime described by Araki et al., (2001). Eight mice were treated 10–21 days previously with MPTP. Single-unit extracellular recordings were made from up to 3 spontaneously firing STN neurons simultaneously. STN neurons in slices from MPTP-lesioned animals fire at 4.23 ± 0.35 Hz (n = 78), significantly slower than those from control animals (9.78 ± 1.16, n = 20; $p < 0.0001$). STN neurons from MPTP-lesioned animals fire irregularly, with an average coefficient of variation of inter-spike interval of 94.4% (n = 78), significantly higher ($p = 0.0007$) than that seen in neurons from control animals (25.8%, n = 33). However, firing in simultaneously recorded STN-STN (20 pairs), STN-GP (8 pairs) and GP-GP neurons (3 pairs) were all uncorrelated. Furthermore, as in control slices, there was no significant change in rate or pattern of firing on application of CNQX (10 μM), AP5 (100 μM) and picrotoxin (50 μM).

6. CONCLUSIONS

An *in vitro* mouse slice preparation from control and MPTP-treated mice in which functional reciprocal GP-STN connectivity is maintained, does not produce oscillatory bursting or synchronous activity neuronal activity. Pharmacological interventions that produce bursting activity do so without concomitant neuronal synchrony, or a requirement for glutamate or GABA transmission. Pre-treatment with MPTP did not alter this behaviour. Thus, we have no evidence that the functionally connected, but isolated, GP – STN network can act as a pacemaker for synchronous correlated activity in the basal ganglia and must conclude that other inputs such as those from cortex and/or striatum are required.

7. ACKNOWLEDGEMENTS

This study was supported by The Wellcome Trust project grants 068818 (IMS) and Research Leave Fellowship 063461 (MGL), The Parkinson's Disease Society and a research grant from the Royal Society. IMS is a MRC Career Establishment Fellow.

8. REFERENCES

Albin, R.L., Young, A.B., and Penney, J.B., 1989, The functional anatomy of basal ganglia disorders, *Trends Neurosci.* **12**:366–375.

Araki, T., Mikami, T., Tanji, H., Matsubara, M., Imai, Y., Mizugaki, M., and Itoyama, Y., 2001, Biochemical and immunohistological changes in the brain of 1-methyl-4-phenyl-1,2,3,6-tetrahydropyridine (MPTP)-treated mouse, *Eur. J. Pharm. Sci.* **12**:231–8.

Bergman, H., Wichmann, T., Karmon, B., and Delong, M.R., 1994, The primate subthalamic nucleus. II. Neuronal activity in the MPTP model of parkinsonism, *J. Neurophysiol*. **72**:507–520.

Beurrier C., Congar P., Bioulac B., Hammond C., 1999, Subthalamic nucleus neurons switch from single-spike activity to burst-firing mode, *J. Neurosci.* **19**:599–609.

Bevan M.D., Wilson C.J., 1999, Mechanisms underlying spontaneous oscillation and rhythmic firing in rat subthalamic neurons, *J. Neurosci.* **19**:7617–7628.

Bevan, M.D., Wilson, C.J., Bolam, J.P., Magill, P.J., 2000, Equilibrium potential of $GABA_A$ current and implications for rebound burst firing in rat subthalamic neurons *in vitro, J. Neurophysiol*. **83**:3169–3172.

Bevan, M.D., Magill, P.J., Hallworth, N.E., Bolam, J.P., and Wilson, C.J. 2002, Regulation of the timing and pattern of action potential generation in rat subthalamic neurons *in vitro* by GABA-A IPSPs, *J. Neurophysiol.* **87**:1348–1362.

Cooper, A.J., Stanford, I.M., 2000, Electrophysiological and morphological characteristics of three subtypes of rat globus pallidus neuron *in vitro, J. Physiol*. **527.2**:291–304.

DeLong, M., 1990, Primate models of movement disorders of basal ganglia origin, *Trends Neurosci*. **13**(7):281–285.

Filion, M., Tremblay, L., 1991, Abnormal spontaneous activity of globus pallidus neurons in monkeys with MPTP-induced parkinsonism, *Brain Res*. **547**:142–151.

Johnson, S.W, Seutin, V., 1997, Bicuculline methiodide potentiates NMDA-dependent burst firing in rat dopamine neurons by blocking apamin-sensitive Ca^{2+}- activated K^+ currents, *Neurosci. Letts*. **231**:13–16.

Kaneoke, Y., Vitek, J.L., 1996, Burst and oscillation as disparate neuronal properties, *J. Neurosci Methods*, **68**:211–223.

Lisman J.E., 1997, Bursts as a unit of neural information: Making unreliable synapses reliable, *Trends Neurosci.* **20**:38–43.

Magill, P.J., Bolam, J.P., Bevan, M.D., 2000, Relationship of activity in the subthalamic nucleus-globus pallidus network to cortical electroencephalogram, *J. Neurosci*. **20**:820–833.

Magill, P.J., Bolam, J.P., Bevan, M.D., 2001, Dopamine regulates the impact of the cerebral cortex on the subthalamic nucleus-globus pallidus network, *Neurosci.* **106**:313–330.

Magnin, M., Morel, A., Jeanmonod, D., 2002, Single unit analysis of the pallidum, thalamus, and subthalamic nucleus in Parkinsonian patients, *Neurosci*. **96**:549–564.

Nakanishi, H., Kita, H., Kitai, S.T. 1987, Electrical membrane properties of rat subthalamic neurons in an *in vitro* slice preparation, *Brain Res*. **437**:35–44.

Nambu, A., Llinás, R., 1994, Electrophysiology of globus pallidus neurons *in vitro, J. Neurophysiol*. **72**:1127–1139.

Nini, A., Feingold, A., Slovin, H. & Bergman, H., 1995, Neurons in the globus pallidus do not show correlated activity in the normal monkey, but phase-locked oscillations appear in the MPTP model of parkinsonism. *J. Neurophysiol*. **74**:1800.

Plenz, D., Kitai, S.T. 1999, A basal ganglia pacemaker formed by the subthalamic nucleus and external globus pallidus, *Nature* **400**:677–682.

Seutin, V., Johnson, S.W., North, R.A., 1993, Apamin increases NMDA-induced burst-firing of rat mesencephalic dopamine neurons, *Brain Res*. **630**:341–344.

Wilson C.J., Weyrick A., Terman D., Hallworth N.E., Bevan M.D., 2004a, A model of reverse spike frequency adaptation and repetitive firing of subthalamic nucleus neurons, *J. Neurophysiol.* **91**:1963–1980.

Wilson C.L., Puntis M., Lacey M.G., 2004b, Overwhelmingly asynchronous firing of rat subthalamic nucleus neurons in brain slices provides little evidence for intrinsic connectivity, *Neurosci.* **123**:187–200.

Raz, A., Vaadia, E., Bergman, H., 2000, Firing Patterns and Correlations of Spontaneous Discharge of Pallidal Neurons in the Normal and the Tremulous 1-Methyl-4-Phenyl-1,2,3,6-Tetrahydropyridine Vervet Model of Parkinsonism, *J. Neurosci*. **20**:8559–8571.

Raz, A., Frechter-Mazar, V., Feingold, A., Abeles, M., Vaadia, E. & Bergman, H., 2001, Activity of pallidal and striatal tonically active neurons is correlated in MPTP-treated monkeys but not in normal monkeys. *J. Neurosci.* **21**:RC128 (1–5).

Zhu, Z.T., Munhall, A., Shen, K.Z., Johnson, S.W., 2004, Calcium-dependent subthreshold oscillations determine bursting activity induced by N-methyl-D-aspartate in rat subthalamic neurons *in vitro*. *Eur. J. Neurosci.* **19**:1296–1304.

Section II

CHOLINERGIC MECHANISMS IN THE STRIATUM

CONVERGENCE AND PLASTICITY OF INPUTS TO STRIATAL CHOLINERGIC INTERNEURONS

The generation of synchronised pauses

John N. J. Reynolds*

1. INTRODUCTION

Electrophysiological studies in behaving animals have added significantly to our understanding of the mechanisms of reward-related learning. From recordings of neural activity made while animals are engaged in a behavioural task, discrete populations of neurons have been described that may mediate particular aspects of task learning or performance. One group that changes its activity during the learning of stimulus-response associations are the Tonically Active Neurons (TANs) located within the striatum of the basal ganglia. It is now well established that the majority of these neurons show little or no change in their tonic firing pattern in response to novel stimuli. However, after repeated pairings of neutral stimuli with a primary reward, these stimuli begin to elicit a transient cessation of TAN firing activity, which has been termed the "conditioned pause response". This change in responsiveness increases in parallel with alterations in behaviour that suggest that a conditioned response to the stimulus is being learned. Once acquired, the pause response remains intact after a prolonged period without exposure to the stimulus or after overtraining, and disappears after the association between stimulus and reward is lost (Aosaki et al., 1994b). Although a correlation between response plasticity and behavioural changes does not establish that changes in TAN firing are causal to the formation of a conditioned response, it is clear that the pause response exhibits many of the features necessary for involvement in a long-term behavioural memory process.

A compelling feature of the pause response is that it is induced in TANs that are sparsely distributed throughout the caudate and putamen (Aosaki et al., 1995). Thus, the conditioned stimulus acts to elicit a pause that is nearly synchronous throughout the whole striatum. Since the TANs identified in behavioural experiments are now believed to be primarily cholinergic interneurons that tonically release acetylcholine, a pause response

* Dept. of Anatomy and Structural Biology and the Neuroscience Research Centre, University of Otago, P.O. Box 913, Dunedin, New Zealand.

initiated simultaneously throughout the striatum would result in a synchronous drop in acetylcholine (ACh) levels. By affecting dopamine release and synaptic plasticity mechanisms in other striatal neurons (Centonze et al., 2003; Rice and Cragg, 2004), this transient notch in ACh tone has been proposed as a temporal signal involved in learning processes at the cellular level (Morris et al., 2004).

To exhibit a global response of similar latency to a discrete stimulus, the cholinergic interneurons, as I will refer to them hereafter, must receive inputs which originate from some common source. The anatomical pathway carrying these inputs must project ubiquitously throughout the striatum since cholinergic interneurons are rare (<1% of striatal neurons) but are scattered fairly uniformly throughout the nucleus (Holt et al., 1997; Oorschot et al., 2002). Activity in these inputs must somehow induce an inhibition of the tonic firing of cholinergic interneurons, either through a direct hyperpolarising effect on the membrane or by activating an interposed inhibitory neuron. Moreover, for the pause response to appear anew after repeated pairings of a neutral stimulus with a reward (or with an aversive stimulus, eg. Blazquez et al., 2002), these inputs must be able to undergo some form of plasticity. A number of pathways exist that could be involved in mediating aspects of the pause response. In this chapter, each of the major afferent pathways will be considered. From my own observations made during *in vivo* intracellular recording experiments on striatal neurons, recent data will be summarised that proposes an important role for the cerebral cortex in initiating and synchronising the conditioned pause response. Finally, a model will be presented for how these pathways may interact in the acquisition and maintenance of conditioned pause responses.

2. DOPAMINERGIC INPUTS TO CHOLINERGIC INTERNEURONS

A close structural and functional relationship exists between the striatal cholinergic interneurons and the dopamine system. The cell bodies of dopamine neurons that project to the dorsal and ventral striatum are situated primarily in the substantia nigra *pars compacta* (SNc) and ventral tegmental area (VTA). Single dopamine axons arborise extensively throughout a large volume of the striatum (Prensa and Parent, 2001). Their axonal branches surround cholinergic interneurons in a distribution suitable for volume transmission of dopamine, as well as forming infrequent synaptic connections on their somata and proximal dendrites (Dimova et al., 1993). Thus, the dopamine system is appropriately situated to play a direct role in pause generation in widely-distributed cholinergic interneurons.

2.1. The Role of Dopamine in the Conditioned Pause Response

It has been well established in behaving animals that the pause response depends on normal striatal dopamine innervation. Direct application to cholinergic interneurons of dopamine receptor antagonists suppresses pause responses that have been previously acquired through reward-related learning (Watanabe and Kimura, 1998). Similarly, depletion of striatal dopamine by lesioning the dopamine projection from the SNc results in a loss of learnt pause responses that can be restored by exogenous dopamine agonists (Aosaki et al., 1994a). These data raise two possibilities for the role of dopamine in pausing the firing of cholinergic interneurons: firstly, that a phasic increase in striatal dopamine release

by the coordinated burst firing of midbrain dopamine cells (Lee et al., 2004) is directly involved in the generation of pause responses, and secondly, that background dopamine "tone" is necessary for the expression of dopamine pauses initiated by some other mechanism. These possibilities will now be considered further.

2.2. Effects of Dopamine Receptor Activation on Cholinergic Interneurons

Determining the role of dopamine in the generation of pause responses requires knowledge of the effect of dopamine on cholinergic interneuron activity. However the evidence available to date from *in vitro* preparations is inconsistent. Cholinergic interneurons express dopamine receptors of both the D1 and D2 families, principally the D5 and D2 subtypes, respectively (Bergson et al., 1995; Alcantara et al., 2003). Dopamine via D1-family receptors depolarises and increases the firing rate of cholinergic interneurons and enhances ACh release (DeBoer and Abercrombie, 1996; Aosaki et al., 1998; Centonze et al., 2003). However, less intense activation of D1/D5 receptors may slow spontaneous firing, by prolonging the fast afterhyperpolarisation (AHP) that follows single spikes, and by enhancing inhibition between intrastriatal GABAergic elements and cholinergic interneurons (Yan and Surmeier, 1997; Bennett and Wilson, 1998).

Activation of D2-family receptors also induces a combination of direct and indirect effects on cholinergic interneuron firing. Both N-type Ca^{2+} conductances (Yan et al., 1997) and the persistent Na^{+} conductance (Maurice et al., 2004) have been shown to be directly inhibited by D2-like receptor activation. Pre-synaptically, D2 receptor agonists reduce synaptic potentials that exert an inhibitory influence on cholinergic interneurons (Pisani et al., 2000). Hence, D2 receptor activation can induce opposing effects: spontaneous firing is directly inhibited by the effect of D2 receptor activation on intrinsic membrane currents, whereas activation of pre-synaptic D2 receptors could potentially have a disinhibitory effect on endogenous firing.

In attempting to make sense of these conflicting *in vitro* findings, a cautionary reminder is necessary. In recent years, it has become apparent that the overall effect of local dopamine release on striatal spiny projection neurons cannot be classified as purely excitatory or inhibitory based only on the predominant dopamine receptor activated. Consideration needs to be given to factors present *in vivo* such as cyclical excitatory input influencing the membrane potential at the time dopamine is released, and to the mode and timing of dopamine application (Reynolds and Wickens, 2002; Wickens and Arbuthnott, 2005). These factors are likely to be equally important when considering the effect of dopamine on cholinergic interneurons. However, emulating these conditions is difficult in the *in vitro* preparation, since endogenous excitation that drives the smallamplitude membrane potential fluctuations in cholinergic interneurons (Wilson, 1993; Reynolds and Wickens, 2004) is absent, as is the phasic burst firing of dopamine cells (Overton and Clark, 1997). Alternatively, testing the effect of dopamine systematically in the *in vivo* preparation is limited by the tremendous difficulty in obtaining intracellular recordings from cholinergic interneurons (Wilson et al., 1990). Notwithstanding these caveats, and taking into account (i) that the direct effect of dopamine on cholinergic cell firing *in vitro* seems, on balance, to be inhibitory and (ii) the fact that anticholinergic treatment improves movement for Parkinson's patients whose brains are depleted of striatal dopamine, it seems that the predominant effect of dopamine *in vivo* is likely to be inhibitory to cholinergic cells.

2.3. Is the Pause Response Secondary to Dopamine Release?

If the dominant effect of direct dopamine application is to inhibit the firing of cholinergic interneurons, it is possible that pauses may be triggered directly by dopamine release. However, this seems unlikely to be the mechanism of pause generation in all situations. Firstly, almost total degeneration of nigrostriatal dopamine terminals does not obliterate established pauses in all cholinergic interneurons in the locally dennervated area, as would be expected if dopamine release was necessary for the pauses (Aosaki et al., 1994a). Instead, dopamine depletion returns the percentage of responding interneurons to the same as before conditioning (approximately 10 to 20%), as if the conditioning had not occurred. Secondly, pauses continue to be generated in cholinergic interneurons in response to fully predicted or aversive stimuli or after the omission of expected stimuli (Morris et al., 2004). Each of these situations have been shown to activate dopamine cells minimally or to suppress tonic dopamine cell firing, hence would not augment (or may, indeed, decrease) dopamine levels in the vicinity of cholinergic interneurons (Morris et al., 2004; Ungless et al., 2004).

Since it is irrefutable that dopamine is required for the expression of conditioned pauses, the above findings point to a role of dopamine as "enabling" rather than initiating cholinergic cell pauses. Hence, another mechanism must be present to initiate pauses in widely-spaced cholinergic interneurons, which requires dopamine for its continued functioning. Since the temporal coding provided by phasic dopamine release would not be necessary for such an enabling role, this mechanism need only respond to tonic striatal dopamine levels provided by single spike firing (Grace and Bunney, 1984).

2.4. Dopamine as a Neuromodulator of Inputs to Cholinergic Interneurons

The proposal that dopamine is facilitating another system to initiate conditioned pauses is consistent with its well-established role as a neuromodulator of excitatory inputs to other striatal neurons. Recent evidence supports such a role in cholinergic interneurons. Using patch-clamp recordings, Suzuki et al. (2001) showed that brief highfrequency stimulation (HFS) induced long-term potentiation (LTP) of cortical and/or thalamic inputs that required activation of D5 dopamine receptors. A similar mechanism has been demonstrated in spiny projection neurons *in vitro* (Kerr and Wickens, 2001) and is involved in the processes of reward-related acquisition of new skills *in vivo* (Reynolds et al., 2001). Hence, dopamine may, in fact, fulfill a dual role in mediating pause responses: phasic release induces synaptic plasticity in excitatory inputs, establishing new pauses in cholinergic interneurons, whereas tonic release maintains the continued expression of newly-acquired pauses. I will now consider the source of these excitatory inputs and their potential role in the conditioned pause response.

3. EXCITATORY INPUTS TO CHOLINERGIC INTERNEURONS

We have to this point considered the effect of dopamine directly on cholinergic interneurons and its potential role in modulating other sources of excitatory input. In now considering the process of initiation and synchronisation of pause responses, it is of special interest that cholinergic interneurons show a high degree of spike synchrony that is not itself dependent on an intact dopamine system (Raz et al., 1996). Since afferent excitatory

activity can modulate the timing of intrinsically-generated spike firing in cholinergic interneurons (Wilson et al., 1990; Bennett and Wilson, 1998) it is possible that a common excitatory source is involved in the initiation of spike firing. This may originate in the thalamus or cortex, since sub-threshold membrane potential fluctuations that underlie spike firing are correlated with corticothalamic EEG activity (Reynolds and Wickens, 2004). It therefore follows that these same excitatory inputs may also be involved in the generation of conditioned pauses, and could also play a vital role in the synchronisation of pauses between cholinergic interneurons. We will now consider both sources of excitatory input.

3.1. Thalamic Inputs to Cholinergic Interneurons

Cholinergic interneurons receive rich synaptic input from the intralaminar nucleus of the thalamus. In primates, this innervation originates in the centromedian-parafascicular (CM-PF) nuclear complex, homologous to the lateral and medial parafascicular (PF) nuclei in the rat (Smith et al., 2004). These areas project in a topographical manner to the striatum, such that in the rat, the lateral PF nucleus projects to lateral sensorimotor areas of the dorsal striatum (Berendse and Groenewegen, 1990). Single thalamostriatal neurons from the PF nucleus arborise extensively within the striatum, innervating a considerable territory (Deschenes et al., 1996). Terminals of thalamic neurons form abundant asymmetric synapses on the somata, proximal and distal dendrites of cholinergic interneurons, which are most likely glutamatergic and excitatory (Wilson et al., 1990; Lapper and Bolam, 1992; Mouroux and Feger, 1993). Thus, the anatomy of the projection from the PF nucleus to the striatum is consistent with the distribution of responses to sensory stimuli to widely-spaced cholinergic interneurons.

Recently, results from a functional study of CM-PF neurons in behaving monkeys elucidated the behavioural conditions that activate the population of thalamostriatal neurons targeting striatal cholinergic interneurons (Matsumoto et al., 2001). Thalamostriatal neurons were excited by a range of visual and auditory stimuli, either within or outside of a behavioural task, and regardless of whether or not the stimuli were associated with reward. They were also excited by unexpected noises that acted as alerting or orienting stimuli, although these responses quickly habituated with repeated presentation. The responses of cholinergic interneurons recorded in the same monkeys contrasted significantly. These interneurons expressed pauses in response to the same stimuli, but the vast majority responded only when the stimuli were associated with reward (Matsumoto et al., 2001). Since the latencies of the responses in PF nucleus neurons particularly were shorter than the latencies of all phases of the pause response in cholinergic interneurons, it follows that neurons of the CM-PF nuclear complex may be driving the pauses in cholinergic interneurons.

Matsumoto et al. (2001) then investigated the effect of inactivating the CM-PF nuclear complex on established conditioned pauses. They focused on the effect of this manipulation on all three components of the conditioned pause response: the period of reduced action potential firing constituting the pause itself, and the two periods of excitation that often flank the pause. Chemical inhibition of the CM-PF almost abolished the pause component and the subsequent rebound excitation, indicating that thalamic inputs to cholinergic interneurons are necessary for the initiation of pause responses. Since thalamic inputs are usually excitatory to striatal neurons, it follows that these inputs must be somehow transduced into inhibitory effects on the firing of cholinergic interneurons. This could be achieved in a number of ways, none of which can be fully discounted at present:

Firstly, an inhibitory neuron may be interposed between the thalamic input and the cholinergic interneuron. This is supported by the finding that strong excitation of excitatory afferent fibres produces a disynaptic inhibitory post-synaptic potential (PSP) in cholinergic interneurons *in vitro* (Suzuki et al., 2001). Also, activation of PF nuclear neurons decreases striatal ACh efflux via inhibitory circuits in the striatum but increases striatal ACh efflux when inhibitory circuits are disabled (Zackheim and Abercrombie, 2005). This suggests that both monosynaptic excitation and disynaptic inhibition of cholinergic interneurons by thalamic inputs co-exist. It is unclear, however, how this disynaptic inhibition is mediated and how it could be involved in the pause response. The firing of spiny projection neurons is incompatible with the timing of the pause response. Alternatively, the firing patterns of GABAergic interneurons during conditioned behaviour are not known, but their synaptic activation *in vivo* induces periods of inhibition in cholinergic interneurons that are likely to be too short-lived to underlie the pause responses directly (Kita, 1993; Reynolds and Wickens, 2004).

Secondly, activation of thalamostriatal inputs may lead to dopamine release via local glutamatergic activation of dopamine terminals, in turn leading to a direct inhibition of cholinergic interneuron firing. This would be an attractive mechanism to explain the requirement for both dopamine and thalamostriatal inputs in the expression of pause responses. However, the lack of spatial convergence of thalamic and dopaminergic synapses at the level of axon terminals, or onto the dendrites of individual cholinergic interneurons, would make glutamate spillover and local dopamine release seem unlikely (Smith et al., 1994).

Thirdly and finally, a membrane hyperpolarisation could be triggered intrinsically, through activity in excitatory inputs. A number of recent observations support the existence of this latter mechanism, and these will be discussed more fully in a later section. Suffice to say here that excitatory activity in thalamic afferents is not transduced directly into pauses, otherwise the patterns of spike activation in CM-PF neurons would be mirrored by the pauses shown by cholinergic interneurons. Clearly, this is not the case, since activity in the thalamic inputs does not require reward association. Another source of input that codes reward association must be integrated with the thalamic inputs at the level of the cholinergic interneurons. A clue to the nature of this input comes from the thalamic inhibition experiment of Matsumoto et al. (2001). Although the pause and rebound excitation were obliterated, there remained an excitation that normally precedes the pause component. Interestingly, this initial excitation is itself modulated by reward association and shows plastic changes through reward-related learning (Aosaki et al., 1995; Matsumoto et al., 2001). The inputs responsible for this component of the pause response presumably originate in the other source of excitatory input to cholinergic interneurons, the cerebral cortex. I will now consider the cortical inputs to cholinergic interneurons as an input source that may initiate pause responses through the temporal convergence with excitatory inputs from the thalamus.

3.2. Cortical Inputs to Cholinergic Interneurons

Cortical afferents to cholinergic interneurons have received less attention as a possible source of inputs necessary for the pause response. The reason for this is mostly due to the anatomical paucity of inputs from the cortex to cholinergic interneurons. Cortical inputs have been difficult to demonstrate, probably because their synaptic connections are located in a dendritic region that is difficult to highlight using standard immunohistochemical procedures (Lapper and Bolam, 1992). Using antibodies against m2 muscarinic receptors

in conjunction with a cortical lesion, Thomas et al. (2000) demonstrated that degenerating cortical terminals made synaptic contact with the distal extremities of the dendrites of large m2-immunoreactive striatal neurons, which have been shown to be cholinergic interneurons (Alcantara et al., 2001). Interestingly, the cortical contacts on these classically aspiny cholinergic interneurons were made with small spines or spine-like appendages, which may have been considered in early studies as originating from neighbouring spiny neurons. Although cortical synaptic contacts have now been demonstrated, they are still relatively rare in comparison with the numerous thalamic synapses located more proximally on the dendrites of cholinergic interneurons (Lapper and Bolam, 1992; Dimova et al., 1993; Thomas et al., 2000).

Despite this pattern of sparse connectivity, functional studies suggest that cortical inputs make a significant impact on the operation of cholinergic interneurons. Firstly, as mentioned above, the cortical inputs probably mediate the residual excitation of cholinergic interneurons after the pause has been obliterated by thalamic inactivation (Matsumoto et al., 2001). Secondly, excitation of cortical inputs is sufficient to elicit striatal ACh release phasically, independent of the tonic release evoked by activity in thalamic inputs (Consolo et al., 1996). Finally, electrophysiological responses to cortical stimulation recorded in cholinergic interneurons are surprisingly large considering this connectivity. In fact, postsynaptic potentials (PSPs) evoked from the contralateral cerebral cortex or the ipsilateral thalamus are similar in size and in ability to elicit spike firing (Wilson et al., 1990). This is unexpected when taking into account the differences in the dendritic location of their synapses and in the number of synaptic connections made by each pathway. These similarities in the response to cortical and thalamic stimulation probably reflect the cellular properties of the cholinergic interneuron, particularly the proximity of its resting membrane potential to firing threshold, its relatively large input resistance and the cable properties of its dendrites (Wilson et al., 1990). Suffice to say that together, the above findings highlight that anatomical scarcity does not necessarily signal redundancy.

3.3. Possible Roles for Cortical Inputs in the Generation of Synchronised Pauses

Recently, we reported a number of findings about cortical inputs to cholinergic interneurons that may be significant to the mechanism of the conditioned pause response (Reynolds et al., 2004; Reynolds and Wickens, 2004). These findings were taken from *in vivo* intracellular recordings from a total sample of 14 cholinergic interneurons, obtained serendipitously during my experiments over a period of six years. Since these experiments were undertaken to study corticostriatal synapses in projection neurons, conditions were correct for a systematic comparison of the cortical inputs to spiny neurons with those of cholinergic interneurons, on the rare occasion that the latter was encountered.

A particularly striking difference was found between the monosynaptic PSPs measured in both neuronal types in response to stimulation of the cortex contralateral to the striatal recording site (see Figure 1). Responses were of a shorter latency in cholinergic interneurons, even when a spiny projection neuron and cholinergic interneuron were recorded from the same rat using the same stimulation electrode and parameters. In contrast, there was no difference in latencies when the ipsilateral corticostriatal inputs were activated by stimulation in the midbrain. These data suggest that there are anatomical differences in the population of corticostriatal neurons that innervate cholinergic interneurons compared to those that innervate spiny projection neurons. Since the differences in latency were only revealed when comparing PSPs elicited by activation of the contralateral cortex, any anatomical

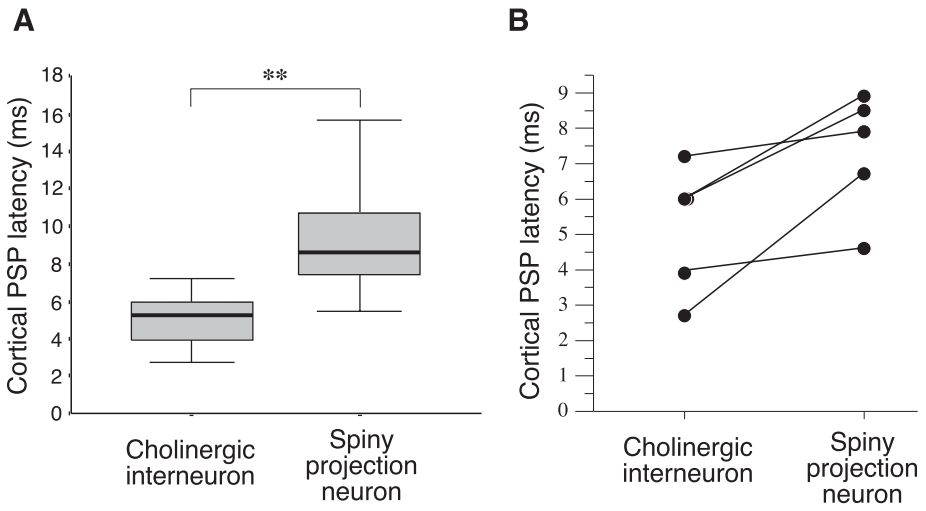

Figure 1. The latency of cortically-evoked PSPs recorded in cholinergic interneurons were shorter than those recorded in spiny projection neurons. (**A**) Test pulse stimulation of the contralateral cortex evoked a PSP of shorter latency in cholinergic interneurons (n = 6) than those measured in spiny projection neurons (n = 12) recorded in different experiments. (**B**) Shorter latency PSPs were also elicited in cholinergic interneurons when compared with a spiny projection neuron from the same animal (n = 5). Adapted from: Reynolds, J.N.J., and Wickens, J.R., 2004, *Brain Res*. **1011**:115–28, with permission from Elsevier Science.

differences must be limited to the population of crossed corticostriatal neurons, which innervate the striata on both sides of the brain (Wilson, 1986). Whether these differences are secondary to the calibre of the axon or its course between the cell body and the target neuron is not known. Whatever the underlying anatomy, this finding does suggest that cholinergic interneurons are targeted by a specialised sub-population of corticostriatal neurons.

Functionally, a faster axonal conduction may be important in ensuring that a cortical event is delivered rapidly to cholinergic interneurons. A fast conduction system could be the means by which the initial excitatory component of the pause response is distributed nearly simultaneously to widely-spaced interneurons. Further, the relatively fast contralateral conduction means that the latencies of contralateral and ipsilaterally-evoked responses are similar, therefore inputs originating in both cortices simultaneously are likely to converge simultaneously. Such an event would lead to a temporal convergence at the level of single cholinergic interneurons, thereby increasing the effective membrane depolarisation.

3.4. The Transduction of Excitation into Pauses

We have reviewed data thus far which indicate that functionally-significant inputs from the thalamus and cortex converge onto the dendrites of cholinergic interneurons. Summation of these inputs, for instance by the temporal convergence of input from the CM-PF nucleus elicited by a neutral stimulus with an input from the cortex coding reward association, could meet the requirements for a signal to initiate the conditioned pause response.

A mechanism is, however, required to convert this period of augmented membrane depolarisation into a pause in action potential firing.

We recently reported that membrane depolarisation can induce a subsequent hyperpolarisation sufficient to pause the tonic firing of cholinergic interneurons (Figure 2). This afterhyperpolarisation (AHP) was elicited using intracellular current injection and therefore represents an intrinsic membrane mechanism (Reynolds et al., 2004). Increasing the number of action potentials elicited by increasing the size of the depolarising current injection increased the size and duration of the AHP, suggesting that the AHP was dependent on the amount of membrane depolarisation. Importantly, action potentials were not necessary for the AHP: subthreshold depolarisations also generated an AHP which was, to a lesser degree, related to the size of the preceding depolarisation. These latter AHPs ranged between 100 ms and 200 ms in duration and were not dependent on preceding action potential firing, and thus shared a number of attributes with the conditioned pause response. In addition, small cortically-evoked excitatory PSPs sometimes elicited an AHP that reduced the probability of action potential firing for a period reminiscent of the pause response in behaving animal experiments (Figure 3B). Thus, membrane depolarisation induced by synaptic excitation can evoke a period of hyperpolarisation that may underlie the pause response.

We also found evidence that suggested that a synaptically-generated AHP can be induced in a cholinergic interneuron that does not exhibit one initially. In experiments involving three cholinergic interneurons, all of which exhibited a cortically-evoked excitatory PSP at baseline but none of which displayed an AHP after the PSP, a plasticity-inducing protocol involving activation of the dopamine cells of the substantia nigra was applied. In all three interneurons, substantia nigra stimulation induced longterm potentiation (LTP) of the cortical response, which was associated with the emergence of a new AHP (see Figure 3A). These findings suggest that strengthening of cortical synapses by the substantia nigra increases the membrane depolarisation achieved by a cortical input and induces an AHP that can transiently suppress tonic spike firing.

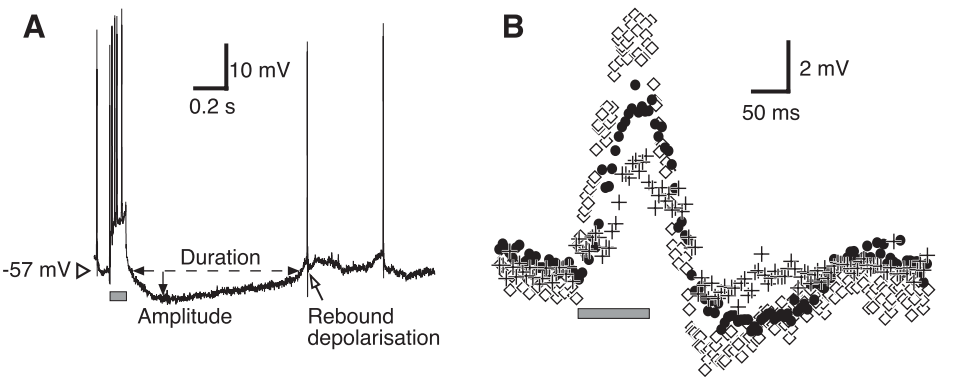

Figure 2. Depolarisation with or without action potentials induces an AHP in cholinergic interneurons. (**A**) Action potentials elicited by suprathreshold intracellular current injection (grey bar) were followed by a prolonged AHP. The duration and amplitude of the AHP was positively correlated with the number of action potentials evoked (data not shown). (**B**) Action potential firing is not essential for the prolonged AHP: subthreshold depolarisation in response to small-amplitude current injection (grey bar) induces a subsequent hyperpolarisation, which is dependent on the level of depolarisation obtained. Adapted from: Reynolds, J.N.J., Hyland, B.I., and Wickens, J.R., 2004, *J. Neurosci*. **24**:9870–7. Copyright 2004 by the Society for Neuroscience.

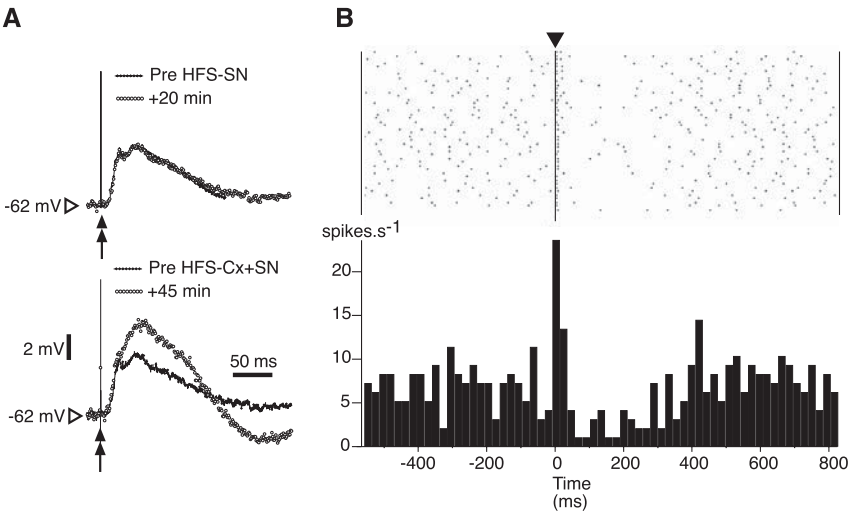

Figure 3. Cortically-evoked PSPs can induce a depolarisation-dependent AHP that pauses the tonic firing of cholinergic interneurons. (**A**) As depicted in these traces from one cholinergic interneuron, HFS of the substantia nigra (HFS-SN) alone did not change the amplitude of the PSP and there is no discernible hyperpolarisation following the PSP (upper traces). However, persistent potentiation was induced in the same interneuron after combined cortical and substantia nigra HFS (HFS-Cx + SN) and was associated with the appearance of an AHP subsequent to the depolarising component of the PSP (lower traces). (**B**) A cortically-evoked response induced a pause in tonic firing in a different interneuron. Each line in the raster (top panel) represents a single sweep aligned to the time of the cortical stimulus (arrowhead). The histogram (bottom panel) shows the firing rate of the neuron summed across sweeps (25 ms bin width). Note the reduction in firing between 100 and 300 ms after the stimulus. Adapted from: Reynolds, J.N.J., Hyland, B.I., and Wickens, J.R., 2004, *J. Neurosci*. **24**:9870–7. Copyright 2004 by the Society for Neuroscience.

The intrinsic membrane mechanisms underlying the AHP have recently been worked out *in vitro* (Wilson, 2005). Interestingly, the AHP that follows a *depolarising* event seems to share the same mechanism as a regenerative hyperpolarisation that is evoked by membrane *hyperpolarisation*. Thus, excitatory synaptic inputs to cholinergic interneurons as well as inhibitory inputs over a certain threshold, can engage a mechanism that produces a fairly stereotypical membrane hyperpolarisation compatible with the timing of the pause response.

4. A MODEL OF THE CONDITIONED PAUSE RESPONSE

Considering as many as possible of the previously reviewed findings, I would like to propose the following model. This makes predictions as to the mechanisms underlying the acquisition, synchronisation and maintenance of pause responses in a number of behavioural situations, which might be tested empirically in future.

a) PRE-CONDITIONING: Before association with reward, a neutral, unpredicted sensory stimulus elicits a pause response in a minority of cholinergic interneurons. Cholinergic

interneurons receive inputs from the thalamus about sensory events. Activity in these inputs is thought to underlie the tonic membrane potential fluctuations of these interneurons and may modulate their spike firing and the tonic release of ACh *in vivo*. The prediction is that in some interneurons sufficient excitation could be induced by the occurrence of a particularly well-defined sensory input to initiate an intrinsic AHP, without requiring pairing with reward-associated excitatory inputs. This may depend on baseline synaptic efficacy and the location on the dendrites of the thalamic synapses concerned.

b) *RANDOM REWARDS: The delivery of a random reward induces a pause in firing.* Pauses in this situation are most likely driven by the phasic activation of dopamine neurons in the SNc and VTA by an unexpected reward. A net hyperpolarising effect of dopamine would reduce excitability for the period of dopamine exposure. The prediction is that a brief hyperpolarisation induced by a short phasic burst of dopamine neurons could be translated into a more stereotypical pause response, due to the action of the conductances underlying the regenerative hyperpolarisation.

c) *ACQUISITION: A neutral sensory stimulus is reliably paired with a primary reward, inducing originally unresponsive cholinergic interneurons to now exhibit a pause.* The majority of cholinergic interneurons will show little response to a nonreward associated stimulus before conditioning. The prediction is that with repeated pairings of the stimulus with reward-related activation of dopamine cells, dopaminedependent potentiation is induced at excitatory inputs on cholinergic interneurons. A further prediction is that this occurs primarily at corticostriatal synapses, potentiating the reward-associated initial excitation component of the pause response. Corticostriatal synapses are located at spine-like appendages on cholinergic interneurons. This relationship between excitatory synapses and dendritic spines is more spatially and, possibly, functionally associated with dopaminergic synapses than is seen with thalamostriatal synapses on striatal neurons (Smith et al., 1994).

d) *OVERTRAINING: Widely-distributed cholinergic interneurons exhibit a pause response of similar latency to the same reward-associated stimulus.* The prediction is that reward-related plasticity will occur at excitatory synapses with cholinergic interneurons throughout the striatum. Since the cholinergic interneurons seem to have specialised, and possibly dedicated, corticostriatal inputs, these interneurons may become effectively linked through strengthened corticostriatal synapses carrying a similar reward-associated initiation signal for the pause response. Since phasic dopamine release is required only to induce the initial corticostriatal plasticity, it is of no consequence that the dopamine signal shifts to earlier more predictable cues with overtraining.

e) *DOPAMINE DEPLETION: Returns the percentage of cholinergic interneurons that respond to the pause to the same as before conditioning.* Tonic dopamine release alone is required to maintain excitatory synaptic efficacy in the striatum, as evidenced by the emergence of synaptic depression following dopamine depletion (Reynolds and Wickens, 2000). Thus, dopamine-depleting lesions are expected to weaken the pause-initiating signal, meaning that only those cholinergic interneurons able to exhibit pauses before conditioning will exhibit pauses after dopamine depletion.

f) OMISSION OF AN EXPECTED REWARD: Cholinergic interneurons that have acquired stimulus-responsiveness exhibit a pause when the reward was predicted. It is difficult to understand how the omission of an expected reward still results in a pause in cholinergic cell firing at the time the predicted reward was expected. The mechanism would probably not involve dopamine, since striatal dopamine levels are likely to be decreased by the pause shown by dopamine cells under the same circumstances (Morris et al., 2004). It is as yet unclear how this is achieved in dopamine cells, although this could involve unopposed activity in striatal spiny projection neurons that send an adaptively timed inhibitory signal to midbrain dopamine cells (Brown et al., 1999). Thus, the prediction is that the pause in cholinergic cell firing in response to reward omission is due to inhibitory inputs exhibiting a similar learned timing mechanism, originating from intrastriatal GABAergic neurons. Intrinsic membrane mechanisms would also amplify short inhibitory inputs into a stereotyped hyperpolarisation.

5. CONCLUSIONS

The mechanisms involved in the acquisition and expression of the conditioned pause response are, without a doubt, multi-factorial. Inputs from the thalamus are necessary for alerting cholinergic interneurons about the arrival of sensory stimuli but themselves do not carry information about reward association. Inputs from the cortex communicate rapid information about the prior association of the stimulus with reward, but by themselves are not sufficient to trigger pauses. A phasic dopamine signal is probably necessary to directly reduce cellular excitability in response to an unexpected reward, but is not activated in every behavioural situation in which pauses are recorded. Thus, all of these inputs to cholinergic interneurons are necessary for the full expression of the pause response, however no one input is sufficient. In this schema, the thalamic inputs can be considered the data lines, the cortical inputs the address lines and dopamine as a switch to enable the functioning of the address lines in computations involving cholinergic interneurons.

6. ACKNOWLEDGEMENTS

I gratefully acknowledge funding from the Marsden Fund of the Royal Society of New Zealand, Lottery Health Research and the Health Research Council of New Zealand. Thanks to my colleagues Prof. Jeff Wickens and Dr. Brian Hyland for their input into this work and to Prof. Gordon Arbuthnott for his comments on the manuscript.

7. REFERENCES

Alcantara, A.A., Chen, V., Herring, B.E., Mendenhall, J.M., and Berlanga, M.L., 2003, Localization of dopamine D2 receptors on cholinergic interneurons of the dorsal striatum and nucleus accumbens of the rat, *Brain Res*. **986**:22–29.

Alcantara, A.A., Mrzljak, L., Jakab, R.L., Levey, A.I., Hersch, S.M., and Goldman-Rakic, P.S., 2001, Muscarinic m1 and m2 receptor proteins in local circuit and projection neurons of the primate striatum: anatomical evidence for cholinergic modulation of glutamatergic prefronto-striatal pathways, *J. Comp. Neurol*. **434**:445–460.

Aosaki, T., Graybiel, A.M., and Kimura, M., 1994a, Effect of the nigrostriatal dopamine system on acquired neural responses in the striatum of behaving monkeys, *Science*. **265**:412–415.

Aosaki, T., Kimura, M., and Graybiel, A.M., 1995, Temporal and spatial characteristics of tonically active neurons of the primate's striatum, *J. Neurophysiol*. **73**:1234–1252.

Aosaki, T., Kiuchi, K., and Kawaguchi, Y., 1998, Dopamine D1-like receptor activation excites rat striatal large aspiny neurons in vitro, *J. Neurosci*. **18**:5180–5190.

Aosaki, T., Tsubokawa, H., Ishida, A., Watanabe, K., Graybiel, A.M., and Kimura, M., 1994b, Responses of tonically active neurons in the primate's striatum undergo systematic changes during behavioral sensorimotor conditioning, *J. Neurosci*. **14**:3969–3984.

Bennett, B.D., and Wilson, C.J., 1998, Synaptic regulation of action potential timing in neostriatal cholinergic interneurons, *J. Neurosci*. **18**:8539–8549.

Berendse, H.W., and Groenewegen, H.J., 1990, Organization of the thalamostriatal projections in the rat, with special emphasis on the ventral striatum, *J. Comp. Neurol*. **299**:187–228.

Bergson, C., Mrzljak, L., Smiley, J.F., Pappy, M., Levenson, R., and Goldman-Rakic, P.S., 1995, Regional, cellular, and subcellular variations in the distribution of D1 and D5 dopamine receptors in primate brain, *J. Neurosci*. **15**:7821–7836.

Blazquez, P.M., Fujii, N., Kojima, J., and Graybiel, A.M., 2002, A network representation of response probability in the striatum, *Neuron*. **33**:973–982.

Brown, J., Bullock, D., and Grossberg, S., 1999, How the basal ganglia use parallel excitatory and inhibitory learning pathways to selectively respond to unexpected rewarding cues, *J. Neurosci*. **19**:10502–10511.

Centonze, D., Grande, C., Usiello, A., Gubellini, P., Erbs, E., Martin, A.B., Pisani, A., Tognazzi, N., Bernardi, G., Moratalla, R., Borrelli, E., and Calabresi, P., 2003, Receptor subtypes involved in the presynaptic and postsynaptic actions of dopamine on striatal interneurons, *J. Neurosci*. **23**:6245–6254.

Consolo, S., Baldi, G., Giorgi, S., and Nannini, L., 1996, The cerebral cortex and parafascicular thalamic nucleus facilitate in vivo acetylcholine release in the rat striatum through distinct glutamate receptor subtypes, *Eur. J. Neurosci*. **8**:2702–2710.

DeBoer, P., and Abercrombie, E.D., 1996, Physiological release of striatal acetylcholine in vivo: modulation by D1 and D2 dopamine receptor subtypes, *J. Pharmacol. Exp. Ther*. **277**:775–783.

Deschenes, M., Bourassa, J., Doan, V.D., and Parent, A., 1996, A single-cell study of the axonal projections arising from the posterior intralaminar thalamic nuclei in the rat, *Eur. J. Neurosci*. **8**:329–343.

Dimova, R., Vuillet, J., Nieoullon, A., and Kerkerian-Le Goff, L., 1993, Ultrastructural features of the choline acetyltransferase-containing neurons and relationships with nigral dopaminergic and cortical afferent pathways in the rat striatum, *Neuroscience* **53**:1059–1071.

Grace, A.A., and Bunney, B.S., 1984, The control of firing pattern in nigral dopamine neurons: single spike firing, *J. Neurosci*. **4**:2866–2876.

Holt, D.J., Graybiel, A.M., and Saper, C.B., 1997, Neurochemical architecture of the human striatum, *J. Comp. Neurol*. **384**:1–25.

Kerr, J.N., and Wickens, J.R., 2001, Dopamine D-1/D-5 receptor activation is required for long-term potentiation in the rat neostriatum in vitro, *J. Neurophysiol*. **85**:117–124.

Kita, H., 1993, GABAergic circuits of the striatum, *Prog. Brain Res*. **99**:51–72.

Lapper, S.R., and Bolam, J.P., 1992, Input from the frontal cortex and the parafascicular nucleus to cholinergic interneurons in the dorsal striatum of the rat, *Neuroscience* **51**:533–545.

Lee, C.R., Abercrombie, E.D., and Tepper, J.M., 2004, Pallidal control of substantia nigra dopaminergic neuron firing pattern and its relation to extracellular neostriatal dopamine levels, *Neuroscience* **129**:481–489.

Matsumoto, N., Minamimoto, T., Graybiel, A.M., and Kimura, M., 2001, Neurons in the thalamic CM-Pf complex supply striatal neurons with information about behaviorally significant sensory events, *J. Neurophysiol*. **85**:960–976.

Maurice, N., Mercer, J., Chan, C.S., Hernandez-Lopez, S., Held, J., Tkatch, T., and Surmeier, D.J., 2004, D2 dopamine receptor-mediated modulation of voltage-dependent Na^+ channels reduces autonomous activity in striatal cholinergic interneurons, *J. Neurosci*. **24**:10289–10301.

Morris, G., Arkadir, D., Nevet, A., Vaadia, E., and Bergman, H., 2004, Coincident but distinct messages of midbrain dopamine and striatal tonically active neurons, *Neuron*. **43**:133–143.

Mouroux, M., and Feger, J., 1993, Evidence that the parafascicular projection to the subthalamic nucleus is glutamatergic, *Neuroreport*. **4**:613–615.

Oorschot, D.E., Tunstall, M.J., and Wickens, J.R., 2002, Local connectivity between striatal spiny projection neurons: a re-evaluation, in: *The Basal Ganglia VII*, L.F.B. Nicholson, and R.L.M. Faull, Plenum Press, New York: pp. 421–434.

Overton, P.G., and Clark, D., 1997, Burst firing in midbrain dopaminergic neurons, *Brain Res. Rev*. **25**:312–334.

Pisani, A., Bonsi, P., Centonze, D., Calabresi, P., and Bernardi, G., 2000, Activation of D2-like dopamine receptors reduces synaptic inputs to striatal cholinergic interneurons, *J. Neurosci*. **20**:RC69.

Prensa, L., and Parent, A., 2001, The nigrostriatal pathway in the rat: A single-axon study of the relationship between dorsal and ventral tier nigral neurons and the striosome/matrix striatal compartments, *J. Neurosci*. **21**:7247–7260.

Raz, A., Feingold, A., Zelanskaya, V., Vaadia, E., and Bergman, H., 1996, Neuronal synchronization of tonically active neurons in the striatum of normal and parkinsonian primates, *J. Neurophysiol*. **76**:2083–2088.

Reynolds, J.N.J., Hyland, B.I., and Wickens, J.R., 2001, A cellular mechanism of reward-related learning, *Nature*. **413**:67–70.

Reynolds, J.N.J., Hyland, B.I., and Wickens, J.R., 2004, Modulation of an afterhyperpolarization by the substantia nigra induces pauses in the tonic firing of striatal cholinergic interneurons, *J. Neurosci*. **24**:9870–9877.

Reynolds, J.N.J., and Wickens, J.R., 2000, Substantia nigra dopamine regulates synaptic plasticity and membrane potential fluctuations in the rat neostriatum, in vivo, *Neuroscience* **99**:199–203.

Reynolds, J.N.J., and Wickens, J.R., 2002, Dopamine-dependent plasticity of corticostriatal synapses, *Neural Netw*. **15**:507–521.

Reynolds, J.N.J., and Wickens, J.R., 2004, The corticostriatal input to giant aspiny interneurons in the rat: a candidate pathway for synchronising the response to reward-related cues, *Brain Res*. **1011**:115–128.

Rice, M.E., and Cragg, S.J., 2004, Nicotine amplifies reward-related dopamine signals in striatum, *Nat. Neurosci*. **7**:583–584.

Smith, Y., Bennett, B.D., Bolam, J.P., Parent, A., and Sadikot, A.F., 1994, Synaptic relationships between dopaminergic afferents and cortical or thalamic input in the sensorimotor territory of the striatum in monkey, *J. Comp. Neurol*. **344**:1–19.

Smith, Y., Raju, D.V., Pare, J.F., and Sidibe, M., 2004, The thalamostriatal system: a highly specific network of the basal ganglia circuitry, *Trends Neurosci*. **27**:520–527.

Suzuki, T., Miura, M., Nishimura, K., and Aosaki, T., 2001, Dopamine-dependent synaptic plasticity in the striatal cholinergic interneurons, *J. Neurosci*. **21**:6492–6501.

Thomas, T.M., Smith, Y., Levey, A.I., and Hersch, S.M., 2000, Cortical inputs to m2-immunoreactive striatal interneurons in rat and monkey, *Synapse*. **37**:252–561.

Ungless, M.A., Magill, P.J., and Bolam, J.P., 2004, Uniform inhibition of dopamine neurons in the ventral tegmental area by aversive stimuli, *Science*. **303**:2040–2042.

Watanabe, K., and Kimura, M., 1998, Dopamine receptor-mediated mechanisms involved in the expression of learned activity of primate striatal neurons, *J. Neurophysiol*. **79**:2568–2580.

Wickens, J.R., and Arbuthnott, G.W., 2005, Structural and functional interactions in the striatum at the receptor level, in: *Handbook of Chemical Neuroanatomy*, **21**: pp. 199–236.

Wilson, C.J., 1986, Postsynaptic potentials evoked in spiny neostriatal projection neurons by stimulation of ipsilateral and contralateral neocortex, *Brain Res*. **367**:201–213.

Wilson, C.J., 1993, The generation of natural firing patterns in neostriatal neurons, *Prog. Brain Res*. **99**:277–297.

Wilson, C.J., 2005, The mechanism of intrinsic amplification of hyperpolarizations and spontaneous bursting in striatal cholinergic interneurons, *Neuron*. **45**:575–585.

Wilson, C.J., Chang, H.T., and Kitai, S.T., 1990, Firing patterns and synaptic potentials of identified giant aspiny interneurons in the rat neostriatum, *J. Neurosci*. **10**:508–519.

Yan, Z., Song, W.J., and Surmeier, J., 1997, D2 dopamine receptors reduce N-type Ca^{2+} currents in rat neostriatal cholinergic interneurons through a membrane-delimited, protein-kinase-C-insensitive pathway, *J. Neurophysiol*. **77**:1003–1015.

Yan, Z., and Surmeier, D.J., 1997, D5 dopamine receptors enhance Zn^{2+}-sensitive GABA(A) currents in striatal cholinergic interneurons through a PKA/PP1 cascade, *Neuron*. **19**:1115–1126.

Zackheim, J., and Abercrombie, E.D., 2005, Thalamic regulation of striatal acetylcholine efflux is both direct and indirect and qualitatively altered in the dopamine-depleted striatum, *Neuroscience* **131**:423–436.

SHORT AND LONG-TERM MODULATION OF SYNAPTIC ACTIVITY IN STRIATAL CHOLINERGIC INTERNEURONS

Paola Bonsi, Massimo Tolu, Franco Lavaroni, Giorgio Bernardi, Paolo Calabresi, and Antonio Pisani*

1. INTRODUCTION

Experimental evidence supports the notion that different classes of striatal neurons are enrolled in distinct aspects of motor, cognitive and motivational functions. Cholinergic interneurons play a crucial role in cognitive aspects of context-dependent motor behaviours. There is now reasonable evidence that cholinergic interneurons correspond to the tonically active neurons (TANs) of the primate striatum, that respond in a temporally related fashion to stimuli that are conditioned by association with primary rewards (Apicella et al., 1991, 1998; Aosaki et al., 1994). The response of TANs to reward-related behavioural signals generally consists of a short-latency depression of firing, often preceded by a pronounced increase after presentation of conditioning stimuli. The mechanisms underlying the TAN pause response are still poorly understood although it is known that synaptic inputs arising from the dopaminergic nigrostriatal system and from thalamic nuclei involved in sensorimotor integration modulate the responsiveness of TANs to reward-related stimuli (Aosaki et al., 1994; Matsumoto et al., 2001). Interestingly, this response to reward-related cues develops through learning and is abolished by inactivating the thalamic inputs to the striatum, though a short-latency corticostriatal excitatory response to reward-related cues remains. Cholinergic interneurons, originally described as large type II giant aspiny neurons (Aosaki et al., 1995), are characterized by a tonic and irregular spontaneous firing activity during *in vitro* intracellular recordings (Wilson et al., 1990; Bennett and Wilson, 1998; Bennett et al., 2000). Moreover, they show a relatively depolarized resting membrane potential, a long-lasting action potential, a high input resistance and a prominent afterhyperpolarization (AHP) (Wilson et al., 1990; Kawaguchi, 1993; Calabresi et al., 1998). Their peculiar intrinsic properties have been proposed to underlie the TAN pause

* Clinica Neurologica, Dipartimento di Neuroscienze, Università Tor Vergata, Via Montpellier 1, 00133 Rome, and C.E.R.C., Fondazione Santa Lucia, 00143 Rome, Italy.

response (Bennett and Wilson, 1998, 1999). However, mechanisms involving GABAergic synaptic transmission have been postulated to play a role in the generation of the pause. Indeed, an activity-dependent long-term potentiation (LTP) of the GABAergic postsynaptic potential has been reported (Suzuki et al., 2001; Bonsi et al., 2004). Moreover, an increase in spontaneous $GABA_A$-dependent synaptic activity has been reported to occur in cholinergic interneurons from rats that have learned a rewarded, externally cued sensorimotor task (Bonsi et al., 2003). Recent findings obtained by means of *in vivo* intracellular recordings from TANs have shown that high-frequency stimulation of the substantia nigra induced potentiation of the cortically evoked excitation and increased the prolonged AHP after the stimulus, suggesting that a substantia nigrainduced AHP produces stimulus-associated firing pauses in cholinergic interneurons (Reynolds et al., 2004). Together, these findings indicate that several mechanisms contribute to the pause response through the modulation both of the intrinsic and synaptic properties of cholinergic interneurons.

2. SYNAPTIC PROPERTIES OF STRIATAL CHOLINERGIC INTERNEURONS RECORDED *IN VITRO*

Cholinergic interneurons are giant polygonal cells (20–50 μm) bearing aspiny dendrites, and representing less than 2% of the entire striatal neuronal population (Fig. 1). These cells show a characteristic combination of electrophysiological properties: depolarized resting potential, large input resistance and spike width, prominent AHP, strong firing accomodation and a hyperpolarization-activated sag conductance (I_h), known to be a unique feature among striatal neuron subtypes (Jiang and North, 1991; Kawaguchi 1993; Kawaguchi et al., 1995). Cholinergic interneurons receive dopaminergic inputs (Kubota et al., 1987) from substantia nigra; likewise, they receive abundant glutamatergic synaptic input from the thalamus at their somata, proximal and distal dendrites, whereas input from the cortex is less represented (Fig. 1) (Lapper and Bolam, 1992; Contant et al., 1996). Electrophysiological recordings performed *in vivo* from these interneurons revealed a tonic, irregular spontaneous firing activity and long-lasting action potentials (Wilson et al., 1990). Yet, striatal cholinergic interneuron activity is regulated by excitatory and inhibitory synaptic inputs. In contrast to the striatal spiny projection neurons, in fact, summation of only two or three excitatory synaptic potentials is sufficient to trigger an action potential in these neurons (Wilson et al., 1990; Wilson, 1993; Bennett and Wilson, 1998). Recent *in vivo* recordings from anesthetized rats have shown that the membrane potential activity of cholinergic interneurons is strongly influenced by spontaneous corticostriatal and/or thalamostriatal glutamatergic activity (Reynolds and Wickens, 2004). These observations suggest that the pharmacological modulation of these synaptic inputs may potentially affect the excitability of cholinergic cells, thereby controlling the tone of striatal ACh. *In vitro* sharp microelectrode recordings have shown that the amplitude both of cortically- and intrastriatally-evoked excitatory synaptic potentials (EPSPs) is largely reduced by both NMDA and AMPA glutamate receptor antagonists; however, the full blockade of the EPSP is achieved by adding to the bathing medium the $GABA_A$ receptor antagonist bicuculline (Calabresi et al., 1998). Interestingly, the complete inhibition of the EPSP by NMDA, AMPA and $GABA_A$ receptor blockers reveals a slow inhibitory synaptic potential (IPSP). This IPSP has been shown to result from an increase

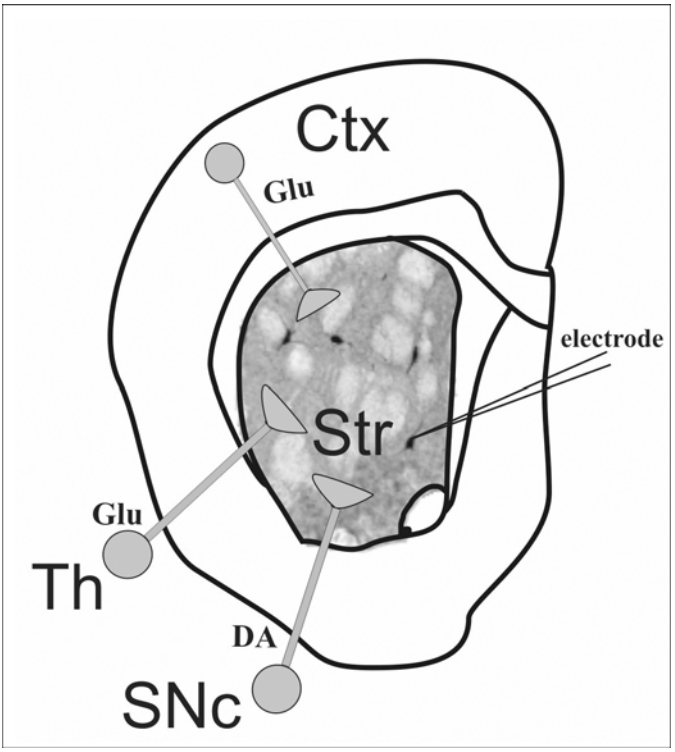

Figure 1. Striatal cholinergic interneurons, putative *tonically active neurons*. Within the striatum (Str), in normal conditions, ACh-containing interneurons (black spots) receive glutamatergic inputs, primarily from the thalamus (Th) and also from the cortex (Ctx), and dopaminergic influence from substantia nigra pars compacta (SNc).

in K^+ conductance as it reverses its polarity close to the equilibrium potential for K^+ (Calabresi et al., 1998). In addition, the IPSP is reversibly blocked by the muscarinic receptor antagonist methoctramine, a selective M2 receptor antagonist (Calabresi et al., 1998), suggesting that these cells may limit their own ACh release by activating M2-like receptors.

Recent observations suggest that a negative feedback of the cortico- and thalamostriatal excitatory drive to cholinergic interneurons is exerted via presynaptic group II metabotropic glutamate (mGlu) receptors. In particular, mGlu2 has been identified in these interneurons, and its activation reduces glutamatergic synaptic input through a selective modulation of P-type HVA calcium channels (Pisani et al., 2002). Likewise, an inhibitory modulation by D2-like DA receptors activation on these synaptic potentials has been described. Bath-applied quinpirole, a D2-like DA receptor agonist, produced a dosedependent presynaptic inhibition of both the $GABA_A$- and ACh-mediated component of the synaptic potentials (Pisani et al., 2000; Momiyama and Koga, 2001). Noteworthy, besides the modulatory activity on synaptic inputs, it cannot be neglected that cholinergic interneurons have been shown to express a variety of functional transmitter receptors able to interfere with their excitability (see Table 1) (Pisani et al., 2003).

Table 1. Neurotransmitter interplay regulates cholinergic interneuron excitability.

Transmitter	Receptor subtype	Mechanism of action
Acetylcholine	M4	membrane hyperpolarization; IPSP; N-, P-type Ca^{2+} current inhibition
Glutamate	NMDA	membrane depolarization/inward current
	AMPA	membrane depolarization/inward current
	Kainate	membrane depolarization
	mGlu 1a and 5	membrane depolarization/inward current; K^+ current inhibition
	mGlu 2	<EPSP/IPSP; <P-type Ca^{2+} channels; <$[Ca^{2+}]_i$; <ACh release
Dopamine	D5	membrane depolarization/inward current; $GABA_A$ current enhancement
	D2	<EPSP, IPSP amplitude; N-type Ca^{2+} currents inhibition
Noradrenaline	β1	membrane depolarization/inward current
γ-Aminobutyric acid	$GABA_A$	membrane depolarization, >ACh release
	$GABA_B$	membrane hyperpolarization, <ACh release

3. LONG-TERM SYNAPTIC PLASTICITY OF CHOLINERGIC INTERNEURONS

Use-dependent long-lasting changes in synaptic efficacy have been proposed as a model for memory and learning. In this respect, the role of TANs appears of primary interest for several reasons. Firstly, these neurons have been shown to modulate the induction of striatal LTP (Calabresi et al., 2000) thereby influencing the final striatal output. Secondly, behavioural correlates show that these cells respond in a temporally-related manner to rewarding stimuli, and are strongly dependent upon the integrity of the nigrostriatal dopaminergic system (Watanabe and Kimura, 1998). Third, these neurons express a form of LTP of synaptic efficacy (Fig. 2). Essential features of the LTP of synaptic transmission observed in these interneurons are represented by: i) D1-like dopamine receptor activation, ii) a critical level of intracellular calcium; iii) integrity of GABAergic inputs. Indeed, in cholinergic interneurons, blockade of the D1-like dopamine receptor by preincubation of the slice with the selective antagonist SCH 23390 fully prevented LTP (Suzuki et al., 2001; Bonsi et al., 2004). Measurement of intracellular calcium rises revealed that tetanic stimulation induced a calcium rise exceeding by fivefold the resting level, which was able to cause a long-lasting enhancement of synaptic transmission. Conversely, stimulation protocols inducing increases in intracellular calcium of lower magnitude failed to cause LTP (Bonsi et al., 2004).

Notably, the pharmacological analysis of the post-tetanic postsynaptic potential revealed that LTP was attributable, to a large extent, to the potentiation of the $GABA_A$-mediated component, whereas the glutamate-dependent component was negligible (Bonsi et al., 2004).

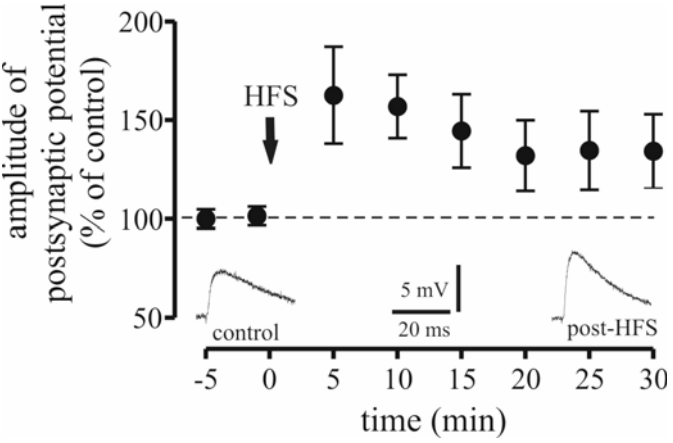

Figure 2. Time-course of long-term synaptic changes in cholinergic interneurons. High-frequency stimulation (HFS) induces a long-lasting increase in the amplitude of synaptic potential recorded from cholinergic interneurons. Note the amplitude of postsynaptic potential before and after delivering HFS (left and right traces, respectively).

4. BEHAVIOURAL LEARNING-INDUCED INCREASE IN SPONTANEOUS $GABA_A$-DEPENDENT SYNAPTIC ACTIVITY

The pause-response to reward-related cues develops through learning, and current evidence appoints a central role to GABAergic inputs for its development. Recently, we have investigated whether long-lasting synaptic changes occur in cholinergic interneurons from rats that have learned a rewarded, externally cued sensorimotor task (Bonsi et al., 2003). Training initially consisted of instrumental conditioning to establish an association between sensory signals and a lever to press. A correct lever press response resulted in the delivery of a single food pellet. The percentage of correct responses showed a progressive improvement of performance, denoted by an increasing number of rewarded trials, from 20–25% recorded at the beginning of the training sessions to 50–55% observed at the last session, before preparation of slices.

Interestingly, recordings from slices prepared from these trained animals showed an increased occurrence of spontaneous bicuculline-sensitive postsynaptic potentials. The frequency of the $GABA_A$-mediated events was increased in comparison to not-conditioned rats, suggesting that an increased GABA influence develops following rewarded sensorimotor paradigm on cholinergic interneurons. The source of such an effect might be represented either by inputs from GABAergic spiny neurons or by GABAergic striatal interneurons impinging onto cholinergic interneurons. This GABA-dependent intrastriatal mechanism might be involved in the pause response of TANs at the presentation of reward-related sensory cues. Accordingly, its cellular correlate might be represented by the LTP observed following tetanic stimulation (Bonsi et al., 2004).

5. CONCLUSIONS

Plastic changes occurring in the basal ganglia involve multiple transmitter systems, each of them playing a particular role. Indeed, the functional anatomy of the basal ganglia ensures this interactive action. Similarly to synaptic plasticity described in striatal medium spiny neurons (Lovinger et al., 1993; Charpier and Deniau, 1997; Calabresi et al., 2000), LTP observed in cholinergic interneurons requires an interplay among different transmitter systems (Suzuki et al., 2001; Bonsi et al., 2004). Dopaminergic inputs from the substantia nigra, glutamatergic fibers arising both from thalamic nuclei and cortical regions and intrastriatal GABAergic input converge onto cholinergic interneurons, shaping their excitability. Recent evidence from behaving monkeys has demonstrated that the dopaminergic signal appears to code the predictive value of various events in relation to reward, whereas the message encoded by TANs would define the temporal frame in which the dopamine signal will be handled. Hence, it is reasonable that several factors contribute to the generation of the peculiar pause response of TANs to stimuli serving as instructions, as triggers for learned behavioural reactions and as signals for reward delivery (Morris et al., 2004).

6. REFERENCES

Apicella, P., Scarnati, E., and Schultz, W., 1991, Tonically discharging neurons of monkey striatum respond to preparatory and rewarding stimuli, *Exp. Brain Res*. **84**:672–675.

Apicella, P., Ravel, S., Sardo, P., and Legallet, E., 1998, Influence of predictive information on responses of tonically active neurons in the monkey striatum, *J. Neurophysiol.* **80**:3341–3344.

Aosaki, T., Graybiel, A.M., and Kimura, M., 1994, Effect of the nigrostriatal dopamine system on acquired neural responses in the striatum of behaving monkeys, *Science* **265**:412–415.

Aosaki, T., Kimura, M., and Graybiel, A.M., 1995, Temporal and spatial characteristics of tonically active neurons of the primate's striatum, *J. Neurophysiol.* **73**:1234–1252.

Bennett, B.D., Callaway, J.C., and Wilson, C.J., 2000, Intrinsic membrane properties underlying spontaneous tonic firing in neostriatal cholinergic interneurons, *J. Neurosci.* **20**:8493–8503.

Bennett, B.D., and Wilson, C.J., 1998, Synaptic regulation of action potential timing in neostriatal cholinergic interneurons, *J. Neurosci.* **18**:8539–8549.

Bennett, B.D., and Wilson, C.J., 1999, Spontaneous activity of neostriatal cholinergic interneurons in vitro, *J. Neurosci.* **19**:5586–5596.

Bolam, J.P., Ingham, C.A., and Smith, A.D., 1984, The section-Golgi-impregrnation procedure. 3. Combination of Golgi-impregnation with enzyme histochemistry and electron microscopy to characterize acetylcholinesterase-containing neurons in the rat neostriatum, *Neuroscience* **12**:687–709.

Bonsi, P., Florio, T., Capozzo, A., Pisani, A., Calabresi, P., Siracusano, A., and Scarnati, E., 2003, Behavioural learning-induced increase in spontaneous GABAA-dependent synaptic activity in rat striatal cholinergic interneurons, *Eur. J. Neurosci.* **17**:174–178.

Bonsi, P., De Persis, C., Calabresi, P., Bernardi, G., and Pisani, A., 2004, Coordinate high-frequency pattern of stimulation and calcium levels control the induction of LTP in striatal cholinergic interneurons, *Learn Mem.* **11**:755–760.

Calabresi, P., Centonze, D., Pisani, A., Sancesario, G., North, R.A., and Bernardi, G., 1998, Muscarinic IPSPs in rat striatal cholinergic interneurons, *J. Physiol.* **510**:421–427.

Calabresi, P., Centonze, D., Gubellini, P., Pisani, A., and Bernardi, G., 2000, Acetylcholine-mediated modulation of striatal function, *Trends Neurosci.* **23**:120–126.

Charpier, S., and Deniau, J.M., 1997, In vivo activity-dependent plasticity at cortico-striatal connections: evidence for physiological long-term potentiation, *Proc. Natl. Acad. Sci. U. S. A.* **94**:7036–7040.

Contant, C., Umbriaco, D., Garcia, S., Watkins, K.C., and Descarries, L., 1996, Ultrastructural characterization of the acetylcholine innervation in adult rat neostriatum, *Neuroscience* **71**:937–947.

Kawaguchi, Y., 1993, Physiological, morphological and histochemical characterization of three classes of interneurons in rat neostriatum, *J. Neurosci.* **13**:4908–4923.

Kawaguchi, Y., Wilson, C.J., Augood, S.J., and Emson, P.C., 1995, Striatal interneurons: chemical, physiological and morphological characterization, *Trends Neurosci.* **18**:527–535.

Kubota, Y., Inagaki, S., Shimada, S., Kito, S., Eckenstein, F., and Tohyama, M., 1987, Neostriatal cholinergic neurons receive direct synaptic inputs from dopaminergic axons, *Brain Res.* **413**:179–184.

Jiang, Z.G., and North, R.A., 1991, Membrane properties and synaptic responses of rat striatal neurones in vitro, *J. Physiol.* **443**:533–553.

Lapper, S.R., and Bolam, J.P., 1992, Input from the frontal cortex and the parafascicular nucleus to cholinergic interneurons in the dorsal striatum of the rat, *Neuroscience* **51**:533–545.

Lovinger, D.M., Tyler, E.C., and Merritt, A., 1993, Short- and long-term synaptic depression in rat neostriatum, *J. Neurophysiol.* **70**:1937–1949.

Matsumoto, N., Minamimoto, T., Graybiel, A.M., and Kimura, M., 2001, Neurons in the thalamic CM-Pf complex supply striatal neurons with information about behaviorally significant sensory events, *J. Neurophysiol.* **85**:960–976.

Momiyama, T., and Koga, E., 2001, Dopamine D2-like receptors selectively block N-type Ca^{2+} channels to reduce GABA release onto rat striatal cholinergic interneurons, *J. Physiol.* **533**:479–492.

Morris, G., Arkadir, D., Nevet, A., Vaadia, E., and Bergman, H., 2004, Coincident but distinct messages of midbrain dopamine and striatal tonically active neurons, *Neuron* **43**:133–143.

Pisani, A., Bonsi, P., Centonze, D., Calabresi, P., and Bernardi, G., 2000, Activation of D2-like dopamine receptors reduces synaptic inputs to striatal cholinergic interneurons, *J. Neurosci.* **20**:RC69.

Pisani, A., Bonsi, P., Catania, M.V., Giuffrida, R., Morari, M., Marti, M., Centonze, D., Bernardi, G., Kingston, A.E., and Calabresi, P., 2002, Metabotropic glutamate 2 receptors modulate synaptic inputs and calcium signals in striatal cholinergic interneurons, *J. Neurosci.* **22**:6176–6185.

Pisani, A., Bonsi, P., Centonze, D., Gubellini, P., Bernardi, G., and Calabresi, P., Targeting striatal cholinergic interneurons in Parkinson's disease: focus on metabotropic glutamate receptors, *Neuropharmacology* **45**:45–56.

Reynolds, J.N., Hyland, B.I., and Wickens, J.R., 2004, Modulation of an afterhyperpolarization by the substantia nigra induces pauses in the tonic firing of striatal cholinergic interneurons, *J. Neurosci.* **24**:9870–9877.

Reynolds, J.N., and Wickens, J.R., 2004, The corticostriatal input to giant aspiny interneurons in the rat: a candidate pathway for synchronising the response to reward-related cues, *Brain Res.* **1011**:115–128.

Suzuki, T., Miura, M., Nishimura, K., and Aosaki, T., 2001, Dopamine-dependent synaptic plasticity in the striatal cholinergic interneurons, *J. Neurosci.* **21**:6492–6501.

Watanabe, K., and Kimura, M., 1998, Dopamine receptor-mediated mechanisms involved in the expression of learned activity of primate striatal neurons, *J. Neurophysiol.* **79**:2568–2580.

Wilson, C.J., 1993, The generation of natural firing patterns in neostriatal neurons, *Prog. Brain Res.* **99**:277–297.

Wilson, C.J., Chang, H.T., and Kitai, S.T., 1990, Firing patterns and synaptic potentials of identified giant aspiny interneurons in rat striatum, *J. Neurosci.* **10**:508–519.

STRIATAL ACETYLCHOLINE CONTROL OF REWARD-RELATED DOPAMINE SIGNALLING

Stephanie J. Cragg, Richard Exley and Michael A. Clements*

1. INTRODUCTION

Nigrostriatal dopaminergic neurons and striatal cholinergic interneurons play key roles in the regulation of normal voluntary movement, as well as the motor dysfunction that occurs in the debilitating disorder, Parkinson's disease (PD). Functional interactions between striatal acetylcholine (ACh) and dopamine (DA) have been recognized as important to basal ganglia function for over 40 years, since clinical observations that striatal ACh was elevated in PD and that the restoration of a balance with the DA afferent system was important in alleviating the motor symptoms of the disease (Katzenschlager et al., 2003; Pisani et al., 2003). More recently, interactions between striatal ACh and DA have emerged as critical to motor response selection, in particular in reward-related learning of stimulus-response associations or habits, acquired through positive reinforcement (Aosaki et al., 1994a,b; Packard and Knowlton, 2002; Zhou et al., 2003; Wickens et al., 2003; Morris et al., 2004; Rice and Cragg, 2004). Our recent data suggest that one such interaction is the regulation by ACh of DA synapse signalling of reward-related activity (Rice and Cragg 2004). Here, we review these data to discuss the consequences for reward-related DA signals of an ACh interneuron 'pause'.

Deficits in either DA or ACh disrupt reward-related procedural learning processes (Knowlton et al., 1996; Matsumoto et al., 1999; Kitabatake et al., 2003). Direct ACh-DA interactions involved in these sensorimotor learning processes (Aosaki et al., 1994a; Packard and Knowlton, 2002; Zhou et al., 2003; Wickens et al., 2003; Morris et al., 2004) include an inverse correlation of neuronal activity (Morris et al., 2004) as well as reciprocal modulation of neurotransmitter release within the striatum. For example, striatal ACh neuron activity and ACh release are inhibited by DA (Drukarch et al., 1989; DeBoer and Abercrombie, 1996; Bennett and Wilson, 1998; Pisani et al., 2000; Reynolds et al., 2004; Maurice et al., 2004) and ACh released from striatal cholinergic interneurons acts at nicotinic ACh receptors (nAChRs) on DA axons to control DA release (Soliakov and Wonnacott, 1996; Jones et al., 2001; Zhou et al., 2001; Champtiaux et al., 2003; Rice and Cragg, 2004;

* All authors: Dept. Pharmacology, Oxford, OX1 3QT, UK. Correspondence: Stephanie.cragg@pharm.ox.ac.uk

Zhang and Sulzer, 2004). This reciprocal influence will be critical to the outcomes of the precise patterning in activity that characterize both mesostriatal DA and striatal ACh neurons.

1.1. Distinct But Coincident Activity in DA and ACh Neurons

Mesostriatal DA neurons and intrastriatal ACh interneurons have tonic activity (Grace and Bunney, 1984; Schultz, 1986; Bennett and Wilson, 1999; Hyland et al., 2002) which is not modified specifically by, or for movement, but rather shows responses to sensory stimuli that have behaviourally significant relevance, 'salience', (e.g. primary reward) or have previously been associated with reward during sensorimotor learning (reward-associated cues) (Graybiel et al., 1994; Aosaki et al., 1994b; Schultz, 2002). The coding of these reward-related functions by these two neuron types is signalled in discrete and opposing manners: Mesostriatal DA neurons signal these events by a phasic burst of activity (~20–100 Hz) lasting up to 100 ms (Schultz, 2002); in contrast, ACh interneurons (tonically active neurons, or 'TANs') respond with a transient suppression or 'pause' of a similar duration, which can be preceded and followed by a brief excitation (Kimura et al., 1984; Aosaki et al., 1994b; Morris et al., 2004). Importantly, these opposing activities coincide with temporal precision (Morris et al., 2004). This temporal coding cannot be without dynamic consequences for the reciprocal modulation of ACh and DA release and their striatal functions. Thus, a fuller understanding of the role of ACh-DA interactions in sensorimotor planning and learning must account for dynamic levels of ACh and their effects on tonic- versus burst-evoked DA release. Here, by using nAChR antagonists, we explore the possible role of an ACh pause on DA signals.

1.2. Regulation of DA Release by nAChRs

Until now, how input from cholinergic interneurons regulates DA release via nicotinic ACh receptors (nAChRs) has been controversial. The long-held view of nicotine addiction in tobacco smokers posits that nicotine elevates striatal dopamine (DA) release (Di Chiara and Imperato, 1988). However, nicotine at concentrations achieved by smokers desensitizes nAChRs on DA neurons (Pidoplichko et al., 1997) and axons (Zhou et al., 2001) in striatum to suppress axonal DA release evoked by a single action potential (Zhou et al., 2001). Our recent data have exemplified the powerful effects that nAChR drugs exert on striatal DA neurotransmission (Rice and Cragg, 2004). These data reveal that nAChRs on dopaminergic axons in striatum are instrumental in gating or filtering how activity in dopaminergic neurons is signalled by corresponding sub-second DA signals (Rice and Cragg, 2004). Thus, nAChR agents may offer a unique ability to boost DA neurotransmission in the parkinsonian striatum, which furthermore, could retain the specific information content of physiological activity in DA neurons.

DA neurons and axon terminals express multiple nAChR subunits including α3–7 and β2–4 (Jones et al., 2001; Klink et al., 2001; Champtiaux et al., 2003). The β2-containing (β2*) nAChRs are the most widely expressed, and molecular and immunological approaches have identified three to four different heteromeric nAChRs in striatal dopaminergic terminal fields: $\alpha4\beta2$*, $\alpha6\beta2$*, $\alpha4\alpha6\beta2$* and $\alpha4\alpha5\beta2$* (Zoli et al., 2002; Champtiaux et al., 2003). Expression of α7 mRNA in DA neurons has been detected but only at low levels (Klink et al., 2001). To date. there is evidence for regulation of DA release by four major nAChR subtypes (Salminen et al., 2004).

Using behaviourally relevant patterns of stimulation with real-time detection of DA release at carbon-fibre microelectrodes, we explored the dynamic properties of DA release by burst versus tonic DA neuron activity and its control by nAChRs. This data has been summarized previously (Rice and Cragg, 2004) with a view to understanding the actions of nicotine on reward-related DA signals. This chapter now explores how, by using nAChR antagonists (as well as nicotine) to suppress nAChR activity, an ACh interneuron pause might similarly gate the dynamic signalling of reward-related DA signals and thus participate in the ACh/DA control of sensorimotor planning, learning and memory.

2. METHODS

2.1. Slice Preparation and Voltammetry

Coronal striatal slices, 400 μm thick, were prepared from male adult guinea-pig brains and maintained in artificial cerebrospinal fluid (containing 2.4 mM Ca^{2+}) as described previously (Cragg, 2003; Rice and Cragg, 2004). $[DA]_o$ was measured using fast-scan cyclic voltammetry with 8 μm carbon-fibre microelectrodes bevelled to a point (exposed tip length, ~30 μm; MPB Electrodes, UK) and a Millar Voltammeter (PD Systems, UK). The applied voltage was a triangular waveform, with a voltage range of –0.7 V to 1.3 V vs. Ag/AgCl at a scan rate of 800 V/s, as used previously (Cragg, 2003; Rice and Cragg, 2004). The sampling frequency was 8–10 Hz. The substance monitored in every evoked release signal was identified as DA by comparison of the potentials for peak oxidation and reduction currents in the signal voltammogram with those of DA in calibration media (typically +500–600 and −200 mV vs. Ag/AgCl respectively). Current sampled at the oxidation peak potential was measured from the baseline of each voltammogram to provide profiles of $[DA]_o$ versus time. This procedure minimizes inclusion of contributions from other electroactive and non-electroactive species to the DA oxidation current. Electrodes were calibrated in 1–2 μM DA in experimental media. The detection limit for $[DA]_o$ was ~20–50 nM depending on the electrode.

2.2. Local Electrical Stimulation and Synaptic Depression

DA release was evoked by surface bipolar electrodes 50 μm apart and ~100 μm from the recording electrode (Cragg et al., 2000; Cragg, 2003). Stimulus pulses (200 μs duration) were generated out-of-phase with FCV scans to eliminate interference with the voltammetric current. Pulses were applied singly or in bursts at a current (0.55–0.8 mA) that was perimaximal for single pulse-evoked release, as described previously (Cragg, 2003; Rice and Cragg, 2004). Stimulation frequencies represented the physiological range of DA neuron firing frequencies (Schultz, 1986; Hyland et al., 2002) and included tonic rates (5–10 Hz) and phasic burst-like frequencies (20–100 Hz) that accompany presentation of a reinforcer or reward-predictor. This physiological stimulus recruits action potentials since release is inhibited by tetrodotoxin (TTX) (Cragg and Greenfield, 1997). Release is also Ca^{2+}-dependent (Chen and Rice, 2001; Cragg, 2003). Although local stimulation will also activate other, non-dopaminergic axons, evoked DA release in this paradigm is not modulated by glutamate or GABA acting at ionotropic receptors on these timescales (Avshalumov et al., 2003; Cragg, 2003; Schmitz et al., 2003).

Carbon-fibre recording microelectrodes detect a population response from multiple release sites. By using stimulation currents that generate 95–99% of maximum DA release with a single pulse release (Cragg, 2003), sources of variability in release, other than those due to local packing density of DA release sites, inherent release probability and plasticity (Cragg, 2003), are kept to a minimum. By decreasing this variability, release from this controlled population as closely as possible resembles on a population level the release from any one site. Release evoked by a single local stimulus using this approach is accompanied by short-term depression of DA release by immediately subsequent stimuli (Cragg, 2003).

2.3. Experimental Design and Analysis

Stimulus pulse paradigms were repeated at a minimum of 2-minute intervals, which ensured stable, consistent release. Drug effects reached a steady-state after 10 minutes application; total exposure times were limited to 90 min. All drug effects were reversible upon prolonged washout. In paired-pulse experiments, single and paired-pulse protocols were alternated at 60 s intervals; at this interval, release is fully reproducible. Release due to the second in a pair of pulses, P_2, was determined by subtracting the average single-pulse response (P_1) from the average summed paired-pulse response (P_{1+2}) at a given site (Cragg, 2003). All data are means ± SEM and sample size, n, represents the number of recording sites. Comparisons for differences in means were assessed by one- or two-way ANOVA and post-hoc multiple comparison t-tests (Newman-Keuls).

3. RESULTS

3.1. Antagonism of nAChRs Enhances the Frequency Sensitivity of DA Release

We explored striatal DA release during reward-like, phasic frequencies of DA pathway activity as well as during non-reward, tonic activity, to determine the effects of nAChR desensitization (by nicotine) or antagonism. The effects of nAChR desensitization or antagonism may be a model for the control of DA release during a reduction in ACh tone e.g. during a pause in activity of striatal ACh interneurons. Striatal extracellular DA concentration ($[DA]_o$) released by single pulses (200-μs duration) was reversibly diminished by nicotine (500 nM) or the nAChR antagonist mecamylamine (Fig. 1a–b). These data are consistent with the facilitation of initial DA release by basal endogenous ACh as well as with the expected nAChR desensitization by nicotine (Zhou et al., 2001). Thus, the neuromodulatory activity of endogenous ACh at nAChR on DA release reflects a basal tone; local cholinergic interneurons are spontaneously active in striatal slice preparations (Bennett and Wilson, 1999) and could provide this background of endogenous ACh (Zhou et al., 2001).

During 5-pulse trains in control measurements, peak extracellular DA concentration ($[DA]_o$) was relatively insensitive to frequency (Fig. 1). However, nicotine, like the antagonist mecamylamine, suppressed release elicited by low, tonic frequencies (″10 Hz) as for single pulses, but enhanced release by higher, phasic bursts (≥25 Hz) (Fig. 1a–c). Thus, nicotine acting by nAChR desensitization or nAChR antagonists, enhanced the contrast between phasic- and tonic-evoked $[DA]_o$ (Fig. 1d).

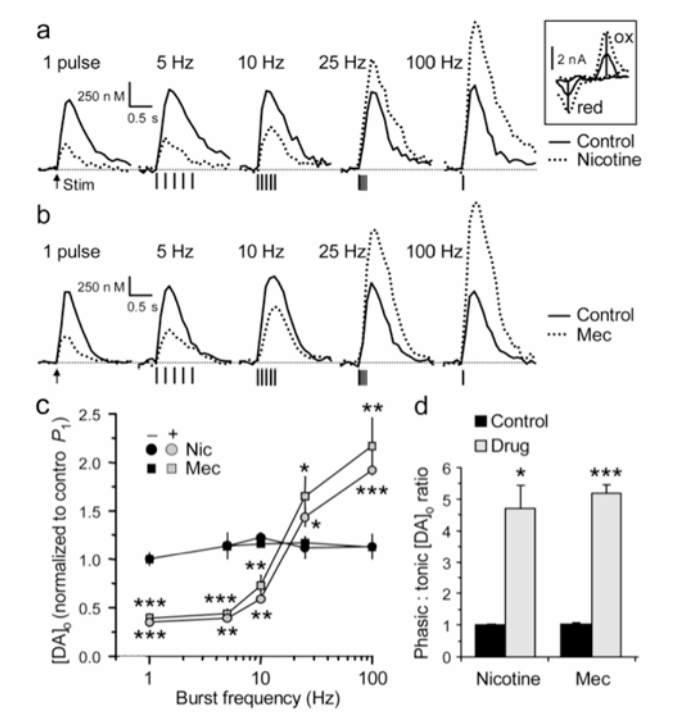

Figure 1. (a,b) Averaged profiles of $[DA]_o$ versus time at a typical site in control and in (a) nicotine (500 nM; n = 3–6 observations) or (b) mecamylamine (Mec; 20 µM; n = 2–11). Boxed inset, Representative cyclic voltammograms elicited by 5 pulses at 100 Hz; DA was identified in control (solid) and in nicotine (dashed) by characteristic oxidation (ox) and reduction (red) peak potentials (+600 and −200 mV vs. Ag/AgCl). (c) Mean peak $[DA]_o$ ± SEM versus frequency in controls, nicotine (500 nM; $n = 3–11$) or mecamylamine (20 µM; $n = 17–19$), normalized to control P_1. Control (–) or with (+) drug. (d) Phasic:tonic ratios of mean peak $[DA]_o$ ± SEM evoked by 5-pulse trains at 100 Hz versus 5 Hz ($n = 3–10$). Versus control: $*P < 0.05$; $**P < 0.01$; $***P < 0.001$. Reproduced with permission, from Rice and Cragg (2004).

3.2. Antagonism of nAChRs Relieves Short-term Depression at High Frequencies

To understand the dual effects of a loss of nAChR activity (enhanced phasic release but a suppression of initial and tonic release), we examined the effect of nicotine and nAChR antagonists on the dynamic release probability of DA (relative release per pulse) within a phasic burst (100 Hz). Under control conditions, there is a negligible 'gain' on DA release evoked by multiple versus single pulses: short-term depression of release is characteristic of striatal synapses (Cragg, 2003) and diminishes release probability at successive pulses (Cragg, 2003; Schmitz et al., 2003) (Fig. 2). In contrast, the suppression of initial pulse-evoked release seen by application of the nAChR antagonists mecamylamine or an antagonist selective for the β2-subunit-containing (β2*) nAChRs expressed on DA axons (Picciotto et al., 1998; Jones et al., 2001), dihydro-β-erythroidine (DHβE) (Figs 1–2), was accompanied by relief of short-term depression: release was equivalent per successive pulse in the burst (Fig. 2). Thus, β2* nAChRs normally gate the dynamic probability of DA

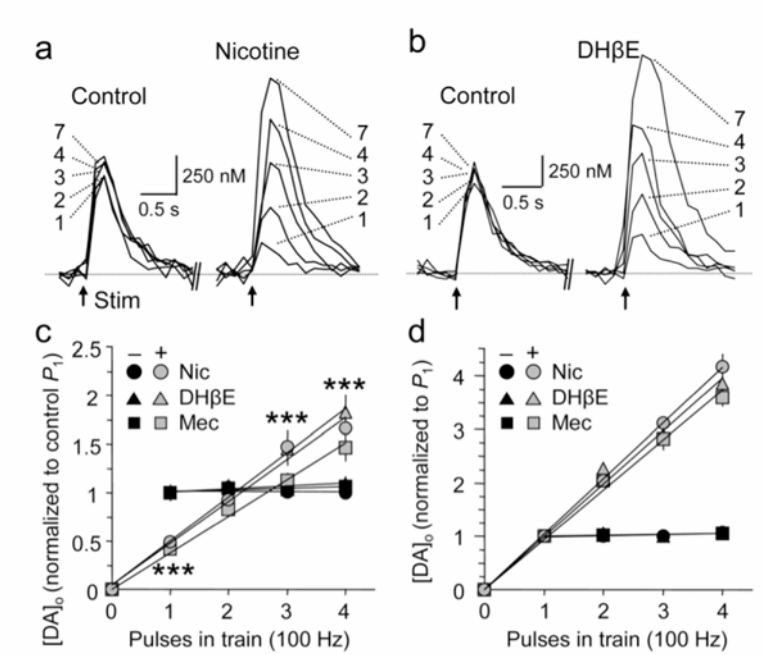

Figure 2. (a,b) Averaged profiles of $[DA]_o$ versus time following 1–7 pulses (*arrows*) at 100 Hz for typical sites in control (*left*) versus (a) nicotine (500 nM) or (b) DHβE (100 nM) (*right*) (n = 2–5). (c,d) Mean peak $[DA]_o$ ± SEM versus number of pulses in 100 Hz bursts in control, nicotine (500 nM; n = 5–46), mecamylamine (Mec, 20 µM; n = 5–23) or DHβE (100 nM; n = 5–26) normalized to (c) control P_1 or (d) drug P_1. Following nAChR desensitization/blockade, $[DA]_o$ became linearly related to pulse number which (c) generated a larger range of $[DA]_o$ (vs. control; ***$P < 0.001$) and (d) restored the slope, or gain, to unity (0.93–1.0; $R^2 > 0.99$). Control (–) or with (+) drug. Reproduced with permission from Rice and Cragg (2004).

release. Removal of nAChR tone, by antagonism or desensitization, reorganizes release probability gated by β2* nAChRs, and relieves short-term depression during phasic bursts.

We further explored the frequency-specific effects of nAChR antagonism (Fig. 1) by determining the interaction between firing frequency and dynamic release probability using paired-pulses at varying inter-pulse intervals. Paired-pulse release ratios (P_2/P_1) showed characteristic short-term depression at the paired-pulse under control conditions (Cragg, 2003) at all inter-pulse intervals (Fig. 3). However, following nAChR desensitization/blockade (nicotine, mecamylamine or DHβE), a change in frequency filtering (Thomson, 2000) occurred at >12.5 Hz (80 ms interval): P_2/P_1 increased with decreasing inter-pulse interval resulting in greater relief of depression at higher frequencies (Fig. 3). Antagonism or desensitization of nAChR tone, switches DA synapses to a high-frequency-pass filter.

The control of evoked DA release by endogenous nAChR activity is not apparently biased by ACh release evoked by the stimulus: similar results were seen in pilot studies in parasaggital slices (15° medial-to-lateral from midline) when DA release was evoked by pathway stimulation (″1000 µm ventrocaudal from the recording electrode) (not illustrated).

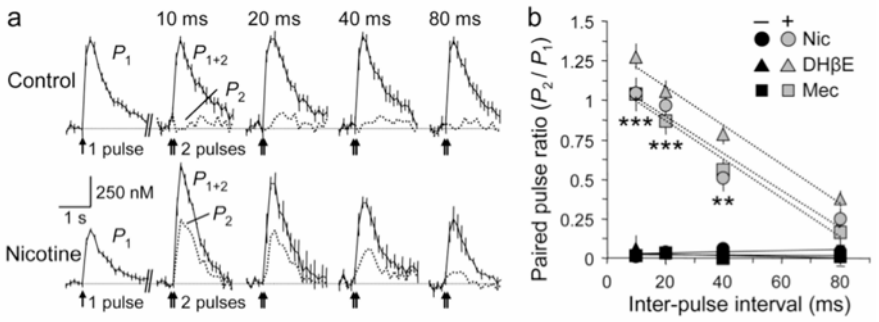

Figure 3. (a) Averaged profiles of $[DA]_o \pm$ SEM versus time elicited by 1 (P_1) or 2 pulses (P_{1+2}) paired at inter-pulse intervals equivalent to 100–12.5 Hz in control (*upper*) versus nicotine (500 nM; $n = 3$–11) (*lower*) at a typical site; P_2 is P_{1+2} minus P_1. (b) Average paired-pulse ratios (P_2/P_1). In control, the slope was not different from zero ($P > 0.05$, $R^2 = 0.05$–0.31). In nAChR desensitization/blockade, linear inverse dependence of P_2/P_1 on pulse interval (*dotted*; slope vs. zero: $P < 0.01$–0.05; $R^2 = 0.92$–0.98; $n = 3$–20). Versus control: $^{**}P < 0.01$; $^{***}P < 0.001$. Control (–) or with (+) drug. Note, selective amplification of high frequencies fails at inter-pulse intervals <10 ms (see Rice and Cragg, 2004). Reproduced with permission from Rice and Cragg (2004).

4. DISCUSSION

Antagonism of β2*-nAChRs or receptor desensitization by nicotine, have powerful consequences for DA release that depend critically on the pattern of DA neuron activity. There are discrete outcomes for β2*-nAChR activity on phasic versus tonic frequency-evoked DA release. Blockade of β2*-nAChRs suppresses DA release during non-reward, low firing frequencies, and conversely, selectively enhances reward-related DA release by relieving short-term depression selectively at higher, reward-related frequencies. These findings indicate an important role for endogenous ACh in striatum in the maintenance of DA tonic levels. Endogenous ACh tone at nAChRs on DA axons presumably arises from the spontaneous, tonic activity of striatal ACh interneurons (Bennett and Wilson, 1999). Although few in number, these interneurons densely arborize to a high varicosity density in the striatum (see Zhou et al., 2002).

These data also suggest that under tonic ACh interneuron activity, ACh minimizes the contrast in $[DA]_o$ when DA neuron activity switches from tonic to phasic, e.g. due to salient primary rewards or conditioned reward predictions (Schultz, 1986). In contrast, a reduction in nAChR tone (also see Section 5) enhances the contrast in $[DA]_o$ when DA neuron activity switches to reward-related bursts. The dependence of nicotine action on DA neuron firing rate reconciles previously conflicting data on nicotine effects (Di Chiara and Imperato, 1988; Zhou et al., 2001) and explains why local actions in striatum have been underestimated (Corrigall et al., 1994). Moreover, these striatal effects provide a neurochemical correlate for the nicotine-enhancement of the reinforcing efficacy of any reward-related stimuli, including non-nicotine conditioned stimuli (e.g. predictive visual cues) that may be essential for nicotine self-administration (e.g. Caggiula et al., 2001). In combination with the actions of nicotine on somatodendritic excitability (Grenhoff et al., 1986; Pidoplichko et al., 1997; Mansvelder et al., 2002), these direct striatal axonal effects will exaggerate dopaminergic mechanisms of reinforcement to provide a powerful 'teaching'

signal (Schultz, 2002) for nicotine-associated learned behaviours, habits and addiction at the synaptic level (Reynolds et al., 2001).

5. CONCLUSIONS

These data reveal how endogenous ACh acts at striatal β2*-nAChRs to govern dynamic dopamine release probability, and frequency filtering by the DA axon. Consequently, not only will the effect of ACh on DA release be dependent on the underlying activity of DA neurons, but moreover, the effect of DA neuron firing rate on the efficacy of synaptic DA release must also depend on the activity of ACh neurons.

What then do these data reveal about the consequences for burst DA signals of an ACh 'pause' (Morris et al., 2004) that together, concomitantly accompany the presentation of a conditioned reward cue? The TAN pause itself might be expected to have consequences for the dynamic probability of DA release if a pause can be presumed, through the rapid hydrolysis of ACh by striatal AChE (Zhang et al., 2004), to result in a corresponding, rapid decline in extracellular ACh concentration. If, in turn, the effects of nAChR antagonism as described here can be used as a model for the transient suppression of ACh release, then the TAN pause will be expected to dramatically enhance the DA release by a concomitant burst when it is of sufficiently high frequency i.e. reward-related activity. The TAN pause will release the DA synapses from short-term depression and perhaps provide a time window to facilitate the DA-dependent corticostriatal plasticity that is critical to striatal learning (Reynolds et al., 2001; Wickens et al., 2003). A possible repertoire of control by the different nAChR subtypes found on DA axons remains to be explored.

In consequence, an ACh pause-facilitation of a DA burst response could feed forward the proposed entraining of the ACh pause response by DA during sensorimotor learning (Reynolds et al., 2004; Maurice et al., 2004). Furthermore, by setting a time window for dynamically filtering DA synapse efficacy, the ACh pause and DA burst response will together permit a sophisticated control of basal ganglia signal integration in the learning of reward-related events.

6. ACKNOWLEDGEMENTS

The authors acknowledge support from Beit Memorial and Paton Fellowships to SC, as well as from the Michael J Fox Foundation, and a BBSRC CASE Studentship.

7. REFERENCES

Aosaki, T., Graybiel, A.M., and Kimura, M., 1994a, Effect of the nigrostriatal dopamine system on acquired neural responses in the striatum of behaving monkeys, *Science* **265**:412.

Aosaki, T., Tsubokawa, H., Ishida, A., Watanabe, K., Graybiel, A.M., and Kimura, M., 1994b, Responses of tonically active neurons in the primate's striatum undergo systematic changes during behavioral sensorimotor conditioning, *J. Neurosci*. **14**:3969.

Avshalumov, M.V., Chen, B.T., Marshall, S.P., Pena, D.M., and Rice, M.E., 2003, Glutamate-dependent inhibition of dopamine release in striatum is mediated by a new diffusible messenger, H2O2, *J. Neurosci*. **23**:2744.

Bennett, B.D., and Wilson, C.J., 1999, Spontaneous activity of neostriatal cholinergic interneurons in vitro, *J. Neurosci*. **19**:5586.

Bennett, B.D., and Wilson, C.J., 1998, Synaptic regulation of action potential timing in neostriatal cholinergic interneurons, *J. Neurosci*. **18**:8539.

Caggiula, A.R., Donny, E.C., White, A.R., Chaudhri, N., Booth, S., Gharib, M.A., Hoffman, A., Perkins, K.A., and Sved, A.F., 2001, Cue dependency of nicotine self-administration and smoking, *Pharmacol. Biochem. Behav*. **70**:515.

Champtiaux, N., Gotti, C., Cordero-Erausquin, M., David, D.J., Przybylski, C., Lena, C., Clementi, F., Moretti, M., Rossi, F.M., Le Novere, N., McIntosh, J.M., Gardier, A.M., and Changeux, J.P., 2003, Subunit composition of functional nicotinic receptors in dopaminergic neurons investigated with knock-out mice, *J. Neurosci*. **23**:7820.

Chen, B.T., and Rice, M.E., 2001, Novel Ca^{2+} dependence and time course of somatodendritic dopamine release: substantia nigra versus striatum, *J. Neurosci*. **21**:7841.

Corrigall, W.A., Coen, K.M., and Adamson, K.L., 1994, Self-administered nicotine activates the mesolimbic dopamine system through the ventral tegmental area, *Brain Res*. **653**:278.

Cragg, S.J., 2003, Variable dopamine release probability and short-term plasticity between functional domains of the primate striatum, *J. Neurosci*. **23**:4378.

Cragg, S.J., and Greenfield, S.A., 1997, Differential autoreceptor control of somatodendritic and axon terminal dopamine release in substantia nigra, ventral tegmental area, and striatum, *J. Neurosci*. **17**:5738.

Cragg, S.J., Hille, C.J., and Greenfield, S.A., 2000, Dopamine release and uptake dynamics within nonhuman primate striatum in vitro, *J. Neurosci*. **20**:8209.

DeBoer, P., and Abercrombie, E.D., 1996, Physiological release of striatal acetylcholine in vivo: modulation by D1 and D2 dopamine receptor subtypes, *J. Pharmacol. Exp. Ther*. **277**:775.

Di Chiara, G., and Imperato, A., 1988, Drugs abused by humans preferentially increase synaptic dopamine concentrations in the mesolimbic system of freely moving rats, *Proc. Natl. Acad. Sci. U. S. A*. **85**:5274.

Drukarch, B., Schepens, E., Schoffelmeer, A.N., and Stoof, J.C., 1989, Stimulation of D-2 dopamine receptors decreases the evoked in vitro release of [3H]acetylcholine from rat neostriatum: role of K^+ and Ca^{2+}, *J. Neurochem*. **52**:1680.

Grace, A.A., and Bunney, B.S., 1984, The control of firing pattern in nigral dopamine neurons: single spike firing, *J. Neurosci*. **4**:2866.

Graybiel, A.M., Aosaki, T., Flaherty, A.W., and Kimura, M., 1994, The basal ganglia and adaptive motor control, *Science* **265**:1826.

Grenhoff, J., Aston-Jones, G., and Svensson, T.H., 1986, Nicotinic effects on the firing pattern of midbrain dopamine neurons, *Acta. Physiol. Scand*. **128**:351.

Hyland, B.I., Reynolds, J.N.J., Hay, J., Perk, C.G., and Miller, R., 2002, Firing modes of midbrain dopamine cells in the freely moving rat, *Neuroscience* **114**:475.

Jones, I.W., Bolam, J.P., and Wonnacott, S., 2001, Presynaptic localisation of the nicotinic acetylcholine receptor beta2 subunit immunoreactivity in rat nigrostriatal dopaminergic neurones, *J. Comp. Neurol*. **439**:235.

Katzenschlager, R., Sampaio, C., Costa, J., and Lees, A., 2003, Anticholinergics for symptomatic management of Parkinson's disease, *Cochrane. Database Syst. Rev.* CD003735.

Kimura, M., Rajkowski, J., and Evarts, E., 1984, Tonically discharging putamen neurons exhibit set-dependent responses, *Proc. Natl. Acad. Sci. U. S. A*. **81**:4998.

Kitabatake, Y., Hikida, T., Watanabe, D., Pastan, I., and Nakanishi, S., 2003, Impairment of reward-related learning by cholinergic cell ablation in the striatum, *Proc. Natl. Acad. Sci. U. S. A*. **100**:7965.

Klink, R., de Kerchove, D.A., Zoli, M., and Changeux, J.P., 2001, Molecular and physiological diversity of nicotinic acetylcholine receptors in the midbrain dopaminergic nuclei, *J. Neurosci*. **21**:1452.

Knowlton, B.J., Mangels, J.A., and Squire, L.R., 1996, A neostriatal habit learning system in humans, *Science* **273**:1399.

Mansvelder, H.D., Keath, J.R., and McGehee, D.S., 2002, Synaptic mechanisms underlie nicotine-induced excitability of brain reward areas, *Neuron*. **33**:905.

Matsumoto, N., Hanakawa, T., Maki, S., Graybiel, A.M., and Kimura, M., 1999, Role of [corrected] nigrostriatal dopamine system in learning to perform sequential motor tasks in a predictive manner, *J. Neurophysiol*. **82**:978.

Maurice, N., Mercer, J., Chan, C.S., Hernandez-Lopez, S., Held, J., Tkatch, T., and Surmeier, D.J., 2004, D2 dopamine receptor-mediated modulation of voltage-dependent Na^+ channels reduces autonomous activity in striatal cholinergic interneurons, *J. Neurosci*. **24**:10289.

Morris, G., Arkadir, D., Nevet, A., Vaadia, E., and Bergman, H., 2004, Coincident but distinct messages of midbrain dopamine and striatal tonically active neurons, *Neuron*. **43**:133.

Packard, M.G., and Knowlton, B.J., 2002, Learning and memory functions of the Basal Ganglia, *Annu. Rev. Neurosci*. **25**:563.

Picciotto, M.R., Zoli, M., Rimondini, R., Lena, C., Marubio, L.M., Pich, E.M., Fuxe, K., and Changeux, J.P., 1998, Acetylcholine receptors containing the beta2 subunit are involved in the reinforcing properties of nicotine, *Nature* **391**:173.

Pidoplichko, V.I., DeBiasi, M., Williams, J.T., and Dani, J.A., 1997, Nicotine activates and desensitizes midbrain dopamine neurons, *Nature* **390**:401.

Pisani, A., Bonsi, P., Centonze, D., Calabresi, P., and Bernardi, G., 2000, Activation of D2-like dopamine receptors reduces synaptic inputs to striatal cholinergic interneurons, *J. Neurosci*. **20**:RC69.

Pisani, A., Bonsi, P., Centonze, D., Gubellini, P., Bernardi, G., and Calabresi, P., 2003, Targeting striatal cholinergic interneurons in Parkinson's disease: focus on metabotropic glutamate receptors, *Neuropharmacology* **45**:45.

Reynolds, J.N., Hyland, B.I., and Wickens, J.R., 2001, A cellular mechanism of reward-related learning, *Nature* **413**:67.

Reynolds, J.N.J., Hyland, B.I., and Wickens, J.R., 2004, Modulation of an afterhyperpolarization by the substantia nigra induces pauses in the tonic firing of striatal cholinergic interneurons, *J. Neurosci*. **24**:9870.

Rice, M.E., and Cragg, S.J., 2004, Nicotine amplifies reward-related dopamine signals in striatum, *Nat. Neurosci*. **7**:583.

Salminen, O., Murphy, K.L., McIntosh, J.M., Drago, J., Marks, M.J., Collins, A.C., and Grady, S.R., 2004, Subunit composition and pharmacology of two classes of striatal presynaptic nicotinic acetylcholine receptors mediating dopamine release in mice, *Mol. Pharmacol*. **65**:1526.

Schmitz, Y., Benoit-Marand, M., Gonon, F., and Sulzer, D., 2003, Presynaptic regulation of dopaminergic neurotransmission, *J. Neurochem*. **87**:273.

Schultz, W., 1986, Responses of midbrain dopamine neurons to behavioral trigger stimuli in the monkey, *J. Neurophysiol*. **56**:1439.

Schultz, W., 2002, Getting formal with dopamine and reward, *Neuron*. **36**:241.

Soliakov, L., and Wonnacott, S., 1996, Voltage-sensitive Ca^{2+} channels involved in nicotinic receptor-mediated [3H]dopamine release from rat striatal synaptosomes, *J. Neurochem*. **67**:163.

Thomson, A.M., 2000, Molecular frequency filters at central synapses, *Prog. Neurobiol*. **62**:159.

Wickens, J.R., Reynolds, J.N., and Hyland, B.I., 2003, Neural mechanisms of reward-related motor learning, *Curr. Opin. Neurobiol*. **13**:685.

Zhang, H., and Sulzer, D., 2004, Frequency-dependent modulation of dopamine release by nicotine, *Nat. Neurosci*. **7**:581.

Zhang, L., Zhou, F.M., and Dani, J.A., 2004, Cholinergic drugs for Alzheimer's disease enhance in vitro dopamine release, *Mol. Pharmacol*. **66**:538.

Zhou, F.M., Liang, Y., and Dani, J.A., 2001, Endogenous nicotinic cholinergic activity regulates dopamine release in the striatum, *Nat. Neurosci*. **4**:1224.

Zhou, F.M., Wilson, C.J., and Dani, J.A., 2002, Cholinergic interneuron characteristics and nicotinic properties in the striatum, *J. Neurobiol*. **53**:590.

Zhou, F.M., Wilson, C.J., and Dani, J.A., 2003, Muscarinic and nicotinic cholinergic mechanisms in the mesostriatal dopamine systems, *Neuroscientist*. **9**:23.

Zoli, M., Moretti, M., Zanardi, A., McIntosh, J.M., Clementi, F., and Gotti, C., 2002, Identification of the Nicotinic Receptor Subtypes Expressed on Dopaminergic Terminals in the Rat Striatum, *J. Neurosci*. **22**:8785.

CHANGES OF GLUTAMATERGIC CONTROL OF STRIATAL ACETYLCHOLINE RELEASE IN EXPERIMENTAL PARKINSONISM

Flora Mela, Matteo Marti, Clementina Bianchi, and Michele Morari*

1. INTRODUCTION

The cholinergic interneurones represent less than 2% of the total striatal cell population. These giant aspiny neurons display an extensive dendritic and axonal network receiving massive inputs from several neurotransmitter systems, and therefore play a fundamental role in the integration and transfer of information between afferent and efferent striatal pathways (Kawaguchi et al., 1995). In particular, the cholinergic interneurones integrate dopaminergic inputs originating in substantia nigra and glutamatergic inputs arising mainly from the cerebral cortex and from the parafascicular nucleus of the thalamus (Consolo et al., 1996; Baldi et al., 1995). Glutamatergic inputs are conveyed by different glutamate (Glu) receptor subtypes, namely ionotropic (iGlu; NMDA and non-NMDA subtypes) and metabotropic (mGlu; group I-III subtypes) which are localized on the membranes of striatal cholinergic interneurones (Tallaksen-Greene et al., 1994; Bernard et al., 1997 Testa et al., 1994; Pisani et al., 2002; Bell et al., 2002). Firing activity and neurosecretion of cholinergic interneurones are affected depending upon which Glu receptor subtype is activated, iGlu or group-I mGlu receptors being facilitatory (Ruzicka and Jhamandas 1993; Di Chiara et al., 1994; Kawaguchi et al., 1995; Calabresi et al., 1998; Morari et al., 1998) and group-II mGlu receptors inhibitory (Pisani et al., 2002; Marti et al., 2001; 2003). Since striatal cholinergic interneurones play a crucial role in the modulation of striatofugal pathways and motor behavior (Di Chiara et al., 1994; Kaneko et al., 2000), much effort has been put into the understanding of the physiopathological mechanisms involved, both at the cellular and circuitry level. In particular, since Glu is the driving force of striatal cholinergic interneurones, it is relevant to investigate whether changes of cholinergic transmission following degeneration of the nigrostriatal dopaminergic pathway during Parkinson's disease (PD; Schwarting and Huston, 1996) are associated with changes in the glutamatergic modulation.

* Flora Mela, Matteo Marti, Clementina Bianchi and Michele Morari, Department of Experimental and Clinical Medicine, Section of Pharmacology, and Neuroscience Centre, University of Ferrara, 44100 Ferrara, Italy.

Therefore, the studies carried out in our laboratories during the last few years were aimed to investigate the effects of selective NMDA, non-NMDA and mGlu receptor agonists and antagonists on endogenous ACh release from rat striatal slices and synaptosomes, and to determine whether iGlu and mGlu receptor mediated regulation of ACh release undergoes plastic changes following disruption of the nigrostriatal pathway with 6-hydroxydopamine (6-OHDA), one of the most established models of PD.

2. IONOTROPIC GLUTAMATE RECEPTORS

Different morphological studies have shown that both NMDA and non-NMDA receptors are localized on striatal cholinergic interneurones. These receptors are differentially assembled from distinct subsets of receptor subunits which confers distinct kinetic properties to the receptor channel complex and makes the cholinergic interneurones unique compared to the other striatal neuronal populations (Chen et al., 1996; Kuppenbender et al., 1999). In particular, by using an in situ hybridization double labelling technique it has been shown that cholinergic interneurones express, in addition to NR1, NR2A and NR2B (as enkephalin-positive GABAergic neurons) also NR2D receptor subunits (Landwehrmeyer et al., 1995). Moreover, cholinergic interneurones selectively express GluR1 and GluR4 subunits (Bernard et al., 1997). Since the first report of Lehmann and Scatton (1982), it has been repeatedly shown that glutamatergic inputs carried by corticostriatal and thalamostriatal afferents facilitate cholinergic transmission via NMDA and non-NMDA receptors although, more recently, evidence that stimulation of the thalamostriatal pathway hyperpolarizes striatal cholinergic interneurones by activating inhibitory GABAergic neurons has been presented (Zackheim and Abercrombie, 2005). The cholinergic interneurones respond to cortical stimulation with a depolarizing synaptic potential that is blocked by both NMDA and AMPA receptor antagonists; accordingly, exogenously applied NMDA and AMPA are able to evoke membrane depolarization in the recorded cells (Calabresi et al., 1998; Richardson et al., 2000). Both NMDA and non-NMDA iGlu receptor agonists have been reported to facilitate ACh release from rat striatal slices (Cai et al., 1991; Ulus et al., 1992; Jin and Fredholm, 1994; Nicolas et al., 1994; Nankai et al., 1995, 1996; Hanania and Johnson, 1999). We confirmed this facilitatory effect by monitoring endogenous ACh release from striatal slices (Morari et al., 1998). In addition, we were able to unveil a biphasic effect (excitation followed by long lasting inhibition) at high (100–300 μM) NMDA or AMPA concentrations. It is likely that the NMDA-induced inhibitory phase involved indirect mechanisms and, in particular, activation of NMDA receptors on other subsets of striatal, possibly GABAergic (Zarckheim and Abercrombie, 2005), neurones. The involvement of NO production and/or synthesis has been also demonstrated, since pre-treatment with L-nitroarginine (L-NARG; a NO synthase inhibitor) prevented the NMDA-induced inhibitory phase (Morari et al., 1998). As for the neuronal location of NMDA and AMPA receptors involved in the facilitation of ACh release, a careful analysis with tetrodotoxin (TTX) showed that low agonist concentrations acted via preterminal and/or somatodendritic receptors (TTX-sensitive) while higher agonist concentrations via presynaptic (TTX-insensitive) receptors. Previous studies, on the basis of the TTX-dependence of NMDA or AMPA effects had suggested the presence of NMDA and non-NMDA iGlu receptors on striatal cholinergic terminals (Lehmann and Scatton, 1982; Jin and Fredholm, 1994). We demonstrated it in a straightforward way by employing a preparation of superfused striatal synaptosomes. In this preparation, both NMDA and AMPA facilitated the K^+-stimulated endogenous ACh release, their effects being antagonized by MK-801 and CNQX, respectively. Both agonists displayed a bell-shaped concentration-response curve with effective concentrations close to

K_D values for receptor binding. Thus, glutamatergic control of striatal cholinergic transmission via iGlu receptors was shown for the first time to operate both at the somatodendritic and presynaptic level (Morari et al., 1998).

2.1. Ionotropic Glutamate Receptors in Experimental Parkinsonism

Chronic dopamine (DA) denervation, as in the 6-OHDA rat model of Parkinson's disease, is associated with significant changes of striatal cholinergic markers (enzymes, receptors, ACh levels), although both increases and decreases have been reported (Schwarting and Huston, 1996). Data obtained from our previous studies have shown that DA denervation does not affect spontaneous and stimulus-induced ACh release (from both slices and synaptosomes) but, rather, changes the responsiveness to glutamatergic inputs driven by subtype selective receptor agonists (Marti et al., 1999; Marti et al., 2003). Indeed, by using slices and synaptosomes taken from hemiparkinsonian rats, we have consistently shown that the ability of NMDA to elevate the spontaneous and stimulus-induced endogenous ACh release was enhanced in the lesioned (DA-denervated) compared to the unlesioned striatum (Marti et al., 1999; Marti et al., 2003), as demonstrated by the increase in NMDA efficacy and potency. To strengthen further the physiopathological relevance of this finding, MK-801 depressed the electrically-induced ACh release in the lesioned but not unlesioned striatum, indicating that activation of NMDA receptors by endogenous GLU was enhanced following DA loss. These data are consistent with up-regulation of NMDA receptors (as a change in both the number and/or pharmacological properties of the receptors) in the striatum of hemiparkinsonian rats. Indeed, in the DA-denervated striatum of 6-OHDA lesioned animals, an increase in NMDA receptor binding (Samuel et al., 1990; Wullner et al., 1994), expression of mRNA encoding for the NR1 subunit, NMDA receptor-mediated currents (Zheng et al., 1998) and tyrosine phosphorylation of NR2B subunits (Landwehrmeyer et al. 1995; Menegoz et al., 1995) have been detected. NMDA receptors appeared to be

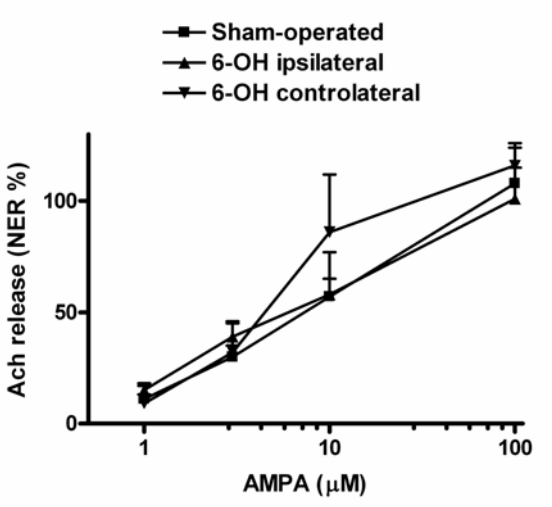

Figure 1. Effect of AMPA (1–100 μM) on spontaneous ACh release from slices taken from the striatum of hemiparkinsonian and sham-operated rats. The lesioned and unlesioned striata were processed separately (For Methods see Morari et al., 1998). Data are mean ± SEM percent net extra release (NER%) from at least six experiments.

selectively affected by DA depletion since, under the same experimental conditions, AMPA receptor evoked ACh release was unaffected. In fact, as shown in Fig. 1, AMPA was equally potent and effective in evoking spontaneous ACh release in the lesioned and unlesioned striatum. In agreement with this finding, AMPA receptor binding was not changed in the striatum of PD patients whereas NMDA receptor binding was increased (Ulas et al., 1994). Moreover, no significant change in GluR1-4 expression in the striatum of 6-OHDA lesioned rats or PD patients has been demonstrated (Bernard et al., 1996), although, in another study (Lai et al., 2003), a decrease in GluR1 expression was observed.

3. METABOTROPIC GLUTAMATE RECEPTORS

In recent years, a new family of Glu receptors, coupled to G-proteins, has been discovered and characterized. To date, eight mGlu receptor subtypes (mGlu1-8; Conn and Pin, 1997; Nishi et al, 2000) have been cloned from mammalian brain and classified into three main groups (I-III) on the basis of sequence homology, pharmacological profile and coupling to second messenger systems. Group-I mGlu receptors, which include mGlu1 and mGlu5, couple primarily to stimulation of phosphoinositide hydrolysis whereas group-II (mGlu2 and mGlu3) and group-III (mGlu4-6-7-8) mGlu receptors couple to inhibition of adenylyl cyclase. Contrary to that reported for iGlu receptors, the role of mGlu receptors in the modulation of striatal ACh release has been less well studied (Cartmell and Schoepp, 2000). The non-selective mGlu receptor agonist 1S,3R-1-amino-cyclopentan-1,3-dicarboxylic acid (1S, 3R-ACPD) increases ACh content in the striatum in vivo (Sacaan et al., 1992) while the group-II agonist (2R,4R)-4-aminopyrrolidine-2,4-dicarboxylate (2R, 4R-APDC) inhibits the NMDA-stimulated ^{3}H-ACh release from striatal slices (Hanania and Johnson, 1999). The first pharmacological characterization of the effects of group-selective mGlu receptor agonists and antagonists on ACh release in vitro was brought by our study on rat striatal synaptosomes (Marti et al., 2001). This study presented strong evidence for differential involvement of presynaptic mGlu receptors in the modulation of neurosecretion at cholinergic interneurones. Indeed, the selective group-I mGlu receptor agonist, (S)-3,5-dihydroxyphenylglycine (DHPG), and group-II mGlu receptor agonist, [(1S,2S,5R,6S)-bicyclo[3.1.0]hexane-2-amino-2,6-dicarboxylic acid] (LY354740), stimulated and inhibited the K^{+}-evoked synaptosomal ACh release, respectively. Conversely, the selective group-III mGlu receptor agonist, L-amino-4-phosphonobutyric acid (L-AP4), was ineffective, overall suggesting that functional opposing group-I and group-II mGlu receptors modulated ACh release presynaptically. Group-I mGlu receptor mRNA (Testa et al., 1994; Kerner et al., 1997) and group-I mGlu receptor immunoreactivity (Tallaksen-Greene et al., 1998; Bell et al., 2002) have been detected in medium spiny projection neurons and striatal interneurones. Interestingly, the DHPG-induced facilitation of synaptosomal ACh release was counteracted to the same extent by both 2-methyl-6-(phenylethynyl)-pyridine (MPEP) and [7-(hydroxyimino) cyclopropa [b] chromen-1a-carboxylate ethyl ester (CPCCOEt), suggesting that functional mGlu1 and mGlu5 receptors were located on cholinergic nerve terminals. Functional mGlu1 and mGlu5 receptors located on the somato-dendritic complex were also found to be involved in the DHPG-induced increase in firing rate of cholinergic interneurones (Pisani et al., 2001). Studies using a combination of non-radioactive in situ hybridization histochemistry (Pisani et al., 2002) and single cell RT-PCR analysis (Bell et al., 2002), demonstrated that the vast majority of ChAT-positive interneurones were mGlu2-mRNA and positive, the mGlu3-mRNA signal being almost absent. These data are in agreement with Testa et al. (1994) who suggested that cholinergic

interneurones express mGlu2 but not mGlu3 group-II receptors. The group-I mGlu receptor facilitation and the group-II mGlu receptor inhibition of ACh release (Marti et al., 2001) were also observed in striatal slices (Marti et al., 2003; Fig. 2 Panel A). It is noteworthy that DHPG evoked the electrically-induced ACh release only when co-applied to the electrical stimulus. The ineffectiveness of DHPG pre-application may be explained with the strong

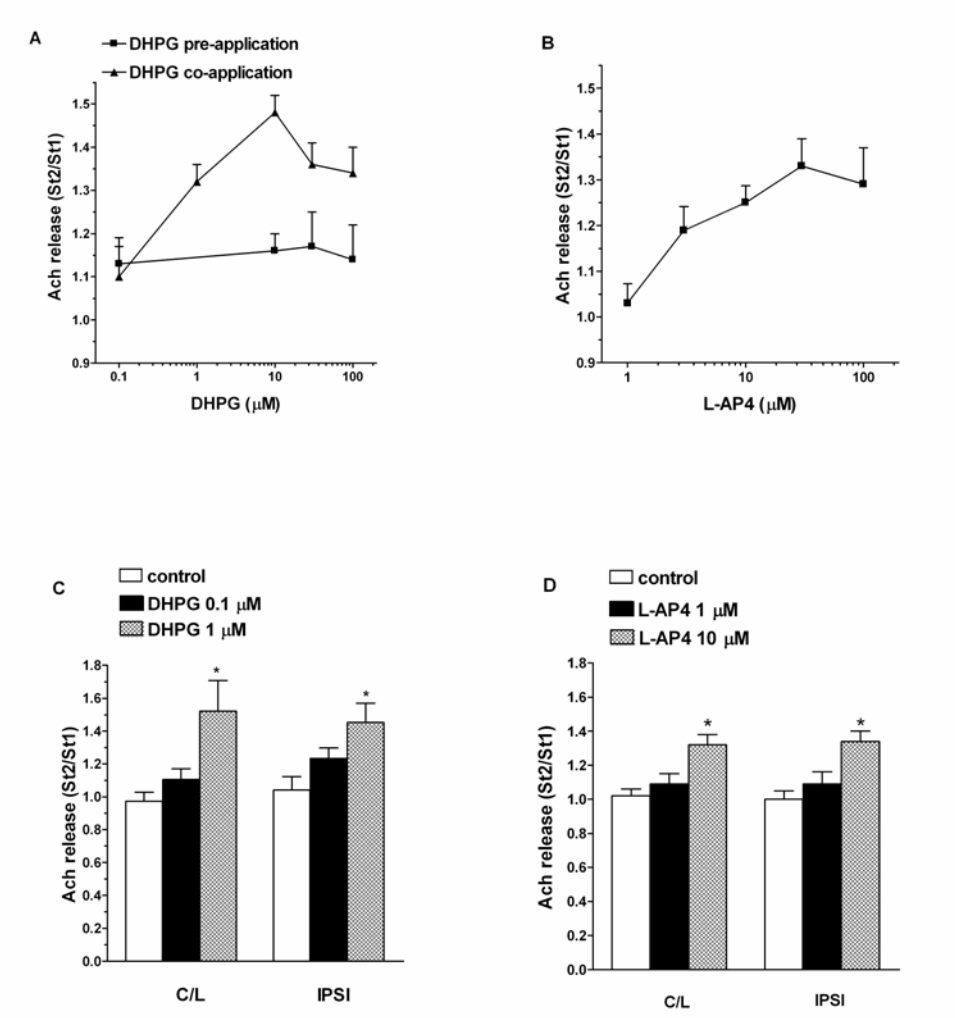

Figure 2. Panel A: Effect of the group-I mGlu receptor agonist DHPG (0.1–100 μM), applied 6 min before or concurrently with St2, on the electrically-stimulated ACh release from rat striatal slices. Panel B: Effect of the group-III mGlu receptor agonist L-AP4 (1–100 μM) on the electrically-stimulated ACh release from rat striatal slices. Panel C: Effect of the group-I mGlu receptor agonist DHPG (0.1–1 μM) on the electrically-stimulated ACh release from striatal slices taken from the striatum of hemiparkinsonian rats. Panel D: Effect of the group-III mGlu receptor agonist L-AP4 (1–10 μM) on the electrically-stimulated ACh release from striatal slices taken from the striatum of hemiparkinsonian rats. The lesioned and unlesioned striata were processed separately (for Methods see Marti et al., 2003). Data (means ± SEM of at least six experiments) are presented as St2/St1 ratio. *$P < 0.05$ different from control. (for Methods see Marti et al., 2003).

tendency of group-I mGlu receptor to desensitize (Rodriguez-Moreno et al., 1998). Overall, the neurochemical data obtained in synaptosomes and slices are consistent with the facilitatory (Takeshita et al., 1996; Calabresi et al., 1999) and the inhibitory (Pisani et al., 2002) role played by group-I and group-II mGlu receptors, respectively, in the modulation of membrane properties of striatal cholinergic interneurones.

As far as group-III mGlu receptors are concerned, the ineffectiveness of L-AP4 in modulating synaptosomal ACh release ruled out the presence of functional presynaptic group-III mGlu receptor on cholinergic terminals. To further confirm this view, L-AP4 did not affect membrane properties of striatal cholinergic cells (Bell et al., 2002). Nonetheless, when applied to striatal slices, L-AP4 facilitated the electrically-stimulated ACh release (Fig. 2 Panel B). This facilitation is likely to involve indirect mechanisms. Indeed, it has been shown that L-AP4 inhibits GABA release in striatal cell cultures (Lafon-Cazal et al., 1999).

3.1. Metabotropic Glutamate Receptors in Experimental Parkinsonism

Contrary to that reported for iGlu receptors, evidence for striatal mGlu receptor plasticity following DA denervation is still limited. In particular, increased expression of mGlu3 and mGlu4 mRNA levels (Rodriguez-Puertas et al., 1999) and up-regulation of presynaptic group-II mGlu receptors located on glutamatergic nerve terminals (Picconi et al., 2002) have been observed in the DA-denervated striatum. In contrast to this finding, we reported loss of group-II mGlu receptor mediated inhibition of ACh release in both slices and synaptosomes taken from the DA-denervated striatum of 6-OHDA rats (Marti et al., 2003). We explained this discrepancy on the basis of different receptor localizations (i.e. pre- vs postsynaptic) and to the fact that activity of glutamatergic projections is increased by DA denervation (Calabresi et al., 2000a). Therefore, to protect against glutamatergic overactivity, presynaptic mGlu2 receptors on glutamatergic terminals are expected to up-regulate while postsynaptic mGlu2 on cholinergic terminals to down-regulate (Marti et al., 2003). Alternatively, since in a different brain area (the substantia nigra) DA-depletion with reserpine or pharmacological DA receptor blockade suppressed the ability of a group-II mGlu receptor agonist to inhibit transmission at excitatory synapses (Wittman et al., 2002), it may be suggested that changes of group II mGlu receptor function are due to loss of direct DA modulation rather than to compensatory changes within the glutamatergic system. At variance with that reported for group-II mGlu and NMDA receptors (Marti et al., 2003), DA-denervation did not affect responses mediated by group-I or group-III mGlu receptors in rat striatal slices, since L-AP4 and DHPG increased ACh release to the same extent in the lesioned and unlesioned striatum (Fig. 2 Panel C-D). Consistently, DA-denervation did not affect the ability of L-AP4 to inhibit corticostriatal EPSPs nor that of DHPG to potentiate NMDA-mediated responses in spiny neurones (Picconi et al., 2002). Again, however, in the substantia nigra, impairment of DA transmission decreased the ability of L-AP4 to inhibit inhibitory synapses (Wittmann et al., 2002).

4. CONCLUDING REMARKS

Experiments performed in slices and synaptosomes have shown that Glu regulates ACh release via multiple receptors, namely NMDA and non-NMDA iGlu and group-I (mGlu1 and mGlu5) and group-II (mGlu2) mGlu receptors. These receptors are located on cholinergic interneurones, both at the somatodendritic and nerve terminals level. This suggests

that glutamatergic regulation of ACh release is finely tuned via interplay between different Glu receptor subtypes. Glu receptors located on non cholinergic cells also indirectly affect ACh release. This is the case of mGlu2 receptors that impair cholinergic transmission also via presynaptic inhibition of Glu release, or group-III mGlu receptors that increase ACh release, possibly via indirect (GABAergic?) mechanisms. Striatal DA denervation as in the 6-OHDA model of Parkinson's disease, is associated with changes in glutamatergic control of striatal ACh release, namely loss of group-II mGlu receptor mediated inhibition and enhancement of NMDA receptor-mediated facilitation. These changes were reversed by chronic treatment with L-DOPA (Marti et al., 2003). Since group I and group-III mGlu receptor mediated transmission was not affected by DA depletion, it can be predicted that loss of mGlu2 inhibition and enhancement of NMDA facilitation will shift the overall glutamatergic control of ACh release in the parkinsonian state toward facilitation, leading to hyperexcitability of cholinergic interneurones. This view may offer a pathogenetic basis to explain dysfunction of the cholinergic system associated with PD (Raz et al., 2001) and suggest that normalization of the cholinergic transmission is one of the mechanisms by which antiparkinsonian drugs could exert their therapeutic effects.

5. ACKNOWLEDGEMENTS

This study has been supported by a FIRB grant from the Italian Ministry of the University to M. Morari.

6. REFERENCES

Baldi, G., Russi, G., Nannini, L., Vezzani, A., and Consolo, S., 1995, Trans-synaptic modulation of striatal ACh release in vivo by the parafascicular thalamic nucleus, *Eur. J. Neurosci*. **7**:1117–1120.

Bell, M.I., Richardson, P.J., and Lee, K., 2002, Functional and molecular characterization of metabotropic glutamate receptors expressed in rat striatal cholinergic interneurones, *J. Neurochem*. **81**:142–149.

Bernard, V., Gardiol, A., Faucheux, B., Bloch, B., Agid, Y., and Hirsch, E.C., 1996, Expression of glutamate receptors in the human and rat basal ganglia: effect of the dopaminergic denervation on AMPA receptor gene expression in the striatopallidal complex in Parkinson's disease and rat with 6-OHDA lesion., *J. Comp. Neurol*. **368(4)**:553–568.

Bernard, V., Somogyi, P., and Bolam J.P., 1997, Cellular, subcellular, and subsynaptic distribution of AMPA-type glutamate receptor subunits in the neostriatum of the rat, *J. Neurosci*. **17**:819–833.

Blanchet, F., Gauchy, C., Perez, S., Soubriè, P., Glowinski, J., and Kemel, M.L., 2000, Control by GABA and tachykinins of the evoked release of acethylcholine in striatal compartments under different modalities of NMDA receptor stimulation. *Brain. Res*. **853**:142–150.

Cai, N.S., Kiss, B., and Erdo, S.L., 1991, Heterogeneity of N-methyl-D-aspartate receptors regulating the release of dopamine and acetylcholine from rat striatal slices, *J. Neurochem*. **57**:2148–2151.

Calabresi, P., Centonze, D., Pisani, A., Sancesario, G., Gubellini, P., Marfia, G.A., and Bernardi, G., 1998, Striatal spiny neurons and cholinergic interneurones express differential ionotropic glutamatergic responses and vulnerability: implication for ischemia and Huntington's disease, *Ann. Neurol*. **43**:586–597.

Calabresi, P., Centonze, D., Pisani, A., and Bernardi, G., 1999, Metabotropic glutamate receptors and cell-type-specific vulnerability in the striatum: implication for ischemia and Huntington's disease, *Exp. Neurol*. **158**:97–108.

Calabresi, P., Centonze, D., and Bernardi, G., 2000a, Electrophysiology of dopamine in normal and denervated striatal neurons, *Trends. Neurosci*. **23**:S57–S63.

Cartmell, J., and Schoepp, D.D., 2000, Regulation of neurotransmitter release by metabotropic glutamate receptors, *J. Neurochem*. **75**:889–907.

Conn, P.J., and Pin, J.P., 1997, Pharmacology and functions of metabotropic glutamate receptors, *Annu. Rev. Pharmacol. Toxicol*. **37**:205–237.

Consolo, S., Baldi, G., Giorgi, S., and Nannini, L., 1996, The cerebral cortex and parafascicular thalamic nucleus facilitate in vivo acetylcholine release in the rat striatum through distinct glutamate receptor subtypes., *Eur. J. Neurosci*. **8**:2702–2710.

Di Chiara, G., Morelli, M., and Consolo, S., 1994, Modulatory functions of neurotransmitters in the striatum: Ach/Dopamine/NMDA interactions, *Trends Neurosci*. **17**:228–232.

Hanania, T., and Johnson, K.M., 1999, Regulation of NMDA-stimulated [14C]GABA and [3H]acetylcholine release by striatal glutamate and dopamine receptors, *Brain Res*. **844**:106–117.

Kaneko, S., Hikida, T., Watanabe, D., Ichinose, H., Nagatsu, T., Kreitman, R.J., Pastan, I., and Nakanishi, S., 2000, Synaptic integration mediated by striatal cholinergic interneurons in basal ganglia functions, *Science*. **289**:633–637.

Kawaguchi, Y., Wilson, C., Augood, S., and Emson, P.C., 1995, Striatal interneurons: chemical, physiological and morphological characterizatio, *Trends Neurosci*. **18**:527–535.

Kerner, J.A., Standaert, D.G., Penney, J.B., Young, A.B., and Landwehrmeyer, B.G., 1997, Expresion of group one of metabotropic glutamate receptor subunit mRNAs in neurochemically identified neurons in the ratneostriatum, neocortex and hippocampus, *Mol. Brain Res*. **48**:259–269.

Kuppenbender, K.D., Albers, D.S., Iadarola, M.J., Landwehrmeyer, G.B., Standaert, D.G., 1999, Localization of alternatively spliced NMDAR1 glutamate receptor isoforms in rat striatal neurons, *J. Comp. Neurol*. 415(2):204–217.

Jin, S., and Fredholm, B.B., 1994, Role of NMDA, AMPA and kainite receptors in mediating glutamate- and 4-AP-induced dopamine and acetylcholine release from rat sriatal slices, *Neuropharmacology*. **33**: 1039–1048.

Lafon-Cazal, M., Viennois, G., Kuhn, R., Malitschek, B., Pin, J.P., Shigemoto, R., and Bockaert, J., 1999, mGluR7-like receptor and GABA(B) receptor activation enhance neurotoxic effects of N-methyl-D-aspartate in cultured mouse striatal GABAergic neurones, *Neuropharmacology*. **38**:1631–1640.

Lai, S.K., Tse, Y.C., Yang, M.S., Wong, C.K., Chan, Y.S., and Yung, K.K., Gene expression of glutamate receptors GluR1 and NR1 is differentially modulated in striatal neurons in rats after 6-hydroxydopamine lesion, *Neurochem. Int*. **43(7)**:639–653.

Landwehrmeyer, G.B., Standaert, D.G., Testa, C.M., Penney, J.B., and Young, A.B., 1995, NMDA receptor subunit mRNA expression by projection neurons and interneuorns in rat sriatum, *J. Neurosci*. **15**:5297–5307.

Lehmann, J., and Scatton, B., 1982, Characterization of the amino acid receptor-mediated release of [3H]acetylcholine from striatal slices, *Brain Res*. **252**:77–89.

Marti, M., Sbrenna, S., Fuxe, K., Bianchi, C., Beani, L., and Morari, M., 1999, In vitro evidence for increased facilitation of striatal acetylcholine release via pre- and postsynaptic NMDA receptors in hemiparkinsonian rats, *J. Neurochem*. **72**:875–878.

Marti, M., Paganini, F., Stocchi, S., Bianchi, C., Beani, L., and Morari, M., 2001, Presynaptic group I and II metabotropic glutamate receptors oppositely modulate striatal acetylcholine release, *Eur. J. Neurosci*. **14**:1181–1184.

Marti, M., Paganini, F., Stocchi, S., Mela, F., Beani, L., Bianchi, C., and Morari, M., 2003, Plasticity of glutamatergic control of striatal acetylcholine release in experimental parkinsonism: opposite changes at group-II metabotropic and NMDA receptors, *J. Neurochem*. **84**:792–802.

Menegoz, M., Lau, L., Hervè, D., Huganir, L.R., and Girault, J., 1995, Tyrosine phosphorylation of NMDA receptor in rat striatum: effects of 6-OH-dopamine lesion, *Neuroreport*. **51**:533–545.

Morari, M., Sbrenna, S., Marti, M., Caliari, F., Bianchi, C., and Beani, L., 1998, NMDA and Non-NMDA ionotropic glutamate receptors modulate striatal acetylcholine release via pre- and postsynaptic mechanisms, *J. Neurochem*. 71:2006–2017.

Nankai, M., Fage, D., and Carter, C., 1995, NMDA receptor subtype selectivity: eliprodil, polyamine spider toxins, dextromethorphan, and desipramine selectively block NMDA-evoked striatal acetylcholine but not spermidine release, *J. Neurochem*. **64**:2043–2048.

Nankai, M., Klarica, M., Fage, D., and Carter, C., 1996, Evidence for native NMDA receptor subtype pharmacology as revealed by differential effects on NMDA-evoked release of striatal neuromodulators: eliprodil, ifenprodil and other native NMDA receptor subtype selective compounds, *Neurochem. Int*. **29**:529–542.

Nicolas, C., Fage, D., and Carter, C., 1994, NMDA receptors with different sensitivities to magnesium and ifenprodil control the release of [14C]acetylcholine and [3H]spermidine from rat striatal slices in vitro, *J. Neurochem*. **62**:1835–1839.

Nishi, N., Odagaki, Y., and Koyama, T., 2000, Pharmacological characterization of metabotropic glutamate receptormediated high-affinity GTPase activity in rat cerebral cortical membranes, *Br. J. Pharmacol*. **130**:1664–1670.

Picconi, B., Pisani, A., Centonze, D., Battaglia, G., Storto, M., Nicoletti, F., Bernardi, G., and Calabresi, P., 2002, Striatal metabotropic glutamate receptor function following experimental parkinsonism and chronic levodopa treatment, *Brain*. **125**:2635–2645.

Pisani, A., Gubellini, P., Bonsi, P., Conquet, F., Picconi, B., Centonze, D., Bernardi, G., and Calabresi, P., 2001. Metabotropic glutamate receptor 5 mediates the potentiation of N-methyl-D-aspartate responses in medium spiny striatal neurons, *Neuroscience*. **106**:579–587.

Pisani, A., Bonsi, P., Catania, M.V., Giuffrida, R., Morari, M., Marti, M., Centonze, D., Bernardi, G., Kingston, A.E., and Calabresi, P., 2002, Metabotropic glutamate 2 receptors modulate synaptic inputs and calcium signals in striatal cholinergic interneurons, *J. Neurosci*. **22**:6176–6185.

Raz, A., Frechter-Mazar, V., Feingold, A., Abeles, M., Vaadia, E., and Bergman, H., 2001, Activity of pallidal and striatal tonically active neurons is correlated in mptp-treated monkeys but not in normal monkeys, *J. Neurosci*. **21**:RC128.

Richardson, P.J., Dixon, A.K., Lee, K., Bell, M.I., Cox, P.J., Williams, R., Pinnock, R.D., and Freeman, T.C., 2000, Correlating physiology with gene expression in striatal cholinergic neurones, *J. Neurochem*. **74**:839–846.

Rodriguez-Moreno, A., Sistiaga, A., Lerma, J., and Sanchez-Prieto, J., 1998, Switch from facilitation to inhibition of excitatory synaptic transmission by group I mGluR desensitization, *Neuron*. **21(6)**:1477–1486.

Rodriguez-Puertas, R., Herrera-Marschitz, M., Koistinaho, J., and Hokfelt, T., 1999, Dopamine D1 receptor modulation of glutamate receptor messenger RNA levels in the neocortex and neostriatum of unilaterally 6-hydroxydopamine-lesioned rats, *Neuroscience*. **89**:781–797.

Ruzicka, B.B., and Jhamandas, K.H., 1993, Excitatory amino acid action on the release of brain neurotransmitters and neuromodulators: biochemical studies, *Prog. Neurobiol*. **40**:223–247.

Sacaan, A.I., Bymaster, F.P., and Schoepp, D.D., 1992, Metabotropic glutamate receptor activation produces extrapyramidal motor system activation that is mediated by striatal dopamine, *J. Neurochem*. **59**:245–251.

Samuel, D., Errami, M., and Nieoullon, A., 1990, Localization of N-methyl-D-aspartate receptors in the rat striatum: effects of specific lesions on the [3H]3-(2-carboxypiperazin-4-yl) propyl-1-phosphonic acid binding, *J. Neurochem*. **54**:1926–1933.

Schwarting, R.K., and Huston, J.P., 1996, The unilateral 6-hydroxydopamine lesion model in behavioral brain research. Analysis of functional deficits, recovery and treatments, *Prog. Neurobiol*. **50**:275–331.

Takeshita, Y., Harata, N., and Akaike, N., 1996, Suppression of K^+ conductance by metabotropic glutamate receptor in acutely dissociated large cholinergic neurons of rat caudate putamen, *J. Neurophysiol*. **76**:1545–1558.

Tallaksen-Greene, S.J., and Albin, R.L., 1994, Localization of AMPA-selective excitatory amino acid receptor subunits in identified populations of striatal neurons, *Neuroscience*. **61**:509–519.

Tallaksen-Greene, S.J., Kaatz, K.W., Romano, C., and Albin, R., 1998, Localization of mGluR1a-like immunoreactivity and mGluR5-like immunoreactivity in identified populations of striatal neurons, *Brain. Res*. **780**:210–217.

Testa C.M., Standaert D.G., Young, A.B., and Penney, J.B., 1994, Metbotrobic glutamate receptor mRNA expression in the basal ganglia of the rat, *J. Neurosci*. **14**:3005–3018.

Testa, C.M., Friberg, I.K., Weiss, S.W., and Standaert, D.G., 1998, Immunohistochemical localization of metabotropic glutamate receptors mGluR1a and mGluR2/3 in the rat basal ganglia, *J. Comp. Neurol*. **390**:5–19.

Ulas, J., and Cotman, C.W., 1996, Dopaminergic denervation in the striatum results in elevated expression of NR2A subunit, *Neuroreport*. **7**:1789–1793.

Wullner, U., Testa, C.M., Catania, M.V., Young, A.B., and Penney, J.B., 1994, Glutamate receptors in striatum and substantia nigra: effects of medial forebrain bundle lesions, *Brain Res*. **645**:98–102.

PEPTIDERGIC REGULATION OF CHOLINERGIC TRANSMISSION IN THE DORSAL STRIATUM

Peptides and acetylcholine in the striatum

Marie-Louise Kemel, Maritza Jabourian, Sylvie Pérez and Jacques Glowinski*

1. INTRODUCTION

The striatum, the main input structure of the basal ganglia, is involved in adaptive control of behavior. Receiving afferents from the entire cerebral cortex, the striatum is a component of multiple cortico-basal ganglia loops that control movement as well as cognitive, motivational and emotional aspects of behavior. In the dorsal striatum (caudate-putamen), in addition to functional territories defined by their specific cortical afferents (McGeorge and Faull 1989; Berendse et al., 1992; Deniau and Thierry, 1997), two main compartments are distinguished the striosomes and the matrix (Graybiel and Ragsdale 1978; Herkenham and Pert 1981; Desban et al., 1989; Gerfen and Wilson 1996). The sensorimotor territory, which occupies the dorsolateral part of the caudateputamen, mainly consists of matrix. It belongs to the sensorimotor cortico-basal ganglia circuits opened onto motor cortical areas. The limbic/prefrontal (PF) territory, which is enriched in striosomes, occupies the rostral part of the caudate-putamen and belongs to frontal cortico-basal ganglia circuits related to the cingulate and orbito-frontal areas (Eblen and Graybiel 1995, Gerfen and Wilson 1996). These latter circuits are specifically altered in fronto-striatal disorders such as Tourette's syndrome, obsessive-compulsive disorders and schizophrenia (Holt et al., 1999; Bradshaw and Sheppard, 2000; Graybiel and Rauch, 2000; Mallet et al., 2002; Saka and Graybiel, 2003).

The striatal network which is composed of a majority of projection neurones and a small proportion of interneurones is characterized by a rather homogeneous cytoarchitecture. Despite their small number, the interneurones play a crucial role in striatal information processing. In particular, the cholinergic interneurones distributed throughout the striatum, possess a large dendritic field which in the limbic/PF territory of the dorsal striatum,

* Marie-Louise Kemel, Maritza jabourian, Sylvie Pérez, INSERM U667, Collège de France, 75231 Paris, France. Jacques Glowinski, Chaire de Neuropharmacologie, INSERM U114, Collège de France, 75231 Paris, France.

Table 1. Localisation of peptide receptors in the dorsal striatum.

					Limbic/PF	
			Neurones	Sensorimotor Matrix	Striosomes	Matrix
Tachykinins	Substance P	NK1	ACh, Som[a]	+++[b]	+[b]	+++[b]
	Neurokinin A	NK2				
	Neurokinin B	NK3	NOs/Som[c]	+[b]	+[b]	+[b]
Opioids	Enkephalin	mu	GABA (DYN)[d]		++++[e]	
			ACh[f]			+[f]
		delta	ACh[g]			
	Dynorphin	kappa	DA terminals[h]			

a, Gerfen and Wilson 1996; b, Tremblay et al., 1992; c, Preston et al., 2000; d, Guttenberg et al., 1996; e, Herkenham and Pert, 1981; Desban et al., 1993; Gerfen and Wilson 1996; f, Jabourian et al., 2005; g, Le Moine et al., 1994; h, Werling et al., 1988; Krebs et al., 1994.

extends into the striosomes and the matrix. These interneurones are innervated not only by the thalamic and cortical glutamatergic neurones but also by the nigral dopaminergic neurones and the peptide-containing terminals originating from recurrent collaterals of striatal efferent neurones (Bolam and Bennett, 1995). Tonically active, cholinergic interneurones are involved in reward related procedural learning and working memory (Graybiel et al., 1994; Aosaki et al., 1995; Apicella, 2002; Kitabatake et al., 2003). A reduction in the density of striatal cholinergic interneurones has been shown to participate to the fronto-striatal dysfunction observed in a subpopulation of schizophrenic patients (Holt et al. 1999). In Parkinson's disease, the degeneration of dopaminergic nigrostriatal neurones induces a deregulation of cholinergic interneurones that contributes to motor impairments (Duvoisin, 1967; Olanow and Koller, 1998).

Neuropeptides, tachykinins (substance P (SP), neurokinin (NK) A and B), and opioids (enkephalins (ENK) and dynorphin (DYN)) are present in GABAergic output neurones of the striatum. In each striatal compartment, these output neurones possess recurrent axon collaterals making synaptic contacts with various striatal neurones including cholinergic interneurones (Bolam and Bennett, 1995). By acting on their respective receptors (Table 1), tachykinin and opioid peptides released from striatal output neurones modulate local circuits and thus participate in striatal functions.

2. INVOLVEMENT OF TACHYKININS IN THE CONTROL OF CHOLINERGIC TRANSMISSION IN THE LIMBIC/PF AND THE SENSORIMOTOR TERRITORIES OF THE RAT DORSAL STRIATUM

Under stimulation of NMDA receptors, *in vitro*, endogenously released tachykinins acting on NK_1 and NK_2 receptors indirectly inhibit the release of ACh through a DA-dependent process. The NK_1-inibitory regulation is found in the limbic/PF territory whereas the NK_2 regulation is present in both the limbic/PF and sensorimotor territories (Blanchet et al., 1998). As shown *in vivo*, endogenously released tachykinins can also facilitate the release of ACh through NK_1 (Anderson et al., 1994; 1995) and NK_2 (Steinberg et al., 1998) receptors when DA/D2 transmission is suppressed. Accordingly, in the sensorimotor territory, a facilitatory effect of tachykinins on the NMDA-evoked release of ACh is also observed after

suppression of DA transmission. Indeed, following acute (presence of α-methyl-p-tyrosine, αMPT, an inhibitor of DA synthesis) or chronic (6-OHDA degeneration of dopaminergic nigrostriatal neurons) suppression of DA transmission, the selective tachykinin receptor antagonists SR140333 (NK_1), SR48968 (NK_2) and SR142801 (NK_3) reduce the NMDA-evoked release of ACh (Table 2, Kemel et al., 2002). Whereas the tachykinin/NK_1 facilitation is directly mediated by NK_1 receptors located on cholinergic interneurones, the tachykinin/NK_2 and NK_3 responses are indirect and require the presence of nitric oxide (Figure 2). Indeed, the SR48968 and SR142801 responses are completely suppressed in the presence of the nitric oxide synthesis inhibitor, L-NMNA, while the reducing effect of the NK_1 antagonist can still be observed (Table 2). These data are in line with the fact that 1- NO depolarizes cholinergic interneurones through a direct postsynaptic action which is independent of substance P regulation (Centonze et al., 2001) 2- NO is involved in the NK_2 but not the NK_1 receptor-mediated facilitation of ACh release *in vivo* (Steinberg et al., 1998).

Different subtypes of NK_1 binding sites, classic, septide-sensitive and new NK_1-sensitive, have been demonstrated in the rat brain (Beaujouan et al., 2000, 2004). In contrast to the classic NK_1 site, the additional NK_1 subsites have a high affinity for NKA, neuropeptide K and neuropeptide gamma. The two non-classic NK_1 subsites are distinguished by their regional distribution and their pharmacological properties. In particular, the tachykinin NK_1 antagonists, GR82334, RP67580 and CP96345, have a low affinity for the "new NK_1-sensitive" binding sites (Beaujouan et al., 2000). As shown by a pharmacological approach, the tachykinin/NK_1 facilitation of the NMDA-evoked release of ACh is mediated through the "new NK_1-sensitive" receptors. Thus, endogenously released SP but also NKA are the ligands of these receptors and in absence of DA transmission, solely some selective tachykinin NK_1 receptor antagonists such as SR140333, SSR240600 and GR205171 are able to reduce the NMDA-evoked release of ACh (Figure 1; Kemel et al., 2003).

In conclusion, after suppression of DA transmission, endogenous tachykinins released from recurrent collaterals of the striatal efferent neurones under stimulation of NMDA receptors, facilitate the release of ACh. This regulation takes place in the sensorimotor but not in the limbic/PF territory of the dorsal striatum. Since endogenous tachykinins participate to the excess of cholinergic transmission observed under deficiency of the dopaminer-

Table 2. Effect of tachykinin receptor antagonists on the NMDA-evoked release of ACh in the sensorimotor territory of the dorsal striatum.

	NMDA D-serine	+SR140333 NK_1	+SR48968 NK_2	+SR142801 NK_3
Control	196 ± 4	202 ± 14	273 ± 21*	217 ± 9
6-OHDA	279 ± 29	180 ± 10*	201 ± 3*	171 ± 22*
αMPT	273 ± 9	192 ± 6*	199 ± 6*	188 ± 7*
αMPT + L-NMNA	218 ± 5	165 ± 5*	237 ± 14	221 ± 10

Superfusion experiments were performed as previously described (Kemel et al., 1989; Blanchet et al., 1997). NMDA (1 mM + 10 µM D-serine) was applied for 2 min, 70 min after the beginning of the washing period. When used, tachykinin antagonists (0.1 µM) and/or αMPT (100 µM) and L-NMNA (0.1 µM) were added to the ACSF from the start of the washing period up to the end of the experiment. In each experiment, the NMDA-evoked release of [^{3}H]-ACh was estimated in 5 min fractions and expressed as a percentage of the mean spontaneous release determined in the two fractions collected before NMDA application. Results are the means ± S.E.M. of data obtained in 8 to 12 experiments. * $P < 0.05$ when NMDA responses obtained in the presence of tachykinin antagonists were compared to the effect of NMDA alone in the various situations, control, 6-OHDA, αMPT or αMPT + L-NMNA.

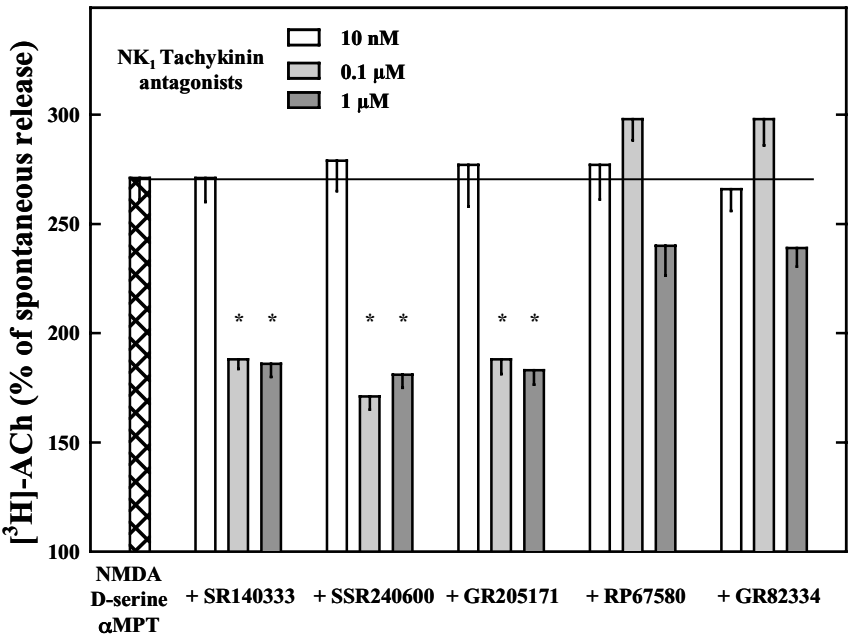

Figure 1. Superfusion experiments were performed as described in table 2. NMDA (1 mM + 10 µM D-serine) was applied for 2 min, 70 min after the beginning of the washing period. When used, tachykinin NK_1 antagonists in the presence of αMPT (100 µM) were added to the ACSF from the start of the washing period up to the end of the experiment. Results are the means ± S.E.M. of data obtained in 8 to 17 experiments. *P < 0.05 when the NMDA responses in the presence of tachykinin antagonists were compared to the effect of NMDA alone.

gic transmission, the selective tachykinin NK_1, NK_2 or NK_3 antagonists could appropriately be used as indirect cholinergic antagonists in the treatment of Parkinson's disease. Due to the main involvement of the tachykinin new NK_1-sensitive receptors in this regulation, solely the tachykinin antagonists having a high affinity for these receptors such as SR140333, GR205171 and particularly SSR240600, a central active nonpeptide antagonist (Emonds-Alt et al., 2002) could be preferentially used as indirect anticholinergic drugs. Such a therapeutic strategy could ameliorate the mental state of Parkinson's patients since there is evidence that these tachykinin receptor antagonists, NK_1 antagonists particularly, exert an antidepressant action (Rupniak and Kramer, 1999).

3. INVOLVEMENT OF ENKEPHALIN IN THE CONTROL OF CHOLINERGIC TRANSMISSION IN THE LIMBIC/PF TERRITORY OF THE DORSAL STRIATUM

Enkephalin is the endogenous ligand of mu opioid receptors (MORs) but also of delta opioid receptors, both present in the striatum (Table 1). In the striatum, MORs exhibit a patchy distribution and their visualization is used to identify striosomes in various species (Herkenham and Pert, 1981; Sharif and Hughes, 1989; Kemel et al., 1992). In rat, MORs visualization has allowed the description of the three dimensional labyrinthine

organization of the striosomal compartment (Desban et al., 1993). At a cellular level, MORs are known to be present on the output neurones of striosomes (Delfs et al., 1994; Guttenberg et al., 1996; Wang et al., 1999). Recently, we have demonstrated that functional MORs are also present in the cholinergic interneurones of the limbic/PF territory in the dorsal striatum; these interneurones being mainly located in the matrix compartment of this territory.

Endogenous ENK regulates the release of ACh by acting on MORs (Lendvai et al., 1993, Jabourian et al., 2004). According to the localisation of MORs in the dorsal striatum, this regulation occurs in the limbic/PF but not in the sensorimotor territory (Jabourian et al., 2004). Interestingly, the stimulation of NMDA receptors provokes an increased release of ENK which in turn inhibits the release of ACh through its action on MORs. The ENK/MOR inhibitory regulation of cholinergic transmission involves two distinct processes, one DA-dependent and another one DA-independent. The DA-dependent MOR regulation of ACh release is indirect, and involves the action of ENK on MORs present on output neurones of the striosomes (Delfs et al., 1994; Guttenberg et al., 1996; Wang et al., 1999) containing GABA and dynorphin which both modulate DA release (Krebs et al., 1994). In contrast, the DA-independent MOR regulation of ACh release is direct and mediated by MORs present on cholinergic interneurones (Figure 2).

Interestingly, the direct ENK/MOR inhibitory regulation of ACh release is only functional in the afternoon (animal sacrificed 7–8 hours after the beginning of the light period). As shown on Table 3, the selective MOR antagonist, β-funaltrexamine (βFNA), dose-dependently facilitates the NMDA-evoked release of ACh; this response being of higher amplitude in the afternoon than in the morning (animal sacrificed 2–3 hours after the beginning of the light period). In addition, after suppression of dopaminergic transmission, the MOR antagonist responses are totally suppressed in the morning but only partially reduced in the afternoon (Table 3, Jabourian et al., 2004).

Consistent with these observations, MOR expression in cholinergic interneurones and the activity of the ENK system follow a parallel diurnal variation. Indeed, whereas only 32% of cholinergic interneurones contain MORs in the morning, most of them, 80%, express these receptors in the afternoon (Jabourian et al., 2005). In addition, in the limbic/PF territory of the dorsal striatum, both the spontaneous and the NMDA-evoked release of ENK are increased in the afternoon (compared to the morning) when ENK tissue levels are reduced (Jabourian et al., 2005). These data are in agreement with previous reports showing fluctuations in the tissue content of ENK with a peak in the night in the striatum (Tang et al., 1984; Kurumaji et al., 1988) and an increase in the release of ENK during the afternoon in the nucleus accumbens (Dauge et al., 1996). The diurnal fluctuation in the number of cholinergic interneurones expressing MORs and in the ENK system could explain why the direct ENK/MOR control of ACh release is functional in the afternoon but not in the morning.

In the limbic/PF territory of the dorsal striatum, cholinergic interneurones containing MORs are mainly located in the matrix. This compartment contains output neurones which integrate and relay cortical information to the output structures of the basal ganglia. Thus, the direct ENK/MOR inhibitory regulation of ACh release which mainly takes place in the matrix of the limbic/PF territory should control information processing in the fronto-cortico-basal ganglia loops. Interestingly, the indirect ENK/MOR regulation involves output neurons of the striosomes and thus may control information send by these output neurons to dopaminergic neurons of the substantia nigra pars compacta (Graybiel, 1990; Desban et al., 1995; Gerfen and Wilson, 1996) or to the serotoninergic neurons of the dorsal raphe

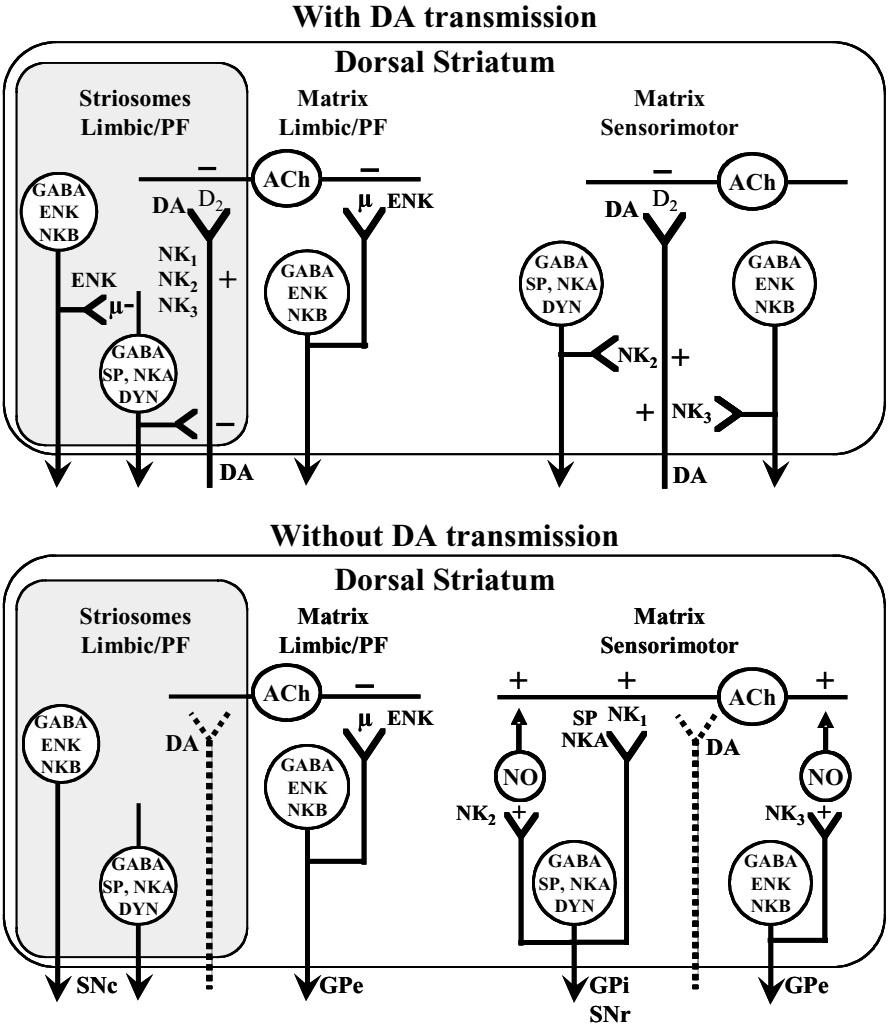

Figure 2. Schematic representation of the tachykinin and opioid peptide regulation of the cholinergic transmission in the limbic/PF and the sensorimotor territories of the dorsal striatum: *top*, in the presence DA transmission; *bottom*, in the absence of DA transmission.

nucleus via the median globus pallidus and the lateral habenula (Herkenham et al., 1979; Reisine et al., 1982; Rujakumar et al., 1993). As previously mentioned, the fronto-cortico-striatal circuits are altered in various neuropsychiatric disorders (Holt et al., 1999; Bradshaw and Sheppard, 2000; Graybiel and Rauch, 2000; Mallet et al., 2002; Saka and Graybiel, 2003). In several of these fronto-striatal disorders, circadian rhythms and opioid systems are also deregulated (Monteleone et al., 1994; McDougle et al., 1999; Pacchierotti et al., 2001). Therefore, by participating in the activity of fronto-basal ganglia circuits, the ENK/MOR inhibitory regulation of cholinergic transmission could be involved in such neuropsychiatric disorders.

Table 3. Effect of MOR antagonists on the NMDA-evoked release of ACh in the limbic/PF territory of the dorsal striatum.

	NMDA D-serine	+βFNA 0.1 nM	+βFNA 10 nM	+βFNA 1 μM
Control, morning	192 ± 6	206 ± 5	284 ± 13*	319 ± 10*
Control, afternoon	197 ± 8	284 ± 10*	361 ± 12*	519 ± 16*
αMPT, morning	333 ± 22	328 ± 14	299 ± 15	317 ± 12
αMPT, afternoon	336 ± 14	411 ± 15*	413 ± 17*	524 ± 21*

Superfusion experiments were performed as described in table 2. NMDA (1 mM + 10 μM D-serine) was applied for 2 min, 70 min after the beginning of the washing period. When used, MOR antagonist, β funaltrexamine (βFNA) and/or α MPT (100 μM) were added to the ACSF from the start of the washing period up to the end of the experiment. Results are the means ± S.E.M. of data obtained in 8 to 17 experiments. * $P < 0.05$ when the NMDA responses in the presence of MOR antagonist were compared to the effect of NMDA alone in various situations, control or α MPT; morning or afternoon.

4. CONCLUSION

In the dorsal striatum, tachykinin and opioid peptides are colocalized in striatal output neurones. When released from recurrent collaterals of these neurones, tachykinins and enkephalin exert a control on cholinergic transmission. This regulation by peptides exhibits a striatal territorial specificity. While ENK is present in the sensorimotor territory, the ENK/MOR regulation of ACh release is only observed in the limbic/PF territory. ENK is the endogenous ligand of MORs but also of delta opioid receptors which are present on striatal cholinergic interneurones. Thus, in addition to the ENK/MOR inhibitory regulation of cholinergic interneurones observed in the limbic/PF territory, an ENK/delta opioid receptors modulation of cholinergic transmission might occur in the sensorimotor territory of the dorsal striatum. Tachykinins participate in the increase in cholinergic transmission observed after degeneration of dopaminergic nigro-striatal neurones but, this regulation is only found in the sensorimotor territory of the dorsal striatum (Figure 2).

Tachykinin and opioid peptides play a major role in the control of the "DA-ACh balance" in the striatum. Interestingly, the suppression of dopaminergic transmission induces major changes in peptide regulations and thus in local circuits involved in the control of striatal cholinergic transmission that contribute to the "DA-ACh imbalance". These observations stress the limits of the current pathophysiological models of Parkinson's disease which only integrate deregulations of the direct postsynaptic control of DA on the striatal output neurones. A better understanding of the role of neuropeptides in the functional territories of the striatum could provide new therapeutic strategies in diseases associated with dysfunctions in sensorimotor and/or frontal cortico-basal ganglia circuits.

5. REFERENCES

Apicella, P., 2002, Tonically active neurons in the primate striatum and their role in the processing of information about motivationally relevant events. *Eur. J. Neurosci*. **16**:2017–2026.

Anderson, J.J., Kuo, S., Chase, T.N., and Engber, T.M., 1994, Dopamine D1 receptor-stimulated release of acetylcholine in rat striatum is mediated indirectly by activation of striatal neurokinin1 receptors. *J. Pharmac. Exp. Ther*. **269**:1144–1151.

Anderson, J.J., Randall, S., and Chase, T., 1995, The neurokinin1 receptor antagonist CP-99,994 reduces catalespsy produced by the dopamine D2 receptor antagonist raclopride: correlation with extracellular acetylcholine levels in striatum. *J. Pharmac. Exp. Ther.* **274**:928–936.

Aosaki, T., Kimura, M., and Graybiel, A.M., 1995, Temporal and spatial characteristics of tonically active neurons of the primate's striatum. *J. Neurophysiol.* 73:1234–1252.

Beaujouan, J.C., Saffroy, M., Torrens, Y., and Glowinski, J., 2000, Different subtypes of tachykinin receptor binding sites are present in the rat brain. *J. Neurochem*. **75**:1015–1026.

Beaujouan, J.C., Torrens, Y., Saffroy, M., Kemel, M.L., and Glowinski, J., 2004, A 25 year adventure in the field of tachykinins. *Peptides*. **25**:339–357.

Berendse, H.W., Galis-de Graaf, Y., and Groenewegen, H.J., 1992, Topographical organization and relationship with ventral striatal compartments of prefrontal corticostriatal projections in the rat. *J. Comp. Neurol*. **316**:314–347.

Blanchet, F., Gauchy, C., Perez, S., Soubrié, P., Glowinski, J., and Kemel, M.L., 1998, Distinct modifications by neurokinin1 (SR140333) and neurokinin2 (SR48968) tachykinin receptor antagonists of the N-Methyl-DAspartate-evoked release of acetylcholine in striosomes and matrix of the rat striatum. *Neuroscience*. **85**:1025–1036.

Blanchet, F., Kemel, M.L., Gauchy, C., Desban, M., Perez, S., and Glowinski, J., 1997, *N*-methyl-D-aspartate-evoked release of [^{3}H]-acetylcholine in striatal compartments of the rat: regulatory roles of dopamine and GABA. *Neuroscience*. **81**:113–127.

Bolam, J.P., and Bennett, B.D., 1995, Microcircuitry of the neostriatum. In: Molecular and cellular mechanisms of neostriatal function (Ariano, M.A., Surmeier, D.J., Eds), pp. 1–19. Austin, TX:Landes.

Bradshaw, J.L., and Sheppard, D.M. (2000) The neurodevelopmental frontostriatal disorders: evolutionary adaptiveness and anomalous lateralization. *Brain Lang*. **73**:297–320.

Centonze, D., Pisani, A., Bonsi, P., Giacomini, P., Bernardi, G., and Calabresi, P., 2001, Stimulation of nitric oxide-cGMP pathway excites striatal cholinergic interneurons via protein kinase G activation. *J. Neurosci*. **21**:1393–1400.

Daugé, V., Mauborgne, A., Cesselin, F., Fournié-Zaluski, M.C., and Roques, B.P., 1996, The dual peptidase inhibitor RB101 induces a long-lasting increase in the extracellular level of Met-enkephalin-like material in the nucleus accumbens of freely moving rats. *J. Neurochem*. **67**:1301–1308.

Delfs, J.M., Kong, H., Mestek, A., Chen, Y., You, L., Reisine, T., and Chesselet, M.F., 1994, Expression of mu opioid receptor mRNA in rat brain: an in situ hybridization study at the single cell level. *J. Comp. Neurol*. **345**:46–68.

Deniau, J.M., and Thierry, A.M., 1997, Anatomical segregation of information processing in the rat substantia nigra pars reticulata. In: *Advances in Neurology*, Lippincott-Raven Publishers, ed. Obeso, J.A., DeLong, M.R., Ohye, C., and Marsden, C.D., vol 74, Philadelphia, pp. 83–96.

Desban, M., Gauchy, C., Glowinski, J., and Kemel, M.L, 1995, Heterogeneous topographical distribution of the striatonigral and striatopallidal neurons in the matrix compartment of the cat caudate nuclues. *J. Comp. Neurol.* **30**:117–133.

Desban, M., Gauchy, C., Kemel, M.L, Besson, M.J., and Glowinski J., 1989, Three-dimensional organization of the striosomal compartment and patchy distribution of striato-nigral projections in the matrix of the cat caudate nucleus Neuroscience, **29**:551–566.

Desban, M., Kemel, M.L., Glowinski, J., and Gauchy, C., 1993, Spatial organization of patch and matrix compartments in the rat striatum. *Neuroscience*. **57**:661–671.

Duvoisin, R., 1967, Cholinergic-anticholinergic antagonists in Parkinsonism. *Arch. Neurol*. **17**:124–36.

Eblen, F., and Graybiel, A.M., 1995, Highly restricted origin of prefrontal cortical inputs to striosomes in the macaque monkey. *J. Neurosci*. **15**:5999–6013.

Emonds-Alt, X., Proietto, V., Steinberg, R., Oury-Donat, F., Vigé, X., Vilain, P., Naline, E., Daoui, S., Advenier, C., Le Fur, G., Maffrand, J.P., Soubrié, P., and Pascal, M., 2002, SSR240600 [(*R*)-2-(1-{2-[3,5-Bis(trifluotomethyl)-phenyl]acetyl}-2-(3,4-dichlorophenyl)-2-morpholinyl]ethyl}-4-piperidinyl)-2-methyl-propanamide], a centrally active nonpeptide antagonist of the tachykinin neurokinin-1 receptor: I. Biochemical and pharmacological characterization. *JPET* **303**:1171–1179.

Gerfen, C.R., and Wilson, C.J., 1996, The basal ganglia. In: *Handbook of Chemical Neuroanatomy, Integrated systems of the CNS*, Part III, vol 12, ed. Swanson, L.W., Bjorklund, A., and Hokfelt, T., Elsevier, Amsterdam pp. 371–468.

Graybiel, A.M., 1990, Neurotransmitters and neuromodulators in the basal ganglia. *Trends Neurosci*. **13**:244–254.

Graybiel, A.M., Aosaki, T., Flaherty, A.W., and Kimura, M., 1994, The basal ganglia and adaptative motor control. *Science*. **265**:1826–1831.

Graybiel, A.M., and Ragsdale, C.W., 1978, Histochemically distinct compartments in the striatum of human, monkey, and cat demonstrated by acetylthiocholinesterase staining. *Proc. Natl. Acad. Sci. USA*. **75**:5723–5726.

Graybiel, A.M., and Rauch, S.L., 2000, Toward a neurobiology of obsessive-compulsive disorder. *Neuron*. **28**:343–347.

Guttenberg, N.D., Klop, H., Minami, M., Satoh, M., and Voorn, P., 1996, Co-localization of mu opioid receptor is greater with dynorphin than enkephalin in rat striatum. *Neuroreport*. 7:2119–2124.

Herkenham, M., and Nauta, W.J.H., 1979, Efferent connections of the habenular nuclei in the rat. *J. Comp. Neurol*. **187**:19–48.

Herkenham, M., and Pert, C.B., 1981, Mosaic distribution of opiate receptors, parafascicular projections and acetylcholinesterase in rat striatum. *Nature*. **291**:415–417.

Holt, D.J., Herman, M.M., Hyde, T.M., Kleinman, J.E., Sinton, C.M., German, D.C., Hersh, L.B., Graybiel, A.M., and Saper, C.B., 1999, Evidence for a deficit in cholinergic interneurons in the striatum in schizophrenia. *Neuroscience*. **94**:21–31.

Jabourian, M., Bourgoin, S., Perez, S., Godeheu, G., Glowinski, J., and Kemel, M.L., 2004, Mu opioid control of the N-methyl-D-aspartate-evoked release of [^{3}H]-acetylcholine in the limbic/PF territory of the rat striatum in vitro: diurnal variations and implication of a dopamine link. *Neuroscience*. **123**:733–742.

Jabourian, M., Venance, L., Bourgoin, S., Ozon, S., Perez, S., Godeheu, G., Glowinski, J., and Kemel, M.L., 2005, Functional mu opioid receptors are expressed in cholinergic interneurones of the rat dorsal striatum. *Eur. J. Neurosci*. In press.

Kemel, M.L., Desban, M., Glowinski, J., and Gauchy, C., 1989, Distinct presynaptic control of dopamine release in striosomal and matrix areas of the cat caudate nucleus. *Proc. Natl. Acad. Sci. USA*. **86**:9006–9010.

Kemel, M.L., Desban, M., Glowinski, J., and Gauchy, C., 1992, Functional heterogeneity of the matrix compartment in the cat caudate nucleus as demonstrated by the cholinergic presynaptic regulation of dopamine release. *Neuroscience*. **50**:597–610.

Kemel, M.L., Pérez, S., Beaujouan, J.C., Jabourian, M., Soubrié, P., and Glowinski, J., 2003, The new neurokinin 1-sensitive receptor mediates the facilitation by endogenous tachykinins of the NMDA-evoked release of acetylcholine after suppression of dopaminergic transmission in the matrix of the rat striatum. *J. Neurochem*. **87**:487–496.

Kemel, M.L., Pérez, S., Godeheu, G., Soubrié, P., and Glowinski, J., 2002, Facilitation by endogenous tachykinins of the NMDA-evoked release of acetylcholine after acute and chronic suppression of dopaminergic transmission in the matrix of the rat striatum. *J. Neurosci*. **22**:1929–1936.

Kitabatake, Y., Hikida, T., Watanabe, D., Pastan, I., and Nakanishi, S., 2003, Impairment of reward-related learning by cholinergic cell ablation in the striatum. *Proc. Natl. Acad. Sci. USA*. **100**:7965–7970.

Krebs, M.O., Gauchy, C., Desban, M., Glowinski, J., and Kemel, M.L., 1994, Role of dynorphin and GABA in the inhibitory regulation of NMDA-induced dopamine release in striosome- and matrix-enriched areas of the rat striatum. *J. Neurosci*. **14**:2435–2443.

Kurumaji, A., Takashima, M., Ohi, K., and Takahashi, K., 1988, Circadian fluctuations in pain responsiveness and brain Met-enkephalin-like immunoreactivity in the rat. *Pharmacol. Biochem. Behav*. **29**:595–599.

Lendvai, B., Sandor, N.T., and Sandor, A., 1993, Influence of selective opiate antagonists on striatal acetylcholine and dopamine release. *Acta. Physiol. Hung*. **81**:19–28.

Mallet, L., Mesnage, V., Houeto, J.L., Pelissolo, A., Yelnik, J., Behar, C., Gargiulo, M., Welter, M.L., Bonnet, A.M., Pillon, B., Cornu, P., Dormont, D., Pidoux, B., Allilaire, J.F., and Agid, Y., 2002, Compulsions, Parkinson's disease, and stimulation. *Lancet*. **360**:1302–1204.

McDougle, C.J., Barr, L.C., Goodman, W.K., and Price, L.H., 1999, Possible role of neuropeptides in obsessive compulsive disorder. *Psychoneuroendocrinology*. **24**:1–24.

McGeorge, A.J., and Faull, R.L.M., 1989, The organization of the projection from the cerebral cortex to the striatum in the rat. *Neuroscience*. **29**:503–537.

Le Moine, C., Kieffer, B., Gaveriaux-Ruff, C., Befort, K., and Bloch, B., 1994, Delta-opioid receptor gene expression in the mouse forebrain: localization in cholinergic neurons of the striatum. *Neuroscience*. **62**:635–640.

Monteleone, P., Catapano, F., Del Buono, G., and Maj, M., 1994, Circadian rhythms of melatonin, cortisol and prolactin in patients with obsessive-compulsive disorder. *Acta. Psychiatr. Scand*. **89**:411–415.

Olanow, C.W., and Koller, W.C., 1998, An algorithm (decision tree) for the management of Parkinson's disease: treatment guidelines. *Neurology*. **50**:S1–57.

Pacchierotti, C., Iapichino, S., Bossini, L., Pieraccini, F., and Castrogiovanni, P., 2001, Melatonin in psychiatric disorders: a review on the melatonin involvement in psychiatry. *Front Neuroendocrinol*. **22**:18–32.

Preston, Z., Richardson, P.J., Pinnock, R.D., and Lee, K., 2000, NK-3 receptors are expressed on mousse striatal gamma-aminobutyric acid-ergic interneurones and evoke [(3)H]gamma-aminobutyric acid release. *Neurosci. Lett.* 284:89–92.

Rajakumar, N., Elisevich, K., and Flumerfelt, B.A., 1993, Compartmental origin of the striato-entopeduncular projection in the rat. *J. Comp. Neurol*. **331**:286–296.

Reisine, T.D., Soubrie, P., Artaud, F., and Glowinski, J., 1982, Involvement of lateralhabenula-dorsal raphe neurons in the differential regulation of striatal and nigral serotonineregic transmission cats. *J. Neurosci*. **2**:1062–1071.

Rupniak, N.M., and Kramer, M.S., 1999, Discovery of the antidepressant and anti-emetic efficacy of substance P receptor (NK_1) antagonists. *Trends Pharmacol. Sci.* **20**:485–490.

Saka, E., and Graybiel, A.M., 2003, Pathophysiology of Tourette's syndrome: striatal pathways revisited. *Brain Dev*. **25**:S15–S19.

Sharif, N.A., and Hughes, J., 1989, Discrete mapping of brain mu and delta opioid receptors using selective peptides: quantitative autoradiography, species differences and comparison with kappa receptors. *Peptides*. **10**:499–522.

Steinberg, R., Souilhac, J., Rodier, D., Alonso, X., Emonds-Alt, X., Le Fur, G., and Soubrié, P., 1998, Facilitation of striatal acetylcholine release by dopamine D1 receptor stimulation: involvement of enhanced nitric oxide production via neurokinin-2 receptor activation. *Neuroscience*. **84**:511–518.

Tang, F., Tang, J., Chou, J., and Costa, E., 1984, Age-related and diurnal changes in Met^5-Enk-Arg^6-Phe^7 and Met^5-enkephalin contents of pituitary and rat brain structures. *Life Sci*. **35**:1005–1014.

Tremblay, L., Kemel, M.L., Desban, M., Gauchy, C., and Glowinski, J., 1992, Distinct presynaptic control of dopamine release in striosomal- and matrix-enriched areas of the rat striatum by selective agonists of NK1, NK2, and NK3 tachykinin receptors. Proc. *Natl. Acad. Sci. USA*, **89**:11214–11218.

Wang, H., Gracy, K.N., and Pickel, V.M., 1999, Mu-opioid and NMDA-type glutamate receptors are often colocalized in spiny neurons within patches of the caudate-putamen nucleus. *J. Comp. Neurol*. **412**:132–146.

Werling, L.L., Frattali, A., Portoghese, P.S., Takemori, A.E., and Cox, B.M., 1988, Kappa receptor regulation of dopamine release from striatum and cortex of rats and guinea pigs. *J. Pharmacol. Exp. Ther*. **246**:282–286.

Section III

PHARMACOLOGICAL AND RECEPTOR STUDIES OF THE BASAL GANGLIA

LOCALIZATION AND FUNCTIONS OF KAINATE RECEPTORS IN THE RAT GLOBUS PALLIDUS

Xiao-Tao Jin and Yoland Smith*

1. INTRODUCTION

Kainate receptors (KARs) are a subtype of ionotropic glutamate receptors composed five subunits (GluR5, GluR6, GluR7, KA1 and KA2) (Hollmann and Heinemann, 1994). Recent studies have demonstrated that activation of KARs mediates a large variety of pre- and post-synaptic effects on neurotransmission. For instance, activation of presynaptic KARs modulates glutamatergic and GABAergic synaptic transmission, while postsynaptic activation induces a small and slow component of glutamatergic response at various synapses in the CNS (for review see Lerma, 2003; Huettner, 2003).

The globus pallidus (GP) plays a central integrative role in the basal ganglia circuitry (Plenz and Kitai, 1999; Bevan et al., 2002). The GP receives glutamatergic inputs from the subthalamic nucleus (STN) and sends GABAergic outputs back to the STN and other basal ganglia nuclei. The hyperactivity of the subthalamofugal glutamatergic projection and changes in the firing pattern of STN and GP neurons are critical in mediating abnormal activity of the basal ganglia circuitry under pathological conditions (Plenz and Kitai, 1999; Bevan et al., 2002).

We have shown that KARs are expressed pre- and post-synaptically in the monkey striatum (Charara et al., 1999; Kieval et al., 2001). Although recent functional studies demonstrated that activation of these receptors by exogenous application of KA modulates glutamatergic transmission in the striatum, none of these studies addressed the role of synaptically activated KARs in the basal ganglia (Casassus and Mulle, 2002; Crowder and Weiner, 2002). Recently, we have demonstrated that KARs immunoreactivity is also expressed in dendrites and glutamatergic axon terminals in the monkey GP (Kane-Jackson and Smith, 2003). These findings pave the way for pre- and post-synaptic KARs-mediated effects in this brain region. To further address this issue, we employed electron microscopic immunocytochemistry and whole cell recording techniques to determine the localization

* X-T. Jin and Y. Smith, Yerkes National Primate Research Center and Department of Neurology, Emory University, Atlanta, GA, USA.

and functions of KARs in rat GP. Consistent with our previous findings in monkeys, we found that GluR6/7 immunoreactivity is expressed in dendrites and glutamatergic terminals in the rat GP. Furthermore, our electrophysiological data provide evidence for KAR-mediated postsynaptic effects and presynaptic regulation of glutamatergic transmission in the rat GP.

2. MATERIALS AND METHODS

2.1. Electron Microscopic Immunocytochemistry

Two adult and two 17-d old Sprague Dawley rats were used in the present study. After deep anesthesia with an overdose of pentobarbital, rats were perfusion-fixed with 500 ml of cold oxygenated Ringer's solution followed by 4% paraformaldehyde and 0.1% glutaraldehyde in phosphate buffer (PB) (0.1 M, pH 7.4). The brains were then cut in 60-μm-thick sections with a vibrating microtome and processed for the immunohistochemical localization of GluR6/7 at the electron microscopic level.

Commercially available affinity-purified polyclonal GluR6/7 antiserum (Upstate Biotech, Lake Placid, NY, dilution 1.5 μg/ml) raised against a synthetic peptide corresponding to the C terminal of GluR6 subunit (TFNDRLPGKETMA) were used in this study. Details of the immunostaining protocols for light and electron microscopy are found in previous studies (Charara et al., 1999; Kieval et al., 2001). Sections processed for immunoperoxidase were stained with diaminobenzidine (DAB) using the avidinbiotin-peroxidase method (ABC, Vector Labs, Burlingame, CA, USA). After immunostaining, sections were processed for electron microscopy, and ultrathin sections of GP region were prepared.

Ultrathin sections collected from immunostained GP were scanned in the electron microscope for the presence of immunoreactive elements. Labeled structures were photographed and characterized on the basis of ultrastructural features described in Peters et al (1990). The total number of labeled elements from a series of ultrathin sections collected from blocks of GP tissue of 4 rats were tabulated and expressed as relative percentages of immunoreactive elements (see Charara et al., 1999; Kieval et al., 2001 for detail).

2.2. Whole-Cell Patch Clamp Recording

Whole-cell patch clamp recordings were performed on slices (300 μm) from 13 to 17-d old Sprague Dawley rats (Charles River Laboratories, Wilmington, MA). Parasagittal slices were made on a Vibratome 3000 (The Vibratome Company, St. Louis, MO) in ice-cold oxygenated sucrose buffer. Slices were stored at room temperature in a chamber containing artificial cerebrospinal fluid (ACSF) (in mM): 124 NaCl, 2.5 KCl, 1.3 $MgSO_4$, 1.0 NaH_2PO_4 and 2.0 $CaCl_2$, 20 glucose, 26 $NaHCO_3$ at pH 7.3–7.4 with 95% O_2, 5% CO_2 bubbling through it. The osmolarity of the ACSF was ~310 mOsm. During the recording, slices were maintained fully submerged in the recording chamber and perfused with oxygenated ACSF. GP neurons were visualized by IR-differential interference contrast microscopy (BX51Wl) using a 40X water immersion objective (Olympus, Pittsburgh, PA). Whole-cell recordings were made with glass pipettes (3–4 mΩ), that contained in (mM): 140 CsCl, 2 $MgCl_2$, 1 $CaCl_2$, 10 EGTA, 10 HEPES, 2 Mg_2ATP, 0.2 GTP, and 0.5% biocytin, pH 7.4 (300–310 mOsm). Cells were characterized as GP neurons if they fulfilled the

electrophysiological criteria established in previous studies (Kita and Kitai, 1991; Nambu and Llinas, 1994; Cooper and Stanford, 2000). Exogenous KA-induced currents were isolated pharmacologically by including 100 μM GYKI 52466, an AMPA receptor antagonist, 50 μM D-AP5, a NMDA receptor antagonist, 50 μM bicuculline, a GABA receptor antagonist and 0.5–1 μM tetrodotoxin (TTX), a Na^+ channel blocker. To record excitatory postsynaptic currents (EPSCs) in GP, a bipolar tungsten stimulation electrode (FHC, Bowdoinham, ME) was placed in the internal capsule. EPSCs were evoked with single pulses that ranged from 3 to 10 V delivered once every 15–20 sec. The paired-pulse facilitation (PPF) of evoked EPSCs was performed as follows: two stimuli of internal capsule were paired with an interstimulus interval of 40–50 ms. The ratio of peak2/peak1 was calculated.

All drugs were purchased from Toris Cookson (Ellisville MO). Signals were filtered at 5 kHz and digitized with a Digidata 1200 analog-to-digital converter (Axon Instruments, Foster City, CA). Data were analyzed off-line using pClamp 6 (Axon Instruments). All values were expressed as means ± SEM. Statistical significance was assessed by Student's *t* tests.

3. RESULTS

3.1. Pre and Postsynaptic Localization of GluR6/7 in the GP

In a first set of experiment, we used commercially available affinity-purified polyclonal antibody to immunohistochemically localize GluR6/7 at the electron microscope level. Consistent with our primate data (Kane-Jackson and Smith, 2003), proximal and distal dendrites were the most common postsynaptic immunoreactive elements encountered in the rat GP. In addition to postsynaptic elements, terminals forming symmetric or asymmetric synapses and small preterminal unmyelinated axons comprised most of the presynaptic labeling (Fig. 1A, B). Although the exact source of the small unmyelinated axons could not be definitively determined, the presence of GluR6/7 on terminals forming asymmetric synapses indicates that GluR6/7 is expressed in presynaptic glutamatergic boutons.

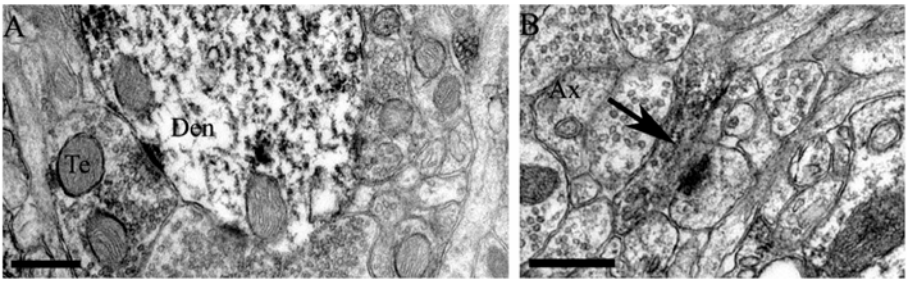

Figure 1. (A) GluR6/7-labeled dendrite (den), an axon terminal (TE) forming an asymmetric synapse. (B) GluR6/7-labeled unmyelinated axon (arrow). Scale bars, 0.5 μm.

3.2. Functional Kainate Receptors are Present on Postsynaptic GP Neurons

Our electron microscopic immunocytochemistry data demonstrate that GluR6/7 immunoreactivity is enriched in postsynaptic elements in the rat GP (Fig. 1A). To test whether these KAR subunits form functional receptors, we measured the amplitude of inward currents induced by bath application of kainate using whole-cell patch-clamp recording techniques. As described previously by others (Kita and Kitai, 1991; Nambu and Llinas, 1994; Cooper and Stanford, 2000) and in a recent study from our laboratory (Poisik et al., 2003), we recorded heterogeneous population of neurons that can be classified into three types on the basis of difference in spike frequency adaptation, timedependent inward rectification, cell's input resistance, and rebound spiking. Since we observed no significant differences in responses to kainate between these different populations of neurons, we combined the results.

GYKI 52466 is a specific AMPA receptor antagonist, which at a concentration of 100 μM, blocks AMPA receptors-mediated currents without significant effects on KARs (Paternain et al., 1995). Bath application of KA (3 μM) induced inward currents in presence of 50 μM D-AP5, 50 μM BIC, 0.5 μM tetrodotoxin (TTX) and 100 μM GYKI 52466. The inward currents evoked by KA were not significantly different in the absence or presence of 100 μM GYKI 52466 (69 ± 4.5 and 59 ± 1.8 pA, respectively. $n = 5$, $p = 0.08$, *t*-test) (Fig. 1A, B). However, it was significantly inhibited by 50 μM CNQX, an AMPA/KAR antagonist (4.4 ± 2.2 pA. $n = 5$, $p < 0.001$) (Fig. 2A, B).

To confirm that 100 μM GYKI 52466 is a selective antagonist for AMPA receptors in the slice of rat GP, we examined the effect of 100 μM GYKI 52466 on AMPAinduced inward currents. Bath application of AMPA (4 μM) induced inward currents that were significantly blocked by pretreatment of 100 μM GYKI 52466 (data not shown). Therefore, 3 μM of KA likely activates KARs and not AMPARs in the presence of 100 μM GYKI 52466. This is consistent with a previous study demonstrating that bath application of KA (1–3 μM) does not induce significant inward currents in nucleus accumbens neurons of GluR6$^{-/-}$ mice (Casassus and Mulle, 2002).

While exogenous application of kainate induces inward whole-cell membrane currents, it is unclear whether synaptically released glutamate can activate these postsynaptic KA receptors. To test this hypothesis, we stimulated the internal capsule medial and ventral to the GP and recorded evoked excitatory post synaptic currents (EPSCs) in presence of 50 μM D-AP5 and 50 μM BIC. Superfusion of slices with 100 μM GYKI 52466 reduced, but did not completely block, the EPSCs ($n = 6$) (Fig. 2C, D). On the other hand, GYKI 52466 plus 50 μM CNQX always produced almost complete inhibition of EPSCs ($n = 6$) (Fig. 2C, D). The remaining EPSC (the amplitude of residual EPSC) after application of GYKI 52466 was 18 ± 4% of control ($n = 6$) (Fig. 2D). The decay time for residual EPSCs was significantly longer than that condition in the absence of GYKI 52466 application.

3.3. Kainate Receptor Activation Reduces Evoked EPSCs

Previous studies from others have demonstrated that a low dose of KA (0.3–1 μM) modulates excitatory synaptic transmission in the striatum (Cassassus and Mulle, 2002; Crowder and Weiner, 2002). We therefore tested KA (0.1–1 μM) on glutamatergic synaptic transmission in GP. EPSCs were evoked every 15 s in GP neurons in presence of 50 μM D-AP5 and 50 μM BIC. Bath application of KA reversibly decreased EPSC amplitude

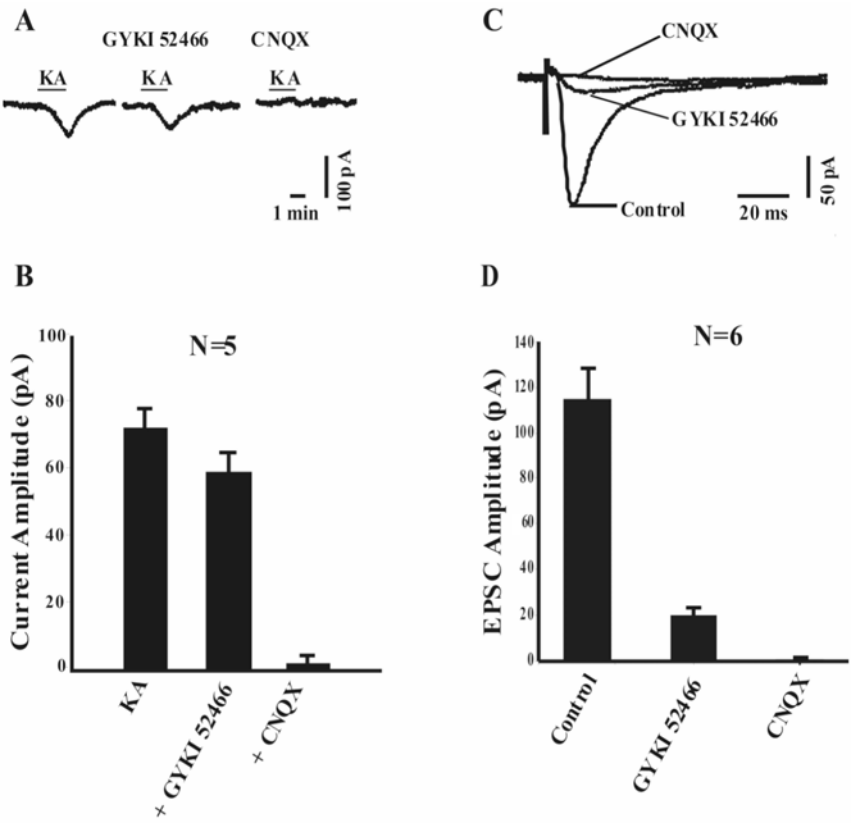

Figure 2. Functional expression of kainate receptors in rat GP. Inward currents evoked by 3 μM kainate in a GP neuron (A) and mean amplitude of inward currents evoked by 3 μM KA (mean ± SEM) (B). Currents were evoked by KA alone, in presence of GYKI 52466 (100 μM) or CNQX (50 μM). Synaptically evoked EPSCs recorded from a GP neuron (C) and mean amplitude of EPSC recorded in control condition and following bath application of GYKI 52466 or CNQX (mean ± SEM) (D).

as shown in figure 3A. On average, 1 μM of KA reduced EPSC amplitude to 43.5 ± 3.7% ($p < 0.001$, $n = 7$) (Fig. 3B). We have demonstrated that 1 μM KA is unlikely to active AMPA receptors under our experimental conditions. This indicates that 1 μM KA-induced EPSC depression is unlikely to be due to activation of AMPA receptors. If this is true, 1 μM KA should also reduce NMDA receptor-mediated EPSCs. Indeed, we found that application of 1 μM KA depressed NMDA receptor-mediated EPSCs to a similar degree as it did for AMPA receptor-mediated EPSCs (46.4 ± 2.9%, $p < 0.001$, $n = 13$) (Fig. 3C, D). However, when slices were pre-treated with AMPA/KA receptor antagonist CNQX, the effects of KA on the NMDAR-mediated EPSCs were abolished (8.4 ± 3.4%, $p = 0.07$, $n = 5$) (Fig. 3C, D). These results suggest that activation of KARs, but not AMPARs, are responsible for KAR activation-induced EPSC depression.

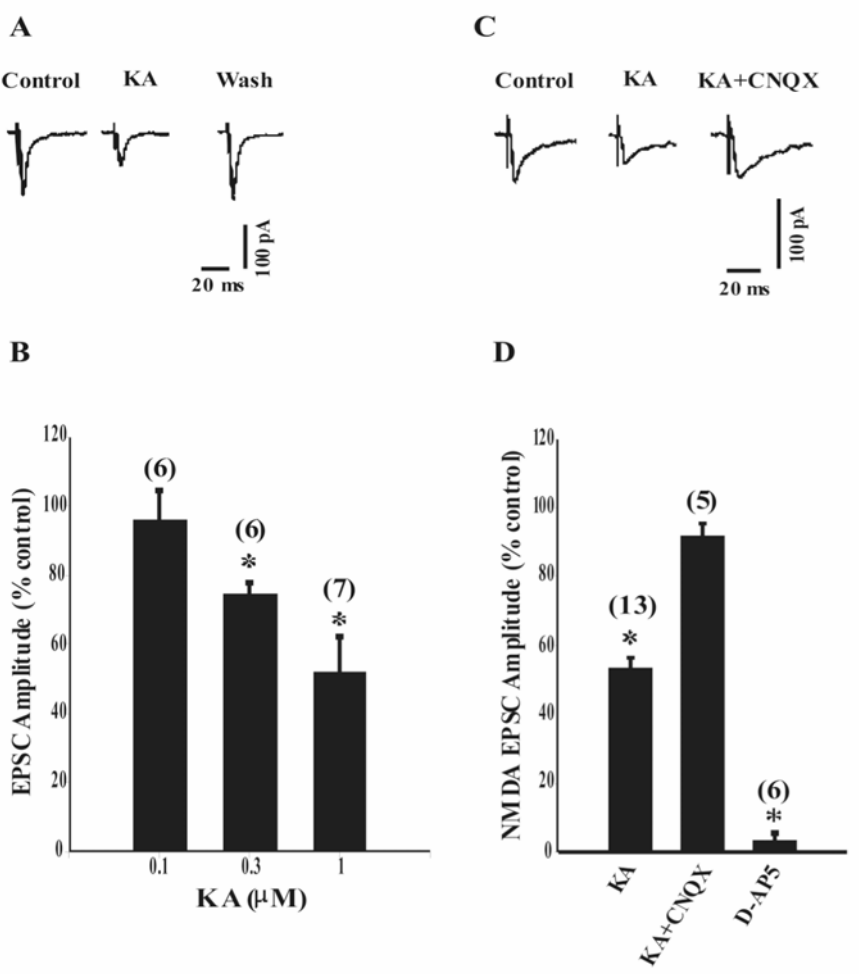

Figure 3. KAR activation inhibits glutamatergic synaptic transmission in rat GP. Application of KA (1 μM) depressed the evoked EPSCs recorded from a GP neuron (A). Summary bar graph showing the effect of bath application of KA (0.1–1 μM) on EPSC amplitude as percent of control (mean ± SEM) (B). NMDA-mediated EPSCs were reduced by KA (1 μM) and this inhibition was blocked by CNQX (C). Bar graph summarizes mean amplitude of NMDA-EPSC in presence KA alone, KA plus CNQX and D-AP5 alone as percent of control ± SEM. All recordings were done in presence of GYKI 52466, and bicuculline. Numbers in parentheses indicate the number of cells tested under each condition; significant difference from control: $*P < 0.001$.

3.4. Kainate Receptor Activation Reduces Evoked EPSCs via a Presynaptic Mechanism

To test whether KA-induced EPSC depression is modulated via a presynaptic mechanism, we studied the effect of KA on paired-pulse facilitation (PPF) ratio of evoked EPSCs. To record paired-EPSCs, two stimuli of internal capsule were paired with an interstimulus interval of 40–50 ms. As shown in figure 4, the peak of the second EPSC is usually larger than the first one. We then calculated the ratio of *peak*2/*peak*1 in the presence or absence

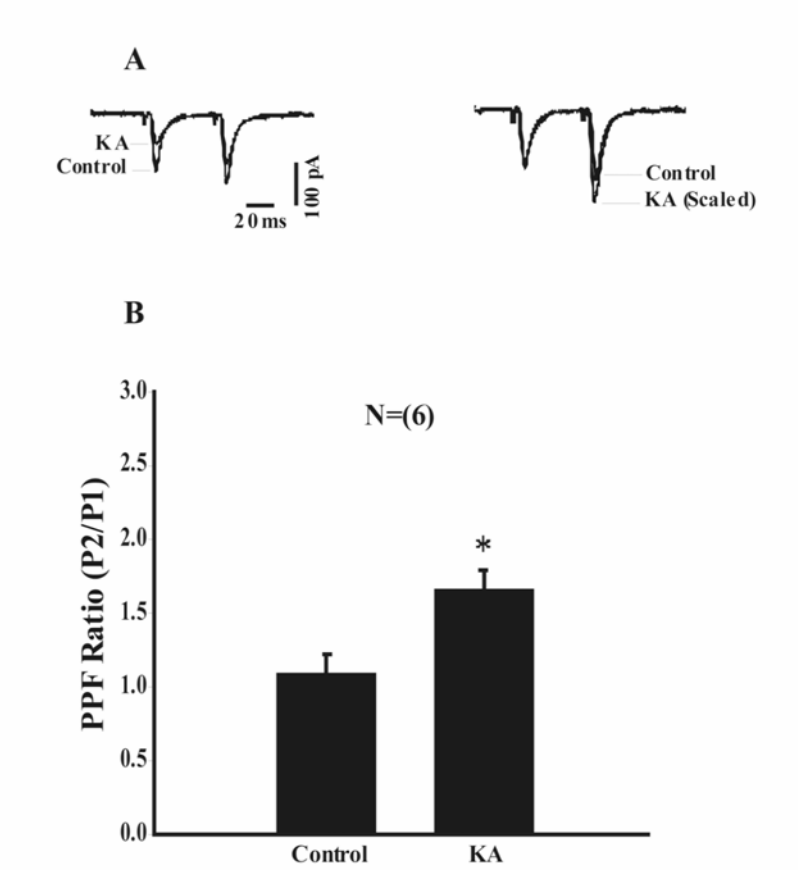

Figure 4. KAR activation increases paired-pulse facilitation (PPF) ratio at glutamatergic synapses in the GP. Effect of KA on paired EPSCs recorded from a GP neuron (A, left traces). The paired-pulse response to KA after scaling to the first EPSC (A, right traces). Bar graph summarizing the PPF ratio of EPSCs, expressed as mean ratio of P2/P1 ± SEM, in the absence or presence of KA. Significant difference from control: $*P < 0.001$.

of KA (1 μM). The ratio of *peak*2/*peak*1 was significantly increased in presence of KA ($p < 0.01$, $n = 6$) (Fig. 4), indicating a presynaptic effect. We also found that at 1 μM concentration, bath application of KA did not significantly change the cell's input resistance (data not shown). Therefore, it seems unlikely that KARs-induced depression of glutamatergic synaptic transmission was due to change in passive membrane properties.

4. DISCUSSION

The data presented in this study provide the first evidence for postsynaptic activation of KARs by exogenous applied KA and synaptic released glutamate in the rat globus pallidus. In line with EM results, we demonstrated that activation of KARs reduces glutamatergic synaptic transmission in GP neurons and that this effect is mediated by a presynaptic mechanism.

Under the condition of blockade of AMPA, NMDA, and $GABA_A$ receptors with their selective antagonists, bath application of 3 μM KA induced an inward current in all recorded GP neurons. Furthermore, these KA-induced currents were completely blocked by CNQX, an AMPA/KA receptor antagonist. The fact that these currents were resistant to AMPA receptor antagonist, but blocked by AMPA/KA receptor antagonist, demonstrates that they were mediated through activation of KARs. These results are consistent with previously published data showing that KA (1–3 μM) does not induce AMPA-mediated inward currents in nucleus accumbens neuron of GluR6-deficient mice (Casassus and Mulle, 2002).

Despite the fact that the amplitude of KAR-mediated EPSCs is much smaller than that of AMPARs-induced EPSC (for review see Lerma, 2003; Huettner, 2003), we recorded small EPSCs evoked by individual stimuli in internal capsule in the presence of AMPA and NMDA receptor antagonists. Consistent with previous reports, we found that this EPSC was resistant to GYKI 52466, but completely blocked by CNQX. Furthermore, the decay time for residual EPSCs were significantly longer than that of AMPAR-mediated EPSCs (Castillo et al., 1997; Kidd and Isaac, 1999; Li and Rogawski, 1998; Li et al., 1999). These results suggest that KARs in rat GP could be activated by synaptically released glutamate.

In line with several studies conducted in hippocampus (Contractor et al., 2000; Kamiya and Ozawa 1998, 2000; Schmitz et al., 2000; Frerking et al., 2001) and nucleus accumbens core region (Crowder and Weiner, 2002; Casassus and Mulle, 2002), our data demonstrate that bath application of KA reduces the amplitude of EPSCs recorded in GP neurons. This effect is likely modulated by KARs because the concentration of KA (1 μM) used in our experiments did not activate AMPA receptors (Casassus and Mulle, 2002). In addition, 1 μM KA also inhibited NMDAR-mediated EPSCs to a similar degree as it did for AMPAR-mediated EPSCs, and this inhibition was insensitive to GYKI 52466, but completely blocked by CNQX.

We next sought to determine the action site of KA on glutamatergic synaptic transmission in rat GP. It has been described in several brain regions that the inhibition of synaptic transmission by KA is modulated, at least in part, by activation of presynaptic KARs (Contractor et al., 2000; Kamiya and Ozawa 1998, 2000; Schmitz et al., 2000; Frerking et al., 2001; Crowder and Weiner, 2002). Our results, indeed, showed that KA inhibition of EPSCs was associated with a significant increase in PPF ratio. Increase in PPF suggests a presynaptic decrease in the probability of neurotransmitter release (Manabe et al., 1993). In line with this result, our electron microscope immunohistochemical data have demonstrated that GluR6/7 immunoreactivity is expressed in putative glutamatergic axon terminals in the rat GP (Fig. 1). In addition to presynaptic modulation, it has been discussed that kainate receptor activation in the postsynaptic neuron reduces the input resistance, which could shunt IPSCs or EPSCs (Contractor et al., 2000; Frerking et al., 1999). However, we did not record a significant amount of inward current following application of 1 μM KA. Thus, we conclude that the reduction of EPSCs induced by KA was modulated by a presynaptic mechanism that did not associate with a significant change in input resistance of GP neurons.

It is known that the STN is by far the main source of glutamatergic inputs to the GP. Thus, KARs-modulated inhibition of EPSCs in rat GP is likely due to activation of KARs in subthalamo-pallidal terminals. However, because a small number of brainstem and thalamic glutamatergic fibers also innervate the GP (Kincaid et al., 1991; Naito and Kita, 1994; Mouroux et al., 1997), we cannot rule out the possibility that activation of KARs at these terminals may also account for the pre-synaptic effect demonstrated in our study.

5. ACKNOWLEDGEMENTS

The authors thank Jean-Francois Paré and Susan Maxson for technical assistance. The work was supported by a grant from the US Army, the Yerkes Primate Center NIH base Grant and Award from Merck/Center for Neurodegenerative Diseases at Emory University.

6. REFERENCES

Bevan, M.D., Magill, P.J., Terman, D., Bolam, J.P., and Wilson, C.J., 2002, Move to the rhythm: Oscillations in the subthalamic nucleus external globus pallidus network. *Trends Neurosci.* **25**:525–531.

Casassus, G., and Mulle, C., 2002, Functional characterization of kainate receptors in the mouse nucleus accumbens. *Neuropharm.* **42**:603–611.

Castillo, P.E., Malenka, R.C., and Nicoll, R.A., 1997, Kainate receptors mediate a slow postsynaptic current in hippocampal CA3 neurons. *Nature.* **388**:182–186.

Charara, A., Blankstein, E., and Smith, Y., 1999, Presynaptic kainate receptors in the monkey striatum. *Neuroscience.* **91**:1195–1200.

Contractor, A., Swanson, G.T., Sailer, A., O'Gorman, S., and Heinemann, S.F., 2000, Identification of the kainate receptor subunits underlying modulation of excitatory synaptic transmission in the CA3 region of the hippocampus. *J. Neurosci.* **20**:8269–8278.

Cooper, A.J., and Stanford, I.M., 2000, Electrophysiological and morphological characteristics of three subtypes of rat globus pallidus neurons in vitro. *J. Physio* (London). **527**:291–304.

Crowder, T.L., and Weiner, J.L., 2002, Functional characterization of kainate receptors in the rat nucleus accumbens core region. *J. Neurophysiol.* **88**:41–48.

Frerking, M., Petersent, C.C., and Nicoll, R.A., 1999, Mechanisms underlying kainate receptor-mediated disinhibition in the hippocampus. *Proc. Natl. Acad. Sci.* U.S.A. **96**:12917–12922.

Frerking, M., Schmitz, D., Zhou, Q., Johansen, J., and Nicoll, R.A., 2001, Kainate receptors depress excitatory synaptic transmission at CA3—CA1 synapses in the hippocampus via a direct presynaptic action. *J. Neurosci.* **21**:2958–2966.

Hollman, M., and Heinemann, S., 1994, Cloned glutamate receptors. *Annu. Rev. Neurosci.* **17**:3–108.

Huettner, J.E., 2003, Kainate receptors and synaptic transmission. *Prog. Neurobiol.* **70**:387–407.

Kamiya, H., and Ozawa, S., 1998, Kainate receptor-mediated inhibition of presynaptic Ca2+ influx and EPSP in area CA1 of the rat hippocampus. *J. Physiol.* (Lond). **509**:833–845.

Kamiya, H., and Ozawa, S., 2000, Kainate receptor-mediated presynaptic inhibition at the mouse hippocampal mossy fiber synapse. *J. Physiol.* (Lond). **523**:653–665.

Kane-Jackson, R., and Smith, Y., 2003, Pre-synaptic kainate receptors in GABAergic and glutamatergic axon terminals in the monkey globus pallidus. *Neuroscience.* **120**:285–289.

Kidd, F.L., and Isaac, J.T., 1999, Development and activity-dependent regulation of kainate receptors at thalamocortical synapses. *Nature.* **400**:569–573.

Kieval, J.Z., Hubert, G.W., Charara, A., Pare, J.F., and Smith, Y., 2001, Subcellular and subsynaptic localization of presynaptic and postsynaptic kainate receptor subunits in the monkey striatum. *J. Neurosci.* **21**:8746–8757.

Kincaid, A.E., Penney, J.B., Young, J.R., and Newman, S.W., 1991, The globus pallidus receive a projection from the parafassicular nucleus in the rat. *Brain. Res.* **553**:18–26.

Kita, H., and Kitai, S.T., 1991, Intracellular study of rat globus pallidus neurons: membrane properties and responses to neostriatal, subthalamic and nigral stimulation. *Brain. Res.* **564**:296–305.

Lerma, J., 2003, Roles and rules of kainate receptors in synaptic transmission. *Nat. Rev. Neurosci*. **4**:481–495.

Li, H., and Rogawski, M.A., 1998, GluR5 kainate receptor mediated synaptic transmission in rat basolateral amygdala in vitro. *Neuropharmacol.* **37**:1279–1286.

Li, P., Wilding, T.J., Kim, S.J., Calejesan, A.A., Huettner, J.E., and Zhuo, M., 1999, Kainate receptormediated sensory synaptic transmission in mammalian spinal cord. *Nature.* **397**:161–164.

Manabe, T, Wyllie, D.J.A., Perkel, D.J., and Nicoll, R.A., 1993, Modulation of synaptic transmission and long-term potentiation: effects on paired pulse facilitation and EPSC variance in the CA1 region of hippocampus. *J. Neurophysiol.* **70**:1451–1459.

Mouroux, M., Hassani, O.K., and Féger, J., 1997, Electrophysiological and Fos immunohistochemical evidence for the excitatory nature of the parafascicular projection to the globus pallidus. *Neuroscience.* **81**: 387–397.

Naito, and Kita, H., 1994, The cortical-pallidal projection in the rat: an anterograde tracing study with biotinylated dextran amine. *Brain. Res*. **653**:251–257.

Nambu, A., and Llinas, R., 1994, Electrophysiology of globus pallidus neurons in vitro. *J. Neurophysiol.* **72**: 1127–1139.

Paternain, A.V., Morales, M., and Lerma, J., 1995, Selective antagonism of AMPA receptors unmasks kainate receptor-mediated responses in hippocampal neurons. *Neuron.* **14**:185–189.

Peters, A., Palay, S.L., and Webster, H. DeF., 1991, The fine structure of the nervous system: Neurons and their supporting cells. Oxford Univ. Press: New York, 494 pp.

Plenz, D., and Kitai, S.T., 1999, A basal ganglia pacemaker formed by the subthalamic nucleus and external globus pallidus. *Nature.* **400**:677–682.

Poisik, O.V., Mannaioni, S., Traynelis, Y., and Smith, Conn. P.G.J., 2003, Distinct functional roles of the metabotropic glutamate receptors 1 and 5 in the rat globus pallidus. *J. Neurosci.* **23**:122–120.

Schmitz, D., Frerking, M., and Nicoll, R.A., 2000, Synaptic activation of presynaptic kainate receptors on hippocampal mossy fiber synapses. *Neuron.* **27**:327–338.

OLIGOMERIZATION OF DOPAMINE D1 AND GLUTAMATE NMDA RECEPTORS: A NEW MECHANISM REGULATING STRIATAL FUNCTION

Chiara Fiorentini, Chiara Busi, Sandra Bontempi, PierFranco Spano, and Cristina Missale[1]

1. INTRODUCTION

The striatum and its ventral extension, the nucleus accumbens, are key areas of the basal ganglia controlling different physiological functions from motor planning to reward seeking and procedural learning (Nicola et al., 2000; Olanow et al., 2000). Essentially the activity of these nuclei are intimately linked to their massive dopaminergic innervation originating in the substantia nigra and the ventral tegmental area. The critical importance of dopamine (DA) in this system is demonstrated by the devastating symptoms of Parkinson's disease, a neurological disorder caused by the degeneration of nigral dopaminergic neurons and the consequent drop of DA levels in the striatum. Dysfunctions of the DA transmission in these areas are also thought to be critical determinants in other neuropsychiatric disorders including schizophrenia and drug addiction. In addition to DA, the striatum receives a major glutamatergic innervation from the cortex conveying sensorimotor information (Smith and Bolam, 1990; Graybiel, 1990) and there is a general agreement that an integrated interplay between DA and glutamate inputs is essential to drive correct motor behaviour. On this line, it has been suggested that the loss of DA neurons in Parkinson's disease is associated with dysregulated glutamate activity. The concurrent modification of these neuronal systems thus appear to play a central role in the development of movement disorders. At the cellular level, glutamatergic and dopaminergic fibres converge on striatal medium spiny projection neurons (Smith and Bolam, 1990) to form a "synaptic triad" at postsynaptic dendritic spines and this close spatial proximity provides an anatomical basis for the coordinated regulation of striatal neuron excitability by these two afferent pathways. The aim of this paper is to overview the molecular mechanisms involved in the post-synaptic cross-talk between DA and glutamate in the basal ganglia.

[1] Division of Pharmacology, Department of Biomedical Sciences and Biotechnology and Centre of Excellence on Diagnostic and Therapeutic Innovation, University of Brescia, 25123 Brescia, Italy

2. FUNCTIONAL INTERACTIONS BETWEEN DA AND GLUTAMATE IN THE STRIATUM

DA interacts with five receptors, belonging to the seven-transmembrane G protein-coupled receptor (GPCR) family, that are divided into D1-like (D1 and D5) and D2-like (D2, D3, D4) subtypes (Missale et al., 1998). Each receptor displays a unique set of properties including affinity for DA, potential for alternative splicing, specificity of G protein coupling and neuronal distribution (Missale et al., 1998; Aizman et al., 2000; Surmeier et al., 1996). In particular, in the striatum the D1 receptor is preferentially expressed in neurons of the direct pathway, that project to the internal globus pallidus (GPi) and the substantia nigra pars reticulata (SNr) and that also express low levels of D3 and D4 receptors (Surmeier et al., 1996). On the other hand, the D2 receptor is selectively expressed in neurons of the indirect pathway, that also express low levels of the D5 receptor and project to the GPi/SNr via the external globus pallidus and the subthalamic nucleus (Surmeier et al., 1996; Aizman et al., 2000). Glutamate exerts its effects at the ionotropic receptors NMDA and AMPA/kainate, as well as at metabotropic receptors (Dingledine et al., 1999; Hollman and Heineman, 1994). NMDA receptors are heteromeric complexes formed by two families of homologous subunits, NR1 and NR2A-D. Further heterogeneity is generated by alternative splicing of the NR1 gene giving rise to a total of eight isoforms with different structural and pharmacological properties (Dingledine et al., 1999; Hollman and Heineman, 1994; Zukin and Bennet, 1995).

DA and glutamate have long been known to interact at multiple levels in the striatum. In particular, the existence of a presynaptic interaction was revealed by the observation that striatal glutamatergic transmission is modulated by DA receptor activation and that DA release is regulated by glutamate (Morari et al., 1998). Moreover dopaminergic and glutamatergic terminals can indirectly interact via interposition of striatal interneurons (Centonze et al., 1999). Medium spiny neurons, on the other hand, present a high degree of co-localization of subtypes of DA and glutamate receptors (Nicola et al., 2000; Landwehmeyer et al., 1995; Surmeier et al., 1996) strongly supporting the existence of a cross-talk between these transmitter systems also at the postsynaptic level. From a functional point of view it is well established that the firing activity of medium spiny neurons, which is determined by cortical glutamate via activation of both AMPA and NMDA receptors, is modulated by DA (Nicola et al., 2000). In particular, there is evidence that DA attenuates the responses associated with activation of non-NMDA receptors, but potentiates those mediated by NMDA receptors (Nicola et al., 2000). This bidirectional modulation depends on the DA receptor subtype preferentially activated. Activation of D2 receptors has been reported, in fact, to inhibit AMPA-mediated responses, while D1 receptors modulate NMDA channel activity (Nicola et al., 2000). In particular, D1 receptor stimulation in medium spiny neurons enhances NMDA-induced whole cell currents (Nicola et al., 2000; Levine et al., 1996) and is a critical requirement for the formation of NMDA-mediated long term potentiation (LTP) at corticostriatal synapses (Nicola et al., 2000; Calabresi et al., 1996; Kerr and Wickens, 2001). Multiple mechanisms contribute to D1 agonist-induced potentiation of NMDA-evoked responses. In particular, activation of L-type voltage-gated Ca^{2+} channels has been implicated in this interaction on the basis of the observations that DA activates these channels via D1 receptors and that selective calcium entry blockers reduce D1-mediated potentiation of NMDA responses (Cepeda et al., 1998; Nicola et al., 2000). Another important mechanism is represented by D1 receptor-mediated phosphorylation of NMDA receptor subunits. In the striatum the D1 receptor activates in fact the cyclic AMP

signalling pathway, modulating protein kinase A (PKA) activity (Missale et al., 1998). PKA both directly and indirectly, through activation of the protein phosphatase inhibitor DARPP-32 (Fienberg et al., 1998), increases the phosphorylation state and activity of many physiological effectors, including the NR1 subunit of NMDA receptor (Blank et al., 1997; Flores-Hernandez et al., 2002; Calabresi et al., 2000), an effect resulting in increased channel activity. On this line, D1 receptor potentiation of NMDAmediated responses is mimicked by other activators of the cAMP-PKA pathway such as forskolin (Blank et al., 1997) and is lost in transgenic mice lacking DARPP-32 (Flores-Hernandez et al., 2002; Calabresi et al., 2000). More recently, it has been reported that D1 receptor activation induces the rapid translocation of NMDA receptor subunits to postsynaptic sites (Dunah and Standaert, 2001) and that activation of NMDA receptors in striatal neurons recruits D1 receptors from cytoplasmic sites to the plasma membrane and dendritic spines (Scott et al., 2002). Thus D1 receptor-mediated reinforcement of NMDA transmission may also rely on the coordinated regulation of receptor trafficking to synaptic sites, resulting in increased number of both NMDA receptors available for neurotransmission and D1 receptors activating the cAMP/PKA pathway. Furthermore, a unique protein-protein coupling between the D1 receptor and NMDA receptor subunits, has been identified in the striatum (Lee et al., 2002; Fiorentini et al., 2003) which adds complexity to the functional cross-talk between these receptor systems.

3. OLIGOMERIZATION, A NEW PARADIGM IN THE REGULATION OF RECEPTOR FUNCTION

The classical idea that GPCRs function as monomeric entities has been unsettled by the emerging concept of hetrodimerization. Recent findings have in fact indicated that many GPCRs can interact not only with closely and distantly related members of the same family, but also with structurally and functionally divergent families of receptors such as ligand-gated channels to form heterodimeric complexes (Angers et al., 2002). In several cases receptors are folded as constitutive multimeric units early after biosynthesis within the endoplasmic reticulum and transported to the cell surface as oligomeric arrays; in this case oligomerization is independent of agonist treatment. Alternatively, receptors may be transported as monomers to the cell membrane where they are assembled into oligomeric complexes in an agonist-dependent way (Devi, 2001). Heterodimerization between receptor subtypes has important functional roles. The pharmacological profile, G protein coupling, downstream signalling and regulatory processes such as internalization have been shown, in fact, to be influenced by the dimeric nature of the receptors. In addition to fundamentally changing our view of the structure and activity of GPCRs, the concept of heterodimerizaton could also have a dramatic impact on drug development and screening.

In the case of the dopaminergic system, it has been reported that the D2 receptors interact with the SST5 somatostatin receptor to form a complex with higher affinity for agonists and higher signalling efficacy (Rochevill et al., 2000), the D1 receptor binds to the adenosine A1 receptor forming a complex with decreased transductional efficiency (Gines et al., 2000), the adenosine A2A receptor antagonistically modulates both affinity and signalling of D2 and D3 receptors by direct protein-protein interaction (Canals et al., 2003; Torvinen et al., 2005) and the D2 and D3 receptors form a heteromeric complex with peculiar pharmacological and signalling properties (Scarselli et al., 2001). Moreover there is evidence that DA receptors also interact with structurally and functionally distant

receptors such as multimeric ligand-gated ion channels. The first example of such an interaction is that involving the GABAA receptor and the D5 receptor and enabling mutually inhibitory functions (Liu et al., 2000). Hetero-oligomerization thus defines a new level of functional diversity in endogenous DA receptor signalling.

4. CO-LOCALIZATION AND CLUSTERING OF D1 AND NMDA RECEPTORS AT CORTICO-STRIATAL SYNAPSES

In the striatum the D1 receptor is mostly localized in GABAergic medium spiny neurons containing substance P and dynorphin; on the other hand, neurons containing preproenkephalin A do not express the D1 mRNA, suggesting a selective association of D1 receptors with the direct output pathway (Missale et al., 1998; Surmeier et al., 1996). Ultrastructural studies have shown that the D1 receptor is present on dendrites and dendritic spines, both in the spine neck and head, and, to a lesser extent in the postsynaptic density (PSD) (Hersch et al., 1995; Yung et al., 1995; Bergson et al., 1995). This highly organized subcellular distribution is typical of the glutamatergic synapse and consists of a complex network of proteins critically involved in synaptic plasticity, including the glutamate NMDA receptors and their scaffolding and signalling proteins (Kennedy, 2000). This partial overlap in the subcellular distribution of NMDA and D1 receptors together with the observation that the delivery of both receptors to synapses is dependent on glutamate transmission (Scott et al., 2002; Barria and Malinov, 2002) led us to investigate whether direct protein-protein interactions may be involved in the trafficking of these receptors to the same subcellular domain.

For this purpose the PSD fraction was isolated from striatal homogenates and analyzed for the content of D1 and NMDA receptors as well as other specific proteins. The results have shown that the D1 receptor is indeed concentrated in this neuronal microdomain, displaying a subcellular distribution that is consistent with the localization of NMDA receptors (Fig. 1). Co-immunoprecipitation studies were also performed to evaluate whether D1 and NMDA receptors interact in striatal PSD. As shown in Fig. 1, a 50 kDa band, that was detected by the anti-D_1 receptor antibody, was present in PSD proteins immunoprecipitated with the antibody against the NR1 subunit of the NMDA receptor. Similarly, the anti-D1 receptor antibody immunoprecipitated a 116 kDa species corresponding to NR1, indicating relevant complex formation between these two holoreceptor moieties.

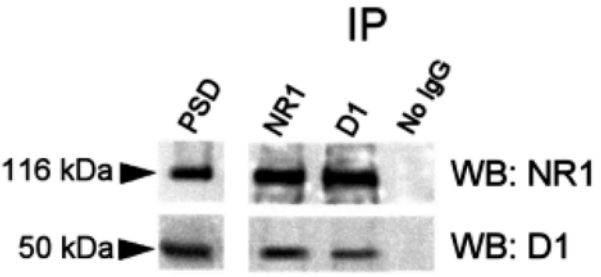

Figure 1. Co-localization and co-clustering of D1 and NMDA receptors in striatal PSD.

Analysis of the domains involved in GPCR interactions has implicated the extracellular, the transmembrane (TM) or the C-terminal regions. For example, TM regions are involved in D2/D3 receptor dimerization (Scarselli et al., 2001), while the Cterminal domains are involved in the interaction between D5 and $GABA_A$ receptors (Liu et al., 2000). Since the D1 receptor has a relatively long C-terminal domain, that is divergent from that of its homologous D5 receptor, thus conferring receptor subtype-selective properties, we evaluated whether this region is involved in the interaction with the NMDA receptor. Pull out experiments were thus performed with GST-fusion proteins containing the C-terminal domains of both D1 and D5 receptors.

The results showed that the C-terminal tail of the D1 receptor, but not that of the D5 receptor, is able to bind to the NR1 subunit of the NMDA channel. By contrast, the NR2A/B subunits were not pulled out from striatal PSD by the D1 receptor C-terminal region indicating that in striatal PSD the D1 receptor selectively interacts with the NR1 subunit of the NMDA channel. The NR1 gene generates eight splice variants, with four possible carboxyltermini[11]. By taking advantage of GST-fusion proteins containing different domains of the NR1 C-terminal tail we demonstrated that both NR1A/B and NR1E/F isoforms may interact with the D1 receptor (Fiorentini et al., 2003). These isoforms differ for their physiological and pharmacological properties and also show different regional and cellular distribution (Landwehrmyer et al., 1995; Zukin and Bennet, 1995). Our results point to the capability of interacting with the D1 receptor as a further difference among these isoforms and suggest that the interaction between D1 and NMDA receptors might be a specific feature of certain neuronal populations.

5. D1 AND NMDA RECEPTORS CONSTITUTIVELY INTERACT IN LIVING CELLS

Fluorescence resonance energy transfer (FRET) and bioluminescence resonance energy transfer (BRET) are newly developed techniques that detect energy transfer between a fluorescent or luminescent donor and a fluorescent acceptor when they are in close proximity. These methods are now considered the systems of choice to study protein-protein interactions since they allow the monitoring of protein oligomerization in living cells without disrupting the natural environment where they are clustered, thus eliminating the possibility of artifactual aggregation that could happen during the solubilization and concentration of membrane proteins (Angers et al., 2002; Devi, 2001). On this line, we evaluated D1 and NMDA receptor interactions in living cells by BRET (Fiorentini et al., 2003). The D1 receptor was fused with *Renilla* luciferase (Rluc) and NR1 was fused with the green fluorescent protein (GFP) and the BRET signal was recorded in COS-7 cells simultaneously or individually expressing these two molecular species. As summarized in Table 1, no BRET signal was detected in cells expressing NR1-GFP and a negligible, non specific signal was detected in cells expressing the D1-Rluc construct. However, tagged D1 receptor and NR1 subunit generated a significant and specific BRET signal when co-transfected in the same cells. This signal did not change in the presence of NR2B suggesting that there is no competition between NR1 and NR2B for interaction with the D1 receptor. Moreover, the BRET signal recorded in cells co-transfected with D1-Rluc, NR1-GFP and NR2B was insensitive to stimulation by 50 μM DA and 100 μM glutamate/10 μM glycine either given alone or in combination. These observations thus point to a constitutive, direct and selective interaction of the D1 receptor with the NR1 subunit of the NMDA channel. To verify

Table 1. Detection of D1 and NMDA receptor interaction by BRET.

	BRET ratio	
	Basal	Agonist stimulation
D1-Rluc	0.03	–
NR1-GFP	0	–
D1-Rluc/NR1-GFP	0.1*	–
D1-Rluc/NR1-GFP/NR2B	0.09*	0.08*

Transfected cells were left untreated or exposed to 50 μM DA and 100 μM glutamate/10 μM glycine.
* $p < 0.001$ vs. D1-Rluc, Student's t test.

whether the D1R/NMDAR interaction is constitutive also in the striatum we treated male Wistar rats with either the D1 antagonist SCH23390 (1 mg/kg, s.c.) or the NMDA channel blocker MK-801 (0.1 mg/kg, s.c.). Co-immunoprecipitation experiments on purified striatal triton-insoluble fractions from these animals, revealed that inhibition of endogenous agonist activation of both D1 and NMDA receptors did not modify their capability to interact, pointing to a constitutive interaction also in the striatum (Fiorentini et al., 2004).

6. FUNCTIONAL IMPLICATIONS OF D1 AND NMDA RECEPTOR OLIGOMERIZATION

It has been suggested that constitutive oligomeric complexes are mostly assembled in the endoplasmic reticulum (ER) and transported to the cell membrane as preformed units. To identify the cellular compartment of D1 and NMDA receptor clustering, HEK293 cells transfected with the D1 receptor and the NR1 subunit were analyzed by confocal microscopy immunofluorescence (Fiorentini et al., 2003). The results indicated that the trafficking of the D1 receptor is substantially modified by its interaction with the NMDA receptor. In particular, in transfected HEK293 cells the D1 receptor was targeted to the plasma membrane, while the NR1 subunit was retained into the ER. These data are consistent with the observation that, in the absence of NR2 subunits, NR1 is usually accumulated into the cytoplasm (Barria and Malinov, 2002) due to the presence of an ER retention motif in its C-terminus (Scott et al., 2001) and that co-expression of NR2 subunits is necessary to drive the NMDA receptor complex to the plasma membrane (Barria and Malinov, 2002). In HEK293 cells co-transfected with the D1 receptor and NR1 subunit, both species were localized into the cytoplasm, suggesting that interaction with NR1 prevents D1 receptor delivery to the plasma membrane. In the presence of the NR2B subunit, however, the cytoplasmic retention of the D1 receptor/NR1 complex was relieved and the D1/NMDA receptor unit was translocated to the plasma membrane. These observations suggest that in striatal medium spiny neurons D1 and NMDA receptors are assembled into the ER as constitutive oligomeric complexes and are delivered to functional sites as preformed units. Interaction with the NMDA receptor may thus represent the mechanism that recruits the D1 receptor to the PSD of cortico-striatal synapses. It is generally accepted that the efficacy of cortico-striatal transmission is dependent on the concurrent activation of D1 and NMDA receptors. (Nicola et al., 2000; Levine et al., 1996; Calabresi et al., 1996; Fienberg et al., 1998; Flores-Hernandez et al., 2002). In this context, the direct interaction between D1 and

NMDA receptors and its influence on D1 receptor trafficking may be crucial to recruit the D1 receptor in the place of synaptic plasticity and to keep it in close proximity of the NMDA receptor to allow rapid cAMP/PKA/DARPP32-mediated potentiation of NMDA transmission (Blank et al., 1997; Calabresi et al., 2000; Flores-Hernandez et al., 2002).

Interestingly, the clustering of D1 and NMDA receptors does not simply represent a chaperon-like strategy to transport the D1 receptor in the place of synaptic plasticity, but also has a functional implication in the regulation of D1 receptor function, by interfering with its adaptive responses to agonist stimulation (Fiorentini et al., 2003). This adaptive mechanisms involve both GRK-mediated phosphorylation, arrestin binding and internalization (Claing et al., 2002). On this line, it has been reported that in striatal medium spiny neurons D1 receptors that are localized in cell bodies and dendrites respond to agonist administration by massive internalization (Dumartin et al., 1998). On the other hand, our data showed that association with the NMDA receptor abolishes agonist-induced D1 receptor cytoplasmic sequestration. The studies performed by confocal microscopy analysis of immunolabelled HEK293 cells transfected with the D1 receptor, as well as receptor binding on purified heavy membrane preparations, showed that exposure to the D1 receptor agonist SKF 81297 induced D1 receptor cytoplasmic sequestration. However, when the D1 receptor was co-expressed with the NMDA channel, made up by the NR1 and NR2B subunits, SKF 81297-induced D1 receptor internalization was lost, indicating that oligomerization with NMDA receptors represents a novel regulatory mechanism modulating D1 receptor function.

In conclusion, these observations suggest that, within a single neuron, D1 receptor plasticity may be subjected to different regulatory mechanisms in different neuronal micro-domains. In particular agonist stimulation apparently induces D1 receptor sequestration in all neuronal compartments but the PSD where this receptor is immobilized at the plasma membrane by its interaction with the NMDA channel. The observation that in striatal medium spiny neurons perisynaptic D1 receptor in dendritic spines do not internalize in response to agonist administration (Dumartin et al., 1998) is consistent with our conclusions. Agonist-induced internalization dynamically calibrates receptor availability for extracellular ligands. Disruption of D1 receptor cytoplasmic sequestration in response to agonist stimulation due to oligomerization with the NMDA receptor, might represent a neuronal mechanism to preserve the optimal synaptic strength at cortico-striatal synapses also in the presence of alterations in the dopamine environment as occurs, for instance, during drug administration or in specific pathological conditions. The data we summarized here may thus provide a new rationale to understand the mechanisms controlling cortico-striatal synaptic transmission in both physiological and pathological conditions.

7. ACKNOWLEDGEMENTS

This work was supported by grants from Ministero dell'Istruzione, Università e Ricerca (MIUR, MM06272753), from MIUR and CNR (FISR-Neurobiotecnologie), from Ministero della Sanità (Ricerca Finalizzata 2000 and 2002), from the University of Brescia.

8. REFERENCES

Aizman, O., Brismar, H., Uhlen, P., Zettergren, E., Levey, A.I., Forssberg, H., Greengard, P., and Aperia, A., 2000, Anatomical and physiological evidence for D1 and D2 dopamine receptor co-localization in neostriatal neurons, *Nat. Neurosci.* **3**:223–230.

Angers, S., Salahpour, A., and Bouvier, M., 2002, Dimerization: an emerging concept for G protein-coupled receptor ontogeny and function, *Annu. Rev. Pharmacol. Toxicol*. **42**:409–435.

Barria, A., and Malinow, R., 2002, Subunit-specific NMDA receptor trafficking to synapses, *Neuron* **35**:345–353.

Bergson, C., Mrzljak, L., Smiley, J.F., Pappy, M., Levenson, R., and Goldman-Rakic, P.S., 1995, Regional, cellular and subcellular variations in the distribution of D1 and D5 dopamine receptors in primate brain, *J. Neurosci.* **15**:7821–7836.

Blank, T., Nijholt, I., Teichert, U., Kugler, H., Behrsing, H., Fienberg, A.A., and Greengard, P., 1997, The phosphoprotein DARPP-32 mediates cAMP-dependent potentiation of striatal N-methyl-D-aspartate responses, *Proc. Natl. Acad. Sci. USA* **94**:14859–14864.

Calabresi, P., Gubellini, P., Centonze, D., Picconi, B., Bernardi, G., Chergui, K., Svenningsson, P., Fienberg, A.A., and Greengard, P., 2000, Dopamine and cAMP-regulated phosphoprotein 32 kDa controls both striatal long-term depression and long-term potentiation, opposing forms of synaptic plasticity, *J. Neurosci.* **20**:8443–8451.

Calabresi, P., Pisani, A., Mercuri, N.B., and Bernardi, G., 1996, The corticostriatal projection: from synaptic plasticity to dysfunctions of the basal ganglia, *Trends Neurosci.* **19**:19–24.

Canals, M., Marcellino, D., Fanelli, F., Ciruela, F., de Benedetti, P., Goldberg, S.R., Neve, K., Fuxe, K., Agnati, L.F., Woods, A.S., Ferre, S., Lluis, C., Bouvier, M., and Franco, R., 2003, Adenosine A2A-dopamine D2 receptor-receptor heteromerization: qualitative and quantitative assessment by fluorescence and bioluminescence energy transfer, *J. Biol. Chem*. **278**:46741–46749.

Centonze, D., Gubellini, P., Bernardi, G., and Calabresi, P., 1999, Permissive role of interneurons in corticostriatal synaptic plasticity, *Brain Res. Rev*. **31**:1–5.

Cepeda, C., Colwell, C.S., Itri, J.N., Chandler, S.H., and Levine, M.S., 1998, Dopaminergic modulation of NMDA-induced whole cell currents in neostriatal neurons in slices: contribution of calcium conductances, *J. Neurophysiol.* **79**:82–94.

Claing, A., Laporte, S.A., Caron, M.G., and Lefkowitz, R.J., 2002, Endocytosis of G protein-coupled receptors: roles of G protein-coupled receptor kinases and beta-arrestin proteins, *Progr. Neurobiol.* **66**:61–79.

Devi, L.A., 2001, Heterodimerization of G-protein-coupled receptors: pharmacology, signalling and trafficking, *Trends Pharmacol. Sci*. **22**:532–537.

Dingledine, R.T., Borges, K., Bowie, D., and Traynelis, S.F., 1999, The glutamate receptor ion channels, *Pharmacol. Rev.* **51**:7–61.

Dumartin, B., Caillé, I., Gonon, F., and Bloch, B., 1998, Internalization of D1 dopamine receptor in striatal neurons in vivo as evidence of activation by dopamine agonists, *J. Neurosci.* **18**:1650–1661.

Dunah, W., and Standaert, D.G., 2001, Dopamine D1 receptor-dependent trafficking of striatal NMDA glutamate receptors to the postsynaptic membrane, *J. Neurosci.* **21**:5546–5558.

Fienberg, A.A., Hiroi, N., Mermelstein, P.G., Song, W., Snyder, G.L., Nishi, A., Cheramy, A., O'Callaghan, J.P., Miller, D.B., Cole, D.G., Corbett, R., Haile, C.N., Cooper, D.C., Onn, S.P., Grace, A.A., Ouimet, C.C., White, F.J., Hyman, S.E., Surmeier, D.J., Girault, J., Nestler, E.J., and Greengard, P., 1998, DARPP-32: regulator of the efficacy of dopaminergic neurotransmission, *Science* **281**:838–842.

Fiorentini, C., Gardoni, F., Spano, P.F., Di Luca, M., and Missale, C., 2003, Regulation of dopamine D1 receptor trafficking and desensitization by oligomerization with glutamate N-methyl-D-aspartate receptors, *J. Biol. Chem.* **278**:20196–20202.

Fiorentini, C., and Missale, C., 2004, Oligomeric assembly of dopamine D1 and glutamate NMDA receptors: molecular mechanisms and functional implications, *Biochem. Soc. Trans.* **32**:1025–1028.

Flores-Hernandez, J., Cepeda, C., Hernandez-Echeagaray, E., Calvert, C.R., Jokel, E.S., Fienberg, A.A., Greengard, P., and Levine, M.S., 2002, Dopamine enhancement of NMDA currents in dissociated medium-sized striatal neurons: role of D1 receptors and DARPP-32, *J. Neurophysiol.* **88**:3010–3020.

Gines, S., Hillion, J., Torvinen, M., Le Crom, S., Casado, V., Canela, E.I., Rondin, S., Lew, J.Y., Watson, S., Zoli, M., Verniera, P., Lluis, C., Ferre, S., Fuxe, K., and Franco, R., 2000, Dopamine D1 and adenosine A1 receptors form functionally interacting heteromeric complexes, *Proc. Natl. Acad. Sci. USA* **97**:8606–8611.

Graybiel, A.M., 1990, Neurotransmitters and neuromodulators in the basal ganglia, *Trends Neurosci.* **13**:133–154.

Hersch, S.M., Ciliax, B.J., Gutekunst, C.A., Rees, H.D., Heilman, C.J., Yung, K.K., Bolam, J.P., Ince, E., Yi, H., and Levey, A.I., 1995, Electron microscopic analysis of D1 and D2 dopamine receptor proteins in the dorsal striatum and their synaptic relationships with motor corticostriatal afferents, *J. Neurosci.* **13**:2237–2248.

Hollmann, M., and Heinemann, S., 1994, Cloned glutamate receptors, *Annu. Rev. Neurosci.* **17**:31–108.

Kennedy, M.B., 2000, Signal-processing machines at the postsynaptic density, *Science* **290**:750–754.

Kerr, J.N.D., and Wickens, J.R., 2001, Dopamine D-1/D-5 receptor activation is required for long-term potentiation in the rat neostriatum in vitro, *J. Neurophysiol.* **85**:117–112.

Landwehrmeyer, G.B., Standaert, D.G., Testa, C.M., Penney, J.B., and Young, A.B., 1995, NMDA Receptor subunit mRNA expression by projection neurons and interneurons in rat striatum, *J. Neurosci*. **15**:5297–5307.

Lee, F.J., Xue, S., Pei, L., Vukusic, B., Chery, N., Wang, Y., Wang, Y.T., Niznik, H.B., Yu, X.M., and Liu, F., 2002, Dual regulation of NMDA receptor function by direct protein-protein interactions with the dopamine D1 receptor, *Cell* **111**:219–230.

Levine, M.S., Altemus, K.L., Cepeda, C., Cromwell, H.C., Crawford, C., Ariano, M.A., Drago, J., Sibley, D.R., and Whestphal, H., 1996, Modulatory actions of dopamine on NMDA receptor-mediated responses are reduced in D1A-deficient mutant mice, *J. Neurosci.* **16**:5870–5882.

Liu, F., Wan, Q., Pristupa, Z.B., Yu, X.M., Wang, Y.T., and Niznik, H.B., 2000, Direct protein-protein coupling enables cross-talk between dopamine D5 and gamma-aminobutyric acid A receptors, *Nature* **403**: 274–280.

Missale, C., Nash, R., Robinson, S.W., Jaber, M., and Caron, M.G., 1998, Dopamine receptors: from structure to function, *Physiol. Rev*. **78**:189–225.

Morari, M., Marti, M., Sbrenna, S., Fuxe, K., Bianchi, C., and Beani, L., 1998, Reciprocal dopamine-glutamate modulation of release in the basal ganglia, *Neurochem. Int.* **33**:383–397.

Nicola, S.M., Surmeier, D.J., and Malenka R.C., 2000, Dopaminergic modulation of neuronal excitability in the striatum and nucleus accumbens, *Annu. Rev. Neurosci*. **23**:185–215.

Olanow, C.W., Obeso, J.A., and Nutt, J.G., eds, 2000, Basal ganglia, Parkinson's disease and levodopa therapy, *Trends Neurosci.* **23**(10, suppl.):S1–S126.

Rocheville, M., Lange, D.C., Kumar, U., Sasi, R., Patel, R.C., and Patel, Y.C., 2000, Receptors for dopamine and somatostatin: formation of hetero-oligomers with enhanced functional activity, *Science* **288**:154–157.

Scarselli, M., Novi, F., Schallmach, E., Lin, R., Bonagli, A., Colzi, A., Griffon, N., Corsini, G.U., Sokoloff, P., Levenson, R., Vogel, Z., and Maggio, R., 2001, D2/D3 dopamine receptor heterodimers exhibit uniquefunctional properties, *J. Biol. Chem.* **276**:30308–30314.

Scott, D.B., Blanpied, T.A., Swanson, G.T., Zhang, C., and Ehlers, M.D., 2001, An NMDA receptor ER retention signal regulated by phosphorylation and alternative splicing, *J. Neurosci.* **21**:3063–3072.

Scott, L., Kruse, M.S., Frossberg, H., Brismar, H., Greengard, P., and Aperia, A., 2002, Selective up-regulation of dopamine D1 receptors in dendritic spines by NMDA receptor activation, *Proc. Natl. Acad. Sci. USA* **99**:1661–1664.

Smith, A.D., and Bolam, J.P., 1990, The neural network of the basal ganglia as revealed by the study of synaptic connections of identified neurons, *Trends Neurosci.* **13**:259–265.

Surmeier, D.J., Song, W.J., and Yan, Z., 1996, Coordinated expression of dopamine receptors in neostriatal medium spiny neurons, *J. Neurosci.* **16**:6579–6591.

Torvinen, M., Marcellino, D., Canals, M., Agnati, L.F., Luis, C., Franco, F., and Fuxe, K., 2005, Adenosine A2A receptor and dopamine D3 receptor interactions: evidence of functional A2A/D3 heteromeric complexes, *Mol. Pharmacol.* **67**:400–407.

Zukin, R.S., and Bennet, M.V.L., 1995, Alternatively spliced isoforms of the NMDAR1 receptor subunit, *Trends Neurosci.* **18**:306–313.

Yung, K.K., Bolam, J.P., Smith, A.D., Hersch, S.M., Ciliax, B.J., and Levey, A.I., 1995, Immunocytochemical localization of D1 and D2 dopamine receptors in the basal ganglia of the rat: light and electron microscopy, *Neuroscience* **65**:709–730.

MODULATORY ROLE OF NK1 RECEPTORS IN THE BASAL GANGLIA. STUDIES IN NK1–/– MICE

Laura Turpín[1], Jorge Boronat[1], Carlos Barcia[1], María Gómez[1], Francisco Ros[1], Virginia García[1], Stephen P Hunt[2], Carmen de Felipe[3], and María-Trinidad Herrero[1]

1. INTRODUCTION

Neurokinin 1 (NK1) receptor is one of the five subtypes of tachykinin receptors (NK1, NK2, NK3, NK3B, and NK4)[1], all of which share a high number of homologous sequences and are G protein-coupled. The receptor proteins contains seven coupled domains in the cell membrane, which act by fosfatidyl inositol hydrolysis, cAMP synthesis and calcium mobilization[2,3]. The receptor is located in the cellular membrane of the soma and dendrites in an inactivated state, but is internalized when neurons are activated[4,5]. Activation of NK receptors excites neurons and induces the release of neurotransmitters[6,7]. Substance P (SP) binds with a high degree of affinity to the NK1 receptor but can also bind to NK3; Neurokinin A (NKA, previously known as Substance K) preferentially binds to NK2, while Neurokinin B (NKB) tends to bind to NK3[8,9,10,11]. NKA and NKB have 100–1000 times lower affinity for NK1 than Substance P[12]. Three types of tachykinin receptors NK1, NK2 and NK3 exhibiting preferences for Substance P, NKA and NKB respectively, have been identified[3]. The tachykinins have the peculiarity of being not highly selective for any given receptor type. Indeed, Substance P binds and activates the G-protein coupled NK1 receptor, but also NK2, NK3 receptors with a lower affinity[13]. In rodents NK1 receptor has been identified in the hypothalamus[14], in the limbic structures[15], in the locus coeruleus[16] and in the dorsal raphe nucleus[17].

Both NK1 and Substance P are abundant in the basal ganglia. NK1 is present in striatal neurons[18,19,20], both in the large cholinergic neurons[20,21], in the somatostatincontaining interneuron and in the medium-sized spiny efferent neurons in the rat[22,23], monkey[24] and human neostriatum[25]. It is also present in the internal and external globus pallidus[26] and in low levels in the substantia nigra *pars reticulata*, where it is difficult to detect except by sensi-

[1] Experimental Neurology & Neurosurgery. School of Medicine. University of Murcia. 30100 Murcia, Spain.
[2] Department of Anatomy & Developmental Biology. University College London. WC1E 6BT London. U.K.
[3] Instituto de Neurociencias. Universitas Miguel Hernández. 03550 Alicante, Spain.

tive techniques[12,26,27]. In rodents, NK1 is the predominant receptor in the entopeduncular nucleus[28], however, in the substantia nigra *pars reticulata* it is almost undetectable and NK3 receptor is by far the most abundantly expressed neurokinin receptor[27,28].

The medium-sized spiny neurons in the striatum that give rise to the direct pathway express high levels of Substance P. The output nuclei of the basal ganglia, entopeduncular nucleus and the substantia nigra *pars reticulata*, are densely innervated by striatal terminals containing substance P in a higher density than in the globus pallidus[29]. In the normal brain, neuronal transmission within the basal ganglia is equally balanced between the direct and indirect pathway, allowing movements to be controlled. However, in Parkinson's disease, due to the loss of the nigrostriatal dopaminergic input, this balance between the indirect and direct pathways is altered. The decreased activity of the GABAergic/Substance P direct pathway induces hyperactivity of GABAergic neurons of the entopeduncular nucleus/internal globus pallidus and in the substantia nigra *pars reticulata*[30,31,32,33]. This effect is mediated by NK1 receptors in the entopeduncular nucleus and by NK3 receptors in the substantia nigra *pars reticulata*[29]. In the present work we functionally dissect the two pathways of the direct circuit, using NK1 receptor knock out mice in an attempt to understand the role of Substance P and its receptors in the basal ganglia circuitry.

2. MATERIAL AND METHODS

Adult young male mice (n = 45) were used for this experiment distributed into three groups: NK1–/– mice (n = 16), NK1+/+, wild type mice (n = 14), and C57Bl6 mice (n = 15) from which NK1–/– mice were created[34,35]. All animals were housed in an environment where light (08:00–20:00), temperature (21 ± 1°C) and humidity were controlled, with food and water provided *ad libitum*. Half of the animals of each group received four injections of MPTP hydrochloride (20 mg/kg per dose, i.p.; Sigma-Aldrich, MO, U.S.A.) or either saline (0.9% NaCl) at 24-hour intervals. Mice were anesthetized and sacrificed 24 hours after the last injection and the brains were immediately removed and fixed for three days in 4% paraformaldehyde in 0.1 M phosphate buffer (PB; pH = 7.4); they were then cryoprotected in 0.1 M PB with 20% sucrose, and frozen in powdered dry ice and kept at –80°C before being serially cut into 40 µm coronal sections on a microtome. The animals were treated in accordance the Guide for Care and Use of Laboratory Animals established by the National Institute of Health and the European Communities Council Directive of 24 November 1986 (86/609 EEC).

2.1. NK1–/– and NK1+/+ mice

Experiments were performed on male mice whose NK1 receptor gene[34,35] had been disrupted. In brief, a genomic DNA clone, containing exon 1 of the mouse NK1 receptor gene was isolated by screening a λ2001 mouse 129 library with a rat NK1 cDNA probe. A cassette containing an internal ribosome entry site and the lacZ coding sequence, together with a neomycin resistance gene from its own promoter, was inserted into the unique Stul site in exon 1. The targeting vector was electroporated into HM1 ES cells (129/Sv) and selected clones were injected into C57Bl6 blastocysts; chimeric males were mated with C57Bl6 females. Transmission of the mutant allele was determined by Southern blot analysis of tail DNA using a probe located outside of the homology region of the gene. Mice homozygous for the NK1 mutation were produced by crossing heterozygotes. Mice for the control recordings were of the same background strain as their litter-mates for the NK1

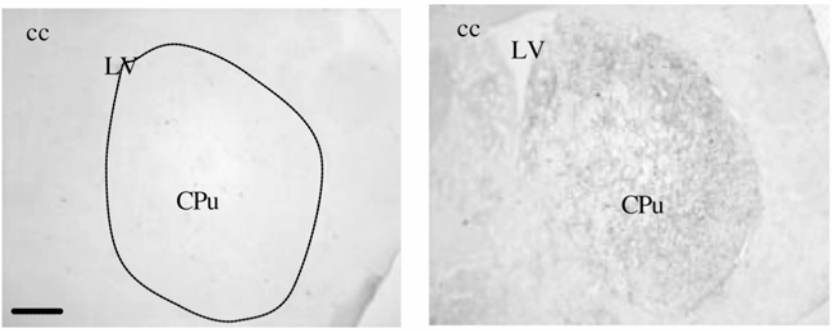

Figure 1. NK1 immunohistochemistry corroborate the lack of NK1 receptor in the striatum of NK1 KO mice (left). Abb.: cc, corpus callosum; CPu, Caudate Putamen (striatum), LV, Lateral Ventricle. Scale Bar = 0.5 mm.

mutation (NK1+/+). Immunocytochemistry using a specific antibody raised against the carboxy terminus receptor of the NK1 receptor indicated, for the first time, that NK1 receptor was absent from the basal ganglia of the NK1−/− mice (Figure 1).

2.2. Tyrosine Hydroxylase (TH) Immunohistochemistry

TH-immunohistochemistry was performed on free-floating sections using a monoclonal antibody against TH (Instar Corporation, Minnesota, U.S.A.) (1/500 dilution, incubated for 48 h at 4°C)[36]. The primary antibody was revealed by the "double-bridge" peroxidase-antiperoxidase (PAP) method, using a goat antimouse antiserum (Nordic, France), at 1/10 dilution, incubated for 30 min, and mouse-PAP (Nordic, France), at 1/500 dilution, incubated for 1 h. The sections were washed again and reacted in 0.05% 3.3-diaminobenzidine tetrahydrochloride (DAB, Sigma) and 0.01% H_2O_2 in 0.1 M phosphate buffer (pH 7.4) for 10–20 minutes to produce a brown reaction product. The sections were washed, mounted on chrome-alum coated slides, rinsed in distilled water, dehydrated through a graded alcohol series to xylene, and coverslipped.

2.3. *In situ* Hybridisation Histochemistry

Following the method described by Fontaine et al. (1988)[37], an S-labelled sense antisense cRNA probe was transcribed from a 2.7-kb cDNA coding for the 67000-kDa human isoform, isolated from a lambda gt-11 human fetal brain library and subcloned in the bluescript M13+ SK vector. The plasmid containing the probe was kindly provided by Dr Tobin. For probe labelling, 1.8 µg of template was added to 20 µl of reaction reagent (DIG RNA Probe Labelling Kit; Roche). The DIG-labelled antisense probe was synthesized by T7 RNA polymerase. A non-radioactive *in situ* hybridisation protocol was devised in our laboratory for use on fixed brain tissue. In brief, sections were washed in DEPC H_2O and saline buffer (PBS) and acetylated (0.25% acetic anhydride in 0.1 M triethanolamine/0.9% NaCl; pH 8) for 10 min. Sections were then washed in PBS, a hydrophobic barrier (PAP pen, Zymed laboratories) drawn to outline the tissue, and rewashed in PBS. The sections were then rinsed in 2 × SSC and 50 ng of antisense probe in 100 mcl of hybridisation buffer contained 46% formamide, 2 × SSC, 1 × 50 Denhardt solution, 10% dextransulfate, 50 mM dithiothreitol (DTT), 250 mcg/ml yeast-RNA, 100 mcg/ml polyadeylic acid and 500 mcg/l

denatured and sheared salmon sperm DNA, which was added just prior to hybridisation. Each section was coverslipped with parafilm and hybridisation was carried out overnight at 37°C. Negative controls were made with non-specific hybridisation mixture added. Sections were then carefully washed in 2 × SSC (1 × 15 min) until coverslips fell off, then in 2 × SSC (2 × 15 min) and 1 × SSC (1 × 15 min) at 37°C, and then at room temperature in 1 × SSC (1 × 15 min) and 0.5 × SSC (1 × 15 min). Immunological detection was then performed on the sections. After 3 washes with Digoxygenin buffer (DB) (10 mM Maleic Acid, 15 mM NaCl, pH = 7.5) for 5 min each, the blocking solution (10%w/v Blocking Reagent (BR), Roche Diagnostics, and 5% normal sheep serum (NSS) in DB), was added before incubating for 1 h at 37°C. Next Anti-DIG-alkaline phosphate antibody (1 : 250 dilution in DB, containing 10% BR and 1% NSS) was added and the sections were incubated for 2 h on a rocking platform at room temperature. The sections were washed in DB (2 × 10 min) and then once in DDB (10 mM Tris, 10 mM NaCl, 5 mM MgCl2, pH = 9.5). The alkaline phosphatase colour reaction buffer mixture was added according to the specifications of the manufacturer (Boehringer Mannheim) (35 mcl NBT, 45 mclBCIP in 10 ml DDB). The sections were incubated overnight (16 h) in a humidified dark box. The colour reaction was then terminated by washing in TE buffer (10 mM Tris, 100 mM NaCl in 1 L DEPC H_2O) (5 min) and distilled water (5 min). The sections were mounted in aquamount solution and coverslipped.

2.4. Analysis and Statistics

The nomenclature and demarcation of the nuclei (substantia nigra *pars compacta*, substantia nigra *pars reticulata* and entopeduncular nucleus) were adopted with reference to the mouse brain atlas[38]. The number of TH-positive cells was measured in 260-µm squares, 200 µm (x) and 200 µm (y) apart, covering the whole surface area of the substantia nigra *pars compacta* using the principle of the optical dissector[39]. Positive cells were counted only when they cut the upper and right hand limit of the square or were inside the square. The results were expressed as the total number of cells analysed. Quantification involved the use of a Zeiss KS 400 image analyser system. To measure the optical density we surrounded every labelled neuron in the entopeduncular nucleus and in the substantia nigra *pars reticulata* from all the slides and substracted the optical density of the nearby background using a suitable software (CoolSnap® digital color video camera software ptp and Scion® Image software) with a Zeiss microscope connected to a digital camera through a Zeiss zoom set at 12.5× and 0.1× adapter.

To assess whether our results showed a normal distribution, the Kolmogorov-Smirnov test was used, while the Levene test was use to check that the variance was equal. Differences between groups and the effect of the MPTP treatment were evaluated with the two-tailed Student's test. When multiple comparisons were made, the results were analyzed using one-way ANOVA and the Bonferroni method. Probability values of less than 0.05 were considered statistically significant.

3. RESULTS

The NK1−/− animals displayed normal behavior with normal feeding and grooming, similar to the wild type animals. In all groups, after the MPTP treatment the animals showed motor alterations but recovered after a few hours.

The optical density of TH immunoreactivity was measured three times at striatal level in each animal, and a significant decrease was observed in the MPTP-treated animals. The quantification of the dopaminergic neurons in the substantia nigra *pars compacta* pointed to a significant decrease in the number of neurons in the MPTP-treated animals in all the experimental groups (in NK1–/– and C57Bl6, $p = 0.005$ and in NK1+/+ $p = 0.016$) (Figure 2). NK1 receptor was detected by immunohistochemistry in the entopeduncular nucleus both in C57Bl6 and in NK1+/+ mice but not in NK1–/– mice or in the substantia nigra *pars reticulata* of any group of mice because of the prevalence of NK3, as observed previously[40,41,42].

The quantitative estimation of GAD mRNA optical density levels showed a significant increase in the substantia nigra *pars reticulata* (Figure 3A) of MPTP-treated groups compared with the corresponding controls ($p < 0.02$). No statistically significant differences were detected between the control groups for NK1–/–, C57Bl6 and NK1+/+, although GAD levels were slightly higher in the NK1–/– control group. However, the optical density of GAD mRNA in the NK1–/– MPTP-treated mice was significantly higher than in the C57Bl6 MPTP-treated mice ($p = 0.005$) and in the NK1 +/+ MPTPtreated animals ($p < 0.05$) when the three MPTP-treated groups were compared. These data may be explained by the higher activity of GABAergic neurons of the substantia nigra *pars reticulata* in the MPTP-treated NK1–/– mice than in the other two groups. As expected, in the entopeduncular nucleus (Figure 3B), a significant increase in GAD mRNA density ($p < 0.05$) was

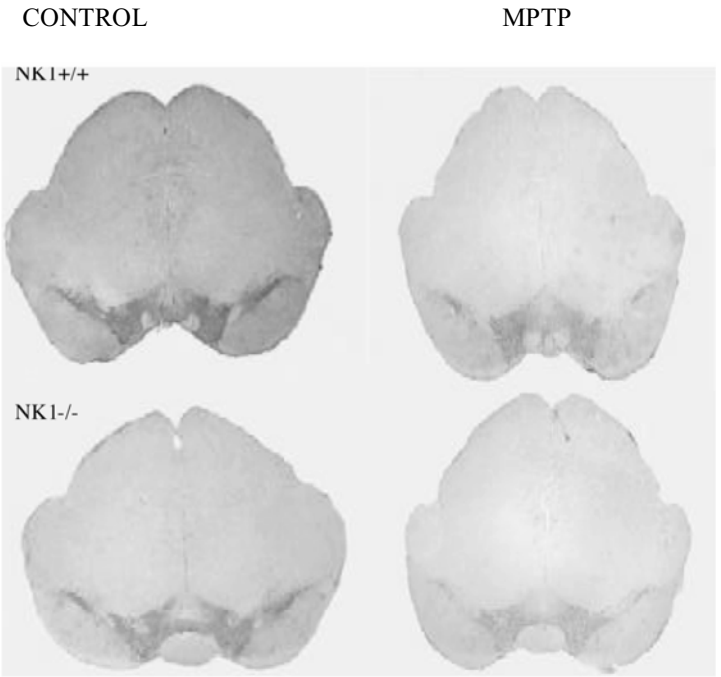

Figure 2. Tyrosine Hydroxylase immunoreactivity in substantia nigra *pars compacta* of NK1+/+ and NK1–/– mice. The number of neurons is significantly decreased in both experimental groups after MPTP treatment. Scale Bar = 0.5 mm.

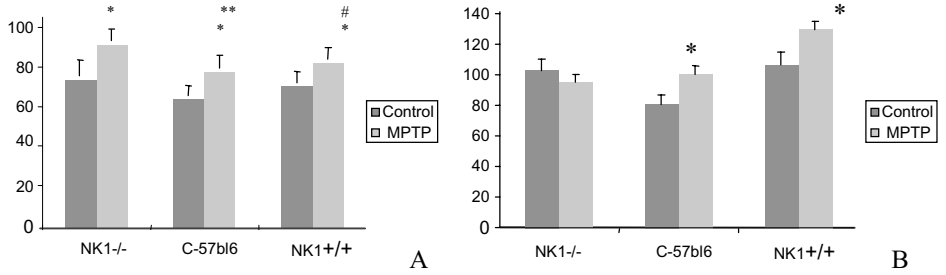

Figure 3. GAD mRNA levels in the substantia nigra *pars reticulata* (SNpr) (A): a significant increase is observed in its expression in MPTP-treated mice (*p < 0.05) over the control groups and in NK1–/– MPTP-treated mice over the NK1+/+ (#p < 0.05) and C57Bl6 (**p < 0.01); GAD mRNA levels in the entopeduncular nucleus (Ent.) (B): a significant increase was observed in the expression in both C57bl6 and NK+/+ after MPTP treatment (*p < 0.05). No differences were observed in NK1–/– MPTP-treated mice compared with its controls.

observed in both NK1 +/+ and C57Bl6 MPTP-treated mice compared with the control groups. However, there were no significant differences between the GAD mRNA optical density of MPTP-treated mice and the corresponding controls in the NK1–/– mice. No statistically significant differences were detected between the three control groups (NK1–/–, C57Bl6 and NK1+/+). The optical density of GAD mRNA in NK1–/– MPTP-treated mice was significantly lower (p = 0.01) than in C57Bl6 MPTP-treated mice and NK1 +/+ MPTP-treated animals (p = 0.0013).

4. DISCUSSION

The fact that GABA activity did not increase in the entopeduncular nucleus of NK1–/– MPTP-treated mice compared with the wild type NK1+/+ and C57Bl6 groups, indicates that the absence of NK1 receptor results in the functional abolition of the direct pathway through the entopeduncular nucleus. However, this does not affect GABA activity in the substantia nigra *pars reticulata* because of the prevalence of Substance P receptor in this nucleus is NK3[41]. It is known that in Parkinson's disease a decrease in Substance P[31,43] is correlated with an increase of its specific receptors[44]. The presence of NK1 receptors in the entopeduncular nucleus suggests that they are involved in the direct pathway in this nucleus and the alteration observed in NK1–/– mice, even before MPTP-treatment, enhances the importance of this neuropeptide in the basal ganglia circuitry. Even though we did not quantify Substance P, we would suggest that the absence of NK1 receptor from birth leads to its increased synthesis in order to compensate the functional deficit or that during animal's development this alteration could be compensated by other neurotransmitters[45].

In Parkinson's disease the activity of output nuclei are increased, resulting in GABAergic inhibition of the thalamus[46,47]. The same results are observed in rhesus monkeys[32,33] and in MPTP-treated mice[48]. In the present study the C57Bl6 and NK1+/+ mice (Figures 3A and 3B) showed a significant increase in GAD mRNA expression, in both the substantia nigra *pars reticulata* and entopeduncular nucleus, which agrees with previous results[48]. On the other hand, no increase in the optical density of GAD mRNA was observed in the entopeduncular nucleus of NK1–/– MPTP-treated mice. Although NK3 has also been

described in the entopeduncular nucleus[28,49], the presence of this receptor for Substance P is not so important as in the substantia nigra *pars reticulata*, where NK3 are the major receptors. This also indicates that the hyperactivity observed in this nucleus is secondary to the activity of Substance P, so the absence of the NK1 receptor in NK1–/– mice does not allow this variation to be seen because substantia nigra *pars reticulata* was not previously inhibited. This leads us to suggest that the absence of NK1 receptor produces an increase in the basal activity of the entopeduncular nucleus because there is no enough inhibition from the striatum by the direct pathway. Then, these results suggest that NK1 receptors could play a crucial role in regulating the function of the output nuclei of the basal ganglia. In fact, the direct pathway could have a wider role in the alteration of the entopeduncular nucleus observed in MPTP-treated mice. According to these results, the activator effect of the subthalamic nucleus may not be as relevant as previously thought[50] and the subthalamic activator effect on the entopeduncular nucleus in a parkinsonism model of NK1 KO mice may have been completely abolished due to the inhibition of the external pallidus. More exhaustive studies in these mice are needed to throw light on the role of Substance P in the organization of the basal ganglia and to increase our understanding of basal ganglia disorders.

5. ACKNOWLEDGEMENTS

The authors would like to thank Mr. Philip Thomas for comments and language suggestions on this manuscript, and wish to extend their gratitude to Prof. Juan Gómez for his help with the statistical analysis and to NJK Tillakaratne, DL Kaufman and AJ Tobin who generously provided the GAD probe. This work was in part supported by grants nos. SAF2001–0479 and FIS PI02/1335.

6. REFERENCES

1. Donalson, L., Haskell, C.A., and Hanley, M.R, 2001, Messenger RNA localisation and further characterization of the putative tachykinin receptor NK4 (NK3B). *Receptors channels* **7**:259–227.
2. Regoli, D., Drapeau, G., Dion, S., and D'Orleans-Juste, P., 1989, Receptors for substance P and related neurokinins. *Pharmacology* **38**:1–15.
3. Nakanishi, S., 1991, Mammalian tachykinin receptors. Annu. Rev. *Neuroscience* **14**:123–136.
4. Li, J.L., Wang, D., Kaneko, T., Shigemoto, R., Nomura, S., and Mizuno, N., 2000, Relationship between neurokinin-1 receptor and substance P in the striatum: light and electron microscopic immunohistochemical study in the rat. *J. Comp. Neurol*. **418**:156–163.
5. Ljungdahl, A., Hökfelt, T., and Nilsson, G., 1978, Distribution of substance P-like immunoreactivity in the central nervous system of the rat–I. Cell bodies and nerve terminals. *Neuroscience* **3**:861–943.
6. Maggio, J.E., Sandberg, B.E.B., Bradley, C.V., Iversen, L., Santikan, S., Williams, B.H., Hunter, J.C., and Hanley, M.R., 1983, Substance K: a novel tachykinin in mammalian spinal cord. In: Substance P. Ed by Skrabanek P. and Powell D. pp. 20–21. Boole, Dublin.
7. Reid, M.S., Herrera-Marschitz, M., Kehr, J., and Ungerstedt, U., 1990, Striatal dopamine and glutamate release: effects of intranigral injections of substance P. *Acta. Physiol. Scand*. **140**:527–537.
8. Patacchini, R., and Maggi, C.A., 1995, Tachykinin receptors and receptor subtypes. *Arch. Int. Pharmacodyn Ther.* **329**:161–184.
9. Saria, A., 1999, The tachykinin NK1 receptor in the brain: pharmacology and putative functions. *Eur. J. Pharmacol*. **375**:51–60.
10. Hökfelt, T., Pernow, B., and Wahren, J., 2001, Substance P: a pioneer amongst neuropeptides. *J. Intern. Med*. **249**:27–40.

11. Mantyh, P.W., 2002, Neurobiology of substance P and the NK1 receptor. *J. Clin. Psychiatry* 63 Suppl **11**:6–10.
12. Whitty, C.J., Walker, P.D., Goebel, D.J., Poosch, M.S., and Bannon, M.J., 1995, Quantitation, cellular localization and regulation of neurokinin receptor gene expression within the rat substantia nigra. *Neuroscience* **64**:419–425.
13. Maggi, C.A., Patacchini, R., Rovero, P., and Giachetti, A., 1993, Tachykinin receptors and tachyikinin receptors antagonist. *J. Auton. Pharmacol*. **13**:23–93.
14. Liu, H.L., Cao, R., Jin, L., and Chen, L.W., 2002, Immunocytochemical localization of substance P receptor in hypothalamic oxytocin-containing neurons of C57 mice. *Brain Res*. **948**:175–179.
15. Beaujouan, J.C., Saffroy, M., Torrens, Y., and Glowinski, J., 2000, Differents subtypes of tachykinin NK1 receptor binding sites are present in the rat brain. *J. Neurochem*. **75**:1015–1026.
16. Chen, L.W., Wei, L.C., Liu, H.L., and Rao, Z.R., 2000, Noradrenergic neurons expressing substance P receptor (NK1) in the locus coeruleus complex: a double immunofluorescence study in the rat. *Brain Res*. **873**:155–159.
17. Commons, K.G., and Valentino, R.S., 2002, Cellular basis for the effects of substance P in the periaqueductal grey and dorsal raphe nucleus. *J. Comp. Neurol*. **39**:1–8.
18. Elde, R., Schalling, M., Ceccatelli, S., Nakanishi, S., and Hökfelt, T., 1990, Localization of neuropeptide receptor mRNA in rat brain: initial observations using probes for neurotensin and substance P receptors. *Neurosci. Lett*. **120**:134–138.
19. Kowall, N.W., Quigley, B.J. Jr, Krause, J.E., Lu, F., Kosofsky, B.E., and Ferrante. R.J., 1993, Substance P and substance P receptor histochemistry in human neurodegenerative diseases. *Regul. Pept.* **46**(1–2):174–185.
20. Gerfen, C.R., 1991, Substance P (neurokinin-1) receptor mRNA is selectively expressed in cholinergic neurons in the striatum and basal forebrain. *Brain Res*. **556**:165–170.
21. Aubry, J.M., Lundstrom, K., Kawashima, E., Ayala, G., Schulz, P., Bartanusz, V., and Kiss, J.Z, 1994, NK1 receptor expression by cholinergic interneurons in human striatum. Neuroreport. 15; **5**(13):1597–1600.
22. Kaneko, T., Shigemoto, R., Nakanishi, S., and Mizuno, N., 1993, Substance P receptor-immunoreactive neurons in the rat neostriatum are segregated into somatostatinergic and cholinergic aspiny neurons. *Brain Res*. **631**:297–303.
23. Shigemoto, R., Nakaya, Y., Nomura, S., Ogawa-Meguro, R., Ohishi, H., Kaneko, T., Nakanishi, S., and Mizuno, N., 1993, Immunocytochemical localization of rat substance P receptor in the striatum. *Neurosci. Lett*. **153**:157–160.
24. Jakab, R.L., Hazrati, L.N., and Golin, P., 1996, Distribution and neurochemical behaviour of substance P receptor (SP immunoreactive striatal neurons of macaque monkey: accumulation of substance P fibers and SPR neurons and dendrites in striocapsules encircled striosomes. *J. Comp. Neurol*. **369**:137–149.
25. Parent, A., Cichtti, F., and Beach, T.G., 1995, Striatal neurons displaying substance P (NK1) receptor immunoreactivity in human and no-human primate. *Neuroreport* **6**:721–724.
26. Mounir, S., and Parent, A., 2002, The expression of neurokinin-1 receptor at striatal and pallidal levels in normal human brain. *Neurosci. Res*. **44**:71–81.
27. Bannon, M.J., and Whitty, C.J., 1995, Neurokinin receptor gene expression in substantia nigra: localization, regulation, and potential physiological significance. *Can J. Physiol. Pharmacol*. **73**:866–870.
28. Mileusnic, D., Lee, J.M., Magnuson, D.J., Hejna, M.J., Krause, J.E., Lorens, J.B., and Lorens, S.A., 1999, Neurokinin-3 receptor distribution in rat and human brain: an immunohistochemical study. *Neuroscience* **89**:1269–1290.
29. Levesque, M., Bedard, A., and Parent, A., 2003, Novel aspect of the chemical anatomy of the striatum and its efferents projections. *J. Chem. Neuroanatomy* **26**:271–281.
30. Levy, R., Hazrati, L.N., Herrero, M.T., Vila, M., Hassani, O.K., Moroux, M., Ruberg, M., Asensi, H., Agid, Y., Feger, J., Obeso, J.A., Parent, A., and Hirsch, E.C., 1997, Re-evaluation of the functional anatomy of the basal ganglia in normal and in Parkinson states. *Neuroscience* **76**:335–343.
31. Herrero, M.T., Augood, S.J., Hirsch, E.C., Javoy-Agid, F., Luquin, M.R., Agid, Y., Obeso, J.A., and Emson, P.C., 1995, Effects of L-DOPA on pre-proenkephalin and pre-protachykinin gene expression in the MPTP-treated monkey striatum. *Neuroscience* **68**:1189–1198.
32. Herrero, M.T., Levy, R., Luquin, M.R., Villares, J., Guillen, J., Faucheux, B., Javoy-Agid, F., Obeso, J.A., and Hirsch, E.C., 1996, Consequence of nigrostriatal denervation and L-dopa therapy on the expression of glutamic acid decarboxylase messenger RNA in the pallidum. *Neurology* **47**:219–224.
33. Vila, M., Levy, R., Herrero, M.T., Ruberg, M., Faucheux, B., Obeso, J.A., Agid, Y., and Hirsch, E.C., 1997, Consequences of nigroestriatal denervation on the functioning of the basal ganglia in human and non human primates: an in situ hybridization study of cytochrome oxydase subunit I mRNA. *J. Neurosci*. **17**:765–773.

34. De Felipe, C., Herrero, J.F., O'Brien, J., Palmer, J., Doyle, C.A., Smith, A., Laird, J.M.A., Belmonte, Cervero, F., and Hunt, S., 1998, Altered nociceptor in analgesia and aggression in mice lacking the receptor for substance P. *Nature* **392**:394–397.
35. Rigual, R., Rico, A., Prieto-Lloret, J., De Felipe, C., and Donnelly, D., 2002, Chemoreceptor activity is normal in mice lacking the NK1 receptor. *Eur. J. Neurosci*. **16**:2078–2084.
36. Herrero, M.T., Hirsch, E.C., Kastner, A., Ruberg, M., Luquin, M.R., Laguna, L., Javoy-Agid, F., Obeso, J.A., and Agid, Y., 1993, Does Neuromelanin contribute to the vulnerability of catecholaminergic neurons in monkeys intoxicated with MPTP? *Neuroscience* **56**:499–511.
37. Fontaine, B., Sassoon, D., Buckingham, M., and Changeux, J.P., 1988, Detection of nicotinic acetylcholine receptor a-subunit mRNA by in situ hybridization at neuromuscular junction of 15 day-old chick striatal muscles, *EMBO J*. **7**:603–609.
38. Paxinos, G., and Franklin, B.J. The mouse brain in stereotaxic coordinates, 2001. Academic Press.
39. Sterio, D.C., 1984, The unbiased estimation of number and sizes of arbitrary particles using the disector. *J. Microsc*.**134**:127–136.
40. Bannon, M.J., and Whitty, C., J., 1995, Neurokinin receptor gene expression in the substantia nigra: location, regulation and potential physiological significant. *Can J. Physiol. Pharmacol*. **73**:866–870.
41. Whitty, C.J., Paul, M.A., and Bannon, M.J., 1997, Neurokinin receptor: mRNA localization in human midbrain dopamine neurons. *J. Comp. Neurol*. **382**:394–400.
42. Saffroy, M., Beaujouan, J.C., Torrens, Y., Besseyre, J., Bergstrom, L., and Glowinski, J., 1988, Localization of tachykinin binding sites (NK1, NK2, NK3 ligands) in the rat brain. *Peptides* **9**:227–241.
43. Mauborgne, A., Javoy-Agid, F., Legrand, J.C., Agid, Y., and Cesselin, F., 1983, Decrease of substance P-like immunoreactivity in the substantia nigra and pallidum of parkinsonian brains. *Brain Res.* **268**:167–170.
44. Rioux, L., and Joyce, J.N., 1993, Substance P receptors are differentially affected in Parkinson's and Alzheimer disease. *J. Neural. Transm. Park Dis. Dement. Sect*. **6**:199–210.
45. Drago, J., Mc Coll, C.D., Horne, M.K., Finkelstein, D.I., and Ross, S.A., 2003, Neuronal nicotinic receptors: insights gained from gene knockout and knock in mutant mice, *Cell Mol. Life Sci*. **60**:1267–1280.
46. Lindefors, N., 1993, Dopaminergic regulation of glutamic acid decarboxylase mRNA expression and GABA release in the striatum: a review. *Prog. Neuropsychopharmacol Biol. Psychiatry* **17**:887–903.
47. Guridi, J., Herrero, M.T., Luquin, M.R., Guillen, J., Ruberg, M., Laguna, J., Vila, M., Javoy-Agid, F., Agid, Y., Hirsch, E., and Obeso, J.A., 1996, Subthalamotomy in parkinsonian monkeys. Behavioural and Biochemical Analysis. *Brain* **119**:1717–1727.
48. Soghomonian, J.J., and Chesselet, M.F., 1992, Effects of nigrostriatal lesion on the levels of messenger RNAs encoding two isoforms of glutamate decarboxylase in the globus pallidus and entopeduncular nucleus of the rat. *Synapse* **11**:124–133.
49. Ding, Y.Q., Zheng, H.X., Wang, D.S., Xu, J.Q., Gong, L.W., Lu, Y., Qin, B.Z., Shi, J., Li, H.L., Li, J.S., Shigemoto, R., Kaneko, T., and Mizuno, N., 1999, The distribution of substance P receptor (NK1)-like immunoreactive neurons in the new-born and adult human spinal cord. *Neurosci. Lett*. **266**:133–136.
50. Maurer, C., Mergner, T., Xie, J., Faist, M., Pollak, P., and Lucking, C.H., 2003, Effect of chronic bilateral subthalamic nucleus (STN) stimulation on postural control in Parkinson's disease. *Brain* **126**:1146–1163.

TRACE AMINES CAUSE MORE THAN ONE EFFECT ON DOPAMINERGIC NEURONS

Raffaella Geracitano[1], Mauro Federici[1], Alessandro Tozzi[1], Patrizia Longone[1], Giorgio Bernardi[1,2], and Nicola B. Mercuri[1,2]

1. INTRODUCTION

Trace amines (TAs) are endogenous amines found in many organisms from plants, bacteria, insects and other invertebrates to mammals, including man. These compounds are detected at low concentrations in peripheral and brain tissues of vertebrates and are also ingested by a diet rich in chocolate, aged cheese and wine (Skerritt, et al., 2000). These amines include: tyramine (TYR), β-phenylethylamine (β-PEA), tryptamine, (TRY) and octopamine (OCT; Fig. 1; Juorio, 1976). TAs are distributed heterogeneously throughout mammalian brain, in particular highest levels of TYR and β-PEA are found in the nigrostriatal and mesolimbic regions, such as the caudate-putamen, olfactory tubercles and nucleus accumbens (Paterson, et al., 1990).

It is likely that TAs are phylogenetically older than classical biogenic amines, dopamine (DA), norepinephrine (NE) and serotonin (5-HT), with whom they share structural proprieties and metabolic pathways (Paterson, et al., 1990), but their physiological roles and mechanisms of action in vertebrates remain unclear (Borowsky, et al., 2001; Bunzow, et al., 2001; Kim and von Zastrow, 2001; Premont, et al., 2001; Branchek and Blackburn, 2003). However, alterations in their amount are associated with various human disorders including schizophrenia, depression, attention deficit hyperactivity disorder (ADHD), Parkinson disease (PD), addiction (Branchek and Blackburn, 2003). Moreover, brain levels of TAs are elevated during inhibition of the monoamine oxidase (MAO) enzyme (MAO-A and MAO-B) or in animals with selective deletion of MAO genes.

TAs are stored in nerve terminals with classical biogenic amines and released together with them; however, they might not be stored in vesicles (Kosa, et al., 2000). Pharmacological studies have suggested that these compounds may function primarily as "endogenous amphetamines" or "false neurotransmitters" which increase catecholamine concentrations by interfering with the transport systems of the active biogenic amines.

[1] Experimental Neurology Laboratory, S. Lucia Foundation I.R.C.C.S., Rome, Italy.
[2] Universita di Tor Vegata, Rome, Italy.

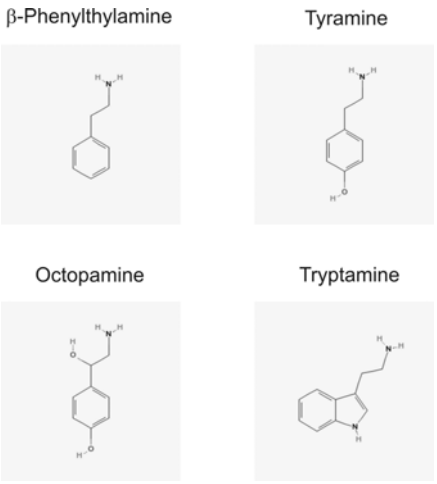

Figure 1. Structure of different trace amines.

Indeed, it has been suggested that TYR and PEA, like amphetamine and other psycostimulants, increase extracellular DA concentrations by competing for uptake of this catecholamine by the plasma membrane DA transporters, inhibiting vesicular monoamine transporters and displacing intracellular pools of catecholamine by promoting reversal of transporter function (Boulton, 1976, 1982; Janssen, et al., 1999; Geracitano, et al., 2004). Thus, many of the effect of TAs are indirect and are caused by the release of endogenous classical amines. However, there is a growing body of evidence suggesting that TAs function independently of classical amine transmitters and mediate some of their effects via the activation of specific receptors (Borowsky, et al., 2001; Bunzow, et al., 2001).

The discovery of a family of G-protein coupled receptors (GPCR) at least some of which appear to be activated by TAs (Paterson, et al., 1990; Borowsky, et al., 2001; Bunzow, et al., 2001), has prompted a resurgence of interest and required a re-evaluation of the potential physiological relevance of these compounds. This new family of TA receptors ($TA_{1–15}$) has been identified by amplifying genomic DNA from humans, rats and mice using degenerate primers in polymerase chain reactions. Cell transfection studies have also indicated that the two receptors so far studied, TA_1 and TA_2 are coupled to an increase in cAMP generation (Borowsky, et al., 2001; Bunzow, et al., 2001) and are particularly sensitive to TYR and PEA. In the central nervous system, the TA_1 and TA_2 receptor proteins can be found sparsely expressed in the substantia nigra/ventral tegmental area, locus coeruleus and dorsal raphe nucleus (Borowsky, et al., 2001). The pharmacological profile of these receptor is intriguing because not only TAs but also numerous psycostimulants and hallucinogenic amphetamines including ecstasy directly activate these receptors (Bunzow, et al., 2001).

Thus, delineation of indirect (transporter-mediated) and direct (GPCR-mediated) effects of TAs is an important issue to better understand the role of these compounds in the physiology and pathology of the dopaminergic system. In the present article we will review our recent results regarding the effects of TAs on dopamine neurons.

1.1. Synthesis and Metabolism of TAs

β-PEA and TYR are formed by the enzymatic decarboxylation of the precursor amino acids L-phenylalanine and L-tyrosine, respectively. This decarboxylation is mediated by the enzyme aromatic L-amino acid decarboxylase (AADC). Metabolism of the TAs is primarily via MAO, with β-PEA the prototypical MAO-B selective substrate. Other TAs show less selectivity and are metabolised by both MAO-A and MAO-B.

2. RESULTS

2.1. Indirect Effects Mediated by TAs

Since TAs appear to be co-released with DA and may further stimulate the efflux of this catecholamine (Schonfeld and Trendelenburg, 1989; Janssen, et al., 1999; Mundorf, et al., 1999), we hypothesised that TAs inhibit DA neurons by increasing DA release and by activating the D2 autoreceptors present on the soma and dendrites of these cells. We further hypothesised that stimulation of DA release by TAs is a result of activation of the DA transporter (DAT). We have thus examined the inhibitory effects of two trace amines (β-PEA and TYR) on the spontaneous discharge and membrane potential of dopamine neurons in ventral midbrain slices. We investigated the sensitivity of this response to antagonism of the D2 receptors, blockade of DAT and depletion of vesicular DA.

The data collected in the present study were obtained from 55 intracellularly recorded "principal" neurons in the SNc and 22 in the VTA that were identified as dopaminergic according to electrophysiological and pharmacological criteria (Johnson and North, 1992; Mercuri, et al., 1995). All neurons fired spontaneous action potentials at a mean rate of 1.2 Hz (range 0.4 to 2.8 Hz) and had a relatively long lasting spike (>1.2 ms).

2.2. TAs Inhibit the Activity of Dopamine Neurons

β-PEA and TYR exerted an inhibitory action on dopamine cells of the ventral mesencephalon. Indeed bath application of β-PEA (100 μM) and TYR (100 μM) caused a reversible inhibition of the spontaneous firing and a hyperpolarisation of the membrane (Fig. 2a and b). The inhibitory effects of TAs on spontaneous activity were concentration-dependent in a range of 10–100 μM. The IC50 for β-PEA was 43.2 ± 13.2 μM (n = 5), while the IC50 for TYR was 39.6 ± 6.7 μM (n = 4; Figure 2c and d) β-PEA (100 μM) and TYR (100 μM) hyperpolarized the neurons by 3.5 ± 2 mV (n = 10) and 6 ± 2 mV (n = 10) respectively. This membrane hyperpolarization caused by both amines, persisted in the presence of tetrodotoxin (TTX) suggesting that TAs-induced effects are independent of neuronal and network activity (Fig. 3a).

In addition, the hyperpolarizing effects of β-PEA and TYR were blocked by the D2 receptor antagonist sulpiride (1–3 μM) (Fig. 3b). Thus, the ability of β-PEA and TYR to inhibit DA cells is related to an activation of the D2-like autoreceptors.

Moreover, cocaine did not affect the membrane hyperpolarization caused by β-PEA or TYR. This suggests that these amines partially stimulate, in an amphetamine-like manner the DAT-mediated efflux of DA from the dendrites of the dopamine cells (Fig. 4a). Interestingly, the DA-induced hyperpolarization of the membrane was not affected by TAs, as would be expected if DAT was inhibited (Fig. 4b).

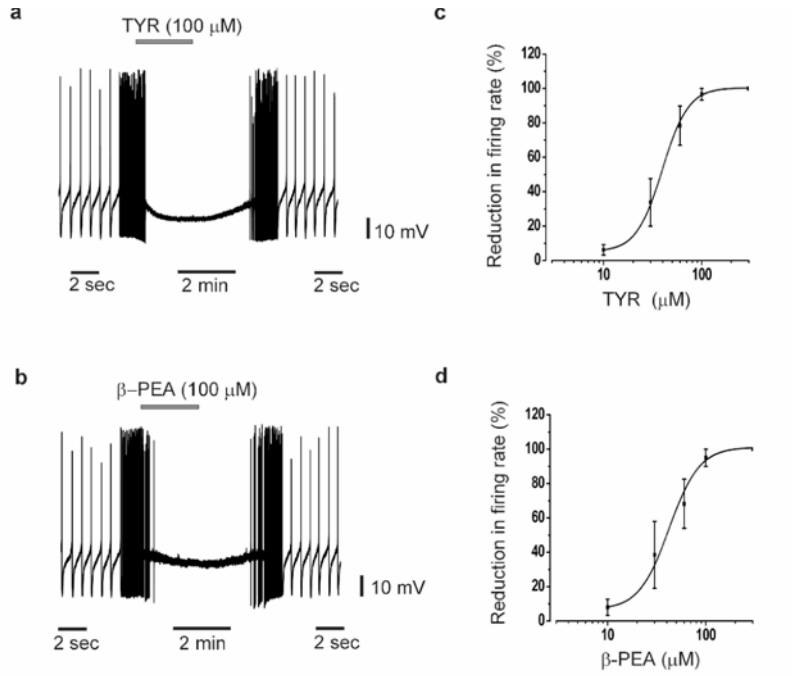

Figure 2. Reversible and concentration-dependent inhibitory effects of β-PEA and TYR on dopamine neuron activity.

2.3. Intracellular DA Depletion Blocks TAs Responses

In reserpine-treated (5–8 mg/kg i.p.) animals, in which intracellular stores of DA were emptied, TAs (100 μM) were still able to inhibit DA cells as in control conditions. Interestingly, when this treatment was combined with the dopa-decarboxylase inhibitor, carbidopa (300 μM). TAs had no effect (Fig. 5a and b). In addition, the inhibitory effect induced by amphetamine was also absent, whereas the response to DA still caused the typical D2-autoreceptors mediated response (Fig. 5c and d). Therefore, these data demonstrate that TAs regulate the activity of DA cells by stimulating the efflux of newly synthesised DA from reserpine-insensitive pools via a carrier-dependent and independent mechanism. The effects reported above could be of crucial importance in the functional processes of the mesolimbic and mesostriatal system suggesting a feasible role for TAs in the physiopathology of altered states such as ADHD, schizophrenia, PD and drug addiction.

3. TAs DEPRESS GABA RESPONSE ON DOPAMINE NEURONS BY INHIBITING GIRK CHANNELS: POSSIBLE ACTIVATION OF TAs RECEPTORS

A specific role for TAs in the ventral midbrain has been recently suggested by the discovery of two subtypes of G protein-coupled TA receptors, TA1 and TA2. They both increase cAMP formation (Borowsky, et al., 2001; Bunzow, et al., 2001) presumably via the G s class of G-proteins in *in vitro* expression systems. Considering that mRNA for the

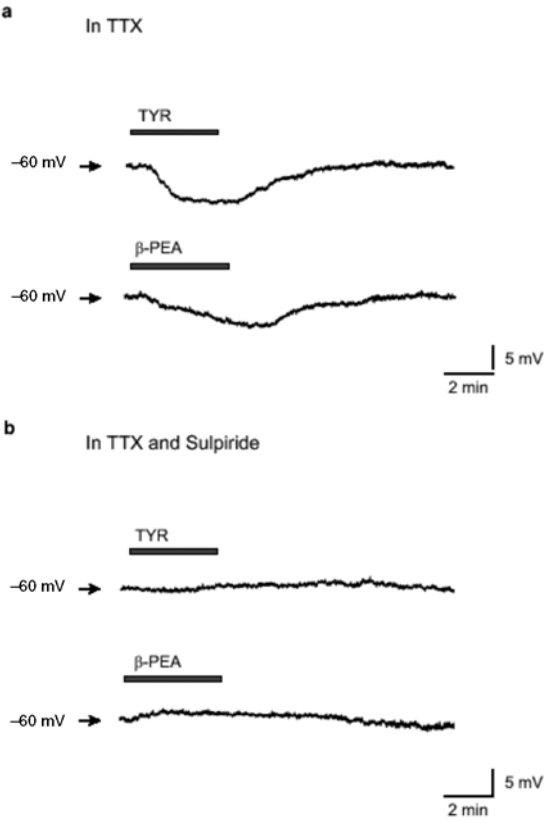

Figure 3. The effects of trace amines occur in the presence of TTX and are antagonized by the D2 antagonist, sulpiride.

TA1 and TA2 receptors is present in the substantia nigra (SN)/ventral tegmental area (VTA) (Borowsky, et al., 2001) and cyclic AMP-dependent protein kinase A (PKA) facilitates $GABA_B$ currents (Cameron and Williams, 1993; Bonci and Williams, 1996; Couve, et al., 2002), we have postulated that the trace amines, β-PEA and TYR, could increase the evoked $GABA_B$-slow inhibitory post synaptic potential (IPSP) in midbrain DA neurons. Unexpectedly, our electrophysiological experiments demonstrated that β-PEA and TYR reduce the $GABA_B$ IPSP by a G-protein coupled postsynaptic mechanism (Federici, et al., 2005).

3.1. TAs Reduce the $GABA_B$ IPSP

Using intracellular recordings with sharp microelectrodes, we studied the effects of TAs on the slow inhibitory transmission mediated by $GABA_B$ receptors on DA cells. Bath application of β-PEA and TYR reduced the amplitude of the $GABA_B$ IPSP (Fig. 6a and b). This depressant action of both TAs was observed in 19 out of 22 cells (86%) peaked in 4–6 min (Fig. 6d) was concentration-dependent (Fig. 6e) and reproducible. The IC50 for β-PEA and TYR were 43.8 ± 6.5 μM (n = 10) and 31.2 ± 3.3 μM (n = 12) respectively. The

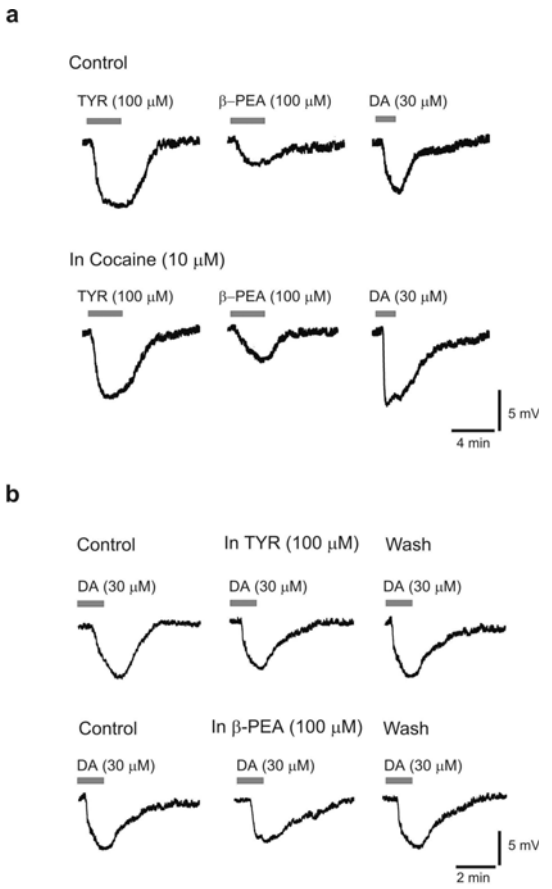

Figure 4. DAT inhibition and store depletion do not change the cellular responses to TAs.

maximal inhibition caused by β-PEA (100 μM) was 41.5 ± 6.6% (n = 10) while that caused by TYR (100 μM) was 60.7 ± 4.5% (n = 12). $GABA_B$ IPSP amplitude was also irreversibly reduced by the adrenergic antagonist phentolamine (30–100 μM) (Fig. 6c). Phentolamine has been recently shown to be a TAs agonist (Bunzow, et al., 2001). The inhibition caused by phentolamine (100 μM) was 30 ± 6.7% (n = 4). Interestingly, neither β-PEA nor TYR (100 μM) affected the amplitude of the evoked fast EPSP or the $GABA_A$ mediated IPSP, not shown. We also tested whether a depletion of DA stores by pretreating the rats with reserpine and then perfusing the slices with carbidopa affects the reduction of the $GABA_B$ IPSP caused by TAs. Under these conditions, β-PEA and TYR still induced a clear-cut, reversible depression of the $GABA_B$ IPSP (not shown).

3.2. TAs Modulate $GABA_B$ Postsynaptic Responses

We have also analyzed the effect of β-PEA and TYR on the $GABA_B$-mediated activation of the GIRK channel by using whole-cell patch-clamp recordings. Pressure applications of the $GABA_B$ agonist baclofen (100 μM, 1s, every 2 min) in the vicinity of the soma

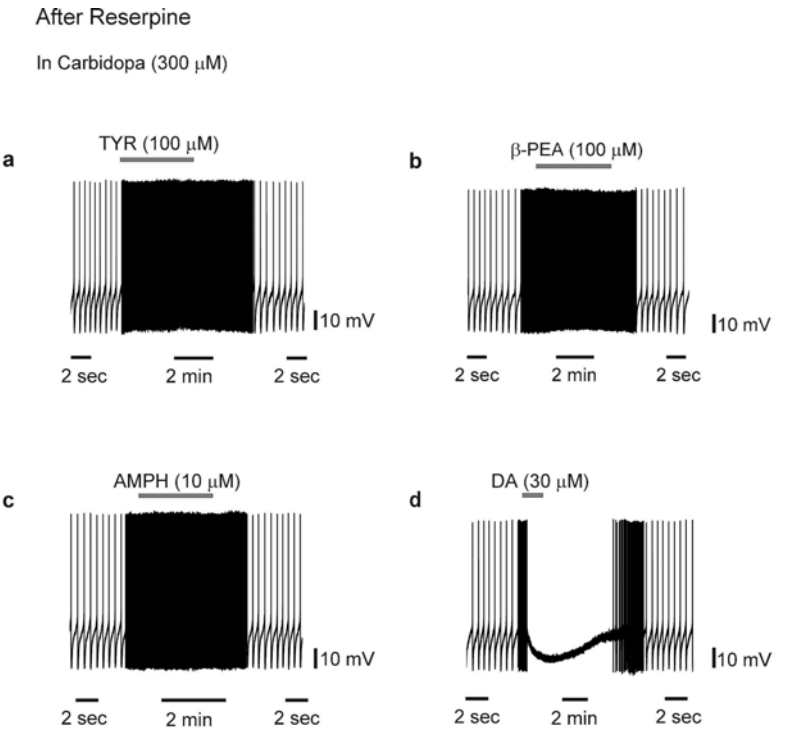

Figure 5. DA depletion prevents the effects of trace amines.

of the recorded neuron (voltage-clamped at −60 mV) caused reproducible outward currents (135.3 ± 13.3 pA; n = 23; Fig. 7a). Bath application of β-PEA (100 μM) and TYR (100 μM) reversibly reduced the baclofen activated outward current (IBac) by 55.6 ± 3.7% (n = 18) and by 31.1 ± 3.9% (n = 10) respectively, in 21 out of 23 cells tested (91%). TAs did not affect IBac responses in 3 cells. The time-course of the effects of β-PEA and TYR on the IBac is shown in Figure 7b. The maximal reduction of the amplitude of the IBac peaked after 4–6 min superfusion of β-PEA and 6–8 min superfusion of TYR. In addition, TAs caused a small inward current (35 ± 22 pA, n = 18) and did not modify membrane resistance. TAs also inhibited the outward current during continuous perfusion of baclofen (10 μM). Thus, brief (3 min) co-application of β-PEA (100 μM) or TYR (100 μM) together with baclofen (10 μM) induced a reversible reduction of the outward current of 30.5 ± 8% and 25 ± 6% respectively (n = 3, Fig. 7c). Interestingly, bath applications of the TA agonist, phentolamine (100 μM) reduced IBac by 62.5 ± 3.4% within 8–10 minutes of perfusion. This effect did not reverse following 30 minutes of washout of the drug from the bath (n = 7; Fig. 7a and b).

3.3. TAs Depress the Interaction of $GABA_B$ Gi/0 with GIRK Channels

To further analyze the mechanisms involved in the attenuation of GIRK by TAs, we loaded the DA neurons with the non-hydrolyzable GTP analog, GTP-γ-S trilithium salt, (GTP-γ-S, 0.3 mM). Whole cell perfusion with GTP-γ-S activated a mean outward current

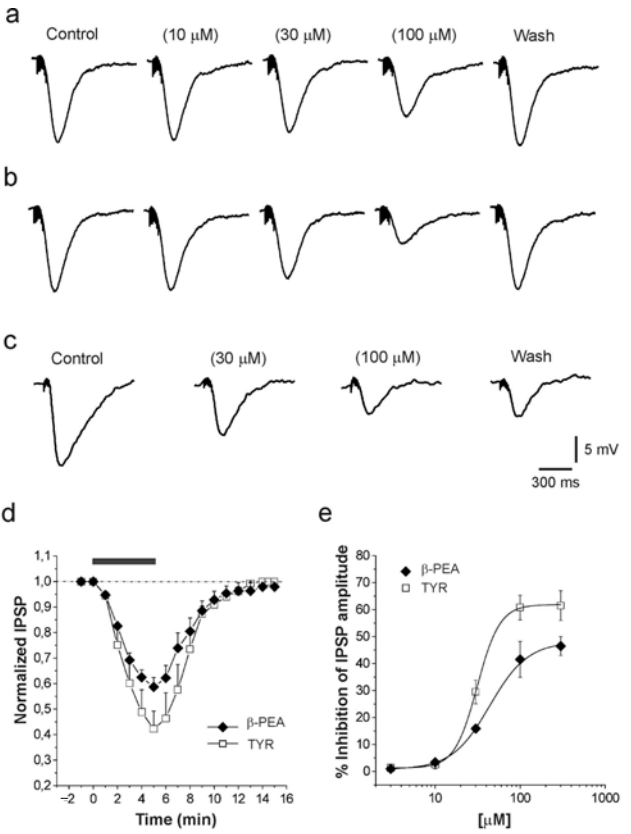

Figure 6. $GABA_B$ synaptic potentials are depressed by trace amines.

of +205 ± 25 pA (n = 6), that gradually occluded non-reversing responses to transient $GABA_B$ receptor activation, indicating the saturated activation of GIRK by G subunits (Fig. 8a and b). Under these conditions the mean holding current (Vhold = −60 mV) was +221 ± 38 pA (n = 13). A subsequent 4–6 minutes bath application of β-PEA (100 μM) or TYR (100 μM) on cells either loaded with GTP-γ-S or also treated with baclofen caused a sustained and non-reversible mean inward current of 202.5 ± 28 pA (n = 7) and 228.2 ± 31 pA (n = 12) respectively. These data indicate that β-PEA and TYR inhibited the GIRK channel which had been tonically activated by the presence of GTP-γ-S and/or $GABA_B$ receptor stimulation. Interestingly, the inward current induced by these TAs did not reverse within the time-course of recordings (up to 20 minutes after washout) in contrast to the reversible effects of TAs using normal GTP (see Fig. 7). Following the TA-induced inward current in GTP-γ-S treated cells, further application of baclofen was without effect (see Fig. 8a and b, n = 11). This suggests that TAs inhibit GIRK through a G protein-dependent mechanism that cannot reverse due to the non-hydrolyzable nature of GTP-γ-S. The inhibition of a tonically activated GIRK conductance by β-PEA and TYR was supported by analysis of the current-voltage relationship (I-V). In neurons loaded with GTP-γ-S, current-voltage relationships were measured before and during bath application of the TAs. The net I-Vs for β-PEA (100 μM, Erev =–102 ± 38 mV, n = 4) and TYR (100 μM, Erev = –104 ± 26 mV, n = 4) indicate that trace amines specifically inhibit a potassium conductance, calculated

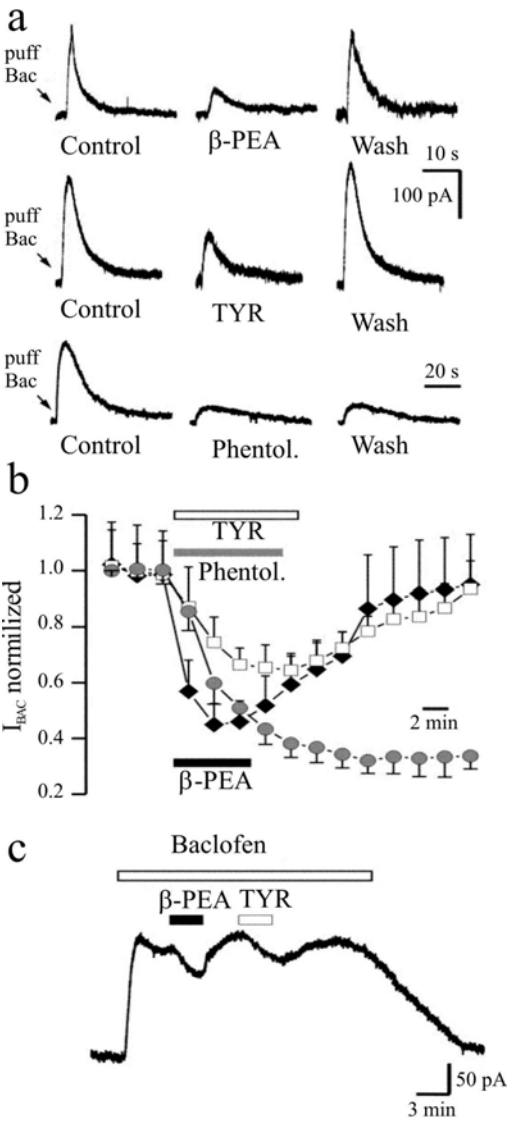

Figure 7. The postsynaptic responses caused by baclofen are reduced by TAs.

reversal potential was −105 mV (Fig. 8c). Consistent with the involvement of the GIRK channel, the β-PEA and TYR conductances showed inward rectification at hyperpolarized potentials (see non-linearity of I-V plot).

3.4. PKA, PKC, PLC and Intracellular Calcium Changes do not Mediate the Effects of TAs

We describe here a series of experiments that do not indicate known intracellular messengers in the actions of TAs, not shown, Activation of TA receptor has been associated

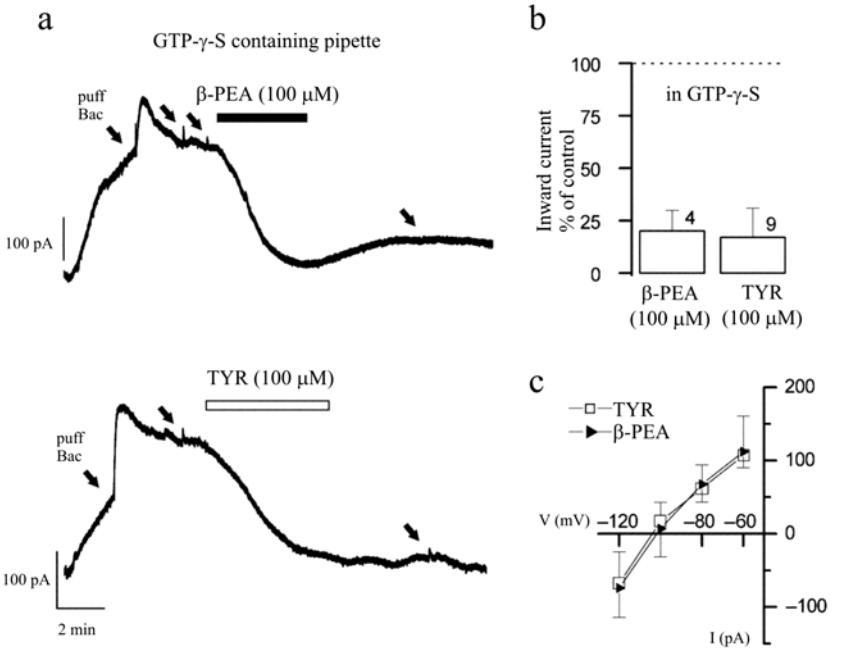

Figure 8. G-proteins are involved in the action of TAs.

with the enhancement of intracellular levels of c-AMP (Borowsky, et al., 2001, Bunzow, et al., 2001). To investigate the possible role of a cAMP-PKA phosphorylation processes (Bonci and Williams, 1996, Couve, et al., 2002) in the inhibition of baclofen responses by TAs, we tested blockers of the adenyl cyclase–cAMP–PKA pathway. Bath application of the adenyl cyclase inhibitor, SQ-22,536 (3 μM), or the PKA-PKC inhibitor, staurosporine (1 μM) or the intracellular dialysis of neurons with the PKA inhibitor c-AMPS-Rp, triethylammonium salt (Rp-cAMPS, 500 μM) had no effect on the inhibition of the baclofen responses caused by either TYR (100 μM) or β-PEA (100 μM).

The possibility that TAs inhibit GIRK channels via stimulation of PLC mediated pathways was excluded by the use of the PLC inhibitor 1-[6-[((17β-3-Methoxyestra-1,3,5[10]-trien-17-yl)amino]hexyl]-1H-pyrrole-2,5-dione (U73122, 20 μM). When it was superfused on the DA cells it did not affect the reduction of IBac by TAs. To investigate whether a PLC-induced depletion of phosphatidylinositol 4,5-bisphosphate (PtIns(4,5)P2), which is thought to be required for activation of GIRK channels (Sui, et al., 1998, Petit-Jacques, et al., 1999), is involved in the TAs-induced depression of the GABAB-activated GIRK channel, we loaded the cells with PtIns(4,5)P2 via the patch pipette (Meyer, et al., 2001). Inclusion of PtIns(4,5)P2 (nominally 500 μM) had no effect on the amplitude or time course of IBac and did not significantly affect the TAs-induced inhibition of the $GABA_B$-activated GIRK. Finally, a separate set of microfluorimetric experiments indicated that TAs did not modify the intracellular concentration of calcium. All together, these results suggest that neither the activation of PKA, PKC, PLC nor changes in cytoplasmatic calcium level represent the signaling step mediating the inhibitory effects of TAs on the $GABA_B$ receptor–activated responses.

3.5. DA Neurons Contain TA Receptor mRNAs

Until now fifteen different TAs receptor isoforms have been identified in rat. In the present study we have focused our attention to the search for mRNA encoding the TA1 and TA2 receptors in DA cells essentially for two reasons. i) The mRNA for these two receptors is sparsely expressed in certain cells of the substantia nigra/ventral tegmental area (Borowsky, et al., 2001). ii) The pharmacological characterization of the TA receptors has focused exclusively on these two members of the TA receptor family. As a first step in the study of the cellular localization of TA receptors in DA cells we examined their tissue expression. Conventional RT-PCR analysis of mRNA isolated from substantia nigra punches revealed the presence of TA1 and TA2 mRNA in this brain area (Fig. 9). We then probed their expression in single DA neurons, after the electrophysiological identification of cells as dopamine-containing. The cytosol of 16 cells was aspirated into patch pipettes and analyzed by single-cell RT-PCR. The presence of TH mRNA was confirmed in 15 cells indicating successful cytosol recovery and RTPCR reaction. Of these 15 TH-positive cells, TA receptor mRNA was detected in 9 cells (60%), 5 of which had both TA1 and TA2 mRNA (33%). One DA (TH-positive) cell had mRNA only for TA1, whereas four cells had message only for TA2. In 6 cells (40%) TA1 and TA2 mRNA was not detected (Fig. 9). These results indicate a nonhomogeneous distribution of TA1 and TA2 receptors in mid-brain DA cells.

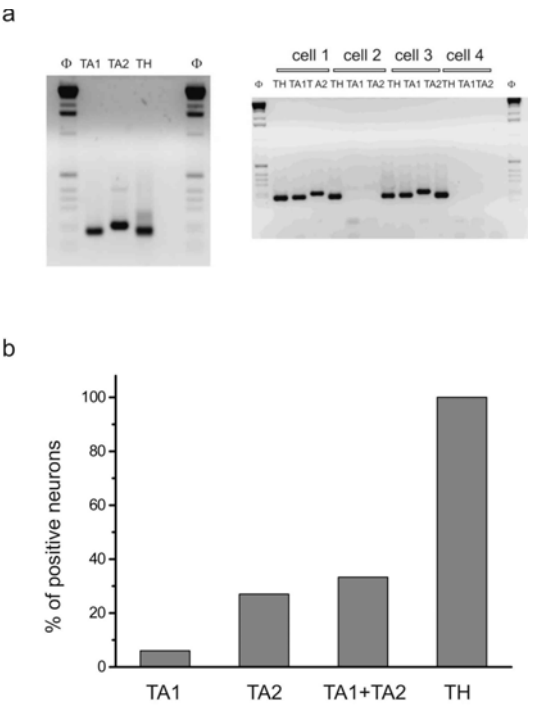

Figure 9. Single-cell RT-PCR analysis of dopamine neurons.

4. DISCUSSION

The present results emphasize the importance of TAs in regulating the function of the DA system of the ventral midbrain.

The experiments in section 1 confirm that β-PEA and TYR have an inhibitory action on DA cells of the ventral mesencephalon. The main finding is that this action is mediated by an activation of the D2 somato-dendritic autoreceptors. Therefore, the ability of β-PEA and TYR to inhibit firing is related to an indirect stimulation of these autoreceptors by an enhanced efflux of DA. This was demonstrated by the fact that the inhibitory effects of TAs were abolished either in the presence of the D2-selective antagonist sulpiride or when a complete intracellular DA depletion was obtained by a combined treatment of reserpine and superfusing midbrain slices with the dopadecarboxylase inhibitor carbidopa.

Since we have observed that the electrophysiological effects of TAs as well as, those induced by amphetamine (Scarponi, et al., 1999), were not reduced by DAT blockade and by a treatment of the rats with reserpine but were abolished by a combined treatment of reserpine and carbidopa, it is possible that TAs mobilize newly-synthesized DA to the extracellular space with modalities similar to the DAT-independent mechanisms operated by amphetamine (Parker and Cubeddu, 1988, Janssen, et al., 1999, Mundorf, et al., 1999). The indirect stimulation of DA receptors which accounts for our electrophysiological data is also in line with behavioral observations reporting that β-PEA induces ipsilateral rotations in rats having 6-hydroxydopamine lesion of the nigrostriatal dopaminergic system (Barroso and Rodriguez, 1996).

In addition to these indirect stimulatory effects on the DA system we have provided evidence that β-PEA and TYR depress the slow $GABA_B$ IPSP in midbrain DA cells, mainly by inhibiting the $GABA_B$-receptor activated GIRK channels. We believe that a TA-induced mobilization of DA from intracellular stores is not the main player in this depression. In fact, we have demonstrated that TAs still depressed the IPSP in reserpine- and carbidopa-treated cells in which the indirect (DA-mediated) effects of TAs are abolished (Geracitano, et al., 2004). Therefore, it might be suggested that the observed effects are mediated by the stimulation of specific TA receptors. In agreement with this, there is the observation that the unspecific and irreversible adrenergic antagonist phentolamine, mimicked the effects of β-PEA and TYR, consistently with its reported agonistic action on TA receptors (Bunzow, et al., 2001).

Because the depression of GIRK by TAs became irreversible in GTP-γ-S-treated cells, we identify a G-protein mediated role for them in modulating synaptic transmission in the mammalian central nervous system. It is generally assumed that GABA acting on $GABA_B$ receptors dissociates the Gαi/0-βγ dimer causing GIRK channel activation (Kunkel and Peralta, 1995; Huang, et al., 1997; Lewohl, et al., 1999). Therefore, in cells loaded with the non-hydrolyzable GTP analogue, GTP-γ-S, the $GABA_B$ agonist, baclofen induced a sustained opening of the GIRK channels that was irreversibly suppressed by TAs. This supports the notion that a) the TA inhibition of $GABA_B$ receptor-activated GIRK is a G protein-dependent process and b) the persistent closure of the GIRK channels by TAs bypasses events taking place upstream of the dissociation of the subunits activated by $GABA_B$ receptors.

Interestingly, the intracellular perfusion of GTP-γ-S initiated a slowly developing outward current in DA neurons even in the absence of exogenous agonist application. This implies that a tonic activated GIRK-linked receptors, due to spontaneous endogenous neu-

rotransmitter release within the slice (e.g. GABAB, nociceptin/orphanin FQ) (Lacey, et al., 1988; Uchida, et al., 2000; Tozzi, et al., 2001), could be modulated by TAs.

Our data also demonstrate that PKA, PKC, PLC or an increase in $[Ca^{2+}]_i$ are not causally involved in the inhibitory actions of TAs on GIRK channels. We therefore reasoned that a negative modulation of the activation the K^+ channels could account for the TAs-induced inhibition of the baclofen-induced current. A similar negative regulatory mechanism has recently been suggested for the orexin-induced depression of neurotransmitter-activated GIRK channels in mammalian neurons (Hoang, et al., 2003).

The single cell PCR approach shows TA1 and TA2 mRNA in the cells containing TH mRNA and supports the hypothesis that trace amines act postsynaptically on TA receptors to reduce GIRK currents. 40% of cells did not show either TA1 or TA2 mRNAs, yet 86 to 91% of DA neurons responded to TYR and β-PEA. It is therefore possible that subpopulations of DA neurons express TAs receptors other than TA1 or TA2, even though their mRNAs have not yet been detected. Therefore, the reduction of the $GABA_B$ IPSP might be principally due to the activation of G protein-coupled trace amine receptors that are stimulated by TYR and β-PEA. Accordingly, saturable, high affinity binding sites for p-[3H]tyramine (Ungar, et al., 1977, Vaccari, 1986, Vaccari and Gessa, 1989) and β-[3H]PEA (Nguyen and Juorio, 1989) have been reported in the nigrostriatal system. Although the IC50 for the reducing effects of trace amines is above the nanomolar range usually found in the brain (Berry, 2004), it could be possible that, under particular metabolic conditions or pharmacological treatments (e.g. MAO inhibition), the synaptic activity of $GABA_B$ receptors is regulated by TAs.

We have recently reported (Geracitano, et al., 2004) that TAs do not affect the gross outward current caused by DA. To explain the different results between the DA- and GABA-induced responses, a specific inhibition of GIRK activated by $GABA_B$ but not D2 receptors can be suggested. However, considering the identity of the GIRK currents activated by $GABA_B$ and D2 receptors on DA cells (Lacey, et al., 1988) this mechanism appears unlikely. We therefore reasoned that the apparent lack of effects of TAs on DA responses could result from a balance between the enhancing and diminishing actions of these endogenous substances, e.g. DA releasing properties, interference with the DA transporter and GIRK channel.

We hope that a more detailed study exploring the interaction between TAs and D_2-mediated GIRK currents will be the subjects of future experiments.

4.1. Functional Implications

We have described two modalities of action of TAs on DA neurons. The first one is the reduction of activity caused by increased DA release: the second one is more complex and shapes the responses to receptor-activated K^+ channels. There is evidence suggesting that trace amines coexist with DA in the DA cells (Juorio, et al., 1991) and activate motor activity by interacting with the DA system (Durden and Philips, 1980). The modulation of the GIRK channels by TAs might have a profound impact on integrative functions of the DA neurons to reduce the postsynaptic hyperpolarization caused by GABA released at inhibitory synapses.

The different actions of biogenic amines on the activity of dopamine neurons might be involved in controlling the extracellular levels of DA in target areas, being therefore of crucial importance in typical physiopathological processes of the dopamine system.

5. ACKNOWLEDGEMENTS

Figures 2 to 5 are taken from Geracitano et al. (2004) published with the consensus of the owner of the copyright, Elsevier. Figures 6 to 8 are taken from Federici et al., (2005) and published with the consensus of the owner of the copyright, ASPET. This study was supported by a COFIN grant (code 2003053445_004) and two Fondo per gli Investimenti della Ricerca di Base grants (codes RBNE01WY7P-010 and RBNE017555-006) to N. B. M.

6. REFERENCES

Barroso, N., and Rodriguez, M., 1996, Action of beta-phenylethylamine and related amines on nigrostriatal dopamine neurotransmission. *Eur. J. Pharmacol.* **297**:195–203.

Berry, M.D., 2004, Mammalian central nervous system trace amines. Pharmacologic amphetamines, physiologic neuromodulators. *J. Neurochem.* **90**:257–271.

Bonci, A., and Williams, J.T., 1996, A common mechanism mediates long-term changes in synaptic transmission after chronic cocaine and morphine. *Neuron.* **16**:631–639.

Borowsky, B., Adham, N., Jones, K.A., Raddatz, R., Artymyshyn, R., Ogozalek, K.L., Durkin, M.M., Lakhlani, P.P., Bonini, J.A., Pathirana, S., Boyle, N., Pu, X., Kouranova, E., Lichtblau, H., Ochoa, F. Y., Branchek, T.A., and Gerald, C., 2001, Trace amines: identification of a family of mammalian G proteincoupled receptors. *Proc. Natl. Acad. Sci. U S A* **98**:8966–8971.

Boulton, A.A., 1976, Identification, distribution, metabolism, and function of meta and para tyramine, phenylethylamine and tryptamine in brain. *Adv. Biochem. Psychopharmacol.* **15**:57–67.

Boulton, A.A., 1982, Some aspects of basic psychopharmacology: the trace amines. *Prog. Neuropsychopharmacol Biol. Psychiatry* **6**:563–570.

Branchek, T.A., and Blackburn, T.P., 2003, Trace amine receptors as targets for novel therapeutics: legend, myth and fact. *Curr. Opin. Pharmacol.* **3**:90–97.

Bunzow, J.R., Sonders, M.S., Arttamangkul, S., Harrison, L.M., Zhang, G., Quigley, D.I., Darland, T., Suchland, K.L., Pasumamula, S., Kennedy, J.L., Olson, S.B., Magenis, R.E., Amara, S. G., and Grandy, D.K., 2001, Amphetamine, 3,4-methylenedioxymethamphetamine, lysergic acid diethylamide, and metabolites of the catecholamine neurotransmitters are agonists of a rat trace amine receptor. *Mol. Pharmacol.* **60**:1181–1188.

Cameron, D.L., and Williams, J.T., 1993, Dopamine D1 receptors facilitate transmitter release. *Nature* **366**:344–347.

Couve, A., Thomas, P., Calver, A.R., Hirst, W.D., Pangalos, M.N., Walsh, F.S., Smart, T.G., and Moss, S.J., 2002, Cyclic AMP-dependent protein kinase phosphorylation facilitates GABA(B) receptor-effector coupling. *Nat. Neurosci.* **5**:415–424.

Durden, D.A., and Philips, S.R., 1980, Kinetic measurements of the turnover rates of phenylethylamine and tryptamine in vivo in the rat brain. *J. Neurochem.* **34**:1725–1732.

Federici, M., Geracitano, R., Tozzi, A., Longone, P., Di Angelantonio, S., Bengtson, C.P., Bernardi, G., and Mercuri, N.B., 2005, Trace amines depress $GABA_B$ response in dopaminergic neurons by inhibiting G-βγ-gated inwardly rectifying potassium channels. *Mol. Pharmacol.* **67**:1283–1290.

Geracitano, R., Federici, M., Prisco, S., Bernardi, G., and Mercuri, N.B., 2004, Inhibitory effects of trace amines on rat midbrain dopaminergic neurons. *Neuropharmacology* **46**:807–814.

Hoang, Q.V., Bajic, D., Yanagisawa, M., Nakajima, S., and Nakajima, Y., 2003, Effects of orexin, hypocretin on GIRK channels. *J. Neurophysiol.* **90**:693–702.

Huang, C.L., Jan, Y.N., and Jan, L.Y., 1997, Binding of the G protein betagamma subunit to multiple regions of G protein-gated inward-rectifying K^+ channels. *FEBS Lett.* **405**:291–298.

Janssen, P.A., Leysen, J.E., Megens, A.A., and Awouters, F.H., 1999, Does phenylethylamine act as an endogenous amphetamine in some patients? *Int. J. Neuropsychopharmcol* **2**:229–240.

Johnson, S.W., and North, R.A., 1992, Two types of neurone in the rat ventral tegmental area and their synaptic inputs. *J. Physiol.* **450**:455–468.

Juorio, A.V., 1976, Presence and metabolism of beta-phenylethylamine, p-tyramine, m-tyramine and tryptamine in the brain of the domestic fowl. *Brain Res.* **111**:442–445.

Juorio, A.V., Paterson, I.A., Zhu, M.Y., and Matte, G., 1991, Electrical stimulation of the substantia nigra and changes of 2-phenylethylamine synthesis in the rat striatum. *J. Neurochem.* **56**:213–220.

Kim, K.A., and von Zastrow, M., 2001, Old drugs learn new tricks: insights from mammalian trace amine receptors. *Mol. Pharmacol.* **60**:1165–1167.

Kosa, E., Marcilhac-Flouriot, A., Fache, M.P., and Siaud, P., 2000, Effects of beta-phenylethylamine on the hypothalamo-pituitary-adrenal axis in the male rat. *Pharmacol. Biochem. Behav.* **67**:527–535.

Kunkel, M.T., and Peralta, E.G., 1995, Identification of domains conferring G protein regulation on inward rectifier potassium channels. *Cell* **83**:443–449.

Lacey, M.G., Mercuri, N.B., and North, R.A., 1988, On the potassium conductance increase activated by $GABA_B$ and dopamine D2 receptors in rat substantia nigra neurones. *J. Physiol.* **401**:437–453.

Lewohl, J.M., Wilson, W.R., Mayfield, R.D., Brozowski, S.J., Morrisett, R.A., and Harris, R.A., 1999, Gprotein-coupled inwardly rectifying potassium channels are targets of alcohol action. *Nat. Neurosci.* **2**:1084–1090.

Mercuri, N.B., Bonci, A., Calabresi, P., Stefani, A., and Bernardi, G., 1995, Properties of the hyperpolarization-activated cation current Ih in rat midbrain dopaminergic neurons. *Eur. J. Neurosci.* **7**:462–469.

Meyer, T., Wellner-Kienitz, M.C., Biewald, A., Bender, K., Eickel, A., and Pott, L., 2001, Depletion of phosphatidylinositol 4,5-bisphosphate by activation of phospholipase C-coupled receptors causes slow inhibition but not desensitization of G protein-gated inward rectifier K^+ current in atrial myocytes. *J. Biol. Chem.* **276**:5650–5658.

Mundorf, M.L., Hochstetler, S.E., and Wightman, R.M., 1999, Amine weak bases disrupt vesicular storage and promote exocytosis in chromaffin cells. *J. Neurochem.* **73**:2397–2405.

Nguyen, T.V., and Juorio, A.V., 1989, Binding sites for brain trace amines. *Cell Mol. Neurobiol.* **9**:297–311.

Parker, E.M., and Cubeddu, L.X., 1988, Comparative effects of amphetamine, phenylethylamine and related drugs on dopamine efflux, dopamine uptake and mazindol binding. *J. Pharmacol. Exp. Ther.* **245**:199–210.

Paterson, I.A., Juorio, A.V., and Boulton, A.A., 1990, 2-Phenylethylamine: a modulator of catecholamine transmission in the mammalian central nervous system? *J. Neurochem.* **55**:1827–1837.

Petit-Jacques, J., Sui, J.L., and Logothetis, D.E., 1999, Synergistic activation of G protein-gated inwardly rectifying potassium channels by the betagamma subunits of G proteins and Na(+) and Mg(2+) ions. *J. Gen. Physiol.* **114**:673–684.

Premont, R.T., Gainetdinov, R.R., and Caron, M.G., 2001, Following the trace of elusive amines. *Proc. Natl. Acad. Sci. U S A* **98**:9474–9475.

Scarponi, M., Bernardi, G., and Mercuri, N.B., 1999, Electrophysiological evidence for a reciprocal interaction between amphetamine and cocaine-related drugs on rat midbrain dopaminergic neurons. *Eur. J. Neurosci.* **11**:593–598.

Schonfeld, C.L., and Trendelenburg, U., 1989, The release of 3H-noradrenaline by p- and m-tyramines and – octopamines, and the effect of deuterium substitution in alpha-position. *Naunyn. Schmiedebergs Arch. Pharmacol.* **339**:433–440.

Skerritt, J.H., Guihot, S.L., McDonald, S.E., and Culvenor, R.A., 2000, Development of immunoassays for tyramine and tryptamine toxins of Phalaris aquatica L. *J. Agric. Food Chem.* **48**:27–32.

Sui, J.L., Petit-Jacques, J., and Logothetis, D.E., 1998, Activation of the atrial KACh channel by the betagamma subunits of G proteins or intracellular Na^+ ions depends on the presence of phosphatidylinositol phosphates. *Proc. Natl. Acad. Sci. U S A* **95**:1307–1312.

Tozzi, A., Guatteo, E., Caputi, L., Bernardi, G., and Mercuri, N.B., 2001, Group I mGluRs coupled to G proteins are regulated by tyrosine kinase in dopamine neurons of the rat midbrain. *J. Neurophysiol.* **85**:2490–2497.

Uchida, S., Akaike, N., and Nabekura, J., 2000, Dopamine activates inward rectifier K^+ channel in acutely dissociated rat substantia nigra neurones. *Neuropharmacology* **39**:191–201.

Ungar, F., Mosnaim, A.D., Ungar, B., and Wolf, M.E., 1977, Tyramine-binding by synaptosomes from rat brain: effect of centrally active drugs. *Biol. Psychiatry* **12**:661–668.

Vaccari, A., 1986, High affinity binding of [3H]-tyramine in the central nervous system. *Br J Pharmacol.* **89**:15–25.

Vaccari, A., and Gessa, G., 1989, [3H]tyramine binding: a comparison with neuronal [3H]dopamine uptake and [3H]mazindol binding processes. *Neurochem. Res.* **14**:949–955.

REGULATION OF DOPAMINE RELEASE AND DOPAMINE CELL ACTIVITY BY ENDOGENOUS H_2O_2: IMPLICATIONS FOR BASAL GANGLIA FUNCTION

Margaret E. Rice, Jyoti Patel, Li Bao, Zsuzsanna S. Pearson, Pullani Shashidharan, Ruth H. Walker, Billy T. Chen, and Marat V. Avshalumov*

1. INTRODUCTION

Reactive oxygen species (ROS) are often considered to be toxic 'byproducts' of cell metabolism. Indeed, increased ROS production and oxidative stress contribute to cell death after acute brain injury, as well as in slowly progressing neurodegenerative disorders, including Parkinson's disease (Olanow and Tatton, 1999; Zhang et al., 2000). This view of ROS is evolving rapidly, however, in light of increasing evidence showing that ROS also act as cellular messengers that can modulate processes from short-term ion-channel activation to gene transcription. Hydrogen peroxide (H_2O_2) is a particularly intriguing candidate as a signaling molecule because it is neutral and membranepermeable (Ramasarma, 1983) and can therefore diffuse freely from a site of generation, characteristics shared with the established diffusible messengers, nitric oxide and carbon monoxide. Moreover, H_2O_2 is not a free radical, unlike superoxide ($\cdot O_2^-$) or the hydroxyl radical ($\cdot$OH), and therefore does not readily cause oxidative damage (Cohen, 1994).

In this chapter we review evidence that endogenously generated H_2O_2 is an important signaling molecule in the nigrostriatal pathway. In dorsolateral striatum, H_2O_2 mediates glutamate-dependent inhibition of axonal DA release. In the substantia nigra pars compacta (SNc), H_2O_2 regulates the spontaneous firing rate of DA neurons and inhibits somatodendritic DA release. All of these effects of H_2O_2 are mediated by ATP-sensitive potassium (K_{ATP}) channels, which are expressed abundantly in both striatum and SNc (Mourre et al., 1990; Xia and Haddad, 1991; Liss et al., 1999).

* Margaret E. Rice, Jyoti Patel, Li Bao, Zsuzsanna S Pearson, Billy T. Chen, and Marat V. Avshalumov, Dept. Physiology and Neuroscience, NYU School of Medicine, New York, NY 10016, USA. Pullani Shashidharan, Dept. Neurology, Mount Sinai School of Medicine, New York, NY 10029, USA. Ruth H. Walker, Dept. Neurology, Veterans Affairs Medical Center, Bronx, NY USA.

2. REGULATION OF DOPAMINE RELEASE BY H_2O_2

2.1. Potential Sources of H_2O_2 Generation

The major source of ROS in neurons, as in all cells, is mitochondrial respiration (Finkel and Holbrook, 2000), although other $\cdot O_2^-$-generating processes, notably NADPH oxidase (Serrano et al., 2003), also contribute. During mitochondrial respiration, $\cdot O_2^-$ is formed from the one electron reduction of O_2; H_2O_2 is generated from $\cdot O_2^-$ by superoxide dismutase (SOD), as well as by spontaneous dismutation (Boveris and Chance, 1973; Cohen, 1994). The amount of H_2O_2 produced by mitochondria is 1–2% of O_2 metabolized (Boveris and Chance, 1973), such that the concentration of H_2O_2 within the restricted volume of a dendrite, for example, could transiently reach mM levels (Chen et al., 2001). Absolute levels of H_2O_2 at any moment in time, however, will depend on the balance between the rate of H_2O_2 generation and the activities of the peroxidase enzymes glutathione (GSH) peroxidase and catalase (Cohen, 1994).

2.2. Endogenous H_2O_2 Inhibits Axonal and Somatodendritic Dopamine Release

Initial studies in our laboratory indicated that transient exposure of guinea-pig striatal slices to exogenous H_2O_2 (15 min, 1.5 mM) causes a reversible 30–40% decrease in evoked extracellular DA concentration ($[DA]_o$), monitored in dorsolateral striatum using carbon-fiber microelectrodes and fast-scan cyclic voltammetry. Suppression of evoked DA release is reversible and is not accompanied by a change in tissue DA content or evidence of oxidative damage (Chen et al., 2001). Subsequently, we discovered that *endogenous* H_2O_2 plays an important role in the physiological regulation of axonal DA release in striatum. Amplification of endogenously generated H_2O_2 by inhibiting GSH peroxidase with mercaptosuccinate (MCS) causes a similar decrease in pulse-train evoked $[DA]_o$ (30 pulses, 10 Hz) to that seen with exogenously applied H_2O_2 (Chen et al., 2002; Avshalumov et al., 2003) (Fig. 1A). Again, no change in DA content is seen (unpublished observations) and DA release suppression is fully reversible upon MCS washout or when the slice is superfused with catalase in the continued presence of MCS (Avshalumov et al., 2003) (Fig. 1A). Moreover, we found that regulation of DA release by endogenous H_2O_2 occurs in the shell of the nucleus accumbens, as well as in dorsolateral striatum (Chen et al., 2002). Importantly, MCS has no effect on $[DA]_o$ evoked by a a single stimulus pulse (Avshalumov et al., 2003), implying that even under conditions of impaired GSH peroxidase activity, basal levels of H_2O_2 in striatum are insufficient to inhibit DA release. Instead, modulatory H_2O_2 must be generated *dynamically* during the first pulse of a stimulus-train and inhibits DA released by subsequent pulses. Additional studies show that H_2O_2 generation is derived from concomitant glutamate release and AMPA receptor activation (discussed in Section 2.3). The time-scale of H_2O_2-dependent DA release suppression is rapid, occurring within a few hundred milliseconds after initiation of a 10 Hz pulse train (Avshalumov et al., 2003).

Somatodendritic DA release in the SNc is also suppressed by endogenous H_2O_2 when GSH peroxidase is inhibited by MCS (Fig. 1B). Strikingly, however, MCS has no effect on evoked DA release in the ventral tegmental area (VTA) (Chen et al., 2002) (Fig. 1B). In addition, the effect of MCS in striatum (and SNc, unpublished observations) persists in the presence of a DA uptake inhibitor (GBR-12909), which confirms that H_2O_2 alters DA release not DA uptake (Avshalumov et al., 2003).

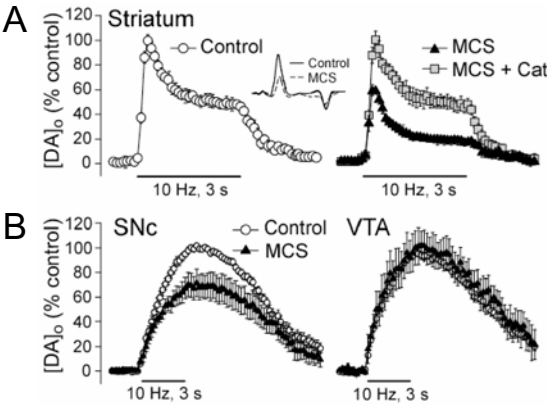

Figure 1. Endogenous H_2O_2 suppresses nigrostriatal DA release. **A.** In guinea-pig striatal slices, inhibition of GSH peroxidase with mercaptosuccinate (MCS, 1 mM) causes a reversible decrease in evoked $[DA]_o$ (30 pulses; 10 Hz) that is reversed by catalase (Cat, 500 IU mL^{-1}); inset shows characteristic DA voltammogram (modified from Avshalumov et al., 2003). **B.** MCS also causes inhibition of DA release in the SNc, but not in the VTA of guinea pig midbrain slices (modified from Chen et al., 2002). Data are means ± SEM, shown a % control; n = 5–8; $p < 0.001$ MCS *vs*. control in striatum and SNc.

What cellular process generates modulatory H_2O_2? Our recent studies indicate that the primary source is mitochondrial respiration: the effect of MCS on DA release in striatum is lost when mitochondrial complex I is inhibited by rotenone (Bao and Rice, 2004). This argues against significant involvement of other $\cdot O_2^-/H_2O_2$ generating pathways, including NADPH oxidase. Additional experiments confirm a lack of involvement of monoamine oxidase (MAO), which produces one molecule of H_2O_2 for each molecule of DA metabolized (Cohen, 1994): a cocktail of MAO inhibitors does not alter evoked $[DA]_o$ *vs*. control or prevent the effect of MCS (Bao and Rice, 2004).

2.3. Regulation of Striatal DA Release by Glutamate Requires H_2O_2

Given the close apposition of mitochondria to presynaptic sites in DA axons (Nirenberg et al., 1997), we intially assumed that modultory H_2O_2 generation in the striatum might occur directly in DA axons, such that activity-dependent H_2O_2 would provide a feedback signal to decrease DA release and thereby "augment the effect of D_2-autoreceptor-mediated inhibition" (Chen et al., 2001). However, our subsequent studies have disproved this hypothesis. The most direct evidence has come from comparisons of the effect of GSH peroxidase inhibition on DA release evoked by local *vs*. distal stimulation in parasagittal slices of striatum, in which DA-axon tracts are preserved for 1–2 mm. In this preparation, as in our usual coronal slices, local stimulation evokes the release of glutamate, GABA and other transmitters, as well as that of DA, whereas distal pathway stimulation selectively activates DA axons to elicit relatively pure DA release. Under these conditions, inhibiting GSH peroxidase with MCS suppressed $[DA]_o$ evoked by local stimulation, as seen previously, but not by distal stimulation (Patel et al., 2004). Also arguing against H_2O_2 generation in DA axons is the finding that H_2O_2-dependent inhibition of DA release requires glutamatergic AMPA receptors (Avshalumov et al., 2003), which are absent from DA axons (Bernard and Bolam, 1998; Chen et al., 1998).

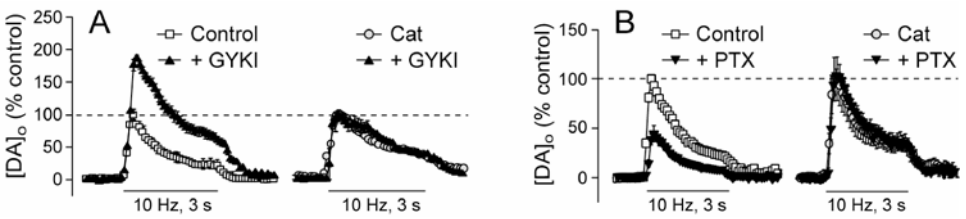

Figure 2. Regulation of striatal DA release by glutamate and GABA requires H_2O_2. **A.** AMPA-receptor blockade by GYKI-52466 (GYKI; 50 µM) causes a ~100% increase in evoked $[DA]_o$ in striatum ($p < 0.001$, $n = 6$). **B.** The effect of AMPA-receptor blockade is prevented by catalase (Cat). **C.** $GABA_A$ receptor blockade by picrotoxin (PTX; 100 µM) causes a ~50% decrease in evoked $[DA]_o$ ($p < 0.001$, $n = 6$). **D.** Catalase abolishes the effect of picrotoxin. Responses in the presence of heat-inactivated catalase were the same as control. Data are means ± SEM, shown as percentage of same-site control (modified from Avshalumov et al., 2003a).

Thus, H_2O_2-mediated inhibition of DA release in striatum is not an auto-regulatory process, but rather represents potent *external* regulation by glutamatergic input to the striatum. Indeed, when striatal AMPA receptors are blocked by a selective antagonist, GYKI-52466, pulse-train evoked $[DA]_o$ increases by 100% (Avshalumov et al., 2003); this effect is completely prevented by catalase, confirming that H_2O_2 is required (Fig. 2A,B). Thus, glutamate released under physiological conditions *inhibits* action potential-dependent DA release in striatum via H_2O_2. Moreover, H_2O_2 amplification by MCS has no effect on DA release in the presence of GYKI-52466, indicating that glutamate acting at AMPA receptors is *required* for generation of modulatory H_2O_2 in striatum (Avshalumov et al., 2003). Consistent with the non-DA axon origin of AMPA-receptor dependent H_2O_2 generation, blockade of AMPA receptors with GYKI-52466 enhanced $[DA]_o$ evoked locally, but had no effect on that evoked distally (Patel et al., 2004). The question of how, or even if, glutamate regulates striatal DA release has been a long-standing source of controversy. Our discovery that glutamate inhibits DA release via H_2O_2 resolves this conundrum.

Regulation of striatal DA release by GABAergic input is also unconventional: blockade of $GABA_A$ receptors by picrotoxin causes a ~50% *decrease* in evoked $[DA]_o$ (Fig. 2C), whereas GABAB-receptor blockade with saclofen has no effect (Avshalumov et al., 2003), indicating that GABA, acting at $GABA_A$ receptors, normally *enhances* DA release. The influence of GABA on DA release, like that of glutamate, must be indirect, since DA axons in striatum do not express $GABA_A$ receptors (Fujiyama et al., 2000). The mediator again proved to be H_2O_2, since the effect of picrotoxin is prevented by catalase (Fig. 2D). Additionally, picrotoxin has no effect on DA release when AMPA receptors are blocked by GYKI-52466 (Avshalumov et al., 2003), indicating that glutamate and GABA act on the same pool of AMPA-receptor dependent H_2O_2.

3. ACTIVITY-DEPENDENT H_2O_2 GENERATION IN MSNS AND DA NEURONS

3.1. H_2O_2 Generation in Striatal Medium Spiny Neurons

Increasing evidence implicates MSNs as the primary cellular source of modulatory H_2O_2 in dorsal striatum. Not only are these the most abundant striatal neurons (90–95%; Kemp and Powell, 1971), but the pattern of sensitivity of DA release to glutamate and

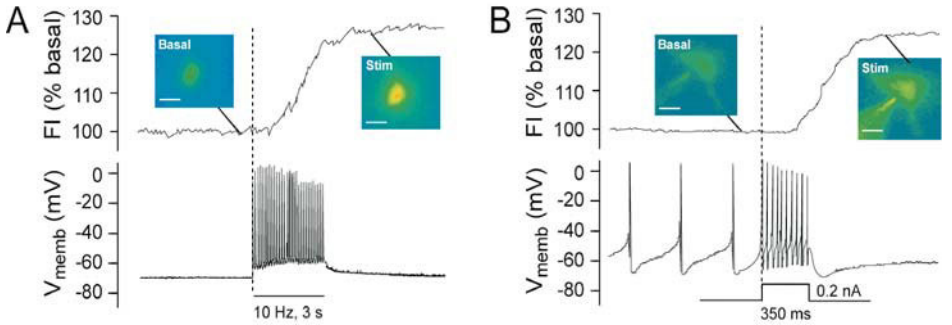

Figure 3. Activity-dependent H_2O_2 generation in striatal medium spiny neurons (MSNs) and in SNc DA neurons in guinea-pig brain slices. **A.** MSN: basal fluorescence intensity (FI) under control conditions and after local stimulation (10 Hz, 30 pulses) with simultaneously recorded membrane voltage (V_{memb}); FI plateau reflects irreversible DCF activation. Images are basal and stimulated (Stim) FI (Patel et al., 2004). **B.** DA neuron: basal FI and after depolarizing current injection with V_{memb} (Avshalumov et al., 2005).

GABA antagonists (Avshalumov et al., 2003) mirrors the electrophysiological responsiveness of these cells (Jiang and North, 1991; Kita, 1996). Moreover, glutamate synapses are closely apposed to DA synapses on MSN dendrites (Smith and Bolam, 1990; Bernard and Bolam, 1998; Chen et al., 1998), such that they are ideally positioned to modulate DA release via postsynaptically generated H_2O_2. Additionally, MSNs express $GABA_A$ receptors at dendritic sites near spines (Fujiyama et al., 2000), which would facilitate GABAergic opposition of glutamatergic excitation and H_2O_2 generation.

Recent studies in our laboratory have confirmed that MSNs are a key cellular source of modulatory H_2O_2 in striatum. In these studies, we used a method we developed for simultaneous whole-cell recording and fluorescence imaging using the H_2O_2-sensitive dye DCF (2′7′-dichlorofluorescein) (Avshalumov et al., 2005). Under control conditions, basal DCF fluorescence is seen in all striatal MSNs, reflecting a basal H_2O_2 tone (Fig. 3A). Local stimulation (with the same 30 pulse, 10 Hz pulse trains used to elicit DA release) causes a ~30% increase in DCF fluorescence in MSNs, which is further enhanced by inhibition of GSH peroxidase with MCS (Patel et al., 2004) (Fig. 3A). Importantly, AMPA-receptor blockade by GYKI-52466 prevented stimulus-induced action potentials, as well as activity-dependent H_2O_2 generation in MSNs.

3.2. H_2O_2 Generation in DA Neurons in the SNc

Both basal and activity-dependent H_2O_2 generation can also be readily detected in DA neurons in the SNc using DCF fluorescence imaging (Avshalumov et al., 2005). Basal DCF fluorescence is detected in all DA neurons (Fig. 3B), indicating tonic H_2O_2 generation during spontaneous pacemaker activity. Activity-dependent H_2O_2 levels are amplified when GSH peroxidase is inhibited by MCS (Avshalumov et al., 2005), which leads to the suppression of somatodendritic DA release in the SNc, as described in Section 2.2. Under normal conditions, we examined activity-dependent H_2O_2 generation by increasing DA cell firing rate with depolarizing current injection. The increase in mean spike frequency to ~32 Hz was accompanied by a significant 25–30% increase in DCF fluorescence that peaked shortly after the pulse ended (Fig. 3B) (Avshalumov et al., 2005). Both basal and

elevated H_2O_2 levels have significant effects on DA cell membrane properties, as discussed in Section 4.

4. H_2O_2 ACTS IN THE NIGROSTRIATAL PATHWAY VIA K_{ATP} CHANNELS

4.1. H_2O_2-Sensitive K_{ATP} Channels Regulate DA Release in Striatum

The mechanism by which H_2O_2 regulates the nigrostriatal pathway is H_2O_2-dependent opening of K_{ATP} channels (Avshalumov et al., 2003; Avshalumov and Rice, 2003). These channels are multimeric proteins composed of an inwardly rectifying poreforming unit, typically Kir 6.2 in neurons (Aschroft and Gribble, 1998), and a sulfonylurea-binding site (SUR1 or SUR2) (Aguilar-Bryan et al., 1998). Previous physiological studies demonstrated that *exogenous* H_2O_2 can cause membrane hyperpolarization by activating a K^+ conductance in a variety of cell types, including pancreatic β-cells (Krippeit-Drews et al., 1999) and CA1 hippocampal neurons (Seutin et al., 1995). Our studies of striatal DA release provided the first evidence that *endogenous* H_2O_2 can activate K_{ATP} channels. Blockade of K_{ATP} channels by tolbutamide or glibenclamide significantly enhances evoked $[DA]_o$ in dorsolateral striatum, indicating that during normal stimulation, K_{ATP}-channel activation causes the inhibition of DA release; these sulfonylureas also prevent the usual pattern of H_2O_2-dependent modulation by MCS, GYKI, and picrotoxin (Avshalumov et al., 2003; Avshalumov and Rice, 2003), demonstrating that K_{ATP} channels are *required* for modulation of DA release by H_2O_2, glutamate, and GABA. Conversely, striatal DA release is decreased by ~40% by either diazoxide, a SUR1-selective K_{ATP}-channel opener, or cromakalim, a SUR2-selective opener. However, diazoxide prevents the effects of MCS, GYKI-52466, and picrotoxin, whereas cromakalim does not, demonstrating that glutamate-dependent H_2O_2 preferentially opens SUR1-based K_{ATP} channels (Avshalumov and Rice, 2003).

4.2. H_2O_2-sensitive K_{ATP} Channels Regulate DA Neuron Excitability in the SNc

Importantly, H_2O_2-sensitive K_{ATP} channels also regulate the activity of DA neurons in the SNc (Avshalumov et al., 2005). As discussed in Section 3.2, basal DCF fluorescence in all DA neurons examined (Fig. 3B) indicates that spontaneous pacemaker activity in these cells produces H_2O_2. These tonic levels have a significant effect on DA cell excitability: depletion of intracellular H_2O_2 by including catalase in the patch-pipette or blockade of K_{ATP} channels by glibenclamide (100 nM) caused a ~40% increase in spontaneous firing rate in all DA neurons tested. Importantly, the backfill solution in these studies contained 3 mM ATP, at which concentration, K_{ATP} channels should be closed (Häusser et al., 1991). Thus, it is unlikely that the resting K_{ATP} channel tone in DA neurons is caused by low ATP. Indeed, previous studies using inside-out membrane patches from cardiac cells have shown a direct, concentration-dependent effect of H_2O_2 on K_{ATP} channel opening by decreasing channel sensitivity to ATP (Ichinari et al., 1996). Whether regulation by H_2O_2 is direct or indirect in DA neurons remains to be elucidated. Regardless of mechanism, regulation of spontaneous activity in all DA neurons suggests that this tonic control is independent of SUR-subunit composition, perhaps implicating a modulatory site on pore-forming subunits.

In companion studies using DCF to visualize intracellular H_2O_2, we found that moderate increases in H_2O_2 (≤25% increase in fluorescence intensity) during partial inhibition of

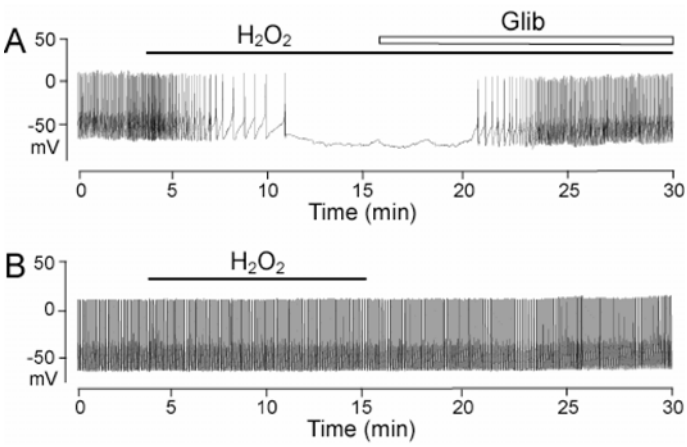

Figure 4. Differential effect of elevated H_2O_2 on DA neurons in the SNc. **A.** Exogenous H_2O_2 (1.5 mM) causes membrane hyperpolarization and inhibition of spontaneous activity in one population of identified DA neurons (responders); this can be reversed by K_{ATP}-channel blockers, here glibenclamide (Glib, 3 μM) or by washout of H_2O_2. **B.** A second population of DA cells (nonresponders) is unaffected by H_2O_2 (Avshalumov et al., 2005).

GSH peroxidase by MCS (0.1–0.3 mM) had no effect on DA neuron firing rate. However, with greater GSH inhibition (1 mM MCS) or application of exogenous H_2O_2 (1.5 mM), 50% of recorded cells, "responders", showed K_{ATP}-channel dependent hyperpolarization (Fig. 4A), whereas 50%, "nonresponders", did not (Fig. 4B) (Avshalumov et al., 2005). This distribution is similar to that of metabolically sensitive and insensitive DA neurons reported previously by Liss et al. (1999), in which greater metabolic sensitivity was found to be conveyed by SUR1-base K_{ATP} channels. Indeed, we found that H_2O_2-responders also hyperpolarize with SUR1-selective diazoxide, but not with SUR1-selective cromakalim, showing that SUR1 expression conveys sensitivity to elevated H_2O_2, as seen also in the striatum (Avshalumov and Rice, 2003). When endogenous H_2O_2 levels were increased by inhibiting catalase, the predominant peroxidase in SNc (Hung and Lee, 1998) with 3-aminotriazole (ATZ), all DA neurons responded with glibenclamide-reversible hyperpolarization. DCF imaging indicated that ATZ rapidly amplified intracellular H_2O_2, whereas MCS caused a slower increase (Avshalumov et al., 2005). Thus, SUR2-based K_{ATP} channels can also be activated by sufficiently high and/or rapid increases in H_2O_2. Overall, these data show that H_2O_2 does serve an auto-regulatory role in SNc DA neurons, in which activity-dependent H_2O_2 generation leads to suppression of neuronal activity via K_{ATP} channels, thus enhancing the reciprocal relationship between metabolism and excitability.

5. SUMMARY AND CONCLUSIONS

The findings discussed in this chapter indicate that H_2O_2 is an endogenous regulator of axonal and somatodendritic DA release, as well as DA neuron activity. Activitydependent H_2O_2 generation is predominantly mitochondrial and occurs in both dopaminergic and non-dopaminergic neurons. In dorsolateral striatum, H_2O_2 is generated downstream from AMPA-receptor activation in MSNs, rather than DA axons, and must therefore diffuse to

DA synapses where it inhibits DA release via opening of SUR1-based K_{ATP} channels. We have proposed that regulation of striatal DA release involves a triad of DA, glutamate, and GABA synapses that are separated by a few micrometers on the dendrites of medium spiny neurons, but bound together functionally by diffusible H_2O_2 (Avshalumov et al., 2003) (Fig. 5). Glutamate input to MSNs increases H_2O_2 production, which inhibits DA release by opening K_{ATP} channels. By decreasing MSN excitability, GABA attenuates H_2O_2 production; however, when $GABA_A$ receptors are blocked (Fig. 5, +PTX), excitation is amplified and H_2O_2 levels increase, leading to greater suppression of DA release. When AMPA receptors are blocked (Fig. 5, +GYKI), H_2O_2 generation is minimal, DA release is uninhibited, and regulation by GABA is lost (Fig. 5, left). Recent studies from our group indicate that regulation of DA release by exogenous agonists of cannabinoid (CB1) receptors may also act through this synaptic triad, via presynaptic modulation of glutamate and GABA release (Pearson and Rice, 2004).

Given the dependence of both axon-terminal and somatodendritic DA release on DA cell firing rate, H_2O_2-dependent regulation of DA cell activity would influence DA release throughout the nigrostriatal pathway. A key finding is that SUR1-containing K_{ATP} channels are required for the inhibition of striatal DA release by endogenous H_2O_2 (Avshalumov and Rice, 2003), as well as for inhibition of DA cell firing when H_2O_2 is elevated above basal levels in the SNc (Avshalumov et al., 2005). Moreover, the 50:50 distribution of H_2O_2-responsive and nonresponsive DA neurons in SNc is reflected in the pattern of functional SUR1- and SUR2-based K_{ATP}-channels in DA axons in striatum. Importantly, AMPA receptor activation in MSNs provides sufficient levels of H_2O_2 to inhibit DA release from ~50% of DA axons; this indicates a new and potentially important mechanism of external regulation of DA release that establishes a formerly "missing link" in the reciprocal relationship between DA and glutamate in striatum. To understand the implications of this for basal ganglia function will require investigation of how SUR1- *vs.* SUR2-expressing DA axons target striatonigral *vs*. striatopallidal MSNs.

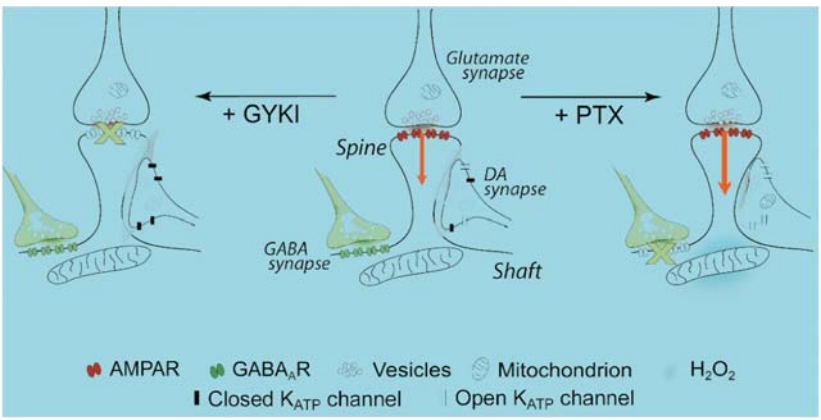

Figure 5. Triad of striatal DA, glutamate and GABA synapses on an MSN dendrite bound together *functionally* by diffusible H_2O_2. Generation of modulatory H_2O_2 when GABA as well as glutamate is released (center); $GABA_A$-receptor ($GABA_AR$) blockade by picrotoxin (+PTX, right), and with AMPA-receptor (AMPAR) blockade by GYKI-52466 (+GYKI, left) (circuitry and locations of receptors and mitochondria are from Smith and Bolam, 1990; Bernard and Bolam, 1998; Chen et al., 1998; Fujiyama et al., 2000).

Lastly, it should be noted that neuromodulation by H_2O_2 is a double-edged sword: an imbalance between H_2O_2 generation and regulation could result in oxidative stress, which has been implicated in nigrostriatal degeneration in Parkinson's disease (Cohen, 1994; Olanow and Tatton, 1999; Zhang et al., 2000). In this light, our finding that inhibition of GSH peroxidase by MCS leads to suppression of somatodendritic DA release in the SNc but not in the VTA (Chen et al., 2002) (Fig. 1B) is potentially important, because of the greater susceptibility of SNc *vs*. VTA DA neurons to degeneration in Parkinson's. Thus, loss of normal H_2O_2 regulation could contribute significantly to nigrostriatal pathology. This may have implications for other basal ganglia disorders, as well; for example, in mice that overexpress a mutated form of TorsinA provide a model for dystonia (Shashidharan et al., 2005), consequences of GSH peroxidase inhibition by MCS on striatal DA release are exacerbated compared to wildtype controls (Walker et al., 2004).

6. ACKNOWLEDGEMENTS

The authors are grateful for support from NIH grants NS-36362 and NS-45325 and the National Parkinson Foundation.

7. REFERENCES

Aguilar-Bryan, L., Clement, J.P.T., Gonzalez, G., Kunjilwar, K., Babenko, A., and Bryan J., 1998, Toward understanding the assembly and structure of K_{ATP} channels, *Physiol. Rev.* **78**:227–245.

Ashcroft, F.M., and Gribble, F.M., 1998, Correlating structure and function in ATP-sensitive K^+ channels. *Trends Neurosci.* **21**:288–294.

Avshalumov, M.V., and Rice, M.E., 2003, Activation of ATP-sensitive K^+ (K_{ATP}) channels by H_2O_2 underlies glutamate-dependent inhibition of striatal dopamine release. *P.N.A.S. (U.S.A.)* **100**:11729–11734.

Avshalumov, M.V., Chen, B.T., Marshall, S.P., Peña, D.M., and Rice, M.E., 2003, Glutamate-dependent inhibition of dopamine release in striatum is mediated by a new diffusible messenger, H_2O_2. *J. Neurosci*. **23**: 2744–2750.

Avshalumov, M.V., Chen, B.T., Koós, T., Tepper, J.M., Rice, M.E., 2005, Endogenous H_2O_2 regulates the excitability of midbrain dopamine neurons via K_{ATP} channels. *J. Neurosci*. **25**: (in press).

Bao, L., and Rice, M.E., 2004, Mitochondrial H_2O_2 mediates glutamate-dependent inhibition of striatal dopamine release, *2004 Abstract Viewer/Itinerary Planner*, Washington, DC: Soc. Neuroscience, 46.7.

Bernard, V., and Bolam, J.P., 1998, Subcellular and subsynaptic distribution of the NR1 subunit of the NMDA receptor in the neostriatum and globus pallidus of the rat: colocalization at synapses with the GluR2/3 subunit of the AMPA receptor, *Eur. J. Neurosci.* **10**:3721–3738.

Boveris, A., and Chance, B., 1973, The mitochondrial generation of hydrogen peroxide. General properties and effect of hyperbaric oxygen, *Biochem. J.* **134**:707–716.

Chen, B.T., Avshalumov, M.V., and Rice, M.E., 2001, H_2O_2 is a novel, endogenous modulator of synaptic dopamine release. *J. Neurophysiol.* **85**:2468–2476.

Chen, B.T., Avshalumov, M.V., and Rice, M.E., 2002, Modulation of somatodendritic dopamine release by endogenous H_2O_2: susceptibility in substantia nigra but resistance in VTA, *J. Neurophysiol*. **87**:1155–1158.

Chen, Q., Veenman, L., Knopp, K., Yan, Z., Medina, L., Song, W.J., Surmeier, D.J., and Reiner, A., 1998, Evidence for the preferential localization of glutamate receptor-1 subunits of AMPA receptors to the dendritic spines of medium spiny neurons in rat striatum, *Neuroscience* **83**:749–761.

Cohen, G., 1994, Enzymatic/nonenzymatic sources of oxyradicals and regulation of antioxidant defenses. *Ann. N.Y. Acad. Sci.* **738**:8–14.

Finkel, T., and Holbrook, N.J., 2000, Oxidants, oxidative stress and the biology of ageing, *Nature* **408**:239–247.

Fujiyama, F., Fritschy, J.M., Stephenson, F.A., and Bolam, J.P., 2000, Synaptic localization of $GABA_A$ receptor subunits in the striatum of the rat. *J. Comp. Neurol*. **416**:158–172.

Häusser, M.A., de Weille, J.R., Lazdunski, M., 1991, Activation by cromakalim of pre- and post-synaptic ATPsensitive K^+ channels in substantia nigra. *Biochem. Biophys. Res. Comm*. **174**:909–914.

Hung, H.C., and Lee, E.H., 1998, MPTP produces differential oxidative stress and antioxidative responses in the nigrostriatal and mesolimbic dopaminergic pathways, *Free Radic. Biol. Med*. **24**:76–84.

Ichinari, K., Kakei, M., Matsuoka, T., Nakashima, H., and Tanaka, H., 1996, Direct activation of the ATPsensitive potassium channel by oxygen free radicals in guinea-pig ventricular cells: its potentiation by MgADP. *J. Mol. Cell. Cardiol.* **28**:1867–1877.

Jiang, Z.G., and North, R.A., 1991, Membrane properties and synaptic responses of rat striatal neurones *in vitro*, *J. Physiol. (Lond.)* **443**:533–553.

Kemp, J.M., and Powell, T.P., 1971, The structure of the caudate nucleus of the cat: light and electron microscopy, *Philos. Trans. R. Soc. Lond. B Biol. Sci*. **262**:383–401.

Kita, H., 1996, Glutamatergic and GABAergic postsynaptic responses of striatal spiny neurons to intrastriatal and cortical stimulation recorded in slice preparations, *Neuroscience* **70**:925–940.

Krippeit-Drews, P., Kramer, C., Welker, S., Lang, F., Ammon, H.P.T., and Drews, G., 1999, Interference of H_2O_2 with stimulus-secretion coupling in mouse pancreatic β-cells, *J. Physiol. (Lond.)* **15**:471–481.

Liss, B., Bruns, R., and Roeper, J., 1999, Alternative sulfonylurea receptor expression defines sensitivity to K_{ATP} channels in dopaminergic midbrain neurons, *EMBO J.* **18**:833–846.

Mourre, C., Smith, M.L., Siesjo, B.K., and Lazdunski, M., 1990, Brain ischemia alters the density of binding sites for glibenclamide, a specific blocker of ATP-sensitive K^+ channels, *Brain Res.* **526**:147–152.

Nirenberg, M.J., Chan, J., Liu, Y., Edwards, R.H., and Pickel, V.M., 1997, Vesicular monoamine transporter-2: immunogold localization in striatal axons and terminals, *Synapse* **26**:194–198.

Olanow, C.W., and Tatton, W.G., 1999, Etiology and pathogenesis of Parkinson's disease, *Annu. Rev. Neurosci.* **22**:123–144.

Patel, J., Avshalumov, M.V., and Rice, M.E., 2004, Glutamate-dependent inhibition of striatal dopamine release is mediated by H_2O_2 generated in medium spiny neurons but not in dopamine terminals, *2004 Abstract Viewer/Itinerary Planner*, Washington, DC: Soc. Neuroscience, 46.6.

Pearson, Z.S., and Rice, M.E., 2004, Cannabinoid receptors modulate dopamine release in guinea-pig dorsal and ventral striatum. *2004 Abstract Viewer/Itinerary Planner*, Washington, DC: Soc. Neuroscience, 953.4.

Ramasarma, T., 1983, Generation of H_2O_2 in biomembranes, *Biochem. Biophys. Acta* **694**:69–93.

Serrano, F., Kolluri, N.S., Wientjes, F.B., Card J.P., and Klann, E., 2003, NADPH oxidase immunoreactivity in the mouse brain. *Brain Research* **988**:193–188.

Shashidharan, P., Sandu, D., Potla, U., Armata, I.A., Walker, R.H., McNaught, K.S., Weisz, D., Sreenath, T., Brin, M.F., and Olanow, C.W., 2005, Transgenic mouse model of early-onset DYT1 dystonia, *Human Mol. Gen*. **14**:125–133.

Seutin, V., Scuvee-Moreau, J., Masotte, L., and Dresse, A., 1995, Hydrogen peroxide hyperpolarizes rat CA1 pyramidal neurons by inducing an increase in potassium conductance, *Brain Res.* **683**:275–278.

Smith, A.D., and Bolam, J.P., 1990, The neural network of the basal ganglia as revealed by the study of synaptic connections of identified neurons, *Trends Neurosci.* **13**:259–265.

Walker, R.H., Bao, L., Rice, M.E., Patel, J., Shashidharan, P., 2004, Effects of torsinA mutation upon dopamine release in mouse brain slices. *International Basal Ganglia Society 8th Triennial Meeting: Crieff, Scotland Abstract Book*; P174.

Xia, Y., and Haddad, G.G., 1991, Major differences in CNS sulfonylurea receptor distribution between the rat (newborn, adult) and turtle, *J. Comp. Neurol.* **314**:278–289.

Zhang, Y., Dawson, V.L., and Dawson, T.M., 2000, Oxidative stress and genetics in the pathogenesis of Parkinson's disease, *Neurobiol. Dis*. **7**:240–250.

NOCICEPTIN/ORPHANIN FQ MODULATES NEUROTRANSMITTER RELEASE IN THE SUBSTANTIA NIGRA: BIOCHEMICAL AND BEHAVIOURAL OUTCOME

Matteo Marti, Massimiliano Manzalini, Clementina Bianchi, Christian Heidbreder, Michele Morari, and Francesco Crespi*#

1. INTRODUCTION

This paper will summarize recent findings on the role that nociceptin/orphanin FQ (N/OFQ) in the substantia nigra (SN) exerts in the control of local neurotransmission and motor behaviour. In addition, new data regarding N/OFQ modulation of nigral serotonin (5-HT) release will be presented. N/OFQ is a recently discovered endogenous neuropeptide (Meunier et al., 1995; Reinscheid et al., 1995) that activates a G-protein coupled receptor of the opioid family named "opioid like-receptor 1" (ORL-1) receptor (Bunzow et al., 1994) or, more recently, NOP receptor (Cox et al., 2000). The N/OFQNOP receptor system is widely represented throughout the CNS of the rodents (Anton et al., 1996; Darland et al., 1998; Neal et al., 1999; Boom et al., 1999; Slowe et al., 2001) and is involved in the modulation of a number of biological actions, among which locomotion (for reviews see Calò et al., 2000; Mogil and Pasternak, 2001). In this respect, i.c.v. administration of N/OFQ has been consistently shown to inhibit spontaneous locomotion (Reinscheid et al., 1995; Devine et al., 1996a, b; Nishi et al., 1997; Noble and Roques, 1997; Stratford et al., 1997; Sandin et al., 1997; Walker et al., 1998; Rizzi et al., 2001; Kuzmin et al., 2004; Narayanan et al., 2004). Motor activity stimulated by pharmacological agents (Di Giannuario et al., 1999; Di Giannuario and Pieretti, 2000; Lutfy et al., 2001) or by exercise (Marti et al., 2004a) also appeared to be impaired by exogenous N/OFQ. Systemic administration of the nonpeptide NOP receptor agonist, Ro 64-6198, mimicked N/OFQ effects,

* Matteo Marti, Massimiliano Manzalini, Clementina Bianchi, and Michele Morari, Department of Experimental and Clinical Medicine, Section of Pharmacology, and Neuroscience Center, University of Ferrara, Italy. Christian Heidbreder and Francesco Crespi, Department of Biology, Center of Excellence for Drug Discovery in Psychiatry, GlaxoSmithKline Pharmaceuticals, 37135 via Fleming 4, Verona, Italy.

# Michele Morari and Francesco Crespi contributed equally to this work.

reducing spontaneous (Higgins et al., 2001; Kuzmin et al., 2004) and exercise-induced motor activity (Jenck et al., 2000; Higgins et al., 2001). More recently, we have shown that also endogenous N/OFQ physiologically inhibits motor behaviour, since pharmacological or genetic blockade of N/OFQergic transmission facilitates locomotion in rodents (Marti et al., 2004a). In particular, we proposed that such inhibition is more relevant under conditions of motor activation rather than at rest (Marti et al., 2004a). Indeed, blockade of N/OFQergic transmission accomplished by selective NOP receptor antagonists (Noda et al., 1998; Calò et al., 2000; Calò et al., 2002; Narayanan et al., 2004; Okabe and Murphy, 2004), antisense oligonucleotides to NOP receptor mRNA (Blakley et al., 2004) or genetic deletion of the NOP receptor gene ($NOP^{-/-}$ mice; Nishi et al., 1997; Murphy et al., 2002; Gavioli et al., 2003; Marti et al., 2004a) does not affect spontaneous but facilitated exercise-induced (Marti et al., 2004a) or pharmacologically-stimulated (Blakley et al., 2004) locomotion. To confirm this view, daily i.c.v. injections of an antisense oligonucleotide to pre-proN/OFQ (Candeletti and Ferri, 2000) or intranigral injection of a high dose of the NOP receptor antagonist UFP-101 (i.e. 30 nmol; Marti et al., 2004a) were needed to cause hyperlocomotion in rats, suggesting that a marked and prolonged blockade of endogenous N/OFQergic transmission is required to unveil N/OFQ inhibitory tone on spontaneous locomotion.

N/OFQ inhibition of motor function is likely due to NOP receptor activation in the basal ganglia (BG; Darland et al., 1998; Neal et al., 1999). In fact, inhibition of motor activity was observed after N/OFQ administration in the nucleus accumbens (NAcc; Narayanan et al., 2004), ventral tegmental area (VTA; Narayanan et al., 2004) and substantia nigra pars reticulata (SNr; Marti et al., 2004a). Until now, motor depressant actions of N/OFQ have been mainly related to N/OFQ ability to modulate dopaminergic (DAergic) transmission along the mesoaccumbal and nigrostriatal pathways. In fact, electrophysiological studies demonstrated that exogenous N/OFQ hyperpolarizes and reduces the firing activity of VTA (Zengh et al., 2002) and SNc (Marti et al., 2004a) DA cells, which express NOP receptors (Norton et al., 2002; Maidment et al., 2002). This action is consistent with microdialysis studies reporting inhibition of DA release in the NAcc (Murphy and Maidment, 1999) or dorsolateral striatum (Marti et al., 2004a) following intrategmental or intranigral N/OFQ injections, respectively. It is noteworthy that, despite the fact that exogenous N/OFQ inhibited both the mesoaccumbal and nigrostriatal DAergic pathways, endogenous N/OFQ may preferentially modulate the nigrostriatal one. In fact, NOP receptor antagonists given in the SNr facilitated DA release in the dorsolateral striatum (Marti et al., 2004a) while NOP antagonists given i.c.v. did not affect DA release in the ventral striatum (Koizumi et al., 2004). The relative contribution of the endogenous N/OFQergic systems in the SNr and VTA to regulation of motor control under different conditions is worthy of more detailed investigation.

Recent evidence indicates that DA may not be the only player involved in the motor response to NOP receptor ligands. We recently reported that intranigral and/or systemic injections of UFP-101 and J-113397 relieved akinesia in 6-hydroxydopamine (6-OHDA) hemilesioned (Marti et al., 2004b) and haloperidol-treated (Marti et al., 2004c) rats, i.e. under conditions of impaired DAergic transmission. In particular, the hypothesis was put forward that these effects were due to modulation of nigral glutamatergic (GLUergic) transmission. The SNr receives an extensive GLUergic innervation, arising from the cerebral cortex (Carter, 1982), the subthalamic (Robledo and Feger, 1980; Rinvik and Ottersen, 1993) and peduncolopontine (Tokuno et al., 1988) nuclei and it has been shown that

changes in nigral GLUergic transmission are associated with physiopathological changes in motor behaviour (Albin et al., 1990; Alexander and Crutcher, 1990): a pathological increase in subthalamonigral GLUergic inputs promotes parkinsonian-like symptoms (e.g. hypokinesia and muscle rigidity) while an impairment of nigral GLUergic transmission is associated with antiparkinsonian effects (Starr, 1995; Blandini and Greenamyre, 1998). In vivo microdialysis studies have shown that N/OFQ regulates GLU release in the mesencephalic areas. Indeed, N/OFQ administration in the VTA (Murphy and Maidment, 1999) or SNr (Marti et al., 2002) enhanced local GLU extracellular levels. However, this effect is not due to activation of presynaptic NOP receptors but likely to modulation of intranigral DAergic and/or GABAergic inputs (Murphy and Maidment, 1999; Marti et al., 2002). More relevant, GLUergic transmission in the SNr appeared to be tonically inhibited by endogenous N/OFQ since intranigral perfusion with [Nphe^1]N/OFQ-NH_2, a NOP receptor antagonist (Calò et al., 2000), decreased local GLU extracellular levels (Marti et al., 2002). This effect was likely DAindependent, since it was induced by systemic administration of the non peptide NOP receptor antagonist J-113397 also in DA-depleted SNr (Marti et al., 2004b). This anti-GLUergic activity may be relevant for the anti-akinetic action displayed by NOP receptor antagonists in experimental models of parkinsonism. In fact, reversal of akinesia induced by intranigral injection of UFP-101 correlated with normalization of nigral GLU release, previously elevated by the neuroleptic (Marti et al., 2004c).

In addition to GLUergic inputs, the SNr receives a large serotonergic innervation from the raphe nuclei (Dray et al., 1978; Imai et al., 1986). These inputs modulate nigral GABAergic efferent pathways and motor behaviour (Jacobs and Fornal, 1997) via both DA-dependent and DA-independent mechanisms (Oberlander et al., 1981). Therefore we sought to investigate whether N/OFQ microinjected in the SNr modulates local serotonin (5-HT) release. To this aim, differential pulse voltammetry (DPV) has been performed in anaesthetised rats. Moreover, to investigate whether inhibition of serotonergic signalling in the SNr results in motor impairment, the non-selective 5-HT_1 and 5-HT_2 receptor antagonist, methiothepin (Hoyer et al., 1994), was microinjected into the SNr of awake rats and motor performance evaluated by the rotarod test.

2. MATERIALS AND METHODS

Male Sprague-Dawley (SD) rats (300–350 g; Stefano Morini, Reggio Emilia, Italy) were kept under regular lighting conditions (12 hr light/dark cycle) and given food and water *ad libitum*. The experimental protocols performed in the present study were approved by the Ethical Committee of the University of Ferrara and adequate measures were taken to minimize animal pain and discomfort. Voltammetry experiments were prereviewed and consented by a local animal care committee in accordance with the guidelines of the "Principles of laboratory animal care" (NIH publication No 86-23, revised 1985), as well as with a Project License obtained according to Italian Law (art. 7, Legislative Decree no. 116, 27 January 1992), which acknowledged the European Directive 86/609/EEC.

2.1. Release Studies

Release experiments were performed in anaesthetised (urethane 1.5 g/kg i.p.) male SD rats using the DPV coupled with nafion-coated carbon fibre micro-electrodes (mCFE;

Crespi et al., 1988). Electrodes were stereotaxically implanted in the right SNr (AP −5.5 mm, ML −2.2 mm, VD −8.3 mm; nose bar positioned at −2.5 mm) and a stainless-steel injector was placed into the SNr near the electrode (~1 mm). Neurochemical detection started 3 hours after the surgery. 5-HT oxidation peak was at +250/270 mV.

2.2. Microinjection Technique

As previously described (Marti et al., 2004a) a guide injection cannula (outer diameter 0.55 mm) was stereotaxically implanted under isoflurane anaesthesia 0.5 mm above the right SNr (AP −5.5 mm, ML −2.2 mm, VD −7.3 mm from bregma, Paxinos and Watson, 1982). Seven days after surgery, methiothepin was injected (0.5 µl volume) through a stainless-steel injector (outer diameter 0.3 mm) protruding 1 mm beyond the cannula tip. At the end of each experiment the placement of the cannula was verified by microscopic examination.

2.3. Studies on Motor Behaviour

As previously reported (Marti et al., 2004a), the fixed-speed rotarod (FSRR) test was employed to investigate the effects of methiothepin on the physiologically-stimulated motor activity. In order to detect both facilitatory and inhibitory effects on motor activity (Marti et al., 2004a) a specific protocol was developed: rats were tested (t_0) at 4 increasing speeds (usually 25, 30, 35 and 40 rpm; 180 sec each), causing a progressive decrement of performance to about 40% of the maximal response (i.e. the experimental cut-off time). A similar response could be reproduced by applying this protocol 50 and 100 min later (t_{50} and t_{100}). Thus, to quantify drug effect on motor behaviour, drugs were administered 10 min prior to t_{50}, and rotarod performance (total time spent on the rotarod) calculated at t_{50} and t_{100} (i.e. 10 and 60 min after injection) as a percent of control (t_0) performance.

2.4. Materials

N/OFQ was synthesized in our laboratories as previously described (Guerrini et al., 1998). Methiothepin was purchased from Tocris Cookson (Bristol, UK). All drugs were freshly dissolved in isosmotic saline solution.

2.5. Data Presentation and Statistical Analysis

5-HT release has been expressed as percentage ± SEM of basal values (calculated as mean of the four samples before the treatment). Motor performance has been presented as percentage ± SEM of the control session. Statistical analysis was performed (GraphPad Prism software, San Diego, CA, USA) on area-under-the-curve (AUC) values (expressed in arbitrary units) by ANOVA followed by the Newman-Keuls test for multiple comparisons. P values <0.05 were considered to be statistically significant.

3. RESULTS

Injection of N/OFQ (0.1–10 nmol) in the SNr dose-dependently inhibited local 5-HT release (Fig. 1). N/OFQ reduced nigral 5HT levels at 0.1 nmol (~15%), 1 nmol (~35%) and

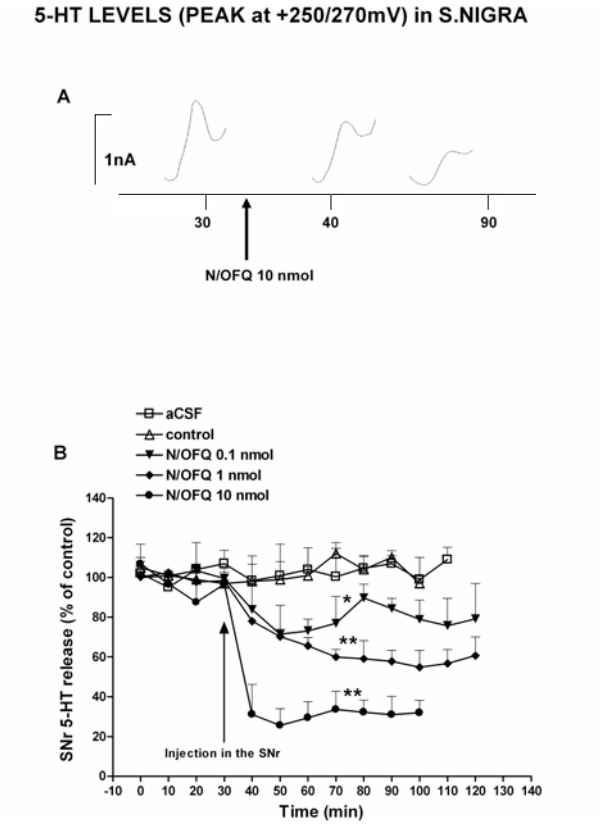

Figure 1. A: Effect of intranigral injection of N/OFQ 10 nmol on 5-HT oxidation peak (+ 250/270 mV). B: Effect of N/OFQ (0.1–10 nmol/0.5 µl) injection in the SNr of anesthetised rats on local 5-HT release (B). Data are expressed as percentages ± SEM of basal pretreatment levels (calculated as the mean of the two samples before the treatment) and are means of 4 determinations. *p < 0.05 and **p < 0.01 significantly different from aCSF.

10 nmol (~75%). The effect was rapid in onset and prolonged. Intranigral injection with saline was ineffective. Behavioural studies showed that intranigral injection of methiothepin (0.01–10 nmol) dose-dependently impaired rat locomotion (Fig. 2).

Methiothepin, ineffective at 0.01 nmol, promptly reduced motor performance at 0.1 (~15%), 1 nmol (~40%) and 10 nmol (~50%; Fig. 2). The highest dose produced marked impairment of motor coordination and flaccid muscle tone, qualitatively similar to that observed after intranigral microinjection of N/OFQ in rats (Marti et al., 2004a).

4. DISCUSSION

The present data show that N/OFQ injected in the SNr of anaesthetized rats reduced local 5-HT release in a range of doses selective for NOP receptor activation in vivo (Marti et al., 2004a). This effect is consistent with the inhibitory action that N/OFQ exerts on

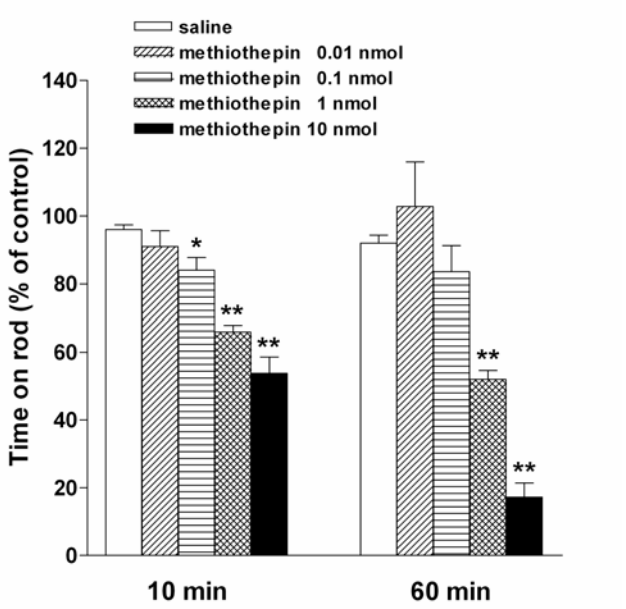

Figure 2. Effect of methiothepin injection (0.01–10 nmol/0.5 µl) in the substantia nigra pars reticulata (SNr) on physiologically-stimulated locomotion in rats. Each experiment consisted in three different sessions: a control session followed (40 min) by other two sessions performed 10 and 60 min after saline or methiothepin injections. Data are expressed as percentages ± SEM of motor activity in the first session and are means of 6–10 determinations. *$p < 0.05$ and **$p < 0.01$ significantly different from saline.

central serotonergic transmission (for a review see Schlicker and Morari, 2000). Indeed, N/OFQ has been consistently demonstrated to reduce both the electrical activity of serotonergic neurons in the dorsal raphe and ventrolateral medulla (Vaughan and Christie, 1996; Chu et al., 1999; Vaughan et al., 2001) and the release of 5-HT from nerve terminals in the target areas (e.g. the cerebral cortex; Sbrenna et al., 2000; Marti et al., 2003; Mela et al., 2004). Although evidence for presynaptic NOP receptors on serotonergic terminals in the SNr is still lacking, the inhibitory effect of N/OFQ on nigral 5-HT release may be due to activation of presynaptic NOP receptors (Dray et al., 1978; Imai et al., 1986), since neurons located in the raphe nucleus express high levels of mRNAs encoding for NOP receptors (Darland et al., 1998; Neal et al., 1999). Modulation of serotonergic transmission by N/OFQ may results in changes of motor activity. Indeed, blockade of nigral serotonergic 5-HT_1 and 5-HT_2 receptors with methiothepin impaired motor performance and muscle tone. Although the possibility that methiothepin reduced motor activity via non serotonergic mechanisms (i.e. D2 receptors; Janssen, 1983) cannot be ruled out, our finding is in line with reports that stimulation of 5-HT receptors (Higgins et al., 1991; Hillegaart et al., 2000) or blockade of 5-HT re-uptake in the SNr (Bata Garcia et al., 2002) facilitated locomotor activity. Thus, inhibition of nigral serotonergic transmission may underlie the motor depressant action induced by intranigral N/OFQ administration. To support this view, the inhibitory action exerted by N/OFQ on nigral 5-HT release occurs in the same range of doses previously reported to depress motor activity in awake freely moving rats (Marti et al., 2004a).

In conclusion, the finding that N/OFQ inhibits 5-HT release in the SNr offers a new biological substrate to interpret the motor depressant effects of this neuropeptide. The overall pattern of neurochemical effects of N/OFQ in the SNr (i.e. reduction of nigrostriatal DAergic transmission and nigral 5-HT release, facilitation of GLU release) strengthens the notion that NOP receptor activation in the SNr impairs motor activity and that NOP receptor antagonists may be beneficial in conditions of hypokinesia associated with increased nigral N/OFQ transmission, such as Parkinson's disease (Norton et al., 2002).

5. ACKNOWLEDEMENTS

We acknowledge the Italian Ministry of the University (COFIN 2002 to C.B.).

6. REFERENCES

Anton, B., Fein, J., To, T., Li, X., Silberstein, L., and Evans, C.J., 1996, Immunohistochemical localization of ORL-1 in the central nervous system of the rat, *J. Comp. Neurol.* **367**:1–23.

Albin, R.A., Young, A.B., and Penney, B., 1989, The functional anatomy of the basal ganglia disorders, *Trends Neurosci*. **12:**366–375.

Alexander, G.E., and Crutcher, M.D., 1990, Functional architecture of basal ganglia circuits: neural substrates of parallel processing, *Trends Neurosci*. **13:**266–271.

Bata-Garcia, J.L., H-Lopez, F.J., A-Cervera, F.J., A-Sandoval G and G-Alfaro JL., 2002, Circling behaviour induced by injection of serotonin reuptake inhibitors in the substantia nigra, *Pharmacol. Biochem. Behavior* **71**:361–371.

Bergquist, F., Shahabi, H.N., Nissbrandt, H., 2003, Somatodendritic dopamine release in rat substantia nigra influences motor performance on the accelerating rod, *Brain Res* **973**:81–91.

Blakley, G.G., Pohorecky, L.A., Benjamin, D., 2004, Behavioral and endocrine changes following antisense oligonucleotide-induced reduction in the rat NOP receptor, *Psychopharmacology* **171**:421–428.

Blandini, F., and Greenamiry, J.T., 1998, Prospects of glutamate antagonists in the therapy of Parkinson's disease, *Fundam. Clin. Pharmacol.***12**:4–12.

Boom, A., Mollereau, C., Meunier, J.C., Vassart, G., Parmentier, M., Vanderhaeghen, J.J., Schiffmann, S.N., 1999, Distribution of the nociceptin and nocistatin precursor transcript in the mouse central nervous system, *Neuroscience* **91**:991–1007.

Bunzow, J.R., Saez, C., Mortrud, M., Bouvier, C., Williams, J.T., Low, M., and Grandy, D.K., 1994, Molecolar cloning and tissue distribution of a putative member of the rat opioid receptor gene family that is not a mu, delta or kappa opioid receptor type. *FEBS lett.* **347**:284–288.

Calò, G., Guerrini, R., Rizzi, A., Salvadori, S., Regoli, D., 2000, Pharmacology of nociceptin and its receptor: a novel therapeutic target, *Br. J. Pharmacol.* **129**:1261–1283.

Calò, G., Rizzi, A., Rizzi, D., Bigoni, R., Guerrini, R., Marzola, G., Marti, M., McDonald, J., Morari, M., Lambert, D.G., Salvadori, S., Regoli, D., 2002, [$Nphe^{1}$,Arg^{14},Lys^{15}]Nociceptin-NH_2, a novel potent and selective antagonist of the nociceptin/orphanin FQ receptor, *Br. J. Pharmacol.* **136**:303–311.

Candeletti, S., and Ferri, S., 2000, Effects of an antisense oligonucleotide to pronociceptin and long-term prevention of morphine actions by nociceptin, *Peptides* **21**:1119–1124.

Carter, C.J., 1982, Topographical distribution of possible glutamatergic pathways from the prefrontal cortex to the striatum and substantia nigra of the rat. *Neuropharmacol*. **21**:379–383.

Chu, X., Xu, N., Li, P., and Wang, J.Q., 1999, The nociceptin receptor-mediated inhibition of the rat rostral ventrolateral medulla neurons in vitro, *Eur. J. Pharmacol.* **364**:49–53.

Cox, B.M., Chavkin, C., Christie, M.J., Civelli, O., Evans, C., Hamon, M.D., Hoellt, V., Kieffer, B., Kitchen, I., Mcknight, A.T., Meunier, J.C., Portoghese, P.S., 2000, Opioid Receptors. In: The IUPHAR Compendium of Receptor Characterization and Classification. (Girdlestone D ed): IUPHAR Media Ltd, London.

Crespi, F., Martin, K.F., and Marsden, C.A., 1988, Measurement of extracellular basal levels of serotonin in vivo using nafion-coated carbon fibre electrodes combined with differential pulse voltammetry, *Neuroscience*. **27**:885–896.

Darland, T., Heinricher, M.M., and Grandy, D.Y., 1998, Orphanin FQ/nociceptin: a role in pain and analgesia, but so much more, *Trends Neurosci.*, **21**:215–221.

Devine, D.P., Taylor, L., Reinscheid, R.K., Monsma, F.J. Jr, Civelli, O., Akil, H., 1996a, Rats rapidly develop tolerance to the locomotor-inhibiting effects of the novel neuropeptide orphanin FQ, *Neurochem. Res.* **21**:1387–1396.

Devine, D.P., Reinscheid, R.K., Monsma, F.J. Jr, Civelli, O., Akil, H., 1996b, The novel neuropeptide orphanin FQ fails to produce conditioned place preference or aversion, *Brain Res.* **727**:225–229.

Di Giannuario, A., Pieretti, S., Catalani, A., Loizzo, A., 1999, Orphanin FQ reduces morphine-induced dopamine release in the nucleus accumbens: a microdialysis study in rats, *Neurosci. Lett.* **272**:183–186.

Di Giannuario, A., and Pieretti, S., 2000, Nociceptin differentially affects morphine-induced dopamine release from the nucleus accumbens and nucleus caudate in rats, *Peptides* **21**:1125–1130.

Dray, A., Davies, J., and Oakley, N.R., Tongroach, P., Vellucci, S., 1978, The dorsal and medial raphe projections to the substantia nigra in the rat: electrophysiological, biochemical and behavioural observations, *Brain Research* **151**:431–442.

Gavioli, E.C., Marzola, G., Guerrini, R., Bertorelli, R., Zucchini, S., De Lima, T.C., Rae, G.A., Salvadori, S., Regoli, D., Calò, G., 2003, Blockade of nociceptin/orphanin FQ-NOP receptor signalling produces antidepressantlike effects: pharmacological and genetic evidences from the mouse forced swimming test, *Eur. J. Neurosci.* **17**:1987–1990.

Guerrini, R., Calò, G., Bigoni, R., Rizzi, A., Varani, K., Toth, G., Gessi, S., Hashiba, E., Hashimoto, Y., Lambert, D.G., Borea, P.A., Tomatis, R., Salvadori, S., Regoli, D., 2000, Further studies on nociceptin-related peptides: discovery of a new chemical template with antagonist activity on the nociceptin receptor, *J. Med. Chem.* **43**:2805–2813.

Higgins, G.A., Jordan, C.C., and Skingle, M., 1991, Evidence that the unilateral actvation of 5-HT_{1D} receptors in the substantia nigra of the guinea-pig elicits contralateral rotation, *Br. J. Pharmacol.* **102**:305–310.

Higgins, G.A., Grottick, A.J., Ballard, T.M., Richards, J.G., Messer, J., Takeshima, H., Pauly-Evers, M., Jenck, F., Adam, G., and Wichmann, J., 2001, Influence of the selective ORL_1 receptor agonist, Ro64–6198, on rodent neurological function, *Neuropharmacology* **41**:97–107.

Hillegaart, V., Magnusson, O., and Ahlenius, S., 2000, A9 and A10 dopamine nuclei as a site of action for effects of 8-OH-DPAT on locomotion in the rat, *Pharmacol. Biochem. Behav.* **67**:55–63.

Hoyer, D., Clarke, D.E., Fozard, J.R., Hartig, P.R., Martin, G.R., Mylecharane, E.J., Saxena, P.R., and Humphrey, P.P.A., 1994, International union of pharmacology classification of receptors for 5-hydroxytryptamine (serotonin), *Pharmacol. Rev.* **46**:157–193.

Imai, H., Steindler, D.A., and Kitai, S.T., 1986, The organization of divergent axonal projections from the midbrain raphe nuclei in the rat, *J. Comp. Neurol.* **15**:363–80.

Jacobs, B.L., and Fornal, C.A., 1997, Serotonin and motor activity. *Curr. Opin. Neurobiol*. **7**:820–825.

Janssen P.A.J., 1983, 5-HT_2 receptor blockade to study serotonin-induced pathology. *TIPS* 198–206.

Jenck, F., Wichmann, J., Dautzenberg, F.M., Moreau, J.L., Ouagazzal, A.M., Martin, J.R., Lundstrom, K., Cesura, A.M., Poli, S.M., Roever, S., Kolczewski, S., Adam, G., and Kilpatrick, G., 2000, A synthetic agonist at the orphanin FQ/nociceptin receptor ORL_1: anxiolytic profile in the rat, *Proc. Natl. Acad. Sci. USA.* **97**:4938–4943.

Koizumi, M., Midorikawa, N., Takeshima, H., and Murphy, N.P., 2004, Exogenous, but not endogenous nociceptin modulates mesolimbic dopamine release in mice, *J. Neurochem.* **89**:257–263.

Kuzmin, A., Sandin, J., Terenius, L., and Ogren, S.O., 2004, Evidence in locomotion test for the functional heterogeneity of ORL-1 receptors, *Br. J. Pharmacol.* **141**:132–140.

Lutfy, K., Do, T., and Maidment, N.T., 2001, Orphanin FQ/nociceptin attenuates motor stimulation and changes in nucleus accumbens extracellular dopamine induced by cocaine in rats, *Psychopharmacology (Berl)* **154**: 1–7.

Maidment, N.T., Chen, Y., Tan, A.M., Murphy, N.P., and Leslie, F.M., 2002, Rat ventral midbrain dopamine neurons express the orphanin FQ/nociceptin receptor ORL-1, *Neuroreport* **13**:1137–1140.

Marti, M., Guerrini, R., Beani, L., Bianchi, C., and Morari, M., 2002, Nociceptin/orphanin FQ receptors modulate glutamate extracellular levels in the substantia nigra pars reticulata. A microdialysis study in the awake freely moving rat, *Neuroscience* **112**:153–160.

Marti, M., Stocchi, S., Paganini, F., Mela, F., De Risi, C., Calò, G., Guerrini, R., Barnes, T.A., Lambert, D.G., Beani, L., Bianchi, C., and Morari, M., 2003, Pharmacological profiles of presynaptic nociceptin/orphanin FQ receptors modulatine 5-hidroxytryptamine and noradrenaline release in the rat neocortex, *Br. J. Pharmacol* **138**:91–98.

Marti, M., Mela, F., Veronesi, C., Guerrini, R., Salvatori, S., Federici, M., Mercuri, N.B., Rizzi, A., Franchi, G., Beani, L., Bianchi, C., and Morari, M., 2004a, Blockade of nociceptin/orphanin FQ receptor signalling in

rat substantia nigra pars reticulata stimulates nigrostriatal dopaminergic transmission and motor behaviour, *J. Neurosci.* **24**:6659–6666.

Marti, M., Mela, F., Trapella, C., Bianchi, C., and Morari, M., 2004b, Blockade of nociceptin/orphanin FQ transmission attenuates hypokinesia in hemiparkinsonian rats, *Mov. Dis.* **19** (Suppl 9), P564.

Marti, M., Mela, F., Guerrini, R., Calò, G., Bianchi, C., and Morari, M., 2004c, Blockade of nociceptin/orphanin FQ transmission in rat substantia nigra reverses haloperidol-induced akinesia and normalizes nigral glutamate release, *J. Neurochem.* **91**:1501–1504.

Mela, F., Marti, M., Ulazzi, L., Vaccai, E., Zucchini, S., Trapella, C., Salvatori, S., Beani, L., Bianchi, C., and Morari, M., 2004, Pharmacological profile of nociceptin/orphanin FQ receptors regulating 5-hydroxytryptamine release in the mouse neocortex, *Eur. J. Neurosci.* **19**:1–8.

Meunier, J.C., Mollereau, C., Toll, L., Suaudeau, C., Moisand, C., Alvinerie, P., Butour, J.L., Guillemot, J.C., Ferrara, P., Monsarrat, B., Mazarguil, H., Vassart, G., Parmentier, M., and Costentin, J., 1995, Isolation and structure of the endogenous agonist of opioid receptor-like ORL_1 receptor, *Nature* **377**:532–535.

Mogil, J.S., and Pasternak, G.W., 2001, The molecular and behavioral pharmacology of the orphanin FQ/Nociceptin peptide and receptor family, *Pharmacol. Rev.* **53**:381–415.

Murphy, N.P., and Maidment, N.T., 1999, Orphanin FQ/nociceptin modulation of mesolimbic dopamine transmission determined by microdialysis, *J. Neurochem.* **73**:179–186.

Murphy, N.P., Lam, H.A., Chen, Z., Pintar, J.E., and Maidment, N.T., 2002, Heroin-induced locomotion and mesolimbic dopamine release is unchanged in mice lacking the ORL.1 receptor gene, *Brain Res.* **953**:276–280.

Narayanan, K., Lam, H., Carroll, I., and Lutfy, K., 2004, OrphaninFQ/nociceptin suppresses motor activity through an action along the mesoaccumbens axis in rats, *Rev. Psychiatr.* **29**:116–123.

Neal C.R. JR, Mansour, A., Reinscheid, R., Nothacker, H.P., Civelli, O., Akil, H., and Watson, S.J., JR., 1999, Opioid receptor-like (ORL_1) receptor distribution in the rat central nervous system: comparison of ORL_1 receptor mRNA expression with ^{125}I-[^{14}Tyr]-orphanin FQ binding, *J. Comp. Neurol.* **412**:563–605.

Nishi, M., Houtani, T., Noda, Y., Mamiya, T., Sato, K., Doi, T., Kuno, J., Takeshima, H., Nukada, T., Nabeshima, T., Yamashita, T., Noda, T., and Sugimoto, T., 1997, Unrestrained nociceptive response and dysregulation of hearing ability in mice lacking the nociceptin/orphaninFQ receptor, *EMBO J.* **16**:1858–1864.

Noble, F., and Roques, B.P., 1997, Association of aminopeptidase N and endopeptidase 24.15 inhibitors potentiate behavioral effects mediated by nociceptin/orphanin FQ in mice, *FEBS Lett.* **401**:227–229.

Noda, Y., Mamiya, T., Nabeshima, T., Nishi, M., Higashioka, M., and Takeshima, H., 1998, Loss of antinociception induced by naloxone benzoylhydrazone in nociceptin receptor-knockout mice, *J. Biol. Chem.* **273**:18047–18051.

Norton, C.S., Neal, C.R., Kumar, S., Akil, H., and Watson, S.J., 2002, Nociceptin/orphanin FQ and opioid receptor-like receptor mRNA expression in dopamine systems, *J. Comp. Neurol.* **444**:358–368.

Oberlander, C., Hunt, P.F., Dumont, C., and Boissier, J.R., 1981, Dopamine independent rotational response to unilateral intranigral injection of serotonin, *Life Sci.* **28**:2595–2601.

Okabe, C., and Murphy, N.P., 2004, Short-term of the nociceptin receptor antagonist Compound B on the development of methamphetamine sensitization in mice: a behavioural and c-fos expression mapping study, *Brain Res.* **1017**:1:12.

Paxinos, G., and Watson, C., 1982, The Rat Brain in Stereotaxic Coordinates. Academic, Sydney.

Reinscheid, R.K., Nothacker, H.P., Bourson, A., Ardati, A., Henningsen, R.A., Bunzow, J.R., Grandy, D.K., Langen, H., Monsma, F.J. Jr, and Civelli, O., 1995, Orphanin FQ: a neuropeptide that activates an opioid-like G protein-coupled receptor, *Science* **270**:792–794.

Rinvik, E., and Ottersen, O.P., 1993, Terminals of subthalamonigral fibres are enriched with glutamate-like immunoreactivity: an electron microscopy, immunogold analysis in the cat, *J. Chem. Neuroanat*. **6**:19–30.

Rizzi, A., Bigoni, R., Marzola, G., Guerrini, R., Salvadori, S., Regoli, D., and Calo', G., 2001, Characterization of the locomotor activity-inhibiting effect of nociceptin/orphanin FQ in mice, *Naunyn Schmiedebergs Arch. Pharmacol.* **363**:161–165.

Robledo, P., and Feger, J., 1990, Excitatory influence of rat subthalamic nucleus to substantia nigra pars reticulata and the pallidal complex: electrophysiologicol data, *Brain Res*. **518**:47–54.

Sandin, J., Georgieva, J., Schott, P.A., Ogren, S.O., and Terenius, L., 1997, Nociceptin/orphanin FQ microinjected into hippocampus impairs spatial learning in rats, *Eur. J. Neurosci.* **9**:194–197.

Sbrenna, S., Marti, M., Morari, M., Calo', G., Guerrini, R., Beani, L., and Bianchi, C., 2000, Modulation of 5-hydroxytryptamine efflux from rat cortical synaptosomes by opioids and nociceptin, *Br. J. Pharmacol.* **130**:425–433.

Schlicker, E., and Morari, M., 2000, Nociceptin/orphanin FQ and neurotransmitter release in the central nervous system, *Peptides* **21**:1023–1029.

Slowe, S.J., Clarke, S., Lena, I., Goody, R.J., Lattanzi, R., Negri, L., Simonin, F., Matthes, H.W., Filliol, D., Kieffer, B.L., and Kitchen, I., 2001, Autoradiographic mapping of the opioid receptor-like 1 (ORL1) receptor in the brains of mu-, delta- or kappa-opioid receptor knockout mice, *Neuroscience* **106**:469–480.

Starr, M.S., 1995, Glutamate/dopamine D1/D2 balance in the basal ganglia and its relevance to Parkinson's disease, *Synapse* **19**:264–293.

Stratford, T.R., Holahan, M.R., and Kelley, A.E., 1997, Injections of nociceptin into nucleus accumbens shell or ventromedial hypothalamic nucleus increase food intake, *Neuroreport* **8**:423–426.

Tokuno, H., Morizumi, T., Kumo, M., and Nakamura, Y., 1988, A morphological evidence for monosynaptic projection from the nucleus peduncolopontinus pars compacta (TPC) to nigrostriatal projection neurons, *Neurosci. Lett*., **85**:1–4.

Ueda, H., Inoue, M., Takeshima, H., and Iwasawa, Y., 2000, Enhanced spinal nociceptin receptor expression develops morphine tolerance and dependence, *J. Neurosci.* **20**:7640–7647.

Vaughan, C.W., and Christie, M.J., 1996, Increase by the ORL_1 receptor (opioid receptor-like1) ligand, nociceptin, of inwardly rectifying K conductance in dorsal raphe nucleus neurones, *Br. J. Pharmacol.* **117**:1609–1611.

Vaughan, C.W., Connor, M., Jennings, E.A., Marinelli, S., Allen, R.G., and Christie, M.J., 2001, Actions of nociceptin/orphanin FQ and other prepronociceptin products on rat rostral ventromedial medulla neurons in vitro, *J. Physiol.* **534**:849–859.

Walker, J.R., Spina, M., Terenius, L., and Koob, G.F., 1998, Nociceptin fails to affect heroin self-administration in the rat, *Neuroreport* **9**:2243–2247.

Zheng, F., Grandy, D.K., and Johnson, S.W., 2002, Actions of orphanin FQ/nociceptin on rat ventral tegmental area neurons in vitro, *Br. J. Pharmacol.* **136**:1065–1071.

MOTOR LEARNING-RELATED GENE REGULATION IN THE STRIATUM: EFFECTS OF COCAINE

Ingo Willuhn and Heinz Steiner*

1. SUMMARY

We investigated the relationship between changes in gene regulation in the striatum and motor learning under the influence of cocaine. Rats were trained on a running wheel for up to 8 days. One day after the training, enduring molecular changes were mapped throughout the striatum. Running-wheel training affected several molecule classes. Challenge-induced expression of the transcription factor c-*fos*, the synaptic plasticity factor Homer 1 and the neuropeptide substance P (but not enkephalin) was enhanced relative to cocaine-treated, non-running controls. These molecular changes were associated with the training phase when rats learn to run on the wheel; they were present after the first training session, peaked after day 2, decreased by day 4, and were absent after 8 days of training. These effects were most robust in the dorsal sensorimotor striatum that receives inputs from the medial agranular (premotor) and sensorimotor cortex. Borderline training effects (c-*fos*, Homer 1) were found when rats trained without cocaine treatment. These findings indicate that motor learning is associated with transiently enhanced inducibility of genes that may participate in restructuring of transstriatal circuits. Cocaine appears to abnormally enhance or alter such learning-related molecular changes. Future studies will have to determine whether these molecular changes are related to motor memory consolidation or other processes of motor learning.

2. INTRODUCTION

Chronic abuse of psychostimulants such as cocaine produces neuroadaptations in the basal ganglia that are implicated in behavioral changes including addiction and dependence. These neuronal changes include alterations in gene expression which are especially pro-

* Dept. of Cell. and Mol. Pharmacology, Rosalind Franklin University of Medicine and Science/The Chicago Medical School, North Chicago, IL 60064, USA. Correspondence to: Heinz.Steiner@rosalindfranklin.edu.

nounced in output neurons of the striatum (Hyman and Nestler, 1996; Harlan and Garcia, 1998; Berke and Hyman, 2000). Evidence indicates that these molecular changes are a consequence of repeated overstimulation of striatal dopamine receptors in interaction with glutamate inputs. Such changes are thought to alter the function of the striatal neurons affected and thus of the cortico-basal ganglia-cortical circuits they participate in (Berke and Hyman, 2000; Graybiel et al., 2000).

Psychostimulant-induced gene regulation in the striatum displays distinct regional variations. Dorsal striatal regions are most profoundly affected by a range of addictive drugs (Steiner and Gerfen, 1993; Harlan and Garcia, 1998; Berke and Hyman, 2000). Little is known regarding the functional significance of these neuronal changes. In order to better define the functional domains altered by psychostimulants, we performed a series of studies in which we mapped psychostimulant-induced changes in gene expression throughout the striatum (Willuhn et al., 2003; Yano and Steiner, 2005a; 2005b). In these studies, we used sampling areas (sectors) designed mostly based on their principal cortical inputs to determine which corticostriatal circuits are affected (see Willuhn et al., 2003).

Initially, we measured changes in gene regulation produced by acute and repeated cocaine treatment in a total of 26 striatal sectors on 4 rostrocaudal levels (Willuhn et al., 2003). Both acute cocaine effects (exemplified by c-*fos* induction), and neuroadaptive changes after repeated cocaine treatment (blunting of c-*fos* response, increase in dynorphin expression) were maximal in dorsal sectors of the middle to caudal striatum (Willuhn et al., 2003). These effects were less pronounced in surrounding sectors, and were relatively minor or absent in rostral and ventral striatal sectors (Willuhn et al., 2003). Further studies showed that acute and repeated treatment with methylphenidate, a psychostimulant with a mode of action similar to cocaine (Volkow et al., 1999), produces changes in striatal gene regulation with a very similar topography (Brandon and Steiner, 2003; Yano and Steiner, 2005a; 2005b). The most affected dorsal striatal sectors receive cortical inputs predominantly from the medial agranular (premotor) and sensorimotor cortex (see Willuhn et al., 2003). These findings thus indicate that sensorimotor corticostriatal circuits under the influence of the medial agranular cortex are most prone to psychostimulant-induced neuroplasticity.

Previous studies showed that psychostimulant-induced gene regulation in the sensorimotor striatum is dependent on cortical input (Cenci and Björklund, 1993; Vargo and Marshall, 1995). Neuronal activity in these corticostriatal circuits is correlated with specific aspects of motor performance (e.g., West et al., 1990; Haracz et al., 1993; Carelli et al., 1997; Jog et al., 1999). We thus asked whether the behavior performed during psychostimulant action (i.e., neuronal activities associated with the execution of this behavior) shapes drug-induced molecular changes in the striatum. The following paragraphs summarize a series of studies performed to answer this question.

3. STRIATAL GENE REGULATION RELATED TO MOTOR LEARNING

3.1. Enhanced c-*fos* Response After Wheel Training Under the Influence of Cocaine

To investigate whether differential behavioral training produced differential molecular changes in the striatum, rats trained on a running wheel were compared with non-running controls (Willuhn et al., 2003). On 4 consecutive days, rats received an injection of cocaine (25 mg/kg) or vehicle and were placed either on a running wheel or in a container, for 1

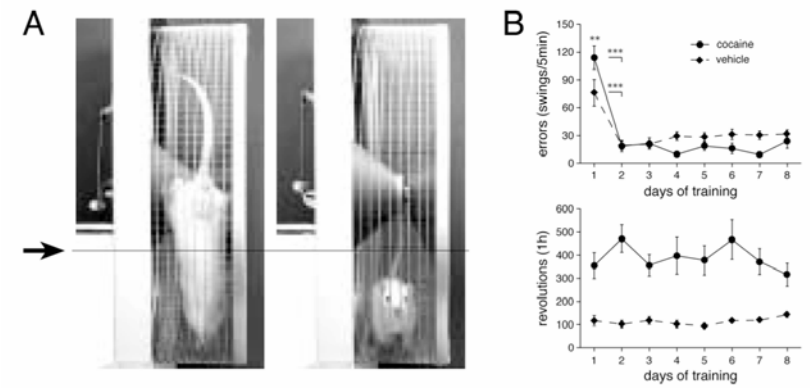

Figure 1. Motor learning during running-wheel training. (**A**) Video stills show a rat committing a running error ("swing", see text) at the beginning of the training (left), and a rat running at the bottom of the wheel after some practicing (right). Rats learn to run with an appropriate speed in order to remain at the bottom. A running error was scored when the rat (body minus tail) interrupted a line marked on the video monitor (arrow). (**B**) Running errors (mean ± SEM) in the first 5-min period (top), and total wheel revolutions per session (bottom) are shown for training sessions 1 to 8, for cocaine- and vehicle-treated animals. ***P < 0.001, **P < 0.01.

hour. Rats on the wheel (Fig. 1) showed mostly running and galloping, whereas rats in the container displayed rearing and locomotion. On day 5, c-*fos* induction by a cocaine challenge was mapped in the 26 striatal sectors. Thus, rats received an injection of cocaine (25 mg/kg) or vehicle, were tested in activity monitors for 30 min, and were then killed. Gene expression was measured with in situ hybridization histochemistry (Willuhn et al., 2003). This challenge test was performed in a different (neutral) room. Thus, the differentially trained groups were tested under physically identical conditions in an environment not associated with the training (see Willuhn et al., 2003, for discussion).

Our results showed that rats trained on the running wheel displayed a greater c-*fos* response to the cocaine challenge than container-trained rats, 24 h after the training under the influence of cocaine (Willuhn et al., 2003). This training-induced difference was regionally selective as it was restricted to 5 sectors, 3 dorsal sensorimotor and 2 adjacent sectors in the middle to caudal striatum (Fig. 2). No effects were seen in animals trained after a vehicle injection. Importantly, the differentially trained groups did not differ in their behavioral response to the cocaine challenge (ambulation, stereotypy counts) (Willuhn et al., 2003), indicating that the differential c-*fos* response was likely not secondary to behavioral activation. Thus, this differential cellular response appeared to reflect enduring neuronal changes produced by the training. Moreover, since no difference in vehicle-treated rats was found, these effects reflected training-associated molecular changes produced (or enhanced) by cocaine.

3.2. Enhanced c-*fos* Response Is Associated with Learning to Run on the Wheel

The enhanced c-*fos* response after the 4-day training could be related to generation of new motor patterns (motor learning), or could reflect neuronal changes produced by extended repetition of motor patterns. Further studies assessed whether the differential c-*fos* induction was associated with the beginning of the running-wheel training (1-, 2-day

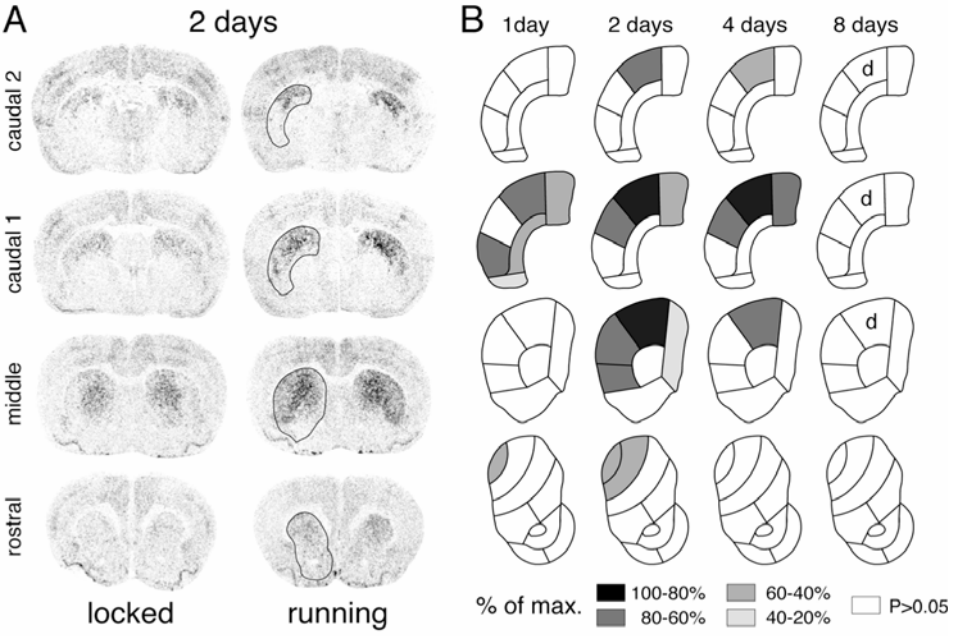

Figure 2. Enhanced c-*fos* response during running-wheel learning. (**A**) Examples of film autoradiograms depict c-*fos* expression in coronal sections from rostral, middle and caudal striatal levels in rats that received a cocaine (25 mg/kg) challenge injection 24 h after a 2-day training on a locked (left) or a running wheel (right) under the influence of cocaine. The left striatum is outlined in the right panels. (**B**) Differences in challengeinduced c-*fos* expression between running wheel-trained rats and non-running controls in the 26 striatal sectors are shown for rats that trained for 1, 2, 4 or 8 days. The differences ($P < 0.05$) are expressed in percentage of the maximal difference (% of max.) found across these regions and days and are coded as indicated. Non-running controls were confined to a locked wheel during the 1-, 2- and 8-day training, or to a container during the 4-day training. Maximal training effects were found in dorsal sectors (d).

training), or with extended training (8 days) (I. Willuhn and H. Steiner, submitted). In these studies, the controls were confined to a locked wheel (rather than a container) to minimize contextual differences between the training situations. The training was videotaped for analysis of behavioral changes that occurred during the course of the training.

Rats will voluntarily run on a wheel given the opportunity (e.g., Sherwin, 1998, for review). However, coordinated running has to be learned. Our video analysis demonstrated that, at the beginning of the training, rats are unable to run with an appropriate speed so as to remain at the bottom of the wheel. The rat is either too fast or too slow relative to the speed of the wheel. Consequently, the rat often "swings". We assessed the number of interruptions (by the rat's body) of a line marked on the video monitor as an index of performance error (Fig. 1). The number of errors (swings) was maximal at the beginning of each session. For both rats under cocaine or vehicle, the error number dropped to a stable, low level within the first 10–15 min of the session (not shown), as the rats learned to adjust and stabilize their running (within-session learning).

Figure 1 shows the running errors in the first 5-min periods of the 8-day training, for cocaine- and vehicle-treated rats. On day 1, rats under the influence of cocaine produced ~50% more errors than vehicle-treated rats (but also ran more than twice as much; Fig. 1).

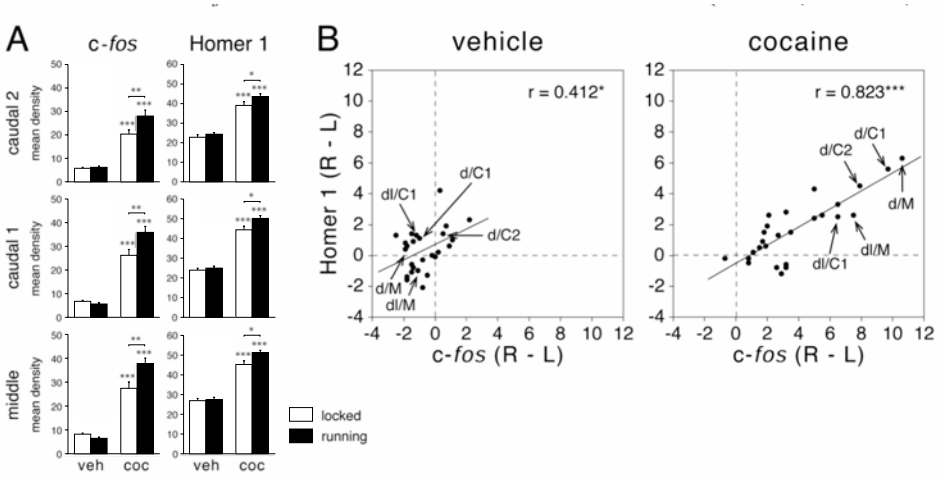

Figure 3. Relationship between enhanced c-*fos* and Homer 1 responses after the 2-day running-wheel training. (**A**) Expression of c-*fos* (left) and Homer 1 (right) (mean density, mean ± SEM) measured in the dorsal sectors on middle to caudal striatal levels are shown for rats that received a cocaine challenge, or vehicle, 24 h after the training on a locked or a running wheel under the influence of cocaine (coc) or vehicle (veh). (**B**) Correlations in training effects (mean density, running wheel-trained minus locked wheel-trained, R-L) between c-*fos* and Homer 1 expression across the 26 striatal sectors are given for vehicle- (left) and cocaine-trained rats (right). Sectors with greatest cocaine-driven increases are marked by arrows. d, dorsal; dl, dorsolateral; M, middle; C1, caudal 1; C2, caudal 2. ***P < 0.001, **P < 0.01, *P < 0.05.

Both groups displayed a significantly improved running performance already on day 2 (between-session learning). However, relative to their initial error rate, cocaine-treated rats improved more and continued to show less errors than vehicle-treated rats despite running more, through the 8-day training period. Thus, cocaine seemed to improve this motor learning, either directly or indirectly by producing more running (exercising).

One day after the 1-, 2- and 8-day training, the c-*fos* response to a cocaine challenge was compared between "running" and "locked" groups. "Running+cocaine"-trained rats again displayed a more robust c-*fos* response than "locked+cocaine"-trained rats, but this effect was dependent on the duration of the training. While present after the 1-day training (6 sectors; Fig. 2), this differential c-*fos* response was maximal and most widespread after the 2-day training. It was found in 10 sectors on 4 rostrocaudal levels (Figs. 2 and 3). On each level, this effect was maximal in the dorsal sensorimotor sector that receives medial agranular and sensorimotor cortical inputs, was smaller in laterally adjacent sensorimotor sectors, and was weakest in medial sectors (receiving input from the anterior cingulate cortex; see Willuhn et al., 2003). In contrast, following the 8-day training, no differential c-*fos* induction was found in any of the 26 striatal sectors (Fig. 2). No statistically significant differences in c-*fos* expression between "running" and "locked" rats treated with vehicle were seen after any of these training durations (but see below).

These results show that the post-training enhanced responsiveness of neurons in the sensorimotor striatum is limited to the beginning of the training when rats learn to run. This effect peaked after the 2-day training and dissipated with longer training duration.

3.3. Molecular Changes in Direct Pathway Neurons Related to Motor Learning

The striatum projects to the basal ganglia output nuclei via two pathways. The *direct* pathway connects the striatum directly to substantia nigra/entopeduncular nucleus, whereas the *indirect* pathway projects via globus pallidus (and subthalamic nucleus) to these output structures (Gerfen and Wilson, 1996). Striatal neurons that give rise to these two pathways differ in receptors and neuropeptides they contain. Direct pathway neurons express predominantly D1 dopamine receptors and the neuropeptides substance P and dynorphin, while indirect pathway (striatopallidal) neurons contain mostly D2 receptors and the peptide enkephalin. Previous studies showed that psychostimulant-induced molecular changes (e.g., c-*fos* induction) occur predominantly in direct pathway neurons (Berretta et al., 1992; Cenci et al., 1992; Kosofsky et al., 1995; Badiani et al., 1999), especially with higher doses (Uslaner et al., 2003; Ferguson et al., 2004), and are principally mediated by D1 receptors (Graybiel et al., 1990; Steiner and Gerfen, 1995; Drago et al., 1996) (see Steiner and Gerfen, 1998, for review). Using neuropeptides as cellular markers, we next investigated whether training-related gene regulation occurred in direct or indirect pathway neurons. Substance P and enkephalin expression were mapped in the 26 striatal sectors 24 h after the 1-, 2- and 8-day training.

Similar to c-*fos*, training-related differential expression of substance P was found after the 1- and 2-day training on all 4 rostrocaudal levels (not shown; I. Willuhn and H. Steiner, submitted). Following the cocaine challenge, "running+cocaine"-trained rats showed higher expression than "locked+cocaine"-trained rats. However, time course and regional patterns varied to some degree compared to c-*fos* expression. Peak increases appeared after the 1-day training (statistically significant in 12 sectors). The most robust differences were again seen in sensorimotor sectors (7 sectors), but medial/central sectors (5) were also affected. After the 2-day training, 9 sectors were affected, including sensorimotor (4) and medial/central sectors (4). Therefore, while training effects on c-*fos* and substance P expression overlapped in sensorimotor sectors, substance P effects were more widespread, as they were also present in medial and central sectors that receive inputs from the anterior cingulate and other prefrontal cortical areas (see Willuhn et al., 2003). Thus, c-*fos* and substance P expression were both affected by motor learning-associated processes, but appear to be differentially regulated to some degree, consistent with earlier findings (Drago et al., 1996; Yano and Steiner, 2005a).

In contrast to c-*fos* and substance P, no training-related increases in enkephalin expression were found (not shown). This is consistent with previous findings showing that enkephalin expression is readily changed by D2 receptor blockade and dopamine depletion (e.g., Steiner and Gerfen, 1999; Steiner and Kitai, 2001), but much less by psychostimulant treatments (cf. Steiner and Gerfen, 1998; Yano and Steiner, 2005a).

Taken together, our results on neuropeptide expression indicate that learning-associated molecular changes occur, at least in part, in the direct pathway.

3.4. Changes in Synaptic Plasticity Factor, Homer 1, Associated With Learning

We investigated whether other plasticity-related molecules were affected by running-wheel training. We assessed effects on the synaptic plasticity factor Homer 1. Homer (Vesl) proteins are scaffolding proteins present at excitatory synapses where they link glutamate receptors to the postsynaptic density and to IP3 receptors in the endoplasmic reticulum (Brakeman et al., 1997; Kato et al., 1997; Xiao et al., 2000; Thomas, 2002). Findings

indicate that Homer proteins are involved in calcium signaling, glutamate receptor clustering and trafficking, spine morphogenesis and other processes of synapse structuring and plasticity. Some splice variants of Homer 1 (Homer 1b/c) are constitutively expressed, others (e.g., Homer 1a) are acutely induced by synaptic activity (Bottai et al., 2002). Homer 1a induction has been found after long-term potentiation, cocaine and other treatments (Brakeman et al., 1997; Kato et al., 1997; Berke et al., 1998; Fujiyama et al., 2003). It has been proposed that Homer 1a regulates synaptic strength by affecting the signaling complex and synapse turnover (Xiao et al., 2000; Thomas, 2002).

Homer 1 is a large gene (~100 kb, 10 exons), and the Homer 1a-specific signal (intron 5) only appears around 30 min after transcription initiation (Bottai et al., 2002). Since in our studies animals were killed 30 min after the cocaine challenge, we used a Homer 1 pan probe (targetting the beginning of the transcript) to produce a more robust signal. Based on previous findings (Brakeman et al., 1997; Bottai et al., 2002; Fujiyama et al., 2003), it is assumed that the cocaine-induced signal obtained with this probe predominantly reflects Homer 1a expression.

Our results showed that Homer 1 induction by cocaine was greater in "running+cocaine"-trained rats than in "locked+cocaine"-trained rats (Fig. 3; I. Willuhn and H. Steiner, in preparation). However, this differential induction was temporally restricted, as it was found after the 2-day training, but not after the 1- or 8-day training. Regionally, it was most robust in the 3 dorsal sectors of the middle to caudal striatum (Fig. 3). Thus, this Homer 1 effect coincided with the most pronounced c-*fos* effects.

We further assessed the relationship between these two factors by a correlation analysis. This analysis showed that, for cocaine-treated animals subjected to the 2-day training, the differences between "running" and "locked" groups were significantly correlated between c-*fos* and Homer 1 across the 26 striatal sectors ($r = 0.823$, $P < 0.001$; Fig. 3). No correlations were seen after the 1- or 8-day training. Interestingly, however, this more sensitive two-marker correlation analysis also revealed a borderline significant training effect in vehicle-treated rats after the 2-day training ($r = 0.412$, $P < 0.05$; Fig. 3). This latter finding suggests enduring molecular changes (c-*fos*, Homer 1) in the striatum associated with running-wheel learning *without* drug treatment. These effects were relatively modest and will need to be confirmed. However, a comparison of the regional patterns between vehicle- and cocaine-trained animals indicates that cocaine produces abnormally robust increases in learning-associated gene expression in dorsal/lateral striatal sectors (Fig. 3B). Earlier work indicated that these sectors participate in procedural learning and habit formation (see below). Increased induction of transcription factors such as c-*fos* may play a role in learning-related protein synthesis (Davis and Squire, 1984; Stork and Welzl, 1999), whereas upregulation of factors that modulate synaptic strength such as Homer 1a (Xiao et al., 2000; Thomas, 2002) may reflect learning-related synapse restructuring.

4. DISCUSSION

The present studies demonstrate molecular changes in the sensorimotor striatum that occur in the first few days of running-wheel training when rats *learn to run* on the wheel. These molecular changes include increased induction of the transcription factor c-*fos*, the synaptic plasticity factor Homer 1a and the neuropeptide substance P. These neuronal changes were found 24 h after the last training session, and thus represent enduring neuronal changes induced by the training.

Previous studies revealed that running affects transmitter release and gene expression in the striatum, but these effects were induced by running *performance*. For example, in vivo microdialysis during running on a motorized treadmill showed increases in striatal dopamine and glutamate release (Hattori et al., 1994; Meeusen et al., 1997). Treadmill running was also found to increase c-*fos* expression in the striatum (Liste et al., 1997). However, Fos levels were similar between previously untrained rats (i.e., after the first 20-min running session) and trained rats (after the seventh daily session), suggesting that c-*fos* was induced by the locomotor activity during the session (Liste et al., 1997). A critical role for dopamine and glutamate/cortical inputs was demonstrated by showing that this c-*fos* response was attenuated by dopamine depletion, D1 (but not D2) receptor antagonists, NMDA receptor blockade, or cortical deafferentation (Liste et al., 1997). Effects on striatal neuropeptide expression were also found. Acute treadmill running increased the expression of substance P and enkephalin (Liste et al., 1999), whereas prolonged wheel running was associated with increased dynorphin expression (Werme et al., 2000).

In contrast to our training effects which were associated with the learning phase, the above effects were found in well-trained animals, often after extended running periods (weeks), and thus likely reflect neuronal changes associated with (extended) performance. However, these effects confirm that such running engages striatal circuits and affects gene regulation in these circuits.

More similar to our studies, Kitsukawa and coworkers recently assessed striatal gene regulation associated with running-wheel *learning* (Kitsukawa et al., 2002; 2004). They investigated effects of learning new stepping patterns (forced gait change on a motorized wheel in well-trained mice) on cortical and striatal c-*fos* expression. Results showed that c-*fos* expression was enhanced in the dorsolateral striatum, preferentially in direct pathway neurons, on the first day of gait change (Kitsukawa et al., 2002). This effect was accompanied by enhanced c-*fos* expression in the motor cortex, specifically in the bilaterally projecting corticostriatal neurons (Kitsukawa et al., 2004), which appear to mainly target direct pathway neurons (Lei et al., 2004). These findings thus also suggest learning-related neuronal changes preferentially in the direct pathway (and its cortical inputs).

While the above effects (Kitsukawa et al., 2002; 2004) indicate molecular changes in the striatum associated with motor learning, they again occurred during wheel performance. In contrast, our findings summarized in this chapter were obtained 24 h after the training and (mostly) in response to a cocaine challenge. Thus, the molecular changes in our studies reflect enduring neuronal changes associated with running-wheel learning. Our results indicate that, for a limited time period during motor learning, striatal projection neurons (probably in the direct pathway) display enhanced inducibility of specific genes, including c-*fos*, Homer 1, and substance P. These molecular changes may participate in restructuring of the corticostriatal circuits subserving such motor patterns (i.e., motor memory consolidation) or in other processes of learning. In our studies, training effects on gene expression were much more pronounced (and different) when the training occurred under the influence of cocaine. Thus, cocaine seems to abnormally enhance/alter such learning-related molecular changes.

5. CONCLUSIONS

According to previous studies, the sensorimotor striatum mediates a form of motor learning (procedural or habit learning; Graybiel, 1995; Knowlton et al., 1996; Packard and Knowlton, 2002). It has been proposed that psychostimulant addiction involves aberrant

motor learning/habit formation, and that this effect is based on drug-induced neuroplasticity in the dorsal striatum (e.g., White, 1996; Berke and Hyman, 2000; Everitt et al., 2001). Our findings are the first to show aberrant gene regulation in the sensorimotor striatum associated with motor learning under the influence of cocaine. Future studies will have to elucidate whether these molecular changes are causally related to the altered motor behavior, and whether they play a role in aberrant habit formation.

6. ACKNOWLEDGEMENTS

This work was supported by grants DA011261 and DA015439 from the National Institute on Drug Abuse. We thank Joel Beverley for excellent technical assistance.

7. REFERENCES

Badiani, A., Oates, M.M., Day, H.E., Watson, S.J., Akil, H., and Robinson, T.E., 1999, Environmental modulation of amphetamine-induced c-fos expression in D1 versus D2 striatal neurons, *Behav. Brain Res.* **103**:203–209.

Berke, J.D., Paletzki, R.F., Aronson, G.J., Hyman, S.E., and Gerfen, C.R., 1998, A complex program of striatal gene expression induced by dopaminergic stimulation, *J. Neurosci.* **18**:5301–5310.

Berke, J.D., and Hyman, S.E., 2000, Addiction, dopamine, and the molecular mechanisms of memory, *Neuron* **25**:515–532.

Berretta, S., Robertson, H.A., and Graybiel, A.M., 1992, Dopamine and glutamate agonists stimulate neuronspecific expression of Fos-like protein in the striatum, *J. Neurophysiol.* **68**:767–777.

Bottai, D., Guzowski, J.F., Schwarz, M.K., Kang, S.H., Xiao, B., Lanahan, A., Worley, P.F., and Seeburg, P.H., 2002, Synaptic activity-induced conversion of intronic to exonic sequence in Homer 1 immediate early gene expression, *J. Neurosci.* **22**:167–175.

Brakeman, P.R., Lanahan, A.A., O'Brien, R., Roche, K., Barnes, C.A., Huganir, R.L., and Worley, P.F., 1997, Homer: a protein that selectively binds metabotropic glutamate receptors, *Nature* **386**:284–288.

Brandon, C.L., and Steiner, H., 2003, Repeated methylphenidate treatment in adolescent rats alters gene regulation in the striatum, *Eur. J. Neurosci.* **18**:1584–1592.

Carelli, R.M., Wolske, M., and West, M.O., 1997, Loss of lever press-related firing of rat striatal forelimb neurons after repeated sessions in a lever pressing task, *J. Neurosci.* **17**:1804–1814.

Cenci, M.A., Campbell, K., Wictorin, K., and Björklund, A., 1992, Striatal c-*fos* induction by cocaine or apomorphine occurs preferentially in output neurons projecting to the substantia nigra in the rat, *Eur. J. Neurosci.* **4**:376–380.

Cenci, M.A., and Björklund, A., 1993, Transection of corticostriatal afferents reduces amphetamine- and apomorphine-induced striatal Fos expression and turning behaviour in unilaterally 6-hydroxydopaminelesioned rats, *Eur. J. Neurosci.* **5**:1062–1070.

Davis, H.P., and Squire, L.R., 1984, Protein synthesis and memory: a review, *Psychol. Bull.* **96**:518–559.

Drago, J., Gerfen, C.R., Westphal, H., and Steiner, H., 1996, D1 dopamine receptor-deficient mouse: Cocaineinduced regulation of immediate-early gene and substance P expression in the striatum, *Neuroscience* **74**:813–823.

Everitt, B.J., Dickinson, A., and Robbins, T.W., 2001, The neuropsychological basis of addictive behaviour, *Brain Res. Rev.* **36**:129–138.

Ferguson, S.M., Thomas, M.J., and Robinson, T.E., 2004, Morphine-induced c-fos mRNA expression in striatofugal circuits: modulation by dose, environmental context, and drug history, *Neuropsychopharmacology* **29**:1664–1674.

Fujiyama, K., Kajii, Y., Hiraoka, S., and Nishikawa, T., 2003, Differential regulation by stimulants of neocortical expression of mrt1, arc, and homer1a mRNA in the rats treated with repeated methamphetamine, *Synapse* **49**:143–149.

Gerfen, C.R., and Wilson, C.J., 1996, The basal ganglia, in: *Handbook of Chemical Neuroanatomy*, L.W. Swanson, A. Björklund and T. Hökfelt, eds., Elsevier, Amsterdam, pp. 371–468.

Graybiel, A.M., Moratalla, R., and Robertson, H.A., 1990, Amphetamine and cocaine induce drug-specific activation of the c-*fos* gene in striosome-matrix compartments and limbic subdivisions of the striatum, *Proc. Natl. Acad. Sci. USA* **87**:6912–6916.

Graybiel, A.M., 1995, Building action repertoires: memory and learning functions of the basal ganglia, *Curr. Opin. Neurobiol.* **5**:733–741.

Graybiel, A.M., Canales, J.J., and Capper-Loup, C., 2000, Levodopa-induced dyskinesias and dopaminedependent stereotypies: a new hypothesis, *Trends Neurosci.* **23**:S71–S77.

Haracz, J.L., Tschanz, J.T., Wang, Z., White, I.M., and Rebec, G.V., 1993, Striatal single-unit responses to amphetamine and neuroleptics in freely moving rats, *Neurosci. Biobehav. Rev.* **17**:1–12.

Harlan, R.E., and Garcia, M.M., 1998, Drugs of abuse and immediate-early genes in the forebrain, *Mol. Neurobiol.* **16**:221–267.

Hattori, S., Naoi, M., and Nishino, H., 1994, Striatal dopamine turnover during treadmill running in the rat: relation to the speed of running, *Brain Res. Bull.* **35**:41–49.

Hyman, S.E., and Nestler, E.J., 1996, Initiation and adaptation: a paradigm for understanding psychotropic drug action, *Am. J. Psychiatry* **153**:151–162.

Jog, M.S., Kubota, Y., Connolly, C.I., Hillegaart, V., and Graybiel, A.M., 1999, Building neural representations of habits, *Science* **286**:1745–1749.

Kato, A., Ozawa, F., Saitoh, Y., Hirai, K., and Inokuchi, K., 1997, Vesl, a gene encoding VASP/Ena family related protein, is upregulated during seizure, long-term potentiation and synaptogenesis, *FEBS Lett.* **412**:183–189.

Kitsukawa, T., Tomioka, R., Utsumi, H., Yanagihara, D., and Yamamori, T., 2002, Histochemical identification of neuronal processing involved in change of running pattern in mice, *Soc. Neurosci. Abstr.* **28**:264.8.

Kitsukawa, T., Yanagihara, D., and Yamamori, T., 2004, Bilaterally projecting cortico-striatal pathway is activated on the stepping-pattern learning in mice, *Soc. Neurosci. Abstr.* **30**:534.5.

Knowlton, B.J., Mangels, J.A., and Squire, L.R., 1996, A neostriatal habit learning system in humans, *Science* **273**:1353–1354.

Kosofsky, B.E., Genova, L.M., and Hyman, S.E., 1995, Substance P phenotype defines specificity of c-*fos* induction by cocaine in developing rat striatum, *J. Comp. Neurol.* **351**:41–50.

Lei, W., Jiao, Y., Del Mar, N., and Reiner, A., 2004, Evidence for differential cortical input to direct pathway versus indirect pathway striatal projection neurons in rats, *J. Neurosci.* **24**:8289–8299.

Liste, I., Guerra, M.J., Caruncho, H.J., and Labandeira-Garcia, J.L., 1997, Treadmill running induces striatal Fos expression via NMDA glutamate and dopamine receptors, *Exp. Brain Res.* **115**:458–468.

Liste, I., Rodriguez-Pallares, J., Caruncho, H.J., and Labandeira-Garcia, J.L., 1999, Locomotor-activityinduced changes in striatal levels of preprotachykinin and preproenkephalin mRNA. Regulation by the dopaminergic and glutamatergic systems, *Mol. Brain Res.* **70**:74–83.

Meeusen, R., Smolders, I., Sarre, S., de Meirleir, K., Keizer, H., Serneels, M., Ebinger, G., and Michotte, Y., 1997, Endurance training effects on neurotransmitter release in rat striatum: an in vivo microdialysis study, *Acta Physiol. Scand.* **159**:335–341.

Packard, M.G., and Knowlton, B.J., 2002, Learning and memory functions of the basal ganglia, *Annu. Rev. Neurosci.* **25**:563–593.

Sherwin, C.M., 1998, Voluntary wheel running: a review and novel interpretation, *Anim. Behav.* **56**:11–27.

Steiner, H., and Gerfen, C.R., 1993, Cocaine-induced c-*fos* messenger RNA is inversely related to dynorphin expression in striatum, *J. Neurosci.* **13**:5066–5081.

Steiner, H., and Gerfen, C.R., 1995, Dynorphin opioid inhibition of cocaine-induced, D1 dopamine receptormediated immediate-early gene expression in the striatum, *J. Comp. Neurol.* **353**:200–212.

Steiner, H., and Gerfen, C.R., 1998, Role of dynorphin and enkephalin in the regulation of striatal output pathways and behavior, *Exp. Brain Res.* **123**:60–76.

Steiner, H., and Gerfen, C.R., 1999, Enkephalin regulates acute D2 dopamine receptor antagonist-induced immediate-early gene expression in striatal neurons, *Neuroscience* **88**:795–810.

Steiner, H., and Kitai, S.T., 2001, Unilateral striatal dopamine depletion: time-dependent effects on cortical function and behavioural correlates, *Eur. J. Neurosci.* **14**:1390–1404.

Stork, O., and Welzl, H., 1999, Memory formation and the regulation of gene expression, *Cell. Mol. Life Sci.* **55**:575–592.

Thomas, U., 2002, Modulation of synaptic signalling complexes by Homer proteins, *J. Neurochem.* **81**:407–413.

Uslaner, J.M., Crombag, H.S., Ferguson, S.M., and Robinson, T.E., 2003, Cocaine-induced psychomotor activity is associated with its ability to induce c-fos mRNA expression in the subthalamic nucleus: effects of dose and repeated treatment, *Eur. J. Neurosci.* **17**:2180–2186.

Vargo, J.M., and Marshall, J.F., 1995, Time-dependent changes in dopamine agonist-induced striatal Fos immunoreactivity are related to sensory neglect and its recovery after unilateral prefrontal cortex injury, *Synapse* **20**:305–315.

Volkow, N.D., Wang, G.J., Fowler, J.S., Fischman, M., Foltin, R., Abumrad, N.N., Gatley, S.J., Logan, J., Wong, C., Gifford, A., Ding, Y.S., Hitzemann, R., and Pappas, N., 1999, Methylphenidate and cocaine have a similar in vivo potency to block dopamine transporters in the human brain, *Life Sci.* **65**:PL7–12.

Werme, M., Thoren, P., Olson, L., and Brene, S., 2000, Running and cocaine both upregulate dynorphin mRNA in medial caudate putamen, *Eur. J. Neurosci.* **12**:2967–2974.

West, M.O., Carelli, R.M., Pomerantz, M., Cohen, S.M., Gardner, J.P., Chapin, J.K., and Woodward, D.J., 1990, A region in the dorsolateral striatum of the rat exhibiting single-unit correlations with specific locomotor limb movements, *J. Neurophysiol.* **64**:1233–1246.

White, N.M., 1996, Addictive drugs as reinforcers: multiple partial actions on memory systems, *Addiction* **91**:921–949.

Willuhn, I., Sun, W., and Steiner, H., 2003, Topography of cocaine-induced gene regulation in the rat striatum: Relationship to cortical inputs and role of behavioural context, *Eur. J. Neurosci.* **17**:1053–1066.

Xiao, B., Tu, J.C., and Worley, P.F., 2000, Homer: a link between neural activity and glutamate receptor function, *Curr. Opin. Neurobiol.* **10**:370–374.

Yana, M., and Steiner, H., 2005a, Topography of methylphenidate (Ritalin)-induced gene regulation in the striatum: differential effects on c-*fos*, substance P and opioid peptides, *Neuropsychopharmacology*, **30**:901–915.

Yana, M., and Steiner, H., 2005b, Methylphenidate (Ritalin) induces Homer 1a and zif 268 expression in specific corticostriatal circuits, *Neuroscience*, **132**:855–865.

OPPOSING SHORT-TERM AND LONG-TERM EFFECTS OF AMPHETAMINE SENSITIZATION ON OPERANT RESPONDING FOR A FOOD REINFORCER

Rebecca E. Nordquist, Pieter Voorn, J.G. de Mooij-van Malsen, R.N.J.M.A. Joosten, Cyriel M.A. Pennartz, and Louk J.M.J. Vanderschuren*

1. ABSTRACT

Repeated exposure to drugs of abuse causes behavioral sensitization, a progressive and persistent increase in the psychomotor response to drugs. Behavioral sensitization is accompanied by altered responses to motivational stimuli and a wide array of neuroadaptations in limbic corticostriatal systems. Interestingly, both the behavioral and neural changes show markedly different effects when tested during induction of sensitization or after a period of drug abstinence. To directly compare short- and long-term effects of repeated drug administration on motivational behavior, we assessed performance of an operant conditioning task in rats either following a three week period of abstinence from amphetamine treatment or during the induction of amphetamine sensitization. We observed a biphasic response pattern for reward, in which operant responding was persistently potentiated following abstinence but transiently decreased when animals were tested during induction. We propose that drug-induced changes in the function of reward-related cortico-striatal systems underlie this pattern of sensitization-induced changes in motivated behavior.

* Author affiliations: Department of Anatomy, Vrije Universiteit Medical Center, Amsterdam (R.E.N., P.V.); Netherlands Institute for Brain Research (R.E.N., J.G.M., R.N.J.M.A.J.); Animal Physiology & Cognitive Neuroscience, Swammerdam Institute for Life Sciences, University of Amsterdam (C.M.A.P.); Rudolf Magnus Institute of Neuroscience, Dept. of Pharmacology and Anatomy, University Medical Center Utrecht (J.G.M., L.J.M.J.V.)

2. INTRODUCTION

Repeated exposure to drugs of abuse causes behavioral sensitization, a progressive and persistent increase in the psychomotor response to drugs (Pierce and Kalivas, 1997; Robinson and Becker, 1986; Robinson and Berridge, 1993; Stewart and Badiani, 1993; Vanderschuren and Kalivas, 2000). This behavioral hypersensitivity is associated with a plethora of neural adaptations in limbic corticostriatal systems (Berke and Hyman, 2000). Given the involvement of these neural circuits affected by sensitization in motivation and reward, it can be predicted that drug sensitization inflicts changes on motivational behaviors. Indeed, repeated psychostimulant exposure causes an increase in reinforcing properties of drug and natural reinforcers after a period of abstinence (Robinson and Berridge, 2003; Taylor and Horger, 1999; Taylor and Jentsch, 2001; Vezina, 2004; Wyvell and Berridge, 2001).

Many of the neural changes induced by sensitization are transient, and are observed only during the drug treatment regimen or in the first few days following cessation of drug treatment, a period generally referred to as induction. These include subsensitivity of D2 dopamine autoreceptors in ventral tegmental area and nucleus accumbens, increased basal levels of dopamine in the ventral tegmental area, and increased excitability of midbrain dopaminergic neurons (for reviews see White and Kalivas, 1998 and Vanderschuren and Kalivas, 2000). Other changes, however, are highly persistent, lasting weeks to months after the last injection of drug. Sensitization of dopamine efflux and altered cellular activity in response to psychostimulants have been repeatedly demonstrated in the striatum weeks to months after induction of sensitization (Canales and Graybiel, 2000; Jaber et al., 1995; Paulson and Robinson, 1995; Robinson et al., 1988; Vanderschuren et al., 2002). In addition, psychostimulant sensitization has been shown to be associated with long-lasting morphological changes of striatal and prefrontal output neurons (Crombag et al., 2005; Li et al., 2003; Robinson and Kolb, 1997; Robinson and Kolb, 1999).

Changes in motivated behavior observed in sensitized animals are thought to be the result of sensitization-associated adaptations in the striatum. Given the specific time course of the neuroadapations described above, we predicted differential effects of sensitization on motivated behaviors when tested during induction of sensitization as compared to testing after a period of abstinence. In order to test this hypothesis, performance of an operant conditioning task was assessed in rats following either a period of abstinence from amphetamine, or during the induction of sensitization.

3. MATERIALS AND METHODS

A total of 40 male Wistar rats (Harlan, Horst, the Netherlands) were housed in facilities and tested in operant chambers as previously described (Nordquist et al., 2003). Behavioral training took place in custom-made operant chambers of $34 \times 33 \times 37$ cm ($l \times w \times h$). The floor of the chamber was composed of bars with bedding under them. The chamber was fitted with a food tray, where food could be dispensed via an automatic feeding device, and a light inside the food tray. A light, loudspeaker, and lever were located on either side of the food tray. Behavioral procedures were run and behavioral data collected through a PC (486-DX2, 55 MHz) with MED-PC software (Version 2.0, 1991, Med Associates, Inc., East Fairfield, VT, USA). All experiments were approved by the Animal Experimentation Committee of the Royal Netherlands Academy of Arts and Sciences and were conducted in

agreement with Dutch laws (Wet op de Dierproeven, 1996) and European regulations (Guideline 86/609/EEC).

Following acclimatization to the reverse day-night cycle in our laboratory facilities and daily handling, one group of animals (n = 12), received 5 daily IP injections of 2.5 mg/kg D-amphetamine (O.P.G., Utrecht, the Netherlands) in the home cages, a procedure which has consistently produced behavioral sensitization in our laboratories (De Vries et al., 1996; Vanderschuren et al., 1999). Sensitization was confirmed in these animals following all testing. The saline pretreated group (n = 8) received IP injections of sterile saline in the home cage on the same days. After 2.5 weeks of drug abstinence and brief training in a shaping procedure, one 30-minute behavioral session per day was conducted in which rats were trained to press a lever to obtain a sucrose pellet reward on a random ratio schedule. Reward probability of each lever press decreased from 1 during the first session through 0.2, 0.1, to a final probability of 0.05 in session 9.

During the second experiment, animals were tested on the Random Ratio task during the induction phase of sensitization. After acclimatization to laboratory facilities, these animals completed a shaping training and started the Random Ratio task procedure as described above, with the modification that these rats were exposed to two training sessions per day. Following 8 days of training (16 training sessions), animals were treated with amphetamine (n = 12) or saline (n = 48) as described above. Amphetamine or saline injections were administered after daily behavioral testing had taken place, so that altered task performance could not be the result of the acute effects of amphetamine.

Data are expressed as mean ±SEM number of lever presses per minute. Data were analyzed using a repeated measures ANOVA with drug treatment as factor. T-tests for independent samples were used to determine in which sessions the saline and amphetamine treated animals differed.

4. RESULTS

The task was readily acquired by all animals, as indicated by the sharp rise in the number of correct lever presses per minute and the low number of incorrect lever presses from sessions 1–10 (Fig. 1 and 2). Significant main effect of session in repeated measures ANOVAs confirmed that both the number of correct lever presses per minute increased ($p < 0.001$) and the number of incorrect lever presses decreased ($p < 0.001$) during both experiments.

4.1. Increased Responding After Drug Abstinence

Consistently higher levels of correct lever pressing were observed in amphetamine-treated animals compared to saline controls (Fig. 1). Rates of correct lever presses were increased by 68% in amphetamine-treated animals: 145.3 ± 13.8 presses per minute in session 45, compared to the 86.3 ± 8.5 presses per minute seen in the saline-treated animals. These differences were reflected in a main effect of drug treatment ($F_{(1,18)} = 9.95$; $p < 0.01$) and a drug treatment x session interaction ($F_{(44,792)} = 2.61$; $p < 0.001$) in a repeated measures ANOVA. T-tests for independent samples showed differences between amphetamine- and saline-treated animals in most sessions from session 9 until the end of the experiment (27 of 37 sessions).

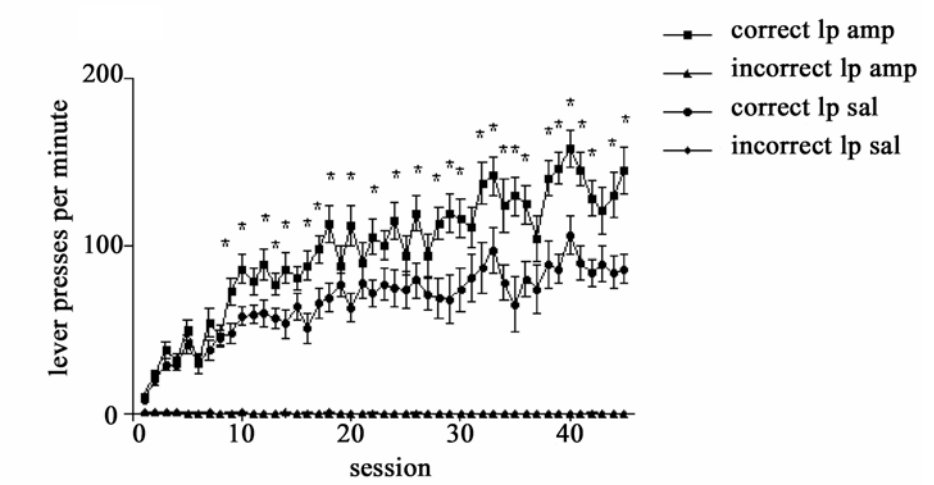

Figure 1. Long-term increase in operant responding after drug abstinence. Number of correct lever presses in random ratio task is higher in amphetamine- than saline-treated animals when training follows a period of drug abstinence. Y-axis represents lever presses per minute during performance of the random ratio task, x-axis represents sessions. Squares represent correct lever presses and triangles represent incorrect lever presses in amphetamine treated animals (n = 12), circles represent correct lever presses and diamonds represent incorrect lever presses in saline treated animals (n = 8). Asterisks indicate sessions in which significant differences are seen between saline- and amphetamine-treated animals in correct response levels.

4.2. Decreased Responding During Sensitization Induction

When comparing the amphetamine- and the saline-treated groups, the most striking feature is the lowered lever pressing levels in the amphetamine-treated group between sessions 20 and 27, a period overlapping the time points that amphetamine was given (Fig. 2). During these sessions, the number of lever presses in the saline-treated animals remained stable (52.3 ± 7.8 in session 19; 47.4 ± 6.4 in session 20; 53.7 ± 9.7 in session 27) while the lever presses in the amphetamine-treated animals dropped from 40.8 ± 6.9 in session 19 to 22.8 ± 2.9 in session 20, and remained considerably lower than the saline treated animals through session 27 when lever pressing was 34.1 ± 2.6. No significant effect of drug treatment or interaction between drug treatment and session was seen in the repeated measures ANOVA taking all sessions into account (treatment: $F_{(1,18)} = 0.816$, not significant; treatment x session: $F_{(44,792)} = 1.27$, not significant). However, pair wise comparisons showed significant differences between amphetamine- and saline-treated groups in sessions 20–24 and 27 ($p < 0.05$).

No differences were observed in incorrect lever pressing between amphetamine- and saline-treated animals for either experiment, as confirmed by a repeated measures ANOVA and pair wise comparisons.

5. DISCUSSION

In the present study, a sensitizing regimen of amphetamine produced opposing short- and long-term effects on motivated behavior. Testing after several weeks of abstinence from

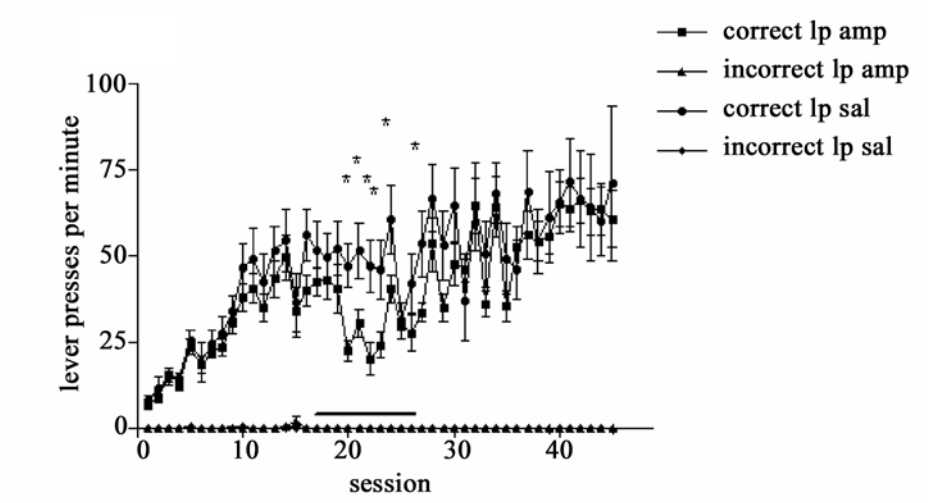

Figure 2. Short-term decrease in operant responding during induction of drug sensitization. Number of correct lever presses is decreased in amphetamine-treated animals when tested during induction of sensitization. Axes and symbols are as in Figure 1. Bar indicates sessions that took place on days that amphetamine was administered.

amphetamine treatment resulted in long-lasting increases, while testing during the induction phase of sensitization caused a transient decrease in operant responding for sucrose. These differential effects indicate that both the neurobiological effects of sensitization that are present during induction and the long-lasting neuroadaptations are reflected in motivated behavior.

In the short-term, withdrawal from chronic amphetamine treatment induces a behavioral profile that is indicative of anxiousness (Cancela et al., 2001) or a negative affective state reminiscent of depressive symptoms (Cryan et al., 2003). During the first days of abstinence from chronic amphetamine, intracranial self-stimulation thresholds are raised, indicating a decrease in rewarding value of self-stimulation (Koob et al., 2004; Lin et al., 2000). This decrease corresponds well with the decreased responding for sucrose observed in the present study, and together these results support the hypothesis that withdrawal from chronic drug administration produces transient symptoms of anhedonia.

After longer periods of abstinence, when increased response levels were seen in the present study, increases are also seen in motivated behaviors for other types of reward such as addictive drugs, sex and conditioned reinforcers (Fiorino and Phillips, 1999; Taylor and Horger, 1999; Vezina, 2004). Overall, the results of the present study add to a large body of evidence showing that repeated treatment with drugs of abuse lead to short-term effects reminiscent of depression, and long-term increases in motivated behaviors. Both effects could contribute to the development of drug addiction, with drug use elicited to relieve a negative motivational state in initial phases of abstinence (Hutcheson et al., 2001; Koob et al., 2004) and increased motivational value of rewarding stimuli increasing the likelihood of drug use after longer periods of abstinence (Robinson and Berridge, 2003).

The opposing effects observed in the responses are reminiscent of the short- and long-term effects of drug sensitization seen on dopamine release. Attenuated dopamine responses to drugs in striatal areas are generally found up to 7 days into drug abstinence (Heidbreder et al., 1996; Kalivas and Duffy, 1993; Segal and Kuczenski, 1992; Segal and Kuczenski, 1992; Wolf et al., 1993), while after four weeks of withdrawal, dopamine responses to drug stimuli are increased (Heidbreder et al., 1996; Kalivas and Duffy, 1993; Vezina, 1996; Wolf et al., 1993). Dopamine release in the striatum is frequently suggested to play an important role in incentive salience attribution and the motivational influence of environmental stimuli on behavior (Cardinal et al., 2002; Robinson and Berridge, 1993; Salamone et al., 2003; Schultz, 2002). Interestingly, recent studies indicate an important role for dopamine in the striatum in gating of glutamate transmission from cortical inputs, with dopamine decreasing release from terminals with a low release probability (Bamford et al., 2004). Thus, behavioral differences observed between animals in induction and following abstinence could be due to changes in cortical control of striatal output.

Although the exact neural substrate underlying effects of sensitization on operant responding remains to be elucidated, the striatum has been implicated in operant responding and shows altered responsivity following drug sensitization, including the changes in dopamine release described above. The dorsal striatum is hypothesized to be involved in habit formation (Mishkin et al., 1984; Packard and Knowlton, 2002; White and McDonald, 2002; Yin et al., 2004) and the ventral striatum involved in reinforcer value and influence of environmental stimuli on motivated behavior (Cardinal et al., 2002; Robinson and Berridge, 1993; Salamone et al., 2003; Schultz, 2002). Alterations in the reactivity of the striatum could lead to changes in motivated behavior as observed in the present study.

Sensitizing regimens of psychostimulant treatment cause many changes in the dorsal striatum, including increased dopamine efflux in response to drug challenges (Paulson and Robinson, 1995), changed expression of various activity markers (Steiner and Gerfen, 1998; Vanderschuren et al., 2002; Willuhn et al., 2003) and changes in neuronal morphology (Li et al., 2003). Within the striatum, a subdivision can be made into "patch" (or striosome) and "matrix" areas in the dorsal striatum (Graybiel, 1983; Graybiel and Ragsdale, 1978), with similar divisions distinguishable in the ventral striatum (Berendse et al., 1992; Gerfen, 1989; Jongen-Rêlo et al., 1994; Voorn et al., 1989; Wright and Groenewegen, 1995), by staining for various neurochemical markers and mapping of anatomical connectivity patterns. Patches have been demonstrated to show heightened reactivity to drug administration following sensitization (Canales and Graybiel, 2000; Vanderschuren et al., 2002). Interactions between the patch and matrix areas have also been speculated to be involved in learning processes (White, 1989), with patches proposed to "train" the matrix to react to reward-associated stimuli through regulation of dopaminergic inputs (Houk et al., 1995). It could thus be hypothesized that drug sensitization initiates distorted flow of information through the segregated cortico-striatal loops that involve patches or matrix in the dorsal striatum (Gerfen, 1992). In this scenario, hyperresponsive dorsal striatal patches would then cause "overtraining" of the matrix, leading to abnormal associative learning that, in turn, results in increased operant responding after drug abstinence. An intriguing possibility is that the changes in motivational value brought about by sensitization could be due to homologous regional changes in neural reactivity in the ventral striatum. Future research should be directed toward elucidation of the importance of striatal differentiation in effects of repeated drug exposure on learning and motivational processes.

In conclusion, drug sensitization has different effects on operant responding that are dependent upon the time period that testing takes place. This may indicate a role for both depressed and increased reward value during different phases of abstinence, potentially with separate contributions to relapse.

6. REFERENCES

Bamford, N.S., Zhang, H., Schmitz, Y., Wu, N.-P., Cepeda, C., Levine, M.S., Schmauss, C., Zakharenko, S.S., Zablow, L., and Sulzer, D., 2004, Heterosynaptic dopamine neurotransmission selects sets of corticostriatal terminals, *Neuron.* **42**:653–663.

Berendse, H.W., Galis-de Graaf, Y., and Groenewegen, H.J., 1992, Topographical organization and relationship with ventral striatal compartments of prefrontal corticostriatal projections in the rat, *J. Comp. Neurol.* **316**: 314–347.

Berke, J.D., and Hyman, S.E., 2000, Addiction, dopamine, and the molecular mechanisms of memory, *Neuron.* **25**:515–532.

Canales, J.J., and Graybiel, A.M., 2000, A measure of striatal function predicts motor stereotypy, *Nat. Neurosci.* **3**:377–383.

Cancela, L.M., Basso, A.M., Martijena, I.D., Capriles, N.R., and Molina, V.A., 2001, A dopaminergic mechanism is involved in the "anxiogenic-like" response induced by chronic amphetamine treatment: a behavioral and neurochemical study, *Brain Res.* **909**:197–186.

Cardinal, R.N., Parkinson, J.A., Hall, J., and Everitt, B.J., 2002, Emotion and motivation: the role of the amygdala, ventral striatum, and prefrontal cortex, *Neurosci. Biobehav. Rev.* **26**:321–352.

Crombag, H.S., Gorny, G., Li, Y., Kolb, B., and Robinson, T.E., 2005, Opposite Effects of Amphetamine Self-administration Experience on Dendritic Spines in the Medial and Orbital Prefrontal Cortex, *Cereb. Cortex.* **15**:341–348.

Cryan, J.F., Hoyer, D., and Markou, A., 2003, Withdrawal from chronic amphetamine induces depressive-like behavioral effects in rodents, *Biol. Psychiatry.* **54**:49–58.

De Vries, T.J., Schoffelmeer, A.N., Tjon, G.H., Nestby, P., Mulder, A.H., and Vanderschuren, L.J., 1996, Mifepristone prevents the expression of long-term behavioural sensitization to amphetamine, *Eur. J. Pharmacol.* **307**: R3–R4.

Fiorino, D.F., and Phillips, A.G., 1999, Facilitation of sexual behavior and enhanced dopamine efflux in the nucleus accumbens of male rats after D-amphetamine-induced behavioral sensitization, *J. Neurosci.* **19**:456–463.

Gerfen, C.R., 1989, The neostriatal mosaic: striatal patch-matrix organization is related to cortical lamination, *Science* **246**:385–388.

Gerfen, C.R., 1992, The neostriatal mosaic: multiple levels of compartmental organization, *Trends Neurosci.* **15**: 133–139.

Graybiel, A.M., 1983, Compartmental organization of the mammalian striatum, *Prog. Brain Res.* **58**:247–256.

Graybiel, A.M., and Ragsdale, C.W., Jr., 1978, Histochemically distinct compartments in the striatum of human, monkeys, and cat demonstrated by acetylthiocholinesterase staining, *Proc. Natl. Acad. Sci. USA* **75**: 5723–5726.

Heidbreder, C.A., Thompson, A.C., and Shippenberg, T.S., 1996, Role of extracellular dopamine in the initiation and long-term expression of behavioral sensitization to cocaine, *J. Pharmacol. Exp. Ther.* **278**:490–502.

Hutcheson, D.M., Everitt, B.J., Robbins, T.W., and Dickinson, A., 2001, The role of withdrawal in heroin addiction: enhances reward or promotes avoidance?, *Nat. Neurosci.* **4**:943–947.

Jaber, M., Cador, M., Dumartin, B., Normand, E., Stinus, L., and Bloch, B., 1995, Acute and chronic amphetamine treatments differently regulate neuropeptide messenger RNA levels and Fos immunoreactivity in rat striatal neurons, *Neuroscience* **65**:1041–1050.

Jongen-Rêlo, A.L., Voorn, P., and Groenewegen, H.J., 1994, Immunohistochemical characterization of the shell and core territories of the nucleus accumbens of the rat, *Eur. J. Neurosci.* **6**:1255–1264.

Kalivas, P.W., and Duffy, P., 1993, Time course of extracellular dopamine and behavioral sensitization to cocaine. I. Dopamine axon terminals, *J. Neurosci.* **13**:266–275.

Koob, G.F., Ahmed, S.H., Boutrel, B., Chen, S.A., Kenny, P.J., Markou, A., O'Dell, L.E., Parsons, L.H., and Sanna, P.P., 2004, Neurobiological mechanisms in the transition from drug use to drug dependence, *Neurosci. Biobehav. Rev.* **27**:739–749.

Li, Y., Kolb, B., and Robinson, T.E., 2003, The location of persistent amphetamine-induced changes in the density of dendritic spines on medium spiny neurons in the nucleus accumbens and caudate-putamen, *Neuropsychopharmacology* **28**:1082–1085.

Lin, D., Koob, G.F., and Markou, A., 2000, Time-dependent alterations in ICSS thresholds associated with repeated amphetamine administrations, *Pharmacol. Biochem. Behav.* **65**:407–417.

Nordquist, R.E., Pennartz, C.M.A., Uylings, H.B., Joosten, R.N.J.M.A., Jonker, A.J., Groenewegen, H.J., and Voorn, P., 2003, C-fos activation patterns in rat prefrontal cortex during acquisition of a cued classical conditioning task, *Behav. Brain. Res.* **146**:65–75.

Packard, M.G., and Knowlton, B.J., 2002, Learning and memory functions of the basal ganglia, *Annual Review of Neuroscience* **25**:563–593.

Paulson, P.E., and Robinson, T.E., 1995, Amphetamine-induced time-dependent sensitization of dopamine neurotransmission in the dorsal and ventral striatum: a microdialysis study in behaving rats, *Synapse.* **19**:56–65.

Pierce, R.C., and Kalivas, P.W., 1997, A circuitry model of the expression of behavioral sensitization to amphetamine-like psychostimulants, *Brain. Res. Brain. Res. Rev.* **25**:192–216.

Robinson, T.E., and Becker, J.B., 1986, Enduring changes in brain and behavior produced by chronic amphetamine administration: a review and evaluation of animal models of amphetamine psychosis, *Brain. Res.* **396**: 157–198.

Robinson, T.E., and Berridge, K.C., 1993, The neural basis of drug craving: an incentive-sensitization theory of addiction, *Brain. Res. Brain. Res. Rev.* **18**:247–291.

Robinson, T.E., and Berridge, K.C., 2003, Addiction, *Annu Rev Psychol* **54**:25–53.

Robinson, T.E., Jurson, P.A., Bennett, J.A., and Bentgen, K.M., 1988, Persistent sensitization of dopamine neurotransmission in ventral striatum (nucleus accumbens) produced by prior experience with (+)-amphetamine: a microdialysis study in freely moving rats, *Brain. Res.* **462**:211–222.

Robinson, T.E., and Kolb, B., 1997, Persistent structural modifications in nucleus accumbens and prefrontal cortex neurons produced by previous experience with amphetamine, *J. Neurosci.* **17**:8491–8497.

Robinson, T.E., and Kolb, B., 1999, Alterations in the morphology of dendrites and dendritic spines in the nucleus accumbens and prefrontal cortex following repeated treatment with amphetamine or cocaine, *Eur. J. Neurosci.* **11**:1598–1604.

Salamone, J.D., Correa, M., Mingote, S., and Weber, S.M., 2003, Nucleus accumbens dopamine and the regulation of effort in food-seeking behavior: Implications for studies of natural motivation, psychiatry, and drug abuse, *J. Pharmacol. Exp. Ther.* **305**:1–8.

Schultz, W., 2002, Getting formal with dopamine and reward, *Neuron.* **36**:241–263.

Segal, D.S., and Kuczenski, R., 1992, In vivo microdialysis reveals a diminished amphetamine-induced DA response corresponding to behavioral sensitization produced by repeated amphetamine pretreatment, *Brain. Res.* **571**:330–337.

Segal, D.S., and Kuczenski, R., 1992, Repeated cocaine administration induces behavioral sensitization and corresponding decreased extracellular dopamine responses in caudate and accumbens, *Brain. Res.* **577**: 351–355.

Steiner, H., and Gerfen, C.R., 1998, Role of dynorphin and enkephalin in the regulation of striatal output pathways and behavior, *Exp. Brain. Res.* **123**:60–76.

Stewart, J., and Badiani, A., 1993, Tolerance and sensitization to the behavioral effects of drugs, *Behav. Pharmacol.* **4**:289–312.

Taylor, J.R., and Horger, B.A., 1999, Enhanced responding for conditioned reward produced by intraaccumbens amphetamine is potentiated after cocaine sensitization, *Psychopharmacology (Berl)* **142**:31–40.

Taylor, J.R., and Jentsch, J.D., 2001, Repeated intermittent administration of psychomotor stimulant drugs alters the acquisition of Pavlovian approach behavior in rats: differential effects of cocaine, damphetamine and 3,4- methylenedioxymethamphetamine ("Ecstasy"), *Biol. Psychiatry* **50**:137–143.

Vanderschuren, L.J.M.J., and Kalivas, P.W., 2000, Alterations in dopaminergic and glutamatergic transmission in the induction and expression of behavioral sensitization: a critical review of preclinical studies, *Psychopharmacology (Berl)* **151**:99–120.

Vanderschuren, L.J.M.J., Schoffelmeer, A.N., Mulder, A.H., and De Vries, T.J., 1999, Dopaminergic mechanisms mediating the long-term expression of locomotor sensitization following pre-exposure to morphine or amphetamine, *Psychopharmacology (Berl)* **143**:244–253.

Vanderschuren, L.J.M.J., Schoffelmeer, A.N, Van Leeuwen, S.D., Hof, L., Jonker, A.J., and Voorn, P., 2002, Compartment-specific changes in striatal neuronal activity during expression of amphetamine sensitization are the result of drug hypersensitivity, *Eur. J. Neurosci.* **16**:2462–2468.

Vezina, P., 1996, D1 dopamine receptor activation is necessary for the induction of sensitization by amphetamine in the ventral tegmental area, *J. Neurosci.* **16**:2411–2420.

Vezina, P., 2004, Sensitization of midbrain dopamine neuron reactivity and the self-administration of psychomotor stimulant drugs, *Neuroscience & Biobehavioral Reviews* **27**:827–839.

Voorn, P., Gerfen, C.R., and Groenewegen, H.J., 1989, Compartmental organization of the ventral striatum of the rat: immunohistochemical distribution of enkephalin, substance P, dopamine, and calcium-binding protein, *J. Comp. Neurol.* **289**:189–201.

White, F.J., and Kalivas, P.W., 1998, Neuroadaptations involved in amphetamine and cocaine addiction, *Drug Alcohol Depend* **51**:141–153.

White, N.M., 1989, A functional hypothesis concerning the striatal matrix and patches: mediation of S-R memory and reward, *Life Sci.* **45**:1943–1957.

White, N.M., and McDonald, R.J., 2002, Multiple parallel memory systems in the brain of the rat, *Neurobiol. Learn Mem.* **77**:125–184.

Willuhn, I., Sun, W., and Steiner, H., 2003, Topography of cocaine-induced gene regulation in the rat striatum: relationship to cortical inputs and role of behavioural context, *Eur. J. Neurosci.* **17**:1053–1066.

Wolf, M.E., White, F.J., Nassar, R., Brooderson, R.J., and Khansa, M.R., 1993, Differential development of autoreceptor subsensitivity and enhanced dopamine release during amphetamine sensitization, *J. Pharmacol. Exp. Ther.* **264**:249–255.

Wright, C.I., and Groenewegen, H.J., 1995, Patterns of convergence and segregation in the medial nucleus accumbens of the rat: relationships of prefrontal cortical, midline thalamic, and basal amygdaloid afferents, *J. Comp. Neurol.* **361**:383–403.

Wyvell, C.L., and Berridge, K.C., 2001, Incentive sensitization by previous amphetamine exposure: increased cue-triggered "wanting" for sucrose reward, *J. Neurosci.* **21**:7831–7840.

Yin, H.H., Knowlton, B.J., and Balleine, B.W., 2004, Lesions of dorsolateral striatum preserve outcome expectancy but disrupt habit formation in instrumental learning, *Eur. J. Neurosci.* **19**:181–189.

ANTEROGRADE TROPHIC MECHANISMS PARTICIPATE IN PATTERN FORMATION IN THE STRIATUM: A ROLE FOR BDNF IN GLUTAMATERGIC AFFERENTS

Abbas F. Sadikot*†, Kenneth Leung, Sandeep Mittal, Vladimir V. Rymar, Mario Alonso-Vanegas, and Kelvin C. Luk

1. ABSTRACT

Increasing evidence suggests that neurotransmitters cooperate with growth factors to promote cell survival in the developing CNS (Aloyz et al., 1999; Blum and Konnerth, 2005). In the striatum, retrograde trophic support from targets, including the ventral midbrain, is important for survival of neurons during postnatal apoptosis (van der Kooy 1996). We hypothesized that anterograde trophic support to the striatum from glutamatergic systems is also an important determinant of neuronal survival during the apoptosis period.

We used the glutamatergic thalamostriatal system (TS) arising from the parafascicular (PF) nucleus as a model. We proposed that anterograde transport of the neurotrophin brain-derived neurotrophic factor (BDNF), occurs in the developing TS system, and cooperates with glutamate to rescue striatal neurons from apoptosis. We demonstrate that early striatal deafferentation by lesioning of the rat PF nucleus at postnatal day 2 (P2) results in: 1) 30% loss of neostriatum neurons by P35 when quantified on Nissl stains using unbiased streology; 2) enhanced apoptosis in the striatum during the first two postnatal weeks measured using Western blots for activated caspase-3; 3) and marked reduction in striatal BDNF content on protein biochemistry. In ongoing work, neuronal loss after P2 PF lesions is markedly reduced by striatal injection of BDNF containing spheres during the first postnatal week.

Anterograde trophic mechanisms play an important role in determining the final complement of striatal neurons. We provide novel evidence indicating that BDNF serves as an

* Department of Neurology and Neurosurgery, Montreal Neurological Institute, McGill University, Montreal, Quebec H3A 2B4, Canada

† To whom correspondence should be addressed. Email: sadikot@bic.mni.mcgill.ca

"anterophin" in developing glutamatergic striatal afferents, and may cooperate with glutamate to promote activity dependent rescue of striatal neurons, thus matching neuronal number with afferent density.

2. INTRODUCTION

The classical neurotrophic hypothesis suggests that developing cells compete for limiting concentrations of growth factors at their targets. Cell death due to limiting concentrations of trophic factor at targets is an important mechanism for specifying the appropriate number and phenotype of neurons in the peripheral and central nervous systems (Davies, 1996). A growing body of evidence suggests that the neurotrophin brain derived neurotrophic factor (BDNF), in addition to its classical role as a target-derived survival factor, also provides trophic support to the developing and mature nervous system by anterograde mechanisms. Further evidence suggests that neurotransmitters cooperate with growth factors to promote cell survival in the developing CNS (Aloyz et al., 1999; Blum and Konnerth, 2005). We are particularly interested in exploring neurotransmitter and growth factor mechanisms that determine the final number of neurons in the mammalian striatum (Luk and Sadikot, 2001; Luk et al., 2003; Luk and Sadikot, 2004). In the present study, we hypothesized that anterograde trophic support to the striatum from glutamatergic systems is an important determinant of neuronal survival during the apoptosis period. As a model, we used early postnatal lesions of the rat thalamic parafascicular (PF) nucleus, a major source of glutamatergic input to the neostriatum (Dube et al., 1988; Sadikot et al., 1992a; Sadikot et al., 1992b; Smith et al., 2004; Castle et al., 2005).

We wished to determine whether the thalamostriatal projection (TS) plays a trophic survival role during the major postnatal period of developmental cell death in the striatum. Expression of mRNA for the neurotrophin brain derived neurotrophic factor (BDNF) is abundant in the PF, but scant in the striatum (Altar et al., 1997; Conner et al., 1997). BDNF is known to exert an important survival effect on striatal neurons in vitro (Ventimiglia et al., 1995), and impaired anterograde trophic mechanisms may be implicated in human pathology such as Huntington's disease (Zuccato et al., 2001). We propose that anterograde transport of BDNF within the TS projection modulates developmental cell death, and plays an important role in determining the final complement of striatal neurons. We provide novel evidence indicating that BDNF serves as an "anterophin" (Nawa and Takei, 2001) in developing glutamatergic striatal afferents. BDNF may cooperate with glutamate and other factors to promote activity dependent rescue of striatal neurons, thus matching neuronal number with afferent density.

3. METHODS

3.1. Experimental Animals

Sprague-Dawley rats received stereotactic lesions of the parafascicular nucleus (PF) of the right thalamus on postnatal day 2 while under anesthesia (Avertin). Unlesioned animals were used as controls. Animals were killed on postnatal day 35 for histology by transcardial perfusion with 4% paraformaldehyde (PFA; in 0.1 M phosphate buffer, pH 7.4) under deep pentobarbital anesthesia. Brains were then removed, postfixed for 24 h and

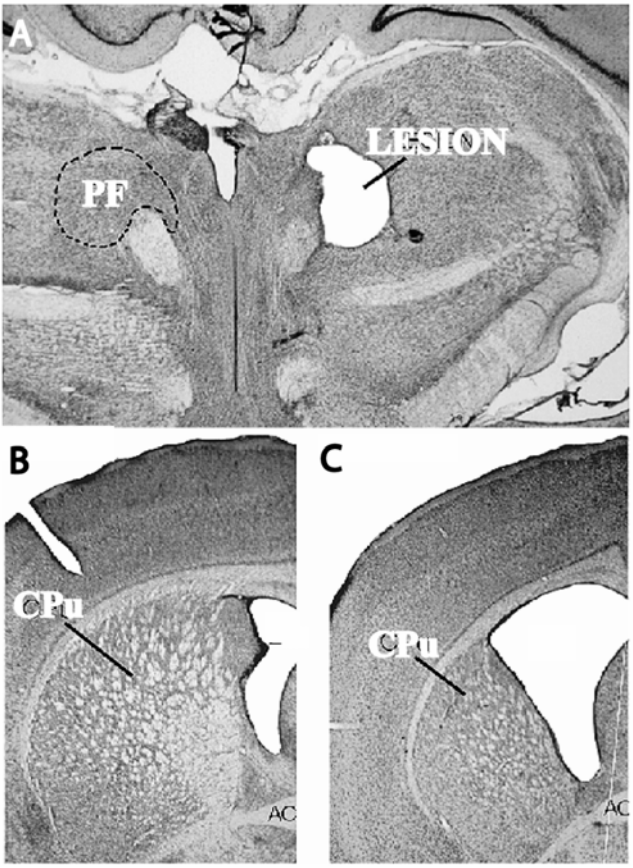

Figure 1. Early deafferentation of the developing thalamostriatal system at P2 prior to maximal apoptosis results in massive loss of surviving striatal neurons in the young adult rat (P35). Representative unilateral lesion of the parafasicular nucleus (PF) (a). Compared to the contralateral striatum (b) volume in the neostriatum ipsilateral to the lesion is markedly decreased (c).

cryoprotected by immersion in buffered sucrose (30%, pH 7.4) for an additional 48 h before cutting. Floating coronal sections were collected in PBS as 6 separate sets. One out of six sections was exposed to cresyl violet as a nissle stain. Location of lesions within the PF was confirmed in thalamic sections with cresyl violet staining (Fig. 1A).

3.2. Stereology

The number of surviving projection neurons in the neostriatum of young adult offspring (P35) was determined using the optical fractionator method (Gundersen et al., 1988). Briefly, coronal sections of the entire adult striatum were cut at 40 µm on a freezing microtome through the rostral and caudal limits of the neostriatum. Every sixth serial section within this volume was examined. In each striatum 10–11 sections were analyzed. The apparatus used consisted of a light microscope (BX40; Olympus, Tokyo, Japan)

coupled with a video camera (DC200; Dage, Michigan City, IN), motorized X-Y stage (BioPoint XYZ; LEP, Hawthorne, NY), *z*-axis indicator (MT12 microcator; Heidenhain, Traunreut, Germany), and a computer running Stereo Investigator software (Microbrightfield, Inc., Colchester, VT). Analysis of Nissl stained sections of the neostriatum was performed by randomly translating a grid (500 × 500 μm) onto the section of interest and applying an optical fractionator (Fig. 2a) (Luk and Sadikot, 2001; Luk et al., 2003; Rymar et al., 2004). Neurons were distinguished using the nucleus as a unique identifier, and

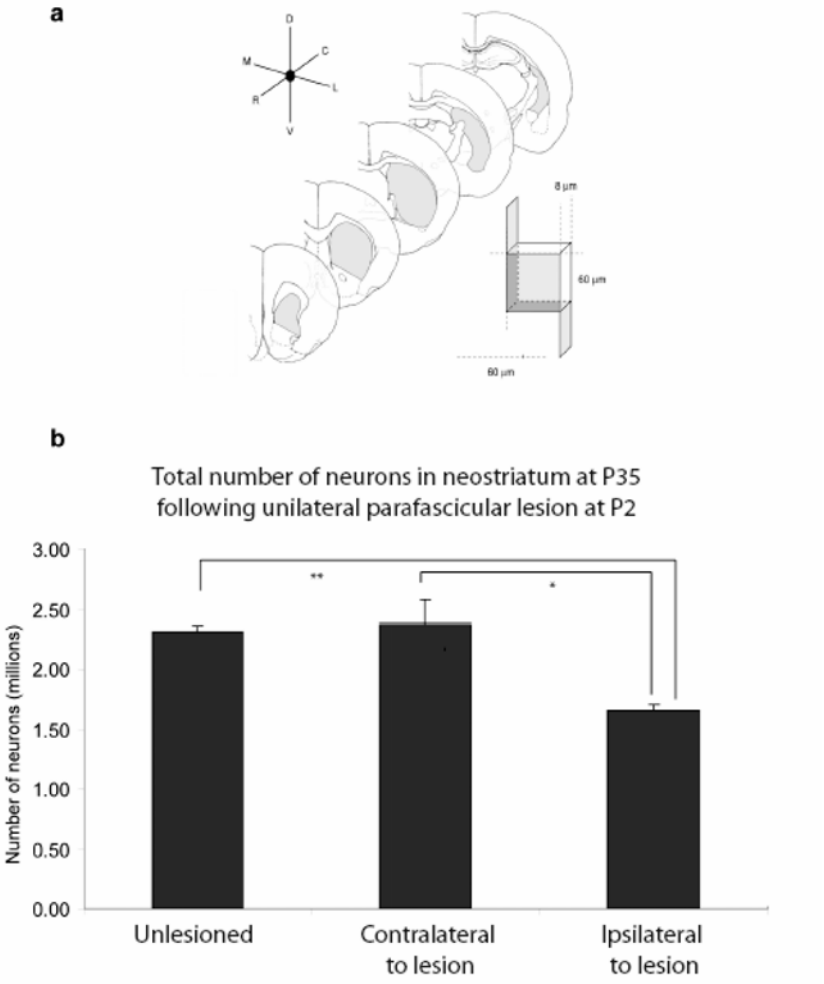

Figure 2. Sampling scheme used for stereological quantification of neostriatum neurons. Ten to eleven coronal sections at regular intervals spanning the entire striatum were selected for stereological analysis (a). Histogram showing stereological estimates of total number of neurons in striatum following unilateral parafascicular lesion at P2. The contralateral neostriatum or neostriatum from unlesioned P35 animals was used as a control. Significant loss (~30%) in ipsilateral lesioned striatum indicates that thalamic afferents are important for neuronal survival (b).

glial cells were excluded on the basis of morphology and by counting only profiles >7 μm in diameter. Each optical dissector therefore consisted of a 60 × 60 × 8 μm brick with three exclusion planes. Calculated estimates of the total number of neurons in each neostriatal and cortical reference volume were determined using the Stereo Investigator software. Analysis of variance (ANOVA) with Tukey's HSD *post hoc* test was used for statistical analysis (SAS v6.12; SAS Institute Inc, Cary, NC or Datasim 1.1; Drake Bradley, Bates College, ME).

3.3. Protein Biochemistry

The time course of apoptosis in the striatum was correlated with histology results by quantifying BDNF content and caspase-3 activation. Punch biopsies of postnatal striatal sections were performed in rapidly frozen (–80°C) fresh tissue (P3, P7, P10, P14, P21, P28, and P35). Lysates from individual control and lesioned animals were analyzed by SDS-PAGE, and the resultant immunoblot was probed with antibodies specific to BDNF (Santa Cruz Biotechnology, Santa Cruz, CA) or activated caspase-3 (Cell Systems Technology, Beverly, MA).

4. RESULTS

Early deafferentation of the developing thalamostriatal system (TS) prior to maximal apoptosis results in massive loss of surviving striatum neurons in the P35 young adult rat (Fig. 1A–C). Total neuron number was quantified using unbiased stereology. In rats receiving PF lesions at P2, the ipsilateral neostriatum contained significantly fewer neurons ($1.66 \pm 0.04 \times 10^6$; all data expressed as mean ± SEM, $n = 3$) compared to either the contralateral neostriatum ($2.37 \pm 0.21 \times 10^6$, $p < 0.05$), or to the neostriatum from unlesioned animals ($2.31 \times 10^6 \pm 0.04$, $n = 3$, $p < 0.01$) (Fig. 2b). Deafferentation prior to the maximum period of striatal apoptosis (Maciejewska et al., 1998) results in massive neuronal loss, indicating a necessary trophic role for thalamostriatal inputs in the postrnatal striatum.

To determine the time course of developmental cell death in postnatal striatum and the effect of thalamostriatal deafferentation, immunoblots were performed for activated caspase-3 at different developmental ages following PF lesion at P2 (Fig. 3a). In unlesioned controls, maximum apoptosis occurs during the first postnatal week. Animals with PF lesions at P2 showed significantly exacerbated developmental cell death during the first postnatal week ($p < 0.05$). To determine developmental changes in BDNF protein in postnatal striatum, and the effect of thalamostriatal deafferentation, immunoblots for BDNF were performed at different developmental ages following PF lesions at P2 (Fig. 3b). BDNF levels rise progressively in the postnatal striatum, and plateau by the third postnatal week. In contrast, P2 lesions result in a significant reduction in BDNF protein content as early as P3, which persists to P35 (Fig. 3b). Since most BDNF in the striatum is produced by extrinsic sources (Conner et al., 1997), and since the PF contains high concentrations of BDNF mRNA, we suggested that anterograde transport of BDNF occurs in the thalamostriatal projection, and may play an important role in determining the final complement of striatal neurons.

Other potential sources of BDNF such as the corticostriatal projection (Altar et al., 1997), may also contribute to striatal BDNF content. Furthermore, the ability of non-

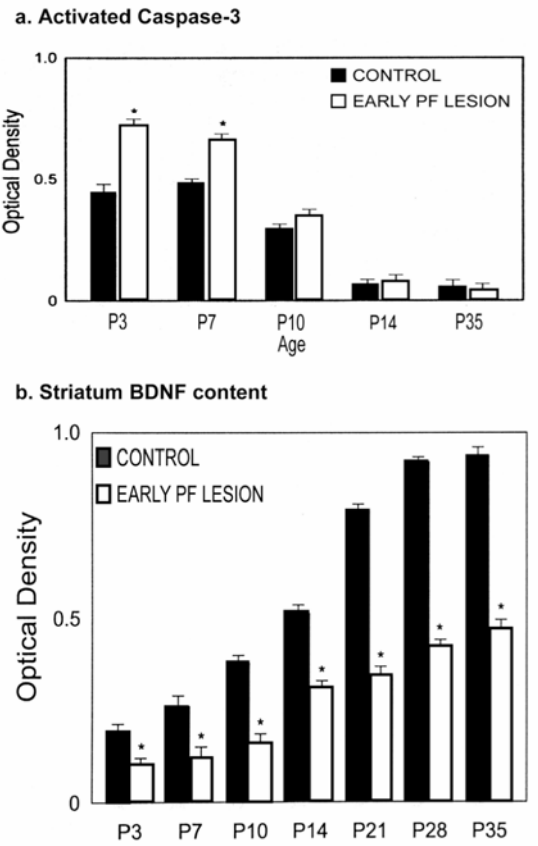

Figure 3. Western blots for relative protein concentrations of activated caspase-3 and BDNF. To determine the time course of developmental cell death in postnatal striatum, and the effect of thalamostriatal deafferentation, immunoblots for activated caspase-3, a marker for apoptosis, were performed at different developmental ages following PF lesions at P2. There is increased cell death by apoptosis during the first postnatal week in striatum from lesioned animals (a). In unlesioned rats BDNF levels are noted to rise progressively in the postnatal striatum, and plateau by the third postnatal week. In contrast, P2 PF lesions result in a significant reduction in striatal BDNF protein content as early as P3 and persisting to P35 (b).

thalamic afferents to contribute to striatum BDNF content may be altered as a result of exacerbated neuronal death following PF lesions. Our preliminary results, published in part in abstract form (Mittal et al., 2000; Mittal et al., 2001), suggest that phosphorylation of the trkB receptor is also reduced in the postnatal striatum following P2 PF lesions, consistent with reduced activation by BDNF. Furthermore, intrastriatal injection of BDNF coated latex spheres at P5 reduces neuronal death in the striatum following P2 PF lesions, indicating a partial rescue effect, and further implicating anterograde transport of BDNF in the thalamostriatal projection as a trophic survival mechanism during striatum pattern formation.

5. DISCUSSION

The classical neurotrophic hypothesis proposes that developing neurons compete for limiting concentrations of neurotrophin at their targets, without which they die (Davies et al., 1994). A novel anterograde signaling mechanism has recently been proposed as an alternative mode by which neurotrophins exert trophic effects (von Bartheld et al., 1995; Altar et al., 1997; Fawcett et al., 1997; Altar and DiStefano, 1998; Alonso-Vanegas et al., 1999; Aloyz et al., 1999). Previous work, has demonstrated that BDNF is concentrated in a vesicular compartment in nerve terminals and is regulated in its release (Fawcett et al., 1997). The BDNF receptor TrkB is present on postsynaptic densities in different brain tissues including the hippocampus and cerebral cortex (Hafidi et al., 1996; Wu et al., 1996), suggesting a functional substrate for vesicular release of BDNF. Furthermore, several CNS pathways show anterograde transport of locally injected ^{125}I-BDNF or recombinant BDNF (von Bartheld et al., 1995). BDNF may therefore function as an "anterophin" in classical neurotransmitter pathways, and exert trophic support in an activity dependent manner (Nawa and Takei, 2001). In recent work, our group has shown that ascending noradrenergic afferents co-localize BDNF in axons and terminals (Fawcett et al., 2000), transport BDNF in an anterograde manner, and release BDNF at noradrenergic targets such as the cerebral cortex in an activity dependant fashion (Aloyz et al., 1999; Fawcett et al., 2000). Pharmacological activation of the noradrenergic system leads to rapid increases in the activated, phosphorylated form of TrkB receptors in the cerebral cortex (Aloyz et al., 1999). These findings support the notion that BDNF release following anterograde transport results in activation of postsynaptic TrkB receptors.

BDNF anterograde transport in the adult CNS may serve a maintenance function. For example, in the adult septum, ascending catecholaminergic projections maintain the phenotype of a subpopulation of septal neurons which express both the calcium-binding protein calbindin-D28k and TrkB receptors (Fawcett et al., 2000). Anterograde transport of BDNF in the developing nervous system may also serve a survival function. As an example, a transgenic mouse that overexpresses BDNF in noradrenergic systems off the dopamine-β-hydroxylase promoter shows a significant increase in number of dopaminergic neurons in the midbrain (Alonso-Vanegas et al., 1999; Aloyz et al., 1999). It is proposed that the increase in dopaminergic cell number is due to rescue from developmental cell death in the perinatal period in BDNF over-expressers (Alonso-Vanegas et al., 1999; Aloyz et al., 1999). Although BDNF is well-established as a potent trophic factor for immature striatal neurons in vitro (Ventimiglia et al., 1995), little information is available on how BDNF may alter survival of neurons in the developing striatum in vivo.

Retrograde transport from striatum targets may also contribute to neuronal survival (van der Kooy, 1996). Anterograde transport of BDNF to the developing striatum has been less well-established. In the adult rat, lesions of the cerebral cortex result in reduced striatal BDNF content and decreased numbers of parvalbumin (PV)-IR neurons in the striatum, suggesting a trophic role for anterograde transport of BDNF in the glutamatergic corticostriatal system (Altar et al., 1997). BDNF anterograde transport in the corticostriatal system also likely plays a maintenance function for striatal dendritic spines in the adult mouse (Baquet et al., 2004).

To investigate the possible role for anterograde transport of BDNF in striatum development, we implemented the glutamatergic (TS) arising from the parafascicular (PF) nucleus as a model. We proposed that anterograde transport of the neurotrophin brain-derived neu-

rotrophic factor (BDNF) occurs in the developing TS system, and cooperates with glutamate to rescue striatal neurons from apoptosis.

The PF is a major source of glutamatergic input to the striatum (Rudkin and Sadikot, 1999). Previous work suggests that the PF contains a high content of the BDNF mRNA (Conner et al., 1997). On the other hand, the striatum contains BDNF protein but little if any BDNF mRNA (Conner et al., 1997). BDNF is well known as a survival and differentiation factor for striatal neurons in vitro (Ventimiglia et al., 1995). Our results support the hypothesis that BDNF anterograde transport in the TS system may play an important role in striatal pattern formation. Indeed, there is a 30% reduction in the number of striatal neurons following PF lesions at P2. In normal development apoptosis in the striatum primarily occurs during the first two postnatal weeks (Maciejewska et al., 1998). Our results using protein biochemistry for activated caspase-3 confirm the previous findings. Thalamostriatal lesions markedly exacerbate apoptosis of striatal neurons during the first two postnatal weeks. Furthermore, increased apoptosis is associated with a marked attenuation of the normal rise of BDNF that occurs during the first three postnatal weeks. In preliminary work, we have also shown that phosphorylation of trkB, the BDNF receptor, is also reduced during the first two postnatal weeks in P2 lesioned animals compared to unlesioned controls (Mittal et al., 2001). Intrastriatal delivery of BDNF during the first postnatal week partially rescues striatal neurons from death following P2 lesions. We conclude that the glutamatergic TS system plays an important neuronal survival role during striatal pattern formation in the postnatal period. A number of factors may mediate the effect, including depolarizing activity and neurotrophic factors. We provide evidence suggesting that the TS projection contributes significantly to BDNF content in the developing striatum, and may play an important role in rescue of striatal neuronal populations. Anterograde transport of BDNF not only has an important functional role in the adult (Nawa and Takei, 2001), but may also play a critical role in rescuing neuronal subpopulations during the developmental cell death period, helping determine the final neuronal complement in the CNS.

6. ACKNOWLEDGEMENTS

This work was supported in part by Canadian Institutes for Health Research (CIHR) and the Parkinson Society of Canada.

7. REFERENCES

Alonso-Vanegas, M.A., Fawcett, J.P., Causing, C.G., Miller, F.D., and Sadikot, A.F., 1999, Characterization of dopaminergic midbrain neurons in a DBH : BDNF transgenic mouse. *J. Comp. Neurol.* **413**:449–462.

Aloyz, R., Fawcett, J.P., Kaplan, D.R., Murphy, R.A., and Miller, F.D., 1999, Activity-dependent activation of TrkB neurotrophin receptors in the adult CNS. *Learn Mem.* **6**:216–231.

Altar, C.A., and DiStefano, P.S., 1998, Neurotrophin trafficking by anterograde transport. *Trends Neurosci.* **21**: 433–437.

Altar, C.A., Cai, N., Bliven, T., Juhasz, M., Conner, J.M., Acheson, A.L., Lindsay, R.M., and Wiegand, S.J., 1997, Anterograde transport of brain-derived neurotrophic factor and its role in the brain. *Nature* **389**:856–860.

Baquet, Z.C., Gorski, J.A., and Jones, K.R., 2004, Early striatal dendrite deficits followed by neuron loss with advanced age in the absence of anterograde cortical brain-derived neurotrophic factor. *J. Neurosci.* **24**: 4250–4258.

Blum, R., and Konnerth, A., 2005, Neurotrophin-mediated rapid signaling in the central nervous system: mechanisms and functions. *Physiology (Bethesda)* **20**:70–78.

Castle, M., Aymerich, M.S., Sanchez-Escobar, C., Gonzalo, N., Obeso, J.A., and Lanciego, J.L., 2005, Thalamic innervation of the direct and indirect basal ganglia pathways in the rat: Ipsi- and contralateral projections. *J. Comp. Neurol.* **483**:143–153.

Conner, J.M., Lauterborn, J.C., Yan, Q., Gall, C.M., and Varon, S., 1997, Distribution of brain-derived neurotrophic factor (BDNF) protein and mRNA in the normal adult rat CNS: evidence for anterograde axonal transport. *J. Neurosci.* **17**:2295–2313.

Davies, A.M., 1996, The neurotrophic hypothesis: where does it stand? *Philos. Trans. R. Soc. Lond B. Biol. Sci.* **351**:389–394.

Dube, L., Smith, A.D., and Bolam, J.P., 1988, Identification of synaptic terminals of thalamic or cortical origin in contact with distinct medium-size spiny neurons in the rat neostriatum. *J. Comp. Neurol.* **267**:455–471.

Fawcett, J.P., Alonso-Vanegas, M.A., Morris, S.J., Miller, F.D., Sadikot, A.F., and Murphy, R.A., 2000, Evidence that brain-derived neurotrophic factor from presynaptic nerve terminals regulates the phenotype of calbindin-containing neurons in the lateral septum. *J. Neurosci.* **20**:274–282.

Fawcett, J.P., Aloyz, R., McLean, J.H., Pareek, S., Miller, F.D., McPherson, P.S., and Murphy, R.A., 1997, Detection of brain-derived neurotrophic factor in a vesicular fraction of brain synaptosomes. *J. Biol. Chem.* **272**: 8837–8840.

Gundersen, H.J., Bagger, P., Bendtsen, T.F., Evans, S.M., Korbo, L., Marcussen, N., Moller, A., Nielsen, K., Nyengaard, J.R., and Pakkenberg, B., et al. 1988, The new stereological tools: disector, fractionator, nucleator and point sampled intercepts and their use in pathological research and diagnosis. *Apmis.* **96**:857–881.

Hafidi, A., Moore, T., and Sanes, D.H., 1996, Regional distribution of neurotrophin receptors in the developing auditory brainstem. *J. Comp. Neurol.* **367**:454–464.

Luk, K.C., and Sadikot, A.F., 2001, GABA promotes survival but not proliferation of parvalbumin-immunoreactive interneurons in rodent neostriatum: an in vivo study with stereology. *Neuroscience* **104**:93–103.

Luk, K.C., and Sadikot, A.F., 2004, Glutamate and regulation of proliferation in the developing mammalian telencephalon. *Dev. Neurosci.* **26**:218–228.

Luk, K.C., Kennedy, T.E., and Sadikot, A.F., 2003, Glutamate promotes proliferation of striatal neuronal progenitors by an NMDA receptor-mediated mechanism. *J. Neurosci.* **23**:2239–2250.

Maciejewska, B., Lipowska, M., Kowianski, P., Domaradzka-Pytel, B., and Morys, J., 1998, Postnatal development of the rat striatum–a study using in situ DNA end labeling technique. *Acta. Neurobiol. Exp. (Wars)* **58**: 23–28.

Mittal, S., Alonso-Vanegas, M.A., Aloyz, R., Miller, F.D., and Sadikot, A., 2001, Thalamostriatal afferents rescue developing striatal neurons from apoptosis. In: Soc for Neurosci Abstr, p 29.19. San Diego.

Mittal, S., Alonso-Vanegas, M., Aloyz, R., Fawcett, J.P., Luk, K.C., Lee, Y.W., Miller, F.D., and Sadikot, A.F., 2000, Glutamatergic afferents provide neurotrophic support to neurons in the developing striatum. In: Society for Neuroscience. New Orleans, LA.

Nawa, H., and Takei, N., 2001, BDNF as an anterophin; a novel neurotrophic relationship between brain neurons. *Trends Neurosci.* **24**:683–684; discussion 684–685.

Rudkin, T.M., and Sadikot, A.F., 1999, Thalamic input to parvalbumin-immunoreactive GABAergic interneurons: organization in normal striatum and effect of neonatal decortication. *Neuroscience* **88**:1165–1175.

Rymar, V.V., Sasseville, R., Luk, K.C., and Sadikot, A.F., 2004, Neurogenesis and stereological morphometry of calretinin-immunoreactive GABAergic interneurons of the neostriatum. *J. Comp. Neurol.* **469**:325–339.

Sadikot, A.F., Parent, A., and Francois, C., 1992a, Efferent connections of the centromedian and parafascicular thalamic nuclei in the squirrel monkey: a PHA-L study of subcortical projections. *J. Comp. Neurol.* **315**: 137–159.

Sadikot, A.F., Parent, A., Smith, Y., and Bolam, J.P., 1992b, Efferent connections of the centromedian and parafascicular thalamic nuclei in the squirrel monkey: a light and electron microscopic study of the thalamostriatal projection in relation to striatal heterogeneity. *J. Comp. Neurol.* **320**:228–242.

Smith, Y., Raju, D.V., Pare, J.F., and Sidibe, M., 2004, The thalamostriatal system: a highly specific network of the basal ganglia circuitry. *Trends Neurosci.* **27**:520–527.

van der Kooy, D., 1996, Early postnatal lesions of the substantia nigra produce massive shrinkage of the rat striatum, disruption of patch neuron distribution, but no loss of patch neurons. *Brain Res. Dev. Brain Res.* **94**: 242–245.

Ventimiglia, R., Mather, P.E., Jones, B.E., and Lindsay, R.M., 1995, The neurotrophins BDNF, NT-3 and NT-4/5 promote survival and morphological and biochemical differentiation of striatal neurons in vitro. *Eur. J. Neurosci.* **7**:213–222.

von Bartheld, C.S., Schober, A., Kinoshita, Y., Williams, R., Ebendal, T., and Bothwell, M., 1995, Noradrenergic neurons in the locus coeruleus of birds express TrkA, transport NGF, and respond to NGF. *J. Neurosci.* **15**:2225–2239.

Wu, K., Xu, J.L., Suen, P.C., Levine, E., Huang, Y.Y., Mount, H.T., Lin, S.Y., and Black, I.B., 1996, Functional trkB neurotrophin receptors are intrinsic components of the adult brain postsynaptic density. *Brain Res. Mol. Brain Res.* **43**:286–290.

Zuccato, C., Ciammola, A., Rigamonti, D., Leavitt, B.R., Goffredo, D., Conti, L., MacDonald, M.E., Friedlander, R.M., Silani, V., Hayden, M.R., Timmusk, T., Sipione, S., and Cattaneo, E., 2001, Loss of huntingtin-mediated BDNF gene transcription in Huntington's disease. *Science* **293**:493–498.

DEVELOPMENTAL ASSEMBLY OF GABA RECEPTORS IN THE RAT SUBSTANTIA NIGRA

Wai K. Lau, Wing H. Yung, Ying-Shing Chan, and Ken K.L. Yung*

1. INTRODUCTION

Gamma-aminobutyric acid (GABA) is a major inhibitory neurotransmitter in neurons of the basal ganglia (Gerfen et al., 1996, Smith et al., 1998). The substantia nigra is a key component of the basal ganglia. Dopaminergic neurons in the substantia nigra pars compacta form an important feedback pathway in the basal ganglia (Gerfen et al., 1996, Smith et al., 1998). The GABAergic neurons in the substantia nigra pars reticulata are the output neurons of the basal ganglia circuitry (Gerfen et al., 1996, Smith et al., 1998). Functions of GABA in the basal ganglia are mediated by $GABA_A$ and $GABA_B$ receptors (Smith et al., 2001). $GABA_A$ receptors are ionotropic receptors and they are responsible for fast GABA transmission (Mohler et al., 1996). $GABA_B$ receptor is the first heteromeric metabotropic receptor cloned (Marshall et al., 1999). It is responsible for slow GABA transmission (Bowery, 1993).

GABA is now known as one of developmental signals in the nervous system (Owens et al., 2002). In response to GABA, GABA receptor clusters are formed during synaptogenesis of GABAergic synapses (Owens et al., 2002, Simeone et al., 2003). Activation of $GABA_A$ receptors are known to cause membrane depolarization in immature neurons and thus closely related to the maturation process of neurons (Owens et al., 2002, Simeone et al., 2003). In addition, $GABA_A$ receptors are also involved in regulation of proliferation of neurons and neuronal differentiation, and both $GABA_A$ and $GABA_B$ receptors are involved in neuronal migration in developing nervous system (Owens et al., 2002, Simeone et al., 2003).

* Wai K. Lau, Department of Biology, Hong Kong Baptist University, Kowloon Tong, Hong Kong (present address: Department of Physiology, The University of Hong Kong, Sassoon Road, Hong Kong). Wing H. Yung, Department of Physiology, The Chinese University of Hong Kong, Shatin, Hong Kong. Ying-Shing Chan, Department of Physiology and Research Center of Heart, Brain, Hormone and Healthy Aging, The University of Hong Kong, Sassoon Road, Hong Kong. Ken K.L. Yung, Department of Biology, Hong Kong Baptist University, Kowloon Tong, Hong Kong. Correspondence to: Ken K.L. Yung at kklyung@hkbu.edu.hk

It is likely different regions in the brain display distinct patterns of GABA receptor expression. Although much is known about the subunit assembly of $GABA_A$ and $GABA_B$ receptors in the substantia nigra in adult mammals (Fritschy et al., 1995, Smith et al., 2001, Fujiyama et al., 2002, Waldvogel et al., 2004), the ontogeny of $GABA_A$ and $GABA_B$ receptor subunits in the nigra during postnatal development is not clear. The objective of the present study was to investigate the developmental expression of GABA receptor subunits ($GABA_A\alpha1$, $\alpha3$ and $\alpha6$; $GABA_BR1$ and R2) in the substantia nigra pars compacta and pars reticulata at four postnatal stages (postnatal day [PND] 1, PND 7, PND 14 and adult). Expression of $GABA_A$ transcripts was studied by reverse transcriptase-polymerase chain reaction. Expression of $GABA_A$ and $GABA_B$ receptor proteins was studed by immunofluorescence. Comparisons between the levels of transcripts and immunoreactivity were made possible. Functional GABA receptors depend on the expression and assembly of subunits. One crucial objective of the present study was to investigate the cellular expression and assembly of GABA receptor subunits in subpopulations of neurons in the substantia nigra. Patterns of postnatal development of GABA receptors in these subpopulations could provide further information about the maturation of the subpopulations of nigral neurons.

2. MATERIALS AND METHODS

2.1. Experimental Animals

Ninety-four Sprague–Dawley rats were used in the present study. Four different groups of rats that were in four stages of postnatal development were used. They were namely, rats at postnatal day one (PND 1; approximately 6 g), rats at PND 7 (10–13 g), rats at PND 14 (19–21 g) and adult rats (>3 month-old, 150–160 g). The handling of rats and all procedures performed on them were approved in accordance with the Animals (Control of Experiments) Ordinance, Hong Kong, China. All efforts were made by the investigators to ensure that both animal numbers and suffering were at its minimal in the experiments.

2.2. Analysis of $GABA_A$ Transcripts

Rats were decapitated and the nigral tissue was dissected. Total RNAs were isolated using TRIZOL Reagent (Gibco, BRL) and isopropyl alcohol as previously described (Lau et al., 2003). Reverse transcriptase-polymerase chain reaction (RT-PCR) was performed in accordance to established method as previously described (Lau et al., 2003). The following primer pairs were used: $GABA_A\alpha1$ (5′-GCAACCAGCTATACCCCTAACTTAGC-3′ and 5′-TTGACTTCTTTCGGTTCTATGGTCG-3′), $\alpha6$ (5′-GCTGTCAACTACTTCACCAATCTCC-3′ and 5′-GCTGGCCTCAGAAGATGGAACG-3′), $\beta2$ (5′-CAGGAGCACAATGCTTGCCTATG-3′ and 5′-CGACTTTTCTTTTGTGCCACATG-3′) and $\beta3$ (5′-GAATGAGGTTGCAGGCAGCG-3′ and 5′-TCTTGTGCGGGATGCTTCTGTC-3′) and GAPDH (5′-ATGGTGAAGGTCGGTGTGAAC-3′ and 5′-GCTGACAATCTTGAGGGAGT-3′) (Liu et al., 1998, Lai et al., 2000). The following amplification cycles were used to compare the levels of $GABA_A$ transcripts: $\alpha1$, 33 cycles; $\alpha6$, 35 cycles; $\beta2$, 35 cycles; $\beta3$, 35 cycles and GAPDH transcript, 35 cycles. Amplification from primers, $\alpha1$, $\alpha6$, $\beta2$, $\beta3$ and GAPDH produces PCR products of 89, 168, 117, 140 and 437 bp in length respectively (Liu et al., 1998). Images of the gels after RT-PCR analyses were digitally captured and semi-quantified by image analyzing software (Metamorph, Universal

Imaging, Downingtown, PA). The relative intensities were measured as averaged gray value and expressed as mean ± S.E.M (Lau et al., 2003). Data of each age group that were obtained from at least three animals from each age were averaged and compared with other groups by analysis of variance (ANOVA) with Duncan's multiple range tests at the 5% error level ($P < 0.05$).

2.3. Analysis of $GABA_A$ and $GABA_B$ Receptor Immunoreactivity

The nigral sections from the animals of all four groups were incubated and reacted in a single reaction for comparison. Rats were perfuse-fixed with 3–4% paraformaldehyde plus 0.01% glutaraldehyde in phosphate buffer (0.1 M, pH 7.4). Immunoreactivity for $GABA_A\alpha1$, $GABA_A\alpha3$, $GABA_A\alpha6$, $GABA_BR1$ and $GABA_BR2$ receptor in the nigral sections of all groups were revealed in one immunofluorescence reaction using commercially available primary antibodies against the following $GABA_A$ subunits: $\alpha1$ (rabbit polyclonal; 0.5–1.0 μg/ml in PBS supplemented with 2% NGS and 0.1% Triton X-100 [PBS-Triton]; Upstate Biotechnology), $\alpha3$ (rabbit polyclonal; 2.5 μg/ml in PBS-Triton; Chemicon), $\alpha6$ (rabbit polyclonal; 2.5 μg/ml in PBS-Triton; Chemicon), and $GABA_BR1$ (guinea pig; 2.5 μg/ml in PBS-Triton; Chemicon) and R2 (guinea pig; 2.5 μg/ml in PBS-Triton; Chemicon). Double immunofluorescence was also performed as previously described (Yung et al., 1999, Ng et al., 2000, Tse et al., 2000a, Ng et al., 2001a). Immunoreactivity for parvalbumin (PV) or tyrosine hydroxylase (TH) was also revealed (PV: mouse monoclonal, 1 : 1000, Sigma, St. Louis, MO; TH: mouse polyclonal, Chemicon Internation, Temcula, CA). Secondary antibodies were used in respect to the origins of primary antibodies (goat-anti-rabbit/goat-anti-guinea pig IgG conjugated with Alexa 488 and goat-anti-mouse IgG conjugated with Alexa 562; 1 : 500 in PBS-Triton; Molecular Probes) 2 h at room temperature. The sections were then observed under the laser scan confocal microscope (LSM 510, Zeiss with an argon-krypton laser with three channels; excitation for Alexa 488: 488 nm; excitation for Alexa 562: 568 nm). Digital images of the double-labeled structures were captured and analyzed. Controls for the single and double immunofluorescence were performed by omission of primary antibodies in turn in the reaction sequences of the labeling experiments as described as in previous studies (Yung et al., 1999, Ng et al., 2000, Ng et al., 2001a).

Image analyses of immunofluorescence were performed as previously described (Lau et al., 2003). Digital images of the substantia nigra were captured under the same parameters in the confocal microscope at low (using a 10× lens) or high (using a 63× lens) magnifications respectively (magnifications of the digital images were: 76.4 pixel/μm^2 (100×); 186.4 pixel/μm^2 (630×); contrast corrections: a gamma value of 0.8 was used; pin hole size: 304 μm; no optical sectioning was performed and all micrographs were captured from a single focal plane). The fluorescent intensity of the confocal microscope images was determined using the image analysis software (Metamorph). The fluorescence intensity was expressed as average gray value as detected in the software. At low magnification, the level of immunofluorescence of at least three random views in the region of substantia nigra, i. e., all the neuropilar elements, was measured (Lau et al., 2003). In each group, at least three sections from each animal and at least 3 animals were used for measurement. At higher magnification, the fluorescent intensities of $GABA_A\alpha1$, $\alpha3$, $\alpha6$, $GABA_BR1$ and R2 immunoreactivity in the perikarya of the double-labeled neurons, i.e., PV- or TH-immunoreactive neurons, were also measured in the doublelabeled sections. The immunofluorescence in the neuropilar elements and immunonegative nuclei were excluded. The fluorescence intensities

were expressed as mean ± S.E.M. Statistical comparisons between the groups were made by ANOVA with Duncan's multiple range tests at the 5% error level ($P < 0.05$).

3. RESULTS

3.1. Differential Modulation of GABA Receptor Transcripts During Postnatal Development

During postnatal development, the level of $GABA_A\alpha1$ mRNA expression was found to be lowest in the nigral tissue. There were no significant differences in the level of expression of α1 mRNA between PND 1, PND 7 and PND 14 rats (Fig. 1). In the adult rats a significant decrease to the lowest level of $GABA_A\alpha1$ immunoreactivity was detected (Fig. 1). In contrast, there were no significant changes in the levels of α6 and β2 mRNAs found during the four postnatal stages (Fig. 1). The level of expression of β3 mRNA was low in PND 1 rats (Fig. 1).

The levels of expression were significantly higher in PND 7 and PND 14 rats (Fig. 1). The level decreased in adult rats to the level similar to that detected in PND 1 rats (Fig. 1).

3.2. Differential Modulation of GABA Receptor Proteins During Postnatal Development

When the primary antibody was omitted, no immunofluorescence was detected in the sections of the substantia nigra (data not shown). On those control sections subjected to double immunofluorescence, the two primary antibodies were omitted in turn during the

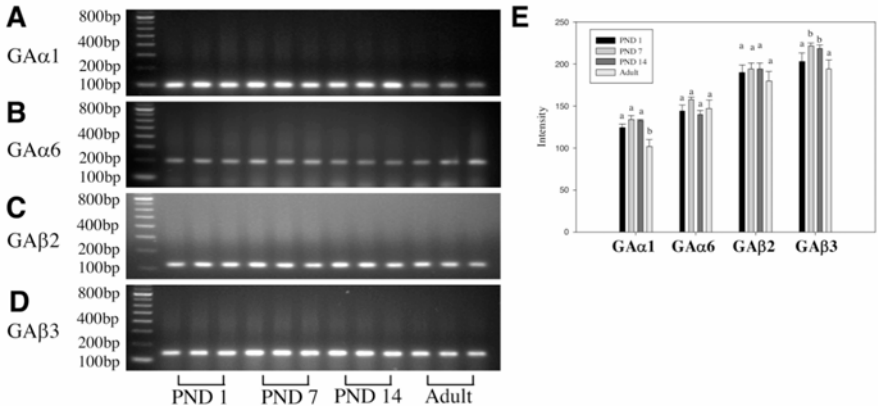

Figure 1. Reverse transcriptase-polymerase chain reaction analysis of the expression of $GABA_A$ receptor transcripts in the rat substantia nigra at four stages of postnatal development.

A–D. Developmental profiles of $GABA_A$ transcripts are shown in triplicates. They are: $GABA_A\alpha1$: 89 bp (**A**); $GABA_A\alpha6$: 168 bp (**B**); $GABA_A\beta2$: 117 bp (**C**): and $GABA_A\beta3$: 140 bp (**D**).

E. Semi-quantitative analyses of the expression of $GABA_A$ receptor subunit transcripts are shown. Bars represent the mean band intensity ± standard error of the mean. Means without the same letter are significantly different at the 5% error level ($P < 0.05$) according to analysis of variance with Duncan's multiple range tests. PND, postnatal day; GA, $GABA_A$ receptor.

Table 1. Semi-quantitative analysis of intensity of immunofluorescence in the rat substantia nigra during postnatal development.

Fluorescent intensity	PND 1 rat	PND 7 rat	PND 14 rat	Adult rat
$GABA_A\alpha1$	39.36 ± 0.92 *a*	46.57 ± 2.17 *b*	45.84 ± 2.33 *b*	39.16 ± 0.20 *a*
$GABA_A\alpha3$	38.68 ± 0.80 *a*	38.38 ± 2.11 *a*	37.34 ± 2.14 *a*	31.55 ± 1.94 *b*
$GABA_A\alpha6$	47.76 ± 1.15 *a*	58.86 ± 2.01 *b*	60.79 ± 2.75 *b*	48.51 ± 0.92 *a*
$GABA_BR1$	43.50 ± 1.90 *a*	60.37 ± 1.77 *b*	55.17 ± 1.76 *b*	44.69 ± 2.67 *a*
$GABA_BR2$	29.68 ± 0.92 *a*	35.52 ± 2.26 *b*	42.23 ± 1.10 *c*	46.27 ± 0.85 *d*

The levels of immunofluorescence were determined in the region of the substantia nigra at low magnification in the confocal microscope. Data were obtained from nine sections from three animals. Means ± S.E.M. without the same letter are significantly different at the 5% error level ($P < 0.05$) according to ANOVA with Duncan's multiple range tests. PND, postnatal day.

labeling procedures. When the first primary antibody in the reaction sequence was omitted, only the second fluorescent labeling was observed (data not shown).

Immunoreactivity for $GABA_A\alpha1$ and $\alpha6$, and $GABA_BR1$ was found to display a transient expression in their levels during postnatal development. Low levels of $\alpha1$ and $\alpha6$, and R1 immunoreactivity was found in PND 1 rat (Table 1). Peak levels of receptor proteins were observed in PND 7 and PND 14 rats (Table 1). In adult rats, the levels were then decreased again to those levels similar to PND 1 (Table 1). In contrast, level of $GABA_A\alpha3$ immunoreactivity was observed to be similar in PND 1, PND 7 and PND 14 rats (Table 1). The level was found to be significantly reduced in adults (Table 1). Unlike the $GABA_BR1$subunit, a general trend of increasing R2 immunoreactivity was detected. Lowest level was detected in PND 1 tissues and the highest level was found in the adult (Table 1).

3.3. Mature TH-positive Neurons Express Primarily $GABA_A\alpha3$, $\alpha6$ and $GABA_BR1$ and R2 Receptors

At higher magnification, TH-immunoreactive perikarya and their proximal dendrites were clearly seen (Fig. 2). In the same sections, immunoreactivity for $GABA_A\alpha1$, $\alpha3$, $\alpha6$, $GABA_BR1$ or R2 was also revealed (Fig. 2). In the TH-immunoreactive neurons, $GABA_A\alpha1$ immunoreactivity was not detected throughout the four developmental stages (Fig. 2A–D and 2A′–D′, Table 2). $GABA_A\alpha3$ immunoreactivity was only detected in more mature TH-immunoreactive neurons in PND 14 and adult rats (Fig. 2E–H, 2E′–H′, Table 2). A transient expression of $GABA_A\alpha6$ and $GABA_BR1$ immunoreactivity was again detected in TH-immunoreactive neurons. The peak levels were found in PND 7 rats ($\alpha6$: Fig. 2I–L, 2I′–L′; R1: Fig. 2M–P, M′–P′, Table 2). In contrast, no $GABA_BR2$ immunoreactivity was seen in the TH-immunoreactive neurons of young rats (Fig. Q–T, 2Q′–T′, Table 2). $GABA_BR2$ immunoreactivity was only detected in adult TH-immunoreactive neurons (Fig. Q–T, 2Q′–T′, Table 2).

3.4. Mature PV-immunoreactive Neurons Express Primarily $GABA_A\alpha1$, $\alpha3$, $\alpha6$ and $GABA_BR1$ and R2 Immunoreactivity

Parvalbumin immunoreactivity was employed in the present study as a neurochemical marker for GABAergic output neurons in the reticulata as previously described (Tse et al.,

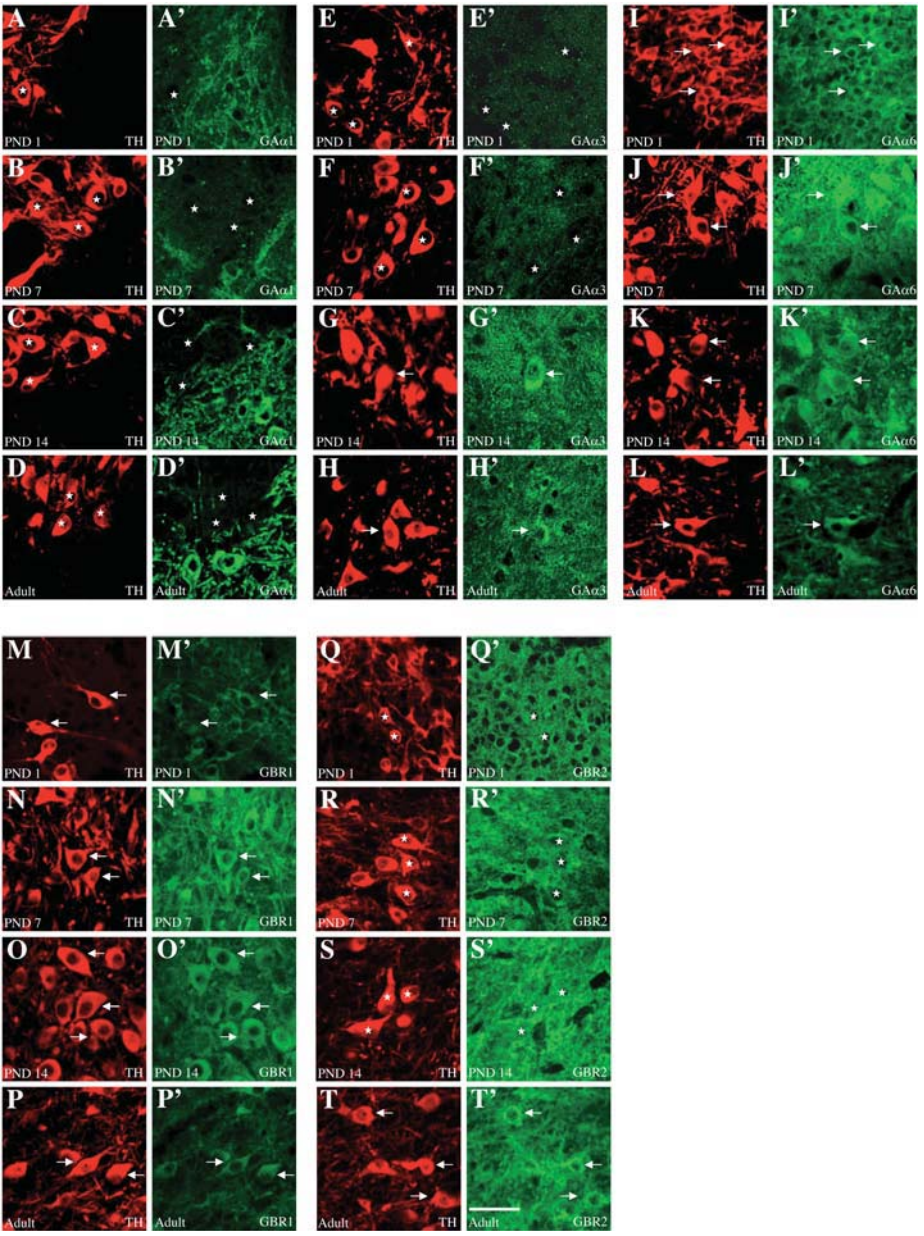
A
PND 1
TH
A'
PND 1
GAα1
E
PND 1
TH
E'
PND 1
GAα3
I
PND 1
TH
I'
PND 1
GAα6
B
PND 7
TH
B'
PND 7
GAα1
F
PND 7
TH
F'
PND 7
GAα3
J
PND 7
TH
J'
PND 7
GAα6
C
PND 14
TH
C'
PND 14
GAα1
G
PND 14
TH
G'
PND 14
GAα3
K
PND 14
TH
K'
PND 14
GAα6
D
Adult
TH
D'
Adult
GAα1
H
Adult
TH
H'
Adult
GAα3
L
Adult
TH
L'
Adult
GAα6
M
PND 1
TH
M'
PND 1
GBR1
Q
PND 1
TH
Q'
PND 1
GBR2
N
PND 7
TH
N'
PND 7
GBR1
R
PND 7
TH
R'
PND 7
GBR2
O
PND 14
TH
O'
PND 14
GBR1
S
PND 14
TH
S'
PND 14
GBR2
P
Adult
TH
P'
Adult
GBR1
T
Adult
TH
T'
Adult
GBR2

Table 2. Semi-quantitative analysis of intensity of immunofluorescence in the rat nigral neuron during postnatal development.

Fluorescence intensity	PND 1 rat	PND 7 rat	PND 14 rat	Adult rat
		TH-immunoreactive neurons		
$GABA_A\alpha1$	Undetectable	Undetectable	Undetectable	Undetectable
$GABA_A\alpha3$	Undetectable	Undetectable	35.31 ± 2.84 *a* (*n* = 38)	34.11 ± 1.23 *a* (*n* = 42)
$GABA_A\alpha6$	49.66 ± 2.44 *a* (*n* = 36)	69.23 ± 1.85 *b* (*n* = 40)	52.98 ± 1.91 *a* (*n* = 41)	44.34 ± 2.33 *c* (*n* = 43)
$GABA_BR1$	28.47 ± 1.40 *a* (*n* = 33)	51.85 ± 2.84 *b* (*n* = 36)	43.70 ± 1.98 *c* (*n* = 40)	29.51 ± 2.49 *a* (*n* = 38)
$GABA_BR2$	Undetectable	Undetectable	Undetectable	54.55 ± 1.81 *a* (*n* = 36)
		PV-immunoreactive neurons		
$GABA_A\alpha1$	Not analyzed	Not analyzed	66.39 ± 1.34 *a* (*n* = 37)	68.94 ± 0.86 *b* (*n* = 41)
$GABA_A\alpha3$	Not analyzed	Not analyzed	57.49 ± 10.66 *a* (*n* = 36)	51.82 ± 1.85 *a* (*n* = 43)
$GABA_A\alpha6$	Not analyzed	Not analyzed	62.86 ± 2.08 *a* (*n* = 40)	60.65 ± 2.19 *a* (*n* = 43)
$GABA_BR1$	Not analyzed	Not analyzed	55.94 ± 2.17 *a* (*n* = 35)	26.09 ± 3.28 *b* (*n* = 38)
$GABA_BR2$	Not analyzed	Not analyzed	53.19 ± 5.20 *a* (*n* = 30)	48.14 ± 1.75 *a* (*n* = 31)

The levels of immunofluorescence were determined in the cytoplasm of nigral neurons of the substantia nigra at high magnification in the confocal microscope. The numbers of neurons measured [n] are given in parentheses. Means ± S.E.M. without the same letter are significantly different at the 5% error level ($P < 0.05$) according to ANOVA with Duncan's multiple range tests. PND, postnatal day.

2000b). At higher magnification, PV immunoreactivity was only found in perikarya in the substantia nigra pars reticulata in rats older than PND 14. Analysis of the expression of GABA receptor immunoreactivity in PV-immunoreactive neurons in young rats was not possible. Unlike TH-immunoreactive neurons, PV-immunoreactive neurons in the substantia

Figure 2. Fluorescent photomicrographs of the rat substantia nigra from four development stages immunostained to reveal immunoreactivity for $GABA_A$ (GA) and $GABA_B$ (GB) subunits. Immunoreactivity for tyrosine hydroxylase (TH) is also revealed in the same section. **A–D and A′–D′**: Less $GABA_A\alpha1$ immunoreactivity (indicated by stars) is observed in the TH-immunoreactive perikarya (also indicated by stars) in the substantia nigra during postnatal development. **E–H and E′–H′**: In young rats (PND 7 and 14), less $GABA_A\alpha3$ immunoreactivity is found in TH-positive neurons (indicated by stars). In older rats, more intense α3 immunoreactivity is observed in TH-positive neurons (indicated by arrows). **I–L and I′–L′**: Moderate levels of $GABA_A\alpha6$ immunoreactivity (indicated by stars) is observed in the TH-immunoreactive perikarya in rats at PND 1. The highest level is detected in rats in PND 7. The level is reduced in rats at PND 14. More reduction is seen in adult rats. **M–P and M′–P′**: Low level of $GABA_BR1$ immunoreactivity is observed in TH-positive neurons (indicated by arrows) in rats at PND 1. The highest level of immunoreactivity for R1 is detected in rats at PND 7. The level is reduced in rats at PND 14. The level is reduced in adult rats. **S–T and S′–T′**: In young rats, low levels of $GABA_BR2$ immunoreactivity is found in the perikarya of TH-positive neurons (indicated by stars) in rats at PND 1. The level is found to increase in later stages of development. In adult rats, R2 immunoreactivity is clearly seen in TH-positive perikarya (indicated by arrows). Scale bar: 20 μm (in T, for all micrographs); PND, postnatal day.

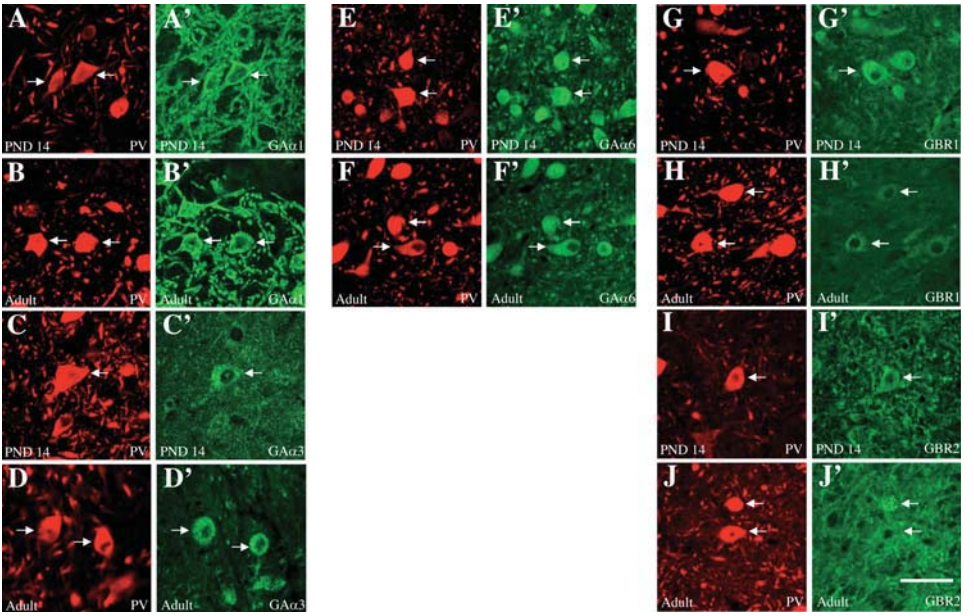

Figure 3. Fluorescent photomicrographs of the rat substantia nigra from four development stages immunostained to reveal immunoreactivity for $GABA_A$ (GA) and $GABA_B$ (GB) subunits. Immunoreactivity for parvalbumin (PV) is also revealed in the same sections. **A–B and A′–B′**: Intense level of $GABA_A\alpha1$ immunoreactivity (indicated by arrows) is observed in the PV-immunoreactive perikarya (indicated by arrows) in the substantia nigra in rats of PND 14 and adulthood. **C–D and C′–D′**: In older rats (PND 14 and adults) strong $GABA_A\alpha3$ immunoreactivity is found in PV-positive neurons (indicated by stars). **E–F and E′–F′**: Intense level of $GABA_A\alpha6$ immunoreactivity is also found in PV-positive neurons (indicated by stars). **G–H and G′–H′**: Intense level of $GABA_BR1$ immunoreactivity is observed in PV-positive (indicated by arrows) in rats at PND 14. In adult rats the level is reduced. **I–J and I′–J′**: Similar levels of $GABA_BR2$ immunoreactivity is found in the perikarya of PV-positive neurons (indicated by stars) in rats at PND 14 and adults. Scale bar: 20 μm (In J, for all micrographs); PND, postnatal day.

nigra pars reticulata displayed high levels of $GABA_A\alpha1$ immunoreactivity (Fig. 3A–B, 3A′–B′, Table 2). Adult PV-immunoreactive neurons expressed the peak level of α1 immunoreactivity. In contrast, similar levels of $GABA_A\alpha3$ (Fig. 3C–D, 3C′–D′, Table 2) and α6 (Fig. 3E–F, 3E′–F′, Table 2), and $GABA_BR2$ (Fig. 3I–J, 3I′–J′, Table 2) immunoreactivity were detected in the PV-immunoreactive neurons. Similar to TH-immunoreactive neurons, a transient level of $GABA_BR1$ immunoreactivity was found and the R1 level was significantly reduced in adult PV-immunoreactive neurons (Fig. 3G–H, 3G′–H′, Table 2).

4. DISCUSSION

Results of the present study provide comprehensive information about the patterns of expression of GABA receptor subunit mRNAs and proteins in the rat substantia nigra during postnatal expression. In addition, postnatal changes in GABA subunit expression in two subpopulations of nigral neurons, namely the TH-positive dopaminergic neuron and PV-positive reticulata neurons (Ng et al., 2000, Tse et al., 2000b), are first reported in the present study.

4.1. GABA Receptors are Differentially Expressed During Postnatal Development of the Substantia Nigra

In the present study, the image analysis that was conducted using low magnification micrographs mainly indicate the receptor immunoreactivity expression in all the cellular components as a whole, i.e., includes both glial and neuronal components. These results may be more compatible to those results that are obtained by RT-PCR method.

During postnatal development, there are differential patterns of expression of the $GABA_A$ subunit transcripts in the substantia nigra. The patterns can be divided into two major trends: 1) a transient expression of the mRNA at birth and decline to lower levels in adult expression in adult ($GABA_A\alpha1$ and $\beta3$); 2) a constant expression of mRNA during these postnatal periods ($\alpha6$ and $\beta2$). These findings indicate that it is likely that robust expressions of major $GABA_A$ transcripts are found shortly after birth. During postnatal development, levels of $GABA_A\alpha1$ and $\beta3$ transcripts reduce during maturation but $\alpha6$ and $\beta2$ transcripts remain stable until later stage of life.

In the whole region of the substantia nigra, the patterns of GABA receptor immunoreactivity expression can also be divided into three major trends: namely, 1) a transient expression in which the peak level is detected at PND 7 or 14 ($GABA_A\alpha1$, $\alpha6$ and $GABA_BR1$); 2) a stable level of expression is found in young rats but the level is reduced in adult ($GABA_A\alpha3$); 3) a progressive increase is found during development ($GABA_BR2$). These results indicate that co-expression of $GABA_A\alpha1$, $\alpha3$ and $\alpha6$ is found in the substantia nigra.

It is well known that the levels of receptor transcripts cannot fully reflect the levels of receptor proteins in neurons, e.g., the pattern of $GABA_A\alpha1$ but not $\alpha6$ immunoreactivity expression found in the present study is consistent to those of transcript expression. These results indicate that there may be post-transcriptional mechanisms that affect the levels of receptor protein in neurons during the maturation of GABA system in the substantia nigra. A previous *in vitro* study has report that there is a 30% decrease of $GABA_A\alpha1$ mRNA in cultured neurons after exposure to GABA (Lyons et al., 2000). The reduction of $\alpha1$ transcript found in the present results may therefore be related to the maturation and synaptogenesis of GABA synapses in the nigra. However, a transient expression of $\alpha1$ protein is found in the nigral region and, only the PV-immunoreactive reticulata neurons are found to express $\alpha1$ subunit. These results again indicate that there are mismatches between transcript levels and protein levels.

The $GABA_BR1$ subunit is expressed transiently in the nigral region. The R2 subunit is found to increase expression during postnatal development. The present results also indicate that although regional overlapping is found, R1 and R2 proteins are in fact differentially expressed by the two subpopulations of nigral neurons (discussed below). A recent study (Fritschy et al., 2004) indicates that an adult-like co-assembly of R1 and R2 is only observed in the rat brain not until the 3rd postnatal week, which is consistent to the present observations in the nigra.

4.2. Subpopulations of Nigral Neurons Display Different GABA Receptor Compositions During Development

Among the $GABA_A\alpha$ subunits studies, dopaminergic neurons in young rats (PND 1 and 7) are found to display high level of $\alpha6$ immunoreactivity only. Interestingly, immunoreactivity for $GABA_A\alpha3$ subunits is only found in dopaminergic neurons after PND 14. Less $GABA_A\alpha1$ subunit is observed in dopaminergic neurons from young to adult stages.

Previous studies has reported that the dopaminergic neurons in the compacta express strong immunoreactivity for $GABA_A\alpha3$, $\alpha2$ (Fritschy et al., 1995) but not $\alpha1$ (Fritschy et al., 1995, Ng et al., 2000, Waldvogel et al., 2004), and $\gamma2$ (Fritschy et al., 1995) subunits in the adult stage. The present results thus extend this previous observation that there is in fact a transient changes in expression of α subunits in dopaminergic neurons. During maturation, the $\alpha3$ subunit is not the dominant α subunit expressed by the dopaminergic neurons despite it is observed in the adult dopaminergic neurons. The functional implications of this transient changes in expression of α subunits await further investigation.

In contrast to $GABA_A$ receptor subunits, the present results indicate that at young postnatal stages, dopaminergic neurons display a high level of $GABA_BR1$ immunoreactivity. No $GABA_BR2$ immunoreactivity is detected initially. However, in adult dopaminergic neurons, a lower level of $GABA_BR1$ immunoreactivity but a higher level of $GABA_BR2$ immunoreactivity is detected, as indicated by our previous study (Ng et al., 2001b). In a recent study, similar trends of R1 and R2 subunit expressions are also seen in the nigral region, although no detailed analysis has been made by the authors in the nigral region (Fritschy et al., 2004). The present results thus indicate that functional $GABA_B$ receptors are only assembled in the dopaminergic neurons in more mature stage of life. Previous physiological studies have indicated that there are robust $GABA_B$ mediated postsynaptic responses found in dopaminergic neurons in older and mature rats (Hausser et al., 1994, Rick et al., 1994, Chan et al., 1998, Tepper et al., 1998, Chan et al., 1999, Paladini et al., 1999a, Paladini et al., 1999b). Little is known about the $GABA_B$ receptor physiology during postnatal development. The present findings thus indicate that the expression of R2 subunit, this enable to assemble a functional $GABA_B$ receptor, is a crucial step to tie up with the maturation of GABA neurotransmission in the dopaminergic neurons.

The present results are also consistent with a previous study (Schlosser et al., 1999), which has demonstrated that no PV-immunoreactive perikarya can be found in the substantia nigra pars reticulata before PND 14. It is therefore impossible to analyze the GABA receptor compositions in the context of the PV-immunoreactive neurons in young rats. Unlike the dopaminergic neurons, all three $GABA_A$ α subunits studied, i.e., $\alpha1$, $\alpha3$ and $\alpha6$, are found to be expressed by PV-positive neurons in older rats. It is likely that there are heterogeneous $GABA_A$ channels in the reticulata neurons during neuronal maturation. The $GABA_A$ channels that are composed of $\alpha3$ and $\alpha6$ subunits are in dominant and relatively fewer $GABA_A$ channels are suggested to contain the $\alpha1$ subunit.

In addition, high level of $GABA_BR1$ and $GABA_BR2$ immunoreactivity is also found in PV-immunoreactive reticulata neurons. The level of $GABA_BR1$ receptor decreases in adult whereas the level of $GABA_BR2$ receptor remains unchanged. These patterns are not similar to those found in dopaminergic neurons (see above). The present studies show that PV-immunoreactive reticulata neuron during maturation express fully functional $GABA_B$ receptors during the postnatal period.

Interestingly, $GABA_B$ receptors and subunit compositions of $GABA_A$ in reticulata neurons are suggested to be related to the control of seizures in young animals (Sperber et al., 1989, Veliskova et al., 1996, Veliskova et al., 2004). In young rat pups, activation of $GABA_B$ receptors by baclofen is found to be protective against seizures (Sperber et al., 1989, Veliskova et al., 1994). The present results thus provide anatomical evidence of the expression of functional $GABA_B$ receptors in young pups and provide support for a role of functional $GABA_B$ receptors in young animals.

In conclusion, our present results demonstrate that there are differential and distinct patterns of expression of GABA receptor subunits in neuronal subpopulations in the region

of the substantia nigra during the course of postnatal development. The specific patterns of GABA receptor expressions are implicated in the maturation and development process in the system.

5. ACKNOWLEDGEMENTS

The present work was supported by HKBU2053/00M, HKBU2148/04M and CUHK4175/02M, Research Grants Council, Hong Kong, and FRG/01-02/II-15, Faculty Research Grant, Hong Kong Baptist University. W.K. Lau was supported by a postgraduate studentship funded by HKBU2053/00M and FRG/01-02/II-15. The authors would like to thank Miss L.Y. Man for technical assistance.

6. REFERENCES

Bowery, N.G., 1993, $GABA_B$ receptor pharmacology, *Annu. Rev. Pharmacol. Toxicol.* **33**:109–147.

Chan, P.K., Leung, C.K., and Yung, W.H., 1998, Differential expression of pre- and postsynaptic $GABA_B$ receptors in rat substantia nigra pars reticulata neurones, *Eur. J. Pharmacol.* **349**:187–197.

Chan, P.K., and Yung, W.H., 1999, Inhibitory postsynaptic currents of rat substantia nigra pars reticulata neurons: role of GABA receptors and GABA uptake, *Brain Res.* **838**:18–26.

Fritschy, J.M., and Mohler, H., 1995, $GABA_A$ receptor heterogeneity in the adult rat brain: differential regional and cellular distribution of seven major subunits, *J. Comp. Neurol.* **359**:154–194.

Fritschy, J.M., Sidler, C., Parpan, F., Gassmann, M., Kaupmann, K., Bettler, B., and Benke, D., 2004, Independent maturation of the $GABA_B$ receptor subunits $GABA_B1$ and $GABA_B2$ during postnatal development in rodent brain, *J. Comp. Neurol.* **477**:235–252.

Fujiyama, F., Stephenson, F.A., and Bolam, J.P., 2002, Synaptic localization of $GABA_A$ receptor subunits in the substantia nigra of the rat: effects of quinolinic acid lesions of the striatum, *Eur. J. Neurosci.* **15**:1961–1975.

Gerfen, C.R., and Wilson, C.J., 1996, *The basal ganglia*, in: *Handbook of chemical neuroanatomy Vol. 12, Integrated systems of the CNS, Part 3*, L.W. Swanson, A. Bjoklund, and T. Hofelt ed., Elsevier, Amsterdam., pp. 371–468.

Hausser, M.A., and Yung, W.H., 1994, Inhibitory synaptic potentials in guinea-pig substantia nigra dopamine neurones in vitro, *J. Physiol. (Lond.)* **479 (Pt 3)**:401–422.

Lai, S.K., Wong, C.K.C., Yang, M.S., and Yung, K.K.L., 2000, Changes in expression of N-methyl-D-aspartate receptor subunits in the rat neostriatum after a single dose of antisense oligonucleotide specific for N-methyl-D-aspartate receptor one subunit, *Neuroscience* **98**:493–500.

Lau, W.K., Lui, P.W., Wong, C.K.C., Chan, Y.S., and Yung, K.K.L., 2003, Differential expression of N-methyl-D-aspartate receptor subunit messenger ribonucleic acids and immunoreactivity in the rat neostriatum during postnatal development, *Neurochem. Int.* **43**:47–65.

Liu, Z.F., and Burt, D.R., 1998, A synthetic standard for competitive RT-PCR quantitation of 13 GABA receptor type A subunit mRNAs in rats and mice, *J. Neurosci. Methods.* **85**:89–98.

Lyons, H.R., Gibbs, T.T., and Farb, D.H., 2000, Turnover and down-regulation of GABA(A) receptor alpha1, beta2S, and gamma1 subunit mRNAs by neurons in culture, *J. Neurochem.* **74**:1041–1048.

Marshall, F.H., Jones, K.A., Kaupmann, K., and Bettler, B., 1999, $GABA_B$ receptors – the first 7TM heterodimers, *Trends Pharmacol. Sci.* **20**:396–399.

Mohler, H., Fritschy, J.M., Luscher, B., Rudolph, U., Benson, J., and Benke, D., 1996, The $GABA_A$ receptors. From subunits to diverse functions, *Ion. Channels.* **4**:89–113.

Ng, T.K.Y., and Yung, K.K.L., 2000, Distinct cellular distribution of GABABR1 and $GABA_A\alpha1$ receptor immunoreactivity in the rat substantia nigra, *Neuroscience* **99**:65–76.

Ng, T.K.Y., and Yung, K.K.L., 2001a, Differential expression of $GABA_BR1$ and $GABA_BR2$ receptor immunoreactivity in neurochemically identified neurons of the rat neostriatum, *J. Comp. Neurol.* **433**:458–470.

Ng, T.K.Y., and Yung, K.K.L., 2001b, Subpopulations of neurons in rat substantia nigra display $GABA_BR2$ receptor immunoreactivity, *Brain Res.* **920**:210–216.

Owens, D.F., and Kriegstein, A.R., 2002, Is there more to GABA than synaptic inhibition?, *Nat. Rev. Neurosci.* **3**:715–727.

Paladini, C.A., Celada, P., and Tepper, J.M., 1999a, Striatal, pallidal, and pars reticulata evoked inhibition of nigrostriatal dopaminergic neurons is mediated by GABA(A) receptors in vivo, *Neuroscience* **89**:799–812.

Paladini, C.A., and Tepper, J.M., 1999b, $GABA_A$ and $GABA_B$ antagonists differentially affect the firing pattern of substantia nigra dopaminergic neurons in vivo, *Synapse.* **32**:165–176.

Rick, C.E., and Lacey, M.G., 1994, Rat substantia nigra pars reticulata neurones are tonically inhibited via $GABA_A$, but not $GABA_B$, receptors in vitro, *Brain Res.* **659**:133–137.

Schlosser, B., Klausa, G., Prime, G., and Ten Bruggencate, G., 1999, Postnatal development of calretinin- and parvalbumin-positive interneurons in the rat neostriatum: an immunohistochemical study, *J. Comp. Neurol.* **405**:185–198.

Simeone, T.A., Donevan, S.D., and Rho, J.M., 2003, Molecular biology and ontogeny of gamma-aminobutyric acid (GABA) receptors in the mammalian central nervous system, *J. Child. Neurol.* **18**:39–48.

Smith, Y., Bevan, M.D., Shink, E., and Bolam, J.P., 1998, Microcircuitry of the direct and indirect pathways of the basal ganglia, *Neuroscience* **86**:353–387.

Smith, Y., Charara, A., Paquet, M., Kieval, J.Z., Pare, J.F., Hanson, J.E., Hubert, G.W., Kuwajima, M., and Levey, A.I., 2001, Ionotropic and metabotropic GABA and glutamate receptors in primate basal ganglia, *J. Chem. Neuroanat.* **22**:13–42.

Sperber, E.F., Wurpel, J.N., and Moshe, S.L., 1989, Evidence for the involvement of nigral $GABA_B$ receptors in seizures of rat pups, *Brain Res. Dev. Brain Res.* **47**:143–146.

Tepper, J.M., Paladini, C.A., and Celada, P., 1998, GABAergic control of the firing pattern of substantia nigra dopaminergic neurons, *Adv. Pharmacol.* **42**:694–699.

Tse, Y.C., and Yung, K.K.L., 2000b, Cellular expression of ionotropic glutamate receptor subunits in subpopulations of neurons in the rat substantia nigra pars reticulata, *Brain Res.* **854**:57–69.

Tse, Y.C., and Yung, K.K.L., 2000a, Cellular expression of ionotropic glutamate receptor subunits in subpopulations of neurons in the rat substantia nigra pars reticulata, *Brain Res.* **854**:57–69.

Veliskova, J., Claudio, O.I., Galanopoulou, A.S., Lado, F.A., Ravizza, T., Velisek, L., and Moshe, S.L., 2004, Seizures in the developing brain, *Epilepsia.* **45 Suppl 8**:6–12.

Veliskova, J., Garant, D.S., Xu, S.G., and Moshe, S.L., 1994, Further evidence of involvement of substantia nigra $GABA_B$ receptors in seizure suppression in developing rats, *Brain Res. Dev. Brain Res.* **79**:297–300.

Veliskova, J., Velisek, L., Nunes, M.L., and Moshe, S.L., 1996, Developmental regulation of regional functionality of substantial nigra $GABA_A$ receptors involved in seizures, *Eur. J. Pharmacol.* **309**:167–173.

Waldvogel, H.J., Billinton, A., White, J.H., Emson, P.C., and Faull, R.L., 2004, Comparative cellular distribution of $GABA_A$ and $GABA_B$ receptors in the human basal ganglia: immunohistochemical colocalization of the alpha 1 subunit of the $GABA_A$ receptor, and the $GABA_B$R1 and $GABA_B$R2 receptor subunits, *J. Comp. Neurol.* **470**:339–356.

Yung, K.K.L., Ng, T.K.Y., and Wong, C.K.C., 1999, Subpopulations of neurons in the rat neostriatum display $GABA_B$R1 receptor immunoreactivity, *Brain Res.* **830**:345–352.

Section IV

DISORDERS OF BASAL GANGLIA FUNCTION I: STUDIES IN ANIMAL MODELS

HIGH FREQUENCY STIMULATION OF THE SUBTHALAMIC NUCLEUS

Electrophysiological and neurochemical aspects

Nicolas Maurice, Jean-Michel Deniau, Bertrand Degos, François Windels, Carole Carcenac, Annie Poupard, and Marc Savasta*

1. INTRODUCTION

The subthalamic nucleus (STN), a major component of the basal ganglia, plays a critical role in the control of movement. It receives direct inputs from the motor, premotor and prefrontal areas of the cerebral cortex and indirect inputs from the entire cortical mantle trough the striatum and the external segment of the globus pallidus (GP). Via its glutamatergic projections, the STN provides a major excitatory drive onto the GABAergic neurons of the substantia nigra pars reticulata (SNR) and the internal segment of globus pallidus (GPi), the basal ganglia output nuclei (Albin et al., 1989; Alexander and Crutcher, 1990). Through this effect, the STN is thought to participate in the scaling of movement and the selection of appropriate motor commands (Mink and Thach, 1993).

In the last decade, STN high frequency stimulation (STN HFS) has become an increasingly used method to treat successfully the parkinsonian motor syndrome. According to the classic patho-physiological model of Parkinson's disease (Albin et al., 1989; DeLong, 1990), the loss of striatal dopamine would induce a bias in the excitability of the two subpopulations of striatal projection neurons from which originate the direct and indirect striato-nigral pathways. This would lead to an over-activity of the STN neurons which, transmitted to the basal ganglia output nuclei, would reinforce the inhibitory influence that they exert on pre-motor networks in thalamus and brainstem (Chevalier and Deniau, 1990). Because HFS of a deep brain structure usually produces an effect similar to a lesion (Benazzouz et al., 1995), the pathophysiological model of Parkinson's disease (PD) suggested the

* N Maurice, B Degos and JM Deniau, Institut National de la Santé et de la Recherche Médicale U.667, Dynamique et Physiopathologie des Réseaux Neuronaux, Collège de France, 11 place Marcelin Berthelot 75231 Paris Cedex 05, France. F Windels, C Carcenac, A Poupard and M Savasta Institut National de la Santé et de la Recherche Médicale U.704, Dynamique des Réseaux Neuronaux, Université Joseph Fourrier, BP-53, 2280 rue de la Piscine, 38041 Grenoble Cedex 09, France.

STN HFS as a neurosurgical treatment of PD. Despite the remarkable efficacy of STN HFS, the neurobiological mechanism by which it exerts its beneficial effect on the parkinsonian motor syndrome is still under debate. *In vitro* studies have shown that STN HFS may silence STN neurons activity via a mechanism of depolarization block (Beurrier et al., 2001; Magarinos-Ascone et al., 2002). However, *in vivo* studies have suggested that HFS may also recruit fiber systems at the level of the STN (Dostrovsky and Lozano, 2002; Vitek, 2002; McIntyre et al., 2004). Functionally, it has been proposed that HFS could act by reshaping the abnormal activity of basal ganglia output nuclei responsible of the motor impairments (Garcia et al., 2003; Bar-Gad et al., 2004).

The present chapter summarizes the studies performed in our laboratories using electrophysiological and neurochemical approaches that gave insights on the mechanisms underlying the beneficial effects of STN HFS. Altogether, our data indicate that STN HFS restores the functionality of basal ganglia system by inhibiting signal transmission through the STN and by inducing remote synaptic events in the basal ganglia circuitry due to the recruitment of excitatory and inhibitory fiber systems.

2. IMPACT OF STN HFS ON THE ELECTROPHYSIOLOGICAL ACTIVITY OF THE SUBSTANTIA NIGRA PARS RETICULATA

The mechanisms by which STN HFS restores the functionality of basal ganglia system was addressed *in vivo* by analyzing the impact of STN HFS on the electrophysiological activity of the basal ganglia output neurons in rats with intact or interrupted dopaminergic (DA) transmission. DA transmission interruption was obtained by a systemic injection of antagonists of both D_1 and D_2 DA receptors at a dose inducing a robust catalepsy in awake rats. This pharmacological approach allowed us to compare in the same SNR cells the changes in activity induced by neuroleptics and the impact of STN HFS on these alterations. Furthermore, STN HFS was applied at parameters that reverse the neuroleptic-induced catalepsy in order to correlate the functional restoration induced by STN HFS with the changes observed in the activity of basal ganglia output nuclei.

2.1. STN HFS Induces a Restoration of SNR Activity

Following interruption of DA transmission by a systemic injection of neuroleptics (SCH-23390, 0.5 $mg \cdot kg^{-1}$; Raclopride, 2 $mg \cdot kg^{-1}$), the firing pattern of SNR cells was dramatically altered. Although the mean firing rate of SNR cells was not significantly modified, they switched from a tonic and regular activity with single spikes to an irregular firing composed of high frequency bursts of spikes and/or pauses (Table 1; Fig. 1). These data support the idea that the akinesia induced by an interruption of DA transmission more likely results from the alteration in the spatio-temporal organization of the discharge pattern of basal ganglia output structures rather than from their overactivity.

Following neuroleptic injection, the transfer of cortical signal to the SNR was also altered (Fig. 1B). The inhibitory component of the response evoked in SNR cells by cortical stimulation, which is due to the activation of the direct striato-nigral pathway, was reduced, whereas the late excitatory component, which results from the activation of the indirect trans-striatal pathway, was potentiated. These changes are in agreement with the prediction from the classical pathophysiological model of Parkinson's disease (PD) that the loss of striatal DA should induce an hypoactivity of the direct striato-nigral pathway and an

Table 1. Effects of neuroleptics and impact of STN HFS on the characteristics of discharge of SNR cells.

	Control	Neuroleptics	STN HFS
Rate of discharge (Hz)	28.6 ± 4.6	28.7 ± 5.3	41.9 ± 8.6*
% of spikes occurring during bursts	9.6 ± 4.5	37.2 ± 7.3*[(a)]	21.8 ± 9.1*[(a)]#
Bursts per minute	13.8 ± 6.5	46.7 ± 7.6*[(b)]	26.0 ± 8.3
Mean duration of the 4 longest pauses (ms)	141.8 ± 22.7	330.9 ± 107.2*[(c)]	157.5 ± 53.4

Each cell (N = 9) was recorded in the three conditions: control, under neuroleptics and during STN HFS applied under neuroleptics. *: the value is statistically different from the control value; #: this value is also statistically different from the value measured following the neuroleptics injection (P = 0.008, Paired t-test). (a): One way RM ANOVA (P ≤ 0.001) followed by a multiple comparison versus control group [Holm Sidak method; P < 0.025 (neuroleptics) and P < 0.05 (STN HFS)]. (b, c): Friedman RM ANOVA on Ranks (P ≤ 0.001) followed by a multiple comparison versus control group Dunn's method; P < 0.05

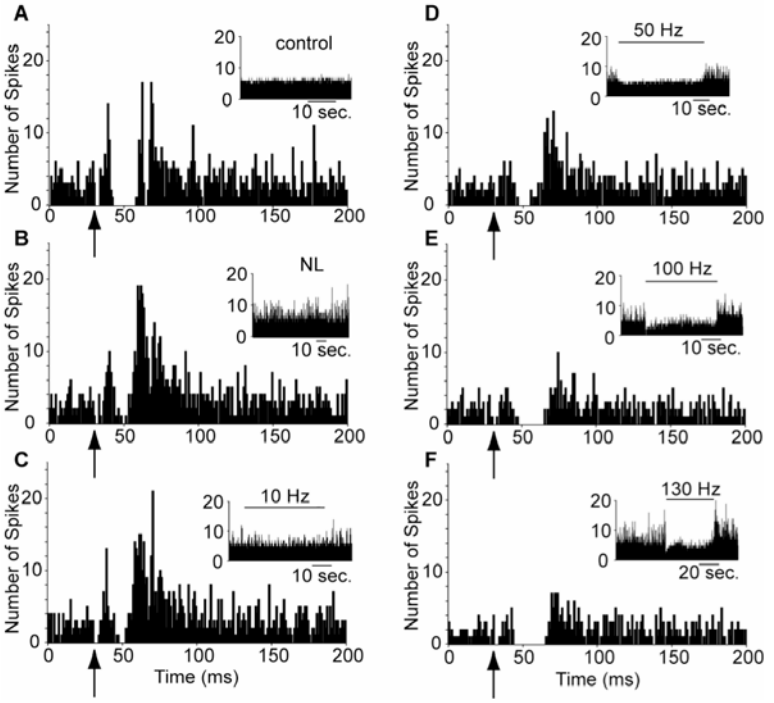

Figure 1. Effect of neuroleptics (NL) and STN HFS on the spontaneous and cortically evoked discharges of a SNR cell. *A*, classical excitatory-inhibitory-excitatory sequence evoked by orofacial sensorimotor cortex stimulation in control conditions; *B*, Following NL injection, the spontaneous SNR discharge was irregular, the inhibitory component of the cortically evoked response presented a marked reduction and the late excitatory component was increased; *C–F*, Increasing the frequency of STN stimulation (2.0 V) produced an increasing inhibition of the cell activity (*Insets*), the inhibitory component of the cortically evoked response was restored and the excitatory components were decreased. *Arrows.* indicate the time of stimulation. Horizontal bars in *Insets.* indicate STN HFS with the corresponding frequency.

hyperactivity of the indirect striato-nigral pathway. To our knowledge, our observation provides the first direct electrophysiological evidence of such an imbalance.

Remarkably, the spontaneous and cortically evoked SNR activities were regularized during STN HFS (Fig. 1). The proportion of SNR cells exhibiting bursting activity and the percentage of spikes contributing to bursts were significantly decreased by the STN stimulation. Moreover, the neuroleptic-induced bias between the direct cortico-striatonigral and the indirect cortico-striato-pallido-subthalamo-nigral circuits was counterbalanced. Through these effects it is expected that STN HFS restores the spatiotemporal shaping of basal ganglia outflow (Kolomiets et al., 2003) which is expected to encode motor commands.

As will be detailed below, the mechanisms contributing to the regularization of spontaneous and cortically evoked SNR cells discharge involve local effects within the STN and remote processes engaged by recruitment of fibers.

2.2. STN HFS Inhibits the Transfer of Cortical Signals Through the STN

Cortical stimulation induces a complex sequence of synaptic events in SNR cells, composed of an inhibition preceded or not by an early excitation and followed or not by a late excitation (Maurice et al., 1999; Kolomiets et al., 2003). The inhibition is due to the activation of the direct striato-nigral pathway whereas the early and late excitations result from the activation of the trans-STN circuits (Maurice et al., 1999). As observed in the control situation (intact DA transmission), STN HFS abolishes the trans-STN excitatory components of the cortically evoked responses. This effect likely results from a functional blockade of signal transmission at the level of the STN since it depends on the intensity of stimulation applied in the STN and is equally observed in SNR cells excited as well as inhibited during STN HFS. This functional blockade certainly contributes to counterbalance the neuroleptic-induced bias in the direct and indirect striato-nigral pathway by reducing the impact of the indirect excitatory striato-nigral pathway. In addition, such a blockade is expected to regularize the SNR spontaneous activity by preventing the propagation of low frequency oscillatory activities through the corticosubthalamo-nigral circuit (Magill et al., 2001). As indicated by *in vitro* and *in vivo* recordings, the functional blockade of the trans-STN circuits may involve several mechanisms including 1- a decreased excitability of STN cells resulting from the activation of the GABAergic pallido-subthalamic fibers; 2- a depolarization block of STN cells; 3- an interruption of signal propagation in STN afferent pathways by a barrage of antidromic spikes generated by the HFS.

2.3. STN HFS Evokes Synaptic Events in SNR Cells Through Fiber Systems Activation

Extracellular electrical stimulation preferentially activates fibers rather than cell bodies. An electrical stimulation may also activate axons while pushing the corresponding cell bodies into a depolarization block (Nowak and Bullier, 1998a, b; McIntyre et al., 2004). Since large axons are more easily activated by electrical current than thinner ones (Ranck, 1975), it is expected that HFS recruits different fiber systems depending of the intensity of stimulation. Accordingly, our data indicate that STN HFS exerts excitatory and

inhibitory synaptic influences on basal ganglia output neurons by recruiting excitatory and inhibitory fibers. In addition, direct evidence of fiber activation induced by STN HFS comes from our observation that STN stimulation evokes antidromic spikes in SNR cells that reliably follow HFS.

The excitation induced by STN HFS likely results from the activation of the glutamatergic subthalamo-nigral pathway. Indeed, the latencies of excitatory responses evoked in nigral cells by single pulse or high frequency STN stimulation were similar to the conduction time of the subthalamo-nigral pathway (Deniau et al., 1978; Kitai and Deniau, 1981). In addition, it has been shown that excitatory responses evoked in SNR by STN stimulation with current intensity <300 μA result from specific activation of the subthalamo-nigral fibers (Hammond et al., 1978).

The inhibition evoked by STN HFS results from the activation of GABA transmission in the SNR since this inhibition was suppressed by iontophoretic application of bicuculline, an antagonist of $GABA_A$ receptors. Thus, the decreased activity of SNR cells induced by STN HFS is not solely due to a functional inhibition of the STN. Different fibers system may account for this GABAergic transmission: (1) The main inhibitory input to the SNR originates from the striatum. However, activation of striato-nigral fibers by spread of current from the STN is unlikely. Indeed, if these fibers were activated, a continuous barrage of antidromic spikes would be generated along the striato-nigral fibers preventing orthodromic volleys from reaching the SNR. As shown by our results, the inhibitory component of the response evoked in SNR cells by cortical stimulation, which is due to the activation of the striato-nigral pathway, was preserved during STN HFS. (2) Another source of inhibition could result from the activation of the intranigral axon collateral network of GABAergic SNR cells, through an axonal reflex (Deniau et al., 1982; Mailly et al., 2003). Several observations favor this hypothesis: – STN stimulation generates antidromic activation of SNR cells (Maurice et al., 2003); – antidromic activation of SNR cells induces, through a local axonal reflex, inhibitory postsynaptic potentials (IPSPs) in SNR cells that follow frequency stimulations at 150–200 Hz (Deniau et al., 1982) and finally – the short duration of these IPSPs is consistent with the phasic inhibitory response observed in nigral cells after STN stimulation at 1 Hz. (3) Finally, the inhibition of nigral cells induced by STN stimulation could also result from the activation of pallido-nigral fibers through an axonal reflex since GABAergic pallido-subthalamic neurons send an axon collateral to the SNR (Kita and Kitai, 1994). Evidence for this hypothesis comes from the neurochemical study detailed in the second part of this chapter.

The combination of excitatory and inhibitory synaptic events as well as antidromic activations that STN HFS exerts on basal ganglia output neurons is expected to provide major contribution to the reshaping of the spatio-temporal structure of neuronal discharge in the basal ganglia output nuclei. Accordingly, a restorative effect was observed in SNR cells that were inhibited as well as excited by STN HFS. Interestingly, when considering the overall population of recorded cells in SNR, the net effect of STN HFS (at an intensity alleviating the neuroleptic-induced catalepsy) was an increase in the mean discharge rate of neuronal population. This observation is in agreement with data from MPTP treated monkeys where the clinical improvements produced by STN HFS correlated with an increased activity in the pallidum (Hashimoto et al., 2003). Altogether, these results suggest that STN HFS produces its beneficial effects via a regularization of discharge pattern of basal ganglia output neurons rather than via a decrease of basal ganglia output due to a functional inhibition of the STN.

3. IMPACT OF STN HFS ON THE EXTRACELLULAR CONTENT OF GLUTAMATE AND GABA IN THE GP AND THE SNr

In this study, the mechanisms by which STN HFS restores the functionality of basal ganglia circuitry in PD were investigated using a neurochemical approach in rats. We have analyzed the effect of STN HFS (in register with the procedures used for treatment of PD) on the extracellular glutamate (Glu) and GABA in GP and SNR, two main STN targets, using *in vivo* intracerebral microdialysis in normal and DA lesioned rats. We also tested the hypothesis that passing fibers are stimulated from pallidal neurons by assessing the effects of STN HFS on Glu and GABA levels in the SNr in normal and hemiparkinsonian rats with a unilateral ibotenate lesion of the GP.

3.1. Basal Levels of Extracellular Glu and GABA in the SNr and GP are Higher in Hemiparkinsonian Rats

Lesioning the SNc with 6-OHDA dramatically increased the basal concentration of Glu in the SNr and the GP, ipsilaterally to the lesion. In the SNr of SNc-lesioned rats ($n = 5$), the mean Glu concentration was 9.5 times ($p < 0.05$) the basal levels previously reported for control intact animals (Windels et al., 2000; Savasta et al., 2002). Glu concentration in the GP ($n = 6$) was 16 times higher ($p < 0.05$) in SNc-lesioned animals than in controls. In contrast, lesioning of the GP ($n = 6$) did not result in significant changes in basal Glu concentrations in the SNr when compared to controls, and did not prevent the increase in Glu concentration induced by 6-OHDA treatment. In GP+SNc- and GP-lesioned rats, Glu concentration was respectively 2.6 and 3.4 times higher than in control. However, increase in Glu contents was significantly lower ($p < 0.05$) in GP+SNc-lesioned rats than in SNc-lesioned animals.

Many studies have shown that the loss of DA nigral neurons in animals and PD patients leads to hyperactivity of the subthalamo-pallidal, subthalamo-nigral and cortico-striatal pathways (DeLong, 1990; Hollerman and Grace, 1992; Calabresi et al., 1993; Levy et al., 2002). The large increase in Glu concentration in the SNr and GP in hemiparkinsonian rats under anesthesia is consistent with previous electrophysiological data showing that SNc-lesioning results in an increase in discharge rate and the appearance of a “bursty” pattern in STN neurons (Hassani et al., 1996). This increase in Glu concentration in the SNr, which may reflect the hyperactivity of STN neurons, cannot be due solely to the removal of pallidal inhibition, because it persists in rats with GP+SNc lesions. Similar conclusions were reached by Hassani et al. (1996), who evaluated the effects of pallidal and SNc lesions on electrophysiological activity in STN neurons. The change in SNr-Glu levels following DA denervation may be due to an effect restricted to the STN or related structures.

Interestingly, 6-OHDA-treatment also doubled the mean basal GABA concentration both in the SNr ($n = 5$) and in the GP ($n = 6$) when compared to intact animals. SNr neurons receive dense GABAergic inputs from the striatum, GP, and SNr neurons themselves, via axon collaterals playing a major role in the regulation of SNr neuron activity (Deniau et al., 1982; Celada et al., 1999). No basal GABA was detected in the SNr of rats with GP lesions, indicating that most of this GABA comes from the GP. This result is consistent with previous electrophysiological data suggesting that pallido-nigral inputs predominate (Celada et al., 1999). GP lesioning did not prevent the increase in basal GABA induced by DA denervation ($n = 6$), but the amount of increase was reduced. Thus, although part of the increase in nigral GABA may result from an increase in the activity of GP neurons

(through the increase in Glu release from STN neuron terminals), other major source of GABA, such as SNr neuron collaterals or other structures, appears to be involved.

3.2. 6-OHDA SNc Lesion Abolishes the Effects of STN HFS on SNr and GP extracellular Glu Contents but not on GABA Contents

We previously reported that STN HFS strongly increases extracellular Glu concentration in the SNr and GP (Windels et al., 2000). In contrast, in SNc-lesioned rats, STN HFS induced no change in the Glu content of both the SNr (n = 5) and the GP (n = 6), on the stimulated (ipsilateral to the SNc lesion) (Fig. 2A) or the unstimulated (contralateral) side (data not shown). Glu concentration remained stable at around baseline values throughout the microdialysis experiment. Thus, lesioning of the SNc abolished the effect of STN stimulation on Glu concentration in the output nuclei, possibly because basal Glu content had already increased considerably. The picture regarding the effect of STN HFS on GABA levels was very different. We showed previously that stimulation of the STN in intact rats increases GABA content in the SNr but not in the GP (Windels et al., 2000). In contrast to what was observed for Glu levels, STN HFS induced a significant increase in extracellular GABA concentration in 6-OHDA-treated rats, in the ipsilateral SNr, during the 1 h HFS period (fractions 8–16). As we reported in intact animals, STN HFS did not affect GABA concentration in the GP in 6-OHDA-treated rats (n = 6, Fig. 2B).

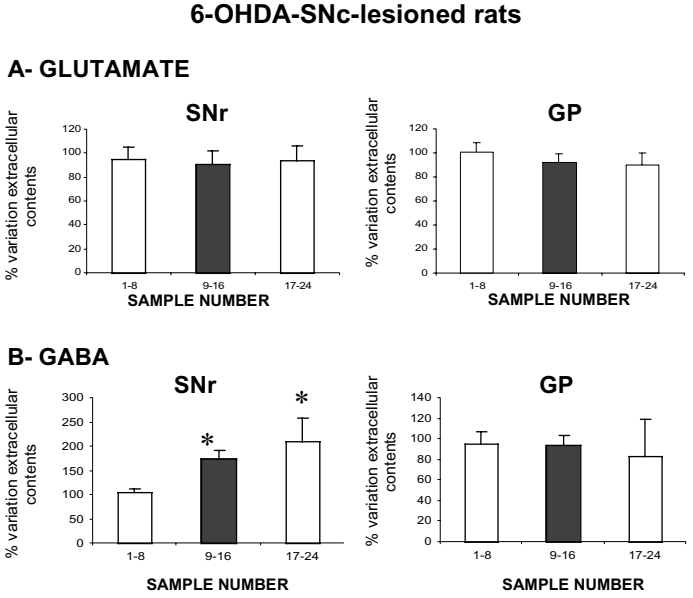

Figure 2. Extracellular glutamate (A) and GABA (B) levels determined at eight-minute intervals in the SNr and GP ipsilateral to the stimulation in 6-0HDA SNc-lesioned rats. The pre-stimulation (fractions 1–8), the stimulation (fractions 9–16) and the post-stimulation periods (fractions 17–24) gave 8 dialysates respectively. The mean ± SEM of the 8 dialysates collected before STN HFS was used as the baseline. Results are expressed as a percentage of variation of this baseline value. Each percentage represents the mean variations ± SEM calculated from six animals. Note that glutamate contents were not significantly affected by STN HFS in the SNr and GP while SNr extracellular GABA concentrations were increased by STN HFS with no significant change in GP.

As described in the introduction, STN HFS is an effective treatment for PD, but the mechanisms involved are unclear. Consistent with the hypothesis discussed above suggesting that HST STN restores the functionality of basal ganglia system by inhibiting signal transmission through the STN and by inducing remote synpatic events in the basal ganglia circuitry due to the recruitment of excitatory and inhibitory fiber systems, we previously reported that extracellular Glu and GABA contents increase in the SNr during STN HFS, thus suggesting the involvement of both excitatory and inhibitory fibers in the action of STN HFS (Windels et al., 2000). We showed here that DA denervation prevented the increase in Glu concentration in both the GP and SNr normally triggered by STN HFS in intact rats. However, an increase in extracellular GABA concentration in the ipsilateral SNr was detected and was even greater in hemiparkinsonian rats. Electrophysiological data presented above and obtained in rats with intact (Maurice et al., 2003) or pharmacologically interrupted DA transmission are in agreement with an increase in GABAergic synaptic transmission by STN HFS.

3.3. The STN HFS-induced Increase in SNr GABA Content Requires an Intact GP

We checked whether the GABA in the SNr originated from pallido-nigral GABAergic fibers, which were probably stimulated by STN HFS, by assessing variations in GABA (and Glu) concentrations in the ipsilateral SNr of GP- and GP+SNc-lesioned rats. Lesioning of the GP did not prevent the increase in Glu concentration in the SNr elicited by STN HFS as shown in Fig 3A ($n = 6$, $p < 0.05$). However the increase in Glu concentration detected here,

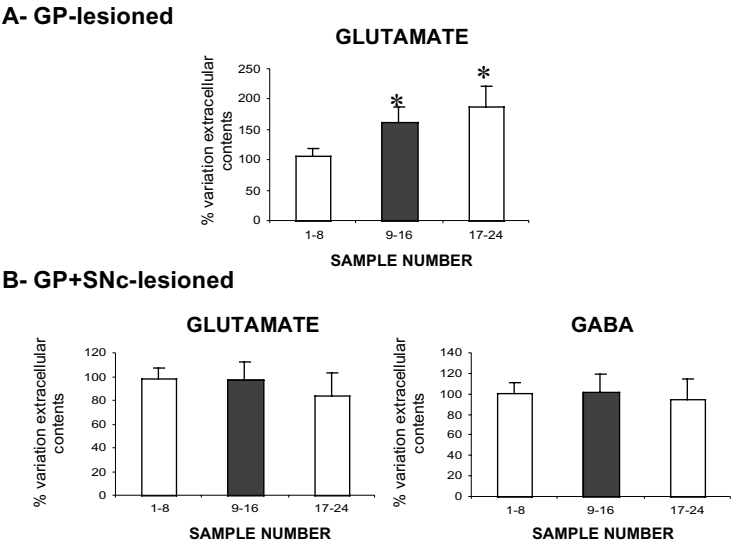

Figure 3. Extracellular Glu concentrations determined at eight-minute intervals in the SNr ipsilateral to stimulation in ibotenic acid GP-lesioned rats (A) and extracellular Glu and GABA levels determined at eight-minute intervals in SNr ipsilateral to stimulation in GP+SNc-lesioned rats (B). The pre-stimulation (fractions 1–8), the stimulation (fractions 9–16) and the post-stimulation periods (fractions 17–24) gave 8 dialysates respectively. The mean ± SEM of the 8 dialysates collected before STN HFS was used as the baseline. Results are expressed as a percentage of variation of this baseline value. Each percentage represents the mean variations ± SEM calculated from five animals. * $p < 0.05$. Note in A the increase in extracellular Glu concentration induced by STN HFS on the ipsilateral, stimulated side while in B, STN HFS did not affect extracellular Glu and GABA concentrations on the ipsilateral, stimulated side.

probably through the excitation of intact subthalamo-nigral neurons, is of lower amplitude in GP-lesioned animals than in controls. Moreover, in GP-lesioned rats, this increase was prevented by 6-OHDA-induced SNc lesions, as in rats with intact GP (n = 6, Fig. 3B).

In contrast, the increase in SNr GABA level induced by STN HFS in intact rats was not observed in GP-lesioned rat and GABA was undetectable before, during and after STN HFS. Similarly, the STN HFS-induced increase in SNr GABA concentration seen in rats with SNc lesions was abolished in rats bearing GP+SNc lesions (Fig. 3B). Therefore, the increase in GABA concentration in the SNr induced by stimulation probably involved stimulation of the GABAergic fibers originating from the GP. Thus, the stimulation of pallido-nigral neurons by STN HFS is sufficient to account for the increase in GABA release in the SNr since GP neurons send axon collaterals to the SNr (Kita and Kitai, 1994). GABAergic GP axons may be activated by synaptic stimulation of GP neurons via the activation of subthalamo-pallidal afferents or by direct stimulation of GABAergic pallido-nigral fibers (Kita and Kitai, 1994). The former possibility is unlikely because STN HFS did not increase Glu levels in the GP in hemiparkinsonian rats. It therefore seems likely that STN HFS activates GABAergic pallido-nigral fibers on their way to SNR or via an axonal reflex, accounting for the STN HFS-induced increase in GABA concentration in the SNr. The role of such a process in the clinical efficacy of STN HFS is unclear, but could at least partly account for the inhibition of SNr neuron activity in vivo by STN HFS in both intact and 6-OHDA-treated rats (Tai et al., 2003).

In conclusion, this neurochemical study indicates that STN HFS increases GABA concentration in the SNr, probably due to an activation of the pallido-nigral GABAergic pathway. This increase in GABA concentration may be actively involved in decreasing the excitatory influence of subthalamic pathways on SNr neurons. Through this action, STN HFS may interact with direct and indirect striato-nigral output circuits, by inhibiting subthalamic circuits. It will be of interest to determine to what extent this interference is involved in counteracting neuronal activity abnormalities within the basal ganglia network caused by DA degeneration in PD, and therefore the exact role of this process in the clinical effects of STN HFS restoring motor functions in parkinsonian patients.

4. ACKNOWLEDGEMENTS

This work was supported by the Institut National de la Santé et de la Recherche Médicale, Centre National de la Recherche Scientifique, the EC (Grant n° QLK6-1999-02173, Fifth Framework Programme for Research and Development), Association France Parkinson, Fondation de France (2002011943), Fondation de la Recherche Médicale and the Ministère de la Recherche et des Nouvelles Technologies (ACI Grant n° 02 2 0409).

5. REFERENCES

Albin, R.L., Young, A.B., and Penney, J.B., 1989, The functional anatomy of basal ganglia disorders, *Trends Neurosci*. **12**:366–375.

Alexander, G.E., and Crutcher, M.D., 1990, Functional architecture of basal ganglia circuits: neural substrates of parallel processing, *Trends. Neurosci*. **13**:266–271.

Bar-Gad, I., Elias, S., Vaadia, E., and Bergman, H., 2004, Complex locking rather than complete cessation of neuronal activity in the globus pallidus of a 1-methyl-4-phenyl-1,2,3,6-tetrahydropyridine-treated primate in response to pallidal microstimulation, *J. Neurosci*. **24**:7410–7419.

Benazzouz, A., Piallat, B., Pollak, P., and Benabid, A.L., 1995, Responses of substantia nigra pars reticulata and globus pallidus complex to high frequency stimulation of the subthalamic nucleus in rats: electrophysiological data, *Neurosci. Lett*. **189**:77–80.

Beurrier, C., Bioulac, B., Audin, J., and Hammond, C., 2001, High-frequency stimulation produces a transient blockade of voltage-gated currents in subthalamic neurons, *J. Neurophysiol*. **85**:1351–1356.

Calabresi, P., Mercuri, N.B., Sancesario, G., and Bernardi, G., 1993, Electrophysiology of dopamine-denervated striatal neurons. Implications for Parkinson's disease, *Brain* **116 (Pt 2)**:433–452.

Celada, P., Paladini, C.A., and Tepper, J.M., 1999, GABAergic control of rat substantia nigra dopaminergic neurons: role of globus pallidus and substantia nigra pars reticulata, *Neuroscience* **89**:813–825.

Chevalier, G., and Deniau, J.M., 1990, Disinhibition as a basic process in the expression of striatal functions, *Trends. Neurosci*. **13**:277–280.

DeLong, M.R., 1990, Primate models of movement disorders of basal ganglia origin, *Trends Neurosci*. **13**:281–285.

Deniau, J.M., Hammond, C., Chevalier, G., and Feger, J., 1978, Evidence for branched subthalamic nucleus projections to substantia nigra, entopeduncular nucleus and globus pallidus, *Neurosci. Lett*. **9**:117–121.

Deniau, J.M., Kitai, S.T., Donoghue, J.P., and Grofova, I., 1982, Neuronal interactions in the substantia nigra pars reticulata through axon collaterals of the projection neurons. An electrophysiological and morphological study, *Exp. Brain Res*. **47**:105–113.

Dostrovsky, J.O., and Lozano, A.M., 2002, Mechanisms of deep brain stimulation, *Mov. Disord*. **17 S3**:S63–68.

Garcia, L., Audin, J., D'Alessandro, G., Bioulac, B., and Hammond, C., 2003, Dual effect of high-frequency stimulation on subthalamic neuron activity, *J. Neurosci*. **23**:8743–8751.

Hammond, C., Deniau, J.M., Rizk, A., and Feger, J., 1978, Electrophysiological demonstration of an excitatory subthalamonigral pathway in the rat, *Brain Res*. **151**:235–244.

Hashimoto, T., Elder, C.M., Okun, M.S., Patrick, S.K., and Vitek, J.L., 2003, Stimulation of the subthalamic nucleus changes the firing pattern of pallidal neurons, *J. Neurosci*. **23**:1916–1923.

Hassani, O.K., Mouroux, M., and Feger, J., 1996, Increased subthalamic neuronal activity after nigral dopaminergic lesion independent of disinhibition via the globus pallidus, *Neuroscience* **72**:105–115.

Hollerman, J.R., and Grace, A.A., 1992, Subthalamic nucleus cell firing in the 6-OHDA-treated rat: basal activity and response to haloperidol, *Brain Res*. **590**:291–299.

Kita, H., and Kitai, S.T., 1994, The morphology of globus pallidus projection neurons in the rat: an intracellular staining study, *Brain Res*. **636**:308–319.

Kitai, S.T., and Deniau, J.M., 1981, Cortical inputs to the subthalamus: intracellular analysis, *Brain Res*. **214**: 411–415.

Kolomiets, B.P., Deniau, J.M., Glowinski, J., and Thierry, A.M., 2003, Basal ganglia and processing of cortical information: functional interactions between trans-striatal and trans-subthalamic circuits in the substantia nigra pars reticulata, *Neuroscience* **117**:931–938.

Levy, R., Ashby, P., Hutchison, W.D., Lang, A.E., Lozano, A.M., and Dostrovsky, J.O., 2002, Dependence of subthalamic nucleus oscillations on movement and dopamine in Parkinson's disease, *Brain* **125**: 1196–1209.

Magarinos-Ascone, C., Pazo, J.H., Macadar, O., and Buno, W., 2002, High-frequency stimulation of the subthalamic nucleus silences subthalamic neurons: a possible cellular mechanism in Parkinson's disease, *Neuroscience* **115**:1109–1117.

Magill, P.J., Bolam, J.P., and Bevan, M.D., 2001, Dopamine regulates the impact of the cerebral cortex on the subthalamic nucleus-globus pallidus network, *Neuroscience* **106**:313–330.

Mailly, P., Charpier, S., Menetrey, A., and Deniau, J.M., 2003, Three-dimensional organization of the recurrent axon collateral network of the substantia nigra pars reticulata neurons in the rat, *J. Neurosci*. **23**: 5247–5257.

Maurice, N., Deniau, J.M., Glowinski, J., and Thierry, A.M., 1999, Relationships between the prefrontal cortex and the basal ganglia in the rat: physiology of the cortico-nigral circuits, *J. Neurosci*. **19**:4674–4681.

Maurice, N., Thierry, A.M., Glowinski, J., and Deniau, J.M., 2003, Spontaneous and evoked activity of substantia nigra pars reticulata neurons during high-frequency stimulation of the subthalamic nucleus, *J. Neurosci*. **23**:9929–9936.

McIntyre, C.C., Savasta, M., Kerkerian-Le Goff, L., and Vitek, J.L., 2004, Uncovering the mechanism(s) of action of deep brain stimulation: activation, inhibition, or both, *Clin. Neurophysiol*. **115**:1239–1248.

Mink, J.W., and Thach, W.T., 1993, Basal ganglia intrinsic circuits and their role in behavior, *Curr. Opin. Neurobiol*. **3**:950–957.

Nowak, L.G., and Bullier, J., 1998a, Axons, but not cell bodies, are activated by electrical stimulation in cortical gray matter. I. Evidence from chronaxie measurements, *Exp. Brain Res*. **118**:477–488.

Nowak, L.G., and Bullier, J., 1998b, Axons, but not cell bodies, are activated by electrical stimulation in cortical gray matter. II. Evidence from selective inactivation of cell bodies and axon initial segments, *Exp. Brain Res*. **118**:489–500.

Ranck, J.B., Jr., 1975, Which elements are excited in electrical stimulation of mammalian central nervous system: a review, *Brain Res*. **98**:417–440.

Savasta, M., Windels, F., Bruet, N., Bertrand, A., and Poupard, A., 2002, Neurochemical modifications induced by high-frequency stimulation of subthalamic nucleus in rats, In: The Basal Ganglia VII (Nicholson LFB and Faull RLM, eds), Kluwer Academic, Plenum Press, New York, pp 581–590.

Tai, C.H., Boraud, T., Bezard, E., Bioulac, B., Gross, C., and Benazzouz, A., 2003, Electrophysiological and metabolic evidence that high-frequency stimulation of the subthalamic nucleus bridles neuronal activity in the subthalamic nucleus and the substantia nigra reticulata, *Faseb. J*. **17**:1820–1830.

Vitek, J.L., 2002, Mechanisms of deep brain stimulation: excitation or inhibition, *Mov. Disord*. **17 Suppl 3**: S69–72.

Windels, F., Bruet, N., Poupard, A., Urbain, N., Chouvet, G., Feuerstein, C., and Savasta, M., 2000, Effects of high frequency stimulation of subthalamic nucleus on extracellular glutamate and GABA in substantia nigra and globus pallidus in the normal rat, *Eur. J. Neurosci*. **12**:4141–4146.

DOWNREGULATION OF A METABOTROPIC GLUTAMATE RECEPTOR IN THE PARKINSONIAN BASAL GANGLIA

Masahiko Takada, Katsuyuki Kaneda, Yoshihisa Tachibana, Michiko Imanishi, Hitoshi Kita, Ryuichi Shigemoto, and Atsushi Nambu*

1. INTRODUCTION

It is well known that nigrostriatal dopamine neuron loss causes Parkinson's disease. Dopamine deficiency in the striatum generates the overactivity of glutamatergic neurons in the subthalamic nucleus (STN; Wichmann and DeLong, 1996; Blandini et al., 2000; Obeso et al., 2000). The enhanced glutamatergic neurotransmission through the subthalamopallidal projection excessively activates GABAergic neurons in the internal segment of the globus pallidus (GPi). The hyperactive pallidal neurons, in turn, suppress the activity of thalamocortical neurons that gain access to the pyramidal tract, thereby developing akinesia, among the cardinal parkinsonian symptoms.

The family of metabotropic glutamate receptors (mGluRs) has been implicated in diverse brain functions (Anwyl, 1999; Rouse et al., 2000). Based on the homology of their amino acid sequences, second messenger systems, and pharmacological characteristics, mGluRs are classified into three groups: group I (mGluR1 and mGluR5), group II (mGluR2 and mGluR3), and group III (mGluR4, mGluR6, mGluR7, and mGluR8) (Pin and Duvoisin, 1995; Conn and Pin, 1997). Accumulated anatomical evidence to date indicates that a variety of mGluRs are expressed in structures of the basal ganglia at presynaptic or postsynaptic locations (Rouse et al., 2000).

* M. Takada, K. Kaneda, M. Imanishi, Dept. of System Neuroscience, Tokyo, Metropolitan Institute for Neuroscience, Tokyo Metropolitan Organization for Medical Research, Fuchu, Tokyo 183-8526, Japan. Y. Tachibana, A. Nambu, Division of System Neurophysiology, National Institute for Physiological Sciences, Okazaki 444-8585, Japan. H. Kita, Dept of Anatomy and Neurobiology, University of Tennessee Memphis, College of Medicine, Memphis, TN 38163, USA. R. Shigemoto, Division of Cerebral Structure, National Institute for Physiological Sciences, Okazaki 444-8585, Japan.

In Parkinson's disease, expression of ionotropic glutamate receptors has been shown to be altered in the basal ganglia (Porter et al., 1994; Ulas et al., 1994; Bernard et al., 1996; Ulas and Cotman, 1996; Betarbet et al., 2000; Dunah et al., 2000). A major question that arises as a consequence of this is whether substantial changes in mGluRs expression occurs in the basal ganglia of a parkinsonian model. To address this issue, we analyzed the immunohistochemical localization of mGluRs in the basal ganglia of monkeys treated with 1-methyl-4-phenyl-1,2,3,6-tetrahydropyridine (MPTP). The results have revealed that in the parkinsonian monkeys, mGluR1α is specifically downregulated in the GPi. In an attempt to elucidate the functional role of mGluR1α in the control of pallidal neuron activity, we further examined the effects of mGluR1-related agents on the spontaneous firing rate of GPi neurons in normal awake monkeys who were later administered with MPTP.

2. CHANGES IN mGluR EXPRESSION IN BASAL GANGLIA OF MPTP-TREATED MONKEYS

The expression patterns of mGluRs in the basal ganglia were examined in normal and MPTP-treated monkeys. To this end, the following antibodies for seven mGluR subtypes were tested here: rabbit anti-mGluR1 (pan mGluR1) antibody, rabbit anti-mGluR1α antibody, mouse anti-mGluR2 antibody, rabbit anti-mGluR2/3 antibody, guinea pig anti-mGluR4a antibody, rabbit anti-mGluR5 antibody, rabbit anti-mGluR7a antibody, or guinea pig anti-mGluR8 antibody (Shigemoto et al., 1993, 1994, 1997; Ohishi et al., 1994, 1995; Kinoshita et al., 1996a,b; Neki et al., 1996).

The immunoreactivity for each subtype was different from structure to structure (Figure 1). Essentially all structures of the basal ganglia were immunostained with anti-mGluR1α antibody (see also Martin et al., 1992; Testa et al., 1998; Hanson and Smith, 1999). In particular, the GPi was enriched with dendritic profiles displaying intense mGluR1α immunoreactivity. The mGluR1α immunoreactivity was further observed strongly in the substantia nigra pars reticulata (SNr) and the substantia nigra pars compacta (SNc), and moderately in the striatum, the external segment of the globus pallidus (GPe), and STN. Likewise, mGluR5 immunoreactivity was seen in all structures of the basal ganglia, with the highest density in the striatum. On the other hand, clear and intense immunoreactivity for mGluR2 or mGluR2/3 was found almost exclusively in the striatum. With respect to mGluR7a, all basal ganglia structures except for the SNc exhibited high levels of the immunoreactivity. In the present experiments, no particular structures of the basal ganglia were intensely immunostained with anti-mGluR1 (pan mGluR1), anti-mGluR4a, or anti-mGluR8 antibodies.

Among the mGluR subtypes, mGluR1α was the only subtype of which expression pattern was changed in the basal ganglia of MPTP-treated monkeys. A significant reduction in mGluR1α immunoreactivity was observed specifically in the pallidal complex (GPi and GPe) and SNr (Figure 1). Our densitometric measurements have revealed that the mGluR1α immunoreactivity was decreased more prominently in the GPi (by 27.2%) than in the SNr (by 19.0%) and GPe (by 15.1%). No substantial changes in the expression of other subtypes of mGluRs, including mGluR5 (another group I mGluR), were detected in the basal ganglia of MPTP-treated monkeys.

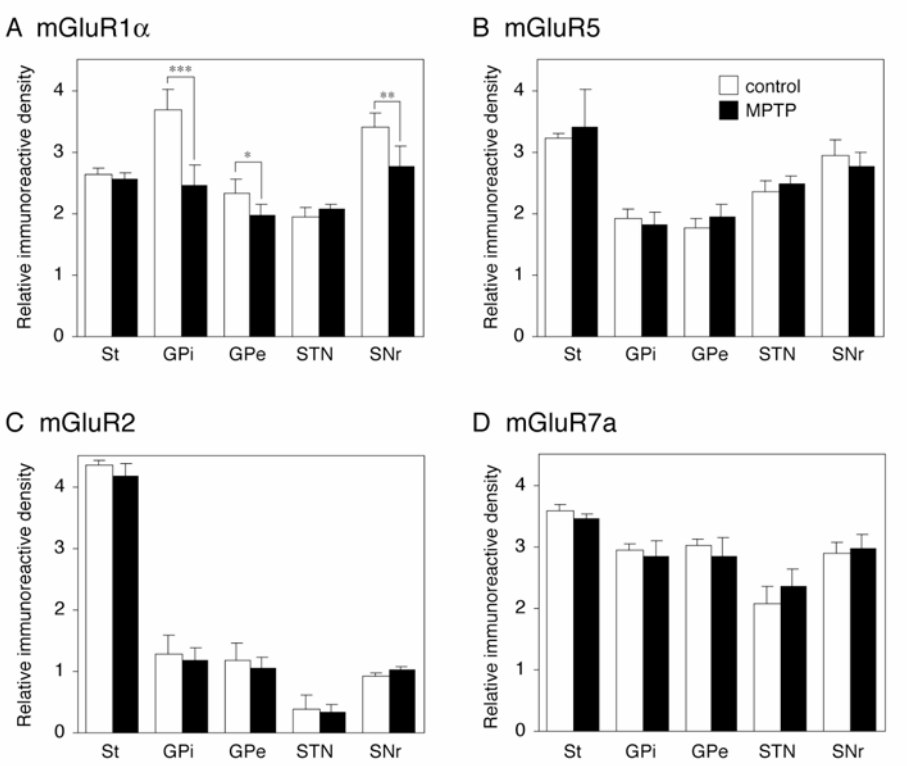

Figure 1. Densitometric measurements of immunoreactivity for mGluR1α (A), mGluR5 (B), mGluR2 (C), and mGluR7a (D) in basal ganglia. The density of immunoreactivity for each subtype was measured by the aid of NIH Image 1.62. For the measurements of the relative immunoreactive densities in the striatum (St) and the pallidal complex (GPi and GPe), two square areas (40,000 μm^2 each) obtained randomly from dorsal and ventral portions three equidistant frontal sections were tested in three representative sections. As for the STN and SNr, three square areas from medial, central, and lateral portions were tested in two representative sections. Thus, the density for each structure of the basal ganglia (D_1) was measured in a total of six square areas, and, as a background, the density for the internal or external capsule (D_0) was measured in the same manner. Then, the relative density was calculated as $(D_1–D_0)/D_0$. In each panel, open columns represent the relative immunoreactive densities in the normal monkey group, while filled columns represent those in the MPTP-treated monkey group. Data are represented as mean ± SD. Significant differences in the relative density between the normal and the MPTP-treated monkey group were statistically analyzed using the two-tailed unpaired t-test: *$p < 0.05$; **$p < 0.01$; ***$p < 0.001$.

3. EFFECTS OF mGluR1-RELATED AGENTS ON PALLIDAL NEURON ACTIVITY

The present immunohistochemical data have indicated that mGluR1α is specifically downregulated in the pallidal complex and SNr of parkinsonian monkeys. To test the hypothesis that mGluR1α is involved in the control of neuronal activity in these structures, we examined the possible changes in spontaneous neuronal firing in the pallidal complex after intrapallidal injections of the following mGluR1-related agents: (RS)-3,5-

dihydroxyphenylglycine (DHPG, a selective agonist of group I mGluRs), (RS)-1-aminoindan-1,5-dicarboxylic acid (AIDA, a selective antagonist of group I mGluRs), and (S)-(+)-α-amino-4-carboxy-2-methylbenzeneacetic acid (LY367385, a selective antagonist of mGluR1). By means of extracellular unit recordings, the rates of pallidal neuron firing were monitored first in normal awake conditions, and then in parkinsonian conditions to explore the alterations in the responsiveness of pallidal neurons to the mGluR1-related agents.

In the normal state, the spontaneous discharge rate of pallidal neurons was 64.2 ± 25.5 or 61.2 ± 28.8 Hz in the GPi (n = 68) and GPe (n = 61), respectively. Following microinjection of DHPG (5–50 mM, 0.05–0.5 µl), an increase in the firing rate occurred shortly after the injection and lasted at least 30–40 min (Figure 2A,B). At the maximum stage, the average discharge rate was increased to 156.1 ± 77.9% (n = 26, mean ± SD, $p < 0.001$, two-tailed paired t-test) or 166.7 ± 94.0% (n = 18, $p < 0.001$) of the preinjection level in the GPi and GPe, respectively (Table 1). By contrast, locally applied AIDA (4.5–20 mM, 0.18–0.5 µl) significantly decreased the rate of pallidal neuron firing (Figure 2C,D). The average discharge rate was decreased to 80.2 ± 24.7% (n = 19, $p < 0.01$) or 81.3 ± 30.3% (n = 27, $p < 0.01$) of the preinjection level in the GPi and GPe, respectively (Table 1). Similarly, LY367385 (0.01–0.1 mM, 0.1–0.5 µl) reduced the average discharge rate to 86.5 ± 25.0% (n = 23, $p < 0.01$) or 82.7 ± 26.3% (n = 16, $p < 0.05$) of the preinjection level in the GPi and GPe, respectively (Figure 2E,F; Table 1).

In the parkinsonian state, the average rate of pallidal neuron firing was 63.7 ± 30.6 or 54.8 ± 23.6 Hz in the GPi (n = 36) and GPe (n = 45), respectively. This suggests that the spontaneous activity of pallidal neurons tends to be enhanced in the GPi and, conversely, suppressed in the GPe. However, no significant differences in the firing rates of either GPi or GPe neurons were statistically detected between normal and parkinsonian conditions ($p > 0.05$, two-tailed unpaired t-test). In MPTP-treated monkeys, intrapallidal injection of DHPG increased the firing rate of pallidal neurons to 129.4 ± 30.9% (n = 18, $p < 0.001$) or 163.2 ± 54.3% (n = 25, $p < 0.001$) of the preinjection level in the GPi and GPe, respectively (Table 1). On the other hand, LY367385 decreased the firing rate to 93.4 ± 15.6% (n = 18, $p < 0.05$) or 90.0 ± 14.6% (n = 20, $p < 0.05$) of the preinjection level in the GPi and GPe, respectively (Table 1). In the parkinsonian state, however, pallidal neuron activity, especially in the GPi, tended to be less severely affected by the mGluR1-related agents than in the normal state.

Table 1. Effects of DHPG, AIDA, and LY367385 on pallidal neuron firing in normal and parkinsonian conditions[a].

	Normal (%)			Parkinson (%)	
	DHPG	AIDA	LY367385	DHPG	LY367385
GPi	156.1 ± 77.9	80.2 ± 24.7	86.5 ± 25.0	129.4 ± 30.9	93.4 ± 15.6
GPe	166.7 ± 94.0	81.3 ± 30.3	82.7 ± 26.3	163.2 ± 54.3	90.0 ± 14.6

[a] For each neuron, the spontaneous firing rate with maximum postinjection change was compared with the preinjection value by using the two-tailed unpaired t-test.

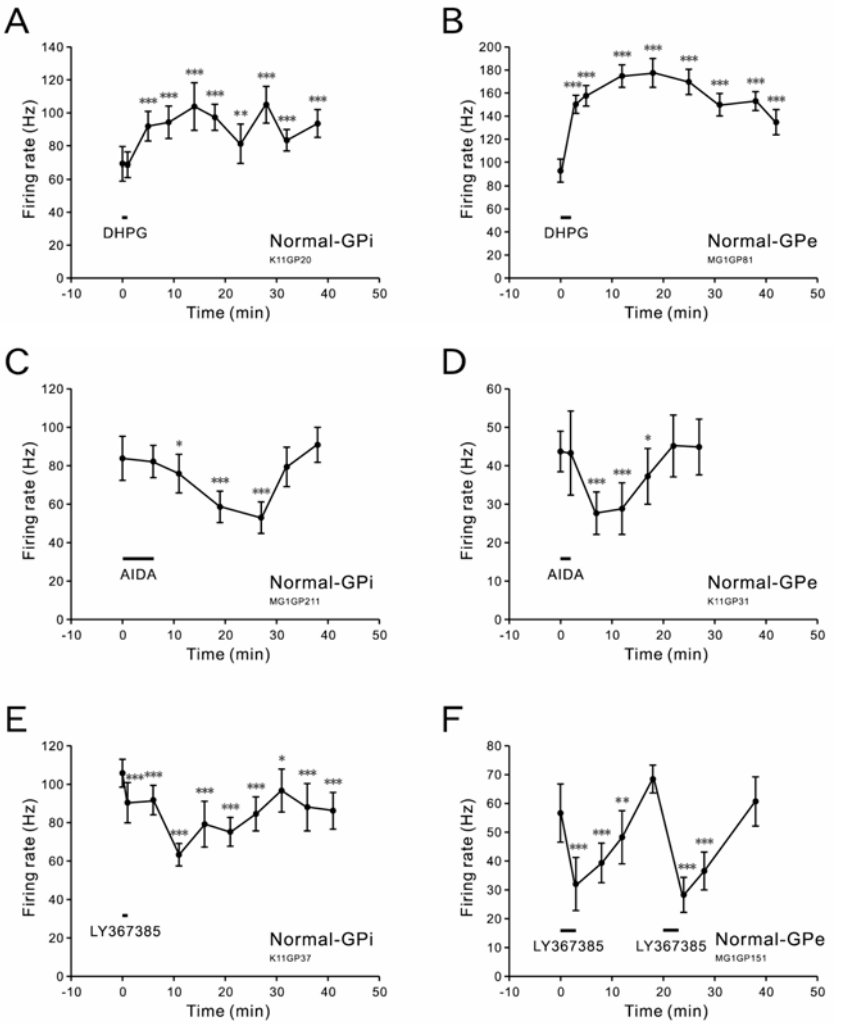

Figure 2. Time course of changes in spontaneous firing rates of representative neurons in GPi (A, C, E) and GPe (B, D, F) by mGluR1-related agents. Intrapallidal injection of DHPG (A, B), AIDA (C, D), or LY367385 (E, F) was made during the period specified by thick line. For microinjections of these agents, a pair of silica capillary tubes (75 μm in inner diameter, 150 μm in outer diameter) were affixed to the electrode beforehand, and each tube was connected to a 25-μl Hamilton microsyringe (see also Nambu et al., 2000; Kita et al., 2004). Activity changes of pallidal neurons were continuously monitored before, during, and after the intrapallidal injection of each agent. When the frequency of spontaneous neuronal firing appeared to be changed, the digital pulses were counted at a bin width of 0.5 sec with a computer, and the firing rate was calculated based on the number of discharges in 20 bins (during 10 sec). Data are indicated as mean ± SD. Statistical analysis was carried out using one-way ANOVA with repeated measures followed by the Bonferroni's post hoc test. Significant differences in the firing rate compared with the preinjection value: *$p < 0.05$; **$p < 0.01$; ***$p < 0.001$.

4. DISCUSSION

Previous studies have demonstrated that the activity of STN neurons is greatly increased in animal models of Parkinson's disease (Miller and DeLong, 1987; Bergman et al., 1994; Hassani et al., 1996; Kreiss et al., 1997). In the present study, we hypothesized that such excessive glutamatergic inputs from the STN might affect the patterns of mGluRs expression in the basal ganglia. Here we provide evidence that, in monkeys rendered parkinsonian by MPTP treatment, mGluR1α is specifically downregulated in the pallidal complex and SNr, each of which is the major target structure of the STN. The decreased expression of mGluR1α was observed most prominently in the GPi, followed by the SNr and then the GPe. Several electrophysiological studies have reported on pallidal and nigral neuron activities in MPTP-treated monkeys (Miller and DeLong, 1987; Filion and Tremblay, 1991; Boraud et al., 1998; Wichmann et al., 1999). They found that (1) the firing rate of GPi neurons is increased, while that of GPe neurons is rather decreased; (2) the number of neurons displaying burst firing is increased more apparently in the GPi than in the GPe and SNr. In the present experiments, however, the changes in pallidal neuron firing were not so marked in MPTP-treated monkeys as previously described (Miller and DeLong, 1987; Filion and Tremblay, 1991; Boraud et al., 1998). Our findings seem comparable with the data of a recent study showing that the spontaneous discharge rate of GPi neurons is not necessarily explicitly increased in parkinsonian monkeys (Wichmann et al., 1999). This can be explained by postulating that mGluR1α expression is downregulated in response to excessive glutamate release. Thus, the specific downregulation of mGluR1α in the GPi might represent a compensatory response to reverse the hyperactivity of STN-derived glutamatergic inputs that is generated in Parkinson's disease.

An additional observation in the present study is the finding that mGluR1 regulates the activity of pallidal neurons in normal awake monkeys. Our extracellular unit recordings revealed that DHPG (an agonist of group I mGluRs) significantly increases the spontaneous firing rate of pallidal neurons. Thus, activation of mGluR1 would be capable of accentuating pallidal neuron activity. However, the possibility cannot as yet be excluded that the excitatory effect of DHPG may also be exerted through mGluR5, because the agent stimulates mGluR5 as well as mGluR1 (Conn and Pin, 1997). In the present study, application of AIDA (an antagonist of group I mGluRs) and LY367385 (a selective antagonist of mGluR1) successfully dampened pallidal neuron activity. This implies that intrinsically released glutamate, which mainly comes from STN terminals, may normally excite pallidal neurons by activating mGluR1.

In the parkinsonian state, excessively released glutamate might make pallidal neurons overactive, which could then be opposed by the downregulated expression of mGluR1α. The present results have indeed shown that the excitatory/inhibitory effects of DHPG and LY367385 on pallidal neuron activity tend to be obscure in the parkinsonian state. It should be emphasized here that the reduction in pharmacologically induced activity changes appear to be evident in GPi neurons, but not in GPe neurons, which fits well the immunohistochemical data showing that mGluR1α expression is decreased more prominently in the GPi than in the GPe of MPTP-treated monkeys.

Clinical as well as experimental manipulations, including surgical lesioning and high-frequency stimulation, that are aimed at the suppression of highly activated neurons in the STN effectively ameliorates parkinsonian motor symptoms (Bergman et al., 1990; Aziz et al., 1991; Benazzouz et al., 1993; Limousin et al., 1995; Guridi et al., 1996; Baron et al., 2002). In addition, blockade of the overactivity of pallidal and nigral neurons is

critical for reversal of Parkinson's disease (Brotchie et al., 1991; Klockgether et al., 1991; Wichmann et al., 2001; Baron et al., 2002; Benabid, 2003). Given that the specific down-regulation of mGluR1α in the pallidal complex and SNr represents a compensatory event against the excessive glutamatergic inputs, selective antagonism of mGluR1α may provide a therapeutic advantage to Parkinson's disease.

5. REFERENCES

Anwyl, R., 1999, Metabotropic glutamate receptors: electrophysiological properties and role in plasticity, *Brain Res. Rev.* **29**:83–120.

Aziz, T.Z., Peggs, D., Sambrook, M.A., and Crossman, A.R., 1991, Lesion of the subthalamic nucleus for the alleviation of 1-methyl-4-phenyl-1,2,3,6-tetrahydropyridine (MPTP)-induced parkinsonism in the primate, *Mov. Disord.* **6**:288–292.

Baron, M.S., Wichmann, T., Ma, D., and DeLong, M.R., 2002, Effects of transient focal inactivation of the basal ganglia in parkinsonian primates, *J. Neurosci.* **22**:592–599.

Benabid, A.L., 2003, Deep brain stimulation for Parkinson's disease, *Curr. Opin. Neurobiol.* **13**:696–706.

Benazzouz, A., Gross, C., Féger, J., Boraud, T., and Bioulac, B., 1993, Reversal of rigidity and improvement in motor performance by subthalamic high-frequency stimulation in MPTP-treated monkeys, *Eur. J. Neurosci.* **5**:382–389.

Bergman, H., Wichmann, T., and DeLong, M.R., 1990, Reversal of experimental parkinsonism by lesions of the subthalamic nucleus, *Science* **249**:1436–1438.

Bergman, H., Wichmann, T., Karmon, B., and DeLong, M.R., 1994, The primate subthalamic nucleus. II. Neuronal activity in the MPTP model of parkinsonism, *J. Neurophysiol.* **72**:507–520.

Bernard, V., Gardiol, A., Faucheux, B., Bloch, B., Agid, Y., and Hirsch, E.C., 1996, Expression of glutamate receptors in the human and rat basal ganglia: effect of the dopaminergic denervation on AMPA receptor gene expression in the striatopallidal complex in Parkinson's disease and rat with 6-OHDA lesion, *J. Comp. Neurol.* **368**:553–568.

Betarbet, R., Porter, R.H., and Greenamyre, J.T., 2000, GluR1 glutamate receptor subunit is regulated differentially in the primate basal ganglia following nigrostriatal dopamine denervation, *J. Neurochem.* **74**:1166–1174.

Blandini, F., Nappi, G., Tassorelli, C., and Martignoni, E., 2000, Functional changes of the basal ganglia circuitry in Parkinson's disease, *Prog. Neurobiol.* **62**:63–88.

Boraud, T., Bezard, E., Guehl, D., Bioulac, B., and Gross, C., 1998, Effects of L-DOPA on neuronal activity of the globus pallidus externalis (GPe) and globus pallidus internalis (GPi) in the MPTP-treated monkey, *Brain Res.* **787**:157–160.

Brotchie, J.M., Mitchell, I.J., Sambrook, M.A., and Crossman, A.R., 1991, Alleviation of parkinsonism by antagonism of excitatory amino acid transmission in the medial segment of the globus pallidus in rat and primate, *Mov. Disord.* **6**:133–138.

Conn, P.J., and Pin, J.P., 1997, Pharmacology and functions of metabotropic glutamate receptors, *Annu. Rev. Pharmacol. Toxicol.* **37**:205–237.

Dunah, A.W., Wang, Y., Yasuda, R.P., Kameyama, K., Huganir, R.L., Wolfe, B.B., and Standaert, D.G., 2000, Alterations in subunit expression, composition, and phosphorylation of striatal N-methyl-d-aspartate glutamate receptors in a rat 6-hydroxydopamine model of Parkinson's disease, *Mol. Pharmacol.* **57**:342–352.

Filion, M., and Tremblay, L., 1991, Abnormal spontaneous activity of globus pallidus neurons in monkeys with MPTP-induced parkinsonism, *Brain Res.* **547**:142–151.

Guridi, J., Herrero, M.T., Luquin, M.R., Guillén, J., Ruberg, M., Laguna, J., Vila, M., Javoy-Agid, F., Agid, Y., Hirsch, E., and Obeso, J.A., 1996, Subthalamotomy in parkinsonian monkeys. Behavioural and biochemical analysis, *Brain* **119**:1717–1727.

Hanson, J.E., and Smith, Y., 1999, Group I metabotropic glutamate receptors at GABAergic synapses in monkeys, *J. Neurosci.* **19**:6488–6496.

Hassani, O.-K., Mouroux, M., and Féger, J., 1996, Increased subthalamic neuronal activity after nigral dopaminergic lesion independent of disinhibition via the globus pallidus, *Neuroscience* **72**:105–115.

Kaneda, K., Imanishi, M., Nambu, A., Shigemoto, R., and Takada, M., 2003, Differential expression patterns of mGluR1α in monkey nigral dopamine neurons, *Neuroreport* **14**:947–950.

Kinoshita, A., Ohishi, H., Neki, A., Nomura, S., Shigemoto, R., Takada, M., Nakanishi, S., and Mizuno, N., 1996a, Presynaptic localization of a metabotropic glutamate receptor, mGluR8, in the rhinencephalic areas: a light and electron microscope study in the rat, *Neurosci. Lett.* **207**:61–64.

Kinoshita, A., Ohishi, H., Nomura, S., Shigemoto, R., Nakanishi, S., and Mizuno, N., 1996b, Presynaptic localization of a metabotropic glutamate receptor, mGluR4a, in the cerebellar cortex: a light and electron microscope study in the rat, *Neurosci. Lett.* **207**:199–202.

Kita, H., Nambu, A., Kaneda, K., Tachibana, Y., and Takada, M., 2004, Role of ionotropic glutamatergic and GABAergic inputs on the firing activity of neurons in the external pallidum in awake monkeys, *J. Neurophysiol.* **92**:3069–3084.

Klockgether, T., Turski, L., Honore, T., Zhang, Z.M., Gash, D.M., Kurlan, R., and Greenamyre, J.T., 1991, The AMPA receptor antagonist NBQX has antiparkinsonian effects in monoamine-depleted rats and MPTP-treated monkeys, *Ann. Neurol.* **30**:717–723.

Kreiss, D.S., Mastropietro, C.W., Rawji, S.S., and Walters, J.R., 1997, The response of subthalamic nucleus neurons to dopamine receptor stimulation in a rodent model of Parkinson's disease, *J. Neurosci.* **17**:6807–6819.

Limousin, P., Pollak, P., Benazzouz, A., Hoffmann, D., Le Bas, J.F., Broussolle, E., Perret, J.E., and Benabid, A.L., 1995, Effect of parkinsonian signs and symptoms of bilateral subthalamic nucleus stimulation, *Lancet* **345**:91–95.

Martin, L.J., Blackstone, C.D., Huganir, R.L., and Price, D.L., 1992, Cellular localization of a metabotropic glutamate receptor in rat brain, *Neuron* **9**:259–270.

Miller, W.C., and DeLong, M.R., 1987, Altered tonic activity of neurons in the globus pallidus and subthalamic nucleus in the primate MPTP model of parkinsonism, in: *The Basal Ganglia II*, M. B. Carpenter, and A. Jayaraman, eds., Plenum Press, New York, pp. 415–427.

Nambu, A., Tokuno, H., Hamada, I., Kita, H., Imanishi, M., Akazawa, T., Ikeuchi, Y., and Hasegawa, N., 2000, Excitatory cortical inputs to pallidal neurons via the subthalamic nucleus in the monkey, *J. Neurophysiol.* **84**:289–300.

Neki, A., Ohishi, H., Kaneko, T., Shigemoto, R., Nakanishi, S., and Mizuno, N., 1996, Pre- and postsynaptic localization of a metabotropic glutamate receptor, mGluR2, in the rat brain: an immunohistochemical study with a monoclonal antibody, *Neurosci. Lett.* **202**:197–200.

Obeso, J.A., Rodríguez-Oroz, M.C., Rodríguez, M., Lanciego, J.L., Artieda, J., Gonzalo, N., and Olanow, C.W., 2000, Pathophysiology of the basal ganglia in Parkinson's disease, *Trends Neurosci.* **23**:S8–19.

Ohishi, H., Nomura, S., Ding, Y.Q., Shigemoto, R., Wada, E., Kinoshita, A., Li, J.L., Neki, A., Nakanishi, S., and Mizuno, N., 1995, Presynaptic localization of a metabotropic glutamate receptor, mGluR7, in the primary afferent neurons: an immunohistochemical study in the rat, *Neurosci. Lett.* **202**:85–88.

Ohishi, H., Ogawa-Meguro, R., Shigemoto, R., Kaneko, T., Nakanishi, S., and Mizuno, N., 1994, Immunohistochemical localization of metabotropic glutamate receptors, mGluR2 and mGluR3, in rat cerebellar cortex, *Neuron* **13**:55–66.

Pin, J.P., and Duvoisin, R., 1995, The metabotropic glutamate receptors: structure and functions, *Neuropharmacology* **34**:1–26.

Porter, R.H., Greene, J.G., Higgins, D.S. Jr., and Greenamyre, J.T., 1994, Polysynaptic regulation of glutamate receptors and mitochondrial enzyme activities in the basal ganglia of rats with unilateral dopamine depletion, *J. Neurosci.* **14**:7192–7199.

Rouse, S.T., Marino, M.J., Bradley, S.R., Awad, H., Wittmann, M., and Conn, P.J., 2000, Distribution and roles of metabotropic glutamate receptors in the basal ganglia motor circuit: implications for treatment of Parkinson's disease and related disorders, *Pharmacol. Ther.* **88**:427–435.

Shigemoto, R., Abe, T., Nomura, S., Nakanishi, S., and Hirano, T., 1994, Antibodies inactivating mGluR1 metabotropic glutamate receptor block long-term depression in cultured Purkinje cells, *Neuron* **12**:1245–1255.

Shigemoto, R., Kinoshita, A., Wada, E., Nomura, S., Ohishi, H., Takada, M., Flor, P.J., Neki, A., Abe, T., Nakanishi, S., and Mizuno, N., 1997, Differential presynaptic localization of metabotropic glutamate receptor subtypes in the rat hippocampus, *J. Neurosci.* **17**:7503–7522.

Shigemoto, R., Nomura, S., Ohishi, H., Sugihara, H., Nakanishi, S., and Mizuno, N., 1993, Immunohistochemical localization of a metabotropic glutamate receptor, mGluR5, in the rat brain, *Neurosci. Lett.* **163**:53–57.

Testa, C.M., Friberg, I.K., Weiss, S.W., and Standaert, D.G., 1998, Immunohistochemical localization of metabotropic glutamate receptors mGluR1a and mGluR2/3 in the rat basal ganglia, *J. Comp. Neurol.* **390**:5–19.

Ulas, J., and Cotman, C.W., 1996, Dopaminergic denervation of striatum results in elevated expression of NR2A subunit, *Neuroreport* **7**:1789–1793.

Ulas, J., Weihmuller, F.B., Brunner, L.C., Joyce, J.N., Marshall, J.F., and Cotman, C.W., 1994, Selective increase of NMDA-sensitive glutamate binding in the striatum of Parkinson's disease, Alzheimer's disease, and mixed Parkinson's disease/Alzheimer's disease patients: an autoradiographic study, *J. Neurosci.* **14**:6317–6324.

Wichmann, T., Bergman, H., Starr, P.A., Subramanian, T., Watts, R.L., and DeLong, M.R., 1999, Comparison of MPTP-induced changes in spontaneous neuronal discharge in the internal pallidal segment and in the substantia nigra pars reticulata in primates, *Exp. Brain Res.* **125**:397–409.

Wichmann, T., and DeLong, M.R., 1996, Functional and pathophysiological models of the basal ganglia, *Curr. Opin. Neurobiol.* **6**:751–758.

Wichmann, T., Kliem, M.A., and DeLong, M.R., 2001, Antiparkinsonian and behavioral effects of inactivation of the substantia nigra pars reticulata in hemiparkinsonian primates, *Exp. Neurol.* **167**:410–424.

PITX3 IS NECESSARY FOR SURVIVAL OF MIDBRAIN DOPAMINERGIC NEURON SUBSETS RELEVANT TO PARKINSON'S DISEASE

Abbas F. Sadikot[1]*, Kelvin C. Luk[1], Pepijn van den Munckhof[2], Vladimir V. Rymar[1], Kenneth Leung[1], Rina Gandhi[1], and Jacques Drouin[2]

1. INTRODUCTION

The pathological hallmark of Parkinson's disease (PD) is progressive loss of midbrain dopaminergic (DA) neurons, accompanied by loss of non-DA populations in more advanced stages (Hassler, 1938; Jellinger, 2001). Midbrain DA neurons are localized in the densely packed substantia nigra (SN) pars compacta, and more loosely packed cells intermingled with GABAergic neurons in the SN pars reticulata, the SN pars lateralis, the ventral tegmental area (VTA) and the retrorubral field (Parent, 1996). The RRF, SN, VTA, are also designated as catecholaminergic areas A8, A9, and 10, respectively (Hökfelt et al., 1984). Three tiers of DA cells are identified in the rodent and primate SN: a dorsal tier of the SN pars compacta (SNc), and the two ventral tiers; one within the SNc proper with the other occupying the SN pars reticulata (SNr). The SN dorsal tier may be distinguished from the ventral tiers by cytological criteria, and expression of the calcium binding proteins calbindin-D-28k (CB) and/or calretinin (CR) in rodents, non-human primates and humans (Coté et al., 1991; Liang et al., 1996; McRitchie et al., 1996).

The pattern of progressive midbrain DA (mDA) neuronal loss in PD is not uniform: mDA subpopulations differ in vulnerability to injury. For example, in the SN, DA neurons that occupy the ventral two tiers ("ventral SN") are lost first, with relative sparing of the DA neurons in the dorsal tier and VTA. While CB expression was initially thought to confer resistance to toxicity (Yamada et al., 1990; Lavoie and Parent, 1991), knockout of CB in transgenic mice does not alter developmental survival of mDA neurons nor enhance

[1] Department of Neurology and Neurosurgery, Montreal Neurological Institute, McGill University, Montreal, Quebec H3A 2B4, Canada.
[2] Unité de recherche en génétique moléculaire, Institut de recherches cliniques de Montréal, Montreal, Quebec H2W 1R7, Canada.
* To whom correspondence should be addressed. Email: sadikot@bic.mni.mcgill.ca.

susceptibility to the DA toxin MPTP (Airaksinen et al., 1997). CB expression is therefore not critical to survival, and may even be an epiphenomenon with respect to toxicity.

We recently discovered that aphakia (*ak*) mice bearing the mutations in the Pitx3 gene shows marked loss of DA neurons in the A9 and A10 nuclear groups (van den Munckhof et al., 2003). Other investigators have provided similar evidence (Hwang et al., 2003; Nunes et al., 2003; Smidt et al., 2004). Our analysis suggested relative sparing of mDA neurons in the dorsal tier group of the SN and in the VTA, and we suggested that the pattern of cell loss resembles that seen in Parkinson's disease (van den Munckhof et al., 2003). The naturally occurring *ak* mutant contains deletions in the promoter and exon-1 of the Pitx3 gene, resulting in failure to express detectable levels of Pitx3 transcript (Semina et al., 2000; Rieger et al., 2001). This homeodomain transcription factor has been reported to contribute to the establishment of the DA phenotype in developing midbrain neurons.

Our imunohistochemical studies have suggested that Pitx3 expression in the mDA system is widespread. However, there is preferential localization of Pitx3 amongst ventral tier neurons with additional expression within intermingled neuronal groups of the VTA. Aphakia mice show loss of the nigrostriatal projection. The mesolimbic projection to the ventral striatum is relatively spared, although innervation of the nucleus accumbens is not normal (van den Munckhof et al., 2003). Furthermore, we demonstrated that *ak* mice, which are blind, show reduced spontaneous locomotor behavior in both light and dark environments (van den Munckhof et al., 2003). The pattern of DA cell loss in the midbrain, striatal denervation with preferential loss of DA terminals in the neostriatum, and relative sparing of mesolimbic DA projections, collectively resembles the pattern of DA loss in PD. We hypothesized that the CB^+ subpopulation of mDA neurons is relatively spared in the *ak* mouse.

Here, we have used unbiased stereology to demonstrate relative sparing of the subpopulation of DA neurons containing CB in the dorsal tier of the SN and in the VTA of *ak* mice. We conclude that Pitx3 is required for the survival of the ventral tier DA subpopulation that is preferentially lost in PD. We therefore propose that malfunction of the transcriptional pathway defined by Pitx3 may be an important factor contributing to preferential DA degeneration in PD.

2. METHODS

All animal procedures were performed in accordance with the Canadian Council on Animal Care guidelines for the use of animals in research and were approved by the McGill University Animal Care Committee. Homozygous male wildtype and aphakia (*ak*) mice were transcardially perfused with 4% paraformaldehyde (PFA; in phosphate buffer, pH 7.4) at postnatal days (P) 35, P100, and P700. Brains were then removed, postfixed for 24 h, and cryoprotected by immersion in buffered sucrose (30%, pH 7.4) for an additional 48 h before cutting. Sectioning was performed using a freezing microtome (Micron, Germany) at 50 µm. Floating coronal sections were collected in PBS as 6 separate sets so that each set contained every sixth serial section.

A series of sections was immunostained for tyrosine hydroxylase (TH), or CB using an avidin-biotin-peroxidase complex (ABC) method as previously described (van den Munckhof et al., 2003; Rymar et al., 2004). Antibodies used included monoclonal anti-TH (1 : 1000; Immunostar, Hudson, WI) and anti-CB (1 : 2000; Sigma, St. Louis, MO), and rabbit anti-TH (1 : 2000; Chemicon, Temecula, CA) and anti-CB (1 : 500; Swant,

Bellinzona, Switzerland). For stereological quantification of TH and CB neurons, floating sections were incubated in rabbit anti-TH or monoclonal anti-CB antibody overnight, washed in phosphate buffered saline (PBS) three times, and incubated for 1 h with biotinylated anti-rabbit or anti-mouse secondary antibody (1 : 200, Vector, Burlinghame, CA). Following another set of washes, avidin-biotin complex (ABC; Vector) was used as per manufacturer's instructions and the final reaction was revealed by 3′3′-diaminobenzidene (DAB) in the presence of 0.006% hydrogen peroxide. Sections were counterstained lightly in 0.1% cresyl violet, dehydrated, and coverslipped. Photographs were captured using a digital camera (Microfire, Optronics, Goleta, CA).

Unbiased estimates of mDA neurons were obtained using the optical dissector method (Gundersen et al., 1988) as previously described (van den Munckhof et al., 2003). The entire rostrocaudal extent of the midbrain, including regions containing A8, 9 and 10 DA cell groups, was examined in a series (1 : 6) of TH- or CB-stained coronal sections using an Olympus BX-40 microscope equipped with a motorized XYZ stage and StereoInvestigator software (Microbrightfield, Colchester, VT). Midbrain DA nuclei were traced at low power. After starting at a random site, 12 µm optical dissectors were applied 2 µm below the surface of the section (guard zone) at counting sites located at 125 µm intervals. TH^+ and CB^+ cell counts were performed at 100× magnification (oil, NA 1.3) using a 60×60 µm counting frame with exclusion edges.

For colocalization experiments, double immunofluorescence for TH and CB was performed by incubating 25 µm sections with polyclonal TH and monoclonal CB antibodies. Labeling was revealed using the appropriate secondary antibodies conjugated to Alexafluor-488 or -596 (1 : 2000; Molecular Probes, Carlsbad, CA), and viewed using suitable filters through a fluorescence microscope (BX-40, Olympus, Tokyo, Japan). 4′,6-Diamidino-2-phenylindole (1 ug/ml) was also used as a nuclear counterstain.

3. RESULTS

We used unbiased stereology to characterize the mDA system of the young adult (P35) and adult (P100) *ak* mice, with specific attention to DA cell loss in mesencephalic subgroups, and quantification of CB^+ neurons in the ventral midbrain. In order to determine the pattern of DA cell loss, P35 wildtype and *ak* mice were immunostained for TH and examined at multiple coronal levels (Fig. 1a–j). As previously reported, *ak* mice show marked DA cell loss at all rostrocaudal levels examined (Fig. 1f–j). TH^+ cell loss was especially pronounced in the SN at all levels examined. In comparison, the VTA showed a less severe decrease in TH^+ cell number. Loss of TH^+ cells was also observed at more caudal levels containing the RRF. Cresyl violet counterstaining indicated accompanying loss of cell bodies, confirming that reduction in TH^+ cell number is not attributable to loss of TH expression, in keeping with our previous report (van den Munckhof et al., 2003). Aphakia mice therefore show significant DA cell loss in the A8, A9 and A10 nuclei.

Previous work indicates that rodent and murine DA neuronal populations undergo extensive developmental cell death primarily in late prenatal and early postnatal periods (Jackson-Lewis et al., 2000). To examine the changes in mDA neuron number that occur with development and maturation, we employed the optical fractionator method in order to quantify total TH^+ cell number in the SNc and VTA of wildtype and *ak* mice at various postnatal ages, in mature mice, and in ageing mice. Here we report the results in adolescent (P35) and adult (P100) mice. In agreement with our previous results, unbiased stereology

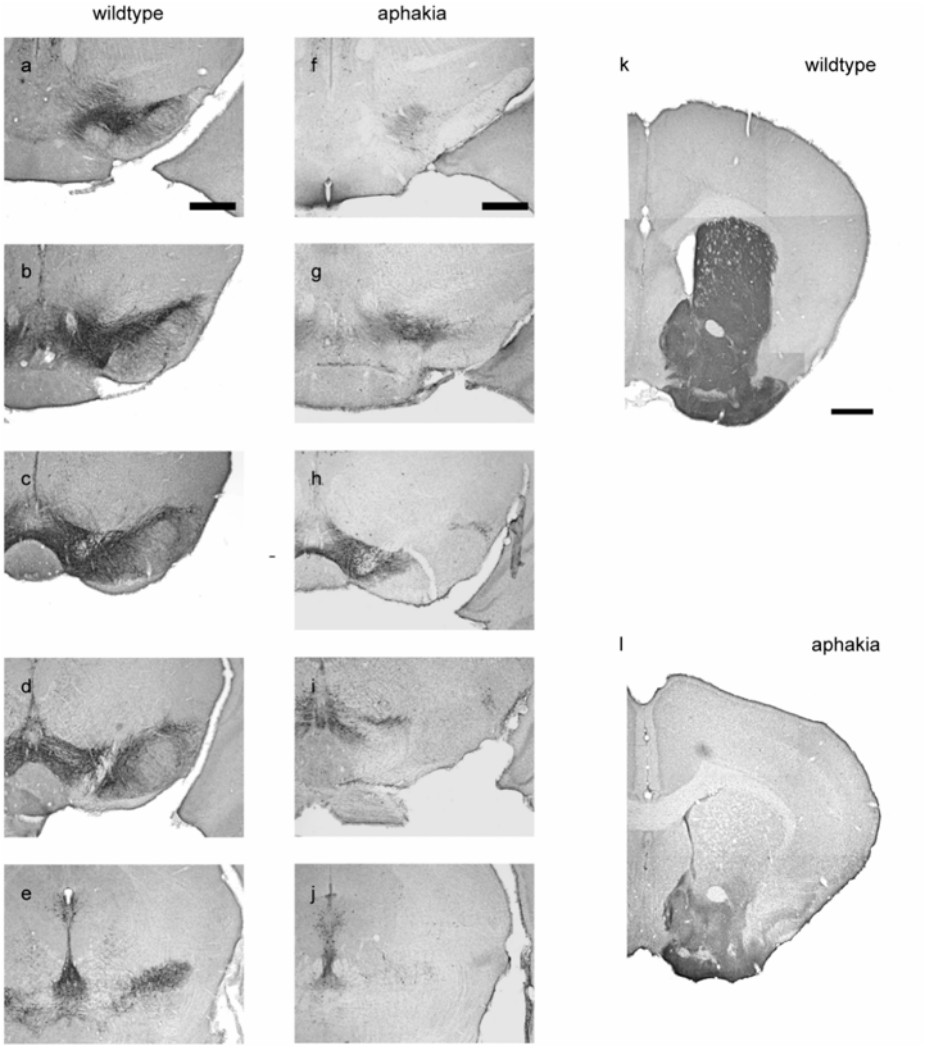

Figure 1. Midbrain dopaminergic cell loss in aphakia mice. Tyrosine hydroxylase immunohistochemistry in wildtype and *ak* mice at P35 demonstrate marked loss of DA neurons in various mDA nuclei. Cell loss is observed in A8, A9, and A10 regions, but is especially pronounced in the first two regions (RRF and SN). In *ak* mice, scant TH^+ populations are detected in SN and RRF, primarily in the medial and dorsal SNc. There is relative sparing of TH^+ in the VTA. Immunostaining in wildtype and *ak* mice at the level of the neostriatum (k,l). Dopaminergic terminals are largely absent in the dorsal striatum of *ak* mice, with relative sparing of the ventral striatal regions, including the nucleus accumbens. Scale bars = 400 μm (a–j), 500 μm (k,l).

revealed an 80% reduction in the number of SNc DA neurons in *ak* mice by P35 (van den Munckhof et al., 2003). Interestingly, we failed to detect any significant alterations in number of DA neurons at P35 and P100, suggesting that most of the DA cell loss occurs in the perinatal and postnatal period, and stabilizes in mature mice (Fig. 2a,b).

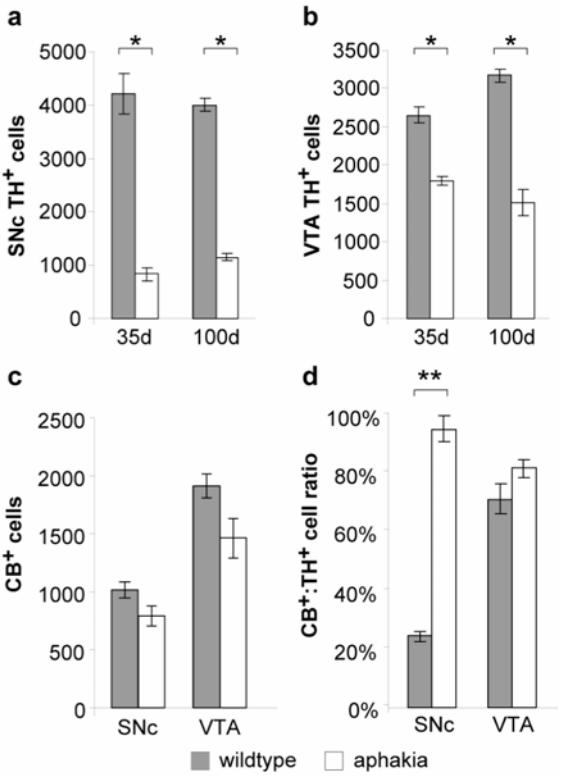

Figure 2. Stereological quantification of midbrain TH and CB neurons. The total number of TH^+ neurons in the VTA and SNc of wildtype and *ak* mice were quantified using the optical dissector method at P35 and P100 (a,b). Reduction of TH^+ cell number in *ak* was in the SNc was over 80%, compared to wildtype animals which did not appear to change with age at P100. In contrast, total TH^+ cell number in the VTA of *ak* mice is comparable to wildtype at birth, but decrease with age (a,b). Total CB^+ neuron number of P100 wildtype and *ak* mice were comparable, suggesting no loss of this subpopulation within the VTA or SNc, suggesting that CB^+ cells are not lost in the absence of Pitx3 (c). Total CB^+ cell numbers in these two areas expressed as a ratio of total TH^+ cell number indicate that CB^+ cells comprise a larger proportion of cells in the VTA than SNc (d). In *ak* mice, CB^+ cell number approaches, but does not exceed, that of TH^+ cells. ($n = 4$ per group; *$p < 0.01$, **$p < 0.05$).

In contrast, total number of TH^+ neurons in the VTA of *ak* mutants is nearly identical to age-matched wildtype mice at birth (van den Munckhof et al., 2003). At the onset of maturation, beginning at P21, there is a gradual reduction in VTA TH^+ cell number so that by P35, a significant reduction could be detected (Fig. 2b). By P100, *ak* mice experienced a 53% loss which remained constant in aging mice even at P700. Collectively, these data suggest that DA cell loss in the SNc precedes that of the VTA. Furthermore, TH^+ cell numbers from both ventral midibrain regions indicate that DA cell loss is complete sometime between the third and fifth postnatal weeks as we observed no further decline with age at P35, P100, or P700 in mice with or lacking Pitx3 expression.

In both mice and rodents, the calcium binding proteins calbindin and calretinin label specific subpopulations of mDA neurons located in the dorsal SNc, SN pars lateralis (SNL), RRF, and parts of the VTA (Baimbridge et al., 1992; Rogers and Resibois, 1992; McRitchie et al., 1996; Nemoto et al., 1999; Gonzalez-Hernandez and Rodriguez, 2000). Furthermore,

subpopulations of mDA neurons that express CB have been reported to be relatively spared in the 1-methyl-4-phenyl-1,2,3,6-tetrahydropyridine (MPTP) model of DA neuron toxicity and in PD (Yamada et al., 1990; Lavoie and Parent, 1991; German et al., 1992). We investigated the chemical identity of the persisting TH^+ population(s) found in *ak* mice postnatally. As previously described, immunohistochemistry for CB revealed a neuronal population in the midbrains of wildtype mice. The pattern of neuronal CB immunostaining in *ak* mice was similar to that seen in wildtype animals, suggesting that these neurons were preserved despite loss of Pitx3 expression.

In order to determine whether the subset of TH^+ neurons expressing CB is preserved in *ak* mice, the total number of TH^+ and CB^+ neurons in the midbrain was quantified in young adult (P35) animals, using unbiased stereology on adjacent sets of sections. Tyrosine hydroxylase immunostaining revealed a similar pattern of cell loss in the SNc, and VTA of mutants, as described above. Significant loss was also detected in the RRF, where there was a 68% reduction of TH^+ cells in P35 *ak* mice, respectively.

In stark contrast to TH^+ cells (which decreased by 80–90%), CB^+ cells were not significantly reduced in *ak* animals. Quantification of adjacent serial sections revealed no significant differences in the total number of CB^+ cells in *ak* or age-matched wild-type mice (Fig. 2c). Whereas the ratio of CB^+:TH^+ cells were approximately 24% and 60% in the SNc and VTA of wildtype mice, this number was nearly 90% in *aphakia* mice, suggesting that the majority of TH^+ neurons remaining in these areas were primarily CB^+ (Fig. 2d). In order to more directly establish that the remaining TH^+ cells in aphakia mice also expressed CB, double immunofluorescence was performed in sections from P100 mice. The majority of remaining TH^+ neurons in *ak* mouse midbrain examined within the SNc and VTA colocalized with CB, including 92% of all TH^+ neurons in the SNc, 87% in the VTA, and 83% in the RRF. The relative sparing in the VTA, which contains a considerable proportion of CB^+ cells, combined with the observation that most TH^+ neurons in *ak* mice also express CB, suggests that CB^+TH^+ cells are relatively resistant to loss of Pitx3 function.

Since CB^+TH^+ positive neurons of the VTA are thought to preferentially project to the nucleus accumbens core, wheareas CB^- neurons project preferentially to the shell (Tan et al., 1999), we determined whether the pattern of TH innervation in the nucleus accumbens reflected the midbrain neuronal pattern. Indeed, the TH^+ neuropil in the core territory of the nucleus accumbens is relatively spared compared to the shell territory in *ak* mice (Fig. 1k,l). On the other hand, both patch and matrix compartment TH staining is lost in the neostriatum. Based on current knowledge of nigrostriatal innervation patterns (Gerfen et al., 1987; Tan et al., 1999), these observations indicate that observed dorsal ventral differences in mDA survival in SN are reflected partially, but not with striking fidelity, in the DA innervation of the striatum of *ak* mice.

4. DISCUSSION

Mesencephalic DA neurons are born at embryonic days (E) 9–11 in the mouse (Bayer et al., 1995). By E15 mDA neurons reach positions in the SN, VTA and retrorubral field (RRF) similar to adults. Over a third of DA neurons die in the late prenatal and early postnatal period (Reisert et al., 1990; Jackson-Lewis et al., 2000). During the last decade, discovery of novel genetic transcriptional pathways has allowed better understanding of factors specifying midbrain morphogenesis. Early midbrain patterning at E7-E9 is associated with expression of the transcription factors Otx2, Pax2, Pax5, Lmx1b, En1/En2, and diffusible

molecules such as Wnt1, sonic hedgehog and FGF8 (see Simon et al., 2003 for review). Mutations in most of these genes result in severe mid/hindbrain malformations that are not specific to DA neurons (Simon et al., 2001; Matsunaga et al., 2002).

Only two transcription factors Pitx3 and Nurr1 (an orphan nuclear receptor), have so far been implicated as playing a direct role in postmitotic survival and specification of mDA neurons (Zetterstrom et al., 1997; Saucedo-Cardenas et al., 1998; van den Munckhof et al., 2003). In mouse, the orphan nuclear receptor Nurr1 is first expressed at E10.5 (Zetterstrom et al., 1997). Pitx3 expression begins at E11, a day after final mitosis of DA progenitors, and expression is maintained throughout adult life (Smidt et al., 1997). Nurr1 and Pitx3 expression is followed by appearance of the rate-limiting enzyme in DA synthesis, tyrosine hydroxylase at E11.5. Nurr1, which is expressed in DA and non-DA midbrain neurons, in addition to areas of the forebrain, is critical for TH expression and maintenance of the DA phenotype (Zetterstrom et al., 1997; Saucedo-Cardenas et al., 1998). In contrast, CNS expression of Pitx3 is limited to mesencephalic DA neurons (Smidt et al., 1997; van den Munckhof et al., 2003). Pitx3 expression is initially maintained in midbrain of Nurr1 null mutants; conversely, Nurr1 expression remains intact in *ak* mice in the initial period before the Pitx3-expressing DA subpopulation is lost (van den Munckhof et al., 2003; Smidt et al., 2004). This suggests independence of the two pathways: in contrast to Nurr1 which appears critical for TH expression and migration of DA neurons, (Zetterstrom et al., 1997) Pitx3 is necessary for survival of a specific subpopulation of midbrain DA neurons.

Pitx3 belongs to a family of transcription factors implicated in major developmental processes such as determination of hindlimb identity (Pitx1) (Lanctot et al., 1999), left-right asymmetry (Pitx2) (Harvey, 1998), craniofacial and pituitary development (Pitx1, Pitx2), or in midbrain and lens morphogenesis (Pitx3) (Drouin et al., 1998; Semina et al., 2000). Recently the Pitx3 gene was mapped to the *ak* locus on mouse chromosome 19, with the human homologue (*PITX3*) on chromosome 10 (Semina et al., 2000; Rieger et al., 2001). In the *ak* mouse, spontaneous deletions in the promoter and exon-1 region, lead to a 95% reduction in Pitx3 transcript levels. Pitx3 protein is undetectable by immuno-histochemistry in brains of *ak* mice (van den Munckhof et al., 2003). Besides midbrain development, Pitx3 is also necessary for morphogenesis of the anterior chamber of the eye, and *ak* homozygotes are easily recognized by their visible lens abnormality.

4.1. CB-Negative mDA Neurons are Preferentially Lost in the Absence of Pitx3

We have previously demonstrated that marked reduction of Pitx3 expression in *ak* mice results in selective loss of mDA neurons (van den Munckhof et al., 2003). Similar results have also been reported by other groups (Hwang et al., 2003; Nunes et al., 2003; Smidt et al., 2004). We proposed that the pattern of DA cell loss resembles that seen in Parkinson's disease. Here we provide detailed evidence suggesting predominant loss of DA neurons occurs in the ventral tiers of the SN, namely the ventrolateral pars compacta and DA populations occupying the SN pars reticulata. Cell loss also occurs in the RRF. In contrast, the dorsal tier of the SN, especially in its medial part, is relatively spared, as are DA neurons in the VTA. The mDA cell loss in *ak* mice is mainly reflected by loss of DA input to the neostriatum, with relative sparing of DA innervation of the nucleus accumbens. It is striking that the overwhelming majority of surviving neurons in the dorsal tier and the VTA in *ak* mice express CB, in comparison to wildtype counterparts. Indeed the number of CB^+ neurons in *ak* and wildtype ventral midbrain are statistically similar. The dopaminergic

deficit resulting from the absence of Pitx3 therefore corresponds mainly to loss of TH^+CB^- neurons.

4.2. Surviving DA Subsets Correspond with Preservation of Mesolimbic Projections

It is of interest to consider the residual pattern of striatal innervation in *ak* mice in the context of the findings presented above. Relative sparing of TH^+CB^+ neurons in the VTA compared to TH^+CB^- neurons would produce preferential innervation of the core territory, based on known projection patterns (Tan et al., 1999). In concordance with this prediction, we note relative sparing of TH-IR in both core and shell territories, but TH-IR in the shell appears less spared than in the core. CB-positive neurons of the dorsal tier of the SN appear to project preferentially to the matrix compartment, whereas CB^- neurons populating the ventral SN project to the patch compartment of the chemically heterogenous neostriatum (Gerfen et al., 1987). Interestingly however, both patch and matrix TH-IR in the neostriatum is lost in *ak* mice, despite the prediction that spared CB^+ DA neurons in the dorsal tier might result in spared innervation to patches, based on proposed anatomy. Further evaluation of DA compartmentalization in dorsal and ventral striatum of *ak* mice is therefore of interest.

4.3. Pitx3 and Disease

Determining the cause of specific vulnerability of the ventral SN group DA group is crucial to understanding mechanisms of mDA degeneration in Parkinson's disease (PD), and may lead to novel therapeutic advances. While CB expression was initially thought to confer resistance to toxicity (Yamada et al., 1990; Lavoie and Parent, 1991), knockout of CB in transgenic mice does not alter developmental survival of mDA neurons nor enhance susceptibility to the DA toxin MPTP (Airaksinen et al., 1997). Dopamine transporter (DAT) mRNA tends to be higher in ventral tier neurons, and may facilitate intracellular entry of the toxic metabolite of MPTP, MPP^+ (Sanghera et al., 1997; Counihan and Penney, 1998).

Our work suggests that ventral tier neurons that are especially vulnerable in PD are lost in *ak* mice which lack the ability to produce Pitx3. Although we have shown locomotor deficits, it is important to emphasize that the mouse is not a strict model of PD. For example, both DA and non-DA systems degenerate in PD (Jellinger, 2001). Furthermore, progressive DA loss in PD occurs in the context of adult degeneration of a motor system that had shown apparently normal function prior to disease onset. The *ak* mouse exhibits early developmental DA loss and therefore should be considered a model of adult neurodegeneration. Nonetheless, the *ak* mouse does reproduce some characteristic features of DA loss in PD, including loss of specific DA subpopulations and preferential denervation of the neostriatum. The pattern of relative preservation of the CB^+ mDA neurons in this developmental model resembles that seen with toxin-induced neuronal degeneration such as the MPTP model, and also resembles patterns of loss seen in human PD (Yamada et al., 1990; Lavoie and Parent, 1991; German et al., 1992). The *ak* mouse is therefore a useful model for vulnerability of DA neuronal subpopulations during development, and mimics some features of PD.

Initial studies by another group using *in situ* hybridization suggest that all mDA neurons contain Pitx3 (Smidt et al., 2004). In contrast, our work using double-

immunofluorescence mapping with TH and Pitx3 antibodies indicates that the protein is preferentially localized in ventral tier SN DA neurons and is intermingled amongst some neurons of the VTA. This localization corresponds well to the pattern of cell loss in the *ak* mutant. We therefore propose that Pitx3 plays a necessary role as part of a developmental pathway important to the survival of the ventral tier subpopulation of DA neurons. The observation that VTA DA neurons in *ak* are virtually normal in number at birth up until the third postnatal week, but later continues to degenerate, suggests an additional maintenance/survival function. We propose that Pitx3 is not only necessary for developmental survival of a subpopulation of mDA neurons, but in the adult, may also play an important role in survival/maintenance of DA populations expressing this factor. Since the Pitx3 dependent population corresponds to a DA subpopulation that degenerates in PD, we propose that a defect in the transcriptional pathway defined by Pitx3 may play an important role in pathogenesis of Parkinson's disease.

5. REFERENCES

Airaksinen, M.S., Thoenen, H., and Meyer, M., 1997, Vulnerability of midbrain dopaminergic neurons in calbindin-D28k-deficient mice, *Eur. J. Neurosci*. **9**:120–127.

Baimbridge, K.G., Celio, M.R., and Rogers, J.H., 1992, Calcium-binding proteins in the nervous system, *Trends Neurosci*. **15**:303–308.

Bayer, S.A., Wills, K.V., Triarhou, L.C., and Ghetti, B., 1995, Time of neuron origin and gradients of neurogenesis in midbrain dopaminergic neurons in the mouse, *Exp. Brain Res*. **105**:191–199.

Coté, P.Y., Sadikot, A.F., and Parent, A., 1991, Complementary Distribution of Calbindin D-28k and Parvalbumin in the Basal Forebrain and Midbrain of the Squirrel Monkey, *Eur. J. Neurosci*. **3**:1316–1329.

Counihan, T.J., and Penney, J.B., Jr., 1998, Regional dopamine transporter gene expression in the substantia nigra from control and Parkinson's disease brains, *J. Neurol. Neurosurg. Psychiatry*. **65**:164–169.

Drouin, J., Lamolet, B., Lamonerie, T., Lanctot, C., and Tremblay, J.J., 1998, The PTX family of homeodomain transcription factors during pituitary developments, *Mol. Cell Endocrinol*. **140**:31–36.

Gerfen, C.R., Baimbridge, K.G., and Thibault, J., 1987, The neostriatal mosaic: III. Biochemical and developmental dissociation of patch-matrix mesostriatal systems, *J. Neurosci*. **7**:3935–3944.

German, D.C., Manaye, K.F., Sonsalla, P.K., and Brooks, B.A., 1992, Midbrain dopaminergic cell loss in Parkinson's disease and MPTP-induced parkinsonism: sparing of calbindin-D28k-containing cells, *Ann. N Y Acad. Sci*. **648**:42–62.

Gonzalez-Hernandez, T., and Rodriguez, M., 2000, Compartmental organization and chemical profile of dopaminergic and GABAergic neurons in the substantia nigra of the rat, *J. Comp. Neurol*. **421**:107–135.

Gundersen, H.J., Bagger, P., Bendtsen, T.F., Evans, S.M., Korbo, L., Marcussen, N., Moller, A., Nielsen, K., Nyengaard, J.R., and Pakkenberg, B., 1988, The new stereological tools: disector, fractionator, nucleator and point sampled intercepts and their use in pathological research and diagnosis, *Apmis*. **96**:857–881.

Harvey, R.P., 1998, Links in the left/right axial pathway, *Cell* **94**:273–276.

Hassler, R., 1938, Zur Pathologie der Paralysis agitans und des postenzephalitischen Parkinsonismus, *J. Psychol. Neurol*. **48**:387–476.

Hökfelt, T., Martensson, R., Bjorklund, A., Kleinau, S., and Goldstein, M., 1984, Distributional maps of tyrosine-hydroxylase-immunoreactive neurons in the rat brain, in: *Classical transmitters in the CNS, part 1*, Bjorklund A, Hökfelt T, eds, Elsevier, Amsterdam, pp 277–378.

Hwang, D.Y., Ardayfio, P., Kang, U.J., Semina, E.V., and Kim, K.S., 2003, Selective loss of dopaminergic neurons in the substantia nigra of Pitx3-deficient aphakia mice, *Brain Res. Mol. Brain Res*. **114**:123–131.

Jackson-Lewis, V., Vila, M., Djaldetti, R., Guegan, C., Liberatore, G., Liu, J., O'Malley, K.L., Burke, R.E., and Przedborski, S., 2000, Developmental cell death in dopaminergic neurons of the substantia nigra of mice, *J. Comp. Neurol*. **424**:476–488.

Jellinger, K.A., 2001, The pathology of Parkinson's disease, *Adv. Neurol*. **86**:55–72.

Lanctot, C., Moreau, A., Chamberland, M., Tremblay, M.L., and Drouin, J., 1999, Hindlimb patterning and mandible development require the Ptx1 gene, *Development* **126**:1805–1810.

Lavoie, B., and Parent, A., 1991, Dopaminergic neurons expressing calbindin in normal and parkinsonian monkeys, *Neuroreport* **2**:601–604.

Liang, C.L., Sinton, C.M., and German, D.C., 1996, Midbrain dopaminergic neurons in the mouse: colocalization with Calbindin-D28K and calretinin, *Neuroscience* **75**:523–533.

Matsunaga, E., Katahira, T., and Nakamura, H., 2002, Role of Lmx1b and Wnt1 in mesencephalon and metencephalon development, *Development* **129**:5269–5277.

McRitchie, D.A., Hardman, C.D., and Halliday, G.M., 1996, Cytoarchitectural distribution of calcium binding proteins in midbrain dopaminergic regions of rats and humans, *J. Comp. Neurol*. **364**:121–150.

Nemoto, C., Hida, T., and Arai, R., 1999, Calretinin and calbindin-D28k in dopaminergic neurons of the rat midbrain: a triple-labeling immunohistochemical study, *Brain Res*. **846**:129–136.

Nunes, I., Tovmasian, L.T., Silva, R.M., Burke, R.E., and Goff, S.P., 2003, Pitx3 is required for development of substantia nigra dopaminergic neurons, *Proc. Natl. Acad. Sci. U S A* **100**:4245–4250.

Parent, A., 1996, The Midbrain, in: *Carpenter's Human Neuroanatomy*, Parent A, ed, Williams and Wilkins, Media, pp 527–582.

Reisert, I., Schuster, R., Zienecker, R., and Pilgrim, C., 1990, Prenatal development of mesencephalic and diencephalic dopaminergic systems in the male and female rat, *Brain Res. Dev. Brain Res*. **53**:222–229.

Rieger, D.K., Reichenberger, E., McLean, W., Sidow, A., and Olsen, B.R., 2001, A double-deletion mutation in the Pitx3 gene causes arrested lens development in aphakia mice, *Genomics*. **72**:61–72.

Rogers, J.H., and Resibois, A., 1992, Calretinin and calbindin-D28k in rat brain: patterns of partial colocalization, *Neuroscience* **51**:843–865.

Rymar, V.V., Sasseville, R., Luk, K.C., and Sadikot, A.F., 2004, Neurogenesis and stereological morphometry of calretinin-immunoreactive GABAergic interneurons of the neostriatum, *J. Comp. Neurol*. **469**:325–339.

Sanghera, M.K., Manaye, K., McMahon, A., Sonsalla, P.K., and German, D.C., 1997, Dopamine transporter mRNA levels are high in midbrain neurons vulnerable to MPTP, *Neuroreport* **8**:3327–3331.

Saucedo-Cardenas, O., Quintana-Hau, J.D., Le, W.D., Smidt, M.P., Cox, J.J., De Mayo, F., Burbach, J.P., and Conneely, O.M., 1998, Nurr1 is essential for the induction of the dopaminergic phenotype and the survival of ventral mesencephalic late dopaminergic precursor neurons, *Proc. Natl. Acad. Sci. U S A* **95**:4013–4018.

Semina, E.V., Murray, J.C., Reiter, R., Hrstka, R.F., and Graw, J., 2000, Deletion in the promoter region and altered expression of Pitx3 homeobox gene in aphakia mice, *Hum. Mol. Genet*. **9**:1575–1585.

Simon, H.H., Saueressig, H., Wurst, W., Goulding, M.D., and O'Leary, D.D., 2001, Fate of midbrain dopaminergic neurons controlled by the engrailed genes, *J. Neurosci*. **21**:3126–3134.

Simon, H.H., Bhatt, L., Gherbassi, D., Sgado, P., and Alberi, L., 2003, Midbrain dopaminergic neurons: determination of their developmental fate by transcription factors, *Ann. N Y Acad. Sci*. **991**:36–47.

Smidt, M.P., Smits, S.M., Bouwmeester, H., Hamers, F.P., van der Linden, A.J., Hellemons, A.J., Graw, J., and Burbach, J.P., 2004, Early developmental failure of substantia nigra dopamine neurons in mice lacking the homeodomain gene Pitx3, *Development* **131**:1145–1155.

Smidt, M.P., van Schaick, H.S., Lanctot, C., Tremblay, J.J., Cox, J.J., van der Kleij, A.A., Wolterink, G., Drouin, J., and Burbach, J.P., 1997, A homeodomain gene Ptx3 has highly restricted brain expression in mesencephalic dopaminergic neurons, *Proc. Natl. Acad. Sci. U S A* **94**:13305–13310.

Tan, Y., Williams, E.S., and Zahm, D.S., 1999, Calbindin-D 28kD immunofluorescence in ventral mesencephalic neurons labeled following injections of Fluoro-Gold in nucleus accumbens subterritories: inverse relationship relative to known neurotoxin vulnerabilities, *Brain Res*. **844**:67–77.

van den Munckhof, P., Luk, K.C., Ste-Marie, L., Montgomery, J., Blanchet, P.J., Sadikot, A.F., and Drouin, J., 2003, Pitx3 is required for motor activity and for survival of a subset of midbrain dopaminergic neurons, *Development* **130**:2535–2542.

Yamada, T., McGeer, P.L., Baimbridge, K.G., and McGeer, E.G., 1990, Relative sparing in Parkinson's disease of substantia nigra dopamine neurons containing calbindin-D28K, *Brain Res*. **526**:303–307.

Zetterstrom, R.H., Solomin, L., Jansson, L., Hoffer, B.J., Olson, L., and Perlmann, T., 1997, Dopamine neuron agenesis in Nurr1-deficient mice, *Science* **276**:248–250.

D1-DOPAMINE RECEPTOR SUPERSENSITIVITY IN THE DOPAMINE-DEPLETED STRIATUM INVOLVES A NOVEL ACTIVATION OF ERK1/2

Charles R. Gerfen*

1. ABSTRACT

A key feature of basal ganglia organization is the existence of the "direct" and "indirect" pathways, which arise from two distinct intermingled populations of medium spiny neurons within the striatum and connect either directly or indirectly with the output nuclei of the basal ganglia. Physiologically, these neuron populations are often indistinguishable as both respond similarly to excitatory inputs from the cortex. On the other hand, they display very distinct responses mediated by signal transduction systems, which are responsible for gene expression changes underlying long term neuronal plasticity. These differences are due to the clear segregation of D1 and D2 dopamine receptor (D1r and D2r) subtypes, respectively to direct and indirect striatal projection neurons. The opposing functional effects of dopamine on these striatal projection neurons is evident following lesions of the nigrostriatal dopamine system, which results in increases in gene expression in the D2 receptor-expressing indirect projection neurons and suppression of gene expression in D1 receptor-expressing direct projection neurons. Treatments with D2 receptor agonists normalize gene expression in indirect projection neurons. However, D1 agonist treatment results in a supersensitive response in direct pathway neurons. This D1 receptor supersensitive response in the dopamine-depleted striatum is distinct from D1 receptor response in the dopamine-intact striatum suggesting that there is an irreversible reorganization of the linkage between the D1 receptor and signal transduction systems. Our studies demonstrate that in the dopamine-depleted striatum the D1 supersensitive response is a consequence of a novel linkage of D1 receptors to the extracellular receptor kinase (ERK1/2).

2. INTRODUCTION

The importance the direct and indirect projection systems of the striatum in basal ganglia function was established by the theory that movement disorders such as Parkinson's

* Charles Gerfen, Section on Neuroanatomy, LSN, NIMH, 35 Convent Dr., Bethesda MD 20892, U.S.A.

Disease and Huntigton Chorea result from imbalances in the activity in these pathways (Albin et al., 1988). Experimental confirmation of this theory (Bergman et al., 1990) led to the initiation of new treatments of Parkinson's Disease, first with lesions of the globus pallidus and then subthalamic nucleus stimulation as effective therapeutic interventions. A critical feature of the basal ganglia model was the discovery that dopamine exerts opposing effects on the direct and indirect striatal pathways due to the segregation of D1r and D2r on the neurons giving rise to these pathways (Gerfen et al., 1990). While this finding was contested initially (Surmeier et al. 1992), it has been confirmed by a variety of methods, including immunohistochemical localization of the D1r and D2r proteins (Hersch et al., 1995) and single cell RT-PCR (Surmeier et al., 1996). Recently, the development of transgenic mice in which large portions of the chromosomes that include either the D1r or D2r genes, have been incorporated into bacterial artificial chromosomes (BACs) and manipulated to express green fluorescent protein (GFP) are incorporated into transgenic mice, have provided definitive confirmation of the segregation of D1r and D2r to the direct and indirect striatal projection neurons (Gong et al., 2002). In these BAC-GFP transgenic mice, GFP is expressed not only in the neuron cell bodies and dendrites, but in their axonal projections as well. In D2-BAC-GFP mice, GFP-positive neurons are densely distributed throughout the striatum, and projection axons are labeled that densely fill the neuropil of the external segment of the globus pallidus. Consistent with the restriction of D2r to the indirect pathway neurons, in the D2-BAC-GFP transgenic mice GFP labeled axons do not extend beyond the globus pallidus. In stark contrast, in D1-BAC-GFP transgenic mice, GFP labeling from striatal neurons extends in axons that spread through the globus pallidus, and extend caudally to fill the internal segment of the globus pallidus and the substantia nigra (Figure 1). This pattern of labeling directly matches the pattern of the distribution of axons of the direct and indirect striatal projection neurons that are observed when individual neurons are filled with tracer by intracellular recording methods (Kawaguchi et al. 1990). Taken together these studies provide definitive evidence of the segregation of D1r and D2r to the direct and indirect striatal projection neurons.

The opposing effects of dopamine on direct and indirect striatal projection neurons was demonstrated by the finding that following lesions of the nigrostriatal dopamine system, levels of mRNA encoding peptides expressed by these neurons were differentially altered (Young et al., 1986). Levels of mRNA encoding enkephalin, which is selectively expressed by indirect projection neurons, were elevated following dopamine lesions of the striatum, whereas levels of mRNA encoding substance P, which is selectively expressed by direct projection neurons, were decreased. The subsequent finding of the co-expression of the D1r with substance P in direct projection neurons, and the co-expression of the D2r with enkephalin in indirect pathway neurons provided an explanation of the changes in peptide levels following dopamine depletion (Gerfen et al., 1990). Treatment of animals with striatal dopamine lesions with selective D1r and D2r agonists normalized the levels of expression of substance P and enkephalin, respectively (Gerfen et al., 1990).

3. DOPAMINE RECEPTOR SUPERSENSITIVITY

While selective D1r and D2r agonist treatments normalize some of the gene changes that result from dopamine-depletion in the striatum, there are other effects that persist. For example, levels of the peptide dynorphin, which is also selectively coexpressed with substance P and D1r in direct pathway neurons, are elevated to very high levels in the

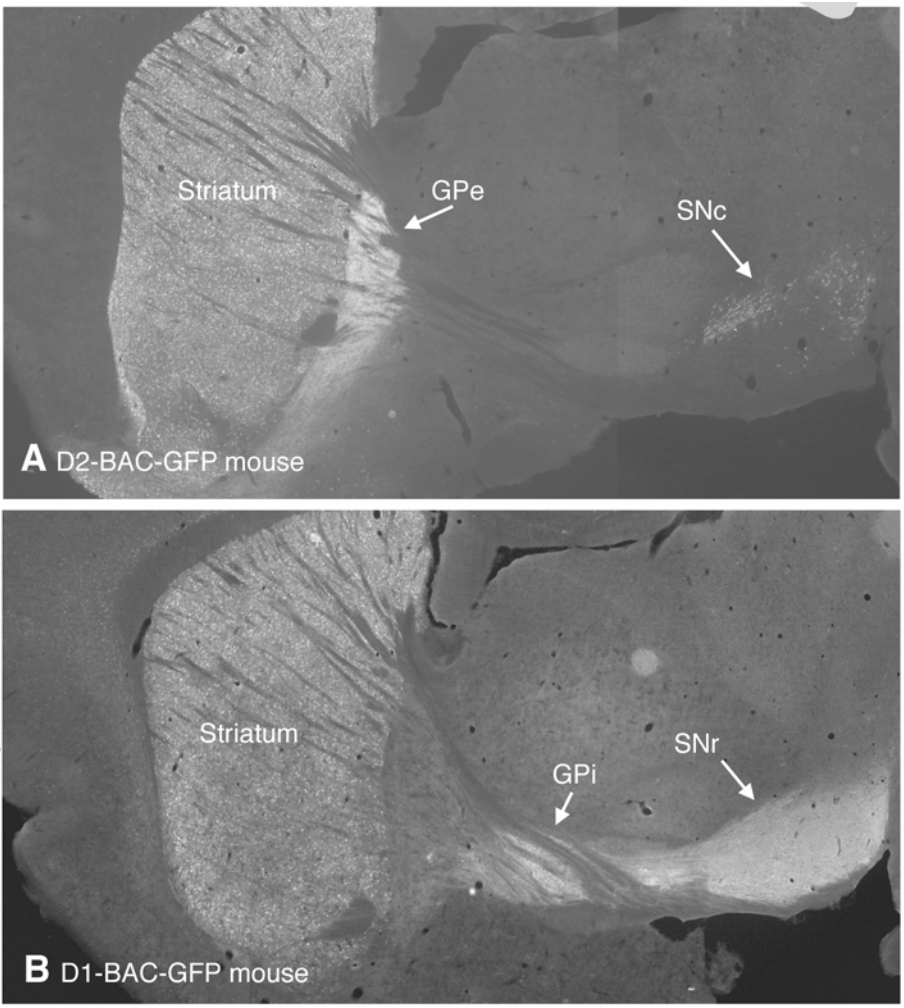

Figure 1. Sagittal sections showing GFP labeling in D2-BAC-GFP (A) and D1-BAC-GFP (B) transgenic mice. A) In D2-BAC-GFP mice indirect pathway striatal projection neurons are labeled throughout the striatum and their axonal projections are seen to terminate within the external segment of the globus pallidus (GPe) but do not extend caudally. Dopamine-neurons in the substantia nigra pars compacta (SNc) are also labeled. B) In D1-BAC-GFP mice direct pathway striatal projection neurons are labeled and their axonal projections are seen to pass through the external segment of the globus pallidus and to provide dense innervation of the internal segment of the globus pallidus (GPi) and substantia nigra pars reticulata (SNr).

dopamine-depleted striatum following D1r agonist treatments (Gerfen et al., 1990). Moreover, D1r agonist treatments result in a very robust induction of immediate early genes (IEGs), such as c-fos in the dopamine-depleted striatum (Berke et al., 1998). This D1r agonist induction of IEGs in the dopamine-depleted striatum is considered to be a supersensitive response as doses of D1r agonists that produce little IEG induction in the dopamine-intact striatum produce a robust IEG induction in the dopamine-depleted

striatum (Gerfen et al., 1995). The concept of dopamine-receptor supersensitivity was first introduced with the unilateral 6-hydroxydopamine (6-OHDA) lesion of the nigrostriatal pathway model by Ungerstedt and his colleagues (Ungerstedt et al., 1975). They made the seminal observation that rats with unilateral dopamine lesions display a postural deviation toward the side of the lesion, and that treatment with dopamine receptor agonists result in a pronounced contralateral rotation away from the lesioned side. This led to the idea that striatal neurons compensated for the loss of dopamine by producing more dopamine receptors, which was responsible for the contralateral rotation. However, following dopamine depletion, levels of mRNA encoding D1r in direct pathway neurons actually decrease while levels of mRNA encoding D2r in indirect pathway neurons increase, as do the genes encoding peptides in these neurons (Gerfen et al., 1990). These changes in gene expression appear to be due to the absence of the effects of dopamine on striatal neurons following dopamine-depletion. Thus, the absence of activation of D1r, which is coupled through the stimulatory G protein to activate adenylate cyclase, results in decreased gene expression, whereas the absence of activation of D2r, which is coupled through the inhibitory G protein to inhibit adenylate cyclase, results in increased gene expression. Following a single treatment of D1r agonist, D1r levels increase above normal, but the D1r supersensitive response occurs prior to this increase. Consequently D1r supersensitive induction is not due to increased D1r, but to some other change in the linkage of the receptor to signal transduction mechanisms.

The D1r supersensitive response in the dopamine-depleted striatum as measured by the induction of IEGs is distinct from the D1r response in the dopamine-intact striatum in a number of ways. First, is the robustness of the response in the dopamine-depleted compared to the dopamine-intact striatum. Doses of D1r agonists that produce little IEG induction in the dopamine-intact striatum induce IEGs in most D1r-bearing direct pathway neurons in the dorsal striatum in the dopamine-lesioned striatum (Gerfen et al., 1995). Induction of IEGs in the dopamine-intact striatum is produced not only by psychostimulant treatments, but by combined D1r and D2r agonists (LaHoste and Marshall, 1993), and by the use of relatively high doses of full D1r agonists, particularly when combined with D2r agonists or scopolamine (Wang and McGinty, 1996). However, these treatments rarely approach the robustness of the IEG response to D1r agonist alone in the dopamine-depleted striatum, in either the level of induction per cell or the number of neurons responding. Second, psychostimulants such as cocaine produce a substantive induction of IEGs, by a D1r-mediated mechanism, in the dopamine-intact dorsal striatum. However, repeated cocaine treatments produce a diminishing IEG response (Steiner and Gerfen, 1993). In contrast, in the dopamine-depleted striatum, the D1r agonist induction of IEGs does not desensitize with repeated treatments (Steiner and Gerfen, 1996). Thirdly, psychostimulant induction of IEGs in the dorsal striatum requires co-activation of both D1r and glutamate NMDA receptors (Konradi et al., 1996), whereas D1r agonist IEG induction in the dopamine-depleted striatum occurs independently of NMDA receptors (Keefe and Gerfen, 1996). Fourth, the cyclic AMP response element-binding protein (CREB) is required for D1r IEG induction in the dopamine-intact striatum, but not in the dopamine-depleted striatum (Andersson et al., 2001). Taken together these results suggest that the linkage of D1r to signal transduction mechanisms responsible for IEG induction is different in the dopamine-intact and – depleted striatum.

Recently we have demonstrated that a novel linkage between D1r and activation of the extracellular receptor kinase (ERK1/2) is responsible for the D1r supersensitive response in the dopamine-depleted dorsal striatum (Gerfen et al., 2002). Activation of ERK1/2 of striatal neurons was first demonstrated in response to corticostriatal stimulation, mediated

by glutamatergic NMDA receptors (Sgambato et al., 1998). Activation of ERK1/2 is demonstrated by immunohistochemical localization of the phosphorylated form of ERK1/2, which occurs when the MAPkinase kinase (MEK) phosphorylated ERK1/2. We investigated the activation of ERK1/2 in the normal and dopamine-depleted striatum in response to D1r agonist treatments. In this experimental paradigm, which reveals D1r supersensitive responses, treatment with the partial D1r agonist SKF 38393 (5 mg/kg), resulted in phospho-ERK1/2 immunoreactive neurons throughout the striatum of the dopamine-depleted striatum, with little to no immunoreactive neurons present in the dopamine-intact striatum (Gerfen et al., 2002). In the dopamine-depleted striatum activated ERK1/2 was specifically localized to direct striatal pathway neurons. Moreover, inhibition of MEK, which is responsible for phosphorylation of ERK1/2, administered either systemically, or directly into the striatum, blocked D1r agonist induction of IEGs in the dopamine-depleted striatum (Figure 2). While these results identified D1r activation of ERK1/2 in the dopaminedepleted D1r supersensitive response, it did not distinguish it from the more than 30 other IEGs and gene products that are activated by D1r-mediated mechanisms in the dopamineintact and –depleted striatum (Berke et al., 1998).

The demonstration that activation of ERK1/2 represents a novel linkage to D1r in the dopamine-depleted striatum was established by using pharmacologic and other treatments that produce activation of the normal linkage of D1r to signal transduction mechanisms to produce IEG induction. In the normal striatum, D1r are linked through stimulatory GTP binding protein complex to the activation of adenylate cyclase, which results in cyclic AMP activation of protein kinase A and subsequent CREB mediated induction of IEGs

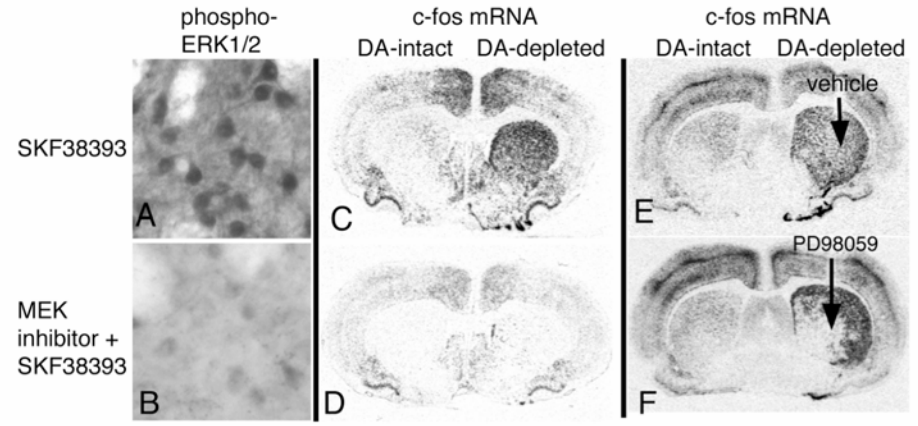

Figure 2. Inhibition by MEK inhibitors of D1r agonist mediated phosphorylation of ERK1/2 and c-fos IEG induction in the dopamine(DA)-depleted striatum. Animals received either saline control or a systemic treatment with the MEK inhibitor SL327 (60 mg/kg/ip) 30 min prior to treatment with the D1r agonist SKF38393 (5 mg/kg). Compared to controls, this MEK inhibitor significantly reduces the phosphorylation of ERK1/2 (A,B) in the dopamine depleted striatum at 15 minutes. This treatment also blocks the later induction of mRNAs encoding the IEGs c-fos (C,D) at 45 minutes following agonist treatment. In a second experiment, either vehicle (E) or the MEK inhibitor PD98059 (F, 100 µM) was infused into the dopamine depleted striatum of animals prior to and following systemic treatment with the D1r agonist SKF38393 (1 mg/kg/ip). Animals were killed 45 min following agoinst treatment. Contrasted with intra-striatal infusion of vehicle (G), MEK inhibitor blocked D1r agonist-induced mRNA encoding c-fos (H) around the infusion site. From Gerfen et al., 2002.

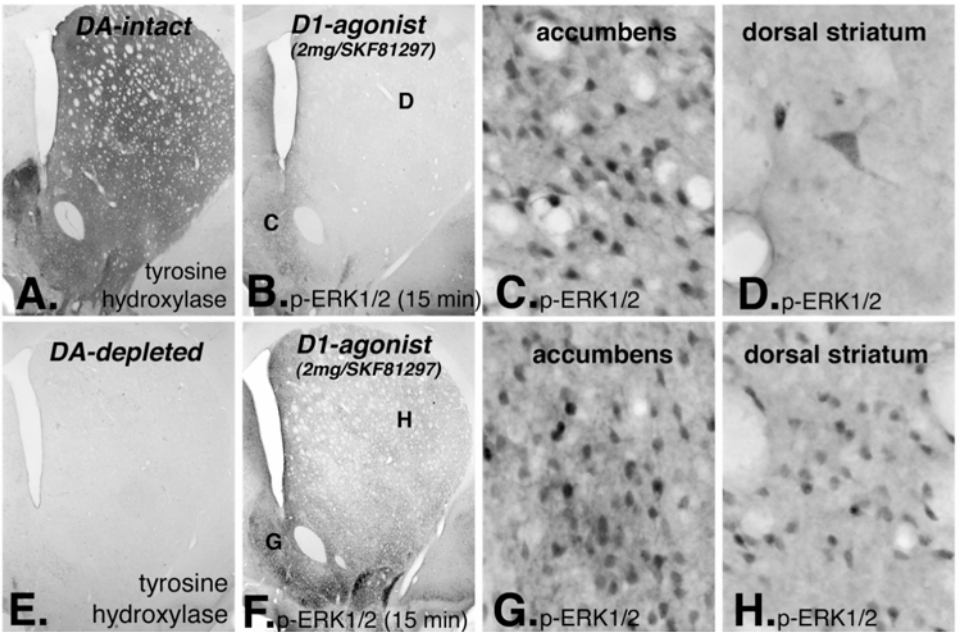

Figure 3. In the dopamine-intact striatum (A, indicated by tyrosine hydroxylase immmunoreactivity), animals killed 15 min after treatment with the full D1r agonist SKF81297 (2.0 mg/kg) display p-ERK1/2 immunoreactivity only in the nucleus accumbens (B). Higher power images reveal numerous immunoreactive projection neurons in the nucleus accumbens (C), whereas in the dorsal striatum, only scattered large immunoreactive neurons are observed (D). In the dopamine-depleted striatum (E, indicated by the absence of tyrosine hydroxylase-immunoreactive fibers), treatment with the full D1r agonist SKF81297 (2.0 mg/kg) display p-ERK1/2 immunoreactivity throughout the nucleus accumbens and dorsal striatum (F). Higher power images reveal numerous immunoreactive medium sized projection neurons in the nucleus accumbens (G) and in the dorsal striatum (H). From Gerfen et al., 2002.

(Konradi et al., 1996; Andersson et al., 2001). While the partial D1r agonist SKF38393 produces little IEG induction in the dopamine-intact striatum, the full D1r agonist, SKF 81297 either alone at doses between 2–5 mg/kg, or when combined with D2r agonists or the muscarinic antagonist scopolamine, produces an IEG response in the dopamine-intact striatum that is comparable to the robust IEG induction in the dopamine-depleted striatum (Wang and McGinty, 1996). Using each of these treatments, we demonstrated that there was a robust induction of the IEG c-fos in most D1r bearing neurons throughout the dopamine-intact striatum, but that activation of ERK1/2 occurred only in the nucleus accumbens (Figure 4). In stark contrast, in the dopamine-depleted striatum, in response to the same treatments, ERK1/2 activation was present in nearly all D1r neurons in the dopamine-depleted dorsal striatum.

To provide a more physiologically relevant test of dopamine-mediated activation of ERK1/2 in the normal striatum, we used an experimental paradigm to stimulate the nigrostriatal dopamine pathway with either electrical or chemical stimuli. Using these paradigms, stimulation of the nigrostriatal dopamine pathway produces robust induction of c-fos

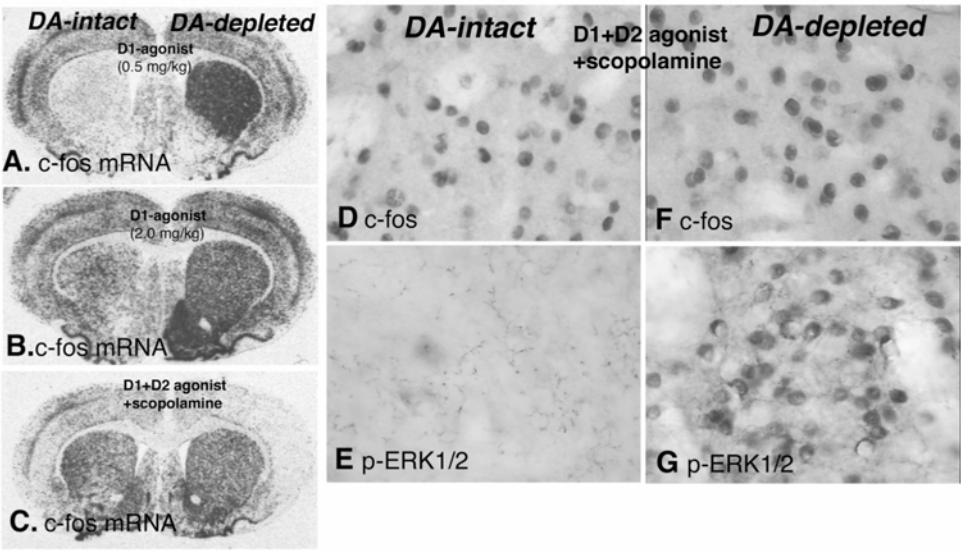

Figure 4. Demonstration of distinct mechanisms of D1r mediated gene regulation in the dopamine (DA)-intact and -depleted striatum, using the full D1r agonist, SKF81297, alone or combined with other drugs. (A–C) In situ hybridization histochemical localization of mRNA encoding c-fos 45 min following different drug combinations: A) SKF81297 (0.5 mg/kg), B) SKF81297 (2.0 mg/kg), C) SKF81297 (2.0 mg/kg) combined with the D2r agonist quinpirole (1 mg/kg) and scopolamine (10 mg/kg). The low dose of agonist alone (A) demonstrates the supersensitive response by the selective induction of c-fos in the dopamine-depleted striatum. Bilateral induction of c-fos IEG in both the dopamine-intact and -depleted striatum follows treatment with high dose of the full d1 agonist alone (B) or in combination with other drugs (C). However, when animals receiving any of these treatments are killed at 15 min, p-ERK1/2-immunoreactive neurons are evident only in the dopamine-depleted striatum, and not in the dopamine-intact striatum (not shown). The treatment combining full D1 agonist with both the D2 agonist and scopolamine produces a robust c-fos IEG response in the dopamine-intact (D) and depleted (F) striatum. This treatment does not activate p-ERK1/2 in neurons in the dopamine-intact striatum (E) but does activate p-ERK1/2 in the dopamine-depleted striatum (G). From Gerfen et al., 2002.

throughout the striatum and nucleus accumbens (Figure 5). However, as with the full D1r agonist treatments, activation of ERK1/2 in striatal projection neurons does not occur throughout the dorsal striatum, but is restricted to the nucleus accumbens. Taken together these results, which employ both pharmacologic treatments with D1r agonists and direct stimulation of the nigrostriatal dopamine pathway, demonstrate that in the normal dopamine-intact dorsal striatum, D1 dopamine receptors are not normally linked to activation of the ERK1/2 signaling pathway. Moreover, D1r activation of ERK1/2 does occur in the normal nucleus accumbens, suggesting a regional differences in the striatum in the mechanisms linking D1r to signal transduction systems (Gerfen et al., 2002).

Several studies have reported that psychostimulants, including cocaine and d-amphetamine, activate ERK1/2 through a D1r-mediated mechanism, primarily in the nucleus accumbens but also in the dorsal striatum (Valjent et al., 2000; 2005). Several points are worth making concerning these reports, which would seem to be at odds with the assertion that in the dorsal striatum, D1r is not normally linked to activation of ERK1/2. First, psychostimulant activation of ERK1/2 appears to be dependent on both D1r and

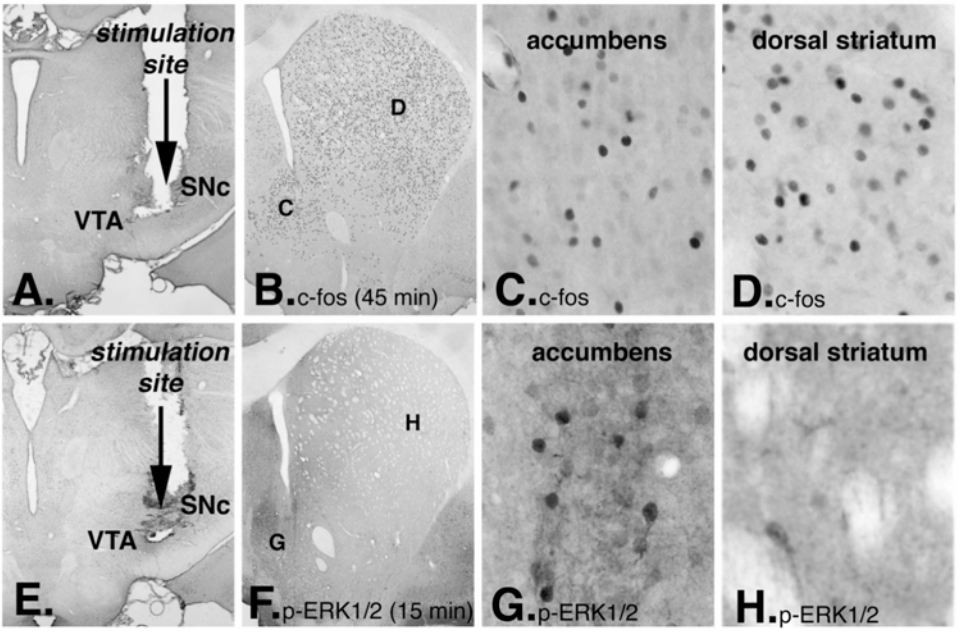

Figure 5. Electrical stimulation of the nigrostriatal pathway results in the induction of the IEG c-fos throughout the striatum and nucleus accumbens, but activation of ERK1/2 occurs only in the nucleus accumbens. Electrodes were placed amongst dopamine neurons in the ventral tegmental area (VTA) and substantia nigra pars compacta (SNc) (A,E). In animals killed 45 minutes after stimulation onset (A–D), the IEG c-fos is induced throughout the dorsal striatum and nucleus accumbens (B). Higher power images reveal c-fos immunoreactive nuclei in the nucleus accumbens (C) and in the dorsal striatum (D). In animals killed 15 minutes after stimulation (E–H), the time point that is optimal for detecting p-ERK1/2, immunoreactive neurons are observed only in the nucleus accumbens (F). Higher power images reveal numerous immunoreactive neurons in the nucleus accumbens (G), whereas in the dorsal striatum, only scattered large neurons are observed (H).

glutamate NMDA receptor mediated mechanisms (Valjent et al., 2000; 2005), while D1r activation of ERK1/2 in the dopamine-depleted striatum is NMDA receptor independent (Gerfen et al., 2002). Second, the doses of psychostimulants required to produce substantive activation of ERK1/2 in the dorsal striatum are relatively high (20–30 mg/kg cocaine and 10 mg/kg d-amphetamine), which raises the possibility of non-dopaminergic mechanisms being involved. Third, psychostimulant treatments may also result in stimulation of corticostriatal or other striatal afferent systems, which are known to be involved in the activation of ERK1/2 (Sgambato et al., 1998). Finally, even at the relatively high doses of psychostimulants used, the proportion of D1r-bearing direct pathway neurons that display activated ERK1/2 is on the order of 10–30% of the total population of these neurons (Valjent et al., 2000), whereas in the dopamine-depleted D1r response, virtually all of D1r bearing neurons display activated ERK/2 (Gerfen et al., 2002). Further studies are required to resolve the discrepancies between psychostimulant activation of ERK1/2 from D1r treatment paradigms. However, both treatment paradigms point to substantive differences in the nucleus accumbens and dorsal striatum in the linkage between D1r and activation of the ERK1/2 signaling system.

Activation of ERK1/2 has been implicated as an important intracellular signaling system that alters transcriptional states thought to underlie long term changes in synaptic plasticity (Impey et al., 1999; Adams and Sweatt, 2002; Thomas and Huganir, 2004). Psychostimulant activation of ERK1/2 has been implicated in the rewarding effects of cocaine, suggesting that its effects on synaptic plasticity may be involved in the addictive properties of psychostimulants (Valjent et al., 2005). Our studies point to important differences between D1r mediated activation of ERK1/2 in the nucleus accumbens and the dorsal striatum in suggesting that such activation is present in the latter region following dopamine-depletion. We propose that the linkage of D1 receptors to activation of ERK1/2 in animal models of Parkinson's Disease results in an abnormal form of neuronal plasticity in the dorsal striatum in direct striatal projection neurons. L-DOPA treatment for Parkinson's disease would result in repeated activation of this abnormal form of neuronal plasticity in direct pathway neurons, which we propose may underlie the development of dyskinesias.

4. REFERENCES

Adams, J.P., and Sweatt, J.D., 2002, Molecular psychology: roles for the ERK MAP kinase cascade in memory, *Annu. Rev. Pharmacol. Toxicol.* **42**:135–163.

Albin, R.L., Young, A.B., and Penney, J.B., 1989, The functional anatomy of basal ganglia disorders, *Trends Neurosci.* **12**:366–375.

Andersson, M., Konradi, C., and Cenci, M.A., 2001, cAMP response element-binding protein is required for dopamine-dependent gene expression in the intact but not the dopamine-denervated striatum, *J. Neurosci*. **21**:9930–9943.

Bergman, H., Wichmann, T., and DeLong, M.R., 1990, Reversal of experimental parkinsonism by lesions of the subthalamic nucleus, *Science* **249**:1436–1438.

Berke, J.D., Paletzki, R.F., Aronson, G.J., Hyman, S.E., and Gerfen, C.R., 1998, A complex program of striatal gene expression induced by dopaminergic stimulation, *J. Neurosci.* **18**:5301–5310.

Gerfen, C.R., Engber, T.M., Mahan, L.C., Susel, Z., Chase, T.N., Monsma, F.J. Jr., and Sibley, D.R., 1990, D1 and D2 dopamine receptor-regulated gene expression of striatonigral and striatopallidal neurons [see comments], *Science* **250**:1429–1432.

Gerfen, C.R., Keefe, K.A., and Gauda, E.B., 1995, D1 and D2 dopamine receptor function in the striatum: coactivation of D1- and D2-dopamine receptors on separate populations of neurons results in potentiated immediate early gene response in D1-containing neurons, *J. Neurosci.* **15**:8167–8176.

Gerfen, C.R., Miyachi, S., Paletzki, R., and Brown, P. 2002, D1 Dopamine receptor supersensitivity in the dopamine-depleted striatum results from a switch in the regulation of ERK1/2/MAP kinase, *J. Neurosci.* **22**:5042–5054.

Gong, S., Zheng, C., Doughty, M.L., Losos, K., Didkovsky, N., Schambra, U.B., Nowak, N.J., Joyner, A., Leblanc, G., Hatten, M.E., and Heintz, N., 2003, A gene expression atlas of the central nervous system based on bacterial artificial chromosomes, *Nature* **425**:917–925.

Hersch, S.M., Ciliax, B.J., Gutekunst, C.A., Rees, H.D., Heilman, C.J., Yung, K.K., Bolam, J.P., Ince, E., Yi, H., and Levey, A.I., 1995, Electron microscopic analysis of D1 and D2 dopamine receptor proteins in the dorsal striatum and their synaptic relationships with motor corticostriatal afferents, *J. Neurosci*. **15**:5222–5237.

Impey, S., Obrietan, K., and Storm, D.R., 1999, Making new connections: role of ERK/MAP kinase signaling in neuronal plasticity, *Neuron* **23**:11–14.

Kawaguchi, Y., Wilson, C.J., and Emson, P.C., 1990, Projection subtypes of rat neostriatal matrix cells revealed by intracellular injection of biocytin, *J. Neurosci*. **10**:3421–3438.

Kebabian, J.W., and Calne, D.B., 1979, Multiple receptors for dopamine, *Nature* **277**:93–96.

Keefe, K.A., and Gerfen, C.R., 1996, D1 dopamine receptor-mediated induction of zif268 and c-fos in the dopamine-depleted striatum: differential regulation and independence from NMDA receptors, *J. Comp. Neurol*. **367**:165–176.

Konradi, C., Leveque, J.C., and Hyman, S.E., 1996, Amphetamine and dopamine-induced immediate early gene expression in striatal neurons depends on postsynaptic NMDA receptors and calcium, *J. Neurosci*. **16**:4231–4239.

LaHoste, G.J., and Marshall, J.F., 1993, Striatal Fos expression is indicative of dopamine D1/D2 synergism and receptor supersensitivity. *Proc. Natl. Acad. Sci. U S A* **90**:7451–7455.

Sgambato, V., Pages, C., Rogard, M., Besson, M.J., and Caboche, J., 1998, Extracellular signal-regulated kinase (ERK) controls immediate early gene induction on corticostriatal stimulation, *J. Neurosci*. **18**:8814–8825.

Steiner, H., and Gerfen, C.R., 1993, Cocaine-induced c-fos messenger RNA is inversely related to dynorphin expression in striatum, *J. Neurosci*. **13**:5066–5081.

Steiner, H., and Gerfen, C.R., 1996, Dynorphin regulates D1 dopamine receptor-mediated responses in the striatum: relative contributions of pre- and postsynaptic mechanisms in dorsal and ventral striatum demonstrated by altered immediate-early gene induction, *J. Comp. Neurol.* **376**:530–541.

Surmeier, D.J., Song, W.J., and Yan, Z., 1996, Coordinated expression of dopamine receptors in neostriatal medium spiny neurons, *J. Neurosci*. **16**:6579–6591.

Surmeier, D.J., Eberwine, J., Wilson, C.J., Cao, Y., Stefani, A., and Kitai, S.T., 1992, Dopamine receptor subtypes colocalize in rat striatonigral neurons, *Proc. Natl. Acad. Sci. U S A* **89**:10178–10182.

Thomas, G.M., and Huganir, R.L., 2004, MAPK cascade signalling and synaptic plasticity, *Nat. Rev. Neurosci*. **5**:173–183.

Ungerstedt, U., Ljungberg, T., Hoffer, B., and Siggins, G., 1975, Dopaminergic supersensitivity in the striatum, *Adv. Neurol*. **9**:57–65.

Valjent, E., Corvol, J.C., Pages, C., Besson, M.J., Maldonado, R., and Caboche, J., 2000, Involvement of the extracellular signal-regulated kinase cascade for cocaine-rewarding properties, *J. Neurosci.* **20**:8701–8709.

Valjent, E., Pascoli, V., Svenningsson, P., Paul, S., Enslen, H., Corvol, J.C., Stipanovich, A., Caboche, J., Lombroso, P.J., Nairn, A.C., Greengard, P., Herve, D., and Girault, J.A. 2005, Regulation of a protein phosphatase cascade allows convergent dopamine and glutamate signals to activate ERK in the striatum, *Proc. Natl. Acad. Sci. U S A* **102**:491–496.

Wang, J.Q., and McGinty, J.F., 1996, Scopolamine augments c-fos and zif/268 messenger RNA expression induced by the full D1 dopamine receptor agonist SKF-82958 in the intact rat striatum, *Neuroscience* **72**:601–616.

DO SYSTEMICALLY ADMINISTERED GLUTAMATE ANTAGONISTS AFFECT SUBTHALAMIC NUCLEUS ACTIVITY?

Relevance to pharmacotherapy of Parkinson's disease

Kelly A. Allers[1], Debra A. Bergstrom, Leyla J. Ghazi, Deborah S. Kreiss[2], and Judith R. Walters*

1. INTRODUCTION

In animal models of Parkinson's disease (PD), subthalamic (STN) neurons have been shown to have increased firing rates and abnormal firing patterns (Miller and DeLong, 1987; Hollerman and Grace, 1992; Bergman et al., 1994; Hassani et al., 1996; Kreiss et al., 1997; Bezard et al., 1999; Allers et al., 2000, 2005; Perier et al., 2000; Villa et al., 2000; Magill et al., 2001; Ni et al., 2001; Tai et al., 2003; Hu et al., 2004; Walters et al., this volume). It is thought that lesion or deep brain stimulation (DBS) of the STN is beneficial in PD because these procedures attenuate or disrupt similar changes in STN firing rates and patterns in PD patients. Ideally, effective attenuation of STN activity could also be induced by pharmacological agents, avoiding the risks associated with surgery. Several observations support the hypothesis that glutamate antagonists may be useful in this regard and may exert effects similar to those induced by STN lesion or DBS (Greenamyre and O'Brien, 1991). This chapter will review these observations and present results from recent studies in a rodent model of PD investigating the neurophysiological effects of glutamate NMDA antagonists on STN neuronal activity.

A number of anatomical considerations support the potential therapeutic benefit of glutamate antagonists in PD. First, STN neurons use glutamate as a neurotransmitter and innervate the basal ganglia output nuclei, the internal globus pallidus and the substantia nigra pars reticulata. Thus, glutamate antagonists have the potential to produce a pharmacological STN lesion as they could block the aberrant glutamate-driven activity in the

* Neurophysiological Pharmacology Section, National Institute of Neurological Disorders and Stroke, National Institutes of Health, Porter Neuroscience Center, Bethesda, MD 20892-3702, USA. Current addresses: [1]Kelly A. Allers, Discovery Biology, Pfizer Ltd., Ramsgate Road, Sandwich, CT13 9NJ, UK and [2]Deborah S. Kreiss, University of Tennessee at Chattanooga, Dept. of Biological and Environmental Sciences, 615 McCallie Avenue, 317H Holt Hall, Chattanooga, TX 37403-2598, USA.

output nuclei. Second, glutamate antagonists could be beneficial in PD by acting in the STN itself to normalize activity. The STN receives glutamatergic projections from the cortex, pedunculopontine nucleus and the thalamus that appear to be more active in PD and in animal models of PD (Orieux et al., 2000; Breit et al., 2001; Pelled et al., 2002). Third, glutamate antagonists could affect basal ganglia activity upstream from the STN. Chronic intermittent stimulation of D1 dopamine receptors, as occurs in PD patients receiving levodopa pharmacotherapy, produces changes in striatal NMDA receptor subunit expression and phosphorylation (Oh et al., 1998, 1999; Dunah et al., 2000). NMDA receptor antagonists can attenuate D1 dopamine receptor-stimulated changes in striatal output (Huang and Walters, 1992; Engber et al., 1994b; Keefe and Gerfen, 1996; Huang et al., 1998; Keefe and Ganguly, 1998; Campbell and Walker, 2001). Through the striatum's indirect output to the STN, via the external globus pallidus, this interaction of D1 receptor and NMDA receptor activities may be reflected in the firing activity of the STN.

Evidence from both the laboratory and the clinic points to the possibility that glutamate antagonists acting at the glutamate NMDA receptor subtype may have antiparkinsonian and antidyskinetic effects (Klockgether and Turski, 1989; Papa et al., 1995; Starr, 1995; Papa and Chase, 1996; Blanchet et al., 1997; Lange et al., 1997; Metman et al., 1998a; Blanchet, 2003). Early studies suggested that NMDA receptor antagonism increases locomotor activity (Clineschmidt et al., 1982), supporting the idea that blocking these receptors could be an effective antiparkinsonian strategy. However, data from animal models of PD have been less than conclusive regarding the behavioral effects of NMDA receptor antagonists, administered alone, as an antiparkinsonian treatment (Starr, 1995). On the other hand, it has been demonstrated that NMDA receptor antagonism alleviates or blocks the development of dopamine agonist-induced motor fluctuations in animal models of PD (Engber et al., 1994b; Papa et al., 1995; Marin et al., 1996: Papa and Chase, 1996; Blanchet et al., 1999; Tahar et al., 2004). Clinically, the hypothesis that NMDA antagonists might be beneficial in the treatment of PD is supported by studies with amantadine. This drug alleviates the dyskinetic side effects of chronic levodopa therapy, while having some antiparkinsonian properties as well (Schwab et al., 1969, 1972; Shannon et al., 1987; Danielczyk, 1995; Metman et al., 1998b, 1999; Luginger et al., 2000; Blanchet et al., 2003). Amantadine's clinical benefit is commonly attributed to its actions at the NMDA receptor, yet it is relatively weak as a noncompetitive NMDA antagonist and may affect other neurotransmitter systems at therapeutically relevant concentrations (Kornhuber et al., 1991; Danysz et al., 1997).

These considerations lead to an interest in the following questions: A) Does systemically administered MK801, a prototypical non-competitive NMDA antagonist, affect STN neuronal firing properties? B) Does systemically administered MK801 attenuate D1 dopamine receptor agonist-induced changes in STN firing properties? C) Does amantadine, an antiparkinsonian agent thought to act as a NMDA antagonist, have effects on STN firing properties and are these effects comparable to MK801? Results from recent neurophysiological studies in a rodent model of PD addressing these questions are discussed below.

2. DOES SYSTEMICALLY ADMINISTERED MK801, A PROTYPICAL NMDA ANTAGONIST, AFFECT STN FIRING PROPERTIES?

MK801 is a prototypical antagonist of the NMDA receptor and has been shown to be a more potent antagonist at this receptor than amantadine. Studies have demonstrated that

systemically administered MK801 reduces rotation behavior induced by levodopa in 6-hydroxydopamine (6-OHDA) lesioned rats and reverses catalepsy induced by dopamine antagonists (Papa et al., 1993, 1995; Engber et al., 1994b; Ossowska, 1994; Marin et al., 1996). MK801 also reverses levodopa-induced changes in cerebral metabolic activity within the STN itself (Engber et al., 1994a). Chronic infusion of MK801 directly into the STN reverses the metabolic changes and behavioural abnormalities induced by dopamine cell lesion (Blandini et al., 2001). These findings provided support for further studies on MK801 effects on the neurophysiology of STN neurons in a rodent PD model.

To examine the hypothesis that MK801-induced blockade of NMDA receptors attenuates dopamine lesion-induced increases and pattern changes in STN activity, single unit recording studies were performed in locally anesthetized, chemically immobilized rats with unilateral 6-OHDA-induced dopamine cell lesion of the substantia nigra pars compacta. MK801 was administered intravenously at a dose of 0.1 mg/kg while STN neuronal activity was recorded extracellularly in lesioned and neurologically intact rats. Overall, mean firing rates were not significantly changed in either group, although individual neurons showed rate increases and decreases (Allers et al., 2005). Two aspects of firing pattern were examined: interspike interval coefficient of variation (ISI CV) and multisecond (2–60 sec) oscillatory activity, a phenomenon frequently observed in the basal ganglia in this preparation (Ruskin et al., 1999a, 1999b, 2001, 2003; Allers et al., 2000, 2002, 2005; Walters et al., 2000). In intact animals, no significant alterations were observed in these measures (Table 1). However, in the dopamine lesioned rats, MK801 had a dramatic effect on the firing rate oscillations: MK801 significantly reduced the incidence of multisecond oscillations (Table 1), as illustrated in Figure 1. Periodic changes in firing rate on the multisecond time scale have been demonstrated in rat, monkey (Wichmann et al., 2002) and man (unpublished observations from recordings obtained from PD patients undergoing DBS surgery). In rat, these become more synchronized across several areas of the basal ganglia following

Table 1. Firing characteristics of STN neuronal activity in intact and dopamine neuron lesioned animals. Data are expressed as mean ± SEM with N in group in brackets. Intact rats: MK801, 0.1 mg/kg; SKF 38393, 20 mg/kg; amantadine, 20 mg/kg. Lesioned rats: MK801, 0.1 mg/kg; SKF 38393, 10 mg/kg; amantadine, 20 mg/kg. [a] significantly different from intact baseline values (t-test). [b] signifycantly different from pre-drug values (repeated measures ANOVA); [c] proportions significantly different compared to pre-drug values (χ^2); [d] significantly different from pre-drug values (paired t-test).

	BASELINE	MK801	SKF 38393t	SKF 38393 WITH MK801
INTACT				
Firing Rate (Hz)	9.0 ± 0.8 (88)	7.0 ± 1.6 (15)	16.1 ± 3.3[d] (14)	16.5 ± 2.8[b] (9)
Coefficient of Variation	1.21 ± 0.05 (88)	1.17 ± 0.09 (15)	1.28 ± 0.14 (14)	0.84 ± 0.09[b] (9)
Multisecond Oscillations (2–60 sec)	22.6 ± 2.1	17.5 ± 3.5	21.5 ± 3.9	N/A
(# *with osc/total N*)	(50/88) 57%	(7/15) 47%	(10/14) 71%	(0/9)*** 0%
LESIONED				
Firing Rate (Hz)	18.5 ± 1.5[a] (98)	20.4 ± 4.9 (10)	29.4 ± 5.0[d] (15)	22.4 ± 6.1 (10)
Coefficient of Variation	1.17 ± 0.06 (98)	0.84 ± 0.12 (10)	0.96 ± 0.08 (15)	0.68 ± 0.08[b] (10)
Multisecond Oscillations (2–60 sec)	20.0 ± 1.5	12.2	11.8 ± 1.8[a]	N/A
(# *with osc/total N*)	(60/98) 61%	(1/10)[c] 10%	(9/15) 60%	(0/10)[c] 0%

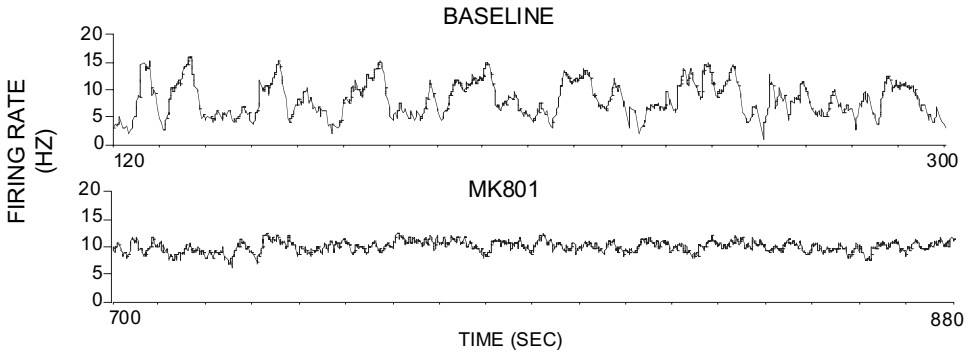

Figure 1. Rate histograms of STN neuronal activity recorded extracellularly in a dopamine cell lesioned rat before and after intravenous MK801 administration. In the pre-drug baseline condition, multisecond oscillatory activity with a cycle of 23.5 sec is present. Following MK801 administration (0.1 mg/kg), multisecond oscillations are eliminated but overall firing rate is unchanged. Data are binned at 2 sec. Periodic oscillatory activity was determined by Lomb periodogram analyses (Kaneoke and Vitek, 1996).

administration of drugs that increase levels of dopamine receptor stimulation (Ruskin et al., 1999a, 1999b, 2001, 2003; Allers et al., 2000; Walters et al., 2000). While the behavioral correlate of this phenomenon is unclear, MK801's ability to reduce the incidence of multisecond oscillations in the dopamine lesioned rats suggests an effect of MK801on basal ganglia network function in this preparation. MK801 also reduced the total power of activity within the theta frequency range in the STN in 6-OHDA lesioned rats (Allers et al., 2005). This latter effect is potentially important in the context of PD, as oscillatory activity in the theta range in the basal ganglia has been linked to tremor in PD patients (Hutchison et al., 1997).

In summary, data from studies investigating effects of MK801 on STN firing properties suggest that NMDA receptor antagonism alters the patterning of STN neuronal firing. In addition, results indicate that the functional effects of blocking these receptors change after dopamine denervation.

3. DOES SYSTEMICALLY ADMINISTERED MK801 ALTER D1 DOPAMINE RECEPTOR AGONIST INDUCED CHANGES IN STN FIRING PROPERTIES?

MK801 has been widely used to investigate dopamine-NMDA receptor interactions. In multiple studies in animal models of PD, MK801 attenuated D1 receptor-mediated effects, a property potentially beneficial in the context of an adjuvant therapy for PD. D1 receptor agonist administration has been shown to increase STN firing rates in neurologically intact rats, and this effect is also observed in 6-OHDA-lesioned rats, where rates are further increased by the D1 agonists beyond the elevated levels associated with the dopamine lesioned state (Kreiss et al., 1996, 1997; Allers et al., 2005).

To test whether NMDA receptor antagonism with MK801 could attenuate the rateincreasing effects of a D1 agonist, SKF38393, STN recordings were performed. The effects of SKF38393 alone were compared to the effects of SKF38393 following pretreatment with

MK801 in both intact and lesioned animals. In intact animals, pretreatment with MK801 had no effect on D1 agonist-induced increases in firing rate (Table 1). However, in lesioned animals, the D1 agonist-induced increases were significantly attenuated by MK801 pretreatment. When changes in firing pattern were examined, neither MK801 nor SKF38393 alone had significant effects on ISI CV or multisecond oscillations in intact rats. In contrast, changes in firing pattern were observed when MK801 and SKF38393 were coadministered to intact animals: ISI CV was significantly decreased by 42%, indicating increased regularity of firing, and multisecond oscillatory activity was eliminated. Similar results were also obtained in dopamine lesioned animals.

These data demonstrate that the combination of glutamate NMDA receptor blockade and D1 receptor stimulation can significantly alter the firing pattern of STN neurons. In addition, they show that in the dopamine denervated state NMDA receptor antagonism can effectively attenuate the marked STN rate increases induced by D1 receptor stimulation, a potentially beneficial effect for an adjuvant PD therapeutic agent.

4. DOES AMANTADINE HAVE EFFECTS ON STN FIRING PROPERTIES AND ARE THESE COMPARABLE TO THE PROTOTYPICAL NONCOMPETITIVE NMDA ANTAGONIST, MK801?

Amantadine has been shown to be an effective adjuvant treatment in PD as it has antiparkinsonian and antidyskinetic properties, and does not block the antiparkinsonian effects of levodopa (Schwab et al., 1969, 1972; Shannon et al., 1987; Danielczyk, 1995; Metman et al., 1998b, 1999; Luginger et al., 2000; Blanchet et al., 2003). Amantadine's clinical effectiveness is commonly attributed to its ability to act as a noncompetitive NMDA antagonist, yet it is relatively weak as an NMDA antagonist, and it may affect several other neurotransmitter systems at therapeutically relevant concentrations as well (Kornhuber et al., 1991; Danysz et al., 1997). These considerations lead to the question of how the effects of amantadine on STN neuronal activity would compare with those of MK801.

Single unit recordings studies showed, surprisingly, that amantadine induced significant increases in firing rates of STN neurons in both intact and dopamine lesioned rats (Figure 2). Mean rate increases of 84% and 96% were detected following administration of amantadine (20 mg/kg, i.v.) to intact (n = 9) and lesioned (n = 8) rats, respectively. The rate increases induced by amantadine in the lesioned rat were notable as they came on top of, and in addition to, the increases in STN firing rates associated with dopamine cell loss. Amantadine had no significant effect on spike regularity or oscillatory activity (Allers et al., 2005). Combined administration of amantadine and SKF38393 (n = 5) did not reduce the incidence of multisecond oscillations as was observed with MK801 and SKF38393 in both intact and lesioned animals. To explore the possibility that amantadine's rate increasing effects could be related to its ability to enhance the release of dopamine and/or block uptake (Bailey and Stone, 1975; Danysz et al., 1997), the effect of blocking D1 receptors on amantadine's rate increasing actions was investigated. Pretreatment with the D1 antagonist SCH23390 (0.5 mg/kg, i.v.) did not attenuate amantadine's rate increasing effects in intact animals; mean rate increases of 92% (n = 8) were still observed following amantadine's administration. In addition, amantadine did not reduce the firing rates of substantia nigra dopamine neurons (n = 6, 10–20 mg/kg, i.v.), suggesting no prominent D2 dopamine receptor stimulating properties. Overall, the effects of amantadine on STN neuronal firing rates are counterintuitive regarding adjuvant therapy for PD in that increased STN firing rates

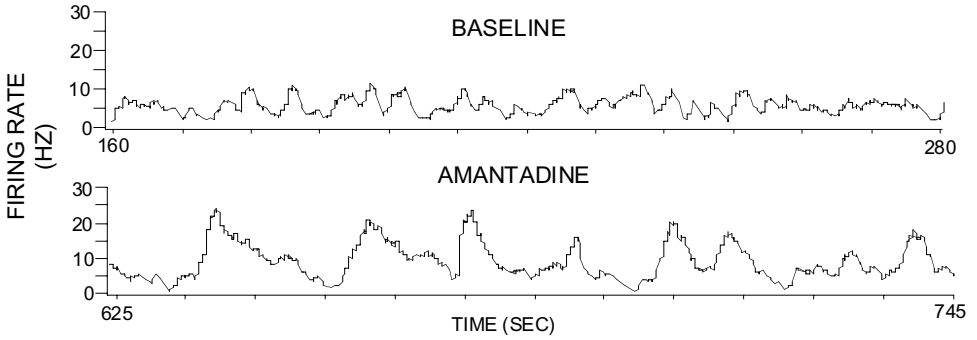

Figure 2. Rate histograms of STN neuronal activity recorded extracellularly in a neurologically intact rat before and after intravenous administration of amantadine. Amantadine (20 mg/kg) markedly increased mean STN neuronal firing. Multisecond oscillations are present in STN neuronal activity in both baseline and following amantadine administration: main spectral periods of 15.5 sec and 17.3 sec for baseline and following amantadine, respectively, were determined by Lomb periodogram (Kaneoke and Vitek, 1996). The large amplitude in multisecond rate fluctuations that emerged following amantadine administration in this STN spike train was typical of the responses of a subpopulation of STN neurons in both intact and lesioned animals. Data are binned at 2 sec.

are typically associated with parkinsonian symptoms. These results suggest that amantadine is not comparable to MK801 with respect to its effects on STN neuronal firing properties even though these two drugs are believed to have similar pharmacological sites of action.

5. DISCUSSION

Taken together, there is a considerable amount of data from animal studies suggesting that NMDA antagonists could be beneficial as a treatment for PD. The single unit recordings studies reviewed here are consistent with this view in some respects. MK801 inhibited D1 receptor-mediated increases in firing rates in the dopamine lesioned animal, which demonstrates inhibition of an effect likely to be deleterious to the PD patient, especially with chronic levodopa therapy (Aubert et al., 2004). In addition, MK801 disrupted slow rhythmic activity and decreased theta frequency activity, which could suggest an ability to reduce dysfunctional synchronization of basal ganglia activity in the PD patient. On the other hand, in the rat model of PD, neither MK801 nor the clinically effective antiparkinsonian agent amantadine significantly attenuated the substantial increase in STN firing rate induced by dopamine cell lesion. In addition, the effects of systemic administration of amantadine, an agent thought to act as a noncompetitive NMDA antagonist, differed considerably from those of the MK801 with respect to other measures of STN neuronal activity.

To the extent that MK801 can be considered a prototypical noncompetitive NMDA antagonist, these results would appear to be relevant to concerns others have raised regarding the actions of agents in this class in PD. One such concern is whether amantadine may be exerting beneficial effects in PD through action on other neurotransmitter receptor systems, such as dopamine, acetylcholine, and $sigma_1$ receptors (Kornhuber et al., 1993; Danysz et al., 1997; Matsubayashi et al., 1997; Peeters et al., 2004). Questions have also

been raised because of the variability in therapeutic benefit reported with other NMDA receptor antagonists (Blanchet et al., 1999; Hallett and Standaert, 2004). It has been pointed out that the effects of NMDA antagonists may vary with the pharmacokinetics of the NMDA antagonist's channel-blocking activity, and the subunit composition of the channel (Blanchet et al., 1999; Rogawski and Wenk, 2003). To this list of caveats regarding NMDA receptor antagonists as therapeutic agents in PD, the present results add caution against using the ability to reduce STN firing rate in animal models as a predictor of clinical efficacy. In fact, the present results raise the possibility that increased STN firing rates might have some benefit, especially in the treatment of levodopa-induced dyskinesias where STN firing rates may be dysfunctionally reduced (Levy et al., 2001). In the future, further definition of the specific attributes of various NMDA receptor antagonists and their relative effects at specific sites of action would be helpful in order to fully explore the potential for these agents as treatments in PD.

6. REFERENCES

Allers, K.A., Kreiss, D.S., and Walters, J.R., 2000, Multisecond oscillations in the subthalamic nucleus: effects of apomorphine and dopamine cell lesion, *Synapse* **38**:38.

Allers, K.A., Ruskin, D.N., Bergstrom, D.A., Freeman, L.E., Ghazi, L.J., Tierney, P.L., and Walters, J.R., 2002, Multisecond periodicities in basal ganglia firing rates correlate with theta bursts in transcortical and hippocampal EEG, *J. Neurophysiol.* **87**:1118.

Allers, K.A., Bergstrom, D.A., Ghazi, L.J., Kreiss, D.S., and Walters, J.R., 2005, MK801 and amantadine exert different effects on subthalamic neuronal activity in a rodent model of Parkinson's disease, *Exptl. Neurol*. **191**:104.

Aubert, I., Guigoni, C., Hakansson, K., Ki, Q., Dovero, S., Barthe, N., Bioulac, B.H., Gross, C.E., Fisone, G., Bloch, B., and Bezard, E., 2004, Increased D1 dopamine receptor signaling in levodopa-induced dyskinesia, *Ann. Neurol*. **57**:17.

Bailey, E.V., and Stone, T.W., 1975, The mechanism of action of amantadine in parkinsonism: a review, *Arch. Int. Pharmacodyn. Ther.* **216**:246.

Bergman, H., Wichmann, T., Karmon, B., and Delong, M.R., 1994, The primate subthalamic nucleus. II. Neuronal activity in the MPTP model of parkinsonism, *J. Neurophysiol.* **72**:507.

Bézard, E., Boraud, T., Bioulac, B., and Gross, C.E., 1999, Involvement of the subthalamic nucleus in glutamatergic compensatory mechanisms, *Eur. J. Neurosci.* **11**:2167.

Blanchet, P.J., Papa, S.M., Metman, L.V., Mouradian, M.M., and Chase, T.N., 1997, Modulation of levodopa-induced motor response complications by NMDA antagonists in Parkinson's disease, *Neurosci. Biobehav. Rev.* **21**:447.

Blanchet, P.J., Konitsiotis, S., Whittemore, E.R., Zhou, Z.L., Woodward, R.M., and Chase, T.N., 1999, Differing effects of N-methyl-D-aspartate receptor subtype selective antagonists on dyskinesias in levodopa-treated 1-methyl-4-phenyl-tetrahydropyridine monkeys, *J. Pharmacol. Exp. Ther.* **290**:1034.

Blanchet, P.J., 2003, The fluctuating parkinsonian patient – clinical and pathophysiological aspects, *Can. J. Neurol. Sci.* **30**:S19.

Blanchet, P.J., Metman, L.V., and Chase, T.N., 2003, Renaissance of amantadine in the treatment of Parkinson's disease, *Adv. Neurol.* **91**:251.

Blanchini, F., Greenamyre, J.T., Fancellu, R., and Nappi, G., 2001, Blockade of subthalamic glutamatergic activity corrects changes in neuronal metabolism and motor behavior in rats with nigrostriatal lesions, *Neurol. Sci*. **22**:49.

Breit, S., Bouali-Benazzouz, R., Benabid, A.L., and Benazzouz, A., 2001, Unilateral lesion of the nigrostriatal pathway induces an increase of neuronal activity of the pedunculopontine nucleus, which is reversed by the lesion of the subthalamic nucleus in the rat, *Eur. J. Neurosci.* **14**:1833.

Campbell, B.M., and Walker, P.D., 2001, MK-801 prevents dopamine D1 but not serotonin 2A stimulation of striatal preprotachykinin mRNA expression, *Neuroreport* **12**:953.

Clineschmidt, B.V., Martin, G.E., Bunting, P.R., and Papp, N.L., 1982, Central sympathomimetic activity of (+)-5-methyl-10,11-dihydro-5H-dibenzo[a,d]cyclohepten-5,10-imine (MK-801), a substance with potent anticonvulsant, central sympathomimetic, and apparent anxiolytic properties, *Drug. Dev. Res*. **2**:135.

Danielczyk, W., 1995, Twenty-five years of amantadine therapy in Parkinson's disease, *J. Neural. Transm. Suppl.* **46**:399.

Danysz, W., Parsons, C.G., Kornhuber, J., Schmidt, W.J., and Quack, G., 1997, Aminoadamantanes as NMDA receptor antagonists and antiparkinsonian agents – preclinical studies, *Neurosci. Biobehav. Rev.* **21**:455.

Dunah, A.W., Wang, Y.H., Yasuda, R.P., Kameyama, K., Huganir, R.L., Wolfe, B.B., and Standaert, D.G., 2000, Alterations in subunit expression, composition, and phosphorylation of striatal N-methyl-Daspartate glutamate receptors in a rat 6-hydroxydopamine model of Parkinson's disease, *Mol. Pharmacol.* **57**:342.

Engber, T.M., Anderson, J.J., Boldry, R.C., Papa, S.M., Kuo, S., and Chase, T.N., 1994a, Excitatory aminoacid receptor antagonists modify regional cerebral metabolic responses to levodopa in 6-hydroxydopamine-lesioned rats, *Neuroscience* **59**:389.

Engber, T.M., Papa, S.M., Boldry, R.C., and Chase, T.N., 1994b, NMDA receptor blockade reverses motor response alterations induced by levodopa, *Neuroreport* **5**:2586.

Greenamyre, J.T., and O'Brien, C.F., 1991, *N*-methyl-D-aspartate antagonists in the treatment of Parkinson's disease, *Arch. Neurol.* **48**:977.

Hallett, P.J., and Standaert, D.G., 2004, Rationale for and use of NMDA receptor antagonists in Parkinson's disease, *Pharmacol. Therap*. **102**:155.

Hassani, O.K., Mouroux, M., and Féger, J., 1996, Increased subthalamic neuronal activity after nigral dopaminergic lesion independent of disinhibition via the globus pallidus, *Neuroscience* **72**:105.

Hollerman, J.R., and Grace, A.A., 1992, Subthalamic nucleus cell firing in the 6-OHDA-treated rat: basal activity and response to haloperidol, *Brain. Res.* **590**:291.

Hu, D., Itoga C.A., Bergstrom, D.A., Parr-Brownlie, L.C., Ghiglieri V., and Walters, J.R., 2004, Increased patterned activity in basal ganglia outputs is organized by coordinated oscillations in the indirect pathway after dopamine loss in anesthetized rats, *Soc. Neurosci. Abstr.* **309**:8.

Huang, K.-X., and Walters, J.R., 1992, D1 receptor stimulation inhibits dopamine cell activity after reserpine treatment but not after chronic SCH 23390: an effect blocked by N-methyl-D-aspartate antagonists, *J. Pharmacol. Exp. Ther.* **260**:409.

Huang, K.-X., Bergstrom, D.A., Ruskin, D.N., and Walters, J.R., 1998, N-methyl-D-aspartate receptor blockade attenuates D1 dopamine receptor modulation of neuronal activity in rat substantia nigra, *Synapse* **30**:18.

Hutchison, W.D., Lozano, A.M., Tasker, R.R., Lang, A.E., and Dostrovsky, J.O., 1997, Identification and characterization of neurons with tremor-frequency activity in human globus pallidus, *Exp. Brain Res.* **113**:557.

Kaneoke, Y., and Vitek, J.L., 1996, Burst and oscillation as disparate neuronal properties, *J. Neurosci. Methods* **68**:211.

Keefe, K.A., and Gerfen, C.R., 1996, D1 dopamine receptor-mediated induction of *zif268* and c-*fos* in the dopamine-depleted striatum: differential regulation and independence from NMDA receptors, *J. Comp. Neurol.* **367**:165.

Keefe, K.A., and Ganguly, A., 1998, Effects of NMDA receptor antagonists on D1 dopamine receptormediated changes in striatal immediate early gene expression: evidence for involvement of pharmacologically distinct NMDA receptors? *Dev. Neurosci.* **20**:216.

Klockgether, T., and Turski, L., 1989, Excitatory amino acids and the basal ganglia-implications for the therapy of Parkinson's disease, *Trends. Neurosci.* **12**:285.

Kornhuber, J., Bormann, J., Hubers, M., Rusche, K., and Riederer, P., 1991, Effects of the 1-amino-adamantanes at the MK-801-binding site of the NMDA-receptor-gated ion channel – a human postmortem brain study, *Eur. J. Pharmacol. – Molec. Pharmacol.* **206**:297.

Kornhuber, J., Schoppmeyer, K., and Riederer, P., 1993, Affinity of 1-aminoadamantanes for the sigma binding site in postmortem human frontalccortex, *Neurosci. Lett.* **163**:129.

Kreiss, D.S., Anderson, L.A., and Walters, J.R., 1996, Apomorphine and dopamine D1 receptor agonists increase the firing rates of subthalamic nucleus neurons, *Neuroscience* **72**:863.

Kreiss, D.S., Mastropietro, C.W., Rawji, S.S., and Walters, J.R., 1997, The response of subthalamic nucleus neurons to dopamine receptor stimulation in a rodent model of Parkinson's disease, *J. Neurosci.* **17**:6807.

Lange, K.W., Kornhuber, J., and Riederer, P., 1997, Dopamine/glutamate interactions in Parkinson's disease, *Neurosci. Biobehav. Rev.* **21**:393.

Levy, R., Dostrovsky, J.O., Land, A.E., Sime, E., Hutchison, W.D., and Lozano, A.M., 2001, Effects of apomorphine on subthalamic nucleus and globus pallidus internus neurons in patients with Parkinson's disease, *J. Neurophysiol*. **86**:249.

Luginger, E., Wenning, G.K., Bosch, S., and Poewe, W., 2000, Beneficial effects of amantadine on L-dopa-induced dyskinesias in Parkinson's disease, *Mov. Disord.* **15**:873.

Magill, P.J., Bolam, J.P., and Bevan, M.D., 2001, Dopamine regulates the impact of the cerebral cortex on the subthalamic nucleus-globus pallidus network, *Neuroscience* **106**:313.

Marin, C., Papa S., Engber, T.M., Bonastre, M., Tolosa, E., and Chase, T.N., 1996, MK-801 prevents levodopa-induced motor response alterations in parkinsonian rats, *Brain Res*. **736**:202.

Matsubayashi, H., Swanson, K.L., and Albuquerque, E.X., 1997, Amantadine inhibits nicotinic acetylcholine receptor function in hippocampal neurons, *J. Pharmacol. Exp. Ther.* **281**:834.

Metman, L.V., Del Dotto, P., Blanchet, P.J., Van den Munckhof, P., and Chase, T.N., 1998a, Blockade of glutamatergic transmission as treatment for dyskinesias and motor fluctuations in Parkinson's disease, *Amino Acids* **14**:75.

Metman, L.V., Del Dotto, P., Van den Munckhof, P., Fang, J., Mouradian, M.M., and Chase, T.N., 1998b, Amantadine as treatment for dyskinesias and motor fluctuations in Parkinson's disease, *Neurology* **50**:1323.

Metman, L.V., Del Dotto, P., LePoole, K., Konitsiotis, S., Fang, J., and Chase, T.N., 1999, Amantadine for levodopa-induced dyskinesias – a 1-year follow- up study, *Arch. Neurol.* **56**:1383.

Miller, W.C., and Delong, M.R., 1987, Altered tonic activity of neurons in the globus pallidus and subthalamic nucleus in the primate MTPTP model of parkinsonism, in: *The Basal Ganglia II*, M.B. Carpenter and A. Jayaraman, eds., Plenum Press, New York, pp. 415–427.

Ni, Z.G., Bouali-Benazzouz, R., Gao, D.M., Benabid, A.L., and Benazzouz, A., 2001, Time-course of changes in firing rates and firing patterns of subthalamic nucleus neuronal activity after 6-OHDA-induced dopamine depletion in rats, *Brain Res.* **899**:142.

Oh, J.D., Russell, D., Vaughan, C.L., and Chase, T.N., 1998, Enhanced tyrosine phosphorylation of striatal NMDA receptor subunits: effect of dopaminergic denervation and L-DOPA administration, *Brain Res.* **813**:150.

Oh, J.D., Vaughan, C.L., and Chase, T.N., 1999, Effect of dopamine denervation and dopamine agonist administration on serine phosphorylation of striatal NMDA receptor subunits, *Brain Res.* **821**:433.

Orieux, G., Francois, C., Feger, J., Yelnik, J., Vila, M., Ruberg, M., Agid, Y., and Hirsch, E.C., 2000, Metabolic activity of excitatory parafascicular and pedunculopontine inputs to the subthalamic nucleus in a rat model of Parkinson's disease, *Neuroscience* **97**:79.

Ossowska, K., 1994, The role of excitatory amino acids in experimental models of Parkinson's disease, *J. Neural. Transm. PD Sect.* **8**:39.

Papa, S.M., Engber, T.M., Boldry, R.C., and Chase, T.N., 1993, Opposite effects of NMDA and AMPA receptor blockade on catalepsy induced by dopamine receptor antagonists, *Eur. J. Pharmacol*. **232**:247.

Papa, S.M., Boldry, R.C., Engber, T.M., Kask, A.M., and Chase, T.N., 1995, Reversal of levodopa-induced motor fluctuations in experimental parkinsonism by NMDA receptor blockade, *Brain Res.* **701**:13.

Papa, S.M., and Chase, T.N., 1996, Levodopa-induced dyskinesias improved by a glutamate antagonist in parkinsonian monkeys, *Ann. Neurol.* **39**:574.

Peeters, M., Romieu, P., Maurice, T., Su, T.P., Maloteaux, J.M., and Hermans, E., 2004, Involvement of the sigma1 receptor in the modulation of dopaminergic transmission by amantadine, *Eur. J. Neurosci.* **19**:2212.

Pelled, G., Bergman, H., and Goelman, G., 2002, Bilateral overactivation of the sensorimotor cortex in the unilateral rodent model of Parkinson's disease – a functional magnetic resonance imaging study, *Eur. J. Neurosci.* **15**:389.

Perier, C., Agid, Y., Hirsch, E.C., and Feger, J., 2000, Ipsilateral and contralateral subthalamic activity after unilateral dopaminergic lesion, *Neuroreport* **11**:3275.

Rogawski, M.A., and Wenk, G.L., 2003, The neuropharmacological basis for the use of memantine in the treatment of Alzheimer's disease, *CNS Drug Rev.* **9**:275.

Ruskin, D.N., Bergstrom, D.A., Kaneoke, Y., Patel, B.N., Twery, M.J., and Walters, J.R., 1999a, Multisecond oscillations in firing rate in the basal ganglia: robust modulation by dopamine receptor and anesthesia., *J. Neurophysiol.* **81**:2046.

Ruskin, D.N., Bergstrom, D.A., and Walters, J.R., 1999b, Multisecond oscillations in firing rate in the globus pallidus: synergistic modulation by D1 nd D2 dopamine receptors, *J. Pharmacol. Exp. Ther.* **290**:1493.

Ruskin, D.N., Bergstrom, D.A., Baek, D., Freeman, L.E., and Walters, J.R., 2001, Cocaine or selective block of dopamine transporters influences multisecond oscillations in firing rate in the globus pallidus, *Neuropsychopharmacology* **25**:28.

Ruskin, D.N., Bergstrom, D.A., Tierney, P.L., and Walters, J.R., 2003, Correlated multisecond oscillations in firing rate in the basal ganglia: modulation by dopamine and the subthalamic nucleus, *Neuroscience* **117**:427.

Schwab, R.S., England, A.C., Jr., Poskanzer, D.C., and Young, R.R., 1969, Amantadine in the treatment of Parkinson's disease, *JAMA.* **208**:1168.

Schwab, R.S., Poskanzer, D.C., England, A.C., Jr., and Young, R.R., 1972, Amantadine in Parkinson's disease. Review of more than two years' experience, *JAMA.* **222**:792.

Shannon, K.M., Goetz, C.G., Carroll, V.S., Tanner, C.M., and Klawans, H.L., 1987, Amantadine and motor fluctuations in chronic Parkinson's disease, *Clin. Neuropharmacol.* **10**:522.

Starr, M.S., 1995, Antiparkinsonian actions of glutamate antagonists-alone and with L-DOPA: a review of evidence and suggestions for possible mechanisms, *J. Neural. Transm – Park Dis. Dement Sect.* **10**:141.

Tahar, A.H., Gregoire, L., Darre, A., Belanger, N., Meltzer, L., and Bedard, P.J., 2004, Effect on a selective glutamate antagonist on 1-dopa-induced dyskinesias in drug-naïve parkinsonian monkeys, *Neurobiol. Dis*. **15**:171.

Tai, C.H., Boraud, T., Bezard, E., Bioulac, B., Gross, C., and Benazzouz, A., 2003, Electrophysiological and metabolic evidence that high-frequency stimulation of the subthalamic nucleus bridles neuronal activity in the subthalamic nucleus and the substantia nigra reticulata, *FASEB J.* **17**:1820.

Vila, M., Perier, C., Feger, J., Yelnik, J., Faucheux, B., Ruberg, M., Raisman-Vozari, R., Agid, Y., and Hirsch, E.C., 2000, Evolution of changes in neuronal activity in the subthalamic nucleus of rats with unilateral lesion of the substantia nigra assessed by metabolic and electrophysiological measurements, *Eur. J. Neurosci.* **12**:337.

Walters, J.R., Ruskin, D.N., Allers, K.A., and Bergstrom, D.A., 2000, Pre- and postsynaptic aspects of dopamine-mediated transmission, *Trends Neurosci.* **23**:S41.

Walters, J.R., Hu, D., Itoga, C.A., Parr-Brownlie, L.C., and Bergstrom, D.A., Do local field potentials reflect synchronized spiking activity of neuronal populations in the basal ganglia? Studies in a rodent model of Parkinson's disease, in: *The Basal Ganglia VIII*, J.P. Bolam, P.J. Magill, and C. Ingham, eds., Springer Science and Business Media, New York, pp 37–46 (This volume).

Wichmann, T., Kliem, M.A., and Soares, J., 2002, Slow oscillatory discharge in the primate basal ganglia, *J. Neurophysiol.* **87**:1145.

STRIATOPALLIDAL CHANGES IN EARLY PARKINSON'S DISEASE

Partial dopamine depletions

Anne E. Grissell and Marjorie A. Ariano*

1. INTRODUCTION

The onset of motor symptoms in Parkinson's disease (PD) develops following substantial loss of striatal dopamine (DA) as a secondary result of degeneration of the cell bodies within the substantia nigra. DA depletion is the principal neurochemical deficit in PD and the keystone measure for patient diagnosis is that L-DOPA therapy improves the cardinal symptoms of the disorder (resting tremor, hypokinesia, bradykinesia and rigidity). Current PD treatments seek to postpone L-DOPA use as long as possible, impeding its induction of unwanted side effects. PD motor symptoms arise from the slowly progressing striatal DA loss and cause differences between the two striatal projection systems such as elevation of D2 DA receptors,[1,2] changes in tertiary spine densities,[3] alterations in dendritic architecture,[4] and augmentation of glutamate responsiveness.[5,6] Partial DA depletion enables modeling the initial stage of PD when DA neurons are undergoing change, but have not degenerated completely in rodents.[7] Evaluation of striatal neurochemistry with respect to the identified projection systems in early PD may reveal mechanisms underlying the functional opposition of these pathways and offer alternative drug therapies to ameliorate symptoms of the disease. We have produced a "premotor" PD rat model of the neurochemically early stage of the disease by unilateral substantia nigra 6-OHDA infusions that partially lesion the nigrostriatal tract. This asymmetrical loss of nigrostriatal DA has been monitored by limb-use behavior in the rat model, which is indicative of their striatal DA imbalance.[8,9] We also assessed residual striatal DA levels four weeks after the 6-OHDA infusion using high pressure liquid chromatography or staining for the rate limiting enzyme tyrosine hydroxylase (TH) and then compared these results with neurochemistry observed in the two striatal projection neuron populations.

* Department of Neuroscience, The Chicago Medical School at Rosalind Franklin University of Medicine and Science, North Chicago, IL 60064-3095, USA. Correspondence to: Marjorie.Ariano@rosalindfranklin.edu.

Novel changes such as striatal caspase 3 activation occurred; its protein staining levels were elevated in DA depleted compared to intact striata. Components upstream (cytochrome C) and downstream (fractin) from activated caspase 3 in the apoptosis cascade also were elevated, indicating involvement of the intrinsic, mitochondria-driven pathway that results from deficiencies in aerobic energy metabolism.[10] These changes were prominent within the striatopallidal output neurons but not in the striatonigral efferents. Elevations in these apoptogens occurred in the absence of cell loss, which was determined using the selective neuronal marker protein, NeuN. These data suggest that enhancements in staining of activated caspase 3 may underlie transient homeostatic imbalances in striatal neurons which are contemporaneous with the DA depletion. These findings indicate that alternative drug intervention schemes to delay or reduce L-DOPA use might focus on mitochondrially driven apoptogenic mechanisms contributing to functional differences in striatal neurochemical deterioration early in PD.

2. METHODS AND PROCEDURES

Male Sprague-Dawley rats (40, 200 g at time of surgery) were used for these studies. All procedures conformed to the *USPHS Guide for the Care and Use of Laboratory Animals* and were approved by the IACUC. Infusion of 6-OHDA (6 μg/μl in 1 μl infusion) into the substantia nigra was used to produce partial or minimal DA lesioned rats, determined on the basis of limb use asymmetry behavior.[8,9] Experiments were terminated at 4 weeks, brains were frozen and stored at −85°C. Sections were cut at 10 μm and immersion-fixed in freshly prepared cold 4% paraformaldehyde in PBS (pH 7.2) for 5 min and then rinsed. Primary antisera were diluted in PBS (TH, 1 : 600; NeuN, 1 : 100; caspase 3, 1 : 200; cytochrome C, 1 : 200; fractin, 1 : 200; substance P, 1 : 30; enkephalin, 1 : 30) and were incubated overnight at 4°C. Unbound primary antisera were rinsed off and secondary fluorescently coupled antisera were diluted 1 : 200 in PBS and incubated for 1.5 h. Sections were examined immediately using fluorescence microscopy. Digitized images for DA intact and depleted striata were matched to similar regions in the dorsal striatum. Acquisition and exposure settings were identical and optimized for staining detected in DA intact striata, normalizing subsequent data from DA depleted striatum.[11]

For western blots, thick (20 μm × 5 each) cryostat sections were made from some of the brain series used to gather the morphological data. The dorsal striatum was dissected on the freeze plate of the cryostat chamber. Sections were placed into cryovials and homogenized in 200 μl ice-cold buffer containing: 10 mM Tris-Cl, pH 7.4 with 50 mM NaF, 10 mM EDTA, 10 mM EGTA, 10 mM $Na_4P_2O_7$, 1 mM Na_3VO_4, 10 units/ml trasylol and sonicated for 3 × 10 seconds. Pepstatin A (1 μM), leupeptin and aprotinin (10 μg/ml), Pefabloc (0.2 mM; 4-(2-aminoethyl)-benzenesulfonyl fluoride), benzamidine (0.1 mg/ml), and calpain inhibitors I and II (8 μg/ml each), also were included in all buffers. Homogenates were centrifuged at 14,000 rpm, 5 min at 4°C and the supernatant was stored at −85°C until assayed. Homogenates were thawed on ice and assayed in SDS-PAGE sample buffer, loaded onto 8% acrylamide gels and run at 150 V for 1 h. Proteins were transferred to PVDF membranes treated with freshly prepared TBS containing 1% BSA and 0.1% Triton X-100 for 1 h at 21°C with constant agitation. Membranes were blocked in filtered 5% nonfat dry milk in 0.1% Tween-20 in TBS containing 1% BSA, 0.1% Triton X-100 and 2 mM $MnCl_2$ for 1 h. Primary antisera were incubated overnight with constant agitation at 4°C. Visualization used HRP-conjugated secondary antisera and ECL chemiluminescence detected using Kodak XAR film. The optical densities were determined using Molecular Analyst™

software (BioRad, Hercules, CA), expressed as a ratio between DA depleted versus DA intact striatum, corrected for protein concentration and used NeuN as a loading control. Blots were run in duplicate, results compared by ANOVA followed by Tukey's test. Significance was $p < 0.05$.

3. LIMB USE ASYMMETRY

Behavioral assessment of partial (N = 18) and minimal (N = 16) DA lesioned rats was videotaped then scored using slow-motion playback. The rats' normal forepaw (ipsilateral to the partial DA loss), the PD forepaw (contralateral to the partial DA loss) and simultaneous forepaw (co-use) placements on the vertical surface of a Plexiglas cylinder were tabulated. Data were collected for the first 20 movements or 5 minutes in each rat, whichever event came first. Scores were plotted as percent use for each limb or co-use per week, and also averaged for total individual forepaw and limb co-use throughout the duration of the experiment. Criteria were: 1) Simultaneous forepaw placement on the cylinder wall was scored as co-use. 2) Opposing limb contact on the wall while the initial forelimb placement was maintained was scored as co-use. 3) Both paws had to be lifted from the wall surface for a subsequent movement score. 4) The movement was not scored if the forepaw handedness or movement category could not be determined (Figure 1).

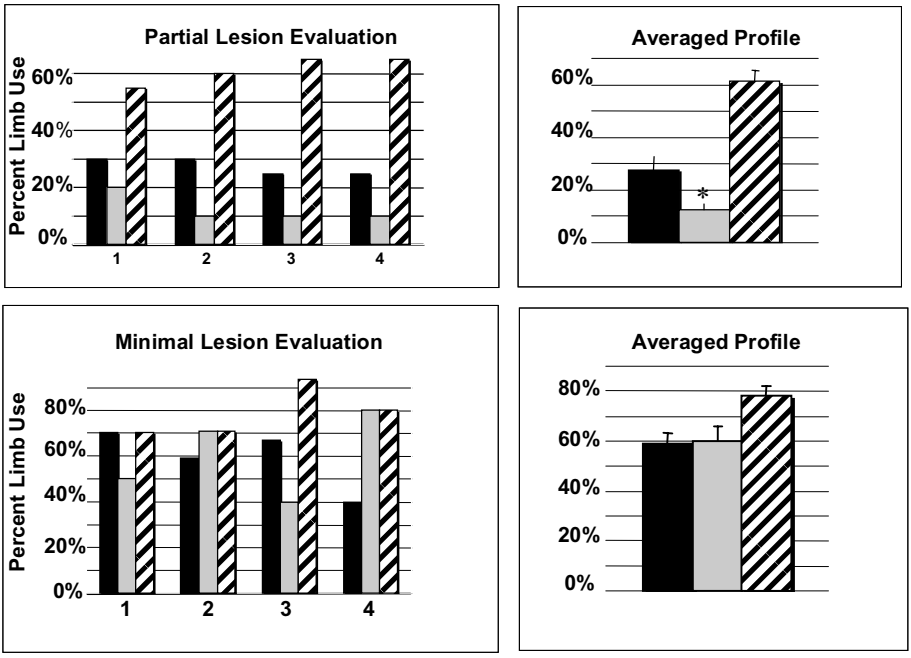

Figure 1. The percentage of movements made by the normal forepaws (black), PD forepaws (grey), or both forepaws (striped) was tabulated. Rats with partial DA loss (range of 25–70% depletion compared to intact side) showed progressive development of hypokinesia in PD forepaws with time. Minimally lesions (DA loss < 20%) showed no consistent decrease in use of the forepaw contralateral to the 6-OHDA infusion. When all movements for each limb were averaged for the full 4 weeks of the study (Averaged Profile plot), significant hypokinesia was detected only in the PD forepaw of the partial DA depleted rat (asterisk, $p < 0.05$).

4. IMMUNOFLUORESCENCE STUDIES

Intensities that provided regional (TH) or cellular staining 20% brighter than the background signal were measured. The background was established from the fluorescence emitted in fiber bundles of the internal capsule that penetrate the striatal parenchyma and were averaged from 3 randomly chosen areas. The median value of the signal for TH was obtained from 60 × 60 pixels square, whereas cellular signals were measured within a 30 pixel circle. Luminosity medians were calculated using the histogram function in Adobe Photoshop as described by Lehr et al.[12] This background signal was subtracted. A counting grid was overlaid on each image, and neurons meeting the criteria of size (enscribed by 30 pixels) and location in the dorsal striatum that intersected the counting grid were measured. Means of individual cellular luminosities and the standard error of the mean for neurons measured in each image from the intact and the DA depleted striata were computed. Results were expressed as the percentage change in mean cellular luminosity between the intact and depleted striata. Immunofluorescence levels were compared by paired two tailed *t*-tests, with significance at $p < 0.001$. All rat striata were evaluated for TH immunohistochemistry to validate the limb use asymmetry behavioral data.

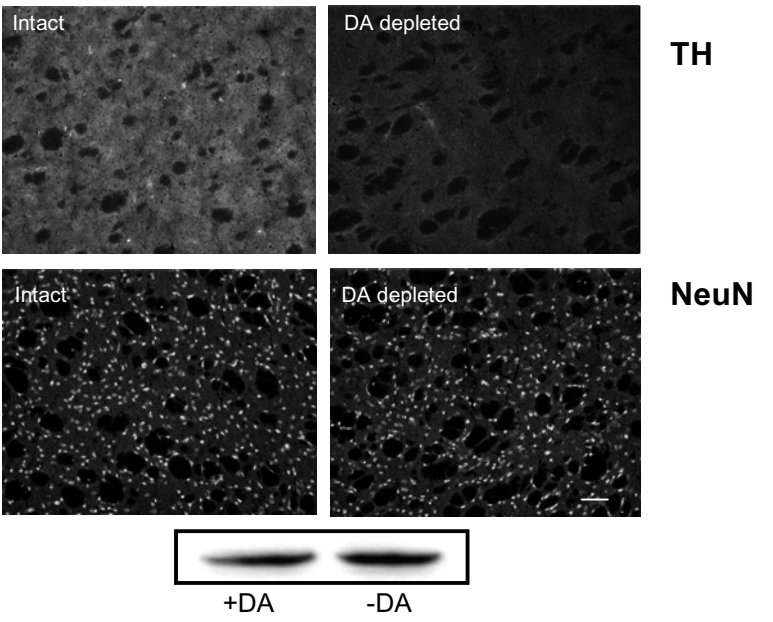

Figure 2. TH immunofluorescence demonstrated ~40% depletion of luminosity values of the neurotransmitter in the DA depleted striatum compared to the intact, whereas there was no loss in cell density, based upon cell counts using NeuN. Calibration bar shows 120 µm and applies to all images. The equivalence of the cell density counts between the intact and DA depleted striata were confirmed using western analysis of NeuN in the intact (+DA) and depleted (–DA) striata.

5. NEURONAL ACTIVATED CASPASE 3 EXPRESSION

While no neuronal losses were measured 4 weeks after the partial DA loss, substantial changes occurred in indices of cellular homeostasis and emphasize the importance of studying the neurochemically early phase of PD in the striatum. Accompanying behavioral limb use asymmetries, the serine protease caspase 3 was activated in neurons after DA loss (Figure 3). At the extreme, activated caspase 3 may execute programmed cell death in severely damaged neurons.[13–17] Since neuronal losses were not detected, the appearance of activated caspase 3 may be a transient event and striatal neurons may recover if given sufficient cellular support and/or time to heal without further insults.

Striatopallidal, enkephalinergic projection neurons show enhanced functioning in PD models of basal ganglia dysfunction,[18] experimentally in 6-OHDA lesioned rats,[1,2,6,19] and in the PD patient.[20,21] Thus, we examined if activated caspase 3 staining was differentially expressed in the two striatal projections systems as an indication of preferential changes in the striatopallidal system (Figure 4). The approach we used was to determine double-labeled immunofluorescence, defining the indirect, striatopallidal pathway by its staining for enkephalin, while the direct, striatonigral projections showed substance P localization; activated caspase 3 was then assessed in these peptideexpressing neurons.

Striatal deteriorations in the projection systems may be demonstrated as changes in intracellular energy homeostasis. Near-total nigrostriatal DA depletion is a substantial insult to the postsynaptic neurons of the striatum and induces a number of changes. Our

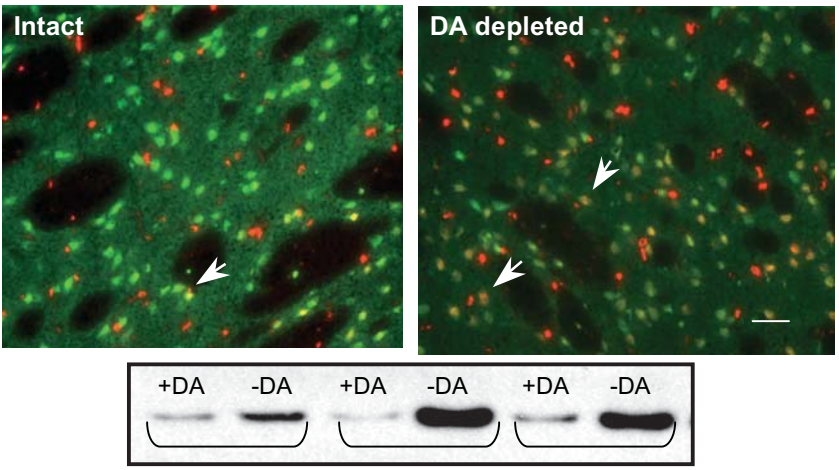

Figure 3. Immunofluorescent experiments were performed using NeuN (green) to mark neuronal elements, while the activated caspase 3 was visualized using a red label. Partial DA depletion caused significant elevation in staining signals (+41%, $p < 0.001$) and in the number of activated caspase-3 stained striatal neurons, (distinguished as yellow cells; arrows), compared to the intact striatum. Calibration bar shows 80 µm. Western blots confirmed that the intact striatum (+DA) contains residual activated caspase-3 protein but robust elevation occurred in depleted (–DA) striata in three different rats. Samples were normalized to protein concentration and showed increases of 230%, 510% and 425% ($p < 0.05$).

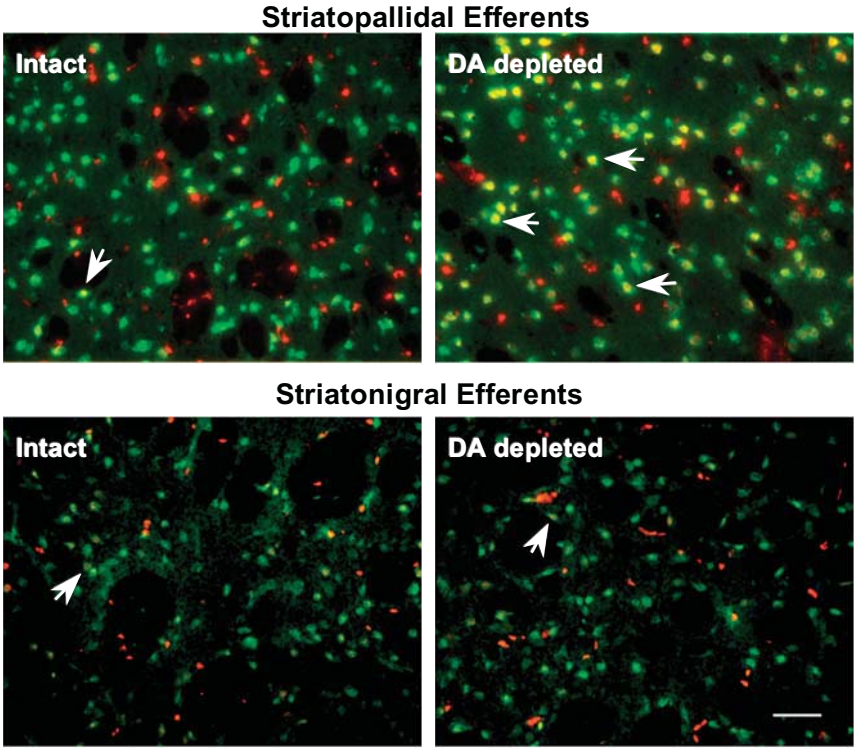

Figure 4. Striatopallidal neurons (enkephalin in green) were evaluated for cleaved caspase 3 (red) staining. More numbers of activated caspase 3 striatopallidal neurons (arrows, yellow) were seen in the DA depleted striatum (TH staining decreased 48%), and cellular caspase 3 staining intensity was increased +40% ($p < 0.001$) compared to intact, 4 weeks after intranigral 6-OHDA. Striatonigral neurons (substance P in green) stained with activated caspase 3 (red) were equivalent in cellular luminosity measurements between the intact and DA depleted striata. Calibration bar shows 80 μm.

data showed that striatal changes in a model of the initial neurochemical DA depletion may be manifested as increased staining for activated caspase 3, a key enzyme in the programmed cell death pathway. Enhanced caspase 3 cleavage has been proposed as a determinant of neurodegeneration in PD patients and experimental rodent and primate models of PD.[13,15–17,22–26] Apaf-1 (***a***poptosis ***p***rotease-***a***ctivating ***f***actor ***1***) coalesces in the neuronal cytoplasm with cleaved caspase 9 and with cytochrome C that has translocated from the mitochondrion, forming the apoptosome, which cleaves the caspase 3 zymogen.[27,28] The appearance of these "upstream" proteins in the apoptosis cascade indicates mitochrondrial energy insufficiency has occurred.[10] We next examined if these early markers of mitochondrially driven energy instability occurred within the striatal projection pathways in our PD rats as defects and changes in mitochondria functioning are hypothesized to be a mechanism for spontaneous PD[29–33] and its genetic variants.[34] In addition, Apaf-1 inhibitors have been used successfully to block the toxic effects of MPTP[35] and may have value in PD gene therapy treatments.[17,36]

6. CYTOCHROME C IN STRIATAL EFFERENTS

Cytochrome C staining in neuropeptide-identified striatal projections was studied to determine if distinctive changes in mitochondrial functioning could be detected after partial DA depletion compared to the intact striatum (Figure 5).

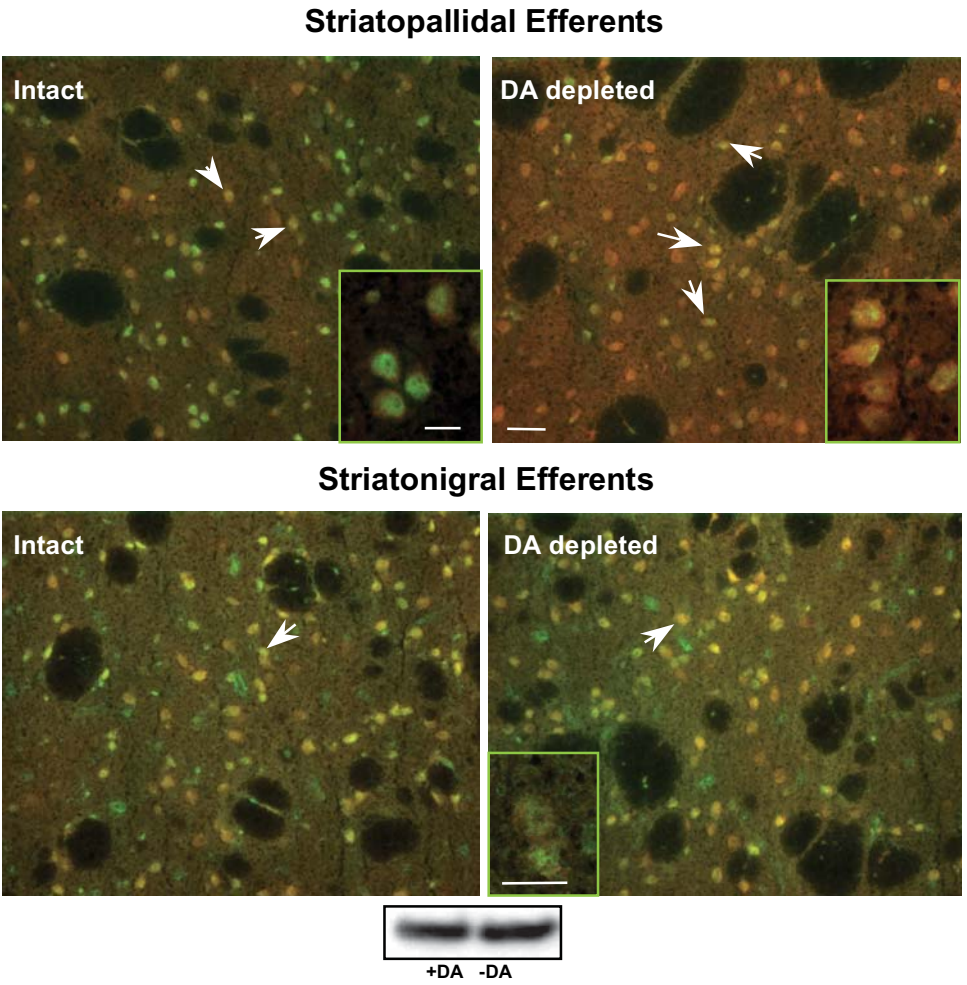

Figure 5. Neuropeptides were detected using Cy2 (green), while cytochrome C staining was visualized using Cy3 (red) in double immunofluorescence experiments. Striatopallidal cytochrome C (yellow, arrows) staining levels were enhanced significantly ($p < 0.001$) within the DA depleted compared to the intact striatum. The inset shows the thin rim of cytoplasmic staining for cytochrome C in enkephalin neurons. Striatonigral cytochrome C (yellow, arrows) was equivalent in cellular luminosity signals between the intact and DA impoverished striata. Inset demonstrates the thin rim of cytoplasmic cytochrome C staining visible in substance P neurons. Calibration bars are equivalent for the lower magnification of the intact and DA depleted images at 60 µm; the inset calibrations are equivalent at 20 µm. These immunofluorescent findings were confirmed in westerns; the DA-depleted striatum (−DA) showed +20% increase in cytochrome C protein levels compared to the intact (+DA) side.

7. FRACTIN EXPRESSION IN STRIATAL EFFERENTS

Actin can be cleaved by activated caspase 3 to form fractin.[25] The enhanced presence of fractin demonstrates that caspase 3 was enzymatically active in addition to demonstrating increased staining signals for the protease (Figures 3, 4). Striatonigral and striatopallidal fractin expression were determined after partial DA loss (Figure 6).

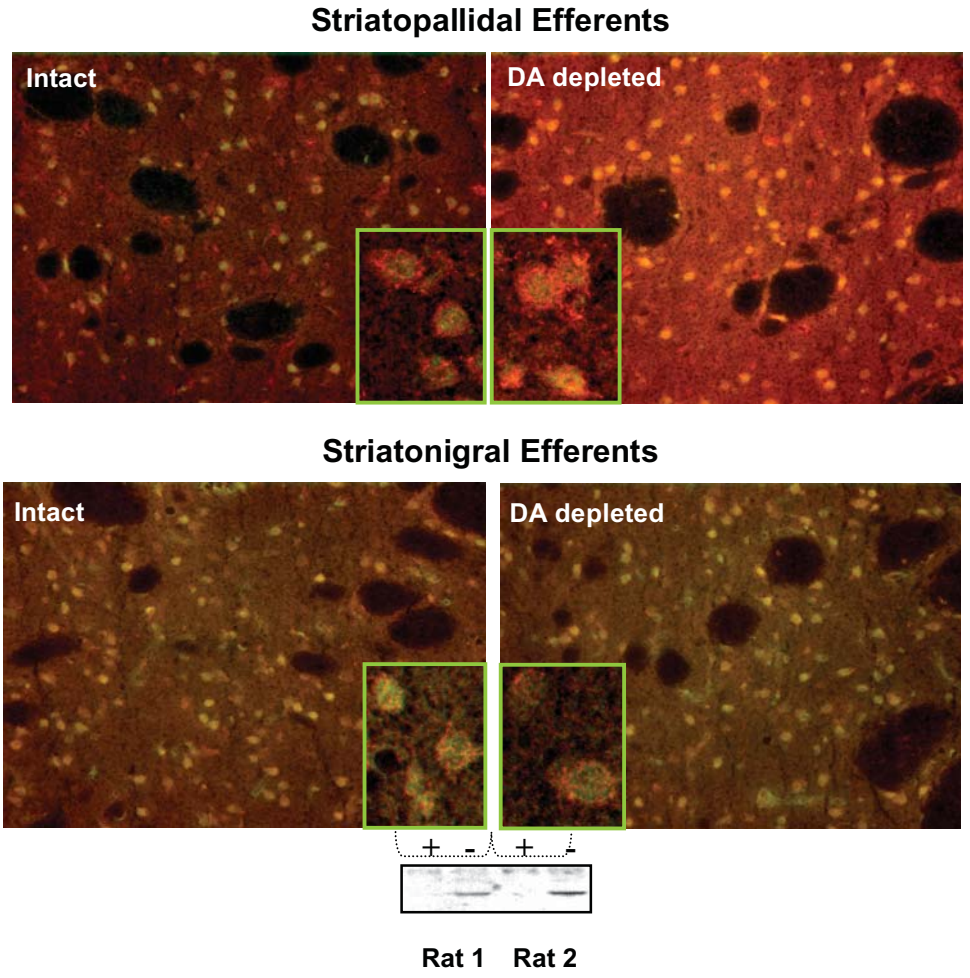

Figure 6. Striatonigral and striatopallidal (green) fractin (red) staining was assessed. Fractin was visible in both striatal projection pathways (arrows) and in the neuropil. No reaction was detected in fiber bundles of the internal capsule. After partial DA depletion, fractin staining was increased significantly ($p < 0.001$) in the striatopallidal but not the striatonigral system. The insets showed the heterogeneous staining pattern for fractin in the cytoplasm of the projection neurons. Calibration bars in lower magnification images represent 60 µm, and insets are 20 µm. The western blot used to determine the quantitative levels of activated caspase 3 (figure 3) was stripped and then re-probed for fractin using the same antisera employed in the morphological studies. In two of the samples, the protein density differences were +220% in rat #1, and +356% in rat #2, and showed significant ($p < 0.05$) striatal fractin levels after partial DA depletion (–) compared to intact (+).

8. CONCLUSIONS

The remarkable observations in this model of early PD were that even mild striatal DA loss could be distinguished as subtle behavioral deficits and at the cellular level of study, had profound and differential effects on the two projection systems. These outcomes would modify the functional neuroplasticity of the basal ganglia circuits. Elements of the intrinsic programmed cell death pathway that may be mobilized through collapse of the mitochondrial membrane potential[37] were enhanced significantly and selectively in the striatopallidal system. Substantial elevations in protein staining and enzymatic activity of activated caspase 3 and constituents upstream (cytochrome C) and downstream (fractin) in the apoptosis cascade were detected. This argued that enzymatic recruitment of the intrinsic (mitochondrial) cell death cascade occurred as an early striatal event in our PD model, well before the overt motor symptoms characteristic of the disorder. The established role for caspase 3 activation is execution of programmed death in severely perturbed cells.[38] Cleavage of the inactive zymogen and appearance of the activated form of caspase 3 have been elicited in experimental models of PD *in vitro* and *in vivo* and have been implicated as a mechanism in nigral DA neurodegeneration in patients.[13–16,24,26] The fact that our studies also detected the robust elevation of activated caspase 3 in the nigrostriatal termination region was unexpected, and leads us to believe that activated caspase 3 underlies another crucial function beyond launching the programmed cell death sequence in early PD.

Activated caspase 3 in many systems may trigger apoptosis but also has a role in neuroprotection after partial insults, similar to that produced in early PD by a fractional DA depletion. Activated caspase 3 was detected in neurons, and specifically in the striatopallidal pathway; no significant changes occurred in the striatonigral pathway. Increased activated caspase 3 protein staining equated to heightened enzymatic activity as one of its catalytic breakdown products, fractin was formed. Fractin staining was elevated in the DA depleted striatum. This would lead to remodeling striatal cytoarchitecture and DA loss will indeed reshape the dendritic structure and spine density of striatal efferents[3,4] altering physiological responsiveness. This supports our hypothesis that partial nigrostriatal disruption causes substantive changes in the striatum.

Models of basal ganglia function derived from experimental and imaging studies support a variety of scenarios for the activity patterns through the striatal outflow pathways in PD,[1,6] but strongly favor increased responsiveness and alterations in firing patterns in the subthalamus, downstream from the striatopallidal neurons of the indirect pathway. Some striatopallidal neurons are particularly sensitive to degeneration via apoptosis in response to manipulation of DA and/or corticosteroid levels.[39] Elucidation of the special character of striatopallidal neurons may contribute to better treatment strategies for basal ganglia movement disorders.

9. ACKNOWLEDGEMENTS

This work was supported in part by the Department of Defense, Neurotoxin Program, DAMD 17-99-1-9542.

10. REFERENCES

1. Gerfen, C.R., Engber, T.M., Mahan, L.C., Susel, Z., Chase, T.N., Monsma, F.J. Jr., and Sibley, D.R., 1990, D1 and D2 dopamine receptor-regulated gene expression of striatonigral and striatopallidal neurons, *Science* **250**:1429–1432.

2. Nisenbaum, L.K., Crowley, W.R., and Kitai, S.T. 1996, Partial striatal dopamine depletion differentially affects striatal substance P and enkephalin messenger RNA expression, *Molec. Brain Res.* **37**:209–216.
3. Arbuthnott, G.W., Ingham, C.A., and Wickens, J.R., 2000, Dopamine and synaptic plasticity in the neostriatum, *J. Anat.* **196**:587–596.
4. Ingham, C.A., Hood, S.H., and Arbuthnott, G.W., 1989, Spine density on neostriatal neurons changes with 6-hydroxydopamine lesions and with age, *Brain Res.* **503**:334–338.
5. Emmi, A., Rajabi, H., and Steward, J., 1996, Behavioral and neurochemical recovery from partial 6-hydroxydopamine lesions of the substantia nigra is blocked by daily treatment with glutamate receptor antagonists MK-801 and CPP, *J. Neurosci.* **16**:5216–5224.
6. Calabresi, P., Centonze, D., and Bernardi, G., 2000, Electrophysiology of dopamine in normal and denervated striatal neurons, *TINS* **23**:S57–S63.
7. Bergstrom, B.P., Schertz, K.E., Weirick, T., Nafziger, B., Takacs, S.A., Lopes, K.O., Massa, K.J., Walker, Q.D., and Garris, P.A., 1991, Partial, graded losses of dopamine terminals in the rat caudate-putamen: an animal model for study of compensatory adaptation in preclinical parkinsonism, *J. Neurosci. Meth.* **106**:15–28.
8. Schallert, T., and Tillerson, J.L., in *Central Nervous System Diseases,* edited by D.F. Emerich, R.L. Dean, III, and P.R. Sanberg (Humana Press, Totowa NJ), pp. 131–151.
9. Tillerson, J.L., Cohen, A.D., Philhower. J., Miller, G.W., Zigmond, M.J., and Schallert, T., 2001, Forced limb-use effects on the behavioral and neurochemical effects of 6-hydroxydopamine, *J. Neurosci.* **21**:4427–4435.
10. Pivovarova, N.B., Nguyen, H.V., Winters, C.A., Brantne, C.A., Smith, C.L., and Andrews, S.B., 2004, Excitotoxic calcium overload in a subpopulation of mitochondria triggers delayed death in hippocampal neurons, *J. Neurosci.* **24**:5611–5622.
11. Ariano, M.A., Cepeda, C., Calvert, C.R., Flores-Hernández, J., Hernández-Echeagaray, E., Klapstein, G.J., Chandler, S.H., Aronin, N., DiFiglia, M., and Levine, M.S., 2004, Striatal potassium channel dysfunction in Huntington's disease transgenic mice, *J. Neurophysiol.* **Epub:** doi:10.1152/jn.00791
12. Lehr, H.A., van der Loos, C.M., Teeling, P., and Gown, A.M., 1999, Complete chromogen separation and analysis in double immunohistochemical stains using Photoshop-based image analysis, *J. Histochem. Cytochem.* **47**:119–126.
13. He, Y., Lee, T., and Leong, S.K., 2000, 6-hydroxydopamine induced apoptosis of dopaminergic cells in the rat sustantia nigra, *Brain Res.* **858**:163–166.
14. Mattson, M.P., 2000, Apoptosis in neurodegenerative disorders, *Nat. Rev. Molec. Cell. Biol.* **1**:120–129.
15. Tatton, N.A., 2000, Increased caspase 3 and Bax immunoreactivity accompany nuclear GAPDH translocation and neuronal apoptosis in Parkinson's disease, *Exp. Neurol.* **166**:29–43.
16. Blum, D., Torch, S., Lambeng, N., Nissou, M., Benabid, A.L., Sadoul, R., and Verna, J.M., 2001, Molecular pathways involved in the neurotoxicity of 6-OHDA, dopamine and MPTP: contribution to the apoptotic theory in Parkinson's disease, *Prog. Neurobiol.* **65**:135–172.
17. Nagatsu, T., 2002, Parkinson's disease: changes in apoptosis-related factors suggesting possible gene therapy, *J. Neural. Trans.* **109**:731–745.
18. Albin, R.L., Young, A.B., and Penney, J.B. Jr., 1989, Functional anatomy of basal ganglia disorders, *TINS* **12**:366–374.
19. Mitchell, I.J., Lawson, S., Moser, B., Laidlaw, S.M., Cooper, A.J., Walkinshaw, G., and Waters, C.M., 1994, Glutamate-induced apoptosis results in a loss of striatal neurons in the Parkinsonian rat, *Neurosci.* **63**:1–5.
20. Obeso, J.A., Rodriguez-Oroz, M.C., Rodriguez, M., Macias, R., Alvarez, L., Guridi, J., Vitek, J., and DeLong, M.R., 2000, Pathophysiologic basis of surgery for Parkinson's disease, *Neurology* **55**:S7–S12.
21. Rodriguez-Oroz, M.C., Rodriguez, M., Guridi, J., Mewes, K., Chockkman, V., Vitek, J., DeLong, M.R., and Obeso, J.A., 2001, The subthalamic nucleus in Parkinson's disease: somatotopic organization and physiological characteristics, *Brain* **124**:1777–1790.
22. Jeon, B.S., Kholodilov, N.G., Oo, T.F., Kim, S.Y., Tomaselli, K.J., Srinivasan, A., Stefanis, L., and Burke, R.E., 1999, Activation of caspase-3 in developmental models of programmed cell death in neurons of the substantia nigra, *J. Neurochem.* **73**:322–333.
23. Lu, C., Fu, W., and Mattson, M.P., 2001, Caspase-mediated suppression of glutamate (AMPA) receptor channel activity in hippocampal neurons in response to DNA damage promotes apoptosis and prevents necrosis: implications for neurological side effects of cancer therapy and neurodegenerative disorders, *Neurobiol. Dis*. **8**:194–206.
24. Hartmann, A., Hunot, S., Michel, P.P., Muriel, M.-P., Vyas, S., Faucheux, B.A., Mouatt-Prigent, A., Turmel, H., Srinivasan, A., Ruberg, M., Evan, G.I., Agid, Y., and Hirsch, E.C., 2000, Caspase-3: a vulnerability

factor and final effector in apoptotic death of dopaminergic neurons in Parkinson's disease, *Proc. Natl. Acad. Sci. USA* **97**:2875–2880.
25. Oo, T.F., Siman, R., and Burke, R.E., 2002, Distinct nuclear and cytoplasmic localization of caspase cleavage products in two models of induced apoptotic death in dopamine neurons of the substantia nigra, *Exp. Neurol.* **175**:1–9.
26. Turmel, H., Hartmann, A., Parain, K., Douhou, A., Srinivasau, A., Agid, Y., and Hirsch, E.C., 2001, Caspase-3 activation in 1-methyl-4-phenyl-1,2,3,6-tetrahydropyridine (MPTP)-treated mice, *Move. Disord.* **16**:185–189.
27. Yoshida, H., Kong, Y.Y., Yoshida, R., Elia, A.J., Hakem, A., Hakem, R., Penninger, J.M., and Mak, T.W., 1998, Apaf1 is required for mitochondrial pathways of apoptosis and brain development, *Cell* **18**:739–350.
27. Zou, H., Henzel, W.J., Liu, X., Lutschg, A., and Wang, X., 1997, Apaf-1, a human protein homologous to C. elegans CED-4, participates in cytochrome c-dependent activation of caspase-3, *Cell* **90**:405–413.
28. Greenamyre, J.T., MacKenzie, G., Peng, T.I., and Stephans, S.E., 1999, Mitochondrial dysfunction in Parkinson's disease, *Biochem. Soc. Symp.* **66**:85–97.
30. Langston, J.W., Ballard, P.A., Tetrud, J.W., and Irwin, I., 1983, Chronic parkinsonism in humans due to a product of meridine-analog synthesis, *Science* **219**:979–980.
31. Nicklas, W.J., and Heikkila, R.E., 1985, Inhibition of NADH-linked oxidation in brain mitochondria by 1-methyl-4-phenyl-1,2,3,6-tetrahydropyridine, *Life Sci.* **36**:2503–2508.
32. Rosenberg, N.L., Myers, J.A., and Martin, W.R.W., 1989, Cyanide-induced parkinsonism: clinical, MRI, and 6-fluorodopa PET studies, *Neurology* **39**:142–144.
33. Sherer, T.B., Betarbet, R., Stout, A.K., Lund, S., Baptista, M., Parnov, A.V., Cookson, M.R., and Greenamyre, J.T., 2002, An *in vitro* model of Parkinson's disease: linking mitochondrial impairment to altered α-synuclein metabolism and oxidative damage, *J. Neurosci.* **22**:7006–7015.
34. Valente, E.M., Abou-Sleiman, P.M., Caputo, V., Muqit, M.M.K., Harvey, K., Gispert, S., Ali, Z., Del Turco, D., Bentivoglio, A.R., Healy, D.G., Albanese, A., Nussbaum, R., Gonzalez-Maldonado, R., Deller, T., Salvi, S., Cortelli, P., Gilks, W.P., Latchman, D.S., Harvey, R.J., Dallapiccola, B., Auburger, G., and Wood, N.W., 2004, Hereditary early-onset Parkinson's disease caused by mutations in *PINK1*, *Science* **304**:1158–1160.
35. Mochizuki, H., Hayakawa, H., Migita, M., Shibata, M., Tanaka, R., Suzuki, A., Shimo-Nakanishi, Y., Urabe, T., Yamada, M., Tamayose, K., Shimada, T., Miura, M., and Mizuno, Y., 2001, An AAV-derived Apaf-1 dominant negative inhibitor prevents MPTP toxicity as anti-apoptotic gene therapy for Parkinson's disease, *Proc. Natl. Acad. Sci. USA* **98**:10918–10923.
36. Waldmeier, P.C., 2003, Prospects for antiapoptotic drug therapy of neurodegenerative diseases, *Prog. Neuropsychopharm. Biol. Psych.* **27**:303–321.
37. Finkel, E., 2001, The mitochondrion: is it central to apoptosis? *Science.* **292**:624–626.
38. Thornberry, N.A., and Lazebnik, Y., 1998, Caspases: enemies within, *Science.* **281**:1312–1316.
39. Mitchell, I.J., Cooper, A.J., and Griffiths, M.R., 1999, The selective vulnerability of striatopallidal neurons, *Prog. Neurobiol.* **59**:691–719.

DYNAMIC MODEL OF BASAL GANGLIA FUNCTIONS AND PARKINSON'S DISEASE

Atsushi Nambu, Yoshihisa Tachibana, Katsuyuki Kaneda,
Hironobu Tokuno, and Masahiko Takada*

1. INTRODUCTION

The loop linking the cerebral cortex and the basal ganglia is important for the control of voluntary movement. Information for movement control is derived from the cortex and is processed in the basal ganglia and returns to the cortex via the thalamus (Alexander and Crutcher, 1990). In the current, standard model of the basal ganglia organization, the striatum receives direct excitatory cortical inputs and projects to two output nuclei, the internal segment of the globus pallidus (GPi) and the substantia nigra pars reticulata (SNr), via two major projection systems, the "direct" and "indirect" pathways (Alexander and Crutcher, 1990). The direct pathway arises from GABAergic striatal neurons containing substance P and projects monosynaptically to the GPi/SNr. The indirect pathway arises from GABAergic striatal neurons containing enkephalin and projects polysynaptically to the GPi/SNr by way of a sequence of connections involving the external segment of the globus pallidus (GPe) and the subthalamic nucleus (STN). The STN is considered to be another input station of the basal ganglia, because the monkey STN receives somatotopically organized direct inputs from the motor-related cortical areas, such as the primary motor cortex, supplementary motor area and premotor cortex (Hartmann-von Monakow et al., 1978; Nambu et al., 1996, 1997), and sends outputs to the GPe and GPi/SNr. The stimulation of the motor-related cortical areas induces an early, short-latency excitation, followed by an inhibition and a late excitation in monkey GPe and GPi neurons (Nambu et al., 1990, 2000; Yoshida et al., 1993). The early excitation is derived from the cortico-STN-pallidal pathway, while the inhibition and late excitation are mediated by the direct and indirect pathways, respectively. These observations suggest the existence of the cortico-STN-GPi/SNr

* Atsushi Nambu, Yoshihisa Tachibana, National Institute for Physiological Sciences, Okazaki, Aichi 444-8585, Japan. Katsuyuki Kaneda, Hironobu Tokuno, Masahiko Takada, Tokyo Metropolitan Institute for Neuroscience, Fuchu, Tokyo 183-8526, Japan

"hyperdirect" pathway. Its conduction velocity is faster than those of direct and indirect pathways.

Integrating the hyperdirect, direct and indirect pathways, we proposed a dynamic model of cortico-basal ganglia functions (Nambu et al., 2000, 2002). In this manuscript, we will briefly introduce this model, and explain the pathophysiology of basal ganglia disorders and the mechanism for the effectiveness of the stereotaxic surgery (functional neurosurgery) based on this model.

2. THE DYNAMIC MODEL OF CORTICO-BASAL GANGLIA FUNCTIONS

Anatomical studies have shown that STN-pallidal fibers arborize more widely and terminate on more proximal neuronal elements of the pallidum than striato-pallidal fibers (Hazrati and Parent, 1992a,b). These findings suggest a "center-surround model" of basal ganglia function, which proposes an inhibition of competing motor programs and focused release of the selected motor program at the level of the thalamus and cerebral cortex (Mink and Thach, 1993; Mink, 1996). The hyperdirect pathway exerts powerful excitatory effects on the output nuclei of the basal ganglia and has shorter signal conduction time from the cerebral cortex than the direct and indirect pathways (Fig. 1A). Based on these observations, we expanded the center-surround model into a "dynamic model" in the *temporal* domain in the regulation of voluntary limb movements (Fig. 1B: Nambu et al., 2002): (1) When a voluntary movement is about to be initiated by cortical mechanisms, a corollary signal is transmitted simultaneously from the motor cortex to the GPi through the hyperdirect pathway, activates GPi neurons and thereby suppresses the large areas of thalamus and

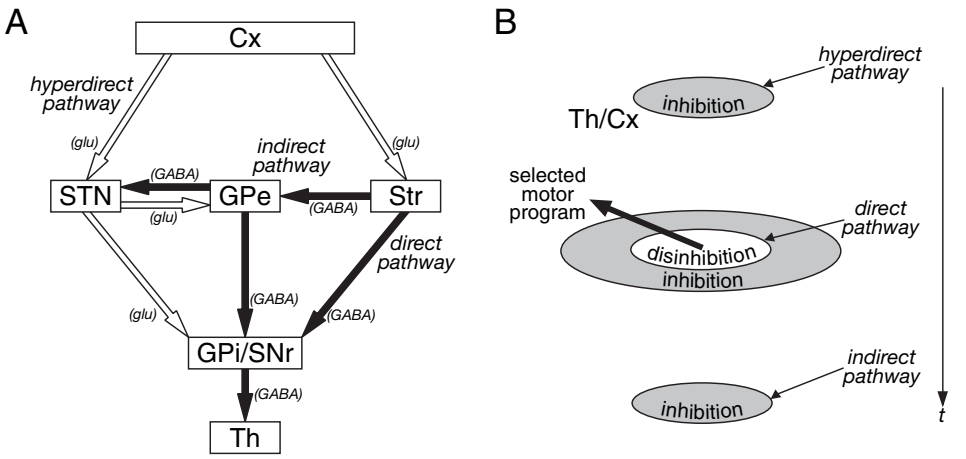

Figure 1. (A) A schematic diagram of the cortico-STN-GPi/SNr "hyperdirect", cortico-striato-GPi/SNr "direct" and cortico-striato-GPe-STN-GPi/SNr "indirect" pathways. Open and filled arrows represent excitatory glutamatergic (glu) and inhibitory GABAergic (GABA) projections, respectively. Cx, cerebral cortex; GPe, external segment of the globus pallidus; GPi, internal segment of the globus pallidus; SNr, substantia nigra pars reticulata; STN, subthalamic nucleus; Str, striatum; Th, thalamus. (B) The dynamic model of basal ganglia function explaining the activity changes in the thalamus and/or cortex (Th/Cx) caused by sequential inputs through the hyperdirect (top), direct (middle) and indirect (bottom) pathways. (Modified from Nambu et al., 2002).

cerebral cortex that are related to both the selected motor program and other competing programs (Fig. 1B, top): (2) Next, another corollary signal through the direct pathway is conveyed to the GPi and inhibits a specific population of pallidal neurons in the center area, resulting in the disinhibition of their targets and release of the selected motor program (Fig. 1B, middle): (3) Finally, the third corollary signal through the indirect pathway reaches the GPi to activate neurons therein and suppresses their targets extensively (Fig. 1B, bottom). Through such sequential information processing, only the selected motor program mediated by pallidal neurons in the center area is initiated, executed and terminated at the selected timing, while other competing motor programs mediated by surrounding pallidal neurons are suppressed.

3. UNDERSTANDING THE PATHOPHYSIOLOGY OF BASAL GANGLIA DISORDERS BY THE DYNAMIC MODEL

The mechanisms underlying hypokinetic and hyperkinetic disorders are currently explained as changes in the *static* state of the basal ganglia: An impaired balance of activity in the direct and indirect pathways causes an increase or decrease in the mean firing rate of GPi/SNr neurons (Albin et al., 1989; DeLong, 1990). According to this model, in parkinsonian state, increased activity along the indirect pathway and reduced activity along the direct pathway enhance the mean firing rate of GPi/SNr neurons, suppress the activity of thalamic and cortical neurons, and finally cause akinesia. Here we would like to suggest that the dynamic model can better explain the pathophysiology of basal ganglia disorders by introducing the *temporal and spatial* aspects of basal ganglia functions.

In normal monkeys, cortical stimulation evokes a triphasic response composed of an early excitation, inhibition and late excitation in GPi neurons. In monkeys rendered parkinsonian by administration of 1-methyl-4-phenyl-1,2,3,6-tetrahydropyridine (MPTP), the duration of inhibition in the GPi evoked by cortical stimulation is reduced, and the amplitude of early and late excitations is increased. The intravenous injection of L-dopa transiently improves parkinsonian akinesia, and the cortically-evoked response pattern in the GPi is restored to the normal triphasic pattern. These observations suggest that when a voluntary movement is about to be initiated by cortical mechanisms, signals through the hyperdirect and indirect pathways expand and suppress not only unwanted motor programs but also the selected motor program (Fig. 2, left). A signal through the direct pathway is reduced, and smaller areas of the thalamus and cortex are disinhibited for shorter period of time than in the normal state. Thus, the selected motor program cannot be released, resulting in akinesia of Parkinson's disease.

The involuntary movement called hemiballism is caused by lesions in the STN or the blockade of STN neuronal activity (Carpenter et al., 1950; Hamada and DeLong, 1992; Nambu et al., 2000). After the blockade of STN neuronal activity, cortical stimulation evokes a long inhibition without excitations in GPi (Nambu et al., 2000). These results suggest that when a voluntary movement is about to be initiated by cortical mechanisms, signals through the hyperdirect and indirect pathways are blocked in the STN, and unwanted motor programs are released. A signal through the direct pathway disinhibits wider areas of the thalamus and cortex for longer periods of time than in the normal state. Thus, not only the selected motor programs, but also unwanted motor programs are released, and the duration of the execution of the selected motor program is prolonged. By these mechanisms,

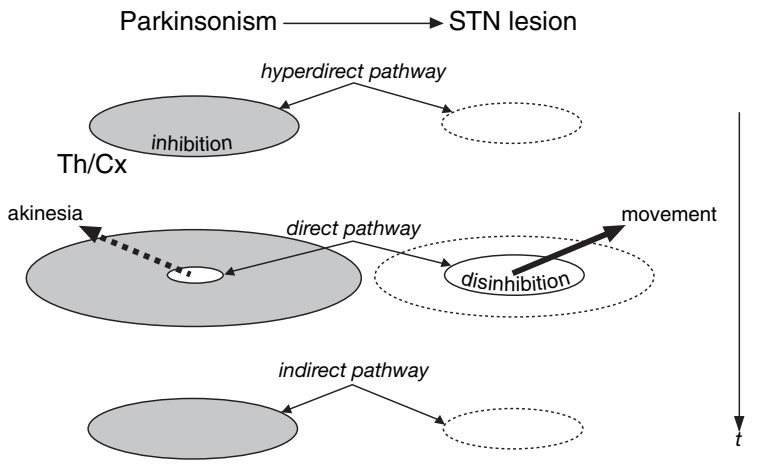

Figure 2. (Left) A schematic diagram showing the activity changes in the Th/Cx during parkinsonian state. Increased signals through the hyperdirect and indirect pathways and a reduced signal through the direct pathway result in reduced disinhibition in the Th/Cx, leading to the akinesia. (Right) A lesion in the STN restores disinhibition in the Th/Cx, and the selected movement can be released.

small excitations in the motor cortex release motor programs randomly, thereby resulting in involuntary movements.

4. MECHANISM FOR THE EFFECTIVENESS OF FUNCTIONAL NEURO SURGERY

Recent advances in functional neurosurgery have highlighted the STN as a target structure. In monkeys and humans, the lesion or high frequency stimulation (HFS) of the STN can ameliorate parkinsonian motor symptoms (Bergman et al., 1990; Jahanshahi et al., 2000, Hashimoto et al., 2003). The blockade of the STN activity by the local injection of $GABA_A$ agonist muscimol also improves motor activity of parkinsonian monkeys. The blockade of the STN diminishes the early and late excitations evoked by cortical stimulation and prolongs the duration of the inhibition in the GPi. According to the dynamic model, a main cause of akinesia is a reduced disinhibition in the thalamus and cortex during movements (Fig. 2, left), and the blockade of the STN restores the disinhibition in the cortex and thalamus during movement and releases the selected motor program (Fig. 2, right).

On the other hand, the mechanism of STN-HFS is not clear. It is open to argument whether HFS excites or inhibits STN neuronal activity (Lozano et al., 2002). In our experiments, not only a single, but also a repetitive stimulation of the STN excites GPi neurons, suggesting that the mechanism of action is the excitation of STN activity rather than inhibition. Because increased GPi and STN activity should make parkinsonian symptoms worse, this observation contradicts the current static model. The triphasic response in the GPi evoked by cortical stimulation is not observed during STN-HFS, suggesting that abnormal neuronal activity through the hyperdirect, direct and indirect pathways during parkinsonian state is not transmitted to GPi during STN-HFS, leading to the amelioration of parkinsonian motor symptoms.

5. CONCLUSIONS

We introduced the dynamic model of basal ganglia functions: Information through the cortico-STN-GPi hyperdirect, direct and indirect pathways dynamically controls the activity of the thalamus and cortex and releases only the selected motor program at the selected timing. The pathophysiology of basal ganglia disorders and the mechanism for the effectiveness of functional neurosurgery can be explained by an increase or decrease in disinhibition and inhibition in the thalamus and cortex in the *temporal and spatial* domains.

6. ACKNOWLEDGEMENTS

This study was supported by Grants-in-Aid for Scientific Research (C) and for Scientific Research on Priority Areas (A) from the Ministry of Education, Culture, Sports, Science and Technology of Japan.

7. REFERENCES

Albin, R.L., Young, A.B., and Penney, J.B., 1989, The functional anatomy of basal ganglia disorders, *Trends Neurosci*. **12**:366–375.

Alexander, G.E., and Crutcher, M.D., 1990, Functional architecture of basal ganglia circuits: neural substrates of parallel processing, *Trends Neurosci*. **13**:266–271.

Bergman, H., Wichmann, T., and DeLong, M.R., 1990, Reversal of experimental parkinsonism by lesions of the subthalamic nucleus, *Science* **249**:1436–1438.

Carpenter, M.B., Whittier, J.R., and Mettler, F.A., 1950, Analysis of choreoid hyperkinesia in the rhesus monkey: surgical and pharmacological analysis of hyperkinesia resulting from lesions in the subthalamic nucleus of Luys, *J. Comp. Neurol*. **92**:293–332.

DeLong, M.R., 1990, Primate models of movement disorders of basal ganglia origin, *Trends Neurosci*. **13**: 281–285.

Hamada, I., and DeLong, M.R., 1992, Excitotoxic acid lesions of the primate subthalamic nucleus result in transient dyskinesias of the contralateral limbs, *J. Neurophysiol*. **68**:1850–1858.

Hartmann-von Monakow, K., Akert, K., and Künzle, H., 1978, Projections of the precentral motor cortex and other cortical areas of the frontal lobe to the subthalamic nucleus in the monkey, *Exp. Brain Res*. **33**: 395–403.

Hashimoto, T., Elder, C.M., Okun, M.S., Patrick, S.K., and Vitek, J.L., 2003, Stimulation of the subthalamic nucleus changes the firing pattern of pallidal neurons, *J. Neurosci*. **23**:1916–1923.

Hazrati, L.-N., and Parent, A., 1992a, Convergence of subthalamic and striatal efferents at pallidal level in primates: an anterograde double-labeling study with biocytin and PHA-L, *Brain Res*. **569**:336–340.

Hazrati, L.-N., and Parent, A., 1992b, Differential patterns of arborization of striatal and subthalamic fibers in the two pallidal segments in primates, *Brain Res*. **598**:311–315.

Jahanshahi, M., Ardouin, C.M.A., Brown, R.G., Rothwell, J.C., Obeso, J., Albanese, A., Rodriguez-Oroz, M.C., Moro, E., Benabid, A.L., Pollak, P., and Limousin-Dowsey, P., 2000, The impact of deep brain stimulation on executive function in Parkinson's disease, *Brain* **123**:1142–1154.

Lozano, A.M., Dostrovsky, J., Chen, R., and Ashby, P., 2002, Deep brain stimulation for Parkinson's disease: disrupting the disruption, *Lancet Neurol.* **1**:225–231.

Mink, J.W., 1996, The basal ganglia: focused selection and inhibition of competing motor programs, *Prog. Neurobiol*. **50**:381–425.

Mink, J.W., and Thach, W.T., 1993, Basal ganglia intrinsic circuits and their role in behavior, *Curr. Opin. Neurobiol*. **3**:950–957.

Nambu, A., Yoshida, S., and Jinnai, K., 1990, Discharge patterns of pallidal neurons with input from various cortical areas during movement in the monkey, *Brain Res*. **519**:183–191.

Nambu, A., Takada, M., Inase, M., and Tokuno, H., 1996, Dual somatotopical representations in the primate subthalamic nucleus: evidence for ordered but reversed body-map transformations from the primary motor cortex and the supplementary motor area, *J. Neurosci*. **16**:2671–2683.

Nambu, A., Tokuno, H., Inase, M., and Takada, M., 1997, Corticosubthalamic input zones from forelimb representations of the dorsal and ventral divisions of the premotor cortex in the macaque monkey: comparison with the input zones from the primary motor cortex and the supplementary motor area, *Neurosci. Lett*. **239**:13–16.

Nambu, A., Tokuno, H., Hamada, I., Kita, H., Imanishi, M., Akazawa, T., Ikeuchi, Y., and Hasegawa, N., 2000, Excitatory cortical inputs to pallidal neurons via the subthalamic nucleus in the monkey, *J. Neurophysiol*. **84**:289–300.

Nambu, A., Tokuno, H., and Takada, M., 2002, Functional significance of the cortico-subthalamo-pallidal "hyperdirect" pathway, *Neurosci. Res*. **43**:111–117.

Yoshida, S., Nambu, A., and Jinnai, K., 1993, The distribution of the globus pallidus neurons with input from various cortical areas in the monkey, *Brain Res*. **611**:170–174.

STRIATAL GRAFTS AND SYNAPTIC PLASTICITY

David Mazzocchi-Jones, Máté Döbrössy, and Stephen Dunnett*

1. INTRODUCTION

Transplanted embryonic tissue into the lesioned striatum of rodents and primates can establish extensive afferent and efferent connections with the host brain (Dunnett et al., 2000). Such transplants have been shown to reduce some of the behaviourally assessed deficits observed post-lesion (Dunnett, 1995; Isacson et al., 1986). Moreover, the demonstration that grafted animals have to relearn previously acquired skills and habits lost following the lesions has been taken to suggest that the grafts may provide a physiological substrate for new learning within integrated graft-host circuits, rather than simply restoring a tonic or enabling influence over motor circuits within the host brain (Brasted et al., 1999). If transplantation of embryonic striatal tissue is to become a viable therapy in the treatment of neurodegenerative conditions such as Huntington's Disease (HD), it must be shown that such transplanted tissue becomes 'functionally integrated'. Much evidence demonstrates that striatal transplants alleviate a degree of the motor deficits observed post-lesion. Yet, there is still only limited data showing that striatal grafts reconnect with the host circuitry, forming fully functional synapses in keeping with the concept of true repair.

In this chapter we review the concept of 'functional integration' of transplanted striatal tissue. Highlighting the anatomical, behavioural and physiological evidence, we will give credence to the hypothesis that embryonic striatal tissue can reform a functionally effective circuit with the host brain that is plastic to changing inputs as required of a neural substrate for new learning.

2. EFFERENT INNERVATION OF EMBRYONIC STRIATAL GRAFTS

It has been well documented that a variety of excitotoxic agents are capable of causing widespread destruction of the cellular population of the striatum (Coyle and Schwarcz, 1976). Though a number of these agents have been used to produce animal models of

* The Brain Repair Group, Cardiff School of Biosciences, Cardiff University, Museum Avenue, PO BOX 911, Cardiff, CF1 3US, UK.

neurodegeneration, the current toxin of choice to mimic the pathology of HD is quinolinic acid. Quinolinic acid over activates *N*-methyl-D-aspartic (NMDA) receptors, causing excessive calcium influx and a selective ablation of medium spiny neurones (MSN's), which constitute both the major cellular, and post-synaptic population of the striatum. Such lesions have been shown to produce behavioural and cognitive deficits, which mimic those seen in human HD patients. Furthermore, the lesions produce a pronounced loss of baseline synaptic transmission, whilst the contralateral intact striatum demonstrates normal synaptic responses.

One of the most striking observations of transplanted embryonic striatal tissue into the lesioned host striatum is that the transplants display a cellular mosaic appearance when distinguished by acetylcholinesterase (AChE) and dopamine- and cyclic AMP-regulated 32 kilodalton phosphoprotein (DARPP-32) immunoreactivity (Graybiel et al., 1989). Such "patch" and "non-patch" zones correspond to areas which contain neurones of striatal morphology, versus areas containing neurones of non-striatal morphology. Patch zones have been shown to demonstrate similar striatal morphology to that of the normal striatum (DiFiglia et al., 1988; Isacson et al., 1987; McAllister et al., 1985), including a significant number of medium spiny neurones, as characterised by positive DARPP-32, γ-aminobutyric acid (GABA) staining (Roberts and DiFiglia, 1990). Furthermore behavioural studies have demonstrated that improved behavioural performance correlates with the density of patch zones found within the graft (Fricker et al., 1997a,b). Non-Patch zones, are shown to stain positive for calbindin and somatostatin, with neuronal features characteristic of pallidal, cortical and amygdala origin.

The transplantation of embryonic striatal tissue into previously lesioned regions has been shown to undergo a certain amount of anatomically assessed reconnection with the host circuitry. A number of studies have demonstrated that for a certain period of time post-transplantation, afferent fibres begin to innervate the graft region (Pritzel et al., 1986; Wictorin et al., 1988, 1989a,b, 1990; Wictorin and Bjorklund, 1989; Xu et al., 1992). Though such transplants receive efferent innervation from nearly all of the input phenotypes, there is a notable variation in the type and density of innervation. Cortical and thalamic inputs appear to initially densely innervate the outer edge of the graft, with a significantly lower innervation of the core regions of the graft. Though over time the fibre ingrowth by such efferents increases, it fails to reach the level observed in the intact striatum. The dopaminergic (DA) afferents from the substantia nigra (SN) appear to form patchy innervation of the transplant, mimicking that of the intact striatum, with similar density of innervation as the transplant matures. Finally, the serotonergic innervation from the mesencephalic raphe appears to innervate the whole transplant, and like DA input from the SN, eventually reaches similar densities to that observed in the intact striatum (see Wictorin, 1992 for a review).

Whilst efferent innervation of the transplant is a critical factor in determining functional efficacy, functional integration is more critically dependant on appropriate "Point-To-Point" reconnection. Whilst it has been shown that the various efferent fibres formed synaptic contacts with transplanted MSN's, not all of these synapses are located on the correct region of the post-synaptic neurones. In a study conducted by Xu et al. (1992) labelled cortical inputs only form synapses with the spines of MSN's roughly 50% of the time, whereas in the normal striatum over 90% of these contacts are found on the spines. Therefore, whilst it is clear that "Point-To-Point" reconnection does occur between host afferents and the transplant, the degree to which this occurs is limited when compared to the intact system.

3. STRIATAL GRAFTS ARE PHYSIOLOGICALLY RESPONSIVE TO HOST STIMULATION

Only a handful of studies exist, in which the function of transplanted embryonic striatal tissue is tested via electrophysiological means. It has been previously shown that transplanted striatal tissue forms functional striatal like neurones which are responsive to stimulation of host efferent fibres (Rutherford et al., 1987; Siviy et al., 1993; Walsh et al., 1988; Xu et al., 1992). These studies report a significant degree of correlation between the electrophysiological characteristics of both transplanted and normal striatal neurones. However, a number of characteristics have emerged which are wholly unique to transplanted embryonic striatal neurones.

Early studies involving the *in vitro* slice preparation demonstrated that following appropriate stimulation of the host cortex, EPSP's could be recorded from transplanted neurones (Rutherford et al., 1987). Later studies conducted *in vivo* showed that the same was true following thalamic stimulation (Xu et al., 1991). It is important to note that on average the maximum amplitude of such EPSP's is smaller from transplanted neurones, than those of the normal striatum. Such observations are consistent with anatomical studies which show a decreased efferent innervation of the transplant, and a lower degree of "Point-To-Point" reconnection (Pritzel et al., 1986; Wictorin et al., 1988, 1989, 1989a, b, 1990; Wictorin and Bjorklund, 1989; Xu et al., 1992). However Xu et al. (1991) report that during intracellular recordings nearly all transplanted neurones displayed excitatory responses to both cortical and thalamic stimulation. This would suggest that nearly all regions of the graft receive sufficient efferent innervation for transplanted neurones to be active to host stimulation. From our own observations, when probing transplanted tissue for extracellular recordings, there appears to be distinct regions which are responsive to host stimulation, with other regions proving non-responsive. Such non-responsive regions remain upon movement of stimulating location, though positioning of the stimulating electrode close to the recording site (within the graft tissue) on some occasions produces non-synaptic fibre volley like responses. This suggests that such non-responsive regions either do not receive host innervation, or do so at insufficient levels to produce synaptic responses. Although it is important to consider that extracellular field recordings require activation of a collection of cells, small efferent innervation may prove sufficient to excite single cells, whilst not being sufficient to activate the multicellular network required for extracellular recordings. It is also important to note that rebound excitation of the neurones within the graft, may be sufficient to generate synaptic activation of graft neurones when recorded at a single cell level, and may not be sufficient at the extracellular level.

The most important difference between normal and transplanted striatal neurons is that transplanted neurones appear to lack the rhythmic depolarising cycles between "Up" and "Down" states (Xu et al., 1991) which in the intact striatum is thought to play a critical role in priming subsections of the striatum for burst firing of action potentials (Wilson and Groves, 1981). Though transplanted neurones display a lack of this rhythmic depolarisation, burst firing of action potentials has been observed following artificial depolarisation (Xu et al., 1991). One such possibility for the lack of rhythmic depolarisation lies in the lower level of cortical efferent innervation of such transplants. It has been documented that the priming of neurones between up and down states occurs on cue with cortical rhythmic oscillations, and is dependant on an intact cortical projection (Wilson and Groves, 1981). It would therefore seem plausible that in the transplant system, where cortical fibre ingrowth is much more limited than the norm, such fluxations would be absent.

4. NEW LEARNING WITHIN STRIATAL GRAFTS

The adult brain is at its most plastic in the period following injury, offering a window of opportunity for therapeutic intervention (Horner and Gage, 2000; Taub et al., 2002). The effects of enriched environment, behavioural experience and grafting can each separately influence neuronal plasticity and recovery of function after brain damage. However, the mechanisms by which these factors interact, so that the environment or training might modify the survival, integration or function of grafted tissues is at present unknown (Dobrossy and Dunnett, 2001). To maximise the positive effects following brain damage, cell replacement therapy must both make use of the endogenous potential for recovery of the host and optimise the external circumstances associated with any intervention. In particular, observations that for some aspects of recovery grafts require training indicates that graft function and experience are not simply independent and additive, but fundamentally interactive. The results of recent experiments studying the idea of "learning to use the graft" suggests that the functions that had been established in the intrinsic circuits of the brain through a lifetime's training and experience prior to lesion need to be re-established – through relearning – using the graft circuitry (Brasted et al., 1999; Coffey et al., 1989, 1990; Mayer et al., 1992). A condition for this to occur is the functional plasticity of the transplanted tissue which is most likely mediated by morphological, cellular and molecular changes, including those that impinge on the mechanisms of plasticity such as long-term potentiation and depression, mechanisms that lend themselves to scrutiny through electrophysiological methods.

"Learning to use a graft" has been investigated in the context of retinal (Coffey et al., 1990; Coffey et al., 2000), and more relevant to this chapter, striatal implants in rats (Brasted et al., 1999; Mayer et al., 1992). Initial experiments employed the '9-hole box' apparatus that allows precise presentation of stimuli and registration of the animals' responses in multiple spatial locations provided by an array of 9 holes in the back wall of the operant box. The animals were trained to hold a nose poke into the central hole and then respond rapidly to brief light stimuli on the left or right sides. Depending on the particular version used, the appropriate response was a nose poke either on the same or the opposite side as the light stimulus. Unilateral excitotoxic lesions of striatal neurones disrupt the initiation of responses on the contralateral side without affecting the animals' ability to detect or attend to the eliciting stimulus (Brasted et al., 1997; Carli et al., 1985). Both the lesioned and grafted rats that have been trained to respond on the opposite side to the stimulus exhibit profound deficits in responding on the contralateral side when returned to the test 4 months later. However, whereas the lesioned rats could not relearn the task, the grafted animals re-acquired the performance with training (Brasted et al., 1999; Mayer et al., 1992). The characteristics of relearning were that it took place over a similar period to that required by naïve rats to learn the task *de novo*, and, as further experiments have since showed, the training needs to be specific in targeting the limb controlled by the damaged striatum with the striatal implant (Dobrossy and Dunnett, 2003).

The gradual behavioural improvement following the training of the grafted animals has been initially demonstrated in complex, high trial number operant behavioural tasks. However, progressive graft-mediated improvement can occur in low repetition nonoperant test such as the skilled paw-reaching task, as well, with far less exposure and practice (Dobrossy and Dunnett, 2005). "Learning to use the graft" implies not only functional plasticity, but also a structural representation of that process within the reconstructed graft-host circuit. Motor skills and habits are acquired and refined throughout development and

a lifetime of experience. To the extent that motor learning (whether expressed in the language of habit formation, procedural or stimulus–response associative learning) is mediated by the striatum, it is not surprising that striatal lesions generate such lasting impairments in a variety of skilled motor tasks. More remarkable is the fact that recovery can be achieved by a process as apparently crude as embryonic striatal cell transplantation, and that the implanted cells not only organise themselves and project appropriately (Bjorklund, 1994; Dunnett, 1995), but retain the physiological plasticity to act as a substrate for new learning. The challenge for the future is to obtain direct evidence that relearning is subserved within the striatal circuitry, and to consider what cellular mechanisms associated with plasticity are involved in, and perhaps responsible for, the functional benefits that striatal graft have been implicated in.

5. STRIATAL GRAFTS DEMONSTRATE BIPHASIC SYNAPTIC PLASTICITY

Previous electrophysiological and neurochemical analysis of graft tissue has demonstrated that transplanted graft neurones display similar electrophysiological properties to the intrinsic cellular population, and that host neurons can signal patterned information to grafted cells (Rutherford et al., 1987; Sirinathsinghji et al., 1988; Siviy et al., 1993; Xu et al., 1991). Behavioural studies have demonstrated that following ablation of MSNs, the striatum fails to learn new tasks, which can be recovered via the transplantation of replacement cells (Brasted et al., 1999). The evidence that such transplants restore the ability to learn new tasks, combined with the evidence demonstrating that such transplanted neurones form functional synapses with the host circuitry, would suggest that graft-host synapses would demonstrate cellular mechanisms of learning and memory. In our own studies, we have been able to demonstrate that grafted cells can transduce changes in afferent input and exhibit stable changes in the form of synaptic plasticity, which is widely considered as the cellular reflection of learning in the whole organism (Bliss and Collingridge, 1993). Utilising the corticostriatal *in vitro* slice preparation, we were able to record extracellular field potentials from the graft region (Fig 1), following stimulation of the host corpus callosum. Such recordings remain relatively stable over a 30 min baseline period, though the magnitude of the response is notably smaller than that observed in the normal striatum. Using high frequency stimulation (HFS) we are able to induce synaptic plasticity from both the normal and grafted striatum. Such plastic behaviour is biphasic, dependant on the presence of Mg^{2+} ions in the perfusate solution, in keeping with the normal system (Calabresi et al., 1992). In the presence of Mg^{2+} ions, HFS produces stable long-term depression (LTD) in both control and graft recordings (Fig 1A, B), though the magnitude of depression observed in graft recordings was lower than that observed in the normal striatum. This is hardly surprising, as the maximal amplitude of graft recordings has been shown to be lower, suggesting that the ability to depress synaptic transmission would be limited.

In the absence of Mg^{2+} ions, HFS results in the predominant expression of long-term potentiation (LTP) within both control and graft recordings (Fig 1C, D). It has been previously suggested that the removal of magnesium leads to NMDA receptor chronic activation, a vital component required in the ability to express corticostriatal LTP. Interestingly, although we observe a slightly lower level of LTP from the graft, there is no significant difference between the level of potentiation in grafts versus control. Though this is unexpected, given the significant difference seen during LTD, it is hardly surprising. We suggest that chronic activation of the NMDA receptor complex leads to a situation where tetanic

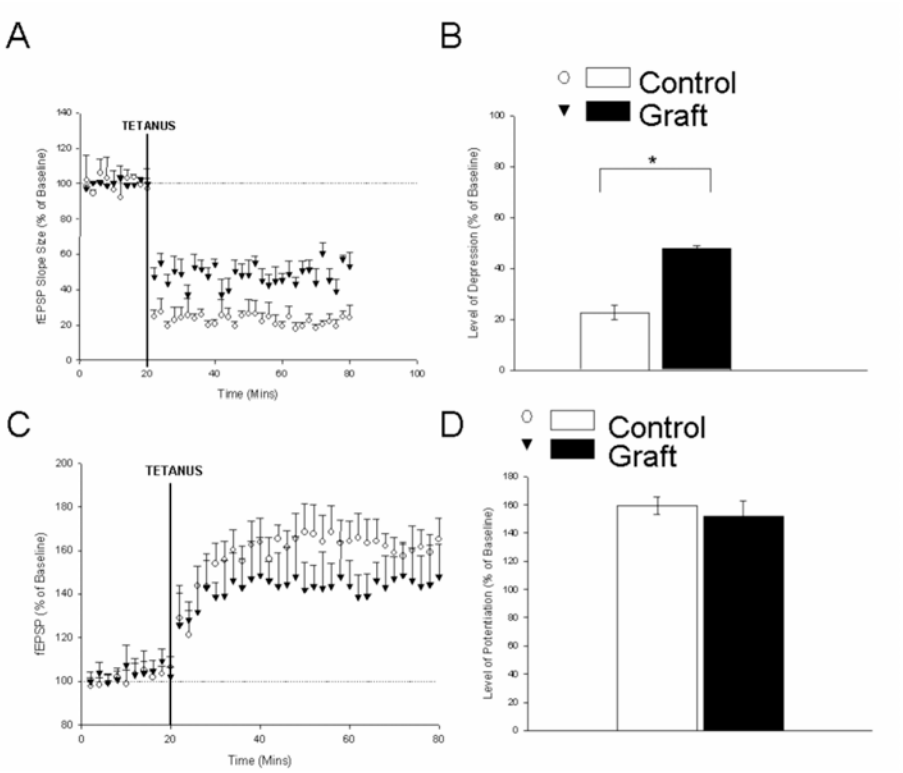

Figure 1. Bi-directional synaptic plasticity in embryonic striatal grafts. (A) Demonstration of LTD in both control and graft recordings, (B) level of depression observed in both control and graft recordings. (C) Demonstration of LTP in graft and control recordings, (D) level of potentiation in graft and control recordings.

stimulation produces a maximal activation of the post-synaptic neurone. Therefore, it is possible that under such conditions the amount of LTP observed would be equal to maximal levels of excitation. Such observations could be confined to the artificial situation represented in the Mg^{2+} *in vitro* slice preparation, and for example may not be seen when LTP is expressed from the graft region *in vivo*.

6. CONCLUSION

Whilst it has been demonstrated previously that embryonic striatal grafts restore the ability of the lesioned striatum to learn new tasks, it has only been recently speculated that this is due to restoration of cellular correlates of learning and memory. We demonstrate that embryonic striatal grafts not only restore baseline transmission, but also display synaptic plasticity, appropriate to that observed within the normal striatum. Our data provides further evidence supporting the hypothesis that embryonic striatal tissue becomes 'functionally integrated' into the host neuronal circuitry, and in doing so restores synaptic

plasticity, which we believe to facilitate striatal transplants to restore the ability to learn new tasks that are lost following striatal lesions.

7. ACKNOWLEDGEMENTS

We gratefully thank P. Chambon for the use of the PrP-L-EGFP-L mouse, our colleagues at the Brain Repair Group, for technical assistance, and Paul Chapman for his initial involvement with this project. This work is supported by an MRC studentship to DMJ.

8. REFERENCES

Bjorklund, A., 1994, Long distance axonal growth in the adult central nervous system, *J Neurol.* **242**:S33.

Bliss, T.V., and Collingridge, G.L., 1993, A synaptic model of memory: long-term potentiation in the hippocampus, *Nature* **361**:31.

Brasted, P.J., Humby, T., Dunnett, S.B., and Robbins, T.W., 1997, Unilateral lesions of the dorsal striatum in rats disrupt responding in egocentric space, *J. Neurosci*. **17**:8919.

Brasted, P.J., Watts, C., Robbins, T.W., and Dunnett, S.B., 1999, Associative plasticity in striatal transplants, *Proc Natl. Acad. Sci. U. S. A*. **96**:10524.

Calabresi, P., Pisani, A., Mercuri, N.B., and Bernardi, G., 1992, Long-term potentiation in the striatum is unmasked by removing the voltage-dependent magnesium block of NMDA receptor channels, *Eur. J. Neurosci*. **4**:929.

Carli, M., Evenden, J.L., and Robbins, T.W., 1985, Depletion of unilateral striatal dopamine impairs initiation of contralateral actions and not sensory attention, *Nature*. **313**:679.

Coffey, P.J., Lund, R.D., and Rawlins, J.N., 1989, Retinal transplant-mediated learning in a conditioned suppression task in rats, *Proc. Natl. Acad. Sci. U. S. A*. **86**:7248.

Coffey, P.J., Lund, R.D., and Rawlins, J.N., 1990, Detecting the world through a retinal implant, *Prog. Brain Res*. **82**:269.

Coffey, P.J., Whiteley, S.J., and Lund, R.D., 2000, Preservation and restoration of vision following transplantation, *Prog. Brain Res*. **127**:489.

Coyle, J.T., and Schwarcz, R., 1976, Lesion of striatal neurones with kainic acid provides a model for Huntington's chorea, *Nature* **263**:244.

DiFiglia, M., Schiff, L., and Deckel, A.W., 1988, Neuronal organization of fetal striatal grafts in kainate- and sham-lesioned rat caudate nucleus: light-and electron-microscopic observations, *J. Neurosci*. **8**:1112.

Dobrossy, M.D., and Dunnett, S.B., 2001, The influence of environment and experience on neural grafts, *Nat. Rev. Neurosci*. **2**:871.

Dobrossy, M.D., and Dunnett, S.B., 2003, Motor training effects on recovery of function after striatal lesions and striatal grafts, *Exp. Neurol*. **184**:274.

Dobrossy, M.D., and and Dunnett, S.B., 2005, Training specificity, graft development and graft mediated functional recovery in a rodent model of Huntington's disease *Neuroscience*. **In Press**.

Dunnett, S.B., 1995, Functional repair of striatal systems by neural transplants: evidence for circuit reconstruction, *Behav. Brain Res*. **66**:133.

Dunnett, S.B., Nathwani, F., and Bjorklund, A., 2000, The integration and function of striatal grafts, *Prog. Brain Res*. **127**:345.

Fricker, R.A., Torres, E.M., and Dunnett, S.B., 1997a, The effects of donor stage on the survival and function of embryonic striatal grafts in the adult rat brain. I. Morphological characteristics, *Neuroscience* **79**:695.

Fricker, R.A., Torres, E.M., Hume, S.P., Myers, R., Opacka-Juffrey, J., Ashworth, S., Brooks, D.J., and Dunnett, S.B., 1997b, The effects of donor stage on the survival and function of embryonic striatal grafts in the adult rat brain. II. Correlation between positron emission tomography and reaching behaviour. *Neuroscience* **79**:711.

Graybiel, A.M., Liu, F.C., and Dunnett, S.B., 1989, Intrastriatal grafts derived from fetal striatal primordia. I. Phenotypy and modular organisation. *J. Neurosci*. **9**:3250.

Horner, P.J., and Gage, F.H., 2000, Regenerating the damaged central nervous system, *Nature*. **407**:963.

Isacson, O., Dunnett, S.B., and Bjorklund, A., 1986, Graft-induced behavioral recovery in an animal model of Huntington disease, *Proc. Natl. Acad. Sci. U. S. A*. **83**:2728.

Isacson, O., Pritzel, M., Dawbarn, D., Brundin, P., Kelly, P.A., Wiklund, L., Emson, P.C., Gage, F.H., Dunnett, S.B., and Bjorklund, A., 1987, Striatal neural transplants in the ibotenic acid-lesioned rat neostriatum. Cellular and functional aspects, *Ann. N. Y. Acad. Sci*. **495**:537.

Mayer, E., Brown, V.J., Dunnett, S.B., and Robbins, T.W., 1992, Striatal graft-associated recovery of a Lesion-Induced performance deficit in the rat requires learning to use the transplant, *Eur. J. Neurosci.* **4**:119.

McAllister, J.P., Walker, P.D., Zemanick, M.C., Weber, A.B., Kaplan, L.I., and Reynolds, M.A., 1985, Morphology of embryonic neostriatal cell suspensions transplanted into adult neostriata, *Brain Res*. **355**:282.

Pritzel, M., Isacson, O., Brundin, P., Wiklund, L., and Bjorklund, A., 1986, Afferent and efferent connections of striatal grafts implanted into the ibotenic acid lesioned neostriatum in adult rats, *Exp. Brain Res*. **65**:112.

Roberts, R.C., and DiFiglia, M., 1990, Long-term survival of GABA-, enkephalin-, NADPH-diaphorase- and calbindin-d28k-containing neurons in fetal striatal grafts, *Brain Res*. **532**:151.

Rutherford, A., Garcia-Munoz, M., Dunnett, S.B., and Arbuthnott, G.W., 1987, Electrophysiological demonstration of host cortical inputs to striatal grafts, *Neurosci. Lett*. **83**:275.

Sirinathsinghji, D.J., Dunnett, S.B., Isacson, O., Clarke, D.J., Kendrick, K., and Bjorklund, A., 1988, Striatal grafts in rats with unilateral neostriatal lesions–II. In vivo monitoring of GABA release in globus pallidus and substantia nigra, *Neuroscience*. **24**:803.

Siviy, S.M., Walsh, J.P., Radisavljevic, Z., Cohen, R.W., Buchwald, N.A., and Levine, M.S., 1993, Evidence for enhanced synaptic excitation in transplanted neostriatal neurons, *Exp. Neurol*. **123**:222.

Taub, E., Uswatte, G., and Elbert, T., 2002, New treatments in neurorehabilitation founded on basic research, *Nat. Rev. Neurosci*. **3**:228.

Walsh, J.P., Zhou, F.C., Hull, C.D., Fisher, R.S., Levine, M.S., and Buchwald, N.A., 1988, Physiological and morphological characterization of striatal neurons transplanted into the striatum of adult rats, *Synapse*. **2**:37.

Wictorin, K., 1992, Anatomy and connectivity of intrastriatal striatal transplants, *Prog. Neurobiol*. **38**:611.

Wictorin, K., and Bjorklund, A., 1989, Connectivity of striatal grafts implanted into the ibotenic acid-lesioned striatum–II. Cortical afferents, *Neuroscience* **30**:297.

Wictorin, K., Clarke, D.J., Bolam, J.P., and Bjorklund, A., 1989a, Host Corticostriatal Fibres Establish Synaptic Connections with Grafted Striatal Neurons in the Ibotenic Acid Lesioned Striatum, *Eur. J. Neurosci.* **1**:189.

Wictorin, K., Clarke, D.J., Bolam, J.P., and Bjorklund, A., 1990, Fetal striatal neurons grafted into the ibotenate lesioned adult striatum: efferent projections and synaptic contacts in the host globus pallidus, *Neuroscience* **37**:301.

Wictorin, K., Isacson, O., Fischer, W., Nothias, F., Peschanski, M., and Bjorklund, A., 1988, Connectivity of striatal grafts implanted into the ibotenic acid-lesioned striatum–I. Subcortical afferents, *Neuroscience* **27**:547.

Wictorin, K., Simerly, R.B., Isacson, O., Swanson, L.W., and Bjorklund, A., 1989b, Connectivity of striatal grafts implanted into the ibotenic acid-lesioned striatum–III. Efferent projecting graft neurons and their relation to host afferents within the grafts, *Neuroscience* **30**:313.

Wilson, C.J., and Groves, P.M., 1981, Spontaneous firing patterns of identified spiny neurons in the rat neostriatum, *Brain Res*. **220**:67.

Xu, Z.C., Wilson, C.J., and Emson, P.C., 1991, Synaptic potentials evoked in spiny neurons in rat neostriatal grafts by cortical and thalamic stimulation, *J. Neurophysiol*. **65**:477.

Xu, Z.C., Wilson, C.J., and Emson, P.C., 1992, Morphology of intracellularly stained spiny neurons in rat striatal grafts, *Neuroscience* **48**:95.

SPONTANEOUS FORMATION OF LEWY BODIES IN A RODENT

J. Nunan, A. Tsiotis-Vais, S. George, C.L. Parish, D.K. Grandy, D.I. Finkelstein, J. Drago, and M.K. Horne[1]

1. INTRODUCTION

Many neurodegenerative disorders are caused by a soluble protein being deposited in an insoluble form, either as fibrils or amorphous precipitates. In the case of Parkinson's disease (PD), α-synuclein (αSN), normally a highly soluble unfolded protein, forms amorphous precipitates to produce hallmark cytoplasmic inclusions known as Lewy Bodies. αSN was linked to PD when mutations in the αSN gene were found in a rare autosomal dominant form of the disease (Polymeropoulos et al., 1997). Interest in αSN became acute when a shortly after, fibrillary αSN was found to be a major component of Lewy Bodies (Spillantini et al., 1998). There is now strong evidence to support 3 other mendelian Parkinson's genes (parkin, PINK1 and DJ-1) with lesser support for 3 others (UCHL1, NR4a2 and synphilin) and linkage data for the existence of at least five as yet undiscovered genes (Healy et al., 2004). At first this may suggest that PD has heterogeneous causes, bound together only because they affect midbrain dopaminergic neurones, hence producing Parkinsonian symptomatology. However a considered examination of the evidence indicates a convergence of two common mechanisms: disturbance in clearance of αSN (through misfolding, over production of αSN or through disturbance in the ubiquitin proteosome system itself) or through oxidative stress (OS). These twin processes lead to abnormal αSN aggregation and production of toxic molecular species and ultimately to the formation of Lewy Bodies in the substantia nigra (SN), a process that is a central element of idiopathic PD. This is not to imply that Lewy Body formation *per se* is the toxic element of PD but

[1] Correspondence to: Professor Malcolm Horne, Email: m.horne@hfi.unimelb.edu.au
J. Nunan, A. Tziotis-Vais, S. George, D.I. Finkelstein, J. Drago, and M.K. Horne. Brian Injury and Repair Group, Howard Florey Institute, University of Melbourne, Parkville 3010, Australia. C.L Parish, Clinical Research Center, Department of Laboratory Medicine, Karolinska Institutet, Stockholm, Sweden. D.K. Grandy, Department of Physiology and Pharmacology, Oregon Health and Science University, Portland, Oregon 97239, USA.

that they are the one element that is an unequivocal marker of idiopathic PD. Thus models of the pathological process leading to PD must also produce Lewy Bodies.

There is ample evidence, accumulated over many years that OS is increased in the SNpc of PD patients, leading to the hypothesis that the formation of reactive oxygen species (ROS) causes to oxidative damage to nigral dopamine (DA) neurones (Zigmond et al., 1990, 2002; Jenner, 1998). Oxidative damage to lipids, proteins and DNA (Alam et al., 1997; Floor and Wetzel, 1998) and the concentration of iron, which catalyzes the formation of hydroxyl radicals from hydrogen peroxide, is elevated in the SN of PD patients (Sofic et al., 1988; Dexter et al., 1989) as is superoxide dismutase (Saggu et al., 1989). In addition, MPTP and roteneone, toxins that cause degeneration of nigral neurones, are complex 1 inhibitors (Langston and Ballard, 1983; Betarbet et al., 2000). PARK6 (Valente et al., 2004) and 7 (Bonifati et al., 2003) point to mitochondrial dysfunction as a key upstream factor in human Parkinsonism and there is also mitochondrial dysfunction and oxidative damage associated with loss of Parkin function (Palacino et al., 2004).

αSN aggregation and OS may be converging mechanisms. When aged in solution, both mutant and wild-type (Wt) αSN aggregate as amyloid-like fibrils similar to those that have been isolated from Lewy Bodies (Conway et al., 1998; El-Agnaf et al., 1998; Hashimoto et al., 1998; Narhi et al., 1999). Mutant and to a lesser extent C-terminally truncated αSN expressed in dopaminergic neuronal cell lines result in enhanced susceptibility to OS (Kanda et al., 2000). Moreover cytochrome c and αSN are colocalised in Lewy Bodies from brains of PD patients (Hashimoto et al., 1999) and increased accumulation of αSN may also lead to mitochondrial alterations that result in OS and eventually cell death (Hsu et al., 2000). On the other hand, it appears that the rate of aggregation of αSN increases when it is incubated in an oxidative system. Gaisson et al (Giasson et al., 2000) provided direct evidence that impairment of cellular antioxidant mechanisms or overproduction of ROS may be a primary event leading to the accumulation of insoluble αSN. They demonstrated extensive accumulation of nitrated αSN in Lewy bodies and in the filamentous building blocks of these inclusions and in the insoluble fractions of affected lesions. Thus there is the potential for "positive feed back" where oxidative stress may lead to aggregation, which in turn, increases vulnerability to oxidative stress (Lotharius, 2002; Lotharius et al., 2002; Petersen, 2002).

Suspicion has fallen on the metabolism of DA itself as a source of ROS including H_2O_2, nitric oxide and other hydroxyl radicals (Graham et al., 1978; Maker, 1981; Zhang et al., 2000). It can also be deaminated by monoamine oxidase (MAO) to produce dihydroxy-phenylacetic acid (DOPAC) and hydrogen peroxide, which can, in turn, be converted to hydroxyl radicals in the presence of iron (Maker, 1981). Furthermore, DA can itself inhibit complex 1 of the electron-transport chain (Ben-Shachar, 1995; Glinka, 1995, 1997, 1998; Gassen, 1996). These factors are particularly relevant in the in the presence of molecular oxygen, which will spontaneously oxidize to yield H_2O_2, superoxide from DA in the cytoplasm whereas within the synaptic vesicle, DA breakdown is retarded as the pH is low and MAO is absent. Importantly, the toxicity of mutant αSN (Lotharius, 2002; Xu et al., 2002) is DA dependent and increased accumulations of αSN may also lead to mitochondrial alterations that result in OS and eventually cell death (Hsu et al., 2000). Thus DA neurones constitutively provide a hostile microenvironment and genetic mutations or aberrations in αSN proteolysis could further jeopardize their survival by leading to OS. In most forms of PD, there is no mutation of αSN to predispose to protein aggregation, but rather, some other circumstances conducive to the formation of amyloid fibrils is present with suspicion that DA metabolism itself is providing that predisposition. We drew the

conclusion that DA neurones with increased DA turnover and hence increased cytosolic DA concentrations are likely to be under a modest but sustained increase in OS that would predispose to protein aggregation and hence the formation of Lewy bodies.

Recent findings (Finkelstein et al., 2000; Finkelstein, 2001; Parish et al., 2001, 2002; Stanic et al., 2003) have provided a model for studying this proposition. In brief we showed that the density of DA terminals in the striatum is regulated by the DA autoreceptor on the DA terminal and that in the normal animal, DA terminal density is regulated by DA concentrations in the synaptic cleft, which is in turn monitored by this receptor (Parish et al., 2001). Thus in the normal animal the terminal arbour is subject to sprouting or pruning so as to modify terminal density in response to changes in synaptic DA concentrations (Finkelstein et al., 2000, 2001; Stanic et al., 2003a, b). In normal nigrostriatal terminals, DA synthesis and release is highly regulated. Pre-synaptic DA 2 receptor (D_2R) inhibits nerve terminal excitability (Bunney et al., 1973; Tepper et al., 1984) and reduces DA release (Ungerstedt et al., 1982; Bowyer and Weiner, 1987), partially mediated via activation of K^+ channels (Lacey et al., 1987; Cass and Zahniser, 1990).

Activation of D_2R by DA reduces cAMP production and thereby reduces DA synthesis by adenylate cyclase dependent phosphorylation of tyrosine hydroxylase (TH), the rate limiting enzyme in the DA synthesis pathway (el Mestikawy et al., 1986; Onali et al., 1988; Lindgren et al., 2001). As DA release is dependent on both newly synthesized and recycled transmitter, this process is likely to play a critical role in the control of striatal dopaminergic transmission. The D_2 autoreceptor is tightly linked to the DA transporter (DAT), both anatomically (Hersch et al., 1995) and functionally (Kimmel et al., 2001; Robinson, 2002). Thus in the normal striatum it appears that the D_2R regulates synaptic DA not only by controlling nerve terminal excitability, DA release, DA synthesis and reuptake but also by regulating DA terminal density. The central role of the D_2R in regulating arbour terminal size was confirmed by administering both selective and nonselective D_1 and D_2 receptor agonists and antagonists to Wt mice and rats and to mutant mice with selective deletion of the D_1R ($D_1(-/-)$) and D_2R ($D_2(-/-)$). The $D_2(-/-)$ mouse provided the greatest density of terminals and the largest terminal arbours (Figure 1). DA release by sprouted terminals is well compensated for but DAT mechanisms are functionally impaired (Stanic et al., 2003). As a consequence of these large arbours and impaired DAT function, each individual

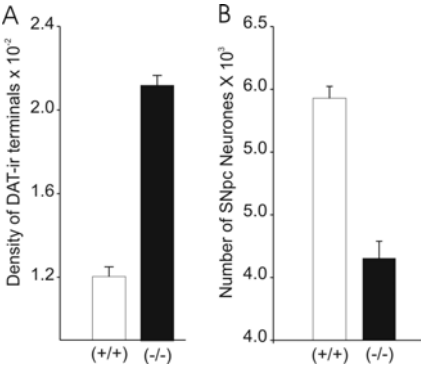

Figure 1. Shows the change in density of dopaminergic terminals in the striatum (A) and cell numbers in the nigra (B) in wild type (white bars) and $D_2(-/-)$ mice (black bars). The mutants have a vastly greater number of terminals serviced by far fewer neurones: i.e. each cell body has a greatly increased terminal arbour. Modified from (Finkelstein, 2001).

neurone must service a larger number of terminals, each producing increased amounts of DA. We therefore predicted that the $D_2(-/-)$ mouse would have increased DA turnover and consequently increased oxidative load and therefore prone to αSN aggregation.

DA turnover was increased in the brain and more specifically in each terminal and cell body of $D_2(-/-)$ mice (Parish et al., 2001). Basal levels of DA and DOPAC in the dorsal striatum of Wt and $D_2(-/-)$ mice were determined and expressed as amount of DA or DOPAC per gram of CPu tissue and DA activity was expressed as the ratio of DOPAC per DA. Although DA levels in the striatum of $D_2(-/-)$ mice were not significantly different from controls, DOPAC levels and DA activity were greatly increased (approximately 2.5 fold in both instances). This suggests normal DA storage but a high DA turnover. DA activity per terminal was calculated by dividing each measure by the estimates of number of DA terminals (based on density). Although striatal DA levels were normal in $D_2(-/-)$ mice, there was a 150% increase in DA activity per terminal in $D_2(-/-)$ mice. OS in these mice was measured using a Colorimetric Lipid Peroxidation Assay (Bioxytech LPO-586, *Oxis* Research, USA) that measures the levels of malondialdehyde (MDA), one of a series of compounds produced by the decomposition of lipid peroxides. The assay was performed on pooled homogenates from the dissected striatum and midbrain of five mice. In $D_2(-/-)$ mice, OS as measured by this assay, was approximately twice the levels of Wt mice.

A cohort of Wt and $D_2(-/-)$ mice were left until they were over 18 months of age whereas a second group was studied when they were between 3 and 4 months of age. Animals in each group were killed and prepared for immunohistochemistry or for Western blotting. For immunohistochemistry thin sections were cut through the midbrain and embedded in paraffin, counterstained with Neutral red and immunoreacted with an antibody to αSN. In young animals αSN immunoreactivity was observed in terminals and in a small number of nuclei. In older $D_2(-/-)$ mice many SNpc neurones showed diffuse cytoplasmic immunoreactivity, which in many instances labeled processes reminiscent of Lewy neuritis (Figure 2B). In addition, dense αSN immunoreactive aggregates were observed. These were

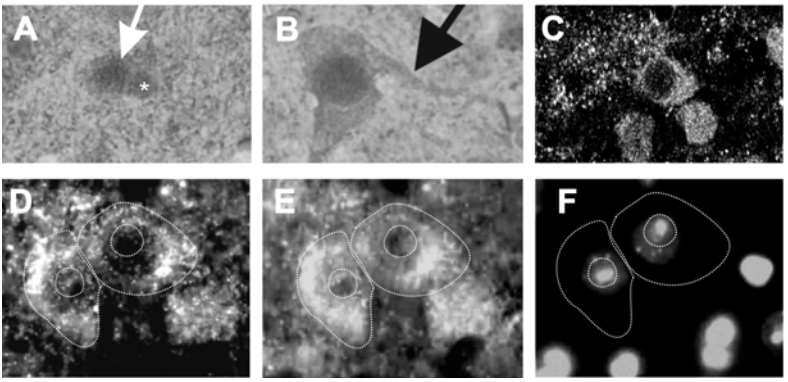

Figure 2. A: αSN immunoreactivity: arrows show cytoplasmic inclusion (arrow) and the adjacent nucleus (asterisk). B: shows a "Lewy neurite". C: is a confocal images showing punctate αSN immunoreactivity in cells with diffuse appearance of αSN immunoreactivity under light microscopy. D, E and F: are confocal images of two cells with diffuse αSN aggregates under light microscopy. D shows αSN immunoreactivity, E ubiquitin immunoreactivity and F is a DAPI nuclear stain.

usually juxtaposed to the nucleus and distorted the shape of the cell and often occupied much of the cytoplasm, thus having the morphological appearance of a Lewy Body (Figure 2A). Although animal numbers are small (n = 8 with age greater than 18 months), the number of Lewy Bodies was increased in very old animals (aged 22 and 24 months). Throughout the SNpc the proportion of cells containing Lewy Bodies was often quite low (2%), however the distribution was not homogeneous and in some regions of the SNpc several Lewy Body containing cells were clumped together. These sections were examined with confocal microscopy and revealed that the large Lewy Body like aggregates under light microscopy were indeed densely aggregated and collocated with ubiquitin (Figure 2E, F and G), whereas cells with diffuse cytoplasmic αSN immunoreactivity had a granular appearance under the confocal microscopes, suggesting micro-aggregates (Figure 2C).

Tissue homogenates from the striatum, SN and cortex from young (3–4 months) and old (18–20 months) $D_2(-/-)$ and WT mice were fractionated according to solubility in buffer, Triton-X 100, SDS and formic acid and αSN immunoreactivity was measured by Western blotting. Detectable levels of αSN were extracted in the S2 (phosphate buffer) and S3 (buffer, Triton-X 100 and SDS) fractions, and, except where noted, ran at a molecular weight of 18 kDa. In the SN, the levels of the highly soluble S2 αSN levels were similar in young Wt and $D_2(-/-)$ mice. However the less soluble αSN extracted from the S3 fraction was significantly increased in the older animals, an elevation that was even more pronounced in older $D_2(-/-)$ mice (Figure 3). The levels of the soluble αSN in the S2 fraction from the striatum was not altered by age or genotype. In the S3 fraction from the striatum, there was a higher MW band of approx 65 kDa, as well as the 18 kDa band. The levels of both bands increased with age, not genotype. In the cortex, all αSN was highly soluble, extracted in the S2 fraction and increased with age.

In summary, it appears that αSN becomes less soluble with age, however, in the nigra this loss of solubility is elevated in $D_2(-/-)$ animals. The total number of TH immunoreactive cells in the SNpc was counted in young and old $D_2(-/-)$ mice. There was no reduction in the number, nor was there an increase in TUNEL positive neurones in the SNpc.

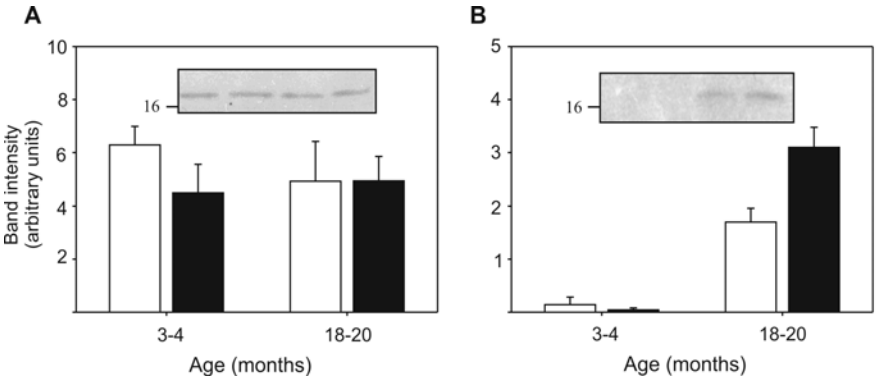

Figure 3. This shows the S2 (A) and S3 (B) fractions of α-synuclein (see text) from the SN of young and old Wt (white bars) and mutant (black bars) mice. The boxes show the Western blots demonstrating fractions that ran at a molecular weight of 18 kDa. There was no difference between Wt and mutant mouse (nor between young and old animals) in the highly soluble S2 αSN levels (A), however the less soluble αSN extracted from the S3 fraction significantly increased in the older animals, an elevation that was even more pronounced in older D_2–/– (B).

2. CONCLUSIONS

These findings support the notion that increased interactions between DA and αSN lead to a propensity to αSN aggregation. In this model dense aggregates were seen in the nigra and striatum but not in the cortex of the $D_2(-/-)$ mice, supporting the hypothesis that the aggregation of αSN depended on increased DA turnover. Further studies are required to establish whether the consequences of increased DA turnover are due to direct DA-αSN interaction, increased oxidative stress or perhaps simply to increased αSN turnover as result of changes in synaptic function. (Singleton et al., 2003)

The dense peri-nuclear aggregates of αSN are consistent with fibrillar αSN aggregates described as juxtanuclear inclusions by Lee and Lee (2002), who also suggest that the small non-fibrillar aggregates are the cellular equivalents of the protofibrils. This would suggest that the small aggregates identified with confocal microscopy are equivalent to these protofibrils, which in cells, seem to be associated with detergentinsoluble structures (Goedert 2001) The diffuse cytoplasmic αSN seems to precede the development of Lewy Body aggregates and is also seen in the aged wild type mice. The Wt αSN in mice is similar to the human A53 mutation and has a greater tendency to aggregate and suggest that were Wt mice to survive longer, they too would also develop Lewy bodies. Because the mutation in the $D_2(-/-)$ mouse hastens the formation Lewy Bodies, it suggests that further increase in cystosolic DA or impaired the handling of OS may further increase the rate of Lewy Body formation. In this animal Lewy Body formation is not associated with increased cell loss. In humans there is a suggestion that the presence of Lewy Bodies may "protect" SNpc DA neurones from injury (Tompkins et al., 1997; Tompkins and Hill, 1997) and that the fibrillar inclusions acts as a "sink" for toxic species of αSN (Goldberg and Lansbury, 2000). This may explain why cell death is not yet apparent in these mice. Where they to survive for longer, the buffering capacity of the Lewy Body may eventually be overwhelmed, and cell death may ensue.

In summary this model provides the opportunity to test various hypotheses such as whether increasing cytoplasmic DA, reducing capacity to handle oxidative stress or altering intracellular iron might lead to increased rate of cell death.

3. ACKNOWLEDGEMENTS

This research was supported by grants from the Bethlehem Griffith Foundation and the Australian National Health and Medical Research Council. J. Drago is an NHMRC Practioner Fellow.

4. REFERENCES

Alam, Z.I., Daniel, S.E., et al., 1997, A generalised increase in protein carbonyls in the brain in Parkinson's but not incidental Lewy body disease, *J. Neurochem*. **69**:1326–1329.

Alam, Z.I., Jenner, A., et al., 1997, Oxidative DNA damage in the parkinsonian brain: an apparent selective increase in 8-hydroxyguanine levels in substantia nigra, *J. Neurochem*. **69**:1196–1203.

Ben-Shachar, D.Z.R., and Glinka, Y., 1995, Dopamine neurotoxicity: inhibition of mitochondrial respiration, *J. Neurochem*. **64**:718–723.

Betarbet, R., Sherer, T.B., et al., 2000, Chronic systemic pesticide exposure reproduces features of Parkinson's disease, *Nat. Neurosci*. **3**:1301–1306.

Bonifati, V., Rizzu, P., et al., 2003, Mutations in the DJ-1 gene associated with autosomal recessive early-onset parkinsonism, *Science* **299**:256–259.

Bowyer, J.F., and Weiner, N., 1987, Modulation of the Ca^{++}-evoked release of [3H]dopamine from striatal synaptosomes by dopamine (D_2) agonists and antagonists, *J. Pharmacol. Exp. Ther*. **241**:27–33.

Bunney, B.S., Aghajanian, G.K., et al., 1973, Comparison of effects of L-dopa, amphetamine and apomorphine on firing rate of rat dopaminergic neurones, *Nat. New Biol*. **245**:123–125.

Cass, W.A., and Zahniser, N.R., 1990, Inhibition of striatal dopamine release by the selective D-2 dopamine receptor agonist N-0437 is blocked by quinine, *Synapse* **5**:336–337.

Conway, K.A., Harper, J.D., et al., 1998, Accelerated in vitro fibril formation by a mutant alpha-synuclein linked to early-onset Parkinson disease, *Nat. Med*. **4**:1318–1320.

Dexter, D.T., Carter, C.J., et al., 1989, Basal lipid peroxidation in substantia nigra is increased in Parkinson's disease, *J. Neurochem*. **52**:381–389.

El-Agnaf, O.M., Jakes, R., et al., 1998, Aggregates from mutant and wild-type alpha-synuclein proteins and NAC peptide induce apoptotic cell death in human neuroblastoma cells by formation of beta-sheet and amyloid-like filaments, *FEBS Lett*. **440**:71–75.

el Mestikawy, S., Glowinski, J., et al., 1986, Presynaptic dopamine autoreceptors control tyrosine hydroxylase activation in depolarized striatal dopaminergic terminals, *J. Neurochem*. **46**:12–22.

Finkelstein, D., Parish, C.L., Stanic, D., Borrelli, E., Drago, J., and Horne, M.K., 2001, The role of Dopamine Receptors in regulating the size of axonal arbours, In: *The Basal Ganglia VII*. Eds. Nicholson L. and Faull R. Kluwer Academic/Plenum Publishers. 313–322.

Finkelstein, D.I., Stanic, D., et al., 2000, Axonal sprouting following lesions of the rat substantia nigra, *Neuroscience* **97**:99–112.

Floor, E., and Wetzel, M.G., 1998, Increased protein oxidation in human substantia nigra pars compacta in comparison with basal ganglia and prefrontal cortex measured with an improved dinitrophenylhydrazine assay. *J. Neurochem*. **70**:268–275.

Gassen, M., Glinka, Y., Pinchasi, B., and Youdim, M.B., 1996, Apomorphine is a highly potent free radical scavenger in rat brain mitochondrial fraction, *Eur. J. Pharmacol*. **308**:219–225.

Giasson, B.I., Duda, J.E., et al., 2000, Oxidative damage linked to neurodegeneration by selective alpha-synuclein nitration in synucleinopathy lesions, *Science* **290**:985–989.

Glinka, Y., Gassen, M., and Youdim, M.D., 1997, Mechanism of 6-hydroxydopamine neurotoxicity. *J. Neural. Transm. Suppl*. **50**:55–66.

Glinka, Y., Tipton, K.F., and Youdim, M.B., 1998, Mechanism of inhibition of mitochondrial respiratory complex I by 6-hydroxydopamine and its prevention by desferrioxamine, *Eur. J. Pharmacol*. **351**:121–129.

Glinka, Y., and Youdim, M.D., 1995, Inhibition of mitochondrial complexes I and IV by 6-hydroxydopamine. *Eur. J. Pharmacol*. **292**:329–332.

Goedert, M., 2001, Alpha-synuclein and neurodegenerative diseases, *Nat. Rev. Neurosci*. **2**:492–501.

Goldberg, M.S., and Lansbury, P.T., Jr., 2000, Is there a cause-and-effect relationship between alpha-synuclein fibrillization and Parkinson's disease? *Nat. Cell Biol.* **2**:E115–E119.

Graham, D.G., Tiffany, S.M., et al., 1978, The toxicity of melanin precursors, *J. Invest. Dermatol*. **70**:113–116.

Hashimoto, M., Hsu, L.J., et al., 1998, Human recombinant NACP/alpha-synuclein is aggregated and fibrillated in vitro: relevance for Lewy body disease, *Brain Res*. **799**:301–306.

Hashimoto, M., Takeda, A., et al., 1999, Role of cytochrome c as a stimulator of alpha-synuclein aggregation in Lewy body disease, *J. Biol. Chem*. **274**:28849–28852.

Healy, D.G., Abou-Sleiman, P.M., et al., 2004, PINK, PANK, or PARK? A clinicians' guide to familial parkinsonism, *Lancet Neurol*. **3**:652–662.

Hersch, S.M., Ciliax, B.J., et al., 1995, Electron microscopic analysis of D_1 and D_2 dopamine receptor proteins in the dorsal striatum and their synaptic relationships with motor corticostriatal afferents, *J. Neurosci*. **15**:5222–237.

Hsu, L.J., Sagara, Y., et al., 2000, alpha-synuclein promotes mitochondrial deficit and oxidative stress, *Am. J. Pathol*. **157**:401–410.

Jenner, P., 1998, Oxidative mechanisms in nigral cell death in Parkinson's disease, *Mov. Disord.* **13 Suppl 1**: 24–34.

Kanda, S., Bishop, J.F., et al., 2000, Enhanced vulnerability to oxidative stress by alpha-synuclein mutations and C-terminal truncation, *Neuroscience* **97**:279–284.

Kimmel, H.L., Joyce, A.R., et al., 2001, Dopamine D_1 and D_2 receptors influence dopamine transporter synthesis and degradation in the rat, *J. Pharmacol. Exp. Ther*. **298**:129–140.

Lacey, M.G., Mercuri, N.B., et al., 1987, Dopamine acts on D_2 receptors to increase potassium conductance in neurones of the rat substantia nigra zona compacta, *J. Physiol*. **392**:397–416.

Langston, J.W., and Ballard, P.A., Jr., 1983, Parkinson's disease in a chemist working with 1-methyl-4-phenyl-1,2,5,6-tetrahydropyridine, *New Eng. J. Med*. **309**:310.

Lee, H.J., and Lee, S.J., 2002, Characterization of cytoplasmic alpha-synuclein aggregates. Fibril formation is tightly linked to the inclusion-forming process in cells, *J. Biol. Chem*. **277**:48976–48983.

Lindgren, N., Xu, Z.Q., et al., 2001, Dopamine D(2) receptors regulate tyrosine hydroxylase activity and phosphorylation at Ser40 in rat striatum, *Eur. J. Neurosci*. **13**:773–780.

Lotharius, J., Barg, S., et al., 2002, Effect of mutant alpha-synuclein on dopamine homeostasis in a new human mesencephalic cell line, *J. Biol. Chem*. **277**:38884–38894.

Lotharius, J., and Brundin, P., 2002, Pathogenesis of Parkinson's disease: dopamine, vesicles and alpha-synuclein, *Nature Rev. Neurosci*. **3**:932–942.

Lotharius, J., and Brundin, P., 2002, Impaired dopamine storage resulting from alpha-synuclein mutations may contribute to the pathogenesis of Parkinson's disease, *Human Mol. Genet*. **1**:2395–2407.

Maker, H.S., W.C., Silides, D.J., and Cohen, G., 1981, Coupling of dopamine oxidation (monoamine oxidase activity) to glutathione oxidation via the generation of hydrogen peroxide in rat brain homogenates, *J. Neurochem*. **36**:589–593.

Narhi, L., Wood, S.J., et al., 1999, Both familial Parkinson's disease mutations accelerate alpha-synuclein aggregation, *J. Biol. Chem*. **274**:9843–9846.

Onali, P., Olianas, M.C., et al., 1988, Evidence that adenosine A2 and dopamine autoreceptors antagonistically regulate tyrosine hydroxylase activity in rat striatal synaptosomes, *Brain Res*. **456**:302–309.

Palacino, J.J., Sagi, D., et al., 2004, Mitochondrial dysfunction and oxidative damage in parkin-deficient mice, *J. Biol. Chem*. **279**:18614–18622.

Parish, C.L., Finkelstein, D.I., et al., 2001, The role of dopamine receptors in regulating the size of axonal arbors, *J. Neurosci*. **21**:5147–5157.

Parish, C.L., Stanic, D., et al., 2002, Effects of long-term treatment with dopamine receptor agonists and antagonists on terminal arbor size, *Eur. J. Neurosci*. **16**:787–794.

Petersen, A., Puschban, Z., Lotharius, J., et al., 2002, Evidence for dysfunction of the nigrostriatal pathway in the R6/1 line of transgenic Huntington's disease mice, *Neurobiol. Dis*. **11**:134–146.

Polymeropoulos, M.H., Lavedan, C., et al., 1997, Mutation in the alpha-synuclein gene identified in families with Parkinson's disease, *Science* **276**:2045–2047.

Robinson, M.B., 2002, Regulated trafficking of neurotransmitter transporters: common notes but different melodies, *J. Neurochem*. **80**:1–11.

Saggu, H., Cooksey, J., et al., 1989, A selective increase in particulate superoxide dismutase activity in parkinsonian substantia nigra, *J. Neurochem*. **53**:692–697.

Singleton, A.B., Farrer, M., et al., 2003, alpha-Synuclein locus triplication causes Parkinson's disease, *Science* **302**:841.

Sofic, E., Riederer, P., et al., 1988, Increased iron (III) and total iron content in post mortem substantia nigra of parkinsonian brain, *J. Neural. Transm*. **74**:199–205.

Spillantini, M.G., Crowther, R.A., et al., 1998, alpha-Synuclein in filamentous inclusions of Lewy bodies from Parkinson's disease and dementia with Lewy bodies, *Proc. Natl. Acad. Sci. USA* **95**:6469–6473.

Stanic, D., Finkelstein, D.I., et al., 2003a, Time course of striatal re-innervation following lesions of dopaminergic SNpc neurons of the rat, *Eur. J. Neurosci*. **18**:1175–1188.

Stanic, D., Parish, C.L., et al., 2003b, Changes in function and ultrastructure of striatal dopaminergic terminals that regenerate following partial lesions of the SNpc, *J. Neurochem*. **86**:329–343.

Tepper, J.M., Nakamura, S., et al., 1984, Autoreceptor-mediated changes in dopaminergic terminal excitability: effects of striatal drug infusions, *Brain Res*. **309**:317–333.

Tompkins, M.M., Basgall, E.J., et al., 1997, Apoptotic-like changes in Lewy-body-associated disorders and normal aging in substantia nigral neurons, *Am. J. Pathol*. **150**:119–131.

Tompkins, M.M., and Hill, W.D., 1997, Contribution of somal Lewy bodies to neuronal death, *Brain Res*. **775**: 24–29.

Ungerstedt, U., Herrera-Marschitz, M., et al., 1982, Models for studying the synaptic mechanisms: correlative measurements of transmitter release and drug altered behaviour. In: *Behavioural Models and the Analysis of Drug Action*. Eds: M.Y. Spiegelstein and A. Levy. Amsterdam, Elsevier: 57–70.

Valente, E.M., Abou-Sleiman, P.M., et al., 2004, Hereditary early-onset Parkinson's disease caused by mutations in PINK1, *Science* **304**:1158–1160.

Xu, J., Kao, S.Y., et al., 2002, Dopamine-dependent neurotoxicity of alpha-synuclein: a mechanism for selective neurodegeneration in Parkinson disease, *Nat. Med*. **8**:600–606.

Zhang, Y., Dawson, V.L., et al., 2000, Oxidative stress and genetics in the pathogenesis of Parkinson's disease, *Neurobiol. Dis*. **7**:240–250.

Zigmond, M., Hastings, T., et al., 2002, Increased dopamine turnover after partial loss of dopaminergic neurons: compensation or toxicity? *Parkinsonism Relat. Disord*. **8**:389.
Zigmond, M.J., Abercrombie, E.D., et al., 1990, Compensations after lesions of central dopaminergic neurons: some clinical and basic implications, *Trends Neurosci*. **13**:290–296.

INTRALAMINAR THALAMIC NUCLEI ARE MAIN REGULATORS OF BASAL GANGLIA

Possible involvement in the pathophysiology of Parkinson's disease

Lydia Kerkerian-Le Goff[1], Jean-Jacques Bacci[1], Pascal Salin[1], Maria S. Aymerich[2], Pedro Barroso-Chinea[2], José A. Obeso[2], and José L. Lanciego[2]*

1. INTRODUCTION

The caudal intralaminar thalamic nuclei, which include the centromedian/parafascicular complex (CM/Pf), are the main source of thalamic afferents to the basal ganglia (BG) in mammals (see Smith et al., 2004). The primary target structure of this system being the striatum, the main input station of BG, thalamic influence on BG functioning has been long viewed as mediated mainly through regulation of striatal outflow. However, there is accumulating electrophysiological and anatomical evidence from studies in rat that CM/Pf represents a complex acting in parallel on individual structures of BG. In addition to striatum, the CM/Pf innervates all the structures of BG, globus pallidus (GP) (Kincaid et al., 1991), subthalamic nucleus (STN) (Sugimoto and Hattori, 1983; Sugimoto et al., 1983) and the output structures of the network, substantia nigra pars reticulata (SNr) and entopeduncular nucleus (ENT, rodent homologous of internal globus pallidus) (Marini et al., 1999). Accordingly, it has been shown that CM/Pf lesions in rat induce a pattern of changes in neurotransmitter-related gene expression in basal ganglia structures that better fit with the removal of direct excitatory thalamic input onto these structures than with changes in intrinsic basal ganglia loops (Bacci et al., 2002). Thalamic afferents have been shown to have direct excitatory effects on GP and STN neurons (Mouroux and Feger, 1993; Mouroux et al., 1995; 1997) and the thalamosubthalamic projection shows, like the thalamostriatal system,

[1] Cellular Interaction, Neurodegeneration and Neuroplasticity Unit. CNRS UMR 6186. Marseilles, France.
[2] Department of Neurosciences, Clinica Universitaria and Medical School, Center for Applied Medical Research, University of Navarra. 31008 Pamplona, Spain.

a high degree of anatomical and functional organisation (see Smith et al., 2004). Although a single cell filling study has shown that some Pf neurons projecting to striatum send collaterals to STN (Deschênes et al., 1996), a dual labelling study has shown that thalamostriatal and thalamosubthalamic projections mostly arise from segregated populations of CM/Pf neurons (Feger et al., 1994), reinforcing the concept of segregated thalamic control of basal ganglia components. On the other hand, whereas both thalamostriatal and thalamosubthalamic projections have been shown to be strictly ipsilateral, there is evidence for thalamic contralateral projections onto SNr (Marini et al., 1999) and STN (Castle et al., 2005), suggesting a role of CM/Pf in interhemispheric regulation of basal ganglia function. Interest for further characterizing the control exerted by thalamic afferents on basal ganglia circuitry is reinforced by the recent data suggesting a critical involvement of CM/Pf in the pathophysiology of PD. The rational for such an involvement is two fold. First, evidence has been provided for increased activity of thalamosubthalamic projection neurons in animals with extensive unilateral lesion of nigral dopamine neurons (Orieux et al., 2000; Hirsch et al., 2000), suggesting that this projection may play a role in the abnormal activation of STN in parkinsonian state. Second, neuropathological studies have shown that CM/Pf represents a major site of non-dopaminergic degeneration in PD (Henderson et al., 2000a,b). The relationship between dopamine neuron and thalamic neuron vulnerability is further exemplified by the experimental data showing neuronal degeneration in midline and intralaminar thalamic nuclei in a MPTP-treated mouse model of PD (Freyaldenhoven et al., 1997), and retrograde degeneration in the Pf after intrastriatal MPP+ administration in a rat model of striatonigral degeneration (Ghorayeb et al., 2002). The functional consequences of thalamic degeneration in PD remain however largely unknown.

In this chapter, we will review recent data from our groups re-evaluating basal ganglia connectivity in relationship with thalamic afferents, and investigating the impact of thalamic lesion on the pathophysiological functioning of basal ganglia in a rat model of PD.

2. THALAMIC INFLUENCE ON BASAL GANGLIA FUNCTION

Current knowledge of basal ganglia circuits has become more complex over the past few years. Recent advances in physiological and anatomical research have provided a more detailed picture that must be integrated within the basal ganglia model. First, basal ganglia circuits are highly collateralized. Second, the formerly known 'indirect pathway' is currently seen as a complex network on its own. Finally, the roles of transverse circuits linking the thalamus with the striatum and the subthalamic nucleus have been largely neglected in most studies dealing with basal ganglia function. Both thalamostriatal and thalamosubthalamic circuits are organized transversally to cortico-basal ganglia-thalamocortical loops and its apparent role, as a positive/negative feedback loop was recently suggested (Obeso et al., 2000).

Recent work carried out in our lab. using multiple tracing paradigms (Gonzalo et al., 2002; Lanciego et al., 2004; Castle et al., 2005) demonstrated that the caudal intralaminar nuclei can exert a complex, multifaceted control of both the direct and indirect basal ganglia pathways at multiple levels. Firstly, thalamic afferents reach striatofugal neurons projecting to either the ENT, substantia nigra pars reticulata (SNr) or GP. Indeed, inhibitory local circuit neurons are also approached by thalamic afferents arising from the rat parafasicular nucleus (PF). Secondly, the STN receives strong glutamatergic innervation from PF neurons, these projections being arranged topographically (Lanciego et al., 2004). Within the STN,

neurons projecting to either ENT, SNr or GP are the apparent postsynaptic target for PF axons. Overall, these data suggest that PF neurons might exert multiple control over basal ganglia output nuclei. On the one hand, the activation of thalamic neurons could excite striatofugal neurons projecting to ENT and SNr, leading to thalamic disinhibition. Indeed, thalamic inputs gaining access to striatopallidal-projecting neurons would led to increased inhibition onto GP neurons projecting to STN, therefore increasing the amount of excitation received by the basal ganglia output nuclei, then resulting in reduced thalamic activity. In other words, thalamostriatal projections reaching both kinds of striatofugal neurons would lead to opposite effects on thalamic functioning, and therefore the final thalamic activity may be seen as a balanced result of both kinds of inputs. On the other hand, one should keep in mind the thalamic influence exerted within the basal ganglia circuitry as a result of thalamo-subthalamic projections. PF neurons send excitatory projections to STN neurons, these neurons mainly project simultaneously to both GP and SNr, via axon collaterals (Castle et al., 2005). The final activity of GP projection neurons is a balance between increased GABA outflow coming from the striatum as a result of thalamic excitatory drive onto striatopallidal neurons and increased glutamate received from STN, the latter being a consequence of PF innervation of subthalamo-pallidal neurons. Just to add more complexity to this already complex scenario, one should keep in mind that PF axons can also gain direct access to GP neurons (Kincaid et al., 1991; Marini et al., 1999; Yasukawa et al., 2004). In summary, the activity of basal ganglia output nuclei is the final result of a complex balance between multiple players: (i) activation, via PF → CPu → ENT/SNr; (ii) inhibition, via PF → CPu → GP → STN → ENT/SNr; (iii) inhibition, via PF → STN → ENT/SNr and (iv) excitation, via PF → STN → GP → STN → ENT/SNr.

Although basal ganglia connectivity is largely sustained by ipsilateral projections, several decussations involving basal ganglia nuclei have already been described. The best-characterized decussation is the crossed nigrostriatal pathway (Fass and Butcher, 1981; Gerfen et al., 1982; Loughlin and Fallon 1982; Altar et al., 1983; Consolazione et al., 1985; Douglas et al., 1987). Crossed thalamic projections arising from either SNr or from the deep mesencephalic nucleus (an SNr analogue) were reported elsewhere (Beckstead et al., 1979; Hekerham, 1979; Rodríguez et al., 2001; González-Hernández et al., 2002). Bilateral nigro-tectal and nigro-pedunculopontine were addressed by Deniau et al. (1977) and by Gerfen et al. (1982), respectively. Efferent PF projections are also a typical source of descending bilateral projections, these projections reaching the raphe nuclei (Marini and Tredici, 1995), SNr (Marini et al., 1999), as well as STN (Castle et al., 2005). Finally, recent data from hodological studies conducted by our group demonstrated that a small population of STN neurons is able to innervate both the contralateral PF and GP, via axon collaterals. An intriguing question is to what extent a small population of STN neurons giving rise to contralateral inputs reaching PF and GP is an idiosyncrasy of the system or does it have a real functional impact on basal ganglia functioning. If this were the case, an exciting implication is to what extent the activity of one STN might be under the indirect control of the contralateral STN, through crossed subthalamo-pallidal projections.

Consistent with these tract-tracing data, unilateral thalamic lesions were found to induce significant bilateral changes in neurotransmitter-related gene expression in most of the components of the BG, but with different time courses between structures (Salin and Kachidian 1998; Bacci et al., 2002). For instance, at 5 days post-lesion, the thalamic lesion-induced changes in SNr and EP were bilateral, whereas those in striatum, GP and STN were ipsilateral. At 12 days post-lesion, the bilateral changes are maintained in SNr and EP, and contralateral responses appear in the striatum and STN; in GP there are contralateral

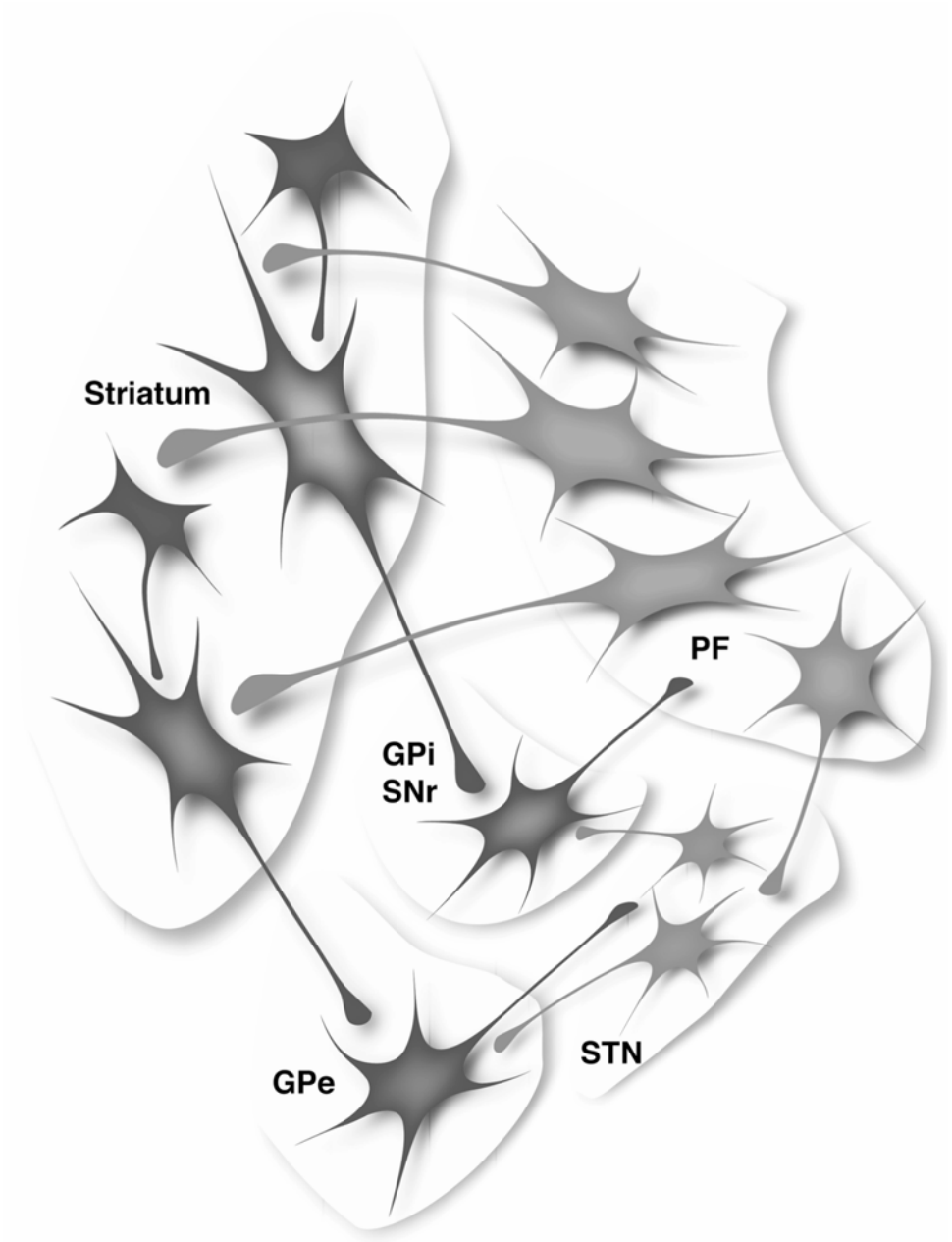

Figure 1. Flow chart illustrating the main pathways supporting the thalamic modulation of basal ganglia nuclei.

tendencies that however did not reach significance. Interestingly, differences are also noticed between the striatal markers examined, as the decrease in cytochrome oxidase subunit I and enkephalin was found to become bilateral, whereas the decrease in GADs was only ipsilateral, suggesting that different direct and indirect mechanisms are involved in these responses. All in all, these data provide evidence for a multimodal interhemispheric control of BG network by intralaminar thalamic nuclei.

3. LESION OF INTRALAMINAR THALAMIC NUCLEI PREVENTS MOST OF THE DOPAMINE DENERVATION-INDUCED CELLULAR DEFECTS IN THE BASAL GANGLIA

Given the widespread control exerted by CM/Pf on the basal ganglia network and the neuropathological observations of neuronal loss in CM/Pf in PD, the pathophysiological functioning of basal ganglia in parkinsonian state cannot be fully understood unless more is known about the possible impact of thalamic degeneration. To address this issue, we examined the effects of separate or combined lesions of nigral dopamine neurons and of CM/Pf neurons on gene expression of markers of neuronal activity in the rat basal ganglia, using in situ hybridization histochemistry (Bacci et al., 2004). The extent of neuronal loss in CM/Pf in PD that averages 30–40% has been reported to be independent of the duration and severity of the disease and suggested to be a primary event in the course of the disease (Henderson et al., 2000a,b). Therefore, thalamic and dopamine lesions have been performed simultaneously in the combined lesion condition.

The markers of neuronal activity examined were mRNA levels of: i) the isoforms of glutamate decarboxylase (GAD67 and GAD 65) in the GABAegic structures of basal ganglia: striatum, GP, SNr and EP; ii) the precursors of the striatal neuropeptides enkephalin and substance P to distinguish the activity of the two main striatal populations of efferent neurons; iii) cytochrome oxidase subunit I (CoI) a neuronal marker encoded by the mitochondrial genome to assess the metabolic activity of subthalamic nucleus (STN) neurons. Unilateral lesion of nigral dopamine neurons was performed by stereotactic injection of 6-hydroxydopamine (8 µg in 4 µl of NaCl 0.9% containing 01% ascorbic acid) in the left substantia nigra pars compacta, and CM:Pf lesion by local injection of ibotenic acid (6 nmol/0.6 µl) on the same brain side. In the combined condition, the two types of injection were made in the same surgical session.

The effects of these lesions were investigated after a two weeks post-lesion delay. The extent of dopamine lesion was assessed by analysis of ^{3}H-mazindol binding to dopamine uptake sites in the striatum (>90% depletion in the selected animals), and thalamic lesion site examined on cresyl violet-stained sections. In situ hybridization histochemistry was performed using ^{35}S-radiolabelled synthetic DNA probes (GADs, enkephalin, substance P) or riboprobes (CoI). Analysis was done for striatum at structural level on film autoradiograms by optical density (OD) measurement, and for the other structures at cellular level on emulsion-coated sections by counting the number of silver grains per labelled neurons.

Results show that thalamic and dopamine lesion, considered separately, have mostly opposite consequences on neurotransmitter-related gene expression in BG. For instance, thalamic lesion decreases, whereas dopamine lesion increases, mRNA levels of enkephalin and GAD67 in the striatum, GAD67 and GAD65 in GP, CoI in STN and GAD67 in EP. In SNr, whereas dopamine lesion increases both isoforms of GAD, thalamic lesion decreases

Table 1. Effects of separate or combined thalamic and dopamine lesion on gene expression of striatal neuropeptides, of GADs in striatum, GP, SNr and EP, and of CoI in STN. The data are the means ± SD of the values determined from the side ipsilateral to surgery in the n animals per condition (5 controls, 5 thalamic lesion, 4 6-OHDA lesion and 5 with combined lesions) and are expressed as percent of the corresponding mean control value. Statistical analyses were performed using a one way analysis of variance followed by Scheffé's test for multiple group comparisons. ** $p < 0.01$ compared with control values; $$ $p < 0.01$ compared with values obtained in rats with 6-OHDA lesion alone.

			Thalamic lesion (12d)	DA lesion	Combined lesions
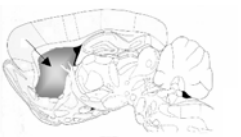	**Striatum**	SP	97.32 + 7.13	54.86 + 3.33**	66.54 + 4.16**
		Enk	68.23 + 7.21**	152.70 + 7.72**	108.33 + 6.56$$
		GAD_{67}	68.89 + 4.65**	145.25 + 5.03**	104.50 + 7.24$$
		GAD_{65}	92.01 + 5.54	98.33 + 8.65	89.42 + 9.24
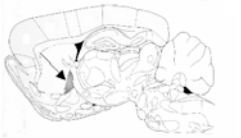	**GP**	GAD_{67}	77.57 + 8.02**	162.85 + 10.6**	95.20 + 6.40$$
		GAD_{65}	64.08 + 5.68**	139.60 + 7.95**	96.54 + 3.72$$
	**STN**	CoI	53.35 + 6.78**	124.20 + 4.32**	87.08 + 3.87$$
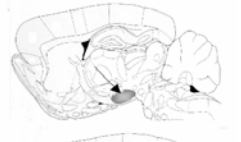	**SNr**	GAD_{67}	94.44 + 8.82	120.55 + 3.44**	114.46 + 2.36**
		GAD_{65}	53.96 + 4.41**	118.96 + 5.76**	90.27 + 6.29$$
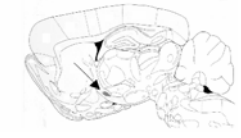	**EP**	GAD_{67}	53.33 + 5.25**	169.94 + 6.50**	73.81 + 3.64**$$
		GAD_{65}	98.86 + 3.52	121.29 + 4.74**	93.68 + 3.19$$

only GAD65. Finally, striatal expression of substance P which is decreased by the dopamine denervation is unaffected by the thalamic lesion, suggesting a preferential influence of thalamic neurons on the neurons of the indirect versus the direct pathway. The effects of the combined lesions globally correspond to an addition of the effects of each lesion considered separately. Indeed, thalamic lesion prevents the dopamine denervation-induced increases in striatal enkephalin and GAD67 mRNA levels in the striatum, in both GAD67 and GAD65 at GP and EP levels, in GAD65 but not GAD67 in SNr and in CoI in STN, without modifying the decreases in substance P mRNA expression. In EP, thalamic lesion even induces a bilateral decrease compared to controls. Therefore, contrasting with the widespread effects of the dopamine denervation alone, the only dopamine lesion-mediated changes still expressed in the combined dopamine/thalamic lesion condition are the decrease in striatal substance P and the increase in nigral GAD67 mRNA levels, suggesting maintenance of the hypoactivity of the direct striatonigral pathway.

Taken together, the present data show that 1) the thalamic and nigral dopaminergic inputs have antagonistic influence on markers of neuronal activity in the indirect pathway

connecting the striatum to the basal ganglia output structures, and 2) extensive lesion of CM/Pf counteracts most of the cellular effects of dopamine denervation within the basal ganglia network. These data raise several important issues. First, the preferential impact of thalamic denervation on striatal neurons at the origin of the indirect pathway appears paradoxical in view of the data showing that striatal neurons projecting to GPe are not preferential target of thalamic projections in primates (Sibide and Smith, 1996). On the other hand, several lines of evidence indicate that the increase in striatal enkephalin expression in response to dopamine lesion is linked to overactive corticostriatal glutamate transmission. Therefore, are the striatal effects of thalamic lesion indirectly mediated through regulation of corticostriatal transmission? Further experiments examining the effects of thalamic lesion alone or combined with dopamine lesion on corticostriatal glutamate transmission are needed to answer this issue. Second, what hypotheses can be drawn about the consequences of thalamic degeneration on the pathophysiological functioning of basal ganglia in PD? Based on the observation of partial and early neuronal loss in CM/Pf in Parkinson's disease, the present data led us to suggest that thalamic degeneration may be a factor contributing to delay the expression of the impact of the progressive dopamine loss on basal ganglia functioning and further to the late appearance of the symptoms of the disease. For instance, partial thalamic neuron loss may counteract the effects of partial dopamine neuron loss in early stages of degeneration, but this effect may be overwhelmed with the progression of dopamine degeneration. Then, how to explain the presumed role of thalamic input in STN overactivity, a landmark feature of the pathophysiological functioning of basal ganglia in PD state? It could be that a secondary hyperactivity of the spared thalamic neurons may on the contrary reinforce the effects of dopamine degeneration at later stages of the disease. It also could be that degeneration affects mainly the ascending thalamic projections to the striatum, GP and cortex and relatively spares the projections to STN and basal ganglia output structures.

4. CONCLUDING REMARKS

There is little doubt that the caudal intralaminar nuclei might modulate basal ganglia transmission at mutiple levels. Although thalamostriatal and thalamosubthalamic projections have largely been neglected in most studies dealing with basal ganglia pathophysiology, the data presented here, as well as data coming from other studies, call for a re-evaluation of the position of the thalamic intralaminar nuclei within the basal ganglia model. The anatomical and metabolic data discussed in this communication clearly support the idea that the intralaminar nuclei cannot longer be seen as a simply relay station between the basal ganglia output nuclei and the cortex. The primary, non-dopaminergic neurodegeneration observed in the caudal intralaminar nuclei might play a key role on the pathophysiology of basal ganglia in PD. Indeed, we suggest that the initial neuronal loss observed within CM-Pf may be a kind of self-compensatory mechanism in early stages of dopamine loss.

5. ACKNOWLEDGEMENTS

This work was supported by grants from the CNRS and the Université de la Méditerranée, as well as by the Michael J. Fox Foundation, Fondo de Investigaciones Sanitarias ref FIS01/0237, Ministerio de Ciencia y Tecnología ref BFI2003-02033, and by the UTE

project/Foundation for Applied Medical Research. JJ Bacci was supported by a fellowship from the France Parkinson Association.

6. REFERENCES

Altar, A., Neve, K.A., Loughlin, S.E., Marshall, J.F., and Fallon, J.H., 1983, The crossed mesostriatal projection : neurochemistry and development response to lesion, *Brain Res*. **279**:1–8.

Bacci, J.J., Kerkerian-Le Goff, L., and Salin, P., 2002, Effects of intralaminar thalamic nuclei lesion on glutamic acid decarboxylase (GAD65 and GAD67) and cytochrome oxidase subunit I mRNA expression in the basal ganglia of the rat, *Eur. J. Neurosci.* **15**:1918–1928.

Bacci, J.J., Kachidian, P., Kerkerian-Le Goff, L., and Salin, P., 2004, Intralaminar thalamic nuclei lesions : widespread impact on dopamine denervation-mediated cellular defects in the rat basal ganglia, *J. Neuropathol. Exp. Neurol.* **63**:20–31.

Beckstead, R.M., Domesik, V.B., and Nauta, W.J., 1979, Efferent connections of the substantia nigra and ventral tegmental area in the rat. *Brain Res.* **175**:191–217.

Castle, M., Aymerich, M.S., Sanchez-Escobar, C., Gonzalo, N., Obeso, J.A., and Lanciego, J.L., 2005, Thalamic innervation of the direct and indirect basal ganglia pathways in the rat : ipsi- and contralateral projections, *J. Comp. Neurol.* **483**:143–153.

Consolazione, A., Bentivoglio, M., Goldstein, M., and Toffano, G., 1985, Evidence for crossed catecholaminergic nigrostriatal projections by combining wheat germ agglutinin-horseradish peroxidase retrograde transport and tyrosine hydroxylase immunocytochemistry, *Brain Res*. **338**:140–143.

Deschênes, M., Bourassa, J., Van Diep, D., and Parent, A., 1996, A single-cell study of the axonal projection arising from the posterior intralaminar thalamic nuclei in the rat, *Eur. J. Neurosci*. **8**:329–343.

Douglas, R., Kellaway, L., Mintz, M., and van Wageningen, G., 1987, The crossed nigrostriatal projection decussates in the ventral tegmental decussation. *Brain Res.* **418**:111–121.

Fass, B., and Butcher, L.L., 1981, Evidence for a crossed nigrostriatal pathway in rats, *Neurosci. Lett*. **22**:109–113.

Feger, J., Bevan, M., and Crossman, A.R., 1994, The projections from the parafascicular thalamic nucleus to the subthalamic nucleus and the striatum arise from separated neuronal populations: a comparison with the corticostriatal and corticosubthalamic efferents in a retrograde fluorescent double-labelling study, *Neuroscience* **60**:125–132.

Freyaldenhoven, T.E., Ali, S.F., and Schmued, L.C., 1997, Systemic administration of MPTP induces thalamic neuronal degeneration in mice. *Brain Res.* **759**:9–17.

Gerfen, C.R., Staines, W.A., Arbuthnott, G.W., and Fibiger, H.C., 1982, Crossed connections of the substantia nigra in the rat, *J. Comp. Neurol.* **207**:283–303.

Ghorayeb, I., Fernagut, P.O., Hervier, L., Labattu, B., Bioulac, B., and Tison, F., 2002, A 'single toxin-double lesion' rat model of striatonigral degeneration by intrastriatal 1-methyl-4-phenylpyridinium ion injection: a motor behavioural analysis, *Neuroscience* **115**:533–46.

González-Hernández, T., Barroso-Chinea, P., Pérez de la Cruz, M.A., Valera, P., Dopico, J.G., and Rodríguez, M., 2002, Response of GABAergic cells in the deep mesencephalic nucleus to dopaminergic cell degeneration : an electrophysiological and in situ hybridization study, *Neuroscience* **113**:311–321.

Gonzalo, N., Lanciego, J.L., Castle, M., Vázquez, A., Erro, E., and Obeso, J.A., 2002, The parafascicular thalamic complex and basal ganglia circuitry : further complexity to the basal ganglia model, *Thalamus & Rel. Sys.* **1**:341–348.

Hekerham, M., 1979, The afferent and efferent connections of the ventromedial thalamus in the rat, *J. Comp. Neurol*. **183**:487–517.

Henderson, J.M., Carpenter, K., Cartwright, H., and Halliday, G.M., 2000, Loss of thalamic intralaminar nuclei in progressive supranuclear palsy and Parkinson's disease: clinical and therapeutic implications, *Brain* **123**:1410–1421.

Henderson, J.M., Carpenter, K., Cartwright, H., and Halliday, G.M., 2000, Degeneration of the centre median-parafascicular complex in Parkinson's disease, *Ann. Neurol*. **47**:345–352.

Hirsch, E.C., Perier, C., Orieux, G. et al., 2000, Metabolic effects of nigrostriatal denervation in basal ganglia, *Trends Neurosci*. **23**:S78–S85.

Kincaid, A.E., Penney, J.B. Jr, Young, A.B., and Newman, S.W., 1991, The globus pallidus receives a projection from the parafascicular nucleus in the rat, *Brain Res.* **553**:18–26.

Lanciego, J.L., Gonzalo, N., Castle, M., Sánchez-Escobar, C., and Aymerich, M.S., Obeso, J.A., 2004, Thalamic innervation of striatal and subthalamic neurons projecting to the rat entopeduncular nucleus, *Eur. J. Neurosci*. **19**:1267–1277.

Loughlin, S.E., and Fallon, J.H., 1982, Mesostriatal projections from ventral tegmentum and dorsal raphe cells project ipsilaterally or contralaterally but not bilaterally, *Neurosci. Lett*. **32**:11–16.

Marini, G., and Tredici, G., 1995, Parafascicular nucleus-raphe projections and termination patterns in the rat, *Brain Res.* **690**:177–184.

Marini, G., Pianca, L., and Tredici, G., 1999, Descending projections arising from the parafascicular nucleus in rats: trajectory of fibers, projection pattern and mapping of terminations, *Somatosens. Mot. Res*. **16**:207–222.

Mouroux, M., and Feger, J., 1993, Evidence that the parafascicular projection to the subthalamic nucleus is glutamatergic, *Neuroreport* **4**:613–615.

Mouroux, M., Hassani, O.-K., and Feger, J., 1995, Electrophysiological study of the excitatory parafascicular projection to the subthalamic nucleus and evidence for ipsi- and contralateral controls, *Neuroscience* **67**:399–407.

Mouroux, M., Hassani, O.-K., and Feger, J., 1997, Electrophysiological and Fos immunohistochemical evidences for the excitatory nature of the parafascicular projection to the globus pallidus, *Neuroscience* **81**:387–397.

Obeso, J.A., Rodríguez-Oroz, M.C., Rodríguez, M., Lanciego, J.L., Artieda, J., Gonzalo, N., and Olanow, C.W., 2000, Pathophysiology of the basal ganglia in Parkinson's disease, *Trends Neurosci*. **23**:S8–S19.

Orieux, G., François, C., Féger, J., Yelnik, J., Vila, M., Ruberg, M., Agid, Y., and Hirsch, E.C., 2000, Metabolic activity of excitatory parafascicular and pedunculopontine inputs to the subthalamic nucleus in a rat model of Parkinson's disease, *Neuroscience* **97**:79–88.

Rodríguez, M., Abdala, P., Barroso-Chinea, P., and González-Hernández, T., 2001, The deep mesencephalic nucleus as an output center of basal ganglia : morphological and electrophysiological similarities with the substantia nigra, *J. Comp. Neurol*. **438**:12–31.

Salin, P., and Kachidian, P., 1998, Thalamo-striatal deafferentation affects preproenkephalin but not preprotachykinin gene expression in the rat striatum, *Mol. Brain Res*. **57**:257–65.

Sidibe, M., and Smith, Y., 1996, Differential synaptic innervation of striatofugal neurones projecting to the internal or external segments of the globus pallidus by thalamic afferents in the squirrel monkey, *J. Comp. Neurol*. **365**:445–65.

Smith, Y., Raju, D.V., Pare, J.F., and Sidibe, M., 2004, The thalamostriatal system: a highly specific network of the basal ganglia circuitry, *Trends Neurosci.* **27**:520–527.

Sugimoto, T., and Hattori, T., 1983, Confirmation of thalamosubthalamic projections by electron microscopic autoradiography, *Brain Res.* **264**:335–339.

Sugimoto, T., Hattori, T., Mizunp, N., Itoh, K., and Sato, M., 1983, Direct projection from the centre median-parafascicular complex to the subthalamic nucleus in the cat and rat, *J. Comp. Neurol.* **214**:209–216.

Yasukawa, T., Kita, T., Xue, Y., and Kita, H., 2004, Rat intralaminar thalamic nuclei projections to the globus pallidus : a biotinylated dextran amine anterograde tracing study, *J. Comp. Neurol.* **471**:153–167.

ACTIVATED MICROGLIA PERSIST IN THE SUBSTANTIA NIGRA OF A CHRONIC MPTP MOUSE MODEL OF PARKINSON'S DISEASE

Gloria E. Meredith, Adrian G. Dervan, and Susan Totterdell*

1. INTRODUCTION

Parkinson's disease (PD) involves the slow loss of dopaminergic neurons from the substantia nigra pars compacta (SNpc). During disease progression, affected neurons show oxidative stress, have reduced energy stores and disturbed proteolysis (Meredith et al., 2004). Moreover, cytoplasmic inclusions containing α-synuclein are found postmortem in some dopaminergic neurons (Spillantini et al., 1997). Microglia, the resident immune cells in the brain, have been implicated in PD pathology (McGeer et al., 1988, Liu et al., 2003). These cells have been found in a reactive state in postmortem tissue taken from PD brains. Once activated, microglia release reactive oxygen species, inducible nitric oxide and pro-inflammatory cytokines that exacerbate neuronal injury. Moreover, activated cells become phagocytic and increase inflammation by recruiting other immune cells to the injury site. Nevertheless, evidence for the role of microglia in PD is primarily circumstantial, and it is largely unknown whether activated microglia harm dopaminergic cells or merely phagocytose dying neurons. Using MPTP and probenecid (MPTP/p), we have established a chronic mouse model of PD (Petroske et al., 2001). Our model shows many of the hallmarks of PD, including progressive and persistent dopamine loss as well as granular, α-synuclein-immunoreactive inclusions (Petroske et al., 2001; Meredith et al., 2002). As a first step to elucidate the contributory role of microglia to dopamine neuron demise and inclusion formation, we studied these cells in the SN of chronically MPTP/p-treated mice and compared results to vehicle-treated controls. In order to control for an aging effect in microglial proliferation, we included a set of untreated, age-matched controls.

* Gloria E. Meredith, Chicago Medical School, Rosalind Franklin University, North Chicago, Illinois 60064, USA. Adrian G. Dervan, Trinity College, University of Dublin, Dublin, Ireland. Susan Totterdell, University of Oxford, Oxford OX1 3QT, United Kingdom.

2. METHODS

Forty adult C57/bl mice were treated twice weekly with *either* MPTP hydrochloride (25 mg/kg s.c. in saline; total dose of 250 mg/kg) and probenecid (250 mg/kg in DMSO, i.p.) (MPTP/p) *or* vehicle (probenecid or saline) alone (control groups). A third group of untreated, age-matched C57/bl mice were included as controls. All mice were tested behaviorally with a forepaw rigidity test (grid test) before and one month after treatment. From 1–10 months following final treatment, animals were anesthetized (pentobarbital, 130 mg/kg) and fixed by perfusion with 0.1 M PBS followed by 4% paraformaldehyde in 0.1 M PB.

2.1. Immunohistochemistry

For light microscopy (LM), 50 µm serial sections cut through the midbrain on a freezing microtome, were immunoreacted with rat anti-Mac-1 (1 : 1000, Boehringer Mannheim, Germany) in 0.1 M PBS with 0.1% Triton X-100, 2) or mouse anti-tyrosine hydroxylase (TH), 1 : 2000 (Diasorin, Stillwater, MN) in 0.1M PBS. All sections were incubated in appropriate IgG (1 : 300, Vector Labs) followed by ABC and immuno-labeling visualized using diaminobenzidine (DAB) as the chromogen. To investigate the relationship between microglia and dopamine-containing neurons in the midbrain, another set of sections were immunolabeled with rat anti-MAC-1 (1 : 2000) with DAB-Nickel (0.05% nickel ammonium sulfate) as the chromogen (blue-black color), and then incubated with mouse anti-TH (1 : 2000) and developed with DAB (brown).

For electron microscopy, 50 µm thick sections cut on a Vibratome were immunoreacted in mouse anti-TH, diluted in 0.1 M PBS, and processed using the ABC protocol with DAB as the chromogen. Sections were flattened, treated in 1% osmium tetroxide in 0.1 M PB for 30 min, dehydrated and embedded in Araldite resin on glass slides. Regions of interest, selected during light microscopic examination, were excised as small blocks from the resin and mounted on pre-cured plastic blocks. Serial, ultrathin sections were mounted onto copper slot grids, contrasted with lead citrate, and images captured digitally from a Philips 400 electron microscope using a Multiscan camera (Gatan, UK).

2.2. Design-Based Stereology

The optical fractionator was used to determine the total number of microglia in the SN of MPTP/p-treated and probenecid controls at one and six months after treatment. Counts were also made in age-matched, untreated animals. The entire SN, comprising the SNpc and pars reticulata (SNpr), was included in the analysis. The investigator was blind to each animal's treatment.

It is important to define boundaries that can be recognized reliably from one animal to another. For this study, the dorsal boundary was a line extending along the ventral border of the medial lemniscus to the lateral surface of the brain and the medial boundary was defined by a line through the medial limit of the cerebral peduncle. Lateral and ventral borders were taken as the edges of the brain. After a random start, every fifth section from the entire rostrocaudal extent (1500 m) of the SN was analyzed. Mac-1- immunopositive microglial cell bodies were counted with a semi-automated system (StereoInvestigator, MicroBrightfield, Colchester, VT) and using a 100X oil objective with a 1.35 NA. Following a pilot study, the SN in each selected section was outlined and overlaid with a 140 µm

× 140 µm grid to produce 20–50 sampling sites. A counting frame (40 µm × 40 µm) with a disector height of 8 µm was used to count Mac-1 immunopositive profiles. A profile was only counted if a 'top' appeared in the counting 'brick' and a clearly defined, perikaryal membrane and nucleus were present. Section thickness was measured at every third sampling site, such that the derived fractionator values were expressed per weighted section thickness. Finally, the somal volume of each cell body was calculated using the nucleator probe.

3. RESULTS

As we have shown previously (Petroske et al., 2001; Meredith et al., 2002), treatment with MPTP/p results in a long lasting depletion of TH-immunoreactive and Nissl-stained neurons in the SN and a significant deficit in forepaw agility with the grid test, adapted from Tillerson and colleagues (2003). There is however some evidence of recovery, especially in the TH-immunoreactive processes by 6 months following treatment. In untreated and probenecid-treated control animals, microglia, typically in a resting state, were observed throughout the SN. They had small cell bodies that gave rise to several fine, highly branched processes (Fig 1A,B,D,E). Following MPTP/p treatment, Mac-1 immunopositive profiles were shorter and thicker (Fig 1C,F), a morphology associated with activated microglia. In some cases, microglial processes were found in close association to TH-immunoreactive neurons. In the electron microscope, following treatment with MPTP/p, microglial pro-

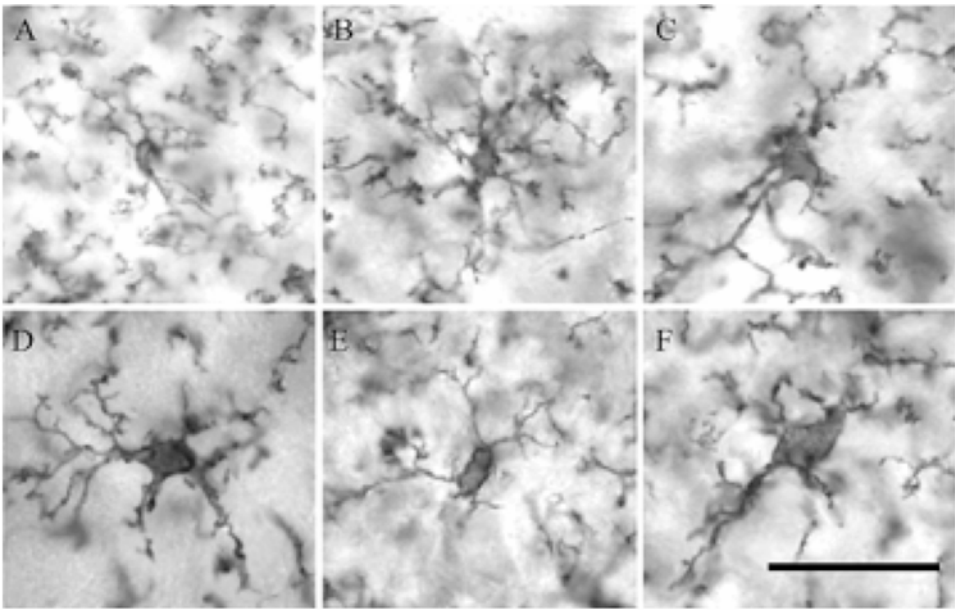

Figure 1. Mac-1-immunopositive microglial cells from the SN of aged matched controls (A, D), probenecid- (B, E) and MPTP/p- (C, F) treated animals, one (A–C) and six (D–F) months after treatment. Note the increased cell body size of microglia from MPTP/p-treated animals (C, F). Scale bar in F is valid for all and equals 20 µm.

cesses were frequently located near either degenerating, and occasionally inclusion-filled (Fig 2A,B,D) or TH-immunoreactive profiles (Fig 2C). The total volume of the SN and the total number of microglia and their size were estimated in sections from mice one month after treatment and compared with untreated control mice of comparable age (Table 1). To determine whether the effects on microglia are chronic, these parameters were also measured in mice 6 months after treatment. Numbers of microglia increased by 11% one month after MPTP/p treatment, an increase that was determined to be significant (Table 1). In addition, microglia in MPTP/p-treated mice were significantly larger than those in controls, and age-matched, untreated mice (Table 1). There was a trend towards increased numbers of microglia with time, both in controls and in MPTP/p-treated animals. By 6 months post-treatment, the number of microglia had increased in all groups but was similar in MPTP/p-treated animals and controls. Nevertheless, the significant difference in the size of microglia persisted in MPTP/p-treated mice compared to controls at 6 months post-treatment. Despite the increase in microglia somal volume and number following MPTP/p treatment, there

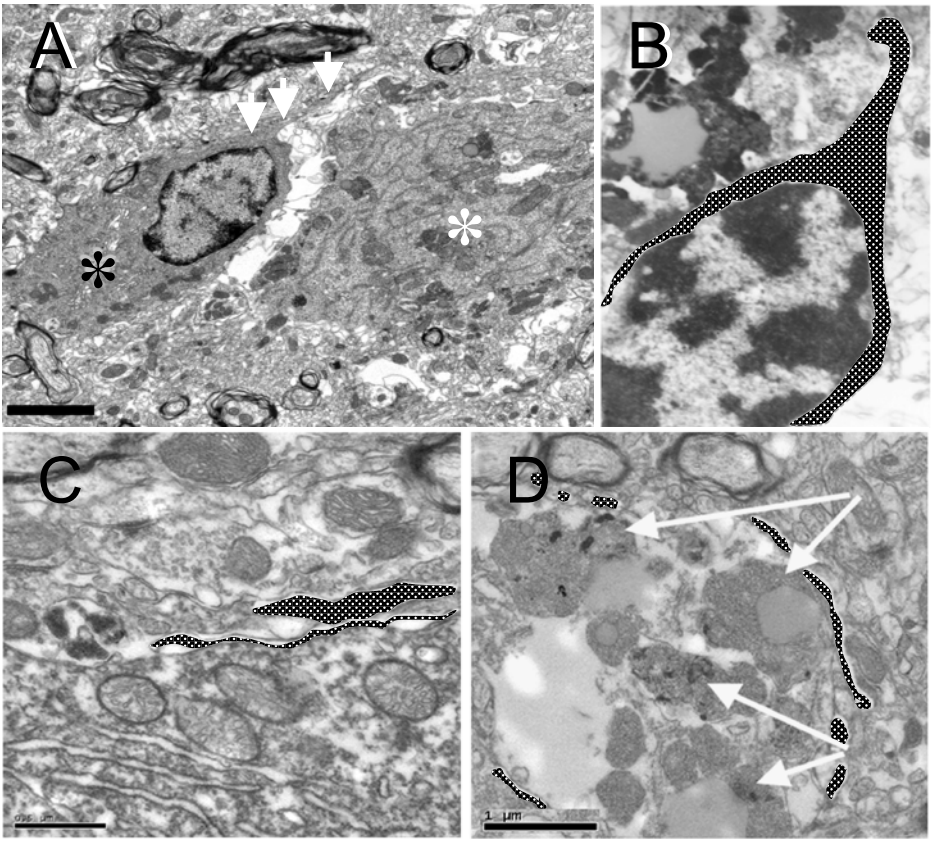

Figure 2. (A) Microglia (black asterisk) closely appose neurons (white asterisk) that contain inclusions containing lipid. (B) microglia with process (hatching) apposed to a degenerating profile containing lipid and dark lipofuscin. (C) Glial processes (hatching) abut a TH-immunoreactive cell (DAB deposits). (D) Inclusion bodies with lipid cores (white arrows) are surrounded by glial processes (hatching). Scales: A,C 0.25 µm, B, D 1 µm (scale applies to both).

Table 1. Number and size of microglia in the SN of MPTP/p-treated and control (vehicle and age-matched) mice.

Controls	Chronic MPTP/p	Volume of SN (mm^3)	CE	Total number $N \times 10^4$	CE	Density $N_v \times 10^4/mm^3$	Somal volume (μm^3)
Age-matched Mean ± SE		0.731 ± 0.030	0.06	1.76 ± 0.05	0.09	2.42 ± 0.09	234 ± 7
Vehicle-treated Mean ± SE		0.739 ± 0.022	0.08	1.75 ± 0.05	0.09	2.37 ± 0.05	232 ± 11
	MPTP/p Mean ± SE	0.704 ± 0.008[a]	0.06	1.95 ± 0.05[b]	0.09	2.76 ± 0.11[c]	274 ± 12[d]

[a] No significant difference when compared to both control groups.
[b] $p =< 0.05$ (one-way ANOVA, Student–Newman-Keuls *post hoc*); significantly greater than both control groups.
[c] $p =< 0.05$ (one-way ANOVA, Student–Newman-Keuls *post hoc*); significantly greater than both control groups.
[d] $p =< 0.001$ (Kruskal-Wallis ANOVA on Ranks); significantly greater than both control groups.

was no change in total volume of the SN at one and six months post-treatment suggesting that glial size and number changes were not due to a change in tissue volume.

4. DISCUSSION

This study continues our work with a chronic mouse model of Parkinson's disease. We show that, in addition to the loss of TH-positive, presumably dopaminergic neurons, and the progressive appearance of inclusion bodies, treated mice display an increase in reactive microglia, as determined by their appearance and size (Fig. 1, Table 1), which persists for at least 6 months after the end of treatment.

During development, microglia have a characteristic amoeboid form and they scavenge dead and dying cells that result from programmed cell death. In normal adult brain they display a more ramified morphology and, together with astrocytes, play a key role in the immune response. When the brain suffers an infection, a toxic insult or trauma, glia proliferate and move from the resting to the activated state. In the case of microglia, this involves a shortening of processes and an increase in somal volume, accompanied by an upregulation of cell surface molecules such as complement receptors, and secretion of a range of neurotrophic molecules (Nakajima and Kohsaka, 2001). A number of harmful factors are released by activated microglia. These include superoxide, nitric oxide and pro-inflammatory cytokines (Liu et al., 2000). Proposed as a key feature of PD, it is possible that free radicals and other reactive oxygen species are a direct result of microglial activation. Cell death may result from toxic molecules acting cooperatively to disrupt normal function. A current view of microglial activation in PD points to an ongoing, self-reinforcing cycle of inflammation that arises from toxin exposure or possibly infectious agents (Liu et al., 2003). Nigral dopaminergic neurons may be selectively at risk due to the high levels of microglia in this brain region (Lawson et al., 1990; Kim et al., 2000). Thus, conditions that result in the activation of microglia might produce an additional toxic burden to already vulnerable dopaminergic neurons.

We have shown that chronic exposure to MPTP results in an increase in numbers and size of microglia in the SN and a change in their morphology that is consistent with their being in an activated state. We also find microglial processes in close association with degenerating profiles, some of which contain granular inclusions, thereby supporting a role for them in the scavenging of dead and dying cells. Microglial activation must also precede neuronal degeneration and may hasten cell death through the release of toxic molecules (Liberatore et al., 1999). On the other hand, *in vitro* studies point to a microglial role in neuron survival, because they produce neurotrophins, including brain derived neurotrophic factor and neurotrophin 4/5 (Miwa et al., 1997). These data raise the question as to whether activated microglia are harmful or helpful.

The chronic inflammatory response seen in the MPTP/p model is consistent with that described for human PD (McGeer, et al., 1988, 2001) but differs from that observed in other animal models. Using a more acute MPTP administration, microglial activation isv transient (Liberatore et al., 1999), and in rats treated with rotenone, activated cells were found even though no dopaminergic cells were lost (Sherer et al., 2003), suggesting that the effects of rotenone on glial proliferation might be independent of its mitochondrial toxicity.

In conclusion, it seems that MPTP/p treatment is accompanied by the chronic activation of microglia. Such activation may be accompanied by the release of pro-inflammatory molecules and free radicals, which would exacerbate the toxic insult and contribute further to dopaminergic neuronal loss in the SN. Our data further support the validity of the MPTP/p model as a useful tool for understanding the inflammatory process in PD.

5. ACKNOWLEDGEMENTS

This work was supported by a NIH-NINDS NS41799 grant and a Wellcome Trust Biomedical Collaboration grant.

6. REFERENCES

Kim, W.G., Mohney, R.P., Wilson, B., Jeohn, G.H., Liu, B., and Hong, J.S., 2000, Regional difference in susceptibility to lipopolysaccharide-induced neurotoxicity in the rat brain: role of microglia, *J. Neurosci.* **20**: 6309–6316.

Lawson, L.J., Perry, V.H., Dri, P., and Gordon, S., 1990, Heterogeneity in the distribution and morphology of microglia in the normal adult mouse brain, *Neuroscience* **39**:151–170.

Liberatore, G.T., Jackson-Lewis, V., Vukosavic, S., Mandir, A.S., Vila, M., McAuliffe, W.G., Dawson, V.L., Dawson, T.M., and Przedborski, S., 1999, Inducible nitric oxide synthase stimulates dopaminergic neurodegeneration in the MPTP model of Parkinson disease, *Nat. Med.* **5**:1403–1409.

Liu, B., Du, L., and Hong, J.-S., 2000, Naloxone protects rat dopaminergic neurons against inflammatory damage through inhibition of microglia activation and superoxide generation, *J. Pharmacol. Exp. Ther.* **293:** 607–617.

Liu, B., Gao, H.M., and Hong, J.S., 2003, Parkinson's disease and exposure to infectious agents and pesticides and the occurrence of brain injuries: role of neuroinflammation, *Environ. Health Perspec.* **111**: 1065–1073.

McGeer, P.L., Itagaki, S., Boyes, B.E., and McGeer, E.G., 1988, Reactive microglia are positive for HLA-DR in the substantia nigra of Parkinson's and Alzheimer's disease brains, *Neurol.* **38**:1285–1291.

McGeer, P.L., Yasojima, K., and McGeer, E.G., 2001, Inflammation in Parkinson's disease, *Adv. Neurol.* **86**: 83–89.

Meredith, G.E., Totterdell, S., Petroske, E., Santa Cruz, K., Callison Jr, R.C., and Lau. Y-S., 2002, Lysosomal malfunction accompanies alpha synuclein aggregation in a progressive mouse model of Parkinson's disease, *Brain Res.* **956**:156–165.

Meredith, G.E., Halliday, G.M., Totterdell, S., 2004, A critical review of the development and importance of proteinaceous aggregates in animal models of Parkinson's disease: New insights into Lewy body formation, *Parkinsonism Rel. Dis.* **10**:191–202.

Miwa, T., Furukawa, S., Nakajima, K., Furukawa, Y., and Kohsaka, S., 1997, Lipopolysaccharide enhances synthesis of brain-derived neurotrophic factor in cultured rat microglia, *J. Neurosci. Res.* **50**:1023–9.

Nakajima, K., and Kohsaka, S., 2001, Microglia: activation and their significance in the central nervous system, *J. Biochem.* **130**:169–175.

Petroske, E., Meredith, G.E., Callen, S., Totterdell, S., and Lau, Y-S., 2001, Mouse model of Parkinsonism: a comparison between subacute MPTP and chronic MPTP/probenecid treatment, *Neuroscience* **106**: 589–601.

Sherer, T.B., Betarbet, R., Kim, J.H., and Greenamyre, J.T., 2003, Selective microglial activation in the rat rotenone model of Parkinson's disease, *Neurosci. Letts.* **341**:87–90.

Spillantini, M.G., Schmidt, M.L., Lee, V.M., Trojanowski, J.Q., Jakes, R., and Goedert, M., 1997, Alpha-synuclein in Lewy bodies, *Nature* **388**:839–840.

Tillerson, J.L., and Miller, G.W., 2003, Grid performance test to measure behavioral impairment in the MPTP-treated-mouse model of parkinsonism, *J. Neurosci. Methods* **123**:189–200.

EARLY BEHAVIORAL PHENOTYPES IN MOUSE MODELS OF HUNTINGTON'S AND PARKINSON'S DISEASES

Marie-Francoise Chesselet, Miriam A. Hickey, Sheila M. Fleming, and Pierre-Olivier Fernagut*

1. INTRODUCTION

Huntington's (HD) and Parkinson's (PD) diseases are two of the major neurological diseases affecting the basal ganglia. For several decades, animal models of these diseases have relied upon the use of selective neurotoxins that mimic the cell loss found in patients (Dauer and Przedborski, 2003; Hickey and Chesselet, 2003a). However, these models have considerable limitations. First, they are relatively acute and do not reproduce the lengthy disease process that occurs in humans; second, they cause the loss of only a subset of neurons affected in the disease; third, and perhaps most importantly, it is unclear that they kill cells by the mechanism(s) that operate in the human disease. A major breakthrough in animal models of HD and PD was the discovery of mutations causing these diseases. This allowed for the development of mice expressing these mutations in various ways. Of course, the situation is very different for HD and PD. HD is a genetic disorder caused by a single mutation (an expanded polyglutamine repeat in the gene encoding huntingtin) with 100% penetrance in the majority of cases (Huntington's Disease Collaborative Research Group, 1993). In contrast, PD is most often sporadic. However, rare familial forms offer the opportunity to examine how particular mechanisms lead to the disease in humans. So far, mutations or abnormal expression of 6 genes have been shown to cause PD. In most cases, their function relates to anomalies previously detected in sporadic PD. Therefore, it is reasonable to assume that insights gained from their studies in mice will shed light to mechanisms relevant to sporadic PD.

In this chapter, we will briefly review efforts from our laboratory to identify early behavioral phenotypes in mouse models of HD and PD. It is important to identify the earliest manifestations caused by the mutations because it helps determine when to perform

* Chesselet M-F, Hickey MA, Fleming SM, Fernagut P-O, Departments of Neurology and Neurobiology, David Geffen School of Medicine, University of California Los Angeles, Los Angeles California, 90095 USA.

more time consuming and invasive experiments to elucidate the mechanisms involved, and because these anomalies can serve as useful end point measures for preclinical testing of new therapies.

Experience has shown that most traditional behavioral tests, designed to detect behavioral deficits caused by massive neuronal loss, are not suitable to identify the much more subtle anomalies caused by the mutations at the early stages of the disease. Furthermore, many behavioral tests developed for rats are not yet widely available for mice. Therefore, a significant aspect of this work was the development or adaptation of novel tests of deficits sensitive to mild dysfunction of the basal ganglia.

2. HUNTINGTON'S DISEASE

The main pathological characteristic of HD is a massive loss of medium sized spiny neurons in the caudate and putamen, although the cerebral cortex and other brain regions are also affected (Vonsattel, et al., 1985). Interestingly, very long CAG repeats, which trigger an earlier onset disease than more moderate expansions, cause more widespread pathology with cell loss in the hippocampus and cerebellum in addition to those regions affected in middle-age onset disease. Therefore, the regional selectivity of the neuropathology in HD is relative.

Patients with HD exhibit a triad of emotional, cognitive and motor impairments (Harper, 1996). The age of onset is usually in midlife, but pathological changes and subtle motor symptoms have been detected in mutant allele carriers, occurring many years prior to calculated age of onset (Smith, et al., 2000; Gomez-Tortosa, et al., 2001). Little is known, however of the earliest effects of the mutation since most post-mortem studies are performed in patients who exhibit late stage disease (Vonsattel, et al., 1985).

Since the identification of the mutation causing HD in 1993 (Huntington's Disease Collaborative Research Group, 1993), numerous mouse models have been generated using a variety of techniques (Menalled and Chesselet, 2002; Hickey and Chesselet, 2003b). Our laboratory has focused on the detection of behavioral anomalies in young transgenic (TG) mice which express exon 1 of a human mutant huntingtin gene, carrying 119–130 CAG repeats in our colony (R6/2 mice, Mangiarini, et al., 1996), and on young knock-in (KI) mice with either 94 or 140 CAG repeats inserted into their huntingtin gene homologue (CAG94, CAG140, Menalled, et al., 2002, 2003). These models are highly complementary: the TG model, which has been extensively characterized by many laboratories, has a rapid disease progression and dies around 14 weeks of age; in contrast, the KI mice live up to two years of age and show slowly progressive anomalies. These KI mice have the advantage of expressing the mutation in the context of the full-length protein and under the normal promoter. As indicated below, the line we have studied demonstrates early behavioral anomalies, which does not seem to be the case for all KI lines, perhaps due to differences in mouse strain or construct (Hickey and Chesselet, 2003b).

2.1. Behavioral Anomalies in Young Knock-in Mice

The CAG140 and CAG94 KI mice carry a chimeric human/mouse exon 1 expressing 94 or 140 CAG repeats within their huntingtin gene. Thus, expression levels of the mutant protein are controlled by the endogenous murine *huntingtin* homologue promotor and are equivalent with normal expression levels (Menalled, et al., 2003). Study of these mice

Table 1. Early behavioral deficits in R6/2 TG and CAG140 KI mice.

	R6/2[g]				CAG140[h]				
Age	1	1.5	2	3	1	1.5	4	6	20
Running wheel (dark phase)	↓↓	nd	↓↓	↓↓↓[a]	=	=	=	↓♂[b]	nd
Climbing[c]	↓	nd	↓↓	nd	nd	↓	=	↓↓	nd
Activity (open field)	↓	nd	↓	nd	↑[i]	nd	↓[i]	=[i]	nd
Body weight	=	=	=	↓	=	=	=	=	↓
Rotarod	=	=	↓↓	nd	nd	nd	nd	nd	nd
Phenotype (tremor)	=	=	↑	↑↑	=	=	=	=	↑[d]
Light dark box[e]	↑	nd	=	nd	nd	↑	nd	=	nd
Pole task[f]	nd	nd	nd	nd	nd	nd	↑	=	nd

= Not different from WT; ↑ Increased, ↑↑ profoundly increased compared to WT; ↓ Decreased, ↓↓ profoundly decreased compared to WT; nd Not determined. [a] Pilot experiment TG n = 2, WT n = 2. [b] Female KI mice show reduced dark phase running wheel activity by 8 months. [c] Time with all paws off the floor. [d] KI mice show uncoordinated gait. [e] Latency to enter light. [f] Latency to descend. Data from Hickey et al., in press[g]; Hickey et al., 2004[h]; Menalled et al., 2003[i].

reveals a CAG repeat length dependent effect on progression of disease, with mice carrying 140 repeats showing earlier behavioral signs and more severe and widespread pathology than their counterparts that express 94 repeats (Menalled, et al., 2002, 2003). Both show hyperactivity in a novel environment at early ages (1 month for CAG140s, 2 months for CAG94s), followed by later hypoactivity, in agreement with other genetic models of HD (Menalled and Chesselet, 2002; Hickey and Chesselet, 2003b) At a much later age, the CAG140 mice show gait abnormalities (Menalled, et al., 2003) which are also noted, at a late phase, in other genetic HD models (Hickey and Chesselet, 2003b).

We have recently found that CAG140 KI mice display several other anomalies, such as reduced climbing, anxiety, impaired sensorimotor function (vertical beam descent, or "pole test") and reduced running wheel activity (Hickey, et al., 2004) (Table 1). Decreased climbing and increased anxiety were observed as early as 1.5 months of age, confirming an early phenotype in these mice. Climbing in particular is an easy test that does not require costly equipment. Therefore, it is amenable to rapid screening. Evidence for increased anxiety is of interest because affective disorders are frequent in HD and often precede overt motor symptoms (Kirkwood, et al., 2002). Reduced activity in the running wheel did not appear under our experimental conditions until 6 months of age, perhaps because this deficit corresponds to the later phase of hypoactivity observed after 4 months of age in the open field. The major advantage of this test, however, is that it can be completely automated which makes it practical for drug testing.

2.2. Behavioral Anomalies in Young R6/2 Mice

Many laboratories have identified behavioral deficits in R6/2 mice, some detected as early as 3 weeks of age (Lione, et al., 1999; Lüesse, et al., 2001). Like the KI mice, these mice have hyper-, followed by hypoactivity (Lüesse, et al., 2001). However, in agreement with the fast course of disease in these mice, the hypoactive phase occurs at a much younger age than in KI mice. This prompted us to examine the possibility that these mice are defective in the running wheel at an early age. Indeed, we found a reduced activity in the running

wheel during the dark (active) phase of the diurnal cycle as early as 1 month of age, the earliest age tested, in the R6/2 mice (Hickey, et al., in press). The deficits worsen, and begin to be detected during the day, at later ages. In addition to an overall decrease in running activity, R6/2 mice show more breaks while on the wheel (Hickey, et al., in press).

2.3. Relationship of Behavioral Anomalies to Neuropathology in HD Mice

Noticeably, the two genetic models we have examined show very similar phenotypes, despite different genetic manipulations and strain backgrounds. This strongly suggests that the behavioral anomalies exhibited by these mice are related to the presence of the HD-causing mutation. The more severe phenotype of the R6/2 mice is likely due to the presence of a truncated form of the pathological protein. Indeed, short fragments of mutant huntingtin are more toxic in vitro than the full-length protein (Hickey and Chesselet, 2003a). Furthermore, cleavage products are detected early in disease process and protection from cleavage is protective (Wellington, et al., 2002; Gafni, et al., 2004). Conversely, KI technology generates full-length proteins under the control of appropriate promoters. With their slower progression of disease and more subtle symptoms, the KI mice present a longer, more realistic window for therapeutic action than other more severe models. This longer timeframe also allows for longer safety and tolerability trials for new interventions.

These mice exhibit degenerative changes very reminiscent of HD patient pathology including loss of striatal volume, loss of medium spiny neuron arborisation, presence of dark neurons and development of intranuclear and neuropil aggregates of mutant huntingtin (Hickey and Chesselet, 2003a). Specifically, the KI mice display reduced striatal volume without cell loss, thus suggesting loss of arborisation and spine density, as has been shown in other models (Klapstein, et al., 2001; Menalled, et al., 2002; Spires, et al., 2004). Accordingly, these models allow focus on early stages of the disease, thus providing insight into pathological mechanisms *leading* to cell death.

Nuclear and neuropil aggregates are an important pathological consequence of expression of mutated, elongated triplet repeats (Hickey and Chesselet, 2003a), however it is possible that different forms of aggregates are more toxic than others (Arrasate, et al., 2004). In the CAG140 KI mice, aggregates develop initially in areas of dopaminergic innervation and in olfactory-related areas (Menalled, et al., 2003). In the same mice, the layers of the cortex are differentially affected with some layers showing inclusion formation, while others show only neuropil aggregates. It is interesting to note that olfaction is an early impairment in HD, and cortical degeneration is layer selective in the HD patient (Moberg, et al., 1987; Hedreen, et al., 1991; Hamilton, et al., 1999; Selemon, et al., 2004). In our CAG94 mice, striatal microaggregate formation shows selectivity for striosomes, an area that shows early neuronal loss in HD (Hedreen and Folstein, 1995; Menalled, et al., 2002).

Although aggregates are important markers of pathology, the behavioral signs described earlier precede overt aggregate formation in our mice (Menalled, et al., 2002, 2003; Hickey, et al., 2004). Furthermore, by 4 months of age, when there is variable presence of aggregates, CAG94 mice show >50% loss of striatal mRNA for enkephalin (Menalled, et al., 2000). The presence of behavioral changes indicates the presence of neuronal dysfunction and indeed, synaptic communication is impaired in very young HD mutant animals (Starling, et al., 2003). Several other model systems have also shown early deficits in transcription and transport (Sipione, et al., 2002; Szebenyi, et al., 2003), both of which could severely affect neuronal function. Thus, neuronal dysfuntion is an important component of

the disease process, and not necessarily dependent on aggregation. The behavioral anomalies we have uncovered at early ages both in KI and TG mice provide a novel way to assess this phase of the disease, which should be the focus of therapy development since it precedes irreversible loss of neurons.

3. PARKINSON'S DISEASE

The first mutation found to cause PD was identified in the gene encoding a vesicular protein, α-synuclein. Of particular interest is the fact that α-synuclein has been linked to both familial and sporadic PD. Although specific mutations in α-synuclein have been found to cause familial PD in very rare families (Polymeropoulos, et al., 1997; Kruger, et al., 1998), the importance of this protein in sporadic PD is underscored by its presence in Lewy bodies, the pathological hallmark of idiopathic PD (Spillantini, et al., 1997). In addition, increased levels of normal α-synuclein due to gene duplication or triplication also lead to early onset familial PD (Singleton, et al., 2003; Ibanez, et al., 2004). Studies in post-mortem human brain revealed widespread pathology in brain regions known to eventually degenerate in PD, and led to the concept that incidental Lewy body disease is actually a presymptomatic form of PD (Forno, 1969; Braak, et al., 2003). Whether this is the case or not, this work points to the fact, well-known from clinicians, that PD is a systemic disease that affects multiple regions of the central and peripheral nervous systems in addition to the canonical loss of nigro-striatal dopaminergic neurons (Lang and Obeso, 2004).

A major limitation of traditional models of PD based on toxin injections is that their focus was to reproduce solely, or primarily, the loss of nigrostriatal dopamine (DA) neurons. The multi-system pathology that characterizes PD calls for new models of the disease. A systemically expressed mutation in mice is more likely to reproduce the true spectrum of lesions found in humans. The most extensively studied genetic mouse models of PD to date express mutations in α-synuclein (Fernagut and Chesselet, 2004) or parkin, an E3 ligase, which is mutated in numerous cases of early onset, recessive familial PD (Goldberg, et al., 2003; Itier, et al., 2003; Palacino, et al., 2004; Von Coelln, et al., 2004; Perez and Palmiter, 2005). Of the mutations more recently identified to cause familial PD (UCHL-1, DJ-1, PINK-1 and LRKK2), only the loss of DJ-1 activity has so far been reproduced in a published mouse model (Goldberg, et al., 2005).

Considering the involvement of the olfactory bulb, medulla, and locus coeruleus before or at the same time as the susbtantia nigra pars compacta in PD, it is not surprising that patients often present with olfactory deficits, sleep and affective disorders, often before the onset of the typical motor symptoms of akinesia, rigidity, tremor, and postural instability (McDonald, et al., 2003; Pal, et al., 2004; Ponsen, et al., 2004). Furthermore, patients show pervasive autonomic and digestive dysfunction, which may be of central or peripheral origin, in view of the presence of Lewy bodies in visceral centers of the medulla as well as in the myenteric plexus (Wakabayashi, et al., 1993; Siddiqui, et al., 2002; Pfeiffer, 2003). Genetic mouse models allow us, for the first time, to study the whole disease, including the early symptoms that often precede the cardinal motor symptoms.

3.1. Behavioral Anomalies in PD Mice

Our laboratory has focused on the detection of early behavioral symptoms in mice overexpressing human wildtype α-synuclein under the Thy1 promoter, generated by E.

Masliah and E. Rockenstein, UCSD (Rockenstein, et al., 2002), and in mice with a deletion of exon 3 of the parkin gene, parkin knock out (KO), generated by J. Shen and M. Goldberg at Bringham and Women's Hospital (Goldberg, et al., 2003). Both α-synuclein over-expressors and parkin KO mice have mutations similar to those found in familial PD. In addition, we have examined the behavioral phenotype of Pitx3-/-aphakia mice, which lose dopaminergic neurons early in development, generated by K-S Kim and D.-Y. Hwang at Mc Lean Hospital.

Using sensitive DA-dependent tests we have shown that α-synuclein over-expressors display impairments in beam walking, on the pole test, in hindlimb stepping, response to sensory stimuli, and in bin cotton use (Figure 1; see Fleming, et al., 2004a, Fleming and Chesselet, 2005) for extensive description of these tests). Both beam walking and bin cotton use impairments worsen with age (Fleming, et al., 2004a). In addition, these mice have an abnormal response to dopaminergic agents including L-DOPA, apomorphine, and amphetamine (Fleming, et al., 2004b). Similar to the α-synuclein over-expressors, parkin KO mice display impairments in beam walking and response to sensory stimuli (Goldberg, et al., 2003) (although more subtle). Preliminary data show that these mice also have a decreased grooming in response to local injection of DA in their striatum (Fleming, et al., unpublished observation), and a separate line of mice with a similar mutation showed a decreased response to amphetamine (Itier, et al., 2003).

These results show that behavioral deficits can be detected in mouse models of PD even though these mice do not have a loss of DA neurons. The involvement of the nigrostriatal pathway in these effects is suggested by the similarity with the behavioral deficits we have observed by using the same tests in Pitx3-/-akaphia mice. These mice, which have a very selective loss of nigrostriatal dopaminergic neurons (in addition to blindness) due to the loss of the homeobox transcription factor Pitx3, show impairments in beam walking, on the pole test, and in rearing. In these mice, most sensorimotor impairments are reversed with L-DOPA (Hwang, et al., 2005). In agreement with a 90% reduction in DA content in the dorsal striatum, these mice show a strong induction of c-fos expression in the dorsal striatum after L-DOPA (Hwang, et al., 2003; Hwang, et al., 2005), an indication of denervation supersensitivity.

It should be noted that although similar, the behavioral profile of these mice is not identical to that found in mice expressing mutations known to cause PD, suggesting that in the latter, dysfunction in additional brain regions may contribute to some of the observed

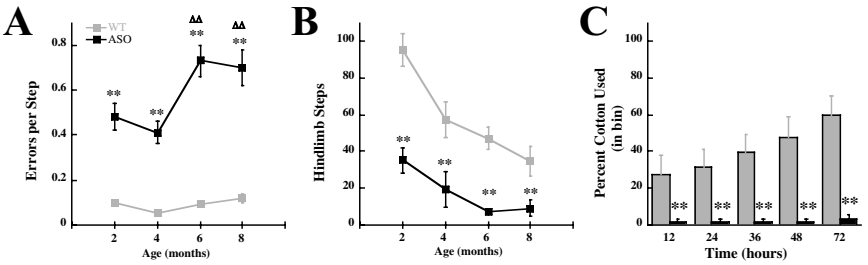

Figure 1. Sensorimotor function in α-synuclein over-expressing (ASO) mice. ASO mice have impairments in beam walking (A), hindlimb stepping (B) and in bin cotton use (C). ** indicates $p < 0.01$ compared to wild-type mice. ΔΔ indicates $p < 0.01$ compared to ASO at 2 and 4 months. Analysis was done using ANOVA followed by Fisher's LSD. Reproduced from Fleming et al., 2004a with permission (copyright 2004 by the Society for Neuroscience).

Table 2. Behavioral Impairments in AK, ASO, and PK Mice.

Behavioral Test	DA Loss	DA Dysfunction	
	AK	ASO	PK
Beam			
Errors	–	+	+
Steps	+	+	–
Time	+	+	–
Cylinder			
Rears	+	+	+
Forelimb Steps	–	+	–
Hindlimb Steps	–	+	–
Grooming	–	+	–
Response to Sensory Stimuli	+	+	+

+ indicates impairment. – indicates no impairment. AK: Pitx3-/- akaphia mice; ASO: α-synuclein over-expressor mice; PK: parkin knock-out mice; see Fleming et al., 2004a, b for a description of the tests.

impairments, in agreement with the more widespread pathology in PD discussed earlier (Table 2).

3.2. Relationship of Sensorimotor Deficits to Other Anomalies in Mouse Models of PD

Although α-synuclein over-expressors and parkin KO mice do not have a loss of nigrostriatal dopaminergic neurons they do have alterations within the nigrostriatal dopaminergic system. Following administration of the neurotoxin MPTP the overexpressors but not wildtype mice show an increase in mitochondrial size, axonal degeneration, and filamentous neuritic aggregations in the substantia nigra suggesting that the nigrostriatal DA system may be compromised in these mice (Song, et al., 2004). Furthermore, we have observed a small but significant decrease in binding to both the cytoplasmic and vesicular dopamine transporters in these mice (Fernagut et al. in preparation). Recent data from our collaborators N. Maidment and M. Levine indicate that these mice have altered dopamine release and synaptic function in the striatum (unpublished observations).

One of the most compelling aspects of α-synuclein over-expressors, however, is the presence of widespread α-synuclein pathology in brain. They have high expression of α-synuclein in thalamus, basal ganglia, substantia nigra, and brainstem (Rockenstein, et al., 2002; Hutson et al., in preparation). This prompted us to examine the possibility that these mice may exhibit non-motor signs similar to those observed in early stages of PD. Indeed, preliminary data indicate that these mice have an early and progressive olfactory deficit and evidence of apathic behavior in the light-dark box (Fleming et al. in preparation). Furthermore, in collaboration with Y. Tache and collaborators at UCLA, we have obtained evidence for digestive deficits in these mice (Wang, et al., 2005). Thus, the α-synuclein over-expressors may represent the first animal model of PD to reproduce a wide range of symptoms characteristic of the disease, in addition to sensorimotor dysfunction.

The parkin KO mice also show alterations in nigrostriatal function. These mice have increased extracellular DA in the striatum and a reduction in synaptic excitability in medium spiny neurons in the striatum (Goldberg, et al., 2003). They also show evidence of oxidative stress in proteomic studies (Palacino, et al., 2004). Interestingly, parkin KO

mice expressing different mutations appear to have distinct phenotypes (Von Coelln, et al., 2004; Perez and Palmiter, 2005). At this time, it remains unclear whether this is due to the type of mutation, genetic background of the mice, or the sensitivity of the tests.

4. CONCLUSIONS

Mouse models of HD and PD have begun to provide extremely valuable tools to examine the effects of the disease-causing mutations in a mammalian organism, in vivo. This level of analysis is less amenable to mechanistic or genetic analyses than in vitro models, or other model organisms such as *Drosophila*, *C. elegans*, or zebra fish. However, it is necessary to assess the role of anatomical connections in disease pathology and for preclinical drug testing. For this purpose, it is essential to develop batteries of sensitive behavioral tests to detect early and robust phenotypes amenable to easy and cost-effective drug trials. We have shown that despite the absence of the massive neuronal cell loss observed during the symptomatic phase of the human diseases, such behavioral phenotypes can be identified, at an early age in several, genetically distinct, mouse models of both HD and PD.

5. REFERENCES

Arrasate, M., Mitra, S., Schweitzer, E.S., Segal, M.R., and Finkbeiner, S., 2004, Inclusion body formation reduces levels of mutant huntingtin and the risk of neuronal death, *Nature.* **431**:805–810.

Braak, H., Del Tredici, K., Rub, U., de Vos, R.A., Jansen Steur, E.N., and Braak, E., 2003, Staging of brain pathology related to sporadic Parkinson's disease, *Neurobiol Aging.* **24**:197–211.

Dauer, W., and Przedborski, S., 2003, Parkinson's disease: mechanisms and models., *Neuron.* **39**:889–909.

Fernagut, P.-O., and Chesselet, M.-F., 2004, Alpha-synuclein and transgenic mouse models, *Neurobiol Dis.* **17**:123–130.

Fleming, S.M., and Chesselet, M.-F., Phenotypical characterization of genetic mouse models of Parkinson's disease, 2005, Phenotypical characterization of genetic mouse models of Parkinson's disease, in: *Animal Models of Movement Disorders*, M. LeDoux, ed., pp 183–192.

Fleming, S.M., Salcedo, J., Fernagut, P.-O., Rockenstein, E., Masliah, E., Levine, M.S., and Chesselet, M.-F., 2004a, Early and progressive sensorimotor anomalies in mice overexpressing wild-type human alpha-synuclein, *J. Neurosci.* **24**:9434–9440.

Fleming, S.M., Salcedo, J., Hutson, C.B., Fernagut, P.-O., Masliah, E., Levine, M.S., and Chesselet, M.-F., 2004b, L-Dopa, apomorphine and amphetamine alter sensorimotor function in mice overexpressing human alpha-synuclein., *Society for Neuroscience, Abstract viewer/Itinery planner*, San Diego, Program No. 561.3.

Forno, L.S., 1969, Concentric hyalin intraneuronal inclusions of Lewy type in the brains of elderly persons (50 incidental cases): relationship to parkinsonism, *J. Am. Geriatr. Soc.* **17**:557–575.

Gafni, J., Hermel, E., Young, J.E., Wellington, C.L., Hayden, M.R., and Ellerby, L.M., 2004, Inhibition of calpain cleavage of huntingtin reduces toxicity: accumulation of calpain/caspase fragments in the nucleus, *J. Biol. Chem.* **279**:20211–20220.

Goldberg, M.S., Fleming, S.M., Palacino, J.J., Cepeda, C., Lam, H.A., Bhatnagar, A., Meloni, E.G., Wu, N., Ackerson, L.C., Klapstein, G.J., Gajendiran, M., Roth, B.L., Chesselet, M.-F., Maidment, N.T., Levine, M.S., and Shen, J., 2003, Parkin-deficient mice exhibit nigrostriatal deficits but not loss of dopaminergic neurons, *J. Biol. Chem.* **278**:43628–43635.

Goldberg, M.S., Pisani, A., Haburcak, M., Vortherms, T.A., Kitada, T., Costa, C., Tong, Y., Martella, G., Tscherter, A., Martins, A., Bernardi, G., Roth, B.L., Pothos, E.N., Calabresi, P., and Shen, J., 2005, Nigrostriatal dopaminergic deficits and hypokinesia caused by inactivation of the familial Parkinsonism-linked gene DJ-1, *Neuron.* **45**:489–496.

Gomez-Tortosa, E., MacDonald, M.E., Friend, J.C., Taylor, S.A., Weiler, L.J., Cupples, L.A., Srinidhi, J., Gusella, J.F., Bird, E.D., Vonsattel, J.P., and Myers, R.H., 2001, Quantitative neuropathological changes in presymptomatic Huntington's disease, *Ann. Neurol.* **49**:29–34.

Hamilton, J.M., Murphy, C., and Paulsen, J.S., 1999, Odor detection, learning, and memory in Huntington's disease, *J. Int. Neuropsychol. Soc.* **5**:609–615.

Harper, P.S., 1996, *Huntington's Disease*, Saunders, London.

Hedreen, J.C., and Folstein, S.E., 1995, Early loss of neostriatal striosome neurons in Huntington's disease, *J. Neuropathol. Exp. Neurol.* **54**:105–120.

Hedreen, J.C., Peyser, C.E., Folstein, S.E., and Ross, C.A., 1991, Neuronal loss in layers V and VI of cerebral cortex in Huntington's disease, *Neurosci. Lett.* **133**:257–261.

Hickey, M.A., and Chesselet, M.-F., 2003a, Apoptosis in Huntington's disease, *Prog. Neuropsychopharmacol. Biol. Psychiatry.* **27**:255–265.

Hickey, M.A., and Chesselet, M.-F., 2003b, The use of transgenic and knock-in mice to study Huntington's disease, *Cytogenet. Genome. Res.* **100**:276–286.

Hickey, M.A., Gallant, K., Gross, G.G., Levine, M.S., and Chesselet, M.-F., in press, Early Behavioral Deficits in R6/2 Mice Suitable for Use in Preclinical Drug Testing, *Neurobiol. Dis.*

Hickey, M.A., Gallant, K., Levine, M.S., and Chesselet, M.-F., 2004, Automated testing of mouse models of Huntington's disease, *Society for Neuroscience Abstract Viewer/Itinerary viewer*, San Diego, Program No. 564.14.

Huntington's Collaborative Research Group, 1993, A novel gene containing a trinucleotide repeat that is expanded and unstable on Huntington's disease chromosomes, *Cell.* **72**:971–983.

Hwang, D.Y., Ardayfio, P., Kang, U.J., Semina, E.V., and Kim, K.S., 2003, Selective loss of dopaminergic neurons in the substantia nigra of Pitx3-deficient aphakia mice, *Brain Res. Mol. Brain Res.* **114**:123–131.

Hwang, D.Y., Fleming, S.M., Ardayfio, P., Moran-Gates, T., Kim, H., Tarazi, F.I., and Chesselet, M.-F., 2005, L-DOPA reverses the motor deficits in Pitx-3-deficient aphakia mice: Behavioral characterization of a novel genetic model of Parkinson's disease, *J. Neurosci.* **25**(8):2132–2137.

Ibanez, P., Bonnet, A.M., Debarges, B., Lohmann, E., Tison, F., Pollak, P., Agid, Y., Durr, A., and Brice, A., 2004, Causal relation between alpha-synuclein gene duplication and familial Parkinson's disease, *Lancet.* **364**: 1169–1171.

Itier, J.M., Ibanez, P., Mena, M.A., Abbas, N., Cohen-Salmon, C., Bohme, G.A., Laville, M., Pratt, J., Corti, O., Pradier, L., Ret, G., Joubert, C., Periquet, M., Araujo, F., Negroni, J., Casarejos, M.J., Canals, S., Solano, R., Serrano, A., Gallego, E., Sanchez, M., Denefle, P., Benavides, J., Tremp, G., Rooney, T.A., Brice, A., and Garcia de Yebenes, J., 2003, Parkin gene inactivation alters behaviour and dopamine neurotransmission in the mouse, *Hum. Mol. Genet.* **12**:2277–2291.

Kirkwood, S.C., Siemers, E., Viken, R., Hodes, M.E., Conneally, P.M., Christian, J.C., and Foroud, T., 2002, Longitudinal personality changes among presymptomatic Huntington disease gene carriers, *Neuropsychiatry Neuropsychol. Behav. Neurol.* **15**:192–197.

Klapstein, G.J., Fisher, R.S., Zanjani, H., Cepeda, C., Jokel, E.S., Chesselet, M.-F., and Levine, M.S., 2001, Electrophysiological and morphological changes in striatal spiny neurons in R6/2 Huntington's disease transgenic mice, *J. Neurophysiol.* **86**:2667–2677.

Kruger, R., Kuhn, W., Muller, T., Woitalla, D., Graeber, M., Kosel, S., Przuntek, H., Epplen, J.T., Schols, L., and Riess, O., 1998, Ala30Pro mutation in the gene encoding alpha-synuclein in Parkinson's disease, *Nat. Genet.* **18**:106–108.

Lang, A.E., and Obeso, J.A., 2004, Time to move beyond nigrostriatal dopamine deficiency in Parkinson's disease, *Ann. Neurol.* **55**:761–765.

Lione, L.A., Carter, R.J., Hunt, M.J., Bates, G.P., Morton, A.J., and Dunnett, S.B., 1999, Selective discrimination learning impairments in mice expressing the human Huntington's disease mutation, *J. Neurosci.* **19**: 10428–10437.

Lüesse, H.G., Schiefer, J., Spruenken, A., Puls, C., Block, F., and Kosinski, C.M., 2001, Evaluation of R6/2 HD transgenic mice for therapeutic studies in Huntington's disease: behavioral testing and impact of diabetes mellitus, *Behav. Brain Res.* **126**:185–195.

Mangiarini, L., Sathasivam, K., Seller, M., Cozens, B., Harper, A., Hetherington, C., Lawton, M., Trottier, Y., Lehrach, H., Davies, S.W., and Bates, G.P., 1996, Exon 1 of the HD gene with an expanded CAG repeat is sufficient to cause a progressive neurological phenotype in transgenic mice, *Cell.* **87**:493–506.

McDonald, W.M., Richard, I.H., and DeLong, M.R., 2003, Prevalence, etiology, and treatment of depression in Parkinson's disease, *Biol. Psychiatry.* **54**:363–375.

Menalled, L., Zanjani, H., MacKenzie, L., Koppel, A., Carpenter, E., Zeitlin, S., and Chesselet, M.-F., 2000, Decrease in striatal enkephalin mRNA in mouse models of Huntington's disease, *Exp. Neurol.* **162**: 328–342.

Menalled, L.B., and Chesselet, M.-F., 2002, Mouse models of Huntington's disease, *Trends Pharmacol. Sci.* **23**:32–39.

Menalled, L.B., Sison, J.D., Dragatsis, I., Zeitlin, S., and Chesselet, M.-F., 2003, Time course of early motor and neuropathological anomalies in a knock-in mouse model of Huntington's disease with 140 CAG repeats, *J. Comp. Neurol.* **465**:11–26.

Menalled, L.B., Sison, J.D., Wu, Y., Olivieri, M., Li, X.J., Li, H., Zeitlin, S., and Chesselet, M.-F., 2002, Early motor dysfunction and striosomal distribution of huntingtin microaggregates in Huntington's disease knock-in mice, *J. Neurosci.* **22**:8266–8276.

Moberg, P.J., Pearlson, G.D., Speedie, L.J., Lipsey, J.R., Strauss, M.E., and Folstein, S.E., 1987, Olfactory recognition: differential impairments in early and late Huntington's and Alzheimer's diseases, *J. Clin. Exp. Neuropsychol.* **9**:650–664.

Pal, P.K., Thennarasu, K., Fleming, J., Schulzer, M., Brown, T., and Calne, S.M., 2004, Nocturnal sleep disturbances and daytime dysfunction in patients with Parkinson's disease and in their caregivers, *Parkinsonism Relat. Disord.* **10**:157–168.

Palacino, J.J., Sagi, D., Goldberg, M.S., Krauss, S., Motz, C., Wacker, M., Klose, J., and Shen, J., 2004, Mitochondrial dysfunction and oxidative damage in parkin-deficient mice, *J. Biol. Chem.* **279**:18614–18622.

Perez, F.A., and Palmiter, R.D., 2005, Parkin-deficient mice are not a robust model of parkinsonism, *Proc. Natl. Acad. Sci. USA.* **102**:2174–2179.

Pfeiffer, R.F., 2003, Gastrointestinal dysfunction in Parkinson's disease, *Lancet Neurol.* **2**:107–116.

Polymeropoulos, M.H., Lavedan, C., Leroy, E., Ide, S.E., Dehejia, A., Dutra, A., Pike, B., Root, H., Rubenstein, J., Boyer, R., Stenroos, E.S., Chandrasekharappa, S., Athanassiadou, A., Papapetropoulos, T., Johnson, W.G., Lazzarini, A.M., Duvoisin, R.C., Di Iorio, G., Golbe, L.I., and Nussbaum, R.L., 1997, Mutation in the alpha-synuclein gene identified in families with Parkinson's disease, *Science.* **276**:2045–2047.

Ponsen, M.M., Stoffers, D., Booij, J., van Eck-Smit, B.L., Wolters, E., and Berendse, H.W., 2004, Idiopathic hyposmia as a preclinical sign of Parkinson's disease, *Ann. Neurol.* **56**:173–181.

Rockenstein, E., Mallory, M., Hashimoto, M., Song, D., Shults, C.W., Lang, I., and Masliah, E., 2002, Differential neuropathological alterations in transgenic mice expressing alpha-synuclein from the plateletderived growth factor and Thy-1 promoters, *J. Neurosci. Res.* **68**:568–578.

Selemon, L.D., Rajkowska, G., and Goldman-Rakic, P.S., 2004, Evidence for progression in frontal cortical pathology in late-stage Huntington's disease, *J. Comp. Neurol.* **468**:190–204.

Siddiqui, M.F., Rast, S., Lynn, M.J., Auchus, A.P., and Pfeiffer, R.F., 2002, Autonomic dysfunction in Parkinson's disease: a comprehensive symptom survey, *Parkinsonism Relat. Disord.* **8**:277–284.

Singleton, A.B., Farrer, M., Johnson, J., Singleton, A., Hague, S., Kachergus, J., Hulihan, M., Peuralinna, T., Dutra, A., Nussbaum, R., Lincoln, S., Crawley, A., Hanson, M., Maraganore, D., Adler, C., Cookson, M.R., Muenter, M., Baptista, M., Miller, D., Blancato, J., Hardy, J., and Gwinn-Hardy, K., 2003, alpha- Synuclein locus triplication causes Parkinson's disease, *Science.* **302**:841.

Sipione, S., Rigamonti, D., Valenza, M., Zuccato, C., Conti, L., Pritchard, J., Kooperberg, C., Olson, J.M., and Cattaneo, E., 2002, Early transcriptional profiles in huntingtin-inducible striatal cells by microarray analyses, *Hum. Mol. Genet.* **11**:1953–1965.

Smith, M.A., Brandt, J., and Shadmehr, R., 2000, Motor disorder in Huntington's disease begins as a dysfunction in error feedback control, *Nature.* **403**:544–549.

Song, D.D., Shults, C.W., Sisk, A., Rockenstein, E., and Masliah, E., 2004, Enhanced substantia nigra mitochondrial pathology in human alpha-synuclein transgenic mice after treatment with MPTP, *Exp. Neurol.* **186**:158–172.

Spillantini, M.G., Schmidt, M.L., Lee, V.M., Trojanowski, J.Q., Jakes, R., and Goedert, M., 1997, Alpha-synuclein in Lewy bodies, *Nature.* **388**:839–840.

Spires, T.L., Grote, H.E., Garry, S., Cordery, P.M., Van Dellen, A., Blakemore, C., and Hannan, A.J., 2004, Dendritic spine pathology and deficits in experience-dependent dendritic plasticity in R6/1 Huntington's disease transgenic mice, *Eur. J. Neurosci.* **19**:2799–2807.

Starling, A.J., Chandler, S.H., Cepeda, C., and Levine, M.S., 2003, Alterations in NMDA and magnesium sensitivity occur early in development in the R6/2 mouse model of Huntington's disease, *Society for Neuroscience Abstract Viewer/Itinerary planner*, San Diego, Program No. 206.3.

Szebenyi, G., Morfini, G.A., Babcock, A., Gould, M., Selkoe, K., Stenoien, D.L., Young, M., Faber, P.W., MacDonald, M.E., McPhaul, M.J., and Brady, S.T., 2003, Neuropathogenic forms of huntingtin and androgen receptor inhibit fast axonal transport, *Neuron.* **40**:41–52.

Von Coelln, R., Thomas, B., Savitt, J.M., Lim, K.L., Sasaki, M., Hess, E.J., Dawson, V.L., and Dawson, T.M., 2004, Loss of locus coeruleus neurons and reduced startle in parkin null mice, *Proc. Natl. Acad. Sci. USA.* **101**:10744–10749.

Vonsattel, J.P., Myers, R.H., Stevens, T.J., Ferrante, R.J., Bird, E.D., and Richardson, E.P., Jr., 1985, Neuropathological classification of Huntington's disease, *J. Neuropathol. Exp. Neurol.* **44**:559–577.

Wakabayashi, K., Takahashi, H., Ohama, E., Takeda, S., and Ikuta, F., 1993, Lewy bodies in the visceral autonomic nervous system in Parkinson's disease, *Adv. Neurol.* **60**:609–612.

Wang, L., Fleming, S.M., Mulugeta, M., Fernagut, P.-O., Chesselet, M.-F., and Taché, Y., 2005, Abnormal Colonic Motility in Mice Overexpressing Human Wildtype Alpha-Synuclein: An Animal Model of Parkinson's Disease., *Digestive Disease Week*, Chicago, IL.

Wellington, C.L., Ellerby, L.M., Gutekunst, C.A., Rogers, D., Warby, S., Graham, R.K., Loubser, O., van Raamsdonk, J., Singaraja, R., Yang, Y.Z., Gafni, J., Bredesen, D., Hersch, S.M., Leavitt, B.R., Roy, S., Nicholson, D.W., and Hayden, M.R., 2002, Caspase cleavage of mutant huntingtin precedes neurodegeneration in Huntington's disease, *J. Neurosci.* **22**:7862–7872.

SYNAPTIC ALTERATIONS IN GENETIC MOUSE MODELS OF HUNTINGTON'S AND PARKINSON'S DISEASES: IS THERE A COMMON THREAD?

Carlos Cepeda, Nanping Wu, Véronique M. André,
and Michael S. Levine*

1. INTRODUCTION

In terms of motor symptoms, Huntington's and Parkinson's diseases (HD, PD) are situated at the opposite ends of the spectrum. HD is characterized by hyperkinesia and uncontrollable movements (chorea), whereas PD is characterized by brady- or akinesia, rigidity and resting tremor (Albin et al., 1989). Similarly, the genetic contribution differs in each disease. In HD, a single mutation in exon 1 of the HD gene, manifested as an expansion of CAG (glutamine) repeats, leads to the development of the disease. In contrast, PD is idiopathic and the weight of genetic factors appears much less than in HD, except in some familial forms. Consequently, a single mutation in the HD gene triggers symptomatology, whereas various genes (e.g., α-synuclein, parkin, Nurr1, DJ-1) are involved in familial forms of PD (Huang et al., 2004). Despite these differences, there are commonalities. First, in both diseases there is protein misfolding and aggregation that may be involved in cell death, in the striatum in the case of HD, or in the substantia nigra in PD (Agorogiannis et al., 2004; Gasser, 2001). Second, although the function of the proteins involved in HD and in familial forms of PD is still unknown, there are indications that they may be involved in vesicle transport and synaptic transmission. In fact, in the case of HD, the question has been raised as to whether or not this disease is a synaptopathy (Li et al., 2003). Finally, and probably as a consequence of altered synaptic transmission in the basal ganglia loop, both diseases can manifest similar cognitive and motor deficits. For example, bradykinesia, a hallmark of PD, can also be observed in some stages of HD.

Before the advent of genetic mouse models of neurodegenerative diseases, emphasis had been placed on neuronal death as the primary etiological factor in the emergence of symptoms. In contrast, mouse models have demonstrated that symptoms may develop in

* Mental Retardation Research Center, David Geffen School of Medicine. Universiy of California Los Angeles, Los Angeles, CA, USA.

the absence of pronounced cell death and that cell dysfunction is sufficient to initiate cognitive, motor and physiological abnormalities (Levine et al., 2004). Furthermore, morphological and functional abnormalities may not be solely restricted to the areas of prominent cell degeneration. Other regions projecting to, or receiving inputs from the most affected areas are concomitantly affected. Not surprisingly, protein aggregation can be seen in areas other than the striatum in HD, or the substantia nigra in PD.

In this chapter we will describe recent results from our laboratory emphasizing significant alterations in synaptic transmission in genetic mouse models of HD and PD. In particular, changes along the corticostriatal pathway occur in these models and these changes may lead to alterations at both the pre- and postsynaptic levels. We have examined synaptic transmission in cortex and striatum of several HD and PD models. A common alteration was the reduced ability of striatal neurons to respond to activation of excitatory inputs, particularly in HD models.

2. THE CORTICOSTRIATAL PATHWAY

Striatal medium-sized spiny neurons (MSSNs) receive their main excitatory input from the cortex and, to a lesser degree, from the thalamus (Smith and Bolam, 1990). MSSNs remain hyperpolarized and quiescent unless activated by glutamatergic inputs from the corticostriatal pathway (Hull et al., 1970; Wilson and Kawaguchi, 1996). Stimulation of the substantia nigra can also depolarize MSSNs (Hull et al., 1970; Kitai et al., 1976), either by a slow, direct action of dopamine (DA) or, alternatively, by concurrent release of glutamate from DA neurons (Chuhma et al., 2004). The corticostriatal pathway conveys information from cortical neurons relevant for the control of movements (Graybiel et al., 1994). Striatal MSSNs integrate this information and through their GABAergic outputs, coordinate motor behavior using a direct and an indirect pathway to basal ganglia output nuclei (Gerfen, 2000). Cortical lesions disrupt striatal function and induce compensatory changes (Cromwell et al., 1995). Similarly, substantia nigra lesions affect the flow of information along the corticostriatal pathway.

3. DA MODULATION OF GLUTAMATE NEUROTRANSMISSION

The release of glutamate along the corticostriatal pathway is modulated prominently by DA receptors and this modulation is relevant to understanding striatal function and dysfunction. Early biochemical studies indicated that activation of D2 receptors, located on corticostriatal terminals, reduced the release of glutamate (Maura et al., 1988). Electrophysiological and cellular imaging studies have confirmed this finding (Bamford et al., 2004; Cepeda et al., 2001; Flores-Hernández et al., 1997; Hsu et al., 1995). DA also modulates glutamate responses postsynaptically. The topography and dynamics of cortical and nigral inputs allow this type of interaction in the striatum. Although the existence of DA modulation of glutamate responses in the dorsal striatum has been challenged (Nicola et al., 2000), there is now ample evidence that this modulation occurs, not only in dorsal striatum but also in the cerebral cortex and other structures (for reviews see Cepeda and Levine, 1998; Seamans and Yang, 2004, who provide a number of reasons why some investigators did not find modulation of glutamate responses). According to our model of DA function in the striatum, the outcome of DA modulation of glutamate

responses depends on a number of factors and principally on the subtype of glutamate and DA receptors involved. Thus DA, via D1 receptors, enhances glutamate responses, particularly those mediated by activation of NMDA receptors and, via D2 receptors, reduces glutamate responses, particularly those mediated by AMPA receptors (Cepeda et al., 1993). Because in the striatum there is considerable segregation of DA receptors in MSSNs comprising the direct and indirect pathways, a natural extension of our model is that DA will preferentially enhance glutamate responses in MSSNs belonging to the direct pathway (cells expressing predominantly D1 receptors) and conversely, it will decrease glutamate responses in cells belonging to the indirect pathway (cells expressing predominantly D2 receptors). Preliminary evidence from electrophysiological studies in dissociated MSSNs expressing green fluorescent protein as a reporter for cells containing D1 or D2 receptors supports the concept that D1 agonists preferentially, though not exclusively, enhance NMDA responses in cells expressing D1 receptors, whereas D2 agonists produce greater reduction of NMDA responses in cells expressing D2 receptors (Cepeda et al., 2004).

Thus, alterations in DA function will affect the release of glutamate and the responses along the corticostriatal pathway. Obviously, because of the loss of DA neurons in PD, important changes in neurotransmission along this pathway can be expected. Less obvious though is the fact that in HD, the nigrostriatal pathway is also significantly compromised (Ariano et al., 2002; Petersen et al., 2002). Thus, in PD and HD, alterations in DA inputs, receptor numbers and sensitivity can alter corticostriatal transmission.

4. GENETIC MOUSE MODELS OF HD

The use of genetic mouse models for understanding the progression of HD and PD is becoming widespread. In spite of the fact that these models do not replicate the massive cell loss of striatal and DA neurons occurring in humans with these diseases, mouse models have shed considerable light on the pathophysiological mechanisms of these neurodegenerative disorders (Levine et al., 2004). Mouse models of HD include transgenics, in which a portion of the mutated gene is expressed under the control of various promoters and knock-ins in which an expanded CAG repeat is introduced into the endogenous mouse HD gene. In addition, Yeast Artificial Chromosomes (YAC) have been used to express full length or portions of the mutated genes. Several reviews have been published that examine the phenotypes of these mouse models in more detail (Hickey and Chesselet, 2003; Levine et al., 2004).

All mouse models of HD, including many knock-in mice, display early and progressive motor anomalies that can be used as phenotypic markers. Disease progression is particularly fast in the most frequently studied model, the R6/2 transgenic mouse, which carries exon 1 of the HD gene with ~155 CAG repeats (Mangiarini et al., 1996). These mice display subtle abnormal behavior at 5 weeks of age or earlier, overt symptoms by 8 weeks, and usually die between 12 and 15 weeks. Behavioral alterations include motor (Carter et al., 1999) and learning deficits (Lione et al., 1999; Murphy et al., 2000). In contrast, the R6/1 line has a much slower progression. YAC mice with 72 and 128 repeats both show a biphasic motor phenotype with hyperactivity followed by hypoactivity (Hodgson et al., 1999; Slow et al., 2003). A biphasic progression of behavioral anomalies also characterizes knock-in mice in which human exon 1 has been inserted into the mouse HD gene (Menalled et al., 2003).

Although the function of huntingtin is still unknown, evidence indicates it is a multidomain protein which is involved in transcriptional regulation, the endosome-lysosome pathway and intracellular transport (Landles and Bates, 2004). Normal huntingtin associates with vesicle membranes and interacts with proteins involved in vesicle transport (Velier et al., 1998), whereas mutant huntingtin impairs axonal trafficking (Trushina et al., 2004). Thus, in HD, alterations in synaptic transmission can be expected.

4.1. Synaptic Function in Mouse Models of HD

Electrophysiological studies provide critical information on neuronal dysfunction and circuit changes that may underlie HD symptoms. Intrinsic membrane properties of MSSNs are affected in some of the models. Beginning at 5 weeks of age an increase in input resistance occurs in the R6/2, which probably reflects progressive loss of conductive membrane channels (Cepeda et al., 2001a; Klapstein et al., 2001). Consistent with this observation, cell capacitance is reduced and there is decreased inward rectification (Ariano et al., 2004). Consequently, many MSSNs have depolarized resting membrane potentials (Klapstein et al., 2001).

The connections between the cortex and the striatum are also affected. Early degeneration of the corticostriatal pathway may occur in conjunction with the accumulation of mutant huntingtin in axonal swellings in striatal neuropil and in the cytoplasm of cortical neurons (Sapp et al., 1999). Defective neurotransmission in HD is supported by observations suggesting early impairment of proteins involved in the control of neurotransmitter release, such as a decrease in complexin II, a presynaptic protein (Morton and Edwardson, 2001). Furthermore, the association of mutant huntingtin with synaptic vesicles has been hypothesized to impair glutamate release (Li et al., 2003). Our own work confirms a reduction in pre- and postsynaptic markers, synaptophysin and PSD-95, in the R6/2 model (Cepeda et al., 2003).

An early indication of electrophysiological changes along the corticostriatal pathway in R6/2 mice is the transient expression of large spontaneous synaptic inward currents at ~5 weeks that coincides with the onset of behavioral symptoms (Cepeda et al., 2003). These events may reflect dysregulation of glutamate release and/or increase in cortical synchronization. In conjunction, a progressive reduction in the frequency of low amplitude spontaneous excitatory postsynaptic currents occurs which probably causes the increase in the stimulus intensity necessary to evoke an excitatory postsynaptic potential in MSSNs (Klapstein et al., 2001; Laforet et al., 2001). This suggests the cortex may become disconnected from some of its striatal targets, thus depriving striatal cells of trophic factors such as BDNF (Zucatto et al., 2001).

Compensatory changes in synaptic transmission also occur in the striatum. Reduced glutamatergic transmission is accompanied by increases in GABA neurotransmission in R6 mice and this increase can be partially reversed by acute application of BDNF (Cepeda et al., 2004a). Reduced glutamatergic and increased GABAergic neurotransmission will severely limit striatal outputs to target cells in the basal ganglia producing a functional ablation. This could explain why in R6 mice cell death is not required to produce HD-like symptomatology.

Alterations of intrinsic cortical circuits can also be observed in R6 mice, leading to cortical hyperexcitability. Although spontaneous synaptic activity does not seem to be altered, application of $GABA_A$ receptor antagonists produces greater synchronous activity

in mutant mice (Uzgil et al., 2004). Increased cortical excitability enhances seizure susceptibility and can help explain the occurrence of spontaneous epileptic seizures in some HD mouse models.

Altered receptor sensitivity or release of glutamate has been hypothesized to underlie degenerative alterations in HD. Because spontaneous excitatory synaptic activity in the corticostriatal pathway decreases progressively, enhanced glutamatergic activity can not explain cell atrophy. Increased sensitivity of glutamate postsynaptic receptors is another possibility. Due to the critical role played by striatal N-methyl-D-aspartate (NMDA) receptors in excitotoxicity this receptor subtype has been examined in many of the models. There is accumulating evidence that subsets of MSSNs are more sensitive to application of NMDA in virtually all models (Levine et al., 1999). Subpopulations of MSSNs from transgenic animals display larger NMDA currents and Ca^{2+} influx (Cepeda et al., 2001a; Laforet et al., 2001), as well as reduced Mg^{2+} sensitivity (Cepeda et al., 2001a). Evidence from dissociated MSSNs indicates that reduced Mg^{2+} sensitivity occurs very early, before overt symptoms, in the R6/2 model (Starling et al., 2003). Increased NMDA receptor sensitivity also occurs very early in YAC models and there is a critical role of NMDA receptors containing NR2B subunits (Zeron et al., 2002; Li et al., 2004).

There is a growing body of evidence that alterations in the corticostriatal pathway in mouse models of HD may lead to changes in receptor sensitivity at the postsynaptic level (Cepeda et al., 2003). Also, it has been suggested that the more vulnerable striatal cells are those that receive more cortical innervation (Fusco et al., 1999). Alterations in synaptic transmission along the corticostriatal pathway may initiate a cascade of events that eventually leads to neuronal dysfunction and cell death. Because the number of synaptic contacts may be reduced in HD, extrasynaptic glutamate receptors and their interacting proteins may play an increasingly important role. For example, stimulation of extrasynaptic NMDA receptors causes loss of mitochondrial membrane potential and cell death (Hardingham et al., 2002). Thus, activation of these receptors may facilitate cell dysfunction in HD.

5. GENETIC MOUSE MODELS OF PD

Mouse models of PD permit identification of early pathogenic processes in neurodegeneration. A variety of transgenic and knock-out mice have begun to provide this information, but because these mice have only recently been developed there is less research available. A rare mutation in α-synuclein was the first genetic anomaly found to cause familial PD (Polymeropoulos et al., 1997), leading to the identification of α-synuclein, a vesicular protein, as a major component of Lewy bodies, even in sporadic PD (Spillantini et al., 1997). Mice overexpressing the normal or mutated forms of α-synuclein model aspects of PD but display a highly variable phenotype (Hashimoto et al., 2003). A major determinant of severity seems to be the promoter used for the transgene. In view of the indisputable role of α-synuclein in both familial and sporadic PD, as ascertained by its accumulation in Lewy bodies, these mice provide a compelling model to identify their role. The second type of mutation shown to cause familial PD occurs in the gene encoding parkin, an E3 ligase (Shimura et al., 2000). Many different mutations have now been described in parkin and they account for a large proportion of early onset PD, although they are also found, more rarely, in cases with late onset.

Parkin mutations are loss-of-function mutations, therefore models have focused on parkin knock-outs. In general, these mice show subtle anomalies (Goldberg et al., 2003; Itier et al., 2003). Parkin knock-outs with a defective exon 3 show progressive motor anomalies as well as deficits in sensorimotor integration, starting as early as 2–4 months of age, but paradoxically have increased basal release of striatal dopamine (Goldberg et al., 2003). Similar alterations were observed in another line of mice with an exon 3 mutation (Itier et al., 2003). Deletion of exon 7 produced loss of locus coeruleus neurons and reduced startle response (Von Coelln et al., 2004), whereas deletion of exon 2 produced no evidence of neurological or cognitive dysfunction and striatal DA was normal (Perez and Palmiter, 2005).

Both α-synuclein and parkin play a role in synaptic transmission (Clayton and George, 1998). Available evidence, e.g., vesicle binding and similar pattern of expression as synaptophysin (Jensen et al., 1998; Murphy et al., 2000), indicates that α-synuclein participates in vesicular function at the synaptic terminal. Parkin also associates with synaptic vesicles (Kubo et al., 2001). In particular, parkin increases DA uptake by enhancing cell surface expression of the DA transporter and through this action it refines the precision of DA transmission (Jiang et al., 2004). In contrast, mutated forms of parkin lose this function possibly leading to increases in extracellular DA in the limbic system and the striatum (Goldberg et al., 2003; Itier et al., 2003).

5.1. Synaptic Function in Models of PD

Compared with HD models, much less is known about changes in synaptic transmission in genetic models of PD. There are however several studies on changes in corticostriatal transmission after neurotoxic or electrolytic lesions of the substantia nigra in rats. The findings indicate that loss of DA leads to increases in spontaneous glutamatergic synaptic activity (Galarraga et al., 1987; Cepeda et al., 1989; Calabresi et al., 2000). Interestingly, an increase in striatal electrotonic communication also occurs, suggesting that one function of DA in the striatum is the uncoupling of gap junctions (Cepeda et al., 1989).

In α-synuclein deficient mice, alterations in DA release and reduction in striatal DA occur, and it has been suggested that this protein exerts a negative regulation of DA neurotransmission (Abeliovich et al., 2000). Furthermore, mice lacking α-synuclein displayed selective deficiency of undocked vesicles and impaired hippocampal synaptic responses to prolonged trains of repetitive stimulation (Cabin et al., 2002).

In parkin knock-out mice there is evidence for a decrease in glutamate release in the CA1 region of the hippocampus (Itier et al., 2003). In the striatum, a deficit in excitatory transmission also occurs (Goldberg et al., 2003). This result is exactly opposite to the effect of DA-depleting manipulations and could be explained by the increased basal release of DA observed in parkin knock-out mice. Interestingly, a recently generated DJ-1 knock-out shows hypoactivity and reduced evoked DA overflow, probably as a result of increased reuptake (Goldberg et al., 2005). Furthermore, although corticostriatal synaptic responses appear normal, long-term depression is absent in DJ-1 knock-outs, suggesting impairment in D2 receptors (Goldberg et al., 2005). None of these models, however, reproduces the loss of DA neurons, therefore the possible significance and applicability of these findings to the human disease remain unclear. Electrophysiological studies in new genetic models, such as the Pitx3-deficient mouse that exhibits major loss of DA neurons, DA deficiency and receptor supersensitivity (Hwang et al., 2005), will shed additional light on synaptic dysfunction in PD.

6. CONCLUSION

The principal function of neurons is to communicate messages via the release of neurotransmitters, neuromodulators and trophic factors. Impaired synaptic transmission leads to cognitive and motor abnormalities. Huntingtin, α-synuclein and parkin play an important role in vesicle transport and synaptic transmission, so that mutations in these proteins impair neuronal communication and lead to a characteristic phenotype. Understanding the function of these proteins in physiological and pathological conditions will further our knowledge of the processes leading to neurodegenerative disorders and the possibility of finding new rational therapies.

7. ACKNOWLEDGEMENTS

This work has been possible thanks to the support of the Hereditary Disease Foundation, the Cure HD initiative, the HiQ Foundation and NIH grants NS 33538, NS 41574, ES 12078 (Center for Gene-Environment Studies in PD) and NS 38367 (Udall Center of Excellence for PD Research).

8. REFERENCES

Abeliovich, A., Schmitz, Y., Farinas, I., Choi-Lundberg, D., Ho, W.H., Castillo, P.E., Shinsky, N., Verdugo, J.M., Armanini, M., Ryan, A., Hynes, M., Phillips, H., Sulzer, D., and Rosenthal, A., 2000, Mice lacking alpha-synuclein display functional deficits in the nigrostriatal dopamine system. *Neuron.* **25**:239–252.

Agorogiannis, E.I., Agorogiannis, G.I., Papadimitriou, A., and Hadjigeorgiou, G.M., 2004, Protein misfolding in neurodegenerative diseases. *Neuropathol. Appl. Neurobiol.* **30**:215–224.

Albin, R.L., Young, A.B., and Penney, J.B., 1989, The functional anatomy of basal ganglia disorders. *Trends Neurosci.* **12**:366–375.

Ariano, M.A., Aronin, N., DiFiglia, M., Tagle, D.A., Sibley, D.R., Leavitt, B.R., Hayden, M.R., and Levine, M.S., 2002, Striatal neurochemical changes in transgenic models of Huntington's disease. *J. Neurosci. Res.* **68**:716–729.

Ariano, M.A., Cepeda, C., Calvert, C.R., Flores-Hernandez, J., Hernandez-Echeagaray, E., Klapstein, G.J., Chandler, S.H., Aronin, N., DiFiglia, M., and Levine, M.S., 2004, Striatal potassium channel dysfunction in Huntington's disease transgenic mice. *J. Neurophysiol.* Dec 29; [Epub ahead of print].

Bamford, N.S., Zhang, H., Schmitz, Y., Wu, N.P., Cepeda, C., Levine, M.S., Schmauss, C., Zakharenko, S.S., Zablow, L., and Sulzer, D., 2004, Heterosynaptic dopamine neurotransmission selects sets of corticostriatal terminals. *Neuron* **42**:653–663.

Cabin, D.E., Shimazu, K., Murphy, D., Cole, N.B., Gottschalk, W., McIlwain, K.L., Orrison, B., Chen, A., Ellis, C.E., Paylor, R., Lu, B., and Nussbaum, R.L., 2002, Synaptic vesicle depletion correlates with attenuated synaptic responses to prolonged repetitive stimulation in mice lacking alpha-synuclein. *J. Neurosci.* **22**:8797–8807.

Calabresi, P., Centonze, D., and Bernardi, G., 2000, Electrophysiology of dopamine in normal and denervated striatal neurons. *Trends Neurosci.* **23**(10 Suppl.):S57–63.

Carter, R.J., Lione, L.A., Humby, T., Mangiarini, L., Mahal, A., Bates, G.P., Dunnett, S.B., and Morton, A.J., 1999, Characterization of progressive motor deficits in mice transgenic for the human Huntington's disease mutation. *J. Neurosci.* **19**:3248–3257.

Cepeda, C., Walsh, J.P., Hull, C.D., Howard, S.G., Buchwald, N.A., and Levine, M.S., 1989, Dye-coupling in the neostriatum of the rat: I. Modulation by dopamine-depleting lesions. *Synapse* **4**:229–237.

Cepeda, C., Buchwald, N.A., and Levine, M.S., 1993, Neuromodulatory actions of dopamine in the neostriatum are dependent upon the excitatory amino acid receptor subtypes activated. *Proc. Natl. Acad. Sci. USA* **90**:9576–9580.

Cepeda, C., and Levine, M.S., 1998, Dopamine and N-methyl-D-aspartate receptor interactions in the neostriatum. *Dev. Neurosci.* **20**:1–18.

Cepeda, C., Hurst, R.S., Altemus, K.L., Flores-Hernandez, J., Calvert, C.R., Jokel, E.S., Grandy, D.K., Low, M.J., Rubinstein, M., Ariano, M.A., and Levine, M.S., 2001, Facilitated glutamatergic transmission in the striatum of D2 dopamine receptor-deficient mice. *J. Neurophysiol.* **85**:659–670.

Cepeda, C., Ariano, M.A., Calvert, C.R., Flores-Hernandez, J., Chandler, S.H., Leavitt, B.R., Hayden, M.R., and Levine, M.S., 2001a, NMDA receptor function in mouse models of Huntington disease. *J. Neurosci. Res.* **66**:525–539.

Cepeda, C., Hurst, R.S., Calvert, C.R., Hernandez-Echeagaray, E., Nguyen, O.K., Jocoy, E., Christian, L.J. Ariano MA, and Levine MS., 2003, Transient and progressive electrophysiological alterations in the corticostriatal pathway in a mouse model of Huntington's disease. *J. Neurosci.* **23**:961–969.

Cepeda, C., Starling, A.J., Wu, N., Soda, T., Lobo, M.K., Yang, X.W., and Levine, M.S., 2004, Defining electrophysiological properties of subpopulations of striatal neurons using genetic expression of enhanced green fluroscent protein. *Soc. Neurosci. Abst.* **30**:307.4.

Cepeda, C., Starling, A.J., Wu, N., Nguyen, O.K., Uzgil, B., Soda, T., André, V.M., Ariano, M.A., and Levine, M.S., 2004a, Increased GABAergic function in mouse models of Huntington's disease: reversal by BDNF. *J. Neurosci. Res.* **78**:855–867.

Chuhma, N., Zhang, H., Masson, J., Zhuang, X., Sulzer, D., Hen, R., and Rayport, S., 2004, Dopamine neurons mediate a fast excitatory signal via their glutamatergic synapses. *J. Neurosci.* **24**:972–981.

Clayton, D.F., and George, J.M., 1998, The synucleins: a family of proteins involved in synaptic function, plasticity, neurodegeneration and disease. *Trends Neurosci.* **21**:249–254.

Cromwell, H.C., Buchwald, N.A., and Levine, M.S., 1995, Decortication decreases paired-pulse facilitation in the neostriatal slice of the rat. *Neurosci. Lett.* **192**:213–217.

Flores-Hernandez, J., Galarraga, E., and Bargas, J., 1997, Dopamine selects glutamatergic inputs to neostriatal neurons. *Synapse* **25**:185–195.

Fusco, F.R., Chen, Q., Lamoreaux, W.J., Figueredo-Cardenas, G., Jiao, Y., Coffman, J.A., Surmeier, D.J., Honig, M.G., Carlock, L.R., and Reiner, A., 1999, Cellular localization of huntingtin in striatal and cortical neurons in rats: lack of correlation with neuronal vulnerability in Huntington's disease. *J. Neurosci.* **19**:1189–1202.

Galarraga, E., Bargas, J., Martinez-Fong, D., and Aceves, J., 1987, Spontaneous synaptic potentials in dopamine-denervated neostriatal neurons. *Neurosci. Lett.* **81**:351–355.

Gasser, T., 2001, Genetics of Parkinson's disease. *J. Neurol.* **248**:833–840.

Gerfen, C.R., 2000, Molecular effects of dopamine on striatal-projection pathways. *Trends Neurosci.* **23**:S64–70.

Goldberg, M.S., Fleming, S.M., Palacino, J.J., Cepeda, C., Lam, H.A., Bhatnagar, A., Meloni, E.G., Wu, N., Ackerson, L.C., Klapstein, G.J., Gajendiran, M., Roth, B.L., Chesselet, M.F., Maidment, N.T., Levine, M.S., and Shen, J., 2003, Parkin-deficient mice exhibit nigrostriatal deficits but not loss of dopaminergic neurons. *J. Biol. Chem.* **278**:43628–43235.

Goldberg, M.S., Pisani, A., Haburcak, M., Vortherms, T.A., Kitada, T., Costa, C., Tong, Y., Martella, G., Tscherter, A., Martins, A., Bernardi, G., Roth, B.L., Pothos, E.N., Calabresi, P., and Shen, J., 2005, Nigrostriatal dopaminergic deficits and hypokinesia caused by inactivation of the familial Parkinsonismlinked gene DJ-1. *Neuron* **45**:489–496.

Graybiel, A.M., Aosaki, T., Flaherty, A.W., and Kimura, M., 1994, The basal ganglia and adaptive motor control. *Science* **265**:1826–1831.

Hardingham, G.E., Fukunaga, Y., and Bading, H., 2002, Extrasynaptic NMDARs oppose synaptic NMDARs by triggering CREB shut-off and cell death pathways. *Nat. Neurosci.* **5**:405–414.

Hashimoto, M., Rockenstein, E., and Masliah, E., 2003, Transgenic models of alpha-synuclein pathology: past, present, and future. *Ann. N Y Acad. Sci.* **991**:171–188.

Hickey, M.A., and Chesselet, M.F., 2003, The use of transgenic and knock-in mice to study Huntington's disease. *Cytogenet. Genome. Res.* **100**:276–286.

Hodgson, J.G., Agopyan, N., Gutekunst, C.A., Leavitt, B.R., LePiane, F., Singaraja, R., Smith, D.J., Bissada, N., McCutcheon, K., Nasir, J., Jamot, L., Li, X.J., Stevens, M.E., Rosemond, E., Roder, J.C., Phillips, A.G., Rubin, E.M., Hersch, S.M., and Hayden, M.R., 1999, A YAC mouse model for Huntington's disease with full-length mutant huntingtin, cytoplasmic toxicity, and selective striatal neurodegeneration. *Neuron* **23**:181–192.

Hsu, K.S., Huang, C.C., Yang, C.H., and Gean, P.W., 1995, Presynaptic D2 dopaminergic receptors mediate inhibition of excitatory synaptic transmission in rat neostriatum. *Brain Res.* **690**:264–268.

Huang, Y., Cheung, L., Rowe, D., and Halliday, G., 2004, Genetic contributions to Parkinson's disease. *Brain Res. Brain Res. Rev.* **46**:44–70.

Hull, C.D., Bernardi, G., and Buchwald, N.A., 1970, Intracellular responses of caudate neurons to brain stem stimulation. *Brain Res.* **22**:163–179.

Hwang, D.Y., Fleming, S.M., Ardayfio, P., Moran-Gates, T., Kim, H., Tarazi, F.I., Chesselet, M.F., and Kim, K.S., 2005, 3,4-Dihydrophenylalanine reverses the motor deficits in Pitx3-deficient Aphakia mice: behavioral characterization of a novel genetic model of Parkinson's disease. *J. Neurosci.* **25**:2132–2137.

Itier, J.M., Ibanez, P., Mena, M.A., Abbas, N., Cohen-Salmon, C., Bohme, G.A., Laville, M., Pratt, J., Corti, O., Pradier, L., Ret, G., Joubert, C., Periquet, M., Araujo, F., Negroni, J., Casarejos, M.J., Canals, S., Solano, R., Serrano, A., Gallego, E., Sanchez, M., Denefle, P., Benavides, J., Tremp, G., Rooney, T.A., Brice, A., and Garcia de Yebenes, J., 2003, Parkin gene inactivation alters behaviour and dopamine neurotransmission in the mouse. *Hum. Mol. Genet.* **12**:2277–2291.

Jensen, P.H., Nielsen, M.S., Jakes, R., Dotti, C.G., and Goedert, M., 1998, Binding of alpha-synuclein to brain vesicles is abolished by familial Parkinson's disease mutation. *J. Biol. Chem.* **273**:26292–26294.

Jiang, H., Jiang, Q., and Feng, J., 2004, Parkin increases dopamine uptake by enhancing the cell surface expression of dopamine transporter. *J. Biol. Chem.* **279**:54380–54386.

Kitai, S.T., Sugimori, M., and Kocsis, J.D., 1976, Excitatory nature of dopamine in the nigro-caudate pathway. *Exp. Brain Res.* **24**:351–363.

Klapstein, G.J., Fisher, R.S., Zanjani, H., Cepeda, C., Jokel, E.S., Chesselet, M.F., and Levine MS., 2001, Electrophysiological and morphological changes in striatal spiny neurons in R6/2 Huntington's disease transgenic mice. *J. Neurophysiol.* **86**:2667–2677.

Kubo, S.I., Kitami, T., Noda, S., Shimura, H., Uchiyama, Y., Asakawa, S., Minoshima, S., Shimizu, N., Mizuno, Y., and Hattori, N., 2001, Parkin is associated with cellular vesicles. *J. Neurochem.* **78**:42–54.

Laforet, G.A., Sapp, E., Chase, K., McIntyre, C., Boyce, F.M., Campbell, M., Cadigan, B.A., Warzecki, L., Tagle, D.A., Reddy, P.H., Cepeda, C., Calvert, C.R., Jokel, E.S., Klapstein, G.J., Ariano, M.A., Levine, M.S., DiFiglia, M., and Aronin, N., 2001, Changes in cortical and striatal neurons predict behavioral and electrophysiological abnormalities in a transgenic murine model of Huntington's disease. *J. Neurosci.* **21**:9112–9123.

Landles, C., and Bates, G.P., 2004, Huntingtin and the molecular pathogenesis of Huntington's disease. *EMBO Reports* **5**:958–963.

Levine, M.S., Klapstein, G.J., Koppel, A., Gruen, E., Cepeda, C., Vargas, M.E., Jokel, E.S., Carpenter, E.M., Zanjani, H., Hurst, R.S., Efstratiadis, A., Zeitlin, S., and Chesselet, M.F., 1999, Enhanced sensitivity to N-methyl-D-aspartate receptor activation in transgenic and knockin mouse models of Huntington's disease. *J. Neurosci. Res*. **58**:515–532.

Levine, M.S., Cepeda, C., Hickey, M.A., Fleming, S.M., and Chesselet, M.F., 2004, Genetic mouse models of Huntington's and Parkinson's diseases: illuminating but imperfect. *Trends Neurosci.* **27**:691–697.

Li, H., Wyman, T., Yu, Z.X., Li, S.H., and Li, X.J., 2003, Abnormal association of mutant huntingtin with synaptic vesicles inhibits glutamate release. *Hum. Mol. Genet.* **12**:2021–2030.

Li, J.Y., Plomann, M., and Brundin P., 2003, Huntington's disease: a synaptopathy? *Trends Mol. Med.* **9**:414–420.

Li, L., Murphy, T.H., Hayden, M.R., and Raymond, L.A., 2004, Enhanced striatal NR2B-containing N-methyl-D-aspartate receptor-mediated synaptic currents in a mouse model of Huntington disease. *J. Neurophysiol.* **92**:2738–2746.

Lione, L.A., Carter, R.J., Hunt, M.J., Bates, G.P., Morton, A.J., and Dunnett, S.B., 1999, Selective discrimination learning impairments in mice expressing the human Huntington's disease mutation. *J. Neurosci.* **19**:10428–10437.

Mangiarini, L., Sathasivam, K., Seller, M., Cozens, B., Harper, A., Hetherington, C., Lawton, M., Trottier, Y., Lehrach, H., Davies, S.W., and Bates, G.P., 1996, Exon 1 of the HD gene with an expanded CAG repeat is sufficient to cause a progressive neurological phenotype in transgenic mice. *Cell* **87**:493–506.

Maura, G., Giardi, A., and Raiteri, M., 1988, Release-regulating D-2 dopamine receptors are located on striatal glutamatergic nerve terminals. *J. Pharmacol. Exp. Ther.* **247**:680–684.

Menalled, L.B., Sison, J.D., Dragatsis, I., Zeitlin, S., and Chesselet, M.F., 2003, Time course of early motor and neuropathological anomalies in a knock-in mouse model of Huntington's disease with 140 CAG repeats. *J. Comp. Neurol.* **465**:11–26.

Morton, A.J., and Edwardson, J.M., 2001, Progressive depletion of complexin II in a transgenic mouse model of Huntington's disease. *J. Neurochem.* **76**:166–172.

Murphy, D.D., Rueter, S.M., Trojanowski, J.Q., and Lee, V.M., 2000, Synucleins are developmentally expressed, and α-synuclein regulates the size of the presynaptic vesicular pool in primary hippocampal neurons. *J. Neurosci.* **20**:3214–3220.

Murphy, K.P., Carter, R.J., Lione, L.A., Mangiarini, L., Mahal, A., Bates, G.P., Dunnett, S.B., and Morton, A.J., 2000, Abnormal synaptic plasticity and impaired spatial cognition in mice transgenic for exon 1 of the human Huntington's disease mutation. *J. Neurosci.* **20**:5115–5123.

Nicola, S.M., Surmeier, J., and Malenka, R.C., 2000, Dopaminergic modulation of neuronal excitability in the striatum and nucleus accumbens. *Annu. Rev. Neurosci.* **23**:185–215.

Perez, F.A., and Palmiter, R.D., 2005, Parkin-deficient mice are not a robust model of parkinsonism. *Proc. Natl. Acad. Sci. USA* **102**:2174–2179.

Petersen, A., Puschban, Z., Lotharius, J., NicNiocaill, B., Wiekop, P., O'Connor, W.T., and Brundin, P., 2002, Evidence for dysfunction of the nigrostriatal pathway in the R6/1 line of transgenic Huntington's disease mice. *Neurobiol. Dis.* **11**:134–146.

Polymeropoulos, M.H., Lavedan, C., Leroy, E., Ide, S.E., Dehejia, A., Dutra, A., Pike, B., Root, H., Rubenstein, J., Boyer, R., Stenroos, E.S., Chandrasekharappa, S., Athanassiadou, A., Papapetropoulos, T., Johnson, W.G., Lazzarini, A.M., Duvoisin, R.C., Di Iorio, G., Golbe, L.I., and Nussbaum, R.L., 1997, Mutation in the alpha-synuclein gene identified in families with Parkinson's disease. *Science* **276**:2045–2047.

Sapp, E., Penney, J., Young, A., Aronin, N., Vonsattel, J.P., and DiFiglia, M., 1999, Axonal transport of N-terminal huntingtin suggests early pathology of corticostriatal projections in Huntington disease. *J. Neuropathol. Exp. Neurol.* **58**:165–173.

Seamans, J.K., and Yang, C.R., 2004, The principal features and mechanisms of dopamine modulation in the prefrontal cortex. *Prog. Neurobiol.* **74**:1–58.

Shimura, H., Hattori, N., Kubo, S., Mizuno, Y., Asakawa, S., Minoshima, S., Shimizu, N., Iwai, K., Chiba, T., Tanaka, K., and Suzuki, T., 2000, Familial Parkinson disease gene product, parkin, is a ubiquitin-protein ligase. *Nat. Genet*. **25**:302–305.

Slow, E.J., van Raamsdonk, J., Rogers, D., Coleman, S.H., Graham, R.K., Deng, Y., Oh, R., Bissada, N., Hossain, S.M., Yang, Y.Z., Li, X.J., Simpson, E.M., Gutekunst, C.A., Leavitt, B.R., and Hayden, M.R., 2003, Selective striatal neuronal loss in a YAC128 mouse model of Huntington disease. *Hum. Mol. Genet*. **12**:1555–1567.

Smith, A.D., and Bolam, J.P., 1990, The neural network of the basal ganglia as revealed by the study of synaptic connections of identified neurones. *Trends Neurosci.* **13**:259–265.

Spillantini, M.G., Schmidt, M.L., Lee, V.M., Trojanowski, J.Q., Jakes, R., and Goedert, M., 1997, Alpha-synuclein in Lewy bodies. *Nature* **388**:839–840.

Starling, A.J., Chandler, S.H., Cepeda, C., and Levine, M.S., 2003, Alterations in NMDA magnesium sensitivity occurs early in development in the R6/2 mouse model of Huntington's disease. *Soc. Neurosci. Abst.* **29**:206.3.

Trushina, E., Dyer, R.B., Badger, J.D.2nd., Ure, D., Eide, L., Tran, D.D., Vrieze, B.T., Legendre-Guillemin, V., McPherson, P.S., Mandavilli, B.S., Van Houten, B., Zeitlin, S., McNiven, M., Aebersold, R., Hayden, M., Parisi, J.E., Seeberg, E., Dragatsis, I., Doyle, K., Bender, A., Chacko, C., and McMurray, C.T., 2004, Mutant huntingtin impairs axonal trafficking in mammalian neurons in vivo and in vitro. *Mol. Cell Biol.* **24**:8195–8209.

Uzgil, B., Cepeda, C., Wu, N., Buchwald, N.A., and Levine, M.S., 2004, Increased cortical excitability in the R6/2 model of Huntington's disease. *Soc. Neurosci. Abst.* **30**:564.2.

Velier, J., Kim, M., Schwarz, C., Kim, T.W., Sapp, E., Chase, K., Aronin, N., and DiFiglia, M., 1998, Wildtype and mutant huntingtins function in vesicle trafficking in the secretory and endocytic pathways. *Exp. Neurol.* **152**:34–40.

Von Coelln, R., Thomas, B., Savitt, J.M., Lim, K.L., Sasaki, M., Hess, E.J., Dawson, V.L., and Dawson, T.M., 2004, Loss of locus coeruleus neurons and reduced startle in parkin null mice. *Proc. Natl. Acad. Sci. USA* **101**:10744–10749.

Wilson, C.J., and Kawaguchi, Y., 1996, The origins of two-state spontaneous membrane potential fluctuations of neostriatal spiny neurons. *J. Neurosci.* **16**:2397–2410.

Zeron, M.M., Hansson, O., Chen, N., Wellington, C.L., Leavitt, B.R., Brundin, P., Hayden, M.R., and Raymond, L.A., 2002, Increased sensitivity to N-methyl-D-aspartate receptor-mediated excitotoxicity in a mouse model of Huntington's disease. *Neuron* **33**:849–860.

Zuccato, C., Ciammola, A., Rigamonti, D., Leavitt, B.R., Goffredo, D., Conti, L., MacDonald, M.E., Friedlander, R.M., Silani, V., Hayden, M.R., Timmusk, T., Sipione, S., and Cattaneo, E., 2001, Loss of huntingtin-mediated BDNF gene transcription in Huntington's disease. *Science* **293**:493–498.

CHANGES IN THE EXPRESSION OF TONIC AND PHASIC NEUROCHEMICAL MARKERS OF ACTIVITY IN A RAT MODEL OF L-DOPA INDUCED DYSKINESIA

Anna R. Carta, Annalisa Pinna, Elisabetta Tronci, and Micaela Morelli*

1. INTRODUCTION

In experimental models of Parkinson's disease, chronic intermittent L-DOPA treatment triggers a complex cascade of functional alterations in the basal ganglia circuit, which have been related to motor side effects associated with prolonged L-DOPA therapy, as dyskinetic movements. Such alterations include changes of gene expression and have been reported in neurons of both the direct and indirect pathway. Thus, chronic L-DOPA induces increased dynorphin, enkephalin and GAD67 mRNA levels in the striatum and globus pallidus (Carta et al., 2002; Cenci et al., 1998; Henry et al., 2003; Nielsen and Soghomonian, 2004; Soghomonian et al., 1996), suggesting that an altered neuronal activity of striatonigral as well as striatopallidal and pallidal neurons is associated with this treatment (Figs 1, 2).

This altered pattern of gene expression is accompanied by an abnormal neuronal activity downstream the striatum, in nuclei of the indirect pathway. Changes in frequency and pattern of firing of individual neurons, have been reported in the globus pallidus and subthalamic nucleus of dyskinetic animals (Benabid et al., 2000; Boraud et al., 1998; Carta et al., 2003; Filion et al., 1991; Hutchison et al., 1997; Levy et al., 2001; Lozano et al., 2000; Nielsen and Soghomonian, 2004; Soghomonian et al., 1996).

All together these changes would result in a pathophysiological imbalance in the modulation operated by direct and indirect pathways on basal ganglia output nuclei, resulting in an excessive reduction in neuronal activity and firing frequency of the Gpi/substantia nigra reticulata (Carta et al., 2003; Boroud et al., 2001; Papa et al., 1999; Herrero et al., 1996). Accordingly, we reported decreased levels of GAD67 mRNA in the substantia nigra reticulata of rats subchronically treated with L-DOPA (Fig. 2).

An aspect of changes in gene expression investigated so far in the striatum of dyskinetic animals is their enduring nature. In previous studies we found that increases in

* Dept Toxicology, Cagliari, Italy, 09124.

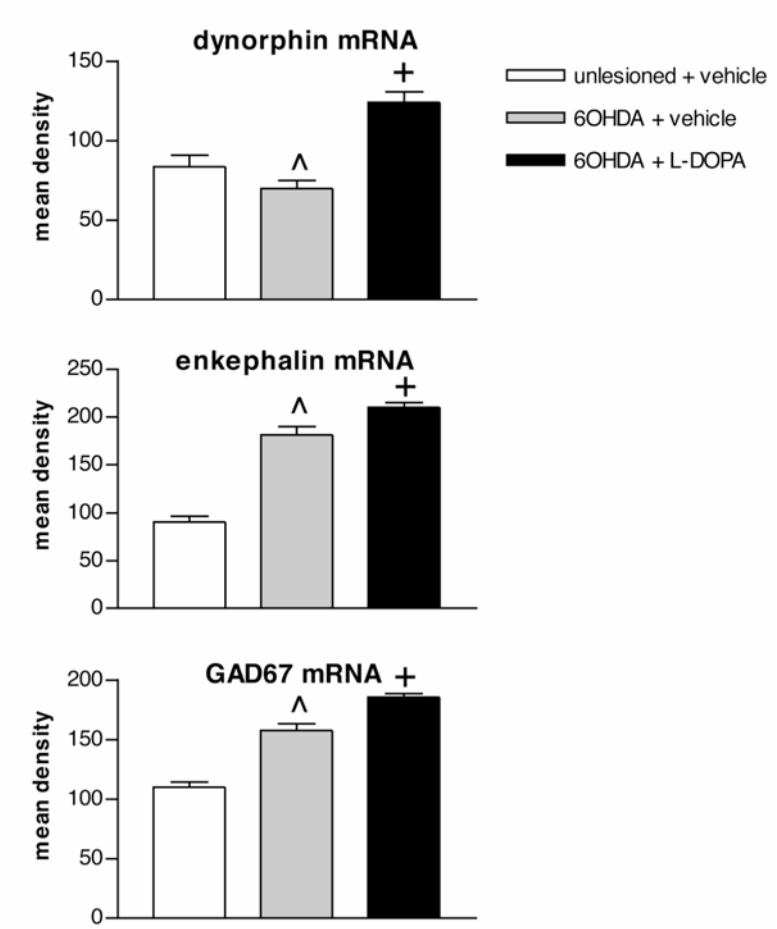

Figure 1. Changes in dynorphin, enkephalin and GAD67 mRNA in the striatum of 6-OHDA lesioned rats, 3 days after discontinuation of subchronic treatment with L-DOPA or vehicle. ^ $P < 0.05$ versus unlesioned + vehicle. + $P < 0.05$ versus unlesioned + vehicle and 6-OHDA + vehicle. From Carta et al., 2001.

GAD67, dynorphin and enkephalin after chronic intermittent L-DOPA are long-lasting, as they can be detected days after discontinuation of L-DOPA treatment (Carta et al., 2002). These changes do not reflect the acute response of striatal neurons to the drug, they are rather "tonic" changes which might represent a mechanism of neuroadaptation to the repeated stimulus.

An important open question is how the responsiveness of striatal neurons to an acute L-DOPA challenge is affected by a chronic L-DOPA treatment. Dyskinetic movements only arise contextually to L-DOPA administration, therefore the responsiveness of striatal neurons upon drug administration is a crucial point to be elucidated for understanding the mechanism of dyskinesia. In front of an increasing amount of data reporting an altered "phasic" response to prolonged L-DOPA in neurons of areas downstream of the striatum, similar evidences of "phasic" changes in striatal neurons activity are still missing. Early genes response, as *c-fos* or *zif-268*, is one of the most widely used tools to evaluate neuronal

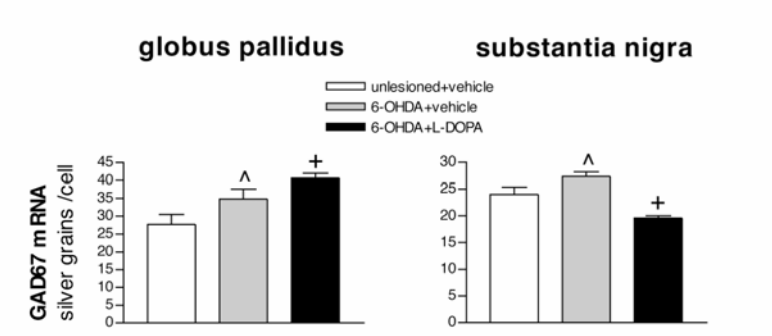

Figure 2. Mean of GAD67 mRNA silver grains per cell in the globus pallidus and substantia nigra reticulata of 6-OHDA lesioned rats, 3 days after discontinuation of subchronic treatment with L-DOPA or vehicle. ^ $P < 0.05$ versus unlesioned + vehicle. + $P < 0.05$ versus unlesioned + vehicle and 6-OHDA + vehicle. From Carta et al., 2003.

responsiveness in basal ganglia (Morgan and Curran, 1991; Sheng and Greenberg, 1990; Wang et al., 1995). Whereas reports exist on early genes induction by acute or chronic L-DOPA in the striatum (Asin et al., 1995, Doucet et al., 1996; Khan et al., 1999; Morelli et al., 1993; Mura et al., 2002; Robertson et al., 1989), the selective response of striatonigral and striatopallidal neurons has not been investigated as yet.

The objective of the present study was to assess changes in the response of striatal neurons to L-DOPA, after a subchronic dyskinetic L-DOPA treatment. To this aim *zif-268* mRNA was measured in striatal neurons one hour after a L-DOPA administration to rats previously treated with subchronic intermittent L-DOPA or vehicle. *Zif-268* positive neurons were double-labelled with either dynorphin or enkephalin mRNA to assess the responsiveness of striatonigral, dynorphin (+) neurons, and striatopallidal, enkephalin (+) neurons.

2. METHODS

6-Hydroxydopamine (6-OHDA) was injected in the left medial forebrain bundle (8 µg/4 µl of saline containing 0.05% ascorbic acid). Rats were pretreated with desipramine to prevent damage to noradrenergic neurons.

19 days after 6-OHDA lesion, rats were primed with L-DOPA (50 mg/kg i.p.) plus benserazide (30 mg/kg i.p.). Seven days after priming rats were subchronically treated twice a day for nineteen days with L-DOPA (6 mg/kg i.p.) plus benserazide (6 mg/kg i.p.) or with saline. Contralateral rotation was evaluated on the 1st and 19th day of treatment for one hour after drug injection. Three days after the last injection rats received a L-DOPA challenge (6 mg/kg i.p.) and were sacrificed after 1 hour.

Cryostat coronal sections were processed as described and hybridized with a [35S]-labelled ribonucleotide probe complementary to *zif-268* mRNA and digoxigenin-labelled ribonucleotide probes complementary to mRNA encoding for dynorphin or enkephalin (Carta et al., 2003b). Slides were dipped in a photographic emulsion and exposed for three weeks at −20°C in the dark. Thereafter slides were developed and counterstained with thionin.

For *zif-268* silver grains counting, adjacent sections were digitised at 400X. About 250 neurons from the dorsolateral striatum were analysed, and grains above each cell were

automatically counted with an image analyser (Zeiss KS 300). A frequency distribution of silver grains per cell was obtained, in which neurons were classified as "no labelling" (0–3 grains/cell), "medium labelling" (4–10 grains/cell), "high labelling" (>10 grains/cell). Inside each class, the effect of drug treatment was determined with a one factor ANOVA followed by Tukey HSD test for comparison between individual groups.

3. RESULTS

On the 19th day of treatment, 6-OHDA lesioned rats subchronically treated with L-DOPA showed a sensitized turning behaviour as compared to the first day of treatment and to the acute L-DOPA injection in rats subchronically treated with vehicle.

Both dynorphin (+) and enkephalin (+) neurons in the lesioned striatum of vehicle treated rats, displayed a low *zif-268* mRNA expression. After acute L-DOPA administration to vehicle pretreated rats, about 80% of dynorphin (+) neurons showed a medium (20%) to high (60%) level of *zif-268* mRNA labelling (Fig. 3), whereas among enkephalin (+) neurons, a smaller but significant population (about 20%) showed medium/high levels of labelling (Fig. 3).

After subchronic intermittent L-DOPA treatment, a L-DOPA challenge induced *zif-268* mRNA expression in a large number of dynorphinergic neurons (about 70%), although most of them at a medium level of labelling (50%) (Fig. 3). In contrast, enkephalin (+) neurons did not show any significant *zif-268* mRNA labelling after the subchronic treatment (Fig. 3).

4. DISCUSSION

The present study describes for the first time the effect of a subchronic dyskinetic L-DOPA treatment on the responsiveness of striatal neurons to L-DOPA at single cell level.

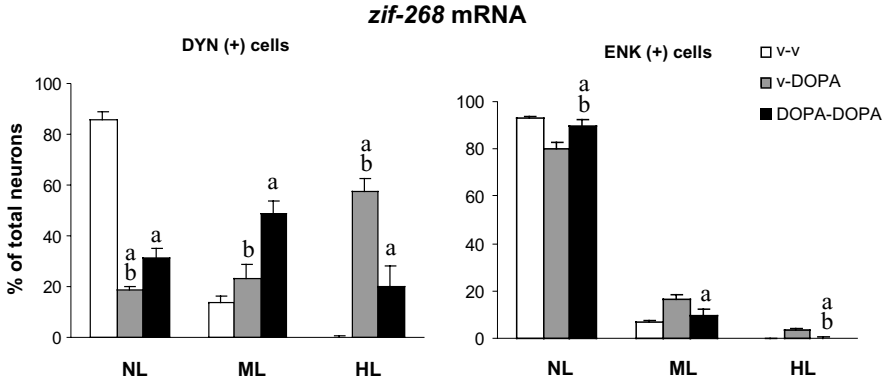

Figure 3. Frequency distribution of the amount of *zif-268* mRNA expressed as number of silver grains per neuron, in dynorphin (+) and enkephalin (+) neurons from the 6-OHDA lesioned dorsolateral striatum. Rats were treated with vehicle, acute or repeated L-DOPA followed, three days after the last injection, by a challenge with L-DOPA. Neurons were grouped based on the number of silver grains in: no labelling, medium labelling and high labelling. a = $p < 0.05$ vs v-v group; b = $p < 0.05$ vs DOPA-DOPA group.

By means of *zif-268* mRNA analysis, we found a different response of striatonigral and striatopallidal neurons to a L-DOPA challenge when given after a subchronic treatment with L-DOPA or vehicle. When given acutelly, to vehicle pretreated rats, L-DOPA elicited *zif-268* mRNA expression in both striatonigral and striatopallidal neurons, even though to a different extent. In contrast, after a subchronic L-DOPA treatment *zif-268* mRNA was increased by a L-DOPA challenge in striatonigral but not in striatopallidal neurons.

An important point raised by these results, is that changes in the *zif-268* response to L-DOPA induced by a subchronic treatment, do not correlate with changes in the expression of GAD67, dynorphin and enkephalin mRNA found in either striatonigral or striatopallidal neurons. A number of studies have reported that a long-lasting overexpression of dynorphin, enkephalin and GAD67 mRNA is associated with chronic L-DOPA treatment but not with an acute administration, suggesting that an overactivity of both striatonigral and striatopallidal neurons might underlie dyskinesia (Carta et al., 2002; Cenci et al., 1998; Henry et al., 2003; Nielsen and Soghomonian, 2004) (Fig. 1).

In contrast, the present results suggest that direct pathway neurons display a sensitized response after subchronic as well as acute L-DOPA, whereas, indirect pathway neuron response is desensitized after repeated L-DOPA, in spite of the increased expression of GAD67 and enkephalin mRNA observed previously.

Induction of transcription factors, as *zif-268*, is a measure of the "phasic" functional response of the neuron, related to dopamine receptor stimulation by L-DOPA, which precedes changes in the expression of other genes, included peptides. In contrast, changes in peptides and GAD67, which are long-lasting in nature, might be indicative of an altered "tonic" activity occurring in striatal neurons after repeated L-DOPA.

In normal rats, a role of dynorphin and enkephalin in counteracting the excessive activation of striatonigral or striatopallidal neurons respectively, has been proposed (Steiner and Gerfen, 1993; 1999). Similarly, in the lesioned striatum these peptides and, possibly, GAD67, may represent a "tonic" long-lasting neuroadaptive mechanism which would tend to counteract the abnormal increase in "phasic" activity observed both in striatonigral and striatopallidal neurons after acute L-DOPA. In line with this suggestion, one L-DOPA or dopamine receptor agonist priming, produces a long-lasting reversal of the decreased dynorphin mRNA levels produced by 6-OHDA lesion, and an increase in GAD67 mRNA levels in the lesioned striatum (Van De Witte et al., 1998; Carta et al., 2003).

Interestingly, in the unlesioned striatum increased levels of dynorphin induced by repeated cocaine, correlate with a downregulation in *c-fos* response in the same area (Steiner and Gerfen, 1993). The present results show that in the 6-OHDA lesioned striatum the number of striatonigral neurons displaying a *zif-268* sensitized response after acute and subchronic L-DOPA was similar, in spite of an abnormal dynorphin increase after the subchronic treatment. Thus, after dopamine denervation, direct pathway neurons seem to loose the property of counteracting their excessive activation, remaining in a sensitized state even after repeated stimulation.

This result supports the recent finding that, in the lesioned striatum, immediate early gene induction in striatonigral neurons is dependent on the abnormal regulation of the MAPKinase / Erk1/2 pathway, rather than on the normally used PKA / CREB pathway, which may account for the sustained hypersensitivity (Gerfen, 2002). In contrast, striatopallidal neurons displayed an increased *zif-268* response after acute L-DOPA (about 20%), whereas were downregulated after the subchronic treatment.

The present data suggest that subchronic L-DOPA treatment results in a profound imbalance in the responsiveness of striatal output pathways to L-DOPA. A balanced

activation of striatopallidal and striatonigral pathways is critical for a correct modulation of the activity of substantia nigra reticulata, whereas an excessive inhibition of the substantia nigra has been related to dyskinetic movements in animals chronically treated with L-DOPA or dopamine agonists (Carta et al., 2003; Boroud et al., 2001; Papa et al., 1999; Herrero et al., 1996).

The persistent sensitized response of striatonigral neurons found in the present study, together with the downregulation of striatopallidal neurons, might account for an excessive inhibition of the substantia nigra, and correlate with the onset of dyskinetic movements. Conversely, an acute L-DOPA administration, eliciting a more balanced response of striatal output pathways, would result in a moderate inhibition of the substantia nigra reticulata and, in turn, in a coordinated behavioural response.

Changes in the level of expression of markers of "tonic" neuronal activity do not concord with the classical model of basal ganglia circuitry, which envisage a reciprocal control of striatopallidal and pallidostriatal neurons (Obeso, 2000). Thus, after chronic L-DOPA, which is associated with increased enkephalin and GAD67 mRNA levels both in striatopallidal and pallidal neurons, the striatum and globus pallidus do not seem to drive each others activity (Fig. 4).

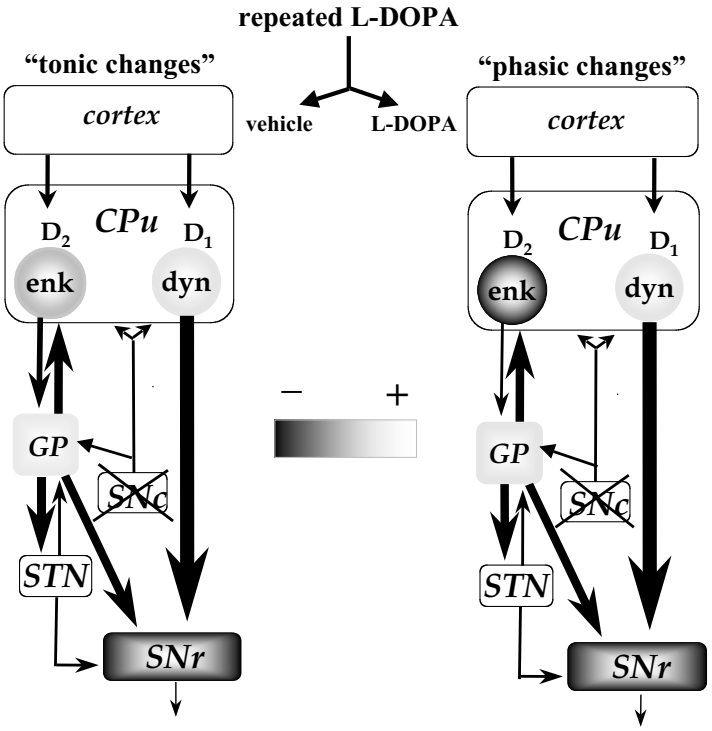

Figure 4. Schematic diagram of "tonic" and "phasic" changes in dopamine basal ganglia upon administration of vehicle or L-DOPA, after repeated L-DOPA treatment. Gray levels reflect the relative increase (light gray) or decrease (dark gray) in "tonic" and "phasic" changes in the different basal ganglia nuclei. White areas were not analysed in the present study.

Conversely, striatal changes in *zif-268* mRNA expression concord with the classical basal ganglia scheme, since striatopallidal neurons are completely downregulated after chronic L-DOPA (Fig. 4). A decreased activity of this neuronal population is in line with several studies reporting an increase in the firing rate of globus pallidus neurons after apomorphine or dopamine agonist therapy in parkinsonian humans and primates (Boraud et al., 2001; Filion et al., 1991; Hutchinson et al., 1997; Lozano et al., 2000). In agreement with electrophysiological studies, in progress experiments show increased levels of *zif-268* mRNA in the globus pallidus of lesioned rats repeatedly treated with L-DOPA. In conclusion, following repeated L-DOPA treatment, evaluation of expression of striatal markers of the direct (dynorphin, substance P) and indirect (enkephalin) pathway do not always correlate with the activity of basal ganglia nuclei connected to the striatum. In contrast, modifications in markers of "phasic" neuronal activity, as *zif-268*, seem to better reflect functional changes of striatum in relation to other basal ganglia structures.

5. REFERENCES

Andersson M., Konradi C., and Cenci M.A., 2001, cAMP response element-binding protein is required for dopamine dependent gene expression in the intact but not the dopamine-denervated striatum, *J. Neurosci*. **21**:9930.

Asin, K.E., Bednarz, L., Nikkel, A., and Perner, R., 1995, Rotation and striatal c-fos expression after repeated, daily treatment with selective dopamine receptor agonists and levodopa., *J. Pharmacol. Exp. Ther*. **273**:1483.

Benabid, A.L., Benazzouz, A., Limousin, P., Koudsie, A., Krack, P., Piallat, B., and Pollak, P., 2000, Dyskinesias and the subthalamic nucleus., *Ann. Neurol*. **47**:S189.

Boraud, T., Bezard, E., Guehl, D., Bioulac, B., and Gross, C., 1998, Effects of L-DOPA on neuronal activity of the globus pallidus externalis (GPe) and globus pallidus internalis (GPi) in the MPTP-treated monkey, *Brain Res*. **787**:157.

Boraud, T., Bezard, E., Bioulac, B., and Gross, C.E., 2001, Dopamine agonist-induced dyskinesias are correlated to both firing pattern and frequency alterations of pallidal neurones in the MPTP-treated monkey, *Brain* **124**:546.

Carta, A.R., Pinna, A., Cauli, O., and Morelli, M., 2002, Differential regulation of GAD67, enkephalin and dynorphin mRNAs by chronic-intermittent L-DOPA and A2A receptor blockade plus L-DOPA in dopamine-denervated rats, *Synapse*. **44**:166.

Carta, A.R., Tabrizi, M.A., Baraldi, P.G., Pinna, A., Pala, P., and Morelli, M., 2003, Blockade of A2A receptors plus L-DOPA after nigrostriatal lesion results in GAD67 mRNA changes different from L-DOPA alone in the rat globus pallidus and substantia nigra reticulata, *Exp. Neurol*. **184**:679.

Carta, A.R., Fenu, S., Pala, P., Tronci, E., and Morelli, M., 2003b, Selective modifications in GAD67 mRNA levels in striatonigral and striatopallidal pathways correlate to dopamine agonist priming in 6-hydroxydopamine-lesioned rats, *Eur. J. Neurosci*. **18**:2563.

Cenci, M.A., Lee, C.S., and Bjorklund, A., 1998, L-DOPA-induced dyskinesia in the rat is associated with striatal overexpression of prodynorphin- and glutamic acid decarboxylase mRNA., *Eur. J. Neurosci*. **10**:2694.

Doucet, J.P., Nakabeppu, Y., Bedard, P.J., Hope, B.T., Nestler, E.J., Jasmin, B.J., Chen, J.S., Iadarola, M.J., St-Jean, M., Wigle, N., Blanchet, P., Grondin, R., and Robertson, G.S., 1996, Chronic alterations in dopaminergic neurotransmission produce a persistent elevation of deltaFosB-like protein(s) in both the rodent and primate striatum, *Eur. J. Neurosci*. **8**:81.

Filion, M., Tremblay, L., and Bedard, P.J., 1991, Effects of dopamine agonists on the spontaneous activity of globus pallidus neurons in monkeys with MPTP-induced parkinsonism, *Brain Res*. **547**:152.

Gerfen, C.R., Miyachi, S., Paletzki, R., and Brown, P., 2002, D1 dopamine receptor supersensitivity in the dopaminedepleted striatum results from a switch in the rgulation of ERK1/2 MAPkinase, *J. Neurosci*. **22**:5042.

Henry, B., Duty, S., Fox, S.H., Crossman, A.R., and Brotchie, J.M., 2003, Increased striatal pre-proenkephalin B expression is associated with dyskinesia in Parkinson's disease, *Exp. Neurol*. **183**:458.

Herrero, M.T., Levy, R., Ruberg, M., Luquin, M.R., Villares, J., Guillen, J., Faucheux, B., Javoy-Agid, F., Guridi, J., Agid, Y., Obeso, J.A., and Hirsch, E.C., 1996, Consequence of nigrostriatal denervation and

L-DOPA therapy on the expression of glutamic acid decarboxylase messenger RNA in the pallidum, *Neurology* **47**:219.

Hutchinson, W.D., Levy, R., Dostrovsky, J.O., Lozano, A.M., and Lang, A.E., 1997, Effects of apomorphine on globus pallidus neurons in parkinsonian patients, *Ann. Neurol*. **42**:767.

Khan, S.M., Smith, T.S., and Bennett, J.P. Jr., 1999, Effects of single and multiple treatments with L-dihydroxyphenylalanine (L-DOPA) on dopamine receptor-G protein interactions and supersensitive immediate early gene responses in striata of rats after reserpine treatment or with unilateral nigrostriatal lesions, *J. Neurosci. Res.* **55**:71.

Levy, R., Dostrovsky, J.O., Lang, A.E., Sime, E., Hutchison, W.D., and Lozano, A.M., 2001, Effects of apomorphine on subthalamic nucleus and globus pallidus internus neurons in patients with Parkinson's disease, *J. Neurophysiol*. **86**:249.

Lozano, A.M., Lang, A.E., Levy, R., Hutchison, W., and Dostrovsky, J., 2000, Neuronal recordings in Parkinson's disease patients with dyskinesias induced by apomorphine, *Ann. Neurol*. **47**:S141.

Morelli, M., Cozzolino, A., Pinna, A., Fenu, S., Carta, A., and Di Chiara, G., 1993, L-DOPA stimulates c-fos expression in dopamine denervated striatum by combined activation of D-1 and D-2 receptors, *Brain Res*. **623**:334.

Morgan, J.I., and Curran, T., 1991, Stimulus-transcription coupling in the nervous system: involvement of the inducible proto-oncogenes fos and jun, *Annu. Rev. Neurosci*. **14**:421.

Mura, A., Mintz, M., and Feldon, J., 2002, Behavioral and anatomical effects of long-term L-dihydroxyphenylalanine (L-DOPA) administration in rats with unilateral lesion of the nigrostriatal system, *Exp. Neurol*. **177**:252.

Nielsen, K.M., and Soghomonian, J.J., 2004, Normalization of glutamate decarboxylase gene expression in the entopeduncular nucleus of rats with a unilateral 6-hydroxydopamine lesion correlates with increased GABAergic input following intermittent but not continuous levodopa, *Neuroscience* **123**:31.

Obeso, J.A., Rodriguez-Oroz, M.C., Rodriguez, M., DeLong, M.R., and Olanow, C.W., 2000, Pathophysiology of levodopa-induced dyskinesias in Parkinson's disease: problems with the current model, *Ann. Neurol*. **47**:S22.

Papa, S.M., Desimone, R., Fiorani, M., and Oldfield, E.H., 1999, Internal globus pallidus discharge is nearly suppressed during levodopa-induced dyskinesias, *Ann. Neurol*. **46**:732.

Robertson, G.S., Herrera, D.G., Dragunow, M., and Robertson, H.A., 1989, L-DOPA activates c-fos in the striatum ipsilateral to a 6-hydroxydopamine lesion of the substantia nigra, *Eur. J. Pharmacol*. **159**:99.

Sheng, M., and Greenberg, M.E., 1990, The regulation and function of c-fos and other immediate early genes in the nervous system, *Neuron*. **4**:477.

Soghomonian, J.J., Pedneault, S., Blanchet, P.J., Goulet, M., Di Paolo, T., and Bedard, P.J., 1996, L-DOPA regulates glutamate decarboxylases mRNA levels in MPTP-treated monkeys. *Brain Res. Mol. Brain Res*. **39**:237.

Steiner, H., and Gerfen, C.R., 1993, Cocaine-induced *c-fos* messanger RNA is inversely related to dynorphin expression in striatum. *J. Neurosci*. **13**:5066.

Steiner, H., and Gerfen, C.R., 1999, Enkephalin regulates acute D2 dopamine receptor antagonist-induced immediate-early gene expression in striatal neurons. *Neuroscience* **88**:795.

Van de Witte, S.V., Groenewegen, H.J., and Voorn, P., 2002, MK-801 alters the effects of priming with L-DOPA on dopamine D_1 receptor-induced changes in neuropeptide mRNA levels in the rat striatal output neurons, *Synapse* **43**:1.

Wang, J.Q., Smith, A.J.W., and McGinty, J.F., 1995, A single injection of amphetamine or methamphetamine induced dynamic alterations in *c-fos*, *zif/268* and preprodynorphin messenger RNA expression in rat forebrain, *Neuroscience* **68**:83.

Section V

DISORDERS OF BASAL GANGLIA FUNCTION II: CLINICAL STUDIES

BILATERAL SOMATOSENSORY RESPONSES OF PALLIDAL NEURONS IN HUMANS STUDIED WITH MICRORECORDING

Chihiro Ohye, Tohru Shibazaki, and Sumito Sato*

1. INTRODUCTION

In the previous IBAGS Meeting and on other occasions, we reported several behaviours of neuronal activities of the globus pallidus (GP) in relation to active and passive limb movement, especially in the internal segment of GP (GPi), in Parkinson's disease during the course of stereotactic pallidotomy (Ohye, 1995; Ohye et al., 1994, 1996). It was revealed that although most of them were related to active movement of limbs, often activated bilaterally, some of them responded to passive movement.

Interested in such somatosensory responses of the GPi neuron to the natural somatosensory stimuli, we had one parkinsonian case of thalamotomy with microrecording. In this particular case, the recording electrode incidentally passed through a part of GPi prior to come in the thalamic ventralis intermedius (Vim) nucleus, the somatosensory responses were found both in GPi and Vim by the similar natural stimuli. In this case, at the level of GPi, we found an isolated spike(s) responding to bilateral passive movement of elbow, wrist and ankle joint, and also other response to tapping on the contralateral forearm. Further advancing the recording electrode into the Vim nucleus, we found again the kinesthetic response as usually the case, and a response to tapping on the similar contralateral part of forearm.

Therefore, taking this rare opportunity, we tried later to compare some aspects of these sensory responses in GPi and Vim by the response pattern and latency, our special attention being focused on bilateral response and the tap response.

* Chihiro Ohye, Tohru Shibazaki, Sumito Sato: Functional and Gamma Knife Surgery Center, Hidaka Hospital, Takasaki, Gunma, 370-0001 Japan

2. SUBJECTS AND METHODS

This is a case study from a particular case of Parkinson's disease with tremor and rigidity. In this case of 63 year-old lady, the the right sided thalamotomy was planned because of insufficient effect of drugs. Using Leksell's stereotactic apparatus, the operation was done under local anesthesia. As usually, depth microrecording was carried out prior to making a coagulative lesion (Ohye, 1998a, 1998b). The recording electrode is a concentric bipolar needle type, outer diameter 0.4 mm, tip about 10 μm, interpolar distance 0.1–0.2 mm, electrical resistance about 100 Kohm. The electrode was oriented to the lower border of thalamic Vim nucleus as tentative zero point, with the aid of Leksell's surgiplan and referring to the anterior and posterior commissures determined on MRI of heavy T2 and proton images. In this patient, the trajectory was somewhat more laterally inclined (about 10 degrees to the midline) to avoid cortical veins at entrance point, so that it passed through the putamen and GP instead of usual caudate nucleus to come into the thalamic nuclei. The electrode was introduced slowly into the cerebral depth by an electric micromanipulator in micron steps, the step and speed being controlled as we required. The depth electrical activity was recorded continuously along the trajectory, and it was further led to monitor oscilloscope, heat pen–writing EEG machine and DAT tape, together with corresponding surface EMG record. The recorded data were later studied by a data analyzer (Powerlab).

3. RESULTS

3.1. Recording Site

In this case, theoretically the recording electrode would pass cerebral cortex, white matter (internal capsule), a part of GP, white matter, dorsal thalamus and ventral thalamus (Vim nucleus). As these structures showed respectively different electrical activity as already described (Ohye, 1998b), the position of the tip of electrode is identified rather clearly by the background activity and characteristic spike discharge (Gross et al., 1999; Vitek et al., 1998). For example, white matter is characterized by small positive spikes, GPi by continuous high frequency spikes, and Vim by high amplitude spikes responding to kinesthetic stimuli or rhythmic burst discharge of tremor frequency if any. So, in this case, at around 1000 μm from zero point, background activity increased telling that the electrode is in GPi probably through internal capsule. This was verified after the operation, by MRI examination that revealed the passage of the electrode really at the dorsal corner of GPi before coming into the thalamus, at corresponding distance ($982 \times 10\,\mu m$) from supposed zero point.

3.2. Physiological Study

In fact, at $982 \times 10\,\mu m$, an interesting neuronal activity was found, responding to multi-joint passive movement, stretching biceps, triceps, forearm flexor, extensor muscles, also tibialis anterior and gastrocnemius muscles. Moreover, not only the contralateral stimulation but also ipsilateral stimuli at symmetric site were equally effective (Figure 1).

This kind of bilateral multijoint response is known to be characteristic of GPi neuronal activity in Parkinson disease (Filion et al., 1988; Ohye et al., 1996).

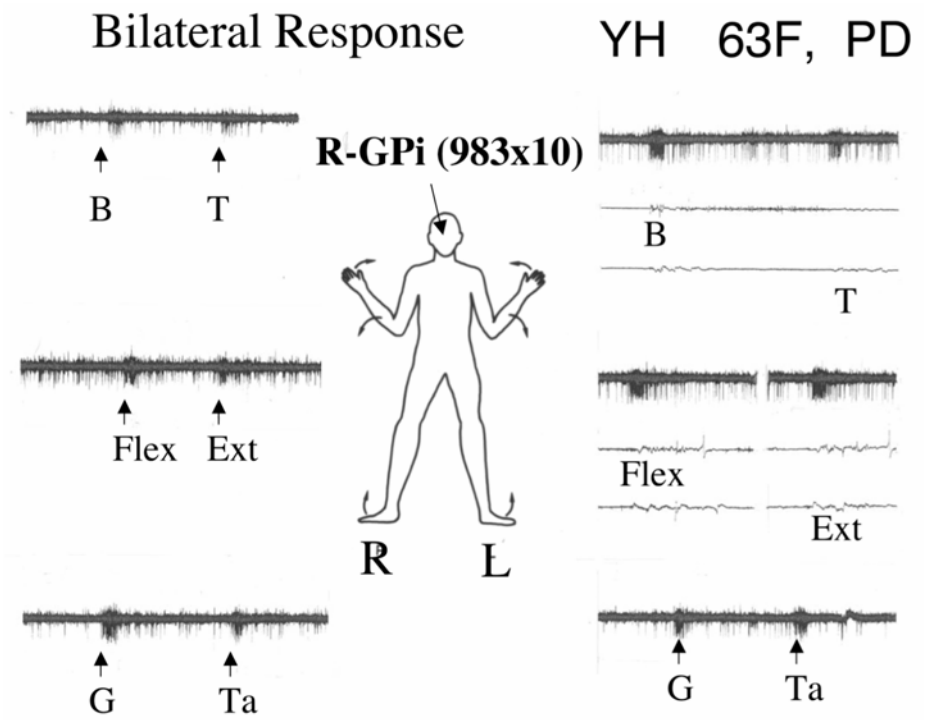

Figure 1. Bilateral multijoint response recorded in the right GPi (at 983 × 10 μm). In the left column are shown responses evoked by the contralateral left side stimulation. In the right column, responses evoked by the ipsilateral stimulation. A: figure in the center illustrates the recorded side (a straight arrow in the right head) and bilateral passive movement (curved arrows). B: biceps brachii muscle, T: triceps brachii, Flex: forearm flexor muscle, Ext: forearm extensor muscle, G: gastrocnemius, Ta: tibialis anterior.

At this point, there was a repetitive spike response to tap on the forearm flexor as shown in Figure 1 and 2. This tap response in GPi was later compared with the same kind of tap response found in the thalamic Vim nucleus. In this supposed GPi area slightly deeper point at 930 × 10 μm, another multijoint response to passive stretch of biceps, triceps, forearm flexor and extensor muscle was recorded.

Further introducing the recording electrode deeper area toward the thalamus, finally from 779 × 10 μm, there was marked increase of background activity with high amplitude spikes of Vim nucleus. There, several kinesthetic responses such as stretching biceps, triceps, and forearm muscles were found as usually the case. And at 300 × 10 μm, the response to tap on the forearm flexor was again recorded. The response recorded on EEG machine by slow paper speed (for example 2.5 cm/sec or 5.0 cm/sec) showed a sharp spike of large positive and negative potential as seen in Figure 2, but its expanded record on oscilloscope revealed slow positive-negative potential of about 10 msec each, superimposed by small spikes on it (Figure 3). In this regard, it is quite different from tap response in GPi, which consisted of a group of negative spike train as shown also in Figure 3.

In this observation, although the stimulation of tap was given by examiner's finger without any particular device, the latency of tap response could be measured roughly by mechanical deflection of EMG record as a trigger point. Thus, the latency from hand to

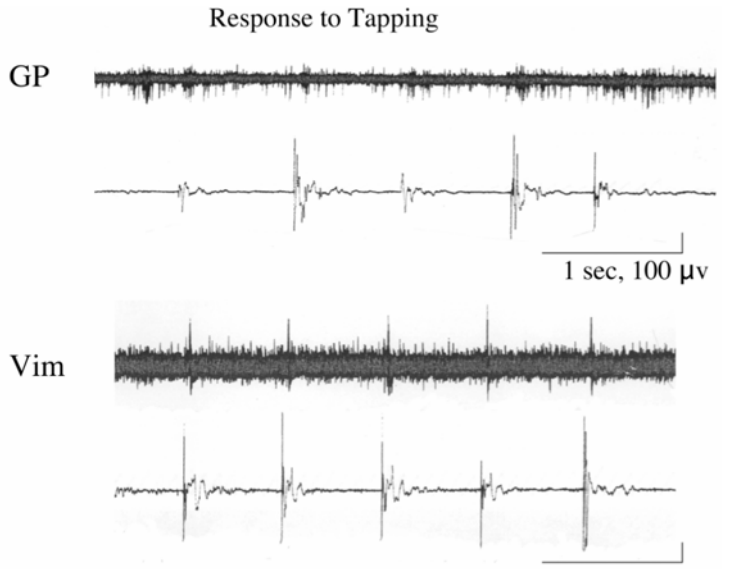

Figure 2. Examples of responses in the right GPi (upper two traces) and Vim (lower two traces) to tapping on the left forearm flexor side. In each pair of traces, upper one is the response, respectively, and the lower one denotes tapping signal (mechanogram of surface EMG was used).

GPi is 59.1 ± 11.5 msec, and from hand to Vim is 15.4 ± 2.6 msec, respectively. The tap response in GPi showed longer latency with more variations than that in Vim, as expected. This was more clearly shown by the latency histogram in Figure 4, in which individual value of latency measured in each 10 trials, hand to Vim and hand to GPi, was plotted.

4. DISCUSSION

Data presented here are obtained in one particular case with Parkinson disease, and therefore a small number study. But it was really a rare occasion to record responses in GPi and Vim from one and the same tracking by the similar peripheral maneuver. So the data are very important and valuable.

Bilateral multijoint responses are characteristic of GP in Parkinson's disease in experimental animal model, first described by Filion et al., (1988) and later found in Parkinson's disease in humans (Sterio et al., 1994; Taha et al., 1996) and also by ourselves (Ohye et al., 1996). As shown here, it is interesting to note that responses were evoked bilaterally by passive movement of the symmetric joint. This phenomena probably related to the impaired selection of movement in Parkinson's disease as suggested previously (Filion, et al., 1988; Ohye et al., 1996). Filion (2001) discussed this point further in his synthesis.

Tap response in GP was not expected in view of that there is no direct sensory input from periphery to GP. As mentioned above, the Vim receives the same information from tapping, and therefore, tap response in GP could be due to further extension of the thalamic response through some transcortical route. The latency study in this paper is a preliminary

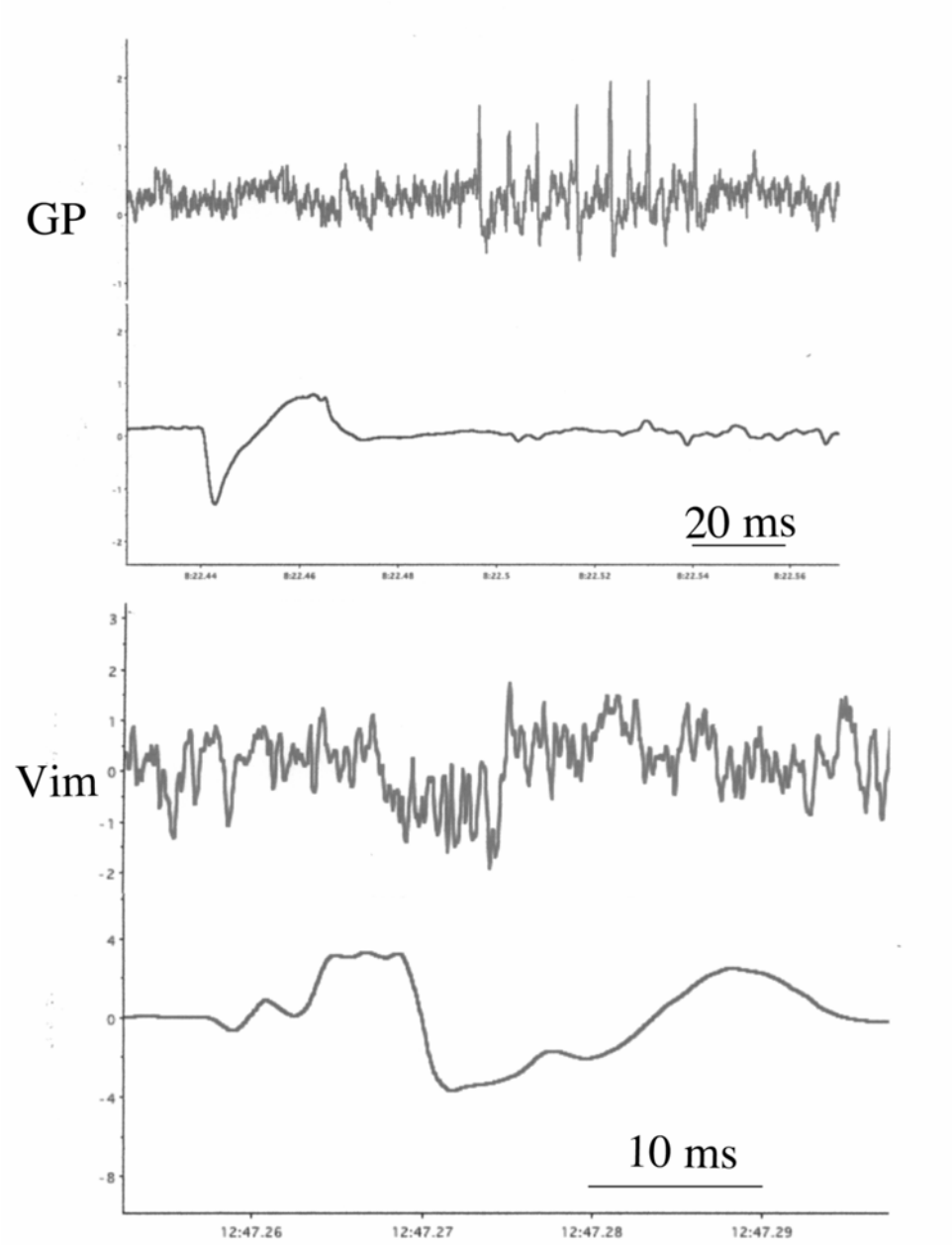

Figure 3. Enlarged, expanded record of the tap response in GPi (upper set) and Vim (lower set) to show latency measurement from the deflexion of the mechanogram (lower one of each pair of traces). In this figure, negativity is shown as upward and positivity as downward deflexion.

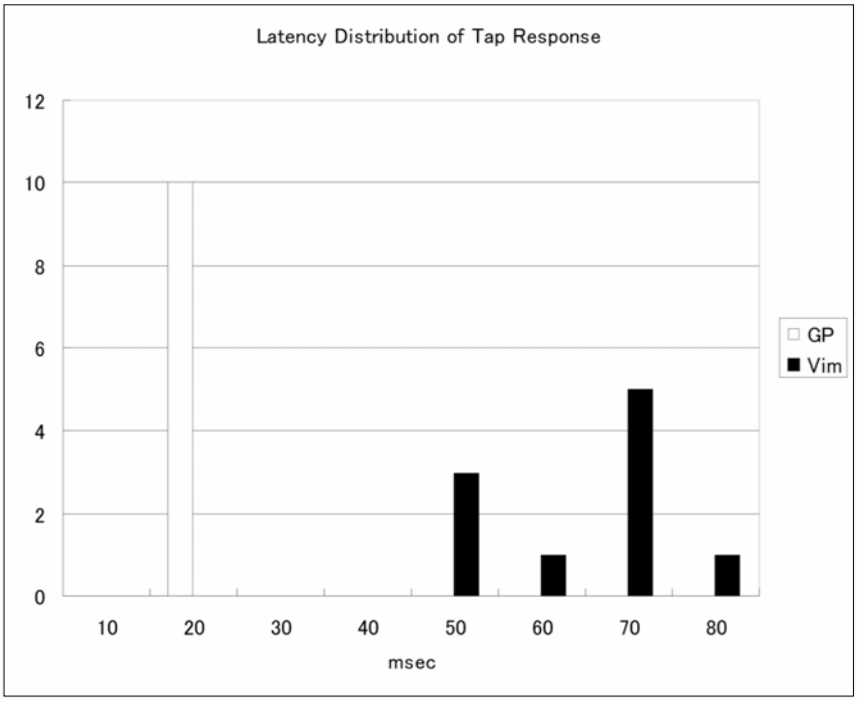

Figure 4. Latency distribution of the tap response in GPi and Vim.

small number study but it revealed a variable value around 50 msec, contrasting to that in Vim which is about 15–20 msec with almost fixed value as shown in Figure 4. In animal experiment there are also only a few systematic study on the latency of somatosensory response in GP. For example, Akazawa et al. (2000) reported electrical stimulation of the median nerve produced GP response with the latency of 24 msec with wide variations in monkey, if not tap response.

On the contrary, tap response in Vim is not so surprising as this thalamic zone is the projection area of kinesthetic sense from the contra lateral peripheral side (Ohye et al., 1989; Ohye, 1997). But, up to date, there is no report about the response by such modality of tapping in the human thalamus. The precise projection area (anatomy), peripheral receptor in the skin and latency study (physiology) are now going on. In this context, referring to the basic study of mechanoreceptor in human skin (Johansson and Vallbo, 1983; Kaas, 1990; Reznik, 1996), either Meissner corpuscle or Pacinian corpuscle could be the candidate responsible for this kind of fast adapting reaction. We are now studying this point also by more precise stimulation method.

5. REFERENCES

Akazawa, T., Takada, M., and Nambu, A., 2003, Activity and distribution patterns of monkey pallidal neurons in response to peripheral nerve stimulation. *Neurosci. Lett*. **339**:16.

Filion, M., Tremblay and Bedard, P.J., 1988, Abnormal influence of passive limb movement on the activity of globus pallidus neurons in parkinsonian monkeys. *Brain Res*. **444**:165.

Filion, M., 2001, Physiology of globus pallidus neurons in movement disorders. in: *Basal Ganglia and Thalamus in Health and Movement Disorders.* K. Kultus-Ilinsky and I. A Ilinsky, eds., Kluver Academic/Plenum, New York, Boston, Dordrecht, London, Moscow, pp. 241–248.

Gross, R.E., Lombardi, W.J., Lang, A.E., Duff, J., Hutchison, W.D., Saint-Cyr, J.A., Tasker, R.R., and Lozano, A.M., 1999, Relationship of lesion location to clinical outcome following microelectrode guided pallidotomy for Parkinson's disease. *Brain.* **122**:405.

Johansson, R.S., and Vallbo, A.B., 1983, Tactile sensory coding in the glabrous skin of the human hand *TINS.* **6**:27.

Kaas, J.H., 1990, Somatosensory System, in: *The Human Nervous System,* George Paxinos, ed., Academic Press, San Diego, New York, Boston, London, Sydney, Tokyo, Toronto, pp. 813–844.

Ohye, C., 1995, Activity of the pallidal neurons related to voluntary and involuntary movements in humans. in: Functions of Cortico-Basal Ganglia Loop. M. Kimura. and A. Graybiel, eds., Springer Verlag, Tokyo, pp. 190–200.

Ohye, C, 1997, Functional organization of the human thalamus: stereotactic intervention. in *Thalamus, Vol II,* M. Steriade, E.G. Jones, D.A. McCormick, eds. Elsevier, Amsterdam, pp. 517–542.

Ohye, C., 1998a, Thalamotomy for Parkinson's disease and other types of tremor. Part 1, Historical background and technique. in: *Textbook of Stereotactic and Functional Neurosurgery.* P.L. Gildenberg, and R.R. Tasker, eds. MacGraw Hill, New York, pp. 1167–1178.

Ohye, C., 1998b, Neural Noise Recording in Functional Neurosurgery. in *Textbook of Stereotactic and Functional Neurosurgery.* P.L. Gildenberg and R.R. Tasker, eds., MacGraw-Hill, New York, pp. 941–947.

Ohye, C., Hirato, M., Takahashi, A., Watanabe K., and Murata, H., 1996, Physiological study of the pallidal neurons in Parkinson's disease. in *The Basal Ganglia V,* C. Ohye, M. Kimura, J.S. McKenzie, eds., Plenum, New York-London, pp. 317–324.

Ohye, C., Hirato, M., Kawashima, Y., Hayase, N., and Takahashi, A., 1994, Neuronal activity of the human basal ganglia in parkinsonism compared to other motor disorders. in: *The Basal Ganglia IV.* G. Percheron, J.S. McKenzie, J. Feger, eds., Plenum, New York-London, pp. 83–391.

Ohye, C., Shibazaki, T., Hirai, T., Wada, H., Hirato, M., and Kawashima, Y., 1989, Further physiological observations on the ventralis intermedias neurons in the human thalamus. *J. Neurophysiol.* **61**:488.

Reznik, M., 1996, Structure and function of the cutaneous nervous system. *Pathol. Biol.* (*Paris*) **44**:331.

Sterio, D., Betric, A., Dogali, M., Fazzini, E., Alfaro, G., and Devinsky, O., 1994, Neurophysiological properties of pallidal neurons in Parkinson's disease. *Ann. Neurol.* **35**:586.

Taha, J.M., Favre J., Baumann, T.K., and Burchiel, K.J., 1996, Characteristics and somatotopic organization of kinesthetic cells in the globus pallidus of patients with Parkinson's disease. *J. Neurosurg.* **85**:1005.

Vitek, J.L., Bakay, R.A.E., Hashimoto, T., Kaneko, Y., Mewes, K., Zhang, j., Rye, D., Starr, P., Turner, R., and DeLong, M.R. 1998, *J. Neurosurg.* **88**:1027.

ALTERATIONS IN GLOBUS PALLIDUS INTERNUS FIRING PATTERNS ARE ASSOCIATED WITH DIFFERENT MOVEMENT DISORDERS

Joyce K.H. Tang, Neil Mahant, William D. Hutchison, Elena Moro, Andres M. Lozano, Anthony E. Lang, and Jonathan O. Dostrovsky*

1. ABSTRACT

Differences in neuronal firing rates of the globus pallidus internus (GPi) in hypokinetic and hyperkinetic movement disorders are thought to play an important role in mediating the contrasting motor symptoms. However, deep brain stimulation (DBS) in the GPi can alleviate both types of disturbances. This suggests that DBS might work by changing the pattern of GPi output, instead of the overall rate. In this study we examined whether GPi firing patterns are altered in various movement disorders involving basal ganglia pathology. We analyzed the neuronal firing patterns in the GPi of 14 Parkinson's disease (PD; n = 188) patients, 3 patients with multiple system atrophy (MSA; n = 26) and 10 patients with varying degrees of hyperkinetic disorders. This hyperkinetic group consisted of six cervical dystonia (CD; n = 183) patients, two idiopathic generalized dystonia (GD; n = 72) patients with the DYT1 mutation and two Huntington's disease (HD; n = 42) patients. The studies were approved by the local research ethics board and patients gave informed consent. Comparisons using different measurements of burstiness such as the burst index (BI), coefficient of variation (COV) and percentage of spikes in bursts (%SB) showed that the burstiness was lowest in the HD group (2.1 ± 0.2, 0.7 ± 0.05, and 6.3 ± 1.3; BI, COV, and %SB, respectively; mean ± SEM), followed by PD (2.6 ± 0.1, 0.9 ± 0.02, and 12.7 ± 0.9), MSA (2.9 ± 0.7, 0.9 ± 0.1, and 12.6 ± 3.4), CD (3.4 ± 0.1, 1.0 ± 0.02, and 15.5 ± 1.0) and GD (3.4 ± 0.3, 1.2 ± 0.07, and 22.4 ± 2.6), which had the highest burstiness. This demonstrates that each disease is associated with a different degree of neuronal firing burstiness and supports the hypothesis that differences in neuronal firing patterns are related to the different movement disorders.

* Joyce K.H. Tang, Neil Mahant and Jonathan O. Dostrovsky, University of Toronto, Toronto, Canada M5S 1A8. William D. Hutchison, Elena Moro, Andres M. Lozano and Anthony E. Lang, Toronto Western Hospital, Toronto, Canada M5T 2S8.

2. INTRODUCTION

The rate-based model of basal ganglia thalamo-cortical circuitry attempts to explain motor symptoms on the basis of the intensity of basal ganglia (BG) output. Specifically, the hypokinesia (impairment of voluntary movement) of Parkinson's disease (PD) is predicted to be due to elevated basal ganglia output, with an increased firing rate in the globus pallidus internus (GPi). In contrast, in hyperkinetic movement disorders such as Huntington's disease (HD), where there are excessive, involuntary movements, this output should be reduced (Albin et al., 1989; DeLong, 1990). The model also proposes an explanation for the success of GPi surgery for PD: reducing the abnormally elevated output of this nucleus results in improved motor function. Although the BG rate model seemed to offer plausible explanations for the pathophysiology of the symptoms in movement disorders, the therapeutic effects obtained by lesioning (Ford, 2004) or DBS (Krauss et al., 2004) in dystonic patients and incongruent findings relating to the firing rates of GPi neurons in dystonic patients (Hutchison et al., 2003; Lenz et al., 1998; Merello et al., 2004; Vitek et al., 1999) cast doubts on the dependability of the rate model in explaining motor symptoms.

Another feature of neuronal firing is firing pattern. The MPTP model of PD has shown that the neuronal firing pattern of the GPi becomes burstier (more irregular) than in normal controls (Filion and Tremblay, 1991). Similarly, the dystonic dt(sz) hamster also exhibits a burstier neuronal firing pattern in the GPi than in normals (Gernert et al., 2002). In humans, however, it is not known how GPi firing patterns are altered in the diseased states due to a lack of control subjects. But in general, GPi neuronal firing patterns are described as bursty or irregular in PD (Hutchison et al., 1994; Schiff et al., 2002) and dystonic patients (Sanghera et al., 2003).

The aim of this study was to investigate whether the firing patterns of neurons in the GPi are different in different groups of movement disorder patients. Recordings of the firing activity of single GPi neurons were made in patients with PD, multiple system atrophy (MSA), cervical dystonia (CD), generalized dystonia (GD) or HD. A general description of these pathologies is presented in Table 1.

Table 1. General description of pathologies studied.

Condition	Key structural changes within the basal ganglia	Key motor signs
Parkinson's disease	Degeneration of dopaminergic neurons located in the substantia nigra pars compacta	Bradykinesia, rigidity and tremor
Multiple system atrophy	Striatal atrophy	Bradykinesia and rigidity
Cervical dystonia	Not evident	Involuntary contraction of neck muscles
Generalized dystonia	Not evident	Involuntary co-contraction of agonist and antagonist muscles
Huntington's disease	Degeneration of striatal medium spiny neurons	Abnormal involuntary movements such as chorea and dystonia

3. METHODS

3.1. Patient Groups

This study included 27 patients with different forms of movement disorders. Of the 27 patients, nine males and five female patients were diagnosed with PD. The mean age was 62 years at the time of surgery. All PD patients had a good clinical levodopa response and the main reason for GPi surgery in these patients was the presence of LDOPA-induced dyskinesias and motor fluctuations. Three of the 27 patients were diagnosed with MSA due to limited response to levodopa therapy and signs of atrophy as determined by magnetic resonance images. Their mean age was 49 years and the mean disease duration of 5 years. Six patients were included in the cervical dystonia (CD) group, with a mean age of 49 years. Two female patients of age 13 and 32 were included in the generalized dystonia (GD) group. Finally, the HD group consisted of one male and one female patient of age 43 and 32, respectively. Their respective durations of onset were 8 and 6 years. All patients experienced motor symptoms that were either medically intractable or were experiencing severe side-effects from medications, thereby demonstrating the need for stereotactic surgery for pallidotomy or implantation of deep brain stimulating electrodes in the GPi. All patients were awake and no sedative was used during recordings.

3.2. Surgical Procedure and Micro-Recordings

The methods of microelectrode-guided stereotactic surgery for the implantation of DBS electrodes into the GPi or pallidotomy have been previously described (Lozano and Hutchison, 2002b). Briefly, recordings were made using Parylene-coated tungsten microelectrodes with an exposed tip size of 15–25 μm. Microelectrode tips were plated with gold and platinum to reduce the impedance to ~0.2 MΩ at 1 kHz. In some patients a pair of closely spaced (250 or 600 um apart) microelectrodes were inserted allowing simultaneous recordings from neuronal pairs. Signals were amplified and filtered using the Guideline System GS3000 (Axon Instruments, Foster City, CA). Action potentials arising from a single neuron were discriminated using template-matching, spike-sorting software (Spike2; Cambridge Electronic Design, Cambridge, UK). Only single-cell recordings that were either longer than 20 seconds in duration or consisted of more than 280 consecutive spikes and that occurred when the patient was at rest were included in the analysis. Recordings of peripallidal border cells were excluded from the analysis.

Locations of the recording sites were reconstructed from the predicted trajectory of the electrode using the Schaltenbrand and Wahren stereotactic atlas (Schaltenbrand and Wahren, 1977), scaled to fit the patient's anterior and posterior commissures and adjusted, if necessary, to correspond with the physiologically determined landmarks. These landmarks were obtained from the single unit recordings and microstimulation data which allowed identification of regions with and without cellular activity (gray vs. white matter), peripallidal border cells, optic tract and internal capsule (Lozano et al., 1996; Lozano and Hutchison, 2002a). From these reconstructions, locations of the recorded neurons were identified.

3.3. Data Analysis

To compare activities of GPi neurons between the two patient groups, mean firing rates and several measures of firing patterns in terms of their burstiness were determined.

For burst analyses, the following methods were utilized: burst index (a ratio of mean interspike interval to the mode interspike interval) and coefficient of variation. In addition, percentages of spikes participating in bursts, durations and frequencies of bursts, and intra-bursts rates in which bursts were detected by an algorithm called the Poisson surprise method as described by Legendy and Salcman (Legendy and Salcman, 1985) were used. In the surprise method, only epochs of elevated discharge rate in a spike train with a surprise value greater than or equal to 5 were considered to be bursts.

3.4. Statistical Analysis

Since the data of the different groups were either not normally distributed or did not posses equal variance, neuronal firing rates and pattern measurements were subjected to Kruskal-Wallis analyses of variance (ANOVA) on ranks followed by *post-hoc* mean tests using the Dunn's method of all pairwise multiple comparison. Mann-Whitney rank sum tests were performed to obtain P-values from pairs that were detected as significantly different by the post-hoc tests and were not normally distributed; otherwise, t-tests were performed to obtain P-values. All statistical analyses were carried out by use of the SigmaStat software (version 3.00, SPSS Inc.). For comparisons of means at different distances from the optic tract, two-way ANOVA followed by Dunn's method of all pairwise multiple comparison were used. A P-value of less than 0.05 was considered to be a significant difference. Values are expressed as the mean ± SEM.

4. RESULTS

A total of 523 GPi neuronal recordings were analyzed. 188 of the recordings were made from the PD group; 26 from the MSA group; 195 from the CD group; 72 from the GD group; and 42 from the HD group.

4.1. Firing Rates

The mean firing rate of neurons recorded from the PD group was significantly higher than those obtained from the MSA and CD groups (Figure 1A; means PD: 91.8 ± 2.7 Hz; MSA: 62.1 ± 9.1 Hz; CD: 72.3 ± 2.0 Hz; $P =< 0.001$ for both; t-test and Mann-Whitney rank sum test, respectively). Figure 1B plots the mean firing rates of neurons recorded in 2-mm intervals as a function of the location above the physiologically identified optic tract. This plot demonstrates that the differences in firing rates only occurred in the ventral part of the GPi (two-way ANOVA). Specifically, a significant difference was found at 2 mm dorsal to the optic tract between the PD and MSA groups ($P =< 0.001$; t-test); 2 and 4 mm dorsal to the optic tract between PD and GD ($P =< 0.001$ and $P = 0.005$, respectively; Mann-Whitney rank sum test); and 2, 4 and 6 mm dorsal to the optic tract between PD and CD ($P =< 0.001$, $P =< 0.001$ and $P = 0.002$, respectively; Mann-Whitney rank sum test).

4.2. Firing Patterns

All three measurements of firing irregularity (or burstiness) demonstrated differences amongst the five groups. Both comparisons of BI and coefficient of variation showed that

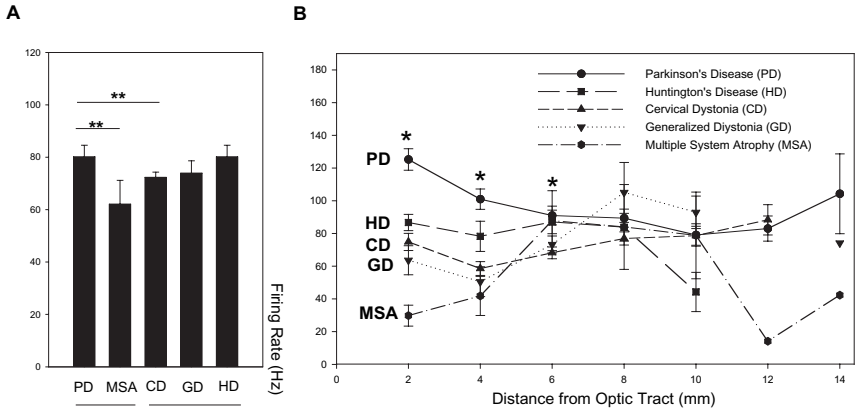

Figure 1. Comparison of neuronal firing rates.

the CD and GD groups have significantly higher values than those in the PD, MSA and HD groups (Figure 2 A and B). On the other hand, comparison by use of percentages of spikes participating in bursts revealed that the GD group had a significantly higher percentage than in the PD, MSA and HD groups, and that there was a significant difference between PD and HD (Figure 2 C). Figure 3 plots the mean burst index, coefficient of variation and percentage of spikes in bursts of neurons recorded in 2-mm intervals as a function of the location above the physiologically identified optic tract. Although the three plots demonstrate significant differences in different areas of the GPi, the differences were all within the ventral portion of the GPi. In general, the patterns of activities recorded from HD patients were the most regular, followed by MSA, PD, GD and CD. The different outcome yielded by different measurements suggests that some measurements might be more sensitive towards one aspect of firing pattern than others.

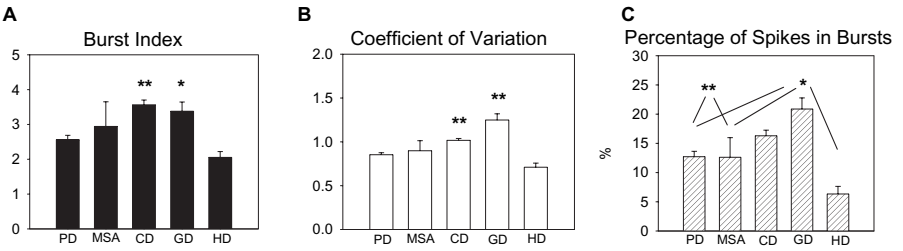

Figure 2. Comparisons of "bustiness" measurements amongst the five tested groups. *denotes P =< 0.05. **denotes P =< 0.001. (ANOVA on ranks followed by Mann-Whitney rank sum test.)

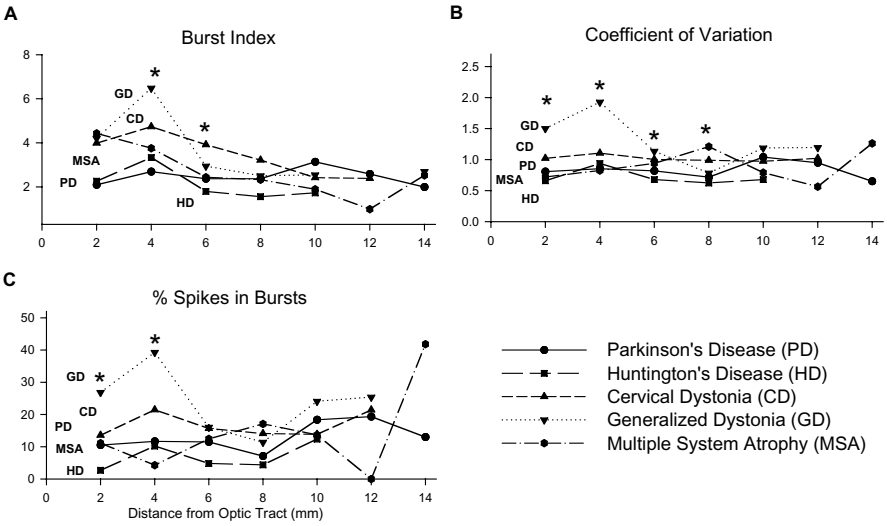

Figure 3. Comparisons of (A) mean burst index, (B) coefficient of variation and (C) percentage of spikes in bursts of neurons recorded in 2-mm intervals as a function of the location above the physiologically identified optic tract. * denotes P =< 0.05. (Two-way ANOVA and Mann-Whitney rank sum test.)

5. DISCUSSION

Our results show that (1) mean GPi firing rates can be similar in different disorders in contrast to the predictions of the rate-based model for hypo- and hyperkinetic disorders, (2) neuronal firing patterns are different in the GPi of patients with different movement disorders, and (3) these differences were limited to the ventral part of the GPi.

5.1. Significance of Firing Rate Findings

The finding of similar GPi neuronal firing rates is in support of the view that the now classical rate-model cannot fully explain the pathophysiology of basal ganglia-related movement disorders. However, we did observe a difference in firing rate between PD and CD, a group with focal manifestation of dystonic symptoms. Considering the focal manifestation of dystonic symptoms in CD, it is possible that large regions of the GPi remain close to normal. The observation of significantly higher firing rates in PD compared to CD suggests that firing rates might indeed be elevated in PD compared to normal. However, this interpretation is complicated by the observation of low firing rates in MSA, a disorder in which patients present with PD-like symptoms. Furthermore, firing rates of GPi neurons in GD and HD patients were similar to those in PD.

5.2. Significance of Firing Pattern Findings

Another interesting finding of this study was the differences in firing patterns. From the MPTP monkey model of PD, it has been shown that neuronal firing patterns of GPi neurons become more bursty (irregular) compared to the normal state (Filion and Tremblay, 1991). However, our results show that the neuronal firing pattern of the GPi can be even

more bursty during dystonic states (GD and CD). Again, if most regions of the GPi are relatively normal in CD, then this finding would suggest that neuronal firing pattern is bursty in the normal state, which contrasts with animal findings.

Our findings regarding firing patterns might reflect the connectivity of the different subnuclei of the basal ganglia network. In neurodegenerative disorders such as MSA and HD, the firing patterns of GPi neurons were very regular. This regularity in output might be due to the degeneration of striatal projections to the GPe leading to a disconnected system, thereby preventing the dynamic interactions between the nuclei of the BG and leading to a static system with regular output produced by intrinsic spontaneous firing of GPi neurons. On the other hand, a loss of dopamine in PD might lead to plasticity changes in the system which promotes dynamic interactions within the BG. This interpretation would also be consistent with the previous finding that administration of the dopamine agonist, apomorphine (APO), which partially normalizes the functioning of the basal ganglia by restoring part of the incomplete network, leads to elevation in burstiness of GPi neurons in PD patients (Levy et al., 2001). In the same study, APO-induced dyskinesias occurred in some cases when the GPi neurons had depressed firing rates and elevated burstiness. Compared to our current observations in the two HD patients in which chorea (clinically similar to medication-induced dyskinesia in PD) was present under a much higher GPi neuronal firing frequency and low burstiness, this suggests that the neuronal firing rates and patterns observed were not a consequence or cause of the motor activity. In basal ganglia dysfunctions that do not involve structural degeneration such as in CD and GD, firing patterns were very bursty, perhaps reflecting the dynamic interactions within the basal ganglia. However, the mechanism of how altered firing pattern can contribute to the generation of clinical symptoms remains unclear.

5.3. Topography

The basal ganglia are known to have a parallel organization, with segregated loops related to different functions (motor, associative, limbic, and oculomotor) passing through them (Alexander et al., 1990; Alexander and Crutcher, 1990; Hoover and Strick, 1993). In this study, the differences in firing rates and patterns were detected within the ventral portion of the GPi. Since the ventral portion of the GPi is part of the motor circuit (Flaherty and Graybiel, 1991; Flaherty and Graybiel, 1993), our finding of differences in firing rates and patterns within the ventral portion of the GPi suggest that the pathophysiological changes in these patient groups primarily involved motor circuits and is consistent with their marked movement disorders. Lastly, our findings suggest that when characterizing properties of GPi neurons, it might not be appropriate to pool the results obtained from different areas of the GPi.

6. REFERENCES

Albin, R.L., Young, A.B., and Penney, J.B., 1989, The functional anatomy of basal ganglia disorders, *Trends Neurosci.* **12**:366–375.

Alexander, G.E., and Crutcher, M.D., 1990, Functional architecture of basal ganglia circuits: neural substrates of parallel processing, *Trends Neurosci.* **13**:266–271.

Alexander, G.E., Crutcher, M.D., and DeLong, M.R., 1990, Basal ganglia-thalamocortical circuits: parallel substrates for motor, oculomotor, "prefrontal" and "limbic" functions, *Prog. Brain Res.* **85**:119–146.

DeLong, M.R., 1990, Primate models of movement disorders of basal ganglia origin, *Trends Neurosci.* **13**:281–285.

Filion, M., and Tremblay, L., 1991, Abnormal spontaneous activity of globus pallidus neurons in monkeys with MPTP-induced parkinsonism, *Brain Res.* **547**:142–151.

Flaherty, A.W., and Graybiel, A.M., 1991, Corticostriatal transformations in the primate somatosensory system. Projections from physiologically mapped body-part representations, *J. Neurophysiol.* **66**:1249–1263.

Flaherty, A.W., and Graybiel, A.M., 1993, Two input systems for body representations in the primate striatal matrix: experimental evidence in the squirrel monkey, *J. Neurosci.* **13**:1120–1137.

Ford, B., 2004, Pallidotomy for generalized dystonia, *Adv. Neurol.* **94**:287–299.

Gernert, M., Bennay, M., Fedrowitz, M., Rehders, J.H., and Richter, A., 2002, Altered discharge pattern of basal ganglia output neurons in an animal model of idiopathic dystonia, *J. Neurosci.* **22**:7244–7253.

Hoover, J.E., and Strick, P.L., 1993, Multiple output channels in the basal ganglia, *Science.* **259**:819–821.

Hutchison, W.D., Lang, A.E., Dostrovsky, J.O., and Lozano, A.M., 2003, Pallidal neuronal activity: implications for models of dystonia, *Ann. Neurol.* **53**:480–488.

Hutchison, W.D., Lozano, A.M., Davis, K.D., Saint-Cyr, J.A., Lang, A.E., and Dostrovsky, J.O., 1994, Differential neuronal activity in segments of globus pallidus in Parkinson's disease patients, *Neuroreport.* **5**:1533–1537.

Krauss, J.K., Yianni, J., Loher, T.J., and Aziz, T.Z., 2004, Deep brain stimulation for dystonia, *J. Clin. Neurophysiol.* **21**:18–30.

Legendy, C.R., and Salcman, M., 1985, Bursts and recurrences of bursts in the spike trains of spontaneously active striate cortex neurons, *J. Neurophysiol.* **53**:926–939.

Lenz, F.A., Suarez, J.I., Metman, L.V., Reich, S.G., Karp, B.I., Hallett, M., Rowland, L.H., and Dougherty, P.M., 1998, Pallidal activity during dystonia: somatosensory reorganisation and changes with severity, *J. Neurol. Neurosurg Psychiatry.* **65**:767–770.

Levy, R., Dostrovsky, J.O., Lang, A.E., Sime, E., Hutchison, W.D., and Lozano, A.M., 2001, Effects of apomorphine on subthalamic nucleus and globus pallidus internus neurons in patients with Parkinson's disease, *J. Neurophysiol.* **86**:249–260.

Lozano, A., Hutchison, W., Kiss, Z., Tasker, R., Davis, K., and Dostrovsky, J., 1996, Methods for microelectrode-guided posteroventral pallidotomy, *J. Neurosurg.* **84**:194–202.

Lozano, A.M., and Hutchison, W.D., 2002a, Microelectrode recordings in the pallidum, *Mov. Disord.* **17 Suppl 3**: S150–S154.

Lozano, A.M., and Hutchison, W.D., 2002b, Microelectrode recordings in the pallidum, *Mov. Disord.* **17 Suppl 3**: S150–S154.

Merello, M., Cerquetti, D., Cammarota, A., Tenca, E., Artes, C., Antico, J., and Leiguarda, R., 2004, Neuronal globus pallidus activity in patients with generalised dystonia, *Mov. Disord.* **19**:548–554.

Sanghera, M.K., Grossman, R.G., Kalhorn, C.G., Hamilton, W.J., Ondo, W.G., and Jankovic, J., 2003, Basal ganglia neuronal discharge in primary and secondary dystonia in patients undergoing pallidotomy, *Neurosurgery.* **52**:1358–1370.

Schaltenbrand, G., and Wahren, W., 1977, Atlas for Stereotaxy of the Human Brain, Thieme, Stuttgart, Germany.

Schiff, S.J., Dunagan, B.K., and Worth, R.M., 2002, Failure of single-unit neuronal activity to differentiate globus pallidus internus and externus in Parkinson disease, *J. Neurosurg.* **97**:119–128.

Vitek, J.L., Chockkan, V., Zhang, J.Y., Kaneoke, Y., Evatt, M., DeLong, M.R., Triche, S., Mewes, K., Hashimoto, T., and Bakay, R.A., 1999, Neuronal activity in the basal ganglia in patients with generalized dystonia and hemiballismus, *Ann. Neurol.* **46**:22–35.

BIOCHEMICAL MARKERS OF DBS-INDUCED TRANSITION FROM "OFF" TO "ON" STATE IN PARKINSONIAN PATIENTS

Salvatore Galati, Antonio Pisani, Alessandro Stefani, Ernesto Fedele, Maurizio Raiteri, Olimpia Pepicelli, Giuseppe Gattoni, Giorgio Bernardi, Paolo Mazzone, and Paolo Stanzione.*

1. INTRODUCTION

Biochemical changes associated with motor improvement induced by deep brain stimulation (DBS) of the subthalamic nucleus (STN) have been assessed in animal models of Parkinson's disease (PD), but poorly investigated in human PD (Windels et al., 2000). Consistent with the functional organization of the "direct" and "indirect" pathways, loss of dopaminergic projections to the striatum occurring in PD, results in decreased inhibitory striatal input to STN via globus pallidus externalis (GPe) (Albin et al., 1989; Alexander and Crutcher, 1990). Thus, the STN hyperactivity leads to the increased activity of globus pallidus internalis (GPi) resulting in an aberrant tonic inhibition of thalamic nuclei (DeLong, 1990). This assumption has been confirmed in the MPTP primate model of PD (Miller and DeLong, 1987; Bergman et al., 1990; Benazzouz et al., 1995a).

Clinical and experimental evidence suggested that STN-DBS effects are due to high frequency stimulation (HFS)-induced inactivation of the STN (Welter et al., 2004; Filali et al., 2004; Benazzouz et al., 1995b). Indeed, recent findings obtained from a 6-hydroxydopamine-denervated rat model have shown that STN-DBS decreased the firing rate of substantia nigra pars reticulata (SNr), resulting in a disinhibition of thalamic motor nuclei (Benazzouz et al., 2000). On the other hand, Hashimoto and co-workers (2003) reported an increase of GPi activity during HFS of STN in MPTP-treated monkeys. Different hypotheses have been proposed to explain these apparent discrepancies. One possibility is

* Salvatore Galati, Antonio Pisani, Alessandro Stefani, Giuseppe Gattoni, Giorgio Bernardi, and Paolo Stanzione I.R.C.C.S. Fondazione S. Lucia, Roma, Italy, and Clinica Neurologica, Dipartimento di Neuroscienze, Università di Roma Tor Vergata, Roma, Italy. Ernesto Fedele, Maurizio Raiteri, Olimpia Pepicelli Dip. Medicina Sperimentale, Sezione di Farmacologia e Tossicologia, Università degli Studi di Genova, Italy and Centro di Eccellenza per la Ricerca Biomedica, Università degli Studi di Genova, Italy. Paolo Mazzone Div. Neurochirurgia, Osp. CTO, Roma, Italy.

that a decrease of firing rate at cell soma level may co-exist with an HFS driven increased activity of the output fibres, leading to increased glutamate release in the target area (GPI and SNr) (Filali et al., 2004; McIntyre et al., 2004). Another possibility is represented by a specific change in the firing pattern of neurons of the GPi and STN rather than a change in their firing frequency (Allers et al., 2000; Stefani et al., 2002; Welter et al., 2004). In addition, an in vitro study has also suggested that while stimulation at low frequencies did not significantly modify ongoing STN activity, at therapeutically effective frequencies of stimulation, HFS suppresses STN spontaneous activity generating a pattern of recurrent burst of spike time locked to a stimulus pulse (Garcia et al., 2003). Together, these observations suggest that differences both in firing rate and pattern of firing discharge may occur during STN-DBS.

Neurochemical changes produced by clinically effective STN-DBS are completely unknown in human PD. We have recently shown that STN-DBS largely increases glutamate-dependent cyclic GMP (cGMP) in the GPi (Stefani et al., 2005), which could be the effect at GPi level of an increased glutamatergic driving from STN. However, neurochemical changes following STN-DBS in the basal ganglia main target (ventrolateral thalamic nucleus, VL and ventro anterior thalamic nucleus, VA) and at the level of the main basal ganglia input (putamen, PUT) are lacking in human PD. Therefore, by means of microdialysis in human PD patients, we evaluated the extracellular contents of cGMP in PUT and extracellular levels of GABA in the VL during STN-DBS.

2. METHODS

Advanced PD patients were involved in this study (six out of ten). The selection criteria have been previously described (Fedele et al., 2001; Stefani et al., 2002, 2005; Peppe et al., 2004). Permanent stimulating electrodes were placed both in the STN and in the GPi. Electrode implantation in the two hemispheres was carried out in separate surgical sessions (Fedele et al., 2001; Peppe et al., 2004). Microdialysis sampling was performed only in one of the two sessions. Demographic and clinical features of PD patients are reported in Table 1. The Local Ethics Committee approved the protocol and consent form. Informed, written consent was obtained from each patient involved in the study.

Table 1. Demographic and clinical features of PD patients.

Patient n°	Age (years)	Disease Duration (years)	LD Therapy (years)	LTTS Duration (years)	LD Therapy before DBS (mg)
1	68	11	9	5	750
2	70	10	7	3	1000
3	52	9	7	3	600
4	49	14	10	5	1000
5	59	13	12	2	700
6	56	8	7	2	800
Mean	**59.00**	**10.83**	**8.67**	**3.33**	**808.33**
SEM	**8.49**	**2.32**	**2.07**	**1.37**	**162.53**

Identification of the target areas, STN and GPi, was performed in each surgical session either preoperatively by means of ventriculography or intra-operatively by performing single unit recordings on two different trajectories (Peppe et al., 2004). In order to access STN via the VL, the STN trajectory was targeted at 11.0 mm of laterality, −4 mm with respect to the CA-PC plane, and 2–4 mm posterior to the mid point of the CA-PC line. In the sagittal plane, this trajectory had an angle of 80°–75°, and of 80°–75° in the coronal plane. Considering these angles in the coronal and sagittal planes, at 11.5 mm above the target, at the level of the top of VL, the trajectory had a laterality of 13.0 mm. Its antero-posterior position was between −2.5 and −0.5 with respect to the midpoint of the intercommissural line. Position of VL was assessed in keeping with the Guiot scheme that on the Shaltenbrand atlas provided these coordinates: laterality between 13.0 mm and 9.0 mm, deepness between + 7.75 mm and +1 mm with respect to the intercommissural plane, antero-posterior between 0 mm and −7.0 mm. Proper positioning of both probes and electrode were verified during surgical session by means of X-ray. Following electrophysiological identification of the target regions, the recording electrode in the GPi was replaced by a microdialysis probe. Along the same trajectory, a second probe was placed in the PUT. Another probe was positioned in the STN trajectory at the level of VL. Probe perfusion (5 µl/min) for stabilization (90 min) then began (Fedele et al., 2001). During this phase the permanent stimulating electrode was implanted in ipsilateral STN. Then, samples of 50 µl each were collected every 10 minutes. The first 5 collected fractions were considered as basal measurements both for GABA (VL probe) and for cGMP (GPi and PUT probes). Once the electrodes were stably implanted (Medtronic mod 3389), STN-DBS was turned on (130–160 Hz, pulse width 60–90 µs). Voltage was gradually raised by steps of 0.1 V up to the appearance of undesired, though tolerable side effects, such as paresthaesias. In this case, stimulation was decreased.

High performance liquid chromatography (HPLC) and radio-immuno assay (RIA) were utilized to measure GABA and cGMP concentration, respectively (Fedele et al., 2001; Bassi et al., 2002). Single measurements of cGMP and GABA obtained in basal conditions, during STN-DBS and during recovery conditions were averaged, and means were compared by non-parametric Friedman ANOVA followed by Wilcoxon test. In some patients (four out of ten), cGMP basal values were below the RIA detection limit (<1 fmol/100 µL) and, therefore, data were not included. In the remaining six patients, cGMP basal concentrations were clearly detectable with a similar profile among patients (see Table 2). In order to establish significance of variations in the single fractions after switching DBS on or off, single fraction values were compared to the previous mean (i.e basal or DBS means; Wilcoxon test). Throughout the session, an expert neurologist, blind to the stimulus intensity, assessed clinical changes, by utilizing selected items of UPDRS (Fahn et al., 1987) (rigidity 0–4, finger tapping 0–4, hand movement 0–4; tot. 0 normal-12 maximum score). We observed a significant clinical improvement in all the patients of more than 30% without side effects at an intensity between 2 and 3 V. STN-DBS intensity was maintained constant thereafter and fractions were collected in course of one hour of stimulation. UPDRS was continuously assessed to ensure persistence of the clinical effect. Clinical scores are reported every ten minutes as microdialysis values. Then means of basal vs DBS-On vs post DBS were compared by non-parametric Friedman ANOVA followed by Wilcoxon test. To assess significance of variations in the single fractions after switching DBS on or off, single fraction values were compared to the previous mean (i.e basal or DBS means). In all the selected patients STN-DBS produced a significant decrease of the UPDRS score contralaterally. The Friedman ANOVA showed a significant difference

Table 2. Biochemical changes of cGMP extracellular concentration in the GPi and PUT, extracellular levels of GABA in the VL and clinical score before, during and after STN-DBS.

Fractions	BASAL						STN-DBS							RECOVERY							Friedman
Patient n°	1	2	3	4	5		1	2	3	4	5	6		1	2	3	4	5	6		ANOVA
											cGMP GPi										
1	2,40	2,20	1,90	2,40	2,10	**2,20**	4,40	9,70	24,50	22,10	29,70	30,10	**20,08**	28,50	2,40	1,30	1,10	2,10	2,30	**6,28**	
2	1,70	1,30	1,70	1,50	1,40	**1,52**	2,70	2,30	2,50	3,20	3,10	3,40	**2,87**	3,90	2,10	1,50	1,40	1,20	1,30	**1,90**	
3	2,50	1,90	2,40	1,60	2,00	**2,08**	3,00	2,70	2,30	2,30	2,50	2,90	**2,62**	3,20	2,00	1,50	1,10	2,10	2,30	**2,03**	
4	1,00	1,50	1,10	1,00	1,00	**1,12**	2,50	9,40	10,70	12,60	10,90	11,20	**9,55**	12,10	1,90	1,10	1,40	1,10	1,40	**3,17**	
5	1,00	1,10	1,50	1,00	1,00	**1,12**	3,50	3,30	5,20	6,90	8,20	9,60	**6,12**	8,20	2,30	1,20	1,80	1,10	1,70	**2,72**	
6	1,90	2,10	2,80	2,30	2,40	**2,30**	3,10	2,80	3,50	5,90	6,40	5,10	**4,47**	13,40	2,70	1,80	1,50	2,20	1,50	**3,85**	
Mean	**1,75**	**1,68**	**1,90**	**1,63**	**1,65**	**1,72**	**3,20**	**5,03**	**8,12**	**8,83**	**10,13**	**10,38**	**7,62***	**11,55**	**2,23**	**1,40**	**1,38**	**1,63**	**1,75**	**3,33**	$p < 0.01$
SD	**0,65**	**0,45**	**0,62**	**0,61**	**0,60**	**0,54**	**0,68**	**3,51**	**8,61**	**7,44**	**10,09**	**10,22**	**6,62**	**9,28**	**0,29**	**0,25**	**0,26**	**0,55**	**0,45**	**1,62**	
											GABA VL										
1	4,30	4,00	4,50	4,90	4,30	**4,40**	3,90	3,70	3,20	3,60	3,20	3,20	**3,47**	3,70	3,70	3,90	4,00	4,20	4,30	**3,97**	
2	4,90	4,30	4,10	4,50	4,70	**4,50**	4,10	4,20	3,90	3,80	4,10	4,10	**4,03**	1,50	2,30	3,00	3,50	4,00	3,40	**2,95**	
3	4,00	3,90	3,70	4,30	4,10	**4,00**	3,00	4,00	3,50	3,90	3,20	3,00	**3,43**	3,00	3,30	4,10	5,40	6,30	5,00	**4,16**	
4	5,10	4,70	4,50	4,80	5,30	**4,88**	3,20	3,10	3,30	3,50	3,40	3,10	**3,27**	3,70	3,80	4,00	4,00	4,20	4,50	**4,03**	
5	4,90	5,30	5,50	5,10	5,60	**5,28**	3,90	3,70	4,00	3,50	3,40	3,10	**3,60**	4,00	4,20	5,10	6,60	4,30	6,70	**5,15**	
6	5,10	5,60	5,40	5,30	5,50	**5,38**	3,50	2,09	2,00	2,04	2,13	1,70	**2,24**	5,00	5,00	5,50	5,30	6,30	6,00	**5,52**	
Mean	**4,72**	**4,63**	**4,62**	**4,82**	**4,92**	**4,74**	**3,60**	**3,46**	**3,32**	**3,39**	**3,24**	**3,03**	**3,34***	**3,48**	**3,72**	**4,27**	**4,80**	**4,60**	**4,98**	**4,30**	$p < 0.05$
SD	**0,46**	**0,70**	**0,71**	**0,37**	**0,64**	**0,54**	**0,44**	**0,77**	**0,72**	**0,68**	**0,64**	**0,77**	**0,60**	**1,17**	**0,90**	**0,90**	**1,17**	**0,96**	**1,20**	**0,92**	
											cGMP PUT										
1	1,10	1,50	1,90	1,60	1,20	**1,46**	2,00	3,50	5,40	4,40	5,50	4,70	**4,25**	4,30	1,40	1,00	1,90	1,40	1,50	**1,92**	
2	1,90	1,70	1,20	1,30	1,30	**1,48**	1,50	1,60	1,40	1,70	2,10	2,10	**1,73**	2,20	1,50	1,70	1,10	1,20	1,50	**1,53**	
3	1,40	1,10	1,40	1,30	1,20	**1,28**	1,70	2,20	2,70	2,50	2,80	2,30	**2,37**	2,90	2,10	1,60	1,10	1,40	1,70	**1,80**	
4	1,70	1,50	1,70	1,40	1,30	**1,52**	1,40	2,30	2,50	2,30	3,20	3,50	**2,53**	3,20	1,40	1,50	1,70	1,70	1,60	**1,85**	
5	1,40	1,10	1,10	1,10	1,20	**1,18**	1,50	2,00	1,90	2,10	2,00	2,10	**1,93**	1,70	1,20	1,50	1,00	1,10	1,30	**1,30**	
6	1,40	1,50	1,60	1,30	1,50	**1,46**	1,40	5,60	6,40	5,90	6,90	6,30	**5,42**	6,10	2,10	1,40	1,50	1,00	1,50	**2,27**	
Mean	**1,48**	**1,40**	**1,48**	**1,33**	**1,28**	**1,40**	**1,58**	**2,87**	**3,38**	**3,15**	**3,75**	**3,50**	**3,04***	**3,40**	**1,62**	**1,45**	**1,38**	**1,30**	**1,52**	**1,78**	$p < 0.01$
SD	**0,28**	**0,24**	**0,31**	**0,16**	**0,12**	**0,13**	**0,23**	**1,48**	**2,03**	**1,64**	**2,00**	**1,71**	**1,47**	**1,59**	**0,39**	**0,24**	**0,37**	**0,25**	**0,13**	**0,33**	
											UPDRS										
1	7,0	8,0	7,0	7,0	8,0	**7,4**	6,0	5,0	5,0	5,0	5,0	5,0	**5,2**	5,0	8,0	8,0	8,0	8,0	9,0	**7,7**	
2	8,0	7,0	7,0	8,0	8,0	**7,6**	7,0	6,0	5,0	5,0	5,0	5,0	**5,5**	5,0	8,0	7,0	8,0	8,0	8,0	**7,3**	
3	9,0	10,0	10,0	9,0	11,0	**9,8**	9,0	7,0	7,0	6,0	6,0	6,0	**6,8**	6,0	9,0	9,0	10,0	11,0	11,0	**9,3**	
4	8,0	7,0	8,0	8,0	8,0	**7,8**	6,0	6,0	5,0	5,0	5,0	5,0	**5,3**	6,0	8,0	8,0	7,0	8,0	9,0	**7,7**	
5	9,0	8,0	8,0	9,0	9,0	**8,6**	7,0	6,0	6,0	5,0	5,0	5,0	**5,7**	6,0	8,0	8,0	9,0	8,0	9,0	**8,0**	
6	7,0	8,0	7,0	8,0	8,0	**7,6**	5,0	5,0	5,0	5,0	5,0	5,0	**5,0**	5,0	8,0	7,0	8,0	8,0	8,0	**7,3**	
Mean	**8,0**	**8,0**	**7,8**	**8,2**	**8,7**	**8,1**	**6,7**	**5,8**	**5,5**	**5,2**	**5,2**	**5,2**	**5,6***	**5,5**	**8,2**	**7,8**	**8,3**	**8,5**	**9,0**	**7,9**	$p < 0.001$
SD	**0,9**	**1,1**	**1,2**	**0,8**	**1,2**	**0,9**	**1,4**	**0,8**	**0,8**	**0,4**	**0,4**	**0,4**	**0,7**	**0,5**	**0,4**	**0,8**	**1,0**	**1,2**	**1,1**	**0,8**	

*$p < 0.05$ *post hoc* Wilcoxon

ANOVA = analysis of variance; SD = standard deviation

between the basal, DBS-ON and post DBS scores (Chi2 10.33, $p < 0.001$). The mean basal score (8.1 ± 0.9) significantly (Wilcoxon test, $Z = 2.52$, $p < 0.05$) decreased to 6.7 ± 1.4 after only ten minutes of STN-DBS. The average score during the 60 minutes of DBS, 5.6 ± 0.7, was significantly lower than basal and post DBS score (Wilcoxon test, $Z = 2.52$, $p < 0.05$). After DBS off, the first score significantly (Wilcoxon test, $Z = 2.52$, $p < 0.05$) different from the mean score during DBS was the second score (8.2 ± 0.4). The mean post DBS score during the 60 minutes of recovery (7.9 ± 0.8) was not statistically different from the basal mean. Then STN-DBS was discontinued and 10 minute fractions were collected for one additional hour. After ending microdialysis, a Medtronic mod. 3387 stimulating electrode was positioned in the GPi. Since probe stabilization was performed during STN electrode positioning and test stimulation during surgery is a routine procedure, the whole microdialysis procedure prolonged surgery only because of post stimulation recovery.

3. RESULTS

3.1. STN-DBS Increases Extracellular cGMP in the GPi

STN-DBS produced a significant change in cGMP concentration in the GPi ($n = 6$, mean +442%. Friedman ANOVA Ch2 = 10.33, $p < 0.01$). The mean ± SD basal value was 1.72 ± 0.54 fMol/50 µL. The rise in cGMP in each patient was significant (Wilcoxon test, $Z = 2.20$, $p < 0.05$) from the first fraction (3.20 ± 0.68 fMol/50 µL) following DBS-ON (Table 2). During DBS-ON the mean value of cGMP, 7.62 ± 6.62 fMol/50 µL, was significantly higher than basal and recovery values (Wilcoxon test, $Z = 2.20$, $p < 0.05$). Noticeably, these changes paralleled the amelioration of clinical performance (Fig. 1). After cessation of DBS elevated cGMP concentration, was maintained for 10–20 minutes in all the six subjects. Therefore the mean recovery value (3.33 ± 1.62 fMol/50 µL) was significantly (Wilcoxon test, $Z = 2.20$, $p < 0.05$) lower than DBS-ON value but higher (Wilcoxon test, $Z = 1.99$, $p < 0.05$) than basal value, showing an incomplete recovery within the examination time of 60 minutes after DBS.

3.2. STN-DBS Decreases Extracellular GABA in the VL

STN-DBS produced a significant change of GABA concentration in the VL ($n = 8$, mean −28%, Friedman ANOVA Ch2 = 7.00, $p < 0.05$). The mean basal value was 4.74 ± 0.54 pMol/50 µL. The decrease in GABA concentration was significant (Wilcoxon test $Z = 2.20$, $p < 0.05$) from the first fraction (3.60 ± 0.44 pMol/50 µL) following DBS-ON in comparison to the mean basal value (Table 2). During DBS on the mean value of GABA concentration, 3.34 ± 0.60 pMol/50 µL, was significantly (Wilcoxon test $Z = 2.20$, $p < 0.05$) lower than basal mean value. These changes also paralleled the amelioration of clinical performance (Fig. 1). After cessation of DBS decreased GABA levels were maintained for at least 20–30 minutes in all the subjects. The first significant (Wilcoxon test, $Z = 1.99$, $p < 0.05$) recovery was obtained in the fifth fraction (4.60 ± 0.96 pMol/50 µL). The mean recovery concentration (4.30 ± 0.92 pMol/50 µL), was higher than the DBS-ON mean and slightly lower than basal value. However both differences were not significant demonstrating a prolonged effect and a not complete recovery.

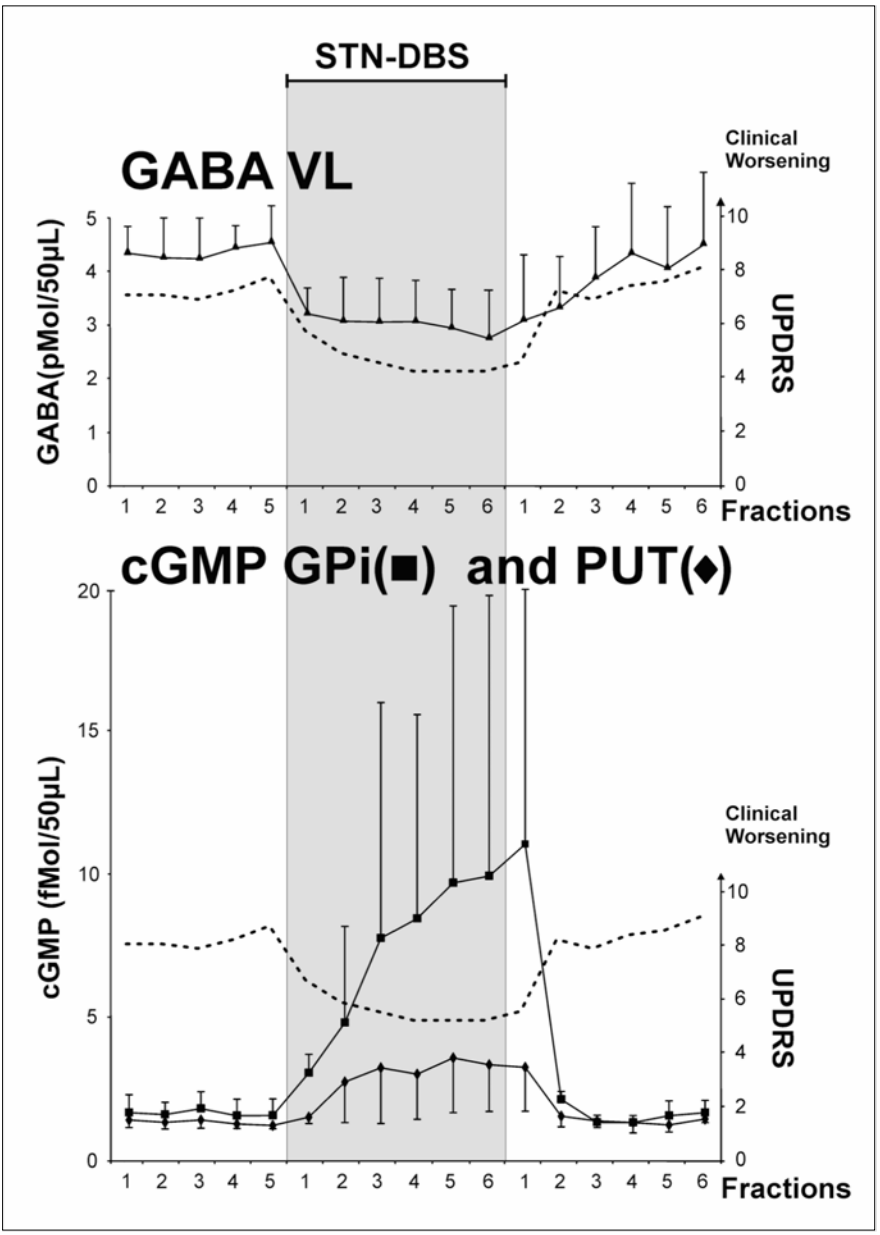

Figure 1. Upper panel. Time course of (triangles) GABA extracellular concentrations in the VL during one hour of clinically effective STN-DBS (shaded area). (Dotted line represents the average UPDRS clinical score of rigidity and akinesia of the contralateral arm: 0 = normal; 12 = maximum score). Note the decrease in GABA extracellular concentrations during clinical amelioration by STN-DBS.
Lower panel. Time course of cGMP extracellular concentrations in the GPi (filled squares) and in the PUT (filled rhombs) during one hour of clinically effective STN-DBS (shaded area). Note the increase in cGMP in both structures during effective STN-DBS.

3.3. STN-DBS Increases Extracellular cGMP in the PUT

STN-DBS also produced a significant change in cGMP concentration in the PUT (n = 6, mean +217%, Freidman ANOVA Ch2 = 12.00 $p < 0.01$). The mean basal value was 1.40 ± 0.13 fMol/50 µL. The rise in cGMP in each patient was significant from only the second fraction (2.87 ± 1.48 fMol/50 µL) following DBS-ON (Table 2). During DBS-ON the mean value of cGMP, 3.04 ± 1.47 fMol/50 µL, was significantly (Wilcoxon test, $Z = 2.20$, $p < 0.05$) higher than basal and recovery (1.78 ± 0.33 fMol/50 µL) values. Noticeably, these changes paralleled the amelioration and worsening of clinical performance during and after DBS (Fig. 1A). After cessation of DBS elevated cGMP concentration, was maintained only for 10 minutes in all the eight subjects as clinical amelioration. The mean recovery value was significantly (Wilcoxon test, $Z = 2.20$, $p < 0.05$) higher than basal value demonstrating a not complete recovery.

4. DISCUSSION

In the present study we confirm our previous observation that clinically effective STN-DBS induced a significant increase in cGMP concentration in the GPi. In addition, evidence is provided that STN-DBS also causes: i) a significant decrease in GABA content in the VL; ii) a large increase of the cGMP in the PUT.

STN-DBS has recently become an important therapeutic option in patients suffering from severe PD. Current notion on the efficacy of STN-DBS on PD patients appoints a central role to DBS-induced inactivation of STN since both STN lesion (Gill et al., 2003) and STN inactivation by local injection of lidocaine or muscimol (Levy et al., 2001), alleviate the parkinsonian symptoms.

Previous findings have shown that clinically effective STN-DBS produces a significant increase in cGMP concentration in the GPi, probably due to an increased glutamate release from the stimulated STN (Stefani et al., in press). The currently reported rise in cGMP in GPi could be the biochemical counterpart of the enhanced GPi firing activity induced by STN-DBS in MPTP-treated monkeys (Hashimoto et al., 2003). Moreover, our results appear in agreement with a recent PET study in humans, showing that STN-DBS induces an increase in blood flow in the GPi, suggesting higher metabolic activity in this area (Hershey et al., 2003). Recent studies have shown that during STNDBS in humans, STN firing rate decreases with a parallel appearance of a burst-like firing pattern (Welter et al., 2004; Filali et al., 2004). These findings are only apparently at odds with our present data. In fact, both groups acknowledge that inhibition of cell body does not preclude a simultaneous axon excitation. Accordingly, it has been recently suggested that suprathreshold stimulation of STN suppresses somatic firing, but generates efferent output at the stimulus frequency in the axon (McIntyre et al., 2004). Indeed, both the axonal firing rate and the shift to a bursting activity might promote a larger glutamate release, leading to an increased cGMP concentrations in the GPi.

VA-VL thalamic relay nuclei form a crucial link between the basal ganglia and cortex by conveying outputs to specific frontal cortical areas (Parent and Hazrati, 1995). Our findings suggest that motor improvement by STN-DBS is paralleled by a decrease of GABA in motor thalamus. These results are in agreement with electrophysiological data showing that STN-HFS enhances firing activity in rat motor thalamus (Benazzouz et al., 2000). Accordingly, Fukada and colleagues (2001) showed an increased blood flow in the VL

during GPi-DBS in humans. The thalamic disinhibition by STN-DBS is likely to produce an increased excitatory thalamic driving toward the cortex, as previously demonstrated by PET studies (Limousin et al., 1997). Similarly, cortical re-activation has been observed in PD patients during DBS (Pierantozzi et al., 1999; Pierantozzi et al., 2002) or after l-dopa administration (Rossini et al., 1993; Stanzione et al., 1991; Pierantozzi et al., 2001). Together, these findings support the hypothesis that both dopaminergic treatment and DBS lead to a normalization of cortical activity in PD patients when "on" state is obtained. As a consequence, this stabilization in cortical activity might re-activate cortico-subcortico-cortical loop.

Finally, our data demonstrate an increased excitation in the PUT during STN-DBS. Previous studies in the rat striatum have provided evidence that after chronic dopamine depletion by 6-hydroxydopamine lesions, the number of glutamatergic synapses is increased, though glutamate basal release is decreased (Meshul et al., 1999). Interestingly, l-dopa may increase glutamate release in the lesioned striatum (Jonkers et al., 2002). Although our study is focused on DBS rather than on l-dopa effects, we found an increase of the glutamate second messenger cGMP in the PUT which resembles the rise in l-dopa-induced glutamate reported in animal models. The increase of cGMP content in the PUT might be explained by an increased excitatory drive (i.e. glutamate and/or cholinergic transmission) or by a decreased inhibitory (GABAergic) activity. PUT is a very complex structure in which several transmitters systems are linked, balanced or in feed-back relationship. A large glutamate input comes from the cortex as well as from the centromedian parafascicular thalamic nuclei (Parent and Hazrati, 1995).

Functional PET studies assessed putaminal activity in PD following l-dopa administration (Feigin et al., 2001) reporting a decreased glucose metabolism in the PUT. They measured the overall metabolic activity within PUT. However, changes of this activity are the result of the algebraic sum of positive and negative changes within that area. It is not surprising that, although cortical input may be largely changed, a net difference is not appreciated, perhaps due to rebalancing mechanisms produced by other transmitters, i.e. acetylcholine, GABA, etc., within the PUT. The hypothesis that cGMP increase in the PUT is related to a larger cortical and/or thalamic glutamatergic inputs is in line with the classical view of the basal ganglia organization and with the concept that basal ganglia form a loop with the cortex.

We can conclude that: i) motor improvement in PD is linked or due to a disinhibition of the thalamo-cortical pathway; ii) both pharmacological and DBS treatments appear to share a common mechanism of action, in agreement with the evidence that in operated patients DBS and pharmacological stimulation produce clinical effects that cannot be summed (Peppe et al., 2004); iii) a key event is a reactivation of putaminal activity, marked by cGMP level increase, as a consequence of an unknown mechanism which is probably linked to an increased cortico-striatal or thalamo-striatal activity.

5. REFERENCES

Albin, R.L., Young, A.B., and Penney, J.B., 1989, The functional anatomy of basal ganglia disorders, *Trends Neurosci.* **12**:366–375.

Alexander, G.E., and Crutcher, M.D., 1990, Functional architecture of basal ganglia circuits: neural substrate of parallel processing, *Trends Neurosci.* **13**:266–271.

Allers, K.A., Kreiss, D.S., and Walters, J.R., 2000, Multisecond oscillations in the subthalamic nucleus: effects of apomorphine and dopamine cell lesion, *Synapse.* **38**:38–50.

Bassi, A., Fedele, E., Peppe, A., Pierantozzi, M., Gattoni, G., Bernardi, G., Stanzione, P., and Stefani, A., 2002, Elettrophysiological and biochemical changes related to high frequency deep brain stimulation in Parkinson's disease, in: *The Basal Ganglia VIII. Structure and Function* – R. Faull and L. Nicholson ed., Pergamon Press.

Benazzouz, A., Gao, D.M., Ni, Z.G., Piallat, B., Bouali-Benazzouz, R., and Benabid, A.L., 2000, Effect of high-frequency stimulation of the subthalamic nucleus on the neuronal activities of the substantia nigra pars reticulata and ventrolateral nucleus of the thalamus in the rat, *Neuroscience* **99**:289–295.

Benazzouz, A., Gross, C., Féger, J., Boraud, T., and Bioulac, B., 1995a, Reversal of rigidity and improvement in motor performance by subthalamic high frequency stimulation in MPTP- treated monkeys, *Eur. J. Neurosci.* **5**:382–389.

Benazzouz, A., Piallat, B., Pollak, P., and Benabid, A.L., 1995b, Responses of substantia nigra pars reticulate and globus pallidus complex to high frequency stimulation of the STN in rats: electrophysiological data, *Neurosci. Lett.* **189**:77–80.

Bergman, H., Wichmann, T., and DeLong, M.R., 1990, Reversal of experimental parkinsonism by lesion of the subthalamic nucleus, *Science* **249**:1436–1438.

DeLong, M.R., 1990, Primate models of movement disorders of basal ganglia origin, *Trend Neurosci* **13**:281–285.

Fahn, S., Elton, R.L., and Members of the UPDRS development committee: The Unified Parkinson's disease rating scale. In: Fahn S, Mardsen CD, Goldstein M, Calne DB, eds.: Recent developments in Parkinson's disease, Florham Park, NJ: Mac Millan Healthcare Information, 1987, pp 153–163.

Fedele, E., Mazzone, P., Stefani, A., Bassi, A., Ansaldo, M.A., Reiteri, M., Altibrandi, M.G., Pierantozzi, M., Giacobini, P., Bernardi, G., and Stanzione, P., 2001, Microdialysis in Parkinsonian patient basal ganglia: acute apomorphine-induced clinical and electrophysiological effects not paralleled by changes in the release of neuroactive amino acids, *Exp. Neurol.* **167**:356–365.

Feigin, A., Fukada, M., Dhawan, V., Przedborski, S., Jackson-Lewis, V., Mentis, M.J., Moeller, J.R., and Eidelberg, D., 2001, Metabolic correlates of levodopa response in Parkinson's disease, *Neurology* **57**:2083–2088.

Filali, M., Hutchison, W.D., Palter, V.N., Lozano, A.M., and Dostrovsky, J.O., 2004, Stimulation-induced inhibition of neuronal firing in human subthalamic nucleus, *Exp. Brain Res.* **156**:274–281.

Garcia, L., Audin, J., D'alessandro, G., Bioulac, B., and Hammond, C., 2003, Dual effect of high-frequency stimulation on Subthalamic neuron activity, *J. Neurosci.* **23**:8743–8751.

Gill, S.S., and Heywood, P., 1997, Bilateral dorsolateral subthalamotomy for advanced Parkinson's disease, *Lancet* **350**:1224.

Hashimoto, T., Elder, C.M., Okun, M.S., Patrick, S.K., and Vitek, J.L., 2003, Stimulation of the subthalamic nucleus changes the firing pattern of pallidal neurons, *J. Neurosci* **23**:1916–1923.

Hershey, T., Revilla, F.J., Wernle, A.R., McGee-Minnich, L., Antenor, J.V., Videen, T.O., Dowling, J.L., Mink, J.W., and Perlmutter, J.S., 2003, Cortical and subcortical blood flow effects of subthalamic nucleus stimulation in PD. *Neurology* **61**:816–821.

Jonkers, N., Sarre, S., Ebinger, G., and Michotte, Y., 2002, MK801 suppresses the L-DOPA-induced increase of glutamate in striatum of hemi-parkinsonian rata, *Brain Res.* **926**:149–155.

Levy, R., Lang, A.E., Dostrovsky, J.O., Pahapill, P., Romas, J., Saint-Cyr, J., Hutchison, W.D., and Lozano, A.M., 2001, Lidocaine and muscimole microinjections in STN reverse parkinsonian symptoms, *Brain* **124**:2105–2118.

Limousin, P., Gree, J., Pollak, P., Rothwell, J., Benabid, A.L., and Frackowiak, R., 1997, Changes in cerebral activity pattern due to STN or GPi stimulation in Parkinson's disease, *Ann. Neurol.* **42**:283–291.

McIntyre, C.C., Savasta, M., Kerkerian-Le Goff, L., and Vitek, J.L., 2004, Uncovering the mechanism, s, of action of deep brain stimulation: activation, inhibition, or both, *Clin. Neurophysiol.* **115**:1239–1248.

Meshul, C.K., Emre, N., Nakamura, C.M., Allen, C., Donohue, M.K., and Buckman, J.F., 1999, Time-dependent changes in striatal glutamate synapses following a 6-hydroxydopamine lesion, *Neuroscience* **88**:1–16.

Miller, W.C., and DeLong, M.R., 1987, Altered tonic activity of neurons in the globus pallidus and Subthalamic nucleus in the primate model of parkinsonism, in: *The Basal Ganglia II*. Structure and Function: current concepts, ed. Carpenter, M.B., and Jayaraman A. New York, Plenum Press, pp 415–427.

Parent, A., and Hazrati, L.N., 1995, Functional anatomy of the basal ganglia. I. The cortico- basal ganglia-thalamo- cortical loop, *Brain Res. Rev.* **20**:91–127.

Peppe, A., Pierantozzi, M., Bassi, A., Altibrandi, M.G., Brusa, L., Stefani, A., Stanzione, P., and Mazzone, P., 2004, Stimulation of the subthalamic nucleus compared with the globus pallidus internus in patients with Parkinson disease, *J. Neurosurg.* **101**:195–200.

Pierantozzi, M., Mazzone, P., Bassi, A., Rossini, P.M., Peppe, A., Altibrandi, M.G., Stefani, A., Bernardi, G., and Stanzione, P., 1999, The effect of deep brain stimulation on the frontal N30 component of somatosensory evoked potentials in advanced Parkinson's disease patients, *Clin. Neurophysiol.* **110**:1700–1007.

Pierantozzi, M., Palmieri, M.G., Marciani, M.G., Bernardi, G., Giacomini, P., and Stanzione, P., 2001, Effect of apomorphine on cortical inhibition in Parkinson's disease patients: a transcranial magnetic stimulation study, *Exp. Brain Res.* **141**:52–62.

Pierantozzi, M., Palmieri, M.G., Mazzone, P., Marciani, M.G., Rossini, P.M., Stefani, A., Giacomini, P., Peppe, A., and Stanzione, P., 2002, Deep brain stimulation of both subthalamic nucleus and internal globus pallidus restores intracortical inhibition in Parkinson's disease paralleling apomorphine effects: a paired magnetic stimulation study, *Clin. Neurophysiol.* **113**:108–113.

Rossini, P.M., Traversa, R., Boccasena, P., Martino, G., Passarelli, S., Pacifici, L., Bernardi, G., and Stanzione, P., 1993, Parkinson's Disease and Somatosensory Evoked Potentials: Apomorphine induced transient potentation of frontal components, *Neurology* **43**:2495–2500.

Stanzione, P., Fattapposta, F., Giunti, P., D'Alessio, C., Tagliati, M., Affricano, C., and Amabile, G., 1991, P300 variations in parkinsonian patients before and during dopaminergic monotherapy: a suggested dopamine component in P300, *Electroencephalogr Clin. Neurophysiol.* **80**:446–453.

Stefani, A., Bassi, A., Mazzone, P., Pierantozzi, M., Gattoni, G., Altibrandi, M.G., Giacomini, P., Peppe, A., Bernardi, G., and Stanzione, P., 2002, Subdyskinetic apomorphine responses in globus pallidus and subthalamus of parkinsonian patients: lack of clear evidence for the 'indirect pathway', *Clin. Neurophysiol.* **113**:91–100.

Stefani, A., Fedele, E., Galati, S., Pedicelli, O., Frasca, S., Pierantozzi, M., Peppe, A., Brusa, L., Hainsworth, A.H., Gattoni, G., Stanzione, P., Bernardi, G., Reiteri, M., and Mazzone, P., 2005, STN stimulation activates internal pallidus: cGMP microdialysis in Parkinson's disease patients, *Ann. Neurol*. **57**:448–452.

Welter, M.L., Houeto, J.L., Bonnet, A.M., Bejjani, P.B., Mesnage, V., Dormont, D., Navarro, S., Cornu, P., Agid, Y., and Pidoux, B., 2004, Effects of high-frequency stimulation on subthalamic neuronal activity in parkinsonian patients, *Arch. Neurol.* **61**:89–96.

Windels, F., Bruet, N., Poupard, A., Urbain, N., Chouvet, G., Feuerstein, C., and Savasta, M., 2000, Effects of high frequency stimulation of subthalamic nucleus on extracellular glutamate and GABA in substantia nigra and globus pallidus in the normal rat, *Eur. J. Neurosci.* **12**:4141–4146.

EFFECT OF DEEP BRAIN STIMULATION ON TREMOR

Fusako Yokochi, Ryoichi Okiyama, Makoto Taniguchi, Hiroshi Takahashi, and Ikuma Hamada*

1. INTRODUCTION

From experiences during stereotactic surgery, tremor is synchronized by the lowfrequency electrical stimulation of the ventralis intermedius nucleus of the thalamus (Vim) at a frequency lower than 10 Hz and suppressed by high-frequency electrical stimulation (Okuma et al., 1986). The surgical treatment of Vim results in a marked suppression of tremor. The high-frequency deep brain stimulation (DBS) of Vim has a similar and immediate effect of Vim coagulation. It is considered that Vim is part of the tremor circuit. On the other hand, DBS of the subthalamic nucleus (STN) suppresses parkinsonian tremor, but not immediately after the start of DBS.

Neuronal activities synchronized with a tremor rhythm are observed in Vim and correlate to the tremor of the extremities. Neuronal activities synchronized with a tremor rhythm are also observed in the dorsal part of the STN, but the relationship between tremor rhythm and the tremor of the extremities is not as close as that in the case of Vim. It is presumed that the DBSs of the two nuclei have different effects on tremor.

2. METHODS

The effects of DBS on tremor were examined in terms of the early effect of DBS and the effect of DBS frequency. The early effect means the clinical changes in tremor following switching off and switching on DBS observed within one month after the operation. The effect of DBS frequency was observed on the basis of changes in tremor frequency caused

* Department of Neurology, Department of Neurosurgery, Tokyo Metropolitan Neurological Hospital, Tokyo, Japan. I. Hamada, Department of Neurophysiology, Tokyo Metropolitan Institute for Neuroscience, Fuchu, Tokyo, Japan.

Table 1. Parameters of DBS.

	Active contact	Frequency (Hz)	Pulse width (μs)	Voltage
(1) Early effect of DBS				
1. PD: STN DBS	0–, 1–, 2+	160	60	3.5
2. PD: STN DBS	2–	130	60	2
3. PD: STN DBS	0–, 1–	185	60	2.6
4. PD: Vim DBS	1–, 3+	160	60	2
5. PD: Vim DBS	2–, 3+	160	60	2
6. ET: Vim DBS	2–	100	60	0.8
7. ET: Vim DBS	1–, 2+	100	60	2
(2) Effect od DBS frequency				
8. PD: STN DBS	1–, 2–	160	60	2.5
9. PD: STN DBS	1–, 2–	160	60	2.2
10. PD: STN DBS	2–	160	60	2
12. PD: Vim DBS	1–, 2+	160	60	2.6
13. PD: Vim DBS	1–, 2–	160	60	2.1

by DBS frequency, which is one of the DBS parameters. The examinations were performed by surface electromyography of the upper extremity of the side with a more severe tremor. The electrodes were attached to four muscles: the biceps, triceps, and flexors and extensors of the forearm. The parameters of DBS indicating the good clinical effect of DBS on each subject are shown in Table 1 and the same parameters were used in the two examinations.

2.1. Early Effect of DBS

Five patients with Parkinson's disease (PD; mean age, 59.2 years old; mean disease duration, 6.2 years) and two patients with essential tremor (ET; mean age, 49 years old; mean disease duration, 15.5 years) receiving DBS for the relief of tremor were examined by surface electromyography of an upper extremity within one month after the start of DBS. Three patients with PD and two patients with ET were treated by Vim DBS, and two patients with PD were treated by STN DBS. DBS was switched on and off during the surface electromyography.

2.2. Effect of DBS Frequency

Five patients with PD (mean age, 64.6 years old; mean disease duration, 7.0 years) were examined more than one year after the start of DBS. Three patients were treated by STN DBS, and the other two patients by Vim DBS. Before the surface electromyography, DBS was switched off in each patient. Tremor in the off period of DBS was observed for more than one hour and recorded for 5 minutes. After completely observing tremor, DBS was restarted at low frequencies. The frequency of DBS was changed from 5 Hz to 185 Hz using an IPG programmer. Surface electromyography was performed for 30 seconds at each DBS frequency. Tremor frequency was examined on the basis of the surface electromyography record obtained during the last 10 seconds at each frequency and measured in the period between the grouping discharges of surface electromyography activities in the flexor muscles of the forearm. Other parameters of DBS were the same as those used in conventional therapy.

3. RESULTS

3.1. Early Effect of DBS

The effect of Vim DBS on tremor in the patients with PD and ET, that is, the suppression of surface electromyography activities of tremor, appeared within 5 seconds after switching on. The tremor reappeared 10 seconds or more after switching off; the period was particularly longer in the patients with ET than in those with PD (Fig. 1). Tremor of all muscles in the upper extremity stopped after switching on and appeared after switching off with the same periods without changes in the amplitudes of grouping discharges. This phenomenon was observed similarly in both the resting and postural types of tremor. On the other hand, the surface electromyography activities in the patients with PD treated by STN DBS showed different patterns from those in patients treated by Vim DBS. The amplitudes of grouping discharges gradually decreased after switching on and increased after switching off. Moreover, the grouping discharges of surface electromyography activities in the upper extremity did not stop or reappear with the same periods as shown in Fig. 2. The effect of switching on was not immediate in two of the three patients treated by STN DBS, and tremor in these patients was completely suppressed following hand movements; the suppression continued after the cessation of hand movements as shown in Fig. 3.

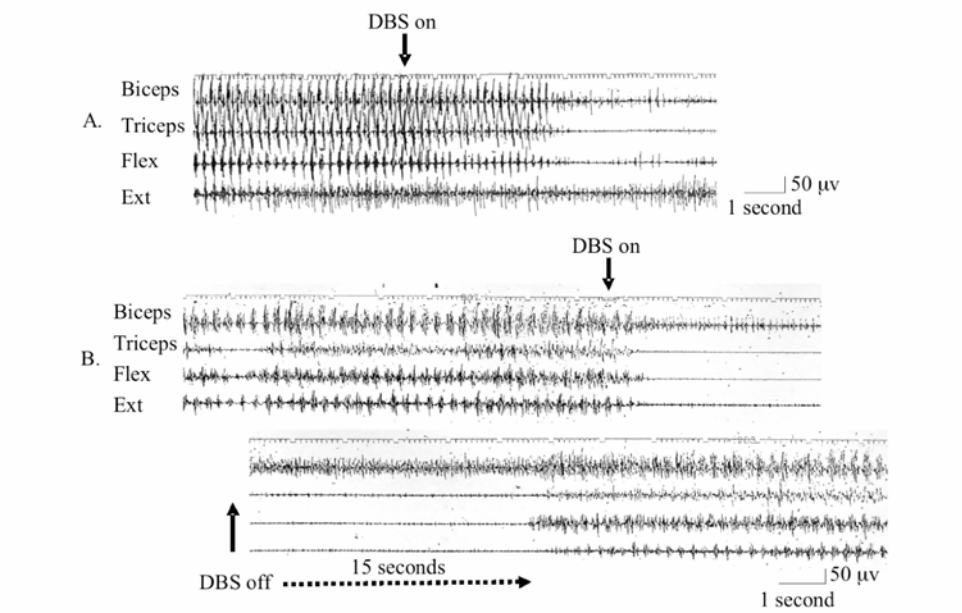

Figure 1. EMG recording during switching on and off Vim DBS. A is the surface electromyography recording of tremor in PD and resting tremor. B is the recording of tremor in ET and postural tremor in the finger-nose test. Lower recording of ET shows after switching off showing that tremor reappeared 15 seconds later. Biceps, biceps brachii; Triceps, triceps brachii; Flex, flexor; Ext, extensor.

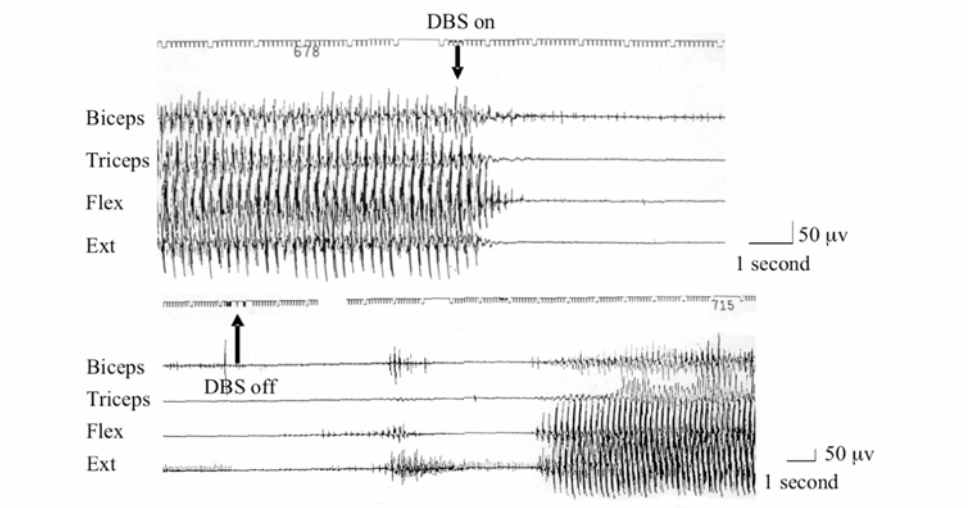

Figure 2. EMG recording during switching on and off STN DBS.

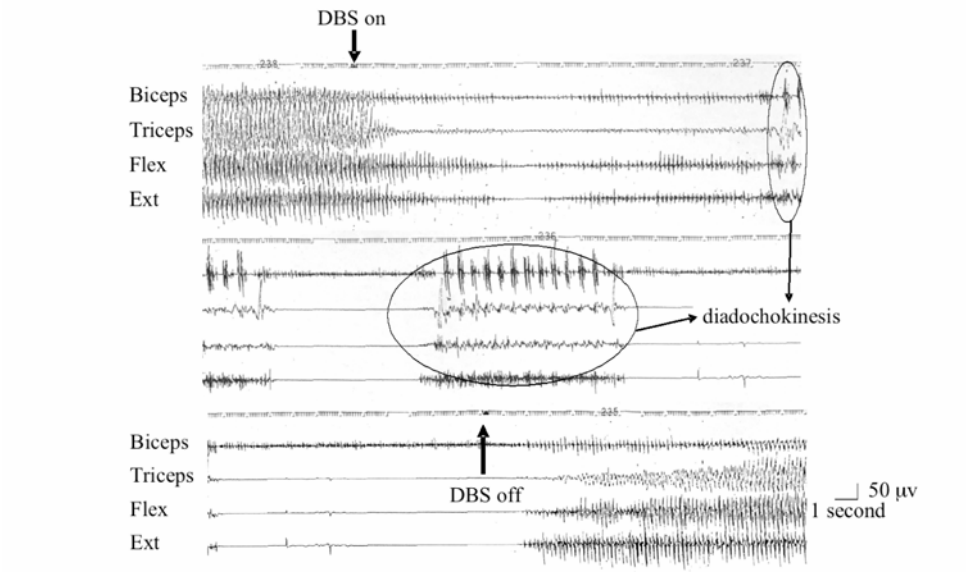

Figure 3. EMG recording of STN DBS. A series of three recordings show that hand movements suppress tremor. In the upper recording, tremor was not suppressed after switching on DBS. Diadochokinesis was continuously performed, and tremor was suppressed after switching off DBS.

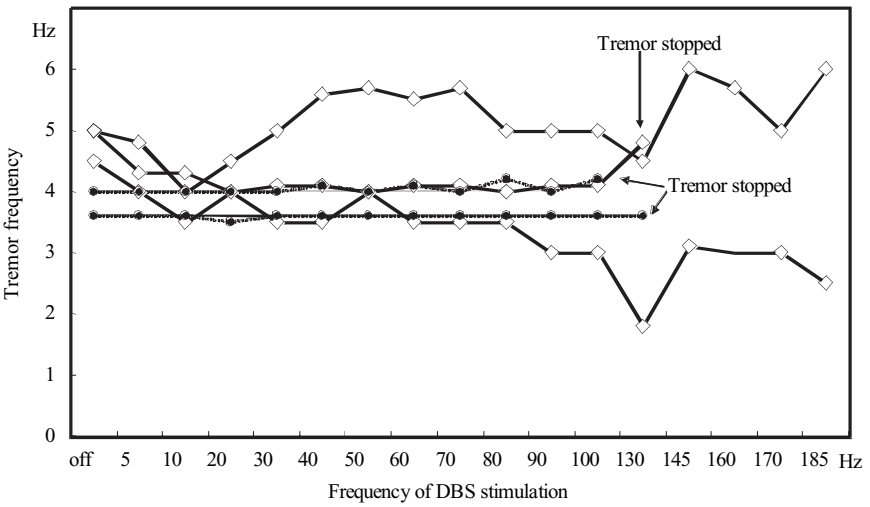

Figure 4. Relationship between tremor frequency and DBS frequency. The open squares connected by the solid line show the results of STN DBS, and the closed circles connected by the dotted line show the results of Vim.

3.2. Effect of DBS Frequency

The effects of switching on and off DBS on tremor more than one year after the start of DBS, that is, the late stage, were different from those at the early stage after DBS. The reappearance of tremor was not immediate in the patients who were treated by STN DBS as well as by Vim DBS. Tremor was not observed for 12 hours after switching off in the state of off-medication in two patients treated by STN DBS. The gradual increase or decrease in the number of grouping discharges of surface electromyography activities on switching on and off was not observed in all patients treated by STN DBS, which was recorded in the early stage after the start of STN DBS.

The changes in DBS frequency had no effect on tremor frequency in the patients treated by Vim DBS, but tremor frequency slightly changed in the patients treated by STN DBS. The high-frequency stimulation increased tremor frequency from the baseline of 4.5 Hz to about 3 Hz in one patient. Figure 4 shows the frequencies of tremor and DBS in the patients treated by STN DBS and Vim DBS.

4. SUMMARY

The effect of Vim DBS on tremor was equivalent to that of thalamotomy. It was immediate and reliable. DBS at various frequencies did not change tremor frequency. The early and late effects on tremor after DBS were the same.

During STN DBS, tremor stopped and reappeared according to changes in the grouping discharges of surface electromyography activities with a gradual increase or decrease in amplitude at the early stage after DBS, but these patterns were not observed in the late stage. The tremor suppression by STN DBS was influenced by the voluntary movements

of the extremity with tremor. The frequency of DBS changed the frequency of grouping discharges, that is, the latter was increased or decreased.

5. DISCUSSION

Tremor is suppressed by Vim DBS or STN DBS. For some time, the target for abolishing tremor was only Vim, but now the selection of the target for the treatment of tremor by DBS is extended. The Vim nucleus of the thalamus, the subthalamic nucleus and the internal pallidum are targets for the improvement of parkinsonian symptoms. It is difficult to determine which target of stimulation has the best effect on tremor. It is generally accepted that Vim is part of the tremor circuit or closely related to the tremor circuit. Rhythmic firing discharges related to tremor are recorded in Vim, and a coagulated lesion or electrical high-frequency stimulation in this area immediately suppresses tremor. Recently, it has been found that a lesion of STN in MPTP monkeys improves parkinsonian symptoms including tremor, and STN DBS has been started as an effective therapy for Parkinson's disease. Many studies showed that neuronal discharges in relation to tremor have been recorded in STN as well as in Vim. Are the mechanisms underlying the suppression of tremor by the therapeutic stimulation of the two nuclei Vim and STN similar? From our observations, the pattern of surface electromyography activities induced by DBS differs between the two nuclei. Switching on Vim DBS immediately suppressed surface electromyography activities of the arm muscles, which reappeared after switching off Vim DBS. On the other hand, surface electromyography activities suppressed by STN DBS showed oscillatory changes. This pattern of surface electromyography activities was supposed to modulate the tremor circuit. The change in tremor frequency induced by the frequency of STN DBS was also presumed as the mechanism of STN as a modulator. Voluntary movements during STN DBS suppressed tremor. It could be presumed that another pathway contributes to the suppression of tremor. STN has a direct projection from motor-related cortical areas, which is called the hyperdirect pathway, and powerful excitatory effects on the basal ganglia via STN. It is suggested that a voluntary movement initiated by cortical mechanisms conveyed through the cortico-subthalamo-pallidal 'hyperdirect' pathway inhibits large areas of the thalamus and cerebral cortex. Is it possible that this pathway modulates the tremor circuit?

6. CONCLUSIONS

Our clinical observations by surface electromyography show that the effects of Vim DBS and STN DBS on tremor are different. It might be postulated that Vim DBS inhibits the current rising tremor, whereas STN DBS modulates the tremor circuit. This investigation is preliminary and it is as yet very difficult to speculate the mechanisms underlying the modulation of the tremor circuit and the mechanisms of Vim and STN. Further clinical investigations should be carried out.

7. REFERENCES

Benabid, A.L., Pollak, P., Louveau, A., Henry, S., and de Rougemont, J., 1987, Combined (thalamotomy and stimulation) stereotactic surgery of the VIM thalamic nucleus for bilateral Parkinson disease, *Appl. Neurophysiol*. **50**:344.

Bergman, H., Wichmann, T., and DeLong, M.R., 1990, Reversal of experimental parkinsonism by lesions of the subthalamic nucleus, *Science* **249**:1436.

Nambu, A., Tokuno, H., and Takada, M., 2002, Functional significance of the cortico-subthalamo-pallidal 'hyperdirect' pathway, *Neurosci. Res.* **43**:111.

Okuma, Y., Yokochi, F., Endo, T., Oshima, T., and Narabayashi, H., 1991, Motor effects of low-frequency thalamic (VIM) stimulation in patients with extrapyramidal symptoms, 10th International Symposium on Parkinson's Disease held in Tokyo (October 27–30, 1991).

Takahashi, A., Watanabe, K., Satake, K., Hirato, M., and Ohye, C., 1998, Effect of electrical stimulation of the thalamic Vim nucleus on hand tremor during stereotactic thalamotomy, *Electroencephalogr Clin. Neurophysiol.* **109**:376.

THALAMIC AND CORTICAL CHANGES IN PARKINSONIAN DISORDERS

Jasmine M. Henderson,* Virginia Macdonald, and Glenda M. Halliday

1. INTRODUCTION

Both Parkinson's disease (PD) and progressive supranuclear palsy (PSP) are characterized as parkinsonian disorders and share some overlapping clinical features including symptoms such as bradykinesia and muscular rigidity (Gelb et al., 1999; Litvan et al., 1997; Parkinson, 1817). Pathologically, both conditions exhibit substantial loss of dopaminergic neurons from the substantia nigra (Fearnley and Lees, 1991; Halliday et al., 1996; Hardman et al., 1997a). In PD, dopamine replacement with the precursor L-dopa improves parkinsonism in PD (Gelb et al., 1999) but has little sustained effect in PSP (Litvan et al., 1997), assisting the differential diagnosis. In addition, patients with PSP manifest other distinguishing symptoms such as early falls and supranuclear gaze palsy, but generally do not have significant resting tremor, unlike PD patients (Litvan, 1998; Litvan et al., 1996a; Litvan et al., 1997). Such differences likely reflect the differential contribution of non-dopaminergic degeneration in other brain regions. A key feature of the pathophysiology of PD is that the loss of dopamine is associated with increased activation of the subthalamic nucleus and consequently of its targets, the basal ganglia output nuclei (internal globus pallidus and subtantia nigra pars reticulata), which are thought to overinhibit motor-related thalamic regions, resulting in underactivation of cortical targets and the appearance of parkinsonian symptoms (DeLong, 1990). Until recently, it was assumed that the latter regions were preserved in PD. In this chapter we examine the pathological involvement of the thalamus and cortex and the possible clinical significance in both PD and PSP.

* Jasmine M. Henderson. Dept of Pharmacology, Room 211d, Bosch Building, University of Sydney, NSW 2006, Australia. jasmine@med.usyd.edu.au Glenda M. Halliday and Virginia MacDonald, Neuropathology Lab. Prince of Wales Medical Research Institute, Barker Street, Randwick, NSW 2031, Australia.

1.1. Pathological Features of PD and PSP

Apart from the loss of dopaminergic neurons from the substantia nigra pars compacta (SNc) and presence of α-synuclein-immunoreactive Lewy bodies (Lewy, 1913) in remaining neurons (Gelb et al., 1999) several non-dopaminergic cell groups degenerate in PD including the noradrenergic locus coeruleus, cholinergic pedunculopontine tegmentum, serotonergic median raphe nucleus, dorsal motor nucleus of the vagus, central nucleus of the amygdala and hippocampus (Forno, 1996; Gai et al., 1991; Halliday et al., 1990; Harding et al., 2002; Hirsch et al., 1987; Jellinger, 1988; Zweig et al., 1987). Such changes may contribute to several other deficits commonly observed in PD such as subtle attentional deficits, mood dysfunction, autonomic and locomotor changes and microsmia.

The pathological inclusions observed in PSP are different to those observed in PD and are composed of tau-immunoreactive neurofibrillary tangles, glial tangles, tufted astrocytes and threads. Like PD, the cholinergic pedunculopontine tegmentum is also affected in PSP (Gai et al., 1991; Hirsch et al., 1987; Jellinger, 1988), but several critical basal ganglia regions – striatum, internal and external globus pallidus, subthalamic nucleus and substantia nigra pars reticulata, degenerate in PSP (Hardman and Halliday, 1999a; Hardman and Halliday, 1999b; Hardman et al., 1997a; Hardman et al., 1996; Hardman et al., 1997b; Litvan et al., 1996b). In this case, loss of the excitatory subthalamic nucleus and basal ganglia output nuclei would be expected to have opposite effects to PD, yet PSP patients paradoxically exhibit parkinsonian features. It is possible that differential degenerative changes further upstream, at the level of the thalamus and cortex, may contribute to this apparent discrepancy.

We have also recently reported selective degeneration within the thalamus (Henderson et al., 2000a; Henderson et al., 2000b) and cortex (MacDonald and Halliday, 2002) highly complicated brain regions which amongst other functions, relay and process motor information. Neuronal loss from degenerating thalamic and cortical regions also affects many target regions which do not degenerate *per se* but which undergo neurochemical changes and/or alterations in receptor activity which are thought to contribute to the symptoms.

1.2. Thalamic and Cortical Motor Circuitry

The thalamus is a highly complex structure composed of many subregions involved in a variety of functions such as sleep-wake cycle, mood, emotion, memory, movement and sensation (Jones, 1985; Macchi and Jones, 1997). The "motor" (ventral) thalamus comprises the ventral anterior (VA), ventral lateral posterior (VLp) and ventral lateral anterior (VLa) subregions (Macchi and Jones, 1997). The internal globus pallidus largely projects to the ventrolateral anterior (VLa) nucleus and to some extent, the ventral anterior nucleus (VA) which receives substantial inputs from the substantia nigra pars reticulata (Jones, 1985; Kim et al., 1976; Schell and Strick, 1984). VLa and VA project to the supplementary motor area (SMA), anterior cingulate and premotor cortices (Jones, 1985; Schell and Strick, 1984). The deep cerebellar nuclei (dentate, interpositus and fastigial nuclei) project to VLp which in turn projects to the motor cortices (Jones, 1985; Schell and Strick, 1984). The VA and VL nuclei also project to a lesser extent to the dorsal "motor" striatum (McFarland and Haber, 2000).

Studies of the connectivity of the centromedian-parafascicular complex (CM-Pf) of the thalamus demonstrate prominent reciprocal connections with the basal ganglia. The

CM-Pf may not simply serve as a relay, but may also exert a modulatory role over basal ganglia function itself. The centromedian nucleus (CM) forms part of the Nauta-Mehler loop which is a sensorimotor processing loop involving collateral projections from the internal globus pallidus to the centromedian nucleus and back to the striatum (Nauta and Mehler, 1966). CM is also reciprocally connected with the supplementary motor area and motor cortices (Fénelon et al., 1991; Fénelon et al., 1994). The parafascicular nucleus (Pf) projects to most basal ganglia structures: caudate nucleus, globus pallidus and STN (Féger et al., 1994; Fénelon et al., 1991; Nakano et al., 1991; Sadikot et al., 1992). The projections from the CM-Pf are glutamatergic (Mouroux and Féger, 1993) and therefore excitatory and constitute the main thalamostriatal projection (Jones, 1985; Sidibé et al., 2002). The thalamic inputs modulate N-methyl-D-aspartate receptors (NMDA) receptors located on medium spiny projection neurons. Therefore the glutamatergic CM-Pf modulates striatal activity and are also well-placed to influence several other key nuclei in the basal ganglia and motor-related cortical regions implicated in circuitry thought to underlie PD symptoms (Smith et al., 2004).

A number of specialised areas make up the motor cortices, each of which receives different cortical and thalamic inputs (Dum and Strick, 2002; Geyer et al., 2000; Naidich et al., 2001; Picard and Strick, 2001). The primary (1°) motor cortex receives thalamic input from VLp and cortical input from the sensory cortices, SMA and dorsolateral premotor region (DPC, Geyer et al., 2000; Naidich et al., 2001). The 1° motor cortex contains approximately 40% of spinally-projecting cortical neurons and is somototopically organized, controlling kinematic and dynamic parameters of voluntary movements (Geyer et al., 2000; Naidich et al., 2001). Most of the remaining spinally-projecting neurons are contained in the non-1° motor cortices which lie anterior to the precentral gyrus and comprise SMA and pre-SMA on the posterior-mesial surface of the frontal lobe, the DPC on the dorsolateral convexity of the frontal lobe, and the ventrolateral premotor cortex on the lateral convexity. SMA is involved in the initiation and correct performance of movements, whereas pre-SMA is involved in selection and preparation for specific movements required (Dum and Strick, 2002; Geyer et al., 2000; Naidich et al., 2001; Picard and Strick, 2001). Unlike the other motor regions, pre-SMA does not project either to the 1° motor cortex or directly to the spinal cord but rather to SMA and DPC (Geyer et al., 2000; Naidich et al., 2001). Pathology affecting these motor-related cortical regions would be expected to contribute to parkinsonian motor deficits.

2. THALAMIC AND CORTICAL PATHOLOGY IN PD AND PSP

Until recently, there have been few detailed pathological studies of the thalamus in parkinsonian disorders. Degeneration of CM had previously been observed in patients with PD, but was attributed to ageing (Xuereb et al., 1991). In order to establish the nature and location of any pathological involvement of the thalamic and cortical structures in parkinsonism, we recently performed detailed cellular quantitation of a variety of thalamic and cortical structures in 9 PD, 6 PSP and 10 age-matched control cases. Regions analysed via unbiased stereological methods included “limbic” (mediodorsal – MD, and anteroventral – AV nuclei), “motor” (VA, VLa and VLp) and caudal intralaminar (CM-Pf) thalamic nuclei, and cortical regions including SMA, pre- SMA, 1° motor cortex and DPC.

2.1. Thalamic Degeneration in Parkinsonian Disorders

In both PD and PSP we identified substantial degenerative changes in both the thalamus and cortex. Whilst the limbic thalamus (MD and AV) was preserved in both PD and PSP, relative to age-matched controls, substantial cell loss in CM-Pf was present in both diseases with an average neuronal loss of 40% in the PD and 55% in PSP (Henderson et al., 2000a; Henderson et al., 2000b). Although α-synuclein positive Lewy bodies were observed in this region in PD, they were found in less than 1% of remaining neurons in CM-Pf, and were found in other nearby thalamic regions which did not degenerate, suggesting that the presence of Lewy bodies was not primarily responsible for thalamic neuronal death in PD. Tangle formation has been previously described in the thalamus in PSP (Steele et al., 1964), and we also observed tau-immunoreactive pathology in our PSP cases including neurofibrillary tangles, glial tangles and neuropil threads. Intracellular neurofibrillary tangle formation was present in ″10% of remaining neurons in affected regions in PSP, again suggesting that other factor(s) were also involved in cell loss.

Calcium binding proteins buffer intracellular calcium levels. When intracellular calcium rises this can contribute to excitotoxicity mechanisms. Differential distribution of these proteins throughout thalamic and basal ganglia subregions may play a role in differential vulnerability of neuronal subpopulations (Jones and Hendry, 1989; Münkle et al., 1999). Further analysis of neuronal subtypes in thalamic regions by immunohistochemistry for EF hand calcium binding proteins and stereological estimation of neuronal numbers, found it was the parvalbumin-immunoreactive neurons in Pf which predominantly degenerated (by 70%), whereas it was a discrete neuronal subpopulation which did not contain either of the calcium-binding proteins parvalbumin or calbindin which degenerated in CM (Henderson et al., 2000a).

Unlike PD cases in whom there was no significant degeneration in any of the motor thalamic regions studied (VA, VLa or VLp compared to controls), PSP cases exhibited selective degeneration of VLp (Fig. 1) with 22% atrophy and approximately 30% neuronal loss (Halliday, Macdonald and Henderson, submitted). VA and VLa were not significantly different in volume or total neuronal number to either controls or PD cases. Further analysis of neuronal subpopulations affected in thalamic subregions is underway.

2.2. Cortical Degeneration in Parkinsonian Disorders

Whilst there was no significant degeneration of the 1° motor cortex, DPC or SMA in PD cases, relative to controls, the pre-SMA exhibited an overall trend towards cell loss (32% of cresyl violet-stained neurons). Different populations of cortical interneurons contain calcium binding proteins so that virtually all interneurons can be identified using immunohistochemistry for calbindin, calretinin and parvalbumin. Since immunohistochemistry for SMI32 can be used to identify a population of pyramidal neurons (and Betz cells, which contain the non-phosphorylated 200 kDa neurofilament protein), the remaining pyramidal neurons can be calculated by subtracting the total number of interneurons identified from the total number of cresyl violet stained neurons (which stains all neurons) in the region of interest. Using this approach, it was found that there was a highly selective loss of 88% of the corticocortical non-SMI32- immunoreactive pyramidal neurons in the pre-SMA in PD cases (Macdonald and Halliday, 2002).

Similar to PD, PSP cases exhibited not only a similar degree of loss (82%) of corticocortical non-SMI32-immunoreactive pyramidal neurons in the pre-SMA but an additional

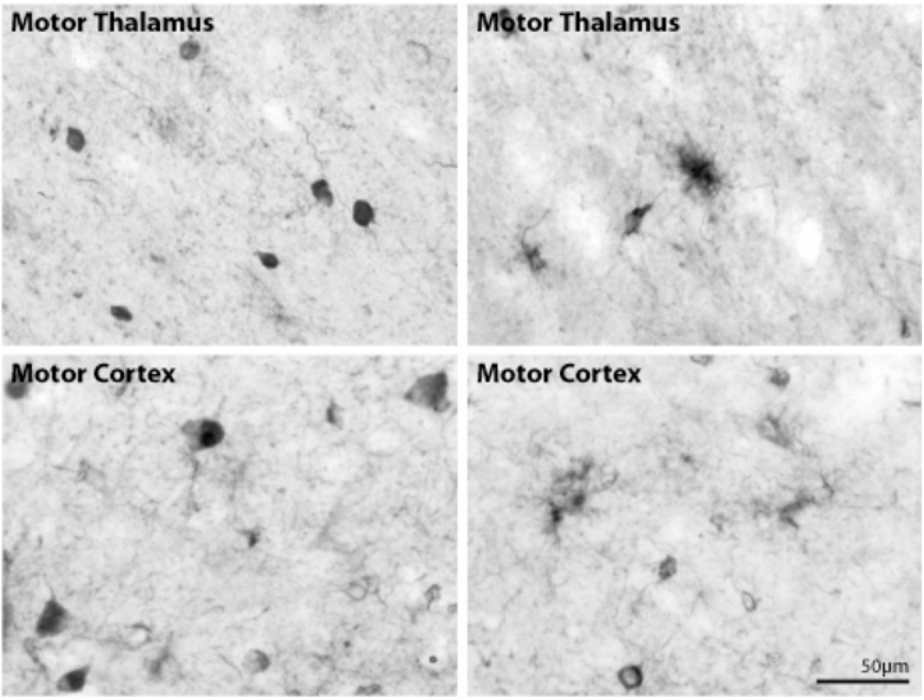

Figure 1. Sections stained immunohistochemically for tau protein from the motor thalamus (upper panels) and motor cortex (lower panels) from PSP cases. Note the tau-immunoreactive neurofibrillary tangles, glial tangles, tufted astrocytes and threads.

31% loss of interneurons (relative to controls, Halliday, Macdonald and Henderson, submitted). PSP cases also exhibited an average of 55% loss of neurons from the 1° motor cortex, which was largely due to loss of inhibitory interneurons (49%). In contrast, there was no cell loss in the DPC in PSP. Tau-positive neurofibrillary and glial tangles and tufted astrocytes were observed throughout the motor cortices in PSP cases (Fig. 1), consistent with other reports (Hanihara et al., 1995; Hauw et al., 1990; Li et al., 1998; Nishimura et al., 1995; Vermesch et al., 1994; Verny et al., 1996).

3. POSSIBLE IMPLICATIONS OF THALAMIC AND CORTICAL PATHOLOGY IN PD AND PSP

In the thalamus, the magnitude of CM-Pf cell loss was similar irrespective of disease duration (Hoehn and Yahr stages 2/3 vs 4/5) or severity of symptoms, suggesting that the degenerative changes are not a late feature of both diseases. The CM-Pf cell loss was similar irrespective of whether the PD cases studied had either resting tremor or not, suggesting that these disturbances are not related to degeneration of this complex (Henderson et al., 2000a). In support of this, whilst none of the PSP cases exhibited tremor all had significant degeneration in this region (Henderson et al., 2000b). All patients studied in both groups had some degree of bradykinesia, rigidity and postural instability making further clinico-

pathological correlations difficult but not discounting a possible contribution from CM-Pf degeneration to one or more of these common parkinsonian symptoms.

Detailed tracing studies of the connectivity of CM-Pf in non-human primates have shown that CM neurons mainly project to the putamen and motor cortices, and it is the parvalbumin-containing Pf neurons which innervate the striatum (Sidibé et al., 2002; Sidibé and Smith, 1999). This suggests that the neurons regulating both striatal (Pf) and cortical motor regions (CM) are affected and would contribute to basal ganglia dysfunction and thalamocortical underactivation in both diseases.

The only other thalamic region found to degenerate was the VLp in PSP cases. Further factor analysis suggested that these changes related to the degree of tau-immunoreactive pathology in both the VLP and the motor cortices and the degree of cell loss in the 1° motor cortex, increasing in amount over the course of the disease (Halliday, Macdonald and Henderson, submitted). The degeneration in VLp in PSP is consistent with a previous descriptive study of the thalamus in this disorder (Amano et al., 1992) and with scanning studies reporting reduced thalamic signal (Blin et al., 1990; Foster et al., 1988; Hanyu et al., 2001) altered glucose metabolism (Blin et al., 1990; Juh et al., 2004) and the loss of synaptophysin (a marker for synapses) in the 1° motor cortex (Bigio et al., 2001) and the progressive atrophy of the superior cerebellar peduncle in PSP (Tsuboi et al., 2003). It is conceivable that degeneration of these cerebellothalamocortical pathways could contribute to the appearance of early falls in PSP (Litvan et al., 1997; Wenning et al., 1999).

In PD resting tremor is thought to result from abnormal activation of cerebellothalamocortical circuitry. Thalamotomy or high frequency stimulation involving the ventral intermediate nucleus (VIM) which forms part of VLp (Macchi and Jones, 1997) is effective for treating resting tremor (Benabid et al., 1991; Ohye et al., 1993). Another possibility, whilst speculative, is that VLp degeneration in PSP may help protect against resting tremor which is not commonly observed in such patients (Litvan et al., 1997).

Significant cortical changes were observed in both diseases with a similar magnitude of loss of pre-SMA corticocortical projection neurons (MacDonald and Halliday, 2002). Selective loss of pyramidal neurons in pre-SMA may underlie the observed perfusion deficits (Fukuda et al., 2001; Sabatini et al., 2000; Thobois et al., 2000) and impaired cortical connectivity (Berardelli et al., 1998; Rowe et al., 2002) reported in PD. Perfusion deficits also occur in both the pre-SMA and primary motor cortex in PSP (Okuda et al., 2000; Piccini et al., 2001; Salmon et al., 1997), consistent with loss of cortical neurons found in these regions in our recent study (Halliday, Macdonald and Henderson, submitted) and with atrophy of these motor cortical regions (Cordato et al., 2000). Overall these changes are likely to have a significant impact at the level of motor cortex excitability apart from any changes resulting from alterations in basal ganglia functioning.

Unlike PD, additional cortical cellular changes were found in PSP with significant loss of cortical interneurons in the pre-SMA and 1° motor cortices, with the degree of cell loss related across these regions. Since the internal globus pallidus also degenerates in PSP, this would reduce inhibitory input to the thalamus (Hardman and Halliday, 1999b) and combined with the loss of inhibitory cortical interneurons, could result in overactivity of cortical projection neurons. In support of this, enlarged cortical somatosensory evoked potentials and an absence of long latency reflexes have been observed in PSP (Kofler et al., 2000; Kuhn et al., 2004).

Overall the thalamic and cortical changes observed in PD and PSP are likely to contribute along with basal ganglia dysfunction to the symptomatology of each disease. The similar degree of involvement of CM-Pf is likely to alter striatal activity and decrease

motor-related cortical activation. The differential involvement of VLp is likely to contribute to some clinical differences, possibly early falls and absence of resting tremor in PSP, as opposed to PD where this structure is preserved. Loss of cortico-cortical pyramidal projection neurons from the pre-SMA in both diseases would be expected to contribute to a reduction in co-ordinated cortical excitation prior to movement onset (MacDonald and Halliday, 2002), exacerbating akinesia and bradykinesia which are observed in both disorders. Whilst there is loss of thalamic inputs to motor related cortical areas (1° motor cortex and SMA), the additional involvement of the interneurons in 1° motor cortex and pre-SMA may produce intracortical disinhibition in these structures in PSP. Further research is required to address the nature of the clinical deficits arising from these thalamic and cortical pathologies.

4. ACKNOWLEDGEMENTS

We would like to acknowledge the generosity of the Eloise Troxel Memorial Grant from the American Society for Progressive Supranuclear Palsy, Australian Research Council, National Health and Medical Research Council and the Australian Brain Foundation for funding for our pathological studies. We acknowledge Ms Katherine Carpenter, Dr Craig Hardman and Dr Antony Harding and Mrs Heidi Cartwright for technical assistance. We would also like to thank the brain tissue donors and their families.

5. REFERENCES

Amano, N., Nagatomo, H., Yokoi, S., Yagishita, S., Siatoh, A., and Mizutani, T., 1992, The thalamic changes in progressive supranuclear palsy, *No To Shinkei* **44**(5):421–428.

Benabid, A., Pollak, P., Gervason, C., Hoffmann, D., Gao, D., Hommel, M., Perret, J., and de Rougemont, J., 1991, Long-term suppression of tremor by chronic stimulation of the ventral intermediate thalamic nucleus, *Lancet* **337**:403–406.

Berardelli, A., Rothwell, J.C., Hallett, M., Thompson, P.D., Manfredi, M., and Marsden, C.D., 1998, The pathophysiology of primary dystonia, *Brain* **121**:1195–1212.

Bigio, E.H., Vono, M.B., Satumtira, S., Adamson, J., Sontag, E., Hynan, L.S., White, C.L., Baker, M., and Hutton, M., 2001, Cortical synapse loss in progressive supranuclear palsy, *J. Neuropatho. Exp. Neurol.* **60**(5):403–410.

Blin, J., Baron, J.C., Dubois, B., Pillon, B., Cambon, H., Cambier, J., and Agid, Y., 1990, Positron emission topography study in progressive supranuclear palsy, Brain hypometabolic pattern and clinicometabolic correlations, *Arch. Neurol.* **47**:747–752.

Cordato, N.J., Halliday, G.M., Harding, A.J., Hely, M.A., and Morris, J.G.L., 2000, Regional brain atrophy in progressive supranuclear palsy and Lewy body disease, *Ann. Neurol.* **47**:718–728.

DeLong, M.R., 1990, Primate models of movement disorders of basal ganglia origin, *Trends Neurosci*. **13**:281–285.

Dum, R.P., and Strick, P.L., 2002, Motor areas in the frontal lobe of the primate, *Physiol. Behav.* **77**:677–682.

Fearnley, J., and Lees, A., 1991, Ageing and Parkinson's disease: substantia nigra regional selectivity, *Brain* **114**:2283–2301.

Féger, J., Bevan, M., and Crossman, A., 1994, The projections from the parafascicular thalamic nucleus to the subthalamic nucleus and the striatum arise from separate neuronal populations: a comparison with the corticostriatal and corticosubthalamic efferents in a retrograde fluorescent double-labelling study, *Neuroscience* **60**:125–132.

Fénelon, G., François, C., Percheron, G., and Yelnik, J., 1991, Topographic distribution of the neurons of the central complex (centre médian-parafascicular complex) and of other thalamic neurons projecting to the striatum in macaques, *Neuroscience* **45**:495–510.

Fénelon, G., Yelnik, J., François, C., and Percheron, G., 1994, Central complex of the primate thalamus: a quantitative analysis of neuronal morphology, *J. Comp. Neurol*. **342**:463–479.

Forno, L.S., 1996, Neuropathology of Parkinson's disease, *J. Neuropathol. Exp. Neurol.* **55**(3):259–272.

Foster, N.L., Gilman, S., Berent, S., Morin, E.M., Brown, M.B., and Koeppe, R.A., 1988, Cerebral hypometabolism in progressive supranuclear palsy studied with positron emission tomography, *Ann. Neurol.* **24**:399–406.

Fukuda, M., Mentis, M., Ma, Y., Antonini, A., Lang, A.E., Lozano, A., et al., 2001, Networks mediating the clinical effects of pallidal brain stimulation for Parkinson's disease: A PET study of resting-state glucose metabolism, *Brain* **124**:1601–1609.

Gai, W.P., Halliday, G.M., Blumbergs, P.C., Geffen, L.B., and Blessing, W.W., 1991, Substance P-containing neurons in the mesopontine tegmentum are severely affected in Parkinson's disease, *Brain* **114**:2253–2267.

Gelb, D.J., Oliver, E., and Gilman, S., 1999, Diagnostic criteria for Parkinson's disease, *Arch. Neurol.* **56**:33–39.

Geyer, S., Matelli, M., Luppino, G., and Zilles, K., 2000, Functional neuroanatomy of the primate isocortical motor system, *Anat. Embryol*. **202**:443–474.

Halliday, G.M., Blumbergs, P.C., Cotton, R.G.H., Blessing, W.W., and Geffen, L.B., 1990, Loss of brainstem serotonin- and substance P-containing neurons in Parkinson's disease, *Brain Res.* **510**:104–107.

Halliday, G.M., McRitchie, D.A., Cartwright, H.R., Pamphlett, R.S., Hely, M.A., and Morris, J.G.L., 1996, Midbrain neuropathology in idiopathic Parkinson's disease and diffuse Lewy body disease, *J. Clin. Neurosci.* **3**:52–60.

Hanihara, T., Amano, N., Takahashi, T., Nagatomo, H., and Yagashita, S., 1995, Distribution of tangles and threads in the cerebral cortex in progressive supranuclear palsy, *Neuropath. Appl. Neurobiol.* **21**:319–326.

Hanyu, H., Asano, T., Sakurai, H., Takasaki, M., Shindo, H., and Abe, K., 2001, Magnetisation transfer measurements of the subcortical grey and white matter in Parkinson's disease with and without dementia and in progressive supranuclear palsy, *Neuroradiology* **43**(7):542–546.

Harding, A.J., Stimson, E., Henderson, J.M., and Halliday, G.M., 2002, Clinical correlates of selective pathology in the amygdala of patients with Parkinson's disease, *Brain* **125**:2431–2445.

Hardman, C.D., and Halliday, G.M., 1999a, The external globus pallidus in patients with Parkinson's disease and progressive supranuclear palsy, *Mov. Disord.* **14**:626–633.

Hardman, C.D., and Halliday, G.M., 1999b, The internal globus pallidus is affected in progressive supranuclear palsy and Parkinson's disease, *Exp. Neurol.* **158**:135–142.

Hardman, C.D., Halliday, G.M., McRitchie, D.A., Cartwright, H.R., and Morris, J.G.L., 1997a, Progressive supranuclear palsy affects both the substantia nigra pars compacta and reticulata, *Exp. Neurol.* **144**:183–192.

Hardman, C.D., McRitchie, D.A., Halliday, G.M., Cartwright, H.R., and Morris, J.G.L., 1996, The substantia nigra pars reticulata in Parkinson's disease, *Neurodegeneration* **5**:49–55.

Hardman, C.D., McRitchie, D.A., Halliday, G.M., and Morris, J.G.L., 1997b, The subthalamic nucleus in Parkinson's disease and progressive supranuclear palsy, *J. Neuropathol. Exp. Neurol.* **56**:132–142.

Hauw, J., Verny, M., Delaere, P., Cervera, P., He, Y., and Duyckaerts, C., 1990, Constant neurofibrillary changes in the neocortex in progressive supranuclear palsy: Basic differences with Alzheimer's disease and aging, *Neurosci. Lett.* **119**:182–186.

Henderson, J.M., Carpenter, K., Cartwright, H., and Halliday, G.M., 2000a, Degeneration of the centre median-parafascicular complex in Parkinson's disease, *Ann. Neurol.* **47**:345–352.

Henderson, J.M., Carpenter, K., Cartwright, H., and Halliday, G.M., 2000b, Loss of thalamic intralaminar nuclei in progressive supranuclear palsy and Parkinson's disease: clinical and therapeutic implications, *Brain* **123**:1410–1421.

Hirsch, E.C., Graybiel, A.M., Duyckaerts, C., and Javoy-Agid, F., 1987, Neuronal loss in the pedunculopontine tegmental nucleus in Parkinson's disease and progressive supranuclear palsy, *Proc. Natl. Acad. Sci. U.S.A.* **84**:5976–5981.

Jellinger, K., 1988, The pedunculopontine nucleus in Parkinson's disease, progressive supranuclear palsy and Alzheimer's disease, *J. Neurol. Neurosurg. Psychiatry* **51**:540–543.

Jones, E.G., 1985, The Thalamus, New York: Plenum Press.

Jones, E.G., and Hendry, S.H.C., 1989, Differential calcium binding protein immunoreactivity distinguishes classes of relay neurons in monkey thalamic nuclei, *Eur. J. Neurosci.* **1**(3):222–246.

Juh, R., Kim, J., Moon, D., Choe, B., and Suh, T., 2004, Different metabolic patterns analysis of Parkinsonism on the [18]F-FDG PET, *Eur. J. Radiol.* **51**:223–233.

Kim, R., Nakano, K., Jayaraman, A., and Carpenter, M.B., 1976, Projections of the globus pallidus and adjacent structures: an autoradiographic study in the monkey, *J. Comp. Neurol.* **1976**:263–290.

Kofler, M.J.M., Reggiani, L., and Wenning, G.K., 2000, Somatosensory evoked potentials in progressive supranuclear palsy, *J. Neurol. Sci.* **179**:85–91.

Kuhn, A.A., Grosse, P., Holtz, K., Brown, P., Meyer, B.U., and Kupsch, A., 2004, Patterns of abnormal motor cortex excitability in atypical parkinsonian syndromes, *Clin. Neurophysiol.* **115**:1786–1795.

Lewy, F.H., 1913, Zur pathologischen anatomie der Paralysis Agitans, *Dtsh. Z. Nervenheilk.* **50**:50–55.

Li, F., Iseki, E., Odawara, T., Kosaka, K., Yagashita, S., and Amano, N., 1998, Regional quantitative analysis of tau-positive neurons in progressive supranuclear palsy: comparison with Alzheimer's disease, *J. Neurol. Sci.* **159**:73–81.

Litvan, I., 1998, Progressive supranuclear palsy revisited, *Acta Neurol. Scand.* **98**:73–84.

Litvan, I., Agid, Y., Calne, D., Campbell, G., Dubois, B., Duvoisin, R.C., Goetz, C., Golbe, L.I., Grafman, J., Growdon, J.H., Hallet, M., Jankovic, J., Quinn, N.P., Tolosa, E., and Zee, D.S., 1996a, Clinical research criteria for the diagnosis of progressive supranuclear palsy (Steele-Richardson-Olszewski syndrome): report of the NINDS-SPSP international workshop, *Neurology* **47**:1–9.

Litvan, I., Campbell, G., Mangone, C.A., Verny, M., McKee, A., Chaudhuri, K.R., Jellinger, K., Pearce, R.K.B., and D'Olhaberriague, L., 1997, Which clinical features differentiate progressive supranuclear palsy (Steele-Richardson-Olszewski syndrome) from related disorders? A clinicopathological study, *Brain* **120**:65–74.

Litvan, I., Hauw, J.J., Bartko, J.J., Lantos, P.L., Daniel, S.E., Horoupian, D.S., McKee, A., Dickson, D., Bancher, C., Tabaton, M., Jellinger, K., and Anderson, D.W., 1996b, Validity and reliability of the preliminary NINDS neuropathologic criteria for progressive supranuclear palsy and related disorders, *J. Neuropathol. Exp. Neurol.* **55**:97–105.

Macchi, G., and Jones, E.G., 1997, Toward an agreement on terminology of nuclear and subnuclear divisions of the motor thalamus, *J. Neurosurg.* **86**:670–685.

MacDonald, V., and Halliday, G.M., 2002, Selective loss of pyramidal neurons in the pre-supplementary motor cortex in Parkinson's disease, *Mov. Disord.* **17**(6):1166–1173.

McFarland, N.R., and Haber, S.N., 2000, Convergent inputs from thalamic motor nuclei and frontal cortical areas to the dorsal striatum in the primate, *J. Neurosci.* **20**(10):3798–3813.

Mouroux, M., and Féger, J., 1993, Evidence that the parafascicular projection to the subthalamic nucleus is glutaminergic, *NeuroReport* **4**:613–615.

Münkle, M.C., Waldvogel, H.J., and Faull, R.L.M., 1999, Calcium binding protein immunoreactivity delineates the intralaminar nuclei of the thalamus in the human brain, *Neuroscience* **90**:485–491.

Naidich, T.P., Hof, P.R., Yousry, T.A., and Yousry, I., 2001, The motor cortex: anatomic substrates of function, *Neuroimaging Clin. N. Am.* **11**:171–193.

Nakano, K., Hasegawa, Y., Kayahara, T., and Kuga, Y., 1991, Topographical organisation of the thalamostriatal projection in the Japanese monkey, *Macaca fuscata*, with special reference to the centremedian-parafascicular and motor thalamic nuclei, In: Beradi, G., Carpenter, M.B., Di Chiara, G., Morelli, M., and Stanzione, P., editors, The Basal Ganglia III, New York: Plenum Press, p 6–72.

Nauta, W., and Mehler, W., 1966, Projections of the lentiform nuclei in the monkey, *Brain Res.* **1**:3–42.

Nishimura, T., Ikeda, K., Akiyama, H., Kondo, H., Kato, M., Li, F., et al., 1995, Immunohistochemical investigation of tau-positive structures in the cerebral cortex of patients with progressive supranuclear palsy, *Neurosci. Lett.* **210**:123–126.

Ohye, C., Shibazaki, T., Hirai, T., Kawashima, Y., Hirato, M., and Matsumura, M., 1993, Tremor-mediating thalamic zone studied in humans and in monkeys, *Stereotact. Funct. Neurosurg.* **60**:136–145.

Okuda, B., Tachibana, H., Kawabata, K., Takeda, M., and Sugita, M., 2000, Cerebral blood flow in corticobasal degeneration and progressive supranuclear palsy, *Alzheimer Dis. Assoc. Disord.* **14**:46–52.

Parkinson, J., 1817, Essay on the Shaking Palsy, London: Sherwood, Neely and Jones.

Picard, N., and Strick, P.L., 2001, Imaging the premotor areas, *Curr. Opin. Neurobiol.* **11**:663–672.

Piccini, P., Yebenez, J., Lees, A.J., Ceravolo, R., Turjanski, N., Pramstaller, P., et al., 2001, Familial progressive supranuclear palsy: detection of subclinical cases using 18F-dopa and 18fluorodeoxyglucose positron emission tomography, *Arch. Neurol.* **58**:1846–1851.

Rowe, J., Stephen, K.E., Friston, K., Frackowiak, R., Lees, A., and Passingham, R., 2002, Attention to action in Parkinson's disease. Impaired effective connectivity among frontal cortical regions, *Brain* **125**:276–289.

Sabatini, U., Boulanouar, K., Martin, F., Carel, C., Colonese, C., Bozzao, L., et al., 2000, Cortical motor reorganisation in akinetic patients with Parkinson's disease: A functional MRI study, *Brain* **123**:394–403.

Sadikot, A., Parent, A., and Francois, C., 1992, Efferent connections of the centromedian and parafascicular thalamic nuclei in the squirrel monkey: a PHA-L study of subcortical projections, *J. Comp. Neurol.* **315**:137–159.

Salmon, E., Van der Linden, M., and Franck, G., 1997, Anterior cingulate and motor network impairment in progressive supranuclear palsy, *Neuroimage* **5**:173–178.

Schell, G.R., and Strick, P.L., 1984, The origin of thalamic inputs to the arcuate premotor and supplementary motor areas, *J. Neurosci.* **4**(2):539–560.

Sidibé, M., Paré, J-F., Raju, D., and Smith, Y., 2002, Anatomical and functional relationships between intralaminar thalamic nuclei and basal ganglia in monkeys. In: Nicholson LB, and Faull RLM, editors. The basal ganglia VII, New York: Kluver Academic/Plenum Publishers, p 409–420.

Sidibé, M., and Smith, Y., 1999, Thalamic inputs to striatal interneurons in monkeys: synaptic organization and co-localization of calcium binding proteins, *Neuroscience* **89**(4):1189–1208.

Smith, Y., Raju, D.V., Paré, J-F., and Sidibé, M., 2004, The thalamostriatal system: a highly specific network of the basal ganglia circuitry, *Trends Neurosci.* **27**(9):520–527.

Steele, J.C., Richardson, J.C., and Olszewski, J., 1964, Progressive supranuclear palsy: a heterogeneous degeneration involving the brainstem, basal ganglia and cerebellum with vertical gaze and pseudobulbar palsy, nuchal dystonia and dementia, *Arch. Neurol.* **10**:333–359.

Thobois, S., Dominey, P., Decety, J., Pollak, P., Gregoire, M., Le Bars, D., et al., 2000, Motor imagery in normal subjects and in asymmetrical Parkinson's disease: A PET study, *Neurology* **55**:996–1002.

Tsuboi, Y., Slowinski, J., Josephs, K.A., Honer, W.G., Wszolek, Z.K., and Dickson, D.W., 2003, Atrophy of superior cerebellar peduncle in progressive supranuclear palsy, *Neurology* **60**:1766–1769.

Vermesch, P., Robitaille, Y., Bernier, L., Wattez, A., Gauvreau, D., and Delacourte, A., 1994, Biochemical mapping of neurofibrillary degeneration in a case of progressive supranuclear palsy: evidence for general cortical involvement, *Acta Neuropathol.* **87**:572–577.

Verny, M., Duyckaerts, C., Agid, Y., and Hauw, J.J., 1996, The significance of cortical pathology in progressive supranuclear palsy. Clinico-pathological data in 10 cases, *Brain* **119**:1123–1136.

Wenning, G.K., Ebersbach, G., Verny, M., Chaudhuri, K.R., Jellinger, K., McKee, A., Poewe, W., and Litvan, I., 1999, Progression of falls in postmortem-confirmed parkinsonian disorders, *Mov. Disord.* **14**(6):947–950.

Xuereb, J.H., Perry, R.H., Candy, J.M., Perry, E.K., Marshall, E., and Bonham, J.R., 1991, Nerve cell loss in the thalamus in Alzheimer's disease and Parkinson's disease, *Brain* **114**:1363–1379.

Zweig, R.M., Whitehouse, P.J., Casanova, M.F., Walker, L.C., Jankel, W.R., and Price, D.L., 1987, Loss of pedunculopontine neurons in progressive supranuclear palsy, *Ann. Neurol.* **22**:18–25.

NEUROGENESIS IN THE BASAL GANGLIA IN HUNTINGTON'S DISEASE IN THE HUMAN BRAIN AND IN AN ANIMAL MODEL

Maurice A. Curtis, Andrew S. Tattersfield, Monica Kam, Ellen B. Penney, Ryan J. Croon, Yin Wai Liu, Michael Dragunow, Richard L. M. Faull, and Bronwen Connor*

1. INTRODUCTION

The vast majority of neurons in the mammalian brain are produced during embryonic development. However, continued neurogenesis is observed in distinct regions of the adult mammalian brain. In the hippocampus, new neurons are produced from progenitor cells residing in the subgranular zone (SGZ) of the dentate gyrus (Altman and Das, 1965; Kaplan and Hinds, 1977; Eriksson et al., 1998; Gould et al., 1999; Kornack and Rakic, 1999). Similarly, progenitor cells persist and continue to proliferate in the subventricular zone (SVZ) / subependymal layer (SEL) lining the lateral ventricles (Altman, 1969; Kaplan and Hinds, 1977; Lois and Alvarez-Buylla, 1994; Lois et al., 1996; Thomas et al., 1996). However, unlike the dentate gyrus, SVZ/SEL neuronal precursor cells in rodents and non-human primates migrate long distances via the rostral migratory stream (RMS) to their final destination in the olfactory bulb where they differentiate into granule and periglomular neurons (Luskin, 1993; Lois and Alvarez-Buylla, 1994; Lois et al., 1996; Thomas et al., 1996).

The presence of ongoing neurogenesis in the adult mammalian brain raises the exciting possibility that endogenous progenitor cells may be able to generate new neurons to replace cells lost through brain injury or neurodegenerative disease. However, relatively little is known regarding the response of endogenous progenitor cells to cerebral injury and their potential involvement in the pathophysiology of neurodegenerative disease. Recent studies of the adult rodent dentate gyrus have demonstrated that progenitor cells in this region respond to a range of injuries including excitotoxic or mechanical lesions, focal ischemic

* Maurice Curtis, Monica Kam, Ellen Penney, Yin Wai Liu and Richard Faull, Dept of Anatomy with Radiology, Faculty of Medical and Health Sciences, University of Auckland, Auckland, New Zealand. Andrew Tattersfield, Ryan Croon, Michael Dragunow and Bronwen Connor, Dept of Pharmacology and Clinical Pharmacology, Faculty of Medical and Health Sciences, University of Auckland, Auckland, New Zealand.

injury or chemoconvulsant-induced seizure activity by increasing neurogenesis (Gould and Tanapat, 1997; Parent et al., 1997; Liu et al., 1998; Jin et al., 2001). An increase in SVZ progenitor cell proliferation has also been observed in various injury models including aspiration or transection lesions of the forebrain, inflammatory or chemical demyelination, percussion trauma, chemoconvulsant-induced seizure activity and focal ischemic injury of the adult rodent brain (Willis et al., 1976; Szele and Chesselet, 1996; Weinstein et al., 1996; Holmin et al., 1997; Calza et al., 1998; Nait-Oumesmar et al., 1999; Jin et al., 2001; Arvidsson et al., 2002; Parent et al., 2002; Parent et al., 2002). Furthermore, recent studies by Parent and colleagues (2002a; 2002b) and Arvidsson and colleagues (2002) have demonstrated an increase in SVZ neurogenesis following focal ischemic injury or chemoconvulsant-induced seizure activity, leading to the migration of neuroblasts from the SVZ to damaged areas of the striatum, where they express markers of developing and mature striatal medium-sized spiny neurons.

Neurogenesis was also recently been demonstrated in the normal adult human brain (Eriksson et al., 1998). However, the response of neural progenitor cells in the SVZ/SEL of the adult human brain in response to neurodegenerative diseases, such as Huntington's disease (HD), had never been previously demonstrated. This chapter reviews our recent studies examining whether progenitor cell proliferation and neurogenesis occurs in the SVZ/SEL adjacent to the caudate nucleus in response to the loss of GABAergic medium spiny striatal projection neurons in both the adult human HD brain and the quinolinic acid (QA) lesion rodent model of HD.

2. NEUROGENESIS IN THE ADULT HUMAN HUNTINGTON'S DISEASE BRAIN

We compared the number of proliferating progenitor cells in the SEL of control (n = 6) and HD (n = 9) human brains by using antibodies to the cell-cycle marker proliferating cell nuclear antigen (PCNA) which labels cells in the S phase of cell division. While we detected a small number of PCNA-positive cells in the SEL of control human brains, the number of PCNA-positive cells was considerably increased in HD brains (Figure 1). Using a 5-point qualitative PCNA grading scale, the thickness of the SEL and the number of PCNA-positive cells in the SEL in control and HD brains were rated by an observer blind to the case numbers. The results showed a significant difference (Mann-Whitney *U* test; $P < 0.0008$) in the thickness of the SEL and the number of PCNA-positive cells in the SEL between control and HD brains (Figure 1; Curtis et al., 2003). Statistical analysis also revealed that the grade of PCNA staining in HD cases significantly (Spearman rank correlation; $P < 0.003$) correlated with the HD neuropathological grade and the number of CAG repeats in the expanded allele of the HD IT15 gene (Spearman rank correlation; $P < 0.02$) (Figure 1; Curtis et al., 2003). No correlation was found between the PCNA grade and the age, sex or postmortem delay of the cases.

To investigate the fate of PCNA-positive cells in the SEL of the diseased adult human brain, we applied double label immunofluorescence techniques using antibodies against βIII-tubulin which labels neurons early in their development, and the glial cell marker GFAP. Using fluorescent confocal microscopy, we detected colocalisation of the PCNA-positive cells with the early neuronal marker βIII-tubulin in the SEL of HD cases (Figure 2; Curtis et al., 2003). We used a Hoechst nuclear DNA stain to confirm that PCNA-positive staining was located in the nuclear region of the βIII-tubulin-positive cells.

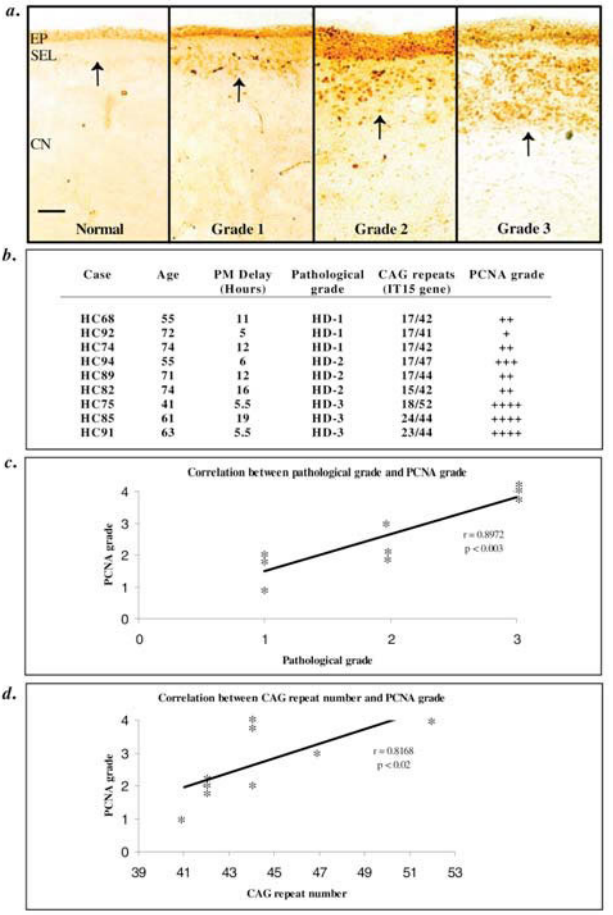

Case	Age	PM Delay (Hours)	Pathological grade	CAG repeats (IT15 gene)	PCNA grade
HC68	55	11	HD-1	17/42	++
HC92	72	5	HD-1	17/41	+
HC74	74	12	HD-1	17/42	++
HC94	55	6	HD-2	17/47	+++
HC89	71	12	HD-2	17/44	++
HC82	74	16	HD-2	15/42	++
HC75	41	5.5	HD-3	18/52	++++
HC85	61	19	HD-3	24/44	++++
HC91	63	5.5	HD-3	23/44	++++

Figure 1. PCNA immunoreactivity is increased in the SEL in HD cases. (a) Table summerising the age, post-mortem delay, pathological grade, CAG trinucleotide repeat length in the IT15 gene, and PCNA grade for each HD case. For each HD case, the level of PCNA immunoreactivity in the SEL was assessed by using a qualitative 5-point grading scale (PCNA grade: 0 = small; + = few; ++ = moderate, +++ = many; ++++ = large number of PCNA-positive cells). (b) Compared with control brain, the thickness of the SEL and the number of PCNA-positive cells in the SEL are increased as the pathological grade of HD increases (grade 1 to grade 3). In each case, the boundary of the SEL with the caudate nucleus (CN) is indicated by an arrow. (EP, ependymal layer; LV, lateral ventricle). (c) Graph showing a significant correlation between pathological grade and PCNA grade in the HD cases (Spearman rank correlation, $r = 0.8972$, $P \leq 0.003$). (d) Graph showing a significant correlation between CAG trinucleotide repeat length in the IT15 gene and PCNA grade in the HD cases (Spearman rank correlation, $r = 0.8168$, $P \leq 0.02$). (Scale bar = 80 μm). Reprinted with permission from PNAS, Curtis et al., 2003.

The demonstration that βIII-tubulin stained processes colocalised with PCNA-positive cell nuclei in the HD SEL indicates that these PCNA-positive cells exhibit a neuronal phenotype (Figure 2; Curtis et al., 2003). The PNCA/βIII-tubulin-positive cells were located mainly in the deeper regions of the SEL adjacent to the caudate nucleus and comprised in order of 5% of the PCNA-positive cells in the SEL (Curtis et al., 2003). Fluorescent confocal microscopy using antibodies against PCNA and GFAP combined with a Hoechst

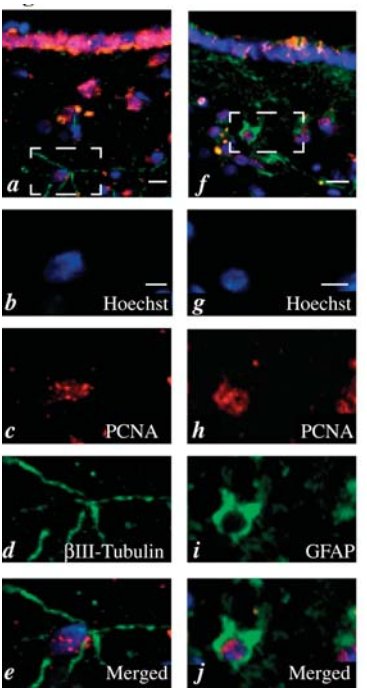

Figure 2. Newly generated cells in the SEL of the HD brain exhibit either a neuronal or glial phenotype. ***a.*** Confocal microscopy demonstrates that the SEL of the HD brain contains newly generated cells that co-express PCNA, βIII-tubulin and stain with a Hoechst stain. The new neurons are located in the lower part of the SEL. Scale bar = 6 μm. ***b–d;*** Higher magnification of the neuron outlined with a box in ***a***. Scale bar = 3 μm. ***b.*** Hoechst (blue) stains the nucleus of cells in the SEL. ***c.*** PCNA (red) labels the nucleus of a new cell and has a granular appearance. ***d.*** βIII-tubulin (green) labels the cytoplasm of neurons early in their development. ***e.*** The merged image demonstrates co-expression of PCNA and βIII-tubulin in the same cell that displays a Hoechst stain indicating that neurogenesis occurs in the SEL of the HD brain. ***f.*** Confocal microscopy demonstrates that the SEL of the HD brain also contains newly generated cells that co-express PCNA and GFAP and stain with a Hoechst stain. These new glial cells are located in the upper part of the SEL in the HD brain. Scale bar = 18 μm. ***g–i;*** Higher magnification of the glial cell outlined with a box in ***f***. Scale bar = 9 μm. ***g.*** Hoechst (blue) stains the nucleus of cells in the SEL. ***h.*** PCNA (red) labels the nucleus of the cell with punctate staining. ***i.*** The astrocytic marker GFAP (green) labels the cytoplasm of the cell. ***j.*** The merged image demonstrates co-expression of PCNA and GFAP in the same cell that displays a Hoechst stain indicating the occurrence of gliogenesis. Reprinted with permission from PNAS, Curtis et al., 2003.

stain demonstrated large numbers of cells in the SEL had intense GFAP cytoplasmic staining, with the nuclear region clearly delineated by PCNA and Hoechst staining (Figure 2; Curtis et al., 2003). The demonstration that the GFAP-stained cytoplasm colocalised with PCNA-positive nuclei in the HD SEL (Figure 2) indicates that these PCNA-positive cells exhibit a glial phenotype (Curtis et al., 2003). The PCNA/GFAP-positive cells were identified mainly in the more superficial region of the SEL adjacent to the ependymal layer (Figure 2) and comprised approximately 50% of the PCNA-positive cells in the SEL (Curtis et al., 2003).

3. NEUROGENESIS IN THE STRIATUM OF THE QUINOLINIC ACID LESION RODENT MODEL OF HUNTINGTON'S DISEASE

In order to better understand the potential role of endogenous neuronal replacement in neurodegenerative disorders and extend our initial observations in the human HD brain, we also examined the effect of striatal cell loss on neurogenesis in the SVZ of the adult rodent forebrain using the quinolinic acid (QA) lesion rat model of HD. To determine the effect of QA lesioning on SVZ neurogenesis, we first examined whether the loss of GABAergic medium spiny projection neurons in the QA-lesioned striatum induced SVZ cell proliferation. Rats received a single injection of the mitotic marker bromodeoxyuridine (BrdU; 200 mg/kg i.p.) on days 1, 3, 7, 14, 21 and 28 after a direct striatal infusion of QA or vehicle solution and were killed 24 h later. In the contralateral and sham-lesioned hemisphere, BrdU labelling was confined to the SVZ. In contrast, at all time points examined BrdU labelling was increased in the SVZ in the lesioned hemisphere and BrdU-positive cells were also observed in the adjacent striatum (Tattersfield et al., 2004). Quantification revealed that QA lesion-induced striatal cell loss produced a significant increase in the area of BrdU immunoreactivity from 1 to 14 days post-lesion compared with sham-lesioned animals ($P \leq 0.05$) with the greatest increase in BrdU immunoreactivity observed at 7 days post-lesion ($P < 0.004$) (Tattersfield et al., 2004). This indicates that the loss of GABAergic medium spiny projection neurons in the QA-lesioned striatum increases SVZ progenitor cell proliferation and results in the expansion of the SVZ, possibly due to the accumulation of cells in the SVZ due to accelerated proliferation.

We next examined whether the expansion of the SVZ observed following QA lesioning corresponded to an increase in the number of immature neurons in the lesioned hemisphere. Rats were given a total of four injections of BrdU (200 mg/kg i.p. per injection) 24 h apart on days 6–9 after QA lesioning. This interval of BrdU labelling was chosen based on the results of our proliferation study, which demonstrated maximal increase in SVZ cell proliferation at 7 days after QA infusion. The rats were then killed 1, 7, 14, 21 and 28 days after the last BrdU injection (days 10, 16, 23, 30 and 37 after QA lesioning). The marker doublecortin (Dcx), a microtubule-associated protein present in migrating neuronal precursors (neuroblasts) was used to detect neuroblasts after QA lesioning. In the contralateral and sham-lesioned hemispheres, Dcx was expressed in the SVZ and RMS with no Dcx-expressing cells present in the striatum. In contrast, Dcx-immunoreactivity was greatly increased in the SVZ ipsilateral to the QA-lesioned striatum at all time points examined (Tattersfield et al., 2004). In addition, large numbers of Dcx-immunoreactive cells were observed in the QA-lesioned striatum, in both the transition zone and the lesion core, and demonstrated morphological characteristics of both migrating (elongated and leading processes) and non-migrating cells (symmetric with several processes in different directions) (Tattersfield et al., 2004). In order to confirm that the cells detected in the lesioned striatum expressing Dcx were newly generated immature neurons we used BrdU labelling and double label immunofluorescence for cell-type specific markers. At 10 days post QA lesion we observed that the majority (95%) of BrdU-positive cells in the ipsilateral SVZ co-expressed Dcx. While we continued to observe Dcx-positive cells in the ipsilateral SVZ until 37 days post lesion, none of the Dcx-positive cells detected in the ipsilateral SVZ co-expressed BrdU after 10 days post QA lesion indicating the migration of BrdU labelled cells from the SVZ (Tattersfield et al., 2004). At each of the time points examined we also observed that BrdU-positive cells within the QA lesioned striatum co-expressed Dcx demonstrating the presence of newly generated immature neurons (Tattersfield et al., 2004).

Dcx-immunoreactive cells detected in the QA lesioned striatum were confirmed to be neuronal as they co-expressed the neuron-specific marker MAP2 within 10 days post QA lesion (Figure 3; Tattersfield et al., 2004). The Dcx-MAP2-double labelled cells typically exhibited morphologies consistent with migrating neuroblasts, including elongated cell

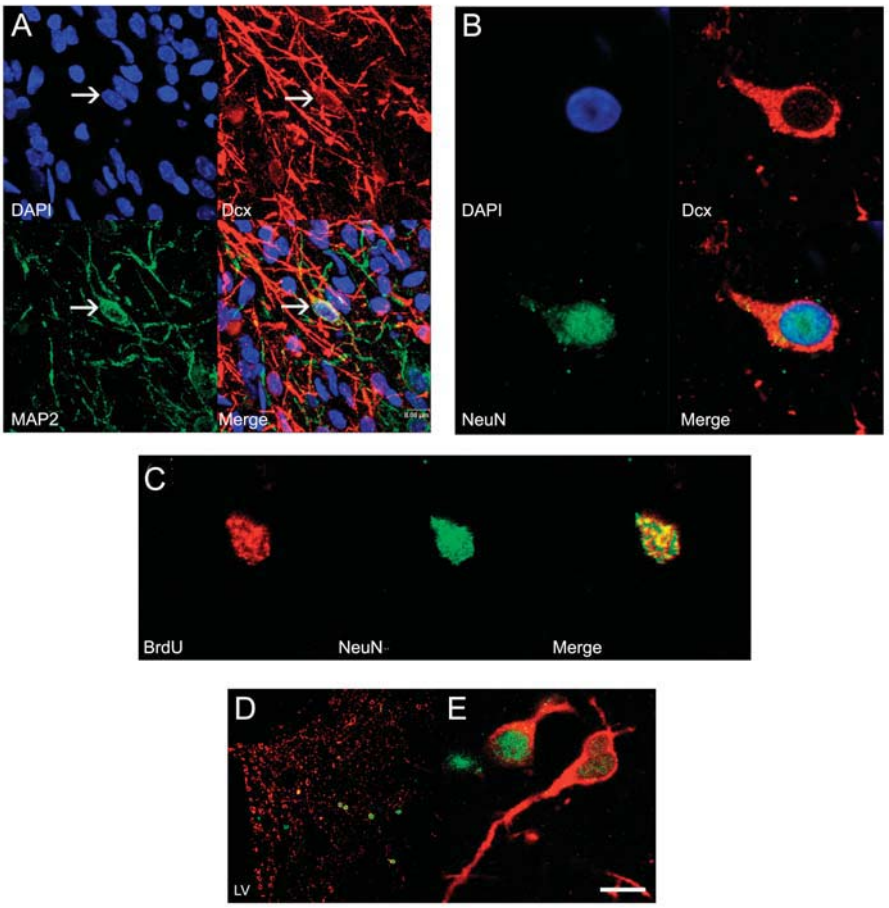

Figure 3. Newly generated cells in the QA lesioned striatum exhibit neuronal morphology. (A) Confocal microscopy demonstrating that newly generated cells in the QA lesioned striatum co-express Dcx (red) and the neuronal marker MAP2 (green) and stain with a nuclear stain, DAPI (blue) 10 days post lesion. The merged image demonstrates co-expression of Dcx and MAP2 in the same cell that displays a DAPI stain (arrow). (B) Confocal microscopy demonstrating that newly generated cells in the QA lesioned striatum co-express Dcx (red) and the mature neuronal marker NeuN (green) and stain with a nuclear stain, DAPI (blue) 16 days post lesion. The merged image demonstrates co-expression of Dcx and NeuN in the same cell that displays a DAPI stain. (C) Confocal microscopy demonstrates that BrdU-labelled cells (red) in the QA lesioned striatum co-express the mature neuronal marker NeuN (green) 37 days post lesion. (D) Low magnification confocal image of the QA lesioned striatum demonstrating the presence of Dcx-positive cells (red) co-expressing NeuN (green) in the transition zone of the lesion 37 days post lesion. (E) High magnification confocal image of two neurons in the QA lesioned striatum co-expressing Dcx (red) and NeuN (green). Scale bar: 24 µm for A, 10 µm for B and E, 20 µm for C and 70 µm for D. LV = lateral ventricle. Reprinted with permission from Elsevier, Tattersfield et al., 2004.

bodies and bipolar processes. These data indicate that QA lesion-induced striatal cell loss expands the rostral forebrain SVZ neuroblast population and that selective striatal cell loss induced by the QA lesion stimulates neurogenesis in the lesioned striatum at the time points examined. Furthermore, we propose that SVZ neuroblasts undergo putative migration from the SVZ to regions of neuronal cell loss in the QA lesioned striatum.

We then examined whether Dcx-positive cells located in the lesioned striatum also co-expressed the mature neuronal marker NeuN in order to determine whether Dcx-positive neuroblasts located in the lesioned striatum generate new mature neurons and whether these new neurons persist in the lesioned striatum. As demonstrated by fluorescent confocal analysis, within 16 days post QA lesion, a subpopulation (~5%) of Dcx-positive cells within the lesioned striatum co-expressed the mature neuronal marker, NeuN (Figure 3; Tattersfield et al., 2004). These cells were found in the dorsomedial striatum and extending into the transition zone of neuronal cell loss in the lesioned striatum. By 23 days post QA lesion approximately 10–20% of Dcx-positive cells exhibited neuronal morphologies and were immunoreactive for the mature neuronal marker NeuN (Tattersfield et al., 2004). The presence of Dcx/NeuN co-expressing cells within the QA lesioned striatum was observed to persist up to 37 days post lesion (Figure 3; Tattersfield et al., 2004). Survival of newly generated neurons in the QA lesioned striatum was further supported by the presence of cells double labelled with BrdU and NeuN at 37 days post lesion (Figure 3; Tattersfield et al., 2004). Cells co-expressing BrdU and NeuN were observed to extend into the transition zone of neuronal cell loss in the lesioned striatum. These findings demonstrate the presence of newly generated mature neurons in the QA lesioned striatum, which persist up to 37 days post lesion. At present however, the integration of these cells into the lesioned striatum remains unknown and further studies are being undertaken to determine whether the newly generated neurons differentiate into striatal neuronal subtypes.

4. CONCLUSION

Our findings indicate a high level of neural plasticity in the adult human brain in response to the degenerating environment that is present in HD. We have demonstrated increased cell proliferation and the generation of new neurons in the HD human brain (Curtis et al., 2003). In support of these observations, we have also demonstrated that the loss of GABAergic medium spiny projection neurons following QA striatal lesioning of the adult rat brain increases SVZ progenitor cell proliferation and leads to the putative migration and formation of new neurons in the lesioned striatum (Tattersfield et al., 2004). Due to the close proximity of the SVZ/SEL with the adjacent striatum, we believe HD is a prime candidate for the augmentation of striatal neurogenesis in response to neuronal cell loss. Since, in early neuronal development, cells migrate from the SVZ/SEL to form the caudate nucleus, it would not be unreasonable to suggest that these immature neurons have the potential to migrate to the caudate nucleus in response to neuronal cell loss occurring in the HD brain. Furthermore, the observation of increased numbers of progenitor cells in the SEL with advancing neuropathological grades of HD would indicate that proliferation is a response to greater numbers of degenerating neurons in the caudate nucleus. However, it is apparent that the level of neurogenesis observed in the HD brain is insufficient to compensate for the progressive cell loss observed in the degenerating adult brain. In the QA lesion rat model, the initial generation of neuroblasts following QA lesioning far exceeds the final number of new mature neurons generated in the lesioned striatum, indicat-

ing that many of these neuroblasts fail to survive and/or differentiate in the damaged striatum possibly due to inadequate levels of local microenvironment signals necessary for neuronal differentiation and survival or the presence of inhibitory factors. A variety of growth factors (e.g. EGF, FGF-2, BDNF; Kuhn et al., 1997; Zigova et al., 1998; Benraiss et al., 2001; Yoshimura et al., 2001) and pharmaceutical agents (e.g. lithium; Chen et al., 2000) have been shown to induced proliferation and neurogenesis. If the potential for endogenous neural replacement could be augmented pharmacologically with the use of exogenous growth factors or pharmaceutical agents that increased the rate of proliferation and directed neuronal migration and differentiation, then the rate of cell loss may be slowed, and clinical improvements may be observed. We believe that the discovery that the diseased adult human brain is capable of neuronal regeneration in response to neuronal cell loss will be of major relevance for the development of therapeutic approaches in the treatment of neurodegenerative diseases.

5. ACKNOWLEDGEMENTS

This work was supported by grants from the Health Research Council of New Zealand and the Neurological Foundation of New Zealand. Imaging was carried out in the Biomedical Imaging Research Unit located at the Faculty of Medical and Health Sciences.

6. REFERENCES

Altman, J., 1969, Autoradiographic and histological studies of postnatal neurogenesis. IV. Cell proloferation and migration in the anterior forebrain, with special reference to persisting neurogenesis in the olfactory bulb, *J. Comp. Neurol*. **137**:433–457.

Altman, J., and Das, G.D., 1965, Autoradiographic and histological evidence of postnatal neurogenesis in rats, *J. Comp. Neurol.* **124**:319–335.

Arvidsson, A., Collin, T., Kirik, D., Kokaia, Z., and Lindvall, O., 2002, Neuronal replacement from endogenous precursors in the adult brain after stroke, *Nature Med*. **8**:963–970.

Benraiss, A., Chmielnicki, E., Lerner, K., Roh, D., and Goldman, S.A., 2001, Adenoviral brain-derived neurotrophic factor induces both neostriatal and olfactory recruitment from endogenous progenitor cells in the adult forebrain, *J. Neurosci*. **21**:6718–6731.

Calza, L., Giardino, L., Pozza, M., Bettelli, C., Micera, A., and Aloe, L., 1998, Proliferation and phenotype regulation in the subventricular zone during experimental allergic encephalomyelitis: in vitro evidence of a role for nerve growth factor, *PNAS* **95**:3209–3214.

Chen, G., Rajkowska, G., Du, R., Seraji-Bozorgzad, N., and Manj, H.K., 2000, Enhancement of hippocampal neurogenesis by lithium, *J. Neurochem*. **75**:1729–1734.

Curtis, M.A., Penney, E.B., Pearson, A.G., van Roon-Mom, W.M.C., Butterworth, N.J., Dragunow, M., Connor, B., and Faull, R.L.M., 2003, Increased cell proliferation and neurogenesis in the adult human Huntington's disease brain, *PNAS* **100**:9023–9027.

Eriksson, P.S., Perfilieva, E., Bjork-Eriksson, T., Alborn, A-M., Nordborg, C., Peterson, D.A., and Gage, F.H., 1998, Neurogenesis in the adult human hippocampus, *Nature Med*. **4**:1313–1317.

Gould, E., Reeves, A.J., Graziano, M.S.A., and Gross, C.G., 1999, Neurogenesis in the neocortex of adult primates, *Science* **286**:548–552.

Gould, E., and Tanapat, P., 1997, Lesion-induced proliferation of neuronal progenitors in the dentate gyrus of the adult rat, *Neuroscience* **80**:427–436.

Holmin, S., Almqvist, P., Lendahl, U., and Mathiesen, T., 1997, Adult nestin-expressing subependymal cells differentiate to astrocytes in response to brain injury, *Eur. J. Neurosci*. **9**:65–75.

Jin, K., Minami, M., Lan, J.Q., Mao, X.Q., Batteur, S., Simon, R.P., and Greenberg, D.A., 2001, Neurogenesis in dentate subgranular zone and rostral subventricular zone after focal ischemia in the rat, *PNAS* **98**:4710–4715.

Kaplan, M.S., and Hinds, J.W., 1977, Neurogenesis in the adult rat: electron microscopic analysis of light radioautographs, *Science* **197**:1092–1094.

Kornack, D.R., and Rakic, P., 1999, Continuation of neurogenesis in the hippocampus of the adult macaque monkey, *PNAS* **96**:5768–5773.

Kuhn, H.G., Winkler, J., Kempermann, G., Thal, L.J., and Gage, F.H., 1997, Epidermal growth factor and fibroblast growth factor-2 have different effects on neural progenitors in the adult rat brain, *J. Neurosci*. **17**:5820–5829.

Liu, J., Solway, K., Messing, R.O., and Sharp, F.R., 1998, Increased neurogenesis in the dentate gyrus after transcient global ischemia in gerbils, *J. Neurosci*. **18**:7768–7778.

Lois, C., and Alvarez-Buylla, A., 1994, Long-distance neuronal migration in the adult mammalian brain, *Science* **264**:1145–1147.

Lois, C., Garcia-Verdugo, J-M., and Alvarez-Buylla, A., 1996, Chain migration of neuronal precursors, *Science* **271**:978–981.

Luskin, M.B., 1993, Restricted proliferation and migration of postnatally generated neurons derived from the forebrain subventricular zone, *Neuron* **11**:173–189.

Nait-Oumesmar, B., Decker, L., Lachapelle, F., Avellana-Adalid, V., Bachoud-Levi, A-C., and van Evercooren, A.B., 1999, Progenitor cells of the adult mouse subventricular zone proliferate, migrate and differentiate into oligodendrocytes after demyelination, *Eur. J. Neurosci*. **11**:4357–4366.

Parent, J.M., Valentin, V.V., and Lowenstein, D.H., 2002a, Prolonged seizures increase proliferating neuroblasts in the adult rat subventricular zone-olfactory bulb pathway, *J. Neurosci*. **22**:3174–3188.

Parent, J.M., Vexler, Z.S., Gong, C., Derugin, N., and Ferriero, D.M., 2002b, Rat forebrain neurogenesis and striatal neuron replacement after focal stroke, *Ann. Neurol*. **52**:802–813.

Parent, J.M., Yu, T.W., Leibowitz, R.T., Geschwind, D.H., Sloviter, R.S., and Lowenstein, D.H., 1997, Dentate granule cell neurogenesis is increased by seizures and contributes to aberrant network reorganization in the adult rat hippocampus, *J. Neurosci*. **17**:3727–3738.

Szele, F.G., and Chesselet, M-F., 1996, Cortical lesions induce an increase in cell number and PSA-NCAM expression in the subventricular zone of adult rats, *J. Comp. Neurol*. **368**:439–454.

Tattersfield, A.S., Croon, R.J., Liu, Y.W., Kells, A.P., Faull, R.L.M., and Connor, B., 2004, Neurogenesis in the striatum of the quinolinic acid lesion model of Huntington's disease, *Neuroscience* **127**:319–332.

Thomas, L.B., Gates, M.A., and Steindler, D.A., 1996, Young neurons from the adult subependymal zone proliferate and migrate along an astrocyte, extracellular martix-rich pathway, *Glia* **17**:1–14.

Weinstein, D.E., Burrola, P., and Kilpatrick, T.J., 1996, Increased proliferation of precursor cells in the adult rat brain after targeted lesioning, *Brain Res*. **743**:11–16.

Willis, P., Berry, M., and Riches, A.C., 1976, Effects of trauma on cell proliferation in the subependymal layer of the rat neocortex, *Neuropath. App. Neurobio*. **2**:377–388.

Yoshimura, S., Takagi, Y., Harada, J., Teramoto, T., Thomas, S.S., Waeber, C., Bakowska, J.C., Breakefield, X.O., and Moskowitz, M.A., 2001, FGF-2 regulation of neurogenesis in adult hippocampus after brain injury, *PNAS* **98**:5874–5879.

Zigova, T., Pencea, V., Wiegand, S.J., and Luskin, M.B., 1998, Intraventricular administration of BDNF increases the number of newly generated neurons in the adult olfactory bulb, *Molec. Cell. Neurosci*. **11**:234–245.

Section VI

PHYSIOLOGICAL AND ANATOMICAL STUDIES OF THE FUNCTIONAL ORGANISATION OF THE BASAL GANGLIA

THE VENTRAL/DORSAL DIVIDE: TO INTEGRATE OR SEPARATE

Suzanne N. Haber, Jean-Michel Deniau, Henk J. Groenewegen, Patricio O'Donnell, Jacqueline F. McGinty, and Christelle Baunez*

The basal ganglia (BG) work in concert with cortex to orchestrate and execute planned, motivated behaviors requiring motor, cognitive, and limbic circuits. While the BG are best known for their motor functions, they are involved in several aspects of goal-directed behaviors, including not only the expression through the control of movement, but also the processes that lead to movement, including the elements that drive actions, such as emotions, motivation, and cognition. Regions within each of the BG nuclei are anatomically and physiologically associated with each of these functional circuits. Ventral regions of the basal ganglia play a key role in reward and reinforcement and are important in the development of addictive behaviors and habit formation (Hollerman et al., 1998; Everitt and Wolf, 2002; Elliott et al., 2003). Central basal ganglia areas are involved in cognitive functions such as procedural learning and working memory tasks (Jueptner et al., 1997; Levy et al., 1997; Jog et al., 1999). Finally, the dorsolateral portion of the striatum, caudal to the anterior commissure is associated with the control of movement. Projections from frontal cortex form a "functional gradient of inputs" from the ventromedial sector through the dorsolateral striatum, with the medial and orbital prefrontal cortex terminating in the ventromedial part, and the motor cortex terminating in the dorsolateral region. Furthermore, afferents from interconnected and functionally associated thalamic and cortical regions terminate in the same striatal area, resulting in a tight, anatomical and functional organization of the striatum. The functional topography of cortex that is maintained through cortical connections

* S. Haber, Dept. Pharm. & Physiol., University of Rochester School of Medicine, Rochester, NY, 14642, USA; H. Groenewegen Dept. Anatomy, Research Institute Neurosciences, Vrije Universiteit, Amsterdam, The Netherlands; J-M Deniau, INSERM U667 Dynamique et Physiopathologie des Réseaux Neuronaux, Collège de France, 11 Place Marcelin Berthelot, Paris, France; Patricio O'Donnell, Dept. Neuropharmacology & Neuroscience, Albany Medical College, 47 New Scotland Ave., Albany, NY 12208; J. McGinty, Dept. Neurosciences, Medical University of South Carolina, Charleston, SC, USA; C. Baunez, Laboratoire de Neurobiologie de la Cognition, CNRS, 31, chemin Joseph Aiguier, 13402 Marseille, France.

to the striatum, is likely to be continued from the striatum to the pallidum/SNr, from these output structures to the thalamus, and finally, back to cortex. Consistent with this topography, diseases affecting mental health, including schizophrenia, drug addiction, and obsessive compulsive disorder, are all linked to pathology in the basal ganglia, as are diseases affecting motor control (McGuire et al., 1994; Koob and Nestler, 1997; Pantelis et al., 1997; Menon et al., 2001; Rauch et al., 2001). The basal ganglia are connected with frontal cortex in a series of functional modules that maintain a relative consistent anatomical and physiological organization, leading to the concept of parallel processing of cortical information through segregated BG circuits (Alexander et al., 1986).

Recent evidence demonstrates that the BG are critical in mediating the learning process by reinforcing new behavioral-guiding rules (Owen et al., 1993; Aosaki et al., 1994; Passingham, 1995). This requires communication across functionally distinct circuits in order to continually evaluate and adjust to stimuli throughout the development of behaviors. Models based solely on parallel processing do not address how information can be transformed across functional regions in order to help implement the learning and adaptability that is necessary in the development of goal-directed behaviors. An emerging literature in primates as well as in rodents supports the idea that there are pathways by which information from separate cortico-basal ganglia loops can influence each other.

Using different approaches, this chapter outlines several nodal points at which integration between functional regions can take place. The first section (Haber) describes two neural networks that provide a mechanism for information to flow from limbic to associative areas, to affect motor outcome. In the second section, Deniau and Groenewegen use 3D reconstructions of the substantia nigra and electrophysiology to demonstrate that striato-nigro-striatal circuits in the rodent are organized in both open and closed loops. The open component allows interaction between segregated cortico-striatal channels through non-reciprocal connections to the substantia nigra. The directionality in these projections indicates that in addition to a 'ventral-to-dorsal' spiral, dorsal-to-ventral transfer of information may also occur. In the third section, O'Donnell demonstrates that in the accumbens core, the 'spiraling' inputs arriving from the hippocampus and amygdala (which target primarily shell neurons) can gate inputs from the core loop. Thus, in addition to a limbic-to-motor transfer by way of thalamic and nigra connections, there is a limbic-to-motor transfer in the manner inputs interact in driving membrane properties of medium spiny neurons. Pharmacological data presented in section four (McGinty) uses gene expression data following drug administration, to demonstrate potential convergent interactions between dorsal and ventral striatal circuitries in rodents. These may occur through similar mechanisms to those demonstrated in the primates. In the fifth section Baunez presents evidence for increased motivation for food and decreased motivation for cocaine after STN lesions. This data highlights the involvement of STN, a structure considered to be part of the dorsal basal ganglia, in motivation. It raises the issue of the existence either a separate motivational sub-circuit or integration of circuits via the STN.

1. INTEGRATIVE NETWORKS OF THE PRIMATE BASAL GANGLIA
(S.N. Haber)

Frontal cortex is divided into several functional regions: the orbital and anterior cingulate prefrontal cortex, involved in emotions and motivation; the dorsolateral prefrontal cortex (DLPFC), involved in higher cognitive processes or 'executive functions'; and the

premotor and motor areas, involved in motor planning, motor control and execution. These areas, along with the thalamic nuclei also associated with these functions, project topographically to the striatum. While BG pathways are generally functionally organized separate loops through the one-way cortico-BG circuits, other parts of the neural network argue against parallel processing as the only organizational rule, indicating cross-talk between adjacent functional regions (Percheron and Filion, 1991; Smith et al., 1998). The data presented here demonstrate two neuronal network systems that extend beyond connecting adjacent regions: 1. the striato-nigro-striatal network and 2. thalamo-cortico-thalamic network (Haber et al., 2000; McFarland and Haber, 2002). These networks provide a feedforward mechanism of information flow so that motor outcome can be influenced by cognitive and motivational input. In this way, limbic pathways interact with cognitive pathways, which, in turn, can affect motor outcome.

1.1. The Striato-Nigro-Striatal Network

The idea that the limbic striatum could influence motor output was first demonstrated in rodents via the striato-nigro-striatal (SNS) pathway (Nauta et al., 1978; Somogyi et al., 1981). In primates, the midbrain dopamine neurons are divided into two tiers: a dorsal tier and a ventral tier (Figure 2) (Lavoie and Parent, 1991; Haber et al., 1995; Francois et al., 1999). The organization of the midbrain-striatal projection has an inverse dorsal-ventral topography. The dorsal dopamine cells project to the ventral striatum, while the ventral cells project dorsally. In addition to an inverse topography there is also a differential ratio of dopamine projections to the different striatal areas. The dorsolateral striatum receives the largest midbrain projection, while the ventral striatum receives the most limited dopamine cell input. Projections from the striatum to the midbrain are also arranged topographically, having an inverse dorsal-ventral topography. The dorsal aspects of the striatum terminate in the ventral regions of the midbrain, while the ventral areas terminate dorsally. Projections from the ventral striatum to the midbrain is the largest and terminates throughout an extensive dorsal region. In contrast, the dorsolateral striatal projection is the smallest and terminates in the ventrolateral midbrain in the pars reticulata and in the dopaminergic cell columns that extend into this region (Szabo, 1979; Hedreen and DeLong, 1991; Parent and Hazrati, 1994; Haber et al., 2000). Taken together, the ventral striatum receives a limited midbrain input, but projects to a large region. The dorsolateral striatum receives a wide input, but projects to a limited region. Thus the ventral striatum influences a wide range of dopamine neurons, but is itself influenced by a relatively limited group of dopamine cells. In contrast, the dorsolateral striatum influences a limited midbrain region, but is affected by a relatively large midbrain region. For each striatal region there is one reciprocal and two nonreciprocal connections with the midbrain. Dorsal to the reciprocal connection lies a group of cells that project to the striatal region, but does not receive projections from it. Ventral to the reciprocal component lies efferent terminals without an ascending reciprocal connection. With this arrangement, information from the limbic system can reach the motor system through a series of connections. The ventral striatum, which receives input from the orbital and anterior cingulate cortices sends an efferent projection to the midbrain that extends beyond it reciprocal connection, terminating lateral and ventral to it. This terminal region projects to the central (or associative) striatum. The central striatum is reciprocally connected to the densocellular region but also projects to the ventral region and thus is in a position to interact with cell projecting to the dorsolateral (or motor) striatum. Taken together, the interface between different striatal regions via the midbrain DA cells is

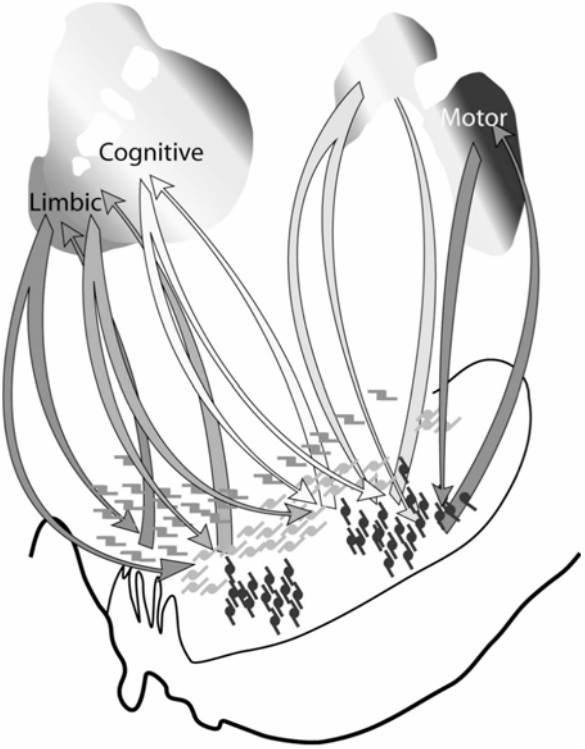

Figure 1. Diagram of the organization of striato-nigro-striatal (SNS) projections in which there are both reciprocal and non-reciprocal connections between different functional regions of the striatum via the midbrain.

organized in an ascending spiral interconnecting different functional regions of the striatum and creating a feed forward organization (Figure 1). Information can thus be channeled from the shell to the core, to the central striatum, and finally to the dorsolateral striatum. In this way, information flows from limbic to cognitive to motor circuits (Haber et al., 2000).

1.2. Thalamo-Cortico-Thalamic Interface

The thalamo-cortical pathway is the last link in the circuit and is often treated as a simple 'one-way relay' back to cortex. However, like the SNS system, the thalamo-cortico-thalamic system is in a critical position for integrating information across functional circuits. While corticothalamic projections to specific relay nuclei are thought to follow a general rule of reciprocity, corticothalamic projections to VA/VL and central MD sites are more extensive than thalamocortical projections (Deschenes et al., 1998; Darian-Smith et al., 1999; McFarland and Haber, 2002). Furthermore, they are derived from areas not innervated by the same thalamic region, indicating non-reciprocal corticothalamic projections to specific basal ganglia relay nuclei. Although each thalamic nucleus completes the cortico-basal ganglia segregated circuit, the non-reciprocal component is derived from a functionally distinct frontal cortical area. For example, the central MD has reciprocal con-

nections with the lateral and orbital prefrontal areas and also a non-reciprocal input from medial prefrontal areas; VA has reciprocal connections with dorsal premotor areas, and caudal area DLPFC and also a non-reciprocal connection from medial prefrontal areas; and VLo has reciprocal connections with caudal motor areas along with a non-reciprocal connection from rostral motor regions. The potential for relaying information between circuits through thalamic connections, therefore, is accomplished through the non-reciprocal cortico-thalamic pathways (Figure 2). Thus, similar to the basal ganglia thalamic relay nuclei appear to mediate information flow from higher cortical "association" areas of the prefrontal cortex to rostral motor areas involved in "cognitive" or integrative aspects of motor control to primary motor areas that direct movement execution.

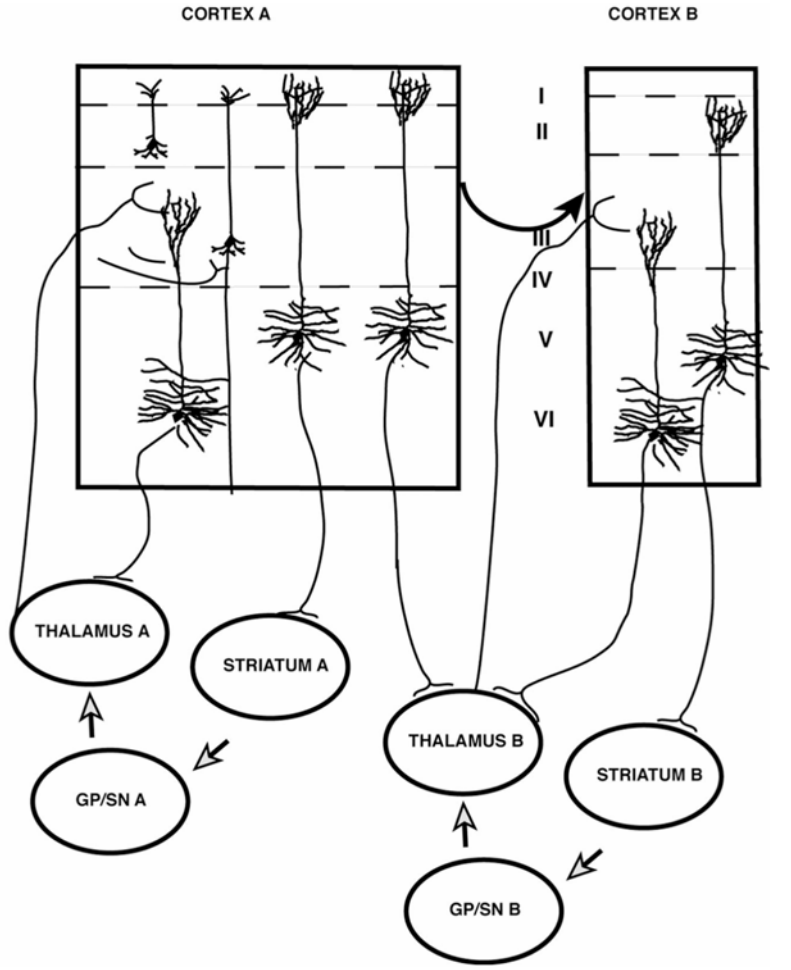

Figure 2. Diagram of the organization of thalamo-cortico-thalamic projections demonstrating how a non-reciprocal cortico-thalamic projection (from cortex A) interfaces with an other cortico-basal circuit (cortex B).

1.3. A Role for Both Parallel Circuit and Integrative Networks

Basal ganglia structures are tographically organized to maintain functional continuity through each circuit and have reciprocal connections that link regions associated with similar functions (maintaining parallel networks). These parallel circuits are important, allowing the coordinated behaviors to be maintained, and focused (via parallel networks). Behaviors must be also be modified and changed according the appropriate external and internal stimuli (via integrative networks). One way in which the basal ganglia works with cortex in the development and modification of goal-directed behaviors is through non-reciprocal connections that link regions that are associated with different cortical-BG circuits. The feedforward organization of both the striato-nigral connections and the thalamo-cortical connections is a mechanism by which information can be channeled from limbic, to cognitive, to motor circuits, allowing action decision-making processes by these different elements, allowing the animal to respond appropriate to environmental cues.

2. RECIPROCAL AND NON-RECIPROCAL COMPONENTS IN THE STRIATO-NIGRO-STRIATAL CIRCUITS

(Y.C. van Dongen, P. Mailly, B. Kolomiets, A.M. Thierry, H.J. Groenewegen and J.M. Deniau)

The striatum and the dopaminergic (DA) neurons of the substantia nigra pars compacta/ventral tegmental area (SNC/VTA) complex are intimately interconnected through loop circuits. The striatum, via its projections to the substantia nigra and VTA provides a direct innervation to the nigro-striatal neurons. In addition, the striatum can also influence the DA neurons via an indirect circuit involving the intranigral projections of the GABAergic neurons of the substantia nigra pars reticulata (SNR) to the DA neurons of the SNC. In turn, the DA neurons of the VTA/SNC collectively innervate the entire striatum where they regulate the integration of cortical signals. These loop circuits constitute potential mechanisms of integration across various components of the parallel cortico-basal ganglia circuits. In particular, since the pioneering anatomical studies by Nauta et al. (Nauta and Cole, 1978) describing that the nucleus accumbens provides a massive innervation of the VTA and SNC, DA neurons have been regarded as a potential link between the limbic circuits of the ventral striatum and the sensorimotor circuits of the dorsal striatum.

Although anatomical evidence for non-reciprocal arrangements in the striato-nigro-striatal loop circuits have been provided (Somogyi et al., 1981; Haber and Fudge, 1997; Joel and Weiner, 2000), the way various components of the functional striatal mosaic communicate via the DA system remains poorly understood. Certainly, one of the major difficulties in defining rules of communication in the striato-nigro-striatal loop circuits lies in the complex spatial arrangement of both striato-nigral projections and nigrostriatal neurons that cannot be easily schematized in two-dimensional maps using cardinal coordinates. Thus, if it is true that the population of nigrostriatal neurons display some kind of medio-lateral topography (for review see Joel and Weiner, 2000), this trend does not adequately describe the organization of the nigro-striatal relationships. In fact, as shown in the rat, the nigro-striatal neurons innervating the lateral sensori-motor striatum distribute throughout the latero-medial extent of the SNC and partially overlap populations of neurons projecting to medial limbic/prefrontal striatal subdivisions (Maurin et al., 1999). A similar remark holds true for the striato-nigral projections. These projections were described in term of medio-lateral and inverted dorso-ventral topographic register (see for review (Joel

and Weiner, 2000) but the various functional sub-territories of the striatum innervate the SNR in the form of longitudinal and curved lamellae arranged in an onion like manner (Gerfen, 1985; Deniau et al., 1996). This organization transcends the medio-lateral and dorso-ventral cardinal subdivisions. Actually, the architecture of the striato-nigro-striatal circuits has to be analyzed at a three-dimensional level using the volume of the substantia nigra as a common frame of reference to describe the relative arrangement of nigro-striatal neurons and striato-nigral projections. We review here some preliminary data on the possible mode of communication between the limbic ventral striatum and the sensori-motor dorso-lateral striatum obtained using this three-dimensional approach in the rat brain.

2.1. Spatial Relationships between Nigro-Striatal Neurons and Striato-Nigral Projections: A Basis for an Indirect Link between Limbic and Sensori-Motor Circuits

Combined three-dimensional analysis of retrogradely labelled neurons in the VTA/SNC complex and of anterogradely labelled fibers in the SNR following WGAHRP injection in distinct functional sub-territories of the striatum and core of nucleus accumbens revealed that each striatal sub-territory is innervated by a sub-population of nigral neurons that can be subdivided in two components (Maurin et al., 1999). The first one, termed the "proximal" population, occupies a position in register with the striatonigral projections in the subjacent SNR. This cell population is topographically organized and in view of its close spatial relationship with the striato-nigral projections, is likely involved in a reciprocal striato-nigro-striatal feedback circuit. The second one, termed the "distal" population, is located more medially and dorsally in the SNC and VTA and is likely to be involved in non-reciprocal connections with the striatum. By contributing to open striato-nigro-striatal loops these "distal" neurons might provide a mechanism for the integration between distinct functional components of the corticostriatal circuits. Since the populations of nigro-striatal neurons extend medially but never laterally to the projections originating from the striatal sub-territory they innervate, this spatial arrangement imposes a defined medio-lateral polarity in the non-reciprocal relation of these neurons with the stiatum. These observations support the concept originally proposed by (Haber et al., 2000) of a spiralling mechanism by which the shell of the nucleus accumbens would indirectly influence the dorso-lateral sensori-motor striatum via a series of feed-forward striato-nigro-striatal circuits. Indeed, as observed by (Haber et al., 2000) in monkeys, the projections issued from the shell of nucleus accumbens are not focused on the region of the VTA projecting back to the shell. Shell projections extend laterally in a region where neurons project to the core of nucleus accumbens (Figure 3). In turn, the core of nucleus accumbens innervates a dorso-medial region of the SNR that is overlaid by SNC neurons projecting not only to the nucleus accumbens core but also to sub-territories of the dorsal striatum affiliated to medial and lateral prefrontal cortical areas. Finally, the striato-nigral projections originating from these latter striatal regions are overlaid by SNC neurons projecting to various sub-territories of the sensori-motor striatum.

Even though it seems clear that the spatial arrangement of striato-nigral projections and nigro-striatal neurons imposes a defined polarity in the transmission of striatal information, from limbic to sensori-motor, the precise mode of interactions between the various components of the functional striatal mosaic remains to be established. In fact, as already mentioned above, the functional striatal mosaic is represented in the SNR along a complex array of curved lamellae and it is not yet known how the dendrites of the various sub-populations of nigro-striatal neurons conform to the lamellar geometry of striatonigral projections. In addition to receiving direct striatal innervation through their dendritic field

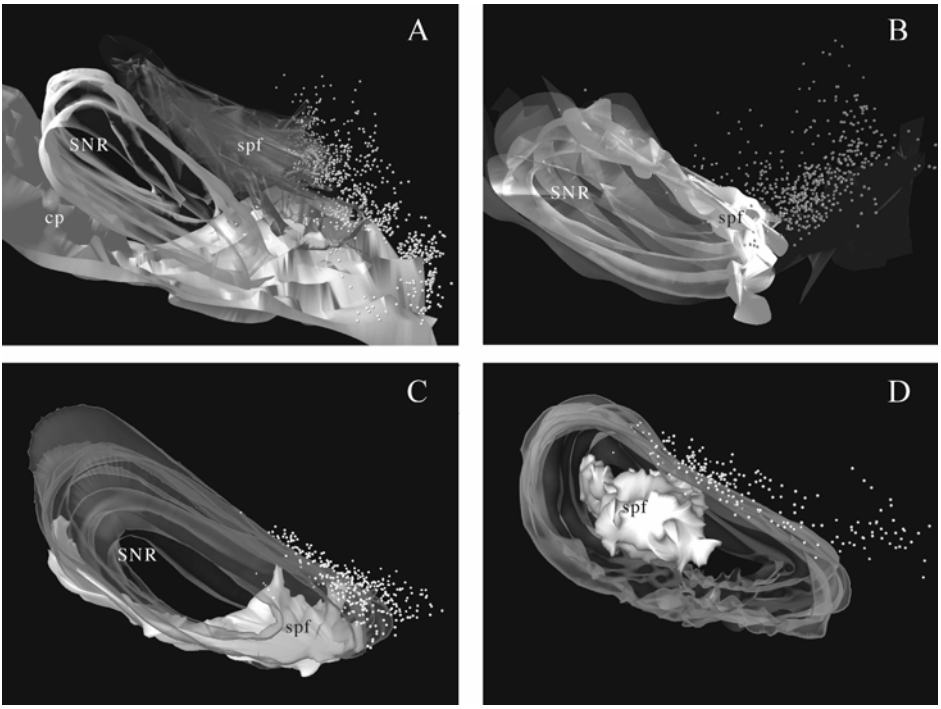

Figure 3. Three dimensional reconstructions of striatal projection fields (spf) within the substantia nigra and distribution of retrogradely labelled neurons (white spheres) following injections of WGA-HRP in different functional sub territories of striatum. A, case of injection in the shell of nucleus accumbens; B, injection in the core of the nucleus accumbens; C, injection in the visual-cingulate striatal sub-territory; D, injection in the sensory-motor orofacial sub territory. SNR: substantia nigra pars reticulata; cp: cerebral peduncle.

in SNR, nigro-striatal neurons receive an indirect striatal input via a disynaptic circuit involving the GABAergic neurons of the SNR. Indeed, most of the output neurons of the SNR provide a recurrent axon collateral network that innervates both the SNR and the SNC (Grofova, 1982; Mailly et al., 2003). Because this indirect striato-nigral circuit is composed of two successive GABAergic links, it is expected to exert a disinhibitory influence opposite to the inhibitory function of the direct striato-nigral pathway. Understanding how the striato-nigral circuits contribute to the integration of information flow across striatal regions will require a precise knowledge on the mode of interaction between the direct and indirect striato-nigral circuits at the level of the SNC. From our current knowledge on the three dimensional organization of the intranigral axonal projections of SNR cells, SNR neurons that receive afferents from a given striatal sub-territory seems to preferentially innervate the region of the SNC in which the nigro-striatal neurons are situated that project back to the corresponding striatal territory (Mailly et al., 2003).

2.2. A Direct Functional Link between the Limbic and the Sensorimotor Striatum

The shell of the nucleus accumbens, a major component of the limbic striatum, provides an extensive innervation of the DA system spanning from the VTA to lateral regions

of the SNC (Groenewegen et al., 1994). This pattern of projections led to the suggestion that DA neurons provide a direct link between the limbic striatum and the sensori-motor circuits of the dorsal striatum. Although this concept is widely considered as a classical notion, experimental evidence demonstrating the existence of such a functional link is still lacking. A previous anatomical study has shown that axons from shell neurons terminate on the dendrites of nigro-striatal neurons innervating the dorsal striatum (Somogyi et al., 1981). However, in this study the sites of projections of the nigro-striatal neurons within the dorsal striatum were not precisely identified. As known, the dorsal striatum is not specifically innervated by the sensori-motor cortex but receives also afferents from the medial and lateral prefrontal cortical areas.

Using an electrophysiological approach, DA nigro-striatal neurons projecting to the striatal sub-territory innervated by the orofacial motor cortical area were identified by antidromic activation and their response to stimulation of the shell of the nucleus accumbens were examined. In 69 of 152 DA cells antidromically activated responded to the stimulation of the shell by a short duration inhibition (38.8 ms ± 3.0 ms) with a mean latency (17.8 ± 0.9 ms) corresponding to the conduction time of the shell-VTA/SNC pathway (16.7 ± 0.2 ms) (Figure 4).

Interestingly, these neurons were mostly located in the dorsal parts of the lateral VTA and the medial SNC in which the distal subpopulation of nigro-striatal neurons is situated

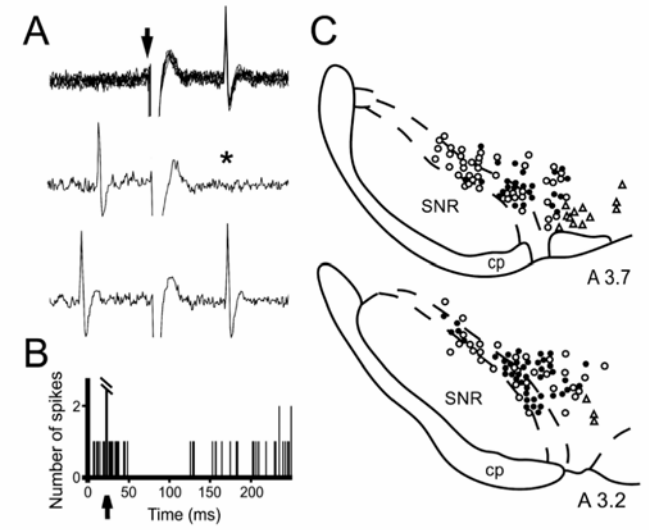

Figure 4. Inhibitory response evoked by electrical stimulation of the shell of nucleus accumbens on electrophysiologically identified dopaminergic nigro-striatal neurons projecting to the sensori-motor orofacial sub-territory of the dorsolateral striatum. A, antidromic activation of the DA neuron following stimulation of the dorso-lateral striatum. Arrow indicates the time of application of the stimulation. The star indicates the lack of the antidromic spike due to collision with a spontaneous discharge. B, post-stimulus time histogram showing the inhibitory effect induced by stimulation of the shell of nucleus accumbens on the DA nigro-striatal neuron illustrated in A; Arrow indicates the time of application of the stimulation. C, distribution of neurons antidromically activated from the shell of nucleus accumbens (open triangles), neurons antidromically activated from the dorso-lateral and receiving an inhibitory influence from the shell (filled circles) or antidromically activated from the dorso-lateral striatum but not inhibited from the shell (open circles).

that innervates the orofacial sensori-motor sub-territory of the dorsal striatum. By contrast, nigro-striatal neurons of the proximal group were not influenced by stimulation of the shell. This suggests that integration between limbic and sensori-motor components of the cortico-striatal circuits occurs via a specific sub-population of nigro-striatal neurons.

In a parallel series of anatomical tracing experiments, the retrograde tracer Fluorogold (FG) was injected in the orofacial sub-territory of the caudate-putamen, using the same stereotaxic coordinates as for the electrophysiological experiments, and an injection of the anterograde tracer biotinylated dextran amine (BDA) was positioned in the shell of the nucleus accumbens. Retrogradely labeled neurons could be identified in the sensori-motor cortex, as well as over virtually the entire mediolateral extent of SNC as well as in the dorsolateral part of the VTA. Neurons located in the medial and dorsal SNC as well as in the VTA were in general more lightly labelled than those in more lateral parts of SNC. These neurons belong to the 'distal' group of DA neurons. In double-stained sections for both FG and BDA, the anterogradely labelled fibers and terminals originating from the shell of the nucleus accumbens could be observed to overlap primarily the labelled neurons of this 'distal' group of SNC/VTA neurons projecting to the sensori-motor striatum (Figure 5). Frequently, close appositions could be observed between anterogradely labeled boutons and retrogradely neuronal cell bodies and dendrites, providing the presumptive morphological substrate for the above-described electrophysiological observations.

In conclusion, the various functional sub-territories of the striatum and their dopaminergic nigro-striatal afferent neurons are engaged in both closed and open loops allowing interactions between segregated cortico-striatal circuits. Interactions between the ventral limbic and the dorso-lateral sensory-motor subdivisions of the striatum have a definite ventro-dorsal polarity and appear to involve a defined subpopulation of nigrostriatal neurons that is not engaged in reciprocal connections with the sensori-motor striatum.

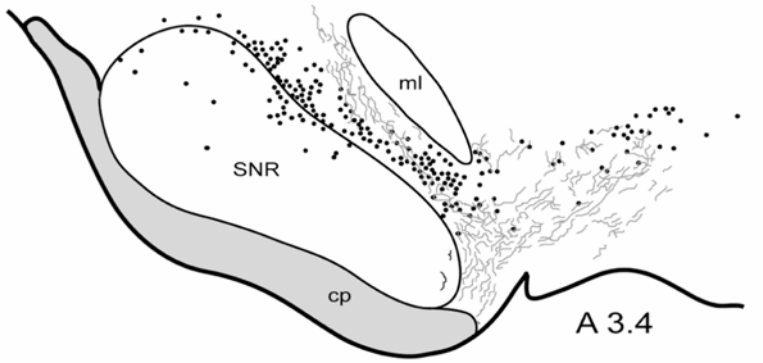

Figure 5. Chartings of BDA-labelled fibers and terminals in the SNC/VTA (injection in the shell of the nucleus accumbens) in combination with retrogradely labeled FG-containing neurons (dots) following an injection in the oro-facial sub-territory of the caudate-putamen. The anterograde labelling in three adjacent sections was compiled. Note the intermingling of anterogradely labelled fibers and retrogradely labelled neurons in the lateral VTA and the dorsal tier of the medial half of the SNC.

3. INTERACTIONS AMONG SYNAPTIC INPUTS TO STRIATAL NEURONS ALLOWS FOR A LIMBIC-TO-MOTOR TRANSFER OF INFORMATION

(P. O'Donnell)

The spiraling organization of basal ganglia loops may also be present in corticostriatal projections, providing a means by which limbic cortical activity exerts an impact on cognitive and motor striatal regions. In fact, striatal medium spiny neurons (MSN) do receive converging inputs from several cortical areas in addition to those reported as forming part of "closed" loops. This has been shown first using electrophysiological techniques: in vivo intracellular recordings revealed monosynaptic responses to stimulation of the hippocampus, amygdala and medial prefrontal cortex in individual ventral striatal MSN (O'Donnell and Grace, 1995), and single MSN responded with action potential firing to stimulation of those diverse afferents in extracellular studies (Finch, 1996). Although tract tracing had revealed some extent of segregation in the distribution of labeled axon terminals originated from prefrontal cortical (PFC) and limbic sources (Wright and Groenewegen, 1996), it was deemed possible that MSN dendrites could extend covering fields receiving inputs from different sources. Anatomical confirmation of single MSN having synaptic contacts with axons from different cortical afferents was provided only recently (French and Totterdell, 2002, 2003). Anterograde tracers in combination with serial reconstruction of a Neurobiotin-injected neuron revealed that MSN do receive synaptic contacts from diverse cortical sources. Thus, ventral striatal MSN can be activated from cortical projections related to the "closed" loop in which they are involved, but also from other cortical inputs.

The concept of spiraling circuits is important for a limbic-to-motor transfer of information. The nature of the electrophysiological impact these diverse inputs may have on MSN may provide clues as to how this transfer takes place. In vivo intracellular recordings have been conducted in the core of the rat nucleus accumbens while stimulating with series of electrical pulses the medial prefrontal cortex and limbic afferents (i.e., the basolateral amygdala and ventral hippocampus) (O'Donnell and Grace, 1995; Goto and O'Donnell, 2002). This pairing could represent an exploration of the influences on striatal cell physiology of the "closed" loop in which the recorded neuron participates (in this case, the prelimbic PFC) and of a set of inputs from cortical areas that primarily target MSN participating in other, more "limbic" loops (in this case, the amygdala or hippocampus, which establish projections primarily to the accumbens shell). This type of recording reveals that activation of hippocampal afferents could set accumbens core MSN into a persistent depolarization (up state) while PFC afferents do not (O'Donnell and Grace, 1995). However, PFC inputs that could not evoke a measurable response on their own are able to elicit action potential firing during the hippocampal-evoked depolarization (O'Donnell and Grace, 1995). This finding was interpreted as evidence of a gating mechanism by which limbic inputs can allow prefrontal inputs to activate accumbens neurons. More recently, the synaptic responses evoked by single-pulse stimulation of the amygdala, hippocampus and medial PFC were examined in neurons in the core region of the nucleus accumbens. Activation of PFC inputs was paired with activation of one of the limbic structures, either by simultaneous stimulation or with 100 ms delays (alternating the order of stimulation). Consistent with previous findings, stimulating the hippocampus prior to PFC activation enhanced the amplitude of the cortical response (Goto and O'Donnell, 2002). Activation of the basolateral amygdala also enhanced responses to subsequent PFC stimulation. When the order of stimulation was reversed, all responses to limbic afferents were reduced in amplitude if tested 100 ms after PFC stimulation (Goto and O'Donnell, 2002). These results are consistent with the notion

that limbic afferents can gate prefrontal afferents to the accumbens core. They also indicate that once the PFC afferents are strongly activated, the responsivity to limbic inputs is transiently reduced in accumbens neurons, allowing for a reset in the gating mechanism. One could also interpret these results in the light of the spiraling basal ganglia organization. If these findings can be generalized to all striatal circuits, the "limbic-to-motor" transfer proposed to occur in the spiraling model may take the form of a gating mechanism in which limbic inputs gate or enhance associative inputs, associative afferents gate motor afferents, and so on. When one of the loops is strongly activated by its set of direct cortical afferents, this lateral transfer of information is reduced, so associative activation can override limbic gating and motor activation can override associative activation.

4. $GABA_B$ RECEPTOR INTERACTIONS IN THE DORSAL AND VENTRAL STRIATUM SUGGEST CONVERGENCE OF MOTOR INFORMATION PROCESSING

(J.F. McGinty)

Convergent interactions between dorsal and ventral striatal circuitries in rodents are suggested by gene expression data following intra-cerebral administration of drugs that interfere with the stimulatory effects of amphetamine. Acute administration of amphetamine causes direct stimulation of dopamine (DA) release from mesoaccumbal and nigrostriatal terminals (Zetterstrom et al., 1983; Sharp et al., 1987). The increased dopamine release leads to a cascade of events that involves the activation of neuropeptides in postsynaptic striatal neurons. The induction of striatal neuropeptides, preprodynorphin (PPD), preprotachychinin (PPT), and preproenkephalin (PPE), is well documented after acute administration of amphetamine (Wang and McGinty, 1995a, b; Zhou et al., 2004). After binding to their corresponding receptors, these peptides are able to modulate the release of DA, glutamate, and acetylcholine in the striatum (Heijna et al., 1990; Guzman et al., 1993; Anderson et al., 1994; Gray et al., 1999; Rawls and McGinty, 2000). Thus, neuropeptides expressed by medium spiny neurons are able to modify the changes in striatal neurotransmission caused by psychostimulants.

In addition to neuropeptides, GABA is known to interact with and modulate DA neurotransmission in the nigrostriatal (Engberg et al., 1993) and the mesolimbic dopaminergic pathways (Kalivas et al., 1990). Although $GABA_A$ receptors are relatively ubiquitous, $GABA_B$ receptors are enriched in areas of the brain that mediate the rewarding and activating effects of psychostimulants (Chu et al., 1990; Lopez-Bendito et al., 2002). $GABA_B$ receptors are G_i/G_o protein-coupled receptors that modulate signal transduction pathways, e.g. inhibiting adenylate cyclase, stimulating phospholipase A2, activating K^+ channels, inhibiting voltage dependent Ca^{2+} channels and regulating inositol phospholipid hydrolysis (Bowery, 1993; Misgeld et al., 1995). Several investigators have demonstrated that the selective $GABA_B$ receptor agonist, baclofen, attenuates cocaine self-administration across a wide range of conditions, including multiple schedule (Shoaib et al., 1998), progressive ratio (Roberts et al., 1996), fixed ratio (Campbell et al., 1999), concurrent access (Brebner et al., 2000), and discrete trial schedules of reinforcement (Roberts and Andrews, 1997).

However, much less is known about the effects of $GABA_B$ receptor stimulation on amphetamine-induced behavioral and neurochemical responses. Recently, we demonstrated

that systemic $GABA_B$ receptor activation by (+)-baclofen (2.5 mg/kg, i.p.) blocked amphetamine-induced rearing, decreased the peak level of striatal DA release, and blocked mRNA expression of medium spiny peptides in the striatum (Zhou et al., 2004). Therefore, we hypothesized that $GABA_B$ receptor stimulation within key nodes of the dorsal and ventral striatal circuitries would decrease amphetamine-induced hyperactivity and striatal neuropeptide gene expression. We found that intra-VTA infusion of baclofen (75 ng/side) completely blocked, whereas intra-NA and intra-SN infusion of baclofen attenuated, amphetamine-induced vertical activity (without affecting amphetamine-induced total distance traveled) and medium spiny peptide gene expression in the dorsal striatum (Zhou et al. in press). Baclofen microinfusions in to the medial prefrontal cortex or the causate-putamen had no effect.

Recent evidence indicates that the presynaptic distribution of $GABA_B$ receptors in the dorsal and ventral striatum of rodents agrees with that found in primates. $GABA_B$ immunoreactivity is expressed primarily in striatal boutons that make asymmetric contacts with labeled and unlabeled dendritic spines in primates (Charara et al., 2000) and in rats (Paul Bolam, personal communication). The presynaptic localization in glutamatergic afferents is consistent with electrophysiological evidence that the predominant effect of baclofen in the striatum is to decrease excitatory synaptic input (Nisenbaum et al., 1993). In addition, $GABA_B$ receptors are expressed by striatonigral, striatopallidal, and glutamatergic afferents as well as by dopamine and GABA neurons in the SN and VTA (Sugita et al., 1992; Charara et al., 2000; Boyes and Bolam, 2003). However, the amphetamine-suppressing effect of baclofen in the ventral mesencephalon is most consistent with a direct action on dopamine neurons. Baclofen decreases burst firing of dopamine neurons that is associated with phasic dopamine release in the SN and VTA (Engberg et al. 1993; Erhardt et al. 2002). How can baclofen decrease amphetamine-induced dopamine release in the striatum by decreasing burst firing of dopamine neurons? Amphetamine triggers dopamine release by reversing the dopamine transporter. However, we have demonstrated by *in vivo* microdialysis that approximately 40–50% of the acute amphetamine-induced increase in extracellular dopamine levels in the striatum is calcium and tetrodotoxin-dependent (Gray et al., 1999; Paredes et al., 2001), suggesting that dopamine neuronal firing contributes to amphetamine-induced dopamine release *in vivo*. This line of reasoning is consistent with the fact that systemic baclofen decreases cocaine or amphetamine-induced dopamine levels in the striatum by ~40–50% (Fadda et al., 2003; Zhou et al., 2004). Thus, although the neural substrates that mediate amphetamineinduced rearing and gene expression are incompletely understood, this study suggests that pre- and postsynaptic $GABA_B$ receptors in the VTA, SN, and NA are differentially involved.

With regard to the dorsal/ventral divide, the question remains as to why baclofen infusions into the VTA or NA would affect dorsal striatal gene expression or infusion into the SN would affect NA gene expression. One possible explanation is that these interactions may be mediated by the often overlooked, direct GABAergic projection from the NA core to the SN and the dopaminergic projection from the VTA to ventromedial CPu (Zahm and Heimer, 1993). These convergent connections that allow information to flow between dorsal and ventral striatal circuitries of rodents may be similar to those more recently described in the primate as “spirals” (Haber et al., 2000). By way of this convergence, $GABA_B$ receptors have several presynaptic and postsynaptic targets in VTA, SN, and NA through which they can exert their effects on amphetamine-induced behavior and striatal neuropeptide gene expression (Figure 6).

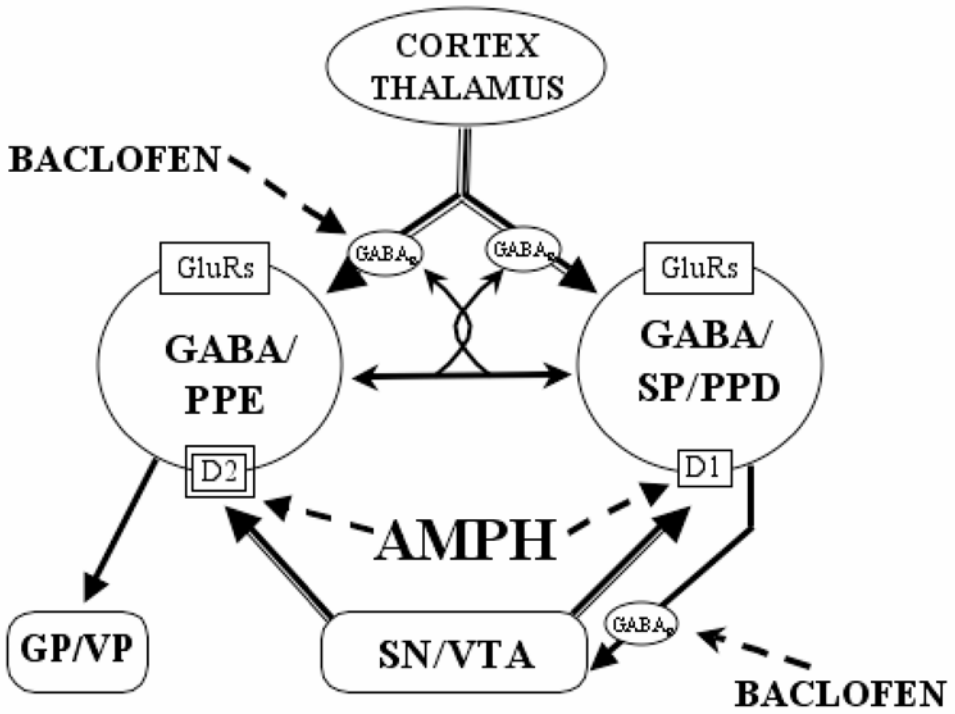

Figure 6. Schematic illustration of the dorsal and ventral striatal circuitry emphasizing the putative location of $GABA_B$ receptors that mediate the effects of baclofen on amphetamine-induced behavior and striatal neuropeptide gene expression.

5. THE SUBTHALAMIC NUCLEUS WITHIN THE "VENTRAL CIRCUIT": INVOLVEMENT IN MOTIVATIONAL PROCESSES

(C. Baunez)

In the "motor loop" of the basal ganglia, the subthalamic nucleus (STN) is a motor relay in so-called "indirect pathway" (DeLong, 1990). The STN is absent from the other loops described by Alexander et al., (Alexander et al., 1990), and was part of the "motor output" box on the schematic diagram proposed by Mogenson et al. (Mogenson et al., 1980) positioning the nucleus accumbens at the interface from motivation to action. However, the STN has more recently been shown to have connections within a loop involving the prefrontal cortex, the nucleus accumbens and ventral pallidum (Groenewegen and Berendse, 1990; Maurice et al., 1998; Maurice et al., 1999) see figure 7). This connectivity suggests that the STN should also be involved in frontal processes such as attention, disinhibition and motivation.

Over the last few years, we have shown that STN lesions affect various cognitive processes such as those involved in response preparation and selection (Baunez et al., 1995, 2001), or in attention (Baunez and Robbins, 1997) and that the direct input from the prefrontal cortex plays a critical role in the attentional deficits observed after STN lesions (Chudasama et al., 2003). Since most of the structures involved in this circuit have been

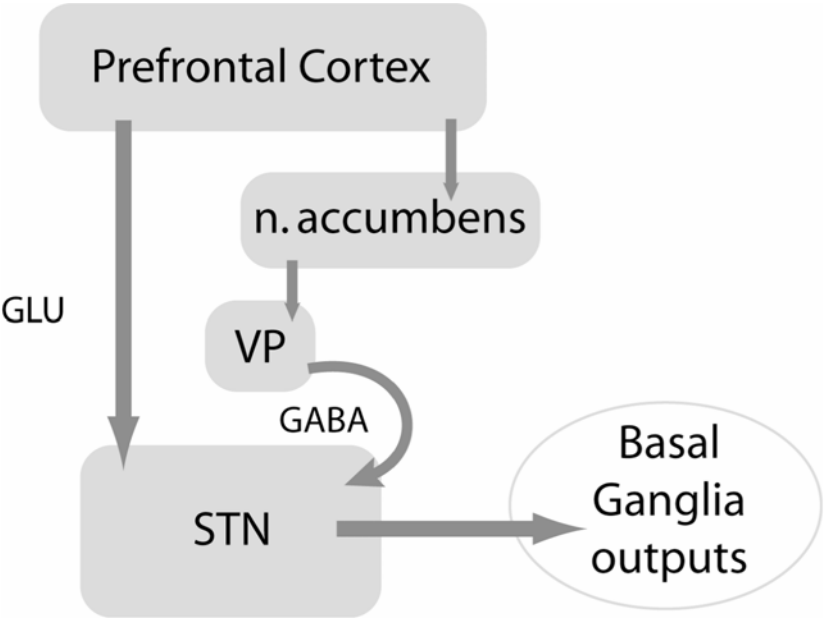

Figure 7. Schematic diagram of the "limbic connectivity" of the Subthalamic nucleus (STN). GLU: glutamate, VP: Ventral Pallidum

shown to mediate motivational information, the effects of STN lesions have been assessed in rats. In a first set of experiments, we have shown that STN lesions increase motivation for food in rats, by showing a higher reactivity to stimuli predicting food reward, while no effect was found on consummatory behaviour (Baunez et al., 2002). This observation was particularly interesting in line with clinical observations reporting hyperphagia after a tumor in the STN (Barutca et al., 2003) or weight gain in parkinsonian patients treated with high frequency stimulation in the STN, supposedly mimicking an inactivation of the STN (Moro et al., 1999; Barichella et al., 2003; Macia et al., 2004). If motivation for food can be increased by STN inactivation, and since the motivational circuit for natural rewards and drugs of abuse is classically considered as unique, we assessed the effects of STN lesions on motivation for drugs of abuse such as cocaine. No difference was observed between sham-lesioned animals and STN-lesioned animals on cocaine intake in a task in which each lever press is followed by an intraveinous injection of cocaine. However, when working load was increased to obtain a cocaine injection, STN lesioned rats worked less than sham animals (Baunez et al., 2005), as illustrated in figure 8.

A similar dissociation has been also observed in a conditioned place preference paradigm in which the animals associate a specific environment with food or cocaine (Baunez et al., 2005). Furthermore, a dose-response study has shown that the decreased motivation for cocaine after STN lesions cannot be attributed to a change in dose-sensitivity (Baunez et al., 2005).

This striking dissociation between natural and drug reinforcement has recently been highlighted by electrophysiological studies. Selective neuronal subpopulations of the nucleus accumbens (ventral striatum) recorded in freely moving rats are found to be

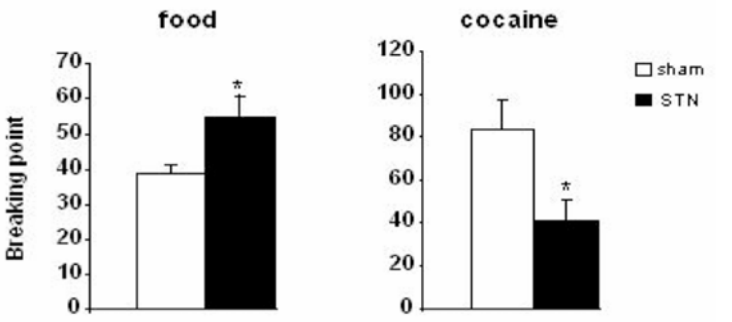

Figure 8. Willingness of the animals to work for either 2 sucrose pellets (left) or intraveinous injection of cocaine (250 µg) assessed by the breaking point in a progressive ratio schedule of reinforcement. In this task, the rats are required to press a lever an increasing number of times (i.e. ratio) to obtain a specific reward. The breaking point is the last ratio reached in average during 5 daily sessions.

differentially activated by "natural reward" (water and food) or by cocaine reinforcement (Carelli et al., 2000, 2002). In addition, the activity of ventral striatal neurons was markedly different between cocaine and juice reward in monkeys performing a reaction time task (Bowman et al., 1996). These findings have important functional implications as they suggest that various parallel microcircuits mediate responses for natural reward versus cocaine. Since the ventral striatum is indirectly connected to the STN (Maurice et al., 1998), these microcircuits are likely to be represented at the level of the STN. Indeed, as mentioned above, the STN participates in a "ventral loop" encompassing the prefrontal cortex, nucleus accumbens, ventral pallidum and STN. More specifically, the core region of the nucleus accumbens projects to that ventral pallidal area which projects to the medial part of the STN. There are successive GABA-ergic connections from the core region to the STN (via the ventral pallidum). Therefore, STN lesions could disrupt these microcircuits and thus differentially affect the reward value of food and cocaine. This interpretation is consistent with the fact that, via its connections to the different sub-loops of the topographically organized cortico-basal ganglia conveying motor, cognitive and limbic informations, the STN may differentially influence goal-directed behaviors for natural or drug reward.

An alternative explanation for this dissociation relies on recent evidence showing that severe serotonin (5-HT) depletion reduces cocaine-seeking behavior while increasing food-seeking behavior (Tran Nguyen et al., 2001). Other reports have shown that 5-HT depletion decreases cocaine craving or seeking (Satel et al., 1995; Tran Nguyen et al., 1999) and increases breaking point in progressive ratio for food and cocaine (Roberts et al., 1994). Interestingly, the STN receives a massive 5-HT innervation from the dorsal raphe nucleus. The lack of 5-HT control in STN lesioned rats may therefore be responsible for the present effects on cocaine motivational reinforcing properties. In line with this, KO mice lacking DA transporter are still able to self-administer cocaine, suggesting that cocaine rewarding effects are mediated by 5-HT transporters (Rocha et al., 1998). The exact contribution of the 5-HT contingent to the STN on motivation remains to be further investigated.

Mesolimbic and neostriatal dopamine projections have been suggested to serve as a common neural currency for rewards (Wise, 1996; Koob and Le Moal, 1997; Berridge and Robinson, 1998; Schultz, 2002). Therefore, modification of the activity of mesencephalic dopaminergic (DA) neurons is an additional potential mechanism through which the STN

could decrease the response to cocaine. In line with this, pharmacological modulation of the DA system with a D3 receptor agonist was recently shown to produce no change in cocaine self-administration for low work load and diminished cocaine intake for high work load (Di Ciano et al., 2003), as found after STN lesions. According to current theories of drug addiction, drugs activate and, via neuroadaptive processes, change dopaminergic neurotransmission in the nucleus accumbens and its related circuitry (Koob and Le Moal, 1997; Everitt et al., 2001). It has been shown that inactivating the transmission between STN and SN induces a biphasic response in DA neurons in the ventral midbrain (Smith and Grace, 1992): a short excitation followed by a reduced firing rate. The loss of excitatory input of the STN after the lesion could ultimately dysregulate their reactivity to reward.

In conclusion, the involvement of STN in motivational processes highlights its functional contribution within the "ventral system". Furthermore, its specific modulation on motivation for natural rewards and drug abuse opens new perspectives for developing specific and efficient treatments of drug abuse.

6. REFERENCES

Alexander, G.E., Crutcher, M.D., and DeLong, M.R., 1990, Basal ganglia-thalamocortical circuits: Parallel substrates for motor, oculomotor, "prefrontal" and "limbic" functions, *Prog. Brain Res.* **85**:119–110.

Alexander, G.E., DeLong, M.R., and Strick, P.L., 1986, Parallel organization of functionally segregated circuits linking basal ganglia and cortex, *Annual Review of Neuroscience* **9**:357–381.

Anderson, J.J., Kuo, S., Chase, T.N., and Engber, T.M., 1994, Dopamine D1 receptor-stimulated release of acetylcholine in rat striatum is mediated indirectly by activation of striatal neurokinin1 receptors, *J. Pharmacol. Exp. Ther.* **269**:1144–1151.

Aosaki, T., Graybiel, A.M., and Kimura, M., 1994, Effect of the nigrostriatal dopamine system on acquired neural responses in the striatum of behaving monkeys, *Science* **265**:412–410.

Baunez, C., Amalric, M., and Robbins, T.W., 2002, Enhanced food-related motivation after bilateral lesions of the subthalamic nucleus, *J. Neurosci.* **22**:562–568.

Baunez, C., Dias, C., Cador, M., and Amalric, M., 2005, The subthalamic nucleus exerts opposite control on cocaine and 'natural' rewards, *Nat. Neurosci.* **8**:484–489.

Baunez, C., Humby, T., Eagle, D.M., Ryan, L.J., Dunnett, S.B., and Robbins, T.W., 2001, Effects of STN lesions on simple vs choice reaction time tasks in the rat: preserved motor readiness, but impaired response selection, *Eur. J. Neurosci.* **13**:1609–1616.

Baunez, C., Nieoullon, A., and Amalric, M., 1995, In a rat model of Parkinsonism, lesions of the subthalamic nucleus reverse increases of reaction time but induce a dramatic premature responding deficit, *J. Neurosci.* **15**:6531–6541.

Baunez, C., and Robbins, T.W., 1997, Bilateral lesions of the subthalamic nucleus induce multiple deficits in an attentional task in rats, *Eur. J. Neurosci.* **9**:2086–2099.

Berridge, K.C., and Robinson, T.E., 1998, What is the role of dopamine in reward: hedonic impact, reward learning, or incentive salience?, *Brain Res. Brain Res. Rev.* **28**:309–369.

Bowery, N.G., 1993, GABAB receptor pharmacology, *Annu. Rev. Pharmacol. Toxicol.* **33**:109–147.

Bowman, E.M., Aigner, T.G., and Richmond, B.J., 1996, Neural signals in the monkey ventral striatum related to motivation for juice and cocaine rewards, *Journal of Neurophysiology* **75**:1061–1073.

Brebner, K., Phelan, R., and Roberts, D.C., 2000, Effect of baclofen on cocaine self-administration in rats reinforced under fixed-ratio 1 and progressive-ratio schedules, *Psychopharmacology (Berl)* **148**:314–321.

Campbell, U.C., Lac, S.T., and Carroll, M.E., 1999, Effects of baclofen on maintenance and reinstatement of intravenous cocaine self-administration in rats, *Psychopharmacology (Berl)* **143**:209–214.

Carelli, R.M., 2002, Nucleus accumbens cell firing during goal-directed behaviors for cocaine vs. 'natural' reinforcement, *Physiol. Behav.* **76**:379–387.

Carelli, R.M., Ijames, S.G., and Crumling, A.J., 2000, Evidence that separate neural circuits in the nucleus accumbens encode cocaine versus "natural" (water and food) reward, *Journal of Neuroscience* **20**: 4255–4266.

Chu, D.C., Albin, R.L., Young, A.B., and Penney, J.B., 1990, Distribution and kinetics of GABAB binding sites in rat central nervous system: a quantitative autoradiographic study, *Neuroscience* **34**:341–357.

Darian-Smith, C., Tan, A., and Edwards, S., 1999, Comparing thalamocortical and corticothalamic microstructure and spatial reciprocity in the macaque ventral posterolateral nucleus (VPLc) and medial pulvinar, *Journal of Comparative Neurology* **410**:211–234.

DeLong, M.R., 1990, Primate models of movement disorders of basal ganglia origin, *Trends Neurosci.* **13**:281–285.

Deniau, J.M., Menetrey, A., and Charpier, S., 1996, The lamellar organization of the rat substantia nigra pars reticulata: segregated patterns of striatal afferents and relationship to the topography of corticostriatal projections, *Neuroscience* **73**:761–781.

Deschenes, M., Veinante, P., and Zhang, Z.W., 1998, The organization of corticothalamic projections: reciprocity versus parity, *Brain Research – Brain Research Reviews* **28**:286–308.

Elliott, R., Newman, J.L., Longe, O.A., and Deakin, J.F., 2003, Differential response patterns in the striatum and orbitofrontal cortex to financial reward in humans: a parametric functional magnetic resonance imaging study, *J. Neurosci.* **23**:303–307.

Engberg, G., Kling-Petersen, T., and Nissbrandt, H., 1993, GABAB-receptor activation alters the firing pattern of dopamine neurons in the rat substantia nigra, *Synapse.* **15**:229–238.

Everitt, B.J., Dickinson, A., and Robbins, T.W., 2001, The neuropsychological basis of addictive behaviour, *Brain Res. Brain Res. Rev.* **36**:129–138.

Everitt, B.J., and Wolf, M.E., 2002, Psychomotor stimulant addiction: a neural systems perspective, *The Journal of Neuroscience* **22**:3312–3320.

Finch, D.M., 1996, Neurophysiology of converging synaptic inputs from the rat prefrontal cortex, amygdala, midline thalamus, and hippocampal formation onto single neurons of the caudate/putamen and nucleus accumbens, *Hippocampus* **6**:495–512.

Francois, C., Yelnik, J., Tande, D., Agid, Y., and Hirsch, E.C., 1999, Dopaminergic cell group A8 in the monkey: anatomical organization and projections to the striatum, *Journal of Comparative Neurology* **414**:334–347.

French, S.J., and Totterdell, S., 2002, Hippocampal and prefrontal cortical inputs monosynaptically converge with individual projection neurons of the nucleus accumbens, *J. Comp. Neurol.* **446**:151–165.

French, S.J., and Totterdell, S., 2003, Individual nucleus accumbens-projection neurons receive both basolateral amygdala and ventral subicular afferents in rats, *Neuroscience* **119**:19–31.

Gerfen, C.R., 1985, The neostriatal mosaic. I. Compartmental organization of projections from the striatum to the substantia nigra in the rat, *Journal of Comparative Neurology* **236**:454–476.

Goto, Y., and O'Donnell, P., 2002, Timing-dependent limbic-motor synaptic integration in the nucleus accumbens, *Proc. Natl. Acad. Sci. U. S. A.* **99**:13189–13193.

Gray, A.M., Rawls, S.M., Shippenberg, T.S., and McGinty, J.F., 1999, The kappa-opioid agonist, U-69593, decreases acute amphetamine-evoked behaviors and calcium-dependent dialysate levels of dopamine and glutamate in the ventral striatum, *J. Neurochem.* **73**:1066–1074.

Groenewegen, H.J., and Berendse, H.W., 1990, Connections of the subthalamic nucleus with ventral striatopallidal parts of the basal ganglia in the rat, *J. Comp. Neurol.* **294**:607–622.

Grofova, I., 1982, Morphology of the substantia nigra pars retucilata projection neurons intracellularly labeled with HRP, *J. Comp. Neurol.* **208**:352–368.

Guzman, R.G., Kendrick, K.M., and Emson, P.C., 1993, Effect of substance P on acetylcholine and dopamine release in the rat striatum: a microdialysis study, *Brain Research* **622**:147–154.

Haber, S.N., and Fudge, J.L., 1997, The primate substantia nigra and VTA: Integrative circuitry and function, *Crit. Rev. Neurobiol.* **11(4)**:323–342.

Haber, S.N., Fudge, J.L., and McFarland, N.R., 2000, Striatonigrostriatal pathways in primates form an ascending spiral from the shell to the dorsolateral striatum, *Journal of Neuroscience* **20**:2369–2382.

Haber, S.N., Ryoo, H., Cox, C., and Lu, W., 1995, Subsets of midbrain dopaminergic neurons in monkeys are distinguished by different levels of mRNA for the dopamine transporter: Comparison with the mRNA for the D2 receptor, tyrosine hydroxylase and calbindin immunoreactivity, *J. Comp. Neurol.* **362**:400–410.

Hedreen, J.C., and DeLong, M.R., 1991, Organization of striatopallidal, striatonigal, and nigrostriatal projections in the Macaque, *J. Comp. Neurol.* **304**:569–595.

Heijna, M.H., Padt, M., Hogenboom, F., Portoghese, P.S., Mulder, A.H., and Schoffelmeer, A.N., 1990, Opioid receptor-mediated inhibition of dopamine and acetylcholine release from slices of rat nucleus accumbens, olfactory tubercle and frontal cortex, *Eur. J. Pharmacol.* **181**:267–278.

Hollerman, J.R., Tremblay, L., and Schultz, W., 1998, Influence of reward expectation on behavior-related neuronal activity in primate striatum, *Journal of Neurophysiology* **80**:947–963.

Joel, D., and Weiner, I., 2000, The connections of the dopaminergic system with the striatum in rats and primates: an analysis with respect to the functional and compartmental organization of the striatum, *Neuroscience* **96**:451–474.

Jog, M.S., Kubota, Y., Connolly, C.I., Hillegaart, V., and Graybiel, A.M., 1999, Building neural representations of habits, *Science* **286**:1745–1749.

Jueptner, M., Frith, C.D., Brooks, D.J., Frackowiak, R.S., and Passingham, R.E., 1997, Anatomy of motor learning. II. Subcortical structures and learning by trial and error, *Journal of Neurophysiology* **77**:1325–1337.

Kalivas, P.W., Duffy, P., and Eberhardt, H., 1990, Modulation of A10 dopamine neurons by gammaaminobutyric acid agonists, *J. Pharmacol. Exp. Ther.* **253**:858–866.

Koob, G.F., and Le Moal, M., 1997, Drug abuse: hedonic homeostatic dysregulation, *Science* **278**:52–58.

Koob, G.F., and Nestler, E.J., 1997, The Neurobiology of Drug Addiction, *The Journal of Neuropsychiatry and Clinical Neurosciences* **9**:482–497.

Lavoie, B., and Parent, A., 1991, Dopaminergic neurons expressing calbindin in normal and parkinsonian monkeys, *Neuroreport.* **2**, **No**. **10**:601–604.

Levy, R., Friedman, H.R., Davachi, L., and Goldman-Rakic, P.S., 1997, Differential activation of the caudate nucleus in primates performing spatial and nonspatial working memory tasks, *Journal of Neuroscience* **17**.

Lopez-Bendito, G., Shigemoto, R., Kulik, A., Paulsen, O., Fairen, A., and Lujan, R., 2002, Expression and distribution of metabotropic GABA receptor subtypes GABABR1 and GABABR2 during rat neocortical development, *Eur. J. Neurosci.* **15**:1766–1778.

Mailly, P., Charpier, S., Menetrey, A., and Deniau, J.M., 2003, Three-dimensional organization of the recurrent axon collateral network of the substantia nigra pars reticulata neurons in the rat, *J. Neurosci.* **23**:5247–5257.

Maurice, N., Deniau, J.M., Glowinski, J., and Thierry, A.M., 1999, Relationships between the prefrontal cortex and the basal ganglia in the rat: physiology of the cortico-nigral circuits, *Journal of Neuroscience* **19**:4674–4681.

Maurice, N., Deniau, J.M., Menetrey, A., Glowinski, J., and Thierry, A.M., 1998, Prefrontal cortex-basal ganglia circuits in the rat: involvement of ventral pallidum and subthalamic nucleus, *Synapse* **29**:363–370.

McFarland, N.R., and Haber, S.N., 2002, Thalamic relay nuclei of the basal ganglia form both reciprocal and nonreciprocal cortical connections, linking multiple frontal cortical areas, *The Journal of Neuroscience* **22**:8117–8132.

McGuire, P.K., Bench, C.J., Frith, C.D., Marks, I.M., Frackowiak, R.S., and Dolan, R.J., 1994, Functional anatomy of obsessive-compulsive phenomena, *British Journal of Psychiatry* **164**:459–468.

Menon, V., Anagnoson, R.T., Glover, G.H., and Pfefferbaum, A., 2001, Functional magnetic resonance imaging evidence for disrupted basal ganglia function in schizophrenia, *Am. J. Psychiatry* **158**:646–649.

Misgeld, U., Bijak, M., and Jarolimek, W., 1995, A physiological role for GABAB receptors and the effects of baclofen in the mammalian central nervous system, *Prog. Neurobiol.* **46**:423–462.

Mogenson, G.J., Jones, D.L., and Yim, C.Y., 1980, From motivation to action: Functional interface between the limbic system and the motor system, *Prog. Neurobiol.* **14**:69–97.

Nauta, H.J.W., and Cole, M., 1978, Efferent projections of the subthalamic nucleus: An autoradiographic study in monkey and cat, *J. Comp. Neurol.* **180**:1–16.

Nauta, W.J.H., Smith, G.P., Faull, R.L.M., and Domesick, V.B., 1978, Efferent connections and nigral afferents of the nucleus accumbens septi in the rat, *Neuroscience* **3**:385–401.

Nisenbaum, E.S., Berger, T.W., and Grace, A.A., 1993, Depression of glutamatergic and GABAergic synaptic responses in striatal spiny neurons by stimulation of presynaptic GABAB receptors, *Synapse* **14**:221–242.

O'Donnell, P., and Grace, A.A., 1995, Synaptic interactions among excitatory afferents to nucleus accumbens neurons: Hippocampal gating of prefrontal cortical input, *J. Neurosci.* **15**:3622–3639.

Owen, A.M., Roberts, A.C., Hodges, J.R., Summers, B.A., Polkey, C.E., and Robbins, T.W., 1993, Contrasting mechanisms of impaired attentional set-shifting in patients with frontal lobe damage or Parkinson's disease, *Brain* **116**:1159–1175.

Pantelis, C., Barnes, T.R., Nelson, H.E., Tanner, S., Weatherley, L., Owen, A.M., and Robbins, T.W., 1997, Frontal-striatal cognitive deficits in patients with chronic schizophrenia, *Brain* **120**:1823–1843.

Parent, A., and Hazrati, L.-N., 1994, Multiple striatal representation in primate substantia nigra, *J. Comp. Neurol.* **344**:305–320.

Passingham, R.E., 1995, The Frontal Lobes and Voluntary Action, in: *Oxford Psychology Series: Vol. 21.*, OUP, Oxford, pp. 1–304.

Percheron, G., and Filion, M., 1991, Parallel processing in the basal ganglia: Up to a point, *Trends Neurosci.* **14**:55–59.

Rauch, S.L., Whalen, P.J., Curran, T., Shin, L.M., Coffey, B.J., Savage, C.R., McInerney, S.C., Baer, L., and Jenike, M.A., 2001, Probing striato-thalamic function in obsessive-compulsive disorder and Tourette syndrome using neuroimaging methods, *Advances in Neurology* **85**:207–224.

Rawls, S.M., and McGinty, J.F., 2000, Delta opioid receptors regulate calcium-dependent, amphetamineevoked glutamate levels in the rat striatum: an in vivo microdialysis study, *Brain Res.* **861**:296–304.

Roberts, D.C., and Andrews, M.M., 1997, Baclofen suppression of cocaine self-administration: demonstration using a discrete trials procedure, *Psychopharmacology (Berl)* **131**:271–277.

Roberts, D.C., Andrews, M.M., and Vickers, G.J., 1996, Baclofen attenuates the reinforcing effects of cocaine in rats, *Neuropsychopharmacology* **15**:417–423.

Schultz, W., 2002, Getting formal with dopamine and reward, *Neuron.* **36**:241–263.

Sharp, T., Zetterstrom, T., Ljungberg, T., and Ungerstedt, U., 1987, A direct comparison of amphetamine-induced behaviours and regional brain dopamine release in the rat using intracerebral dialysis, *Brain Res.* **401**:322–330.

Shoaib, M., Swanner, L.S., Beyer, C.E., Goldberg, S.R., and Schindler, C.W., 1998, The GABAB agonist baclofen modifies cocaine self-administration in rats, *Behav. Pharmacol.* **9**:195–206.

Smith, I.D., and Grace, A.A., 1992, Role of subthalamic nucleus in the regulation of nigral dopamine neuron activity, *Synapse* **12**:287–303.

Smith, Y., Bevan, M.D., Shink, E., and Bolam, J.P., 1998, Microcircuitry of the direct and indirect pathways of the basal ganglia, *Neuroscience* **86**:353–387.

Somogyi, P., Bolam, J.P., Totterdell, S., and Smith, A.D., 1981, Monosynaptic input from the nucleus accumbens-ventral striatum region to retrogradely labelled nigrostriatal neurones, *Brain Res.* **217**:245–263.

Szabo, J., 1979, Strionigral and nigrostriatal connections. Anatomical studies, *Applied Neurophysiology* **42**:9–12.

Wang, J.Q., and McGinty, J.F., 1995a, Alterations in striatal zif/268, preprodynorphin and preproenkephalin mRNA expression induced by repeated amphetamine administration in rats, *Brain Res.* **673**:262–274.

Wang, J.Q., and McGinty, J.F., 1995b, Dose-dependent alteration in zif/268 and preprodynorphin mRNA expression induced by amphetamine or methamphetamine in rat forebrain, *J. Pharmacol. Exp. Ther.* **273**:909–917.

Wise, R.A., 1996, Addictive drugs and brain stimulation reward, *Annual Review of Neuroscience* **19**:319–340.

Wright, C.I., and Groenewegen, H.J., 1996, Patterns of overlap and segregation between insular cortical, intermediodorsal thalamic and basal amygdaliod afferents in the nucleus accumbens of the rat, *Neuroscience* **73**:359–373.

Zahm, D.S., and Heimer, L., 1993, Specificity in the efferent projections of the nucleus accumbens in the rat: Comparison of the rostral pole projection patterns with those of the core and shell, *J. Comp. Neurol.* **327**:220–232.

Zetterstrom, T., Sharp, T., Marsden, C.A., and Ungerstedt, U., 1983, In vivo measurement of dopamine and its metabolites by intracerebral dialysis: changes after d-amphetamine, *J. Neurochem.* **41**:1769–1773.

Zhou, W., Mailloux, A.W., Jung, B.J., Edmunds, H.S., Jr., and McGinty, J.F., 2004, GABAB receptor stimulation decreases amphetamine-induced behavior and neuropeptide gene expression in the striatum, *Brain Res.* **1004**:18–28.

FEEDFORWARD AND FEEDBACK INHIBITION IN THE NEOSTRIATUM

James M. Tepper, Tibor Koós, and Charles J. Wilson*

1. INTRODUCTION

The neostriatum is the principal input structure of the basal ganglia and plays the greatest role in integrating and transducing the excitatory input that derives from the cortex and thalamus. The principal neuron, the GABAergic spiny projection neuron, comprises the majority of the striatal neurons, ranging from slightly less than 80% of all striatal neurons in primates (Graveland and DiFiglia, 1985) to almost 98% in rodents (Luk and Sadikot, 2001; Rymar et al., 2004). The remainder of the neuronal population consists of at least 3 distinct types of GABAergic and one cholinergic interneuron.

The somatodendritic morphology and existence of a local axonal arborization of the spiny neuron was well described in the earliest Golgi studies but the nature and full extent of the local axon collateral plexus was not completely appreciated until the advent of in vivo intracellular staining of striatal neurons with horseradish peroxidase in the late 1970s and early 1980s (Wilson, 1979; Preston et al., 1980; Wilson and Groves, 1980; Bishop et al., 1982). These studies revealed that the main axon of the spiny cell branched within a few tens of micrometers from the soma of origin to form a relatively dense and homogeneous local arborization that in most cases overlapped and extended slightly beyond the dendritic field of the parent neuron. In some cases the local collateral arborization extended for great distances beyond the parent dendritic field.

Around the same time it became clear from electron microscopic analysis of intracellularly or retrogradely labeled material that the principal targets of the spiny cell local axon collaterals were the surrounding spiny neurons (Wilson and Groves, 1980; Somogyi et al., 1981). This was not unexpected given the numerical predominance of the spiny cells in the striatum, and the finding led rather naturally to the inference that the functional organization of the neostriatum would incorporate a powerful lateral inhibitory modulation of spiny neurons by their local collaterals (Groves, 1983). Several other independent lines

* James M. Tepper, Center for Molecular and Behavioral Neuroscience, Rutgers University, Newark, NJ 07102. Tibor Koós, Section of Neurobiology, Yale University School of Medicine, New Haven, CT 06510. Charles J. Wilson, Division of Life Science, University of Texas at San Antonio, San Antonio, TX, 78249, USA.

of evidence supported this view. For example, most neostriatal neurons exhibited very little spontaneous activity in vivo and many did not fire spontaneously at all (Richardson et al., 1977; Levine et al., 1982), even in locally anesthetized preparations (Wilson and Groves, 1980, 1981). However, local application of a $GABA_A$ antagonist produced a dramatic increase in the firing rate of a subpopulation of spiny neurons (Nisenbaum and Berger, 1992), providing evidence for a substantial GABAergic tone in vivo. Local stimulation in striatal slices readily elicited GABAergic IPSPs in spiny neurons presumed to be mediated by the local collaterals (Lighthall and Kitai, 1981). Stimulation of the entopeduncular nucleus in decorticate and thalamic-lesioned cats, which was expected to cause antidromic activation of striatal spiny neurons, led to inhibition of striatal units in extracellular recordings in cats, an effect that could be blocked by iontophoretic application of bicuculline (Katayama et al., 1981). Finally, action potentials evoked by depolarizing current injections in spiny neurons were found to reduce the size of EPSPs evoked by stimulation of substantia nigra, an effect that was eliminated by systemic administration of bicuculline and which was attributed to the activation of axon collaterals synapsing back onto the parent cell (Park et al., 1980).

Thus, as biologically-based computational models of the neostriatum were applied to understanding the functioning of the basal ganglia, a common attribute of many striatal models came to be the instantiation of the spiny cell local axon collateral synapses as a "winner-take-all" lateral inhibition which acted to strengthen and sharpen the output of the most strongly excited neurons by inhibiting their neighbors which in turn would lead to disinhibition of the strongly excited cells (e.g., Wickens et al., 1995; Beiser and Houk, 1998; Redgrave et al., 1999; Wickens and Oorschot, 2000; Bar-Gad and Bergman, 2001).

Experiments designed to detect collateral inhibition directly failed to do so. Antidromic activation of spiny neurons while recording intracellularly in vivo or in vitro failed to produce a detectable IPSP but cortical stimulation subthreshold for eliciting orthodromic spikes in spiny neurons could evoke IPSPs in spiny neurons in slices (Wilson et al., 1989), in vivo in neonates (Tepper and Trent, 1993) and in neostriatal grafts (Xu et al., 1991). However, simultaneous recording of pairs of cells located within each other's axon collateral field failed to reveal synaptic responses, even with spike-triggered averaging (Jaeger et al., 1994). The difficulty in demonstrating collateral inhibition in striatum, despite the incontrovertible anatomical evidence for the existence of the synapses, was, however, consistent with results from in vivo extracellular recordings in behaving monkeys or rats where little or no correlation among spiking in nearby neurons was observed (Jaeger et al., 1995; Woodward et al., 1995) and with results from in vivo intracellular recordings which showed that although the up and down state transitions of nearby spiny neurons were highly correlated, action potentials were not (Stern et al., 1998). These data led to the suggestion that collateral interactions among spiny neurons are not a source of powerful inhibition in the striatum but rather might play a more subtle modulatory role and that the strong GABAergic inhibition observed after local or cortical stimulation was likely mediated by GABAergic interneurons (Jaeger et al., 1994).

2. INTERNEURONAL GABAERGIC INHIBITION IN STRIATUM

The earliest Golgi studies of neostriatum showed the presence, albeit in small number, of a large aspiny neuron and one or more medium sized aspiny neurons that clearly differed from the medium sized spiny neuron in somatic size, shape and/or dendritic arborization.

The ability of medium-sized aspiny neurons to take up radiolabeled GABA showed that at least some of these were GABAergic (Bolam et al., 1983). Subsequent studies utilizing immunocytochemical labeling revealed three distinct types of GABAergic interneurons that colocalized, respectively, parvalbumin (PV), calretinin (CR) or neuropeptide Y (NPY), somatostatin (SOM) and nitric oxide synthase (Takagi et al., 1983; Cowan et al., 1990; Bennett and Bolam, 1993; Kawguchi, 1993; Rymar et al., 2004). Two of these (the parvalbumin and the NPY expressing neurons) have been characterized electrophysiologically and termed FS and PLTS interneurons, respectively (Kawaguchi, 1993; Koós and Tepper 1999). Recordings from an infrequently encountered and immunocytochemically or morphologically unidentified GABAergic interneuron, termed the LTS neuron, have been reported (Koós and Tepper, 1999, 2002) which might correspond to the calretinin-containing GABAergic interneuron (Tepper and Bolam, 2004), or represent a physiological variant of SOM-expressing PLTS neurons. This classification is likely overly simplistic considering the morphological and physiological diversity of the PV interneurons (Kawaguchi, 1993; Koós and Tepper, 1999), and the comparison with cortical (Markram et al., 2004; Monyer and Markram, 2004) and hippocampal (Freund and Buzsaki, 1995) interneuron populations which is particularly relevant in the light of the shared developmental origin of certain cortical GABAergic interneurons with their striatal counterparts (Marin et al., 2000).

In recordings from brain slices, the striatal PV-expressing neuron was found to exhibit very narrow spikes with a large, rapid AHP, little or no spike frequency accommodation even at high firing rates (>200 Hz) and intermittent firing in short bursts which arise from subthreshold membrane potential oscillations in response to lower amplitude depolarizing pulses (Kawaguchi, 1993; Kawaguchi et al., 1995; Koós and Tepper, 1999, 2002; Bracci et al., 2003). These electrophysiological characteristics are similar or identical to the so-called fast-spiking (FS) interneuron previously described in cortex and hippocampus (Freund and Buzsaki, 1995), a subclass of which also expresses parvalbumin). Similar results were obtained in striatal organotypic cell co-cultures (Plenz and Aertsen, 1996; Plenz and Kitai, 1998). The somatostatin neuron was also shown to exhibit distinguishing electrophysiological features including a low-threshold spike and prolonged plateau depolarizations (Kawaguchi, 1993; Kawaguchi et al., 1995).

The expected role of these interneurons in mediating intrastriatal GABAergic inhibition was first demonstrated directly by simultaneous whole cell recordings of FS interneurons and spiny neurons in striatal slices (Koós and Tepper, 1999; 2002). These recordings revealed that action potentials in FS interneurons produced monosynaptic GABAA-mediated IPSPs in roughly 25% of spiny neurons within a 250 μm radius of the presynaptic neuron. The IPSPs were notable in several respects. They were large; single spikes in a FS interneuron produced hyperpolarizing IPSPs over 1 mV in amplitude in spiny neurons at their maximal subthreshold up state membrane potential. Summation was very effective and short bursts of action potentials led to IPSPs up to 7 mV in amplitude (Koós and Tepper, 1999). The IPSP was also very effective at delaying or even abolishing evoked spikes in postsynaptic spiny neurons; single presynaptic spikes produced a delay of almost 6 ms in spiny cell spike timing and short bursts could completely block spiking (Koós and Tepper, 1999). The IPSP was also extremely reliable, showing an overall failure rate of less than 1% (Koós and Tepper, 1999; Tepper et al., 2004). In addition, the FS interneurons were also found to be electrotonically coupled, as predicted by the electron microscopic visualization of gap junctions (Kita et al., 1990), and therefore presumed to form a sort of syncytium of GABAergic interneurons that could act to generate IPSPs in a large number of spiny neurons simultaneously.

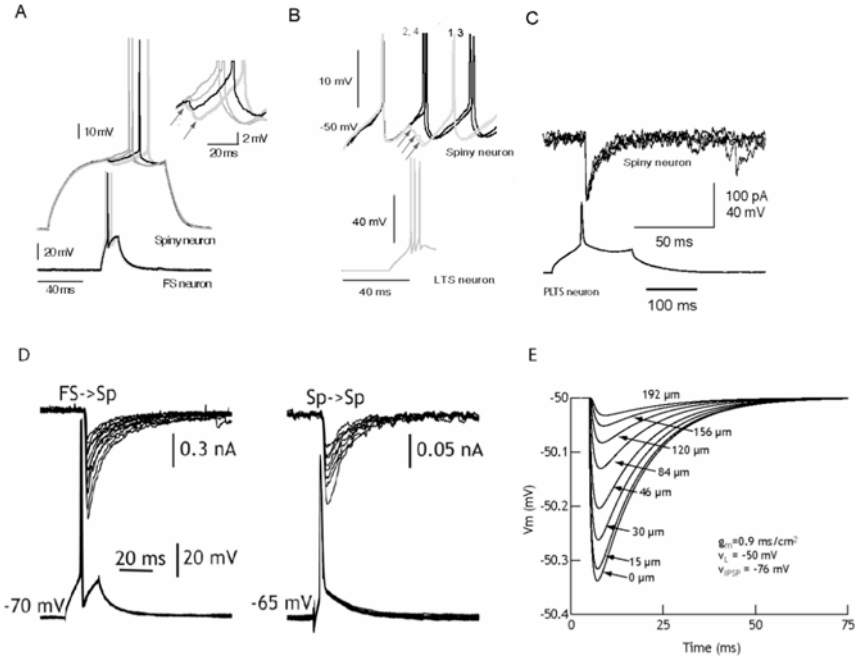

Figure 1. A. IPSP/Cs evoked by interneurons and spiny neurons (Sp). Depolarization-elicited spike in a spiny neuron (2 upper light gray traces) is delayed by IPSPs evoked by single spikes (lower black trace) or a spike doublet (lower gray trace) of an FS interneuron. Inset shows IPSPs and spike delays at higher gain. **B**. Burst of three spikes evoked in a LTS neuron delays firing of depolarization-induced spiking of a spiny neuron. The LTS evokes compound IPSPs (upper gray traces 1, 3) that prevent the firing of the spiny neuron (black traces 2, 4). **C**. Single spike in a PLTS neuron elicits an IPSC in a spiny neuron. **D**. Comparison of IPSCs evoked in spiny neurons by spiny cells (Sp->Sp) and by fast spiking cells (FS->Sp). Typical IPSCs in whole cell recordings after replacement of K^+ by Cs^+. The time course of the IPSCs are similar, but the FS-evoked IPSC is about 6 times larger than the Sp->Sp IPSC. Note difference in scales. **E**. Computer simulation of spiny cell IPSPs with the synapse at varying distances from the somatic recording site.

Similarly powerful and effective IPSPs in spiny cells were elicited by spiking in LTS neurons (Koós and Tepper, 1999; 2002). Although also monosynaptically connected to spiny neurons, PLTS neurons may primarily provide dendritic inhibition since PLTS neurons in the striatum target primarily the dendrites of spiny cells (Kubota and Kawaguchi, 2000), similar to SOM^+ interneurons in the hippocampus (Katona et al., 1999).

Thus, while neostriatal interneurons are probably functionally heterogeneous, at least 2 classes appear specialized for providing powerful feed-forward inhibition onto spiny cells. Given the effectiveness of the evoked IPSPs at delaying or abolishing spiking in spiny neurons (Figure 1), these feed-forward GABAergic inputs appear to be the principal mediators of the GABAergic modulation of spike timing in the spiny neurons.

3. SPINY NEURON AXON COLLATERALS

Direct demonstration of the spiny neuron axon collateral IPSP was first reported with paired intracellular current clamp recordings in striatal slices (Tunstall et al., 2002). Evoked

action potentials in one spiny neuron produced a small IPSP in a second spiny neuron in 9 of 45 pairs recorded an average of 264 μm apart. The IPSP had a mean of about 277 μV, excluding failures, or only about 1/6 the amplitude of IPSPs generated in spiny cells by interneurons under reasonably similar postsynaptic conditions of membrane potential, input resistance and chloride concentration (Koós and Tepper, 1999). Individual IPSPs could sometimes be seen, but usually required averages of 200 sweeps for reliable detection. The probability of synaptic connection was relatively low, only 9/90 or 10% and there were no reciprocally connected pairs in the sample. In addition, the IPSP exhibited a rather high (38%) mean failure rate. Like the interneuronal IPSP, the collateral IPSP was mediated by $GABA_A$ receptors.

Soon after, the spiny cell collateral IPSP was detected with paired whole cell recordings in cortical-striatal-nigral co-cultures (Czubayko and Plenz, 2002). While many of the characteristics of the IPSP were the same as those reported by Tunstall et al. (2002) in the slice, the amplitude of the IPSP was much larger (~2 mV) in the co-cultures. In addition, the probability of connection also significantly greater (24.6%), and reciprocal connections were observed in 31% (8/26) of the connected pairs, suggesting that a greater connectivity exists among neurons in the co-cultures than in acute slices, where the probability of synaptic connectivity ranged between 10 and 18% (Koós et al., 2004; Tunstall et al., 2002; Taverna et al., 2004, 2005). Nevertheless, if the IPSPs of Czubayko and Plenz (2002) were normalized to those of Tunstall et al. (2002) by correcting for differences in input resistance and membrane potential, the IPSP amplitudes in the two studies were similar (Tepper et al., 2004).

Subsequent reports using voltage clamp in acute slices reported collateral IPSCs in spiny neurons under a variety of different conditions (principally Cs^+ substitution for K^+ and/or high Cl^+ in the internal solution) intended to optimize the size of the chloride-mediated synaptic response (Koós et al., 2004; Guzman et al., 2003; Taverna et al., 2004; Venance et al., 2004). When the peak conductance and decay time constants of the IPSCs were used in a single compartment model to simulate the IPSP that would be recorded near the maximal subthreshold up-state membrane potential (−47 mV), the results (−171 to 340 μV; Tepper et al., 2004) were very close to those reported by Tunstall et al. (2002). These data seemed to indicate that the spiny cell axon collateral IPSP was several fold smaller in amplitude than the feedforward IPSP originating from striatal interneurons (Koós and Tepper, 1999), but direct comparison was difficult because of the large number of methodological differences among the different studies. Therefore we compared the characteristics of the feedforward and feedback synaptic responses directly by measuring IPSCs originating from the axon collaterals and from the GABAergic interneurons with dual whole cell or perforated patch recordings in identical preparations under the same recording conditions.

4. COMPARISON OF AXON COLLATERAL AND INTERNEURONAL INHIBITION

Whole cell recordings were obtained in striatal slices from adult rats from neuron pairs consisting of two spiny neurons or one FS interneuron and one spiny neuron (Koós et al., 2004). The presynaptic neuron was recorded in current clamp using a standard internal solution and the postsynaptic neuron was recorded in voltage clamp using an internal based on 140 mM CsCl. Under these conditions the FS → spiny cell IPSC was 269 ± 213 pA

Table 1

Group	Peak Current (pA)	Rise Time (msec)	Half-width (msec)	N release sites	q* (pA)	p_r
spiny → spiny	51 + 39	1.3 + 0.6	12.9 + 3.4	2.9 + 1.6	43 + 16	0.76 + 0.18
FS → spiny	269 + 213	1.6 + 1.0	11.6 + 3.8	6.7 + 7.8	64 + 17	0.57 + 0.24

(n = 9). Under identical recording conditions, the spiny → spiny IPSC was 51 ± 39 pA (n = 26) or a little less than 1/5 as large. If recorded with the same chloride concentration in the internal but without Cs^+ ions (which block K^+ channels and greatly reduces the effects of electrotonic attenuation), the IPSC was only 18.3 ± 13.8 pA (n = 3). This suggests that one important factor contributing to the difference is the location of the synapse. Immunocytochemical studies show that PV^+ terminals make the majority of their synapses proximally, often forming pericellular baskets around the soma and proximal dendrites of spiny neurons (Kita et al., 1990; Bennett and Bolam, 1994). In contrast, electron microscopy of intracellularly labeled spiny cell axons shows that 88% of the synapses are located in the spiny (i.e., intermediate and distal) regions of the dendrites (Wilson and Groves, 1980). Spines give the dendrites of the spiny cell approximately twice the electrotonic length of a similarly sized, aspiny dendrite (Wilson et al., 1983). This coupled with the strong inward rectification which gives the spiny cell a very low resting input resistance makes location a large factor in synaptic efficacy in these neurons, and is responsible for decreasing the somatic effects of the collateral IPSP by about a factor of 3 (Koós et al., 2004).

In addition to location, the differences in the amplitudes of the spiny → spiny IPSC and the FS → spiny cell IPSC could be due to a variety of presynaptic factors including release probability, quantal size and/or the number of presynaptic release sites (active synapses). To distinguish among these possibilities, the data were subjected to variancemean analysis (Clements and Silver, 2000) and nonstationary PSC analysis (Scheuss et al., 2002) from which the release probability (p), quantal current (q*) and the number of release sites (N) can be extracted. The results of this analysis are shown in Table 1.

The two IPSCs were quite similar, differing only in amplitude, as expected, and in the number of release sites (Figure 2). The difference in number of release sites is in actuality likely greater than our data suggest. When we searched for pairs of spiny neurons for recording and analysis we biased our sample towards pairs which showed the largest and most robust synaptic connection. This likely resulted in our sample having a larger N than is representative of the entire population. In any event, it is this difference in the number of release sites that accounts for the greatest fraction of the difference in amplitude between the FS → spiny and spiny → spiny synapses (Koós et al., 2004). The difference in N is also responsible for the much greater failure rate of the spiny → spiny synapse than the FS → spiny synapse which fails completely less than 1% of the time (Koós and Tepper, 1999).

5. FUNCTIONAL IMPLICATIONS

The connectivity of the feedforward and feedback circuits also exhibits important differences. Using estimates for the interneuron population based on the number of highly GAD_{67} positive neurons (3–5%), the convergence of GABAergic interneurons onto spiny

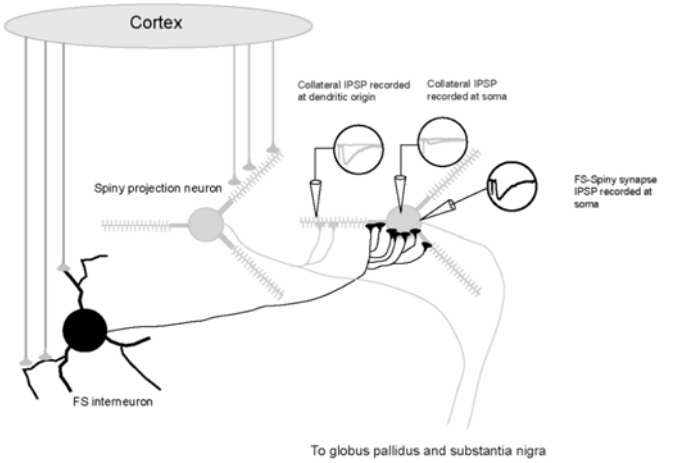

Figure 2. Simplified schematic illustration of the organization of the feedforward and feedback GABAergic pathways in neostriatum and their major differences. The somatic amplitude of the FS → SP IPSC is many times larger than that of the SP → SP IPSC. In addition, the SP → SP IPSC has a high failure rate while the FS → SP IPSC fails <1% of the time. The difference in failure rate and part of the difference in amplitude is due to the number of synapses each presynaptic neuron makes. Each spiny neuron typically makes 2 or 3 synapses on each postsynaptic spiny neuron while each FS interneuron typically makes 6 or more synapses on each postsynaptic spiny cell. The rest of the amplitude difference is due to the distal location of the SP → SP synapses in contrast to the proximal location of the FS → SP synapses.

neurons is between 4 and 27 (Koós & Tepper, 1999; Kubota and Kawaguchi, 2000). If the calculations are made based on more recent unbiased stereological cell counts of immunolabeled PV, CR and SOM positive neurons (2%, Rymar et al., 2004) the convergence becomes smaller and if only FS interneurons are considered is between 4 and 1 (Tepper et al., 2004). But even a single presynaptic GABAergic interneuron exerts a powerful enough IPSP to block spiking in a spiny neuron (Koós and Tepper, 1999). Thus the feedforward inhibitory system has the appropriate characteristics to precisely and powerfully modify both the overall firing rate and the timing of single action potentials in spiny neurons.

This stands in sharp contrast to the situation with respect to feedback inhibition. The influence of a single projection neuron on the spike timing of its postsynaptic targets can be estimated through a comparison with the same effect of FS interneurons, since the magnitude of the delay of postsynaptic action potentials is approximately linearly related to the somatic amplitude of the IPSP. Thus even in the presence of the relatively high *in vitro* somatic input resistance of spiny neurons, a single 0.05–0.3 mV collateral IPSP (Figure 1E) would cause a spike delay of only 0.25–1.5 ms if the postsynaptic neurons fire at physiological rates (20–50 Hz). Consequently, the influence of a single collateral input on the firing rate of its targets is largely negligible. Along with the rarity or absence of reciprocal collateral inhibition (Tunstall et al., 2002; Koós et al., 2004; Taverna et al., 2004), this indicates that the axon collaterals are not well-suited to create the type of winner-take-all lateral inhibition widely proposed to occur in the neostriatum. Rather, since the IPSP generated by single projection neurons is expected to be much stronger at their dendritic site of origin, both unitary connections as well as their populations can be instrumental in and specialized for controlling distal dendritic events perhaps including modulation of

synaptic plasticity, spike backpropagation and the integrative properties of the distal dendrites (Kerr and Plenz, 2002, 2004; Vergara et al., 2003; Koós et al., 2004).

At the population level, however, despite the weak effect of unitary collateral inputs, feedback inhibition may contribute significantly to firing rate control due to the convergence of numerous inputs onto single postsynaptic cells. Based on the observed probability of connectivity among spiny neurons in vitro, a convergence of 407–518 presynaptic projection neurons innervating each postsynaptic cell can be estimated, which, depending on the population size and exact convergence of FS and other interneurons (see above), translates into approximately 16 to over 125 times more presynaptic MS neurons than interneurons innervating each projection cell (see also Guzman et. al., 2003; Tepper et al., 2004), and represents a 3–25 times larger net synaptic conductance associated with the feedback circuitry (Koós et al., 2004).

Consequently, it is likely that both the feed-forward and the feedback circuits contribute to the net inhibitory control of the firing rate of neostriatal projection neurons, but through significantly different input circuits and biophysical mechanisms.

6. ACKNOWLEDGEMENTS

Supported by NS34865 (JMT) and NS20743 (CJW).

7. REFERENCES

Bar-Gad, I., and Bergman, H., 2001, Stepping out of the box: information processing in the neural networks of the basal ganglia, *Curr. Opin. Neurobiol.* **71**:439–473.

Beiser, D.G., and Houk, J.C., 1998, Model of cortical-basal ganglionic processing: encoding the serial order of sensory events, *J. Neurophysiol.* **79**:3168.

Bennett, B.D., and Bolam, J.P., 1994, Synaptic input and output of parvalbumin-immunoreactive neurons in the neostriatum of the rat, *Neuroscience* **62**:707–719.

Bennett, B.D., and Bolam, J.P., 1993, Characterization of calretinin-immunoreactive structures in the striatum of the rat, *Brain Res*. **609**:137–148.

Bishop, G.A., Chang, H.T., and Kitai, S.T., 1982, Morphological and physiological properties of neostriatal neurons: An intracellular horseradish peroxidase study in the rat, *Neuroscience* **7**:179–191.

Bolam, J.P., Clarke, D.J., Smith, A.D., and Somogyi, P., 1983, A type of aspiny neuron in the rat neostriatum accumulates [3H]γ-aminobutyric acid: Combination of golgi-staining, autoradiography, and electron microscopy, *J. Comp. Neurol.* **213**:121–134.

Bracci, E., Centonze, D., Bernardi, G., and Calabresi, P., 2003, Voltage-dependent membrane potential oscillations of rat striatal fast-spiking interneurons. *J. Physiol*. **549**:121.

Cowan, R.L., Wilson, C.J., Emson, P.C., and Heizmann, C.W., 1990, Parvalbumin-containing GABAergic interneurons in the rat neostriatum, *J. Comp. Neurol.* **302**:197–205

Czubayko, U., and Plenz, D., 2002, Fast synaptic transmission between striatal spiny projection neurons, *Proc. Natl. Acad. Sci. U.S.A.* **99**:15764.

Clements, J.D., and Silver, R.A., 2000, Unveiling synaptic plasticity: a new graphical and analytical approach, *Trends Neurosci.* **23**:105–113.

Freund, T.F., and Buzsáki, G., 1996, Interneurons of the hippocampus, *Hippocampus* **6**:347–470.

Graveland, G.A., and DiFiglia, M., 1985. The frequency and distribution of medium-sized neurons with indented nuclei in the primate and rodent neostriatum, Br*ain Res.* **327**:307–311.

Groves, P.M., 1983, A theory of the functional organization of the neostriatum and the neostriatal control of voluntary movement, *Brain Res. Rev.* **5**:109–132.

Guzman, J.N., Hernandez, A., Galarraga, E., Tapia, D., Laville, A., Vergara, R., Aceves, J., and Bargas, J., 2003, Dopaminergic modulation of axon collaterals interconnecting spiny neurons of the rat striatum, *J. Neurosci.* **23**:8931–8940.

Jaeger, D., Kita, H., and Wilson, C.J., 1994, Surround inhibition among projection neurons is weak or nonexistent in the rat neostriatum, *J. Neurophysiol.* **72**:1–4.

Katayama, Y., Miyazaki, S., and Tsubokawa, T., 1981, Electrophysiological evidence favoring intracaudate axon collaterals of GABAergic caudate output neurons in the cat, *Brain Res.* **216**:180–186.

Katona, I., Acsády, L., and Freund, T.F., 1999, Postsynaptic targets of somatostatin immunreactive interneurons in the rat hippocampus, *Neuroscience* **88**:37–55

Kawaguchi, Y., 1993, Physiological, morphological and histochemical characterization of three classes of interneurons in rat neostriatum, *J. Neurosci.* **13**:4908–4923.

Kawaguchi, Y., Wilson, C.J., Augood, S.J., and Emson, P.C., 1995, Striatal interneurones: chemical, physiological and morphological characterization, *Trends Neurosci.* **18**:12:527–535.

Kerr, J.N., and Plenz, D., 2002, Dendritic calcium encodes striatal neuron output during up-states, *J. Neurosci.* **22**:1499–1512.

Kerr, J.N., and Plenz, D., 2004, Action potential timing determines dendritic calcium during striatal up-states, *J. Neurosci.* **24**:1877–885.

Kita, H., Kosaka, T., and Heizmann, C.W., 1990, Parvalbumin-immunoreactive neurons in the rat neostriatum: a light and electron microscopic study, *Brain Res.* **536**:1–15.

Koós, T., and Tepper, J.M., 1999, Inhibitory control of neostriatal projection neurons by GABAergic interneurons, *Nat. Neurosci.* **2**:467–472.

Koós, T., and Tepper, J.M., 2002, Dual cholinergic control of fast spiking interneurons in the neostriatum, *J. Neurosci.* **22**:529–535.

Koós, T., Tepper, J.M., and Wilson, C.J., 2004, Comparison of IPSCs evoked by spiny and fast-spiking neurons in the neostriatum, *J. Neurosci.* **24**;7916–7922.

Kubota, Y., and Kawaguchi, Y., 2000, Dependence of GABA ergic synaptic areas on the interneuron type and target size, *J. Neurosci.* **20**:375–386.

Levine, M.S., Fisher, R.S., Hull, C.D., and Buchwald, N.A., 1982, Development of spontaneous neuronal activity in the caudate nucleus, globus pallidus-entopeduncular nucleus, and substantia nigra of the cat, *Dev. Brain Res*. **3**:429–441.

Lighthall, J.W., and Kitai, S.T., 1983, A short duration GABAergic inhibition in identified neostriatal medium spiny neurons: in vitro slice study, *Brain Res.Bull.* **11**:103.

Luk, K.C., and Sadikot, A.F., 2001, GABA promotes survival but not proliferation of parvalbumin-immunoreactive interneurons in rodent neostriatum: An in vivo study with stereology, *Neuroscience* **104**:93–103.

Marin, O., Anderson, S.A., Rubenstein, J.L., 2000, Origin and molecular specification of striatal interneurons, *J. Neurosci.* **20**:6063–6076.

Markram, H., Toledo-Rodriguez, M., Wang, Y., Gupta, A., Silberger, G., and Wu, C., 2004, Interneurons of the neocortical inhibitory system, *Nat. Rev. Neurosci*. **5**:793–807.

Monyer, H., and Markram, H., 2004, Interneuron diversity series: Molecular and genetic tools to study GABAergic interneuron diversity and function, *Trends Neurosci.* **27**:90–97

Nisenbaum, E.S., and Berger, T.W., 1992, Functionally distinct subpopulations of striatal neurons are differentially regulated by GABAergic and dopaminergic inputs–I. In vivo analysis, *Neuroscience* **48**:561–578.

Park, M.R., Lighthall, J.W., and Kitai, S.T., 1980, Recurrent inhibition in the rat neostriatum, *Brain Res*. **194**:359–369.

Plenz, D., 2003, When inhibition goes incognito: feedback interaction between spiny projection neurons in striatal function. *Trends Neurosci*. **26**:436–443.

Plenz, D., and Aertsen, A., 1996, Neural dynamics in cortex-striatum co-cultures–I. anatomy and electrophysiology of neuronal cell types, *Neuroscience* **70**:861–891.

Plenz, D., and Kitai, S.T., 1998, Up and down states in striatal medium spiny neurons simultaneously recorded with spontaneous activity in fast-spiking interneurons studied in cortex-striatum-substantia nigra organotypic cultures, *J. Neurosci.* **18**:266–283.

Preston, R.J., Bishop, G.A., and Kitai, S.T., 1980, Medium spiny neuron projection from the rat striatum: an intracellular horseradish peroxidase study. *Brain. Res*. **183**:253–263.

Redgrave, P., Prescott, T.J., and Gurney, K., 1999, The basal ganglia: a vertebrate solution to the selection problem?, *Neuroscience* **89**:1009.

Richardson, T.L., Miller, J.J., and McLennan, H., 1977, Mechanisms of excitation and inhibition in the nigrostriatal system, *Brain Res*. **127**:219–234.

Rymar, V.V., Sasseville, R, Luk, K.C., and Sadikot, A.F., 2004, Neurogenesis and stereological morphometry of calretinin-immunoreactive GABAergic interneurons of the neostriatum. *J. Comp. Neurol.* **469**:325–339.

Scheuss, V., Schneggenburger, R., and Neher, E., 2002, Separation of presynaptic and postsynaptic contributions to depression by covariance analysis of successive EPSCs at the calyx of Held synapse, *J. Neurosci.* **22**:728–739.

Somogyi, P., Bolam, J.P., and Smith, A.D., 1981, Monosynaptic cortical input and local axon collaterals of identified striatonigral neurons. A light and electron microscopic study using the Golgi-peroxidase transport-degeneration procedure, *J. Comp. Neurol*. **195**:567–584.

Stern, E.A., Jaeger, D., and Wilson, C.J., 1998, Membrane potential synchrony of simultaneously recorded striatal spiny neurons in vivo, *Nature* **394**:475–478.

Takagi, H., Somogyi, P., Somogyi, J., and Smith, A.D., 1983, Fine structural studies on a type of somatostatin-immunoreactive neuron and its synaptic connections in the rat neostriatum: a correlated light and electron microscopic study. *J. Comp. Neurol.* **214**:1–16.

Taverna, S., Canciani, B., and Pennartz, C.M., 2005, Dopamine D1-receptors modulate lateral inhibition between principal cells of the nucleus accumbens, *J. Neurophysiol*. **93**:1816–1819.

Taverna, S., van Dongen, Y.C., Groenewegen, H.J., and Pennartz, C.M., 2004, Direct physiological evidence for synaptic connectivity between medium-sized spiny neurons in rat nucleus accumbens in situ, *J. Neurophysiol.* **91**:1111–1121.

Tepper, J.M., and Bolam, J.P., 2004, Functional diversity and specificity of neostriatal interneurons, *Curr. Opin. Neurobiol.* **14**:685–692.

Tepper, J.M., Koós, T., and Wilson, C.J., 2004, GABAergic microcircuits in the neostriatum, *Trends Neurosci*. **27**:662–669.

Tepper, J.M., and Trent, F., 1993, In vivo studies of the postnatal development of rat neostriatal neurons, in: *Chemical Signalling in the Basal Ganglia* G.W. Arbuthnott, P.C. Emson, eds., Elsevier Science Publishers, Progress in Brain Research Vol. 99, pp. 35–50.

Tunstall, M.J., Oorschot, D.E., Kean, A., and Wickens, J.R., 2002, Inhibitory interactions between spiny projection neurons in the rat neostriatum, *J. Neurophysiol.* **88**:1263–1269.

Venance, L., Glowinski, J., and Giaume, C., 2004, Electrical and chemical transmission between striatal GABAergic output neurones in rat brain slices, *J. Physiol.*, **559**:215–230.

Vergara, R., Rick, C., Hernandez-Lopez, S., Laville, J.A., Guzman, J.N., Galarraga, E., Surmeier, D.J., and Bargas, J., 2003, Spontaneous voltage oscillations in striatal projection neurons in a rat corticostriatal slice, *J. Physiol., (Lond.)* **553**:169–182.

Wickens, J.R., Kotter, R., and Alexander, M.E., 1995, Effects of local connectivity on striatal function: stimulation and analysis of a model, *Synapse* **20**:281–298.

Wickens, J.R., and Oorschot, D.E., 2000, Neural dynamics and surround inhibition in the neostriatum: A possible connection, in Conceptual Advances in Brain Research, Dynamics and the Striatal Complex, R. Miller and J.R. Wickens, eds., Gordon and Breach, Reading, UK, pp. 141–150.

Wilson, C.J., 1979, Light and electron microscopic observations on neurons of the rat caudate-putamen stained by intracellular injection of horseradish peroxidase. *Anat. Rec*. **193**:722–723.

Wilson, C.J., 1995, Dynamic modification of dendritic cable properties and synaptic transmission by voltagegated potassium channels, *J. Computational Neurosci.* **2**:91–115.

Wilson, C.J., Groves, P.M., Kitai, S.T., and Linder, J.C., 1983, Three-Dimensional Structure of Dendritic Spines in the Rat Neostriatum, *J. Neurosci.* **3**:383–398.

Wilson, C.J., Kita, H., and Kawaguchi, Y., 1989, GABAergic interneurons rather than spiny cell axon collaterals are responsible for the IPSP responses to afferent stimulation in neostriatal spiny neurons, *Soc. Neurosci. Abstr.* **15**:907.

Wilson, C.J., and Groves, P.M., 1980, Fine structure and synaptic connections of the common spiny neuron of the rat neostriatum: A study employing intracellular injection of horseradish peroxidase. *J. Comp. Neurol*. **194**:599–615.

Wilson, C.J., and Groves, P.M., 1981, Spontaneous firing patterns of identified spiny neurons in the rat neostriatum, *Brain Res.* **220**:67–80.

Woodward, D.J., Kirillov, A.B., Myre, C.D., and Sawyer, S.F., 1995, Neostriatal circuitry as a scalar memory: Modeling and ensemble neuron recording. In: *Models of Information Processing in the Basal Ganglia*, edited by J.C Houk, J.L. Davis and D.G. Beiser (MIT Press, Cambridge, 1995), pp. 315–336.

Xu, Z.C., Wilson, C.J., and Emson, P.C., 1991, Synaptic potentials evoked in spiny neurons in rat neostriatal grafts by cortical and thalamic stimulation, *J. Neurophysiol.* **65**:477–493.

DOPAMINERGIC MODULATION OF CORTICAL AND STRIATAL UP STATES

Kuei Y. Tseng and Patricio O'Donnell*

1. INTRODUCTION

Cortical and striatal neurons recorded *in vivo* exhibit spontaneous membrane potential fluctuations. A very negative and quiescent down state is periodically interrupted by synchronous plateau depolarizations (up states; Fig. 1). Up and down states are readily observed in anesthetized animals and during slow wave sleep (for review see Steriade et al., 2001; O'Donnell, 2003); there is some debate, however, on whether such oscillations are present in awake animals. Until recently, elucidating this issue was beyond available technical means; nowadays, several groups can perform intracellular recordings from awake animals that have been trained to remain quiet with their heads attached to a stereotaxic apparatus by way of a device attached to their skull. Some of those studies reported that upon awakening, cat cortical neurons enter a persistent up state (Steriade et al., 2001) suggesting that down states may be a feature of slow wave sleep. A more recent *in vivo* study demonstrated that up-down transitions do exist in the sensory cortex of awake rats and mice, and that up states are triggered by natural sensory inputs, which makes them important for sensory integration (Petersen et al., 2003). Thus, although anesthetics may induce a slow, periodic oscillation between up and down states that mimics slow-wave sleep, it is likely that in awake conditions up and down state transitions also occur, although their duration and frequency may be quite variable (and even non-synchronous). Whether they last for a few hundred ms and repeat every second under anesthesia or they last for several seconds or minutes and signal awake or, more likely, alert conditions, up states are important cellular elements in corticostriatal information processing, probably determining the ensembles of active neurons at any given moment (O'Donnell, 2003).

Despite their obvious importance, little is known about the mechanisms contributing to sustaining up states. The onset of these events requires strong excitatory synaptic inputs to overcome the tight hold the inwardly rectifying K^+ current provides to the membrane potential during down states. The periodicity observed in striatal medium spiny neurons

* Kuei-Yuan Tseng and Patricio O'Donnell, Center for Neuropharmacology & Neuroscience, 47 New Scotland Avenue, Albany Medical College (MC-136), Albany NY 12208, USA.

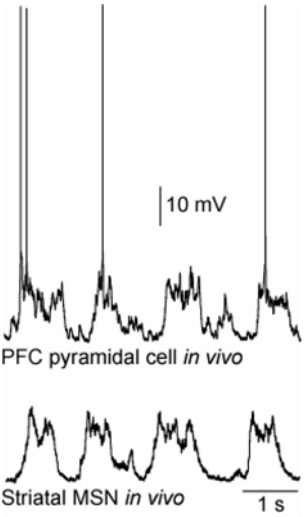

Figure 1. Representative traces of spontaneous membrane potential up-down state transitions recorded *in vivo* from a medial PFC pyramidal cell (*top*) and a striatal MSN (*bottom*).

(MSN) *in vivo* is dependent on the electrical activity of cortical neurons providing such inputs (Goto and O'Donnell, 2001b; Mahon et al., 2001). There is an ongoing debate regarding whether up states are sustained by continuous glutamatergic inputs, intrinsic voltage-gated conductances, or both. Cortical and striatal neurons may differ in this regard. There is ample evidence of intrinsic currents sustaining plateau depolarizations in pyramidal cortical neurons; striatal MSN, on the other hand, seem more dependent on at least a combination of persistent afferent activity and intrinsic currents. It is possible that neuromodulators in both regions sustain plateau depolarizations by activating/inactivating intrinsic voltage-gated channels and by modulating the strength of local glutamatergic excitation. Among these neurotransmitters, dopamine (DA) stands out as one of the major players because of its known role in modulating cortical and striatal glutamatergic transmission as well as calcium and sodium currents. In this chapter, we will discuss recent findings suggesting a strong role of DA in the modulation of cortical and striatal up states.

2. CORTICAL UP STATES AND DOPAMINE

Up states in pyramidal cortical neurons are driven by excitatory inputs. Several *in vivo* studies have produced evidence suggesting intra-cortical networks may be responsible for this glutamatergic drive. For example, thalamic stimulation does not evoke cortical up states (Lewis and O'Donnell, 2000) and these events can be observed even in cortical "slabs", which are disconnected from other areas (Timofeev et al., 2000). To determine whether intrinsic ionic currents can contribute to sustain up states initiated by glutamatergic afferent activity cannot be directly studied *in vivo*, and *in vitro* preparations generally lack sufficient neuronal activity to provide the drive necessary for up states. Several recent *in vitro* studies, however, revealed that neocortical pyramidal neurons can exhibit persistent depolarizing activity resembling up states under certain conditions. Pyramidal neurons recorded from visual and prefrontal cortices in mice and ferrets exhibited spontaneous plateau depolarizations when a bath solution reflecting more closely the K^+ concentration of brain interstitial

fluid *in situ* was used (Sanchez-Vives and McCormick, 2000; Cossart et al., 2003). This persistent activity in cortical slices seems to be driven by local synaptic activity, but it also requires intracellular Ca^{++}, as indicated by Ca^{++} transients observed during the plateau depolarizations (Cossart et al., 2003). In the rat prefrontal cortex, calcium (specifically via L-type channels) is critical for plateau depolarizations elicited by co-administration of NMDA and a D_1 agonist (Tseng and O'Donnell, 2005). Such depolarizations are the consequence of enhanced local network activation, as evidenced by their blockade by AMPA antagonists (Tseng and O'Donnell, 2005). However, if Ca^{++} signaling is blocked only in the recorded cell, one is left with synaptic responses of shorter duration occurring at a frequency similar to that of plateaus. This strongly argues for cortical up states being driven by local network excitatory activity and sustained by Ca^{++} and slow Na^{+} currents.

The prefrontal cortex (PFC) receives an extensive DA innervation that may play an important role in shaping up states. *In vivo* intracellular recordings revealed that chemical and electrical stimulation of the ventral tegmental area (VTA) can evoke prolonged plateau depolarizations in PFC pyramidal neurons. The dependence of this evoked plateau on DA was demonstrated by its shortening following systemic administration of the D_1 antagonist SCH23390 (Lewis and O'Donnell, 2000). Furthermore, transient VTA inactivation with lidocaine decreased synchrony among PFC up states *in vivo* (Peters et al., 2004). Because the VTA also contains GABA projection neurons (Steffensen et al., 1998), and DA targets cortical neurons other than deep-layer pyramidals, it is difficult to unequivocally determine the mechanisms by which DA may facilitate PFC up states using *in vivo* experiments.

In vitro recordings allow for a better controlled cellular pharmacology, but do not typically allow up states. As mentioned above, under certain conditions plateau depolarizations can be observed in slices. For example, whole-cell recordings from PFC pyramidal neurons yield occasional (i.e., every 10 or 20 min.) short depolarizations (Tseng and O'Donnell, 2005); these depolarizations may correspond to synchronous Ca^{++} events detected in a changing array of neurons in cortical slices (Cossart et al., 2003), which have been termed "cortical songs" (Ikegaya et al., 2004). If a D_1 agonist is added to the bath, the duration of those depolarizations increases significantly, suggesting that DA may sustain the depolarization. We have also recently reported that by co-activating D_1 and NMDA receptors, PFC network activity is enhanced, causing spontaneous plateau depolarizations (up states; Fig. 2) in individual neurons (Tseng and O'Donnell, 2005). These plateaus were eliminated by the D_1 antagonist SCH23390 and the NMDA antagonist APV. Bath application of the PKA inhibitor KT-5720 or the L-type Ca^{++} channel blocker nifedipine also prevented the plateaus. These results are consistent with the notion that a D_1 enhancement of NMDA function in the PFC can result in recurrent plateau depolarizations via a PKA-dependent pathway and activation of postsynaptic Ca^{++} channels. On the other hand, we also observed that interrupting local synaptic activity with TTX or CNQX eliminated these plateaus, suggesting that recurrent depolarizations induced by D_1-NMDA reflect an enhancement of local network activity. Adding the Ca^{++} chelator BAPTA or the Na^{+} channel blocker QX-314 to the recording electrodes also disrupted the depolarizations, indicating that co-activation of D_1 and NMDA receptors can promote recurrent plateau depolarizations in individual neurons by a combination of increased network activity and activation of intrinsic currents (voltage-gated Na^{+} and Ca^{++} channels). These interactions cannot be observed in slices obtained from young (prepubertal) animals; they are only seen in the adult PFC (Tseng and O'Donnell, 2005). Thus, DA sustains PFC up states *in vitro*, but only after puberty.

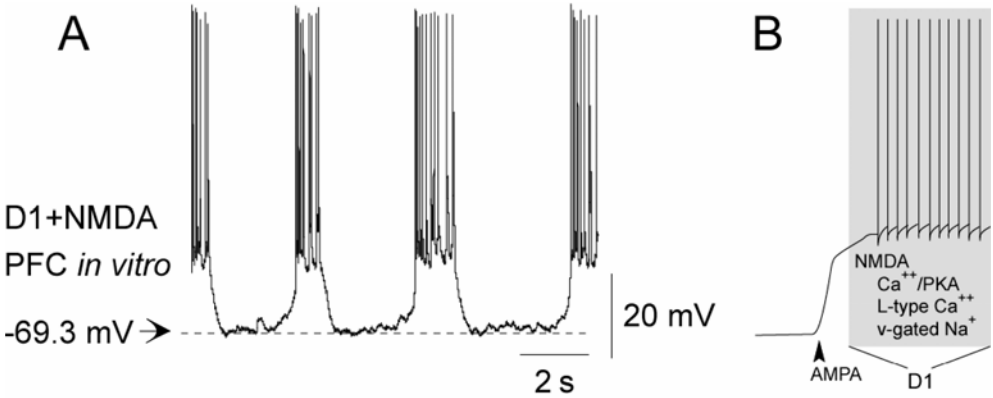

Figure 2. D_1-NMDA receptor co-activation evoked recurrent plateau depolarizations resembling *in vivo* up states in PFC pyramidal neurons. **A.** Representative trace recorded from a PFC pyramidal neuron in presence of D_1 + NMDA showing the plateau depolarizations. In this example, the membrane potential was held to baseline value (~70 mV) by somatic current injection. **B.** Simplified diagram illustrating the proposed DA-dependent mechanisms that drive plateau depolarizations in PFC pyramidal neurons. The transition to the up states is mediated by non-NMDA receptors. DA could contribute to sustain the plateau depolarizations through a combination of increased network activity induced by a D_1 enhancement of NMDA function and activation of intrinsic currents (e.g., voltage-gated Na^+ channels).

3. STRIATAL UP STATES AND DOPAMINE

Up states recorded in MSN are clearly driven by synchronous excitatory cortical inputs. Electrical stimulation of the ventral hippocampus evokes up states in ventral striatal neurons (O'Donnell and Grace, 1995), and a transection of the fimbria-fornix (the fiber bundle carrying hippocampal afferents to the nucleus accumbens) or a lesion of the ventral hippocampus eliminate accumbens up states (O'Donnell and Grace, 1995; Goto and O'Donnell, 2002). Furthermore, accumbens up states are synchronous with field potential deflections in the hippocampus (Goto and O'Donnell, 2001a). Similar paired recordings from dorsal striatal neurons and neocortical field potentials have revealed a dependence of MSN up states on cortical events (Wilson, 1993; Mahon et al., 2001; Tseng et al., 2001). Thus, MSN appear to follow closely the barrages of cortical inputs they receive and this may drive their own membrane potential oscillations.

The observation of MSN up states in slices has been even more elusive than in cortical regions. Many *in vitro* studies from dorsal and ventral striatal MSN have explicitly described these neurons as having a negative membrane potential devoid of any sign of spontaneous synaptic activity. Only one recent report described MSN up states in a brain slice following repeated cortical afferent stimulation (Vergara et al., 2003). However, because the slices contained the cortical area providing the afferents, it cannot be ruled out that the oscillations were driven by cortical activation in a fashion similar to what was described in the previous section.

There is also evidence that DA contributes to sustain striatal up states. For example, VTA stimulation with trains of 5 pulses at 20 Hz (mimicking DA neuron burst firing) evokes plateau depolarizations resembling spontaneous up states in ventral striatal MSN (Goto and O'Donnell, 2001b). Although DA antagonists fail to block the onset of the response, they

reduced the duration of the evoked plateau, suggesting that DA does not mediate the transition to the up states, but sustains the depolarization. Unlike the PFC, where D_1 blockade was sufficient to shorten VTA-evoked up states, in the ventral striatum both D_1 and D_2 receptors had to be blocked to induce this effect. This suggests that when a surge of DA in the striatum is coincident with strong excitatory inputs, the glutamate-driven depolarization can be prolonged by mechanisms dependent on both D_1 and D_2 receptors.

Several mechanisms may account for DA-dependent up states in striatal MSN. A recent work by West and Grace (2002) with local administration of drugs via reverse dialysis while conducting intracellular recordings showed that striatal D_1 and D_2 receptors have opposite effects on MSN membrane potential up-down transitions *in vivo*. Local administration of the D_1 antagonist SCH23390 significantly reduced the amplitude of striatal up states and MSN excitability without affecting corticostriatal synaptic responses. In contrast, D_2 receptor blockade failed to modify striatal up states, but enhanced MSN excitability as well as the synaptic response to cortical stimulation. These results suggest that the D_2-mediated inhibition may control the impact of the converging corticostriatal excitatory drive whereas D_1-mediated excitation may facilitate MSN up states. Several findings are consistent with these possibilities: first, a D_2 decrease in the efficacy of corticostriatal synaptic response has been repeatedly found (Calabresi et al., 1988). In the ventral striatum, D_2 receptors downregulate PFC synaptic inputs (O'Donnell and Grace, 1994; Brady and O'Donnell, 2004) but D_1 receptors seem involved in controlling other glutamatergic afferents (Charara and Grace, 2003). Second, a D_1 enhancement of glutamatergic function has been repeatedly observed. Specifically, D_1 receptors enhance NMDA currents (Levine and Cepeda, 1998; O'Donnell, 2003), probably via a PKA-dependent phosphorylation of NMDA receptor subunits (Cepeda and Levine, 1998; Cepeda et al., 1998). In addition, DA is known to modulate a number of voltage-gated ion channels in MSN. DA can activate voltage-gated Ca^{++} currents (Surmeier et al., 1995; Galarraga et al., 1997; Hernandez-Lopez et al., 1997; Vergara et al., 2003) or persistent Na^{+} currents (Carr et al., 2003). Another mechanism by which D1 receptors can enhance NMDA function is by inducing trafficking of NMDA receptor subunits to the postsynaptic membrane (Dunah and Standaert, 2001). Thus, combined D1 effects on postsynaptic Ca^{++} and NMDA function via a PKA-dependent signaling pathway could contribute to sustain striatal up states initiated by non-NMDA receptors.

4. FUNCTIONAL IMPLICATIONS

Activation of the mesolimbic/mesocortical DA system has been associated with a wide variety of PFC-related cognitive functions including working memory, attention and reward (Goldman-Rakic et al., 2000; Horvitz, 2000; Schultz, 2002). These actions of DA may depend on the interactions among specific DA and glutamate receptors. For example, it has been shown that PFC D_1 receptors are important for memory retrieval performance (Floresco and Phillips, 2001), and co-activation of D_1 and NMDA receptors in the PFC is necessary for appetitive instrumental learning (Baldwin et al., 2002). Although the precise neural basis responsible of this DA action is not entirely clear, it has been postulated that a D_1 potentiation of NMDA-dependent synaptic plasticity may facilitate the acquisition of cognitive abilities in the PFC by enhancing context-relevant inputs to drive the system (O'Donnell, 2003; Jay, 2003). This is consistent with studies showing that D_1 activation facilitates hippocampal-PFC long-term potentiation, a phenomenon that requires intact DA mesocortical projections (Gurden et al., 1999, 2000). It is possible that DA synchronizes

clusters of cortical neurons into the up states through a D_1 enhancement of NMDA functions by a number of mechanisms including activation of intrinsic voltage-gated channels, postsynaptic PKA and Ca^{++} signaling (Tseng and O'Donnell, 2005). In addition, a DA modulation of local GABAergic transmission may also contribute to coordinate cortical activity (Tseng and O'Donnell, 2004) by determining the timing and spatial selectivity of pyramidal cells firing. The information encoded in this ensemble of cortical neurons would be reinforced (or suppressed) and transmitted to the striatum, depending on the strength of coincident excitatory inputs arriving from other cortical areas that synchronize neuronal firing during the up states. If the emergence of this cortical activity was coordinated with a phasic DA signal reaching the striatum (e.g., in presence of salient stimuli; Schulz, 2002), NMDA currents would be facilitated by local D_1 receptors and the ongoing striatal activity would be enhanced by setting appropriate cortico-MSN ensembles into synchronous up states (O'Donnell, 2003). A DA control of glutamate-driven up states may be critical for establishing proper temporal coordination between neuronal ensembles across different corticostriatal axes, which in turn may be relevant for the production of specific goal-directed behaviors.

5. ACKNOWLEDGEMENTS

Supported by USPHS grant MH57683 (PO'D) and a NARSAD Independent Investigator Award (PO'D).

6. REFERENCES

Baldwin, A.E., Sadeghian, K., and Kelley, A.E., 2002, Appetitive instrumental learning requires coincident activation of NMDA and dopamine D1 receptors within the medial prefrontal cortex. *J. Neurosci*. **22**:1063.

Brady, A.M., and O'Donnell, P., 2004, Dopaminergic modulation of prefrontal cortical input to nucleus accumbens neurons in vivo. *J. Neurosci*. **24**:1040.

Calabresi, P., Benedetti, M., Mercuri, N.B., and Bernardi, G., 1988, Endogenous dopamine and dopaminergic agonists modulate synaptic excitation in neostriatum: intracellular studies from naíve and catecholaminedepleted rats. *Neuroscience* **27**:145.

Carr, D.B., Day, M., Cantrell, A.R., Held, J., Scheuer, T., Catterall, W.A., and Surmeier, D.J., 2003, Transmitter modulation of slow, activity-dependent alterations in sodium channel availability endows neurons with a novel form of cellular plasticity. *Neuron* **39**:793.

Cepeda, C., Colwell, C.S., Itri, J.N., Chandler, S.H., and Levine, M.S., 1998, Dopaminergic modulation of NMDA-induced whole cell currents in neostriatal neurons in slices: contribution of calcium conductances. *J. Neurophysiol*. **79**:82.

Cepeda, C., and Levine, M.S., 1998, Dopamine and N-methyl-D-aspartate receptor interactions in the neostriatum. *Dev. Neurosci*. **20**:1.

Charara, A., and Grace, A.A., 2003, Dopamine receptor subtypes selectively modulate excitatory afferents from the hippocampus and amygdala to rat nucleus accumbens neurons. *Neuropsychopharmacol.* **28**:1412.

Cossart, R., Aronov, D., and Yuste, R., 2003, Attractor dynamics of network UP states in the neocortex. *Nature.* **423**:283.

DeFrance, J.F., Marchand, J.F., Sikes, R.W., Chronister, R.B., and Hubbard, J.I., 1985, Characterization of fimbria input to nucleus accumbens. *J. Neurophysiol*. **54**:1553.

DeFrance, J.F., Sikes, R.W., and Chronister, R.B., 1985, Dopamine action in the nucleus accumbens. *J. Neurophysiol*. **54**:1568.

Dunah, A.W., and Standaert, D.G., 2001, Dopamine D1 receptor-dependent trafficking of striatal NMDA glutamate receptors to the postsynaptic membrane. *J. Neurosci*. **21**:5546.

Floresco, S.B., and Phillips, A.G., 2001, Delay-dependent modulation of memory retrieval by infusion of a dopamine D1 agonist into the rat medial prefrontal cortex. *Behav. Neurosci*. **115**:934.

Galarraga, E., Hernandez-Lopez, S., Reyes, A., Barral, J., and Bargas, J., 1997, Dopamine facilitates striatal EPSPs through an L-type Ca2+ conductance. *Neuroreport*. **8**:2183.

Goldman-Rakic, P.S., Muly, E.C. 3rd, and Williams, G.V., 2000, D(1) receptors in prefrontal cells and circuits. *Brain Res. Brain Res. Rev.* **31**:295.

Gonon, F., 1997, Prolonged and extrasynaptic excitatory action of dopamine mediated by D1 receptors in the rat striatum in vivo. *J. Neurosci*. **17**:5972.

Goto, Y., and O'Donnell, P., 2001a, Network synchrony in the nucleus accumbens in vivo. *J. Neurosci*. **21**:4498.

Goto, Y., and O'Donnell, P., 2001b, Synchronous activity in the hippocampus and nucleus accumbens in vivo. *J. Neurosci*. **21**:RC131.

Goto, Y., and O'Donnell, P. 2002, Delayed mesolimbic alteration in a developmental animal model of schizophrenia. *J. Neurosci.* **22**:9070.

Gurden, H., Takita, M., and Jay, T.M., 2000, Essential role of D1 but not D2 receptors in the NMDA receptordependent long-term potentiation at hippocampal-prefrontal cortex synapses in vivo. *J. Neurosci.* **20**:RC106.

Gurden, H., Tassin, J.P., and Jay, T.M., 1999, Integrity of the mesocortical dopaminergic system is necessary for complete expression of in vivo hippocampal-prefrontal cortex long-term potentiation. *Neuroscience.* **94**:1019.

Hernandez-Lopez, S., Bargas, J., Surmeier, D.J., Reyes, A., and Galarraga, E., 1997, D1 receptor activation enhances evoked discharge in neostriatal medium spiny neurons by modulating an L-type Ca2+ conductance. *J. Neurosci*. **17**:3334.

Horvitz, J.C., 2000, Mesolimbocortical and nigrostriatal dopamine responses to salient non-reward events. *Neuroscience*. **96**:651.

Ikegaya, Y., Aaron, G., Cossart, R., Aronov, D., Lampl, I., Ferster, D., and Yuste, R., 2004, Synfire chains and cortical songs: temporal modules of cortical activity. *Science* **304**:559.

Jay, T.M., 2003, Dopamine: a potential substrate for synaptic plasticity and memory mechanisms. *Prog. Neurobiol*. **69**:375.

Levine, M.S., and Cepeda, C., 1998, Dopamine modulation of responses mediated by excitatory amino acids in the neostriatum. *Adv. Pharmacol*. **42**:724.

Lewis, B.L., and O'Donnell, P., 2000, Ventral tegmental area afferents to the prefrontal cortex maintain membrane potential 'up' states in pyramidal neurons via D1 dopamine receptors. *Cereb. Cortex*. **10**:1168.

Mahon, S., Deniau, J.M., and Charpier, S., 2001 Relationship between EEG potentials and intracellular activity of striatal and cortico-striatal neurons: an in vivo study under different anesthetics. *Cereb. Cortex.* **11**:360.

O'Donnell, P., 2003, Dopamine gating of forebrain neural ensembles. *Eur. J. Neurosci*. **17**:429.

O'Donnell, P., and Grace, A.A., 1995, Synaptic interactions among excitatory afferents to nucleus accumbens neurons: hippocampal gating of prefrontal cortical input. *J. Neurosci*. **15**:3622.

O'Donnell, P., and Grace, A.A., 1996, Dopaminergic reduction of excitability in nucleus accumbens neurons recorded in vitro. *Neuropsychopharmacology*. **15**:87.

O'Donnell, P., Greene, J., Pabello, N., Lewis, B.L., and Grace, A.A., 1999, Modulation of cell firing in the nucleus accumbens. *Ann. N. Y. Acad. Sci*. **877**:157.

Ohyama, T., Horvitz, J.C., Drew, M.R., Gibbon, J., Malapani, C., and Balsam, P.D., 2000, Conditioned and unconditioned behavioral-cognitive effects of a dopamine antagonist in rats. *Behav. Neurosci*. **114**:1251.

Peters, Y., Barnhardt, N.E., and O'Donnell, P., 2004, Prefrontal cortical up states are synchronized with ventral tegmental area activity. *Synapse*. **52**:143.

Petersen, C.C., Hahn, T.T., Mehta, M., Grinvald, A., and Sakmann, B., 2003, Interaction of sensory responses with spontaneous depolarization in layer 2/3 barrel cortex. *Proc. Natl. Acad. Sci. U. S. A*. **100**:13638.

Sanchez-Vives, M.V., and McCormick, D.A., 2000, Cellular and network mechanisms of rhythmic recurrent activity in neocortex. *Nat. Neurosci*. **3**:1027.

Schultz, W., 2002, Getting formal with dopamine and reward. *Neuron*. **36**:241.

Steffensen, S.C., Svingos, A.L., Pickel, V.M. and Henriksen, S.J., 1998, Electrophysiological characterization of GABAergic neurons in the ventral tegmental area. *J. Neurosci.* **18**:8003.

Steriade, M., Timofeev, I., and Grenier, F. 2001, Natural waking and sleep states: a view from inside neocortical neurons. *J. Neurophysiol*. **85**:1969.

Surmeier, D.J., Bargas, J., Hemmings, H.C., Jr., Nairn, A.C., and Greengard, P., 1995, Modulation of calcium currents by a D1 dopaminergic protein kinase/phosphatase cascade in rat neostriatal neurons. *Neuron.* **14**:385.

Timofeev, I., Grenier, F., Bazhenov, M., Sejnowski, T.J., and Steriade, M., 2000, Origin of slow oscillations in deafferented cortical slabs. *Cereb. Cortex* **10**:1185.

Tseng, K.Y., Kasanetz, F., Kargieman, L., Riquelme, L.A., and Murer, M.G., 2001, Cortical slow oscillatory activity is reflected in the membrane potential and spike trains of striatal neurons in rats with chronic nigrostriatal lesions. *J. Neurosci*. **21**:6430.

Tseng, K.Y., and O'Donnell, P., 2004, Dopamine-glutamate interactions controlling prefrontal cortical pyramidal cell excitability involve multiple signaling mechanisms. *J. Neurosci*. **24**:5131.

Tseng, K.Y., and O'Donnell, P., 2005, Post-pubertal emergence of prefrontal cortical up states induced by D1-NMDA co-activation. *Cereb. Cortex*. **15**:49.

Vergara, R., Rick, C., Hernandez-Lopez, S., Laville, J.A., Guzman, J.N., Galarraga, E., Surmeier, D.J., and Bargas, J., 2003, Spontaneous voltage oscillations in striatal projection neurons in a rat corticostriatal slice. *J. Physiol*. **553**:169.

West, A.R., and Grace, A.A., 2002, Opposite influences of endogenous dopamine D1 and D2 receptor activation on activity states and electrophysiological properties of striatal neurons: studies combining in vivo intracellular recordings and reverse microdialysis. *J. Neurosci*. **22**:294.

Wilson, C.J., 1993, The generation of natural firing patterns in neostriatal neurons. *Prog. Brain Res*. **99**:277.

INTEGRATION OF CORTICAL ACTIVITY BY STRIATAL MEDIUM SPINY NEURONS

Fernando Kasanetz and M. Gustavo Murer*

1. INTRODUCTION

Striatal Medium-size Spiny Neurons (MSNs) are projection cells and constitute the main link between cortical and thalamic inputs and the remaining Basal Ganglia (BG) structures (Bolam et al., 2000; Wilson, 2004). Far from being just a relay station, MSNs are supposed to perform integrative computations that are essential for cortico-BG functions. Much of our thinking regarding MSN function is derived from the well-known anatomical organisation of the corticostriatal system. Almost all cortical regions project, in a topographically-ordered fashion, to the striatal complex. In the rat, sensorimotor and cognitive-limbic afferents arrive to the dorsolateral and ventromedial striatum respectively (McGeorge and Faull, 1989). This organization presumably allows parallel processing across cortico-BG channels, where modality-related cortices converge and non-related cortices presumably diverge in the striatal space (Alexander et al., 1990; Flaherty and Graybiel, 1994; Alloway et al., 2000).

The simultaneous *in vivo* recording of cortical field potentials (LFP) and the membrane potential (V_m) of MSNs has proven to be an interesting approach for the study of striatal representation of cortical activity (Tseng et al., 2001, Mahon et al., 2001, Kasanetz et al., 2002). Intracellular recordings are almost unfeasible without rigorously restraining the animals, so we worked with an anaesthetised preparation. Although the need of anaesthesia might seem unfortunate at first sight, it provides the advantage of allowing some control on the animal brain activity state. The V_m of neurones recorded intracellularly *in vivo* reflects the interplay between intrinsic membrane currents and barrages of synaptic inputs, with the latter conditioned by the activity state of the network (Destexhe et al., 2003), which is, in our preparation, driven by the anaesthetic agent. Because MSNs receive their main input from the cortex, and several thousand cortical neurones converge onto a single MSN, the simultaneous cortical LFP and striatal recordings allowed us to analyse the integration that takes place in a single neuron and its afferent "functional" connectivity.

* Laboratorio de Fisiología de Circuitos Neuronales, Departamento de Fisiología, Facultad de Medicina, Universidad de Buenos Aires, Argentina. E-mail: neurofis@fmed.uba.ar

Numerous studies have shown that the MSN V_m alternates between two preferred values, a polarised resting DOWN state and a depolarised "active" UP state (Figure 1) (Wilson and Groves, 1981; Stern et al., 1997, 1998; Reynolds and Wickens, 1999; Tseng et al., 2001, Mahon et al., 2001; Kasanetz et al., 2002). It has been shown that the transition to the UP state is driven by cortical activity. When MSNs are deprived of excitatory inputs, inward rectifier potassium currents hold the V_m at values close to the reversal potential for that ion, as it is observed during DOWN states or in brain slices (where cortical inputs were removed) (Wilson, 1993). When presynaptic activity increases, the V_m rises and is sustained in the UP state for as long as the combined forces of synaptic drive and voltage-dependent intrinsic currents remain strong enough. During that time, the V_m is held close to action potential threshold and a mix of synaptic currents and intrinsic sodium, calcium and potassium conductances modulate firing probability (Nicola et al., 2000). As spontaneous action potential firing is only possible during UP states, the transition to that condition has been perceived as a gating mechanism that allows information to flow across the striatum (O'Donnell and Grace, 1995).

Recently, more evidence has come forward concerning the influence of cortical activity on driving MSN UP states. Simultaneous recordings of the MSN V_m and electrocorticogram (ECoG, or cortical local field potential – LFP) demonstrated that the oscillatory trait of UP-DOWN state transitions (~1 Hz) is correlated to slow wave activity in the ECoG (Figure 1) (Tseng et al., 2001; Mahon et al., 2001; Kasanetz et al., 2002). This evidence suggests that MSNs are not only set in a ready-to-fire condition by cortical inputs, but that they are engaged by the slow rhythms generated by the thalamo-cortical network. Interestingly, it is known that the cerebral cortex can display LFP oscillatory activity at a variety of frequencies depending on the phase of the wake-sleep cycle, the behavioural condition, and the influence of drugs (reviewed by Steriade, 2000), raising the possibility that MSNs show distinct V_m features depending on circumstances.

Here we review recent data from our laboratory that increased our insight on the influence of the temporal structure of cortical network activity on MSN subthreshold fluctuations (Kasanetz et al., 2002). In addition, we present preliminary experiments extending the time domain analysis to high frequency bands, and showing how the spatial organisation of cortical network activity impacts on the MSN V_m.

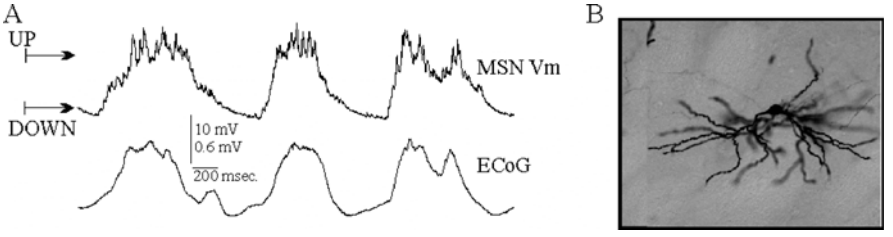

Figure 1. A. Simultaneous recording of a MSN *V*m and the frontal ECoG in an urethane-anaesthetised rat. Note the tight correlation between the occurrence of UP states and the positive phase of the cortical waves, which in our recordings indicate population firing of cortical neurones. **B.** Microphotograph of a striatal neurone filled with neurobiotine after the recording, depicting the typical morphology of a MSN.

2. THE MSN V_m TWO-STATE ALTERNATION IS DISRUPTED DURING CORTICAL DESYNCHRONIZATION

For more than twenty years, MSN UP states have been extensively explored and their cortical dependence is now not a point of discussion (Wilson, 1993; O'Donnell and Grace, 1995; Stern et al., 1997; Tseng et al., 2001; Mahon et al., 2001). The temporal structure of the MSN UP-DOWN fluctuation reflects the correlated activity of excitatory synaptic inputs and the postsynaptic integration that takes place in the MSN dendritic tree and cell body. Most cortical pyramidal neurones (Amzica and Steriade, 1995; Lewis and O'Donnell, 2000), as well as corticostriatal neurones (Stern et al., 1997, Mahon et al., 2001), display rhythmic UP-DOWN alternation in anaesthetised animals. This alternation is synchronised across an extensive cortical neuronal population and gives rise to the slow wave activity of the ECoG (Amzica and Steriade, 1995). This coherent cortical UP state is a window of opportunity for correlated corticostriatal neurone firing that results in the recruitment of MSNs into the oscillatory synchronised pattern that governs most of the forebrain.

During "activated cortical states" pyramidal neurones may remain depolarised for long periods of time (Steriade et al., 1993; Steriade et al. 2001) and the ECoG displays the pattern classically known as "desynchronisation". To determine how the MSN V_m behaves under the influence of a "desynchronised" cortical network, we recorded simultaneously the frontal ECoG and the MSN V_m in rats anaesthetised with urethane. When the intracellular recording was established, we manipulated the degree of synchronisation of the ECoG in different ways. We found that striatal UP-DOWN alternation occurred synchronously with slow wave activity in the ECoG, and is unfailingly disrupted during episodes of ECoG desynchronisation. Accordingly, the typical V_m two state alternation of MSNs is disrupted when, in order to induce cortical desynchronisation (Steriade et al., 1993), a train of electrical pulses was applied to the Mesopontine Tegmentum (MT) (Figure 2A, vertical arrow). After the stimulus, UP-DOWN transitions were replaced by a persistent depolarisation that lasted for many seconds, until the ECoG resumed the slow wave activity. Typically, an all-points histogram of the MSN V_m shows a bimodal distribution for the epoch of ECoG synchronisation, which means that the MSN spent most of the time at any of the two preferred V_m values (Figure 2C, left). But a similar histogram for the desynchronised ECoG epoch displays an unimodal distribution, where the V_m range is not statistically different from that corresponding to the UP states in the bimodal distribution (Figure 2C, right). Time series analysis (Figure 2B) revealed that both signals oscillate synchronously with a period of 1 second during ECoG synchronisation, and there is an obvious interruption of such correlation for the time segment where the ECoG is desynchronised.

The above findings can be generalised to other cortical desynchronised states (Kasanetz et al., 2002). First, by applying sensory stimuli (tail or hind limb pressure) it is possible to disrupt cortical slow wave activity. In these cases, MSNs displayed a "persistent UP state" accompanying the episode of ECoG desynchronisation (Figure 2D). Interestingly, when a sensory stimulus failed to change the cortical activity state (as assessed through the frontal cortex ECoG) no stimulus dependent response was seen in the MSN V_m, suggesting that the shape of the V_m depended on the ability of the sensory stimulus to set the network in a desynchronised state rather than on stimulus features (duration, localisation). Finally, more evidence comes from brief episodes of ECoG desynchronisation that take place spontaneously during long lasting recordings. Such episodes are invariably associated with MSN persistent depolarisations (Figure 2E) and share the properties described for MT induced desynchronisation.

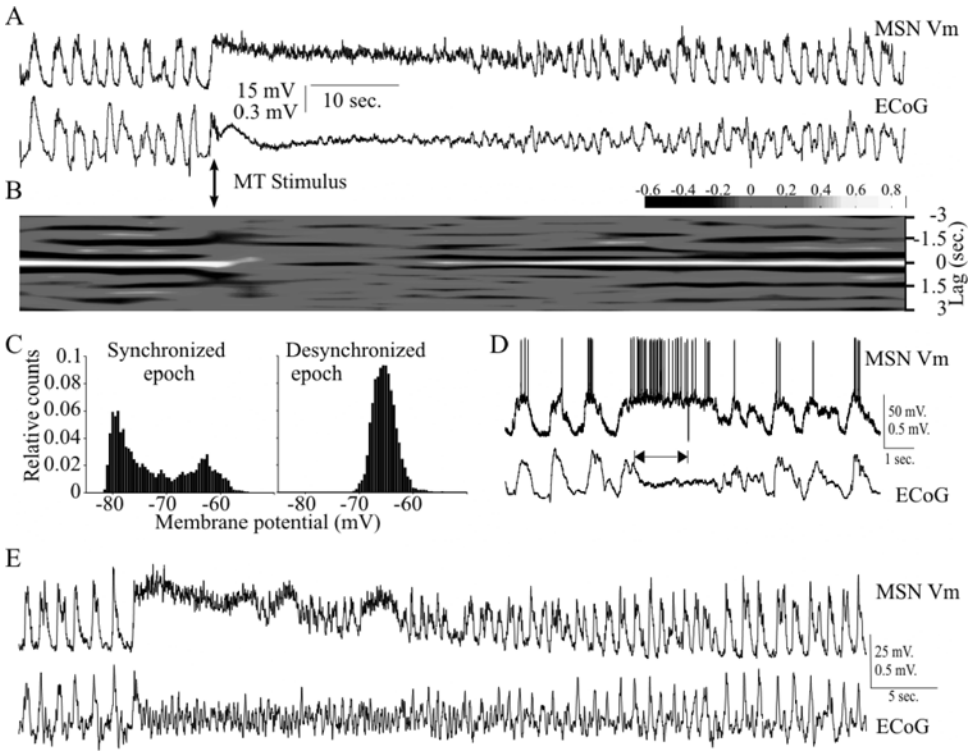

Figure 2. A. Traces of a simultaneous recording of a MSN and the frontal ECoG. The double headed arrow indicates the time at which a 500 ms train of electrical pulses (0.3 ms, 40 Hz, 0.8 mA) was applied to the MT in order to induced cortical desynchronisation. **B.** Contour graph showing the time function cross-correlation between the signals displayed in A. The *x* axis is time and is matched with that of the signal above, the *y* axis is the lag of the cross-correlation and the grey scale represent the correlation coefficient as indicated in the calibration bar. The graph was constructed from 6 s sliding windows overlapped 75 % in order to obtain a good time resolution. **C.** All points histograms of the MSN *V*m for signal segments of synchronised (before MT stimulus) or desynchronised epochs. **D.** A segment of a simultaneous MSN *V*m and ECoG recording where desynchronisation was induced by a sensory stimulation. The arrow indicates the duration of the stimulus (tail pinch). **E.** An episode of spontaneous desynchronisation of the ECoG accompanied by a complex waveform in the MSN *V*m recording.

Altogether, these experiments show that two-state V_m alternation is not the sole pattern of activity that MSNs can display. Instead, our results support the view that the prevailing cortical activity state shapes the MSN V_m. On the one hand, when the ECoG is oscillating synchronously at a low frequency, MSNs are recruited by the thalamo-cortical network and alternate synchronously between active (UP) and resting (DOWN) states. This is seen under anaesthesia and presumably takes place during other cortical activity states, both physiological and pathological, which are characterised by strong oscillatory synchronisation, like slow wave sleep and seizures (see Slaght et al., 2004). On the other hand, MSNs encode the sustained depolarisation and change of firing pattern of cortical neurones that underlies ECoG desynchronisation (Steriade, 1993; Steriade et al., 2001) as persistent depolarisation ("persistent UP state"). If we accept that MSN UP states are enabling events that allow specific sets of cortical inputs (which are embedded in the massive input that drives the

UP state) to be translated into sequences of action potentials, our results suggest that cortical activated states modulate the time window during which striatal information processing channels are operational.

3. DO THE MSN UP STATES ENCODE INFORMATION REGARDING THE SPATIAL LOCALISATION OF ACTIVE CORTICAL NETWORKS?

The anatomical arrangement of the corticostriatal pathway supports the proposal that multiple segregated cortico-BG channels are involved in processing information related to distinct functions (Alexander et al., 1990). Spike recordings showed that the activity of striatal neurones is functionally-related to that of the cortical territory that provides the major projection to the striatal region from which they were recorded (Crutcher and DeLong, 1984; Alexander and DeLong, 1985). But it is also clear that striatal neurones are often modulated by a combination of the sensorimotor, cognitive and motivational aspects of behaviour (Hollerman et al., 1998; Kawagoe et al, 1998). The simultaneous recording of cortical network and striatal subthreshold activities can provide valuable information on the functional connectivity and integration processes that take place in the corticostriatal network.

On the basis of the results presented above, we hypothesise that local activity at a given cortical territory will govern the subthreshold behaviour of the MSNs located in the striatal region that receives its major input from that cortical territory. In the rat, the V_m recorded from a dorsolateral striatal MSN would be highly correlated to motor cortex ECoG and less correlated to the ECoG of cortices that subserve other functions. To investigate if the coupling of MSN UP states to cortical LFPs reflects the spatial arrangement of corticostriatal connectivity, we have made intracellular recordings of dorsolateral striatal MSN while measuring simultaneously the LFP at three distant and functionally different cortical regions, the primary motor (mot), somatosensory barrel (sen) and medial frontal prelimbic (prl) cortices.

To begin with, we compared the degree of coupling among the three ECoG – MSN V_m pairs during periods of strong ECoG low frequency synchronisation (Figure 3A). By visual inspection of the raw signals, it becomes evident that the slow oscillation occurs in a highly synchronous way in the three ECoG channels. This fact was true for all the animals used in the experiments. As a consequence, UP-DOWN alternation in MSNs is typically significantly correlated with slow wave activity at all the three ECoG recordings. Figure 3B shows an example of the analysis of a 90 seconds recording of one MSN with the concomitant ECoGs. The cross-correlations demonstrated the oscillatory nature and the strong synchronisation of activity for all the three ECoG – MSN pairs. Nevertheless, it was possible to discriminate a preferred coupling of a given MSN with an ECoG channel by analysing the stability of indexes of coupling computed from short time windows (encompassing just a few oscillatory cycles) passed over long signal segments. We assumed that two tightly coupled signals will maintain a less variable correlation and phase relationship over time. The population results for 16 MSNs are summarised in Figure 3C. The mean correlation coefficient (computed from 6 seconds sliding windows) for the MSN-motor cortex pairs was significantly higher than that of the other two MSN-cortex pairs (Figure 3C, *upper*). In addition, the MSN-motor cortex pairs showed the less variable phase relationship measured as circular dispersion (Figure 3C, *lower*). This difference can be readily appreciated in the polar graphs of the phase angle histograms, where the phase lags for the MSN-motor

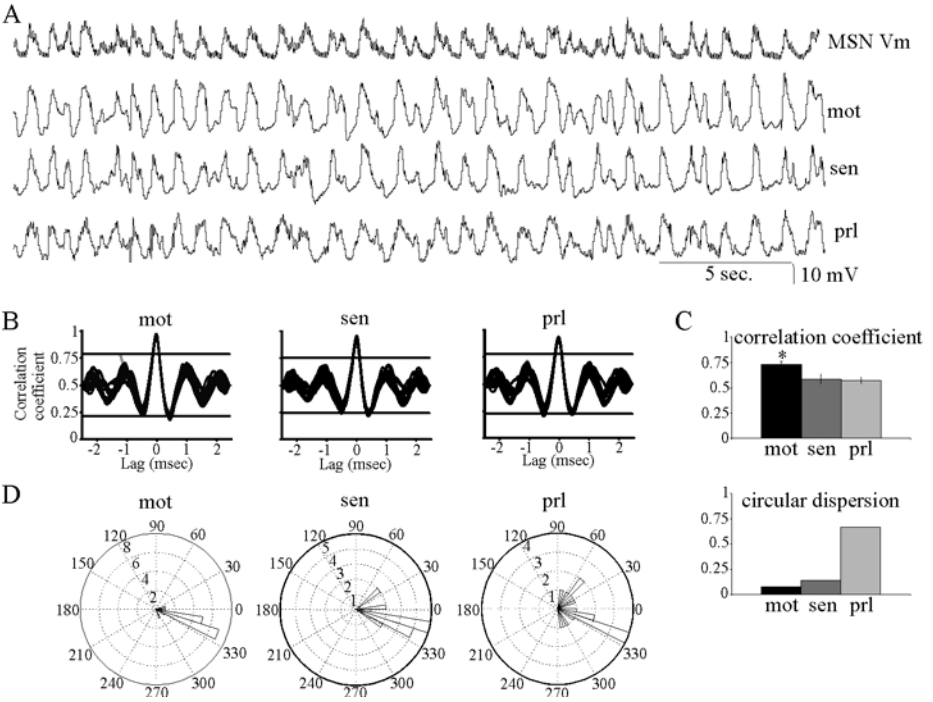

Figure 3. A. Simultaneous recording of a MSN and the LFP from the motor, sensory and prelimbic cortices during a long lasting synchronised epoch. **B.** Cross-correlations between the MSN *V*m and each of the three ECoG channels. Each graph contains, superimposed, the cross-correlations obtained from every 6 s window passed over 90 s of signal with 75% overlap. The straight horizontal lines indicate the confidence interval. **C.** Population results from 16 MSNs. The correlation coefficient was higher (*p < 0.01, Kruskal-Wallis ANOVA) and the dispersion of phase angles smaller for the MSN-mot pairs than for the other pairs. **D.** Polar graph showing the distribution of the mean phase angles for each MSN recorded and the three concomitant ECoGs.

cortex pairs were concentrated in a few angle bins, while those of the other pairs showed a broader distribution (Figure 3D). Preliminary findings suggest that, similarly, the persistent UP states of MSNs located in the dorsolateral striatum are more tightly associated to episodes of ECoG desynchronisation in the motor cortex than in the prelimbic and sensory cortices (not shown).

These data suggest that UP states of MSNs located in the dorsolateral striatum are more tightly coupled to the slow changes of the motor cortex LFP than to prelimbic or sensory cortices LFPs. On this basis it is tempting to predict that if we record MSNs from the ventromedial striatum, for example, their V_m will be more tightly related to ECoG activity of the prelimbic cortex than to that of the motor or sensory cortices. Our preliminary data are in agreement with this prediction.

Although the evidence is still incomplete, our results suggest that the activation of a local cortical network opens a window of firing opportunity in a topographically-matched assembly of MSNs by settling them in the UP state for as long as the cortical network remains in an “active state” (active part of the slow waves, desynchronised state). This striatal assembly represents an “operational” information processing channel, probably modality-specific, which is temporarily able to feed the BG output stage. In this context a

relevant question is, to what extent can a given striatal information processing channel be settled into the operational mode (MSNs in the UP state) independently of other presumably segregated information processing channels? We believe that this would depend on the extent to which the activity of a local cortical network can be decoupled from that of the rest of the cortex. In the urethane-anaesthetised rat, gross uncoupling of the low frequency components of distant cortical LFPs occurs infrequently, for example, during transitions from synchronous network oscillations to desynchronisation. This might indicate that MSN UP states (rhythmic or persistent) take place synchronously throughout the dorsal striatum. In line with this presumption, Stern et al. (1998) have shown that pairs of MSNs recorded simultaneously and separated by up to a millimetre displayed UP states concurrently. These MSNs probably belonged to the same functional striatal domain, remaining to be elucidated if such coupled activity takes place between MSNs located in different striatal domains as well. It is known that the hippocampus can exhibit synchronised rhythms (theta oscillations) while the neocortex displays a desynchronised field potential (Lopes da Silva et al., 1990). This fact suggests that MSNs from the dorsal and ventral striatum might exhibit, at least under certain circumstances, decoupled UP states. Clearly, more experiments are needed to resolve these issues.

4. DOES THE MSN V_m ENCODE FAST CORTICAL RHYTHMS?

In addition to the slow modulations that predict MSN UP state dynamics, the ECoG exhibits fast rhythms. The top of the slow waves is often crowned by high frequency modulations (theta band and above, 6–15 Hz), like the spindles generated by cortico-thalamic interactions (Steriade et al., 2001). During ECoG desynchronisation, low voltage oscillations can achieve higher frequencies, well within the beta (15–30 Hz) and gamma (30–60 Hz) bands (Steriade et al., 2001). Synchrony at such frequencies has been suggested to underlie information processing across cortical (Engel et al., 2001) and striatal (Courtemanche et al., 2003) neuronal assemblies during goal directed behaviour. It is of interest, then, to determine if fast cortical rhythms are transferred to MSNs and what is their impact on MSN physiology.

MSNs display high frequency V_m modulations in the top of the UP states that eventually provoke firing (Stern et al. 1997, 1998; Kasanetz et al., 2002). Even though these modulations most probably reflect integration of strongly correlated afferent inputs, in a previous study we found it very difficult to detect correlation at high frequencies between the frontal ECoG and the V_m of MSNs (see also Mahon et al., 2001). In this early work we performed cross-correlation analysis to time-windows of different duration, sampled randomly from persistent UP states. The long time-windows (>1 sec) did not exhibit significant correlation, but a small number of short time-windows showed coupling at frequencies within the theta range and above. The main features of thesesynchronous ECoG – MSN oscillations were their transient nature and variable frequency. So, the average cross-correlogram of several randomly selected epochs did not show any significant peaks (Kasanetz et al., 2002). In the present set of experiments, we applied short duration sliding windows to long signal segments encompassing synchronised and/or desynchronised cortical LFP epochs, with an aim at revealing episodes of transient high frequency synchronisation between the MSN V_m and any of the simultaneously recorded ECoGs (motor, sensory, prelimbic; see section 3). Preliminary results show that significant cross-correlations take place between MSNs of the dorsolateral striatum and the LFP at any of the three cortical

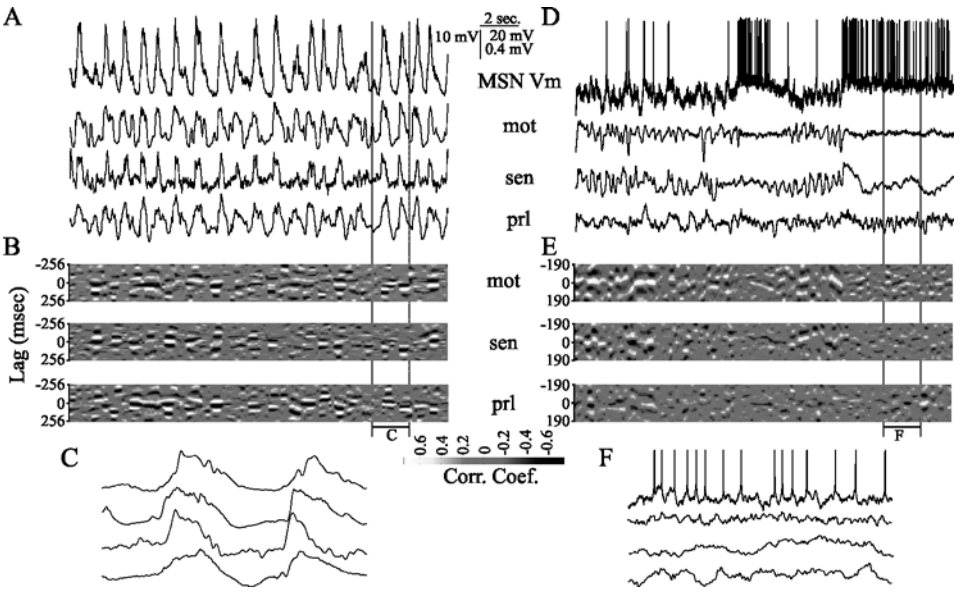

Figure 4. A. Simultaneous MSN *V*m and ECoG recordings showing a 20 second synchronised episode where high frequency modulations are present on the top of the slow waves. **B.** Cross-correlation analysis using short sliding windows (512 ms) between the MSN *V*m and each ECoG showing significant (white or black stripes) correlation in the theta band, probably corresponding to spindles, is typically present concomitantly in several MSN-ECoG pairs. **C.** Amplification of the 2 second segment marked in B to depict the presence of theta activity in the four signals. **D.** Similar as in A, this time for an ECoG desynchronisation with modulations at the theta and beta bands. **E.** The cross-correlation analysis (380 ms sliding windows) shows transient coupling with differ ent ECoG channels at different times and at different frequencies. **F.** Amplification of the 2 second segment marked in E.

regions (Figure 4). Usually, theta band synchrony appears simultaneously in the three MSN-ECoG pairs when spindles are seen on the top of the cortical slow waves (Figure 4A,B,C). When the ECoG looks desynchronised, theta or beta band oscillations appear in various or only one ECoG channel at a time, and sometimes is accompanied by a similar band fluctuation of the MSN V_m, producing high cross-correlation coefficients (Figure 4D,E,F). In the last case, the high frequency synchrony is transient, and it moves through the frequency spectrum, both in the course of time and among the MSN-ECoG channels. For the representative MSN depicted in Figure 4, the V_m seems to reflect cortical oscillations at a specific frequency during very precise short time windows. Further studies are needed to determine what is the functional significance of that fast rhythm corticostriatal transfer.

5. CONCLUSION

In this communication we have reviewed previous data and presented preliminary results from new experiments concerning the influence of cortical activity states on the subthreshold behaviour of MSNs. Overall, our data highlight the dynamic nature of the MSN V_m. Both in the time and space domains, MSN UP states are governed by cortical activity traits. In isolation, even small portions of the cerebral cortex are able to generate

persistent activity states (Sanchez-Vives and McCormick, 2000; Tseng and O'Donnell, 2005). In contrast, the isolated striatal circuitry seems to be almost inactive (Wilson, 1993). On the basis of our results, it is tempting to suggest that an activated modality-specific cortical network can settle into the UP state, for as long as it remains active, a topographically-related MSN assembly. The MSN UP state dependence on local cortical network dynamics would ensure the presence of an operational striatal window (the assembly of MSNs in the UP state) that matches in the space and time domains the operational window of the cortical network that feeds it. This mechanism would allow the "ready-to-fire" MSN assembly to extract relevant information from its main cortical input channel.

The fact that in the anaesthetised rat the degree of low frequency coupling between distant ECoG recordings is almost invariably high and the number of different global cortical network states low, suggest that, at least under anaesthesia, a large number of the dorsal striatum MSNs can display UP states concomitantly. The fact that LFP activity can exhibit synchronisation across widespread cortical areas under some natural conditions (Steriade et al., 2001; Gervasoni et al., 2004; Massimini et al., 2004) suggest that, to some extent, this inference can be generalised to more physiological circumstances as well.

To finish, we presented preliminary data showing transient coupling between cortical LFPs and the MSN V_m at frequencies within the theta, alpha and beta bands. The possibility that striatal assemblies were recruited during episodes of high frequency synchronisation of local cortical networks suggests new ways to understand how the BG extract specific signals from their massive cortical inputs.

6. ACKNOWLEDGEMENTS

This work was supported by FIRCA RO3 TW6282-01 (P O'Donnell, MG Murer), FONCYT PICT2002-11012 and PME2003-29, Universidad de Buenos Aires y Consejo Nacional de Investigaciones Científicas y Técnicas (Argentina). We thank Luis Riquelme for his assistance with time series analysis and Patricio O'Donnell for helpful discussions and his continuous support.

7. REFERENCES

Alexander, G.E., and DeLong, M.R., 1985, Microstimulation of the primate neostriatum. II. Somatotopic organization of striatal microexcitable zones and their relation to neuronal response properties. *J. Neurophysiol.* **53**:1417–1430.

Alexander, G.E., Crutcher, M.D., and DeLong, M.R., 1990, Basal ganglia-thalamocortical circuits: parallel substrates for motor, oculomotor, "prefrontal" and "limbic" functions. *Prog. Brain Res.* **85**:119–146.

Alloway, K.D., Mutic, J.J., Hoffer, Z.S., and Hoover, J.E., 2000, Overlapping corticostriatal projections from the rodent vibrissal representations in primary and secondary somatosensory cortex. *J. Comp. Neurol.* **428**:51–67.

Amzica, F., and Steriade, M., 1995, Short- and long-range neuronal synchronization of the slow (<1 Hz) cortical oscillation. *J. Neurophysiol.* **73**:20–38.

Bolam, J.P., Hanley, J.J., Booth, P.A.C., and Bevan, M.D., 2000, Synaptic organization of the basal ganglia, *J. Anat.* **196**:527–542.

Courtemanche, R., Fujii, N., and Graybiel, A.M., 2003, Synchronous, focally modulated beta-band oscillations characterize local field potential activity in the striatum of awake behaving monkeys. *J. Neurosci.* **23**:11741–11752.

Crutcher, M.D., and DeLong, M.R., 1984, Single cell studies of the primate putamen. I. Functional organization. *Exp. Brain Res.* **53**:233–243.

Destexhe, A., Rudolph, M., and Pare, D., 2003, The high-conductance state of neocortical neurons in vivo. *Nat. Rev. Neurosc.* **9**:739–751.

Engel, A.K., Fries, P., and Singer, W., 2001, Dynamic predictions: oscillations and synchrony in top-down processing. *Nat. Rev. Neurosci.* **2**:704–716.

Flaherty, A.W., and Graybiel, A.M., 1994, Input-output organization of the sensorimotor striatum in the squirrel monkey. *J. Neurosci.* **2**:599–610.

Gervasoni, D., Lin, S.C., Ribeiro, S., Soares, E.S., Pantoja, J., and Nicolelis, M.A., 2004, Global forebrain dynamics predict rat behavioral states and their transitions. *J. Neurosci.* **24**:11137–11147.

Hollerman, J.R., Tremblay, L., and Schultz, W., 1998, Influence of reward expectation on behavior-related neuronal activity in primate striatum. *J. Neurophysiol.* **80**:947–963.

Kasanetz, F., Riquelme, L.A., and Murer, M.G., 2002, Disruption of the two-state membrane potential of striatal neurones during cortical desynchronisation in anaesthetised rats. *J. Physiol. (London)* **543**:577–589.

Kawagoe, R., Takikawa, Y., and Hikosaka, O., 1998, Expectation of reward modulates cognitive signals in the basal ganglia. *Nat. Neurosci.* **1**:411–416.

Lewis, B.L., and O'Donnell, P., 2000, Ventral tegmental area afferents to the prefrontal cortex maintain membrane potential 'up' states in pyramidal neurons via D1 dopamine receptors. *Cereb. Cortex* **10**:1168–1175.

Lopes da Silva, F.H., Witter, M.P., Boeijinga, P.H., and Lohman, A.H., 1990, Anatomic organization and physiology of the limbic cortex. *Physiol. Rev.* **70**:453–511.

Mahon, S., Deniau, J.M., and Charpier, S., 2001, Relationship between EEG potentials and intracellular activity of striatal and cortico-striatal neurons: an in vivo study under different anesthetics. *Cereb. Cortex* **11**:360–373.

Massimini, M., Huber, R., Ferrarelli, F., Hill, S., and Tononi, G., 2004, The sleep slow oscillation as a traveling wave. *J. Neurosci.* **24**:6862–6870.

McGeorge, A.J., and Faull, R.L.M., 1989, The organization of the projection from the cerebral cortex to the striatum in the rat. *Neuroscience* **29**:503–537.

Nicola, S.M., Surmeier, J., and Malenka, R.C., 2000, Dopaminergic modulation of neuronal excitability in the striatum and nucleus accumbens. *Annu. Rev. Neurosci.* **23**:185–215.

O'Donnell, P., and Grace, A.A., 1995, Synaptic interactions among excitatory afferents to nucleus accumbens neurons: hippocampal gating of prefrontal cortical input. *J. Neurosci.* **15**:3622–3639.

Reynolds, J.N., and Wickens, J.R., 1999, Substantia nigra dopamine regulates synaptic plasticity and membrane potential fluctuations in the rat neostriatum, in vivo. *Neuroscience* **99**:199–203.

Sanchez-Vives, M.V., and McCormick, D.A., 2000, Cellular and network mechanisms of rhythmic recurrent activity in neocortex. *Nat. Neurosci.* **3**:1027–1034.

Slaght, S.J., Paz, T., Chavez, M., Deniau, J.M., Mahon, S., and Charpier, S., 2004, On the activity of the cortico-striatal networks during spike-and-wave discharges in a genetic model of absence epilepsy. *J. Neurosci.* **24**:6816–6825.

Stern, E.A., Kincaid, A.E., and Wilson, C.J., 1997, Spontaneous subthreshold membrane potential fluctuations and action potential variability of rat corticostriatal and striatal neurons in vivo. *J. Neurophysiol.* **77**:1697–1715.

Stern, E.A., Jaeger, D., and Wilson, C.J., 1998, Membrane potential synchrony of simultaneously recorded striatal spiny neurons in vivo. *Nature* **394**:475–478.

Steriade, M., Amzica, F., and Nunez, A., 1993, Cholinergic and noradrenergic modulation of the slow (approximately 0.3 Hz) oscillation in neocortical cells. *J. Neurophysiol.* **70**:1385–1400.

Steriade, M., 2000, Corticothalamic resonance, states of vigilance and mentation. *Neuroscience.* **101**:243–276.

Steriade, M., Timofeev, I., and Grenier, F., 2001, Natural waking and sleep states: a view from inside neocortical neurons. *J. Neurophysiol.* **85**:1969–1985.

Tseng, K.Y., Kasanetz, F., Kargieman, L., Riquelme, L.A., and Murer, M.G., 2001, Cortical slow oscillatory activity is reflected in the membrane potential and spike trains of striatal neurons in rats with chronic nigrostriatal lesions. *J. Neurosci.* **21**:6430–6439.

Tseng, K.Y., and O'Donnell, P., 2005, Post-pubertal emergence of prefrontal cortical up states induced by D1-NMDA co-activation. *Cereb. Cortex* **15**:49–57.

Wilson, C.J., and Groves, P.M., 1981, Spontaneous firing patterns of identified spiny neurons in the rat neostriatum. *Brain Res.* **220**:67–80.

Wilson, C.J., 1993, The generation of natural firing patterns in neostriatal neurons. *Prog. Brain Res*. **99**:277–297.

Wilson, C.J., 2004, Basal Ganglia, in: The synaptic organization of the brain, 5th edition, G. Shepherd, ed., Oxford University Press, New York, 361–413.

ACTIVATION OF NOS INTERNEURONES IN STRIATUM AFTER EXCITOTOXIC LESIONS OF RAT GLOBUS PALLIDUS

Matilde Lombardero Fernandez, Ann K. Wright, and
Gordon W. Arbuthnott*

1. INTRODUCTION

In addition to the well-established descending connections from the rat globus pallidus (GP) to the subthalamic nucleus and the substantia nigra, there is a prominent ascending projection to the striatum (Arbuthnott et al., 1983; Staines and Fibiger, 1984). This pathway arises in a sub-group of the GP neurones with descending projections and seems to preferentially target interneurones in the striatum (Bevan et al., 1998). Because the interneurones are greatly in the minority in the striatum, electrophysiological investigation of this pathway has been difficult *in vivo* and preparations that preserve pallidostriatal connections *in vitro* (when the interneurones could be identified visually) have so far not been studied.

The experiments in this report are a development of a series of experiments designed to look at the descending pallidosubthalamic pathway *in vivo*. We had made lesions in globus pallidus in order to study their effect upon the substantia nigra via the subthalamic nucleus (Wright et al., 2002; Wright et al., 2004) and the present report concerns the results of such lesions upon the striatal interneurones. Two of the interneurone types in the striatum, both the parvalbumin staining (PV) neurones and those neurones containing nitric oxide synthase (NOS) staining with diaphorase were studied histochemically. There is already good evidence that these two groups of interneurones form totally separate populations (Bennett and Bolam, 1994; Kawaguchi, 1993) and that both receive input from the pallidostriatal pathway (Bevan et al., 1998). Our anatomical study suggests that the pallidostriatal pathway is inhibitory upon the NOS interneurones but we could detect no change in the PV interneurones by our immunocytochemical methods.

* M. Lombardero Fernandez, Department of Anatomy and Embryology, Faculty of Veterinary Science, University of Santiago de Compostela, 27002 Lugo – Spain. A.K. Wright and G.W. Arbuthnott, University of Edinburgh Division of Neuroscience, Veterinary Biological Sciences, Summerhall, Edinburgh, EH9 1QL, U.K.

2. METHODS

Fifteen male Sprague Dawley rats weighing 300–320 g (Harlan, UK) were anaesthetised with halothane, placed in a stereotaxic frame and, using co-ordinates from a stereotaxic atlas of rat brain (Paxinos and Watson, 1986), the left globus pallidus was injected with 0.6 µl of a 10 µg/1 µl solution of ibotenic acid made up in phosphate buffered saline pH 7.4 (PBS). The co-ordinates used were 2.8 mm lateral to the midline, 1.1 mm posterior to bregma and 5.7 mm vertical to the cortical surface. The ibotenic acid was injected over a period of 5 min and the needle was left in position for a further 5 min to limit diffusion back along the needle tract. To prevent any seizures in the first few hours after the lesion ketamine 20 mg/kg and xylazine 10 mg/kg were injected i.p. immediately after surgery.

The 22 rats used in this study were in four groups: control group (n = 7), rats sacrificed 3 weeks post lesion (n = 8), rats sacrificed 7 weeks post lesion (n = 7). The brains were dissected out and placed in a 50 : 50 mixture of 20% sucrose solution in PBS and fixative. The forebrains were stored at 4°C until sectioned. Fixative was washed out by immersion in a cryoprotective solution of 10% sucrose in phosphate buffered saline (PBS). Coronal 50 µm thick sections were obtained on a freezing microtome.

2.1. Immunocytochemistry for Parvalbumin (PV)

Serial, sections throughout the striatum were prepared and every second section was processed for immunocytochemical detection of parvalbumin. Free-floating sections were washed in PBS pH 7.4. The pre-treatment (1 h) with 20% normal goat serum (NGS) was followed by incubation overnight at 4°C with agitation in a rabbit polyclonal antiserum raised against rat PV (1 : 2000, a gift from Prof. P.C. Emson) in PBS with 0.3% TritonX100 (TX). After two washes in PBS-TX sections were incubated for 45 min at room temperature in biotinylated goat anti-rabbit secondary antiserum (Vector Laboratories), rinsed in PBS, and incubated in the avidin-biotin peroxidase complex (ABC kit, Vector Laboratories) for 45 min at room temperature. After rinsing in PBS, sections were reacted in a fresh solution containing diaminobenzidine (DAB substrate kit, Vector laboratories). Then sections were rinsed in buffer, mounted on subbed slides, dried overnight (37°C), dehydrated using a graded series of alcohol (70%, 90%, 95%, 2× 100%), cleared in xylene, and mounted.

2.2. Diaphorase Method

Diaphorase method was also performed for detection of NOS-containing neurons. Alternate serial sections from the striata were reacted free floating in multiwell plates. Sections were washed several times in PBS-TX pH 8.0, then were incubated for 45 min at 37°C in a solution made of 0.1 mg/ml nitro blue tetrazolium (Sigma), 1.0 mg/ml β-nicotinamide adenine dinucleotide phosphate reduced form (NADPH) (Sigma) in PBS. They were washed again with PBS-TX and rinsed with PBS several times, mounted on subbed slides and dehydrated in an incubator (37°C) for 48 h, cleared in xylene and coverslipped with DPX.

2.3. Image Analysis

All the sections from PV immunostaining and NADPH-d histochemistry were examined under the light microscope by researchers who were unaware of the origin of the sections.

The PV positive-neuron population was estimated with an unbiased stereological procedure, where counts were made of stained neurons in the right and left striatum (see Ingham et al., 1998), using the fractionator method (Stereoinvestigator – Microbright-field).

The diaphorase staining intensity was estimated in the right and left striatum in each section with the NIH image software package (http://rsb.info.nih.gov). Areas in dorsal and lateral zone of the striatum were measured and the optical density of each was expressed in terms of grey scale intensity.

2.4. Statistical Analysis

The data were analysed using one-way ANOVA to detect differences between each animal group, and paired t-tests to detect differences between right and left striatum.

3. RESULTS

The sections processed by the immunohistochemical technique for parvalbumin displayed an intense staining in the striatum. The PV+ neurons were uniformly dispersed within the striatum, and were clearly visible against the background (Figure 1).

Statistical analysis revealed that there was no significant difference ($P < 0.01$) between the number of PV+ neurons in right and left striatum in the three groups in the study. Values expressed as mean ± S.D are shown in Figure 2.

As nNOS and NADPH-d appear completely co-localized in striatal interneurons in rats (Figueredo-Cardenas et al., 1996), we analyzed optical density in NADPH-d processed striatal sections in order to refer the results to the intensity not only of the nNOS neuronal cell bodies but also of their dendrites and axon terminals. The results displayed in Figure 3, are from a single section from the brain of one of the rats surviving 3 weeks after a lesion of globus pallidus.

Statistical analysis revealed that there were highly significant differences ($p < 0.001$) between the right and left striatum in the group sacrificed 3 weeks post operation. This fact implies a prominent decrease in the staining in the striatum ipsilateral to the injured GP. The difference was also significant ($p < 0.05$) in the group sacrificed 7 weeks post operation but no longer different in the group sacrificed at 12 weeks (data not illustrated). As expected, there was no significant difference between the right and left striatum in the control group.

4. DISCUSSION

In rats with long-term damage to the cells of the GP induced by injection of ibotenic acid we looked for the consequences of the loss of the GP input to interneurones in the striatum. We here demonstrate a reduction of nitric oxide synthase activity in striatum. In the same brains we saw no change in the numbers of the parvalbumin interneurones.

In neurones that synthesise other peptides it is clear that a reduction in stores of peptide is a common consequence of increased activity. In the striatum, inhibition of the synthetic capacity of the interneurones by application of 7NI results in the reduction of intensity of staining by the histochemical technique using the diaphorase reaction (Arbuthnott et al.,

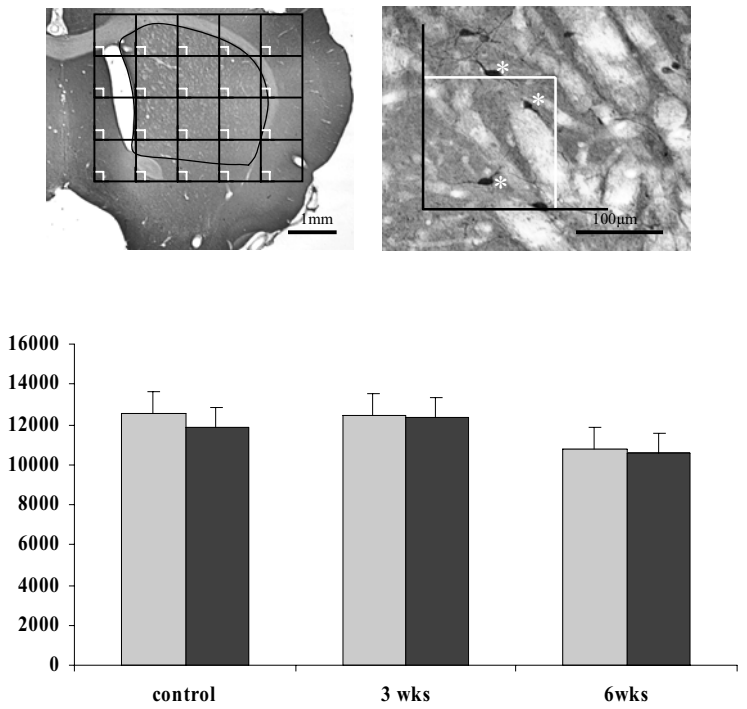

Figure 1. Numbers of PV+ neurons in the striatum of rats. *Upper panel*: Cells were counted in an area delimited by the ventricle, the callosal fibres, and bounded at the ventral edge by a line joining the lowest point of the ventricle with the rhinal fissure. On the left the low power view shows the systematic random distribution of counting frames determined by the computer. On the right a high power view of one frame with cells counted in that frame marked with an *. *Lower panel:* The absolute number of PV+ neurons in the two striata are not different in any group.

1994). In these animals with chronic GP lesions we found a similar reduction in the intensity of the colour reaction in the striatum on the side of the GP lesion. A result which would suggest that the removal of the tonic inhibitory action of the GP connection to these neurones has resulted in a reduction in the stores of active NOS enzyme, perhaps due to hyperactivity in this particular striatal interneuronal population.

We had no similar readout of the activity of the PV interneurones, and had to rely on counts of stained neurones in this instance. Although there are good reasons to suppose that immunocytochemical methods optimised for the detection of antigens might not be suitable to detect changes in amount of antigen, there have been reports of changes in the number of immunoreactive cells detected in striatum after dopamine removal (eg. Kerkerian et al., 1986). Thus either we have so optimised the immunocytochemistry that decreases are not visible – or there are no changes in the turnover of PV in these feedforward inhibitory interneurones of the striatum.

The source of the excitation that is driving the NO release is of interest and some earlier experiments suggest that the source is their usual input from ipsilateral cortex (Staines and Hincke, 1991). At least a short time after the GP lesion, decortication returns the NOS neurone staining towards normal. How does this cortically induced hyper-release

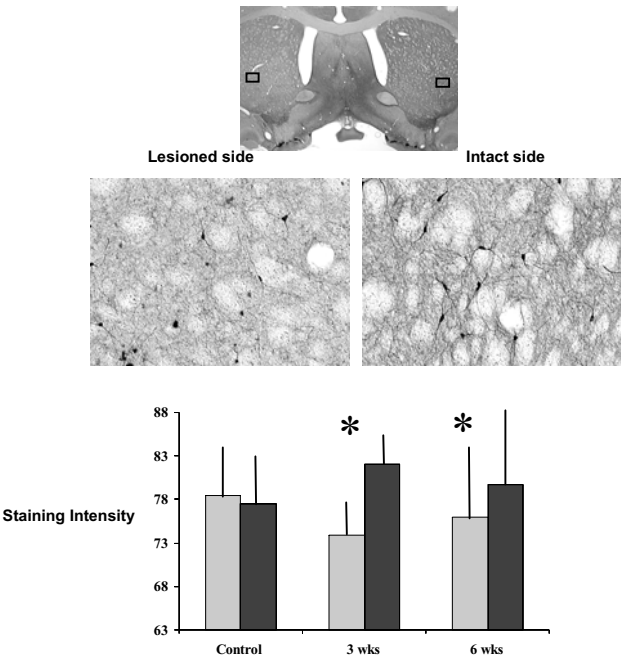

Figure 2. Difference in intensity of diaphorase staining between striata. *Top two panels*: Samples from the striatum of a rat 3 weeks after the GP lesion. Both neurones and background staining is less after lesion. *Lower panel*: Intensity of diaphorase reaction in striata. Pale colour represents lesioned side 3 weeks or 6 weeks after a lesion to GP. Mean ± SEM $*P < 0.01$ paired 't'-test.

of NO change the striatal neurochemical balance? To answer that requires several results that are at present uncertain. We need to know the output from these interneurones. It may be safe to assume them to be presynaptic to spiny neurone dendrites and so to have a post-synaptic action on the firing of spiny neurones rather like the parvalbumin containing cells do. They may, however, be presynaptic to synaptic terminals in striatum and thus be responsible for changes in transmitter release in the striatum. NO is freely diffusible in brain and thus itself unlikely to have a specific synaptic source or limited access to either kind of membrane since pre- or post-synaptic sites are equally accessible to a lipid soluble gas. If the action of NO is dependent on the soluble guanylate cyclase, that is its target in smooth muscle cells, then the actions are likely to be limited by the presence of this substance in neurones in the region of release. However there is some doubt about the cyclase as the only site of action of the gas and so even the evidence of soluble guanylate cyclase in spiny neurones does not guarantee the site of action is limited to those cells.

Recent research has implicated NO in plasticity of the corticostriatal system *in vivo.* Several papers suggest that NO release can cause increased release of acetylcholine (Centonze et al., 2001; Guevara-Guzman et al., 1994) and dopamine (West and Grace, 2000) and also that it is a vital part of the long-term depression that follows trains of stimuli to the corticostriatal system (Calabresi et al., 2000). On the other hand the clear effects of NO on blood flow and the ability of cortical NOS containing interneurones to influence blood vessel diameter directly (Cauli et al., 2004) implicates these interneurones in the control of blood flow in the striatum also (Kawaguchi et al., 1995). Such a seemingly

prosaic mode of action may be just as vital to the efficient working of the corticostriatal system and its control of basal ganglia function as any of the complex transmitter interactions beloved of neurophysiologists.

5. CONCLUSIONS

On the same side of the brain as the ibotenic acid lesion of the globus pallidus we have evidence of a reduction in the activity of diaphorase in the striatum. Such a reduction is compatible with a reduction in the stores of NOS in the cells perhaps as a result of the overproduction of the transmitter NO. We assume that the production of this potentially toxic substance is normally limited by inhibition from the GP. The number of parvalbumin positive neurones does not seem to have been changed by the lesion.

6. ACKNOWLEGEMENTS

M. Lombardero was supported by a research grant from Conselleria de Educación (Xunta de Galicia) – Spain. The Study was supported by the UK Parkinson's Disease Society.

7. REFERENCES

Arbuthnott, G.W., Kelly, P.A.T., and Wright, A.K., 1994, Some consequences of local blockade of nitric-oxide synthase in the rat neostriatum. In: The Basal Ganglia \IV. New ideas and data on structure and function. *Advances in behavioural biology*., (G. Percheron, J.S. McKenzie, J. Feger, eds) pp. 171–178. New York: Plenum Press.

Arbuthnott, G.W., Staines, W.A., Walker, R.H., and Whale, D., 1983, Pallido-striatal neurons with branches to the mesencephalon – electrophysiological evidence in the rat. *J. Physiol.* **346**:33P.

Bennett, B.D., and Bolam, J.P., 1994, Localisation of parvalbumin-immunoreactive structures in primate caudateputamen. *J. Comp. Neurol.* **347**:340–356.

Bevan, M.D., Booth, P.A., Eaton, S.A., and Bolam, J.P., 1998, Selective innervation of neostriatal interneurons by a subclass of neuron in the globus pallidus of the rat. *J. Neurosci.* **18**:9438–9452.

Calabresi, P., Gubellini, P., Centonze, D., Picconi, B., Bernardi, G., Chergui, K., Svenningsson, P., Fienberg, A. A., and Greengard, P., 2000, Dopamine and cAMP-regulated phosphoprotein 32 kDa controls both striatal long-term depression and long-term potentiation, opposing forms of synaptic plasticity. *J. Neurosci.* **20**:8443–8451.

Cauli, B., Tong, X.K., Rancillac, A., Serluca, N., Lambolez, B., Rossier, J., and Hamel, E., 2004, Cortical GABA Interneurons in Neurovascular Coupling: Relays for Subcortical Vasoactive Pathways. *J. Neurosci.* **24**:8940–8949.

Centonze, D., Pisani, A., Bonsi, P., Giacomini, P., Bernardi, G., and Calabresi, P., 2001, Stimulation of Nitric Oxide-cGMP Pathway Excites Striatal Cholinergic Interneurons via Protein Kinase G Activation. *J. Neurosci.* **21**:1393–1400.

Figueredo-Cardenas, G., Morello, M., Sancesario, G., Bernardi, G., and Reiner, A., 1996, Colocalization of somatostatin, neuropeptide Y, neuronal nitric oxide synthase and NADPH-diaphorase in striatal interneurons in rats. *Brain Res.* **735**:317–324.

Guevara-Guzman, R., Emson, P.C., and Kendrick, K.M., 1994, Modulation of in vivo striatal transmitter release by nitric oxide and cyclic GMP. *J. Neurochem.* **62**:807–810.

Ingham, C.A., Hood, S.H., Taggart, P., and Arbuthnott, G.W., 1998, Plasticity of synapses in the rat neostriatum after unilateral lesion of the nigrostriatal dopaminergic pathway. *J. Neurosci.* **18**:4732–4743.

Kawaguchi, Y., 1993, Physiological, morphological, and histochemical characterization of three classes of interneurons in rat neostriatum. *J. Neurosci.* **13**:4908–4923.

Kawaguchi, Y., Wilson, C.J., Augood, S.J., and Emson, P.C., 1995, Striatal interneurones: Chemical, physiological and morphological characterization. *Trends neurosci.* **18**:527–535.

Kerkerian, L., Bosler, O., Pelletier, G., and Nieoullon, A., 1986, Striatal neuropeptide Y neurons are under the influence of the nigrostriatal dopaminergic pathway: immunohistochemical evidence. *Neurosci. Lett.* **66**:106–112.

Paxinos, G., and Watson, C., 1986, The Rat Brain in Stereotaxic Coordinates, New York. Academic Press.

Staines, W.A., and Fibiger, H.C., 1984, Collateral projections of neurons of the rat globus pallidus to the striatum and substantia nigra. *Exp. Brain Res.* **56**:217–220.

Staines, W.A., and Hincke, M.T.C., 1991, Substantial alterations in neurochemical and metabolic indices in select basal ganglia neurons follow lesions of globus pallidus neurons in rats. *Soc. Neurosci. Abstr.* **17**:456–456.

West, A.R., and Grace, A.A., 2000, Striatal nitric oxide signaling regulates the neuronal activity of midbrain dopamine neurons in vivo. *J. Neurophysiol.* **83**:1796–1808.

Wright, A.K., Atherton, J.F., Norrie, L., and Arbuthnott, G.W., 2004, Death of dopaminergic neurones in the rat substantia nigra can be induced by damage to globus pallidus. *Eu. J. Neurosci.* **20**:1737–1744.

Wright, A.K., McLaughlin, K.E., Atherton, J.F., Norrie, L., and Arbuthnott, G.W., 2002, Lesions of the rat globus pallidus, which increase subthalamic nucleus activity, cause dopamine cell death. In The Basal Ganglia: Structure & Function VII. R.L.M. Faull, and L.F.B. Nicholson (eds) pp. 457–464. Kluwer Academic Publishing, Boston.

ELECTRICAL SYNAPSES BETWEEN OUTPUT NEURONES OF THE STRIATUM AND BETWEEN NEURONES OF THE SUBSTANTIA NIGRA PARS COMPACTA

Marie Vandecasteele, Jean-Michel Deniau, Christian Giaume, Jacques Glowinski, and Laurent Venance*

1. INTRODUCTION

The striatum is the main input structure of the basal ganglia while the substantia nigra pars compacta (SNc) contains the group of modulatory dopaminergic cells which project to the striatum. GABAergic striatal output neurones (SONs) receive convergent inputs from the entire cerebral cortex and act as coincidence detectors and integrators to select relevant cortical information (Wickens, 1993; Graybiel et al., 1994; Wilson, 1995). Dopamine (DA) released from the nerve terminals of nigrostriatal neurones potently modulates the processing of corticostriatal information (Reynolds and Wickens, 2002; Guzman et al., 2003). In addition to receiving extrinsic inputs, output neurones from the striatum and from the SNc are engaged in local interactions (chemical and/or electrical synapses) that contribute to shape their discharge, but which have still to be further investigated at a cellular level.

Electrical synapses refer to connections between two neurones through gap junction channels. Gap junction channels allow direct communication between the cytoplasms of adjacent cells. These intercellular channels are permeable to ions with a weak selectivity, and to small molecules (PM < 1.2 kDa) such as second messengers (IP_3, cAMP) or energetic metabolites (glucose 6-phosphate, fructose 6-phosphate), and thus respectively allow electrical and metabolic coupling (Harris, 2001).

The existence of electrical synapses was first hypothesized in the nervous system in the late fifties (Furshpan and Potter, 1959, Sloper, 1972, for review see Bennett, 1977), but growing evidence for functional electrical synapses was obtained during the last five years

* Marie Vandecasteele, Jean-Michel Deniau and Laurent Venance, Institut National de la Santé et de la Recherche Médicale U 667, Dynamique et Physiopathologie des Réseaux Neuronaux; Christian Giaume and Jacques Glowinski, Institut National de la Santé et de la Recherche Médicale U 114, Neurobiologie Pharmacologique, Collège de France, 11 place Marcelin Berthelot 75231 Paris Cedex 05, France.

(for review Bennett and Zukin, 2004). Few junctional channels are required to efficiently connect two neurones (Traub, 1995). Therefore, the demonstration of functional electrical coupling relies on the ability to record very small junctional currents. Technological advances (double patch-clamp combined with infrared microscopy in brain slices), have allowed the demonstration of the existence of functional electrical synapses, especially between sub-populations of GABAergic interneurones (Galarreta and Hestrin, 2001, Bennett and Zukin, 2004). However, little is yet known concerning the existence of functional electrical synapses between output neurones.

Pioneering studies have revealed the existence of dye-coupling between DA neurones and between SONs, suggesting the occurrence of intercellular communication through gap junctions (Grace and Bunney, 1983b, Cepeda et al., 1989, Walsh et al., 1989, O'Donnell and Grace, 1993, Onn and Grace, 1994). However, the existence of functional electrical synapses between these output neurones remained to be demonstrated. In this chapter, we summarize our results concerning local interactions between DA neurones and between SONs (Venance et al., 2004, Vandecasteele et al., 2005).

2. METHODS

2.1. Electrophysiological Recordings

Single and double patch-clamp whole-cell recordings were achieved in Sprague-Dawley rat (postnatal days 5–25) brain slices (350 µm thick), as previously described (Venance et al., 2000, Venance et al., 2004, Vandecasteele et al., 2005). Whole-cell recordings were made using borosilicate glass pipettes containing (mM): 105 K-gluconate, 30 KCl, 10 HEPES, 10 phosphocreatine, 4 ATP-Mg, 0.3 GTP-Na, 0.3 EGTA (adjusted to pH 7.35 with KOH). The composition of the extracellular solution was (mM): 125 NaCl, 2.5 KCl, 25 glucose, 25 NaHCO3, 1.25 NaH2PO4, 2 CaCl2, 1 MgCl2, 10 µM pyruvic acid, bubbled with 95% O_2 and 5% CO_2. All whole-cell recordings were performed at 34°C.

2.2. Data Analysis

Off-line analysis was performed using PulseFit-8.50 (HEKA Elektronik) and Igor Pro (Wavemetrics, Lake Oswego, OR, USA). Results were expressed as mean ± standard error of mean and statistical significance was assessed using the student's t test, or the nonparametric Mann-Whitney test when appropriate, at the significance level $P < 0.05$. Coupling coefficient (*e.g.* k_{12}) was calculated as the ratio of voltage responses of the postsynaptic (receiving) cell (here, cell2) to the presynaptic (stimulated) cell (here, cell1). Junctional conductance (Gj), taking input resistances (R_1 and R_2) into account, was estimated as follows: $Gj_{12} = k_{12} / (R_2 - R_1 k_{12}^2)$. When sinusoidal stimuli were used, 50 to 100 responses were averaged and subjected to a fast Fourier transform to confirm that the main frequency of the response was the frequency of the applied stimulus.

2.3. Tracer Coupling (Biocytin)

Biocytin 5 mg/ml was dissolved in the patch pipette solution and cells were filled during at least 45 min of recording (performed at room temperature). Biocytin crosses gap junctions and therefore diffuses in the recorded neurone but also in coupled cells. Subsequently, slices were fixed overnight in 2% paraformaldehyde at 4°C. Biocytinfilled cells

were visualized using the avidin-HRP reaction (ABC Elite peroxidase kit; Vector laboratories, Burlingame, CA, USA) according to the instructions of the manufacturer.

3. RESULTS

Both DA neurones and SONs were clearly identified by their electrophysiological features (Fig. 1A, B) (Grace and Bunney, 1983a; Kita et al., 1986; Wilson and Groves, 1980; Kawaguchi et al., 1989).

3.1. Tracer Coupling

To assess the occurrence of gap junction communication within each of these two populations of output neurones, tracer coupling experiments were performed during the first postnatal month. In the SNc, tracer coupling was observed in P5-P10 and P15-P25 rats, but was surprisingly absent between P10 and P15 (Fig. 1C). In the striatum, tracer coupling incidence was high during the first two postnatal weeks, and decreased thereafter (Fig. 1D). Tracer coupling was inhibited after carbenoxolone (150 µM) treatment. These results suggest a metabolic coupling within these neuronal populations.

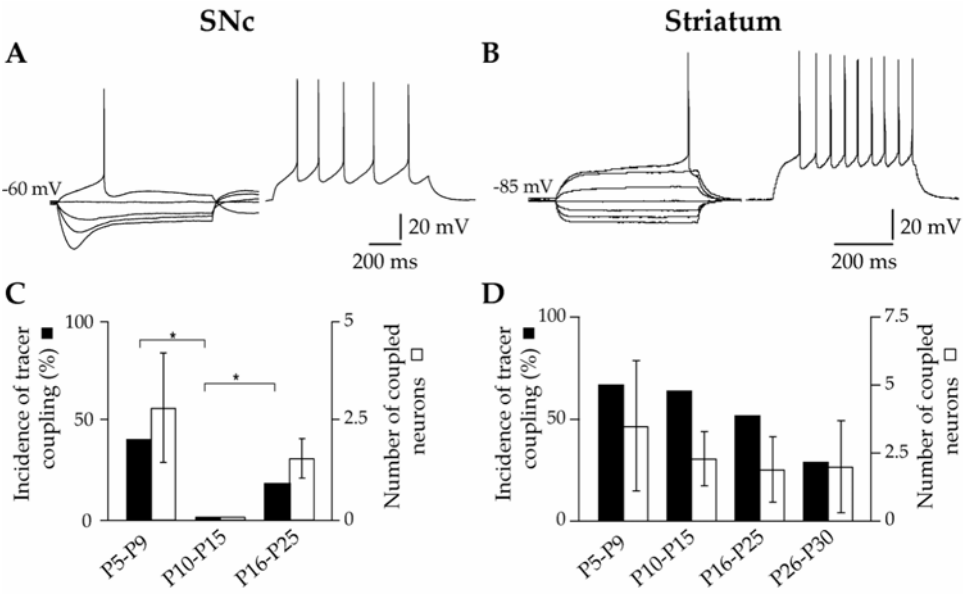

Figure 1. Electrophysiological characterization and tracer coupling of SNc and striatal output neurones. A, B: Responses of a SNc DA neurone (A) and of a SON (B) to current injections. Left panels: –90, –60, –30, 0, +30 pA for the DA neurone, –90, –60, –30, 0, +30, +60, +70 pA for the SON. Right panels: evoked spiking pattern, +40 pA above AP threshold. The DA neurone was held at –60 mV with –50 pA injected current, the SON was at resting membrane potential. Note the characteristic hyperpolarization-induced sag, post-hyperpolarization rebound and the large amplitude AHP for the DA neurone (A), and the characteristic hyperpolarized membrane potential, inward rectification, long depolarizing ramp to spike threshold for the SON (B).C,D: Incidence of tracer coupling and number of coupled neurones during postnatal development between DA neurones (C), and SONs (D). *: Fischer's exact test, $p < 0.05$. Adapted from Venance et al., (2004) and Vandecasteele et al., (2005).

3.2. Electrical Coupling

The existence of electrical synapses was investigated by dual whole-cell patch-clamp recordings. Functional electrical synapses were observed both between DA neurones and between SONs. Indeed, after injection of hyperpolarizing and depolarizing currents in presynaptic cells (stimulated cells), an electrotonic response was detected in postsynaptic cells (receiving cells) (Fig. 2). In the SNc, most of DA neurone pairs were electrically coupled in P7-P10 animals (96%, n = 51; k = 2.3 ± 0.2%, corresponding to Gj of 86.2 ± 7.0 pS) while coupling incidence decreased to 20% (n = 15; k = 1.9 ± 0.3% and Gj = 60.3 ± 0.7 pS) in P17-P21 rats (Fig. 2A). In the striatum, 24% of SONs pairs were electrically

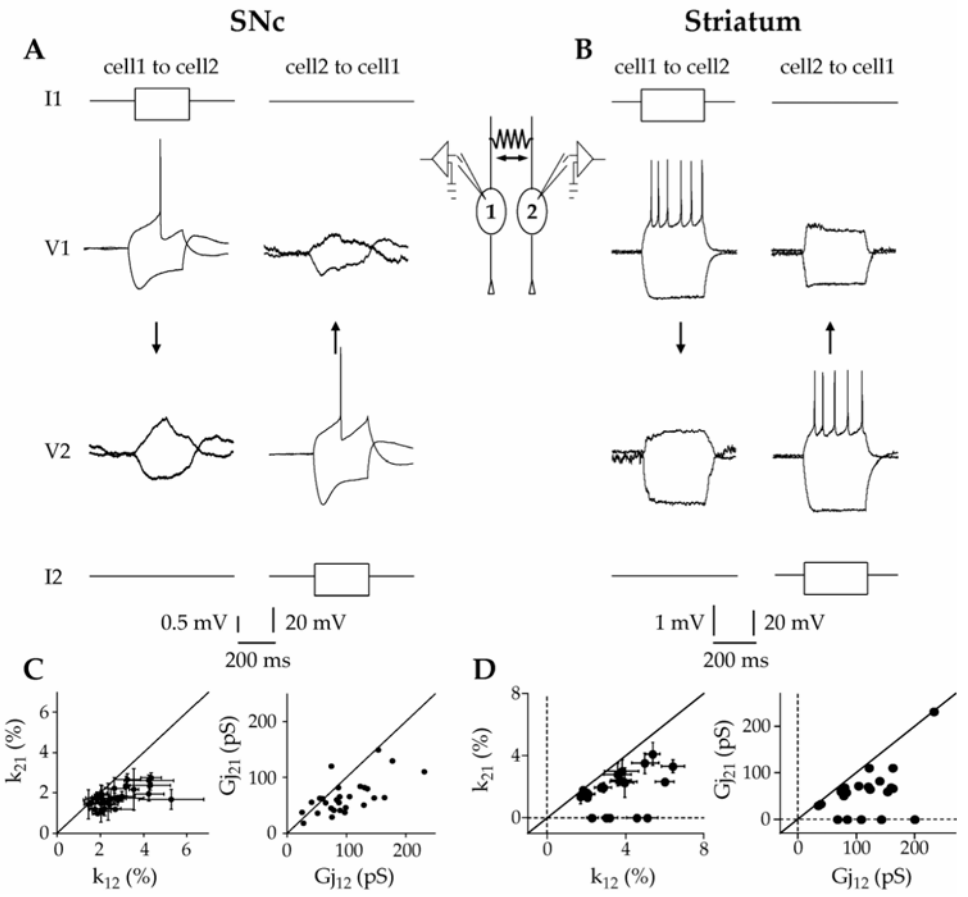

Figure 2. Electrical coupling between DA neurones and between SONs. A, B: Simultaneous patch-clamp recordings from pairs of output neurones in the SNc (A) and in the striatum (B) (I1 and V1 refer to cell1; I2 and V2 to cell2). Junctional currents were observed and estimated after injection of depolarizing (+100 pA for DA neurones, +140 pA for SONs) or hyperpolarizing (−200 pA for DA neurones, −250 pA for SONs) currents. C, D: Comparison of k and Gj in both directions of coupling for each cell pair (C: n = 28 DA neurone pairs, D: n = 22 SON pairs). k values were plotted with k_{12} being the higher k, Gj values were then plotted accordingly. Continous lines indicate identical k or Gj, in both directions, representing a symmetrical coupling. Adapted from Venance et al., (2004) and Vandecasteele et al., (2005).

coupled in P15-P18 animals (n = 91; k = 2.9 ± 0.2% and Gj = 102.2 ± 8.4 pS) (Fig. 2B). Carbenoxolone (200 µM) efficiently abolished junctional currents.

Electrical synapses between DA neurones and between SONs neurones globally shared the same properties. They were voltage-independent, most of them were symmetrical (82% in SNc, 68% in the striatum) and acted as low-pass filters. Indeed, when applying sinusoidal stimuli (Fig. 3), the coupling coefficient decreased and the phase-lag was enhanced with

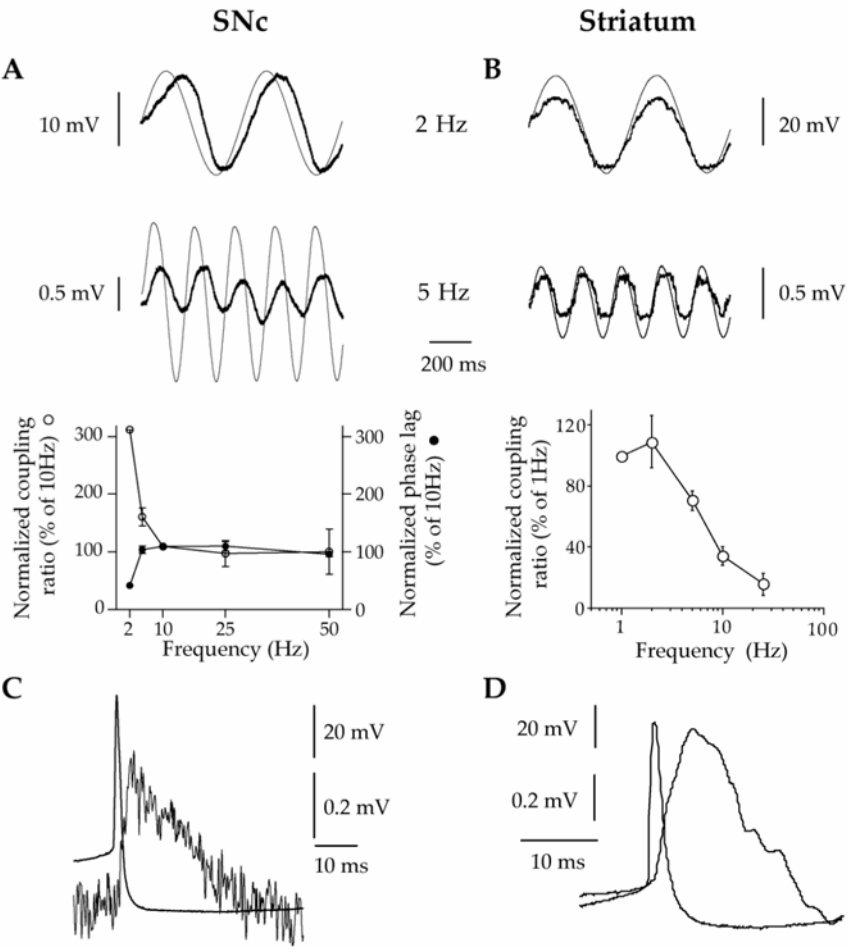

Figure 3. Electrical synapses in SNc (A and C, P7-P10 rats) and in striatum (B and D, P15-P18 rats) act as low-pass filters. A, B: Subthreshold sinusoidal current injections into cell1 of an electrically coupled pair induced membrane potential oscillations in both cell1 (thin traces) and cell2 (thick traces). Upper panels: Two examples are shown for stimuli frequencies of 2 Hz and 10 Hz. Lower panels: Frequency dependency of k (○) and phase-lag (●). In DA neurones (left panel, n = 19 pairs) k and phase-lag values were normalized to the 10 Hz values. In SONs (right panel, n = 5 pairs) normalization was set to the 1 Hz value. C, D: The attenuated transmission of presynaptic spikes is illustrated by superimposing the presynaptic spike over the induced spikelet recorded in the postsynaptic cell of a coupled DA neurone (C) and SON (D) pair. Note the different scale bars for pre- and post-synaptic events. Adapted from Venance et al., (2004) and Vandecasteele et al., (2005).

increasing frequencies of stimulation. This low-pass filtering is illustrated (Fig. 3C, D) by the attenuated transmission of action potentials through electrical synapses. Presynaptic action potentials can generate electrotonic postsynaptic events of small amplitude, named spikelets. Thus, electrical synapses observed between SNc DA neurones and between SONs display the characteristics of electrical synapses described so far in the central nervous system of mammals (Galaretta and Hestrin, 2001; Bennett and Zukin, 2004). However, it should be noted that low-pass filtering properties are much more pronounced in the SNc and in the striatum than those reported for other neurones in other studies.

DA neurones are spontaneously tonically active in slices (Sanghera et al., 1984; Kita et al., 1986). Therefore, we investigated whether the activity of a DA neurone could reverberate on the spontaneous activity of electrically coupled neurones. Hyperpolarization of the presynaptic DA cell slowed down the spontaneous firing frequency of the postsynaptic DA cell. Conversely, a depolarizing step increased the spontaneous firing rate of the postsynaptic neurone (Fig. 4). However, no significant synchronization of the spontaneous discharges of coupled neurones could be observed.

3.3. Chemical Synapses Between SONs

In contrast to DA neurones, in which no evidence of chemical interactions could be observed in our experimental conditions, 19% of SON pairs (n = 62) displayed functional chemical synapses. This chemical transmission was mediated by $GABA_A$ receptors since it was reversibly inhibited by bicuculline (Fig. 5A) and chloride conductances were exclusively responsible for these IPSCs (Fig. 5B). GABAergic synaptic transmission between SONs appeared highly reliable (mean failure rate: 6 ± 3%), precise (variation coefficient of latency: 0.06 ms) and strong (mean IPSC amplitude evoked by a single presynaptic spike:

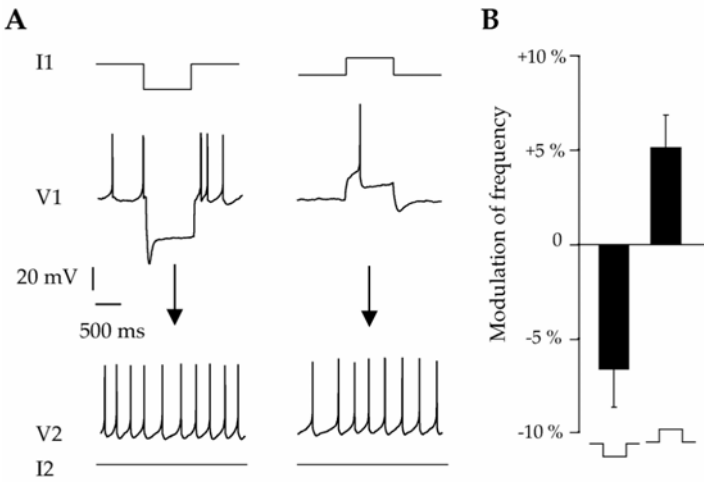

Figure 4. Junctional current can modulate spontaneous firing activity in electrically coupled DA neurone pairs. A: Hyperpolarizing and depolarizing current injections in cell1 (I1) (while no current was injected in cell2 (I2) allowing a spontaneous tonical activity) induce a decrease and an increase in the spontaneous firing rate of cell2 (V2), respectively. B: Mean change in the spontaneous firing rate of the receiving cells for hyperpolarizing pulses (n = 7 DA neurones pairs) and depolarizing pulses (n = 8 DA neurones pairs) applied in the stimulated cells. Adapted from Vandecasteele et al., (2005).

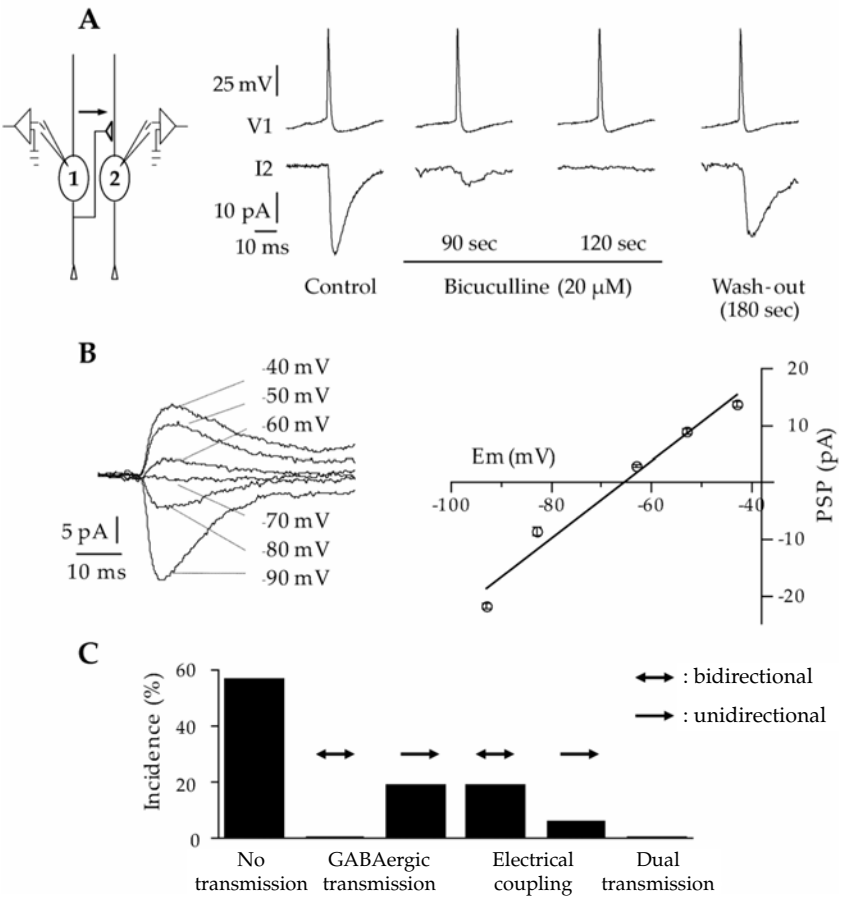

Figure 5. Chemical transmission between SONs. A: presynaptic spikes (top traces) and unitary postsynaptic currents (bottom traces) recorded from two SONs, and its reversible inhibition by bicuculline (20 μM, n = 4). B: averaged postsynaptic currents (n = 11–15) as a function of the membrane potential, with low chloride (10 mM KCl). In this condition, theoretical $E_{Cl} = -65.3$ mV, and experimentally the postsynaptic current reversed at −66 mV (n = 4). C: Summary of the incidences of GABAergic and electrical transmissions between SONs. Unidirectional and bidirectional transmissions are indicated (arrows). Adapted from Venance et al., (2004).

38 ± 12 pA). In all cases, the inhibitory synaptic transmission between SON pairs was unidirectional. Interestingly, chemical and electrical transmissions were mutually exclusive (Fig. 5C). Indeed, chemically-connected cell pairs were never electrically connected, and similarly, none of the electrically-coupled pairs were chemically connected.

4. DISCUSSION

Electrical synapses have been demonstrated mainly between subpopulations of GABAergic interneurones (Galaretta and Hestrin, 2001; Bennett and Zukin, 2004). Computer

modelling studies first suggested the implication of electrical coupling in synchronization of neuronal activity occurring during motor and learning behaviour. Experimental evidence for such a role has been provided using knock-out animals for the neuronal connexin Cx36 (sub-unit constituting the intercellular channels). The invalidation of Cx36 gene impairs the synchronization of gamma range oscillations in hippocampal and cortical interneurones (Hormuzdi et al., 2004; Connors and Long, 2004). Still, the existence of functional electrical synapses between output neurones remains less documented.

Here, we show the existence of functional electrical coupling between two output neuronal populations: the nigrostriatal DA neurones and their target, SONs. These findings highlight the diversity of output neuronal populations expressing functional intercellular channels. Output neurones can be divided into two functional categories: (1) neurones supporting fast transmission (mainly glutamatergic and GABAergic output neurones, including SONs) and (2) neurones underlying a neuromodulatory role (aminergic output neurones, including DA neurones). Considering this functional classification, different roles for electrical synapses within output neurones from the SNc and the striatum can be expected.

DA neurones display two modes of activity, tonic and phasic, resulting in different amounts of DA released in the striatum (Gonon, 1988, Floresco et al., 2003). Tonic activity allows a low but constant release of DA, supporting a general tune-up of the striatal network. Bursting activity causes a marked increase in DA which appears to be spatially-restricted, corresponding to a predictive reward value (Schultz et al., 1997). A computer modelling study proposed that electrically coupled DA neurones would fire synchronously (Komendantov and Canavier 2002). During spontaneous tonic activity (the spontaneous firing mode in slices), a lack of synchronization of action potentials was observed. Nevertheless, the role of intercellular communication between DA neurones remains to be explored during phasic activity. Synchronization of DA peaks in distinct striatal areas could have important functional consequences such as the linkage of reward-related information with different behavioural components in which the striatum is involved.

Concerning SONs, we demonstrated the existence of mutually exclusive bidirectional electrical synapses and unidirectional chemical synapses. It has been proposed that electrical coupling may increase the ability of coincidence detection (Galarreta and Hestrin, 1999; Bartos et al., 2001). SONs acting as coincidence detectors (Wickens, 1993; Graybiel et al., 1994; Wilson, 1995), modulation of electrical coupling (for example by DA) could influence cortico-basal ganglia information processing. Unidirectional GABAergic transmission between SONs could contribute to the lack of synchronization of spiking activity of these cells when recorded *in vivo* (Stern et al., 1998). Moreover, according to the 'winner-takes-all' mechanism proposed by Fukai (1999), unidirectional chemical synapses between SONs could participate to a selection process of relevant cortical information. The next step would be to determine the precise repartition of electrical and chemical synapses in relation with corticostriatal inputs. Indeed, the distribution of these synapses may play a central role in the processing of corticostriatal information. Modulation of these local interactions should induce a remodelling of the striatal network. Indeed, interestingly, dye-coupling between SONs has been shown to be increased in 6-OHDA-lesioned animals as well as after chronic treatment with neuroleptics (Cepeda et al., 1989; Onn and Grace, 1994). Alteration of electrical and/or chemical transmissions in pathological context, such as Parkinson's disease, should be explored for a better understanding of the role of local interactions in the physiology and pathology of basal ganglia.

5. ACKNOWLEDGEMENTS

Figures 1 (A and C), 2 (A and C), 3 (A and C) and 4, Copyright 2005 by the Society for Neuroscience. Figures 1 (B and D), 2 (B and D), 3 (B and D) and 5, Copyright 2004 by The Physiological Society.

6. REFERENCES

Bartos, M., Vida, I., Frotscher, M., Geiger, J.R., and Jonas, P., 2001, Rapid signaling at inhibitory synapses in a dentate gyrus interneuron network, *J. Neurosci.* **21**:2687–2698.

Bennett, M.V., 1977, Electrical transmission: a functional analysis and comparison to chemical transmission, in: *Cellular Biology of Neurons, Handbook of Physiology, The Nervous System*, E.R. Kandel, ed, Williams and Wilkins, Baltimore, pp. 357–416.

Bennett, M.V., and Zukin, R.S., 2004, Electrical coupling and neuronal synchronization in the Mammalian brain, *Neuron* **41**:495–511.

Cepeda, C., Walsh, J.P., Hull, C.D., Howard, S.G., Buchwald, N.A., and Levine, M.S., 1989, Dye-coupling in the neostriatum of the rat: I. Modulation by dopamine-depleting lesions, *Synapse* **4**:229–237.

Connors, B.W., and Long, M.A., 2004, Electrical synapses in the mammalian brain, *Annu. Rev. Neurosci.* **27**:393–418.

Floresco, S.B., West, A.R., Ash, B., Moore, H., and Grace, A.A., 2003, Afferent modulation of dopamine neuron firing differentially regulates tonic and phasic dopamine transmission, *Nat. Neurosci.* **6**:968–973.

Fukai, T., 1999, Sequence generation in arbitrary temporal patterns from theta-nested gamma oscillations: a model of the basal ganglia-thalamo-cortical loops, *Neural. Netw.* **12**:975–987.

Furshpan, E.J., and Potter, D.D., 1959, Transmission at the giant motor synapses of the crayfish, *J. Physiol.* **145**:289–325.

Galarreta, M., and Hestrin, S., 1999, A network of fast-spiking cells in the neocortex connected by electrical synapses, *Nature* **402**:72–75.

Galarreta, M., and Hestrin, S., 2001, Electrical synapses between GABA-releasing interneurons, *Nat. Rev. Neurosci.* **2**:425–433.

Gonon, F.G., 1988, Nonlinear relationship between impulse flow and dopamine released by rat midbrain dopaminergic neurons as studied by in vivo electrochemistry, *Neuroscience* **24**:19–28.

Grace, A.A., and Bunney, B.S., 1983a, Intracellular and extracellular electrophysiology of nigral dopaminergic neurons–1. Identification and characterization, *Neuroscience* **10**:301–315.

Grace, A.A., and Bunney, B.S., 1983b, Intracellular and extracellular electrophysiology of nigral dopaminergic neurons–3. Evidence for electrotonic coupling, *Neuroscience* **10**:333–348.

Graybiel, A.M., Aosaki, T., Flaherty, A.W., and Kimura, M., 1994, The basal ganglia and adaptive motor control, *Science* **265**:1826–1831.

Guzman, J.N., Hernandez, A., Galarraga, E., Tapia, D., Laville, A., Vergara, R., Aceves, J., and Bargas, J., 2003, Dopaminergic modulation of axon collaterals interconnecting spiny neurons of the rat striatum, *J. Neurosci.* **23**:8931–8940.

Harris, A.L., 2001, Emerging issues of connexin channels: biophysics fills the gap, *Q. Rev. Biophys.* **34**: 325–472.

Hormuzdi, S.G., Filippov, M.A., Mitropoulou, G., Monyer, H., and Bruzzone, R., 2004, Electrical synapses: a dynamic signaling system that shapes the activity of neuronal networks, *Biochim. Biophys. Acta.* **1662**:113–137.

Kawaguchi, Y., Wilson, C.J., and Emson, P.C., 1989, Intracellular recording of identified neostriatal patch and matrix spiny cells in a slice preparation preserving cortical inputs, *J. Neurophysiol.* **62**:1052–1068.

Kita, T., Kita, H., and Kitai, S.T., 1986, Electrical membrane properties of rat substantia nigra compacta neurons in an in vitro slice preparation, *Brain Res.* **372**:21–30.

Komendantov, A.O., and Canavier, C.C., 2002, Electrical coupling between model midbrain dopamine neurons: effects on firing pattern and synchrony, *J. Neurophysiol.* **87**:1526–1541.

O'Donnell, P., and Grace, A.A., 1993, Dopaminergic modulation of dye coupling between neurons in the core and shell regions of the nucleus accumbens, *J. Neurosci*. **13**:3456–2471.

Onn, S.P., and Grace, A.A., 1994, Dye coupling between rat striatal neurons recorded in vivo: compartmental organization and modulation by dopamine, *J. Neurophysiol.* **71**:1917–1934.

Reynolds, J.N., and Wickens, J.R., 2002, Dopamine-dependent plasticity of corticostriatal synapses, *Neural Netw.* **15**:507–521.

Schultz, W., Dayan, P., and Montague, P.R., 1997, A neural substrate of prediction and reward, *Science* **275**: 1593–1599.

Sloper, J.J., 1972, Gap junctions between dendrites in the primate neocortex, *Brain Res.* **44**:641–646.

Stern, E.A., Jaeger, D., and Wilson, C.J., 1998, Membrane potential synchrony of simultaneously recorded striatal spiny neurons in vivo, *Nature* **394**:475–478.

Traub, R.D., 1995, Model of synchronized population bursts in electrically coupled interneurons containing active dendritic conductances, *J. Comput. Neurosci.* **2**:283–289.

Vandecasteele, M., Glowinski, J., and Venance, L., 2005, Electrical synapses between dopaminergic neurons of the substantia nigra pars compacta, *J. Neurosci.* **25**:291–298.

Venance, L., Rozov, A., Blatow, M., Burnashev, N., Feldmeyer, D., and Monyer, H., 2000, Connexin expression in electrically coupled postnatal rat brain neurons, *Proc. Natl. Acad. Sci. USA* **97**:10260–10265.

Venance, L., Glowinski, J., and Giaume, C., 2004, Electrical and chemical transmission between striatal GABAergic output neurones in rat brain slices, *J. Physiol.* **559**:215–230.

Walsh, J.P., Cepeda, C., Hull, C.D., Fisher, R.S., Levine, M.S., and Buchwald, N.A., 1989, Dye-coupling in the neostriatum of the rat: II. Decreased coupling between neurons during development, *Synapse* **4**:238–247.

Wickens, J., 1993, *Theory of the Striatum*, series 7, Pergamon *Studies in Neuroscience*, Elsevier Science, Oxford, pp. 1–182.

Wilson, C.J., and Groves, P.M., 1980, Fine structure and synaptic connections of the common spiny neuron of the rat neostriatum: a study employing intracellular inject of horseradish peroxidase, *J. Comp. Neurol.* **194**:599–615.

Wilson, C.J., 1995, The contribution of cortical neurons to the firing pattern of striatal spiny neurons, in: *Model of Information Processing in Basal Ganglia*, J.C. Houk, J.L. David, and D.G. Beiser, eds, MIT Press, Cambridge, pp. 29–50.

NITRIC OXIDE SIGNALING MODULATES THE RESPONSIVENESS OF STRIATAL MEDIUM SPINY NEURONS TO ELECTRICAL STIMULATION OF THE SUBSTANTIA NIGRA

Striatal Nitrergic Signaling

Danting Liu, Stephen Sammut, and Anthony R. West*

1. INTRODUCTION

The basal ganglia are a group of interconnected subcortical nuclei critically involved in the generation of goal-directed voluntary motor behavior.[1–4] The basal ganglia consist of the caudate-putamen (referred to collectively as the striatum), globus pallidus, subthalamic nucleus, and the substantia nigra (SN) pars reticulata and pars compacta. Together, these nuclei give rise to multiple, parallel segregated circuits critically involved in the planning and selection of complex movements and storage and retrieval of motor memory.[4] The importance of these systems for normal motor behavior is underscored by the numerous neuropsychiatric and neurological disorders linked to dysfunction of specific basal ganglia sub-nuclei.

The striatal complex (including the ventral striatum and nucleus accumbens) receives massive excitatory projections from the entire neocortical mantle as well as subregions of the thalamus and other limbic structures such as the amygdala and hippocampus.[5] Information transmitted via these convergent inputs is integrated in functionally coupled networks of striatal principal neurons and interneurons.[6] It is well accepted that 90–95% of striatal neurons are principal neurons termed medium spiny projection neurons (MSNs).[7] Interactions between excitatory, inhibitory and modulatory systems at the level of the MSN dendrites and soma are believed to regulate the membrane properties of these neurons and control striatal output.[7] When studied in the intact animal using *in vivo* intracellular recording techniques, MSNs exhibit characteristic membrane fluctuations which consist of a hyperpolarized "down" state and a relatively depolarized "up" state (two-state membrane

* Department of Neuroscience, The Chicago Medical School at Rosalind Franklin University of Medicine and Science, North Chicago, IL 60064-3095, USA. Correspondence to: Anthony.West@rosalindfranklin.edu.

activity).[8] In most cases, these neurons also tend to fire at relatively low frequencies (<1 Hz) and exhibit short bursts of activity separated by longer periods of quiescence.[8]

In contrast to the MSNs, limited information is available regarding the membrane properties of striatal aspiny interneurons in the intact animal. To date, at least four major subtypes of aspiny interneurons have been characterized in brain slices based on morphology, physiological properties, and neurotransmitter synthesis.[9] Recent studies by Tepper and colleagues have shown that small numbers of electrotonically coupled interneurons can exert a powerful feed-forward regulatory influence over large populations of MSNs recorded *in vitro*.[10] Thus, despite their small number, striatal interneurons have been shown to potently regulate the activity of MSNs. Our recent studies and the work of others have shown that striatal nitric oxide (NO) producing interneurons play an important role in modulating the membrane activity of MSNs and promoting neural plasticity in striatal output pathways.[11–17] Medium aspiny interneurons containing type 1 (neuronal) NO synthase (NOS) are primarily responsible for the generation of NO in the striatal complex.[18] Together with reports indicating an important role for striatal NO neurotransmission in the regulation of dopamine (DA) release[15] and motor behavior,[19,20] these studies suggest that characterization of factors regulating NO synthesis and nitrergic signaling will be essential for understanding normal striatal function and pathophysiological conditions such as Parkinson's disease (PD).

Given the recent evidence that striatal NOS-immunoreactive interneurons receive dense DA innervation from the SN,[21,22] localize D_5 receptors,[23] and respond to $D_{1/5}$ receptor agonist administration with a robust increase in firing activity,[23,24] we hypothesized that NOS activity would be potently stimulated by phasic DAergic transmission. This is supported by histochemical evidence showing that D_1 receptor antagonists decrease NOS activity measured *ex vivo*.[25] Taken together, these studies indicate that DA cell burst firing may stimulate NOS activity in the striatal complex and lead to the robust activation of nitrergic signaling. The current study examined this possibility using NO selective microsensor recordings in intact anesthetized rats to monitor striatal NO efflux prior to and during electrical train stimulation of the SN. *In vivo* extracellular and intracellular recordings were also performed in separate animals to determine the impact of NO efflux evoked during SN stimulation on the membrane activity of striatal MSNs.

2. METHODS

Electrochemical and electrophysiological measurements were made from male Sprague-Dawley rats weighing 275–400 grams. Prior to experimentation, animals were housed two per cage under conditions of constant temperature (21–23°C) and maintained on a 12 : 12 hour light/dark cycle with food and water available *ad libitum*. All animal procedures were approved by the Chicago Medical School Institutional Animal Care and Use Committee and adhere to the *Guide for the Care and Use of Laboratory Animals* published by the USPHS. Prior to surgery, animals were deeply anesthetized with chloral hydrate (400 mg/kg, i.p.) and placed in a stereotaxic apparatus. After drilling a burr hole in the skull overlying the dorsal striatum (coordinates: −0.5–2.0 mm anterior from bregma, 2.0–3.5 mm lateral from the midline), the dura was resected and the microsensor or microdialysis probe was lowered into the striatum using a Narishige micromanipulator. All coordinates were derived from a rat brain stereotaxic atlas.[26] The level of anesthesia was periodically verified via the hind limb compression reflex and maintained using supplemental administration of

anesthetic as previously described.[14,16] Temperature was monitored using a rectal probe and maintained at 37°C with a heating pad. Extracellular and intracellular recordings were performed using microelectrodes filled with either NaCl (2 M) or potassium acetate (3 M) solution containing 2% biocytin, respectively, as described previously.[14,16] In experiments combining intracellular recordings and microdialysis, concentric microdialysis probes were implanted into the dorsal striatum over a 25–30 minute period (3–4 μm/sec) and perfused with artificial cerebral spinal fluid (aCSF) containing (in mM) 145 NaCl, 2.7 KCl, 1.0 $MgCl_2$, 1.2 $CaCl_2$, 2.0 NaH_2PO_4, and 2.0 Na_2HPO_4 at a rate of 2 μL/min as described previously.[16]

3. ELECTROCHEMICAL MICROSENSOR MEASUREMENTS OF STRIATAL NO EFFLUX

NO levels were determined in the intact animal using an NO selective, amperometric microsensor (ISO-NOP200, World Precision Instruments (WPI)). Prior to each experiment, the electrode was calibrated[27] in a temperature controlled chamber using known solutions (0.6–192 nM) of the NO generating compound S-nitroso-N-acetylpenicillamine (SNAP). Calibration curves were constructed prior to each experiment in order to determine the sensitivity and integrity of the NO microelectrode (see Figure 1A). In each experiment, twisted-pair bipolar stimulating electrodes were implanted into the SN (coordinates: 3.7–4.2 mm anterior to lambda, 1.5–2.0 mm lateral to midline, 7.5–8.5 mm ventral to brain

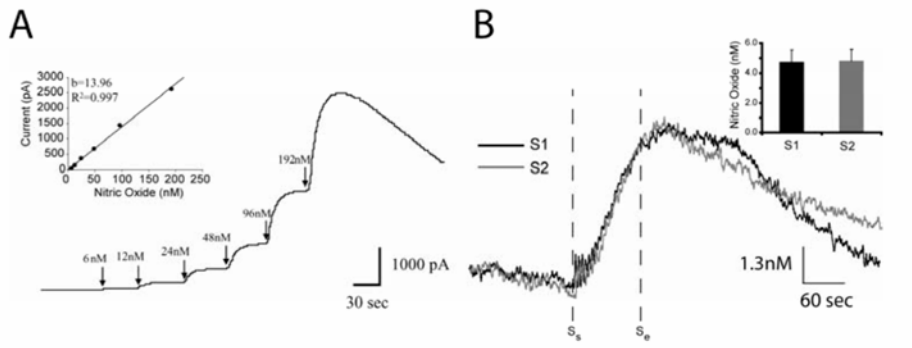

Figure 1. Train stimulation of the substantia nigra increases striatal NO efflux *in vivo*. *A*, Calibration of the NO microsensor *in vitro*. Prior to implantation, NO microelectrodes were calibrated in a temperature controlled (37°C) chamber containing a copper sulfate solution (0.1 M). Known concentrations of NO (6–196 nM as indicated by arrows) were generated from the NO donor S-nitroso-N–acetyl-penicillamine (SNAP, 100 μM) and NO calibration curves were constructed from measures of generated NO oxidation current. ***B***, Two representative recordings showing the NO oxidation signal during the pre-stimulation (0–150 sec.), stimulation (S_s-S_e, 150–250 sec, 750 μA, 0.5 ms, 20 Hz), and the post-stimulation (250–600 sec) periods. High frequency SN stimulation significantly increased striatal NO efflux over pre-stimulation levels in a reproducible manner (S1 and S2 stimulations were performed approximately 15 minutes apart). *Inset:* The magnitude of NO efflux evoked by SN stimulation was not significantly different when repeated 15–30 min after the first stimulation trial ($p > 0.05$, paired t-test, n = 20 paired stimulations from 20 rats).

surface). Electrical stimuli (100 msec ISI) with durations of 500 µs and intensities between 0.1–1.0 mA were generated using a Grass stimulator (S88) and photoelectric constant current/stimulus isolation unit (PSIU6F) and delivered as stimulus trains (20 Hz, 800 ms train duration, 5 sec inter-train interval) for a duration of 100–300 seconds. Next, either a NO microsensor or sharp recording micropipette was implanted into the dorsal striatum (coordinates: 0.7 mm anterior to bregma, 3.0 mm lateral to midline, 6.5 mm ventral to brain surface) ipsilateral to the stimulating electrode. The animal was allowed to recover for approximately 2 hours prior to initiation of the experiment.

To characterize the potential role of phasic DA transmission in modulating striatal NO synthesis, the afferents from the SN were activated using electrical train stimulation (see above) patterned to approximate the natural burst firing activity of midbrain DA neurons. Electrical stimulation of the SN at high frequencies (20 Hz) significantly increased striatal NO efflux over pre-stimulation levels (Figure 1B, n = 20). The facilitatory effect of high frequency SN stimulation on striatal NO efflux was typically transient and reproducible over 30 minute test periods (Figure 1B, inset). Moreover, the signal was derived from neuronal sources of NO since it was attenuated by systemic administration (25 mg/kg, i.p.) of the neuronal NO synthase inhibitor 7-nitroindazole (7-NI, Figure 2, *p < 0.05, paired t-test, n = 6).

4. IMPACT OF SYSTEMIC NEURONAL NOS INHIBITION ON STRIATAL MSN ACTIVITY: EXTRACELLULAR RECORDING STUDIES

To examine the influence of tonic NO on the basal and evoked activity of striatal neurons in the intact system, recordings were made from putative MSNs following systemic administration of either vehicle (10% cremophor EL in physiological saline) or 7-NI (25 mg/kg, i.p.). Extracellular action potentials were biphasic, starting with either a negative or a positive component, followed by the opposite phase (Figure 3A). Comparisons of average firing rate within a 2 min basal recording period revealed no significant differences between the two groups (p > 0.05, t-test, FR ± S.E.M. = 0.623 ± 0.160 Hz, n = 27 for

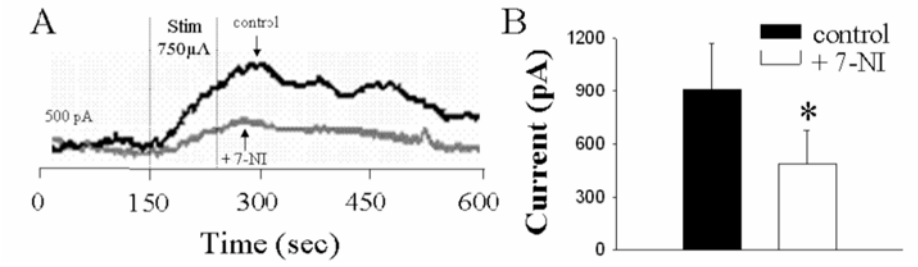

Figure 2. Systemic administration of a neuronal NOS inhibitor attenuates striatal NO efflux evoked during electrical stimulation of the SN. ***A***, A representative recording showing the effects of high frequency stimulation (100 sec, 20 Hz, 750 µA, 0.5 ms) under control conditions (black) and following (≥30 min) systemic administration of 7-nitroindazole (7-NI, 25 mg/kg, i.p.). ***B***, The mean ± S.E.M. increase in NO efflux evoked by SN stimulation was significantly reduced following 7-NI treatment (*p < 0.01, paired t-test, n = 6).

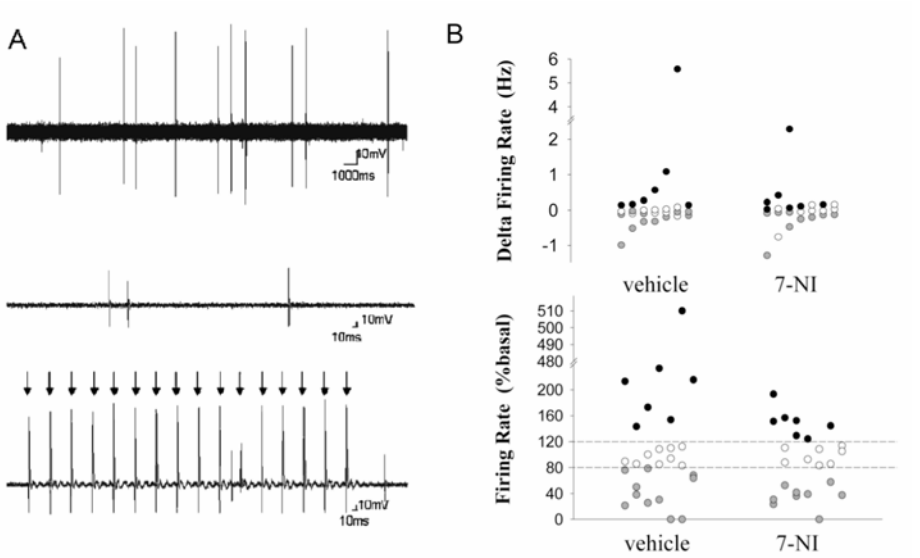

Figure 3. Impact of 7NI on the responsiveness of striatal neurons to electrical stimulation of the SN. ***A***, Representative extracellular recordings under basal conditions (top and middle) and during electrical stimulation (bottom) of the SN (5 min, 20 Hz, 100 µA, 0.5). Arrows indicate the stimulus artifacts. ***B***, The change in firing rate of striatal neurons induced by SN stimulation was not significantly affected by systemic pretreatment with 7-NI ($p > 0.05$, two-way ANOVA, n = 24–27 per group from 16 rats). Black and grey circles represent individual cells which responded to SN stimulation with an increase or decrease (≥20%) in firing rate, respectively. White circles represent cells which were not significantly affected by SN stimulation.

vehicle group; FR ± S.E.M. = 0.971 ± 0.316, n = 24 for 7-NI group). In order to examine the potential intermediary role of NO in SN stimulation-induced changes of striatal neuronal activity, the percent change in firing rate was compared between vehicle and 7-NI groups. Systemic administration of 7-NI did not significantly alter the responsiveness of putative MSNs to SN stimulation (Figure 3, $p > 0.05$, Mann-Whitney Rank Sum Test, n = 27 for vehicle, n = 24 for 7-NI).

5. IMPACT OF LOCAL NEURONAL NOS INHIBITION ON STRIATAL MSN ACTIVITY: INTRACELLULAR RECORDING STUDIES

As mentioned above, MSNs recorded *in vivo* often exhibit characteristic shifts in membrane potential consisting of a depolarized plateau potential or "up state" and a hyperpolarized resting membrane potential termed the "down state"[7] (Figure 4A). Consistent with previous studies,[28,29] we have found that MSNs exhibiting this two-state membrane activity respond to high frequency stimulation of the midbrain (delivered in the down state) with a sustained depolarized-post synaptic plateau potential (dPSP, Figure 4, A, B). In the current study, SN stimulation significantly depolarized all MSNs tested ($^{\#}p < 0.05$, paired t-test, n = 4 cells/rats). To determine the effects of endogenous striatal NO tone on the dPSP evoked during SN stimulation, MSNs were recorded before and after local perfusion of the

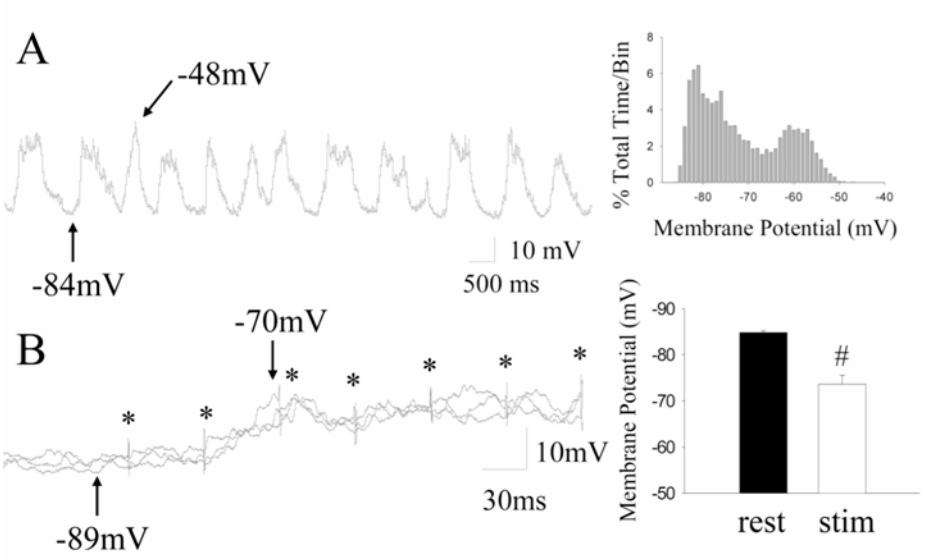

Figure 4. Train stimulation of the SN depolarizes striatal spiny neurons *in vivo*. *A*, Spiny neurons exhibited two-state membrane potential activity (left) and bimodal membrane distributions (right). ***B***, High frequency SN stimulation (20 Hz, 100–200 μA, 0.5 ms, 800 ms train duration, 5 sec inter-train interval), significantly depolarized the membrane of striatal neurons (#$p < 0.05$, paired t-test, n = 4 cells/rats,). *indicates location of stimulus artifacts.

neuronal NOS inhibitor 7-NI (10 μM). Intrastriatal 7-NI infusion did not have a significant impact on the duration of sustained depolarized plateau potentials evoked during SN stimulation (Figure 5, $p > 0.05$, paired t-test). However, local 7-NI infusion significantly reduced the amplitude of dPSPs evoked during SN stimulation (Figure 5, $p < 0.05$, paired t-test), suggesting that activation of NO signaling during SN stimulation facilitates sustained membrane depolarizations and nigrostriatal transmission.

6. SUMMARY AND CONCLUSIONS

Data reported herein indicate that striatal NO signaling may be potently activated by nigrostriatal inputs during DA cell burst firing. These findings are interesting in light of previous studies showing that $D_{1/5}$-like receptor antagonism decreases *ex vivo* histochemical measures of striatal NOS activity.[25] Also, $D_{1/5}$ receptor agonist administration has been shown to stimulate the firing activity of electrophysiologically identified NOS interneurons.[23,24] Given that our experiments were performed in the intact animal using systemic drug administration, it is unclear whether the activation of NOS activity induced during high frequency SN stimulation occurs directly at the level of the striatal NOS interneuron or through indirect circuits. Because the activation of DA $D_{1/5}$ receptors stimulates the activity of cholinergic interneurons[30] known to innervate NOS-interneurons, the potential role of this and other indirect circuits in the SN effect on NOS activity needs to be assessed.

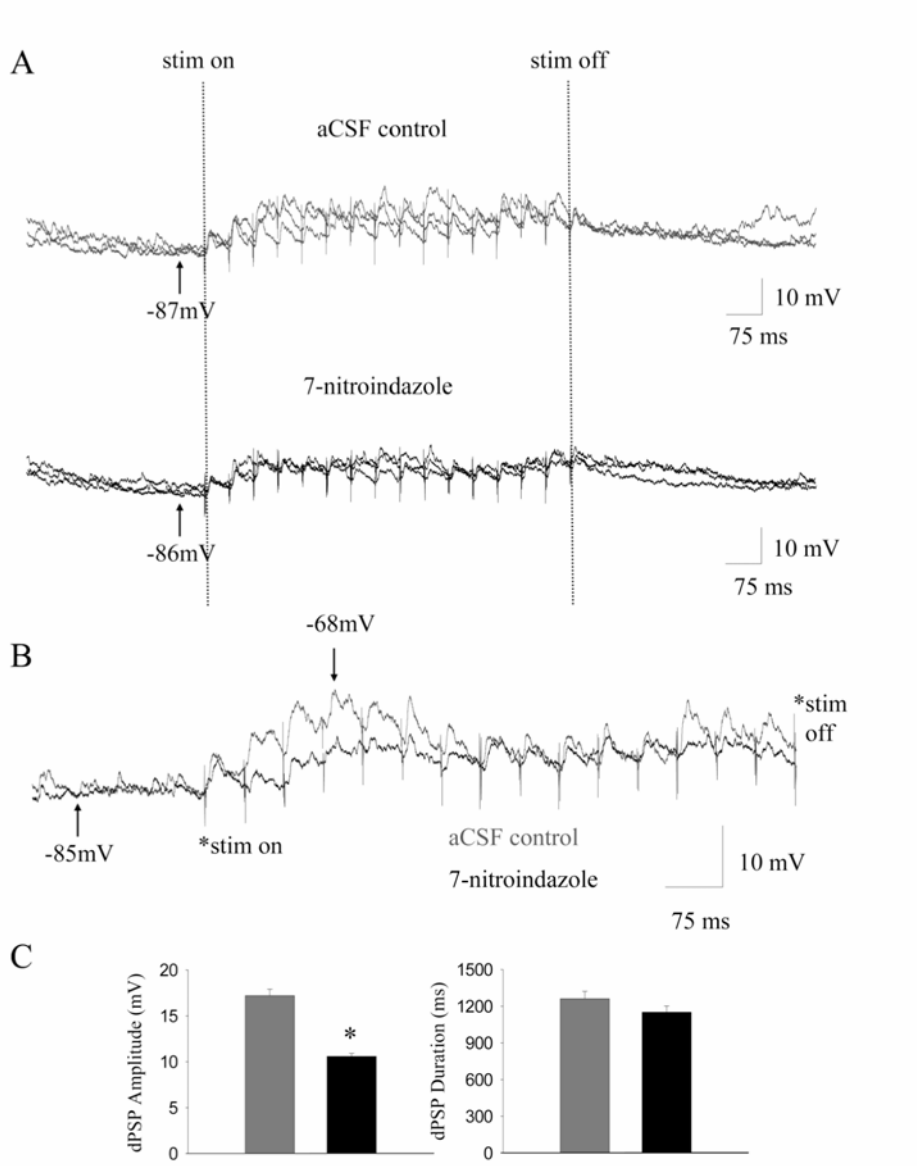

Figure 5. The effects of intrastriatal administration of 7-NI on the responsiveness of striatal spiny neurons to electrical stimulation of the SN. *In vivo* intracellular recordings were performed proximal to a microdialysis probe during aCSF and 7-NI infusion as described above in the Methods section. ***A***, Representative intracellular recordings of the membrane response (overlay of 3 repetitions of SN stimulation) of a single cell to SN stimulation (20 Hz, 200 µA, 0.5 ms) during reverse dialysis of aCSF (top) and during intrastriatal infusion (~15 min) of 7-NI (10 µM, bottom). ***B***, Overlay of single traces of membrane activity recorded during SN stimulation during either aCSF infusion (grey) or following 7-NI (black) infusion (~15 min). ***C***, *Left:* Intrastriatal infusion of 7-NI decreased the mean ± SEM depolarizing postsynaptic potential (dPSP) in response to high frequency SN stimulation (*$p < 0.05$, paired t-test), but not affect the duration of the dPSP (*right*).

Stimulation of the SN has also been shown to antidromically activate corticospinal axons passing through the midbrain which also send axon collaterals to the striatum.[7] Thus, indirect activation of corticostriatal pathways may have contributed to the effects of midbrain stimulation on striatal NO synthesis. We anticipate that our ongoing studies examining the impact of DA antagonists on evoked NO efflux *in vivo* and in *in vitro* brain slice preparations will shed light on these important issues.

Given the above, it is likely that the characterization of the impact of NO signaling on the activity of MSNs will be relevant for understanding information integration in the normal striatum and in pathophysiological conditions such as PD. In initial experiments, we utilized *in vivo* extracellular recording techniques to examine the impact of systemic NOS inhibitor administration on the responsiveness of putative MSNs to SN stimulation. In these studies, no significant differences in firing rate were observed in cells recorded from control and 7-NI treated animals under basal conditions and during SN stimulation. It is possible that the decrease in striatal NOS activity achieved in the current study using an IC_{50} dose of 7-NI was not effective enough to impact on the physiological responsiveness of striatal neurons to SN inputs. It should also be pointed out that the limitations of extracellular recording techniques make it impossible to detect the impact of NOS inhibition on subthreshold membrane responses.

In order to overcome the technical limitations associated with extracellular recordings and enable the examination of the effects of local 7-NI administration on MSN membrane activity, we combined the techniques of *in vivo* intracellular recordings and reverse microdialysis. Our previous studies using this approach indicate that tonic NO signaling may significantly increase the membrane excitability of striatal MSNs by increasing responsiveness to synaptic inputs.[14–16] Consistent with this, disruption of endogenous NO signaling via intrastriatal infusion of the neuronal NOS inhibitor 7-NI significantly reduced the amplitude of dPSPs evoked in MSNs during SN stimulation (Figure 5). As mentioned above, SN stimulation is likely to activate nigrostriatal and corticostriatal pathways in a concurrent manner.[7] Thus, the generation of SN stimulation-evoked dPSPs is likely to involve both DAergic and glutamatergic interactions. Our findings indicating that NO also plays a significant role in the generation of the dPSP is consistent with our previous studies showing that intrastriatal infusion of a NO scavenger reduced both the amplitude of naturally occurring up states and EPSPs evoked by prefrontal cortex stimulation. These studies also showed that that NO interneurons may play a crucial role in modulating the functional states of MSNs and their afferent inputs through activation of the guanylyl cyclase signaling cascade. Two experimental findings substantiate this argument in that intracellular cGMP augmentation induced directly, or indirectly using a PDE inhibitor, increased membrane excitability and prolonged the duration of up events in MSNs.[16] These observations are also consistent with recent studies performed in the nucleus accumbens showing that NO facilitates glutamatergic transmission elicited during electrical stimulation of the hippocampal fimbria via a mechanism involving increased cGMP synthesis.[31] Moreover, high frequency stimulation of the SN (using stimulation parameters found to be optimal for reward-related learning) has been shown to potentiate corticostriatal synaptic activity via a $D_{1/5}$ receptor-dependent mechanism.[32] Interestingly, $D_{1/5}$ receptor agonists have been shown to increase striatal tissue levels of the NO effector cGMP via an unknown mechanism.[33] Thus, while the influence of intrinsic neurotransmitters such as NO on neurotransmission across corticostriatal and nigrostriatal synapses is poorly understood, it is plausible that NO and DA may act in concert to regulate the synaptic activity of MSNs containing guanylyl cyclase, DARPP-32 and/or other NO and DA effector proteins.[15] Further elucidation of the func-

tional interaction between striatal NO interneurons, MSNs, and their glutamatergic and dopaminergic afferents will expand our understanding of information integration and propagation within striatal networks and basal ganglia circuits involved in normal and pathophysiological states such as PD.

7. ACKNOWLEDGEMENTS

The authors thank Mr. John Linardakis for his excellent technical assistance and Mr. Brian Lowry for the development of software (Neuroscope8) used in data acquisition and analysis. The authors also thank Drs. Marjorie Ariano and Heinz Steiner for their valuable assistance and comments regarding this manuscript. This work was supported by the Parkinson's Disease Foundation and by United States Public Health Service grant NS 047452 (ARW).

8. REFERENCES

1. Graybiel, A.M., 2000, The basal ganglia. *Curr. Biol.* **10**(14):R509–R511.
2. Wichmann, T., and DeLong, M.R., 1996, Functional and pathophysiological models of the basal ganglia. *Curr. Opin. Neurobiol.* **6**(6):751–758.
3. Gerfen C.R., 2000, Molecular effects of dopamine on striatal-projection pathways. *Trends Neurosci*. **23**(10 Suppl):S64–S70.
4. Middleton, F.A., and Strick, P.L., Revised neuroanatomy of frontal-subcortical circuits. In: *Frontalsubcortical circuits in psychiatric and neurological disorders*. Edited by D. Lichter, and J. Cummings, (Guilford, New York, 2001), pp. 44–58.
5. Voorn, P., Vanderschuren, L., Groenewegen, H., Robbins, T., and Pennartz, C., 2004, Putting a spin on the dorsalventral divide of the striatum. *TINS* **27**:468–474.
6. Kawaguchi, Y., 1997, Neostriatal cell subtypes and their functional roles. *Neurosci. Res.* **27**:1–8.
7. Wilson, C.J., Basal Ganglia. In: *The synaptic organization of the brain*. Edited by G. Shepherd, (Oxford University Press, Oxford, 2004), pp. 361–414.
8. Wilson, C.J., and Kawaguchi, Y., 1996, The origins of two-state spontaneous membrane potential fluctuations of neostriatal spiny neurons. *J. Neurosci.* **16**(7):2397–2410.
9. Kawaguchi, Y., 1993, Physiological, morphological, and histochemical characterization of three classes of interneurons in rat neostriatum. *J. Neurosci*. **13**:4908–4923.
10. Tepper, J.M., Koós, T., and Wilson, C.J., 2004, GABAergic microcircuits in the neostriatum. *TINS* **27**:662–669.
11. O' Donnell, P., and Grace, A.A., 1997, Cortical afferents modulate striatal gap junction permeability via nitric oxide. *Neurosci*. **76**:1–5.
12. Calabresi, P., Centonze, D., Gubellini, P., Marfia, G.A., and Bernardi, G., 1999a, Glutamate-triggered events inducing corticostriatal long-term depression. *J. Neurosci*. **19**(14):6102–6110.
13. Calabresi, P., Gubellini, P., Centonze, D., Sancesario, G., Morello, M., Giorgi, M., Pisani, A., and Bernardi, G., 1999b, A critical role of the nitric oxide/cGMP pathway in corticostriatal long-term depression. *J. Neurosci.* **19**(7):2489–2499.
14. West, A.R., and Grace, A.A., 2000, Striatal nitric oxide signaling regulates the neuronal activity of midbrain dopamine neurons *in vivo. J. Neurophys*. **83**(4):1796–1808.
15. West, A.R., Galloway, M.P., and Grace, A.A., 2002, Regulation of striatal dopamine neurotransmission by nitric oxide: Effector pathways and signaling mechanisms. *Synapse*. **44**:227–245.
16. West, A.R., and Grace, A.A., 2004, The nitric oxide-guanylyl cyclase signaling pathway modulates membrane activity states and electrophysiological properties of striatal medium spiny neurons recorded *in vivo*. *J. Neurosci.* **24**(8):1924–1935.
17. Di Giovanni, G., Ferraro, G., Sardo, P., Galati, S., Esposito, E., and La Grutta, V., 2003, Nitric oxide modulates striatal neuronal activity via soluble guanylyl cyclase: an in vivo microiontophoretic study in rats. *Synapse*. **48**:100–107.

18. Kharazia, V.N., Schmidt, H.H.W., and Weinberg, R.J., 1997, Type 1 nitric oxide synthase fully accounts for NADPH-diaphorase in rat striatum but not cortex. *Neurosci.* **62**(4):983–987.
19. Mancuso, F., Calignano, A., and Sorrentino, L., 1994, Endogenous nitric oxide modulates the behavioral effects elicited by substance P in rat. *Eur. J. Pharmacol*. **271**:329–333.
20. Stewart, J., Deschamps, S.-E., and Amir, S., 1994, Inhibition of nitric oxide synthase does not block the development of sensitization to the behavioral activating effects of amphetamine. *Brain Res*. **641**:141–144.
21. Fujiyama, F., and Masuko, S., 1996, Association of DAergic terminals and neurons releasing nitric oxide in the rat striatum: An electron microscopic study using NADPH-diaphorase histochemistry and tyrosine hydroxylase immunohistochemistry. *Brain Res. Bull.* **40**(2):121–127.
22. Hidaka, S., and Totterdell, S., 2001, Ultrastructural features of the nitric oxide synthase-containing interneurons in the nucleus accumbens and their relationship with tyrosine hydroxylase containing terminals. *J. Comp. Neurol.* **431**:139–154.
23. Centonze, D., Grande, C., Saulle, E., Martin, A.B., Gubellini, P., Pavon, N., Pisani, A., Bernardi, G., Moratalla, R., and Calabresi, P., 2003, Distinct roles of D_1 and D_5 dopamine receptors in motor activity and striatal synaptic plasticity. *J. Neurosci.* **23**(24):8506–8512.
24. Centonze, D., Bracci, E., Pisani, A., Gubellini, P., Bernardi, G., and Calabresi, P., 2002, Activation of dopamine D_1-like receptors excites LTS interneurons of the striatum. *Eur. J. Neurosci*. **15**:2049–2052.
25. Morris, B.J., Simpson, C.S., Mundell, S., Maceachern, K., Johnston, H.M., and Nolan, A.M., 1997, Dynamic changes in NADPH-diaphorase staining reflect activity of nitric oxide synthase: Evidence for a dopaminergic regulation of striatal nitric oxide release. *Neuropharmac.* **36**(11/12):1589–1599.
26. Paxinos, G., and Watson, C., 1986, *The Rat Brain in Stereotaxic Coordinates*. (Academic Press, New York, 1986).
27. Ohta, K., Rosner, G., and Graf, R., 1996, Nitric oxide generation from sodium nitroprusside and hydroxyamine in brain. *Neuroreport* **8**:2229–2235.
28. Yim, C.Y., and Mogenson, G.J., 1986, Mesolimbic dopamine projection modulates amygdala-evoked EPSP in nucleus accumbens neurons: an in vivo study. *Brain Res*. **369**:347–352.
29. Goto, Y., and O'Donnell, P., 2002, Delayed mesolimbic system alteration in a developmental animal model of schizophrenia. *J. Neurosci*. **22**(20):9070–9077.
30. Aosaki, T., Kiuchi, K., and Kawaguchi, Y., 1998, Dopamine D1-like receptor activation excites rat striatal large aspiny neurons in vitro. *J. Neurosci*. **18**(14):5180–5190.
31. Kraus, M.M., and Prast, H., 2002, Involvement of nitric oxide, cyclic GMP and phosphodiesterase 5 in excitatory amino acid and GABA release in the nucleus accumbens evoked by activation of the hippocampal fimbria. *Neurosci*. **112**(2):331–343.
32. Reynolds, J.N.J., Hyland, B.I., and Wickens, J.R., 2001, A cellular mechanism of reward-related learning. *Nature* **413**:67–70.
33. Altar, C.A., Boyar, W.C., and Kim, H.S., 1990, Discriminatory roles for D1 and D2 dopamine receptor subtypes in the in vivo control of neostriatal cyclic GMP. *Eur. J. Pharm*. **181**:17–21.

CHANDELIER NEURON CARTRIDGES IN THE RAT PREFRONTAL CORTEX CONTACT PYRAMIDAL NEURONS WHICH PROJECT TO THE NUCLEUS ACCUMBENS

Claire Hardwick, Sarah J. French, and Susan Totterdell*

1. INTRODUCTION

Chandelier neurons were first described in Golgi studies in the rat visual cortex (Szentagothai and Arbib, 1974). They form a subclass of cortical interneurons with a specific synaptic target, the axon initial segment (AIS) of pyramidal neurons (Somogyi, 1979; Fairen and Valverde, 1980; Peters et al., 1982). By exerting their inhibition at the site of action potential generation, chandelier neurons are suggested to be in an ideal location to influence profoundly the output of pyramidal cells (Somogyi, 1979). Furthermore, it has been calculated that each chandelier neuron may give rise to between 200–300 cartridges and is hence capable of making contact with 200–300 different target cells (Somogyi et al., 1985) thereby facilitating the synchronisation of large groups of pyramidal neurons (Somogyi et al., 1983). However, there has been no evidence as to whether specific populations of cortical neurons might be subject to this unique inhibition.

It has been suggested that abnormal connectivity of these chandelier neurons may contribute to the symptoms of schizophrenia. Labelling with antibodies to the GABA transporter, GAT-1 in human *post mortem* tissue reveals a 40% reduction (Woo et al., 1998) in the terminal arrays of chandelier neurons, called cartridges, in the prefrontal cortex (PFC) of schizophrenic patients. Such a change may represent an important reduction in inhibition by chandelier neurons of pyramidal neurons, which would have a significant impact on the output of the PFC.

One of the principal projections of the PFC is that to the nucleus accumbens (NAcb) (Christie et al., 1985; Vertes, 2004). The NAcb represents a key site of integration for many regions implicated in schizophrenia (O'Donnell and Grace, 1998). It is considered to be the main site of action of the dopamine antagonists which form the mainstay of the

* Department of Pharmacology, University of Oxford, OX1 3QT, UK.

treatment of this disorder as well as receiving substantial inputs from many of the cortical regions that show pathological changes in this illness, including the projection from the PFC. The PFC projection to the NAcb is known to be regulated by dopamine (Carr et al., 1999) and this regulation is believed to be important in working memory, attention and the effects of stress In contrast to the wealth of information regarding control of this pathway by dopamine, much less is known about a possible role for GABA.

Electrophysiological data has demonstrated that application of GABA agonists in mPFC can affect stress-induced dopamine changes in the NAcb (Doherty and Gratton, 1999; Jayaram and Steketee, 2004). present the anatomical basis for this is unknown: there is no anatomical evidence for GABAergic regulation of PFC-accumbens neurons. In an attempt to address this issue we therefore examined the possible relationship between chandelier neuron cartridges, a major source of GABAergic inhibition, and the PFC pyramidal neurons that project to the core compartment of the NAcb.

2. METHODS

2.1. Injection of Tracer

Environmental conditions for housing of the rats and all procedures that were performed on them were in accordance with the UK Animals (Scientific Procedures) Act 1986, and all efforts were made to minimise the number of animals used and adverse effects. Post-operative observation of the rats indicated minimal levels of distress 24 hours after surgery. The rats were maintained on a 12 h light–dark cycle, with free access to food and water. Male Lister Hooded rats (200–250 g, Harlan, UK) were deeply anaesthetised using Hypnorm and Hypnovel (3 ml/kg i.p. for induction, and 0.2 ml i.m. for maintenance). An iontophoretic injection (7 μA, 7 s on–5 s off, 20 min) of the neuronal tracer Neurobiotin (6% in 0.9% sodium chloride; Vector, UK) was placed into the core of the NAcb of four rats under stereotaxic guidance, using co-ordinates derived from the atlas of Paxinos and Watson (Paxinos, 1986) (Figure 1). After a survival period of 24 hours, the animals were terminally anaesthetised with sodium pentobarbitone and perfused firstly with 100 ml 0.9% saline, and then with 500 ml of 0.2% glutaraldehyde and 4% paraformaldehyde in phos-

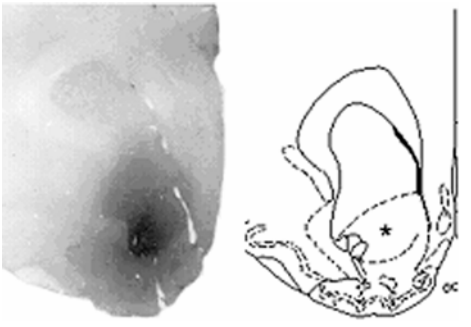

Figure 1. Photomicrograph of injection site into the NAcc core with corresponding atlas drawing taken from Paxinos and Watson, asterisk indicates the injection site.

phate buffer (0.1 M, pH 7.4) for 20 min. After fixation, the brain was removed from the cranium and placed in phosphate buffered saline (PBS; pH 7.4). The injected hemispheres were sectioned coronally on a vibrating microtome (Leica, UK) at 30 μm through the PFC to include the full extent of the NAcb, and sections stored in PBS.

2.2. Visualisation of the Injection Site

To illustrate the injection site, sections containing the NAcb were processed for light microscopy. Sections were incubated in the avidin–biotin–peroxidase complex (ABC) (Vector, UK) with 0.1% Triton X-100 overnight at 4°C. Peroxidase linked to biotinylated tracers by the avidin–biotin bridge was revealed by placing the sections in 0.05 M Tris–HCl buffer (pH 7.6) containing 0.025% 3,3′-diaminobenzidine tetrahydrochloride (DAB) and 0.01% hydrogen peroxidase for 10 min. Rinsing the sections several times in Tris–HCl buffer terminated the reaction. The distribution of GAT-1-immunoreactivity was also examined at the light microscopic level. Sections were incubated with rabbit anti-GAT-1 (1 : 500, Chemicon) in 0.1% Triton-X in PBS overnight, then with biotinylated goat anti-rabbit followed by ABC, with washes in PBS between. Finally the bound peroxidase was revealed using DAB as the chromogen. Sections were mounted on gelatine-coated slides, dehydrated and a coverslip applied with XAM neutral mounting medium.

2.3. Histofluorescence

For double-labelling studies, GAT-1 labelled chandelier cartridges and Neurobiotin labelled projection neurons were visualised using histofluorescence. Firstly, sections were washed in blocking solution (3% goat serum, 2 g/l bovine serum albumin in PBS with 0.5% Triton-X100) to permeabilise the tissue and reduce non-specific labelling. Sections were then incubated in anti-rabbit GAT-1 antibody (Chemicon) and Streptavidin-conjugated Alexafluor 594 (Molecular Probes), both at a concentration of 1:500, with 0.1% Triton X-100 in blocking solution for 48 hours at 4°C.

Following this incubation sections were washed in PBS, and then incubated in 1 : 1000 donkey anti-rabbit Alexafluor 488 (Molecular Probes) and 1 : 500 Streptavidin-conjugated Alexafluor 594 (Molecular Probes) in PBS overnight at 4°C. Finally, sections were washed in PBS and mounted in Vector Shield to reduced bleaching.

Sections were examined using either a fluorescence (Leica, UK) or confocal microscope and images were captured using OpenLab or Leica software. All labelled projection neurons were photographed and examined for possible contact by GAT-1 positive cartridges. Photographs were taken at the same focal plane for each fluorescent channel.

3. RESULTS

3.1. Retrogradely Labelled Neurons

Neurobiotin injections into the core of the NAcb retrogradely labelled projections in layer II and V of the prelimbic subregion of medial PFC (Figure 2A, 3A). In addition to labelled somata, proximal apical and basal dendrites were revealed, as were axon initial segments, emerging from the base of the soma and travelling towards the white matter.

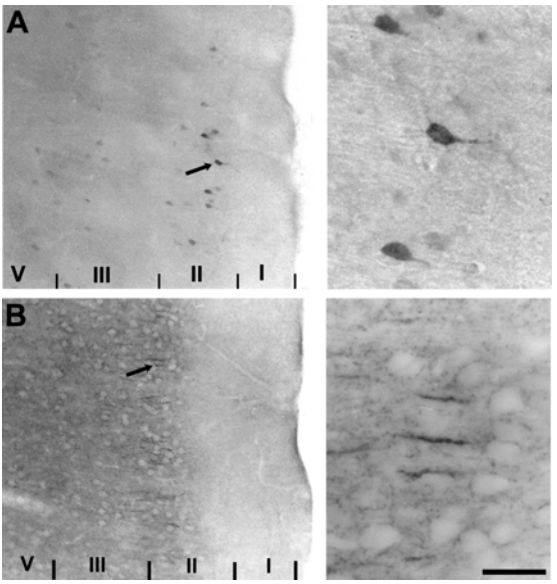

Figure 2. Micrographs of neurobiotin labelling and GAT-1 immunostaining in prelimbic cortex. A. Neurobiotin injection labelled cells in layer II (arrow) and V of prelimbic PFC. B.GAT-1 immunohistochemistry produced punctate staining in all layers of the PFC. Cartridge-like structures (arrow) indicative of chandelier neuron terminals were visible in layers II and III. Scale bar represent 120 µm and 50 µm respectively.

3.2. Immunolabelling with GAT-1

Immunolabelling with GAT-1 antibodies revealed vertically orientated (in relationship to pial surface) rows of boutons, forming cartridge-like structures, which were commonest in layers II and III of all regions of medial PFC. Punctate staining was also observed throughout this region (Figure 2B, 3B), including basket-like arrangements surrounding the cell bodies of some pyramidal neurons.

3.3. Fluorescent Double Labelling

In double labelled tissue, GAT-1-immunnoreactive cartridges were in close apposition with the axon initial segments of retrogradely labelled pyramidal neurons (Figure 3A–C). A fluorescence emission plot taken through an AIS demonstrated peaks for each fluorescent channel in close proximity (data not shown). In certain cases, as well as being aligned to the axon initial segment, GAT-1-positive boutons surrounded the somata of labelled projection neurons (Figure 3B). Analysis of all retrogradely labelled projection neurons showed that about one-third (34.6%) were apparently contacted by GAT-1-immunopositive cartridges.

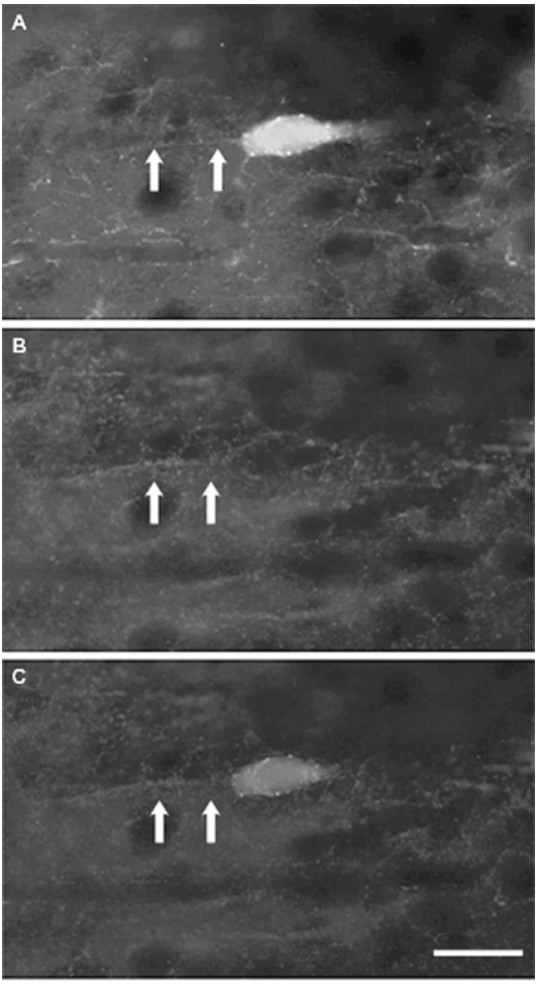

Figure 3. Fluorescence micrographs of duel labelling. A.Cy3 labelled projection neuron with labelled AIS (arrows). B.GAT-1 (Alexafluor 488) labelled puncta and cartridge (arrows). C.Overlay of both channels. Scale bar = 25μm.

4. DISCUSSION

These data represent the first demonstration that chandelier neurons are in a position to regulate a specific population of projection neurons within the mPFC. We show that chandelier neuron cartridges appose PFC neurons projecting to the NAcb. Although we did not examine this material in the electron microscope, other studies have indicated that these cartridges are always synaptic (Soriano et al., 1990). Hence we suggest that chandelier neurons are at least one population of prefrontal cortical interneurons that are in a position to regulate PFC–accumbens projection neuron activity. Since cartridges apposed only about

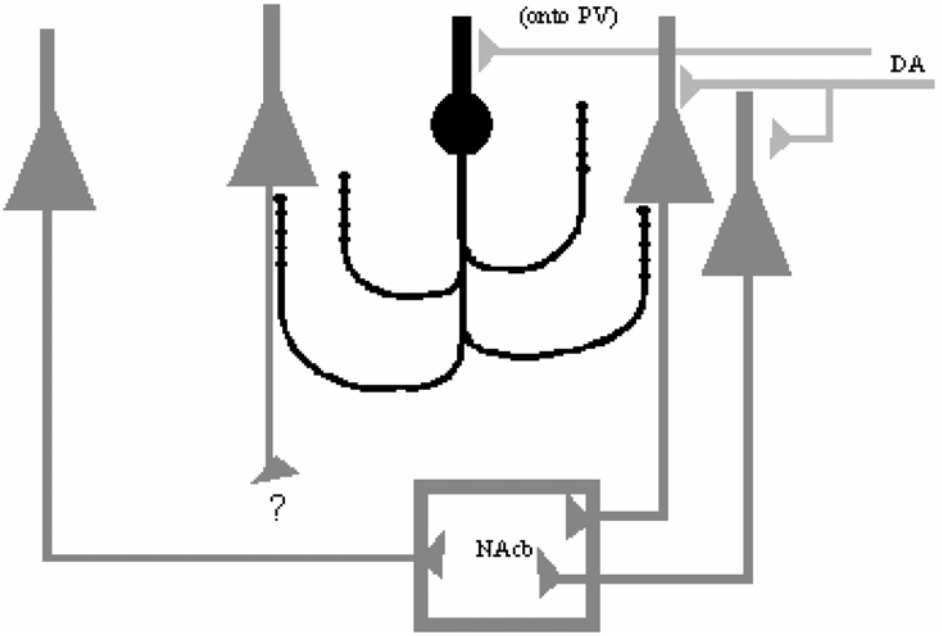

Figure 4. Cartoon summarising the role of chandelier neurons in regulating the PFC – NAcc core projection. Chandelier neurons contact a sub-population of the projection neurons, and may also regulate projections to other unknown regions. Also, shown is the dopaminergic innervation of the parvalbumin sub-class of interneurons, which includes chandelier neurons and the innervation of PFC-NAcc neurons.

one-third of labelled projection neurons, it is likely that only a subset of PFC neurons that project to the NAcb are subject to this type of inhibition.

This study confirms the presence of neurons projecting from PFC to the NAcb in both layers II and V (Ding et al., 2001). As chandelier cartridges are present in Layers II and III (Hardwick et al., 2005) it is the neurons projecting from superficial layers which will be regulated by chandelier neurons. The termination patterns of the two laminar populations are predominantly similar, although the projection from deep layer neurons is more restricted to moderately ENK immunoreactive regions (Berendse et al., 1992; Heidbreder and Groenewegen, 2003). The converging information from superficial and deep cortical neurons within the core of the NAcb might represent an important interface. Nevertheless, the regulation of some layer II projection neurons by chandeliers may present a mechanism by which PFC signal diversity is sustained within the same terminal region. Therefore three types of PFC-accumbens neurons could be present, those projecting from deep layers, those from superficial layers without chandelier input and finally those under this strong inhibition. This classification would provide an additional level of refinement of signalling within the NAcb.

Chandelier cartridges were also seen to impinge on unlabelled pyramidal neurons. This may be a technical issue, since it is quite likely that not all PFC-accumbens neurons were retrogradely labelled. It is quite possible, however, that other populations of cortical projec-

tion neurons may be regulated by chandelier neurons. The PFC is known to project to the VTA (Carr and Sesack, 2000) where it has a role in regulating dopamine release (Rossetti et al., 1998) and it has recently been shown that this regulation may involve GABA (Enrico et al., 1998; Harte and O'Connor, 2005). Chandelier neurons may impinge on neurons projecting to the VTA and therefore regulate dopamine release. As a single chandelier neuron can inhibit several hundred different neurons it is feasible that PFC-accumbens and PFC-VTA neurons could both be under the control of a single chandelier neuron, thereby synchronising the activity of neurons in these disparate regions. Equally possible is that these projections are differentially regulated allowing activation of one pathway with an inhibition of the other.

It has been suggested that the function of chandelier neurons is to control excessive cortical excitation (Zhu et al., 2004), and they may also to play a role in synchronisation of pyramidal neuron firing (Gonzalez-Burgos et al., 2004). Given the specific location of the chandelier neuron input onto the axon initial segment, the sub-population of PFC–accumbens neurons contacted by chandelier neurons is likely to be subject to particularly strong inhibitory control. Moreover, since one chandelier neuron can innervate many axon initial segments, releasing these target neurons simultaneously from this inhibition might result in highly synchronous firing. This is supported by the reports of abnormalities in chandelier neurons associated with epilepsy (Ribak, 1985; DeFelipe, 1999; Arellano et al., 2003). Nevertheless, the function of this interneuronal population is not fully understood, nor has it been possible to differentiate them from other fastspiking neurons on the basis of their electrical activity (Kawaguchi and Kubota, 1997). The rich diversity of cortical interneuron populations (Freund and Buzsaki, 1996) allows for a variety of distinct inhibitory mechanisms possibly subserving distinct roles in information processing; however at present the circuitry involving individual interneuron populations and their mechanisms of signal integration are poorly understood.

The PFC–accumbens projection is known to play a role in reward (Tzschentke, 2000; Tzschentke and Schmidt, 2000). For example, it is important in the sensitisation of cocaine seeking behaviour (McFarland et al., 2003; Jayaram and Steketee, 2004; McFarland et al., 2004). This pathway has previously been shown to be regulated by dopamine, both anatomically and electrophysiologically (O'Donnell and Grace, 1994; Carr et al., 1999). Furthermore, stress-induced increases in cortical dopamine impair certain cognitive processes associated with this brain region (Arnsten and Goldman-Rakic, 1998).

In addition to direct inputs by dopamine onto the prefrontal cortical neurons projecting to the NAcb, there is also evidence for possible indirect control via dopaminergic modulation of a subpopulation of local circuit neurons (Sesack et al., 1998; Sesack et al., 2003). Furthermore, electrophysiological data has demonstrated a role for direct GABAergic inhibition of this pathway, which may be key for cocaine seeking (Miller and Marshall, 2004). This is the first study to assess the anatomical basis for this type of inhibition and demonstrates a role for chandelier neurons in the control of PFC-accumbens processing.

As has previously been mentioned, chandelier neurons are believed to play a particularly significant role in suppression of pyramidal neuron firing, and as such could have an important impact on the signals sent to the NAcb. The NAcb is believed to be a site of motor-limbic integration and within this structure various subregions form parts of loops to which are attributed various functions (Groenewegen et al., 1999). As the chandelier neurons do not apparently regulate all layer II PFC-accumbens neurons it would be interesting to determine if those that are regulated in this manner contribute to one or more of these functional loops.

4.1. Possible Role in Schizophrenia

The presence of chandelier cartridges on the axon initial segments of PFC-accumbens neurons has interesting implications for schizophrenia, as these cartridges are significantly reduced in post-mortem studies of schizophrenic brains (Woo et al., 1998). It might be hypothesized that such a reduction would either lead to disinhibition of this output pathway or to its de-synchronisation. Either way, the information being processed is likely to be significantly distorted and the input to the NAcb disrupted. Such a cortical pathology might be in part responsible for the symptoms of schizophrenia. In this case, the efficacy of dopamine antagonists acting in the NAcb could represent some compensatory mechanism for glutamatergic dysfunction rather than for a primary dopamine abnormality.

5. ACKNOWLEDGEMENTS

Claire Hardwick is supported by a GlaxoSmithKline and MRC CASE studentship award.

6. REFERENCES

Arellano, J.I., Munoz, A., Ballesteros-Yanez, I., Sola, R.G., and DeFelipe, J., 2003, Histopathology and reorganization of chandelier cells in the human epileptic sclerotic hippocampus, *Brain* **127**:45–64.

Arnsten, A.F., and Goldman-Rakic, P.S., 1998, Noise stress impairs prefrontal cortical cognitive function in monkeys: Evidence for a hyperdopaminergic mechanism, *Arch. Gen. Psychiatry* **55**:362–368.

Berendse, H.W., Galis-de Graaf, Y., and Groenewegen, H.J., 1992, Topographical organization and relationship with ventral striatal compartments of prefrontal corticostriatal projections in the rat, *J. Comp. Neurol.* **316**:314–347.

Carr, D.B., O'Donnell, P., Card, J.P., and Sesack, S.R., 1999, Dopamine terminals in the rat prefrontal cortex synapse on pyramidal cells that project to the nucleus accumbens, *J. Neurosci.* **19**:11049–11060.

Carr, D.B., and Sesack, S.R., 2000, Projections from the rat prefrontal cortex to the ventral tegmental area: Target specificity in the synaptic associations with mesoaccumbens and mesocortical neurons, *J. Neurosci.* **20**:3864–3873.

Christie, M.J., James, L.B., and Beart, P.M., 1985, An excitant amino acid projection from the medial prefrontal cortex to the anterior part of nucleus accumbens in the rat, *J. Neurochem.* **45**:477–482.

DeFelipe, J., 1999, Chandelier cells and epilepsy, *Brain* **122(Pt 10)**:1807–1822.

Ding, D.C., Gabbott, P.L., and Totterdell, S., 2001, Differences in the laminar origin of projections from the medial prefrontal cortex to the nucleus accumbens shell and core regions in the rat, *Brain Res.* **917**:81–89.

Doherty, M.D., and Gratton, A., 1999, Effects of medial prefrontal cortical injections of GABA receptor agonists and antagonists on the local and nucleus accumbens dopamine responses to stress, *Synapse* **32**:288–300.

Enrico, P., Bouma, M., de Vries, J.B., and Westerink, B.H., 1998, The role of afferents to the ventral tegmental area in the handling stress-induced increase in the release of dopamine in the medial prefrontal cortex: A dual-probe microdialysis study in the rat brain, *Brain Res.* **779**:205–213.

Fairen, A., and Valverde, F., 1980, A specialized type of neuron in the visual cortex of cat: A Golgi and electron microscope study of chandelier cells, *J. Comp. Neurol.* **194**:761–779.

Freund, T.F., and Buzsaki, G., 1996, Interneurons of the hippocampus, *Hippocampus* **6**:347–470.

Gonzalez-Burgos, G., Krimer, L.S., Povysheva, N.V., Barrionuevo, G., and Lewis, D.A., 2004, Functional properties of fast spiking interneurons and their synaptic connections with pyramidal cells in primate dorsolateral prefrontal cortex, *J. Neurophysiol*. **93**:942–953.

Groenewegen, H.J., Wright, C.I., Beijer, A.V., and Voorn, P., 1999, Convergence and segregation of ventral striatal inputs and outputs, *Ann. N. Y. Acad. Sci.* **877**:49–63.

Hardwick, C., French, S.J., Southam, E., and Totterdell, S., 2005, A comparison of possible markers for chandelier cartridges in rat medial prefrontal cortex and hippocampus, *Brain Res.* **1031**:238–244.

Harte, M., and O'Connor, W.T., 2005, Evidence for a selective prefrontal cortical GABA (B) receptor-mediated inhibition of glutamate release in the ventral tegmental area: A dual probe microdialysis study in the awake rat, *Neuroscience* **130**:215–222.

Heidbreder, C.A., and Groenewegen, H.J., 2003, The medial prefrontal cortex in the rat: Evidence for a dorso-ventral distinction based upon functional and anatomical characteristics, *Neurosci. Biobehav. Rev.* **27**:555–579.

Jayaram, P., and Steketee, J.D., 2004, Effects of repeated cocaine on medial prefrontal cortical gabab receptor modulation of neurotransmission in the mesocorticolimbic dopamine system, *J. Neurochem.* **90**:839–847.

Kawaguchi, Y., and Kubota, Y., 1997, GABAergic cell subtypes and their synaptic connections in rat frontal cortex, *Cereb. Cortex* **7**:476–486.

McFarland, K., Davidge, S.B., Lapish, C.C., and Kalivas, P.W., 2004, Limbic and motor circuitry underlying footshock-induced reinstatement of cocaine-seeking behavior, *J. Neurosci.* **24**:1551–1560.

McFarland, K., Lapish, C.C., and Kalivas, P.W., 2003, Prefrontal glutamate release into the core of the nucleus accumbens mediates cocaine-induced reinstatement of drug-seeking behavior, *J. Neurosci.* **23**:3531–3537.

Miller, C.A., and Marshall, J.F., 2004, Altered prelimbic cortex output during cue-elicited drug seeking, *J. Neurosci.* **24**:6889–6897.

O'Donnell, P., and Grace, A.A., 1994, Tonic D_2-mediated attenuation of cortical excitation in nucleus accumbens neurons recorded in vitro, *Brain Res.* **634**:105–112.

O'Donnell, P., and Grace, A.A., 1998, Dysfunctions in multiple interrelated systems as the neurobiological bases of schizophrenic symptom clusters, *Schizophr. Bull* **24**:267–283.

Paxinos, C.W.G., 1986, The rat brain in stereotaxic coordinates, Academic Press, Inc.

Peters, A., Proskauer, C.C., and Ribak, C.E., 1982, Chandelier cells in rat visual cortex, *J. Comp. Neurol.* **206**:397–416.

Ribak, C.E., 1985, Axon terminals of GABAergic chandelier cells are lost at epileptic foci, *Brain Res.* **326**:251–260.

Rossetti, Z.L., Marcangione, C., and Wise, R.A., 1998, Increase of extracellular glutamate and expression of foslike immunoreactivity in the ventral tegmental area in response to electrical stimulation of the prefrontal cortex, *J. Neurochem.* **70**:1503–1512.

Sesack, S.R., Carr, D.B., Omelchenko, N., and Pinto, A., 2003, Anatomical substrates for glutamate-dopamine interactions: Evidence for specificity of connections and extrasynaptic actions, *Ann. N. Y. Acad. Sci.* **1003**:36–52.

Sesack, S.R., Hawrylak, V.A., Melchitzky, D.S., and Lewis, D.A., 1998, Dopamine innervation of a subclass of local circuit neurons in monkey prefrontal cortex: Ultrastructural analysis of tyrosine hydroxylase and parvalbumin immunoreactive structures, *Cereb. Cortex.* **8**:614–622.

Somogyi, P., 1979, An interneurone making synapses specifically on the axon initial segment of pyramidal cells in the cerebral cortex of the cat [proceedings], *J. Physiol.* **296**:18P–19P.

Somogyi, P., Freund, T.F., Hodgson, A.J., Somogyi, J., Beroukas, D., and Chubb, I.W., 1985, Identified axo-axonic cells are immunoreactive for GABA in the hippocampus and visual cortex of the cat, *Brain Res.* **332**:143–149.

Somogyi, P., Nunzi, M.G., Gorio, A., and Smith, A.D., 1983, A new type of specific interneuron in the monkey hippocampus forming synapses exclusively with the axon initial segments of pyramidal cells, *Brain Res.* **259**:137–142.

Soriano, E., Nitsch, R., and Frotscher, M., 1990, Axo-axonic chandelier cells in the rat fascia dentata: Golgielectron microscopy and immunocytochemical studies, *J. Comp. Neurol.* **293**:1–25.

Szentagothai, J., and Arbib, M.A., 1974, Conceptual models of neural organization, *Neurosci. Res. Program Bull* **12**:305–510.

Tzschentke, T.M., 2000, The medial prefrontal cortex as a part of the brain reward system, *Amino Acids* **19**:211–219.

Tzschentke, T.M., and Schmidt, W.J., 2000, Functional relationship among medial prefrontal cortex, nucleus accumbens, and ventral tegmental area in locomotion and reward, *Crit. Rev. Neurobiol.* **14**:131–142.

Vertes, R.P., 2004, Differential projections of the infralimbic and prelimbic cortex in the rat, *Synapse* **51**:32–58.

Woo, T.U., Whitehead, R.E., Melchitzky, D.S., and Lewis, D.A., 1998, A subclass of prefrontal gamma-aminobutyric acid axon terminals are selectively altered in schizophrenia, *Proc. Natl. Acad. Sci. USA* **95**:5341–5346.

Zhu, Y., Stornetta, R.L., and Zhu, J.J., 2004, Chandelier cells control excessive cortical excitation: Characteristics of whisker-evoked synaptic responses of layer 2/3 nonpyramidal and pyramidal neurons, *J. Neurosci.* **24**:5101–5108.

THE PEDUNCULOPONTINE AND REINFORCEMENT

Helen L. Alderson and Philip Winn*

1. INTRODUCTION

A rather older literature recognized clearly that the pedunculopontine tegmental nucleus (PPTg) was intimately wired into the basal ganglia. For example, the very first article in the very first issue of Brain Research concerned the projections of the lentiform nuclei and showed clearly projections from globus pallidus to PPTg (Nauta and Mehler, 1966). The renewed interest in this part of the brain was largely triggered by the introduction of choline acetyltransferase immunohistochemistry which enabled visualization, description and classification of cholinergic neurons, including those in the mesopontine tegmentum (Mesulam et al., 1983). Most recently, it has again been argued that the PPTg is a member of the basal ganglia family of structures and that understanding of its structure and function can only proceed effectively if we understand its position within this (Mena-Segovia et al., 2004). Functionally, it has been recognized for some time that the PPTg is involved with much more than simply the control of locomotion and sleep, as an older literature suggested. Many studies over the last decade have shown that the PPTg has something to do with reward and reinforcement. The purpose of this brief review is to describe the structure of the PPTg as it relates to the basal ganglia and to examine critically its role in reward and reinforcement.

2. ANATOMY OF THE PPTg

We present here a brief synopsis of what is known of the composition and connections of the PPTg. There are a number of recent reviews describing both the connections and functions of the PPTg (for example, Inglis and Winn, 1995; Pahapill and Lozano, 2000; Mena-Segovia et al., 2004) to which readers are referred for more details. It is also worth observing that the PPTg, like the basal ganglia (Marin et al., 1998), has been very well

* Helen L Alderson, and Philip Winn, School of Psychology, University of St Andrews, St Mary's Quad, South Street, St Andrews, Fife, KY16 9JP, United Kingdom. Email for correspondence: hla@st-and.ac.uk

conserved through evolution. There are many descriptions of its composition and connections in a variety of species (from teleost fish [Brantley and Bass, 1988] to humans [Mesulam et al., 1989]) that indicate its highly conserved nature.

2.1. Composition

The neurons of the PPTg are discriminable morphologically, neurochemically and electrophysiologically. The most obvious population of neurons in PPTg is the Ch5 cholinergic neurons that aggregate at the lateral tip of the superior cerebellar peduncle, though there are many non-cholinergic neurons medially adjacent to and interdigitated with them. Early descriptions of the region suggested that cholinergic and noncholinergic neurons were separated and that the term "PPTg" should be reserved for the cholinergic neurons and "midbrain extrapyramidal area" used to describe the adjacent non-cholinergic neurons. This separation however is not as sharp as was supposed: there are clearly non-cholinergic neurons interdigitated amongst the cholinergic neurons.

PPTg cholinergic neurons contain other neurotransmitters and neuromodulators as well as ACh. Virtually all contain nitric oxide synthase (NOS) for production of the neurotransmitter NO (Vincent and Kimura, 1992) and subsets of the Ch5 group contain amino acid neurotransmitters (glutamate and GABA) or neuropeptides – substance P for example (Vincent et al., 1986; Bevan and Bolam., 1995; Charara et al., 1996). As yet, no systematic pattern of neurotransmitter co-existence has been described. The noncholinergic neurons appear, for the most part, to contain GABA (Ford et al., 1995). Both cholinergic and non-cholinergic neurons appear in small (long axis <20 μm), medium (20–35 μm), and large (>35 μm) types (Takakusaki et al., 1997) and both typically have six primary dendrites. Cholinergic neurons are known to have extensive dendritic fields that often extend outwith the PPTg, and their axons (certainly of the cholinergic neurons) show extensive branching, in some cases with ascending and descending limbs (Semba et al., 1990). Electrophysiologically, populations of neurons differing in terms of ionic mechanism and burst firing properties have been described. For example, using *in vitro* slice preparations, Kitai and his colleagues (Takakusaki et al., 1997) describe two populations of neurons: less common non-cholinergic neurons with low-threshold calcium spikes and a more common type, predominantly but not exclusively cholinergic showing an A-current. Perhaps most interestingly though, when recorded *in vivo*, PPTg neurons show very short response latencies to sensory stimuli (Dormont et al., 1998).

2.2. Connections

There are extensive ipsilateral connections, with good evidence for at least some of the projections traveling to the contralateral hemisphere (Usunoff et al., 1999). The many connections are best described in groups. (i) There are descending connections to the spinal cord (Skinner et al., 1990), the pontine and medullary reticular formations (Jones, 1990; Semba et al., 1990) and the motor trigeminal (Fay and Norgren, 1997). There are also ascending connections to the PPTg from the deep nuclei of the cerebellum that are most likely branches of axons ascending to the thalamus (Hazrati and Parent, 1992). (ii) The Ch5 neurons of PPTg can be considered as archetypal members of the ascending reticular activating system (ARAS) – small numbers of cells giving rise to branched axons spreading over a wide area and having neuromodulatory functions – and, as expected, they are interconnected with other ARAS elements. There are both noradrenergic and serotonergic inputs

(Williams and Reiner, 1993; Honda and Semba, 1994), as well as connections with the contralateral PPTg (Leonard and Llinas, 1990). (iii) There are extensive connections with many nuclei of the thalamus – indeed, en masse, the cholinergic neurons of the mesopontine tegmentum innervate the entire thalamus. Projections from the PPTg have impact on both thalamocortical and thalamostriatal output (Erro et al., 1999). In more functional terms, unilateral stimulation of the posterior PPTg increases *c-fos* activation significantly in the centrolateral and ventrolateral nuclei ipsilaterally, and thalamic reticular nucleus bilaterally (Ainge et al., 2004). Other nuclei, such as the parafascicular have innervation (Kobayashi and Nakamura, 2003) and why these do not show increased Fos expression after posterior PPTg stimulation is unclear. One possible explanation is that different parts of the PPTg make differential innervations of the thalamus. (iv) As well as being able to affect cortical activity through the thalamus, PPTg has impact on sites of non-specific cortical input, including lateral hypothalamus and the basal forebrain. (v) There are extensive connections with corticostriatal and related systems (Figure 1). As well as innervating the thalamus, the PPTg makes a strong innervation of midbrain dopamine (DA) neurons: ACh has excitatory effects on both substantia nigra pars compacta (SNc) and ventral tegmental area (VTA) DA neurons (Bolam et al., 1991; Blaha and Winn, 1993; Blaha et al., 1996). The ability to drive DA neurons gives PPTg indirect control over the structures to which these neurons project, including of course the striatum and prefrontal cortex. In addition to these, there are also direct ascending connections with the subthalamic nucleus (Bevan and Bolam, 1995) and the globus pallidus (Mesulam et al., 1989). The PPTg also receives output from corticos-

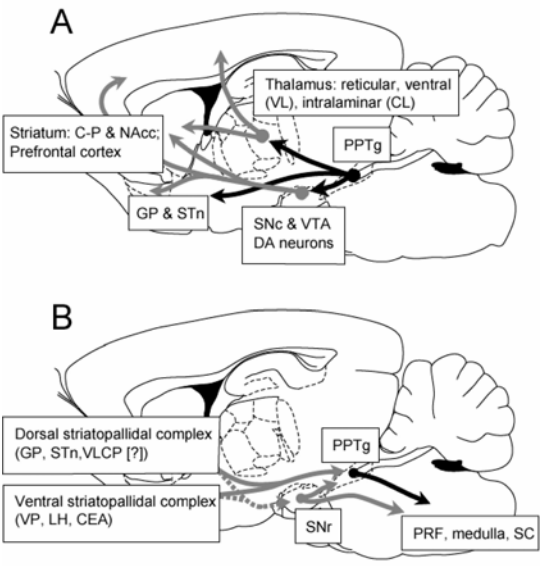

Figure 1. Rat brain sections (Paxinos and Watson, 1997) showing (A) ascending and (B) descending PPTg – corticostriatal connections; black arrows show PPTg. *Abbreviations*: C-P caudate putamen; CEA central extended amygdala; CL centrolateral thalamus; GP globus pallidus; LH lateral hypothalamus; NAcc nucleus accumbens; PPTg pedunculopontine tegmental nucleus; PRF pontine reticular formation; SC spinal cord; STn subthalamic nucleus; SNc substantia nigra, compacta; SNr substantia nigra, reticulata; VP ventral pallidum; VLCP ventrolateral caudate-putamen; VL ventrolateral thalamus.

triatal and related systems: the substantia nigra pars reticulata (SNr), subthalamic nucleus and globus pallidus all project to the PPTg (Moriizumi and Hattori, 1992; Saitoh et al., 2003; Parent and Parent, 2004), as does the ventral pallidum and a significant tranche of the central extended amygdala (Zahm et al., 2001). There are also afferent and efferent connections with superior colliculus (Beninato and Spencer, 1986; Redgrave et al., 1987).

2.3. Functional Implications of PPTg Anatomy

This brief review gives evidence of the fact that the PPTg has a complex internal organization and an extensive set of afferent and efferent connections. The broad pattern of these can be conceptualized as follows: it receives polymodal sensory data that has as yet received little processing – from superior colliculus for example. The PPTg has output to thalamus and corticostriatal systems, as well as sites of nonspecific cortical input. It also receives output from corticostriatal systems and can be considered as an important basal ganglia output station. In addition, PPTg has descending output to sites in brainstem and spinal cord. This suggests that the PPTg is a route for sensory input to thalamus and basal ganglia and, in turn, mediates their output. It seems reasonable, therefore, to consider the functions of the PPTg in terms of the processing that is engaged by corticostriatal and thalamic systems. One of the principal functions of these systems is the analysis of incoming data and the formulation of appropriate behavioral responses. Key to this is learning about the relationships between stimuli and behavior.

3. REWARD AND REINFORCEMENT

The terms “reward” and “reinforcement” are commonly used in behavioural neuroscience, often interchangeably. However, their meanings are very different and it is important to define them. Reward is defined as the appetitive nature of a stimulus – that is, its incentive value, how valuable that stimulus is to the animal. The reward value of a stimulus – food, for example – is not constant, but changes according to the state of the animal. Food has a lower reward value to a sated animal than it does to a hungry one. Reinforcement is defined as the ability of a stimulus to support a learned behaviour. For example, food can be said to be functioning as a reinforcer when it is given following a lever-press, and the animal subsequently increases the rate of lever-pressing in order to receive more food. There is, of course, a relationship between reward and reinforcement: a stimulus that has rewarding properties can support reinforcement learning.

4. APPROACHES TO REWARD, REINFORCEMENT AND THE PPTg

The PPTg has long been associated with reward-related behaviours and a wide variety of methods have been used to investigate them in rats bearing PPTg lesions. These have ranged from simple measures of food and water intake in the home cage, to more complex assessments of the accuracy of reward perception using operant methods. Studies have examined natural rewards – predominantly food – and drug rewards. Interest in the involvement of the PPTg in mediating the rewarding effects of drugs of abuse in particular has been growing in recent times.

The most straightforward reward-related behaviour is the consumption of lab chow and water in the home cage, which is not affected by bilateral excitotoxic lesions of the PPTg (Allen and Winn, 1995). However, PPTg lesioned rats do show altered behavioural responses when given the opportunity to consume a sucrose solution. At low concentration there is no difference between PPTg lesioned rats and controls in the volume of sucrose solution drunk, but at concentrations of 12% and above, PPTg lesioned rats consume significantly more sucrose solution than do controls (Olmstead et al., 1999; Alderson et al., 2001; Keating et al., 2002). There are a number of possible explanations for this altered consumption of high-concentration sucrose solutions. Firstly, that a PPTg lesion somehow results in an alteration in the ability to regulate calorie intake. However, it has been found that PPTg lesioned rats reduce their lab chow consumption when offered high-concentration sucrose solutions so that their calorie intake is the same as when the only food source offered is lab chow (Keating et al., 2002). An alternative explanation for the over-consumption of high-concentration sucrose by PPTg lesioned rats is that they perceive it to be more rewarding than do normal rats. The perception of the reward value of sucrose has been measured using conditioned place preference (CPP) and negative contrast tests, and found to be unchanged by PPTg lesions (Olmstead et al., 1999; Alderson et al., 2001; Keating et al., 2002). It seems most likely that the over-consumption of sucrose by PPTg lesioned rats is due to a lack of behavioral control – a dysregulation of inhibition or switching for example – rather than an alteration in their perception of its reward value. In the context of natural rewards, it must be noted that CPP for food reward has been examined in rats bearing excitotoxic lesions of the PPTg, and it has been suggested that the deprivation state of the rat is an important factor controlling responding. PPTg lesioned rats were impaired in the acquisition of CPP for lab chow when food deprived, but not when they were non-deprived (Bechara and van der Kooy 1992a). However, in other studies deprivation state has not been a critical factor in determining the performance of PPTg lesioned rats (Keating et al., 2002).

Reward perception can also be measured by use of a progressive ratio (PR) schedule of operant responding. This requires the rat to perform an increasing number of leverpresses in an operant chamber in order to gain each successive reward. For example, under a PR5 schedule, the first reward would be delivered after 5 lever-presses, the second after 10, the third after 15, and so on. The point in the schedule at which an animal stops responding is known as the breaking point, and this is taken to reflect the perceived value of the reward to the animal: how hard it is prepared to work for the reward offered. PPTg lesioned rats show a reduced breaking point under a PR schedule of food reward, compared with controls, which might be interpreted as reflecting a reduction in the perceived reward value of the food. However, this reduced breaking point is actually a result of increased responding on the control, non-reinforced, lever and does not appear to indicate changes in reward perception (Alderson et al., 2002). Although responses to natural rewards are changed by PPTg lesions, this does not seem to be as a result of altered reward perception. Therefore, the PPTg does not appear to be involved in mediating the judgment of the rewarding impact of a stimulus such as food.

The rewarding properties of drugs of abuse have also been suggested to be functionally dependent on the PPTg. Several studies have been carried out examining CPP to drugs of abuse in PPTg lesioned rats, with mixed results. PPTg lesions have been found to impair the acquisition of CPP to amphetamine (Bechara and van der Kooy 1989; Olmstead and Franklin, 1994) but not cocaine (Parker and van der Kooy, 1995), a result that is somewhat surprising given the similarities between the mechanism of action drugs.

A number of studies have also found that CPP to morphine is impaired by lesions of the PPTg (Bechara and van der Kooy 1989; 1992b; Olmstead and Franklin 1994). However, in rats that have been made dependent on morphine, PPTg lesions are without effect on CPP to it (Bechara et al., 1992). One possible interpretation of these impairments in CPP following PPTg lesions is that the lesions block the rewarding effect of drugs of abuse, at least under some conditions. However, evidence from studies of intravenous self-administration (IVSA) of drugs of abuse, a more direct measure of drug reward, suggests that this is not the case.

The self-administration of several drugs of abuse has been examined following excitotoxic lesions of the PPTg. IVSA of heroin is impaired by PPTg lesions made before operant training occurs, but not by lesions made afterwards (Olmstead et al., 1998). Similarly, self-administration of *d*-amphetamine under a fixed-ratio schedule by rats bearing PPTg lesions was impaired when no pre-lesion training has been given, but not when an operant response had been acquired prior to lesion surgery (Alderson et al., 2004a). Both these studies suggest that the role of the PPTg is not to mediate the rewarding effect of the self-administered drug, but that the impairment is in the ability to acquire an operant response – that is, impaired reinforcement processes. The role of the PPTg in nicotine self-administration appears to be more complex. Corrigall and his colleagues (1994) reported that lesions restricted to the dorsal PPTg did not affect nicotine IVSA in rats trained prior to lesion surgery. A recent study from our laboratory (Alderson et al., 2004b) compared the effects of lesions of the posterior PPTg (pPPTg; pars compacta) and anterior PPTg (aPPTg; pars dissipata) on nicotine IVSA in rats given operant training prior to being lesioned. There was no effect of aPPTg lesions on nicotine IVSA, while rats bearing pPPTg lesions showed an increase in the number of infusions taken. This increase did not appear to be a result of an alteration in the rewarding impact of nicotine, because these rats showed a normal dose-response to nicotine, albeit responding at a higher level than controls, for all doses and saline.

Manipulation of the PPTg by local drug microinjections have produced mixed results. The μ-opioid receptor agonist DAMGO reduced both cocaine and nicotine IVSA, as did the muscarinic agonist carbachol (Corrigall et al., 1999; 2002) and the GABA agonists muscimol and baclofen (Corrigall et al., 2001). Cocaine IVSA was increased by intra-PPTg microinjection of the nicotinic receptor agonist DHβE (Corrigall et al., 1999). These data are difficult to interpret, beyond suggesting a role for the PPTg in drug self-administration and a complex local synaptology.

4.1. Theories I: Two-Motivational Systems Hypothesis

Derek van der Kooy and his colleagues developed the Two-Separate-Motivational Systems hypothesis of opiate reward, the only theory explicitly suggesting that the rewarding effect of opiates is mediated, under very specific conditions, by the PPTg. The central tenet (Bechara et al., 1998) is that opiate reward is mediated by the PPTg when users are in a drug-naïve state – not dependent on the drug – but by the DA system when in an opiate-dependent state. The authors also suggest that it is possible to use these theories to explain their finding that PPTg lesions impair CPP for food in sated rats, but not in those that are food-deprived. The theory suggests that these two systems operate independently: one takes over from the other once food deprivation or drug dependence (and hence withdrawal in the absence of drug) occurs. This theory is not

supported by experiments from other laboratories, including our own, regarding both the role of the PPTg in reward-related behaviour, and interactions between the PPTg and DA systems. Neurochemical and electrophysiological data support the notion of significant interaction between the PPTg and DA systems. As described above, PPTg innervates DA neurons in the VTA and SNc (Oakman et al., 1995); lesions of the PPTg alter striatal DA function (Blaha and Winn 1993); and PPTg stimulation elicits firing of midbrain DA neurons, leading to increased striatal DA efflux (Floresco et al., 2003; Forster and Blaha 2003). It is important to note here, first, that the relationship is not an opponent one, as the two motivational systems hypothesis implies, but co-operative; and second, that the hypothesis that DA systems are involved in motivation only in particular deprivation / dependent states is not supported (see Berridge and Robinson, 1998).

Behavioral studies, as discussed above, have found that CPP to sucrose was not impaired in PPTg lesioned rats, regardless of deprivation state (Keating et al., 2002), while operant responding for food reward was altered by PPTg lesions, but not in a manner suggestive of alterations in its rewarding effects (Alderson et al., 2002). Additionally, although acquisition of amphetamine was impaired by PPTg lesions, this was ameliorated by a pre-session priming dose of amphetamine, which presumably increased striatal DA levels. This is consistent with there being a close functional relationship between DA systems and the PPTg (Alderson et al., 2004a). Indeed, it may be possible to explain the findings of van der Kooy and his colleagues in terms of changed DA responsiveness rather than deprivation state. The available evidence certainly argues for a close co-operative relationship between the PPTg and midbrain DA system in mediating reward-related behaviour.

4.2. Theories II: Learning About Reward

There is a wealth of evidence from other studies suggesting that the PPTg is critically involved in reinforcement learning rather than in mediating the rewarding effects of stimuli. Midbrain DA neurons are critically involved in reinforcement learning (see Schultz, 2002 for review) and they are dysfunctional following excitotoxic lesions of the PPTg (Blaha and Winn, 1993). We suggest that the functional integrity of the PPTg is necessary for reinforcement learning because of its involvement in modulating midbrain DA activity. A number of studies have found impairments in relatively complex learning following excitotoxic lesions of the PPTg. The acquisition of responding for conditioned reinforcement is impaired (Inglis et al., 1994; Inglis et al., 2000) as are discriminated approaches in an autoshaping paradigm (Inglis et al., 2000). The reduction in breaking point under a progressive schedule of food reward following PPTg lesions can also be interpreted as a learning impairment (Alderson et al., 2002): the breaking point reduction was accompanied by increased responding on the nonreinforced control lever, suggesting a problem in the associative processes linking lever and reward. Evidence for the involvement of the PPTg in reward-related learning also comes from examination of amphetamine self-administration in PPTg lesioned rats (Alderson et al., 2004a). In conditions in which operant behavior had been acquired prior to PPTg lesion surgery, there was no effect of such lesions on amphetamine self-administration. In contrast, if lesions were made prior to training, acquisition of amphetamine self-administration was impaired, a problem ameliorated by noncontingent priming with amphetamine.

5. CONCLUSIONS

Consistent with the role that the PPTg has in the regulation of midbrain DA activity, we conclude that the functional integrity of the PPTg is necessary for reward-related learning but not for the maintenance of previously acquired rewarded behavior. This conclusion is consistent with the connectivity of the PPTg: it makes fast responses to sensory data, relaying this to the thalamus and, via midbrain DA neurons, to corticostriatal systems. It is also an important basal ganglia output station, with descending connections to pontomedullary and spinal cord sites. The structure of PPTg is strongly reminiscent of the substantia nigra: we believe that its function might be too.

6. ACKNOWLEDGEMENTS

Our work is supported by generous grants from the Wellcome Trust and the BBSRC.

7. REFERENCES

Ainge, J.A., Jenkins, T.A., and Winn, P., 2004, Induction of *c-fos* in specific thalamic nuclei following stimulation of the pedunculopontine tegmental nucleus, *Eur. J. Neurosci.* **20**:1827.

Alderson, H.L., Jenkins, T.A., Kozak, R., Latimer, M.P., and Winn, P, 2001, The effects of excitotoxic lesions of the pedunculopontine tegmental nucleus on conditioned place preference to 4%, 12% and 20% sucrose solutions, *Brain Res. Bull.* **56**: 599.

Alderson, H.L., Brown, V.J., Latimer, M.P., Brasted, P.J., Robertson, A.H., and Winn, P., 2002, The effect of excitotoxic lesions of the pedunculopontine tegmental nucleus on performance of a progressive ratio schedule of reinforcement, *Neurosci.* **112**:417.

Alderson, H.L., Latimer, M.P., Blaha, C.D., Phillips, A.G., and Winn, P., 2004a, An examination of d-amphetamine self-administration in pedunculopontine tegmental nucleus-lesioned rats, *Neurosci.* **125**:349.

Alderson, H.L., Latimer, M.P., and Winn, P., 2004b, Differential effects of anterior and posterior pedunculopontine tegmental nucleus lesions on intravenous self-administration of nicotine, *2004 Abstract Viewer/Itinerary Planner*, Society for Neuroscience, Washington D.C., Program no. 575.3.

Allen, L.F., and Winn, P., 1995, Excitotoxic lesions of the pedunculopontine tegmental nucleus disinhibit orofacial behaviours stimulated by microinjections of d-amphetamine into the rat ventrolateral caudateputamen, *Exp. Brain Res*. **104**:262.

Bechara, A., and van der Kooy, D., 1989, The tegmental pedunculopontine nucleus: a brain-stem output of the limbic system critical for the conditioned place preferences produced by morphine and amphetamine, *J. Neurosci.* **9**:3400.

Bechara, A., Harrington, F., Nader, K., and van der Kooy, D., 1992, Neurobiology of motivation: double dissociation of two motivational mechanisms mediating opiate reward in drug-naïve versus drug-dependent animals, *Behav. Neurosci.* **106**:798.

Bechara, A., and van der Kooy, D., 1992a, A single brain stem substrate mediates the motivational effects of both opiates and food in nondeprived rats but not in deprived rats, *Behav. Neurosci.* **106**:351

Bechara, A., and van der Kooy, D., 1992b, Chronic exposure to morphine does not alter the neural tissues subserving its acute rewarding properties: apparent tolerance is overshadowing, *Behav. Neurosci.* **106**:364.

Bechara, A., Nader K., and van der Kooy, D., 1998, A two-separate motivational systems hypothesis of opioid addiction, *Pharm. Biochem. Behav.* **59**:1.

Beninato, M., and Spencer, R.F., 1986, A cholinergic projection to the rat superior colliculus demonstrated by retrograde transport of horseradish peroxidase and choline acetyltransferase immunohistochemistry. *J. Comp. Neurol*. **253**:525.

Berridge, K.C., and Robinson, T.E., 1998, What is the role of dopamine in reward: hedonic impact, reward learning or incentive salience? *Brain Res. Rev*. **28**:309.

Bevan, M.D., and Bolam, J.P., 1995, Cholinergic, GABAergic and glutamate-enriched inputs from the mesopontine tegmentum to the subthalamic nucleus in the rat, *J. Neurosci.* **15**:7105.

Blaha, C. D., and Winn, P., 1993, Modulation of do[amine efflux in the striatum following cholinergic stimulation of the substantia nigra in intact and pedunculopontine tegmental nucleus-lesioned rats, *J. Neurosci.* **13**:1035.

Blaha, C.D., Allen, L.F., Das, S., Inglis, W.L., Latimer, M.P., Vincent, S.R., and Winn, P., 1996, Dopamine efflux in the nucleus accumbens following cholinergic stimulation of the ventral tegmental area in intact, pedunculopontine tegmental nucleus-lesioned and laterodorsal tegmental nucleus-lesioned rats, *J. Neurosci*. **16**:714.

Bolam, J.P., Francis, C.M., and Henderson, Z., 1991, Cholinergic input to dopaminergic neurons in the substantia nigra: a double immunocytochemical study, *Neurosci.* **41**:483.

Brantley, R.K., and Bass, A.H., 1988, Cholinergic neurons in the brain of a teleost fish (Porichthys notatus) located with a monoclonal antibody to choline acetyltransferase, *J. Comp. Neurol.* **275**:87.

Charara, A., Smith, Y., and Parent, A., 1996, Glutamatergic inputs from the pedunculopontine nucleus to midbrain dopaminergic neurons in primates: *Phaseolus vulgaris*-leucoagglutinin anterograde labeling combined with postembedding glutamate and GABA immunohistochemistry, *J. Comp. Neurol.* **364**:254.

Corrigall, W.A., Coen, K.M., and Adamson, K.L., 1994, Self-administered nicotine activates the mesolimbic dopamine system through the ventral tegmental area, *Brain Res.* **653**:278.

Corrigall, W.A., Coen, K.M., Adamson, K.L., and Chow, B.L.C., 1999, Manipulations of mu-opioid and nicotinic cholinergic receptors in the pontine tegmental region alter cocaine self-administration, *Psychopharm.* **145**:412.

Corrigall, W.A., Coen, K.M., Zhang, J., and Adamson, K.L., 2001, GABA mechanisms in the pedunculopontine tegmental nucleus influence particular aspects of nicotine self-administration selectively in the rat, *Psychopharm.* **158**:190.

Corrigall, W.A., Coen, K.M., Zhang, J., and Adamson, K.L., 2002, Pharmacological manipulations of the pedunculopontine tegmental nucleus in the rat reduce self-administration of both nicotine and cocaine, *Psychopharm.* **160**:198.

Dormont, J.F., Condé, H., and Farin, D., 1998, The role of the pedunculopontine tegmental nucleus in relation to conditioned motor performance in the cat. I. Context-dependent and reinforcement-related single unit activity, *Exp. Brain Res*. **121**:401.

Erro, W., Lanciego, J.L., and Giminéz-Amaya, J.M., 1999, Relationships between thalamostriatal neurons and pedunculopontine projections to the thalamus: a neuroanatomical tract-tracing study, *Exp. Brain Res.* **127**:162.

Fay, R.A., and Norgren, R., 1997, Identification of rat brainstem multisynaptic connections to the oral motor nuclei using pseudorabies virus. I. Masticatory muscle motor systems, *Brain Res. Rev.* **25**:255.

Floresco, S.B., West, A.R., Ash, B., Moore, H., and Grace A.A., 2003, Afferent modulation of dopamine neuron firing differentially regulates tonic and phasic dopamine transmission, *Nat. Neurosci.* **6**:968.

Ford, B., Holmes, C.J., Mainville, L., and Jones, B.E., 1995, GABAergic neurons in the rat pontomesencephalic tegmentum: codistribution with cholinergic and other tegmental neurons projecting to the posterior lateral hypothalamus, *J. Comp. Neurol.* **363**:177.

Forster, G.L., and Blaha, C.D., 2003, Pedunculopontine tegmental stimulation evokes striatal dopamine efflux by activation of acetylcholine and glutamate receptors in the midbrain and pons of the rat, *E. J. Neurosci.* **17**:751.

Hazrati, L.N., and Parent, A., 1992, Projection from the deep cerebellar nuclei to the pedunculopontine nucleus in the squirrel monkey, *Brain Res*. **585**:267.

Honda, T., and Semba, K., 1994, Serotonergic synaptic input to cholinergic neurons in the rat mesopontine tegmentum, *Brain Res.* **647**:299.

Inglis, W.L., and Winn P., 1995, The pedunculopontine tegmental nucleus: where the striatum meets the reticular formation, *Prog. Neurobiol.* **47**:1.

Inglis, W.L., Dunbar, J.S., and Winn, P., 1994, Outflow from the nucleus accumbens to the pedunculopontine tegmental nucleus: dissociation between locomotor activity and the acquisition of responding for conditioned reinforcement stimulated by *d*-amphetamine, *Neurosci.* **62**:51.

Inglis, W.L., Olmstead, M.C., and Robbins, T.W., 2000, Pedunculopontine tegmental nucleus lesions impair stimulus-reward learning in autoshaping and conditioned reinforcement paradigms, *Behav. Neurosci.* **114**:285.

Jones, B.E., 1990, Immunohistochemical study of choline acetyltransferase-immunoreactive processes and cells innervating the pontomedullary reticular formation in the rat, *J. Comp. Neurol.* **295**:485.

Keating, G.L., Walker, S.C., and Winn, P., 2002, An examination of the effects of bilateral excitotoxic lesions of the pedunculopontine tegmental nucleus on responding to sucrose reward, *Behav. Brain Res.* **134**:217.

Kobayashi, S., and Nakamura, Y., 2003, Synaptic organization of the rat parafascicular nucleus, with special reference to its afferents from the superior colliculus and the pedunculopontine tegmental nucleus, *Brain Res.* **980**:80.

Leonard, C.S., and Llinás, L,L., 1990, Electrophysiology of mammalian pedunculopontine and laterodorsal tegmental neurons in vitro: implications for the control of REM sleep, in: *Brain Cholinergic Systems* Steriade, M., and Biesold, D., eds., Oxford University Press, Oxford, pp205–223.

Marin, O., Smeets, W.J.A.J., and González, A., 1998 Evolution of the basal ganglia in tetrapods: a new perspective based on recent studies in amphibians, *Trends Neurosci.* **21**:487.

Mena-Segovia, J., Bolam, J.P., and Magill, P.J., 2004, Pedunculopontine nucleus and basal ganglia: distant relatives or part of the same family? *Trends Neurosci.* **27**:565.

Mesulam, M.M., Mufson, E.J., Wainer, B.H., and Levey A.I., 1983, Central cholinergic pathways in the rat: an overview based on an alternative nomenclature (Ch1–Ch6), *Neurosci.* **10**:1185.

Mesulam, M.M., Geula, C., Bothwell, M.A., and Hersh, L.B., 1989, Human reticular formation: cholinergic neurons of the pedunculopontine and laterodorsal tegmental nuclei and some cytochemical comparisons to forebrain cholinergic neurons, *J. Comp. Neurol.* **281**:611.

Moriizumi, T., and Hattori, T., 1992, Separate neuronal projections of the rat globus pallidus projecting to the subthalamic nucleus, auditory cortex and pedunculopontine tegmental area, *Neurosci.* **46**:701.

Nauta, W.J.H., and Mehler, W.R., 1966, Projections of the lentiform nuclei in the monkey, *Brain Res.* **1**:3.

Oakman, S.A., Faris, P.L., Kerr, P.E., Cozzari, C., and Hartman, B.K., 1995, Distribution of pontomesencephalic cholinergic neurons projecting to substantia nigra differs significantly from those projecting to ventral tegmental area, *J. Neurosci.* **15**:5859.

Olmstead, M.C., and Franklin, K.B.J., 1994, Lesions of the pedunculopontine tegmental nucleus block drug-induced reinforcement but not amphetamine-induced locomotion, *Brain Res.* **638**:29.

Olmstead, M.C., Inglis, W.L., Bordeaux, C.P., Clarke, E.J., Wallum, N.P., Everitt, B.J., and Robbins T.W., 1999, Lesions of the pedunculopontine tegmental nucleus increase sucrose consumption but do not affect discrimination or contrast effects, *Behav. Neurosci.* **113**:732.

Pahapill, P.A., and Lozano, A.M., 2000, The pedunculopontine nucleus and Parkinson's disease, *Brain* **123**:1767.

Parent, M., and Parent, A., 2004, The pallidofugal motor system in primates, *Parkinson's Rel. Disord.* **10**:203.

Parker, J.L., and van der Kooy, D., 1995, Tegmental pedunculopontine nucleus lesions do not block cocaine reward, *Pharm. Biochem. Behav.* **52**:77.

Paxinos, G., and Watson, C., 1997, *The Rat Brain In Stereotaxic Co-ordinates*, Academic Press, New York.

Redgrave, P., Mitchell, I.J., and Dean, P., 1987, Further evidence for segregated output channels from superior colliculus in rat: ipsilateral tecto-pontine and tecto-cuneiform projections have different cells of origin, *Brain Res.* **413**: 170.

Saitoh, K., Hattori, S., Song, W-.J., Isa, T., and Takakusaki, K., 2003, Nigral GABAergic inhibition upon cholinergic neurons in the rat pedunculopontine tegmental nucleus, *Eur. J. Neurosci.* **18**:879.

Schultz, W., 2002, Getting formal with dopamine and reward, *Neuron* **36**: 241.

Skinner, R.D., Kinjo, N., Henderson, V., and Garcia-Rill, E., 1990 Locomotor projections from the pedunculopontine tegmental nucleus to the spinal cord, *NeuroReport* **1**:183.

Semba, K., Reiner, P.B., and Fibiger, H.C., 1990, Single cholinergic mesopontine tegmental neurons project to both the pontine reticular formation and the thalamus in the rat, *Neurosci.* **38**:643.

Takakusaki, K., Shiroyama, T., and Kitai, S.T., 1997, Two types of cholinergic neurons in the rat tegmental pedunculopontine nucleus: electrophysiological and morphological characterization, *Neurosci.* **79**:1089.

Usunoff, K.G., Kharazia, V.N., Valtschanoff, J.G., Schmidt, H.H., and Weinberg, R.J., 1999, Nitric oxide synthase-containing projections to the ventrobasal thalamus in the rat, *Anat. Embryol.* **200**:265.

Vincent, S.R., and Kimura, H., 1992, Histochemical mapping of nitric oxide synthase in the rat brain, *Neurosci.* **46**:755.

Vincent, S.R., Satoh, K., Armstrong, D.M., Panula, P., Vale, W., and Fibiger H.C., 1986, Neuropeptides and NADPH-diaphorase activity in the ascending cholinergic reticular system of the rat, *Neurosci.* **17**:167.

Williams, J.A., and Reiner, P.B., 1993, Noradrenaline hyperpolarizes identified rat mesopontine cholinergic neurons in vitro, *J. Neurosci.* **13**:3878.

Zahm, D.S., Williams, E.A., Latimer, M.P., and Winn, P., 2001, Ventral mesopontine projections of the caudomedial shell of the nucleus accumbens and extended amygdala in the rat: double dissociation by organization and development, *J. Comp. Neurol.* **436**:111.

THE PEDUNCULOPONTINE NUCLEUS:
Towards a functional integration with the basal ganglia

Juan Mena-Segovia, Hana M. Ross, Peter J. Magill, and J. Paul Bolam[1]

1. INTRODUCTION

The pedunculopontine tegmental nucleus (PPN) is a neurochemically heterogeneous structure located in the rostral brainstem that forms part of two important regulatory systems of behaviour: the *reticular activating system* and the *mesencephalic locomotor region*. The modulation of the activity of the forebrain and the brainstem underlie the PPN's roles in diverse behavioural functions. The long axonal projections of its neurons reach a wide variety of targets, from the frontal cortex to the thoracic segment of the spinal cord. In addition to these projections, the PPN has a high degree of interconnectivity with the basal ganglia. The anatomical, physiological and behavioural evidence of this close relationship suggests that the PPN and the basal ganglia could be considered as part of the same functional circuit. The aim of this chapter is to present some of the information supporting this notion, focusing on the importance of this relationship for a deeper understanding of basal ganglia function.

2. THE CHALLENGES POSED BY CELLULAR DIVERSITY IN THE PPN

The PPN is composed of a wide variety of cell types. The cholinergic cell population, the best described cell group, only accounts for about 50% of the neurons in the PPN (Manaye et al., 1999). The location of this population has traditionally been used to delineate the boundaries of the PPN. Little is known about the other cell types and whether their cell bodies contribute to the boundary of the PPN as clearly as the cholinergic cells do. It is thus apparent that one of the main difficulties in the study of the PPN lies in the definition of the limits of its extent. Clements and Grant (1990), who first demonstrated the presence of glutamatergic cells in the PPN, showed that the limit of the area occupied by these cells does not correspond to the limits of the cells labelled for nicotinamide adenine

[1] MRC Anatomical Neuropharmacology Unit, University of Oxford, Mansfield Road, Oxford, OX1 3TH.

dinucleotide phosphate (NADPH), which also co-express choline acetyltransferase (ChAT), the synthetic enzyme selectively enriched in cholinergic neurons. By tracing the projections from the PPN and labelling the cholinergic cells, Semba and colleagues (1990) observed that some of the projection cells, which were negative for ChAT, were located dorsal to the population that were positive for ChAT. In other words, classical targets of the PPN receive axons from cells that are located outside of the cholinergic cell population of the PPN. Recent functional studies showed that non-cholinergic cells, whether within or dorsal to the PPN (as defined by the location of ChAT-positive neurons), were activated under the same experimental conditions (Mena-Segovia et al., 2004b, Mena-Segovia and Giordano, 2003).

The cellular diversity of the PPN region further complicates the situation and any possible future redefinition of PPN boundaries. Even amongst the cholinergic cells, it has been shown that differences exist in terms of physiology, connectivity, receptor expression, and neurochemistry. For instance, in terms of physiological membrane properties, three classes of cholinergic neurons have been described in brain slices: cells with low-threshold spikes (LTS type), cells with transient outward current (A-current type), and cells with both characteristics (A+LTS type) (Saitoh et al., 2003). With respect to the receptors expressed, one third of the cholinergic cells express α_{1A} adrenoceptors, whereas half of the cells express α_{2A} adrenoceptors (Hou et al., 2002). The connectivity of each cell type in the PPN also varies according to the input: the GABAergic input from the substantia nigra pars reticulata (SNr), for example, innervates a smaller proportion of cholinergic cells than non-cholinergic cells (Grofova and Zhou, 1998). In terms of neurochemistry, cholinergic cells co-express NADPH (Vincent et al., 1983), and, to varying extents, glutamate (Lavoie and Parent, 1994b) and GABA (Jia et al., 2003). Furthermore, some of the cholinergic cells also express calbindin (Cote and Parent, 1992), while a small sub-population co-express calretinin (Fortin and Parent, 1999). Parvalbumin is also expressed in the PPN (Dun et al., 1995), albeit at lower levels, as are enkephalin and substance P, although their levels of expression in cholinergic cells remains to be determined. This list of heterogeneities of the cholinergic cells is not exhaustive, but has far-reaching implications for the functions of the PPN. Furthermore, a similar degree of heterogeneity exists for the non-cholinergic cell groups.

The non-cholinergic components of the PPN have been less well-studied, even though the glutamatergic and GABAergic neurons were identified more than 10 years ago (Clements and Grant, 1990; Ford et al., 1995). A significant number of noncholinergic neurons are positive for some peptides, and it is likely that there are populations of neurons hitherto undescribed. The lack of a clear definition of the neurochemical natures of the non-cholinergic cells is partly explained by the difficulties in obtaining reliable immunocytochemical signals in the PPN. It is clear, however, that some of these neurons share some characteristics, at least in terms of physiology and connectivity, with the cholinergic cells. Thus, it has been described that approximately 40% of the A-current cell type, and an even higher proportion of LTS and A+LTS cell types, are non-cholinergic (Saitoh et al., 2003). Furthermore, the PPN sends both GABAergic and glutamatergic projections, along with the cholinergic projection, to the subthalamic nucleus (STN; Bevan and Bolam, 1995).

As alluded to above, and despite the large degree of morphological and neurochemical heterogeneity of neuronal populations in the PPN, the physiological characteristics of PPN neurons show a limited number of patterns. *In vitro* studies in brain slices have identified three groups of neurons, one of which is partly made up by cholinergic cells (60%). This

group of cells fires rhythmically and spontaneously (without any distinction between cholinergic or non-cholinergic cells) and has two different characteristics; they possess either short duration action potentials, slow axonal conduction times and high frequencies of discharge, or long action potentials, fast conduction and slow frequencies of discharge. The other two groups consist predominantly of non-rhythmically firing, non-cholinergic neurons (Takakusaki and Kitai, 1997). No other correlation between intrinsic physiological activity and any other neurochemical marker has been described. *In vivo* studies have mainly described two types of activity in PPN neurons; fast, bursting activity and slow, regular activity (Scarnati et al., 1987), both of which are related to cortical activation (Steriade et al., 1990). In addition to these, we have observed tonically-active, fast-firing neurons that do not modify their activity in relation to the activation of the forebrain and cortex (unpublished results). These physiological categories do not represent the entire population of PPN, as some cells remain silent in different conditions (Siegel and McGinty, 1976). Thus, it may be argued that the great cellular diversity in the PPN continues to challenge a ready characterisation of the roles of different PPN neurons in brain function. The questions that arise at this point are whether these physiological characteristics and activity patterns represent different populations of neurons, and whether they are correlated with the wide variety of functions subserved by the PPN.

3. CORRELATION BETWEEN MORPHOLOGY AND PHYSIOLOGY

The problem of cellular heterogeneity of the PPN, coupled with the absence of any apparent sub-nuclei boundaries, is a major issue. The most direct approach to address this is to correlate directly the morphological characteristics, neurochemistry and physiological properties of PPN neurons. The use of juxtacellular recording and labelling allows us to correlate these characteristics at the single-cell level, and thus, to define different subgroups of cells at different functional levels, including their connections.

Cholinergic neurons have medium to large somata, ranging from 20 to 40 μm in their longest axis. Larger cells tend to be fusiform, triangular or multipolar, and give rise to 3–6 thick primary dendrites, whereas medium-sized cells are round or oval and give rise to 2–3 thinner dendrites (Ichinohe et al., 2000; Rye et al., 1987). In contrast, glutamatergic and GABAergic cells usually have a smaller cell body (10–20 μm) and, in the case of the glutamatergic cells, give rise to 2–4 thin dendrites. Some of the glutamatergic and GABAergic cells, however, have larger cell bodies, and this seems to be in accordance with the co-expression of acetylcholine (Clements and Grant, 1990; Ichinohe et al., 2000; Jia et al., 2003). From this evidence, one can assume that larger cells (<20 μm) are cholinergic and smaller cells (<20 μm) are non-cholinergic, a proposal that is in agreement with our observations of juxtacellular labelling combined with immunofluorescence. Figure 1 shows basal firing rates and responses to cortical activation associated with sensory stimulation (hindpaw pinch) of identified PPN neurons in relation to the dimensions of the cell bodies of the recorded cells. The neurons with larger cell bodies, which are presumably cholinergic (some of which were confirmed to be so by immunofluorescence for ChAT) had slower basal firing rates, and most of them increased their activity in relation to cortical activation, a function closely associated with the reticular activating system. Interestingly, some cells with smaller cell bodies, which had faster basal firing rates, also increased their activity in response to cortical activation. This could indicate that the function of a population of non-cholinergic cells is related to

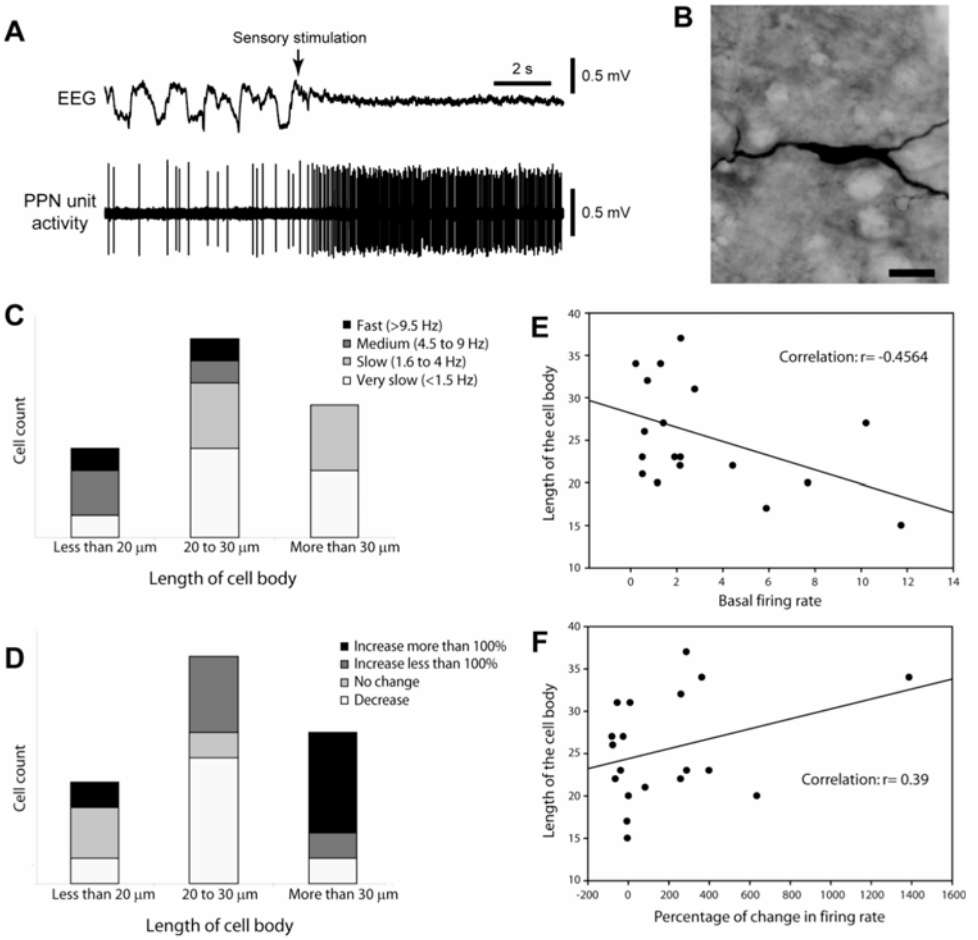

Figure 1. Correlation between physiology and morphology of single PPN neurons recorded and labelled by the juxtacellular method. Extracellular single-unit recordings are used to evaluate the basal firing rate and the change in the firing rate during and after the sensory stimulation; the EEG changes from a slow-wave activity to an activated state characterized by smaller-amplitude, faster-frequency rhythmic activity (A). The recorded cells are then labelled with neurobiotin and their morphology analyzed (B), to correlate the length of the cell body in the longest axis (µm) with the basal firing rate (C, E) and the response to the sensory stimulation (D, F). Scale bar = 20 µm.

cortical activation, and therefore, that cholinergic and non-cholinergic cells are involved in common PPN functions. The fact that some neurons in the PPN are not activated in response to the sensory stimulation is also of importance. Whether these cells have a modulatory function within the PPN, or have projections associated with different functions or brain states is still undetermined, but supports the notion of functional heterogeneity in the PPN.

4. PHYSIOLOGICAL CHARACTERISTICS OF SINGLE CELLS, AND CORRELATION WITH FUNCTION

The *reticular activating system* (RAS; Moruzzi and Magoun, 1949) is located in the brainstem and projects diffusely to the anterior brain. The tonic activity of neurons of the RAS maintains the waking state and is reinforced by sensory inputs. The PPN contributes to this system by its cholinergic projection, and possible glutamatergic projection, to the intralaminar thalamic nuclei. The PPN is in a position to modulate inputs coming from the spinal cord, and then modify the activity of the forebrain through the generation of fast rhythmic activity (see Figure 1A), producing a global activation of the brain. Steriade and colleagues (1991) have shown the involvement of the mesopontine cholinergic nuclei (which include the PPN) in triggering and maintaining the activation of thalamocortical projections, thereby facilitating the activation of the cortex. Stimulation of the PPN is followed by cortical activation, with a 10–20 msec delay, and typically produces a long lasting depolarization of thalamocortical cells that is mediated by muscarinic acetylcholine receptors. This depolarization is associated with prolonged gamma oscillations in the EEG (Steriade et al., 1991), that are indicative of the activated or aroused brain state. PPN stimulation is able to produce a decrease in slower rhythms (0–8 Hz) in the cortex, due to the reduction or suppression of the long-lasting hyperpolarizations of thalamic and cortical cells, as well as to increase the power of fast rhythms (24–33 Hz) (Steriade et al., 1993). This typical cortical activation is obtained following either the electrical stimulation of PPN by pulse trains, or chemical stimulation of PPN by administration of cholinergic or glutamatergic agonists, and is blocked by GABA agonists. In agreement with these observations, changes in the activity of neurons in the PPN are associated with the cortical activation that is observed in particular brain states like wakefulness and REM sleep. Moreover, in addition to the disruption of the oscillations of the thalamocortical projections during slow-wave activity, the PPN is also involved in the generation and maintenance of ponto-geniculo-occipital (PGO) waves. PGO waves are phasic field potentials, of 150 V of amplitude and 100 msec of duration in rats, which originate in the pons and are transferred to the lateral geniculate body and the occipital cortex immediately before the onset of REM sleep. They have been implicated in high-level brain functions, such as sensorimotor integration and learning and memory. PPN neurons contribute to PGO waves by firing in a bursting pattern during the transition from slow-wave activity to the activated state of REM sleep (for a review see Datta, 1997).

In addition to the PPN's role in arousal and the generation of specific thalamic and cortical rhythms as part of the RAS, it is also involved in locomotion (for other PPN functions, see Alderson and Winn's chapter in this book), and indeed forms part of the *mesencephalic locomotor region* (MLR). Stimulation of the MLR produces locomotion, but with a typical delay (2 s) between the stimulation and the movement (stepping). This has led to the suggestion that locomotion is gradually recruited rather than immediately induced (Garcia-Rill, 1991). Garcia-Rill and colleagues (for a review see Garcia-Rill et al., 2004) have shown that rapid stimulation of the PPN produces a startle response, but if the stimulation is ramped, it will produce stepping movements. In fact, the effect of this stimulation is closely dependent on the frequency of the stimuli: the PPN, as well as other mesopontine sites, requires a train of stimuli delivered at 40–60 Hz before locomotion develops, in comparison to other locomotor regions, which require lower frequencies. Similarly, the effect of PPN stimulation on its targets (i.e., pontine reticular neurons) also varies according

to the frequency of stimulation (from no response to a prolonged response), even when the duration of the stimulus remained constant (Garcia-Rill et al., 2001). These variable responses may relate to variations in the co-release of neurotransmitters from PPN terminals. In addition to firing rate, firing pattern is associated with different behaviours; thus, tonic firing is related to initiation or termination of locomotion, whereas burst firing is related to the stepping frequency (Garcia-Rill and Skinner, 1988). Furthermore, there may be a topography of physiological characteristics within the PPN; the proportion of bursting cells seems to increase in the dorsal part of the PPN, whereas tonic neurons predominate in the ventral part. The behavioural response to the stimulation of PPN neurons also seems to vary from a locomotor response to a change in the muscle tone, depending on whether the electrode is within the PPN or surrounding its dorsal or ventral borders (Takakusaki et al., 1997).

The fact that the same PPN neuron types exhibit different firing patterns in relation to different tasks (Kobayashi and Isa, 2002) presents a target for future PPN research. Thus, it is possible that a single PPN neuron fires in a bursting pattern in relation to a particular behaviour (e.g., stepping frequency in locomotion, PGO waves), and then a phasic pattern in response to a sensory stimulus. The different firing patterns probably depend on the activation or inhibition conditions, that is, the combination of neurotransmitters released and the combination of receptors expressed in each neuron. A single PPN neuron could thus be involved in a wide variety of functions, its role being dependent on the inputs activated and its activity history at any particular point in time. In addition, the differences in the physiological features of single cells related to different functions, together with the high degree of neurotransmitter co-expression, raises the possibility that PPN cells could differentially release neurotransmitters depending on their firing pattern.

5. RECIPROCAL CONNECTIONS WITH THE BASAL GANGLIA

Anterograde and retrograde studies conducted over the last two decades have demonstrated that a large number of nuclei receive projections from PPN neurons. Almost every functional system has been reported to receive PPN inputs. Targets of the PPN include nuclei in the basal forebrain, such as the lateral hypothalamus and amygdala, the tectum (superior colliculus), zona incerta, all basal ganglia nuclei, and areas located in the brainstem and spinal cord. Not only does the PPN send out widespread projections, it also receives a varied and extensive input from numerous nuclei, and on many occasions, the projections are reciprocal (for comprehensive reviews, refer to Pahapill and Lozano, 2000; Usunoff et al., 2003).

Accordingly, the axonal projections of these cells are long and far-reaching; some axons are collateralized and contact multiple target nuclei, although to what degree still remains unknown. It is generally considered that the majority of PPN neurons have *either* ascending *or* descending projections, although some studies (including our own unpublished work) have shown that the axons of PPN neurons collateralise and extend in both directions (Semba et al., 1990). The long, ascending projection axons tend to travel by one of two avenues (Shute and Lewis, 1967): dorsally towards the thalamus, or ventrally towards the basal ganglia and rostral forebrain, with many other targets receiving collaterals along the way. In addition to these ascending projection tracts, there are also descending projections. Targets of descending axons include nuclei of the brainstem reticular formation, such as the pontis oralis and caudalis (PnO and PnC, respectively; Grofova and Keane, 1991),

and even the spinal cord. The varied structures served by these numerous pathways are crucially involved in the control of movement and sensorimotor coordination (basal ganglia), sleep-wake mechanisms and arousal (thalamus), and locomotion and autonomic functions (brainstem and spinal cord). With this in mind, it is not surprising that the PPN has been implicated in such a large repertoire of functions. In particular, the importance of the PPN in diverse functions is exemplified by the complex, reciprocal connections that it forms with the basal ganglia (Figure 2; Mena-Segovia et al., 2004a). In light of the cellular heterogeneity of the PPN, and the difficulty in delineating the boundaries of the PPN, it is perhaps more useful to define the PPN, and its possible sub-territories, on the basis of connectivity.

5.1. Connections from the PPN to the Basal Ganglia

In light of the increasing evidence of the importance of non-cholinergic neurons in the PPN, several studies have reported that glutamatergic and GABAergic afferents from the PPN innervate different regions in the basal ganglia. The PPN projects to the SNr and the internal segment of the globus pallidus (GPi), as well as to the substantia nigra pars compacta (SNc; Lavoie and Parent, 1994a; Spann and Grofova, 1989; Spann and Grofova, 1991). The neurons giving rise to these projections have been shown to contain glutamate, in addition to expressing ChAT (Lavoie and Parent, 1994a). Lavoie and Parent (1994c) further showed that most PPN neurons projecting to the substantia nigra in the squirrel monkey are located in the more medial, non-cholinergic area, and that a small proportion

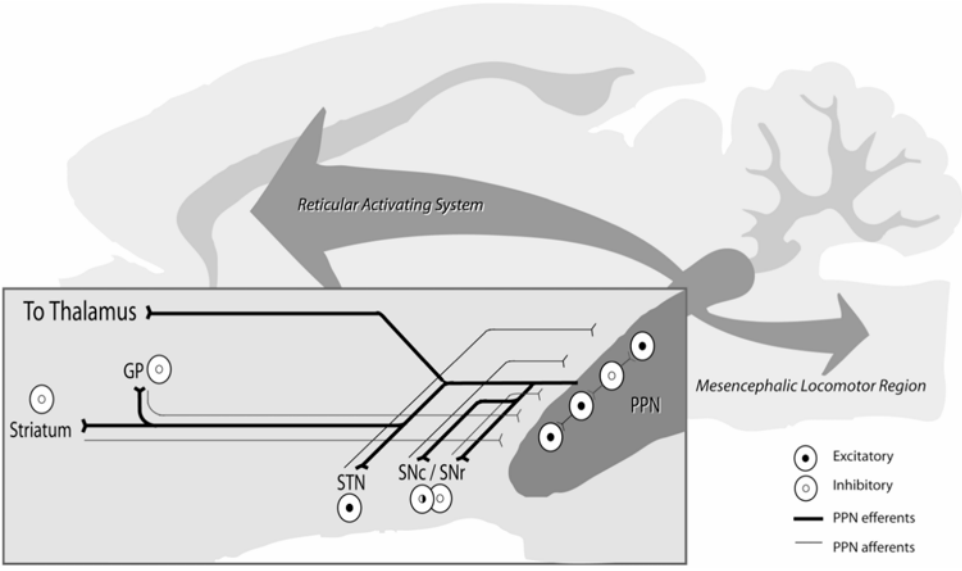

Figure 2. Schematic representation of the main PPN connections. Besides being part of two major behavioral systems, the reticular activating system and the mesencephalic locomotor region, the pedunculopontine nucleus (PPN) is highly interconnected with the basal ganglia. All of the nuclei of the basal ganglia project to, and receive inputs from the PPN. The SNc is represented as a modulatory (excitation/inhibition) connection. SNr, substantia nigra pars reticulata; SNc, substantia nigra pars compacta; STN, subthalamic nucleus; GP, globus pallidus.

are located within the cholinergic cell population; in addition, neurons located in the core of the PPN provide the greatest innervation of the basal ganglia. Similarly, cholinergic terminals in the STN and entopeduncular nucleus (EP, rat equivalent of GPi), which are presumed to be derived from the PPN, contain glutamate (Clarke et al., 1997). At least a component of the mesopontine projection is GABAergic (Bevan and Bolam, 1995). Anterograde tracing, combined with immunolabelling for GABA or glutamate, in primates (Charara et al., 1996), suggests that the PPN has a varied and extensive influence over neurons of the SNc and ventral tegmental area (VTA). Furthermore, dopamine neurons in both regions have been shown to receive input from cholinergic terminals presumed to be derived from the PPN (Bolam et al., 1991; Garzon et al., 1999). We have also shown the existence of glutamatergic and GABAergic projections from the PPN to the VTA at the electron microscopic level using the post-embedding method (Figure 3). Our results showed that 13 of 14 (93%) anterogradely-labelled PPN terminals in the VTA were glutamate immunopositive and completely devoid of GABA immunolabelling (Figure 3A and 3B). In contrast, when the anterograde tracer injection was placed in the area medial to the cholinergic core of the PPN (referred to by some authors as PPN pars dissipata), 5 of 8 (63%) terminals were GABA-immunopositive (Figure 3C and 3D).

5.2. Connections from the Basal Ganglia to the PPN

The basal ganglia output nuclei, SNr and GPi or EP, seem to be the major afferents to the PPN derived from the basal ganglia, providing a prominent GABAergic input to the PPN (Figure 2). Tracing studies combined with immunocytochemistry suggest that nigral GABAergic afferents form synaptic contact mainly with non-cholinergic neurons, some of which have been identified as glutamatergic, and to a lesser extent, the cholinergic neurons (Grofova and Zhou, 1998). These findings are supported by electrophysiological evidence demonstrating an inhibitory effect of the nigral projection, mediated by GABA-A receptors, on the activity of non-cholinergic and cholinergic neurons in the PPN (Saitoh et al., 2003). It is interesting to note that, following injections of tracers both in the SNr in rats and in the GPi of primates, retrogradely labelled neurons in the PPN are sometimes seen to receive input from anterogradely labelled nigral axons, indicating that the interconnections are, at least in part, reciprocal (Grofova and Zhou 1998; Shink et al. 1997). In addition to the output nuclei of the basal ganglia, the STN also provides a prominent, but in this case glutamatergic, innervation of the PPN (Hammond et al., 1983; Steininger et al., 1992).

It should be noted, however, that by virtue of the PPN innervation by the output nuclei, every division of the basal ganglia is in a position, at least indirectly, to influence the activity of neurons in the PPN. Indeed recent functional studies are in support of this (Mena-Segovia et al., 2004b). Although differential inputs and outputs of the PPN in relation to the basal ganglia have been identified, it remains to be established how well the topographical organisation of the cortico-basal ganglia-thalamocortical circuits is maintained at the level of the PPN, or whether the PPN is a major site for the integration of information derived from different functional territories of the basal ganglia (Shink et al., 1997).

5.3. Regulation of the PPN by the Basal Ganglia

The influence of the basal ganglia upon the PPN depends of course on the activity of the direct and indirect pathways. As mentioned above, the major inputs from the basal

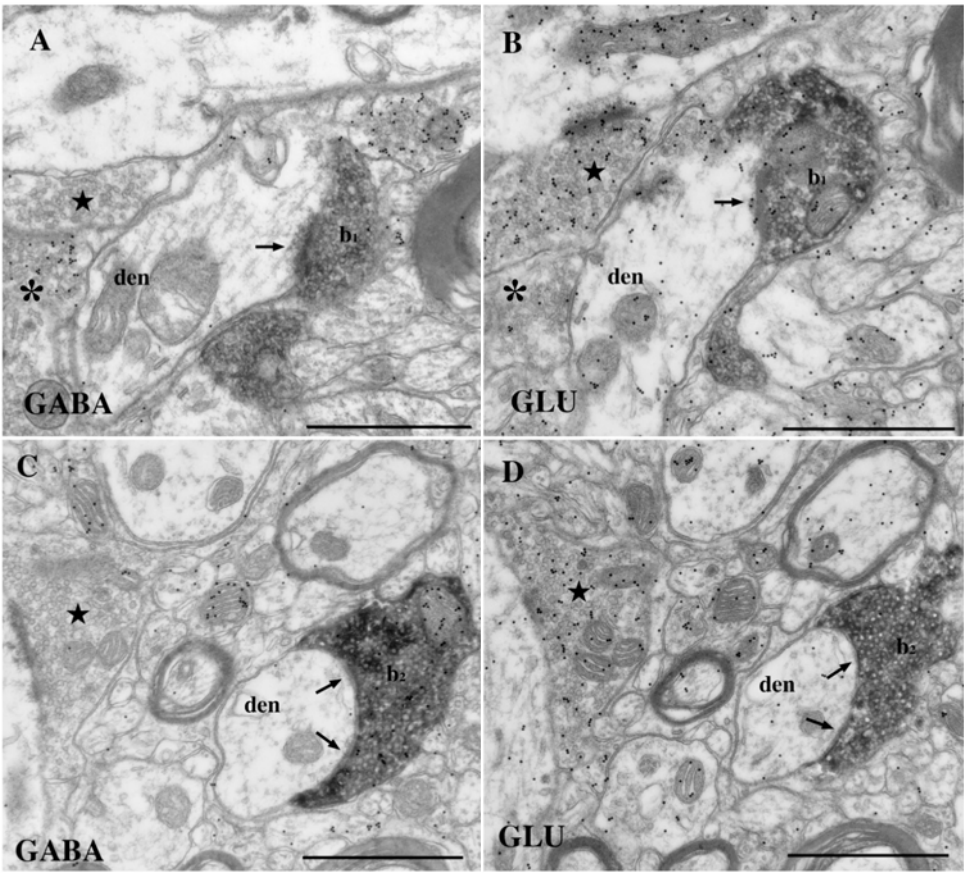

Figure 3. Pairs of electron micrographs of terminals in the VTA that were anterogradely labelled following injections of BDA in the PPN (A, B) and medial to the core of cholinergic neurons in the PPN (C, D). One of each pair of serial sections was immunolabelled to reveal GABA (A, C; GABA) and the other to reveal glutamate (B, D; GLU) using the post-embedding immunogold method. (A, B) The BDA-labelled bouton b_1, is forming an asymmetric synapse (arrow) and is associated with a low level of GABA immunolabelling and a high level of glutamate immunolabelling. Note that adjacent to the BDA-labelled terminal, another unlabelled terminal (star) makes asymmetric synaptic contact with a different dendrite (den) and also has low levels of GABA and high levels of glutamate immunolabelling, while the bouton labelled with an asterisk has high levels of GABA and low levels of glutamate immunolabelling. (C, D) The BDA-labelled bouton b_2, is in symmetrical synaptic contact (arrows) with a dendrite and is associated with a high level of GABA immunolabelling and a low level of glutamate immunolabelling. Note that adjacent to the BDA-labelled terminal, another unlabelled terminal (star), makes asymmetric synaptic contact with a different dendrite and has low levels of GABA and high levels of glutamate immunolabelling. Scale bars = 1 µm. (Data from Ross, Bevan, et al., unpublished.)

ganglia are the glutamatergic projection from the STN and the GABAergic projections from the SNr and GPi/EP. Both pathways and neurotransmitters have been shown to produce significant effects on PPN function: in Parkinson's disease or its models, in which the basal ganglia output is overactive, there are marked changes in PPN neuron activity. In these conditions the PPN is driven by an increased inhibitory input from the basal ganglia

output nuclei and an increased excitatory input from the STN, which is reflected in decreased or increased firing of PPN neurons (for a review see Mena-Segovia et al., 2004a; Pahapill and Lozano, 2000), although the types of cells affected in these ways are unknown. The increased activity of afferents from SNr and STN have also been confirmed in a microdialysis study showing increased extracellular levels of both GABA and glutamate in the PPN following a 6-hydroxydopamine lesion of the SNc (Blanco- Lezcano et al., 2005). These changes have been proposed to underlie the akinesia in Parkinson's disease, which improved following the blockade of GABA-A receptors (Nandi et al., 2002).

6. CONCLUSIONS

The dense interconnections of the PPN and basal ganglia enable the two structures to maintain a close functional relationship that has significant bearing on a wide range of behaviours, including sleep/arousal, locomotion, and posture. Our synthesis of the literature suggests that it is no longer sufficient to view PPN neurons as playing roles in only one of two distinct effector systems, namely the RAS and MLR, but that individual PPN neurons are ideally suited to play central roles in *both* systems. The impact of this hypothesis on our understanding of basal ganglia function is difficult to predict at this time. What is certain, however, is that an appreciation of the functional integration of the PPN and basal ganglia is critical for a better understanding of the roles played by each circuit in behaviour. The cellular heterogeneity present in the PPN indicates that the development of a realistic scheme for functional integration is a major challenge for the future. In meeting this challenge, it is imperative that *correlative* analyses of the physiology, neurochemistry and morphology of the non-cholinergic neurons, as well as the cholinergic neurons, of the PPN are undertaken. Furthermore, it is important that we consider the different functional aspects of the PPN at the level of single *identified* neurons. Using this and other approaches, it will be possible to dissect the influences of the basal ganglia and PPN as they work together as a single 'system', rather than two separate entities.

7. ACKNOWLEDGEMENTS

This work has been supported by grants from the Medical Research Council UK, the Parkinson's Disease Foundation and the Parkinson's Disease Society UK.

8. REFERENCES

Bevan, M.D., and Bolam, J.P., 1995, Cholinergic, GABAergic, and glutamate-enriched inputs from the mesopontine tegmentum to the subthalamic nucleus in the rat, *J. Neurosci.* **15**:7105.

Blanco-Lezcano, L., Rocha-Arrieta, L.L., Alvarez-Gonzalez, L., Martinez-Marti, L., Pavon-Fuentes, N., Gonzalez-Fraguela, M.E., Bauza-Calderin, Y., and Coro-Grave de Peralta, Y., 2005, The effects of lesions in the compact part of the substantia nigra on glutamate and GABA release in the pedunculopontine nucleus, *Rev. Neurol.* **40**:23.

Bolam, J.P., Francis, C.M., and Henderson, Z., 1991, Cholinergic input to dopaminergic neurons in the substantia nigra: a double immunocytochemical study, *Neuroscience* **41**:483.

Charara, A., Smith, Y., and Parent, A., 1996, Glutamatergic inputs from the pedunculopontine nucleus to midbrain dopaminergic neurons in primates: phaseolus vulgaris-leucoagglutinin anterograde labeling combined with postembedding glutamate and GABA immunohistochemistry, *J. Comp. Neurol.* **364**:254.

Clarke, N.P., Bevan, M.D., Cozzari, C., Hartman, B.K., and Bolam, J.P., 1997, Glutamate-enriched cholinergic synaptic terminals in the entopeduncular nucleus and subthalamic nucleus of the rat, *Neuroscience* **81**:371.

Clements, J.R., and Grant, S., 1990, Glutamate-like immunoreactivity in neurons of the laterodorsal tegmental and pedunculopontine nuclei in the rat, *Neurosci. Lett.* **120**:70.

Cote, P.Y., and Parent, A., 1992, Calbindin D-28k and choline acetyltransferase are expressed by different neuronal populations in pedunculopontine nucleus but not in nucleus basalis in squirrel monkeys, *Brain Res.* **593**:245.

Datta, S., 1997, Cellular basis of pontine ponto-geniculo-occipital wave generation and modulation, *Cell Mol. Neurobiol.* **17**:341.

Dun, N.J., Dun, S.L., Hwang, L.L., and Forstermann, U., 1995, Infrequent co-existence of nitric oxide synthase and parvalbumin, calbindin and calretinin immunoreactivity in rat pontine neurons, *Neurosci. Lett.* **191**:165.

Ford, B., Holmes, C.J., Mainville, L., and Jones, B.E., 1995, GABAergic neurons in the rat pontomesencephalic tegmentum: codistribution with cholinergic and other tegmental neurons projecting to the posterior lateral hypothalamus, *J. Comp. Neurol.* **363**:177.

Fortin, M., and Parent, A., 1999, Calretinin-immunoreactive neurons in primate pedunculopontine and laterodorsal tegmental nuclei, *Neuroscience* **88**:535.

Garcia-Rill, E., 1991, The pedunculopontine nucleus, *Prog. Neurobiol.* **36**:363.

Garcia-Rill, E., Homma, Y., and Skinner, R.D., 2004, Arousal mechanisms related to posture and locomotion: 1. Descending modulation, *Prog. Brain Res.* **143**:283.

Garcia-Rill, E., and Skinner, R.D., 1988, Modulation of rhythmic function in the posterior midbrain, *Neuroscience* **27**:639.

Garcia-Rill, E., Skinner, R.D., Miyazato, H., and Homma, Y., 2001, Pedunculopontine stimulation induces prolonged activation of pontine reticular neurons, *Neuroscience* **104**:455.

Garzon, M., Vaughan, R.A., Uhl, G.R., Kuhar, M.J., and Pickel, V.M., 1999, Cholinergic axon terminals in the ventral tegmental area target a subpopulation of neurons expressing low levels of the dopamine transporter, *J. Comp. Neurol.* **410**:197.

Grofova, I., and Keane, S., 1991, Descending brainstem projections of the pedunculopontine tegmental nucleus in the rat, *Anat. Embryol. (Berl).* **184**:275.

Grofova, I., and Zhou, M., 1998, Nigral innervation of cholinergic and glutamatergic cells in the rat mesopontine tegmentum: light and electron microscopic anterograde tracing and immunohistochemical studies, *J. Comp. Neurol.* **395**:359.

Hammond, C., Rouzaire-Dubois, B., Feger, J., Jackson, A., and Crossman, A.R., 1983, Anatomical and electrophysiological studies on the reciprocal projections between the subthalamic nucleus and nucleus tegmenti pedunculopontinus in the rat, *Neuroscience* **9**:41.

Hou, Y.P., Manns, I.D., and Jones, B.E., 2002, Immunostaining of cholinergic pontomesencephalic neurons for alpha 1 versus alpha 2 adrenergic receptors suggests different sleep-wake state activities and roles, *Neuroscience* **114**:517.

Ichinohe, N., Teng, B., and Kitai, S.T., 2000, Morphological study of the tegmental pedunculopontine nucleus, substantia nigra and subthalamic nucleus, and their interconnections in rat organotypic culture, *Anat. Embryol. (Berl).* **201**:435.

Jia, H.G., Yamuy, J., Sampogna, S., Morales, F.R., and Chase, M.H., 2003, Colocalization of gamma-aminobutyric acid and acetylcholine in neurons in the laterodorsal and pedunculopontine tegmental nuclei in the cat: a light and electron microscopic study, *Brain Res.* **992**:205.

Kobayashi, Y., and Isa, T., 2002, Sensory-motor gating and cognitive control by the brainstem cholinergic system, *Neural. Netw.* **15**:731.

Lavoie, B., and Parent, A., 1994a, Pedunculopontine nucleus in the squirrel monkey: cholinergic and glutamatergic projections to the substantia nigra, *J. Comp. Neurol.* **344**:232.

Lavoie, B., and Parent, A., 1994b, Pedunculopontine nucleus in the squirrel monkey: distribution of cholinergic and monoaminergic neurons in the mesopontine tegmentum with evidence for the presence of glutamate in cholinergic neurons, *J. Comp. Neurol.* **344**:190.

Lavoie, B., and Parent, A., 1994c, Pedunculopontine nucleus in the squirrel monkey: projections to the basal ganglia as revealed by anterograde tract-tracing methods, *Journal of Comparative Neurology* **344**:210.

Manaye, K.F., Zweig, R., Wu, D., Hersh, L.B., De Lacalle, S., Saper, C.B., and German, D.C., 1999, Quantification of cholinergic and select non-cholinergic mesopontine neuronal populations in the human brain, *Neuroscience* **89**:759.

Mena-Segovia, J., Bolam, J.P., and Magill, P.J., 2004a, Pedunculopontine nucleus and basal ganglia: distant relatives or part of the same family?, *Trends Neurosci.* **27**:585.

Mena-Segovia, J., Favila, R., and Giordano, M., 2004b, Long-term effects of striatal lesions on c-Fos immunoreactivity in the pedunculopontine nucleus, *Eur. J. Neurosci.* **20**:2367.

Mena-Segovia, J., and Giordano, M., 2003, Striatal dopaminergic stimulation produces c-Fos expression in the PPT and an increase in wakefulness, *Brain Res.* **986**:30.

Moruzzi, G., and Magoun, H.W., 1949, Brain stem reticular formation and activation of the EEG, *Electroencephalogr. Clin. Neurophysiol.* **1**:455.

Nandi, D., Aziz, T.Z., Giladi, N., Winter, J., and Stein, J.F., 2002, Reversal of akinesia in experimental parkinsonism by GABA antagonist microinjections in the pedunculopontine nucleus, *Brain* **125**:2418.

Pahapill, P.A., and Lozano, A.M., 2000, The pedunculopontine nucleus and Parkinson's disease, *Brain* **123**:1767.

Rye, D.B., Saper, C.B., Lee, H.J., and Wainer, B.H., 1987, Pedunculopontine tegmental nucleus of the rat: cytoarchitecture, cytochemistry, and some extrapyramidal connections of the mesopontine tegmentum, *Journal of Comparative Neurology* **259**:483.

Saitoh, K., Hattori, S., Song, W.J., Isa, T., and Takakusaki, K., 2003, Nigral GABAergic inhibition upon cholinergic neurons in the rat pedunculopontine tegmental nucleus, *Eur. J. Neurosci.* **18**:879.

Scarnati, E., Proia, A., Di Loreto, S., and Pacitti, C., 1987, The reciprocal electrophysiological influence between the nucleus tegmenti pedunculopontinus and the substantia nigra in normal and decorticated rats, *Brain Research* **423**:116.

Semba, K., Reiner, P.B., and Fibiger, H.C., 1990, Single cholinergic mesopontine tegmental neurons project to both the pontine reticular formation and the thalamus in the rat, *Neuroscience* **38**:643.

Shute, C.C., and Lewis, P.R., 1967, The ascending cholinergic reticular system: neocortical, olfactory and subcortical projections, *Brain* **90**:497.

Siegel, J.M., and McGinty, D.J., 1976, Brainstem neurons without spontaneous unit discharge, *Science* **193**:240.

Spann, B.M., and Grofova, I., 1989, Origin of ascending and spinal pathways from the nucleus tegmenti pedunculopontinus in the rat, *Journal of Comparative Neurology* **283**:13.

Spann, B.M., and Grofova, I., 1991, Nigropedunculopontine projection in the rat: an anterograde tracing study with *Phaseolus vulgaris*-leucoagglutinin (PHA-L), *J. Comp. Neurol.* **311**:375.

Steininger, T.L., Rye, D.B., and Wainer, B.H., 1992, Afferent projections to the cholinergic pedunculopontine tegmental nucleus and adjacent midbrain extrapyramidal area in the albino rat. I. Retrograde tracing studies, *J. Comp. Neurol.* **321**:515.

Steriade, M., Amzica, F., and Nunez, A., 1993, Cholinergic and noradrenergic modulation of the slow (approximately 0.3 Hz) oscillation in neocortical cells, *J. Neurophysiol.* **70**:1385.

Steriade, M., Datta, S., Pare, D., Oakson, G., and Curro Dossi, R.C., 1990, Neuronal activities in brain-stem cholinergic nuclei related to tonic activation processes in thalamocortical systems, *J. Neurosci.* **10**:2541.

Steriade, M., Dossi, R.C., Pare, D., and Oakson, G., 1991, Fast oscillations (20–40 Hz) in thalamocortical systems and their potentiation by mesopontine cholinergic nuclei in the cat, *Proc. Natl. Acad. Sci. USA* **88**:4396.

Takakusaki, K., Habaguchi, T., Nagaoka, T., and Sakamoto, T., 1997, Stimulus effects of pedunculopontine tegmental nucleus (PPTN) on hindlimb motoneurons in cats, *Soc. Neurosci. Abstr.* **23**:762.

Takakusaki, K., and Kitai, S.T., 1997, Ionic mechanisms involved in the spontaneous firing of tegmental pedunculopontine nucleus neurons of the rat, *Neuroscience* **78**:771.

Usunoff, K.G., Itzev, D.E., Lolov, S.R., and Wree, A., 2003, Pedunculopontine tegmental nucleus. Part I: Cytoarchitecture, transmitters, development and connections, *Biomed Rev.* **14**:95.

Vincent, S.R., Satoh, K., Armstrong, D.M., and Fibiger, H.C., 1983, NADPH-diaphorase: a selective histochemical marker for the cholinergic neurons of the pontine reticular formation, *Neurosci. Lett.* **43**:31.

GLUTAMATERGIC AND GABAERGIC CONTROL OF PALLIDAL ACTIVITY IN MONKEYS

Hitoshi Kita, Yoshihisa Tachibana, and Atsushi Nambu*

1. INTRODUCTION

This article presents our recent investigations on the role of glutamatergic and GABAergic inputs on the control of the firing rate and patterns of pallidal neurons in awake monkeys. A simple basal ganglia connection diagram introduced about 10 years ago is shown in Figure 1A (Kita, 1994). The neostriatum (Str) and the subthalamic nucleus (STN) are considered to be the input nuclei of the basal ganglia. The external segment of the globus pallidus (GPe) is located in the strategic locus in the basal ganglia connections. The GPe receives its main excitatory inputs from the STN and main inhibitory inputs from the Str. It sends GABAergic inhibitory projections mainly to the basal ganglia output nuclei, the internal segments of the globus pallidus (GPi) and the substantia nigra pars reticulata (SNr) and to the GPe itself, through recurrent-collateral axons (Kita and Kitai, 1991; Kita, 1992; Kita, 1994; Kita and Kitai, 1994; Parent and Hazrati, 1995). These connections suggest that information arriving in the input nuclei of the basal ganglia, the Str and the STN, is processed, forwarded to the GPe, and then redistributed to the many nuclei of the basal ganglia (Kita, 1994).

In awake animals, the most frequently encountered type of neuron in the GPe was the high frequency firing with pause type and, in the GPi, the continuous-irregular-high frequency firing type (DeLong 1971; Anderson and Horak 1985; Tremblay et al., 1989; Nambu et al., 2000). The level and pattern of these firing activities change with the development of basal ganglia diseases including Parkinson's disease and hemiballism (Pan and Walters 1988; Tremblay et al., 1989; Nini et al., 1995). Thus, exploring the mechanisms controlling the firing activity of GPe and GPi neurons is important for understanding basal ganglia functions in normal and pathological conditions.

* H. Kita, Dept. of Anatomy and Neurobiol., College of Medicine, Univ. of Tennessee, Memphis, TN 38163, U.S.A. Y. Tachibana and A. Nambu, Division of System Neurophysiol., National Institute for Physiological Sciences, Okazaki, 444-8585, Japan.

In the latter part of this article, we will discuss the responses of pallidal neurons to stimulation of the motor cortex and the STN. Stimulation of the primary motor cortex (M1) or the supplementary motor area evoked a similar sequence of responses in both segments of the pallidum. The sequence typically consisted of an early excitation, an inhibition, and a late excitation (Fig. 1). Several excitatory and inhibitory drives forming this response pattern can be considered based on the major synaptic connections and previous observations on the cortical stimulation induced response in the Str and the STN (Fig. 1B). The early excitation of the GPe and GPi is due to the disynaptic cortico-STNGPe/GPi connection with very fast conducting axons (Kita 1992; Nambu et al., 2000). For the inhibition following the early excitation two synaptic inputs can be considered. The early excitation in the GPe should evoke inhibition in the postsynaptic neurons in both the GPe and GPi. Another is the cortico-Str-GPe/GPi input. Because the conduction velocity of Str axons is slow (Tremblay et al., 1989), the inhibition should arrive a few milliseconds after the arrival of the early excitation. The late excitation was also considered to be of STN origin because stimulation of the cortex also induced a late excitation in STN neurons, with a latency that was a few milliseconds shorter than that of the pallidum, and muscimol blockade of the STN that diminished or abolished both the early and late response in pallidal neurons(Nambu et al., 2000; Kita et al., 2004).

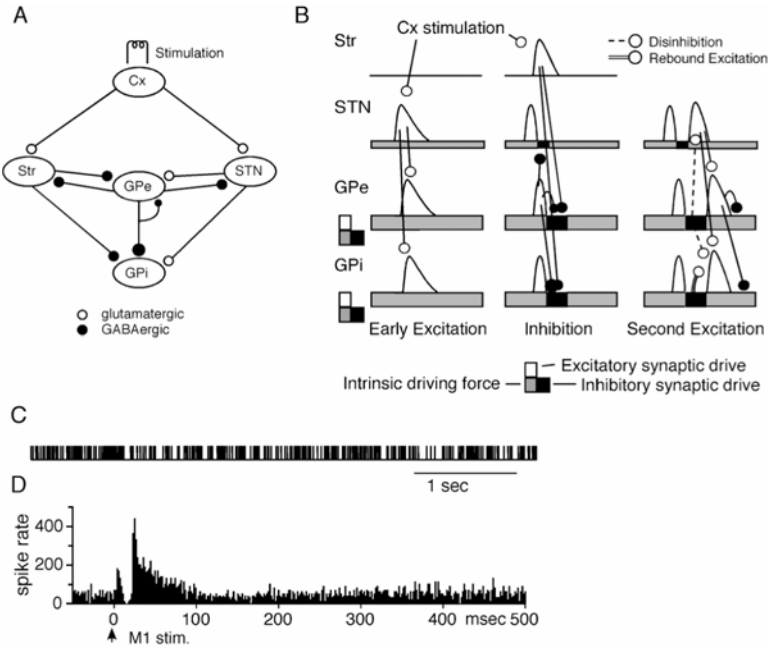

Figure 1. The diagrams show the major connections of the basal ganglia (A) and the time sequence and the major driving forces that evoke a sequence of early excitation, inhibition, and late excitation in pallidal neurons (B). The thickness of base bars represents the level of spontaneous firing that is set by the sum of the strengths of the glutamatergic excitatory component (white column), the GABAergic inhibitory component (black column), and intrinsic driving forces (gray column). C and D: A typical spontaneous firing pattern (C) and a peri-stimulus time histograms (PSTH) of response to cortical stimulation in the GPe.

2. RESULTS

2.1. Glutamatergic and GABAergic Control of Firing Rate and Pattern of Pallidal Neurons

STN neurons in awake animals are highly active while Str projection neurons are quiescent. Thus, it can be expected that both STN-GPe glutamatergic and GPe-GPe/GPi GABAergic inputs play crucial roles in the maintenance of the high level of firing activity and the generation of firing patterns of the pallidal neurons. To examine the contribution of the STN inputs, the GABA agonist muscimol was injected in the STN and unitary activities of the pallidum were recorded in monkeys. The muscimol blockade of STN resulted in dramatic changes in the firing pattern in the GPe (Nambu et al., 2000; Kita et al., 2004). Initially, the STN blockade greatly decreased the firing rate, to complete silence in some neurons. However, 5–10 min after the muscimol injection, the activity began to increase with repeated occurrences of short grouped spike discharges. As time progressed, the activity further increased and developed into repeated occurrences of two to twelve seconds of a very high-frequency active phase and then two to twelve seconds of a completely silent period (Fig. 2A) (Nambu et al., 2000; Kita et al., 2004). Alternatively occurring active and silent phases in GPe neurons were also induced with the injection of the AMPA/kainate blocker NBQX (0.2–1 mM in saline, 0.2 µl) into the vicinity of the pallidal neurons through the electrode assembly that was designed so that injected drugs covered a large somatodendritic space of recorded neurons (Kita et al., 2004). In the GPi, the STN blockade or local injection of NBQX reduced the firing rate and increased the firing regularity (Nambu et al., 2000). Unlike the GPe, GPi neurons did not develop the active and silent phases. The NMDA antagonist CPP also decreased the mean firing rate of pallidal neurons, although the change was less prominent than with NBQX.

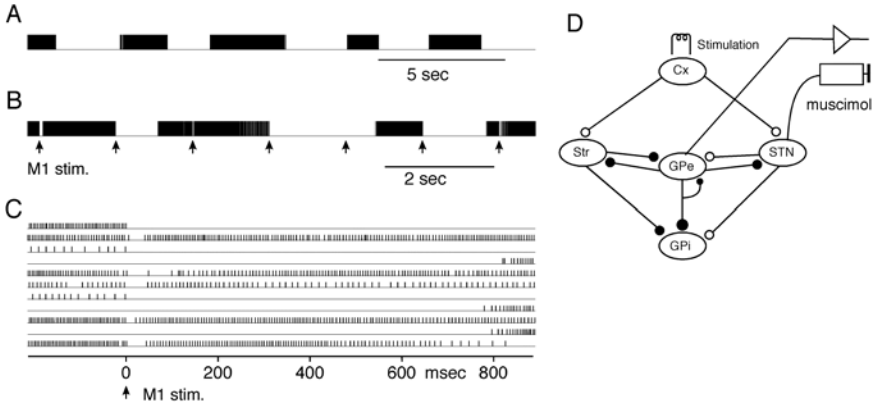

Figure 2. Recording of a GPe neuron obtained after muscimol (0.5 µg/µl saline, 1.0 µl) injection in the STN. A: A digitized spike trace with a slow-sweep speed show the repeated occurrence of active and silent phases. B: A slow sweep record shows that M1 stimulation (marked by arrows) induced different responses depending on the timing of stimulus in the slow oscillation. C: Fast-sweep digitized unit responses to consecutive M1 stimulation. D: The diagram shows experiment setup.

These results suggest that glutamatergic inputs contribute to the high rate and the irregularity of spontaneous activity of GPe and GPi neurons in awake monkeys by not only providing driving forces but also by shifting the membrane potential to express different membrane properties. The mechanisms that underlie the development of active and pause phases in GPe neurons after blockade of glutamatergic inputs are unknown. We speculate that intrinsic mechanisms of GPe neurons may generate the pauses within an appropriate membrane potential range.

To examine the contribution of the GABAergic inputs to the firing activity of the pallidum, the $GABA_A$ receptor blocker, gabazine, was injected into the vicinity of the pallidal neurons. Gabazine increased the firing rate of most of the GPe and GPi neurons examined (Fig. 3). Co-application of NBQX and gabazine greatly increased the firing rate and regularity of most of neurons examined (Figs. 3G and H). These results indicated that

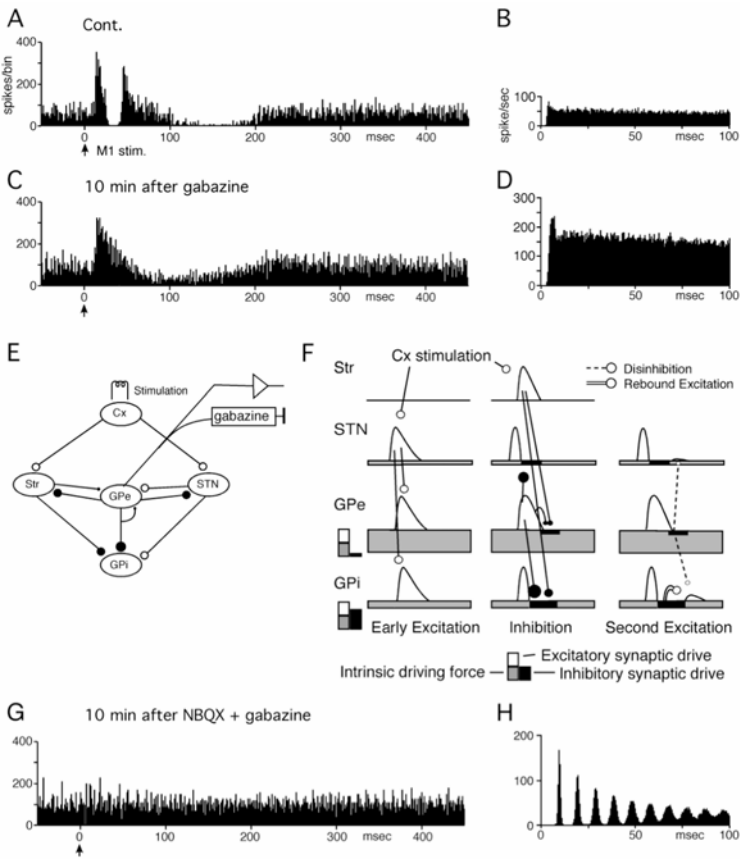

Figure 3. Effects of gabazine on GPe neurons. A–D: PSTHs show M1 stimulation induced responses and autocorrelograms in the control (A and B) and 10 min after gabazine (1 mM in saline, 0.2 µl) injection (C and D). Note that gabazine greatly diminished the inhibition and late excitation. E and F: The diagrams show experiment setup and response sequences in the basal ganglia. G and H: Coapplication of NBQX and gabazine (1 mM each in saline, 0.2 µl) abolished all the responses.

GABAergic inputs are continuously suppressing the firing of GPe and GPi neurons and that GPe and GPi neurons have intrinsic driving forces to support spontaneous firing.

2.2. Cortical Stimulation Induced Responses in Pallidal Neurons

The muscimol blockade of the STN or the local NBQX injection not only changed the rate and pattern of firing but also greatly changed the motor cortex stimulation induced responses of GPe and GPi neurons. As mentioned above, many GPe neurons exhibited alternately occurring active and silent phases after the blockade of the glutamatergic inputs. In these neurons, cortical stimulation induced different responses depending on the phase of the neurons at the time of stimulation (Figs. 2B and C). Stimulation applied during the silent phase triggered the active phase approximately 400–800 msec after the stimulation. Stimulation applied during the active phase induced different responses depending on the intensity and timing of the stimulation. Low intensity stimulation and stimulation applied during an early part of the active phase, often induced short inhibitions. Conversely, strong stimulation and stimulation applied during a late part of the active phase often terminated the active phase. Local injection of gabazine abolished all the inhibitions.

These observations suggested that the loss of glutamatergic inputs not only eliminated excitatory responses but also altered the nature of the inhibitory inputs and/or the response characteristics of GPe neurons. The blockade of STN-pallidal glutamatergic inputs should eliminate the GPe recurrent input. The remaining Str-GPe inhibition may be augmented after STN blockade because of the removal of the tonic presynaptic suppression of GABA release by group III metabotropic glutamate receptors (Matsui and Kita, 2003). This possible trans-synaptic modulation has significant functional implications. Parkinson's disease and hemiballismus have been associated with an increase and a decrease in STN activity, respectively (Bergman et al., 1990; Hassani et al., 1996). These changes might transsynaptically control the information flow of the Str-pallidal projections.

In the GPi, the muscimol blockade of the STN or local injection of NBQX predictably eliminated both the early and late excitations and evoked a 72–88 msec duration inhibition followed by a small rebound excitation.

2.3. Subthalamic Stimulation Induced Responses in Pallidal Neurons

It can be expected from the anatomical connections that an activation of the STN should induce a monosynaptic excitation overlapped by a disynaptic inhibition in both the GPe and GPi (Fig. 4). The latency of the monosynaptic excitation is only few milliseconds shorter than that of disynaptic inhibition (Kita and Kitai, 1991; Nambu et al., 2000). Thus, it can be assumed that the net outcome of the overlapped responses in the GPe and GPi to both single and high frequency burst stimulation of the STN might be critically dependent on the relative strength of the two responses. To investigate this power dominance issue, responses of pallidal neurons to single and burst stimulation of the STN were recorded in unanesthetized monkeys and the responses were characterized by local application of glutamate and GABA receptor blockers. Burst stimulations were used to mimic burst firing of STN neurons and also to address the effects of the continuous high-frequency stimulation of the STN that has been used as a treatment of Parkinson's disease. Our results revealed that responses of GPe and GPi neurons to both single and burst STN stimulation differ greatly from each other, although both nuclei receive anatomically similar monosynaptic

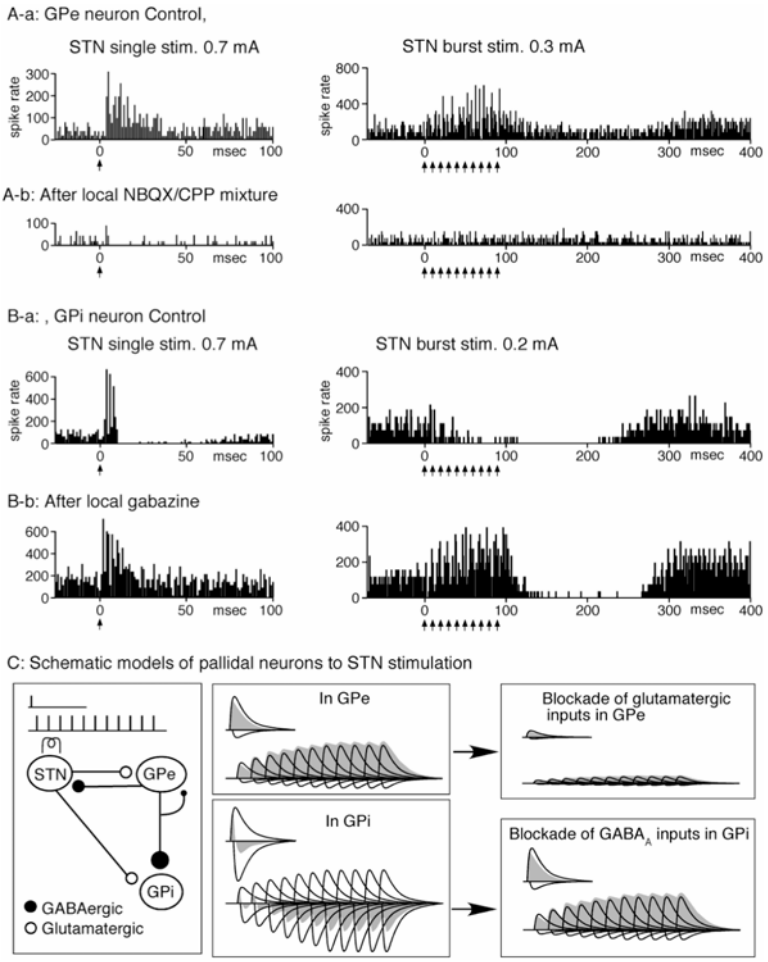

Figure 4. A-a: responses of a GPe neuron to single and burst stimulation of the STN. A-b: Local application of a mixture of NBQX and CPP into GPe (0.5 mM each in saline, 0.2 µl) greatly decreased the rate of spontaneous firing and suppressed the short latency excitation. B-a: Responses of a GPi neuron to single and burst stimulation of the STN. B-b: Local application of the GABAA blocker gabazine into GPi (0.5 mM in saline, 0.2 µl) greatly decreased the inhibition and also increased the rate of spontaneous firing. C: The diagram shows experiment setup and response sequences in the pallidum.

excitatory and disynaptic inhibitory connections. The primary difference was the strength of the disynaptic inhibition.

2.3.1. Responses of GPe Neurons to STN Stimulation

In the GPe, the most frequently observed response to single stimulation of the STN by a concentric-bipolar electrode was an early excitation followed by a weak inhibition. The most frequently observed response to burst stimulation (a burst of 10 repetitive stimuli

with 100 Hz) of the STN consisted of a series of early excitations during stimulation followed either by a late inhibition or by a late excitation (Fig. 4A-a). These results indicated that, in the GPe, the STN-GPe excitation dominates over the STN-GPe-GPe recurrent inhibition to both single and burst stimulation of the STN.

During the burst stimulation, the early excitation to each stimulation showed progressive potentiation, a waxing, and appeared to reach a steady level by the fifth to tenth stimulation (Fig. 4A). This potentiation could be due to a property of the STN-GPe synapses because unitary EPSPs recorded in rat pallidal neurons in slice preparations show similar waxing (Hanson and Jaeger, 2002). As expected from previous studies showing that the STN-GPe projection is glutamatergic (Kita and Kitai, 1991; Kita et al., 2004), local application of ionotropic glutamate blockers greatly diminished or abolished both the excitatory and inhibitory responses to single and burst stimulation of the STN and also greatly decreased the rate of spontaneous firing (Fig. 4A-b).

2.3.2. Responses of GPi Neurons to STN Stimulation

In the GPi, the response to a single stimulation of the STN was an early excitation followed by an inhibition. The duration of the excitation was significantly shorter and the strength of the inhibition was stronger than those of the GPe. Local application of gabazine greatly decreased the inhibition, increased the duration of the early excitation and increased the rate of spontaneous firing (Fig. 4B). The most frequently encountered response pattern to burst stimulation of the STN was a brief 3 to 16 msec early excitation at the beginning of the burst stimulation followed by an inhibition lasting for various durations, from 100 to 300 msec after the termination of the burst stimulation. The inhibition was often abruptly terminated and was followed by a late excitation (Fig. 4B-a). Local application of gabazine completely suppressed the inhibition during burst stimulation and disclosed a series of early excitations. However, gabazine was less effective during the later part of the inhibition that occurred after the termination of the burst stimulation. To block disynaptic STN-GPe-GPi inputs at the GPe and maintain the spontaneous firing level of the GPe, a mixture of NBQX, CPP, and gabazine (0.5 mM each in saline, injection volume 0.4–0.6 µl) was injected into the GPe 5–30 min prior to GPi recording. After the injection, both single and burst stimulation of the STN did not evoke inhibition but did evoke predominantly early excitations in all eight GPi neurons tested.

These results suggest that the disynaptic STN-GPe-GPi input dominates over the monosynaptic STN-GPi input. The reports that high-frequency stimulation of the STN induced both glutamate and GABA release in the GPe and a larger GABA release in the substantia nigra pars reticulata (SNr), the nucleus that has similar inputs as the GPi, are consistent with our present observations (Savasta et al., 2002; Windels et al., 2003).

3. FUNCTIONAL IMPLICATIONS

The results suggest that the level and pattern of activity in both segments of the pallidum are controlled by multiple factors including glutamatergic inputs, GABAergic inputs, and membrane properties. Studies have shown that basal ganglia disorders are accompanied by changes in the level and pattern of pallidal activity. The changes reported in the GPe of parkinsonian patients and of experimental parkinsonian animals include a modest decrease in the firing rate, an increase in the irregularity and bursting, and an increase in the sensory

response such as to the movement of multiple joints (Pan and Walters 1988; Filion and Tremblay 1991). A widely used basal ganglia model of Parkinson's disease assumes an augmentation of the Str-GPe input (Albin et al., 1989; Delong 1990; Nini et al., 1995). The augmented Str-GPe inputs would increase the firing irregularity, an effect opposite to that of gabazine where the firing pattern is greatly regularized.

Dyskinesias can be experimentally induced by various treatments including a lesion or a chemical blockade of the STN, or an application of GABA antagonists in the GPe (Crossman et al., 1988; Robertson et al., 1989; Hamada and DeLong, 1992; Nambu et al., 2000). Dyskinesias induced by blockade of the STN involve a decrease in the firing activity in both GPe and GPi and changes in the firing pattern of the GPe (Hamada and DeLong 1992; Vitek et al., 1999; Nambu et al., 2000). Based on the present study, it can be inferred that application of a GABA antagonist in the GPe increased the firing rate of GPe neurons, and in turn, decreased the rate and regularized firing activity of the GPi. The strong active phases alternating with silent phases that developed in GPe neurons after the STN blockade should also contribute to alter the basal ganglia output nucleus GPi activity and promote the occurrence of dyskinesias, although the precise functional significance of the active and silent phases is unknown at this time.

The most significant implication of the STN stimulation study is that a burst activation or high-frequency stimulation of the STN might inhibit the activity of the majority of neurons in the GPi. STN neurons in parkinsonian patients and experimental parkinsonian animals often show higher frequency firing and increased burst activity (Bergman et al., 1994; Hutchison et al., 1998). The STN burst activity could be induced by both cortical excitatory and pallidal inhibitory synaptic inputs, and could be supported or enhanced by the reciprocal connections with the GPe and membrane properties of STN neurons (Bevan et al., 2002; Magill et al., 2004). The present results suggest that burst activity of the STN would facilitate burst activity in the GPe by inducing monosynaptic excitations. On the other hand, the burst activity of STN may induce a pause and rebound discharges in GPi neurons.

The finding that the activity of a large number of GPi neurons decreased during burst stimulation of the STN opens up new discussions. It has been commonly suggested that over activation of the *indirect* striatal output increases the activity of the STN and then increases the activity of the GPi. This suggestion may not be so simple as long as the disynaptic STN-GPe-GPi projection is functioning normally. First, the increased STN activity might excite the GPe, acting as a negative feedback circuit, shaping activity of the GPe. Secondly, the elevated GPe activity effectively inhibits the GPi as well as the STN. Thus, the *indirect* pathway has built-in feedback systems. Previous studies reported that high-frequency stimulation of the STN inhibited the activity of neurons in the SNr. The inhibition was considered to be due to the suppression of the STN itself or the activation of GABAergic fibers in the STN (Benazzouz et al., 2000; Maurice et al., 2003). The results of the present study add another possibility that the STN-GPe-SNr inhibition may dominate over the STN-SNr excitation.

4. CONCLUSIONS

In summary, the present data indicated 1) that tonic glutamatergic and GABAergic inputs contribute to the control of spontaneous firing activity of most GPe and GPi neurons, 2) that GPe and GPi neurons have intrinsic properties or non-ionotropic glutamatergic tonic

inputs that sustain a fast oscillatory firing, 3) that both single and burst stimulation of the STN evoked different responses in the GPe and GPi, 4) that, in the GPe, the STN-GPe excitatory response dominated over the STN-GPe-GPe recurrent inhibition, and 5) that, conversely in the GPi, the STN-GPe-GPi inhibitory response dominated over the STN-GPi excitatory response.

5. ACKNOWLEDGEMENTS

We thank Ms. Dawn Merrick for editing the manuscript. This study was supported by NIH grants NS-42762, NS-47085, and Grants-in-Aid for Scientific Research (H.K.) and for Scientific Research on Priority Areas (A.N.) from the Ministry of Education, Culture, Sports, Science and Technology of Japan.

6. REFERENCES

Albin, R.L., Young, A.B., and Penney, J.B., 1989, The functional anatomy of basal ganglia disorders. *Trends Neurosci.* **12**:366–375.

Anderson, M.E., and Horak, F.B., 1985, Influence of the globus pallidus on arm movements in monkeys. III. Timing of movement-related information. *J. Neurophysiol.* **54**:433–448.

Benazzouz, A, Gao, D.M., Ni, Z.G., Piallat, B., Bouali-Benazzouz, R., and Benabid, A.L., 2000, Effect of high-frequency stimulation of the subthalamic nucleus on the neuronal activities of the substantia nigra pars reticulata and ventrolateral nucleus of the thalamus in the rat. *Neurosci*. **99**:289–295.

Bergman, H., Wichmann, T., and DeLong, M.R., 1990, Reversal of experimental parkinsonism by lesions of the subthalamic nucleus. *Science.* **249**:1436–1438.

Bergman, H., Wichmann, T., Karmon, B., and DeLong, M.R., 1994, The primate subthalamic nucleus. II. Neuronal activity in the MPTP model of parkinsonism. *J. Neurophysiol.* **72**:507–520.

Bevan, M.D., Magill, P.J., Hallworth, N.E., Bolam, J.P., and Wilson, C.J., 2002, Regulation of the timing and pattern of action potential generation in rat subthalamic neurons in vitro by GABA-A IPSPs. *J. Neurophysiol.* **87**:1348–1362.

Crossman, A.R., Mitchell, I.J., Sambrook, M.A., and Jackson, A., 1988, Chorea and myoclonus in the monkey induced by gamma-aminobutyric acid antagonism in the lentiform complex. The site of drug action and a hypothesis for the neural mechanisms of chorea. *Brain* **111**:1211–1233.

DeLong, M.R., 1971, Activity of pallidal neurons during movement. *J. Neurophysiol.* **34**:414–427.

Filion, M., and Tremblay, L., 1991, Abnormal spontaneous activity of globus pallidus neurons in monkeys with MPTP-induced parkinsonism. *Brain Res.* **547**:142–151.

Hamada, I., and DeLong, M.R., 1992, Excitotoxic acid lesions of the primate subthalamic nucleus result in reduced pallidal neuronal activity during active holding. *J. Neurophysiol.* **68**:1859–1866.

Hanson, J.E., and Jaeger, D., 2002, Short-term plasticity shapes the response to simulated normal and parkinsonian input patterns in the globus pallidus. *J. Neurosci.* **22**:5164–5172.

Hassani, O.K., Mouroux, M., and Feger, J. 1996, Increased subthalamic neuronal activity after nigral dopaminergic lesion independent of disinhibition via the globus pallidus. *Neurosci.* **72**:105–115.

Kita, H. 1992, Responses of globus pallidus neurons to cortical stimulation: intracellular study in the rat. *Brain Res.* **589**:84–90.

Kita, H. 1994, Physiology of two disynaptic pathways from the sensorimotor cortex to the basal ganglia output nuclei. In "*The basal ganglia IV. New ideas and data on structure and function*" G. Percheron., J.S. Mckenzie and J. Feger (eds). Plenum Press. pp 263–276.

Kita, H., and Kitai, S.T., 1994, The morphology of globus pallidus projection neurons in the rat: an intracellular staining study. *Brain Res.* **636**:308–319.

Kita, H., and Kitai, S. T., 1991, Intracellular study of rat globus pallidus neurons: membrane properties and responses to neostriatal, subthalamic and nigral stimulation. *Brain Res.* **564**:296–305.

Kita, H., Nambu, A., Kaneda, K., Tachibana, Y., and Takada M. 2004, Role of ionotropic glutamatergic and GABAergic inputs on the firing activity of neurons in the external pallidum in awake-monkeys. *J. Neurophysiol.* **92**:3069–3084.

Magill, P.J., Sharott, A., Bolam J.P., and Brown, P., 2004, Brain state-dependency of coherent oscillatory activity in the cerebral cortex and basal ganglia of the rat. *J. Neurophysiol.* **92**:2122–2136.

Matsui, T., and Kita, H., 2003, Activation of group III metabotropic glutamate receptors presynaptically reduces both GABAergic and glutamatergic transmission in the rat globus pallidus. *Neuroscience* **122**:727–737.

Maurice, N., Thierry, A.M., Glowinski, J., and Deniau, J.M., 2003, Spontaneous and evoked activity of substantia nigra pars reticulata neurons during high-frequency stimulation of the subthalamic nucleus. *J. Neurosci.* **23**:9929–9936.

Nambu, A., Tokuno, H., Hamada, I., Kita, H., Imanishi, M., Akazawa, T., Ikeuchi, Y., and Hasegawa, N., 2000, Excitatory cortical inputs to pallidal neurons via the subthalamic nucleus in the monkey. *J. Neurophysiol.* **84**:289–300.

Nini, A., Feingold, A., Slovin, H., and Bergman, H., 1995, Neurons in the globus pallidus do not show correlated activity in the normal monkey, but phase-locked oscillations appear in the MPTP model of parkinsonism. *J. Neurophysiol.* **74**:1800–1805.

Pan, H.S., and Walters, J.R., 1988, Unilateral lesion of the nigrostriatal pathway decreases the firing rate and alters the firing pattern of globus pallidus neurons in the rat. *Synapse* **2**:650–656.

Parent, A., and Hazrati, L.N., 1995, Functional anatomy of the basal ganglia. II. The place of subthalamic nucleus and external pallidum in basal ganglia circuitry. *Brain Res. Brain Res. Rev.* **20**:128–154.

Robertson, R.G., Farmery, S.M., Sambrook, M.A., and Crossman, A.R., 1989, Dyskinesia in the primate following injection of an excitatory amino acid antagonist into the medial segment of the globus pallidus. *Brain Res.* **476**:317–322.

Savasta, M., Windels, F., Bruet, N., Bertrand, A., and Poupard, A., 2002, Neurochemical modifications induced by high frequency stimulation of subthalamic nucleus in rats. In: *The basal ganglia VII*, Nicholsson L, ed. New York: Kluwer Academic Plenum Publishers. p 581–590.

Tremblay, L., Filion, M., and Bedard, P.J., 1989, Responses of pallidal neurons to striatal stimulation in monkeys with MPTP-induced parkinsonism. *Brain Res.* **498**:17–33.

Vitek, J.L., Chockkan, V., Zhang, J.Y., Kaneoke, Y., Evatt, M., DeLong, M.R., Triche, S., Mewes, K., Hashimoto, T., and Bakay, R.A., 1999, Neuronal activity in the basal ganglia in patients with generalized dystonia and hemiballismus. *Ann Neurol.* **46**:22–35.

Windels, F., Bruet, N., Poupard, A., Feuerstein, C., Bertrand, A., and Savasta, M., 2003, Influence of the frequency parameter on extracellular glutamate and gamma-aminobutyric acid in substantia nigra and globus pallidus during electrical stimulation of subthalamic nucleus in rats. *J. Neurosci. Res.* **72**:259–267.

COMBINED MODELING AND EXTRACELLULAR RECORDING STUDIES OF UP AND DOWN TRANSITIONS OF NEURONS IN AWAKE OR BEHAVING MONKEYS

Hiroshi Okamoto, Yoshikazu Isomura, Masahiko Takada, and Tomoki Fukai*

1. INTRODUCTION

Accumulating evidence suggests that cortical and striatal neurons show two-state membrane potential fluctuations in slice preparations and in anesthetized animals (Wilson and Kawaguchi, 1996; Anderson et al., 2000; Cossart et al., 2003; Shu et al., 2003). While it was reported that the barrel cortex of awake quiet rats display such spontaneous fluctuations (Petersen et al., 2003), other studies suggested that the hyperpolarizing down state gradually disappears as rats recover from an anesthetized state (Steriade et al., 2001). Thus, whether these fluctuations exist in awake or behaving animals remains controversial. This is partly because intracellular recordings of neuronal activity, by which the subthreshold neuronal states can be studied most directly, are difficult to obtain in behaving animals. Here, we attempt to study whether cortical and/or striatal neurons exhibit the two-state transitions in awake and behaving monkeys using the extracellular recording technique. Such studies may provide only indirect evidence. Nevertheless, they might achieve some insight into how the brain processes information during behaviour when they are combined with computational studies.

* Hiroshi Okamoto, Corporate Research Center, Fuji Xerox Co. Ltd., Nakai-machi, Ashigarakami-gun, Kanagawa 259-0157, Japan, Yoshikazu Isomura, Masahiko Takada, Department of System Neuroscience, Tokyo Metropolitan Institute for Neuroscience, Fuchu, Tokyo 183-8526, Japan, Tomoki Fukai, Lab for Neural Circuit Theory, Brain Science Institute RIKEN, Wako, Saitama 351-0198, Japan.

2. RESULTS

2.1. Striatal Neurons in Awake Quiet Monkeys

We first show some evidence that the membrane potential of striatal medium spiny neurons in awake macaque monkeys likely displays spontaneous transitions between a depolarizing and a hyperpolarizing or resting state (Kitano et al., 2002). To this end, we repeatedly stimulated cortical neurons projecting to the striatum and measured the latency of the earliest spikes elicited from the medium spiny neurons. We demonstrated that the distributions of the earliest spikes show two peaks at short and long latencies separated by 10–20 msec. The results indicated that the medium spiny neurons may possess two distinct subthreshold membrane potential states, both of which may be visited with almost equal probabilities.

We conducted numerical experiments with a realistic model of medium spiny neurons and obtained bimodal distributions quite similar to those obtained in experiments. The feedforward inhibition by GABAergic interneurons delayed the response of the medium spiny neurons by several milliseconds. However, it neither inhibited firing of the medium spiny neurons nor changed the bimodal nature of the earliest spike latency histograms. Moreover, the earliest spikes were delayed only when the model neuron was in the down state, but not in the up state. These experimental and theoretical results strongly suggest that the medium spiny neurons may have two distinct subthreshold membrane potential levels, which presumably correspond to the up and down states. In addition, the feedforward inhibition by GABAergic interneurons modulates the spike timing of medium spiny neurons in a state-dependent manner.

2.2. Temporally Organized Bistable Transitions in Anterior Cingulate Neurons

The two–state membrane potential transitions of the medium spiny neurons are considered to reflect coincident input from many cortical neurons. On the other hand, cortical neurons in vitro exhibit similar membrane potential transitions, which are presumably generated by reverberating synaptic input (Cossart et al., 2003; Shu et al., 2003). The two-state transitions are characteristic of persistent neuronal firing in anesthetized animals, but whether they might engage in cognitive functions, such as working memory, remains elusive. Here, we demonstrate that activity of monkey anterior cingulate neurons exhibits bimodal distributions of firing rate. Moreover, these transitions are temporally organized in such a way that generates a trial averaged activity steadily increasing or decreasing during a delay period of conditional Go/No-go discrimination tasks (Isomura et al., 2003).

We reanalyzed the climbing or descending delay-period activity that was recorded previously from the anterior cingulate cortex (ACC) of macaque monkeys performing the delayed Go/No-go discrimination tasks (Fig. 1a, b). In the analysis, we adopt a new method, i.e., weighted inter-spike-interval (WtISI) histogram, to analyze spike sequence of low frequency firing. To construct the WtISI histogram, we time-aligned spike trains of single neurons in repeated trials to sensory stimuli, and divided the time axis into bins of 1 ms width. In each trial, we assigned the same ISI value to all the bins sandwiched by a spike pair. Then, the distribution of ISI was calculated over trials for each of the consecutive overlapping intervals, which were typically 200 ms long. The WtISI histogram was smoothed by a Gaussian filter ($\sigma = 50$ ms) and was normalized to have an integrated area of unity. In

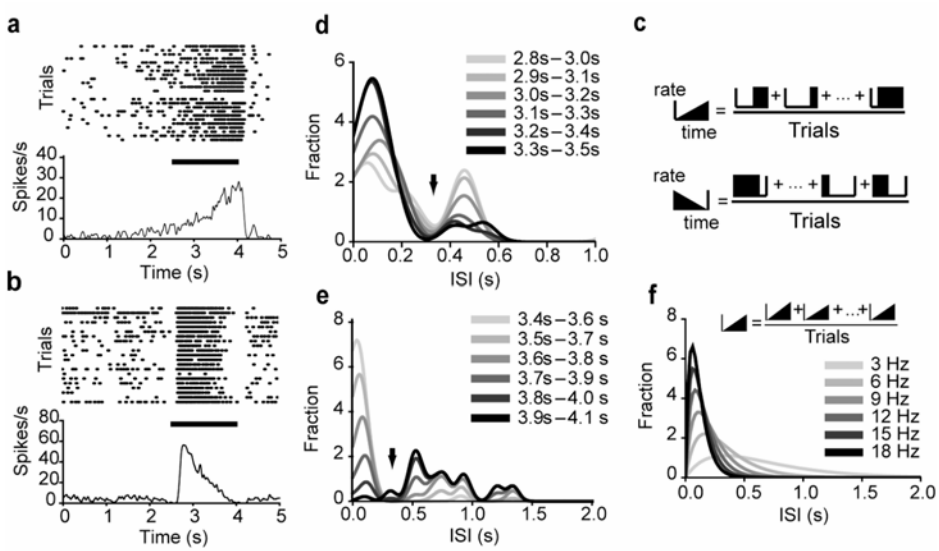

Figure 1. Delay-period (designated by horizontal bars) activity recorded from the monkey ACC. (a, b) Some ACC neurons display steadily climbing or descending delay-period activity. The spike counts were smoothed by a Gaussian filter ($\sigma = 20$ ms). (c) Stepwise increases or decreases in firing rate can underlie climbing (*upper*) or descending (*lower*) activity, respectively. The WtISI distributions smoothed by a Gaussian filter ($\sigma = 50$ ms) are shown for the climbing (d) and descending (e) activities. In both cases, the distinct bimodal distributions indicate the two-state transitions during the delay period. (f) The WtISI distributions display only single peaks for Poisson-distributed spike trains of varying frequencies.

short, the histogram gives the distribution of ISIs weighted by their own interval lengths, reporting the ranges of ISI that dominate any given period of spike firing. The WtISI distributions enabled us to inspect whether the pattern of spike firing in single trials might exhibit stepwise rate changes during the delay period (Fig. 1c). It is remarked that the stepwise rate changes averaged over trials could result in a constant increase or decrease in delay-period activity, if their occurrence was equally probable at arbitrary moments during the period.

In Fig. 1d, the WtISI distributions were calculated for the climbing activity in consecutive, overlapping 200 ms long intervals. In each interval, WtISIs were formed into two clusters, one for short ISIs and one for longer ISIs. The time evolution of these clusters indicated how spike firing shifted from a low- to a high-frequency regime. The descending activity exhibited an opposite evolution pattern (Fig. 1e), representing a shift from high to low frequencies. Importantly, in both cases the two clusters remained separate by a trough (arrow) during the time evolution, to reveal discontinuous rate changes in single trials. The WtISI distributions would display single peaks, if the rate changes during climbing or descending delay-period activity were continuous.

We can consider several possible mechanisms for the stepwise rate changes in ACC neurons. An intriguing possibility is that such transitions reflect the membrane potential fluctuations between ‘up’ and ‘down’ states. Recent findings on such fluctuations in the barrel cortex neurons of anesthetized as well as awake quiet rats may give supportive evidence for this possibility (Petersen et al., 2003). In this study, we employed a simple

mathematical model of the bistable neuronal responses without giving a specific biological mechanism. Since the cortical membrane potential fluctuations are generated by reverberating synaptic input (Cossart et al., 2003; Shu et al., 2003), we examined whether a recurrent network of model neurons endowed with up- and down-like bistable firing states could replicate the essence of the present experimental findings (Fig. 2a). In Fig. 2b, the neurons were initially settled in the 'down' state, and an external input was kept at an elevated level during the simulated delay period. Consistent with the present experiments, the spike count averaged over trials exhibited a steady increase during that period. Descending activity could also be induced in a similar network by a transient external input at the onset of a delay period (Fig. 2c). In both cases, the WtISI distributions of the model showed a remarkable similarity to those of the experiments, with clear distinction between a short- and a long-ISI cluster (Fig. 2d, e).

It is noted that spike trains exhibit a large trial-to-trial variability in the present simulations, as was the case for the ACC neurons tested (see Fig. 1a, b). Our network model consists of identical neurons connected with synaptic connections of uniform strength. Therefore, it has no prescribed order of activation among different neurons. In each trial, the order of neuronal activation is determined solely by a stochastic transition rule, and hence should be different from trial to trial (Fig. 1). This implies that the trial-averaged activity of a single neuron coincides with the single-trial activity averaged over a neuronal ensemble in the present model. By contrast, in some of the previous models of neural integrator circuit (Seung et al., 2000; Koulakov et al., 2002), finely tuned synaptic connec-

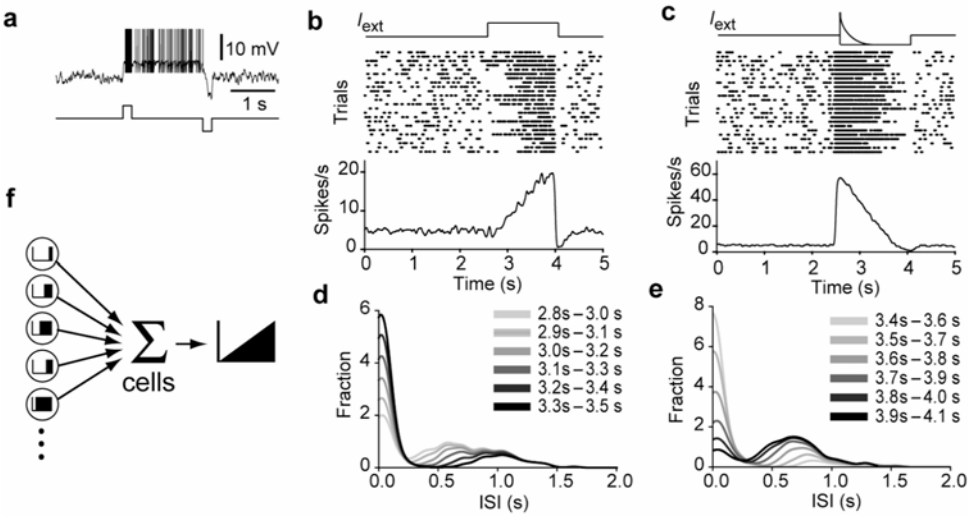

Figure 2. Delay-period activity in a recurrent network model. (**a**) Model excitatory neurons display 'up'- and 'down'-like firing states. See Methods for details. (**b**) Enhancement of external input can induce climbing activity in the network. (**c**) A transient external input could induce descending activity. To replicate the suppressed firing immediately preceding and following the delay period (Fig. 1b), a constant hyperpolarizing component was simultaneously applied during the simulated delay period. (**d**, **e**) As in ACC neurons, the WtISI distributions of the simulated climbing and descending activities display two distinct clusters. (**f**) On a single-trial basis, the climbing (or descending) profile can be decoded from the population activity of model neurons.

tions or cell-dependent activation thresholds would activate different neurons in an approximately fixed order in different trials. A slow synaptic current would result in a large trial-to-trial variability, but the individual neurons would not display abrupt rate changes (Wang 2002).

3. CONCLUSION

We have shown that the medium spiny neurons in awake monkeys exhibit two separated peaks in the earliest spike latency histograms in response to a cortical stimulation, indicating the two-state membrane potential fluctuations in these neurons. In addition, we have demonstrated that delay-period activity in the anterior cingulate cortex consists of temporally organized two-state transitions between high- and low-frequency firing states in behaving monkeys. Whether the two distinct neuronal states found in the present experiments may represent the so-called 'up' and 'down' states in striatal or cortical neurons remains to be further tested by intracellular recordings or calcium imaging. Climbing or descending activity is generally linked with animal's anticipation of, or attention on, forthcoming sensory or motor events (Rainer et al., 1999; Hoshi et al., 2000; Isomura et al., 2003), with recognition of interval timing (Durstewitz, 2003; Kitano et al, 2003; Reutimann et al., 2004), or with perceptual or voluntary decision making (Hanes and Schall, 1996; Reddi and Carpenter, 2000; Shadlen and Newsome, 2001; Usher and McClelland, 2001; Hernandez et al., 2002; Smith and Ratcliff, 2004). Results of the present simulations suggested that climbing or descending activity can be decoded by averaging spike trains over many cortical neurons. Since the striatum receives a massive input from almost all the cortical areas, the decoding of an ensemble cortical activity may be performed by striatal medium spiny neurons during cognitive tasks.

4. METHODS

The detailed experimental methods for extracellular recordings from the monkey ACC can be found in the previous paper (Isomura et al., 2003). Here, we describe only mathematical details of our recurrent network model. Excitatory neurons in our network model show two distinct stable states (bistable states), a depolarizing high-frequency firing state and a resting state, which may correspond to the 'up' state and the 'down' state in cortical neurons. Previous modeling studies suggested that neuronal bistability may arise from a network mechanism (Compte et al., 2003) or a single-cell-based mechanism (Gruber et al., 2003). Our model adopted the latter possibility. Otherwise, the detailed physiological mechanism of the bistability is not crucial for the performance of the model. We consider a recurrent network of 400 excitatory neurons coupled with 100 inhibitory neurons. Each excitatory neuron receives synaptic inputs from about 10% of other excitatory neurons and all the inhibitory neurons. Each inhibitory neuron receives input from all the excitatory neurons.

The dynamics of the membrane potentials are described by leaky-integrate-fire neuron models. An excitatory neuron obeys $CdV/dt = -G_L(V - V_L) - \kappa I_{up/down} - I_{AMPA} - I_{GABA} + I_{ext} + I_{BG}$, where the membrane capacitance $C = 0.5$ nF, the membrane conductance $G_L = 0.025$

ìS and the reversal potential $V_L = -70$ mV. When V reaches threshold, $V_\theta = -52$ mV, it is reset to $V_{\text{reset}} = -62$ mV and is clamped at the same voltage during a refractory period of 2 ms. The bistability of the membrane potential is attained by a current that depends nonlinearly on the membrane potential: $I_{up/down} = A_1/(1 + \exp(-\beta(\bar{V} + 54))) + A_2$, where $\bar{V}$ is obtained by smoothing the time evolution of the membrane potential: $d\bar{V}/dt = (\bar{V} - V)/\tau_{\text{up/down}} + \Delta_{\bar{V}}\delta(t - t_{\text{post}})$, with $\Delta_{\bar{V}} = 4$ mV, τup/down = 70 ms, and t_{post} representing times of postsynaptic spikes. The second term in the right-hand side may encourage the neurons to make transitions to the up state. We assume that $I_{\text{up/down}}$ is only activated during a delay period (with 200 ms lags): $\kappa \to 1$ for 2.5 s < t < 4.0 s and $\kappa \to 0$ otherwise. A rising and a decaying time constant of 100 ms are introduced at the on/off transients of κ. In reality, this input may emerge from modulations of the neuronal excitability by dopamine (O'Donnell, 2003). In the present simulations, the best performance was obtained with $A_1 = 0.115$ nA, $A_2 = -0.135$ nA and $\beta = 3(\text{mV})^{-1}$ for climbing activity (Fig. 2b), or $A_1 =$ 0.3 nA, $A_2 = -135$ nA and $\beta = 0.7(\text{mV})^{-1}$ for descending activity (Fig. 2c). Experimentally observed climbing activity was better replicated, if we reset $\bar{V}$ to V_{reset} in about 70% of randomly selected excitatory neurons at the beginning of climbing activity. This manipulation resets the neurons in the 'down' state.

AMPA receptor-mediated recurrent synaptic input is calculated as $I_{\text{AMPA}} = G_{\text{AMPA}}(V - V_{\text{AMPA}})\Sigma_n p_n$, where $V_{\text{AMPA}} = 0$ mV and the sum is taken over presynaptic neurons. The maximum conductance G_{AMPA} is set to 0.15 nS for climbing activity and 0.125 nS for descending activity. A similar formula is applied to inhibitory neurons, with $G_{\text{AMPA}} = 0.15$ or 0.02 nS for climbing or descending activity. When the n-th presynaptic neuron fires, the gating variable p_n is set to unity; otherwise it obeys $dp_n/dt = -p_n/\tau_{\text{AMPA}}$ with $\tau_{\text{AMPA}} = 5$ ms. GABA-A receptor-mediated synaptic input is calculated in a similar manner: $I_{\text{GABA}} = G_{\text{GABA}}(V - V_{\text{GABA}})\Sigma_n q_n$, where $dq_n/dt = -q_n/\tau_{\text{GABA}}$ with $\tau_{\text{GABA}} = 10$ ms. The parameters are set as $G_{\text{GABA}} = 0.00625$ nS and $V_{\text{GABA}} = -80$ mV.

I_{ext} is an external current during a delay period (Fig. 2b and 2c, top traces): if 2.5 s < t < 4 s, $I_{\text{ext}} = 0.075$ nA for climbing activity, and $I_{\text{ext}} = -0.05 + I_{\text{tr}}$ nA for descending activity. Otherwise, $I_{\text{ext}} = 0$. In the case of descending activity, a transient depolarizing input I_{tr} is included in the external input to activate neurons at the onset of the delay period: $I_{\text{tr}} = 0$ for t < 2.5 s, whereas $I_{\text{tr}} = 0.175 \times e^{-(t-2.5)/\tau_{\text{tr}}}$ nA with $\tau_{\text{tr}} = 220$ ms for $t \geq 2.5$ s (Fig. 2c, top trace). I_{ext} may represent internally or externally driven information that must be temporally integrated during the delay period. Such a temporal integration of input is crucial for various cognitive processes (Reddi and Carpenter, 2000; Mazurek et al., 2003; Smith and Ratcliff, 2004).

I_{BG} represents the background noise from external neuron pools: $I_{BG} = I_E + I_1 + I_0$, where I_E and I_I represent the excitatory and inhibitory inputs mediated by AMPA and GABA-A receptors, respectively, and I_0 is a constant input to tune the spontaneous firing rate of neurons. They are defined as $I_0 = 0.4$ nA, $I_E = -G_E s_E(V - V_{\text{AMPA}})$ and $I_1 = -G_1 S_1(V - V_{\text{GABA}})$ with $G_E = 5$ nS and $G_1 = 1$ nS. The gating variables obey $ds_{E,I}/dt = -s_{E,I}/\tau_{\text{AMPA,GABA}} + X_{E,I}(t)$, with X_E and X_I representing the Poisson processes of rates r_E and r_I, respectively. Here, r_E = 1.9 kHz (climbing) and 2 kHz (descending), and $r_I = 1$ kHz. In Fig. 2a, the bistability of a single neuron was demonstrated by setting $I_{\text{AMPA}} = I_{\text{GABA}} \equiv 0$ in the equation of excitatory neurons.

Similarly, the membrane potential dynamics of an inhibitory neuron are described by a leaky integrate-and-fire neuron model: $CdV/dt = -G_L(V - V_L) - I_{AMPA} + I_{BG}$. The refractory period is 1 ms, and other parameters are set as $C = 0.2$ nF, $G_L = 0.02$ iS, $V_L = -65$ mV, $V_\theta =$ −52 mV, $V_{\text{reset}} = -60$ mV, $G_E = 0.3$ nS, $G_1 = 0.3$ nS, $r_E = r_I = 2$ kHz, and $I_0 = 0.3$ nA.

5. REFERENCES

Anderson, J., Lampl, I., Reichova, I., Carandini, M., and Ferster, D., 2000, Stimulus dependence of two-state fluctuations of membrane potential in cat visual cortex, *Nat. Neurosci.* **3**:617.

Compte, A., Sanchez-Vives, M.V., McCormick, D.A., and Wang, X.J., 2003, Cellular and network mechanisms of slow oscillatory activity (<1 Hz) and wave propagations in a cortical network model, *J. Neurophysiol.* **89**:2707.

Cossart, R., Aronov, D., and Yuste, R., 2003, Attractor dynamics of network UP states in the neocortex, *Nature* **423**:283.

Durstewitz, D., 2003, Self-organizing neural integrator predicts interval times through climbing activity, *J. Neurosci.* **23**:5342.

Gruber, A.J., Solla, S.A., Surmeier, D.J., and Houk, J.C., 2003, Modulation of striatal single units by expected reward: a spiny neuron model displaying dopamine-induced bistability, *J. Neurophysiol.* **90**:1095.

Hanes, D.P., and Schall, J.D., 1996, Neural control of voluntary movement initiation, *Science* **274**:427.

Kitano, K., Cateau, H., Hernandez, A., Zainos, A., and Romo, R., 2002, Temporal evolution of a decision-making process in medial premotor cortex, *Neuron* **33**:959.

Hoshi, E., Shima, K., and Tanji, J., 2000, Neuronal activity in the primate prefrontal cortex in the process of motor selection based on two behavioral rules, *J. Neurophysiol.* **83**:2355.

Isomura, Y., Ito, Y., Akazawa, T., Nambu, A., and Takada, M., 2003, Neural coding of "attention for action" and "response selection" in primate anterior cingulate cortex, *J. Neurosci.* **23**:8002.

Kaneda, K., Nambu, A., Takada, M., and Fukai, T., 2002, Two-state membrane potential transitions of striatal spiny neurons as evidenced by numerical simulations and electrophysiological recordings in awake monkeys, *J. Neurosci.* **22**:RC230.

Kitano, K., Okamoto, H., and Fukai, T., 2003, Time representing cortical activities: two models inspired by prefrontal persistent activity, *Biol Cybern*. **88**:387.

Koulakov, A.A., Raghavachari, S., Kepecs, A., and Lisman, J.E., 2002, Model for a robust neural integrator, *Nat. Neurosci.* **5**:775.

Mazurek, M.E., Roitman, J.D., and Shadlen, M.N., 2003, A role for neural integrators in perceptual decision making, *Cerebral Cortex* **13**:1257.

O'Donnell, P., 2003, Dopamine gating of forebrain neural ensembles, *Eur. J. Neurosci.* **17**:429.

Petersen, C.C., Hahn, T.T., Mehta, M., Grinvald, A., and Sakmann, B., 2003, Interaction of sensory responses with spontaneous depolarization in layer 2/3 barrel cortex, *Proc. Natl. Acad. Sci. USA.* **100**:13638.

Rainer, G., Rao, S.C., and Miller, E.K., 1999, Prospective coding for objects in primate prefrontal cortex, *J. Neurosci.* **19**:5493.

Reddi, B.A., and Carpenter, R.H.S., 2000, The influence of urgency on decision time, *Nat. Neurosci.* **3**:827.

Reutimann, J., Yakovlev, V., Fusi, S., and Senn, W., 2004, Climbing neuronal activity as an event-based cortical representation of time, *J. Neurosci.* **24**:3295.

Seung, H.S., Lee, D.D., Reis, B.Y., and Tank, D.W., 2000, Stability of the memory of eye position in a recurrent network of conductance-based model neurons, *Neuron* **26**:259.

Shadlen, M.N., and Newsome, W.T., 2001, Neural basis of a perceptual decision in the parietal cortex (area LIP) of the rhesus monkey, *J. Neurophysiol.* **86**:1916.

Shu, Y., Hasenstaub, A., and McCormick, D.A., 2003, Turning on and off recurrent balanced cortical activity, *Nature* **423**:288.

Smith, P.L., and Ratcliff, R., 2004, Psychology and neurobiology of simple decisions, *Trends Neurosci*. **27**:161.

Steriade, M., Timofeev, I., and Grenier, F., 2001, Natural waking and sleep states: a view from inside neocortical neurons, *J. Neurophysiol.* **85**:1969.

Usher, M., and McClelland, J.L., 2001, The time course of perceptual choice: the leaky, competing accumulator model, *Psychol. Rev.* **108**:550.

Wang, X.-J., 2002, Probabilistic decision making by slow reverberation in cortical circuits, *Neuron* **36**:955.

Wilson, C.J., and Kawaguchi, Y.J., 1996, The origins of two-state spontaneous membrane potential fluctuations of neostriatal spiny neurons, *J. Neurosci.* **16**:2397.

SEQUENTIAL MOTOR BEHAVIOR AND THE BASAL GANGLIA

Evidence from a serial reaction time task in monkeys

Robert S. Turner, Kevin McCairn, Donn Simmons and Izhar Bar-Gad[1]

1. INTRODUCTION

An important aspect of motor skill lies in the ability to acquire and utilize representations of ordered sequences of motor acts, thereby allowing one to select and execute a sequence of movements as a whole. The importance of this ability becomes evident when one considers alternatives; for instance, having to tie one's shoes every morning based on the conscious selection of each constituent movement of the tying sequence. Understanding the neural control of motor sequences is also important because of the prevalence of human neuropathologies in which movement sequences are impaired differentially [e.g., Parkinson's disease (Benecke et al., 1987)] and because of the widening use of surgical therapies for those disorders (e.g., deep brain stimulation).

The importance of basal ganglia (BG) networks for sequential motor control remains a topic of debate (Marsden, 1984; Mink, 1996). Several lines of research suggest that the motor circuit of the BG plays an important role in sequential behaviors (reviewed recently by Graybiel, 2004; Keele et al., 2003). One of the most prevalent hypotheses is that the BG contributes to the "proceduralization" of action sequences (Eichenbaum and Cohen, 2001). Procedural learning provides the capacity for series of events or actions to be recalled as a whole [i.e., as "chunks" (Graybiel, 1998)] with minimal attentional load. It is possible that the BG contributes both to the laying down of new procedural memories (e.g., as a "teacher") and to the recall or expression of already-learned procedures (Aldridge and Berridge, 1998; Cromwell and Berridge, 1996; Hikosaka et al., 2002a). Several investigators have made a strong case for a role for the BG in switching between components of a familiar sequence (i.e., between the constituent movements of "natural units of action" or

[1] Robert S. Turner, Kevin McCain, Donn Simmons, and Izhar Bar-Gad, Department of Neurological Surgery, UCSF, San Francisco CA 94122.

"chunks") (Aldridge et al., 2004; Brotchie et al., 1991; Graybiel, 1998; Keele et al., 2003). Other investigators have challenged the importance of the BG in this function (Exner et al., 2002; Penhune and Doyon, 2002; Rhodes et al., 2004; Smith et al., 2001; Wenger et al., 1999), especially for the production of short familiar sequences (Verwey et al., 2002).

We have explored BG involvement in the production of familiar sequences using a non-human primate version of the serial reaction time task (Nissen and Bullemer, 1987). The SRTT paradigm has been extremely useful for exploring the psychophysics and functional neuroanatomy of human sequential motor behavior (reviewed by Curran, 1998; Keele et al., 2003). In the prototypical SRTT, a subject is prompted to move her/his hand to a seemingly-random series of target locations. The subject can show learning specific to a surreptitiously-ordered portion of the target series in the absence of awareness of its ordered nature. The primary measure of learning is a reduction in reaction times (RTs; the interval from a "go" signal to the onset of movement), in particular as compared with RTs when the subject is presented later with a random target series. Here we describe an SRTT paradigm for monkeys that shows many similarities to what has been described for humans. We also present preliminary results using this task to explore BG encoding of sequence-related information and the effects on SRTT performance of reversible inactivation of BG output. Our results cast doubt on a major role for the BG motor circuit in selecting constituent movements of sequences that are short and familiar.

2. A PRIMATE MODEL OF THE SERIAL REACTION TIME TASK

Despite its dominance in human studies of sequence learning, SRTT paradigms have seldom been described for non-human primates (Lee and Quessy, 2003; Procyk et al., 2000). The SRTT can be distinguished from other sequence learning paradigms [e.g., trial-and-error learning (Hikosaka et al., 2002b; Miyachi et al., 1997; Rand et al., 1998)] by the absence of external cues indicating whether the series of stimuli is ordered or not, and by no requirement that a subject actually learn anything. SRTT learning can occur incidentally, independent of reward contingency or intention to learn.

We developed an SRTT-like task for macaques that replicates many of the characteristics of the human version. Three rhesus monkeys learned to move a joystickcontrolled cursor into a series of target zones displayed continuously on an LCD monitor (Fig. 1*A*). Visual cues, indicating which target to capture by their spatial location or color, led an animal through a sequence of four out-and-back movements. The actual targets to be captured changed from block-to-block. Typically, 10-trial blocks of "random" sequences were interleaved with 50-trial blocks of "fixed" sequences. For random trials, the four targets changed at random from trial-to-trial, with each target appearing between 0 and 4 times. Two types of "fixed" sequences were presented: 1) Novel fixed sequences were used to study the acquisition and transfer of new sequence knowledge. In these sequences, targets were presented in a fixed order as determined by random selection from all orderings of 4 items with replacement. 2) Over-learned fixed sequences (e.g., Fig. 1*A*) were used to measure the full extent of learning possible and to assess BG involvement in the production of familiar sequences. Over-learned sequences were practiced extensively for weeks prior to collection of the data reported here. Different over-learned sequences were used at different times in each animal.

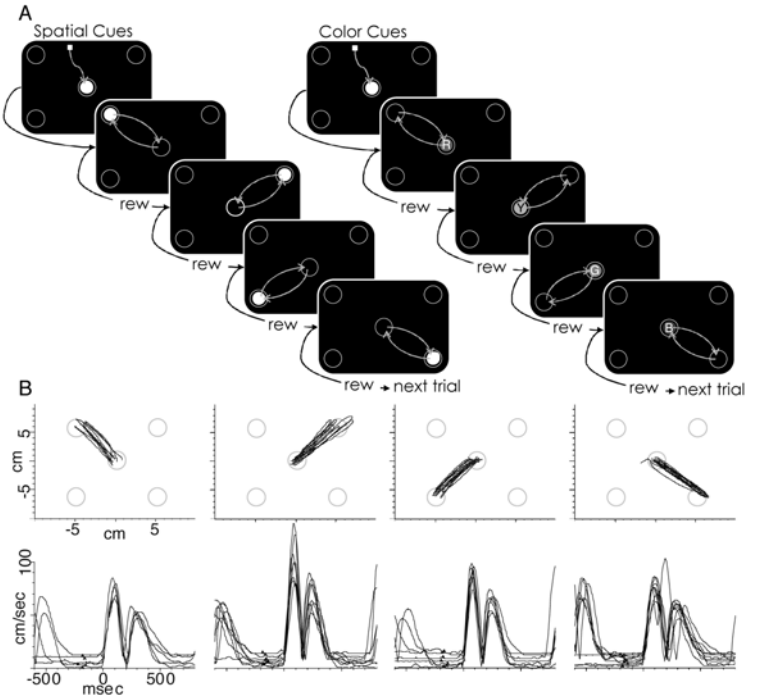

Figure 1. *A*. Schematic of the SRTT paradigm is shown. Animals moved an on-screen cursor through four outand-back movements between a central fixation target and four peripheral targets (*gray open circles*). Each successful out-and-back movement was rewarded (*rew*). Instructions for which target to capture were delivered through a cue's spatial location (*left*) or its color (*right*). *R*, red; *Y*, yellow; *G*, green; *B*, blue. *B*. Animals performed each out-and-back movement as a whole, with no pause between peripheral-capture and return-tocenter components. Spatial trajectories (*top*) and tangential velocities (*bottom*) are shown for several repetitions of each component of the sequence illustrated in *A*. Single-trial velocities, aligned on movement onsets, show a characteristic two-peaked profile, the first for the outward movement and the second for return-to-center. Early velocity deflections in some trials reflect the terminal portion of preceding out-and-back movements.

2.1. SRTT Learning in the Macaque

For all three animals, RTs shortened gradually following the introduction of a novel fixed sequence (Fig. 2*A*). RTs for random sequence blocks did not deviate significantly from the mean for random trials presented prior to learning. The learning-related reduction in RTs was modeled as a piece-wise linear function of trial number (Fig. 2*A*). The pre-asymptotic slope of the line reflected the rate of learning (msec reduction in RT per sequence trial performed). Across 33 learning sessions in three animals, RTs declined slowly during the initial 200–500 trials of a novel sequence (Fig. 2*B*, *Novel*), after which RTs asymptoted at a significantly lower level (~70 msec below the RTs of random trials). Knowledge acquired on the first day of training aided performance of the same sequence on the following day, as reflected by substantially faster learning rates (Fig. 2*B*, *Recall*).

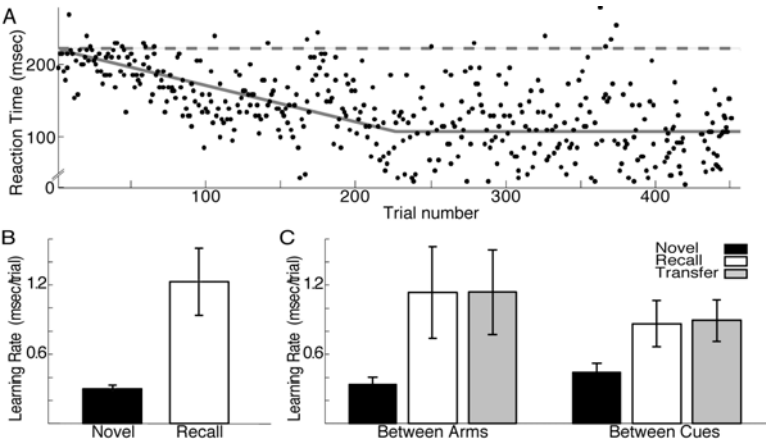

Figure 2. *A*. An example of the slow reduction in RTs following introduction of a novel fixed sequence. •, RTs from single trials. *Horizontal dashed line*, mean RT during random sequences. *Solid gray line*, piece-wise linear fit to the novel sequence RTs. *B*. The mean rate of reduction in RTs (i.e., *Learning Rate*, ±SEM) is plotted. Novel fixed sequences were learned slowly on the day they were first introduced (*Novel*), but recall of the learned sequence led to a rapid fall in RTs on the following day (*Recall*). *C*. Sequence knowledge transferred readily between arms (*left*, *Transfer*) and between color and spatial cues (*right*, *Transfer*).

2.2. Sequence Knowledge Independent of Motor Effectors and Sensory Cues

How sequence knowledge is represented in the CNS has been studied in humans by "transferring" subjects to a different task following an initial session of SRTT learning. By dissociating a task's sensory cues from motor output, these experiments have shown that sequence knowledge is represented centrally as a series of abstract motor responses, independent of any one end-effector. Multiple studies have shown that subjects can utilize previously-acquired sequence knowledge to improve RTs on a transfer task that requires different movements than those executed during initial training (Cohen et al., 1990; Keele et al., 1995). The fact that SRTT learning typically occurs in motor rather than perceptual systems was demonstrated by showing efficient transfer of sequence knowledge to tasks that present different sensory stimuli but require the same motor responses (Willingham et al., 2000; but see Koch and Hoffmann, 2000). Thus, the consensus view from human studies is that sequences are represented as a series of abstract motor responses, independent of the specific end effectors and sensory cues used in a task. We found similar results for SRTT learning in non-human primates.

Transfer experiments were performed on the day following initial learning of a novel sequence. For these experiments, subjects first performed a block of random trials followed by a block of the novel fixed sequence used the previous day. Animals were then transferred to trials in which either the opposite hand was used to move the joystick or the alternate type of visual cues was presented. The rate of learning following either form of transfer was significantly faster than that during initial learning of the novel sequence and it was statistically indistinguishable from that for simple next-day recall of the sequence (Fig. 2*C*). Full transfer between arms indicates that sequence knowledge was equally available to the motor control apparatus of both forelimbs. Combined with similar transfer between cue

types, these results closely parallel what has been described commonly for human SRTT learning. Sequence knowledge is typically represented as a series of motor responses, abstracted from specific movements or effectors.

In summary, our model of SRTT learning in non-human primates provides distinct advantages that supplement other sequence learning paradigms. The SRTT provides a way to study sequence learning independent from confounding factors such as attentional load, sense of effort, strategy, cognitive set, and subject awareness. During SRTT learning, the task stimuli and motor responses remain unchanged and knowledge of results, as far as whether the sequence is being learned correctly, is unavailable. Unlike trial and error learning, only one target is presented at a time and no "wrong" movements are made. Thus, learning-related changes in task performance cannot be attributed to altered performance strategies or movement kinematics. Also, it is unlikely that cognitive set plays a role in SRTT learning because subjects are given no instructions concerning learning and learning can accrue without awareness of the presence of a sequence. Finally, implementation of an animal model of SRTT learning, in which invasive studies can be performed, can work synergistically with ongoing studies of SRTT learning (e.g., Bischoff-Grethe et al., 2004). Below, we provide preliminary results from our studies of BG involvement in the performance gains associated with long-term SRTT training.

3. NEURONAL CORRELATES IN THE PALLIDUM OF SRTT PERFORMANCE

We investigated the prevalence of pallidal task-related activity that differed between random and learned SRTT sequences. Given the many reports of sequence-related activity in the BG (e.g., Aldridge and Berridge, 1998; Jog et al., 1999; Kermadi and Joseph, 1995; Kermadi et al., 1993; Kimura et al., 2003; Miyachi et al., 2002; Mushiake and Strick, 1995; Ueda and Kimura, 1997) and the extensive literature pointing to BG involvement in motor sequencing (see Introduction), it was reasonable to predict that activity in the pallidal motor territory would show a preference for movements performed as a part of a learned sequence. To our surprise, we found little evidence for qualitative differences in pallidal activity related to sequence familiarity.

Standard single unit recording methods were used to sample the extracellular activity of neurons in external and internal segments of the globus pallidus (GPe and GPi, respectively). Recordings were obtained from two animals performing the SRTT paradigm described above. Random and over-learned sequences were presented in separate blocks. The results shown in Fig. 3 serve as an exemplar for a large majority of the >400 cells sampled across the motor territory of both pallidal segments. Despite the presence of clear differences in RTs between learned and random conditions, we found very few sequence-related effects on perimovement discharge. Clearly, this preliminary conclusion must be confirmed through quantitative analysis. The far-reaching implications of the result, if confirmed, are discussed in the general conclusion.

4. SEQUENCE RECALL DURING GPI INACTIVATION

To examine the importance of the BG motor circuit for the recall of familiar sequences, we reversibly inactivated sites in the posterior GPi in two animals as they performed the

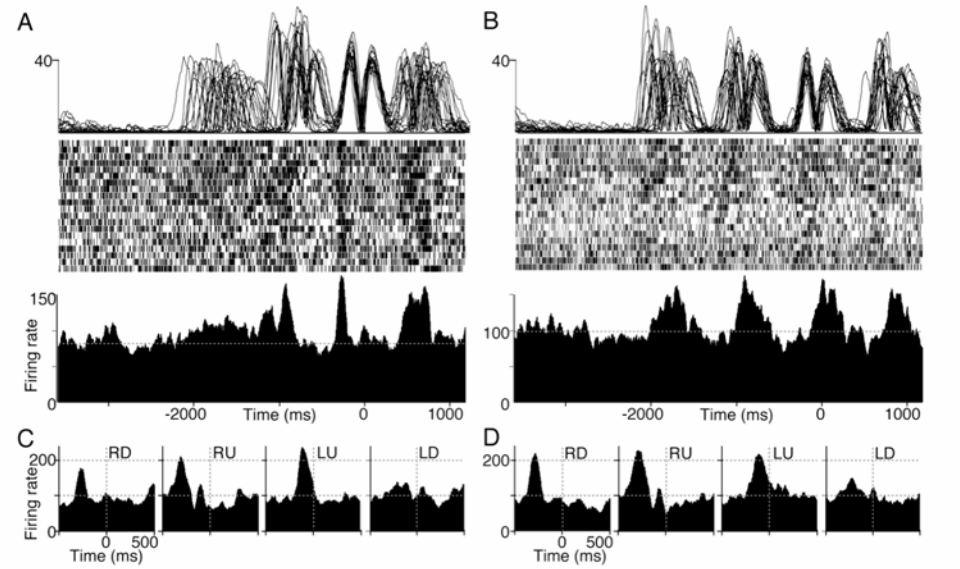

Figure 3. Task-related activity of a GPi neuron is shown during performance of learned and random sequences (*left* and *right*, respectively). Perimovement changes in firing were very similar under the two conditions. All of the data shown in *A* and *B* are aligned on the peripheral target touch of the 3rd movement. Single-trial tangential velocities (*top*) show that transitions from one movement to the next were often very rapid under the learned condition (*A*) in contrast to the clearly-defined pauses between movements under the random condition (*B*). Differences between learned and random conditions are evident in rasters (*middle*) and spike density functions (SDFs, *bottom*), but data from the random condition were not sorted according to peripheral target. *C* and *D*, Perimovement discharge was very similar under learned and random conditions in SDFs sorted according to.

SRTT. Muscimol, a GABAergic agonist, was microinjected at a range of sites throughout the posterior GPi (1 μg/μl, 0.5 μl–2.0 μl). Because this part of GPi constitutes the principal output nucleus of the BG sensorimotor circuit, inactivation here should disrupt motor functions that depend on BG signaling. Injection sites were chosen based on prior microelectrode mapping to identify nuclear boundaries and regions responsive to proprioceptive stimulation.

If the BG motor circuit contributes to the selection of component movements within a learned sequence, then GPi inactivation should interfere with that selection process and thereby block the expression of RT savings. However, among 25 injections performed in two animals, the majority had minimal effects on RTs, independent of whether sequences were over-learned or random (Fig. 4*A*, *left*). In keeping with previous reports (Horak and Anderson, 1984; Inase et al., 1996; Mink and Thach, 1991), GPi inactivation consistently reduced both peak velocity and movement extent (Fig. 4, *right*). Interestingly, a minor fraction of the injections did block RT savings for a learned sequence (Fig. 4*B*). These results indicate that any BG role in selecting sequence components likely involves a subcircuit within the general BG sensorimotor region (Hoover and Strick, 1993). Large parts of the BG motor circuit can be functionally disconnected from downstream motor control areas with no effect on the efficient selection and initiation of component movements within an over-learned sequence.

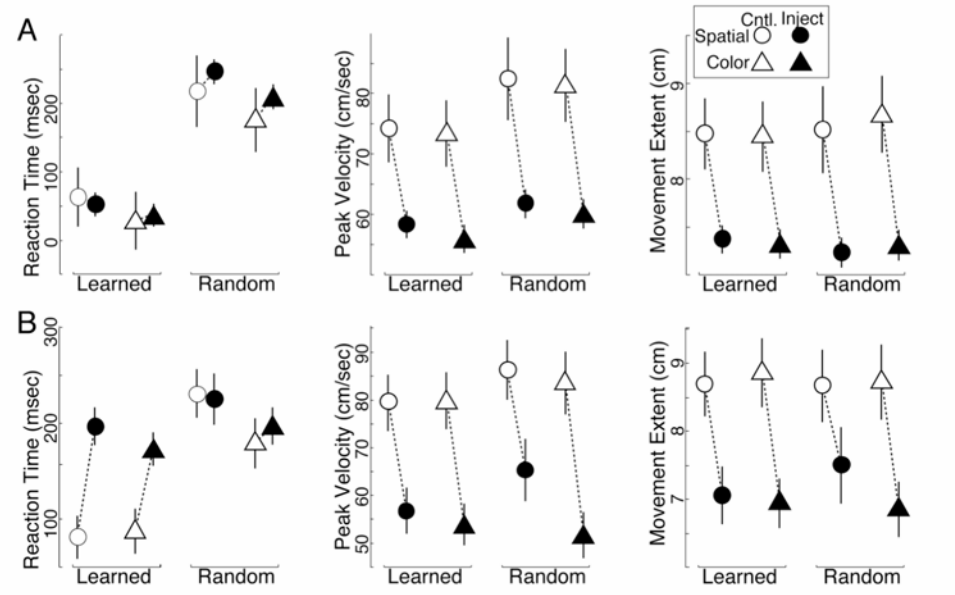

Figure 4. Example data illustrate the two most common effects of muscimol microinjection into the sensorimotor GPi. *A*. In most cases, GPi inactivation had a minimal effect on RTs [*left*, compare pre-injection (*open symbols*) versus post-injection means (*filled symbols*)]. This was true irrespective of whether animals performed over-learned fixed sequences (*Learned*) or random sequences (*Random*), or whether cues provided information by their spatial location (*circles*) or color (*triangles*). In contrast, muscimol injections consistently reduced movement velocity (*middle*) and extent (*right*). *B*. In a minority of cases, GPi inactivation lead to a selective slowing of RTs during performance of over-learned fixed sequences. Error bars ±SEM.

5. CONCLUSION

A variety of experimental approaches will be required to develop a detailed, biologically-grounded model of sequential motor control. Among the approaches used to date, the SRTT has been perhaps the most productive for studying sequence learning in humans. This paradigm has led to the demonstration of a form a procedural learning that can occur incidentally, independent of reward contingency or intention to learn (Nissen and Bullemer, 1987), and the demonstration that this form of learning very likely involves motor control regions of the CNS, including the BG (e.g., Bischoff-Grethe et al., 2004; Grafton et al., 1995; Hazeltine et al., 1997). A central remaining question is whether distinct roles can be assigned to the different components of this network. To address this question there are obvious benefits to replicating the SRTT in a non-human primate. Although SRTT-like learning has been described in non-primate species (e.g., Baunez and Robbins, 1999; Christie and Hersch, 2004), there are clear advantages to using a species with close structural and functional similarities to the human CNS. We have developed an SRTT paradigm for monkeys that shows many similarities to what has been described for humans. Of particular significance is that our model consistently shows a gradual reduction in RTs within one learning session. Gradual reductions in RT like this are a hallmark of SRTT learning in humans when subjects are unaware of the ordered sequence (Keele et al., 2003).

It is notable that other features of the implicit form of SRTT learning in humans were also found in our animal model (i.e., recall of sequence knowledge independent of changes in sensory cues or end effectors). Thus, we conclude that our model of SRTT learning allows investigation of the neural substrates of implicitlike sequence learning in a non-human primate. Here, we have presented preliminary results on involvement of the BG motor circuit in the expression of familiar sequences learned under SRTT conditions.

5.1. BG Contributions to Motor Sequences

With our monkey model of the SRTT, we have address a narrowly-defined hypothesis: that the BG motor circuit contributes a switching type of function that aids automatic chaining from one component to the next within a well-learned sequence of movements (Aldridge et al., 2004; Brotchie et al., 1991; Cromwell and Berridge, 1996; Graybiel, 1998; Keele et al., 2003). We investigated the prevalence in the pallidum of activity related preferentially to the production to familiar sequences based on the rationale that prominent encoding of sequence-related information would suggest an important role in sequence performance. We also investigated the effects of GPi inactivation based on the view that acute blockade of normal BG output should disrupt or alter aspects of behavior that the BG contributes to. Results from both experiments were not strongly supportive of the hypothesis stated above.

Very few pallidal cells in our recording study had perimovement activity related selectively to the performance of familiar sequences. These results should be interpreted with caution given the number of recording studies that describe sequence-related discharge in BG structures (Aldridge and Berridge, 1998; Jog et al., 1999; Kermadi and Joseph, 1995; Kermadi et al., 1993; Kimura et al., 2003; Miyachi et al., 2002; Mushiake and Strick, 1995; Ueda and Kimura, 1997). Most relevant for the present discussion is the study of Mushiake and Strick (1995), who found that some pallidal neurons had activity selective for memory-guided sequential movements. The sequence-specific activity was concentrated in the pallidal region that other studies have shown to project via thalamus to the supplementary motor area (Hoover and Strick, 1993). That study, along with many others, clearly confirms that neuronal activity in the BG can distinguish between a variety of movement contexts including sensory-guided versus memory-guided or sensorytriggered versus self-initiated (Hikosaka and Wurtz, 1983; Kimura et al., 1992; Turner and Anderson, 2005). Previous recording studies, however, do not specifically address the question whether the BG motor circuit is activated preferentially for familiar sequences under SRTT-like conditions. This is not a minor distinction because few tasks aside from the SRTT control for differences in context (e.g., task stimuli, movement kinematics, reward contingencies, knowledge of results) that are unrelated to the expression of procedurally-acquired sequence knowledge. Our recording results suggest that activity in the pallidal motor circuit has little involvement in the expression of sequence knowledge under SRTT conditions.

Our GPi inactivation results also bring into question the importance of the BG motor circuit for the expression of procedural sequence knowledge. In contrast to strong and consistent effects on movement kinematics, GPi inactivation had infrequent and variable effects on the RT savings associated with familiar sequences. These results are not without precedent. It has been shown repeatedly that acute or permanent inactivation of the GPi motor territory in normal primates has a minimal effect on movement initiation (Horak and Anderson, 1984; Inase et al., 1996; Mink and Thach, 1991). More recent work suggested indirectly that motor sequencing might also be preserved following acute pallidal

inactivation (Wenger et al., 1999). Additionally, ablation of the avian equivalent of the BG does not interfere with the execution of already-learned song (a clearly sequential behavior, Bottjer et al., 1984; Nottebohm et al., 1976) although it does interfere with new song acquisition. Finally, many studies in humans have produced results that are consistent. Leaving aside for the moment studies of Parkinson's disease (PD) itself, ablation of the posteroventral GPi (i.e., pallidotomy) is an effective and well-accepted neurosurgical treatment for PD (Baron et al., 1996; Laitinen, 1995; Marsden and Obeso, 1994; Smeding et al., 2005). Despite that fact that pallidotomy ablates a large, sometimes bilateral (Green et al., 2004), portion of the GPi motor territory, few if any motor deficits result (Limousin et al., 1999). Significantly, there is no evidence that pallidotomy disrupts the performance of already-learned sequential behaviors (e.g., hand writing, shoe tying), although some reports suggest that pallidotomy interferes with new procedural learning (Brown et al., 2003; Sage et al., 2003).

How do we harmonize the view laid out above with the well-recognized motor sequencing deficits observed in PD (Benecke et al., 1987, 1986) and with reports that inactivation of the motor striatum interferes with production of already-learned sequences (Cromwell and Berridge, 1996; Miyachi et al., 1997)? One reasonable explanation is that striatal dysfunction is likely to have effects on BG-recipient circuits that are very different from the effects of GPi inactivation. The striatal dysfunctions associated with dopamine depletion lead to abnormally-pattern activity in the GPi (Filion and Tremblay, 1991; Miller and DeLong, 1988). The resultant parkinsonian symptoms can be blocked by temporary or permanent inactivation of the GPi (Baron et al., 2002; Laitinen, 1995). Striatal lesions also induce abnormal pallidal firing patterns (Sachdev et al., 1991), and it is reasonable to predict that GPi inactivation would also block the behavioral abnormalities associated with those lesions. Thus, as has been inferred from the success of ablative therapies for PD, abnormally-patterned BG outflow appears to have far more deleterious effects on the functions of BG-recipient structures than the simple interruption of BG outflow.

In conclusion, our preliminary studies using a monkey model of the SRTT cast doubt on a major role for the BG in the performance enhancements associated with simple familiar sequences. Recently the concept has arisen that motor sequences are represented differently in the CNS depending on the complexity of the sequence (Rhodes et al., 2004). It may be possible to represent short familiar sequences, like the ones we used, at the cortical level, independent of BG involvement (Verwey et al., 2002). Indeed, transient inactivation of the primary motor cortex has been shown recently to selectively disrupt the performance of over-learned motor sequence (Lu and Ashe, 2005). A topic for further research is the possiblility that a subcircuit within the BG motor territory does contribute to the expression of SRTT RT savings, as suggested by the handful of GPi inactivations that did block RT savings. Our primate model of the SRTT will also enable a detailed investigation of the roles played by the BG in the acquisition of new motor sequences under procedural learning conditions.

6. REFERENCES

Aldridge, J.W., and Berridge, K.C., 1998, Coding of serial order by neostriatal neurons: a "natural action" approach to movement sequence, *J. Neurosci*. **18**:2777–2787.

Aldridge, J.W., Berridge, K.C., and Rosen, A.R., 2004, Basal ganglia neural mechanisms of natural movement sequences, *Can J. Physiol. Pharmacol*. **82**:732–739.

Baron, M.S., Vitek, J.L., Bakay, R.A.E., Green, J., Kaneoke, Y., Hashimoto, T., Turner, R.S., Woodard, J.L., Cole, S.A., McDonald, W.M., and DeLong, M.R., 1996, Treatment of advanced Parkinson's disease by posterior GPi pallidotomy: 1-year results of a pilot study, *Ann. Neurol*. **40**:355–366.

Baron, M.S., Wichmann, T., Ma, D., and DeLong, M.R., 2002, Effects of transient focal inactivation of the basal ganglia in parkinsonian primates, *J. Neurosci*. **22**:592–599.

Baunez, C., and Robbins, T.W., 1999, Effects of transient inactivation of the subthalamic nucleus by local muscimol and APV infusions on performance on the five-choice serial reaction time task in rats, *Psychopharmacology* (*Berl.*) **141**:57–65.

Benecke, R., Rothwell, J.C., Dick, J.P.R., Day, B.L., and Marsden, C.D., 1987, Disturbances of sequential movements in patients with Parkinson's disease, *Brain* **110**:361–379.

Benecke, R., Rothwell, J.C., Dick, J.P.R., Day, B.L., and Marsden, C.D., 1986, Performance of simultaneous movements in patients with Parkinson's disease, *Brain* **109**:739–757.

Bischoff-Grethe, A., Goedert, K.M., Willingham, D.T., and Grafton, S.T., 2004, Neural substrates of response-based sequence learning using fMRI, *J. Cogn. Neurosci*. **16**:127–138.

Bottjer, S.W., Miesner, E.A., and Arnold, A.P., 1984, Forebrain lesions disrupt development but not maintenance of song in passerine birds, *Science* **224**:901–903.

Brotchie, P., Iansek, R., and Horne, M.K., 1991, Motor function of the monkey globus pallidus. 2. Cognitive aspects of movement and phasic neuronal activity, *Brain* **114**:1685–1702.

Brown, R.G., Jahanshahi, M., Limousin-Dowsey, P., Thomas, D., Quinn, N.P., and Rothwell, J.C., 2003, Pallidotomy and incidental sequence learning in Parkinson's disease, *Neuroreport* **14**:21–24.

Christie, M.A., and Hersch, S.M., 2004, Demonstration of nondeclarative sequence learning in mice: development of an animal analog of the human serial reaction time task, *Learn Mem*. **11**:720–723.

Cohen, A., Ivry, R.I., and Keele, S.W., 1990, Attention and structure in sequence learning, *J. Exp. Psychol.: Learning Memory Cogn*. **16**:17–30.

Cromwell, H.C., and Berridge, K.C., 1996, Implementation of action sequences by a neostriatal site: a lesion mapping study of grooming syntax, *J. Neurosci*. **16**:3444–3458.

Curran, T., 1998, Implicit sequence learning from a cognitive neuroscience perspective, in: *Handbook of Implicit Learning*, M.A. Stadler and P.A. Frensch, eds., Sage, Thousand Oaks, CA, pp. 365–400.

Eichenbaum, H., and Cohen, N.J., 2001, *From Conditioning to Conscious Recollection: Memory Systems of the Brain*, Oxford University Press, Oxford, New York.

Exner, C., Koschack, J., and Irle, E., 2002, The differential role of premotor frontal cortex and basal ganglia in motor sequence learning: evidence from focal basal ganglia lesions, *Learn Mem*. **9**:376–386.

Filion, M., and Tremblay, L., 1991, Abnormal spontaneous activity of globus pallidus neurons in monkeys with MPTP-induced parkinsonism, *Brain Res*. **547**:142–151.

Grafton, S.T., Hazeltine, E., and Ivry, R., 1995, Functional anatomy of sequence learning in normal humans, *J. Cogn. Neurosci*. **7**:497–510.

Graybiel, A.M., 1998, The basal ganglia and chunking of action repertoires, *Neurobiol. Learn Mem*. **70**:119–136.

Graybiel, A.M., 2004, Network-level neuroplasticity in cortico-basal ganglia pathways, *Parkinsonism Relat. Disord*. **10**:293–296.

Green, A.L., Joint, C., Sethi, H., Bain, P., and Aziz, T.Z., 2004, Cost analysis of unilateral and bilateral pallidotomy for Parkinson's disease, *J. Clin. Neurosci*. **11**:829–834.

Hazeltine, E., Grafton, S.T., and Ivry, R., 1997, Attention and stimulus characteristics determine the locus of motor-sequence encoding. A PET study, *Brain* **120**:123–140.

Hikosaka, O., Nakamura, K., Sakai, K., and Nakahara, H., 2002a, Central mechanisms of motor skill learning, *Curr. Opin. Neurobiol*. **12**:217–222.

Hikosaka, O., Rand, M.K., Nakamura, K., Miyachi, S., Kitaguchi, K., Sakai, K., Lu, X., and Shimo, Y., 2002b, Long-term retention of motor skill in macaque monkeys and humans, *Exp. Brain Res*. **147**:494–504.

Hikosaka, O., and Wurtz, R.H., 1983, Visual and oculomotor functions of monkey substantia nigra pars reticulata. III. Memory-contingent visual and saccade responses, *J. Neurophysiol*. **49**:1268–1284.

Hoover, J.E., and Strick, P.L., 1993, Multiple output channels in the basal ganglia, *Science* **259**:819–821.

Horak, F.B., and Anderson, M.E., 1984, Influence of globus pallidus on arm movements in monkeys. I. Effects of kainic acid-induced lesions, *J. Neurophysiol*. **52**:290–304.

Inase, M., Buford, J.A., and Anderson, M.E., 1996, Changes in the control of arm position, movement, and thalamic discharge during local inactivation in the globus pallidus of the monkey, *J. Neurophysiol*. **75**:1087–1104.

Jog, M.S., Kubota, Y., Connolly, C.I., Hillegaart, V., and Graybiel, A.M., 1999, Building neural representations of habits, *Science* **286**:1745–1749.

Keele, S.W., Ivry, R., Mayr, U., Hazeltine, E., and Heuer, H., 2003, The cognitive and neural architecture of sequence representation, *Psychol. Rev*. **110**:316–339.

Keele, S.W., Jennings, P., Jones, S., Caulton, S., Caulton, D., and Cohen, A., 1995, On the modularity of sequence representation, *J. Motor. Behav*. **27**:17–30.

Kermadi, I., and Joseph, J.P., 1995, Activity in the caudate nucleus of monkey during spatial sequencing, *J. Neurophysiol*. **74**:911–933.

Kermadi, I., Jurquet, Y., Arzi, M., and Joseph, J.P., 1993, Neural activity in the caudate nucleus of monkeys during spatial sequencing, *Exp. Brain Res*. **94**:352–356.

Kimura, M., Aosaki, T., Hu, Y., Ishida, A., and Watanabe, K., 1992, Activity of primate putamen neurons is selective to the mode of voluntary movement: visually guided, self-initiated or memory-guided, *Exp. Brain Res*. **89**:473–477.

Kimura, M., Matsumoto, N., Okahashi, K., Ueda, Y., Satoh, T., Minamimoto, T., Sakamoto, M., and Yamada, H., 2003, Goal-directed, serial and synchronous activation of neurons in the primate striatum, *Neuroreport* **14**:799–802.

Koch, I., and Hoffmann, J., 2000, The role of stimulus-based and response-based spatial information in sequence learning, *J. Exp. Psychol. Learn Mem. Cogn*. **26**:863–882.

Laitinen, L.V., 1995, Pallidotomy for Parkinson's diesease, *Func. Neurol*. **6**:105–112.

Lee, D., and Quessy, S., 2003, Activity in the supplementary motor area related to learning and performance during a sequential visuomotor task, *J. Neurophysiol*. **89**:1039–1056.

Limousin, P., Brown, R.G., Jahanshahi, M., Asselman, P., Quinn, N.P., Thomas, D., Obeso, J.A., and Rothwell, J.C., 1999, The effects of posteroventral pallidotomy on the preparation and execution of voluntary hand and arm movements in Parkinson's disease, *Brain* **122**:315–327.

Lu, X., and Ashe, J., 2005, Anticipatory activity in primary motor cortex codes memorized movement sequences, *Neuron* **45**:967–973.

Marsden, C.D., 1984, Which motor disorder in Parkinson's disease indicates the true motor function of the basal ganglia?, in: *Functions of the Basal Ganglia*, C.F. Symp, ed., Pitman, London, pp. 225–237.

Marsden, C.D., and Obeso, J.A., 1994, The functions of the basal ganglia and the paradox of stereotaxic surgery in Parkinson's disease, *Brain* **117**:877–897.

Miller, W.C., and DeLong, M.R., 1988, Parkinsonian symptomatology: an anatomical and physiological analysis, *Ann. NY Acad. Sci*. **515**:287–302.

Mink, J., 1996, The basal ganglia: focused selection and inhibition of competing motor programs, *Prog. Neurobiol*. **50**:381–425.

Mink, J., and Thach, W., 1991, Basal ganglia motor control. III. pallidal ablation: normal reaction time, muscle cocontraction, and slow movement, *J. Neurophysiol*. **65**:330–351.

Miyachi, S., Hikosaka, O., and Lu, X., 2002, Differential activation of monkey striatal neurons in the early and late stages of procedural learning, *Exp. Brain Res*. **146**:122–126.

Miyachi, S., Hikosaka, O., Miyashita, K., Karadi, Z., and Rand, M.K., 1997, Differential roles of monkey striatum in learning of sequential hand movement, *Exp. Brain Res*. **115**:1–5.

Mushiake, H., and Strick, P.L., 1995, Pallidal neuron activity during sequential arm movements., *J. Neurophysiol*. **74**:2754–2758.

Nissen, M.J., and Bullemer, P., 1987, Attentional requirements of learning: evidence from performance measures, *Cogn. Psychol*. **19**:1–32.

Nottebohm, F., Stokes, T.M., and Leonard, C.M., 1976, Central control of song in the canary, Serinus canarius, *J. Comp. Neurol*. **165**:457–486.

Penhune, V.B., and Doyon, J., 2002, Dynamic cortical and subcortical networks in learning and delayed recall of timed motor sequences, *J. Neurosci*. **22**:1397–1406.

Procyk, E., Ford Dominey, P., Amiez, C., and Joseph, J.P., 2000, The effects of sequence structure and reward schedule on serial reaction time learning in the monkey, *Brain Res. Cogn. Brain Res*. **9**:239–248.

Rand, M.K., Hikosaka, O., Miyachi, S., Lu, X., and Miyashita, K., 1998, Characteristics of a long-term procedural skill in the monkey, *Exp. Brain Res*. **118**:293–297.

Rhodes, B.J., Bullock, D., Verwey, W.B., Averbeck, B.B., and Page, M.P., 2004, Learning and production of movement sequences: behavioral, neurophysiological, and modeling perspectives, *Hum. Mov. Sci*. **23**:699–746.

Sachdev, R.N., Gilman, S., and Aldridge, J.W., 1991, Bursting properties of units in cat globus pallidus and entopeduncular nucleus: the effect of excitotoxic striatal lesions, *Brain Res*. **549**:194–204.

Sage, J.R., Anagnostaras, S.G., Mitchell, S., Bronstein, J.M., De Salles, A., Masterman, D., and Knowlton, B.J., 2003, Analysis of probabilistic classification learning in patients with Parkinson's disease before and after pallidotomy surgery, *Learn Mem*. **10**:226–236.

Smeding, H.M., Esselink, R.A., Schmand, B., Koning-Haanstra, M., Nijhuis, I., Wijnalda, E.M., and Speelman, J.D., 2005, Unilateral pallidotomy versus bilateral subthalamic nucleus stimulation in PD A comparison of neuropsychological effects, *J. Neurol*. **252**:176–182.

Smith, J., Siegert, R.J., McDowall, J., and Abernethy, D., 2001, Preserved implicit learning on both the serial reaction time task and artificial grammar in patients with Parkinson's disease, *Brain Cogn*. **45**:378–391.

Turner, R.S., and Anderson, M.E., 2005, Context-dependent modulation of movement-related discharge in the primate globus pallidus, *J. Neurosci*. **25**:2965–2976.

Ueda, Y., and Kimura, M., 1997, Contrasting properties of activity of primate putamen and primary motor cortex neurons during sequential motor behavior, *Soc. Neurosci. Abstr*. **23**:465.

Verwey, W.B., Lammens, R., and van Honk, J., 2002, On the role of the SMA in the discrete sequence production task: a TMS study. Transcranial Magnetic Stimulation, *Neuropsychologia* **40**:1268–1276.

Wenger, K.K., Musch, K.L., and Mink, J.W., 1999, Impaired reaching and grasping after focal inactivation of globus pallidus pars interna in the monkey, *J. Neurophysiol*. **82**:2049–2060.

Willingham, D.B., Wells, L.A., and Farrell, J.M., 2000, Implicit motor sequence learning is represented in response locations, *Mem. Cognit*. **28**:366–375.

GABAERGIC AND DOPAMINERGIC MODULATION OF BASAL GANGLIA OUTPUT IN PRIMATES

Adriana Galvan, Michele A. Kliem, Yoland Smith,
and Thomas Wichmann[1]

1. INTRODUCTION

The basal ganglia process motor and non-motor information, and are part of larger, segregated circuits which traverse cortex and thalamus. Within the basal ganglia circuitry, the striatum and subthalamic nucleus (STN) are the primary input structures, while the substantia nigra pars reticulata (SNr) and the internal pallidal segment (GPi) are output structures, projecting to the ventral and intralaminar thalamic nuclei, which, in turn, project back to cerebral cortex and striatum, as well as to the brainstem (Ilinsky et al., 1993; Kultas-Ilinsky et al., 1983). While GPi neurons appear to be preferentially concerned with functions related to the control of movement (e.g. Brotchie et al., 1991; Georgopoulos et al., 1983; Mink and Thach, 1991; Turner and Anderson, 1997), the activity of many SNr neurons is closely related to oculomotor (Hikosaka and Wurtz, 1983a,b; 1985) and non-motor functions, such as memory or attention (Wichmann and Kliem, 2004). Neuronal discharge in both structures is strongly altered in movement disorders, such as Parkinson's Disease (PD) (Wichmann et al., 1999). Some of the motor manifestations of PD can be ameliorated by inactivation or lesions of GPi or SNr (Baron et al., 2002; Wichmann et al., 2001), raising the possibility that abnormal activity in GPi or SNr plays a role in the generation of these signs.

Both of the basal ganglia output nuclei receive similar inputs. The main excitatory inputs are glutamatergic and arise in the STN (Bolam et al., 2000; Smith et al., 1998), while the majority of inhibitory inputs to GPi or SNr neurons is GABAergic and originates in the striatum, the external segment of the globus pallidus (GPe), and from local axon collaterals. Both nuclei also receive dopaminergic inputs from the substantia nigra, pars compacta (SNc) (Bjorklund and Lindvall, 1975; Smith and Kieval, 2000; Smith et al., 1989). In primates, the SNc-GPi projection appears to be separate from the nigrostriatal projection,

[1] Yerkes National Primate Research Center and Dept. Neurology, Emory University, Atlanta, GA, 30322, USA.

because few nigrostriatal fibers give rise to axon collaterals to GPi (Smith et al., 1989). The mode of dopamine release in the SNr differs from that in GPi or striatum, because dopamine reaching SNr neurons appears to be released from dendrites (rather than axons) of SNc neurons (Bjorklund and Lindvall, 1975). SNc and SNr interdigitate, so that portions of the dendritic trees of SNc neurons are located in the SNr.

The afferent control of GPi and SNr activity has been studied extensively *in vitro*, but there are few reports studying this issue under the more complex *in vivo* situation. We have begun to carry out such experiments by studying the local effects of compounds acting at GABA receptors and at dopamine D1-like receptors on the neuronal activity in SNr and GPi in awake monkeys.

The actions of GABA are mediated by ionotropic GABA-A and metabotropic GABA-B receptors. Both types of receptors are expressed in pallidal and nigral neurons in humans and non-human primates (Billinton et al., 2000; Bowery et al., 1999; Charara et al., 2000; 2005; Waldvogel et al., 1998; 1999; 2004). GABA-A receptor activation in GPi and SNr induces fast inhibitory post-synaptic potentials (Kita, 2001; Kita and Kitai, 1991; Nakanishi et al., 1985; Rick and Lacey, 1994), while GABA-B receptors have a presynaptic role regulating the release of glutamate and GABA (Chan et al., 2000; Chen et al., 2002; Shen and Johnson, 1997).

Dopamine, on the other hand, acts via two families of receptors, i.e., D1-like receptors (including D1 and D5 receptors) (Clark and White, 1987; Neve and Neve, 1997) and D2-like receptors (including D2, D3, and D4 receptors) (Neve and Neve, 1997). Binding studies show a preponderance of D1-like receptors in the monkey GPi and SNr (Richfield et al., 1987). Electron microscopic studies suggest that these receptors are primarily located on axons and terminals of the GABAergic 'direct' projections arising in the striatum (Barone et al., 1987; Yung et al., 1995). Activation of D1-like receptors at these sites is thought to enhance the release of GABA (Trevitt et al., 2002).

Based on the existing rodent literature, we hypothesized that activation of GABA receptors would reduce basal ganglia output, primarily through postsynaptic actions, and activation of D1-like receptors would inhibit GPi and SNr cells through increased release of GABA. We also carried out experiments with the respective antagonists to examine whether the receptors are tonically activated by the endogenous transmitter.

2. MATERIALS AND METHODS

2.1. Animals and Surgery

All experiments were performed in accordance with the NIH Guide for the Care and Use of Laboratory Animals, and the PHS Policy on Humane Care and Use of Laboratory Animals (amended 2002), and were approved by the Institutional Animal Care and Use Committee at Emory University. Four Rhesus monkeys were used. The animals received stainless steel recording chambers under aseptic conditions and isoflurane anesthesia. The chambers were stereotactically aimed at the globus pallidus at an angle of 50° in the coronal plane, or at the substantia nigra at an angle of 25° in the parasagittal plane. The recording chambers, together with standard metal head holders (Crist Instruments, Hagerstown, MD), were embedded into a dental acrylic 'cap' which was affixed to the animal's skull. The recording and injection experiments began one week after surgery. The animals were awake for the recording experiments.

2.2. Recording-injection System

A combined recording-injection device was used for all of these experiments. This device permits local injections of small quantities (<1 µl) of drug solutions, and extracellular electrophysiologic recording in the immediate vicinity (within 100 µm) of the injection site. As previously described, (Kliem and Wichmann, 2004) the device consists of a tungsten microelectrode (Frederick Haer Co., Bowdoinham, ME; Z = 0.7–2.5 MΩ), and a fused silica tube (Polymicro Technologies, Phoenix, AZ), which are both protected by a polyimide sleeve (O.D. = 0.5 mm; MicroLumen, Tampa, FL). The tip of the electrode extends 50–100 µm beyond the silica tubing. The silica tubing is attached to a gas-tight 1 ml syringe, operated by a pump for delivery of drugs or artificial cerebrospinal fluid (aCSF, comprised of (in mM concentrations) 143 NaCl, 2.8 KCl, 1.2 $CaCl_2$, 1.2 $MgCl_2$, 1 Na_2HPO_4, pH = 7.2–7.4) via a micro-T connector (CMA, Solna, Sweden). A microdrive (MO-95B, Narishige; Tokyo, Japan) was used to lower the system into the brain.

2.3. Recording and Injection Sessions

We carried out initial electrophysiological mapping with standard electrophysiologic methods, using tungsten electrodes (without the silica tubing) to identify GPi and SNr. For these, and all other recording sessions, the neuronal activity was amplified (DAM-80 preamplifier; WPI, Sarasota, FL and MDA-2 amplifier, BAK Mount Airy, MD), filtered (0.4–6.0 kHz, Krohn-Hite, Brockton, MA), displayed on an oscilloscope (DL1540; Yokogawa, Tokyo, Japan), and audio amplified. GPi and SNr were identified by their characteristic high-frequency discharge, waveform, and their spatial relationship to surrounding nuclei. The electrophysiologic mapping information was used to place the recording-injection system to record single pallidal or nigral neurons. Neurons were recorded throughout a control period of at least one minute prior to drug infusion, the infusion period, and an epoch lasting at least five minutes after the injections. The recorded activity was stored to computer disk with a data acquisition system (Spike 2, CED, Cambridge, UK) for off-line analysis.

2.4. Drugs

The following drugs were used: the selective D1 receptor agonist SKF82958 (3 mg/ml; Sigma-Aldrich, St. Louis, MO), the selective D1 receptor antagonist SCH23390 (5 mg/ml; Sigma-Aldrich), the GABA-A receptor agonist muscimol (114 µg/ml; Tocris Cookson, Ellisville, MO), the GABA-B receptor agonist baclofen (213 µg/ml; Sigma-Aldrich); the GABA-A receptor antagonist gabazine (368 µg/ml; Tocris); and the GABA-B receptor antagonist CGP-55845 (402 µg/ml; Tocris). All solutions were filtered using a 250 µm micropore filter (Fisher Scientific, Hampton, NH), and infused at a rate of 0.25–0.3 µl/min for a total volume of 0.5–1 µl.

2.5. Data Analysis

Responses to drug injections began 2–4 minutes after the start of drug infusion. Data collected during the pre-infusion control epoch were compared to the ‘effect’ epoch, a four-minute post-injection segment of data, which started two minutes after the start of the injection. Template-matching spike sorting (Spike 2 or MSD, Alpha Omega, Nazareth,

Israel) was used to isolate action potential waveforms for individual units, and to compute inter-spike intervals (ISIs). The ISI information was used to calculate average discharge rates, ISI distributions, and the incidence of burst discharges for each neuron before, during, and after injections using algorithms in the Matlab programming environment (Mathworks, Natick, MA). The post-drug discharge rates (binned in 15 s-intervals) of the neuron were considered different from the baseline activity if the discharge rate of the recorded neuron changed by two standard deviations (SDs) from the average of the baseline activity.

3. RESULTS

3.1. Control Injections

Control injections of aCSF ($n = 4$, all done in GPi) had no effect on the activity of the recorded neurons.

3.2. Activation and Blockade of GABA-A and GABA-B Receptors in the GPi

The GABA-A receptor agonist muscimol reduced the firing rate in all four GPi neurons tested. An example of this effect is shown in Figure 1. On average, the firing rate decreased by 57% compared to the baseline period. These effects were not seen when the GABA-A receptor antagonist gabazine was given concurrently with muscimol (not shown).

Baclofen, a GABA-B receptor agonist, decreased the discharge rate of all three GPi neurons tested (see example in Figure 2). On average the reduction was 69% from basal. No effect on the firing rate was observed when baclofen was applied in combination with the GABA-B antagonist CGP-55845 (not shown).

Gabazine, administered alone, had no consistent effects on GPi activity. Thus, the drug increased the firing rate in three neurons, but had no effect in two additional cells. When pooled, these results were not statistically different from those of control injections. The

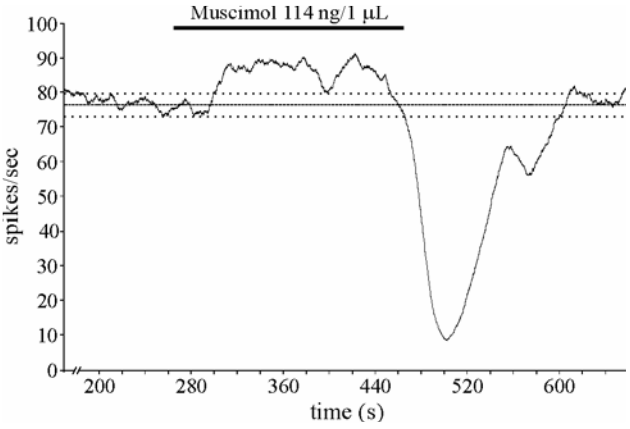

Figure 1. Example of the effect of the GABA-A agonist, muscimol, on the discharge rate of a GPi cell. The duration of drug infusion is indicated by the horizontal bar. Dashed lines represent the mean discharge rate ±2 SDs.

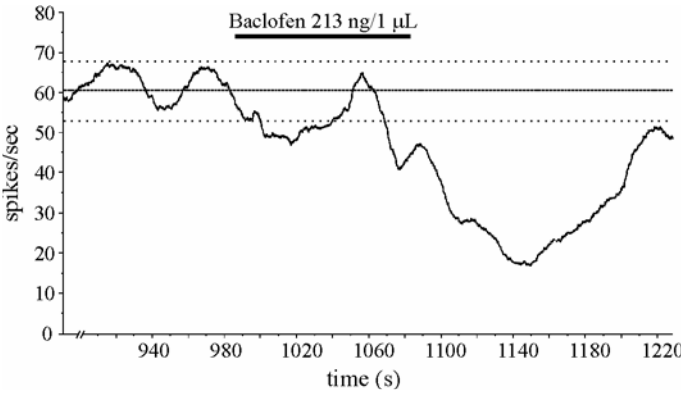

Figure 2. A neuron in the GPi exhibits decreased firing rate after exposure to the GABA-B agonist baclofen. The duration of drug infusion is indicated by the horizontal bar. Dashed lines represent the mean discharge rate ±2 SDs.

GABA-B antagonist CGP-55845 evoked, in 5 of 6 cases, an average increase of 26% in the firing rate of GPi neurons. However, these effects were highly variable among neurons, so that they did not reach statistical significance in the aggregate.

3.3. Activation and Blockade of D1 Receptors in the SNr and GPi

Figure 3 shows the response of an SNr neuron before, during, and after infusion of the D1-like receptor agonist, SKF82958. The nigral cell decreased its discharge rate immediately upon completion of drug delivery. After 120 s, the activity began to return to baseline.

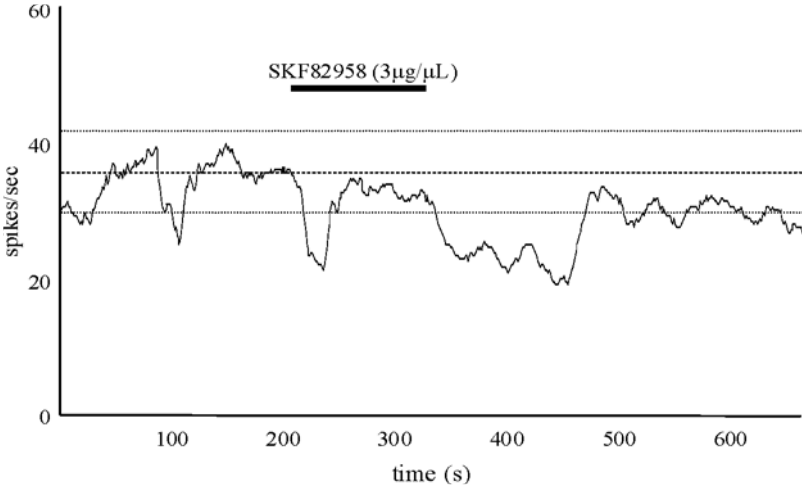

Figure 3. Response of a SNr cell to local administration of the D1-like receptor agonist, SKF82958. The duration of drug infusion is indicated by the horizontal bar. Dashed lines represent the mean discharge rate ±2 SDs.

Such reductions in activity were seen in half of the pallidal cells ($n = 4$), and the majority of nigral cells ($n = 7$) tested with an average decrease in discharge rate of 15.5% and 31.9%, respectively, as compared to the control epoch. Injections of the D1-like receptor antagonist, SCH23390, however, did not alter discharge rates in SNr ($n = 2$).

4. DISCUSSION

SNr and GPi are the primary output nuclei of the basal ganglia, and their activity is thought to strongly modulate motor and non-motor functions. The results presented here indicate that activation of GABA or dopamine receptors affect the activity of neurons in both of these nuclei, although the antagonist experiments did not indicate a significant intrinsic tone of GABA or dopamine.

4.1. GABA Receptor Activation

In agreement with previous studies, (Baron et al., 2002; Kita, 2001; Kita and Kitai, 1991; Nakanishi et al., 1985) we found that activation of GABA-A receptors with muscimol inhibits the firing of GPi cells. In both basal ganglia output nuclei, GABA-A receptors (identified through electron microscopic visualization of subunits) are found in the core of inhibitory synapses and also at non-synaptic sites along plasma membranes of dendrites and cell bodies (Charara et al., 2005; Fujiyama et al., 2002). Thus, the inhibition we observed after muscimol injections may have been mediated through synaptic or extrasynaptic receptors. There is increasing evidence for the existence of functional extrasynaptic ionotropic GABA receptors in the CNS. For instance, in cerebellar and dentate gyrus granule cells, tonic inhibition is mediated by extrasynaptic GABA-A receptors, (Mody and Pearce, 2004; Semyanov et al., 2004) which contain δ and $\alpha4$, $\alpha5$ or $\alpha6$ subunits (Semyanov et al., 2004). In the monkey GPi and SNr, the mRNA for δ and $\alpha4$ subunits is present at moderate to high levels (Kultas-Ilinsky et al., 1983); however, it is not known whether GABA-A receptors composed of these subunits are also extrasynaptic in these brain regions.

Administration of the GABA-B agonist, baclofen, also resulted in a marked decrease of neuronal firing of GPi cells, indicating that activation of GABA-B receptors have an inhibitory effect in GPi in the *in vivo* situation. Ultrastructural studies have shown that GABA-B receptors are located both pre- and postsynaptically in GPi and SNr (Boyes and Bolam, 2003; Charara et al., 2005; Chen et al., 2004). In the rodent SNr, presynaptic GABA-B receptors are found at GABAergic and glutamatergic terminals (Boyes and Bolam, 2003), whereas in the monkey GPi and SNr, these presynaptic receptors are only found in a subset of putative glutamatergic terminals (Charara et al., 2000; 2005). The majority of GABA-B receptors, however, are postsynaptic, and predominately found extrasynaptically (Boyes and Bolam, 2003; Charara et al., 2000; 2005; Chen et al., 2004).

Local injections of GABA-A or GABA-B receptor antagonists did not show any significant changes compared to controls, despite the fact that they readily antagonized the effects of the respective agonists, when given concurrently. These results contrast, with a recent study by Kita et al. (2004) who reported that in experiments which were generally similar to ours, GABA-A receptor antagonists increased the activity of neurons in the monkey GPe. This discrepancy may be due to technical differences in the design of injection devices. The observations made by Kita et al. (2004) may also apply to a specific subset

of pallidal cells, because the sampling of neurons in their study was restricted to cells that responded to electrical stimulation of motor cortex.

4.2. Dopamine Receptor Activation

The selective dopaminergic D1-like receptor agonist, SKF82958, significantly reduced neuronal discharge in both GPi and SNr. Previous studies in rats (Huang and Walters, 1994; Ruskin et al., 2002) reported mixed results in regards to changes in neuronal discharge after injections of dopaminergic agonists in entopeduncular nucleus (the rodent homologue of GPi) or SNr. In these studies, however, the D1-receptor ligands were systemically administered, so that the site(s) of action of these agents remains unclear. In our experiments, the selective ligands were instead locally injected into either GPi or SNr within 100 μm of the isolated neuron.

None of the available agonists is specific for D1 or D5 receptors, but it is likely that the effects seen in our study resulted from activation of D1-receptors. Previous reports have shown that D1-receptors reside presynaptically in GPi and SNr, most likely on axons and terminals of the 'direct' monosynaptic striatal afferents to these regions (Barone et al., 1987; Yung et al., 1995), while a small number of D5-receptors is found postsynaptically on cell bodies of SNr cells (Ciliax et al., 2000). Activation of D5-receptors would be expected to enhance the activity of SNr projecting neurons, which obviously contrasts with the results reported here.

Based on results obtained in rodents, it is thought that activation of D1-like receptors enhances GABA release from terminals of this projection, which, in turn, may affect the neuronal discharge in the vicinity of these GABAergic terminals. This notion is supported by microdialysis experiments in which local activation of D1-like receptors in either SNr (Trevitt et al., 2002) or entopeduncular nucleus in the rat (Ferre et al., 1996; Trevitt et al., 2002) resulted in increased GABA release.

Our data are compatible with the idea that dopamine acts at pre-synaptic sites to enhance GABA release from terminals of direct pathway neurons, resulting in a reduction of basal ganglia output to the thalamus and other targets. Our antagonist experiments did not provide evidence for a dopaminergic tone at the GABAergic output neurons of the basal ganglia. This may indicate that, at rest, the GABAergic output neurons are not reached by significant amounts of dopamine.

Together, our data indicate that the responses of cells in the basal ganglia output nuclei to GABAergic inputs are modulated through pre- and postsynaptically located dopamine and GABA receptors. GABA can then activate synaptic GABA-A receptors or perhaps diffuse out of the synapse and bind to extrasynaptic GABA-A and GABA-B receptors. Furthermore, GABA could reach presynaptic GABA-B heteroreceptors in glutamatergic terminals. At least at the level of the SN, both GABA and glutamate receptors may also alter the activity of dopaminergic cells.

4.3. Relevance for an Understanding of Parkinsonism

It is known that expression of GABA-A and GABA-B receptors is upregulated in GPi and SNr in animal models of PD (Calon et al., 1995; 2000; 2001; Chadha et al., 2000a,b; Johnston and Duty, 2003; Pan et al., 1985), supporting the notion that striatal inhibition to the output nuclei is decreased after striatal dopamine loss (Albin et al., 1989; DeLong, 1990). Despite the loss of dopamine in PD, the relative abundance of D1-like receptors in

these nuclei remains unchanged (Barone et al., 1987). These findings suggest that both groups of receptors may be involved in compensatory mechanisms and/or could be used as therapeutic targets, particularly at the level of the SNr. In fact, the administration of glia-derived neurotrophic factor (GDNF) (Gerhardt et al., 1999) or fetal mesencephalic tissue grafts directed at the SN were shown to ameliorate parkinsonian motor signs in MPTP-treated monkeys (Starr et al., 1999). Both effects are likely mediated via enhanced dopaminergic transmission in the substantia nigra. In addition, some of the beneficial or untoward effects associated with the currently used dopaminergic replacement therapies in parkinsonism may be explainable through effects at nigral or pallidal sites.

The potential antiparkinsonian effects of GABA-receptor active drugs at these sites have not been explored in much detail, although it is clear that global inactivation of basal ganglia output is an effective strategy in the treatment of PD.

5. REFERENCES

Albin, R.L., Young, A.B., and Penney, J.B., 1989, The functional anatomy of basal ganglia disorders. *Trends Neurosci*. **12**:366–375.

Baron, M.S., Wichmann, T., Ma, D., and DeLong, M.R., 2002, Effects of transient focal inactivation of the basal ganglia in parkinsonian primates. *J. Neurosci*. **22**:592–599.

Barone, P., Tucci, I., Parashos, S.A., and Chase, T.N., 1987, D-1 dopamine receptor changes after striatal quinolinic acid lesion. *Eur. J. Pharmacol*. **138**:141–145.

Billinton, A., Ige, A.O., Wise, A., White, J.H., Disney, G.H., Marshall, F.H., Waldvogel, H.J., Faull, R.L., and Emson, P.C., 2000, GABA(B) receptor heterodimer-component localisation in human brain. *Brain Res. Mol. Brain Res*. **77**:111–124.

Bjorklund, A., and Lindvall, O., 1975, Dopamine in dendrites of substantia nigra neurons: suggestions for a role in dendritic terminals. *Brain Res*. **83**:531–537.

Bolam, J.P., Hanley, J.J., Booth, P.A., and Bevan, M.D., 2000, Synaptic organisation of the basal ganglia. *J. Anat*. **196**:527–542.

Bowery, N.G., Parry, K., Goodrich, G., Ilinsky, I., and Kultas-Ilinsky, K., 1999, Distribution of GABA(B) binding sites in the thalamus and basal ganglia of the rhesus monkey (Macaca mulatta). *Neuropharmacology* **38**:1675–1682.

Boyes, J., and Bolam, J.P., 2003. The subcellular localization of GABA(B) receptor subunits in the rat substantia nigra. *Eur. J. Neurosci*. **18**:3279–3293.

Brotchie, P., Iansek, R., and Horne, M.K., 1991, Motor function of the monkey globus pallidus. 2. Cognitive aspects of movement and phasic neuronal activity. *Brain* **114** (Pt 4):1685–1702.

Calon, F., Goulet, M., Blanchet, P.J., Martel, J.C., Piercey, M.F., Bédard, P.J., and Di Paolo, T., 1995, Levodopa or D2 agonist induced dyskinesia in MPTP monkeys: correlation with changes in dopamine and GABAA receptors in the striatopallidal complex. *Brain Res*. **680**:43–52.

Calon, F., Lavertu, N., Lemieux, A.M., Morissette, M., Goulet, M., Grondin, R., Blanchet, P.J., Bedard, P.J., and Di Paolo, T., 2001, Effect of MPTP-induced denervation on basal ganglia GABA(B) receptors: Correlation with dopamine concentrations and dopamine transporter. *Synapse* **40**:225–234.

Calon, F., Morissette, M., Goulet, M., Grondin, R., Blanchet, P.J., Bedard, P.J., and Di Paolo, T., 2000, 125I-CGP 64213 binding to GABA(B) receptors in the brain of monkeys: effect of MPTP and dopaminomimetic treatments. *Exp. Neurol*. **163**:191–199.

Chadha, A., Dawson, L.G., Jenner, P.G., and Duty, S., 2000a, Effect of unilateral 6-hydroxydopamine lesions of the nigrostriatal pathway on GABA(A) receptor subunit gene expression in the rodent basal ganglia and thalamus. *Neuroscience* **95**:119–126.

Chadha, A., Howell, O., Atack, J.R., Sur, C., and Duty, S., 2000b, Changes in [3H]zolpidem and [3H]Ro 15-1788 binding in rat globus pallidus and substantia nigra pars reticulata following a nigrostriatal tract lesion. *Brain Res*. **862**:280–283.

Chan, S.C.Y., Yung, K.K.L., and Yung, W.H., 2000, Pre- and postsynaptic distributions of GABA-B receptors in rat globus pallidus revealed by immunocytochemistry and electrophysiology. *Society for Neuroscience Abstracts* **26**:622.17.

Charara, A., Heilman, T.C., Levey, A.I., and Smith, Y., 2000, Pre- and postsynaptic localization of GABA(B) receptors in the basal ganglia in monkeys. *Neuroscience* **95**:127–140.

Charara, A., Pare, J.F., Levey, A.I., and Smith, Y., 2005, Synaptic and Extrasynaptic GABA-A and GABA-B receptors in the Globus Pallidus: an Electron Microscopic immunogold analysis in monkeys. *Neuroscience* **131**:917–933.

Chen, L., Boyes, J., Yung, W.H., and Bolam, J.P., 2004. Subcellular localization of GABAB receptor subunits in rat globus pallidus. *J. Comp. Neurol*. **474**:340–352.

Chen, L., Chan, S.C.Y., and Yung, W.H., 2002, Rotational behavior and electrophysiological effects induced by GABAB receptor activation in rat globus pallidus. *Neuroscience* **114**:417–425.

Ciliax, B.J., Nash, N., Heilman, C., Sunahara, R., Hartney, A., Tiberi, M., Rye, D.B., Caron, M.G., Niznik, H.B., and Levey, A.I., 2000, Dopamine D(5) receptor immunolocalization in rat and monkey brain. *Synapse* **37**:125–145.

Clark, D., and White, F.J., 1987, D1 dopamine receptor – the search for a function: a critical evaluation of the D1/D2 dopamine receptor classification and its functional implications. *Synapse* **1**:347–388.

DeLong, M.R., 1990, Primate models of movement disorders of basal ganglia origin. *Trends Neurosci*. **13**:281–285.

Ferre, S., O'Connor, W.T., Svenningsson, P., Bjorklund, L., Lindberg, J., Tinner, B., Stromberg, I., Goldstein, M., Ogren, S.O., Ungerstedt, U., Fredholm, B.B., and Fuxe, K., 1996, Dopamine D1 receptor-mediated facilitation of GABAergic neurotransmission in the rat strioentopenduncular pathway and its modulation by adenosine A1 receptor-mediated mechanisms. *European Journal of Neuroscience* **8**:1545–1553.

Fujiyama, F., Stephenson, F.A., and Bolam, J.P., 2002, Synaptic localization of GABA(A) receptor subunits in the substantia nigra of the rat: effects of quinolinic acid lesions of the striatum. *Eur. J. Neurosci*. **15**:1961–1975.

Georgopoulos, A.P., DeLong, M.R., and Crutcher, M.D., 1983, Relations between parameters of step-tracking movements and single cell discharge in the globus pallidus and subthalamic nucleus of the behaving monkey. *J. Neurosci*. **3**:1586–1598.

Gerhardt, G.A., Cass, W.A., Huettl, P., Brock, S., Zhang, Z., and Gash, D.M., 1999, GDNF improves dopamine function in the substantia nigra but not the putamen of unilateral MPTP-lesioned rhesus monkeys. *Brain Res*. **817**:163–171.

Hikosaka, O., and Wurtz, R.H., 1983a, Visual and oculomotor functions of monkey substantia nigra pars reticulata. I. Relation of visual and auditory responses to saccades. *Journal of Neurophysiology* **49**:1230–1253.

Hikosaka, O., and Wurtz, R.H., 1983b, Visual and oculomotor functions of monkey substantia nigra pars reticulata. III. Memory-contingent visual and saccade responses. *Journal of Neurophysiology* **49**:1268–1284.

Hikosaka, O., and Wurtz, R.H., 1985, Modification of saccadic eye movements by GABA-related substances. II. Effects of muscimol in monkey substantia nigra pars reticulata. *Journal of Neurophysiology* **53**:292–308.

Huang, K.X., and Walters, J.R., 1994, Electrophysiological effects of SKF 38393 in rats with reserpine treatment and 6-hydroxydopamine-induced nigrostriatal lesions reveal two types of plasticity in D1 dopamine receptor modulation of basal ganglia output. *J. Pharmacol. Exp. Ther*. **271**:1434–1443.

Ilinsky, I.A., Tourtellotte, W.G., and Kultas-Ilinsky, K., 1993, Anatomical distinctions between the two basal ganglia afferent territories in the primate motor thalamus. *Stereotact. Funct. Neurosurg*. **60**:62–69.

Johnston, T., and Duty, S., 2003, Changes in GABA(B) receptor mRNA expression in the rodent basal ganglia and thalamus following lesion of the nigrostriatal pathway. *Neuroscience* **120**:1027–1035.

Kita, H., Nambu, A., Kaneda, K., Tachibana, Y., and Takada, M., 2004, Role of ionotropic glutamatergic and GABAergic inputs on the firing activity of neurons in the external pallidum in awake monkeys. *J. Neurophysiol*. **92**:3069–3084.

Kita, H., 2001, Neostriatal and globus pallidus stimulation induced inhibitory postsynaptic potentials in entopeduncular neurons in rat brain slice preparations. *Neuroscience* **105**:871–879.

Kita, H., and Kitai, S.T., 1991, Intracellular study of rat globus pallidus neurons: membrane properties and responses to neostriatal, subthalamic and nigral stimulation. *Brain Res*. **564**:296–305.

Kliem, M.A., and Wichmann, T., 2004, A method to record changes in local neuronal discharge in response to infusion of small drug quantities in awake monkeys. *J. Neurosci. Methods* **138**:45–49.

Kultas-Ilinsky, K., Ilinsky, I., Warton, S., and Smith, K.R., 1983, Fine structure of nigral and pallidal afferents in the thalamus: an EM autoradiography study in the cat. *J. Comp. Neurol*. **216**:390–405.

Mink, J.W., and Thach, W.T., 1991, Basal ganglia motor control. I. Nonexclusive relation of pallidal discharge to five movement modes. *J. Neurophysiol*. **65**:273–300.

Mody, I., and Pearce, R.A., 2004, Diversity of inhibitory neurotransmission through GABAA receptors. *Trends in Neurosciences* **27**:569–575.

Nakanishi, H., Hori, N., and Kastuda, N., 1985, Neostriatal evoked inhibition and effects of dopamine on globus pallidal neurons in rat slice preparations. *Brain Res*. **358**:282–286.

Neve, K.A., and Neve, R.L., 1997, *The Dopamine Receptors*. Totowa: Humana Press.

Pan, H.S., Penney, J.B., and Young, A.B., 1985, Gamma-aminobutyric acid and benzodiazepine receptor changes induced by unilateral 6-hydroxydopamine lesions of the medial forebrain bundle. *J. Neurochem*. **45**:1396–1404.

Richfield, E.K., Young, A.B., and Penney, J.B., 1987, Comparative distribution of dopamine D-1 and D-2 receptors in the basal ganglia of turtles, pigeons, rats, cats, and monkeys. *J. Comp. Neurol*. **262**:446–463.

Rick, C.E., and Lacey, M.G., 1994, Rat substantia nigra pars reticulata neurones are tonically inhibited via GABAA, but not GABAB, receptors in vitro. *Brain Research* **659**:133–137.

Ruskin, D.N., Bergstrom, D.A., and Walters, J.R., 2002, Nigrostriatal lesion and dopamine agonists affect firing patterns of rodent entopeduncular nucleus neurons. *Journal of Neurophysiology* **88**:487–496.

Semyanov, A., Walker, M.C., Kullmann, D.M., and Silver, R.A., 2004, Tonically active GABAA receptors: modulating gain and maintaining the tone. *Trends in Neurosciences* **27**:262–269.

Shen, K.Z., and Johnson, S.W., 1997, Presynaptic GABAB and adenosine A1 receptors regulate synaptic transmission to rat substantia nigra reticulata neurones. *J. Physiol.* (*Lond*). **505**:153–163.

Smith, Y., and Kieval, J.Z., 2000, Anatomy of the dopamine system in the basal ganglia. *Trends Neurosci*. **23**: S28–S33.

Smith, Y., Lavoie, B., Dumas, J., and Parent, A., 1989, Evidence for a distinct nigropallidal dopaminergic projection in the squirrel monkey. *Brain Res*. **482**:381–386.

Smith, Y., Shink, E., and Sidibe, M., 1998. Neuronal circuitry and synaptic connectivity of the basal ganglia. *Neurosurgery Clinics of North America* **9**:203–222.

Starr, P.A., Wichmann, T., van Horne, C., and Bakay, R.A., 1999, Intranigral transplantation of fetal substantia nigra allograft in the hemiparkinsonian rhesus monkey. *Cell Transplant* **8**:37–45.

Trevitt, T., Carlson, B., Correa, M., Keene, A., Morales, M., and Salamone, J.D., 2002, Interactions between dopamine D1 receptors and gamma-aminobutyric acid mechanisms in substantia nigra pars reticulata of the rat: neurochemical and behavioral studies. *Psychopharmacology (Berl)*. **159**:229–237.

Turner, R.S., and Anderson, M.E., 1997, Pallidal discharge related to the kinematics of reaching movements in two dimensions. *J. Neurophysiol*. **77**:1051–1074.

Waldvogel, H.J., Billinton, A., White, J.H., Emson, P.C., and Faull, R.L., 2004, Comparative cellular distribution of GABAA and GABAB receptors in the human basal ganglia: Immunohistochemical colocalization of the alpha1 subunit of the GABAA receptor, and the GABABR1 and GABABR2 receptor subunits. *J. Comp. Neurol*. **470**:339–356.

Waldvogel, H.J., Fritschy, J.M., Mohler, H., and Faull, R.L., 1998, GABA(A) receptors in the primate basal ganglia: an autoradiographic and a light and electron microscopic immunohistochemical study of the alpha1 and beta2,3 subunits in the baboon brain. *J. Comp. Neurol*. **397**:297–325.

Waldvogel, H.J., Kubota, Y., Fritschy, J., Mohler, H., and Faull, R.L., 1999, Regional and cellular localisation of GABA(A) receptor subunits in the human basal ganglia: An autoradiographic and immunohistochemical study. *J. Comp. Neurol*. **415**:313–340.

Wichmann, T., Bergman, H., Starr, P.A., Subramanian, T., Watts, R.L., and DeLong, M.R., 1999, Comparison of MPTP-induced changes in spontaneous neuronal discharge in the internal pallidal segment and in the substantia nigra pars reticulata in primates. *Exp. Brain Res*. **125**:397–409.

Wichmann, T., and Kliem, M.A., 2004, Neuronal activity in the primate substantia nigra pars reticulata during the performance of simple and memory-guided elbow movements. *J. Neurophysiol*. **91**:815–827.

Wichmann, T., Kliem, M.A., and DeLong, M.R., 2001, Antiparkinsonian and behavioral effects of inactivation of the substantia nigra pars reticulata in hemiparkinsonian primates. *Exp. Neurol*. **167**:410–424.

Yung, K.K., Bolam, J.P., Smith, A.D., Hersch, S.M., Ciliax, B.J., and Levey, A.I., 1995, Immunocytochemical localization of D1 and D2 dopamine receptors in the basal ganglia of the rat: light and electron microscopy. *Neuroscience* **65**:709–730.

THE BASAL GANGLIA-THALAMOCORTICAL CIRCUIT ORIGINATING IN THE VENTRAL PREMOTOR AREA (PMv) OF THE MACAQUE MONKEY

K. Nakano, T. Kayahara, and E. Nagaoka*

1. INTRODUCTION

It is well known that the basal ganglia-thalamocortical loops remain anatomically and physiologically segregated into the motor, association and limbic loops. The available evidence based on our data suggested that the internal pallidal segment (GPi) contains multiple output channels each of which projects to a distinct cortical area in the frontal lobe (Nakano et al., 2000a,b). Output channels related to the primary motor area (MI) and supplementary motor area proper (SMA pro) appear to be topographically separated from those of the premotor area (PM) and pre-SMA. The former loop is located more caudoventrolaterally than the latter one which is located more rostrodorsomedially in the GPi. The SMA loop appears to be intermediate between the MI and PM loops with overlap. The relationships between the basal ganglia-thalamocortical loops arising from the ventral premotor area (PMv) and the dorsal premotor area (PMd) have not been completely clarified. Using a transneuronal tracing method, Strick and his associates (1995) demonstrated the ventrolateral GPi projection to the PMv through the nucleus ventralis lateralis pars oralis (VLo). In the present paper, we demonstrated a possible circuit of the basal ganglia-thalamocortical sub-loop arising from the PMv, and the region of the GPi and thalamic nuclei relaying this circuit are the ventromedial part of the GPi, the ventral part of nucleus ventralis anterior pars parvicellularis (VApc) and the nucleus ventralis lateralis pars medialis (VLm). We consider the PMv sub-loop may play a crucial role in the manipulation of hand movements.

* K. Nakano, Department of Physical Therapy, Faculty of Health Science, Suzuka University of Medical Science, Suzuka, Mie 510-0293, Japan. T. Kayahara, E., Nagaoka, Department of Anatomy, Faculty of Medicine Mie University, Tsu, Mie 514-8507, Japan.

2. MATERIALS AND METHODS

Sixteen Japanese monkeys (*Macaca fuscata*), weighing 3.0–7.7 kg, were used. All experiments were performed according to the Guideline for Care and Use of Laboratory Animal of the National Institutes of Health, and were approved by the Committee for Animal Research of Mie University. The monkeys were anesthetized with ketamine hydrochloride (10 mg/kg, i.m.), followed by sodium pentobarbital (15–30 mg/kg, i.p.), and the operation was done under aseptic conditions.

In five monkeys, single injections (0.06 µl) of 2% wheatgerm agglutinin-horseradish peroxidase (WGA-HRP) were made stereotaxically into the VApc, and VLm of the thalamus or the ventromedial part of the putamen (Put), and three point injections (a total of 1.2 µl) into the PMv using pneumatic picopump made through a glass micropipette. After a two-day survival period, each animal was deeply anesthetized again and fixed by perfusion of 8% formalin and 0.15% glutaraldehyde in 0.1 M phosphate buffer (pH 7.4). The brains were removed, and saturated with 30% sucrose in the same fresh buffer at 4°C for 2–3 days. Frontal serial sections were cut with a freezing microtome at 50 µm thickness. Some sections were processed for cytoarchitecture using Nissl stain. The remaining sections were processed for HRP reaction using tetramethyl-benzidine (TMB) as the substrate and counter stained with neutral red. In four monkeys, a 0.3–0.4 µl of 5% biotinylated dextran amine (BDA) solution in saline was pressure-injected in the VApc or VLm. After a survival time of 10–16 days, the monkeys were sacrificed. The brain sections were stained histochemically for DAB using Vectastain ABC kit (Vector Laboratories), and then examined by bright- and dark-field microscopy. In seven monkeys, small volumes (0.3–0.5 µl) of ^{3}H-leucine concentrated to 30 µCi/µl were injected slowly into the VApc and VLm of the thalamic nuclei, and or into the ventromedial part of the Put, or in PMv. After 7-day survival, these animals were deeply re-anesthetized, and perfused through the left ventricle by 2000 ml of 10% buffered neutral formalin. Paraffin serial sections were subsequently cut at 7 µm, and processed for autoradiography. Using standard procedures (Cowan et al., 1972), the brain sections were coated with Sakura NR-M2 emulsion, and exposed for 4–28 weeks. After developing in Rendol for 8 min, the sections were counterstained with cresyl violet.

3. RESULTS

3.1. ^{3}H-leucine Injection in the Ventral Part of the Premotor Area (PMv)

An injection site in M123 was localized in the central portion of the rostral PMv, and the injected mass invaded all cortical layers with slight diffusion in the subcortical white matter. Anterogradely labeled fibers arising from the injection site passed through the subcortical white matter dorsal to the claustrum and reached the corpus callosum and the anterior limb of the internal capsule. Labeling fibers traversed the internal capsule and migrated to the striatum and the thalamus. Densely labeled terminals were detected in the ventromedial part of the Put (Fig. 1A) and lesser labeling terminals in the caudate nucleus, especially in the limited area adjoining the internal capsule. Other fibers arising from the injection site coursed ventrally through the external and extreme capsules, and were traceable dorsally to the ventromedial Put. The labeling of the Put was bilateral and almost mirror-like, but much heavier on the side of the injection. Labeling terminals in the Put

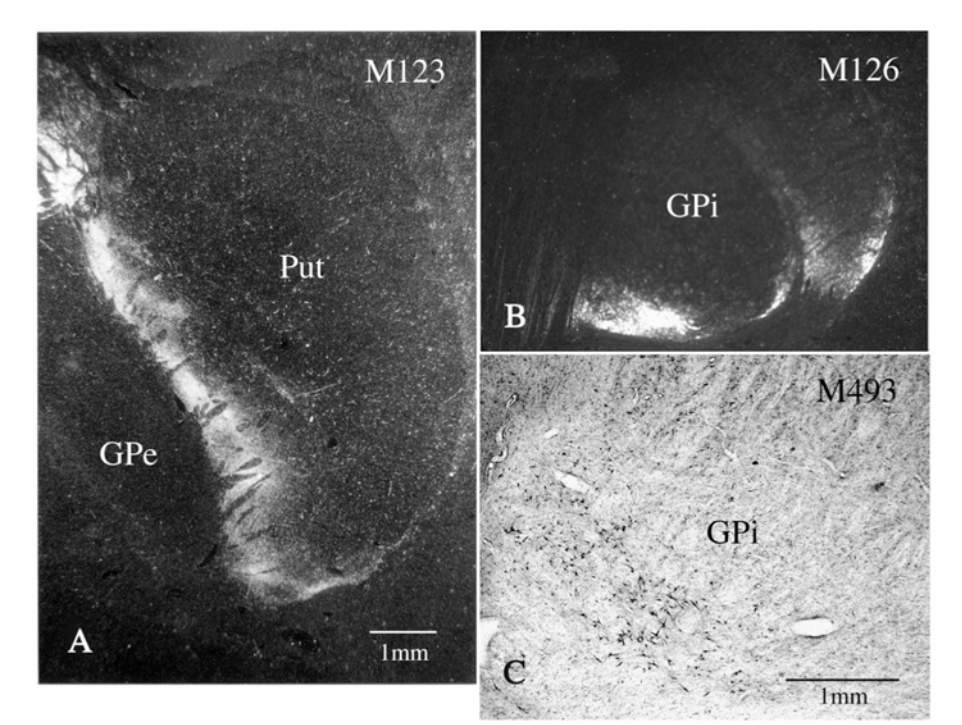

Figure l. Photomicrograph (A) showing anterograde terminal labeling in the ventromedial part of the putamen (Put) following ^{3}H-leucine injection in PMv. Photomicrograph (B) showing anterograde terminal labeling in the ventromedial portions of the internal pallidal segment (GPi) and the external pallidal segment (GPe) following WGA-HRP injection into the ventromedial Put. Photomicrograph (C) showing retrogradely labeled neurons in the medioventral portion of the GPi with a WGA-HAP injection in the ventral part of the nucleus ventralis lateralis pars parvicellularis (VApc) in the thalamus.

were most dense at the levels of the optic chiasm and postcommissural portion, and decreased in number at the level of the mammillary body. Dense labeling terminals were seen also in the ventral portion of the VApc and the dorsomedial part of the VLm in the thalamus.

3.2. WGA-HRP Injection in th e Ventromedial Part of the Postcommissural Put

An injection site of WGA-HRP was made in the ventromedial part of the postcommissural Put. Retrogradely labeled neurons in the frontal lobe were densest in the PMv, and denser in the cingulate motor area (ventral bank and fundus of the cingulate sulcus), and the fundus of the lateral orbital sulcus. A moderate number of labeled neurons were also found in the ventral bank of the principal sulcus in area 46. Anterogradely labeled terminals were dense in the ventromedial corner of the GPi (M438). A similar pattern of terminal labeling was observed in the GPi (Fig. 1B, M126) with ^{3}H-leucine injection in the ventromedial part of the post-commissural Put.

3.3. WGA-HRP Injections in VApc and VLm

In M493, the injection site is highly concentrated in the ventral part of the VApc with partial involvement of the dorsal part of the VLm, and with some spread into the needle tract in the dorsal VApc. Retrogradely labeled neurons were dense in the dorsomedial and medial parts of the GPi (Fig. 1C), mainly at the level of the ansa lenticularis, and only a few labeled neurons were detected in the dorsal part of the GPi at the level of the lenticular fascicle. In M577, the injection site was focused in the medial portion of the VLm and the small ventral part of the VApc. Retrogradely labeled neurons were present mainly in the medial to ventral margins of the GPi.

3.4. WGA-HRP Injections in PMv

Retrogradely labeled neurons in the thalamus were dense in the ventral portion of the VApc and the dorsomedial portion of the VLm, less dense in the ventrolateral part of the nucleus medialis dorsalis pars parvicellularis (MDpc) and paralamellar part (MDpl), the ventral part of the nucleus ventralis lateralis pars caudalis (VLc), and the central lateral intralaminar nucleus (CL), as well as the parafascicular nucleus (Pf) following three point injections in the PMv in M476.

3.5. BDA Injection in VApc and VLm

Following an injection of BDA linearly into the center of the VApc, dense labeling terminals were found in the superficial and deep cortical layers in the PMv, and only limited terminals were seen in the PMd as well as in the pre-SMA and SMA pro. In M792, BDA was injected in the medial part of the VLm and to a lesser extent in the ventral part of VApc. Anterogradely labeled terminals of BDA were dense in the superficial and deep cortical layers in the PMv and arcuate premotor area and partially in the PMd in addition to moderate terminals in the pre-SMA and SMA pro. Labeled terminals were seen in the deep layers in the frontal eye field.

4. DISCUSSION

The present findings raise the possibility of a basal ganglia-thalamo-PMv circuit in which the PMv projects to the ventromedial GPi via the ventromedial Put, and then the ventromedial GPi projects back to the PMv via the ventral VApc and dorsomedial VLm. However, the thalamic area relaying the PMv circuit of the basal ganglia-thalamocortical loops was indicated in the VLo (Strick et al., 1995). On the basis of our data, the VLo mainly relays the MI circuits of the basal ganglia-thalamocoritical loops, and the VApc relays the PM circuit (Nakano et al., 2000a,b). They also demonstrated the ventrolateral zone of the GPi to be the relay region of the PM circuit. In our cases, this relay area is located mainly in the medial portion of the GPi, and small ventral margin (Fig. 1B,C). The projection areas from the pre-SMA and SMA pro are separated rostrocaudally in the striatum. The pre-SMA projects to the lateral portion of the caudate nucleus and the dorsomedial portion of the Put with dense terminations in the cellular bridges in the anterior crus of the internal capsule (Inase et al., 1999). The PMd projects to the lateral CN, and the PMv to

the ventromedial zone of Put (Nakano et al., 2000a,b). Data in the present experiments also confirmed the PMv projection to the ventromedial zone of the Put, and further demonstrated the projection from this zone to the ventromedial GPi.

The topographical organization of the pallidothalamic projection indicated an anterior GPi projection to the VApc through the ansa lenticularis, a posterior GPi projection to the VLo, VLm and the centromedian nucleus through the lenticular fasciclus (Kim et al., 1976) or the medial GPi projection to the VApc through the ansa lenticularis, and the lateral GPi to the VLo through the lenticular fasciuclus (Ilinsky and Kultas-Ilinsky, 1987). The dorso-ventral (Kim et al., 1976; DeVito and Anderson, 1982) and medio-lateral topographies (Ilinsky et al., 1987) were reported in the GPi. In our cases, the dorsomedial part of the rostral GPi projects to the VApc through the ansa lenticularis and the ventrolateral part of the caudal GPi to the VLo through the lenticular fasciclus.

The GPi neurons receiving MI input were located in the ventrolateral part of the more caudal GPi, whereas the neurons receiving the prefrontal cortex (PFC) and PM were in the dorsomedial part of the more rostral GPi, and the neurons receiving input from the SMA-cingulate and arcuate premotor area were located in the intermediate zone of the GPi (Yoshida et al., 1993). The GPi-thalamic neurons projecting to SMA are located mainly in the VApc and the rostral portion of the VLo. The GPi-thalamic neurons projecting to the PM are distributed mainly in the dorsomedial part of the VApc (Jinnai et al., 1993). These findings are well agreement with our findings (Nakano et al., 1993). According to Sidibe et al. (1997), the dorsomedial GPi projects mainly to the VApc and VLd (dorsal part of the ventrolateral nucleus), the ventromedial GPi to the VLa (the anterior part of the ventrolateral nucleus corresponds to the VLo by Olszewski (1952), and the rostromedial pole of the GPi (association GPi) to the VApc and VM (the ventromedial nucleus corresponds to the VLm by Olszewski (1952). In their figure 6, the VLa region receiving the ventromedial GPi input appears to include the ventral part of the VApc. In our experiments, neurons projecting to the pre-SMA were mainly present in the lateral part of the VApc, which receives the GPi afferents from the intermediate zone adjoining the dorsomedial GPi; neurons projecting to the SMA pro were in the rostromedial VLo and the transitional part of the VApc-VLo, which receive the GPi afferents from the intermediate zone adjoining the ventrolateral GPi; and neurons projecting to the PMv are in the ventral part of the VApc and the VLm, which receive the GPi afferent from the ventromedial GPi. Neurons projecting to the PMd are located in the more dorsal portion of the VApc (Nakano et al., 1993). The caudal part of the PM connects with the VLc, and the rostral part of the PM with the VApc (Wiesendanger, 1981). The rostral part of the PMd connects with the more dorsomedial and rostral parts of thalamic neurons than the thalamic neurons connecting to the caudal PMd (Inase et al., 1994). The pallidal information conveyed to the pre-SMA from the VApc appears to be functionally linked to the association cortices (Sakai et al., 2000). The MI and SMA pro appear to be directly linked to movement execution, and the pre-SMA to be implicated in more cognitive aspects of motor behavior (updating motor plans) (Hikosaka et al., 1999).

The PMv has widespread connections with the prefrontal cortex (PFC), MI, SMA and also the sensory-related cortices (Barbas and Pandya, 1987; Matelli et al., 1986). The PMv receives visual input from the visual high order, polysensory areas of the inferior parietal lobule (see review by Boussaoud et al., 1996; Andersen et al., 1990; Cavada and Goldman-Rakic, 1989), and has heavy projections to hand/arm regions of the MI (Matelli et al., 1986). Area 7a is reciprocally interconnected with multiple visual-related areas, and also

receives vestibular input to integrate visual and vestibular information. Area 7a appears to play a role in spatial perception (see Andersen et al., 1990). Area 7ip may be an important source of visual input to the PMv (Fogassi et al., 1996). The object size and shape are coded in the inferior parietal lobule, especially in the caudal part of the lateral bank of the intraparietal sulcus (LIP) (Shikata et al., 1996) and in the anterior intraparietal area (AIP) (Sakata et al., 1995; Taira et al., 1990). The intraparietal sulcal area (IPS) plays a role in spatial perception, reaching and attention, and is implicated in visual and somatosensory integration. The LIP receives inputs from visual, somatosensory, motor, and polysensory areas, and from presumed vestibular- and auditory-related areas. Multimodal integration appears to be strongest in the fundus of the IPS. The medial bank of the IPS is connected with somatosensory and somatomotor areas, and the lateral bank corresponds with visual areas. The fundus has connections with both (for references, see Lewis and Van Essen, 2000).

The AIP has rich connections with the rostral PMv (F5) (Matelli et al., 1994). Neurons in the F5 discharge during goal-directed hand movements (Murata et al., 1997). F5 has visuomotor neurons, codes the object shape, and relates to the presentation of 3-D objects. F5 neurons appear to respond by representing an object description either in visual or motor terms (Murata et al., 1997). F5 has a more direct access to motor output at the spinal level than other regions of the PMv (Dum and Strick, 1991; He et al., 1993), and controls hand movements (Rizzolatti et al., 1981, 1988). The caudal PMv (F4) does not project to the spinal cord and receives substantial thalamic input both from the VLo, and area X (He et al., 1993; Matelli et al., 1989). Periarcuate neurons represent hand movement towards the mouth (Rizzolatti et al., 1981). F4 sends direct connections to arm and mouth fields of F1 (Matelli et al., 1986). There is no representation of distal movements in F4. Most neurons in the F4 code space in somatocentered field to control arm and head movements (Fogassi et al., 1996). F4 has a possible role in providing a spatial framework for the organization of head and arm movements (Fogassi et al., 1996).

The posterior parietal cortex also is a major source of input to the PFC, and provides information to the PFC on the location of objects in extrapersonal space. The dorsolateral PFC and posterior parietal lobule form part of a distributed network subserving spatially guided behavior (Selemon and Goldman-Rakic, 1988). The parietal cortex could provide the PMv with spatial information for on-line guidance of movements in extrapersonal space. The dorsolateral PFC could provide the PMv with spatial information stored in short-term memory for the internal guidance of movements (Selemon and Goldman-Rakic, 1988). The PMv is thought to be primarily involved in the initiation and guiding limb movements in extrapersonal space and in the postural adjustment during skilled movement of the limbs based on visual cues and other sensory information (see Godschalk et al., 1981; Rizzolattie et al., 1988; Gentilucci et al., 1988; 1989). We consider the sub-loop arising from the PMv may play a crucial role for the manipulation of hand movements.

5. CONCLUSION

The PMv projects to the ventromedial zone of the Put, which connects to the medial to ventromedial portions of the GPi. The ventral part of the VApc and the medial part of the VLm receive the basal ganglia output from these GPi regions, and make a final link back to the PMv.

6. ACKNOWLEDGEMENTS

This study was supported in part by a Grant-in-Aid for Scientific Research (C)13680829 from the Ministry of Education, Culture, Sports, Science, and Technology of Japan.

7. REFERENCES

Andersen, R.A., Asanuma, C., Essick, G., and Siegel, R.M., 1990, Corticocortical connections of anatomically and physiologically defined subdivisions within the inferior parietal lobule, *J. Comp. Neurol*. **296**:65–113.

Barbas, H., and Pandya, D.N., 1987, Architecture and frontal cortical connections of the premotor cortex (area 6) in the rhesus monkey, *J. Comp. Neurol*. **256**:211–228.

Boussaoud, D., di Pellegrino, G., and Wise, S.P., 1996, Frontal lobe mechanisms subserving vision-for-action versus vision-for-perception. *Behav. Brain Res*. **72**:1–15.

Cavada, C., and Goldman-Rakic, P.S., 1989, Posterior parietal cortex in rhesus monkey: II. Evidence for segregated corticocortical networks linking sensory and limbic areas with the frontal lobe, *J. Comp. Neurol*. **287**:422–445.

Cowan, W.M., Gottlieb, D.I., Hendrickson, A.E., Price, J.L., and Woolsey, T.A., 1972, The autoradiographic demonstration of axonal connections in the central nervous system, *Brain Research* **37**:21–51.

DeVito, J.L., and Anderson, M.E., 1982, An autoradiographic study of efferent connections of the globus pallidus in *Macaca mulatta*, *Exp. Brain Res*. **46**:107–117.

Dum, P.R., and Strick, P.L., 1991, The origin of corticospinal projections from the premotor areas in the frontal lobe, *J. Neurosci*. **11**:667–689.

Fogassi, L., Gallese, V., Fadiga, L., Luppino, G., Matelli, M., and Rizzolatti, G., 1996, Coding of peripersonal space in inferior premotor cortex (area F4), *J. Neurophysiol*. **76**:141–157.

Gentilucci, M., Fogassi, L., Luppino, G., Matelli, M., Camarda, R., and Rizzolatti, G., 1988, Functional organization of inferior area 6 in the macaque monkey, I. Somatotopy and the control of proximal movements, *Exp. Brain Res*. **71**:475–490.

Gentilucci, M., Fogassi, L., Luppino, G., Matelli, M., Camarda, R, and Rizzolatti, G., 1989, Somatotopic representation in inferior area 6 of the macaque monkey, *Brain Behav. Evol*. **33**:118–121.

Godschalk, M., Lemon, R.N., Nijs, H.G., and Kuypers, H.G.J.M., 1981, Behaviour of neurons in monkey periarcuate and precentral cortex before and during visually guided arm and hand movements, *Exp. Brain Res*. **44**:113–116.

He, S-Q., Dum, R.P., and Strick, P.L., 1993, Topographic organization of corticospinal projections from the frontal lobe: Motor areas on the lateral surface of the hemisphere, *J. Neurosci*. **13**:952–980.

Hikosaka, O., Nakahara, H., Rand, M.K., Sakai, K., Lu, X., Nakamura, K., Miyachi, S., and Doya, K., 1999, Parallel neural networks for learning sequential procedures, *Trends Neurosci*. **22**:464–471.

Ilinsky, I.A., and Kultas-Ilinsky, K., 1987, Sagittal cytoarchitectonic maps of the *Macaca mulatta* thalamus with a revised nomenclature of the motor-related nuclei validated by observations on their connectivity, *J. Comp. Neurol*. **262**:331–364.

Inase, M., and Tanji, J., 1994, Projections from the globus pallidus to the thalamic areas projecting to the dorsal area 6 of the macaque monkey: a multiple tracing study, *Neurosci. Lett*. **180**:135–137.

Inase, M., Tokuno, H., Nambu, A., Akazawa, T., and Takada, M., 1999, Corticostriatal and corticosubthalamic input zones from the presupplementary motor area in the macaque monley: comparison with the input zones from the supplementary motor area, *Brain Res*. **833**:191–201.

Jinnai, K., Nambu, A., Tanibuchi, I., and Yoshida, S., 1993, Cerebello- and pallido-thalamic pathways to areas 6 and 4 in the monkey. *Stereotact. Funct. Neurosurg*. **60**:70–79.

Kim, R., Nakano, K., Jayaraman, A., and Carpenter, M.B., 1976, Projections of the globus pallidus and adjacent structures: an autoradiographic study in the monkey, *J. Comp. Neurol*. **169**:263–290.

Lewis, J.W., and Van Essen, D.C., 2000, Corticocortical connections of visual, sensorimotor, and multimodal processing areas in the parietal lobe of the macaque monkey, *J. Comp. Neurol*. **428**:112–137.

Matelli, M., Camarda, R., Glickstein, M., and Rizzolatti, G., 1986, Afferent and efferent projections of the inferior area 6 in the macaque monkey, *J. Comp. Neurol*. **251**:281–298.

Matelli, M., Luppino, G., Fogassi, L., and Rizzolatti, G., 1989, Thalamic input to inferior area 6 and area 4 in the macaque monkey, *J. Comp. Neurol*. **280**:468–488.

Murata, A., Fadiga, L., Fogassi, L., Gallese, V., Raos, V., and Rizzolatti, G., 1997, Object representation in the ventral premotor cortex (area F5) of the monkey, *J. Neurophysiol*. **78**:2226–2230.

Nakano, K., Hasegawa, Y., Kayahara, T., Tokushige, A., and Kuga, Y., 1993, Cortical connections of the motor thalamic nuclei in the Japanese monkey, *Macaca fuscata*. *Stereotact. Funct. Neurosurg*. **60**:42–61.

Nakano, K., Kayahara, T., Tsutsumi, T., and Ushiro, H., 2000, Neural circuits and functional organization of the striatum, *J. Neurol*. **247** Suppl 5:1–15.

Nakano, K., 2000, Neural circuits and topographic organization of the basal ganglia and related regions, *Brain Dev*. **22** Suppl:S5–S16.

Olszewski, J., 1952, The Thalamus of the Macaca mulatta. An Atlas for Use with the Stereotaxic Instrument, Karger, Basel, 93pp.

Rizzolatti, G., Camarda, R., Fogassi, L., Gentilucci, M., Luppino, G., and Matelli, M., 1988, Functional organization of inferior area 6 in the macaque monkey, II. Area F5 and the control of distal movements. *Exp. Brain Res*. **71**:491–507.

Rizzolatti, G., Scandolara, C., Matelli, M., and Gentilucci, M., 1981, Afferent properties of periarcuate neurons in macaque monkeys, I. Somatosensory responses, *Behav. Brain Res*. **2**:125–146.

Sakai, S.T., Stepniewska, I., Qi, H.X., and Kaas, J.H., 2000, Pallidal and cerebellar afferents to pre-supplementary motor area thalamocortical neurons in the owl monkey: a multiple labeling study, *J. Comp. Neurol*. **417**:164–180.

Sakata, H., Taira, M., Murata, A., and Mine, S., 1995, Neural mechanisms of visual guidance of hand action in the parietal cortex of the monkey, *Cereb. Cortex* **5**:429–438.

Selemon, L.D., and Goldman-Rakic, P.S., 1988, Common cortical and subcortical targets of the dorsolateral prefrontal and posterior parietal cortices in the rhesus monkey: evidence for a distributed neural network subserving spatially guided behavior, *J. Neurosci*. **8**:4049–4068.

Shikata, E., Tanaka, Y., Nakamura, H., Taira, M., and Sakata, H., 1996, Selectivity of the parietal visual neurones in 3D orientation of surface of stereoscopic stimuli, *Neuroreport* **7**:2389–2394.

Sidibe, M., Bevan, M.D., Bolam, J.P., and Smith, Y., 1997, Efferent connections of the internal globus pallidus in the squirrel monkey: I. Topography and synaptic organization of the pallidothalamic projection, *J. Comp. Neurol*. **382**:323–347.

Strick, P.L., Dum, R.P., and Mushiake, H., 1995, Basal ganglia 'loops' with the cerebral cortex, in: Functions of the Cortico-Basal Ganglia Loop, M. Kimura, and, A.M. Graybiel, eds., Springer, New York, pp. 106–124.

Taira, M., Mine, S., Georgopoulos, A.P., Murata, A., and Sakata, H., 1990, Parietal cortex neurons of the monkey related to the visual guidance of hand movement, *Exp. Brain Res*. **83**:29–36.

Wiesendanger, M., 1981, Organization of secondary area of cerebral cortex, in: Handbook of Physiology. The Nervous System, II. Motor Control, Books, V.S., ed. Physiological Society, Washington, pp. 1121–1147.

Yoshida, S., Nambu, A., and Jinnai, K., 1993, The distribution of the globus pallidus neurons with input from various cortical areas in the monkeys, *Brain Res*. **611**:170–174.

THE SUBTHALAMIC REGION OF THE SHEEP

John S. McKenzie, and Michael J. McKinley*

1. INTRODUCTION

Among several functions attributed to the basal ganglia is a suggested role in the organization of habitual learning and behaviour (Graybiel, 1994, 1998; Hikosaka, 1994; Marsden, 1982). For a number of years we have studied different patterns of appetitive behaviour, both learned and instinctive, in the sheep (Weisinger et al., 1993), and in the course of these studies stereotaxic methods of working on the sheep brain were developed (McKenzie and Smith, 1971). During stereotaxically directed stimulation of the deep forebrain and diencephalon (McKenzie and Denton, 1974), some sites in the basal ganglia appeared to elicit elements of ingestive behaviour.

In recent years the subthalamic region has been recognised as making important contributions to the functions of the basal ganglia, going beyond the classical observations of hemiballismus following its pathological damage, to involvement in neurophysiological organisation, behavioural relations, and therapeutic interventions in the basal ganglia system (Levy et al., 1997),

The sheep brain is anatomically intermediate to small laboratory animals and primates, and offers the advantages of relative complexity and modest expense for a range of brain investigations. As part of a detailed anatomical characterisation of the sheep basal ganglia, we have studied the cytology and some histochemical properties of the subthalamic region as limited to its definition by Berman and Jones (1982). Thus limited, the ovine subthalamus contains mainly small to medium sized neuron perikarya (up to about 40 μm diameter), in the subthalamic nucleus of Luys, the zona incerta with separate dorsal and ventral divisions at most levels, and a poorly defined but extensive nucleus of the Fields of Forel. We have examined these components in frozen sections stained for Nissl bodies, for acetylcholinesterase (AChE), or NADPH-diaphorase (NADPH-d), and immunohistochemically for tyrosine hydroxylase (TH), dopamine β-hydroxylase (DBH), or the calcium–binding proteins calbindin, calretinin, and parvalbumin (Parent et al., 1996)

* John S. McKenzie, Department of Physiology, and Michael J. McKinley, Howard Florey Institute, University of Melbourne, Victoria 3010, Australia.

2. METHODS

Four Merino ewes were killed by intravenous injection of sodium pentobarbital (100 mg/kg), and the brains perfused via the carotid arteries with 4% paraformaldehyde in phosphate buffered saline. Brains were cryoprotected by immersion for several days in phosphate buffer containing 20% sucrose, and frozen sections then cut at 40 or 50 μm. Free-floating sections were histochemically stained for NADPH-d (Popeski et al., 1999), or subjected to standard immunohistochemical procedures using primary polyclonal antisera (obtained from Chemicon International) against calbindin, calretinin, parvalbumin, tyrosine hydroxylase, or dopamine β-hydroxylase. Other ewes supplied 60 or 80 μm frozen sections stained on the slide for Nissl bodies with cresyl fast violet (Conn et al., 1960) or for AChE (Paxinos and Watson, 1986).

3. RESULTS

3.1. Topography of Subthalamic Region in Sheep

In stereotaxic frontal sections the subthalamus of the sheep (Fig. 1) resembles that of the dog (Rioch, 1929; Adrianov and Mering, 1959).

The subthalamic nucleus lies above the dorsomedial surface of the cerebral peduncle as a band of neurons extending from the lateral mamillary nuclei ventromedially, to the most dorsal corner of the peduncle. Its lateral extremity is narrow, and an expanded middle section sits in a depression on the peduncular surface. Rostro-caudally it extends for about 3 mm. The zona incerta nucleus lies dorsal to the lateral half of the subthalamic nucleus, separated from it by the fibrous band of the fasciculus lenticularis, and from the overlying thalamus by the external capsule and the fasciculus thalamicus. At most levels the zona incerta is clearly separated into dorsal and ventral subdivisions by bands of nerve fibres (Fig. 1), except at its rostral and caudal ends, where it is undivided (as is almost all the nucleus in dogs). The dorsal and ventral divisions are fused medially, next to the field H of Forel. This is an ill defined cellular area pierced by many fibres, in which lies the extensive nucleus of the fields of Forel, associated with the subthalamic reaches of the fasciculus retroflexus caudally, and continuing rostrally up to the lateral hypothalamus.

No immuno-histochemical staining for DBH was observed in the subthalamic region of the sheep. However, in the bed nucleus of the stria terminalis lying against the anterior commissure and in some small regions of the ventral and periventricular hypothalamus, sharply stained small neurons and neuropil were found. The neurons of the magnocellular red nucleus were weakly stained for DBH.

3.2. Subthalamic Nucleus

The subthalamic nucleus (STN) is made up mainly of closely packed medium-sized neurons with ovoid or polygonal perikarya, of about 28 μm diameter, with some smaller neurons (Fig. 2A). In its middle expanded section, the STN displays structurally distinct regions, dorsal, dorsolateral with darker and slightly larger neurons, a large mid zone, and a thin ventral section. The cells are similar in all zones, differing in packing density, except in the round dorsolateral zone, in which the cells are somewhat larger; this zone expands

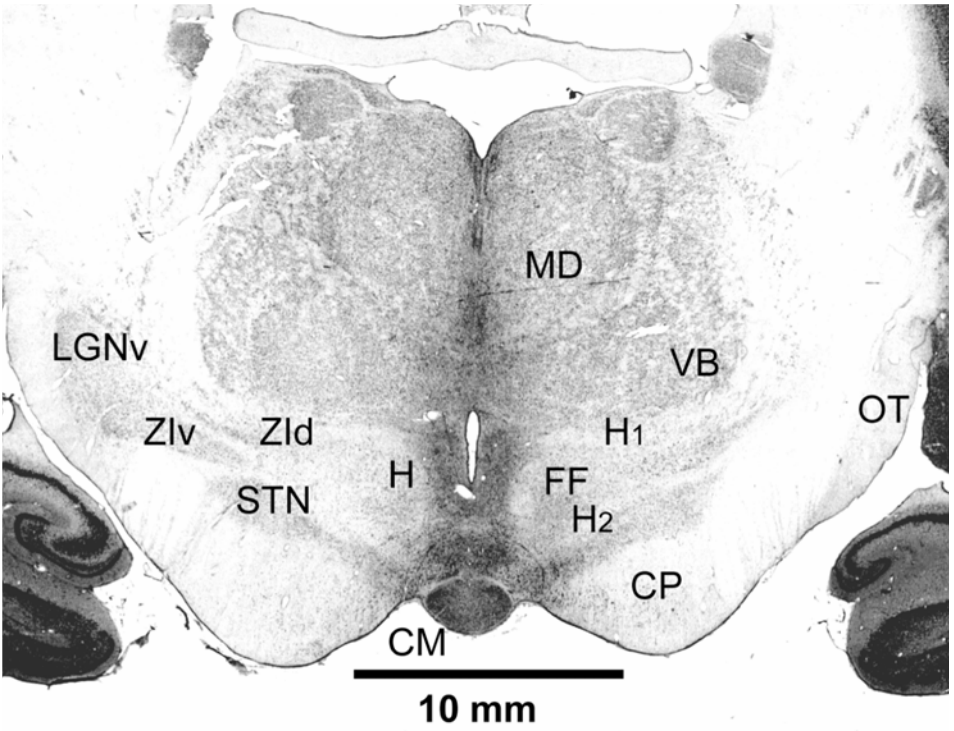

Figure 1. Thalamus and subthalamus of sheep brain, coronal Nissl section. CM: corpus mamillare; CP: cerebral peduncle; FF: nucleus of Fields of Forel; LGNv: ventral lateral geniculate nucleus; MD: dorsomedial thalamic nucleus; OT: optic tract; STN: subthalamic nucleus of Luys; VB: ventrobasal thalamic nucleus; ZId, ZIv: zona incerta pars dorsalis, pars ventralis.

in area more rostrally. An almost rectangular zone in frontal sections extends ventromedially towards the lateral mamillary nuclei, with cells more densely packed than in the main sectors of the nucleus. Near its most rostral sector, STN is intersected by neuron strands in diagonal arches that pass between the supramammillary area and the ventral lateral mamillary area at the medial cerebral peduncle (Fig. 1). STN neurons were deeply stained for NADPH-d, against a strongly stained background neuropil (Fig. 2D), and their proximal dendrites strongly stained for AChE (Fig. 2B, C).

Tyrosine hydroxylase staining demonstrated dense fibres covering the dorso-medial sector of STN, becoming sparse towards the cerebral peduncles and in more dorsal parts of zona incerta. At high power, the short TH fibre bundles in STN showed deeply staining terminal-like swellings as described by McKenzie et al., (2002). No neuron perikarya in STN demonstrated staining for calbindin or parvalbumin, but the entire nucleus contained deeply staining parvalbumin neuropil, with some fine apparent preterminals. With calretinin there were weakly stained small cells in the medial sector of STN and scattered in the subjacent cerebral peduncle. With calbindin, some stained fibres appeared to enter from (or into) the peduncle, against an unstained background.

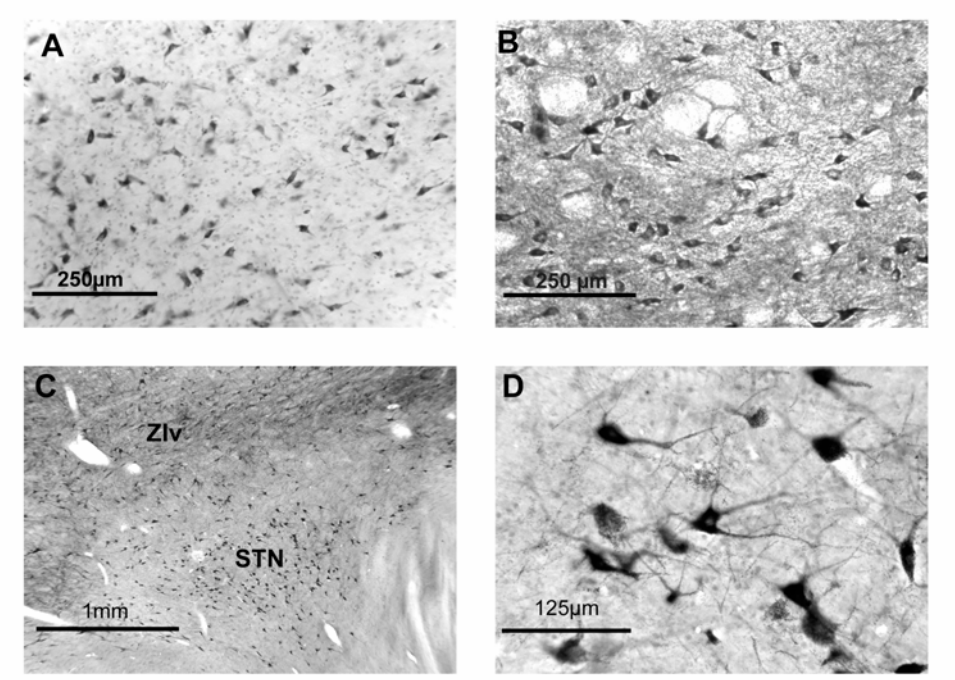

Figure 2. Subthalamic nucleus, different stains. A: Nissl; B: NADPH-d; C,D: Acetylcholinesterase, see Fig. 1.

3.3. Zona Incerta

The zona incerta (ZI) arises caudally in the pre-rubral field, where lateral neurons have the appearance of medium sized ZI cells found more rostrally. It contains neurons of heterogeneous size and shape, with perikarya of small (about 15 µm) to medium (about 40 µm) diameter (Fig. 3A). Caudally ZI is not divided into dorsal and ventral sections. It extends from the region of dorsal FF towards the reticular thalamic nucleus as dark medium cells among smaller neurons in Nissl sections. A separate ventral (ZIv) nucleus appears as a large area of smaller cells abutting the ventral lateral geniculate nucleus, then joining the dorsal (ZId) component medial to it. Further forward, the (ZId) and (ZIv) divisions arise medially in the same mass of medium sized darkly stained cells (Fig. 1, RHS), which appear similar to those in adjacent parts of the nucleus of the fields of Forel (FF). In ZId more laterally, the medium sized cells give way to a population of smaller and paler neurons, but in ZIv medium cells continue to dominate the appearance of the nucleus. Some medium, darker cells appear in ZId laterally towards the reticular thalamic nucleus (nRT), with which the ZI appears to merge. In some sections, there appears to be a further subdivision of ZId to form a thin dorsal lamina of mainly fusiform cells demarcated ventrally from the rest of ZId by a thin fibre band.

The larger perikarya, in both ZId and ZIv, were deeply stained for AChE, together with their dendrites; many of the smaller neurons appeared to stain more weakly, perhaps merely as a function of their size (Figs. 3B, C). NADPH-d positive neurons were mainly

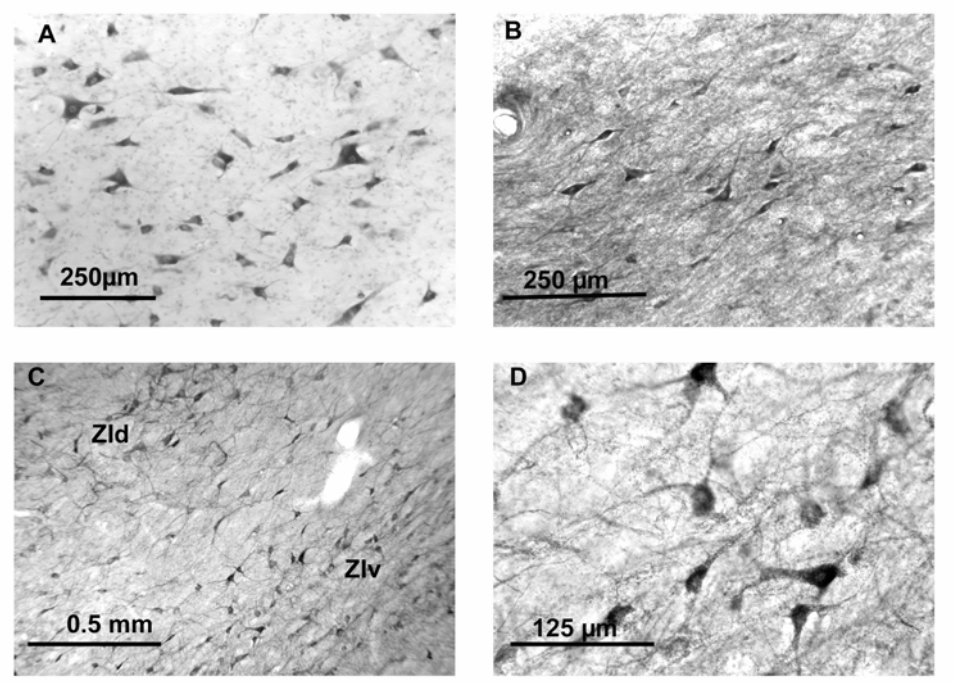

Figure 3. Zona incerta, different stains. A: ZLv, Nissl; B: ZLv, NADPH-d; C: ZId, ZLv, Acetylcholinesterase; D: ZIv, Acetylcholinesterase.

of medium size and relatively sparse in both sectors, lying among a well-stained neuropil (Fig. 3d).

Tyrosine hydroxylase-positive fibre bundles were dense in ZIv, with sparse terminal-like swellings. They were sparse to absent in ZId. Calbindin but not calretinin binding was seen in some scattered neurons in medial ZI, with weak background staining. Neuropil was stained for parvalbumin in both dorsal and ventral ZI, with only a few small cells stained in the lateral region. This contrasted with the plentiful stained neurons in the overlying thalamus as well as in the nRT contiguous with lateral ZI.

3.4. Fields of Forel

In the region adjacent to the fasciculus retroflexus, the FF contains dense groups of ovoid or fusiform neurons of medium size mixed with many smaller neurons (Fig. 4A). At some levels the medium cells are continuous with those of ZIv, or are scattered laterally with small cells towards ZId. In many FF cells, perikarya and dendrites were stained deeply for tyrosine hydroxylase among more widespread TH-positive neuropil (Figs. 4C, D). There were scattered small cells positive for NADPH-d in a positive neuropil. Ventral FF neuropil with many small neurons was heavily stained for AChE, but staining in dorsal field H1 was weaker. Among scattered calbindin positive cells in FF was a fairly compact group in which perikarya and dendrites were stained more deeply than background neuropil

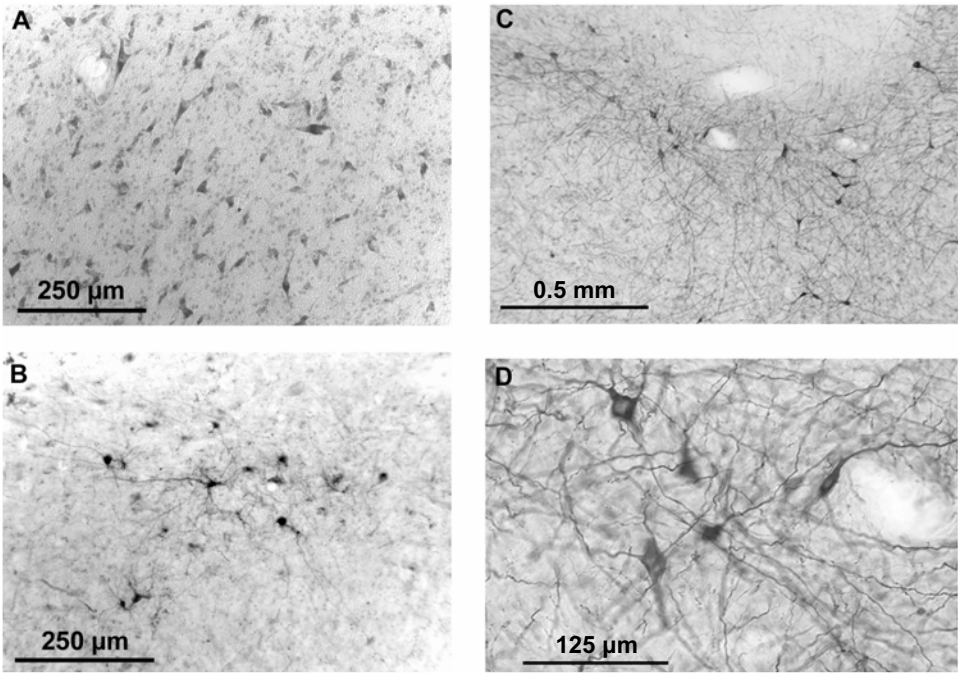

Figure 4. Nucleus of Fields of Forel, different stains. A: Nissl; B: Calbindin; C,D: Tyrosine hydroxylase.

(Fig. 4B). A few perikarya were stained weakly for calretinin through the FF region. Parvalbumin stained neuropil was present in most of the FF, with occasional positive small neurons and their dendrites.

4. DISCUSSION

4.1. Cytoarchitecture

Overall, the cell structure of the subthalamus is similar in sheep and other mammals. Heterogeneities of cytoarchitecture in STN lead some accounts to demarcate the ventromedial strip as posterior hypothalamus, but in the sheep there is gradual transition of cell density from central STN to this more closely packed sector (Fig. 1). Such difference is less marked in cat (Berman and Jones, 1982) and dog (Adrianov and Mering, 1959). The structure of ZI in sheep appears more complex than in rat (Paxinos and Watson, 1986), cat, and dog, with dorso-ventral and medio-lateral variations in cell size and density, dependent on rostro-caudal level. There are also differences in the relations of H1 and H2 fasciculi with the ZI nuclei, in that at different levels both ZId and ZIv appear to be further subdivided by small fibre bundles. The sheep's FF nucleus is relatively large in comparison with that of the cat (Berman and Jones, 1982; Bleier, 1961), and there is greater prominence of the medium sized cell groups, especially those merging with medial ZI. Because boundaries are often vague, its ventromedial cell group is sometimes included with posterior hypothalamus.

4.2. Functional Aspects

The connections of STN with other basal ganglia structures have been reviewed in detail by Parent and Hazrati (1995). The excitatory afferents from thalamic parafascicular nucleus (Féger et al., 1994) provide possible access to STN for non-specific somatic afferent information. Strong tyrosine hydroxylase staining of fibres in the dorsal part of STN and in ZIv indicate the presence of dopamine, since no dopamine β-hydroxylase staining was found in the subthalamic region, though it was strongly present in a few sites firther rostrally, in both cell bodies and axons (e.g. bed nucleus of stria terminalis). Dopaminergic innervation of the STN has been described in recent years (Parent and Hazrati, 1995), and the observations in sheep now suggest that the dopaminergic pathway extends terminals also to the ventral zona incerta. Such direct nigro-incertal innervation if significant in rats could provide a basis for the increase in functional activity of zona incerta neurons found by Périer et al. (2000) to follow 6-hydroxydopamine lesions of the substantia nigra.

The multifarious and reciprocal connections of ZI with virtually all major brain structures, summarized by Mitrofanis (2005), impose difficulties in attributing functions at present. The location of some chemical markers described for other mammals were only partly reproduced in sheep, where the density of parvalbumin stained cells was lower, and the distribution of NOS cells (indexed in sheep by NADPH-d staining) was wider and denser. GABAergic outputs of ZI appear to gate the responses to somatic input of some thalamic neurons (Trageser and Keller, 2004). The FF nucleus receives input from internal pallidum, from spinal cord, and brain stem reticular nuclei (Berman and Jones, 1982) with multiple neurophysiological pathways for somatic afferents (Denavit and Kosinski, 1968). Localised cooling in FF of cats has indicated that the nucleus plays a part in maintenance of vigilance (Naquet et al., 1966).

The functions of calcium-binding proteins in the brain are largely unknown, with much speculation. Parvalbumin staining of neurons has been correlated with GABAergic properties, but the correlation is imperfect (Parent and Hazrati, 1995). Its presence in STN neuropil of sheep is consistent with GABAergic pallido-Luysian pathways. The extensive NADPH-d staining in the subthalamus suggests an as yet unspecified role for NO on a broad scale.

5. REFERENCES

Adrianov, O.C., and Mering, T.A., 1959, *Atlas Mozga Sobaki*, State Pub. Med. Lit., Moscow, pp. 71–77.

Berman, A.L., and Jones, E.G., 1982, *The Thalamus and Basal Telencephalon of the Cat*, Univ. Wisconsin Press, p. 28.

Bleier, R. 1961, *The Hypothalamus of the Cat*, Johns Hopkins Press, Baltimore.

Conn, H.J., Darrow, M.A., and Emmels, V.M., 1960, *Staining Procedures Used by the Biological Stain Commission*, Williams and Wilkins, Baltimore, pp. 93–94.

Denavit, M., and Kosinski, E., 1968, Somatic afferents to the cat subthalamus, *Arch. Ital. Biol*. **106**:391–411.

Féger, J., Mouroux, M., Benazzouz, A., Borand, T., Gross, C., and Crossman, A., 1994, The subthalamic nucleus: a more complex structure than expected, in: *The Basal Ganglia IV*, G. Percheron et al., eds., Plenum Press, New York, pp. 371–382.

Graybiel, A.M., 1998, The basal ganglia and chunking of action repertoires, *Neurobiol. Learn. Mem*. **70**:119–136.

Graybiel, A.M., Aosakka, T., Flaherty, A.W., and Kimura, M., 1994, The basal ganglia and adaptive motor control, *Science* **265**:1826–1831.

Hikosaka, O., 1994, Role of basal ganglia in control of innate movements, learned behavior and cognition – a hypothesis, in: *The Basal* Ganglia *IV*, G. Percheron, et al., eds., Plenum Press, new York, pp. 579–588.

Levy, R., Hazzrati, L.-N., Herrero, M.-T., Vila, M., Hassani, O.-K., Mouroux, M., Ruberg, M., Asensi, H., Agid, Y., Féger, J., Obeso, J.A., Parent, A., and Hirsch, E.C., 1997, Re-evaluation of the functional anatomy of the basal ganglia in normal and parkinsonian states, *Neurosci*. **76**:335–343.

Marsden, C.D., 1982, The mysterious motor function of the basal ganglia: the Robert Wartenberg lecture, *Neurol*. **32**:514–538.

McKenzie, J.S., and Denton, D.A., 1974, Salt ingestion responses to diencephalic stimulation in the unrestrained conscious sheep, *Brain Res*. **70**:449–466.

McKenzie, J.S., and Smith, M.H., 1971, Stereotaxic method and variability data for the brain of the merino sheep, *J. f. Hirnforsch*. **14**:355–366.

McKenzie, J.S., Chai, S.Y., Giles, M., and McKinley, M.J., (2002), Dopaminergic system in the basal ganglia of sheep, in: *The Basal Ganglia VII*, L.F.B. Nicholson and R.L.M. Faull, eds. Kluver Academic/Plenum Publishers, New York, pp. 107–116.

Mitrofanis, J., 2005, Some certainty for the "zone of uncertainty"? Exploring the function of the zona incerta, *Neuroscience* **130**:128–154.

Naquet, R., Denavit, M., and Albe-Fessard, D., 1966, Comparaison entre le role du subthalamus et celui des différentes structures bulbomésencéphaliques dans le maintien de la vigilance, *Electroenceph. Clin. Neurophysiol*. **20**:149–164.

Parent, A., and Hazrati, L.-N., 1995, Functional anatomy of the basal ganglia. II. The place of subthalamic nucleus and external pallidum in basal ganglia circuitry, *Brain Res. Rev*. **20**:128–154.

Parent, A., Fortin, M., Côté, P.-Y., and Ciccheti, F., 1996, Calcium-binding proteins in primate basal ganglia, *Neurosci. Res*. **25**:309–334.

Paxinos, G., and Watson, C., 1986, *The Rat Brain in Stereotaxic Coordinates, second edn*. Academic Press, Sydney, p. ix.

Périer, C., Vila, M., Féger, J., Agid, Y., and Hirsch, E.C., 2000, Functional activity of zona incerta neurons is altered after nigrostriatal denervation in hemiparkinsonian rats, *Exp. Neurol*. **162:**215–224.

Popeski N., Amir S., Woodside, B., 1999, Changes in NADPH-d staining in the paraventricular and supraoptic nuclei during pregnancy and lactation in rats: role of ovarian steroids and oxytocin, *J. Neuroendoc*. **11**:53–61.

Rioch, D. McK., 1931, Studies on the diencephalon of carnivora, part III, *J. Comp. Neurol*. **53**:319–388.

Simpson, J.B., 1993, Forebrain lesions that disrupt water homeostasis do not

Trageser, J.C., and Keller, A., 2004, Reducing the uncertainty: gating of peripheral inputs by zona incerta, *J. Neurosci*. **24**:8911–8915.

Weisinger, R.S., Denton, D.A., McKinley, M.J., Miselis, R.R., Park, R.G., and Simpson, J.B., 1993, Forebrain lesions that disrupt water homeostasis do not eliminate the sodium appetite of sodium deficient sheep, *Brain Res*. **628:**166–178.

DIFFERENTIAL LOCALIZATION OF VESICULAR GLUTAMATE TRANSPORTERS 1 AND 2 IN THE RAT STRIATUM

Dinesh V. Raju and Yoland Smith*

1. INTRODUCTION

Glutamate is the most ubiquitous excitatory neurotransmitter in the central nervous system. Glutamate neurotransmission is involved in various brain functions, including motor control, learning and memory, cognition and neural development. Abnormal glutamatergic transmission also underlies many brain diseases, such as epilepsy, stroke, Parkinson's Disease (PD) and Huntington's Disease (Bleich et al., 2003). Despite these critical functions, the identification of glutamatergic neurons has been difficult. Glutamate and glutaminase immunostaining approaches have failed to conclusively identify glutamatergic neurons because glutamate is a common metabolite and precursor for the neurotransmitter γ-aminobutyric acid (GABA), and glutaminase, a glutamate-generating enzyme, is colocalized in some GABAergic neurons (Kaneko et al., 2002).

Recently, vesicular glutamate transporters (vGluTs) have been used to identify glutamatergic neurons because vGluT1 and vGluT2 have been shown to package glutamate into vesicles (Bellocchio et al., 2000; Takamori et al., 2001) and confer glutamatergic activity to GABAergic neurons (Takamori et al., 2000, 2001). Although vGluT1 and vGluT2 appear to have a complementary distribution in the rat CNS (Fremeau et al., 2001; Herzog et al., 2001; Kaneko et al., 2002; Varoqui et al., 2002), very little is known about the exact sources of axon terminals that express these transporters in the basal ganglia.

The striatum, the primary input nucleus of the basal ganglia, is rich in glutamatergic innervation from the cortex and thalamus (McGeorge and Faull, 1989; Berendse and Groenewegen, 1990). Medium spiny neurons (MSNs) are the projection neurons of the striatum. They have a 10–20 μm diameter soma, express GABA as their primary neurotransmitter, and are innervated by cortical and thalamic afferents (Kawaguchi, 1997; Cicchetti

* Yerkes National Primate Research Center and Dept. of Neurology, Emory University, 954 Gatewood RD NE, Atlanta, GA 30322, USA.

et al., 2000). Originating from layers III and V of virtually all cortical regions, corticostriatal afferents form asymmetric synapses onto dendritic spines of MSNs. Unlike cortical inputs, thalamostriatal afferents, which arise predominantly from the caudal intralaminar nuclei, form asymmetric synapses onto dendritic shafts (Dube et al., 1988; Sadikot et al., 1992). In light of previous tract tracing studies, a large proportion of terminals that innervate spines are thought to arise from sensorimotor cortices, whereas those that innervate dendrites originate predominantly from the parafascicular nucleus (PF), a caudal intralaminar thalamic nucleus (Somogyi et al., 1981; Dube et al., 1988; Berendse and Groenewegen, 1990).

The discrete synaptic localization of vGluT1 and vGluT2 suggests that these transporters are highly segregated and identify unique subpopulations of terminals and neurons in the striatum (Fremeau et al., 2001; Herzog et al., 2001; Kaneko et al., 2002; Varoqui et al., 2002). In this chapter, we highlight our recent findings of vGluT1 and vGluT2 electron microscopic localization in the rat striatum and discuss their relevance as selective markers of corticostriatal and thalamostriatal pathways.

2. VESICULAR GLUTAMATE TRANSPORTERS

Anatomically, the complementary distribution of vGluTs in nonoverlapping regions suggests that each isoform subserves particular regions of the central nervous system. *In situ* hybridization for vGluT1 mRNA shows strong signals in all layers of the cortex, hippocampal formation, lateral and basolateral amygdala, and the granule layer of the cerebellum (Hisano et al., 2000; Fremeau et al., 2001; Herzog et al., 2001). In contrast, vGluT2 mRNA is abundant in the thalamus, medial and central amygdala, and deep cerebellar nuclei (Hisano et al., 2000; Fremeau et al., 2001; Herzog et al., 2001).

Although there is no direct evidence for the existence of either vGluT protein in cortical or thalamic neurons projecting to the striatum, Hur and Zaborszky recently reported that vGluT2 mRNA is expressed in the majority of thalamocortical neurons projecting to the neocortex (Hur and Zaborszky, 2005). Immunocytochemistry for vGluTs shows complementary distribution in the neuropil of the rat CNS. For example, in the neocortex, all layers, except layer IV, express vGluT1 protein, whereas vGluT2 is abundant in layer IV (Fremeau et al., 2001; Varoqui et al., 2002). In the thalamus, the ventromedial and posterior nuclei are rich in vGluT1 protein, whereas the paraventricular, anterodorsal and reticular thalamic nuclei contain mostly vGluT2 protein (Varoqui et al., 2002). In the cerebellum, parallel fibers exclusively express vGluT1 in the adult rat, whereas the climbing fibers express only vGluT2 protein (Fremeau et al., 2001). Both vGluT1 and vGluT2 proteins are also observed in the neuropil of the striatum (Fremeau et al., 2001). At the ultrastructural level, vGluT1 and vGluT2 are exclusively expressed in terminals forming asymmetric synapses (Fremeau et al., 2001).

3. METHODS

3.1. Primary Antibodies

Two new anti-vGluT1 and anti-vGluT2 antibodies were generated. For anti-vGluT1 antibody, a peptide was generated to the COOH terminus of the rat vesicular glutamate

transporter 1 (rvGluT1), corresponding to amino acids 543–560 (cATHSTVQP-PRPPPPVRDY). The epitope is absolutely conserved in the mouse vGluT1 sequence and has one site of divergence in the human sequence (underlined above). For anti-vGluT2, a peptide was generated to the COOH terminus of the rat vesicular glutamate transporter 2 (rvGluT2), corresponding to amino acids 569–582 (cAQDAYSYKDRDDYS). This epitope shares 93% sequence homology with the mouse sequence and 71% homology with the human sequence. For each sequence, a cysteine was added to aid in conjugation to the protein carrier keyhole limpet hemocyanin (KLH; Pierce). Antisera were obtained from rabbits (Covance) immunized with the conjugated peptide and the IgG fraction was recovered by ammonium sulfate precipitation as follows: Sera was first treated with 25% ammonium sulfate to remove any proteins that might precipitate at low ionic concentrations and incubated with stirring overnight at 4°C. Following a 3000 g × 30 minute spin, the supernatant was removed and transferred to a clean tube. Ammonium sulfate was added to a final concentration of 50% saturation. After another overnight incubation at 4°C, the IgG fraction was isolated in the pellet by centrifugation at 3000 g × 30 minute. The pellet was resuspended in PBS and dialyzed overnight with 3 buffer changes. A polyclonal guinea pig anti-vGluT1 antiserum (Chemicon International, Temecula, CA) was also used.

3.2. Western Immunoblots

Fresh frozen brain tissue from one rhesus monkey (*M. mulatta*) and two Sprague-Dawley rats (Charles River Laboratories, Wilmington, MA) was homogenized, resolved by SDS-PAGE, and subjected to Western blot analysis with anti-vGluT1 (0.2 µg/ml) and anti-vGluT2 (0.2 µg/ml) antibodies. Immunoreactive bands were detected with the enhanced chemiluminescence detection system (Pierce, Rockford, IL) with horseradish peroxidase-conjugated goat anti-rabbit secondary antibody (1 : 4,000; Amersham Biosciences, Little Chalfont, United Kingdom). Preadsorbtion of primary antibody with synthetic peptide (0.2–0.4 µg/ml) overnight at 4°C abolished immunoreactivity, while preadsorbtion with a similar but non-identical peptide preserved immunoreactivity.

3.3. Tract-tracing

After being anesthetized with ketamine (60–100 mg/Kg) and dormitor (0.1 mg/Kg), six Sprague-Dawley rats were fixed in a stereotaxic frame. A glass micropipette (25–40 µm tip diameter), containing *Phaseolus vulgaris* leucoagglutinin (PHA-L) was placed in the PF or primary motor cortex (M1) (as per coordinates of Paxinos and Watson, 1998,) and iontophoretic delivery was performed with a 7 µA positive current for 20 minutes by a 7 sec ON/7 sec OFF cycle. Seven to ten days later, the rats were sacrificed.

3.4. Immunocytochemistry

All immunocytochemistry for vGluT1 and vGluT2 was performed on striatal tissue from normal Sprague Dawley rats (n = 3) and for PHA-L in rats with M1 (n = 3) and PF (n = 3) injections. For light microscopy, tissue was incubated with primary antibodies against the two transporters overnight at room temperature. Next, the primary antibodies (0.2 µg/ml for vGluT1, vGluT2; 0.5 µg/ml for anti-PHA-L) were reacted with species specific biotinylated secondary antibodies (0.4 µg/ml, Vector Labs, Burlingame, CA) which, in turn, were complexed with avidin/peroxidase (ABC Kit, Vector) to ultimately form an

avidin-biotin-peroxidase complex. In the presence of the chromogen 3,3′-diaminobenzidine tetrahydrochloride (DAB) and hydrogen peroxide, a diffusible reaction product forms to identify immunoreactivity for the transporter. At the light microscopic level, DAB appears as a brown deposit. Preadsorbtion tests were identical to those described above (see 3.2).

For single pre-embedding immunoperoxidase, tissue was incubated with primary antibodies against the two transporters for 48 hours at 4°C. Subsequent incubations were identical to those of the light microscopy protocol. After DAB revelation, the tissue was treated with osmium tetroxide and dehydrated with an increasing gradient of ethanol. During the dehydration, the sections were washed with uranyl acetate to improve contrast of the tissue at the electron microscope (EM). Next, the tissue was treated with propylene oxide, embedded in epoxy resin (Fluka) for 12 hours, mounted on slides and placed in an oven (60°C) for 48 hours. Striatal tissue was cut from the brain slices and mounted onto resin blocks. Using an ultramicrotome (Leica), the blocks were cut into 60 nm thick sections and placed onto copper grids. The ultrathin sections were stained with lead citrate and examined with a Zeiss EM-10C electron microscope at 25,000X magnification.

For double pre-embedding immunogold and immunoperoxidase, tissue was incubated with pooled primary antibodies for 24 hours, reacted with species specific 1.4 nm gold-conjugated (Nanoprobes, Yaphank, NY) and biotinylated (Vector) secondary antibodies, and washed with sodium acetate solution. The gold particles were intensified, which appear as 30–50 nm-sized electron-dense particles, using silver intensification (HQ Kit; Nanoprobes). Subsequent incubations and tissue processing was identical to that of the single immunoperoxidase procedure.

4. RESULTS

4.1. Antibody Specificity

Prior to performing immunocytochemical localization of vGluTs, antibody specificity was examined using Western blot analysis and preadsorbtion tests on rat striatal tissue for two recently generated antibodies (MAB Technologies, Atlanta, GA). All anti-vGluT antibodies used in this study recognized proteins of size similar to that of published values (~60 kDa) in striatal tissue, and preabsorbtion with antigenic peptide eliminated detection in Western immunoblots and in immunocytochemistry (Figure 1). Immunocytochemistry for all anti-vGluT antibodies used in this study in rat striatum was consistent with previously published studies (Fremeau et al., 2001; Herzog et al., 2001; Varoqui et al., 2002). Furthermore, minimal background labeling was detected on rat striatal tissue when the primary antibodies were omitted from the incubation solution. The specificity of the guinea pig anti-vGluT1 antibody (Chemicon) was previously shown with both immunoblotting and immunocytochemical analyses (Todd et al., 2003).

4.2. vGluT-Immunolabeling is Mainly in Terminals Forming Axo-spinous Synapses

At the light microscopic level, both anti-vGluT1 and anti-vGluT2 antibodies labeled exclusively the neuropil. Neuropil immunoreactivity was maintained at varying concentrations of primary antibodies (1–0.01 µg/ml for anti-vGluT1; 1–0.17 µg/ml for anti-vGluT2). Cell body labeling was never detected.

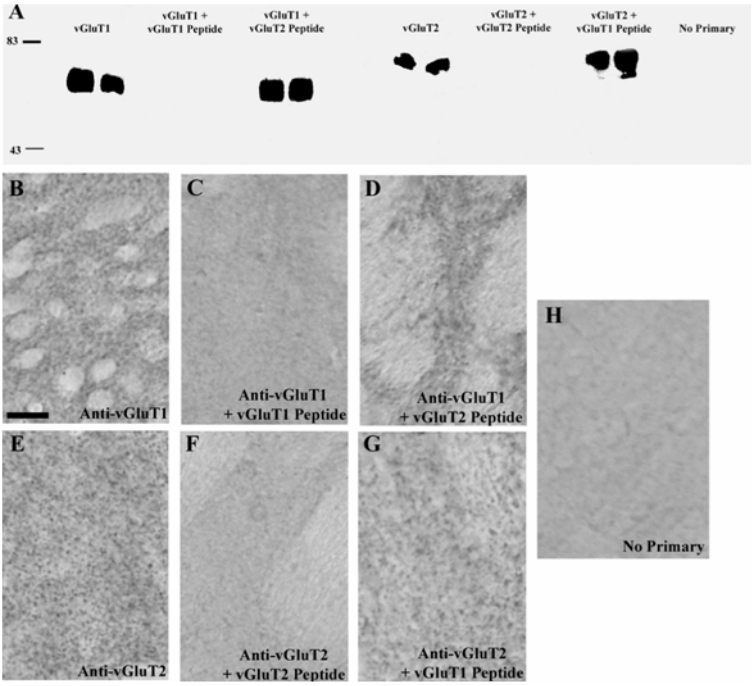

Figure 1. vGluT1 and vGluT2 antibody specificity. Anti-vGluT1 and anti-vGluT2 antibodies detected proteins of ≈60 kDa corresponding to the molecular weight predicted for vGluT1 and vGluT2 proteins (A). Immunoreactivity is completely abolished when antibodies are preadsorbed with the synthetic vGluT1 or vGluT2 peptide prior to immunoblotting (A). Immunoreactivity is preserved when anti-vGluT1 antibody is preabsorbed with synthetic vGluT2 peptide or when anti-vGluT2 antibody is preadsorbed with synthetic vGluT1 peptide (A). Light microscopic examination of striatal tissue with anti-vGluT1 and anti-vGluT2 antibodies demonstrates neuropil immunoreactivity (B, E), which is abolished when antibodies are preadsorbed with their corresponding synthetic peptides (C, F). Immunoreactivity is preserved when antibodies are preadsorbed with similar but non-identical synthetic peptides (D, G). Immunostaining of striatal tissue without primary antibodies is shown for reference (H). Molecular weight standards are indicated on the left (in kDa). Scale bar represents 50 μm for B-H.

Pre-embedding immunoperoxidase was performed to determine which types of terminals contain vGluT1 and vGluT2 in the rat striatum. All vGluT1- and vGluT2-immunopositive terminals formed asymmetric synapses (Figure 2). Furthermore, all synapses involved either dendrites or spines but not the soma. Most vGluT1- (<95%) and vGluT2-labeled (~80%) terminals formed asymmetric synapses onto spines. In addition, a sizable minority (~20%) of vGluT2-labeled boutons synapsed onto dendrites.

4.3. vGluT1 and vGluT2 are Rarely Co-Localized

Double pre-embedding immunoperoxidase and immunogold was performed to determine the degree of co-localization of the two vGluTs (Figure 3). The majority of all labeled terminals were immunopositive for vGluT1 (~78%), and colabeling for vGluT1 and vGluT2 was extremely low (~1.4%).

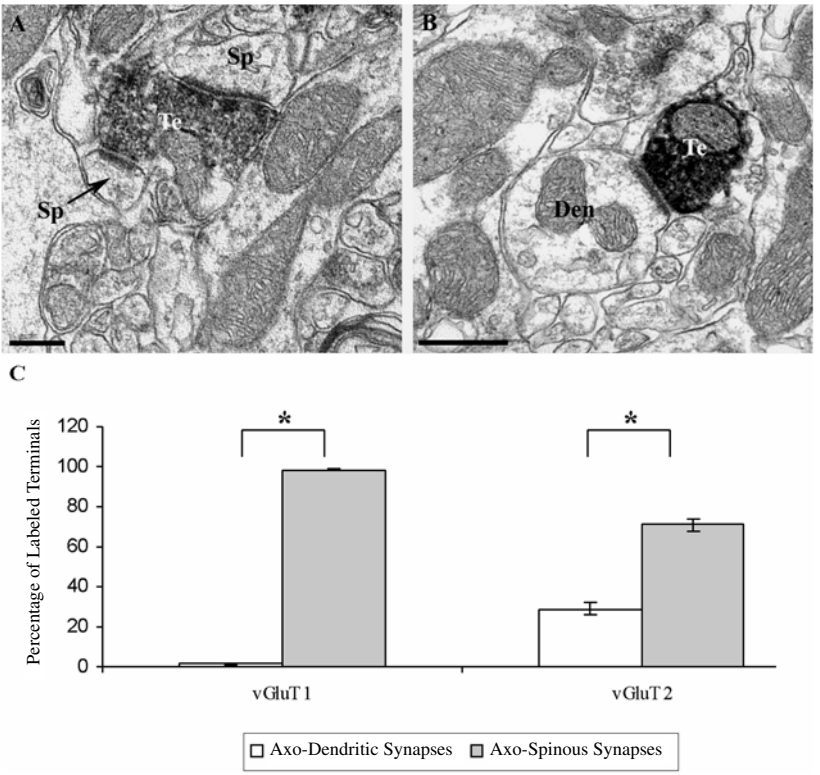

Figure 2. vGluT1 (A) and vGluT2 (B) in the striatum are expressed in terminals (Te) that form asymmetric synapses onto dendrites (Den) and spines (Sp). No labeled terminals forming symmetric synapses were detected. Pre-embedding immunoperoxidase using antibodies raised against two different epitopes of vGluT1 and vGluT2 generated similar results. As summarized in C, most vGluT1- and vGluT2-labeled terminals with Mab Technologies antibodies form synapses onto spines, though a substantial proportion of vGluT2-labeled terminals also form synapses onto dendrites (n vGluT1 = 323, vGluT2 = 234 labeled terminals). * Indicates statistically significant difference between the percentage of axo-dendritic and axo-spinous synapses (Student's t-test, $p < 0.05$). Error bars indicate SEM in C. Scale bars represent 0.5 µm for both A and B.

4.4. How does vGluT1/vGluT2 Distribution Compare to Corticostriatal and Thalamostriatal Projections?

To address this issue, PHA-L was iontophoretically injected into the M1 or PF. Pre-embedding immunoperoxidase for PHA-L was performed to identify the synaptology of afferents arising from M1 (n = 3) and PF (n = 3) in the striatum. Most corticostriatal afferents from M1 (~95%) formed axo-spinous synapses, while most thalamostriatal afferents from the PF (~83%) formed axo-dendritic synapses. These results confirm previous reports examining the synaptology of corticostriatal and thalamostriatal afferents in rats (Somogyi et al., 1981; Dube et al., 1988). The distribution of vGluT1-immunolabeled axon terminals is similar to that of corticostriatal afferents, whereas the distribution of vGluT2-immunolabeled axon terminals differs from that of thalamostriatal afferents described above (Sec 4.2; Figures 2 and 4).

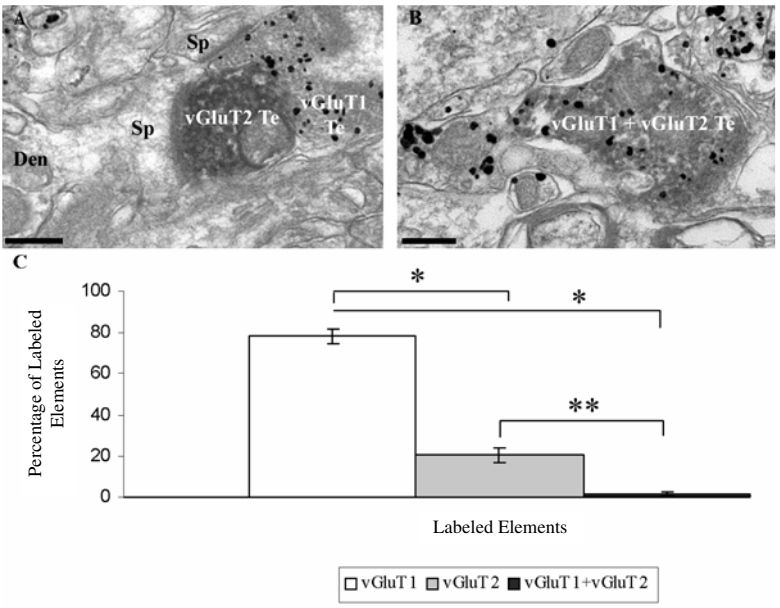

Figure 3. Immunoreactivity for vGluT1 and vGluT2 is rarely colocalized in the striatum. vGluT1 (labeled with immunogold) and vGluT2 (labeled with immunoperoxidase) immunostaining identifies separate populations of axon terminals (A, C). Immunoreactivity for vGluT1 and vGluT2 is found occasionally in the same terminal (B, C). Histogram for vGluT1 and vGluT2 immunoreactivity shows the relative abundance of vGluT1, vGluT2 and double labeled elements (n = 693 labeled elements, C). *, ** indicates statistically significant differences (One-way ANOVA $F(2,6) = 197.195$, $p < 0.001$; Tukey's post-hoc test, * $p < 0.001$; **, $p < 0.01$). Error bars indicate SEM in C. Scale bars represent 0.25 μm for both A and B.

5. DISCUSSION

In this study, we used highly specific polyclonal antibodies to characterize the synaptic connectivity of vGluT1- and vGluT2-containing terminals in the rat striatum. The main conclusions that can be proposed from the EM data are the following: First, both vGluT1- and vGlut2-labeled terminals form asymmetric synapses preferentially onto dendritic spines, though almost 20% of vGluT2-labeled terminals contact dendritic shafts. Second, vGluT1 and vGluT2 are largely segregated onto separate populations of axon terminals. Third, although vGluT1-labeled boutons display a pattern of synaptic connectivity similar to that of corticostriatal afferents, such is not the case for vGluT2-labeled boutons and the thalamostriatal projections from the PF. In the following account, we will briefly discuss the functional significance of these observations and relate their importance for a deeper understanding of glutamatergic modulation of striatal outflow.

The abundance of vGluT1 mRNA in the cortex and the large proportion of both vGluT1-immunoreactive terminals and motor cortical afferents forming axo-spinous synapses suggest that corticostriatal afferents express vGluT1. On the other hand, although a majority of vGluT2-labeled boutons form axo-spinous synapses, it is unlikely that vGluT2 identifies corticostriatal afferents because mRNA for this transporter is very sparse in the neocortex.

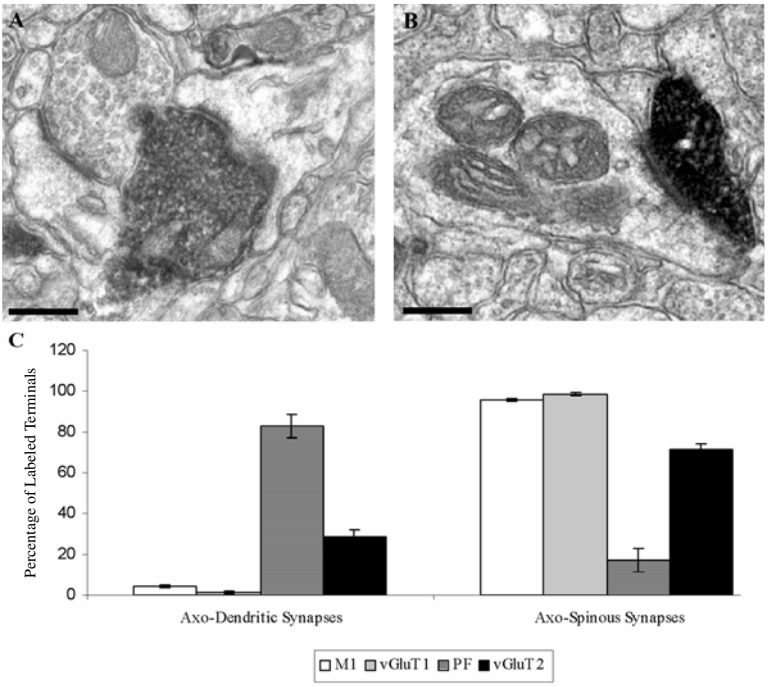

Figure 4. Comparison of the specific connectivity of PHA-L-labeled terminals from M1 or PF with vGluT1- and vGluT2-labeled boutons in rat striatum. Pre-embedding immunoperoxidase for PHA-L shows that corticostriatal projections from M1 (A, C) form predominantly axo-spinous synapses, and thalamostriatal afferents from PF (B, C) form predominantly axo-dendritic synapses. However, both vGluT1- and vGluT2-immunolabeled terminals mostly form synapses onto spines. n: M1 = 155, PF = 154, vGluT1 = 323, vGluT2 = 234 labeled terminals. Error bars indicate SEM in C. Scale bars represent 0.3 µm for both A and B.

In light of the preponderance of vGluT2 mRNA in the thalamus and the discrete populations of axon terminals identified by the two transporters (Figure 3), the large proportion of vGluT2-labeled axon terminals forming synapses onto spines suggests that specific thalamostriatal projections form axo-spinous synapses in the rat striatum. A reexamination of thalamostriatal projections from the PF showed that about 20% of axon terminals from this nucleus form axo-spinous synapses, a finding consistent with previous studies in rat and monkey (Dube et al., 1988; Sadikot et al., 1992). However, this relatively small proportion cannot account for the substantially larger number of vGluT2-immunopositive terminals that form axo-spinous synapses in the rat striatum. These results suggest that, in contrast to PF, other thalamic nuclei projecting to the striatum form mainly axo-spinous synapses. In line with this hypothesis, anterograde tract tracing studies of the central lateral nucleus showed that thalamostriatal afferents from this rostral intralaminar nucleus forms predominantly axo-spinous synapses in rats (Xu et al., 1991).

The functional significance of segregated glutamatergic inputs onto different compartments of striatal MSNs remains poorly understood. Similarly, the role of the thalamostriatal system in the functional circuitry of the basal ganglia is still a matter of speculation. The MSNs exist in “down” and “up” states, and while in the depolarized “up” state, the neuron is more likely to fire. Glutamatergic inputs from the neocortex are thought to bring striatal

neurons to a more depolarized state, where functionally grouped cortical inputs activate ensembles of "up" state MSNs to fire (Wilson, 1995; Kitano et al., 2001). Although highly simplified, this model does not include thalamostriatal input (Kitano et al., 2001). It is possible that individual thalamic nuclei bring specific MSNs to the "up" state, a situation that could then allow incoming cortical input to activate these striatofugal neurons. The spatio-temporal occurrence of excitation to depolarize the MSNs and subsequent excitation to activate the MSNs are likely to depend on the location of synapses (Kitano et al., 2001). For example, axo-dendritic synapses formed by PF afferents may play a more significant role than afferents from other thalamic nuclei forming axo-spinous synapses because depolarization of dendritic compartments and subsequent activation of neighboring spines are more likely to activate MSNs than depolarization and subsequent activation of a group of neighboring spines.

Although it is not as thoroughly characterized as in other brain regions, there is good evidence for localization/function relationships of specific inputs onto MSNs. For instance, it is well established that corticostriatal and nigrostriatal axon terminals converge onto the head and neck of dendritic spines of MSNs, respectively, creating a substrate for complex functional interplay between dopaminergic and cortical afferent regulation of MSN activity (Carlsson and Carlsson, 1990; Smith and Bolam, 1990; Smith et al., 1994). Evidence that thalamostriatal afferents form axo-spinous synapses would suggest that specific thalamostriatal afferents may also interact with nigrostriatal dopaminergic inputs, an interaction which may be of particular relevance for the understanding of the pathophysiology of PD (Ingham et al., 1998). It is noteworthy that previous studies from our laboratory have demonstrated that axo-dendritic thalamic inputs from the CM/Pf do not display any particular relationship with dopaminergic terminals in the monkey striatum (Smith et al., 1994). Whether the tight anatomical convergence between dopaminergic and glutamatergic inputs on spines of MSNs is specific for cortical afferents or possibly applies to other thalamostriatal afferents remains to be established.

6. ACKNOWLEDGEMENTS

This work was supported by grants from the NIH. We thank Mr. Marc Verrault for technical advice in performing stereotactic surgeries.

7. REFERENCES

Bellocchio, E.E., Reimer, R.J., Fremeau, R.T., Jr., and Edwards, R.H., 2000, Uptake of glutamate into synaptic vesicles by an inorganic phosphate transporter, *Science* **289**:957–960.

Berendse, H.W., and Groenewegen, H.J., 1990, Organization of the thalamostriatal projections in the rat, with special emphasis on the ventral striatum, *J. Comp. Neurol*. **299**:187–228.

Bleich, S., Romer, K., Wiltfang, J., and Kornhuber, J., 2003, Glutamate and the glutamate receptor system: a target for drug action, *Int. J. Geriatr. Psychiatry* **18**:S33–S40.

Carlsson, M., and Carlsson, A., 1990, Interactions between glutamatergic and monoaminergic systems within the basal ganglia–implications for schizophrenia and Parkinson's disease, *Trends Neurosci*. **13**:272–276.

Cicchetti, F., Prensa, L., Wu, Y., and Parent, A., 2000, Chemical anatomy of striatal interneurons in normal individuals and in patients with Huntington's disease, *Brain Res. Brain Res. Rev.* **34**:80–101.

Dube, L., Smith, A.D., and Bolam, J.P., 1988, Identification of synaptic terminals of thalamic or cortical origin in contact with distinct medium-size spiny neurons in the rat neostriatum, *J. Comp. Neurol*. **267**:455–471.

Fremeau, R.T., Jr., Troyer, M.D., Pahner, I., Nygaard, G.O., Tran, C.H., Reimer, R.J., Bellocchio, E.E., Fortin D., Storm-Mathisen, J., and Edwards, R.H., 2001, The expression of vesicular glutamate transporters defines two classes of excitatory synapse, *Neuron* **31**:247–260.

Herzog, E., Bellenchi, G.C., Gras, C., Bernard, V., Ravassard, P., Bedet, C., Gasnier, B., Giros, B., and El Mestikawy, S., 2001, The existence of a second vesicular glutamate transporter specifies subpopulations of glutamatergic neurons, *J. Neurosci*. **21**:RC181.

Hisano, S., Hoshi, K., Ikeda, Y., Maruyama, D., Kanemoto, M., Ichijo, H., Kojima, I., Takeda, J., and Nogami, H., 2000, Regional expression of a gene encoding a neuron-specific Na(+)-dependent inorganic phosphate cotransporter (DNPI) in the rat forebrain, *Brain Res. Mol. Brain Res*. **83**:34–43.

Hur, E.E., and Zaborszky, L., 2005, Vglut2 afferents to the medial prefrontal and primary somatosensory cortices: A combined retrograde tracing in situ hybridization, *J. Comp. Neurol.* **483**:351–373.

Ingham, C.A., Hood, S.H., Taggart, P., and Arbuthnott, G.W., 1998, Plasticity of synapses in the rat neostriatum after unilateral lesion of the nigrostriatal dopaminergic pathway, *J. Neurosci.* **18**:4732–4743.

Kaneko, T., Fujiyama, F., and Hioki, H., 2002, Immunohistochemical localization of candidates for vesicular glutamate transporters in the rat brain, *J. Comp. Neurol.* **444**:39–62.

Kawaguchi, Y., 1997, Neostriatal cell subtypes and their functional roles, *Neurosci. Res.* **27**:1–8.

Kitano, K., Aoyagi, T., and Fukai, T., 2001, A possible functional organization of the corticostriatal input within the weakly-correlated striatal activity: a modeling study, *Neurosci. Res*. **40**:87–96.

McGeorge, A.J., and Faull, R.L., 1989, The organization of the projection from the cerebral cortex to the striatum in the rat, *Neuroscience* **29**:503–537.

Sadikot, A.F., Parent, A., Smith, Y., and Bolam, J.P., 1992, Efferent connections of the centromedian and parafascicular thalamic nuclei in the squirrel monkey: a light and electron microscopic study of the thalamostriatal projection in relation to striatal heterogeneity, *J. Comp. Neurol.* **320**:228–242.

Smith, A.D., and Bolam, J.P., 1990, The neural network of the basal ganglia as revealed by the study of synaptic connections of identified neurones, *Trends Neurosci.* **13**:259–265.

Smith, Y., Bennett, B.D., Bolam, J.P., Parent, A., and Sadikot, A.F., 1994, Synaptic relationships between dopaminergic afferents and cortical or thalamic input in the sensorimotor territory of the striatum in monkey, *J. Comp. Neurol*. **344**:1–19.

Somogyi, P., Bolam, J.P., and Smith, A.D., 1981, Monosynaptic cortical input and local axon collaterals of identified striatonigral neurons, A light and electron microscopic study using the Golgi-peroxidase transport-degeneration procedure, *J. Comp. Neurol.* **195**:567–584.

Takamori, S., Rhee, J.S., Rosenmund, C., and Jahn, R., 2000, Identification of a vesicular glutamate transporter that defines a glutamatergic phenotype in neurons, *Nature* **407**:189–194.

Takamori, S., Rhee, J.S., Rosenmund, C., and Jahn, R., 2001, Identification of differentiation-associated brain-specific phosphate transporter as a second vesicular glutamate transporter (VGLUT2), *J. Neurosci.* **21**: RC182.

Todd, A.J., Hughes, D.I., Polgar, E., Nagy, G.G., Mackie, M., Ottersen, O.P., and Maxwell, D.J., 2003, The expression of vesicular glutamate transporters VGLUT1 and VGLUT2 in neurochemically defined axonal populations in the rat spinal cord with emphasis on the dorsal horn, *Eur. J. Neurosci.* **17**:13–27.

Varoqui, H., Schafer, M.K., Zhu, H., Weihe, E., and Erickson, J.D., 2002, Identification of the differentiation-associated Na+/PI transporter as a novel vesicular glutamate transporter expressed in a distinct set of glutamatergic synapses, *J. Neurosci.* **22**:142–155.

Wilson, C.J., 1995, The contribution of cortical neurons to the firing pattern of striatal spiny neurons, in: Models of Information Processing in the Basal Ganglia, D.G. Beiser, ed., MIT Press, Cambridge, pp. 29–50.

Xu, Z.C., Wilson, C.J., and Emson, P.C., 1991, Restoration of thalamostriatal projections in rat neostriatal grafts: an electron microscopic analysis, *J. Comp. Neurol.* **303**:22–34.

LOCAL CONNECTIVITY BETWEEN NEURONS OF THE RAT GLOBUS PALLIDUS

Ahmed-Ramadan Sadek, Peter J. Magill, and J. Paul Bolam*

1. INTRODUCTION

The globus pallidus (GP), or globus pallidus externa (GPe) in primates, is located in a central position in the macrocircuits of the cortico-basal ganglia-thalamo-cortical loops. Traditionally, the GP was considered as a relay between the striatum and the output nuclei, via its connection to the subthalamic nucleus (STN), and thus, part of the so-called 'indirect pathway' (Albin et al., 1989; DeLong, 1990). However, the morphology of GP neurons is not consistent with the simple unidirectional transmission of striatal information proposed in the now classic direct/indirect pathways model of basal ganglia organisation (Albin et al., 1989; DeLong, 1990). It is now known that the GP transmits topographically- and functionally-diverse information to all other nuclei of the basal ganglia. Indeed, single GP neurons, in addition to projecting to the STN, project to all the more caudal nuclei of the basal ganglia, and about a quarter to a third of the neurons also project back to the striatum (Nauta, 1979; Iwahori and Mizuno, 1981; Smith and Bolam, 1989, 1990; Kita and Kitai, 1994; Bevan et al., 1997, 1998; Sato et al., 2000; Kita and Kita, 2001). Globus pallidus neurons generally innervate their target neurons in their most proximal domains (Smith et al., 1998; Bolam et al., 2000). Thus, GP neurons are in a position to powerfully influence network activity and the flow of cortical information at many levels in the basal ganglia (Bolam and Smith, 1992; Bevan et al., 1996, 1997, 1998; Shink et al., 1996; Celada et al., 1999; Paladini et al., 1999). In addition to their long axonal projections, GP neurons also possess local axon collaterals. These local axonal collaterals are likely to play a critical role in the processing of striatal, subthalamic and other afferent information within the GP, and thus in sculpting the responses of GP neurons to these inputs.

* MRC Anatomical Neuropharmacology Unit, Mansfield Road, Oxford, OX1 3TH, U.K.

2. EVIDENCE OF LOCAL CONNECTIVITY WITHIN THE GP

The results of early Golgi-impregnation studies in the mouse, rat and primate demonstrated the presence of local axon collaterals arising from neurons of the GP (Iwahori and Mizuno, 1981; Francois et al., 1984; Millhouse, 1986). Similarly, intracellular labelling, juxtacellular labelling, single-axon tracing studies (Park et al., 1982; Kita and Kitai, 1994; Bevan et al., 1998; Sato et al., 2000) and immunohistochemical labelling techniques (Kita, 1994) have revealed the presence of local axon collaterals of GP neurons that give rise to terminal arborisations and boutons that appose unlabelled structures, some of which could be identified as perikarya. Whilst these studies have been instrumental in qualitatively characterising the local axon collaterals of GP neurons, a quantitative characterisation is critical in defining their role within the GP.

We have performed a detailed single-cell juxtacellular labelling study of GP neurons and their local collaterals in the rat (Sadek et al., 2003, 2004; Sadek, Magill and Bolam, 2005 *in preparation*). Following the juxtacellular labelling and recovery of the neurons we digitally reconstructed them in three dimensions using the Neurolucida system, obtained quantitative anatomical data and performed an electron microscopic analysis of their local collaterals. These analyses revealed that all GP neurons possess organised and extensive local axonal arborisations, but may be divided into two groups on the basis of their location within the GP and the number of boutons contained within their local axonal arborisations. One group is located in a band apposing the striatum (within ~100 μm of the striatal border) i.e., the lateral and rostral poles of the GP (hereafter referred to as 'lateral neurons'). The second group is located in the more medial and caudal aspects of the GP (hereafter referred to as 'medial neurons'). Neurons in both groups possess extensive local axonal arborisations and there is a correlation between the location of the neurons and the numbers of boutons in the arborisations, such that lateral neurons possess an average of 264 boutons whereas medial neurons possess an average of 581 boutons (Table 1). The local axonal arborisations are not homogeneously distributed within the GP but are divided into subregions that are located at different positions with respect to the parent cell body. The axons of both groups possess an arborisation located within the parent dendritic arborisation (hereafter referred to as the *proximal arborisation*) and an arborisation that is located caudo-ventro-medial to the soma (hereafter referred to as the *distal arborisation*), along the course taken by the striatofugal fibre bundles passing through the GP. Medial neurons also possess an intermediate axonal arborisation located within or very close to the dendritic arborisation, but it will be considered together with the proximal arborisation for the purposes of this discussion. The numbers of boutons contained within the different arborisations are summarised in Table 1.

Electron microscopic analysis of the local axonal arborisations revealed that the boutons identified at the light microscopic level, are indeed synaptic boutons, forming symmetrical synapses with the dendrites and perikarya of other GP neurons. This analysis revealed that the majority of terminals form synaptic contact with perikarya and proximal (first order) dendrites (61% for lateral neurons and 72% for medial neurons). This is consistent with the light microscopic observations because boutons of the local arbours are often seen closely associated with unstained perikarya and large diameter proximal dendrites. Thus, like the synapses formed by GP neurons in other regions of the basal ganglia, local axon collaterals predominantly make contact with such proximal domains of neighbouring GP neurons. The remainder of the synapses are formed at a greater distance from the perikaryon i.e., on higher-order dendrites.

Table 1. Quantitative model of connectivity between GP neurons.

Lateral Neurons	
1. Mean number of boutons in the local axonal arborisation	264
2. Mean number of boutons in the proximal axonal arborisation	166 (63%)
3. Mean number of boutons in the distal axonal arborisation	98 (37%)
4. Mean number of contacts with proximal domains formed by the proximal arborisation	133 (80%)
5. Mean number of contacts with distal dendrites formed by the proximal arborisation	33 (20%)
6. Maximum number of boutons from one GP neuron contacting the dendrite of another GP neuron (Park et al., 1982)	9
7. Maximum number of boutons from one GP neuron contacting the proximal domain of another GP neuron	14
8. Numbers of neurons contacted in their proximal domains by the proximal arborisation of a lateral neuron (i.e. minimum: #4 divided by #7; maximum: #4 divided 3)	10–44
9. Number of neurons receiving contacts onto their dendrites from the proximal arborisation of a lateral neuron (minimum: #5 divided by #6; maximum: #5 divided by 3)	4–11
10. Theoretical total number of GP neurons innervated by the proximal arborisation of a lateral neuron (sum of maxima and minima in #8 and #9)	14–55
11. Mean number of contacts with proximal domains formed by the distal arborisation	63 (64%)
12. Mean number of contacts with dendrites formed by the distal arborisation	35 (36%)
13. Numbers of neurons receiving contacts onto proximal domains formed by the distal arborisation of a lateral neuron (minimum: #11 divided by #7; maximum: #11 divided by 3)	5–21
14. Numbers of neurons receiving contacts onto their dendrites from the distal arborisation of one lateral neuron (minimum: #12 divided by #6; maximum: #12 divided by 3)	4–12
15. Theoretical total number of GP neurons innervated by the distal arborisation of one lateral neuron (sum of maxima and minima in #13 and #14)	9–33
16. Totalnumber of neurons a single lateral neuron may contact through its local axonal collaterals (sum of maxima and minima in #10 and #15)	**23–88**
Medial Neurons	
18. Mean number of boutons in the local axonal arborisation	581
19. Mean number of boutons in the proximal axonal arborisation	447 (77%)
20. Mean number of boutons in the distal axonal arborisation	134 (33%)
21. Mean number of contacts with proximal domains formed by the proximal arborisation	215 (48%)
22. Mean number of contacts with distal dendrites formed by the proximal arborisation	232 (52%)
23. Numbers of neurons contacted in their proximal domains by the proximal arborisation of a medial neuron (i.e. minimum: #21 divided by #7; maximum: #21 divided by 3)	15–72
24. Number of neurons receiving contacts onto their dendrites from the proximal arborisation of a medial neuron (minimum: #22 divided by #6; maximum: #22 divided by 3)	26–77
25. Theoretical total number of GP neurons innervated by the proximal arborisation of one medial neuron (sum of maxima and minima in #23 and #24)	41–149
26. Mean number of contacts with proximal domains formed by the distal arborisation	99 (74%)
27. Mean number of contacts with dendrites formed by the distal arborisation	35 (26%)
28. Numbers of neurons receiving contacts onto proximal domains formed by the distal arborisation of a medial neuron (minimum: #26 divided by #7 and a maximum: #26 divided by 3)	7–33
29. Number of neurons receiving contacts onto their dendrites from the distal collateral of one medial neuron (minimum: #27 divided by #6; maximum: #27/3)	4–12
30. Theoretical total number of GP neurons innervated by the distal collateral of one medial neuron (sum of maxima and minima in #28 and #29)	11–45
32. Totalnumber of neurons a single medial neuron may contact through its local axonal collaterals (sum of maxima and minima in #25 and #30)	**52–194**

3. QUANTITATIVE ESTIMATES OF LOCAL CONNECTIVITY

With knowledge of the numbers of axon terminals in a local axonal arborisation, and knowledge of their synaptic targets and pattern of innervation, we can make estimates of the degree of connectivity between GP neurons. However, certain assumptions have to be made.

3.1. Assumptions

3.1.1. Number of Contacts Formed by a Single GP Local Axon on a Single Postsynaptic Neuron

The facts that lateral neurons possess a mean of 264 boutons in their axonal arbour and medial neurons possess a mean of 581 boutons indicate that the maximum number of neurons that each cell type could contact is 264 and 581, respectively, if their local axon collaterals give rise to only a single synapse per target neuron. However, this is clearly not the case because both light and electron microscopic analyses indicate that single GP axons make multiple appositions or synapses with their targets (Park et al., 1982; Kita, 1994; Sadek et al., 2003, 2004; Sadek, Magill and Bolam, 2005 *in preparation*). We frequently observe single axons making multiple appositions to the proximal domains of target neurons at the light microscopic level and on higher order dendrites in the electron microscope. The maximum number of boutons from a single axon apposed to the proximal domains (defined as the primary dendrites and soma) of a single target neuron that we have observed is 14, of which 10 have been shown to make synapses (Sadek et al., 2003, 2004; Sadek, Magill and Bolam, 2005 *in preparation*). An earlier electron microscopic study identified that a single axon can form up to 9 boutons onto a single dendrite (Park et al., 1982). We thus make the assumption that the maximum numbers of synapses formed by a single axon on the proximal domains and higher-order dendrites of a single postsynaptic neuron are 14 and 9, respectively. It is difficult to define a hard figure for the minimum number of contacts formed by a single axon with a single postsynaptic neuron without complete reconstruction and identification of the postsynaptic structures of individual labelled axons. From our light and electron microscopic analyses we estimate that an individual axon will make a minimum of 3 synapses with an individual postsynaptic neuron. This assumption is not without at least a degree of risk. It could perhaps be argued that the most conservative minimum estimate is that an individual axon only makes a single synaptic contact with any other neuron. However, we consider this conservative estimate to be too low for the reasons stated above, and because an axon may contact more that one dendrite of a postsynaptic neuron. We also assume that the connectivity is the same for the two classes of neurons.

3.1.2. Volume of GP Occupied by Proximal Axonal Arborisation

Previous studies have touched upon the issue of finding an accurate method of elucidating the volume of an axonal arborisation (Kincaid et al., 1998; Zheng and Wilson, 2002). This is not the physical volume of the axonal arborisation, but rather the volume of tissue in which it can potentially make contacts. The best analogy to describe this is the volume enclosed by a net thrown over the branches of a tree. The total volume of the branches themselves is not of interest here, but rather the empty volume enclosed by the net is most

instructive; the latter could be equivalent to the volume of GP innervated by a single axonal arbour. The volume of the axonal arborisation, or the bouton cloud, is difficult to obtain without mathematical cluster analysis, as it depends on the spatial distribution of boutons. However, we know that the proximal axonal arborisations of GP neurons are located within the volume of GP occupied by the dendritic arborisations. Because of the characteristic shape of the dendritic arborisations of GP neurons we can estimate the volume of GP that the dendrites occupy by approximating their shape to either a rectangle or circle for lateral and medial neurons, respectively, and assigning a depth. This is an approximation of the volume occupied by the principal plane of each neuronal type. Estimates made from 5 neurons of each type (Sadek, Magill and Bolam, 2005 *in preparation*) give the mean volume occupied by a lateral neuron as $0.015\,mm^3$ (s.d. = $0.002\,mm^3$) and that of a medial neuron as $0.028\,mm^3$ (s.d. = $0.003\,mm^3$). Of course, the axonal arborisation does not occupy the *whole* volume occupied by the dendritic arborisation; we estimate that the axonal arborisation occupies 20% of that volume occupied by the dendritic tree. Thus, any GP neuron within this volume is a potential target of the axonal arborisation.

3.1.3. Number of Neurons in the Volume Occupied by the Proximal Axonal Arborisations

The distribution of the 45,960 neurons within the rat GP (Oorschot, 1996) is not homogeneous (Kita and Kita, 2001). The neuronal density in the lateral regions of the GP is lower than that in the more medial regions. The lateral regions contain 15,264 neurons/mm^3 whereas the medial regions contain 18,708 neurons/mm^3 (Kita and Kita, 2001). On the basis of these figures, the number of neurons with somata located within the dendritic arborisation of a lateral neuron is 229, and that number within the dendritic arborisation of a medial neuron is 523. Because we estimate that the proximal axonal arborisation probably only occupies about 20% of this volume (see section 3.1.2), the maximum number of neurons that an average lateral and an average medial neuron may contact through their proximal axonal arborisation is 46 and 105, respectively. This figure of course does not take into account neurons with cell bodies located outside of this region but whose dendrites course through the arborisation.

3.1.4. Volume of GP Occupied by the Distal Axonal Arborisations

The spatial organisation of the distal axonal arborisation of both lateral and medial neurons is not as well defined as that of the proximal axonal arborisation and is not contained within the dendritic arborisation. Furthermore, the shape of the arborisation is qualitatively different between neurons of both groups. We have thus not attempted at this stage to make estimates of its volume.

3.2. Connectivity of the *Proximal Arborisation* of Lateral Neurons

On average, the proximal axonal arborisation of a lateral neuron possesses 166 boutons, of which 133 (80%) form contacts onto the proximal domains of other GP neurons and 33 form contacts onto higher-order dendrites (Table 1; Sadek, 2004; Sadek, Magill and Bolam, 2005 *in preparation*). Based on the assumptions described above we estimate that the proximal arborisation of a lateral neuron may contact between 10 and 44 neurons in their proximal domains, and between 4 and 11 neurons on their higher-order dendrites. Thus, taking into account both proximal and distal dendritic contacts, lateral neurons are in a

position to form synapses with 14–55 neurons through their proximal axonal arborisation. This represents between 30% and 100% of the neurons within the volume occupied by the proximal axonal arborisation and between 6 and 24% of the neurons located within the dendritic arborisation (see Table 1 for calculations).

3.3. Connectivity of the *Proximal Arborisation* of Medial Neurons

For medial neurons, the proximal axonal arborisation possesses an average of 447 boutons, of which 215 (48%) form synapses with the proximal domains of other medial GP neurons and 232 with higher-order dendrites (Table 1). Hence between 15 and 72 neurons may be contacted in their proximal domains by the proximal axonal arborisation of a medial neuron and 26 to 77 neurons on their higher-order dendrites. Thus the total number of neurons the proximal axonal arborisation of a medial neuron may contact is in the range of 41 to 149. This represents between 39% and 100% of the neurons within the volume occupied by the proximal axonal arborisation of a medial neuron and 8 to 28% of the neurons within the dendritic arborisation (see Table 1 for calculations).

3.4. Connectivity of the *Distal Arborisation* of Lateral Neurons

Of the mean of 98 boutons contained within the distal axonal arborisation of a lateral neuron, 63 (64%) make synaptic contact with the proximal domains of other GP neurons and the remaining 35 make contact with higher-order dendrites. Boutons forming contacts with the proximal domains of neighbouring neurons could innervate 5 to 21 different neurons, whereas boutons in contact with distal dendrites may innervate another 4 to 12 neurons. Thus the distal axonal arborisation of a lateral neuron may contact between 9 to 33 (medial) neurons located caudo-ventro-medially in the GP (see Table 1 for calculations).

3.5. Connectivity of the *Distal Arborisation* of Medial Neurons

The distal axonal arborisation of medial neurons give rise on average to 134 boutons, 99 (74%) of which make contact proximal domains of their targets and 35 (26%) with higher-order dendrites. The boutons in the distal arborisation may thus contact 7 to 33 neurons in their proximal domains and 4 to 12 neurons at the level of higher-order dendrites. Thus, the distal axonal arborisation of a medial neuron is in a position to contact 11 to 45 other medial neurons (see Table 1 for calculations).

4. SUMMARY AND CONCLUDING REMARKS

- All GP neurons give rise to exten.sive and complex local axonal arborisations.
- There are quantitative differences between the local axonal arborisations of lateral and medial neurons.
- The local axonal arbours of lateral neurons are in a position to contact between 23 and 88 other GP neurons when considering the arborisation as a whole. Their proximal arborisations are in a position to contact between 14 and 55 neurons, which accounts for

between 30% and 100% of the neurons with somata located inside the volume occupied by that part of the arborisation.

- The local axonal arbours of medial neurons are in a position to contact between 52 and 194 other GP neurons when considering the arborisation as a whole. Their proximal arborisations are in a position to contact between 41 and 149 neurons i.e. between 39% and 100% of the neurons with somata located within the volume occupied by that part of the arborisation.

- These findings predict that for a neuron in the lateral GP there is a 6–24% chance of it being connected to another GP neuron within its dendritic arborisation and this figure rises to 30–100% chance for neurons located within the volume occupied by its proximal axonal arborisation. Similarly, for a neuron in the medial GP there is a 8–28% chance of it being connected to another GP neuron within its dendritic arborisation and this figure rises to 39–100% chance for neurons located within the volume occupied by its proximal axonal arborisation.

- Since the average number of boutons in the proximal arborisation of a lateral GP neuron is 166, then, if we assume that connectivity is homogeneous across the GP (which of course may not be the case), a lateral GP neuron will *receive* an average of 166 synaptic boutons from neighbouring GP neurons.

- Similarly, because the average number of boutons in the proximal arborisation of a medial GP neuron is 447, a medial GP neuron will thus *receive* an average of 447 synaptic boutons from neighbouring GP neurons *plus* any additional boutons derived from the distal arborisation of lateral neurons.

- The degree of convergence of local axons of GP neurons onto other GP neurons is given by the number of neurons that are estimated to be contacted within an arborisation. Thus lateral neurons will receive convergent input from 14 to 55 other GP neurons. Medial neurons on the other hand, will receive convergent input from 41 to 149 other GP neurons *plus* any additional convergence carried by the distal arborisations of lateral neurons.

- The complex local circuitry, the quantitative and qualitative differences in the connectivity of lateral and medial neurons, and the rostro-lateral to caudo-medial organisation of the distal axonal arborisations implies complex information processing within the GP. These data, together with the known connections of individual GP neurons with all other regions of the basal ganglia, suggest that the GP should not be considered as an homogeneous relay nucleus transmitting striatal information to the subthalamic nucleus and basal ganglia output nuclei, but rather a nucleus that is involved in complex information processing within its borders and the spatio-temporal selection of neurons at every level of the basal ganglia.

- These data call for the re-examination and redefinition of current models of GP, and the basal ganglia in general, to incorporate intra-pallidal connectivity.

- Finally, it should be emphasised that the quantitative features of connectivity that we calculate are necessarily based upon many assumptions. These assumptions may ulti-

mately prove to be inadequate or inaccurate. With the availability of new data in the future, the calculations presented here can be revised and incorporated into new and more precise models of the local connectivity of GP neurons.

5. ACKNOWLEDGEMENTS

This work was supported by the Medical Research Council UK. We are grateful to Justin Boyes, Kevin Gurney and Rob Stewart for their insightful comments, and to Ben Micklem for his help with the digital reconstruction technique.

6. REFERENCES

Albin, R.L., Young, A.B., and Penney, J.B., 1989, The functional anatomy of basal ganglia disorders. *Trends Neurosci.* **12**:366–375.

Bevan, M.D., Smith, A.D., and Bolam, J.P., 1996, The substantia nigra as a site of synaptic integration of functionally diverse information arising from the ventral pallidum and the globus pallidus in the rat. *Neuroscience* **75**:5–12.

Bevan, M.D., Clarke, N.P., and Bolam, J.P., 1997, Synaptic integration of functionally diverse pallidal information in the entopeduncular nucleus and subthalamic nucleus in the rat. *J. Neurosci.* **17**:308–324.

Bevan, M.D., Booth, P.A.C., Eaton, S.A., and Bolam, J.P., 1998, Selective innervation of neostriatal interneurons by a subclass of neuron in the globus pallidus of the rat. *J. Neurosci.* **18**:9438–9452.

Bolam, J.P., Booth, P.A.C., Hanley, J.J., and Bevan, M.D., 2000, Synaptic organisation of the basal ganglia, *J. Anatomy* **196**:527–542.

Bolam, J.P., and Smith, Y., 1992, The striatum and the globus pallidus send convergent synaptic inputs onto single cells in the entopeduncular nucleus of the rat: a double anterograde labeling study combined with post-embedding immunocytochemistry for GABA. *J. Comp. Neurol.* **321**:456–476.

Celada, P., Paladini, C.A., and Tepper, J.M., 1999, GABAergic control of rat substantia nigra dopaminergic neurons: Role of globus pallidus and substantia nigra pars reticulata. *Neuroscience* **89**:813–825.

Chung, Y.W., and Hassler, R.G., 1984, Types of synapses in the pallidum and their differential degeneration following lesions of pallidal afferents in squirrel monkey (*Saimiri sciureus*). *New York: Raven Press*.

DeLong, M.R., 1990. Primate models of movement disorders of basal ganglia origin. *Trends Neurosci.* **13**:281–285.

DiFiglia, M., Pasik, P., and Pasik, T., 1982, A Golgi and ultrastructural study of the monkey globus pallidus. *J. Comp. Neurol.* **212**:53–75.

Falls, W.M., and Park, M.R., 1981, Light and EM analysis of rat globus pallidus neurons intracellularly recorded and labelled with HRP. *Anat. Rec.* **199**:79A–80A.

Fox, C.A., Andrade, A.N., Lu Qui, I.J., and Rafols, J.A., 1974, The primate globus pallidus: a Golgi and electron microscopic study. *J. Hirnforsch.* **15**:75–93.

Francois, C., Percheron, G., Yelnik, J., and Heyner, S., 1984, A Golgi analysis of the primate globus pallidus. I. Inconstant processes of large neurons, other neuronal types, and afferent axons. *J. Comp. Neurol.* **227**:182–199.

Iwahori, N., and Mizuno, N., 1981, A Golgi study on the globus pallidus of the mouse. *J. Comp. Neurol.* **197**:29–43.

Kincaid, A.E., Zheng, T., and Wilson, C.J., 1998, Connectivity and convergence of single corticostriatal axons. *J. Neurosci.* **18**:4722–4731.

Kita, H., 1994, Parvalbumin-immunopositive neurons in rat globus pallidus: a light and electron microscopic study. *Brain Res.* **657**:31–41.

Kita, H., and Kitai, S.T., 1994, The morphology of globus pallidus projection neurons in the rat: an intracellular staining study. *Brain Res.* **636**:308–319.

Kita, H., and Kita, T., 2001, Number, origins, and chemical types of rat pallidostriatal projection neurons. *J. Comp. Neurol.* **437**:438–448.

Millhouse, O.E., 1986, Pallidal neurons in the rat. *J. Comp. Neurol.* **254**:209–227.

Nauta, H.J.W., 1979, Projections of the pallidal complex: An autoradiographic study in the cat. *Neuroscience* **4**:1853–1873.

Oorschot, D.E., 1996, Total number of neurons in the neostriatal, pallidal, subthalamic, and substantia nigral nuclei of the rat basal ganglia: a stereological study using the Cavalieri and optical dissector methods. *J. Comp. Neurol.* **366**:580–599.

Paladini, C.A., Iribe, Y., and Tepper, J.M., 1999, $GABA_A$ receptor stimulation blocks NMDA-induced bursting of dopaminergic neurons in vitro by decreasing input resistance. *Brain Res.* **832**:145–151.

Park, M.R., Falls, W.M., and Kitai, S.T., 1982, An intracellular HRP study of the rat globus pallidus. I. Responses and light microscopic analysis. *J. Comp. Neurol.* **211**:284–294.

Sadek, A.R., Magill, P.J., and Bolam, J.P., 2003, The morphology, connectivity and neurochemistry of single cells in the globus pallidus of the rat, *Soc. Neurosci. Abs.* **29**:601.10

Sadek, A.R., Magill, P.J., and Bolam, J.P., 2004, Local axonal collaterals of neurons of the rat globus pallidus. *IBAGS* Abstr:51.

Sadek, A.R., Magill, P.J., and Bolam, J.P., 2005, Morphology and connectivity of single neurons in the globus pallidus of the rat. *In preparation*.

Sato, F., Lavallée, P., Lévesque, M., and Parent, A., 2000, Single-axon tracing study of neurons of the external segment of the globus pallidus in primate. *J. Comp. Neurol.* **417**:17–31.

Shink, E., and Smith, Y., 1995, Differential synaptic innervation of neurons in the internal and external segments of the globus pallidus by the GABA- and glutamate-containing terminals in the squirrel monkey. *J. Comp. Neurol.* **358**:119–141.

Shink, E., Bevan, M.D., Bolam, J.P., and Smith, Y., 1996, The subthalamic nucleus and the external pallidum: two tightly interconnected structures that control the output of the basal ganglia in the monkey. *Neuroscience* **73**:335–357.

Smith, Y., Bevan, M.D., Shink, E., and Bolam, J.P., 1998, Microcircuitry of the direct and indirect pathways of the basal ganglia, *Neuroscience* **86**:353–387.

Smith, Y., and Bolam, J.P., 1989, Neurons of the substantia nigra reticulata receive a dense GABA-containing input from the globus pallidus in the rat, *Brain Res*. **493**:160–167.

Smith, Y., and Bolam, J.P., 1990, The output neurones and the dopaminergic neurones of the substantia nigra receive a GABA-containing input from the globus pallidus in the rat, *J. Comp. Neurol*. **296**:47–64.

Zheng, T., and Wilson, C.J., 2002, Corticostriatal combinatorics: the implications of corticostriatal axonal arborizations. *J. Neurophysiol.* **87**:1007–1017.

AUTHOR INDEX

SUBJECT INDEX

D

E

F

G

H

I

K

L

M

N

O

P

Q

R

S

T